



सत्यमेव जयते

INDIAN AGRICULTURAL  
RESEARCH INSTITUTE, NEW DELHI.

**L A. R. I. 6.**

MGIPC—S1—6 AR/54—7-7-54—10,000.







THE  
LONDON, EDINBURGH, AND DUBLIN  
PHILOSOPHICAL MAGAZINE  
AND  
JOURNAL OF SCIENCE.

CONDUCTED BY

SIR OLIVER JOSEPH LODGE, D.Sc., LL.D., F.R.S.  
JOSEPH JOHN THOMSON, O.M., M.A., Sc.D., LL.D., F.R.  
JOHN JOLY, M.A., D.Sc., F.R.S., F.G.S.  
RICHARD TAUNTON FRANCIS, F.R.S.E.

AND

WILLIAM FRANCIS, F.I.S.

---

"Nec araneorum sane textus ideo melior quia ex se fila gignunt, nec noster  
vilior quia ex alienis libamus ut apes." JUST. LIPS. *Polit. lib. i. cap. l. Not.*

---

VOL. IX.—SEVENTH SERIES.

JANUARY—JUNE 1930.

28124/136

LONDON:

TAYLOR AND FRANCIS, RED LION COURT, FLEET STREET.

SOLD BY SMITH AND SON, GLASGOW;—HODGES, FIGGIS, AND CO., DUBLIN;—  
AND VEUVE J. BOYVEAU, PARIS.



THE  
LONDON, EDINBURGH, AND DUBLIN  
PHILOSOPHICAL MAGAZINE  
AND  
JOURNAL OF SCIENCE.

CONDUCTED BY

SIR OLIVER JOSEPH LODGE, D.Sc., LL.D., F.R.S.  
SIR JOSEPH JOHN THOMSON, O.M., M.A., Sc.D., LL.D., F.R.S.  
JOHN JOLY, M.A., D.Sc., F.R.S., F.G.S.  
RICHARD TAUNTON FRANCIS, F.R.S.E.

AND

WILLIAM FRANCIS, F.I.S.

---

"Nec aranearum sane textus ideo melior quia ex se fila gignunt, nec noster  
vilior quia ex alienis libamus ut apes." JUST. LIPS. *Polit. lib. i. cap. l. Not.*

---

VOL. IX.—SEVENTH SERIES.

JANUARY—JUNE 1930.

28124/136

LONDON:

TAYLOR AND FRANCIS, RED LION COURT, FLEET STREET.

SOLD BY SMITH AND SON, GLASGOW;—HODGES, FIGGIS, AND CO., DUBLIN;—  
AND VEUVE J. BOYVEAU, PARIS.

“Meditationis est perscrutari occulta ; contemplationis est admirari perspicua . . . . Admiratio generat quæstionem, quæstio investigationem investigatio inventionem.”—*Hugo de S. Victore.*

---

—“Cur spirent venti, cur terra dehiscat,  
Cur mare turgescat, pelago cur tantus amaror,  
Cur caput obscura Phœbus ferrugine condât,  
Quid toties diros cogat flagrare cometas,  
Quid pariat nubes, veniant cur fulmina cœlo.  
Quo micet igne Iris, superos quis conciat orbes  
Tam vario motu.”

*J. B. Pinelli ad Mazonium*



# CONTENTS OF VOL. IX.

(SEVENTH SERIES).

NUMBER LV.—JANUARY 1930.

	Page
Mr. S. Davies and Prof. E. J. Evans on the Damping produced by Eddy Currents induced in Metal Spheres and Cylinders Oscillating in a Non-Uniform Magnetic Field, and its Application to the Determination of Resistivity.....	1
Mr. E. S. Keeping on the Damped Oscillation of a Conductor in a Non-Uniform Magnetic Field .....	16
Mr. A. E. Bate on the Determination of the End Correction and Conductance at the Mouth of a Stopped Organ (Flue) Pipe ....	23
Messrs. Edward S. Lamar and W. Edwards Deeming on Temperature Distribution along a Heated Filament used as a Catalyst ..	28
Dr. D. B. Deodhar on New Bands in the Secondary Spectrum of Hydrogen.—Part II. ....	37
Dr. Ludwik Silberstein on Illuminated Spacetime: Optical Effects of Isotropic Radiation Spread over Elliptic Space .....	50
Dr. A. Claassen on the Calculation of Absorption in X-Ray Powder-Photographs and the Scattering Power of Tungsten.....	57
Dr. William Hume-Rothery on the Crystal Structures of the Elements of the B Sub-Groups and their Connexion with the Periodic Table and Atomic Structures .....	65
Mr. Hrishikesh Rakshit on the Distribution of Space Charge between a Plane Hot Cathode and a Parallel Anode.....	80
Messrs. D. Banerji and R. Ganguli on the Generation of Pulses in Vibrating Strings. (Plate I.) .....	88
Dr. G. F. C. Searle on the Mutual Action of a Pair of Rational Current Elements .....	92
Dr. A. E. Martin on the Determination of the Variation with Pressure of the Force between Two Plates at Different Temperatures at Low Pressures, with a View to the Determination of Molecular Mean Free Paths.....	97
Mr. F. J. Garrick on Studies in Coordination. Part I.—Ion Hydrates .....	131
Mr. W. R. Morgans on the Kirchhoff Formula extended to a Moving Surface.....	141
Dr. J. Lockwood Taylor on some Hydrodynamical Inertia Coefficients .....	161
Prof. Seiichi Higuchi on some Closed Algebraic Curves and their Application to Dynamical Problems.—Part I. ....	184
Notices respecting New Books:—	
Mr. V. Bush's Operational Circuit Analysis .....	191
Mr. G. Birtwistle's La Nouvelle Mécanique de Quanta.....	191
Prof. H. A. Lorentz's Vorlesungen über Theoretische Physik .	192

## NUMBER LVI.—FEBRUARY.

Mr. G. W. Brindley on the Amplitude of Vibration of Ions in the Crystals NaCl, NaF, LiF, and KCl .....	193
Mr. G. W. Brindley on a Note on the Scattering Power of the Carbon Atom in Diamond for X-Rays .....	204
Prof. N. A. Kolossowsky on the Principle of Inaccessibility of the Absolute Zero .....	208
Mr. Ziró Tuzi on the Effect of a Circular Hole on the Stress Distribution in a Beam under Uniform Bending Moment. (Plate II.) ..	210
Mr. T. L. Eckersley on The Critical Frequency in an Ionized Medium. Steady Magnetic Force Present. ....	225
Prof. T. M. Lowry and Mr. M. A. Vernon on the Electronic Theory of Valency.—Part VII. (Plates III. & IV.) ..	233
Dr. George Green on some Problems in the Conduction of Heat ..	241
Prof. W. M. Thornton on the Propagation of Flame in Gaseous Explosions .....	260
Mr. A. C. Banerji on the Scattering of $\alpha$ -particles by Light Atoms. ..	273
Mr. S. Chandrasekhar on the Ionization-Formula and the New Statistics .....	292
Dr. S. L. Ziemecki and Mr. K. Narkiewicz-Jodko on the Raman-Effect in the Proximity of the Critical Point. ....	299
Dr. Kulesh Chandra Kar and Mr. Mohinimohon Ghosh on the Theory of the Pianoforte String struck by a Hard Hammer.—Part I. ....	306
Dr. K. C. Kar and Mr. M. Ghosh on the Theory of the Pianoforte String struck by a Hard Hammer.—Part II. ....	321
Mr. Andrew Robertson on the Critical Stress for Tubular Struts ..	324
Proceedings of the Geological Society :—	
Dr. P. K. Ghosh on the Carnmenellis Granite: its Petrology, Metamorphism, and Tectonics .....	326
Mr. Richard Dixon Oldham on Historic Changes of Level in the Delta of the Rhone .....	327
Major Arthur Richard Derryhouse on the Glaciation of Clun Forest, Radnor Forest, and some Adjoining Districts .....	328

## NUMBER LVII.—MARCH.

Mr. Sydney Thomas on Vibrations damped by Solid Friction .....	329
Dr. Eric J. Irons on the Free Periods of Resonators .....	346
Mr. R. W. Roberts on the Paramagnetic Rotatory Dispersion of Aqueous Solutions of Cobalt Sulphate in the Visible and Ultra-Violet Regions of the Spectrum .....	361
Prof. W. T. David and Mr. W. Davies on Luminosity in Gaseous Combustion. (Plates V.—VIII.) .....	390
Prof. W. T. David and Mr. W. Davies on Temperature Measurements in Gaseous Combustion. (Plate IX.) .....	402
Prof. J. B. Seth and Messrs. Chetan Anand and Girdhari Lal Puri on some Experiments with Carbon Line Resistances .....	415
Dr. A. R. Martin on the Effect of a Permanent Electrical Dipole on the Internal Latent Heat of Vaporization of a Liquid .....	422
Dr. W. H. Brooks on Problems of determining Initial and Maximum Stresses in Ties and Struts under Elastic or Rigid End Constraints.—Part II. ....	426

	Page
Dr. A. L. Reimann and Mr. R. Murgoci on Thermionic Emission and Electrical Conductivity of Oxide Cathodes . . . . .	440
Miss Hazel M. Fletcher on the Effect of Occluded Gases and Moisture on the Resistance of Air Condensers at Radio Frequencies . . . . .	464
Prof. H. Saegusa and Mr. S. Shimizu on an Anomalous After-Effect of Dielectrics for their Apparent Resistivity . . . . .	474
Prof. H. Levy and Mr. S. G. Hooker on the Vortex System in the Wake of a Cylinder in a Fluid . . . . .	489
Mr. F. E. Hoare on the Damping of a Pendulum by Viscous Media (Aniline) . . . . .	502
Mr. Wilfred W. Barkas on Positive and Negative Photophoresis of Colloidal Particles in Aqueous Solutions . . . . .	505
Messrs. S. Barratt and A. R. Bonar on the Band Spectra of Cadmium and Bismuth . . . . .	519
Dr. J. Brentano on Precision Measurement of X-Ray Reflexions from Crystal Powders . . . . .	525

## NUMBER LVIII.—APRIL.

Mr. C. Childs on the Cathode Dark Space in the Geissler Discharge . . . . .	529
Mr. Emlyn Stephens on the Hall Effect, Electrical Conductivity, and Thermoelectric Power of the Lead-Antimony Series of Alloys . . . . .	547
Prof. V. A. Bailey on the Behaviour of Electrons in Magnetic Fields . . . . .	560
Mr. D. Meksyn on Hamilton's Principle and the Field Equations of Radiation . . . . .	568
Prof. P. E. Shaw on Frictional Electricity . . . . .	577
Prof. Meghnad Saha and Ramesh Chandra Majumdar on new Methods in Statistical Mechanics . . . . .	584
Messrs. J. A. C. Teegan and K. G. Krishnan on Application of the Photoelectric Cell to the Measurement of Small Displacements . . . . .	589
Mr. J. P. Andrews on the Theory of Collision of Spheres of Soft Metals . . . . .	593
Mr. William Stone on some Phenomena of the Contact of Solids . . . . .	610
Mr. S. Chandrasekhar on the Probability Method in the New Statistics . . . . .	621
Prof. V. A. Bailey on the Behaviour of Electrons in Magnetic Fields . . . . .	625
Prof. P. E. Shaw on the Nature of Friction . . . . .	628
Mr. P. Cormac on a Skew Double-Slider-Crank Mechanism . . . . .	639
Mr. Paul White on the Scattering and Diffraction of Cathode-Rays . . . . .	641
Mr. W. G. Penney on Hydrogen and Helium Lines as Standards of Wave-length . . . . .	661
Prof. A. Ogg on the Space-Group of the Alkaline Sulphates, with a Note by Dr. A. E. H. Tutton . . . . .	665
Mr. H. Carrington on Critical Stresses for Tubular Struts . . . . .	668
Notices respecting New Books:—	
Prof. D. E. Smith's Source Books in the History of the Sciences . . . . .	668
Prof. H. W. Turnbull's The Great Mathematicians . . . . .	669
Mr. F. C. S. Schiller's Logic for Use . . . . .	669
Messrs. W. Wien and F. Harms's Handbuch der Experimental Physik . . . . .	670
Mr. F. Bouny's Leçons de Mécanique Rationnelle, Tome deuxième . . . . .	671
Proceedings of the Geological Society:—	
Prof. Beeby Thompson on the Upper Estuarine Series of Northamptonshire and Northern Oxfordshire . . . . .	671



## NUMBER LIX.—MAY (SUPPLEMENT).

Prof. W. M. Hicks on an Analysis of the Spectrum of Hg II . . . .	673
Mr. K. F. Herzfeld on the Scattering of Sound-Waves by small Elastic Spheres . . . . .	741
Mr. K. F. Herzfeld on the Propagation of Sound in Suspensions .	752
Miss Dorothy A. Newton on the Investigation of the Cataphoresis of small Particles in Water . . . . .	769
Dr. L. Silberstein and Mr. A. P. H. Trivelli on the Quantum Theory of X-Ray Exposures on Photographic Emulsions. (Plate X.) .	787
Mr. J. P. Den Hartog on Forced Vibrations with combined Viscous and Coulomb Damping . . . . .	801
Messrs. P. A. Macdonald and John F. Allen on the Psychophysical Law.—I. The Sense of Vision . . . . .	817
Messrs. P. A. Macdonald and John F. Allen on the Psychophysical Law.—II. The Sense of Audition . . . . .	827
Mr. John F. Allen on the Depression and Enhancement of Auditory Sensitivity . . . . .	834
Dr. W. N. Bond: Concerning Electrical and other Dimensions . .	842
Dr. F. C. Chalklin on the Soft X-Rays of Manganese . . . . .	847
Mr. A. F. Dufton on the Effective Temperature of a Warmed Room. (Plate XI.) . . . . .	858
Notices respecting New Books:—	
Dr. J. W. Mellor's A Comprehensive Treatment on Inorganic and Theoretical Chemistry . . . . .	861
Dr. H. Banister's Elementary Applications of Statistical Method . . . . .	862
Prof. R. H. Fowler's The Elementary Differential Geometry of Plane Curves . . . . .	862
Proceedings of the Geological Society:—	
Dr. Edward Greenly on Foliation in its Relation to Folding in the Mona Complex at Rhoscolyn (Anglesey) . . . . .	863
Dr. Frederick Walker on the Geology of the Shiant Isles . .	864

## NUMBER LX.—MAY.

Mr. S. Whitehead on Dipoles in Relation to the Anomalous Properties of Dielectrics . . . . .	865
Mr. A. G. Warren on the Free and Forced Symmetrical Oscillations of Thin Bars, Circular Diaphragms, and Annuli . .	881
Mr. A. T. Starr on Lag in a Thermometer when the Temperature of the External Medium is Varying . . . . .	901
Mr. G. A. Tomlinson on a Molecular Theory of Elastic Hysteresis . . . . .	913
Prof. Hermann Weyl on Redshift and Relativistic Cosmology. . .	936
Dr. Edmund C. Stoner on the Equilibrium of Dense Stars. . . . .	944
Mr. D. B. Mair on Second Order Expressions for the Potentials of a Sphere . . . . .	964
Dr. E. C. Rhodes on Reducing Observations by the Method of Minimum Deviations . . . . .	974
Messrs. E. Vyron Howells and W. Morris Jones on an X-ray Investigation of the Copper-Antimony System of Alloys . . . . .	993
Mr. E. H. Synge on a Method of Investigating the Higher Atmosphere . . . . .	1014
Dr. F. E. King and Prof. J. R. Partington on Measurements of Sound-Velocities in Air, Oxygen, and Carbon Dioxide at Temperatures from 900° C. to 1200° C., with special reference to the Temperature-Coefficients of Molecular Heats . . . . .	1020

	Page
Mr. F. Tyler on the Magnetic Characteristics of Nickel .....	1026
Drs. N. A. V. Piercy and E. G. Richardson on the Turbulence in front of a Body moving through a Viscous Fluid .....	1038
Dr. P. Monteagle Barlow on Experiments on the Apparent Deviation from Ohm's Law for Metals at High Current Densities. ....	1041
Notices respecting New Books:—	
Dr. Harvey Fletcher's Speech and Hearing.....	1055
Lady T. Mary Lockyer and Miss Winifred L. Lockyer's The Life and Work of Sir Norman Lockyer .....	1057
His Majesty's Stationery Office—National Physical Laboratory Collected Researches .....	1057
Prof. P. Debye's Dipolmoment und Chemische Struktur ....	1058
Mr. Rudolf Peierls's Einführung in die Wellenmechanik, Louis de Broglie .....	1058
Proceedings of the Geological Society:—	
Mr. John Vernon Harrison on the Geology of some Salt-Plugs in Laristan (Southern Persia) .....	1059
Prof. J. W. Gregory on Geological History of the Pacific Ocean .....	1060
Mr. Sydney Ewart Hollingworth on the Glaciation of Western Edenside and Adjoining Areas, and the Drumlins of Edenside and the Solway Basin .....	1062
Prof. W. T. Gordon: Exhibition of a set of Cellulose 'Pulls' from Coal-Balls .....	1063

NUMBER LXI.—JUNE.

Prof. Alfred W. Porter: Notes on Surface-Tension .....	1065
Dr. Gorakh Prasad on the Numerical Solution of Partial Differ- ential Equations .....	1074
Mr. G. W. Brindley on the Scattering Powers of the Atoms in Magnesium Oxide for X-Rays and some Related Properties....	1081
Dr. W. H. Brooks on the Problems of determining Initial and Maximum Stresses in Ties and Struts under Elastic or Rigid End Constraints.—Part III. ....	1094
Mr. E. Tyler on a Hot-Wire Amplifier Method for the Measure- ment of the Distribution of Vortices behind Obstacles .....	1113
Dr. R. A. Houstoun on the Mathematical Representation of Sensi- bility to Difference of Colour .....	1130
Prof. J. S. Townsend on the Energies of Electrons in Gases .....	1145
Dr. R. N. Ghosh on the Elastic Impact of a Pianoforte Hammer. (Plate XII.) .....	1174
Sir J. J. Thomson on the Relation of Electronic Waves to Light Quanta and to Planck's Law .....	1185
Notices respecting New Books:—	
Sir Henry A. Miers's An Introduction to the Scientific Study of Minerals. Second Edition, revised by H. L. Bowman ..	1194
Lewis's Catalogue of Medical and Scientific Circulating Library	1196
Proceedings of the Geological Society:—	
Mr. Roy Woodhouse Pocock on the Age of the Midland Basalts .....	1196
Dr. Thomas Robertson on the Origin of the Etruria Marl....	1197
Mr. Walter Campbell Smith on a Classification of some Rhyolites, Trachytes, and Phonolites from part of Kenya Colony, with a Note on some associated Basaltic Rocks ..	1198
Prof. Léon W. Collet on the Structure of the Canadian Rockies	1199
Index .....	1200

## P L A T E S.

- I. Illustrative of Messrs. D. Banerji and R. Ganguli's Paper on the Generation of Pulses in Vibrating Strings.
- II. Illustrative of Mr. Z. Tuzi's Paper on the Effect of a Circular Hole on the Stress Distribution in a Beam under Uniform Bending Moment.
- III. & IV. Illustrative of Prof. T. M. Lowry and Mr. A. Vernon's Paper on the Electronic Theory of Valency.
- V.-VIII. Illustrative of Prof. W. T. David and Mr. W. Davies's Paper on Luminosity in Gaseous Combustion.
- IX. Illustrative of Prof. W. T. David and Mr. W. Davies's Paper on Temperature Measurements in Gaseous Combustion.
- X. Illustrative of Dr. L. Silberstein and Mr. A. P. H. Trivelli's Paper on the Quantum Theory of X-Ray Exposures on Photographic Emulsions.
- XI. Illustrative of Mr. A. F. Dufton's Paper on the Effective Temperature of a Warmed Room.
- XII. Illustrative of Dr. R. N. Ghosh's Paper on the Elastic Impact of a Pianoforte Hammer.

---

ERRATUM.

Vol. VIII., p. 990 (December 1929), line 21,  
*for*  $10^{-12}$  ampere *read*  $10^{-8}$  ampere.

---

THE  
LONDON, EDINBURGH, AND DUBLIN  
PHILOSOPHICAL MAGAZINE  
AND  
JOURNAL OF SCIENCE.

---

[SEVENTH SERIES.]

---

JANUARY 1930.

---

- I. *The Damping produced by Eddy Currents induced in Metal Spheres and Cylinders Oscillating in a Non-Uniform Magnetic Field, and its Application to the Determination of Resistivity.* By S. DAVIES, B.Sc., and E. J. EVANS, D.Sc., University College of Swansea\*.

*Introduction.*

IT is well known that the resistivity of a conductor can be measured by swinging a magnetic needle over the conductor, or by oscillating the conductor about a vertical axis in a uniform magnetic field. Both methods were employed by F. Himstedt †, who also considered the problem from the theoretical standpoint. In the first method a magnetic system was set swinging near a fixed copper sphere, and the damping produced by the induced currents was measured. In the second method the damping was determined when the copper sphere was set oscillating about a vertical axis in a uniform magnetic field. Warburg ‡ emphasized the importance of considering the effect of hysteresis when a magnetic needle is set swinging over magnetic substances. When a needle swings over an iron plate the damping is greater than would be expected from its specific resistance. Weber § also employed the same two

\* Communicated by Prof. E. J. Evans.

† Wied. Ann. ii. p. 812 (1880).

‡ Wied. Ann. xiii. p. 159 (1881).

§ Wied. Ann. lxviii. p. 705 (1899).

$$\begin{aligned}
 \log \text{dec}_1 - \log \text{dec}_2 &= \frac{1}{4} k_2 T \\
 &= \frac{3K}{2\pi} \left( \frac{dH}{ds} \right)^2 \cdot \frac{D^2}{\rho} \cdot \frac{1}{d} \cdot T \\
 &= C \left( \frac{dH}{ds} \right)^2 \cdot \frac{D^2}{\rho} \cdot \frac{1}{d} \cdot T, \quad \dots (6)
 \end{aligned}$$

where

$$C = \frac{3}{2} \frac{K}{\pi} = \frac{1}{160} = \cdot 00625.$$

(b) *Cylinders.*

(1) The pendulum bobs were cylinders of copper or brass swinging with their axes vertical in the horizontal magnetic field between the pole-pieces of the electromagnet. The lines of magnetic force were perpendicular to the axes of the cylinders.

In this case the experimental results in conjunction with the theory of dimensions show that

$$\log \text{dec}_1 - \log \text{dec}_2 = K \left( \frac{dH}{ds} \right)^2 \cdot \frac{f(D \cdot l)}{\rho} \cdot \frac{1}{d} \cdot T, \quad \dots (7)$$

where  $K$  is a constant and  $f(D \cdot l)$  is of dimensions  $L^2$ .

(2) The pendulum bobs were cylinders supported by a bifilar suspension of fine silk, and swinging with their axes parallel to the lines of force.

The experimental results indicate that the difference of  $\log \text{dec}$  is independent of the lengths of the cylinders, and it therefore follows from the theory of dimensions that

$$\log \text{dec}_1 - \log \text{dec}_2 = C_1 \left( \frac{dH}{ds} \right)^2 \cdot \frac{D^2}{\rho} \cdot \frac{1}{d} \cdot T, \quad \dots (8)$$

where  $C_1$  is a constant.

According to Keeping\* the value of  $C_1 = \frac{1}{128} = \cdot 00781$ .

*Experimental Work.*

According to equation (6) deduced for a sphere, oscillating between the poles of the electromagnet, the difference of logarithmic decrement with and without the magnetic field is given by

$$\log \text{dec}_1 - \log \text{dec}_2 = C \left( \frac{dH}{ds} \right)^2 \cdot \frac{1}{\rho} \cdot \frac{1}{d} \cdot D^2 \cdot T.$$

\* *Loc. cit.*

The experimental work therefore involves the measurement of  $\frac{dH}{ds}$ , the rate of variation of the magnetic field along the line of vibration of the pendulum, the resistivity  $\rho$ , the density  $d$ , the diameter  $D$ , and the period of swing  $T$ , together with the difference of logarithmic decrement with and without field. In order to test the various relationships involved in the above equation, spherical pendulum bobs were made of copper, aluminium, tin, zinc, lead, mercury, brass, and an alloy of tin and lead. In the case of copper, four spheres of diameters 2.48, 2.12, 1.715, and 1.263 cm. respectively were made. The smallest sphere of diameter 1.263 cm. was turned from a rod of very pure copper, and its resistivity was determined by measuring the resistance of the rod with the Kelvin bridge. This measured value of the resistivity was used in the application of the above equation to the measurement of resistivity.

The spheres of other materials were turned from rods or from cylinders of the materials specially cast for the purpose. With the exception of zinc and mercury, the actual resistivities of the materials employed in the preparation of the spheres were actually measured.

### *Resistivities.*

The resistances of the various materials to be measured varied from about 0.0000670 ohm for the copper rod to .00149 ohm for the lead rod. An accurate method for the determination of low resistances was therefore necessary, and for this reason the measurements were made with a Kelvin bridge constructed by the Cambridge Instrument Company. The method is well known, and no description is therefore necessary.

### *Logarithmic Decrement.*

The metallic spheres were suspended by a fine silk thread, thus forming a simple pendulum. Behind the thread on the top of one of the pole-pieces, and parallel with the line of swing of the pendulum, was fixed a centimetre scale with its middle point opposite the centre of the magnetic field between the pole-pieces. The pendulum and scale were viewed by a telescope placed at a distance of about 4 feet from the magnet. The logarithmic decrement was then determined in the usual way.

*Measurement of the Intensity of the Magnetic Field at the Centre of Swing and the Variation of the Field along the Line of Swing.*

The electromagnet was designed to give a strong and uniform magnet field over a comparatively large area, and the pole-faces were of rectangular cross-section, having a length of 16.5 cm. and a breadth of 5.0 cm.

In the present experiments, measurements of  $H$  and  $\frac{dH}{ds}$  were carried out with the distance between the pole-pieces tapering from 3.96 cm. at one end to 3.46 cm. at the other end, and also with the same distance tapering from 4.45 cm. at one end to 3.45 cm. at the other end. Three points, A, B, and C, were selected along the line of swing of the simple pendulum, and the intensities of the magnetic fields at B, the point of rest of the pendulum bob, were determined for 2, 3, 4, 5, and 6 amperes passing through the magnet coils by means of a search coil or fluxmeter. The values of  $\frac{dH}{ds}$ , corresponding to various values of the current passing through the magnet, could then be calculated from the deflexions observed when the search coil was placed at A and C respectively. The points A and C were situated on opposite sides of B, and at a distance of 2 cm. from it. The values of  $\frac{dH}{ds}$  determined in this way were accurate to within about 4 per cent., and within the limits of experimental error the deflexions at A, B, and C indicated that  $\frac{dH}{ds}$  was constant over the distance AC.

With the pole-faces adjusted for the larger taper a more accurate value of  $\frac{dH}{ds}$  was obtained when a current of 5 amperes was passed through the electromagnet. Two small coils of equal mean area, and whose centres were at a distance apart of 4 cm., were connected up in series with the fluxmeter so that the E.M.F.'s induced were in opposition when the coils were simultaneously removed from the fields at A and C. The value of  $\frac{dH}{ds}$  obtained in this way was about 3 per cent. higher than that obtained by the previous method, and will be used later in the determination of the values of the constants C and  $C_1$  in equations (6) and (8).

## Experimental Results for Spheres.

TABLE I.

Magnet pole-faces tapering from 3.46 cm. at one extremity to 3.96 cm. at other extremity.

Nature of pendulum bob.	Diam. of bob in cm.	Current in amps. through magnet.	Field in gauss at B, the centre of swing.	Period of swing in secs.	Temperature in degrees centigrade of air between poles.	Log dec with field—log dec without field.
Copper .....	1.263	5.0	5660	1.0	23.0	.00158
" .....	"	"	"	1.5	22.5	.00238
" .....	"	"	"	2.0	23.8	.00312
" .....	1.715	"	"	1.5	17.7	.00434
" .....	2.120	"	"	"	18.8	.00653
" .....	2.480	"	"	"	17.7	.00901
Brass.....	1.723	"	"	"	23.8	.00125
Zinc .....	1.174	"	"	1.0	19.1	.00103
" .....	"	"	"	1.5	"	.00154
" .....	"	"	"	2.0	"	.00204
" .....	2.485	"	"	1.5	21.2	.00310

TABLE II.

Magnet pole-faces tapering from 3.45 cm. at one extremity to 4.45 cm. at other extremity.

Nature of pendulum bob.	Diam. of bob in cm.	Current in amps. through magnet.	Field in gauss at B, the centre of swing.	Period of swing in secs.	Temperature in degrees centigrade of air between poles.	Log dec with field—log dec without field.
Copper .....	1.263	5.0	4993	1.5	21.2	.00712
Aluminium...	1.232	2.0	2152	"	22.5	.00247
" .....	"	3.0	3207	"	"	.00525
" .....	"	4.0	4218	"	"	.00900
" .....	"	5.0	4993	"	"	.01290
" .....	"	6.0	5445	"	"	.01610
" .....	2.19	5.0	4993	"	22.0	.04110
Lead .....	1.26	5.0	4993	1.5	22.5	.00046
" .....	2.48	"	"	"	21.4	.00177
Tin .....	1.703	"	"	"	23.7	.00229
Lead-Tin alloy. }	1.713	"	"	"	20.1	.00122
Mercury .....	2.16	"	"	"	19.0	.00024



*Discussion of Results.*

According to equation (6) the difference between logarithmic decrement with the field and without the field is given by

$$C \cdot \left( \frac{dH}{ds} \right)^2 \cdot \frac{D^2}{\rho} \cdot \frac{T}{d}.$$

The variation of the difference of log dec with the various quantities concerned will now be considered.

TABLE III.

Variation with T. (Field at centre of swing = 5660 gauss.)

Nature of pendulum bob.	Period of swing in seconds.	Log dec with field — log dec without field.	$\frac{\text{Log dec}_1 - \text{log dec}_2}{T}$
Copper, 1.263 cm. ....	1.0	.00158	.00158
„ ..... 1.5	1.5	.00238	.00158
„ ..... 2.0	2.0	.00312	.00156
Zinc, 1.714 cm. ....	1.0	.00103	.00103
„ ..... 1.5	1.5	.00154	.00103
„ ..... 2.0	2.0	.00204	.00102

The results show that for a given pendulum bob, keeping the field at each point constant, the value of  $\text{log dec}_1 - \text{log dec}_2$  is directly proportional to the period of swing.

TABLE IV.

Variation with Diameter “D.”

Period T = 1.5 seconds in all cases, 5 amperes passing through magnet and distance between pole-faces tapering from 3.46 cm. at one end to 3.96 cm. at other end.

Nature of pendulum bob.	Diameter “D” in cm.	Field in gauss at centre of swing.	$\frac{\text{Log dec}_1 - \text{log dec}_2}{D^2}$
Copper .....	1.263	5660	.00149
„ .....	1.715	„	.00148
„ .....	2.120	„	.00145
„ .....	2.480	„	.00147

The results given in Table IV. show, for spheres of the same material oscillating in the same magnetic field with the same period of swing, that  $(\log \text{dec}_1 - \log \text{dec}_2)$  is proportional to the square of the diameter.

TABLE V.

Variation with  $\frac{dH}{ds}$ .

Aluminium sphere of diameter 1.23 cm., and the distance between pole-faces tapering from 3.45 cm. at one end to 4.45 cm. at other end.

Current through magnet in amperes.	Field in gauss at centre of swing.	$\frac{dH}{ds}$ in gauss per cm.	Relative values of $\left(\frac{dH}{ds}\right)^2$ .	Relative values of $\log \text{dec}_1 - \log \text{dec}_2$ .
2	2152	36.1	1	1
3	3207	54.0	2.24	2.13
4	4218	69.0	3.65	3.64
5	4993	83.4	5.34	5.22
6	5445	91.6	6.43	6.52

The above results show that the difference of logarithmic decrement with field and without field is proportional to  $\left(\frac{dH}{ds}\right)^2$  when the current passing through the magnet is changed.

*Measurements of the Resistivities of the various Conductors by comparison with the Resistivity of the Material from which the small Copper Sphere of Diameter 1.263 cm. was turned.*

Let  $d_{Cu}$ ,  $\rho_{Cu}$ ,  $D_{Cu}$ , and  $(\log \text{dec}_1 - \log \text{dec}_2)_{Cu}$  represent the values of the density, resistivity, diameter, and the difference of log dec with and without the magnet field in the case of copper, and  $d_m$ ,  $\rho_m$ ,  $D_m$ ,  $(\log \text{dec}_1 - \log \text{dec}_2)_m$  the corresponding quantities in the case of the material examined.

It follows then, from equation (6) when  $\frac{dH}{ds}$  and T are the same for both, that

$$\rho_m = \frac{D_{Cu}^2}{D_m^2} \cdot \frac{d_{Cu}}{d_m} \cdot \frac{(\log \text{dec}_1 - \log \text{dec}_2)_{Cu}}{(\log \text{dec}_1 - \log \text{dec}_2)_m} \cdot \rho_{Cu}.$$

The resistivities of the various substances calculated from the above equation are collected in Table IV. The values of the resistivities have been calculated from the results given for  $(\log \text{dec}_1 - \log \text{dec}_2)$  in Tables I. and II. when a current of 5 amperes passed through the magnet and  $T=1.5$  seconds.

The resistivity of the copper from which the small sphere was turned equals 1.703 microhms per cm.<sup>2</sup> at 16.7° C. The resistivities in all cases can be reduced to 18° C. from the known values of the temperature coefficients of resistance.

TABLE VI.

Nature of sphere.	Diameter of sphere in cm.	Density of material in grams per c.c.	Resistivity in microns per cm. <sup>2</sup> at 18° C. determined from pendulum experiments.	Resistivity in microns per cm. <sup>2</sup> at 18° C. determined directly.
Aluminium ... {	1.23	2.71	2.95	2.91
	2.19		2.92	2.91
Zinc ..... {	1.714	7.18	6.15	6.10
	2.485		6.17	6.10
Brass ..... {	1.723	8.40	6.50	6.29
Lead ..... {	1.26	11.37	20.9	21.5
	2.48		21.20	21.5
Tin ..... {	1.703	7.22	11.92	12.0
Lead-Tin alloy ... {	1.713	9.04	18.5	18.2
Mercury ..... {	2.16	13.6	96.6	95.6

The resistivities determined from the pendulum experiments agree within about 2 per cent. with those determined directly with the Kelvin bridge.

#### *Determinations of the Constant "C."*

The determination of the constant "C" in the equation

$$\log \text{dec}_1 - \log \text{dec}_2 = C \left( \frac{dH}{ds} \right)^2 \cdot \frac{D^2}{\rho} \cdot \frac{1}{d} \cdot T$$

is rendered fairly difficult owing to the smallness of the quantity  $\frac{dH}{ds}$ . The value of  $\frac{dH}{ds}$  was therefore re-determined when the distance between the pole-faces varied from 3.45 cm. at one end to 4.45 cm. at the other end, and a current of 5 amperes passed through the electromagnet. Two coils of equal mean area, whose centres were 4 cm. apart, were connected in series with the fluxmeter, so that the E.M.F.'s induced in the coils opposed one another when removed simultaneously from the field between the pole-pieces. The value of  $\frac{dH}{ds}$  obtained in this way was 86 gauss per cm., and was about 3 per cent. higher than 83.4 gauss per cm. previously obtained.

Considering the results obtained with the small copper sphere of diameter 1.263 cm., we find:—

Difference of log dec = .00712.

Density of copper = 8.92 gm. per c.c.

Resistivity of copper at 21.2° C. =  $1.733 \times 10^{-6}$  ohm  
per cm.\*  
=  $1.773 \times 10^9$  c.g.s. units.

T = 1.5 seconds and  $\frac{dH}{ds} = 86$  gauss per cm.

Putting these values into the above equation, the constant "C" is found to be equal to .00622.

The value obtained by Keeping\*, from theoretical considerations, is .00625.

### *Discussion of Results.*

#### *Variation with T.*

An inspection of the results contained in Table VII. for the copper cylinder of length 2.57 cm. and diameter 1.270 cm., with a current of 5 amperes passing through the magnet, shows that the difference of log dec is approximately proportional to T.

#### *Variation with $\left(\frac{dH}{ds}\right)^2$ .*

Taking the results for the copper cylinder 1.279 cm. long and 1.270 cm. diameter in conjunction with the values of

\* *Loc. cit.*

*Experiments with Cylinders.*

- (a) Cylinders oscillating in the horizontal magnetic field with their axes vertical, and the distance between the pole-faces varying from 3.45 cm. at one end to 4.45 cm. at the other.

TABLE VII.

Material of cylinder.	Length in cm.	Diameter in cm.	Current in amperes through magnet.	Field in gauss at centre of swing.	Period of swing in seconds.	Temperature in degrees centigrade between poles.	Log dec with field—log dec without field.
Copper...	1.279	1.270	2	2152	1.5	21.5	.00172
" ...	"	"	3	3207	"	"	.00361
" ...	"	"	4	4218	"	"	.00623
" ...	"	"	5	4993	"	"	.00886
" ...	"	"	6	5445	"	"	.01064
Copper...	2.57	1.270	5	4993	1.5	17.5	.01315
" ...	"	"	6	5445	"	"	.01606
" ...	"	"	5	4993	1.0	23.0	.00860
" ...	"	"	5	4993	2.0	22.5	.01760
Copper...	1.29	1.907	5	4993	1.5	23.5	.01279
" ...	"	"	6	5445	"	"	.01550
Copper...	2.57	1.910	5	4993	1.5	22.5	.02484
" ...	"	"	6	5445	"	"	.03069
Brass ...	1.271	1.279	5	4993	1.5	18.5	.00269
" ...	"	"	6	5445	"	"	.00331
Brass ...	2.57	1.27	5	4993	1.5	22.0	.00105
" ...	"	"	6	5445	"	"	.00475
Brass ...	1.27	1.925	5	4993	1.5	20.5	.00395
" ...	"	"	6	5445	"	"	.00482
Brass ...	2.57	1.925	5	4993	1.5	19.5	.00776
" ...	"	"	6	5445	"	"	.00937

$\left(\frac{dH}{ds}\right)^2$  contained in Table V., it can be shown that the difference of log dec is approximately proportional to  $\left(\frac{dH}{ds}\right)^2$ .

*Variation of Difference of log dec with Dimensions of Cylinders.*

The experimental results given in Table VII. show that the difference of log dec for a cylinder with its axis perpendicular to the magnetic field depends upon both the length and diameter of the cylinder, but is not proportional to their product. The experimental results, coupled with the theory of dimensions, suggest the following equation:—

$$\log \text{dec}_1 - \log \text{dec}_2 = \text{constant} \left( \frac{dH}{ds} \right)^2 \cdot \frac{f(l, D)}{\rho} \cdot \frac{1}{d} \cdot T,$$

where  $l$  and  $D$  represent the length and diameter of the cylinder, and  $f(l, D)$  is of dimension  $L^2$ .

*Determination of Resistivity.*

The resistivities of brass and copper can be compared for cylinders of the same dimensions by means of the equation :

$$\frac{(\log \text{dec}_1 - \log \text{dec}_2)_{\text{copper}}}{(\log \text{dec}_1 - \log \text{dec}_2)_{\text{brass}}} \cdot \frac{d_{\text{copper}}}{d_{\text{brass}}} = \frac{\rho_{\text{brass}}}{\rho_{\text{copper}}}.$$

*Experiments with Cylinders.*

(b) Cylinders with bifilar suspension oscillating with their axes parallel to the lines of magnetic force.

TABLE VIII.

Material of cylinder.	Length in cm.	Diameter in cm.	Current in amperes through magnet.	Field in gauss at centre of swing.	Period of swing in seconds.	Temperature in degrees centigrade between poles.	log dec with field — log dec without field.
Brass ...	2.57	1.925	5	4993	1.5	15.2	.00625
" ...	"	"	"	"	1.0	"	.00423
Copper...	2.57	1.910	2	2152	1.5	16.5	.00404
" ...	"	"	3	3207	"	"	.00924
" ...	"	"	4	4218	"	"	.01537
" ...	"	"	5	4993	"	"	.02148
" ...	"	"	6	5445	"	"	.0262
Copper...	1.29	1.907	5	4993	1.5	15.5	.0214
" ...	"	"	"	"	1.0	16.0	.0142
" ...	"	"	"	"	2.0	17.5	.0284
Copper...	1.279	1.27	5	4993	1.5	18.0	.00960

Using the results for cylinders of length 2.57 cm. and diameter 1.27 cm. in Table VII. and the resistivity of copper at 20° C. (1.73 microhms per cm.<sup>3</sup>), the resistivity of brass calculated from the above equation is 6 microhms per cm.<sup>3</sup> This result is in fair agreement with the value determined by the Kelvin bridge, viz. 6.3 microhms per cm.<sup>3</sup>

### *Discussion of Results.*

#### *Variation with T.*

Inspection of Table IX. shows that for a given substance and a given current passing through the magnet the difference of log dec is proportional to the period of swing T.

#### *Variation with Dimensions of the Cylinders.*

(i.) An examination of Table IX. also shows that for a given substance the difference of log dec is practically independent of the length of the cylinder when the latter is oscillating with its axis parallel to the lines of force.

(ii.) A comparison of the differences of log dec for copper cylinders of diameters 1.27 cm. and 1.907 cm. shows that the difference of log dec is directly proportional to  $D^2$ .

#### *Variation with $\left(\frac{dH}{ds}\right)^2$ .*

If the differences of log dec for the copper cylinder of length 2.57 cm and diameter 1.910 cm. given in Table VIII. are examined in relation to the values of  $\left(\frac{dH}{ds}\right)^2$  given in Table V., it can be shown that the difference of log dec is proportional to  $\left(\frac{dH}{ds}\right)^2$ .

### *Determination of Resistivity.*

If the resistivity of copper be known, the resistivity of brass can be determined from the values of the difference of log dec for brass and copper cylinders of known dimensions and densities. Taking the values from Table VIII. for brass and copper cylinders of diameters 1.925 and 1.910 cm. respectively, the resistivity of brass works out to be 6.4 microhms per cm.<sup>3</sup> This value is in fair agreement with the experimental value 6.3 ohms per cm.<sup>3</sup>

The experimental results for cylinders oscillating with their axes parallel to the lines of magnetic force show that

$$\log \text{dec}_1 - \log \text{dec}_2 = C_1 \left( \frac{dH}{ds} \right)^2 \cdot \frac{D^2}{\rho} \cdot \frac{1}{d} \cdot T.$$

*Determination of the Constant  $C_1$ .*

Considering the results for the copper cylinder of length 1.29 cm. and diameter 1.907 cm., it follows that

$$\left( \frac{dH}{ds} \right) = 86 \text{ gauss per cm.},$$

$$\log \text{dec}_1 - \log \text{dec}_2 = .0213,$$

$$d = 8.92 \text{ grams per c.c.},$$

$$T = 1.5 \text{ seconds},$$

$$\rho = 1.70 \times 10^{-6} \text{ ohm per cm.}^3 = 1.70 \times 10^3 \text{ c.g.s. units.}$$

The value of  $C_1$  calculated from the above equation = .00802.

Taking the results for the copper cylinder of diameter 1.910 cm., the value of  $C_1 = .00804$ .

The mean value of  $C_1 = .00803 = \frac{1}{125}$  approx.

The value of  $C_1$  deduced theoretically by Keeping\* is  $\frac{1}{128}$ .

*Summary of Results.*

1. The logarithmic decrements with and without the magnetic field have been measured for spheres and cylinders of conducting material swinging as pendulums between the pole-pieces of an electromagnet. The pole-pieces, which were of rectangular cross-section, were mounted with a slight taper, so that the spheres and cylinders were oscillating in a non-uniform field. Measurements showed that, for a given current passing through the magnetic coils, the value of  $\frac{dH}{ds}$  along the line of swing was constant.

2. It has been shown in the case of oscillating spheres that the difference of log dec with field and without field is given by

$$C \left( \frac{dH}{ds} \right)^2 \cdot \frac{D^2}{\rho} \cdot \frac{1}{d} \cdot T,$$



where  $D$  is the diameter of the sphere,  $\rho$  the specific resistance of the material composing the sphere,  $d$  the density,  $T$  the period of swing, and  $C$  a constant equal to .00625.

3. For cylinders oscillating with their axes perpendicular to the magnetic field, the difference of log dec is given by

$$\text{constant} \left( \frac{dH}{ds} \right)^2 \cdot \frac{f(lD)}{\rho} \cdot \frac{1}{d} \cdot T,$$

where  $l$  represents the length of the cylinder and  $f(lD)$  is of dimensions  $L^2$ .

4. For cylinders oscillating with their axes parallel to the magnetic field, the difference of log dec is given by

$$C_1 \left( \frac{dH}{ds} \right)^2 \cdot \frac{D^2}{\rho} \cdot \frac{1}{d} \cdot T,$$

where the constant  $C_1$  is equal to  $\frac{1}{128}$  or .00781.

5. The method can be used for comparing the resistances of conductors in the form of spheres and cylinders or for determining resistivities absolutely.

## II. On the Damped Oscillation of a Conductor in a Non-uniform Magnetic Field. By E. S. KEEPING, B.Sc., D.I.C. (University College of Swansea) \*.

THIS note is intended as a supplement to the preceding paper by Mr. S. Davies and Prof. E. J. Evans<sup>(1)</sup> on the damping produced in metal spheres and cylinders oscillating in a non-uniform magnetic field and its application to the determination of resistivity. It gives a theoretical deduction of certain formulæ quoted in that paper.

There exists an extensive literature on the induction of eddy-currents in moving conductors, and the particular problems of the torsional oscillations of a suspended sphere and of a suspended cylinder with its axis vertical in a uniform

\* Communicated by Prof. E. J. Evans.

field have been investigated by various writers<sup>(2)</sup>. The to-and-fro pendulum motion in a non-uniform field does not appear, however, to have been previously discussed. The only cases treated here are those of the sphere and the cylinder with its axis along the lines of force. The corresponding problem of the cylinder with axis perpendicular to the field presents great analytical difficulties.

Taking the origin of Cartesian coordinates at the centre of gravity of the pendulum bob when at rest, and the axis of  $x$  vertically upwards, the motion may, for small oscillations, be taken as simple harmonic along the  $y$ -axis. The magnetic lines of force are then practically parallel to the  $z$ -axis, and the strength of field increases uniformly along the  $y$ -axis, the gradient being produced in practice by slightly inclining the plane-poles of an electromagnet. The problem of the moving bob is then practically identical with that of the same bob at rest in a magnetic field fluctuating harmonically. If  $h$  is the amplitude of oscillation of the bob, the field at its centre fluctuates between the limits  $H_0 \pm h \, dH/dy$ . The magnetic field is not constant over the whole of the bob, but the extent of the fluctuation is the same at all points, and as the induced currents depend entirely on the variable part of the field, we can regard the eddy-currents actually produced as due to a uniform but harmonically oscillating field  $h \, dH/dy \cos pt$ .

If  $E$ ,  $M$  are the electric and magnetic field strengths in a medium of unit permeability and conductivity  $\sigma$ ,

$$\left. \begin{aligned} \text{curl } M &= 4\pi\sigma E, \\ \text{curl } E &= -dM/dt, \\ \text{div } M &= 0, \\ \text{div } E &= 0, \end{aligned} \right\} \dots \dots (1)$$

the units being electromagnetic. These equations may be solved in particular cases by the method given by Bromwich<sup>(3)</sup>. The solutions must satisfy the boundary conditions that the tangential and normal components of magnetic field strength are continuous across the boundary. This type of solution has been used by Marcus<sup>(4)</sup> for the analogous problem of a rotating sphere.

### *Spherical Conductor.*

Let  $a$  be the radius of the sphere. The axis of  $z$  is one of symmetry, and may be taken as the axis of spherical polar coordinates. A solution of (1) is

$$\left. \begin{aligned}
 M_r &= \frac{\partial^2 U}{\partial r^2} - 4\pi\sigma \frac{\partial U}{\partial t}, \\
 M_\theta &= \frac{1}{r} \frac{\partial^2 U}{\partial r \partial \theta}, \\
 M_\phi &= \frac{1}{r \sin \theta} \frac{\partial^2 U}{\partial r \partial \phi}, \\
 E_r &= 0, \\
 E_\theta &= \frac{1}{r \sin \theta} \frac{\partial}{\partial \phi} \left( \frac{\partial U}{\partial t} \right), \\
 E_\phi &= -\frac{1}{r} \frac{\partial}{\partial \theta} \left( \frac{\partial U}{\partial t} \right),
 \end{aligned} \right\} \dots \dots (2)$$

where  $V$  is any solution of the equation

$$\frac{\partial^2 U}{\partial r^2} + \frac{1}{r^2 \sin \theta} \frac{\partial}{\partial \theta} \left( \sin \theta \frac{\partial U}{\partial \theta} \right) + \frac{1}{r^2 \sin^2 \theta} \frac{\partial^2 U}{\partial \phi^2} = 4\pi\sigma \frac{\partial U}{\partial t}. \quad (3)$$

If we write  $U = V(r, \theta, \phi) e^{igt}$ , the equation becomes

$$(\nabla^2 + k^2) V = 0, \dots \dots (4)$$

$$\text{where} \quad k^2 = -4\pi i \sigma g. \dots \dots (5)$$

A solution of (4) is

$$V = A \cos \theta [(\sin kr)/kr - \cos kr],$$

whence from (2)

$$\begin{aligned}
 M_r &= 2A \cdot \cos \theta \cdot e^{igt} [(\sin kr)/kr^3 - (\cos kr)/r^2], \\
 M_\theta &= -A/r \cdot \sin \theta \cdot e^{igt} [\cos kr/r - \sin kr/kr^2 + k \sin kr], \\
 M_\phi &= 0, \\
 E_r &= 0, \\
 E_\theta &= 0, \\
 E_\phi &= A/r \cdot \sin \theta \cdot ig e^{igt} [(\sin kr)/kr - \cos kr]. \dots \dots (6)
 \end{aligned}$$

Outside the sphere the part of the magnetic field arising from the induced currents is derivable from a potential  $\chi$ , which satisfies the relation

$$\nabla^2 \chi = 0. \dots \dots (7)$$

The appropriate form of  $\chi$  is  $Y_n/r^{n+1}$ , where  $Y_n$  is a spherical harmonic, and the particular solution corresponding to (6) is given by

$$\chi = B/r^2 \cdot \cos \theta. \dots \dots (8)$$

The magnetic field arising from this is

$$\left. \begin{aligned} M_r' &= 2B/r^3 \cdot \cos \theta \cdot e^{iqt}, \\ M_\theta' &= B/r^3 \cdot \sin \theta \cdot e^{iqt}, \\ M_\phi' &= 0. \end{aligned} \right\} \dots \dots (9)$$

The external inducing field is given by

$$\left. \begin{aligned} H_r &= h \, dH/dy \cdot \cos pt \cdot \cos \theta, \\ H_\theta &= -h \, dH/dy \cdot \cos pt \cdot \sin \theta, \\ H_\phi &= 0, \end{aligned} \right\} \dots \dots (10)$$

which may be written, in conformity with (6) and (9),

$$\left. \begin{aligned} H_r &= \Sigma \frac{1}{2} h \, dH/dy \, e^{iqt} \cdot \cos \theta, \\ H_\theta &= \Sigma -\frac{1}{2} h \, dH/dy \, e^{iqt} \cdot \sin \theta, \\ H_\phi &= 0, \end{aligned} \right\} \dots \dots (11)$$

the summation being over the two values of  $q = \pm p$ .

The boundary conditions at  $r=a$  give

$$\begin{aligned} 2A[(\sin ka)/ka^3 - (\cos ka)/a^2] &= 2B/a^3 + \frac{1}{2} h \, dH/dy \\ A/a[(\cos ka)/a - (\sin ka)/ka^2 + k \sin ka] \\ &= -B/a^3 + \frac{1}{2} h \, dH/dy, \end{aligned}$$

whence 
$$A = \frac{3ha}{4k \sin ka} \, dH/dy \dots \dots (12)$$

and

$$E_\phi = \Sigma \frac{3ha}{4k \sin ka} \cdot \frac{dH}{dy} \cdot \frac{\sin \theta}{r} \, i q e^{iqt} \left[ \frac{\sin kr}{kr} - \cos kr \right]. \quad (13)$$

The two values of  $k$  in this summation are

$$\left. \begin{aligned} k_1 &= (1-i) \sqrt{2\pi\sigma p}, \\ k_2 &= (1+i) \sqrt{2\pi\sigma p}. \end{aligned} \right\} \dots \dots (14)$$

Now in the experimental work  $\sqrt{2\pi\sigma p} \cdot a$  is of the order of 1/10, so that it is permissible to the degree of approximation justified by the data to neglect terms of the third and higher orders in the expansion of  $(\sin kr)/kr$  and  $\cos kr$ . We then obtain, on adding together the two expressions for  $E_\phi$ ,

$$E_\phi = \frac{1}{2} h \cdot dH/dy \cdot p \sin pt \cdot r \sin \theta. \dots (15)$$

The work done per second by the eddy-currents in the sphere is given by

$$W = \iiint \sigma E_{\phi}^2 dt, \quad . \quad . \quad . \quad (16)$$

integrated throughout the volume of the sphere. This gives

$$\begin{aligned} W &= 2/15 \cdot \pi \sigma a^5 (dH/dy)^2 h^2 p^2 \sin^2 pt. \\ &= 2/15 \cdot \pi \sigma \cdot a^5 \cdot (dH/dy)^2 \cdot \dot{y}^2, \quad . \quad . \quad . \quad (17) \end{aligned}$$

$\dot{y}$  being the instantaneous velocity of the sphere.

If  $F$  is the instantaneous force per unit mass acting on the sphere due to eddy-currents,

$$W = 4/3 \cdot \pi \rho a^3 \cdot F \dot{y},$$

so that

$$F = 1/10 \cdot \sigma / \rho \cdot a^2 (dH/dy)^2 \dot{y} = 2x\dot{y},$$

where  $\rho$  is the density of the material of the bob.

The logarithmic decrement of the oscillations is, therefore,

$$\kappa T/2 = T/40 \cdot \sigma / \rho a^2 \cdot (dH/dy)^2, \quad . \quad . \quad . \quad (18)$$

where  $T$  is the period of swing of the pendulum.

It is clear from the discussion of results in the paper of Davies and Evans above that this formula is in satisfactory agreement with experiment.

### *Cylindrical Conductor, with Axis along Lines of Force.*

Taking the axis of  $z$  as that of cylindrical coordinates,  $\rho, \phi, z$ , with the origin at the centre of the cylinder, we find as solution of (1),

$$\left. \begin{aligned} M_{\theta} &= \frac{\partial^2 U}{\partial z \partial \rho}, \\ M_{\phi} &= \frac{1}{\rho} \frac{\partial^2 U}{\partial \phi \partial z}, \\ M_z &= \frac{\partial^2 U}{\partial z^2} - 4\pi\sigma \frac{\partial U}{\partial t}, \\ E_{\rho} &= -\frac{1}{\rho} \frac{\partial^2 U}{\partial \phi \partial t}, \\ E_{\phi} &= \frac{\partial^2 U}{\partial \rho \partial t}, \\ E_z &= 0, \end{aligned} \right\} \quad . \quad . \quad . \quad (19)$$

where  $U$  is any solution of the equation,

$$\frac{\partial^2 U}{\partial \rho^2} + \frac{1}{\rho} \frac{\partial U}{\partial \rho} + \frac{1}{\rho^2} \frac{\partial^2 U}{\partial \phi^2} + \frac{\partial^2 U}{\partial z^2} - 4\pi\sigma \frac{\partial U}{\partial t} = 0. \quad (20)$$

Noting that there is symmetry about the  $z$ -axis, and putting  $U = Ve^{igt}$ , we find for  $V$  the equation

$$\frac{\partial^2 V}{\partial \rho^2} + \frac{1}{\rho} \frac{\partial V}{\partial \rho} + \frac{\partial^2 V}{\partial z^2} + k^2 V = 0, \quad \dots \quad (21)$$

where, as before,

$$k^2 = -4\pi i \sigma q.$$

A solution of (21) is

$$V = A J_0(\alpha \rho) e^{-\sqrt{\alpha^2 - k^2} \cdot z}, \quad \dots \quad (22)$$

whence

$$\left. \begin{aligned} M_\rho &= -A \alpha \sqrt{\alpha^2 - k^2} J_0'(\alpha \rho) e^{-\sqrt{\alpha^2 - k^2} \cdot z} \cdot e^{igt}, \\ M_z &= \alpha^2 A J_0(\alpha \rho) e^{-\sqrt{\alpha^2 - k^2} \cdot z} \cdot e^{igt}, \\ E_\phi &= i q \alpha A J_0'(\alpha \rho) e^{-\sqrt{\alpha^2 - k^2} \cdot z} \cdot e^{igt}, \\ M_\phi &= E_\rho = E_z = 0. \end{aligned} \right\} \quad \dots \quad (24)$$

The magnetic potential  $\chi$  of the field in outside space arising from the induced currents may be written

$$\chi = B J_0(\beta \rho) \cdot e^{-\beta z} e^{igt}, \quad \dots \quad (25)$$

whence

$$\left. \begin{aligned} M_\rho' &= -B J_0'(\beta \rho) \beta \cdot e^{-\beta z} e^{igt}, \\ M_z' &= B \beta J_0(\beta \rho) e^{-\beta z} e^{igt}, \\ M_\phi' &= 0. \end{aligned} \right\} \quad \dots \quad (26)$$

The external inducing field is

$$\left. \begin{aligned} H_\rho &= H_\phi = 0, \\ H_z &= \frac{1}{2} h \frac{dH}{dy} \Sigma e^{igt}. \end{aligned} \right\} \quad \dots \quad (27)$$

The boundary conditions at the curved surface of the cylinder,  $\rho = a$ , are

$$\left. \begin{aligned} -A \alpha \sqrt{\alpha^2 - k^2} \cdot J_0'(\alpha a) e^{-\sqrt{\alpha^2 - k^2} \cdot z} &= -B J_0'(\beta a) \beta e^{-\beta z}, \\ \alpha^2 A J_0(\alpha a) e^{-\sqrt{\alpha^2 - k^2} \cdot z} &= B \beta J_0(\beta a) \cdot e^{-\beta z} + \frac{1}{2} h \frac{dH}{dy}, \end{aligned} \right\} \quad \dots \quad (28)$$

which are satisfied by putting

$$\beta = \sqrt{\alpha^2 - k^2} = 0.$$

Hence

$$E_\phi = \Sigma i q e^{igt} A \cdot k J_0'(k \rho) \cdot \dots \quad (29)$$

Expanding the Bessel functions in series, and retaining terms up to the third order, the expression for  $E$  reduces, after some manipulation, to

$$E_{\phi} = \frac{1}{2} p h \rho \frac{dH}{dy} \cdot [2 \sin pt + \cos pt \cdot \pi \sigma p (2a^2 + \rho^2)]. \quad (30)$$

The work  $W$  done per second is therefore given by

$$\begin{aligned} W = 2b\sigma \int_0^a \int_0^{2\pi} & \left( \frac{1}{2} p h \rho \frac{dH}{dy} \right)^2 \cdot [\sin pt \\ & + \frac{1}{2} \pi \sigma p (2a^2 + \rho^2) \cos pt]^2 d\rho \cdot \rho d\phi \\ = \frac{1}{4} \pi a^2 b \sigma p^2 h^2 \sin^2 pt & \left( \frac{dH}{dy} \right)^2 + \text{terms of higher order in} \\ & \sigma p \text{ which are negligible. } (b \text{ denotes the half-} \\ & \text{length of the cylinder.}) \end{aligned}$$

The force per unit mass acting on the cylinder is therefore given by

$$F = 1/8 \cdot \sigma / \rho a^2 \cdot \dot{y} = 2\kappa \dot{y}, \quad . \quad . \quad . \quad (31)$$

and the logarithmic decrement of the oscillations is

$$\kappa T/2 = 1/32 \sigma / \rho a^2 \left( \frac{dH}{dy} \right)^2, \quad . \quad . \quad . \quad (32)$$

which again is in satisfactory agreement with experiment.

In the above working the boundary conditions at the flat ends of the cylinder have been ignored. Two of these are satisfied by the solution given, but the third appears to be incapable of being exactly satisfied by a solution of this type. It is clear, however, from the symmetry of the problem that the eddy-currents will flow in concentric circles in planes perpendicular to the axis, so that the effect of the finite length of the cylinder will be very small. That this is so is proved by the experimental work of Davies and Evans<sup>(6)</sup>.

### *References.*

- (1) S. Davies and E. J. Evans, *suprà*, p. 1.
- (2) E. g., Lamb, *Phil. Trans.* clxxiv. p. 519 (1883); Lamb, *Proc. Lond. Math. Soc.* xv. pp. 139 & 270 (1884); Hertz, *Inaug. Diss.* ('Collected Works', i. p. 37); Himstedt, *Gott. Nach.* p. 491 (1880). Himstedt, *Ann. der Phys.* xi. p. 812 (1880); Larmor, *Phil. Mag.* xvii. p. 1 (1884); J. J. Thomson, *Mess. Math.* xiv. p. 37 (1884); Kern, *Ann. der Phys.* xlii. p. 460 (1913); Gans, *Arch. für Elektrotechnik*, ix. p. 413 (1921); Marcus, *Phys. Rev.* xxiv. p. 68 (1924).
- (3) T. J. I'a. Bromwich, *Phil. Mag.* xxxvii. p. 407 (1919).
- (4) *Loc. cit.* note (2).
- (5) *Loc. cit.* note (1).

III. *Determination of the End Correction and Conductance at the Mouth of a Stopped Organ (Flue) Pipe.* By A. E. BATE, M.Sc., Northern Polytechnic, London\*.

§ 1. **I**N a previous communication† an account was given of the effect of variation in the pressure of the air and of the dimensions of the mouth of a stopped organ-pipe on the frequency of the pipe. It was shown that, after the length of the pipe had been suitably adjusted, the most stable note was obtained when these factors were connected by the equation

$$\frac{V}{nh} = \frac{74}{3} (0.3 - s), \quad . . . . . (I.)$$

in which  $V$  stands for the velocity of the air in feet per second,

$n$  „ „ frequency,

$h$  „ „ height of the mouth in feet, and

$s$  „ „ the width in inches of the slit from which the air issues.

The pipe referred to had its mouth in a plate which otherwise closed one end of the pipe, and in consequence the air had to be blown across the pipe instead of along it; this enabled the height of the mouth to be altered without altering the length of the air column.

The same pipe was used to obtain the results given in this paper, but in this case the slit width was .05 inch throughout, so the formula becomes

$$\frac{V}{nh} = 6.167, \quad . . . . . (I.a)$$

and from this the air pressures were calculated which were required to make the pipe speak with maximum stability at frequencies of 128, 256, 288, 320, and 340 respectively, and with heights of mouth equal to 0.35, 0.5, 0.65, and 0.8 inch in each case.

§ 2. The correction was obtained by subtracting the length of the pipe (measured from the lip to the inner face of the plate closing the end) from one quarter of the corresponding wave-length. This correction was found for each frequency for each height of mouth, the air pressure having been

\* Communicated by Reg. S. Clay, D.Sc.

† Phil. Mag. viii. p. 750 (1929).



adjusted to its appropriate value each time. The length of the pipe was found at which it gave four beats per second with the fork used as standard, *i. e.*, until the frequency of the pipe was  $n-4$ , where  $n$  is the frequency of the fork. The length of the pipe was then altered until it had a frequency of  $n+4$ , accurate counting of beats being assured by means of a metronome set at four ticks per second. Both lengths of pipe were measured and the arithmetic mean taken as the length of the pipe of frequency  $n$ . Actually the harmonic mean should be taken, but this is equal to the arithmetic mean to the degree of accuracy attained in the experiments. The method of beats was used, as it is practically impossible to obtain true agreement of frequencies directly.

§ 3. Lord Rayleigh \* gives the equation

$$\tan \frac{2\pi L}{\lambda} = \frac{\lambda \cdot c}{2\pi \cdot A} \quad \dots \dots (II.)$$

for a cylindrical resonator without a neck, in which  $L$  is the length,  $A$  the cross-section,  $\lambda$  is the wave-length of the natural frequency, and  $c$  is the conductance of the orifice, which is assumed to be circular. He stated that  $c$  is of linear dimension, and equals the diameter of the orifice if circular, or  $2\sqrt{\frac{\omega}{\pi}}$  if approximately circular, where  $\omega$  stands for the area of the orifice. This quantity is referred to in the present paper as the equivalent diameter.

Another formula given by Lamb† for the same type of resonator is

$$\cot \frac{2\pi L}{\lambda} = \frac{2\pi}{\lambda} \cdot \alpha, \quad \dots \dots (III.)$$

in which  $\alpha$  is the end correction, *i. e.*, the amount by which  $L$  falls short of  $\lambda/4$ ; the other symbols are as in (II.). It follows that, since (II.) may be written:

$$\cot \frac{2\pi L}{\lambda} = \frac{2\pi}{\lambda} \cdot \frac{A}{c},$$

$$\text{that} \quad \alpha = \frac{A}{c}$$

$$\text{or} \quad c = \frac{A}{\alpha} \quad \dots \dots (IV.)$$

\* Irons, *Phil. Mag.* p. 879 (May 1929).

† Lamb, 'Dynamical Theory of Sound,' Art. 86.

This indicates that, provided  $A$  remains unchanged, the product  $\alpha c$  should be constant for all frequencies; hence, for a given area of mouth, *i.e.*, for a given value of  $c$ ,  $\alpha$  should also remain constant at all frequencies.

§ 4. Since the equation

$$\tan \frac{2\pi L}{\lambda} = \frac{\lambda}{2\pi} \frac{c}{A}$$

is satisfied by any one of a series of values of  $L$  increasing by  $\lambda/2$ , it follows that for each of these values the same frequency and mouth conditions should hold, as indicated in the previous paper.

§ 5. TABLE I.

Measured values of  $\alpha$  corresponding to varying frequencies and heights of mouth. (All lengths in inches.)

Height of mouth.	Frequencies.				
	128	256	288	320	340
0.35	—	3.83	3.71	3.41	3.36
0.5	—	3.20	3.19	3.01	2.92
0.65	2.88	2.85	2.83	2.67	—
0.8	2.53	2.53	—	—	—

Table I. gives the values of the end correction obtained by direct measurement. The results missing from the second column were unobtainable, as the appropriate pressures were too low to cause the pipe to speak. The other missing values required pressures well above 4 ins. of water and are omitted, as such pressures increase the effect of the alteration of the density of the air in the jet beyond the limit taken in obtaining expression (1.).

It will be seen that the values are practically constant at the lower frequencies, and increase with decrease in the height of the mouth. As the frequencies increase, however, the correction gets smaller. This is attributed to the decrease in the volume of the pipe owing to the decrease in wavelength, which thereby invalidates the assumption that the orifice is small in comparison with the volume of the resonator.

## § 6.

## TABLE II.

Conductances calculated from the measurements  
given in Table I.

Height of mouth.	Frequencies.					Equivalent diameters.
	128	256	288	320	340	
0.35	—	0.86	0.88	0.95	0.95	0.83
0.5	—	1.05	1.04	1.10	1.13	0.98
0.65	1.21	1.19	1.19	1.26	—	1.11
0.8	1.39	1.36	—	—	—	1.24

The values of the conductances of the mouths given in Table II. were calculated from the results quoted in Table I. by Rayleigh's formula (II.). For the purposes of comparison the equivalent diameters are included; these were obtained as indicated in § 3, the width of the mouth being 1.5 ins. in each case. The table shows that the actual conductances with rectangular orifices are larger than the calculated equivalent diameters; other workers have shown that this is the case with circular orifices\*.

## § 7.

## TABLE III.

Calculated values of  $\alpha$ , the end correction.

Height of mouth.	Frequencies.				
	128	256	288	320	340
0.35	—	4.12	4.05	3.74	3.72
0.5	—	3.38	3.40	3.24	3.15
0.65	2.92	2.98	2.98	2.82	—
0.8	2.56	2.61	—	—	—

The end-corrections were calculated from equation (III.). It will be noticed that the discrepancies between the results in Tables I. and III. diminish with increase in height of mouth, and also with increase of wave-length. The latter variation is explained in § 5; the other effect appears to be due to alteration in the shape of the mouth.

\* Irons, *ibid.* p. 886.

§ 8.

TABLE IV.

Conductances calculated from equation (IV.),  
using the measured end-corrections.

Height of mouth.	Frequencies.				
	128	256	288	320	340
0.35	—	0.93	0.93	1.04	1.06
0.5	—	1.11	1.11	1.18	1.21
0.65	1.23	1.25	1.25	1.33	—
0.8	1.40	1.40	—	—	—

Since  $c$  is the only quantity in equation (IV.) which is not directly measured, the values of  $c$  were calculated from it, using the results in Table I. for  $\alpha$ ; the diameter of the pipe was  $2\frac{1}{8}$  ins.

The results are given in Table IV. On comparing these with the values of  $c$  given in Table II., it will be seen that they agree more closely as the mouth is made larger, *i. e.*, as the mouth becomes more nearly square. This indicates that the approximation suggested by Rayleigh\*—that any orifice may be treated as circular if it does not differ too much from a circle—is only valid in the case of a rectangle which is practically square. Even then the conductance is greater than the equivalent diameter. At first this was thought to be due to the shape of the orifice, but this cannot be the case in those instances in which the mouth is 0.8 inch in height, as the results in Tables II. and IV. agree so closely for this value.

§ 9.

TABLE V.

End-corrections for different heights of mouth with added lengths of pipe equal to  $\lambda/2$  and  $\lambda$  respectively, for a frequency of 256.

Height of mouth.	Normal length.	Normal + $\lambda/2$ .	Normal + $\lambda$ .
0.35	3.83	3.79	3.85
0.5	3.20	3.18	3.18
0.65	2.85	2.77	2.78
0.8	2.53	2.50	2.46

\* Rayleigh, 'Scientific Papers,' i. Art. 5, p. 53, equation (26).

The theoretical conclusions of §4 were tested for a frequency of 256 by lengthening the stopped pipe speaking with this frequency, by approximately one half-wave-length, and adjusting it by the method described in §2. In this way the actual lengths of pipe required to produce a frequency of 256 with heights of mouth equal to the four values previously used were found. Within the limits of experimental error, the results indicate that the increase is one half-wave-length for each height of mouth. Repetition with a further addition of one half-wave-length gave similar results.

The end-corrections for each set of results are given in Table V., and were obtained by subtracting the actual lengths of pipe from three-quarters and five-fourths of the wave-length in each case respectively. The close agreement for each height of mouth shows that the conductances are unaltered.

#### §10. CONCLUSIONS.

A stopped organ-pipe behaves in exactly the same way as a cylindrical resonator without a neck, provided that the edge-tone set up by the vortex system in the air-stream at the mouth of the pipe synchronizes with the natural frequency of the air-column in the pipe. It follows that the usual resonator formulæ may be applied, and from these the equation  $A = c.a$  is deduced, and is shown to hold experimentally if  $c$  is regarded as being somewhat larger than the equivalent diameter of the orifice.

The author desires to acknowledge his indebtedness to Dr. Clay for the interest he has shown in this research, and for the facilities provided.

#### IV. *Temperature Distribution along a Heated Filament used as a Catalyst.* By EDWARD S. LAMAR and W. EDWARDS DEMING, *Bureau of Chemistry and Soils, Washington, D.C.\**

##### *Abstract.*

AN expression was found for the temperature gradient at any point along a heated molybdenum filament used

\* Communicated by C. H. Kunsman. The basis of some of the work presented in this paper was used by E. S. Lamar to satisfy the dissertation requirements of George Washington University for the degree of M.A., 1928.

as a catalyst in the decomposition of ammonia. The temperature at any point along the length was obtained by graphical integration of this expression. The integrated resistance for the whole length of filament was compared with the measured resistance and found to agree within .27 per cent. at four different temperatures. Knowing the distribution of temperature, it was possible to determine the equivalent length of the filament effective as a catalyst at the maximum temperature. From considerations of the thermal losses to the gas, a value of the heat of dissociation of ammonia was found that was in good agreement with that obtained by Lewis and Randall from Haber's data.

---

*Introduction.*

IN the course of some investigations made by C. H. Kunsman\* on the catalytic decomposition of ammonia, it was feared that the equivalent length effective at the given maximum temperature of the heated filament used as a catalyst varied with the maximum temperature owing to the cooling at the ends. The present paper concerns an attempt to determine the distribution of temperature along a cylindrical molybdenum filament, to obtain its length effective as a catalyst, and to determine the heat of dissociation of ammonia.

*Theory.*

If the radial temperature gradient is zero, the steady thermal state of the filament can be represented by

$$\pi r^2 \left[ K(T) \frac{d^2 T}{dx^2} + \frac{dK(T)}{dT} \left( \frac{dT}{dx} \right)^2 \right] dx + 2\pi r S(T) dx + \frac{R(T) l^2}{\pi r^2} dx = 0. \quad (1)$$

The term in brackets represents the gain in heat by the element of length  $dx$  at  $x$  in unit time by metallic conduction along the axis. The second term represents the gain in heat through the surface of the element, and the third term is the gain in heat due to the flow of an electric current through the element.  $r$  is the radius of the

\* C. H. Kunsman, J. Am. Chem. Soc. 1. p. 2100 (1928); li. p. 688 (1929).

filament,  $T$  the temperature of the surface, and  $K(T)$  is the thermal conductivity of the metal,  $S(T)$  the heat gained by unit surface in unit time,  $R(T)$  the electrical resistivity, all at temperature  $T$ , and  $I$  the current. When the steady state is reached, the net gain in heat per unit time in the element of length  $dx$  is zero.

If  $\left(\frac{dx}{dT}\right)^2 [K(T)]^2$  in equation (1) be replaced by  $U$ , the differential equation becomes

$$\frac{dU}{dT} + \frac{4K(T)S(T)}{r} + \frac{2K(T)R(T)}{\pi^2 r^4} I^2 = 0, \quad \dots (2)$$

from which

$$U = -(4/r) \int K(T)S(T) dT - (2I^2/\pi^2 r^4) \int K(T)R(T) dT + C = 0. \quad \dots (3)$$

Going back to the original variables,

$$\begin{aligned} \frac{dx}{dT} = K(T) \left\{ -(4/r) \int K(T)S(T) dT \right. \\ \left. - (2I^2/\pi^2 r^4) \int K(T)R(T) dT + C \right\}^{-\frac{1}{2}}. \quad \dots (4) \end{aligned}$$

The second integration can be performed graphically. If  $T$  is the temperature on an element at  $x$  and  $T + \Delta T$  is the temperature on an element at  $x + \Delta x$ , then

$$x + \Delta x = x + \frac{dx}{dT} \cdot \Delta T, \quad \dots (5)$$

closely if  $\Delta T$  is small. The derivative  $dx/dT$  is to be evaluated at  $T + \frac{1}{2} \Delta T$ , as indicated.

### *Values of the Necessary Constants and Functions.*

The only measurements on the thermal conductivity of molybdenum seem to be those of Barratt\* at  $0^\circ$  and  $100^\circ$  C. The equation  $K(T) = 3.455 \cdot 10^7 T^{-1.533}$  satisfies his two values when expressed in C.G.S. units, and is used for  $K(T)$ . From the data of A. G. Worthing† it was found that the heat lost by radiation could be represented quite accurately as  $AT^n = 12.4 T^{4.9} \times 10^{-16}$  watt per  $\text{cm}^2$ . Worthing found that the temperature coefficient of resistance was the same for two specimens of the same

\* T. Barratt, Proc. Phys. Soc. xxvi. p. 347, August 1914.

† A. G. Worthing, Phys. Rev. xxviii. p. 190, July 1926.

purity. His measurements on the resistivity of molybdenum, over the temperature range used in our experiment, fit the equation  $\rho = R_0 T^{1.17}$  ohm cm. This also fits accurately the temperature variation of the resistivity of our filament from  $0^\circ$  to  $100^\circ$  C., so we feel justified in using 1.17 as the exponent of  $T$ . Our values of resistivity give  $R_0 = 7.893 \times 10^{-9}$ ; so we used  $\rho = 7.893 \times 10^{-9} T^{-1.17}$  ohm cm.

Along a short length in the middle of the filament, where the temperature gradient is zero, the heat delivered to the surrounding gas is equal to that generated by the current less that lost by radiation. By plotting the logarithm of the heat delivered to the gas against  $\log (T - T_0)$  a straight line of slope 2 is obtained ( $T_0$  is the temperature of the water surrounding the tube), so we used  $B(T - T_0)^2$  to represent the heat delivered per second to the gas. Thus

$$S(T) = -\{12.4 \times 10^{-16} T^{4.9} + B(T - T_0)^2\}.$$

Substituting the functions and constants thus far determined into equation (4) and performing the two simple integrations inside the brace, we have

$$\begin{aligned} \frac{dx}{dT} = & \{1.6211 \times 10^{-14} T^{6.0533} + B(26.392 T^{3.1533} \\ & - 81.366 T_0 T^{2.1533} + 88.732 T_0^2 T^{1.1533}) \\ & - .0040493 I^2 T^{2.3233} \div C T^{3.066}\}^{-\frac{1}{2}}. \quad \dots (6) \end{aligned}$$

This is used in equation (5) for the graphical integration to get  $T$  as a function of  $x$ .

The constant  $B$  was determined in each case by assuming the first term of equation (1) to be zero at the maximum temperature and solving for  $B$  in  $S(T)$ . The assumption made seems justifiable because the filament was of uniform temperature for quite a distance along its length. The constant  $C$  for each case was obtained by setting  $\frac{dT}{dx}$  equal to zero, that is to say, by setting the quantity in the brace in equation (4) equal to zero for the maximum temperature and solving for  $C$ , the only unknown left.

### *Apparatus.*

The experimental set-up was that described by Kunsman\* with the exception that the filament was made

\* C. H. Kunsman, J. Am. Chem. Soc. 1. p. 2100 (1928); li. p. 688 (1929).



one arm of a Kelvin double bridge rather than of a Wheatstone bridge, as the absolute value of the filament resistance was desired.

The principal use of the tube was to measure the rate of decomposition of ammonia as a function of temperature. The temperature distribution along the filament was to be measured under the conditions of the experiment as a means of determining the equivalent length effective at the given maximum temperature. The maximum temperature was obtained by means of a rare metal thermocouple spot welded to the centre of the filament. These wires were two mils in diameter, and there was apparently no cooling at the junction. It was found that wires of such small diameter could be sealed successfully through pyrex glass. Cooling fins were attached to each end of the filament, and the assumption was made that the temperature of the ends was that of the water bath surrounding the tube. Preliminary investigations in air seemed to justify this assumption when the fins were made sufficiently large.

### *Experimental Procedure.*

The tube was first pumped out, and the pumping system was then closed off from the tube by means of a mercury trap. Ammonia to a pressure of 26.6 cm. Hg was then admitted to the tube. Before starting a run, the ratio was set on the Kelvin bridge to produce the desired temperature. During the run simultaneous observations were made on the increase in pressure as the reaction progressed, on the current flowing in the filament, on the thermocouple E.M.F., and on the time.

The change in the maximum temperature of the filament from the beginning to the end of a decomposition run was less than five degrees. From this fact, and the fact that the resistance was kept constant, it is reasonable to assume that the distribution of temperature, and thus the effective length of the filament, did not vary appreciably during a single decomposition run.

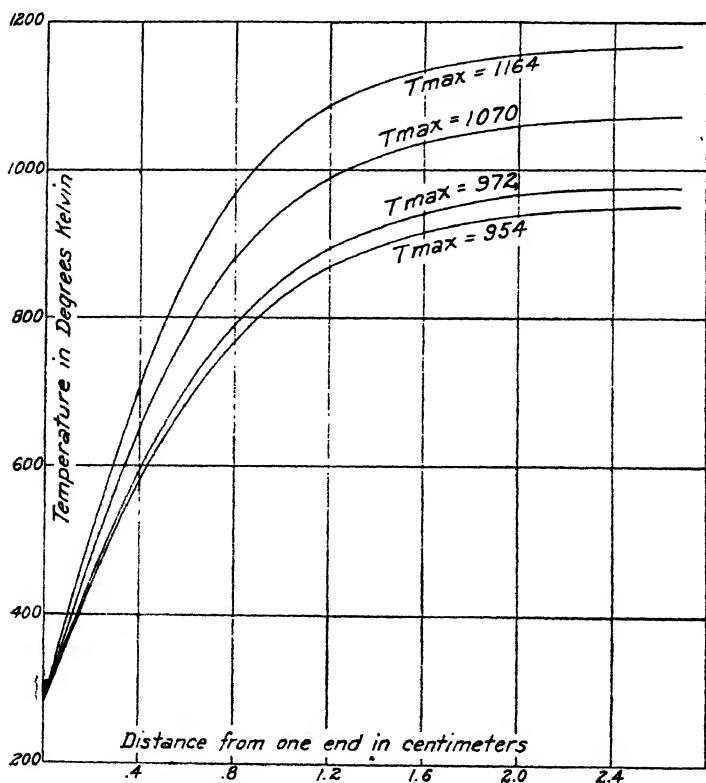
The results of the graphical integration, giving the temperature as a function of the distance from one end of the filament, are shown in the figure for four different maximum temperatures. As a check on the accuracy of the work, the integrated resistance was compared with

the measured resistance and the results are shown in Table I.

The effective length of filament was determined by means of the expression

$$l = \Sigma k \Delta x / \bar{k},$$

where  $k$  is the rate of reaction for the temperature of the element  $\Delta x$ , and  $\bar{k}$  is the rate at the maximum temperature.



*Results of the Graphical Integration.  
Temperature along the Filament as a Function  
of the Distance from one End*

The rates of reaction for each of the temperatures used in the integration were obtained from a  $\log k$  against  $T^{-1}$  plot of the experimental data.

Table I. gives the measured resistance, the computed resistance, the resistance that the filament would have if its entire length had been at the maximum temperature, and the effective length.

TABLE I.

T. °K.	Measured resistance.	Computed resistance.	Computed resistance. uncorrected.	Effective length = $\Sigma k \Delta x / \bar{k}$ .
1164	·6969	·6988	·7398	15·23
1070	·6324	·6330	·6642	14·85
972	·5661	·5652	·5933	14·37
954	·5533	·5518	·5804	14·21

*Heat of Dissociation of Ammonia.*

As has been shown above, over the temperature range investigated the thermal losses to the gas in the tube could be represented as  $W \equiv B(T - T_0)^2$ . Lorenz \* found empirically that the thermal losses from a filament to a gas could be represented by  $B(T - T_0)^{5/4}$  over quite a wide range of temperatures. In the present work, it was thought that the discrepancy between the two empirical laws could be accounted for on the basis of the fact that the gas was reacting chemically. Irving Langmuir †, in his work on the thermal conductivity of hydrogen, expressed the losses to the gas as  $S(\phi_2 - \phi_1)$ , where  $S$  is a constant known as the shape factor, and

$$\phi_2 - \phi_1 = \int_{T_1}^{T_2} K dT,$$

where  $K$  is the thermal conductivity of the gas at the temperature  $T$ .  $T_1$  and  $T_2$  are the temperatures of the water-bath and of the surface of the metal. The function of convection, as postulated by Langmuir, is to maintain the boundary of an enveloping layer of gas practically at the temperature  $T_1$ . Langmuir's results are in agreement with the empirical law given by Lorenz. In the present work, the losses to the gas can be expressed as the sum of two terms, the first the conduction and convection loss, and the second the loss due to the chemical reaction. This second term should be proportional to the rate of reaction, so

$$W = S(\phi_2 - \phi_1) + qk_0, \quad . \quad . \quad . \quad . \quad (7)$$

where  $k_0$  is the rate of reaction at the beginning of the run,

\* L. Lorenz, *Ann. Phys.* xiii. p. 582 (1881).

† Irving Langmuir, *Phys. Rev.* xxxiv. p. 401, June 1912.

and  $q$  is the heat of dissociation of ammonia. The experimental values of  $B$  were plotted against total pressure in the tube, and the smoothed curves were extended back to the beginnings of the decomposition runs to determine the values of  $W$  when the concentration of the products of the reaction were zero. The values of  $k$  at the beginnings of the runs were determined by plotting  $1/k$  against  $p_1/p_0$  and extending the straight lines back to the  $1/k$  axis, where  $p_1/p_0=0$ , as described by Kunsman, Lamar, and Deming\*.  $p_1$  is the partial pressure of hydrogen, and  $p_0$  is that of ammonia.

The formula  $K=a\eta c_v$  was used for the thermal conductivity of ammonia in the calculation of  $\phi_2-\phi_1$ .  $a$  is a constant,  $\eta$  is the viscosity, and  $c_v$  the specific heat at constant volume. Sutherland's formula,

$$\eta=\eta_0 T^{\frac{1}{2}}/(1+c/T),$$

was used with  $c=370$ , as given in the International Critical Tables.  $c_p$  is given in these tables by the formula

$$c_p=8.62+0.002(T-273)+7.2 \times 10^{-9}(T-273)^2$$

calories per mol per degree. The last term was neglected. The pressure of the ammonia was 26.6 cm. Hg at the beginning of each run and its temperature next to the filament was in the neighbourhood of  $1000^\circ\text{K}$ , so we think the assumption that  $c_p-c_v=\text{constant}$  is justifiable. The ratio  $c_p/c_v$  at  $15^\circ\text{C}$ . is given in the tables as 1.31. This allows  $c_v$  to be calculated at  $15^\circ\text{C}$ ., and assuming  $c_p-c_v=\text{constant}$  to be true for all temperatures,  $c_v$  is known at all temperatures. The constant  $a$  was computed using  $K$  as given for  $100^\circ\text{C}$ . in the Critical Tables, and  $\eta$  and  $c_v$  as given by the above formulas (remembering to reduce them all to the same units), whence  $K=a\eta c_v$  becomes

$$K=35.05 \times 10^{-6} T^{\frac{1}{2}} \{1+0.000304(T-273)\} / (1+370/T) \\ \text{joules/cm. deg.} \quad \dots \dots \dots (8)$$

Table II. furnishes eight observations on equation (7). The values of  $q$  and  $S$  that render

$$\sum_{i=1}^8 \{(\phi_2-\phi_1)_i - W_i(1/S) + k_{0i}(q/S)\}^2$$

\* Kunsman, Lamar, and Deming, "Rates and Temperature Coefficients of the Catalytic Decomposition of Ammonia over Molybdenum, Tungsten, and Promoted Iron," to be published soon.

### 36 *The Temperature Distribution along a Heated Filament.*

a minimum were found. Thus the entire adjustment is thrown on to  $\phi_2 - \phi_1$  for each temperature, which is fair enough because the experimental values of  $k$  and  $W$  are much more reliable than the determinations of  $\phi_2 - \phi_1$ . The least-square computation yields  $q=50,513$  joules per mol = 12,067 calories per mol, and  $S=32.83$ .

TABLE II.

$W$  is the power in watts supplied to a length of filament that has an area of one square centimetre, as computed from the observed current and the calculated resistance, minus the calculated loss by radiation.  $\phi_2 - \phi_1$  is calculated using  $K$  given in eq. (7). The values of  $k$  are smoothed values of the observed reaction rate, in mols per second per square centimetre.

T °K.	$W(\text{watts/cm.}^2)$ ,	$(\phi_2 - \phi_1) \times 10^2$ .	$k \times 10^6 \frac{\text{mols}}{\text{sec. cm.}^2}$ .
1164	26.08	63.22	121.20
1121	22.93	57.52	79.10
1081	20.27	53.17	52.80
1070	19.47	51.82	46.22
1043	17.90	49.17	31.48
1007	15.85	45.49	14.00
972	14.16	42.27	6.59
954	12.92	40.27	3.50

Thus 12,067 calories per mol is found to be the average heat of dissociation of ammonia for the temperature interval 954° to 1164° K. Lewis and Randall\* give a formula, based on Haber's data, that yields  $q=13,375$  calories per mol over this temperature range. The agreement justifies the assumption that the discrepancy in the empirical law for the thermal loss to the gas was due to the progress of the chemical reaction.

The authors desire to thank Professor T. B. Brown of the George Washington University and Dr. C. H. Kunsman of this laboratory for several helpful suggestions made during the progress of this work.

\* Lewis and Randall, 'Thermodynamics,' Chapt. xxxix.

V. *New Bands in the Secondary Spectrum of Hydrogen.*—  
Part II. By D. B. DEODHAR, M.Sc., Ph.D., *Physics*  
*Department, Lucknow University, India* \*.

THE investigation of the secondary spectrum of hydrogen has been continued in the Physics Department of the Lucknow University, and it has brought to light a large number of new band-groups in the blue and the violet region of the spectrum similar to those in the yellow region, which were dealt with in detail in my last paper †. In the present paper I propose to set forth a system of seven new bands in the blue region which I have been able to examine thoroughly.

The band-groups in the yellow, blue, etc. region start respectively on the short-wave length side of  $H_{\alpha}$ ,  $H_{\beta}$ , etc., and extend further towards the violet end of the spectrum. In picking up band-lines use is made of the microphotograph of a typical first-type discharge spectrogram of hydrogen taken by Moll's self-registering photometer.

There is a large mass of lines in the blue and the violet region of the first-type spectrum whose intensity gradation on the photograph indicates the presence of regularities in a very conspicuous way. Many of these lines appear to be extensions of the systems developed by Professor O. W. Richardson ‡. There are some lines which have been grouped by Allen and Sandeman § as belonging to triatomic hydrogen. However, there are several lines which are not yet ordered, and which show regularities according to the microphotograph.

The leading lines have been picked up from the first-type spectrogram. The accurate picking of relevant lines has been further facilitated by the wave-length tables of hydrogen lines recently published by Gale, Monk, and Lee ||. These authors have resolved several strong lines into their components with the help of a 21-foot concave grating, and the measurement of standard lines was made by them by means of a Fabry-Perot interferometer giving a high accuracy to the values of the interpolated lines.

\* Communicated by the Author.

† Phil. Mag. vii. pp. 466-479 (1928).

‡ Roy. Soc. Proc. A, cxiii. pp. 368-419 (1926).

§ Roy. Soc. Proc. A, cxiv. pp. 293-313 (1927).

|| Astro. Phys. Journ. lxvii. pp. 89-113 (1928).

The P(2)-lines of all the blue bands are about 150 wave-numbers apart, as in the case of P(2)-lines of the yellow bands, and the vertical differences of the various P, Q, and R branches are approximately of the same order as those of the yellow ones. These bands are named as  $D'_1$ ,  $D'_2$ ,  $D'_3$ ,  $D'_4$ ,  $D'_5$ ,  $D'_6$ , and  $D'_7$ , the D's representing their similarity to the yellow bands. The signifying letter D is dashed to distinguish the blue group from the yellow group. The frequencies, properties, and other details of these bands are given in Table I. The band-lines are represented by their frequencies. The values of frequencies are taken from the tables of Gale, Monk, and Lee in general, and from the tables of Merton and Barratt\*, Tanaka†, or Deodhar‡ in the case of those lines which do not occur in the list of Gale, Monk, and Lee. The frequency of the line is followed by (1) the intensity estimate according to Gale, Monk, and Lee, and (2) the intensity estimate made by the author on the first-type spectrogram. It may be pointed out that the estimate of intensity in the list of Gale, Monk, and Lee is much higher than the intensity estimate in the lists of Merton and Barratt, Tanaka, or Deodhar.

Many ( $r$ ) and ( $rd$ ) lines in Tanaka's and Deodhar's lists appear as (0) and (1) lines in G., M., and L.'s tables. However, in this paper I have used G., M., and L.'s estimates for the sake of quick reference. Underneath the frequency value of the line are given the H.P., L.P., C.D., He, Z, and S properties according to Merton and Barratt's tables, where the letters have their usual meaning. These properties are followed in the same line by other claims, if any, made by other systems. The first and second differences are given in the next two columns. The horizontal and the vertical differences are given in Tables II. and III. respectively.

It will be seen from Table I. that the first-type property is exhibited by a majority of the band-lines in the blue region. There are also very few important claims by other systems. The line  $D_3P(2)$  appears as Richardson's § 111 P(6) and 11 R(5), but Richardson considers it to be too strong for either of these two series.  $D'_3R(2)$  figures as  $3\gamma_4Q(4)$ , but here Richardson || appears to be in doubt about the proper assignment of the line as  $3\gamma_4Q(4)$ ;  $D'_1R(1)$  is claimed as  $D'_3Q(4)$ , and  $D'_1R(3)$  appears as  $D'_3Q(3)$ . Nothing definite

\* Phil. Trans. Roy. Soc. A, ccxxii. pp. 369-400 (1922).

† Roy. Soc. Proc. A, cviii. pp. 592, 606 (1925).

‡ Roy. Soc. Proc. A, cxiii. pp. 420-432 (1926).

§ Roy. Soc. Proc. A, cix. pp. 43, 44 (1925).

|| Roy. Soc. Proc. A, cxiii. p. 388 (1926).

TABLE I.

$D'_1P(m).$			$D'_1Q(m).$			$D'_1R(m).$		
$m.$	$\Delta_1.$	$\Delta_2.$	$m.$	$\Delta_1.$	$\Delta_2.$	$m.$	$\Delta_1.$	$\Delta_2.$
2.	21112.23 (0h) (o)	> 98.34	1.	21298.72 (1) (ab)	> 29.01	1.	21456.53 (0) (0)	> 28.99
3.	21013.94 (1) (2)	> 114.32	2.	21260.71 (0) (ab)	> 11.24	2.	21485.52 (6) (2)	> 11.75
4.	20899.62 (Q', a) (0)	> 16.61	3.	21229.46 (1) (1)	> 15.60	3.	21502.76 (0) (0)	> 17.24
5.	2050 (Q)(3)	> 130.93	4.	21173.61 (3) (0)	> 55.85	4.	21507.70 (0, a) (0)	> 4.94
	20768.69 (7) (2)		5.	21102.54 (0) (<0)	> 71.07			
	L.P. +							
$D'_2P(m).$			$D'_2Q(m).$			$D'_2(Rm).$		
$m.$	$\Delta_1.$	$\Delta_2.$	$m.$	$\Delta_1.$	$\Delta_2.$	$m.$	$\Delta_1.$	$\Delta_2.$
2.	21262.87 (2) (1)	> 103.95	1.	21424.74 (0) (ab)	> 26.97	1.	21559.99 (1) (<0)	> 38.28
3.	21158.92 (4) (2)	> 15.18	2.	21397.77 (1) (0)	> 11.21	2.	21598.27 (1) (prob. ab)	> 6.03
	L.P. +	> 119.13	3.	21359.59 (5) (1)	> 38.18	3.	21630.52 (0) (ab)	> 32.25
4.	21039.79 (4) (1)	> 16.67		L.P. +, 3.33 Q(1)	> 48.82	4.	21655.44 (00) (ab)	> 24.92
	H.P. +, 8.	> 135.80	4.	21310.77 (1) (0)	> 14.07			
5.	20903.99(1, a) (ab)		5.	21247.88 (3) (1)	> 62.89			



TABLE I. (*cont.*).

$D'_3P(m)$ .		$D'_3Q(m)$ .		$D'_3R(m)$ .	
$m$ .	$\Delta_1, \Delta_2$	$m$ .	$\Delta_1, \Delta_2$	$m$ .	$\Delta_1, \Delta_2$
2.	21410.61 (3) (1) H.P. +, 111 P (6)	1.	21562.97 (r) (ab) D.	1.	21690.06 (00) (<0) 5 $\gamma$ 2 Q(1)
3.	21300.46 (0) (0)	2.	21537.93 (r) (ab) D.	2.	21740.19 (3) (0) H.P. + +, He + + 3 $\gamma$ 4 Q(4) ?
4.	21178.30 (1, a) (<0)	3.	21502.76 (0) (0) D <sub>1</sub> R(5)	3.	21780.80 (1) (<0)
5.	21035.46 (0) (ab)	4.	21456.53 (0) (0)	4.	21820.64 (4) (2) H.P. + +, He + +
		5.	21399.47 (1) (1)		
$D'_4P(m)$ .		$D'_4Q(m)$ .		$D'_4R(m)$ .	
$m$ .	$\Delta_1, \Delta_2$	$m$ .	$\Delta_1, \Delta_2$	$m$ .	$\Delta_1, \Delta_2$
2.	21557.79 (0h) (0)	1.	21709.81 (0) (ab)	1.	21837.43 (6) (0)
3.	21440.31 (8) (3) L.P. +	2.	21686.28 (r) (ab) D.	2.	21901.17 (1) (ab) 2 $\gamma$ 3 Q(4) ?
4.	21315.17 (7) (1) H.P. +, 082 Q(2)	3.	21655.44 (00) (<0) He + +	3.	21956.51 (0) (ab)
5.	21173.61 (3) (0)	4.	21616.85 (0) (ab) 4 $\gamma$ 5 Q(1)	4.	22005.96 (1) (ab)
		5.	21562.97 (r) (ab) D <sub>3</sub> Q(1)		

TABLE I. (cont.).

$D'_6P(m).$		$D'_6Q(m).$		$D'_6R(m).$	
$m.$	$\Delta_1, \Delta_2.$	$m.$	$\Delta_1, \Delta_2.$	$m.$	$\Delta_1, \Delta_2.$
2. $D.$	21702.52 ( $r$ ) (?)	1. 21869.77 (0) ( $ab$ )	> 22.68	1. 22014.85 (2) (1)	H.P. +
3. $D.$	21579.44 ( $q$ ) (?)	2. 21847.14 (0) (1)	> 31.53	2. 22083.53 (0) (0)	> 68.68
4. 21449.88 (00 $b$ ) ( $ab$ )	> 129.56	3. 21815.61 (10) (3)	> 39.51	3. 22141.31 (2) (0)	> 57.78
5. 21306.76 (5) (1)	> 143.12	4. 21776.10 ( $r$ ) ( $ab$ )	> 47.09	4. 22198.54 (00) ( $ab$ )	> 57.23
0.02 Q(3), 56R(4)		5. 21729.01 (1) (0)			
$D'_6P(m).$		$D'_6Q(m).$		$D'_6R(m).$	
$m.$	$\Delta_1, \Delta_2.$	$m.$	$\Delta_1, \Delta_2.$	$m.$	$\Delta_1, \Delta_2.$
2. 21844.49 (1) (1)	> 124.86	1. 22047.14 (1) (0)	> 22.31	1. 22227.98 (3) (0)	He +
3. 21719.63 ( $r$ ) (0)	> 11.15	2. 22024.93 (5) (2)	> 31.10	2. 22299.80 (00) (< 9)	> 71.82
T.	> 136.01	H.P. + +, Z.	> 37.22	3. 22367.39 (0) (0)	> 67.59
4. 21583.62 (9) (6)	> 151.69	D.	> 44.60	4. 22435.59 (2) (1)	> 68.20
He +, Z.		4. 21956.51 (0) ( $ab$ )			
5. 21431.93 (1) (< 0)		5. 21911.91 (1) (0)			

$D'_7P(m).$			$D'_7Q(m).$			$D'_7R(m).$		
$m.$	$\Delta_1.$	$\Delta_2.$	$m.$	$\Delta_1.$	$\Delta_2.$	$m.$	$\Delta_1.$	$\Delta_2.$
2.	21985.24 (1) (1)	$> 132.14$	1.	22241.08 (1) (<0)	$> 21.14$	1.	22476.06 (6) (2)	$> 83.38$
3.	21853.10 (0) (0)	$> 145.35$	2.	22219.94 (00) (0)	$> 28.16$	2.	22559.44 (1) (0)	$> -0.93$
4.	21707.75 (2) (1)	$> 7.46$	3.	22191.78 (1) (0)	$> 3.41$	3.	22643.75 (3) (ab)	$> 84.31$
	H.P. +, He+	$> 152.81$		L.P. +, He + +, O $_2^3Q(4)$	$> 31.57$		He + +, Z, S	$> 78.90$
5.	21554.94 (00) (ab)		4.	22160.21 (1) (0)	$> 10.73$	4.	22722.65 (1) (ab)	
			5.	22117.91 (3) (prob. ab.)	$> 42.30$			
				He + +, Z, S				

TABLE II.

Horizontal Differences of P(m)'s, Q(m)'s, and R(m)'s.

	D' <sub>2</sub> -D' <sub>1</sub> .	D' <sub>3</sub> -D' <sub>2</sub> .	D' <sub>4</sub> -D' <sub>3</sub> .	D' <sub>5</sub> -D' <sub>4</sub> .	D' <sub>6</sub> -D' <sub>5</sub> .	D' <sub>7</sub> -D' <sub>6</sub> .
P(2).....	150·59	147·74	147·18	144·73	141·97	140·75
P(3).....	144·98	141·54	139·85	139·13	140·19	133·47
P(4).....	140·17	138·51	136·87	134·71	133·74	124·13
P(5).....	135·30	131·47	138·15	133·15	125·17	123·01
Q(1).....	126·02	138·23	146·84	159·96	177·37	193·94
Q(2).....	128·06	140·16	148·35	160·86	177·79	195·01
Q(3).....	130·13	143·17	152·68	160·17	178·12	198·05
Q(4).....	137·16	145·76	160·32	159·25	180·41	203·70
Q(5).....	145·34	151·59	163·50	166·04	182·90	206·00
R(1).....	103·46	130·07	147·37	177·42	213·13	248·08
R(2).....	112·75	141·92	160·98	182·36	216·27	259·64
R(3).....	127·76	150·28	175·71	184·80	226·08	276·36
R(4).....	147·74	165·20	185·32	192·58	237·05	287·06

TABLE III.

Vertical Differences of P(m), Q(m), and R(m) lines.

Band.	P(2)-P(3).	P(3)-P(4).	P(4)-P(5).		
D' <sub>1</sub> .....	98·34	114·32	130·93		
D' <sub>2</sub> .....	103·95	119·13	135·80		
D' <sub>3</sub> .....	110·15	122·16	142·84		
D' <sub>4</sub> .....	117·48	125·14	141·56		
D' <sub>5</sub> .....	123·03	129·56	143·12		
D' <sub>6</sub> .....	124·86	136·01	151·69		
D' <sub>7</sub> .....	132·14	145·35	152·81		
	Q(1)-Q(2).	Q(2)-Q(3).	Q(3)-Q(4).	Q(4)-Q(5).	
D' <sub>1</sub> .....	29·01	40·25	55·85	71·07	
D' <sub>2</sub> .....	26·97	38·18	48·82	62·89	
D' <sub>3</sub> .....	24·04	35·17	46·23	57·06	
D' <sub>4</sub> .....	23·53	30·84	38·59	53·58	
D' <sub>5</sub> .....	22·63	31·53	39·51	47·09	
D' <sub>6</sub> .....	22·31	31·10	37·22	44·60	
D' <sub>7</sub> .....	21·14	28·16	31·57	42·30	
	R(2)-R(1).	R(3)-R(2).	R(4)-R(3).		
D' <sub>1</sub> .....	28·99	17·24	4·94		
D' <sub>2</sub> .....	38·38	32·25	24·92		
D' <sub>3</sub> .....	50·13	40·61	39·84		
D' <sub>4</sub> .....	63·74	55·34	49·45		
D' <sub>5</sub> .....	68·68	57·78	57·23		
D' <sub>6</sub> .....	71·82	67·59	68·20		
D' <sub>7</sub> .....	83·38	84·31	78·90		

can be said about this double claim ; but these lines do not so far appear to be claimed by any other published series.  $D'_4R(2)$  figures as Richardson's  $2\gamma_3Q(4)$ , but here also Richardson seems to be uncertain about the correctness of the line belonging there. The line 21306·76, which is  $D'_5P(5)$  in the present paper, has been claimed as  $0\delta 2Q(3)$  and  $56R(4)$  by Richardson. The line is rather strong for its place as  $D'_5P(5)$  ; it also appears to be strong for  $56R(4)$ .  $D'_6Q(2)$  figures as Allen and Sandeman's \* II A.C.Q(2). Its first-type property is certainly favourable for its place as  $D'_6Q(2)$ , and its high-pressure nature may demand its position in Allen and Sandeman's series as well.  $D'_7Q(5)$  is given as Allen and Sandeman's II<sub>A</sub>. *d*. Q(2). Its intensity is a bit strong for its assignment as  $D'_7Q(5)$ ; but it shows helium effect, which favours its place there. Its probable absence, that is to say its extreme weakening in the first-type spectrum, speaks favourably for its place in Allen and Sandeman's series. The intensities of  $D'_5P(2)$  and  $D'_5P(3)$  cannot be exactly given on the judgment of the first-type plate, and this is indicated by making a query in the bracket for intensity ;  $D'_5P(2)$  is 21702·52(*r*)D, and it is very close to 21699·61, which is broad, and possesses intensity (1).  $D'_5P(3)$  is 21579·44(*q*)D, and is quite close to 21583·62, which is (7) in intensity on the first-type plate.

The horizontal and vertical differences of  $P(m)$ ,  $Q(m)$ , and  $R(m)$  lines are arranged in Tables II. and III. It will be seen from Table II. that the successive horizontal differences have a fairly systematic run. The value in wave-numbers of these differences for P's, Q's, and R's are roughly of the same order as for those in the case of the yellow bands. The run of the vertical differences in Table III. is very systematic. It is also interesting to compare the vertical differences of P's, Q's, and R's of all the bands of the blue with those in the yellow. For instance, the  $P(2) - P(3)$  difference in the yellow gradually rises from 99 for the first band to 130 for the last band ; and in the case of the blue bands it gradually rises from 98 for the first to 132 for the seventh band.  $Q(1) - Q(2)$  for the yellow gradually decreases from 30 to 21, and for the blue it is 29 for the first band and then gradually goes down to 21 for the last band. The  $R(2) - R(1)$  value of the yellow bands steadily rises from 26 to 82 approximately, while that of the blue bands also shows a gradual increase from 29 to 83.

\* Roy. Soc. Proc. A, cxiv. p. 301 (1927).

The usual combination principle, such as  $Q(m+1) + Q(m) = P(m+1) + R(m)$  is obeyed throughout by the P, Q, and R branches of all the seven bands. The accuracy with which the combination principle is satisfied can also be easily seen by looking to the initial and the final term differences which are tabulated in Tables IV. and V. respectively. The frequencies of the null lines, the moments of inertia, and other band-constants are given in Table VI. The properties of lines involved in all these bands and the systematic variation of the successive differences from band to band show that these bands are related to each other. The run of the null-line frequencies and the gradual variation of values of the initial and the final moments of inertia from  $D'_1$  to  $D'_7$  lend further support to this view.

As usual, the emission of the  $R(m)$  line is the result of a quantum jump  $m+1 \rightarrow m$ ; the  $P(m)$  line is due to a  $m-1 \rightarrow m$  jump, and the  $Q(m)$  line is due to a  $m \rightarrow m$  jump.

$$\begin{aligned}\text{Thus} \quad R(m) &= \nu_0 + (Fm1) - f(m), \\ Q(m) &= \nu_0 + F(m) - f(m), \\ P(m) &= \nu_0 + F(m-1) - f(m).\end{aligned}$$

Here  $\nu_0$  is the frequency of the null lines and  $F$  and  $f$  represent the initial and the final states respectively of the molecule. From these equations the initial and the final differences can be easily calculated. The differences obtained in the above manner are tabulated in Tables IV. and V. With the help of the term-differences we can calculate the initial and the final moments of inertia of the emitters of the bands. We can also calculate Kratzer's correction terms  $P$  and  $\rho$ , representing the effect of the angular momentum due to electrons in the initial and the final state from relations of the form  $F(m) = B(m-P)^2$  and  $f(m) = b(m-\rho)^2$ , where  $B$  and  $b$  can be easily shown to be equal to  $\frac{1}{2}\{(F(3) - F(2)) - (F(2) - F(1))\}$  and  $\frac{1}{2}\{(f(3) - f(2)) - (f(2) - f(1))\}$  respectively. The evaluation of  $P$  and  $\rho$  gives a clue to the determination of the terms from which we can directly calculate the frequencies of the null lines of the various bands. The details of the process of these calculations have been already worked out in the paper on the yellow bands, and to avoid repetition it is assumed that that paper is available for reference. The values of  $\nu_0$ 's calculated for each band from  $Q(1)$ ,  $P(2)$ , and  $R(1)$ , and the values of the final and the initial terms, etc.,

TABLE IV.

## Initial Terms.

Band.	<i>m</i> .	$\frac{R(m)}{Q(m+1)}$	$\frac{Q(m+1)}{-P(m+1)}$	Means.	Term diff.	2nd diff.
$D'_1$	1 ...	157·81	157·43	157·62	$F(2) - F(1)$	
	2 ...	215·81	215·52	215·66	$F(3) - F(2)$	> 58·04
	3 ...	273·30	273·99	273·64	$F(4) - F(3)$	> 57·98
	4 ...	334·09	333·85	333·97	$F(5) - F(4)$	> 60·33
$D_2$	1 ...	135·25	134·90	135·08	$F(2) - F(1)$	
	2 ...	200·50	200·67	200·58	$F(3) - F(2)$	> 65·50
	3 ...	270·93	270·93	270·95	$F(4) - F(3)$	> 70·37
	4 ...	344·67	343·89	344·28	$F(5) - F(4)$	> 73·33
$D'_3$	1 ...	127·09	127·32	127·20	$F(2) - F(1)$	
	2 ...	202·26	202·30	202·28	$F(3) - F(2)$	> 75·08
	3 ...	278·04	278·23	278·14	$F(4) - F(3)$	> 75·86
	4 ...	364·11	364·01	364·06	$F(5) - F(4)$	> 85·92
$D'_4$	1 ...	127·62	128·49	128·05	$F(2) - F(1)$	
	2 ...	214·89	215·13	215·01	$F(3) - F(2)$	> 86·96
	3 ...	301·07	301·68	301·38	$F(4) - F(3)$	> 88·37
	4 ...	389·11	389·36	389·24	$F(5) - F(4)$	> 87·86
$D'_5$	1 ...	145·08	144·62	144·85	$F(2) - F(1)$	
	2 ...	236·39	236·17	236·28	$F(3) - F(2)$	> 91·43
	3 ...	325·70	326·22	325·96	$F(4) - F(3)$	> 89·68
	4 ...	422·44	422·25	422·35	$F(5) - F(4)$	> 96·39
$D'_6$	1 ...	180·84	180·44	180·64	$F(2) - F(1)$	
	2 ...	274·87	274·10	274·49	$F(3) - F(2)$	> 93·85
	3 ...	373·66	372·89	373·27	$F(4) - F(3)$	> 98·78
	4 ...	479·08	479·98	479·53	$F(5) - F(4)$	> 106·26
$D'_7$	1 ...	234·98	234·70	234·84	$F(2) - F(1)$	
	2 ...	339·50	338·68	339·09	$F(3) - F(2)$	> 104·25
	3 ...	451·97	452·46	452·21	$F(4) - F(3)$	> 113·12
	4 ...	562·45	562·97	562·71	$F(5) - F(4)$	> 110·50

TABLE V.

Final Terms.

Band.	<i>m</i> .	$\frac{R(m)}{-(Q(m+1))}$	$\frac{Q(m)}{-P(m+1)}$	Means.	Term diff.	2nd diff.
$D'_1$	1 ...	186·82	186·44	186·61	$f(2)-f(1)$	
	2 ...	256·06	255·77	255·91	$f(3)-f(2)$	> 69·30
	3 ...	329·15	329·84	329·50	$f(4)-f(3)$	> 73·59
	4 ...	405·16	404·92	405·04	$f(5)-f(4)$	> 75·54
$D'_2$	1 ...	162·22	161·87	162·05	$f(2)-f(1)$	
	2 ...	238·68	238·85	238·76	$f(3)-f(2)$	> 76·71
	3 ...	319·75	319·80	319·77	$f(4)-f(3)$	> 81·01
	4 ...	407·56	406·78	407·17	$f(5)-f(4)$	> 87·40
$D'_3$	1 ...	152·13	152·36	152·25	$f(2)-f(1)$	
	2 ...	237·43	237·47	237·45	$f(3)-f(2)$	> 85·20
	3 ...	324·27	324·46	324·37	$f(4)-f(3)$	> 86·92
	4 ...	421·17	421·07	421·12	$f(5)-f(4)$	> 96·75
$D'_4$	1 ...	151·15	152·02	151·59	$f(2)-f(1)$	
	2 ...	245·73	245·97	245·85	$f(3)-f(2)$	> 94·26
	3 ...	339·66	340·27	339·96	$f(4)-f(3)$	> 94·11
	4 ...	442·99	443·24	443·11	$f(5)-f(4)$	> 103·15
$D'_5$	1 ...	167·71	167·25	167·48	$f(2)-f(1)$	
	2 ...	267·92	267·70	267·81	$f(3)-f(2)$	> 100·33
	3 ...	365·21	365·73	365·47	$f(4)-f(3)$	> 97·66
	4 ...	469·53	469·34	469·44	$f(5)-f(4)$	> 103·97
$D'_6$	1 ...	203·05	202·65	202·85	$f(2)-f(1)$	
	2 ...	306·07	305·30	305·68	$f(3)-f(2)$	> 102·83
	3 ...	410·88	410·11	410·50	$f(4)-f(3)$	> 104·82
	4 ...	523·68	524·58	524·13	$f(5)-f(4)$	> 113·63
$D'_7$	1 ...	256·12	255·84	255·98	$f(2)-f(1)$	
	2 ...	367·66	366·84	367·25	$f(3)-f(2)$	> 111·27
	3 ...	483·54	484·03	483·78	$f(4)-f(3)$	> 116·53
	4 ...	604·74	605·27	605·00	$f(5)-f(4)$	> 121·22



TABLE VI.—Band Constants.

Band.	From Q(1).	From P(2).	From R(1).	F(2).	F(1).	f(2).	f(1).	P.	$\rho$ .	Initial Moment of Inertia.	Final Moment of Inertia.
D <sub>1</sub> ...	21323·17	21323·14	21323·69	299·02	141·74	352·60	186·18	-1·21	-1·06	$9·41 \times 10^{-41}$ gm. cm. <sup>2</sup>	$7·60 \times 10^{-41}$ gm. cm. <sup>2</sup>
D <sub>2</sub> ...	21444·45	21444·41	21444·77	214·63	79·70	261·24	99·40	-0·56	-0·61	7·95 "	0·78 "
D <sub>3</sub> ...	21580·70	21580·65	21580·90	180·05	53·16	223·40	70·89	-0·19	-0·29	7·02 "	5·62 "
D <sub>4</sub> ...	21716·22	21715·96	21715·57	189·93	51·66	209·83	58·07	-0·06	-0·11	6·36 "	5·59 "
D <sub>5</sub> ...	21885·13	21885·44	21885·77	197·76	53·32	236·24	68·68	-0·08	-0·17	5·99 "	5·50 "
D <sub>6</sub> ...	22063·62	22063·53	22064·29	274·78	94·61	313·65	111·09	-0·42	-0·47	5·56 "	5·17 "
D <sub>7</sub> ...	22261·70	22261·76	22262·14	394·16	159·62	433·14	180·24	-0·75	-0·80	5·07 "	4·76 "

are all assembled in Table VI. in the same order as was done in the previous paper. The values of  $F(2)$ 's and  $f(1)$ 's are given in that table to facilitate the work of checking the accuracy of the values.

The frequency of the null line is separately determined by using Q(1), P(2), and R(1) members of each band. Table IV. shows that the three values of  $\nu_0$  for each band obtained from three different sources are in perfect agreement with one another, and that  $\nu_0$  steadily increases from  $D'_1$  to  $D'_7$ . The initial moment of inertia is larger than the final moment of inertia for each band, and the value of the moment of inertia steadily decreases from the first band to the last. The gradual decrease in the moment of inertia from band to band, and the systematic increase in the  $\nu_0$  values from set to set clearly indicate that these bands are related to each other.

A majority of band-lines in Table I. come up in the "first-type" discharge, which is known to favour the emission of spectrum by an excited molecule of hydrogen ( $H_2$ ), and, looking to the values of the moment of inertia which are in the neighbourhood of the values given by Dieke\* and by Richardson †, it appears that the emitter of the bands given in the present paper is an excited hydrogen molecule ( $H_2$ ).

A group of bands similar to the yellow and the blue ones appears to be present in the violet region of the first-type spectrum. It is being investigated, and I hope to deal with it in another communication. A comparison of the moment of inertia values of the yellow and the blue bands seems to suggest that these two groups may be related to each other. However, at this stage it is rather difficult to express a definite view about this point. Perhaps the investigation in the violet region may give some clue in this direction.

Physics Department,  
Lucknow University, India.

\* Proc. Amsterdam Acad. Sci. xxvii. p. 490 (1924).

† Roy. Soc. Proc. A, cxiii. p. 410 (1926).

28124/136

VI. *Illuminated Spacetime: Optical Effects of Isotropic Radiation Spread over Elliptic Space.* By LUDWIK SILBERSTEIN, Ph.D. (Communication No. 385.) \*

THE solution of Einstein's amplified ("cosmological") equations of the gravitational field,

$$R_{\mu\nu} - \frac{1}{2}(R - 2\lambda)g_{\mu\nu} = -\kappa T_{\mu\nu}, \quad . \quad . \quad . \quad (1)$$

found by de Sitter, and represented by the line-element

$$ds^2 = \cos^2 \sigma \cdot c^2 dt^2 - [dr^2 + R^2 \sin^2 \sigma (d\phi^2 + \sin^2 \phi d\theta^2)], \quad (2)$$

$\sigma = r/R$ , corresponds to an empty spacetime, *i. e.*, one devoid of matter proper and of energy as well, in fine for  $T_{\mu\nu} = 0$ .

Now, although stray particles of (palpable) matter, as molecules, atoms, protons, or electrons, are very scarce † in interstellar, and—no doubt—still more so in intergalactic regions, *radiant energy*, or plainly "light," visible and invisible, emitted by stars and nebulae, can, without exaggeration, be said to be omnipresent, spread all over the space. Nay, its total mass-equivalent ( $E/c^2$ ) amounts to an astounding figure. To realize this it is enough to recall that our own sun alone radiates at the very least (*i. e.*, not counting ultra-violet and X-rays)  $3.8 \cdot 10^{33}$  ergs per second, or  $1.33 \cdot 10^9$  grams per year, and since it is pretty certain that it has done this, and even more lavishly, at least during the last two thousand million years, and since but very little of this radiation has been intercepted, it is certain that the mass-equivalent of solar radiation now abroad in space is not less than

$$2.66 \cdot 10^{29} \text{ grams,}$$

which, though only  $5.4 \cdot 10^{-4}$  suns (mass unit), is in itself an imposing mass. Our galaxy consists of, say,  $1.5 \cdot 10^9$  stars, of which many are more lavish than the sun. Thus the mass of radiant energy originally emitted during that time by all these stars and now abroad, partly within the galaxy and partly outside, in intergalactic regions, has the prodigious mass of 800,000 suns. And then there are certainly a good many millions of such, and perhaps bigger, galaxies. It is true that all this "radiant mass" (to have a brief name for

\* Communicated by the Author. From the Kodak Research Laboratories.

† Cf., for instance, A. S. Eddington's 'Internal Constitution of the Stars' (Cambridge University Press, 1926).

$E/c^2$ ) is distributed over a huge volume, viz.,  $V = \pi^2 R^3$ , so that its mean density does not amount to very much\*. Yet it would be unwise, and somewhat repugnant, to neglect it.

It has, therefore, seemed by all means worth the trouble to take account of this stray light, so to speak. In other words, while de Sitter himself, and other writers, considered an empty, *dark* spacetime or world, we propose here to investigate an *illuminated* world. And as this "illumination" is actually provided by myriads of celestial bodies distributed more or less haphazardly, it is reasonable to treat it as *isotropic radiation*, in the generally accepted sense of the word.

Now such a radiation has the capital property that the light pressure, a hydrostatic pressure, associated with it is just *one-third* of the energy-density, say,

$$p = \frac{1}{3}\rho. \quad . \quad . \quad . \quad . \quad . \quad (3)$$

The corresponding energy-tension is, therefore, in orthogonal coordinates,

$$T_{ii} = \frac{1}{3}\rho g_{ii}, \quad T_{44} = \rho g_{44}, \quad i = 1, 2, 3, \quad . \quad (4)$$

and has the remarkable property that its scalar, or invariant,  $T = \rho - 3p$ , *vanishes*. (This, by the way, is also the property of every electromagnetic energy-tensor.) Thus the field-equations (1), which give without trouble

$$\lambda = \frac{1}{4}R = \frac{1}{4}g^{ik}R_{ik},$$

become

$$\left. \begin{aligned} R_{ii} &= \left( \frac{1}{4}R + \frac{\kappa\rho}{3} \right) g_{ii}, \\ R_{44} &= \left( \frac{1}{4}R - \kappa\rho \right) g_{44}. \end{aligned} \right\} \quad . \quad . \quad . \quad . \quad (5)$$

Let us try to solve this system of equations by the radially-symmetrical form of the line-element,

$$ds^2 = g_{11} dx^2 - x^2(d\phi^2 + \sin^2\phi d\theta^2) + g_{44} dt^2, \quad . \quad (6)$$

assuming, that is,  $\rho$  as function of  $x$  alone, and thus a *globe*, of any radius, filled with isotropic radiation. (This radius

may, if we like, be made equal to  $\frac{\pi}{2}R$ , when *the whole*

\* According to Eddington's quotation (*loc. cit.*) the total density of radiation "received by us from the stars" is  $7.7 \cdot 10^{-13}$  erg/cm.<sup>3</sup>, whence the corresponding mass-density,  $\rho = 8.6 \cdot 10^{-34}$  gr./cm.<sup>3</sup>. The italicized words imply, of course, that this density holds in interstellar regions, within our galaxy. Somewhere half-way between the Milky Way and the nebula in Andromeda, say, the density  $\rho$  may be a good deal smaller.

elliptic space will be full of radiation, as very likely it is.) The problem consists in finding  $g_{11}$ ,  $g_{44}$ , and  $\rho$  as functions of  $x$ .

Now, putting  $h_1 = \log g_{11}$ ,  $h_4 = \log g_{44}$ , and denoting derivations with respect to  $x$  by dashes, we can write the second of equations (5)

$$-R_{22} = 1 + \frac{1}{g_{11}} \left[ 1 + \frac{x}{2} (h_1' - h_4') \right] = - \left( \frac{R}{4} + \frac{\kappa\rho}{3} \right) x^2. \quad (7)$$

The third says the same thing (for  $R_{33} = R_{22} \sin^2 \phi$ ); the fourth is

$$\begin{aligned} R_{44} &= \frac{g_{44}}{g_{11}} \left[ R_{11} + \frac{1}{x} (h_1' + h_4') \right] \\ &= \left( \frac{1}{4}R - \kappa\rho \right) g_{44}, \end{aligned}$$

or, replacing  $R_{11}$  by its value given in (5),

$$h_1' + h_4' = -\frac{4}{3}\kappa\rho x g_{11} \quad . \quad . \quad . \quad (8)$$

Instead of the first of (5) it is more convenient to apply the first of the so-called equations of matter, which are known to be but a consequence of the gravitational field-equations, and this gives, without trouble,  $\rho \sqrt{g_{44}} = \text{const.}$  Since, without any loss to generality, we can put  $g_{44}(0) = 1$ , we have

$$\rho = \frac{\rho_0}{\sqrt{g_{44}}},$$

where  $\rho_0$  is the value of  $\rho$  (*system density* of radiant mass) at the origin  $O$  of the coordinates.

It remains to substitute this expression in the differential equations (7) and (8), and to solve them for  $g_{11}$ ,  $g_{44}$  as functions of  $x$ .

Subtracting (8) from (7), one finds

$$\frac{d}{dx} \left( 1 + \frac{1}{g_{11}} \right) + \frac{1}{x} \left( 1 + \frac{1}{g_{11}} \right) = \left( \frac{1}{4}R + \kappa\rho \right) x,$$

whence, in absence of a singularity (mass-centre) at  $O$ ,

$$-\frac{1}{g_{11}} = 1 - x^2/R^2, \quad R^2 = \frac{3}{\lambda + \kappa\rho} \quad . \quad . \quad . \quad (9)$$

It remains to find  $g_{44}$  from (8). Now, this equation can be written

$$\frac{d \sqrt{g_{44}}}{dx} + \left( \frac{d}{dx} \log \sqrt{-g_{11}} \right) \cdot \sqrt{g_{44}} = -\frac{4}{3}\kappa\rho_0 x g_{11},$$

which is Euler's linear equation. Its complete solution is

$$\sqrt{g_{44}} = e^{-\int d \log \sqrt{-g_{11}}} \cdot \left\{ C - \frac{2}{3} \kappa \rho_0 \int x g_{11} e^{\int d \log \sqrt{-g_{11}}} dx \right\},$$

where  $C$  is an arbitrary constant, or

$$\sqrt{g_{44}} = \frac{1}{\sqrt{-g_{11}}} \left\{ C - \frac{2i}{3} \kappa \rho_0 \int x g_{11}^{3/2} dx \right\}, \quad (10)$$

where  $i = \sqrt{-1}$ , while  $g_{11}$  is given by (9) and  $\rho = \rho_0 / \sqrt{g_{44}}$ . Thus, however,  $R$ , which contains  $\rho$  and  $\lambda = \frac{1}{2} R = \frac{1}{2} g^{\kappa\kappa} R_{\kappa\kappa}$ , might depend on  $g_{44}$  and directly on  $x$ , and the actual evaluation of  $g_{44}$  from (10) would be a highly complicated affair, possibly a hopeless task.

Fortunately, however, the combination  $\lambda + \kappa\rho$  is a constant. In fact, we may write

$$\begin{aligned} R &= \frac{1}{g_{11}} R_{11} + \frac{2}{g_{22}} R_{22} + \frac{1}{g_{44}} R_{44} \\ &= \frac{2}{g_{11}} R_{11} - \frac{2}{x^2} R_{22} + \frac{h_1' + h_4'}{x g_{11}}, \\ \lambda = \frac{1}{2} R &= \frac{1}{x^2 g_{11}} \left\{ 1 + \frac{x}{2} (h_4' - h_1') \right\} + \frac{1}{x^2} + \frac{h_1' + h_4'}{2x g_{11}} + \frac{1}{2} \kappa \rho, \end{aligned}$$

or, after some simple reductions,

$$\lambda = \kappa \rho + \frac{3}{2} \frac{g_{44}'}{x g_{11} g_{44}},$$

and, eliminating  $g_{44}'$  with the aid of (8),

$$\begin{aligned} \lambda &= -\kappa \rho + \frac{3}{2x} \frac{d}{dx} \left( \frac{1}{g_{11}} \right) \\ &= -\kappa \rho + \frac{3}{R^2} \left[ 1 - \frac{x}{R} \frac{dR}{dx} \right], \end{aligned}$$

the latter by (9). Thus

$$\frac{1}{R^2} = \frac{1}{3} (\lambda + \kappa \rho) = \frac{1}{R^2} \left[ 1 - \frac{x}{R} \frac{dR}{dx} \right],$$

from which we see two things: first, that  $dR/dx = 0$ , i. e., that  $R$  is *constant* throughout the space; and second, that *its numerical value remains free*, that is to say, is not determined by the density  $\rho$  or  $\rho_0$  of the radiant energy. The value of  $R$  (the curvature radius of spacetime) is thus to be explored independently, by means of observations (viz., the Doppler effect of stars).

Under these circumstances ( $R = \text{const.}$ ) the evaluation of the integral in formula (10) becomes a perfectly easy matter. In fact, put

$$x = R \sin \sigma, \quad \sigma = r/R.$$

Then, by (8),

$$g_{11} = -\sec^2 \sigma, \quad \frac{1}{\sqrt{g_{11}}} = i \cos \sigma,$$

so that

$$\int x g_{11}^{3/2} dx = i R^2 \int \frac{\sin \sigma}{\cos^2 \sigma} d\sigma = i R^2 \sec \sigma,$$

and (10) gives

$$\sqrt{g_{44}} = C \cdot \cos \sigma + \frac{2}{3} \kappa \rho_0 R^2;$$

or, since  $g_{44}(0) = 1$ ,

$$\sqrt{g_{44}} = \cos \sigma + \frac{2}{3} \kappa \rho_0 R^2 (1 - \cos \sigma). \quad . \quad . \quad (11)$$

Again,

$$dx = R \cos \sigma \cdot d\sigma = \cos \sigma dr,$$

so that

$$g_{11} dx^2 = -dr^2,$$

and the required solution, of form (6), ultimately becomes

$$ds^2 = g_{44} c^2 dt^2 - dl^2, \quad . \quad . \quad . \quad (12)$$

where  $g_{44}$  is as in (11) and

$$dl^2 = dr^2 + R^2 \sin^2 \sigma (d\phi^2 + \sin^2 \phi d\theta^2),$$

i. e., the familiar line-element of an elliptic three-space of curvature radius  $R$ . As we have just seen, this radius is, exactly as in empty space, *constant*, while its value is in no way predetermined by the intensity of illumination.

Since  $\kappa = 8\pi k/c^2$ , where  $k$  is the gravitation constant, we have

$$\frac{2}{3} \kappa \rho_0 = \frac{16\pi}{3} \cdot \frac{k\rho_0}{c^2}.$$

The second factor, being the "gravitation radius" of the radiant mass per unit volume, has the dimensions of

$$\frac{\text{length}}{\text{volume}}$$

or of a reciprocal area. Thus, if  $\lambda_0$  be a length and we put

$$\frac{k\rho_0}{c^2} = \frac{1}{\lambda_0^2},$$

the last expression becomes  $\frac{16\pi}{3} \frac{R^2}{\lambda_0^2}$ , and

$$\sqrt{g_{44}} = \cos \sigma + \frac{16\pi}{3} \left(\frac{R}{\lambda_0}\right)^2 (1 - \cos \sigma). \quad (11a)$$

Needless to say, all the optical and kinetical properties of the spacetime thus illuminated are fully determined by the line-element (12) with this value of  $g_{44}$ .

For  $\rho_0=0$  ( $\lambda_0=\infty$ ) our solution reduces to that found by de Sitter, viz.,  $g_{44}=\cos^2 \sigma$ , as it should.

With regard to the density of distribution of the radiant energy or its mass-equivalent, it is important to notice that  $\rho$ , for which we have found the value  $\rho_0/\sqrt{g_{44}}$ , is the system density. The *natural measure* of density can readily be shown to be  $\rho\sqrt{g_{44}}$ , and is, therefore, in our case *constant*, namely,  $\rho_0$  itself.

All the physical consequences of the solution just obtained can readily be derived, remembering that  $ds=0$  gives the propagation of light, and  $\delta \int ds=0$  the motion of a free particle inserted in the illuminated world.

Here, however, it will be enough to consider the Doppler effect, for a star and an observer in relative free (inertial) motion, as influenced by the illumination.

By a reasoning given in the writer's 'Theory of Relativity' (1924, chap. XVI.), and in symbols there explained, the Doppler effect is

$$D \equiv \frac{\delta \lambda}{\lambda} = \frac{ds}{ds'} - 1,$$

and if the origin of coordinates is placed in the star,

$$c dt - ds' = \frac{1}{\sqrt{g_{44}}} dr$$

or

$$c dt \left[ 1 - \frac{1}{\sqrt{g_{44}}} \frac{dr}{c dt} \right] = ds'.$$

Further, since the observing station (sun) is supposed to have a free, inertial motion,

$$g_{44} c \frac{dt}{ds} = k = \text{const.}$$

Thus

$$\frac{ds}{ds'} = \frac{g_{44}/k}{1 - \frac{1}{\sqrt{g_{44}}} \frac{dr}{c dt}},$$



and ultimately, the required formula for the Doppler effect,

$$D + 1 \equiv \frac{\delta\lambda}{\lambda} + 1 = \frac{g_{44}}{k \left\{ 1 - \frac{1}{\sqrt{g_{44}}} \frac{dr}{c dt} \right\}}, \quad . \quad . \quad (13)$$

where  $dr/dt$  is the radial velocity of the observer relatively to the star or *vice versa*. This follows readily from the developed form of  $\delta \int ds = 0$ , which gives

$$\frac{1}{c} \frac{dr}{dt} = \sqrt{g_{44}} \cdot \sqrt{1 - \frac{g_{44}}{k^2} - \frac{p^2 g_{44}}{k^2 R^2 \sin^2 \sigma}}, \quad . \quad (14)$$

where  $p = R^2 \sin^2 \sigma \, d\theta/ds = \text{const.}$  is (besides  $g_{44} c dt/ds = k$ ) a first integral of the equations of free motion. Thus the Doppler effect is given, rigorously, by (13) and (14), where  $r$  and  $dr/dt$  refer to the instant of receiving the light.

For small values of  $\sigma = r/R$ , that is to say, neglecting  $\sigma^4$  in presence of unity, also  $\sigma^2 r^2/c^2$ , the Doppler effect reduces to

$$D = \frac{v_r}{c} = \pm \sqrt{g_{44}} \cdot \sqrt{1 - \frac{g_{44}}{k^2} - \frac{p^2 g_{44}}{k^2 R^2}}, \quad . \quad (15)$$

where

$$k = \frac{g_0}{\sqrt{g_0 - \beta_0^2}}, \quad p = \frac{\beta_0 R \sin \sigma_0}{\sqrt{g_0 - \beta_0^2}}. \quad . \quad . \quad (16)$$

Here  $\beta_0, \sigma_0$  refer to the perihelion of the star's orbit,  $g_0$  is written for  $g_{44}(\sigma_0)$ , and  $\beta$  for  $v/c$ . The positive sign in (15) corresponds to a receding, and the negative to an approaching star.

Developing the rigorous expressions (16) to the said degree of approximation, one finds, after simple reductions,

$$D^2 = \frac{v_r^2}{c^2} = \left(1 - \frac{r_0^2}{r^2}\right) \{\beta_0^2 + N\sigma^2\}. \quad . \quad . \quad (17)$$

where

$$N = 1 - \frac{16\pi}{3} \frac{R^2}{\lambda_0^2}.$$

The only difference, with the Doppler-effect formula for dark spacetime, is that  $\sigma^2$  in the second factor is replaced by  $N\sigma^2$ , i. e.,  $r^2/R^2$  by  $r^2 N/R^2$ . In fine,  $R$ , as evaluated from radial velocities of celestial objects of known distance, is replaced by

$$R' = \frac{R}{\sqrt{N}} = \frac{R}{\sqrt{1 - \frac{16\pi}{3} \frac{R^2}{\lambda_0^2}}}. \quad . \quad . \quad (18)$$

Thus what we have determined, say from the Cepheid Variables and the O-stars\*, is  $R'$ . Having found  $R'$ , we can determine  $R$  ( $\lambda_0$  being assumed to be known), viz. :

$$R = \frac{R'}{\sqrt{1 + \frac{16\pi}{3} \left(\frac{R'}{\lambda_0}\right)^2}}. \quad \dots \quad (18 a)$$

While  $R'$  is of the order of  $10^{11}$  to  $10^{12}$  astronomical units,  $\lambda_0$  is some ten or hundred thousand times greater. In fact, according to Eddington's quotation (*loc. cit.*), the "total density of radiation received by us from the stars," *i. e.* valid for interstellar regions, is  $7 \cdot 7 \cdot 10^{-13}$  erg/cm.<sup>3</sup>, whence

$$k\rho_0 = 5 \cdot 73 \cdot 10^{-41} \text{ astr. mass units per cm.}^3,$$

and

$$\lambda_0 = \frac{c}{\sqrt{k\rho_0}} = 2 \cdot 65 \cdot 10^{17} \text{ astr. units.}$$

Possibly, if ultra-violet and X-rays were taken into account,  $\rho_0$  would be several times greater, and  $\lambda_0$  might drop to the order of  $10^{16}$  or even  $10^{15}$  a.u. At any rate, however, formula (18 a) can be safely replaced by

$$R = R' \left\{ 1 - \frac{8\pi}{3} \left(\frac{R'}{\lambda_0}\right)^2 \right\}.$$

Rochester, N.Y.

February 15, 1929.

## VII. The Calculation of Absorption in X-Ray Powder-Photographs and the Scattering Power of Tungsten. By Dr. A. CLAASSEN †.

1. **Q**UANTITATIVE intensity measurements obtained from powder photographs have to be corrected for absorption in the powder rod. This correction has been made in special cases by Debye and Scherrer ‡ and Greenwood § by means of graphical integration. As this is a very tedious proceeding, it is probably worth while to

\* Cf. 'The Size of the Universe,' now in the course of printing at the Oxford University Press.

† Communicated by the Author.

‡ P. Debye and P. Scherrer, *Phys. Zeitschr.* xix. p. 474 (1918).

§ G. Greenwood, *Phil. Mag.* i. p. 963 (1927).

give some data \* with which it is possible to calculate the absorption-coefficient in any particular case. This will be done in the following, and the results will be applied to the determination of the scattering power of tungsten.

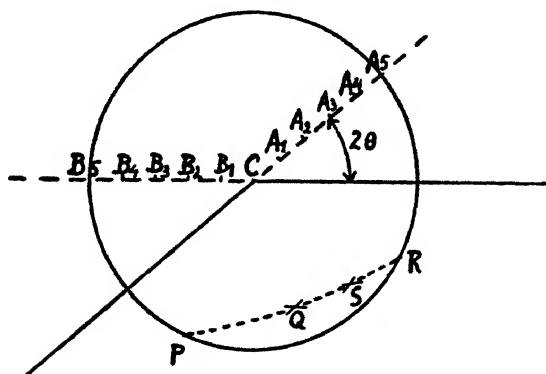
2. Let the circle of fig. 1 represent the cross-section of the rod of crystal powder, and let its centre be at C and its radius be equal to R.

The absorption-factor A, i. e. the ratio between the intensity of the diffracted beam and the intensity of the beam uninfluenced by absorption, is given by

$$A = \frac{1}{\pi R^2} \iint e^{-\mu a} dO, \quad . . . . . (1)$$

in which  $a$  = length of the path of the ray through the rod ;

Fig. 1.



$\mu$  = absorption-coefficient of the crystal powder;  $dO$  = surface-element of C. The integration must be carried out all over C. The rod is supposed to be bathed in a parallel beam of X-rays.

It is impossible to evaluate this integral, but it can be solved graphically. To this purpose C is divided into strips of size  $\Delta O$ , such that rays diffracted by points in  $\Delta O$  traverse a distance between  $a$  and  $a + \Delta a$  through the rod. We have then approximately

$$A = \frac{1}{\pi R^2} \sum e^{-\mu a} \Delta O. \quad . . . . . (2)$$

This division into strips can easily be carried out geometrically. Let in fig. 1 the incident beam be parallel to BC and the reflected beam parallel to CA. Let, further,  $MA_1 = A_1A_2 = \dots$

\* A. Claassen, Dissertation, Amsterdam, 1926.

$A_4A_5 = 1/5 R$  and  $MB_1 = B_1B_2 = \dots = B_4B_5 = 1/5 R$ , and suppose that  $S$  is the point of intersection of two circles, each with radius  $R$ , erected in the points  $A_3$  and  $B_1$ . Then the ray scattered in  $S$  has traversed a distance equal to  $3/5 R + 1/5 R = 4/5 R$  through the rod. In the same way the ray scattered in  $Q$  (circles erected in  $A_2$  and  $B_2$ ) has traversed also a distance  $4/5 R$ . Thus the line  $PR$  is constructed as the locus of all points in which rays are scattered, which traverse a distance  $4/5 R$  through the rod. Let us call these points for shortness "points  $4/5 R$ ," generally "points  $a$ ."

By constructing the loci for several values of  $a$ , the size of the strips  $\Delta O$  belonging to these values of  $a$  can be readily obtained by measuring their area with a planimeter.

When in (1) we put  $x = \frac{a}{R}$ , then the area  $\Delta s$  (expressed in the total area of  $C$  as unity) containing all points from  $x$  to  $x + \Delta x$  is a function of  $x$  only. Hence (1) becomes

$$A = \sum e^{-\mu R x} \Delta s. \quad (3)$$

Table I. gives values of  $\Delta s$  for four different glancing-angles and with  $\Delta x = 0.2$ .

TABLE I.

$x$ .	$\Delta s \cdot 10^2$ .				
	$\theta = 0^\circ$ .	$\theta = 22\frac{1}{2}^\circ$ .	$\theta = 45^\circ$ .	$\theta = 67\frac{1}{2}^\circ$ .	$\theta = 90^\circ$ .
0	0.04	0.78	2.64	4.94	6.22
0.2	0.32	1.41	3.36	4.86	6.47
0.4	0.84	2.04	4.05	5.80	6.43
0.6	1.90	2.72	4.65	6.04	6.18
0.8	2.68	3.58	5.38	6.50	6.38
1.0	4.58	4.61	6.10	6.44	6.18
1.2	7.10	5.95	6.88	6.40	6.18
1.4	11.10	7.95	7.52	6.64	5.98
1.6	17.84	15.35	8.46	6.30	5.44
1.8	53.60	22.20	9.60	6.40	5.44
2.0	—	33.30	10.20	6.34	5.44
2.2	—	—	11.00	6.20	5.04
2.4	—	—	9.90	5.90	5.04
2.6	—	—	8.88	5.36	4.86
2.8	—	—	1.30	4.88	4.20
3.0	—	—	—	4.44	4.12
3.2	—	—	—	3.22	3.50
3.4	—	—	—	2.70	3.22
3.6	—	—	—	0.60	2.47
3.8	—	—	—	—	1.24

Calculation of (3) from this table gives the absorption-factor for these glancing-angles. For other glancing-angles

the absorption-factors can be obtained with sufficient accuracy by graphical interpolation.

3. The calculation of  $A$ , according to (3), is not possible when  $\mu$  becomes very large, because the factor  $e^{-\mu R x}$  changes so rapidly in one strip that it cannot be considered as a constant. This difficulty could be overcome by taking  $\Delta x$  much smaller than 0.2, but then the exact evaluation of  $\Delta s$  for small values of  $x$  (by which  $A$  is practically entirely determined) is very difficult. A better method is the following one:—

Let the area containing all points  $< x$  be equal to  $f(x)$ . This  $f(x)$  can be calculated from Table I. It appears that for values of  $x$  smaller than 1,  $f(x)$  can be represented by the first three terms of a power-series:

$$f(x) = \alpha x + \beta x^2 + \gamma x^3 + \dots \quad (4)$$

Now  $ds = \frac{df}{dx} dx$ , and substitution in (1) gives

$$A = \int e^{-\mu R x} \frac{df}{dx} dx = \int e^{-\mu R x} (\alpha + 2\beta x + 3\gamma x^2 + \dots) dx. \quad (5)$$

If  $\mu$  is large, we may integrate from  $\mu = 0$  to  $\mu = \infty$ , and we get

$$A = \frac{1}{\mu R} \left\{ \alpha + \frac{2\beta}{\mu R} + \frac{6\gamma}{\mu^2 R^2} + \dots \right\} \quad (6)$$

( $R$  expressed in cm.)

Table II. gives the values of  $\alpha$ ,  $\beta$ , and  $\gamma$ .

TABLE II.

$\theta$ .	$\alpha \cdot 10^2$ .	$\beta \cdot 10^2$ .	$\gamma \cdot 10^3$ .
0	0	3.0	5.0
$22\frac{1}{2}$	3.1	4.0	4.0
45	11.4	9.0	0
$67\frac{1}{2}$	23.2	5.0	0
90	31.1	0.7	0

For exceedingly heavy powders the terms containing  $\beta$  and  $\gamma$  in (6) may be neglected, and in this case the absorption-factor is simply proportional to  $\alpha$ . For this limiting case of  $\mu = \infty$  the absorption can also be calculated directly, which gives a check on the values of  $\alpha$  derived from Table I.

For a plane powder surface the absorption-factor for very large  $\mu$  is easily seen to be proportional to

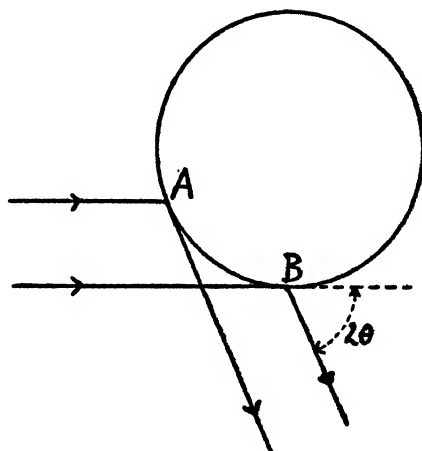
$$\int_0^\infty \exp. \mu x \left\{ \frac{1}{\sin \phi} + \frac{1}{\sin (2\theta - \phi)} \right\} dx,$$

with  $\phi$  = angle of incidence,

$$\text{or} \quad A_\phi^\theta \sim \frac{\sin \phi \sin (2\theta - \phi)}{\sin \phi + \sin (2\theta - \phi)}. \quad \dots \quad (7)$$

For a cylindrical rod of a very heavy powder it is evident that only the portion AB of the surface (see fig. 2) is effective in scattering.

Fig. 2.



The angle of incidence for the surface elements of AB varies from  $\phi = 0$  in B to  $\phi = 2\theta$  in A. Thus the total absorption-factor for a glancing-angle  $\theta$  becomes

$$A_\theta = \int_0^{2\theta} A_\phi^\theta d\phi = \int_0^{2\theta} \frac{\sin \phi \sin (2\theta - \phi)}{\sin \phi + \sin (2\theta - \phi)} d\phi. \quad \dots \quad (8)$$

This integral can be evaluated graphically or numerically. The values of  $\alpha$  in Table II. are corrected by means of the values of  $A_\theta$  calculated from (8).

All these absorption-factors have been calculated supposing a perfectly circular rod. In practice this often will not be the case, but if the rod is rotated during exposure these calculations are still valid.

## 4. The scattering power of tungsten.

The crystal structure of tungsten is cubic, body-centred with  $a = 3.158 \text{ \AA}^*$ . Powder photographs were made with  $\text{CuK } \alpha$ -rays. The diameter of the rod was about  $0.8 \text{ mm.}$ , while the tungsten powder was enclosed in a glass tube of  $\pm 5\mu$  thickness. The rod was rotated continuously during exposure. The powder particles were smaller than  $\pm 5\mu$ , so that primary extinction may be assumed to be absent  $\dagger$ .

The intensities of the reflexions were measured with a Moll self-registering photometer, applying the usual corrections. The blackening curve of the films used has been determined by van Arkel and Burgers  $\ddagger$ . The blackening of the strongest lines never exceeded 1.

Table III. gives the observed intensities (average from 5 films, accuracy from 5–10 per cent.).

The intensity of a line in a powder photograph is given by

$$I \sim \frac{A\nu F^2(1 + \cos^2 2\theta)}{\sin^2 \theta \cos \theta} e^{-2M} \S,$$

TABLE III.

Indices.	Sin $\theta$ .	$\frac{\nu(1+\cos^2 2\theta)}{\sin^2 \theta \cos \theta}$	A.	$e^{-2M}$ .	$I_{\text{obs.}}$	$F_{\text{rel.}}$	$F_{\text{abs.}}$
110	0.346	170.4	2.5	1.00	108	51	61
200	0.489	36.2	5.0	0.95	37	46	55
211	0.599	91.0	7.8	0.93	118	42	50
220	0.690	34.9	10.9	0.91	57	41	48
310	0.772	65.8	14.3	0.89	125	39	46
222	0.845	25.0	18.3	0.86	50	35	42
321	0.912	202.1	22.2	0.85	420	33	40
400	0.975	50.9	28.3	0.82	136	31	37

in which  $A$  = absorption-factor,  $\nu$  = plane-number factor,  $F$  = structure factor (in this case the scattering power of tungsten), and  $e^{-2M}$  the Debye || temperature factor as

\* A. E. van Arkel, *Zeitschr. für Krystall.* lxvii. p. 235 (1928).

† See J. Brentano, *Phil. Mag.* iv. p. 620 (1927).

‡ A. E. van Arkel and W. G. Burgers, *Zeitschr. für Phys.* xlviii. p. 690 (1928).

§ P. Debye and P. Scherrer, *Phys. Zeitschr.* xix. p. 474 (1918). G. C. Darwin, *Phil. Mag.* xliii. p. 800 (1922). J. M. Bijvoet, *Rec. Trav. Chim.* xlii. p. 886 (1924).

|| P. Debye, *Ann. der Phys.* xliii. p. 49 (1914).

modified by Waller\*. In this expression  $M$  is given by

$$M = \frac{6h^2}{\mu k \Theta} \left( \frac{\phi(x)}{x} + \frac{1}{4} \right) \frac{\sin^2 \theta}{\lambda^2},$$

with  $\mu$  the mass of the tungsten atom,  $h$  Planck's constant,  $k$  the gas constant per molecule,  $\Theta$  the characteristic temperature of the crystal which occurs in the theory of specific heats;  $x = \Theta/T$ , where  $T$  is the absolute temperature and  $\phi(x)$  is a certain function of  $x$ , which Debye evaluates. Zero-point energy is assumed according to Waller and James†.

The absorption-coefficient of tungsten for  $\text{CuK } \alpha$ -rays amounts to about 3500, so that  $A$  in Table III. has been taken equal to  $\alpha$  in Table I.

To evaluate  $M$  the approximate value  $\Theta = 280^\circ$  was calculated from Lindemann's‡ formula, giving  $M = 0, 10 \sin^2 \theta$ .

In the 7th column of Table III. the values of  $F$  calculated from (8) are given. As only relative intensities have been measured, these values are only relative ones. To arrive at the absolute  $F$ -values we have extrapolated the relative  $F$ -values to  $\sin \theta = 0$ , and assigned to the number so obtained the absolute value 74, *i.e.* the number of electrons in a tungsten atom. This extrapolation is, of course, rather uncertain, but in any case it will give an approximate idea of the decline of scattering power with increasing glancing-angle for a heavy atom. The  $F$ -curve obtained in this way is reproduced in fig. 3. Table IV. gives  $F$ -values for various values of  $\frac{\sin \theta}{\lambda}$ .

TABLE IV.

$\frac{\sin \theta}{\lambda}$ .....	0	0.1	0.2	0.3	0.4	0.5	0.6
$F_{\text{exp}}$ ..	74	70	63	57	51	45	39
$F_{\text{Thomas}}$ .....	74	68	61	53	47	42	37

A theoretical  $F$ -curve can be calculated according to Bragg and West§ from an atomic model calculated by Thomas||. In this model it is assumed that the effective

\* I. Waller, Dissertation, Upsala, 1925; *Ann. der. Phys.* lxxxiii. p. 154 (1927).

† I. Waller and R. W. James, *Proc. Roy. Soc.* cxvii. p. 214 (1927).

‡ See, *e.g.*, M. Born, 'Atomtheorie des festen Zustandes,' p. 630, or

⁴ *Handbuch der Experimentalphysik*, viii. p. 250.

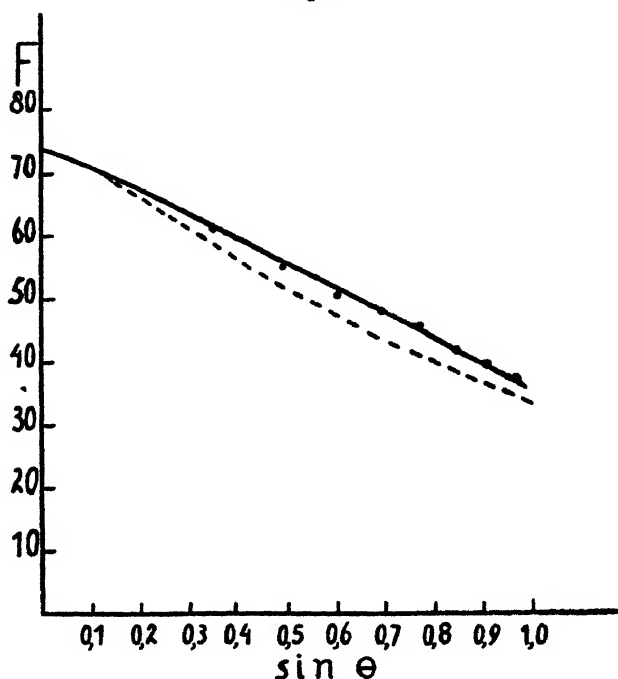
§ W. L. Bragg and J. West, *Zeitschr. für Krystall.* lxxix. p. 118 (1928).

|| L. Thomas, *Proc. Cambridge Soc.* xxiii. p. 542 (1927).



field in an atom is given by a potential  $V$  depending only on the distance  $r$  from the nucleus; that the electrons are distributed uniformly in the six-dimensional phase-space for the motion of an electron at the rate of two for each  $h^3$  of six-dimensional volume; and that this potential  $V$  is itself determined by the nuclear charge and the distribution of electrons. With these assumptions Thomas solves numerically a differential equation in  $V$  which gives the density of electrons at a distance  $r$  from the nucleus as a function of the atomic number. Thomas calculated the electron distribution for

Fig. 3.



caesium. From the form of Thomas's equation it follows that the electron distribution for any other atom can be simply calculated if it is known for a given atom (*in casu caesium*). These theoretical  $F$ -curves should be quite accurate, especially for atoms of high atomic number; even in the case of light elements the difference with the experimental results is not great\*.

The dotted line in fig. 3 gives the  $F$ -curve for tungsten calculated in this way from Thomas's figures. Table IV. compares the numerical values.

\* W. L. Bragg and J. West, *Zeitschr. für Krystall.* lxix. p. 118 (1928).

It is seen that the agreement is rather satisfactory, considering the rough way in which the experimental F-values have been obtained.

On the other hand, this agreement proves to a certain extent the validity of our calculated absorption-coefficients.

*Summary.*

This paper describes the calculation of absorption in X-ray powder photographs. For heavy powders a simple formula is deduced. The results are applied to the reflexion intensities of tungsten. The experimental scattering power of tungsten agrees approximately with the F-curve calculated from the Thomas model of the atom.

I wish to thank Dr. W. G. Burgers for having the powder photographs made.

Natuurkundig Laboratorium der  
N. V. Philips's Gloeilampenfabrieken,  
Eindhoven, Aug. 1929.

---

VIII. *The Crystal Structures of the Elements of the B Sub-Groups and their Connexion with the Periodic Table and Atomic Structures.* By WILLIAM HUME-ROTHERY, M.A., Ph.D.\*

1. *Introductory.*

THE general factors affecting crystal structure are at present comparatively little understood except for simple ionized structures such as those of the halide salts, and correspondingly simple covalent structures such as that of the diamond. In a series of most interesting papers Goldschmidt† has recently examined the inter-atomic distances in a large number of crystals, and has used these in order to deduce a series of "atomic radii" which are characteristic of the different elements under similar conditions, but which may vary with the degree of "coordination," i. e., the number of atoms which surround

\* Communicated by Prof. W. L. Bragg, F.R.S.

† Goldschmidt, *Z. Phys. Chem.* cxxxiii. p. 397 (1928).

selenium in Group VI. In this case the above rules require each atom to have  $8-6=2$  neighbours. The actual structure is hexagonal with space-group  $D_3^4$  or  $D_3^6$  (enantiomorphous), the atoms being in spiral chains, in which each atom has two close neighbours at a distance of 2.35 Å. the remaining interatomic distances being considerably greater.

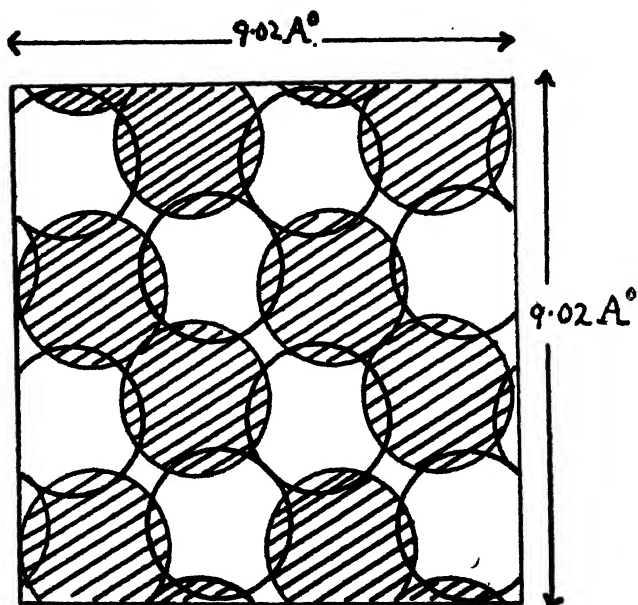
Turning now to arsenic in Group V., the above rules require each atom to have  $8-5=3$  neighbours. Actually arsenic crystallizes in the rhombohedral hexagonal type, space-group  $D_3^5d$ , in which each atom has three close neighbours at a distance of 2.51 Å., the remaining distances being considerably greater. Germanium in Group IV. crystallizes in the tetrahedral diamond type of structure, in which each atom has four neighbours, in agreement with the above rules, the interatomic distance being 2.44 Å., which lies between those of selenium and arsenic.

In the case of gallium (Group III.), if the above rules be correct, the structure should be such that each atom is surrounded by  $8-3=5$  neighbours, which at first sight appears improbable. In actual fact, however, the structure deduced by Jaegar, Terpstra, and Westenbrink\* is precisely that which is required. Gallium crystallizes with di-tetragonal bi-pyramidal symmetry, and the structure deduced by X-ray measurements has space-group  $D_2^1h$ , and is a curious double-layer structure in which each atom is in close contact with one other in its own layer, and with four others in the next layer, the interatomic distances being 2.56 Å. If the atoms are assumed to be spherical (which is, of course, a pure assumption) the double layers are not in contact with one another, but would be so if the distance between the double layers were reduced by 0.14 Å. If this structure be correct, it is of the greatest interest, since the tendency for the atom to surround itself by (8-N) neighbours is still clear, whilst it can also be seen from the figure that the structure is beginning to resemble a much distorted close-packed arrangement. In a private communication, Professor Bragg has kindly told the present author that, while the structure deduced by Jaegar, Terpstra, and Westenbrink may well be correct, the evidence is not as completely conclusive as in the case

\* Jaegar, Terpstra, and Westenbrink, *Proc. Akad. Amsterdam*, xxix. p. 1193 (1926).

of the structures in Groups IV. to VI. It will be noted that the closest distance of approach in gallium is the same as that in copper ( $2.56 \text{ \AA}$ ). This is in contrast to the second and third long periods, in which the interatomic distances in the Group III. metals indium and thallium are considerably greater than those in the corresponding Group I. elements silver and gold (see p. 75).

Turning now to zinc, the structure is one of close-packed prolate spheroids, each atom being surrounded by six others in its own layer at a distance of  $2.67 \text{ \AA}$ , and by six



The figure shows one of the double layers in the structure deduced for gallium by Jaeger, Terpstra, and Westenbrink. The atoms in one layer are shaded, and those in the next are left white. Four atoms in one layer form a trapezium, in the centre of which fits the atom of the adjacent layer, whilst in its own layer each atom is in close contact with one other at a distance equal to that which separates it from the four in the adjacent layer. The next double layer has an identical structure except that it is turned through  $90^\circ$ . The interatomic distances between the double layers are greater than the closest distances of approach within the double layer, so that, if spherical atoms be assumed, the double layers are separated by gaps.

others (three in the layer above, and three in that below) at a distance of  $2.92 \text{ \AA}$ . In sections 4-5 we shall discuss the question as to how far the presence of six neighbours

in zinc and of five in gallium is a real continuation of the (8-N) process which is so clear in the later groups. Finally, in copper the structure is one of simple close-packed spheres.

(b) *The Second Long Period.*

In this period the crystal structure of iodine has been determined, and the whole process from iodine to silver can be examined.

In Group VII., iodine, the structure deduced by Harris, Mack, and Blake \* shows the unit cell to possess orthorhombic bi-pyramidal symmetry, space-group  $V_8^{16}$  case  $f$ , the atoms being arranged in pairs, which the above authors took to be  $I_2$  molecules, the closest distance of approach being  $2.70 \text{ \AA}$ . Each atom, therefore, has one neighbour in accordance with the general principle.

In Groups VI. and V. tellurium and antimony crystallize with the same structures as selenium and arsenic respectively, the atoms having two neighbours in Group VI. and three in Group V. The closest distances of approach are  $2.87 \text{ \AA}$ . for both tellurium and antimony.

In Group IV. grey tin has the tetrahedral structure, with four neighbours at a distance of  $2.80 \text{ \AA}$ . In this period, however, the tendency to form the pure (8-N) type of structure has diminished, and the tetrahedral form is accompanied by another modification, white tin, in which each atom is still surrounded by four others, but the distance is considerably greater,  $3.07 \text{ \AA}$ ., as compared with  $2.80 \text{ \AA}$ . in the grey modification. The tetrahedral arrangement is also much distorted, and besides the four near neighbours there are two others at a slightly greater distance,  $3.16 \text{ \AA}$ .

The next metal, indium, possesses a very curious and interesting structure which is face-centred tetragonal, but the axial ratio is only 1.06, so that it is only a very slightly distorted form of the close-packed face-centred cubic arrangement. Each neighbour has four neighbours at a distance of  $3.24 \text{ \AA}$ ., and eight others at  $3.33 \text{ \AA}$ ., so that the structure is very nearly that of close-packed spheres, the distances being very much greater than in grey tin.

\* Harris, Mack and Blake, J. Amer. Chem. Soc. 1. p. 1583 (1928).

† Actually it is a possible close packing of spheroids with axes in the ratio 1.06:1.

In this period, therefore, the tendency to form an (8-N) structure has disappeared in Group III., and is replaced by the formation of a close-packed structure.

Cadmium and silver crystallize with the same structures as zinc and copper, and we shall discuss later the meaning of the six grouping in cadmium. The interatomic distance in silver is  $2.88 \text{ \AA}$ ., and is thus much less than in indium.

(c) *The Third Long Period.*

Here the tendency to form the pure (8-N) kind of structure has diminished so greatly that it is found only for bismuth, which has the same structure as arsenic and antimony, each atom being surrounded by three others at a distance of  $3.10 \text{ \AA}$ . In this period the tendency to form close-packed structures is much greater, and thallium (Group III.) has the structure corresponding to the hexagonal close packing of spheres, and lead (Group IV) the face-centred cubic close packing of spheres, the interatomic distances being  $3.40 \text{ \AA}$ . (Tl) and  $3.48 \text{ \AA}$  (Pb), both of which are considerably greater than the closest distance of approach in bismuth ( $3.10 \text{ \AA}$ ).

Mercury, like the other Group II. elements, crystallizes so that each atom is surrounded by  $8-3=6$  others, but structure is here simple rhombohedral instead of that of the close-packed prolate spheroids characteristic of zinc and cadmium. Gold resembles copper and silver, and has the face-centred cubic close-packed structure, the closest distance of approach being  $2.88 \text{ \AA}$ , which is much less than that in thallium.

From the above description it can be seen how all these apparently complex and different structures can be regarded as the outcome of two simple opposing tendencies. There is first the tendency to form structures in which each atom is surrounded by (8-N) others, and this diminishes as we pass from the first to the third long period. There is, secondly, the tendency to form close-packed structures, which diminishes as we proceed from Group I. to Group VIII., and increases as we pass from the first to the third long period.

In the remaining sections it is proposed to discuss the theoretical interpretations of these general principles, and later to compare the conclusions which are drawn with those of J. D. Bernal and other previous investigators.

#### 4. The Covalent, Molecular and Metallic Linkages.

For Groups IV. to VII. the most obvious explanation of the (8-N) rule described above is that, just as in the covalent compounds of chemistry an atom of Group N immediately preceding an inert gas completes its octet of electrons by sharing one electron with each of (8-N) other atoms, so in the crystal of the elements the octet is completed by the atom taking (8-N) neighbours and sharing one electron with each. In this way the presence of one, two, three, and four neighbours to each atom in the crystals of the elements of Groups VII., VI., V., and IV. respectively is readily accounted for. Reference to the literature shows that in the original pioneer work of A. J. Bradley \* this explanation was already realized. for this author states†: "... in the normal crystalline forms of ... germanium, grey tin, arsenic, antimony, bismuth, selenium, and tellurium, electron sharing takes place until the outer shell of each atom has its full quota of electrons. In this way each atom of these elements is in close contact with as many neighbours as it has negative valencies."

In Group IV. this conception accounts for the linkages throughout the crystal, since the tetrahedral arrangement throughout space enables the whole crystal to be bound together. But in the remaining groups this is not the case, and, while it seems clear that each atom is completing its octet by sharing with one, two, or three others, some additional forces must be postulated in order to account for the complete structure, and it seems probable that these are of a *molecular* nature. This suggestion is not in any way an *ad hoc* assumption, for it seems to be perfectly clear that in the case of iodine the pairs of atoms are  $I_2$  molecules, and since it is a fact that these are held together in the solid crystal, it does not seem unreasonable to assume that similar forces are present in the case of Group VI. where there exist chains of atoms each with two neighbours, and Group V., where there are layers of atoms which give each atom three neighbours. The alternative view of J. D. Bernal, that the additional forces are metallic in nature, will be discussed later.

It is when we come to deal with the retention of the (8-N) rule in Groups III. and II. that difficulty arises, for

\* A. J. Bradley, *Phil. Mag.* xlviii. p. 477 (1924).

† *Ibid.* p. 496.

here it seems clear that the presence of simple covalent linkages will not account for the fact that each atom has five or six neighbours. Since each gallium atom has only three valency electrons, it cannot share one electron with each of five others, because there are not enough electrons available. The position is rather like that met with in connexion with the hydrides of the elements of the first short period, where we can readily account for  $\text{OH}_2$ ,  $\text{NH}_3$ , and  $\text{CH}_4$ , but where the hydride of boron,  $\text{B}_2\text{H}_6$ , presents difficulty. It is suggested that we have here the real underlying cause of the formation of the *metallic linkage* in the crystals of the solid elements. When there are not sufficient valency electrons per atom to enable the octet to be completed by each atom sharing one electron with each of its neighbours, the need arises for a new kind of bond, in which an electron can serve for more than two atoms, and so the metallic linkage comes into being, and is apparently favoured by three structures, the body-centred cubic, the face-centred cubic, and the hexagonal close-packed structures.

It is here that the structure of gallium is so particularly interesting, if the work of Jaeger, Terpstra, and Westenberg be correct. For, in spite of the fact that the full number of electrons necessary to form an octet by simple covalent linkages is no longer available, the tendency to form the (8-N) type of structure is still found, and at the same time the tendency to form a distorted close-packed structure is so very apparent. It seems, however, to be almost certain that most of the linkages are covalent, because (1) the metal shows marked diamagnetism, contraction and fall in resistance on melting, etc., just as with bismuth and antimony, and (2) the closest distance of approach in gallium does not show the marked increase which is found when we pass from the covalent linkage in grey tin (2.80 Å.) and bismuth (3.10 Å.) to the preceding close-packed metallic structures in indium (3.24 Å.) and lead (3.48 Å.). Further, as we have already indicated, the closest distances of approach in indium and thallium are much greater than in the preceding univalent metals silver and gold, whereas in the case of gallium and copper the distances are almost the same (see p. 69). But whether the remaining linkages in gallium are metallic, as suggested by J. D. Bernal\*, or molecular appears less certain. As

\* J. D. Bernal, *Trans. Faraday, Soc.* (1929).



we have already indicated (p. 68), the structure of gallium is not yet absolutely certain, so that discussion of this point is not carried further.

The structures of the Group II. elements will be considered separately in the next section. In the case of the Group I. B-elements, we find typical close packed-structures which clearly correspond to the purely metallic linkages. It is considered unwise to attempt to give anything in the way of a mechanical picture of this kind of binding, in view of the fact that the whole tendency of modern atomic theory is to avoid the precise mechanical pictures of the older dynamics. The essential points are that the metallic linkage comes into being when the number of valency electrons in the atom is insufficient to allow the (8-N) type of structure to be produced by simple covalency electron sharing, and that the characteristic of the linkage is that one electron can serve for more than two atoms. Alternative views are that of the electron lattice\* of Lindemann, in which the electrons are conceived of as vibrating about fixed centres, so that they may be said to be shared by the surrounding atoms. As shown by the present author, this conception is in many ways attractive†, but it is sometimes considered too static in nature, and the new theories of Bloch‡, in which the valency electrons are regarded as moving in a three-dimensional periodic field characteristic of the crystal as a whole, may perhaps be considered as an attempt to express our general idea in more precise terms.

From this point of view, therefore, the metallic bond is to be looked upon as of a homopolar nature, in which one electron may be associated with many atoms. In support of this conclusion we may note that the interatomic distances in copper, silver, and gold are of the same order as those of the covalent linkages in the same long period, the actual values being as follows :—

Copper ...	2.56 Å.	Covalent linkages Ga-Se ...	2.56 Å.-2.35 Å.
Silver ...	2.88 Å.	„ „ Sn-I .....	2.87 Å-2.70 Å.
Gold .....	2.88 Å.	„ „ Bi .....	3.10 Å.

\* It should be noted that an electron lattice may be considered either as an ionic structure of electrons and ions, or as a homopolar structure in which the electrons on the lattice are shared by the surrounding atoms.

† Hume-Rothery, *Phil. Mag.* iv. p. 1017 (1927).

‡ Bloch, *Z. Physik*, lii. p. 555 (1928-29).

It is not to be expected that these distances will be exactly equal, because an allowance must presumably be made for the degree of coordination, and also for the effect of atomic number upon the dimensions of the electronic orbits. It is, however, noteworthy that in the case of gallium, where the covalent bonds are accompanied by what is nearly a close-packed structure, the closest distance of approach is the same as in the case of the purely metallic copper in Group I.

It remains now to account for the sudden expansion of the interatomic distances in indium, thallium, and lead, to which we have assigned metallic structures, and it is just here that the theory of atomic structure gives the necessary support. According to the generally accepted theory, the building up of a group of eight electrons takes place in steps of 2, 2, and 4 electrons respectively. The outer electron groupings in atoms *in the free state* of the Group III. and Group IV. metals are thus (18) (2) (1) and (18) (2) (2) respectively, and the whole of the facts of chemistry indicate that the relative stability of the underlying (18) (2) group increases as we go down the periods. Thus in aluminium only trivalent salts are stable, whilst with thallium the univalent  $(18)(2)^+$  salts are stable, and the trivalent  $(18)^{+++}$  salts relatively unstable. It is, therefore, quite to be expected that in indium, thallium, lead and, possibly, also in white tin we have in the metal crystal only one free electron per atom in Group III. and two in Group IV., in which case the remaining atomic cores which are responsible for the repulsive forces will be larger than in the case of silver and gold, where the cores contain only the group of (18). But, on the other hand, it is just this group of (18) which remains in the covalent structures, so that the difference is at once accounted for. The fact that in indium the structure is not quite that of close-packed spheres is not in contradiction to this point of view, since there is no reason to suppose that a group of (18) (2) electrons will retain spherical symmetry in the crystal structure, even though it may do so in the free state.

### *5. The Structure of the Group II. Elements.*

We have already indicated that, although the Group II. elements obey the (8-N) rule, there is reason for thinking that the process is here different from that met with in

Groups IV. to VII. Bernal has suggested that in the B-Group elements we have purely metallic structures in Group I., purely homopolar structures in germanium and grey tin, and structures containing both metallic and homopolar bonds in most of the remaining elements. He also concludes that zinc and cadmium are not to be looked upon as possessing merely a distorted form of close-packed structure. At first it might be suggested that these are larger lattices in which the atoms in each layer are bound together by homopolar bonds, but if this be so, it is clear that the "homopolar bonds" must be different from the covalent bonds which we have suggested for Groups IV. to VII.\*, since there are not enough electrons present to form these. The alternative view which is suggested here is that both zinc and cadmium are true metals in which the atoms are held together solely by metallic linkages, but that only one electron per atom is free to form the metallic bond. The fact that we have close-packed spheroids instead of spheres is, then, the result of there being one electron above the (18) group attached to the positive ions, which are thus readily polarizable in the structure, and so no longer correspond to spheres. In support of this rather unexpected conclusion the following points may be noted :—

(1) In the A groups, when we pass from the univalent alkalis to the divalent alkaline earths, the melting-points rise, and the interatomic distances diminish. In the B groups the reverse is the case.

(2) The electrode potentials change in opposite directions in the A and B groups when passing from Group I. to Group II.

(3) The photoelectric threshold frequencies of the alkaline earths are much higher than those of the alkalis, whilst in the B sub-groups the threshold frequencies are much the same for Groups I. and II.

These, and other abnormalities, are explained if zinc and cadmium are only singly ionized in the metallic state, the ions being larger than those of the preceding univalent metal, and in the crystal structure much less symmetrical.

\* In Group IV. the "covalent linkages" of the present paper are identical with the "homopolar bonds" of Bernal. In the other groups Bernal's "homopolar bonds" are less clear.

The structure of mercury is quite abnormal, but the interatomic distances ( $2.99 \text{ \AA.}$ ) are greater than those of gold ( $2.88 \text{ \AA.}$ ), and here again it is suggested that the solid metal is univalent, giving one free electron per atom to form the metallic linkage.

#### 6. *The Question of Electrical Conductivity.*

The most obvious objection to the above suggestions is that if the elements in Groups IV. to VII., to which we have assigned covalent and molecular structures, are really of this nature, they should be non-conductors, since all the valency electrons are required for the covalent bonds. In this connexion it is interesting to note that for germanium and grey tin, which possess the tetrahedral structure, it has already been concluded by Kapitza\*, from work on the properties of metals in strong magnetic fields, that these metals (and also silicon) are really not normal metallic conductors at all, and this point of view was accepted by Bernal. It has, in fact, been suggested by Kapitza that if these metals could be obtained quite free from impurities they would, at any rate at low temperatures, be non-conductors, and that the actual conductivity observed is due to traces of impurities upsetting the regularity of the lattice, and so liberating some electrons, a process which is assisted by rise of temperature which increases the atomic vibrations. These metals have, in fact, very abnormal properties as regards the electrical conductivity. Thus silicon has a negative temperature coefficient of resistance up to a high temperature, at which polymorphic changes occur. Germanium shows the phenomenon of a minimum resistance at  $-116^{\circ} \text{C.}$ , and Bidwell† has concluded that the same may be true for the elements of Groups V. and VI., and also that silicon would attain a minimum resistance at a high temperature if it were not for the polymorphic change. The phenomenon of a minimum resistance is, of course, quite in agreement with the above view, since on raising the temperature from the absolute zero we may expect the resistance first to diminish owing to the gradual liberation of electrons; but later the increasing amplitude of the atomic vibrations will interfere with the motion of the electrons in the

\* Kapitza, Proc. Roy. Soc. cxiii. p. 292 (1929).

† Bidwell, Physical Review, xix. p. 447 (1922).

ordinary way. From this point of view, since the covalent linkage becomes less stable as we pass from the first to the third long period, we should expect the minimum resistance to occur at a lower temperature, which is in agreement with the fact. The metals silicon, germanium, and grey tin may be said to form the critical test in this connexion. If once it be admitted that these are purely covalent (Bernal "purely homopolar"), in spite of their conductivity and other metallic properties, then the present theory cannot be attacked on this ground, whilst it is, of course, well known that other electrical properties, such as the Hall Effect, thermoelectric power, etc., are very abnormal for these elements, and for those of Groups V. and VI.

Once, however, we get the purely metallic bond, conductivity is obviously possible, since the electrons are no longer required to be bound to two particular atoms. It may be noted that supraconductivity is shown by none of the metals to which we have assigned covalent and molecular structures: it is white, and not grey, tin which is supraconducting.

### *7. The Relation of the Present Work to that of Bernal.*

We have already discussed the suggestions of Bernal with reference to the structure of the Group II. elements, and we may now refer to other points in the most stimulating paper by this author. The chief point made by Bernal in connexion with the structure of the B-group elements was that we have here to deal with both homopolar and metallic bonds in the same crystal. In the structure of selenium, for example, the atoms are regarded as bound by homopolar bonds into the zigzag chains (each having two neighbours), and the chains themselves are regarded as held together by metallic bonds. A similar suggestion was made for Group V. It is suggested that the present view of covalent and molecular linkages is more probably correct for the following reasons:—

(1) If the "homopolar" bonds are the covalent bonds which have been suggested here, it seems impossible to provide the free electrons necessary to form the metallic linkage. Each selenium atom has completed its octet by

sharing with two others, and if it is to give further free electrons to provide a metallic linkage, the octet will be broken up. This might be overcome by assuming that the metallic linkage does not involve the conductivity electrons at all, but is the same as what has been called the "molecular linkage" in the present paper; but the properties as regards plasticity, etc., are not the same, and the evidence that the conductivity electrons are concerned in the metallic bond appears considerable.

(2) Alternatively, if it be assumed that the "homopolar bond" is not the covalent bond described above, we are at a loss to account for the (8-N) rule, which appears such a characteristic feature.

It is suggested, therefore, that the present view, which regards the metallic bond as never appearing in Groups V. and VI., and only in the second and third long periods in Group IV., is more probably correct, as well as the conclusions that zinc, cadmium, mercury, and indium are true metals, but with distorted ions. Apart from these points, Bernal's arguments concerning diamagnetism, etc., are fully accepted as indicating the presence of covalent bonds, and no claim is made that the suggestion of covalent bonds in these metals is a novel one, and, as we have already indicated, this suggestion was, in part at any rate, anticipated in the original work of Bradley.

### 8. *Conclusion.*

It is hoped that the above paper will assist in giving a general indication of the relations between the crystal structures of the B-group Elements, and the Periodic Table and Atomic structures. It must be emphasized, however, that we have dealt here solely with the pure elements, and that the principles described need not necessarily always apply in alloys. When, for example, we have suggested that zinc, cadmium, and indium are univalent in the pure metal, there is no suggestion that this necessarily applies in alloys. It is hoped to deal later with the regularities underlying the formation of solid solutions and intermetallic compounds, and particularly with the question as to the conditions under which an atom preserves a "constant radius."

## 9. Acknowledgments.

The author must express his thanks to Professor F. Soddy, F.R.S., for giving laboratory accommodation which enables him to work in Oxford. and to Professor W. L. Bragg, F.R.S., Dr. A. J. Bradley, and Dr. T. V. Barker for help and criticism. He must also thank the Armourers' and Brasiers' Company for election to a Research Fellowship.

The Old Chemistry Department,  
The Museum, Oxford.

---

## IX. *On the Distribution of Space Charge between a Plane Hot Cathode and a Parallel Anode.* By HRISHIKESH RAKSHIT, M.Sc., Khaira Research Scholar in Physics\*.

### *Introduction.*

WHEN a metal is heated, electrons are emitted from it according to Richardson's law. The emitted electrons are mostly concentrated near the surface of the hot metal, and thus an atmosphere of electrons is set up near it. The negative space charge thus created repels the electrons subsequently emitted and presses the slowly moving ones into the hot metal. After some time an equilibrium condition is reached when the number of electrons emitted in unit time is the same as the number pressed back into the hot metal by the space charge. In such an equilibrium condition the distribution of potential near the hot surface when it is plane and infinitely extended has been worked out by Richardson<sup>†</sup> and Laue<sup>‡</sup>. Similar calculations have been made by Epstein<sup>§</sup>, Fry<sup>||</sup>, and Adams<sup>¶</sup> for the case when the potential distribution is altered, due to the presence of a parallel positively charged plate of infinite extent near the hot surface. The corresponding problem of determining the distribution of electron density near a heated surface has been solved only in the case of a plate of infinite extent

\* Communicated by Prof. S. K. Mitra, D.Sc.

† Phil. Trans. A, cci. p. 516 (1903).

‡ *Jahrb. d. Radioakt. u. Elektronik*, xv. p. 205 (1918).

§ *Ber. d. Deut. Phys. Ges.* xxi. p. 85 (1919).

|| Phys. Rev., April 1921.

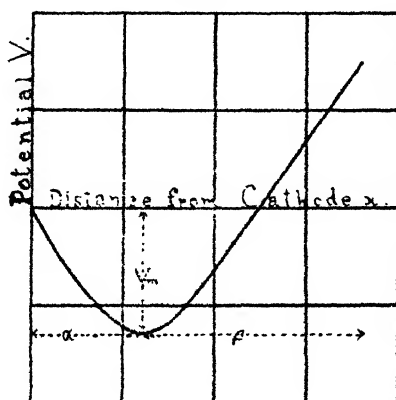
¶ Not published; cf. Langmuir, Phys. Rev., April 1923.

without any external field\*. The case of altered distribution of electron density when a current flows between the cathode and the anode, though often met with in practice, has not received adequate attention from workers in this field. It is proposed in this paper to determine this altered distribution of electron density in the simple case of two parallel infinite plates, and to give quantitative results for a few typical cases.

### Mathematical Discussion.

In any case of thermionic emission, when the current between the cathode and anode is less than the saturation current, there is a region of negative potential gradient near the cathode. The general nature of potential distribution is

Fig. 1



shown in fig. 1. The potential becomes more and more negative as the distance from the cathode increases; it attains a certain minimum value  $V_m$  and then increases, being ultimately positive at greater distances from the cathode. With Fry let us denote the region between the cathode and the surface of minimum potential as the region  $\alpha$ , and the rest of the region to the anode as region  $\beta$ .

Let  $dN$  be the number of electrons emitted per unit time per unit area, having emission velocities normal to the cathode between the limits  $v_0$  and  $v_0 + dv_0$ . Then, in accordance with Maxwell's law,

$$dN = N \cdot \frac{mv_0}{kT} \cdot e^{-\frac{mv_0^2}{2kT}} \cdot dv_0,$$

\* Langmuir, Phys. Rev., April 1923.



where  $N$  is the total number of electrons emitted per unit time per unit area from the cathode at temperature  $T^\circ \text{K}$ . The emitted electrons have velocities ranging from zero to infinity, and it is therefore evident that the slowly moving ones will go only a certain distance from the cathode and then be stopped and turned back to the cathode by the retarding field in region  $\alpha$ . Thus in this region there are two groups of electrons, those going away from the cathode and those returning back to the cathode; but in region  $\beta$  the electrons are only moving away from the cathode. Let us consider a point in region  $\alpha$  whose distance from the cathode is  $x$ . If  $V$  is the potential of this point (with respect to the cathode), the electrons that are emitted with velocities, normal to the cathode, lower than  $\sqrt{\frac{2Ve}{m}}$  do not reach  $x$ ; those with emission velocities lying between  $\sqrt{\frac{2Ve}{m}}$  and  $\sqrt{\frac{2V_m e}{m}}$  reach and pass  $x$ , but are stopped before reaching the surface of minimum potential and turned back by the retarding field; the electrons with emission velocities higher than  $\sqrt{\frac{2V_m e}{m}}$  pass  $x$ , but do not return after passing,  $V_m$  being the minimum potential between cathode and anode. If, now,  $v$  is the actual velocity of the electrons  $dN$ , the contribution of these to the space-charge density  $\rho$  is given by

$$d\rho = \frac{dN}{v} \cdot e.$$

This takes into account only the absolute value of  $v$ , and not its direction. Thus each of the two equally dense streams of electrons in region  $\alpha$ , with emission velocities lying between  $\sqrt{\frac{2Ve}{m}}$  and  $\sqrt{\frac{2V_m e}{m}}$ , but moving in opposite directions, contributes to the space charge  $\rho_\alpha$ , which can thus be expressed in the form

$$\begin{aligned} \rho_\alpha = 2e \int_{\sqrt{\frac{2Ve}{m}}}^{\sqrt{\frac{2V_m e}{m}}} \frac{N}{v} \cdot \frac{mv_0}{kT} \cdot e^{-\frac{mv_0^2}{2kT}} \cdot dv_0 \\ + e \int_{\sqrt{\frac{2V_m e}{m}}}^{\infty} \frac{N}{v} \cdot \frac{mv_0}{kT} \cdot e^{-\frac{mv_0^2}{2kT}} \cdot dv_0, \quad \dots \quad (1) \end{aligned}$$

where  $v$  is the velocity of an electron at a point whose potential with respect to the cathode is  $V$ , and  $v_0$  is the emission velocity of this electron.

Let us now put  $A$  for  $Nem/kT$ , which is equal to  $i_0m/kT$ ,  $i_0$  being the saturation current per sq. cm. of the cathode, and  $\theta$  for  $\frac{m}{2kT}$ ; then eqn. (1) becomes

$$\rho_\alpha = 2A \int_{\sqrt{\frac{2Ve}{m}}}^{\infty} \frac{v_0 \cdot e^{-\theta v_0^2}}{v} \cdot dv_0 - A \int_{\sqrt{\frac{2V_m e}{m}}}^{\infty} \frac{v_0 \cdot e^{-\theta v_0^2}}{v} \cdot dv_0. \quad (2)$$

Now

$$v^2 = v_0^2 + \frac{2Ve}{m},$$

the numerical value of  $e$  being taken ;

$$\therefore v dv = v_0 dv_0. \quad \dots \dots (3)$$

Substituting (3) in (2), changing the variable, and remembering that, in region  $\alpha$ ,  $V$  is negative, we get

$$\rho_\alpha = 2A \cdot e^{\frac{2\theta Ve}{m}} \int_0^{\infty} e^{-\theta v^2} dv - A \cdot e^{\frac{2\theta V_e}{m}} \int_{\sqrt{\frac{2e}{m}(V_m+V)}}^{\infty} \frac{e^{-\theta v^2}}{v} dv,$$

where the numerical value of  $V_m$  is to be taken.

Putting  $\sqrt{\theta} \cdot v = z$ , this further reduces to the form

$$\rho_\alpha = \frac{2A}{\sqrt{\theta}} \cdot e^{\frac{2\theta Ve}{m}} \int_0^{\infty} e^{-z^2} dz - \frac{A}{\sqrt{\theta}} \cdot e^{\frac{2\theta V_e}{m}} \int_{\sqrt{\frac{2e}{m}(V_m+V)}}^{\infty} \frac{e^{-z^2}}{z} dz. \quad (4)$$

In region  $\beta$  only those electrons are present which have emission velocities greater than or at least equal to  $\sqrt{\frac{2V_m e}{m}}$ . Hence

$$\rho_\beta = e \int_{\sqrt{\frac{2V_m e}{m}}}^{\infty} \frac{N}{v} \cdot \frac{mv_0}{kT} \cdot e^{-\frac{mv_0^2}{2kT}} \cdot dv_0. \quad \dots (5)$$

Proceeding as above, this reduces to the form

$$\rho_\beta = \frac{A}{\sqrt{\theta}} \cdot e^{\frac{2\theta V_e}{m}} \int_{\sqrt{\frac{2e}{m}(V_m+V)}}^{\infty} \frac{e^{-z^2}}{z} dz. \quad \dots (6)$$

The integrals involved in equations (4) and (6) are of well-known type, and can be evaluated by means of tables of Probability Integrals when the limits are known. To determine the limits it is necessary to find the potential distribution between the plates.

Suppose that the cathode is a large flat surface at a known temperature and the anode is a parallel surface at a certain distance from the cathode. With this position of the plates, when a steady current flows between the two, the potential distribution can be found, after some laborious calculations, according to the method indicated by Langmuir\*. This will give the values of  $V_m$  and  $V$ , the latter being different for different distances from the cathode. The next step is to find the distance  $x_m$  of the surface of minimum potential from the cathode, by which we can know whether any chosen point is in region  $\alpha$  or  $\beta$ . To find the density of space charge at this point, formula (4) or (6) is applied, according as the case may be.

#### *Numerical Results for a Typical Case.*

Suppose that the cathode is a flat tungsten surface at temperature  $2400^\circ \text{K}$ ., and the anode is a parallel surface at a distance of 0.5 cm. With Fry we assume that the saturation current  $i_0$  per sq. cm. of the cathode is 0.16 ampere at  $2400^\circ \text{K}$ . Let us consider the case in which the current  $i$  between the plates is 0.00016 ampere per sq. cm. of the cathode. Proceeding, as indicated by Langmuir, we get, for this case

$$x_m = 0.074 \text{ cm.},$$

$$V_m = -1.4292 \text{ volts.}$$

The distribution of potential is also worked out for this case. Knowing the potential  $V$  at any point, the value of

$$z = \sqrt{\frac{2\theta e}{m}(V_m + V)} = \sqrt{4.833(1.4292 + V)}$$

is found out, and from the tables of probability integrals the value of  $\int_z^\infty e^{-z^2} dz$  is obtained by interpolation. When  $z$  is large, the value of  $\int_z^\infty e^{-z^2} dz$  is obtained from the equation

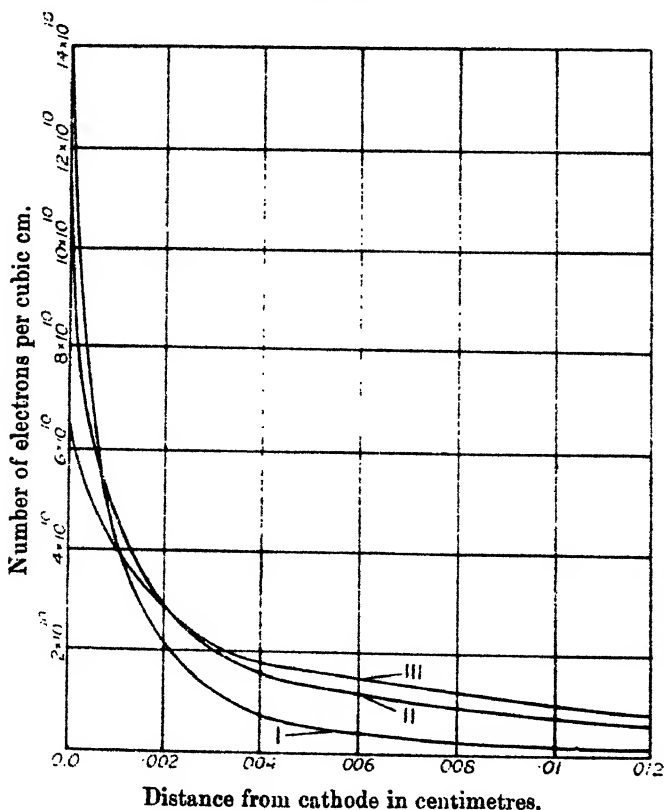
$$\int_z^\infty e^{-z^2} dz = \frac{e^{-z^2}}{2z} \left[ 1 - \frac{1}{2z^2} + \frac{1.3}{(2z^2)^2} - \dots \right].$$

\* Langmuir, Phys. Rev., April 1923.

Next the value of  $\epsilon^{\frac{20e}{m} \times V} = \epsilon^{4.833 \times V}$  is found, and the density  $\rho$  of space charge at the point under consideration is obtained from formula (4) or (6), according as  $x < \text{or} > x_m$ . The distribution of electron density for different values of the current  $i$  is given in the following tables, together with the distribution when there is no external field.

Curves in fig. 2 show the distribution of electron density

Fig. 2.



between the cathode and the anode for different values of thermionic current between the plates. It will be seen that immediately near the surface of the cathode the electron density diminishes as the current increases, but at greater distances it increases with the current. Also, the steepness of the curves immediately near the cathode diminishes with increase of current, but at greater distances the curves are very nearly parallel to the axis of  $x$  (distance from the cathode) for all values of the current—the effect of increasing

the current being merely to raise this portion of the curve higher.

In fig. 2, curve I. shows the distribution when there is no external field, *i.e.*, when the current is zero; curve II. shows the distribution when the current is 0.08 ampere per sq. cm. of the cathode, *i.e.*, half the saturation current; and curve III. when the current is saturated. The curves for the cases when the current is 0.00016, 0.0016, and 0.016 respectively have not been drawn, for they follow curve I. very closely.

### CASE I.

$i = 0$ . (No external field.)

$x$ (cm.).	$V$ (volts).	$\rho$ (e. s. u.).	Number of electrons/c.e.
0	0	62.938	$13.18 \times 10^{10}$
0.0001	-0.03026	54.388	$11.39 \times 10^{10}$
0.001	-0.23330	20.380	$4.27 \times 10^{10}$
0.003	-0.49060	5.878	$1.23 \times 10^{10}$
0.005	-0.64790	2.747	$5.75 \times 10^9$
0.007	-0.76190	1.585	$3.32 \times 10^9$
0.01	-0.88920	0.856	$1.79 \times 10^9$
0.1	-1.79600	0.011	$2.24 \times 10^7$
0.2	-2.08100	0.003	$5.67 \times 10^6$

### CASE II.

$i = 0.08$  amp. per sq. cm.;  $x_m = 0.0018347$  cm.  
 $V_m = -0.1434$  volt.

$x$ (cm.).	$V$ (volts).	$\rho$ (e. s. u.).	Number of electrons/c.e.
0.	0	55.405	$11.605 \times 10^{10}$
0.0001	-0.01872	49.670	$10.400 \times 10^{10}$
0.001	-0.12663	22.400	$4.691 \times 10^{10}$
0.003	-0.10860	10.462	$2.192 \times 10^{10}$
0.005	+0.07050	6.651	$1.393 \times 10^{10}$
0.007	+0.35230	4.952	$1.037 \times 10^{10}$
0.01	+0.91177	3.630	$7.603 \times 10^9$
0.1	+42.82900	0.691	$1.447 \times 10^9$
0.2	+113.78400	0.505	$1.058 \times 10^9$

Tables showing the electron density and the potential at various distances from the cathode are given for curves I., II., and III.

### CASE III.

$i = 0.16$  amp. per sq. cm. ;  $x_m = 0$  cm. ;  $V_m = 0$  volt.

$x$ (cm.).	$V$ (volts).	$\rho$ (e. s. u.).	Number of electrons/c.c.
0	0	31.464	$6.590 \times 10^{10}$
0.0001	+0.00058	29.646	$6.210 \times 10^{10}$
0.001	+0.05028	19.487	$4.083 \times 10^{10}$
0.003	+0.35520	11.193	$2.344 \times 10^{10}$
0.005	+0.83480	8.022	$1.681 \times 10^{10}$
0.007	+1.43720	6.348	$1.329 \times 10^{10}$
0.01	+2.51624	4.907	$1.028 \times 10^{10}$
0.1	+71.56550	1.231	$2.579 \times 10^9$

### *Conclusion.*

The distribution of electron density between a plane-heated cathode and a parallel anode has been calculated when a thermionic current flows between the two. Numerical results for a few typical cases are given. It is found that when a current flows the electron density diminishes immediately near the hot surface, but increases at a greater distance from it. Curves showing the variation of electron density are given for various values of electronic current flowing between the cathode and the anode.

My best thanks are due to Prof. S. K. Mitra, D.Sc., for having suggested the problem to me and for taking keen and helpful interest during the progress of the work.

Wireless Laboratory,  
University College of Science,  
92 Upper Circular Road,  
Calcutta, India.

May 21, 1929.

X. *On the Generation of Pulses in Vibrating Strings.* By D. BANERJĪ, M.Sc., Lecturer in Physics, Calcutta University, and R. GANGULĪ, Lecturer in Physics, Serampore College, Bengal\*.

[Plate I.]

*Introduction.*

THE vibrations of long strings, stretched between their ends and excited by vibrations of shorter segments of their own, present many acoustical peculiarities which do not appear to have received any attention from workers in this field.

The experiment is suggested by an art of finger-playing (known as "Abataran Ash") on the strings of the Indian musical instrument "Vina" †. This is a sudden drop of the tone-frequency from a high to a low value by a brisk movement of the finger-tip from one position to another, which increases the vibrating length of the string. The other form of "Ash," namely, the "Arohan Ash," is the converse of "Abataran Ash" just described, inasmuch as here the length of the vibrating string is suddenly diminished instead of increased, as in the former case. The latter form of "Ash" is easier to comprehend from the known acoustical principles of vibrating strings, but the effect of the former cannot be estimated *a priori* without a detailed examination of the mode of vibration of the string immediately after release of the finger-tip. Although such an art is recognized by Indian musicians to be unique in its musical effect, and is, therefore, very often resorted to for the adornment of instrumental music, yet no scientific study has been made of the exact nature of the transition of the mode of vibration from one of higher frequency to another of lower frequency or *vice versa*. It is proposed to give in the following lines the results of an investigation to bring out the characteristics of the vibrations of a stretched string clamped at different points on its length by a mechanical device which can suddenly be released after excitation of one of the segments of division by gentle plucking. Although such an arrangement differs in details from an actual "Vina," inasmuch as the points of clamping are not those where the frets are actually placed, yet the sudden release of the clamp, while one segment of the string is

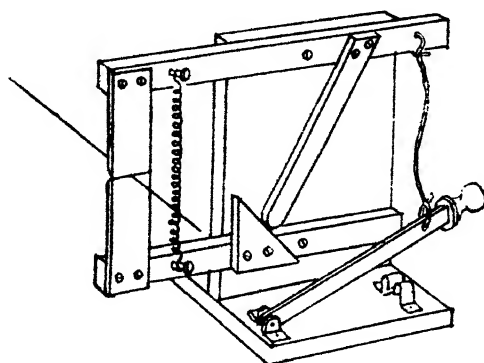
\* Communicated by Prof. S. K. Mitra, D.Sc.

† For description of "Vina," see an article by C. V. Raman, Proc. Ind. Assoc. Cult. of Science, vii. pp. 29-33 (1921).

executing its natural vibration, is a sufficient imitation of the process of "Abataran Ash," previously described. It is also expected that the investigation will throw light on the main issue of the problem, namely, how the form of the string-vibration changes suddenly from one of higher frequency to another of lower frequency.

*Experiment.*

With the above object in view, a steel wire was tied at one end to a rigid support, and from the other end, which passed over a pulley, weights were hung to put it under proper tension. A scissor-like clamp, specially designed for the purpose, and shown in the adjoining figure, could be adjusted



to clamp the string in any desired position, and by the application of a lever-hammer attached to its framework the blades of the clamp could be suddenly separated without disturbing the string. The form of vibration of one segment of the string when it is plucked with the finger-tips over a finite length, so as to elicit only the fundamental of the segment, together with the complex tone on transition to the lower frequency of the complete length just after release of the clamp, can thus both be depicted photographically on a sensitive paper moving uniformly at the focus of a point of the segment of the string.

*Results and Discussion.*

In fig. 1 (Pl. I.) the clamp was at a point  $> 1/2$ .

" 2	"	"	" the mid-point.
" 3 (a) & (b)	"	"	between $1/2$ and $1/3$ .
" 4	"	"	at $1/3$ .
" 5	"	"	" $1/5$ .
" 6	"	"	" $1/7$ .



The main results of observations are stated below :—

(a) When the clamp is applied so as to divide the string into two segments in the ratios of  $1 : 1$ ,  $1 : 2$ ,  $1 : 3$ , and so on, and the shorter segment is made to vibrate by plucking over a finite length, the unexcited part takes up a less intense vibration from the excited part, and is divided into segments of lengths equal to that of the excited part. Care is taken to pluck the string gently over a finite length to elicit only the gravest component of the Fourier Series. This phenomenon of leakage of oscillation, which is due to the effect of resonance, is particularly noticeable when the clamped point is exactly in the position of nodal division of the string, and is completely minimized on shifting the clamp on either side of this position. The clamp takes up the oscillation of the shorter segment and communicates it to the other segment of commensurable period.

(b) The time-displacement curve of the complete length immediately after the clamp is removed presents peculiarities in that, whenever the excited shorter segment is an aliquot fraction of its total length, its total amplitude is equal to the amplitude of the exciting oscillation. There is one important exception, namely, when the position of the clamp is near  $1/7$  the amplitude is increased. This anomalous increase of amplitude near  $1/7$  may have some bearing with similarly observed phenomena in struck strings, of which no satisfactory explanation has been offered. The time-displacement curves, especially at smaller ratios of division, make it clear that the original exciting vibration tends to persist in the final motion, and seems, though slightly modified by the presence of very weak upper partials, to repeat after intervals of rest-positions of the string equal to its fundamental period.

(c) The transition from the original oscillation of higher frequency to the graver fundamental of the string is as sudden as the release of the clamp, and may take effect at any phase of the former. The number of partials excited by the transition appears to be limited by the fundamental of the shorter segment. The relative intensities of the partials which are sufficiently strong at  $1/2$  and  $1/3$  do not seem to be altered appreciably by slightly shifting the position of the clamp on either side of the nodal points. If the total energy content of the string before the release of the clamp is distributed without loss over the partials generated by the release of the clamp, then, according to a well-known energy principle, the relation between the

amplitudes of the vibrations before and after the release of the clamp will be as below :

$$\frac{\Sigma A_i^2}{a^2} = \frac{m}{M} \frac{\Sigma T_i^2}{t^2}$$

(where  $m$  and  $M$  are the respective masses of the shorter segment and of the whole string,  $t$  and  $T_i$  the respective periods of the shorter segment and of the whole string vibrating in its  $i$ th harmonic component, and  $a$  and  $A_i$  the corresponding amplitudes). Such a relation, however, fails to correspond with facts, and the calculated and observed values of the final amplitudes differ considerably for all cases. The amplitude of the original simple vibration is nucleated in pulses of equal amplitude repeating at intervals of the period of the fundamental of the total length of the string. The effect can be explained if we remember that the clamp, in communicating the vibration from one side to the other, is itself thrown in a state of vibration. The result of the sudden removal of the clamp is on the one hand the disappearance of a certain amount of energy which was in the clamp, and on the other hand the cessation of communication of energy from the excited to the unexcited segment. The consequence is that the displaced form of the shorter segment at the moment of release of the clamp is propagated along the length of the string in the form of a pulse which travels to and fro between the two ends of the string. This can easily be verified by the measurements of the distances between the pulses in the plate.

This probably explains the use of the "Abataran Ash" by musicians in India. The sudden change of length of the vibrating string produces pulses which bring in a peculiar richness in the tonal quality which is not otherwise possible.

### *Summary and Conclusion.*

Experiments are made to imitate the common practice (technically known as "Abataran Ash") of exciting the string of the Indian musical instrument "Vina." This consists of a sudden drop of the tone-frequency from a higher to a lower value by suddenly removing the finger tip so as to increase the length of the vibrating string. A string stretched between its ends is clamped at points of aliquot division of the string, and the shorter segment is excited by plucking. On releasing the clamp suddenly the original high-frequency oscillation appears to be nucleated in pulses which move to and fro between the ends of the

string. It seems, therefore, that "Abataran Ash" is only a technique of exciting pulses in the vibrating string of the "Vina." The pulses, which are well known to be rich in harmonics, help to produce the peculiar musical effect.

In conclusion, we desire to express our best thanks to Prof. S. K. Mitra for his kind interest in our work and much useful help.

University College of Science,  
92 Upper Circular Road, Calcutta, India.  
29th May, 1929.

XI. *The Mutual Action of a Pair of Rational Current Elements.* By G. F. C. SEARLE, Sc.D., F.R.S., University Lecturer in Experimental Physics, Cambridge\*.

THE "rational current element" devised by Oliver Heaviside consists of an elementary line of length  $ds$  conveying an electric current  $i$ , the current flowing out at the positive end of the element into an infinite medium, as from a point-source, and flowing in at the negative end. The current density in the medium is that due to the two radial currents. Two rational elements,  $i_1 ds_1$  and  $i_2 ds_2$ , in any given positions will give rise to a magnetic field, and  $T$ , the magnetic energy of the field, will be a homogeneous quadratic function of  $i_1$  and  $i_2$ . Heaviside calculated the part of  $T$  which depends upon the product  $i_1 i_2$ , and has termed it the "mutual action" of the two elements. He stated the results in his 'Electrical Papers,' vol. ii. pp. 501, 502, but he did not give a proof. An indication of the method is given in vol. ii. p. 506. A recent inquiry leads me to give an elementary account of the calculation.

If  $H$  be the magnetic force and  $\mu$  the magnetic permeability, we have

$$T = \frac{1}{8\pi} \iiint \mu H^2 dx dy dz, \quad \dots \quad (1)$$

where the integration extends through all space. We can replace (1) by

$$T = \frac{1}{2} \iiint \text{SAC} dx dy dz, \quad \dots \quad (2)$$

where  $\text{SAC}$  is the scalar product of the vector potential  $\mathbf{A}$  and the current density  $\mathbf{C}$ , and the integration again extends through all space. We have  $\text{SAC} = AC \cos \psi$ , where  $A, C$

\* Communicated by the Author.

are the magnitudes of  $\mathbf{A}$ ,  $\mathbf{C}$ , and  $\psi$  is the angle between their forward directions. Vector symbols are printed in Clarendon type.

We may write  $\mathbf{A} = \mathbf{A}_1 + \mathbf{A}_2$ ,  $\mathbf{C} = \mathbf{C}_1 + \mathbf{C}_2$ , where  $\mathbf{A}_1$ ,  $\mathbf{C}_1$  are the vector potential and the current density due to the element  $i_1 ds_1$  and  $\mathbf{A}_2$ ,  $\mathbf{C}_2$  are due to  $i_2 ds_2$ . If  $T_{12}$  be the part of  $T$  which depends upon the product  $i_1 i_2$ , we have

$$T_{12} = \frac{1}{2} I_1 + \frac{1}{2} I_2, \quad \dots \quad (3)$$

where

$$I_1 = \iiint S \mathbf{A}_1 \mathbf{C}_1 dx dy dz, \quad I_2 = \iiint S \mathbf{A}_2 \mathbf{C}_2 dx dy dz. \quad (4)$$

The vector potential due to the vector element  $i_1 ds_1$  at a point at a distance  $r$  from the element is  $\mathbf{A}_1 = \mu i_1 ds_1 / r$ , the two vectors being parallel and having the same positive direction. Similarly  $\mathbf{A}_2 = \mu i_2 ds_2 / r$ .

If  $\alpha_2$  be the cross-section of the element  $i_2 ds_2$ , and if  $\mathbf{C}_2$  be the current density in the element,  $i_2 = \mathbf{C}_2 \alpha_2$ , and thus, if  $dv_2$  be the infinitesimal volume occupied by  $ds_2$ , we have  $\mathbf{C}_2 dv_2 = i_2 ds_2$ . Throughout  $dv_2$  we may treat  $\mathbf{A}_1$  as constant, and thus the contribution of  $dv_2$  to the integral  $I_1$  is

$$\mu i_1 i_2 ds_1 ds_2 \cos \epsilon / r, \quad \dots \quad (5)$$

where  $r$  is the distance between the two elements and  $\epsilon$  is the angle between the positive directions of the elements.

The evaluation of the integrals in (4) will be found to depend on the integral

$$\int (R^2 / \rho) \cos \psi d\omega$$

taken over the surface of a sphere of centre  $O_2$  and radius  $R$ . Here  $d\omega$  is an elementary solid angle,  $\rho$  is the distance from the surface element  $R^2 d\omega$  at  $Q$  on the sphere to a fixed point  $O_1$ , and  $\psi$  is the angle between  $O_2 Q$  and a straight line  $O_2 F_2$ , which is parallel to and has the same forward direction as a fixed straight line  $O_1 F_1$ . The value of the integral depends upon whether  $R$  is less or greater than  $r$ , where  $r = O_1 O_2$ . We shall write

$$G = \int (R^2 / \rho) \cos \psi d\omega, \quad \text{when } R < r, \quad \dots \quad (6)$$

$$J = \int (R^2 / \rho) \cos \psi d\omega, \quad \text{when } R > r. \quad \dots \quad (7)$$

If a sphere of radius  $R$  and density  $k^{-1}$  be centred at  $O_2$ , and a second sphere of radius  $R$  and density  $-k^{-1}$  be centred at  $O_2'$  on  $O_2 F_2$ , where  $O_2' O_2 = k$  and  $O_2' O_2$  has the same forward direction as  $O_2 F_2$ , the spheres neutralize each other except in those parts where they do not overlap. When  $k$  is very small, the radial thickness at  $Q$  of the un-neutralized part

is  $k \cos \psi$ . The "surface density" is thus  $k^{-1} \cdot k \cos \psi$  or  $\cos \psi$ . Hence  $G$  (or  $J$ ), the potential at  $O_1$  of the layer of surface density  $\cos \psi$ , is also the potential at  $O_1$  of the system of the two spheres. We note that, when  $k$  is infinitesimal,

$$O_1 O_2 - O_1 O_2' = k \cos O_2 O_1 F_1. \quad \dots \quad (8)$$

If we take the positive direction of  $O_1 F_1$  to coincide with the positive direction of the element  $ds_1$ , we have

$$\cos O_2 O_1 F_1 = -dr/ds_1. \quad \dots \quad (9)$$

At distance  $r$  from the centre of a sphere of radius  $R$  and density  $k^{-1}$ , the potential is  $4\pi R^3/3kr$ , when  $R < r$ . Hence, when  $R < r$ , we have, by (8) and (9),

$$G = \frac{4\pi R^3}{3k} \left( \frac{1}{O_1 O_2} - \frac{1}{O_1 O_2'} \right) = \frac{4\pi R^3}{3r^2} \cdot \frac{dr}{ds_1}. \quad \dots \quad (10)$$

When  $R > r$ ,  $O_1$  lies inside the sphere centred at  $O_2$ . The potential at  $O_1$  of that part of the sphere which lies within a distance  $r$  from  $O_2$  is  $4\pi r^3/(3kr)$  or  $4\pi r^2/3k$ . The potential within the sphere of radius  $r$  and centre  $O_2$  due to the shell of radii  $R$  and  $r$  is constant and equal to the potential at  $O_2$ , and thus equals

$$\int_r^R \frac{4\pi R^2 dR}{kR} = \frac{4\pi}{k} \cdot \frac{R^2 - r^2}{2}.$$

Thus the potential at  $O_1$  of the sphere of radius  $R$  centred at  $O_2$  is

$$\frac{4\pi}{k} \left( \frac{r^2}{3} + \frac{R^2 - r^2}{2} \right) = \frac{2\pi}{k} \left( R^2 - \frac{r^2}{3} \right).$$

Hence  $J$ , the potential at  $O_1$  of the layer of surface density  $\cos \psi$ , when  $R > r$ , is given, through (8) and (9), by

$$\begin{aligned} J &= -\frac{2\pi}{3k} (O_1 O_2^2 - O_1 O_2'^2) = \frac{2\pi}{3k} (O_1 O_2 + O_1 O_2') k \frac{dr}{ds_1} \\ &= \frac{4\pi r}{3} \cdot \frac{dr}{ds_1}. \quad \dots \quad (11) \end{aligned}$$

The values of  $G$  and  $J$  agree when  $R = r$ .

We will now return to the electrical problem and, using the values of  $G$  and  $J$ , will find the part of the integral  $I_1$  arising from the radial current flowing out of  $P_2$ , the positive end of  $ds_2$ ; we suppose  $P_2$  to be at  $O_2$ . The element  $i_1 ds_1$  is at  $O_1$ , and, as in (9), we take  $O_1 F_1$  to coincide with the forward direction of  $ds_1$ . The current density,  $C_2$ , due to

$i_2$  is  $i_2/4\pi R^2$  at Q at the distance R from  $P_2$ , and thus, since  $O_1Q=\rho$ ,

$$\begin{aligned} SA_1C_2 \cdot R^2 d\omega &= \frac{\mu i_1 ds_1}{\rho} \cdot \frac{i_2}{4\pi R^2} \cos \psi \cdot R^2 d\omega \\ &= \frac{\mu i_1 i_2 ds_1}{4\pi R^2} \cdot \frac{R^2 \cos \psi d\omega}{\rho}. \end{aligned}$$

The contribution of the shell of radii R and  $R+dR$  to the integral  $I_1$  is

$$dR \cdot \int SA_1C_2 \cdot R^2 d\omega = \frac{\mu i_1 i_2 ds_1}{4\pi R^2} G dR, \quad \text{when } R < r, \quad (12)$$

$$dR \cdot \int SA_1C_2 \cdot R^2 d\omega = \frac{\mu i_1 i_2 ds_1}{4\pi R^2} J dR, \quad \text{when } R > r. \quad (13)$$

Hence the part of  $I_1$  due to the current flowing out at  $P_2$  is

$$\frac{\mu i_1 i_2 ds_1}{4\pi} \left\{ \int_0^r \frac{G dR}{R^2} + \int_r^\infty \frac{J dR}{R^2} \right\} = \frac{1}{2} \mu i_1 i_2 ds_1 \cdot \frac{dr}{ds_1}. \quad (14)$$

At  $N_2$ , the negative end of  $ds_2$ , the arc of which  $ds_2$  is a part is less than at  $P_2$  by  $ds_2$ . Hence the part of  $I_1$  due to the current flowing in at  $N_2$  is

$$-\frac{1}{2} \mu i_1 i_2 ds_1 \left\{ \frac{dr}{ds_1} - \frac{d}{ds_2} \frac{dr}{ds_1} \cdot ds_2 \right\}. \quad (15)$$

Adding the two expressions (14) and (15), we find that the part of  $I_1$  due to the two radial currents is

$$\frac{1}{2} \mu i_1 i_2 ds_1 ds_2 \cdot d^2 r / ds_2 ds_1. \quad (16)$$

Adding the expression (5), we find

$$I_1 = \left( \frac{\cos \epsilon}{r} + \frac{1}{2} \frac{d^2 r}{ds_2 ds_1} \right) \mu i_1 i_2 ds_1 ds_2. \quad (17)$$

Since  $d^2 r / ds_1 ds_2 = d^2 r / ds_2 ds_1$ ,  $I_2 = I_1$ , and thus, by (3), we obtain Heaviside's result \*,

$$T_{12} = \mu i_1 i_2 \left( \frac{\cos \epsilon}{r} + \frac{1}{2} \frac{d^2 r}{ds_1 ds_2} \right) ds_1 ds_2. \quad (18)$$

We can express  $d^2 r / ds_1 ds_2$  in another form. Let the coordinates of  $O_1$ ,  $O_2$ , the centres of the elements, be  $x_1, y_1, z_1$  and  $x_2, y_2, z_2$ , and let  $\xi_1, \eta_1, \zeta_1$  and  $\xi_2, \eta_2, \zeta_2$  be the coordinates of points on the elements relative to  $O_1, O_2$ . Then  $r^2 = a^2 + b^2 + c^2$ , where

$$a = x_2 + \xi_2 - x_1 - \xi_1, \quad b = y_2 + \eta_2 - y_1 - \eta_1, \quad c = z_2 + \zeta_2 - z_1 - \zeta_1.$$

\* 'Electrical Papers,' vol. ii. p. 501.

## 96 Mutual Action of a Pair of Rational Current Elements.

Since  $\xi_1, \eta_1, \zeta_1$  and  $d\xi_1/ds_1, d\eta_1/ds_1, d\zeta_1/ds_1$  are independent of  $s_2$ , we have

$$\begin{aligned} r \frac{dr}{ds_2} &= a \frac{d\xi_2}{ds_2} + b \frac{d\eta_2}{ds_2} + c \frac{d\zeta_2}{ds_2}, \\ r \frac{dr}{ds_1} &= - \left( a \frac{d\xi_1}{ds_1} + b \frac{d\eta_1}{ds_1} + c \frac{d\zeta_1}{ds_1} \right), \\ r \frac{d^2r}{ds_1 ds_2} &= - \left( \frac{d\xi_1}{ds_1} \frac{d\xi_2}{ds_2} + \frac{d\eta_1}{ds_1} \frac{d\eta_2}{ds_2} + \frac{d\zeta_1}{ds_1} \frac{d\zeta_2}{ds_2} \right) - \frac{dr}{ds_1} \frac{dr}{ds_2}. \end{aligned}$$

We now evaluate the differential coefficients when

$$\xi_1 = \eta_1 = \zeta_1 = 0 \quad \text{and} \quad \xi_2 = \eta_2 = \zeta_2 = 0.$$

The direction cosines of the vector  $O_1O_2$  are  $a/r, b/r, c/r$ , those of the vector  $ds_1$  are  $d\xi_1/ds_1$ , etc., and those of the vector  $ds_2$  are  $d\xi_2/ds_2$ , etc. Then

$$rd^2r/ds_1 ds_2 = -\cos \epsilon + \cos \phi_1 \cos \phi_2,$$

where  $\phi_1$  and  $\phi_2$  are the angles between the vector  $O_1O_2$  and the vectors  $ds_1$  and  $ds_2$  respectively. Hence, by (18),

$$T_{12} = \frac{1}{2} \mu i_1 i_2 r^{-1} (\cos \epsilon + \cos \phi_1 \cos \phi_2) ds_1 ds_2. \quad (19)$$

Following Heaviside, we now take the axis of  $x$  along  $O_1O_2$ . If the direction cosines of the elements be  $l_1, m_1, n_1$  and  $l_2, m_2, n_2$ , we have

$$\cos \phi_1 = l_1, \quad \cos \phi_2 = l_2, \quad \cos \epsilon = l_1 l_2 + m_1 m_2 + n_1 n_2,$$

and then we obtain Heaviside's result \*,

$$T_{12} = \frac{1}{2} \mu i_1 i_2 r^{-1} (2l_1 l_2 + m_1 m_2 + n_1 n_2) ds_1 ds_2. \quad (20)$$

If the currents  $i_1, i_2$ , instead of flowing in two elements, flow in two finite unclosed arcs  $N_1P_1, N_2P_2$ , we integrate with respect to  $ds_1$  and also with respect to  $ds_2$ . We obtain

$$\begin{aligned} \iint \frac{d^2r}{ds_1 ds_2} ds_1 ds_2 &= \int \left( \frac{dr}{ds_2} \text{ at } P_1 - \frac{dr}{ds_2} \text{ at } N_1 \right) ds_2 \\ &= P_1 P_2 - P_1 N_2 - P_2 N_1 + N_2 N_1, \end{aligned}$$

and thus, by (18), as Heaviside found †,

$$T_{12} = \mu i_1 i_2 \left\{ \iint r^{-1} \cos \epsilon ds_1 ds_2 + \frac{1}{2} (P_1 P_2 + N_1 N_2 - P_1 N_2 - P_2 N_1) \right\}. \quad (21)$$

If the second circuit be closed,  $N_2$  is identical with  $P_2$ , and then, whether the first circuit be closed or unclosed, (21) becomes

$$T_{12} = \mu i_1 i_2 \iint r^{-1} \cos \epsilon ds_1 ds_2. \quad (22)$$

\* 'Electrical Papers,' vol. ii. p. 501.

† 'Electrical Papers,' vol. ii. p. 502.

**XII. Determination of the Variation with Pressure of the Force between Two Plates at Different Temperatures at Low Pressures, with a View to the Determination of Molecular Mean Free Paths. By A. E. MARTIN, Ph.D.\***

**1. Introduction.**

THE object of the work to be described was to measure the force between two small, plane, parallel plates, due to difference of temperature between them at low pressures, and to study the variation of the force with the pressure and nature of the gas, the temperature difference, and the distance between the plates. Simple considerations show that at pressures so low that the mean free path of the gas molecules is large compared with the distance between the plates, other factors remaining constant, the force between the plates is proportional to the pressure, and this, indeed, is the basis of the Knudsen low-pressure gauge; but at higher pressures, when the distance between the plates and the mean free path are comparable, this linear relation is no longer followed, and an attempt has been made to determine the mean free path from the observed deviations. Measurements of the heat conducted from a heated surface at low pressures are also given, and here again the deviations from a linear relation could be used to determine the mean free path, although this has not yet been attempted.

**2. Description of Apparatus.**

The apparatus is shown diagrammatically in fig. 1, and consisted of a glass bulb containing heater and suspended system, a modified McLeod pressure-gauge, vacuum-pumps, and an arrangement for admitting the gas to be investigated into the apparatus to any desired pressure not less than .001 mm. Hg.

The glass bulb B (fig. 1) was about 10 cm. diameter, and to it was sealed a wide glass tube, fitted with a ground-glass stopper. Just below the stopper was placed a short length of glass tubing, kept in place by dents in the outer tube, and between the two tubes was wedged a piece of copper strip C, bent as shown in fig. 2. To this strip was

\* Communicated by Prof. J. R. Partington, D.Sc.



attached a piece of copper wire D, from which was suspended a quartz fibre F, about 20 cm. long, the attachment being effected by means of a minute quantity of Faraday wax. The bulb also contained the heater, the platinum leads to which were sealed into a glass tube passing into the bulb.

Fig. 1.

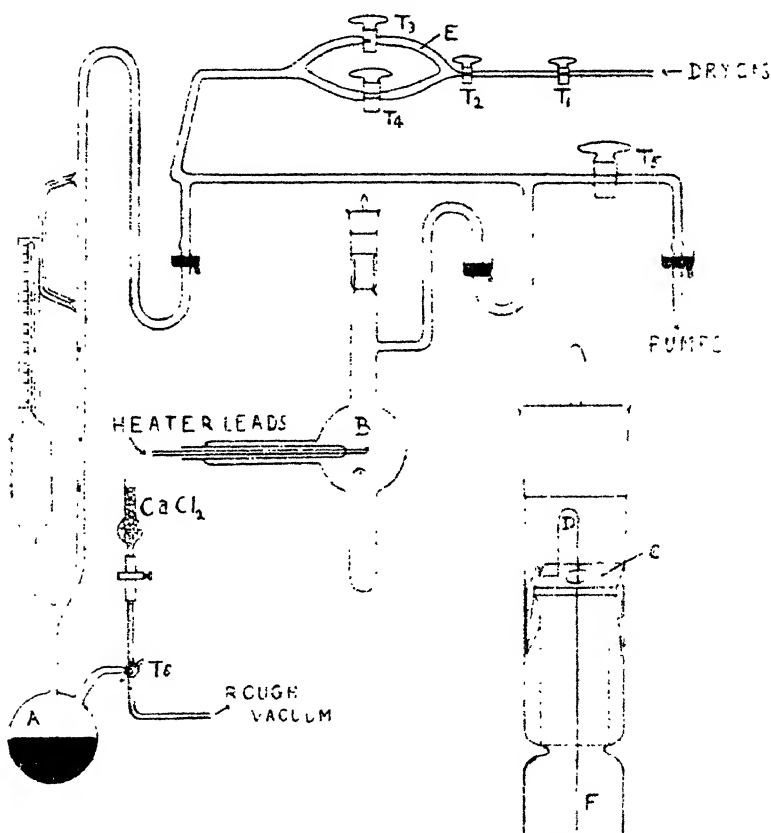


Fig. 2.

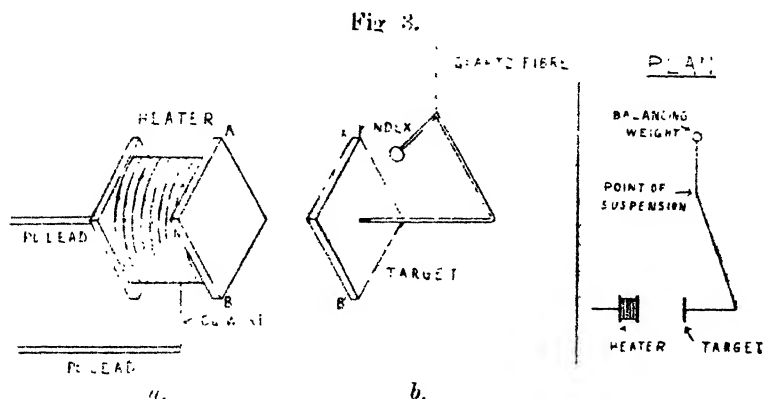
The heater (fig. 3a) consisted of a copper bobbin on which was wound, as non-inductively as possible, about 1 yard of No. 47 gauge enamelled copper wire, the ends of which were attached to the platinum leads.

One of the leads supported the bobbin, the free face of which, a copper plate 2 mm. square, formed the heated surface from which gas molecules were reflected. The temperature of this plate was taken as being the same as

that of the heating coil, which was used as a resistance thermometer. This coil was made one arm of a resistance bridge, and resistance measurements were made in the usual way except that a valve amplifier and telephones were used instead of a galvanometer.

The bulb containing the heater was almost completely surrounded by a water-jacket, and the temperature of the water was taken at frequent intervals during each experiment.

The target (fig. 3*b*) was a copper plate 2 mm. square, similar to that forming part of the heater, and was attached to an arm of thin copper wire, which was in turn attached to the quartz-fibre suspension by means of a trace of Faraday wax. The target was counterbalanced by a small



blob of solder. The upper end of the quartz fibre was attached to a kind of torsion head, already described, by means of which the position of rest of the target could be altered. Before any particular experiment the target was arranged so that when deflected during the experiment it would be directly opposite and parallel to the heater surface. It was desired to carry out experiments under such conditions that all molecules which travelled direct from heater surface to target traversed the same distance, and to this end the heater surface and target were made as small as possible. The distance between the heater surface and target was varied from 3 to 8 mm. during the course of the work, but could not be altered outside these limits. To enable the deflexions of the target to be accurately measured an index of phosphor-bronze strip

( $0.1 \times 0.01$  mm.) was attached to the target, so that when viewed through a microscope the thin edge was visible. The heater surface and target were mounted, each having a diagonal vertical, so that when the microscope was in position any one of the diagonal corners could be focussed by moving the microscope up and down or from side to side. In this way both the distance between the two upper corners, A and A', and between the lower corners, B and B' (figs. 3a and 3b) could be measured. The mean of these two measurements is given as  $s$  in the tables of measurements. All deflexions and distances were determined to  $.01$  mm.

In order to prevent any shift of the suspended system during experiments the whole apparatus was securely clamped at a number of places; also, as the suspended system was very susceptible to vibration, it was necessary to avoid any disturbance in the neighbourhood of the apparatus while readings were being taken. All readings were taken late at night, when vibration was at a minimum, and as the apparatus was unavoidably disturbed to some extent when pressure and other readings were taken, it was necessary to leave the apparatus entirely alone for some minutes after any adjustment before the position of the image of the target index on the eyepiece-scale could be determined. All pumps were shut off while measurements were being taken, except when it was necessary to use the filter-pump for a few seconds partially to exhaust the reservoir, which, besides being employed in conjunction with the filter-pump to provide a rough vacuum for the first stage of the two diffusion-pumps used to evacuate the apparatus, served to operate the pressure-gauge. This gauge was provided with a mercury reservoir A (fig. 1), which communicated with the rough vacuum while the apparatus was being evacuated. In order to take a pressure reading, the tap  $T_6$  was turned so as to cut off A from the rough vacuum, and air was admitted through a drying-tube, its rate of entry being controlled by means of a screw clip and pressure tubing. When the surface of the mercury in the open capillary was level with the top of the closed capillary the air was shut off and the length of the gas column in the closed capillary read off on a mirror scale. The pressure in the apparatus was calculated in the usual way, the capillary having been calibrated by means of a mercury thread during the construction of the

gauge, and the volume of the bulb being known from the weight of water required to fill it at a known temperature.

The gas pressure in the apparatus during an experiment was altered by means of tap  $T_3$  (fig. 1). The plug of this tap had a hole bored halfway through, the volume of the hole being about 10 cu. mm.; gas filled the cavity at atmospheric pressure when the tap was turned so that the bore communicated with the tube E, and this gas was discharged into the apparatus by turning the tap through  $180^\circ$ , the pressure being thereby increased by  $\cdot 01$  mm. The pressure could also be increased by  $\cdot 001$  mm. at a time by admitting gas at atmospheric pressure from the tube connecting  $T_1$  and  $T_2$  to the tubes connecting  $T_2$  to  $T_3$  and  $T_4$ , previously evacuated, and then admitting this gas into the apparatus as before by tap  $T_3$ . The tubes mentioned were exhausted at the commencement of each experiment through tap  $T_4$ ; this tap was then turned off, and gas, free from moisture and carbon dioxide, admitted through  $T_1$ . The gases investigated were air and hydrogen. The various pieces of apparatus were connected by means of ground joints, fitted with mercury seals.

### 3. *Mode of Experiment.*

The apparatus at the commencement of each experiment was exhausted to a pressure certainly below  $10^{-4}$  mm. The pressure-gauge indicated  $10^{-5}$  mm. ignoring any vapours present, and a similar value is obtained from considerations involving the speed of the pumps and rate of formation of mercury and other vapours in the apparatus.

The apparatus having been exhausted and flushed out with dry gas, the pumping was continued for about twenty minutes, the pumps then being shut off from the apparatus by means of  $T_5$  and stopped. Gas was immediately admitted into the apparatus to a pressure of  $\cdot 01$  mm. in the case of air and  $\cdot 02$  mm. in the case of hydrogen, it being found impossible to take readings at lower pressures owing to the small amount of damping of the oscillating target. Devices for increasing the damping were tried, but were unsatisfactory and were discarded. After admitting the gas the temperature of the heater was adjusted to a suitable value, and a pressure reading was taken. The position of the image of the target index on the eyepiece-scale was read off as soon as possible

(about fifteen minutes after shutting off the pumps), and this reading was repeated at intervals of some minutes, so that subsequently a correction could be applied for mercury and other vapours in the apparatus, the drift of the target being a measure of the amount of vapour formed.

Readings were then taken at higher pressures, the pressure being increased by  $\cdot 01$  mm. at a time, and the temperature of the heater being suitably adjusted so as to keep the deflexion of the target, and hence the distance between the target and heater, practically constant. It was not found advisable to attempt to keep the deflexion absolutely constant, as after each change of heating current an appreciable time elapsed before equilibrium was attained. Readings were taken up to a pressure of  $\cdot 11$  mm., the limit of the gauge.

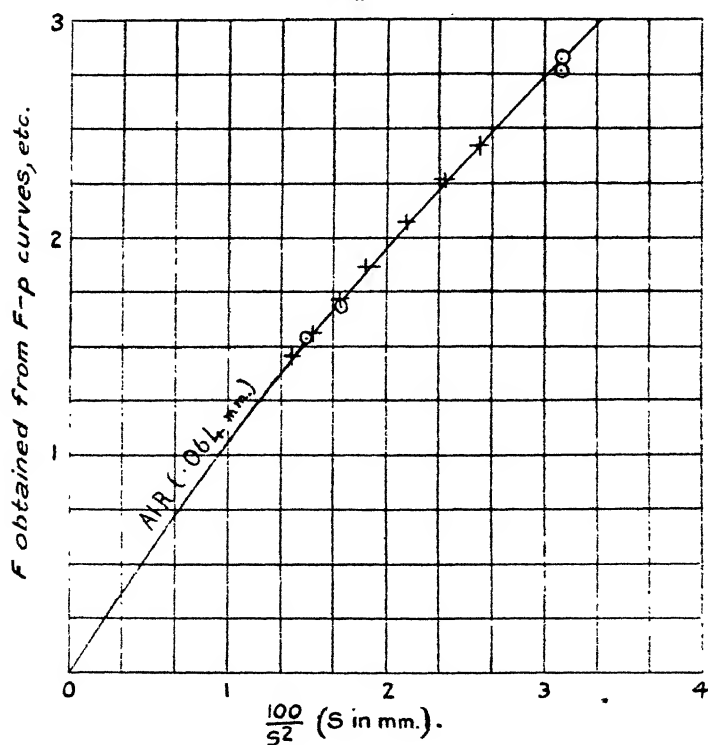
The force acting on the target at any time was proportional to the deflexion, and the torsional constant of the fibre being known, the moment of the force could be calculated, and hence the force itself. The torsional constant of the fibre was obtained by determining the period of torsional oscillation *in vacuo* of a body, of which the moment of inertia could be calculated from its mass and dimensions, attached to the fibre in place of the target. In the Tables absolute values of the force on the target are only given when there is an object in doing so. In the case of fibre 1 the force required to cause a deflexion of 1 mm. was  $\cdot 001208$  dyne; with fibre 2 a force of  $\cdot 00114$  dyne produced the same deflexion. The two fibres were actually identical, except that the target became detached from fibre 1 and had to be replaced.

#### 4. *Variation of Deflecting Force with Temperature Difference between Target and Heater.*

Measurements of the resistance of the heating coil were made at  $0^{\circ}$  C. and at  $100^{\circ}$  C. both before the heater was sealed into the bulb and after the apparatus was dismantled. These two sets of measurements agreed so well that no serious change in the heater could have occurred during the course of the work. For the determination of temperatures from resistance measurements it was assumed that the temperature coefficient of the heating coil was constant between  $0^{\circ}$  C. and  $100^{\circ}$  C. Allowance was made for the leads attached to the heating coil.

The temperature of the target could not be directly measured, but was taken as being equal to that of the water jacket. This is not quite correct, as the target was at a temperature slightly higher than that of its surroundings owing to the heat received from the heater during the course of an experiment; but this difference is so small that it can be safely neglected. If the temperature of the heater is  $\theta_2$  and the resistance of the heating coil is  $R_2$ ,

Fig. 4.



and if the temperature of the water jacket is  $\theta_1$  and the resistance of the heating coil at this temperature is  $R_1$ , then

$$\theta_2 - \theta_1 = 36.61(R_2 - R_1),$$

$\theta_2$  and  $\theta_1$  being in  $^{\circ}\text{C.}$  and the resistances in ohms. In the tables of figures and in the curves given values of  $R_2 - R_1$  are used rather than the corresponding values of  $\theta_2 - \theta_1$ , needless calculation being thus avoided.

It is of interest to determine how the deflecting force varies with  $\theta_2 - \theta_1$  when the gas pressure and distance

between the heater and target are kept constant. This variation cannot be directly determined, since the deflecting force is measured by means of changes in the distance  $s$ , but an indirect method can be used. Values of the quantity  $\frac{\text{Deflexion (mm.)}}{R_2 - R_1}$ , denoted by  $F$ , are plotted

TABLE I.

Quartz fibre 1.		Air.	
No. of Expt.	F.	$s$ , mm.	$\frac{100}{s^2}$ .
3	2.76	5.68	3.10
4	2.81	5.68	3.10
5	3.03	5.46	3.36
6	1.68	7.64	1.714
7	1.54	8.20	1.488

Points plotted from above values are marked  $\odot$  in fig. 4.

Quartz fibre 2.			Air.		
$R_2 - R_1$ , ohms.	Deflexion, mm.	$\frac{\text{Deflexion}}{R_2 - R_1}$ , = $F$ .	$F$ 1.060.	Distance $s$ , mm.	$\frac{100}{s^2}$ .
.866	1.71	1.974	1.863	7.32	1.866
.569	1.25	2.197	2.072	6.86	2.126
.376	0.88	2.395	2.259	6.51	2.360
.226	0.58	2.566	2.421	6.21	2.592
1.507	2.49	1.652	1.559	8.08	1.533
1.842	2.84	1.542	1.454	8.43	1.406
1.129	2.05	1.816	1.713	7.66	1.706

Points plotted from above values are marked  $+$  in fig. 4.

Since the force required for 1 mm. deflexion is different for the two fibres, it is necessary to divide the values of  $F$  in the second series by 1.060 to make them comparable with those in the first series.

against the pressure, small corrections having been applied for small variations in  $s$ , and from the curves obtained values of  $F$  are read off for some particular pressure, and a curve showing the relation between  $F$  and  $s$  at constant pressure is obtained.

The temperature differences corresponding to the values of  $F$  plotted did not greatly differ throughout the series. A

series of readings had previously been taken at the same pressure, but with widely different temperature differences; and it will be seen that the corresponding values of  $F$ , when plotted against  $s$ , fall on the curve previously obtained (fig. 4). This shows, within the limit of experimental error, that, for given values of pressure and distance  $s$ ,  $\frac{\text{Deflexion}}{\theta_2 - \theta_1}$  is constant; i. e., the deflexion is proportional to the temperature difference. These measurements are given in Table I.

### 5. *Variation of Deflecting Force with Pressure, other Factors remaining constant.*

Assuming that  $F$  is independent of temperature difference, it is only necessary to correct the values of  $F$ , obtained from any series of readings, for small variations in the value of  $s$ , and for mercury and other vapours in the apparatus, after which curves showing the variation of deflecting force with pressure can be drawn. The former correction is given later, but the latter will be discussed at this point.

As previously stated, the pressure inside the apparatus at the instant when the pumps were shut off was between  $10^{-5}$  and  $10^{-4}$  mm. This amount can be safely neglected, since the lowest pressure at which readings were taken was  $10^{-2}$  mm. The rate of external leakage under average conditions was measured by exhausting the apparatus and leaving overnight, and was found to be quite negligible. The sole pressure correction arises through the formation of mercury and other vapours in the apparatus after the pumps were shut off. These vapours were, of course, ignored by the McLeod gauge. Experiments were made to find how the rate of formation of vapour varied with the time, and it was found that it fell off almost exponentially, and was, as far as could be ascertained, independent of gas in the apparatus at pressures up to .1 mm. Theoretical considerations lead to a similar result.

Let the amount of mercury, grease, etc. adsorbed on the walls of the apparatus at the instant when the pumps were shut off be  $a$ . Suppose that after time  $t$  this amount has decreased by  $x$ , the vapour formed being proportional to  $x$ ; then the rate at which molecules in the vapour phase strike the walls of the apparatus will also be proportional to  $x$ ,



and, if it is assumed that a constant proportion of such molecules is readsorbed, the rate at which  $x$  is decreasing from this cause will be proportional to  $x$  itself. At the same time  $x$  will be increasing, due to evaporation from the walls of the apparatus, at a rate proportional to the amount of volatile material remaining. Thus we have

$$\frac{dx}{dt} = k_1(a - x) - k_2x = k_1a - kx,$$

where  $k_1$  and  $k_2$  are constants and  $k_1 + k_2 = k$ .

$$\therefore dt = \frac{dx}{k_1a - kx} \quad \text{and} \quad kt = C - \ln(k_1a - kx),$$

$C$  being the integration constant. When  $t=0$ ,  $x=0$ ;

$$\therefore kt = \ln \left( \frac{k_1a}{k_1a - kx} \right)$$

$$\text{and} \quad x = \frac{ak_1}{k} (1 - e^{-kt}). \quad . \quad . \quad . \quad . \quad (1)$$

$a$  will vary from one experiment to another, but  $k$  should remain reasonably constant, since neither the composition of the adsorbed volatile material nor the temperature of the apparatus varied very much during the course of the work. It was found from experiment that the vapour formed during the first hour was double that formed during the second hour, which was in turn double that formed during the third hour, in agreement with equation (1) when  $e^{-k} = \frac{1}{2}$ ,  $t$  being measured in hours.

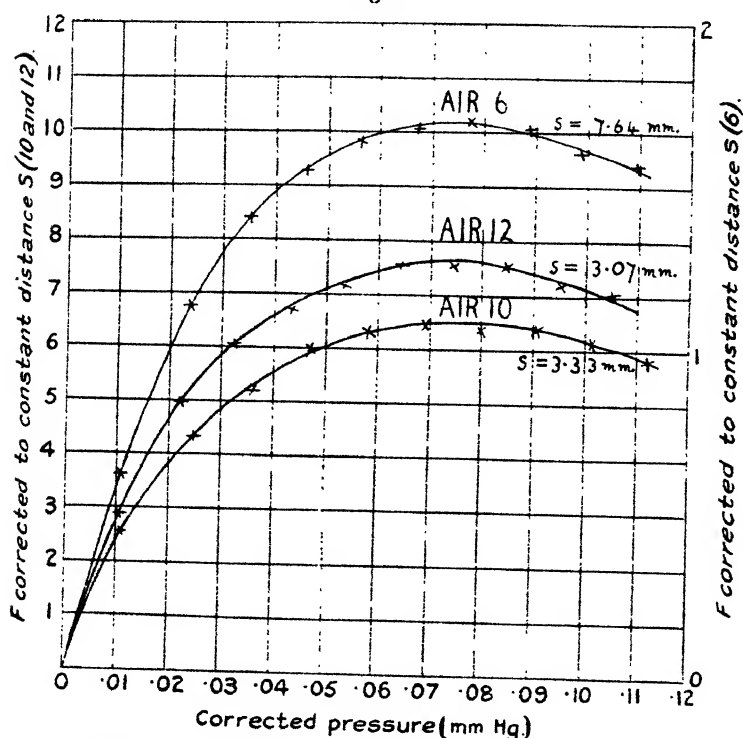
The corrections for vapour pressure are obtained by plotting  $F$  against time, using the measurements taken at the commencement of each experiment, before admitting a second quantity of gas into the apparatus. The curve obtained is completed by making use of the observation that the vapour formed during the first hour is double that formed during the second hour, as previously explained. Over the small pressure range applying to the values of  $F$  obtained from measurements taken at the commence-

ment of an experiment,  $\frac{\delta F}{\delta p}$  is practically constant and can

be obtained from the appropriate  $F-p$  curve; the  $F$  scale in the  $F$ -time curve can be directly converted to pressure, and the vapour formed in the apparatus at any given time can be read off from the curve. This pressure is

added to the gauge pressure, and the total taken as the actual pressure in the apparatus at this particular time. The pressure correction is not, of course, the actual vapour pressure, but the pressure of air or hydrogen to which it is equivalent in these experiments. Figs. 5 and 6 show the variation of the deflecting force with the pressure, other factors remaining constant. These curves are referred to as  $F-p$  curves for convenience.

Fig. 5.



To convert values of  $F$  to dynes multiply by .001208 for (6) and (10), and by .00114 for (12).

#### 6. Relation between $F$ and $s$ at Constant Pressure.

From the  $F-p$  curves for air and hydrogen values of  $F$  and  $s$  at constant pressure were obtained, and curves were drawn showing the relation between  $F$  and  $s$  (fig. 7). These curves were used to correct the values of  $F$

$\left(\frac{\text{Deflexion}}{R_2 - R_1}\right)$  for small variations in  $s$  as follows:—

Suppose that in a given experiment  $F$  and  $s$  have the

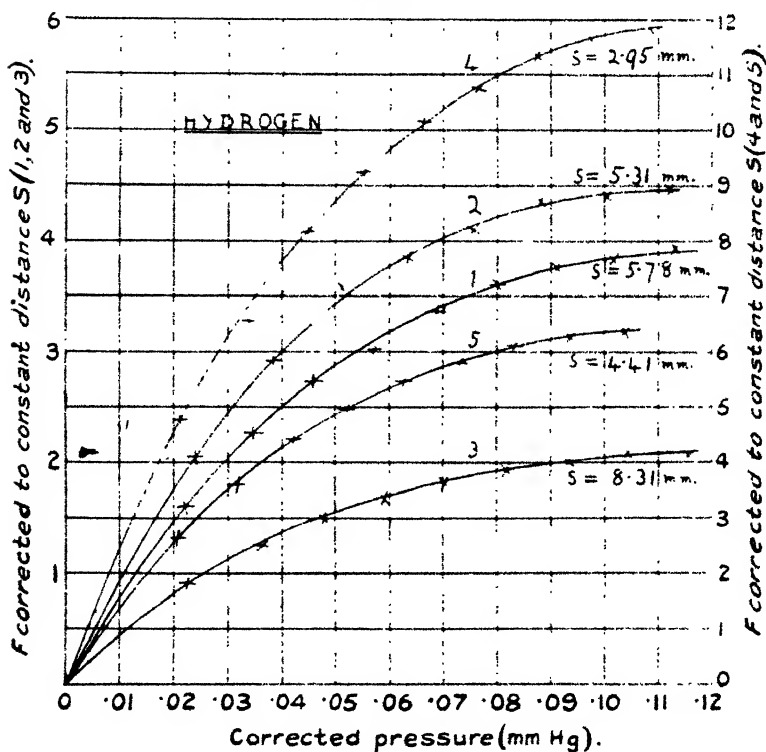
values  $F_1$  and  $s_1$  at a pressure  $p$ , and that it is required to find the change in  $F$ ,  $\delta F_1$ , due to a change in  $s$  of  $\delta s_1$  at the same pressure.

Assuming the relation between  $F_1$ ,  $s_1$ , and  $p$  to be of the form

$$F_1 = f(p)f(s_1),$$

we have 
$$\frac{\delta F_1}{\delta s_1} = f(p)f'(s_1) = F_1 \cdot \frac{f'(s_1)}{f(s_1)}.$$

Fig. 6.



To convert values of  $F$  to dynes multiply by .001208 for (1), (2), and (3), and by .00114 for (4) and (5).

But the slope of the appropriate curve in fig. 7 at any point is

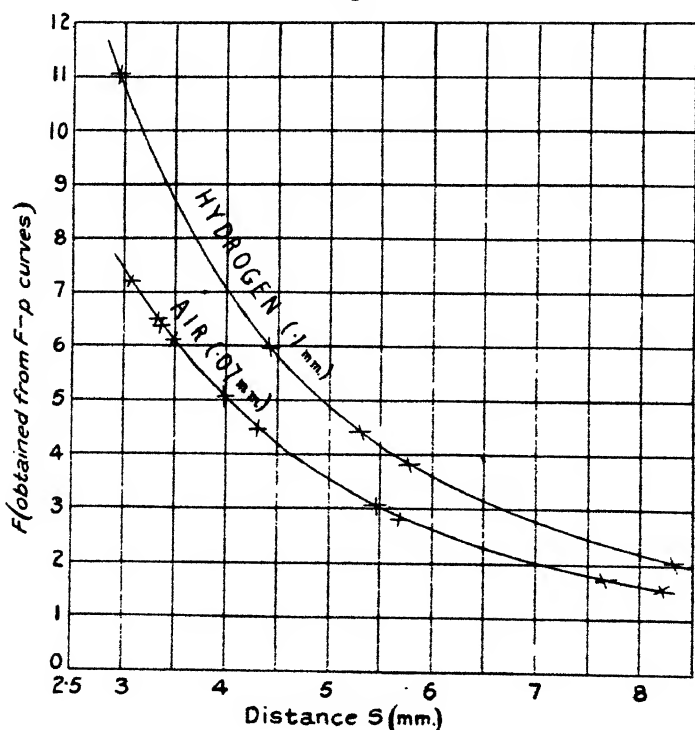
$$\begin{aligned} \frac{\delta F}{\delta s} &= F \frac{f'(s)}{f(s)} \\ &= F_2 \frac{f'(s_1)}{f(s_1)} \end{aligned}$$

at the point where  $s=s_1$ ,  $F_2$  being the corresponding value of  $F$ ,

$$\therefore \frac{\delta F_1}{\delta s_1} = \frac{F_1}{F_2} \frac{\delta F}{\delta s},$$

and since  $\frac{\delta F}{\delta s}$  can be found from the curve,  $\frac{\delta F_1}{\delta s_1}$  can be obtained.

Fig. 7.



The relation between  $F$  and  $s$  at constant pressure is shown better by plotting  $F$  against  $\frac{100}{s^2}$  (fig. 8).

### 7. Discussion of Results.

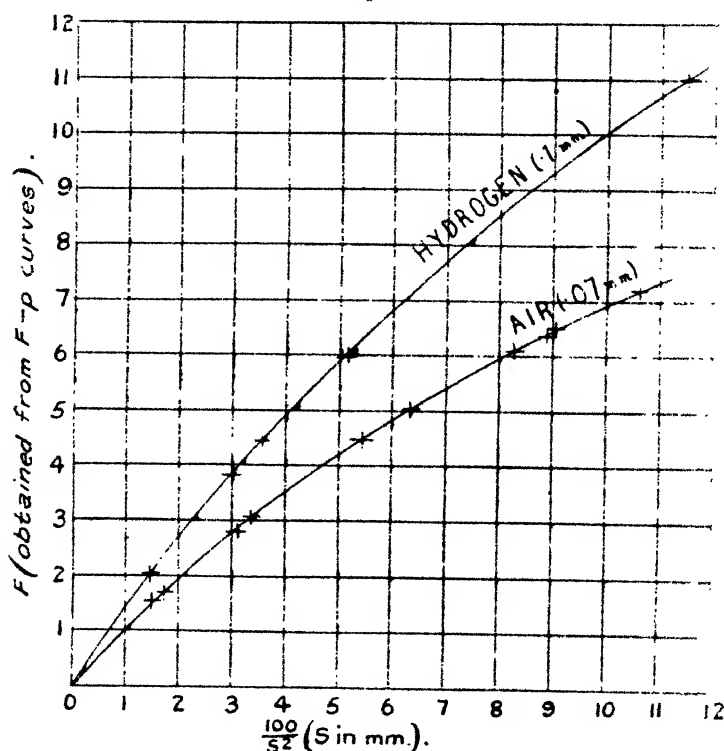
Both for air and hydrogen it is seen that the curves obtained by plotting  $F$  against  $p$ ,  $s$  constant, pass through the origin. It might be supposed that the deflecting force acting on the target is not solely due to the bombarding molecules, and in order to explore this possibility various

forces which might conceivably deflect the target are enumerated below and, as will be seen, finally disregarded.

The possible forces are as follows :—

(1) Gravitational attraction between heater and target. Approximate calculation shows that this force would be less than  $10^{-7}$  dyne, which can be safely neglected, since the smallest readable deflexion was equivalent to  $10^{-5}$  dyne.

Fig. 8.



(2) Deflecting force due to heat radiation falling on target. The rate at which heat was generated in the heater was measured in some experiments, and using these values for approximate calculation, it is found that in no case would the force due to heat radiation exceed  $10^{-6}$  dyne, and this is negligible.

(3) The energy received by the target would cause the face nearer the heater to be at a higher temperature than the other surface. This alone would cause the forces acting

on the two sides to be unequal, so that a deflecting force would be produced. Rough calculation shows that the difference of temperature between the two sides during an experiment would never be greater than  $\frac{1}{10,000}^{\circ}\text{C.}$ , and this is quite incapable of causing any readable deflexion.

(4) Any slight magnetic field due to current circulating in the heating coil might deflect the target, especially if the latter contained any magnetic impurities. A force of this nature can be dismissed, since a powerful electromagnet when brought near to the target produced no observable deflexion.

The fact that the  $F-p$  curves pass through the origin is in agreement with the conclusion that the only deflecting force is due to molecular bombardment.

From the  $F-p$  curves for air it is seen that  $F$  reaches a maximum value at about  $\cdot 07$  mm. pressure, this pressure being independent of  $s$ .

In the case of hydrogen no maxima of  $F$  are obtained, but there is little doubt that such maxima would have been exhibited at about  $\cdot 13$  mm.

The curves obtained for air and hydrogen by plotting  $F$  against  $\frac{100}{s^2}$  at constant pressure (fig. 8) are almost straight lines passing through the origin, which latter would be obtained if  $F$  were proportional to  $\frac{1}{s^2}$ . Thus the inverse square law is obeyed, provided that  $s$  is large compared with the dimensions of heater surface and target.

The above observations admit of quite simple theoretical explanation and are of interest in connexion with the working of the radiometer. In explaining these results, use will be made of some theoretical work due to Einstein\* and Hettner†.

In the case of a vane, the dimensions of which are small compared with the mean free path  $L$ , situated in a gas, pressure  $p$ , in which exists a temperature gradient  $\frac{\delta T}{\delta s}$ , normal to the surface of the vane, area  $\sigma$ , a force given by

\* A. Einstein, *Z. tschr. f. Phys.* xxvii. p. 1 (1924).

† G. Hettner, *loc. cit.* xxvii. p. 12 (1924).

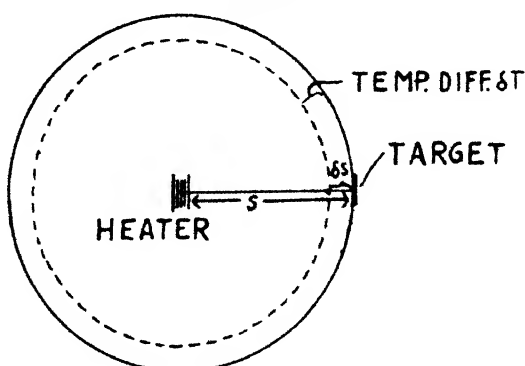
equation (2) will act on the vane, tending to move it in the direction of decreasing temperature.

$$K = \frac{\sigma f}{u} = -\frac{1}{2} p \frac{L}{T} \frac{\delta T}{\delta s} \sigma, \quad . . . . . (2)$$

where  $K$  is the force,  $f$  the heat flow across unit area of the plane containing the vane,  $u$  the mean velocity of the molecules striking the vane, and  $T$  the temperature of the vane. This equation is due to Einstein. In fig. 9, if  $E$  is the heat energy conducted from the heater per second by gas molecules, then

$$E = 4\pi s^2 f,$$

Fig. 9.



and substituting for  $f$  in equation (2) we obtain

$$K = \frac{\sigma E}{4\pi s^2 u} . . . . . (3)$$

This equation agrees with results obtained at low pressures, since  $E$  is proportional to the pressure and to the temperature difference between the heater and surroundings. If  $E$  in equation (3) is replaced by  $E_1$ , the heat conducted at any pressure for a temperature difference of  $36.6^\circ \text{C.}$ , then  $K$  can be replaced by  $F$ , in conformity with previous practice. Equation (3) then becomes

$$F = \frac{\sigma E_1}{4\pi s^2 u} . . . . . (3a)$$

Measurements of the heat conducted from the heater by the gas at various pressures are given later, and from them values of  $E_1$  have been found and used to calculate values of  $F$  from equation (3a).

The calculated values of  $F$  are found to be about five times greater than the observed values in the case of air, and about three times greater in the case of hydrogen. These differences are explained by the fact that Einstein in deriving equation (2) only considered the translational velocities of the molecules, and did not allow for the accommodation coefficient. A further cause for discrepancy lies in the fact that heat is not conducted from the heater equally in all directions as assumed above. The whole question of the force on the target at low pressures is discussed more fully at a later point.

Einstein extends equation (2) to cover the case of a vane of dimensions great compared with the mean free path. Equation (2) applies in this case only to the extreme edges of the vane, over a region of the order of a mean free path wide. Over the remainder of the vane the pressure is the same on both sides. This leads to the equation

$$K = \frac{fL}{u} = -\frac{1}{2}p \frac{L^2}{T} \frac{\delta T}{\delta s}, \quad \dots \dots \dots (4)$$

where  $K$  is now the force per unit-length of edge of the vane. Proceeding as before we obtain

$$K = \frac{EL}{4\pi s^2 u}, \quad \dots \dots \dots (5)$$

where  $E$  is the energy conducted by the gas molecules. If the pressure is sufficiently high, then  $E$  will be proportional to temperature difference but independent of pressure.

Equation (5) can then be modified as follows :—

$$F = \frac{E_2 L l}{4\pi s^2 u}, \quad \dots \dots \dots (5a)$$

where  $E_2$  is the energy conducted for a temperature difference of  $36.6^\circ \text{C.}$ , and  $F$  is the force for the entire length of edge ( $l$ ) of the vane. It is thus seen that at high pressures

$$F \propto \frac{1}{p}.$$

Hettner derives an equation to cover all pressures as follows :—

At high pressures put  $F = \frac{a}{p}$ , and at low pressures put



$F = bp$ ,  $a$  and  $b$  being constants. At any pressure we have approximately

$$\frac{1}{F} = \frac{p}{a} + \frac{1}{bp}, \quad \dots \dots \dots (6)$$

$$\text{or} \quad \frac{p}{F} = \frac{p^2}{a} + \frac{1}{b} \dots \dots \dots (6a)$$

If equation (6a) holds good, then a straight line should be obtained by plotting  $p^2$  along the  $x$  axis and  $\frac{p}{F}$  along the  $y$  axis.

Further, from equation (6)  $F$  is a maximum when

$$p = \sqrt{\frac{a}{b}} = p_0 \text{ (say).}$$

But from equation (6a)

$$p^2 = -\frac{a}{b}, \text{ when } \frac{p}{F} = 0,$$

so that the intercept on the  $x$  axis is

$$-\frac{a}{b} = -p_0^2.$$

Equation (6a) was tested for air and hydrogen in the manner indicated, and it is found that the points plotted lie almost exactly on two straight lines (fig. 10). From these straight lines the following values for  $p_0$  are obtained :—

Air,  $p_0 = 0.07$  mm. ; hydrogen,  $p_0 = 0.11$  mm.

The value for air is identical with that obtained from the corresponding  $F-p$  curve. The  $F-p$  curve for hydrogen does not actually show a maximum, although a value for  $p_0$  in the neighbourhood of 0.13 mm. is indicated.

The value of  $p_0$  for any case can be calculated purely theoretically as follows :—

By comparison of equations (3a) and (5a) with equation (6) we obtain

$$a = \frac{E_2 L p}{4\pi s^2 u} \quad \text{and} \quad b = \frac{\sigma E_1}{4\pi s^2 u p},$$

whence

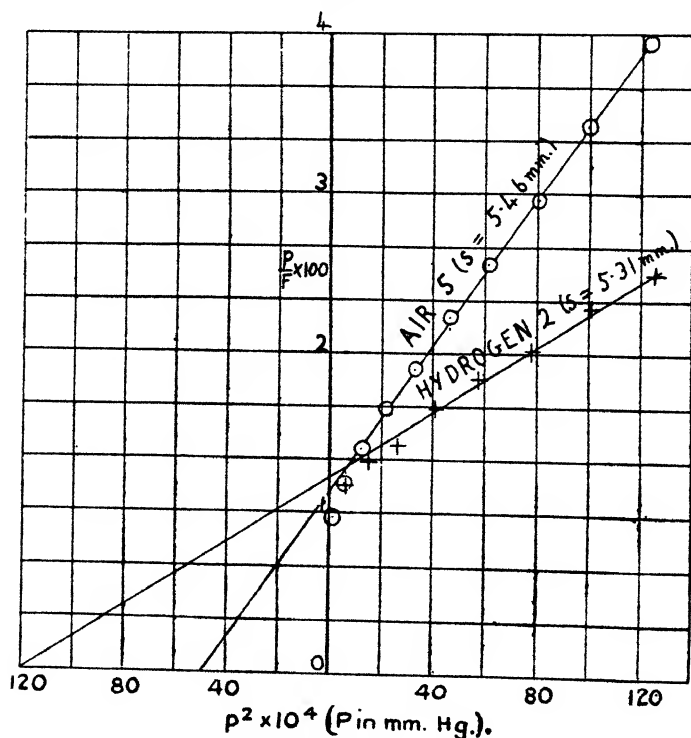
$$\frac{a}{b} = \frac{E_2 L p^2}{\sigma E_1}$$

and

$$p_0 = p \sqrt{\frac{L E_2}{\sigma E_1}} \dots \dots \dots (7)$$

Equation (7) shows that  $p_0$  is independent of  $s$ , which is in accord with experimental results.  $E_1$  and  $E_2$  were found for air and hydrogen from measurements of heat conduction, and by substituting these values together with the values for  $L$ , usually given, in equation (7), the values of  $p_0$  for air and hydrogen are found to be .09 mm. and .16 mm., respectively. These values agree quite well with the observed values, and this agreement proves the correctness of equation (4), at least as regards order of magnitude.

Fig. 10.



It should be noted that equations (2) and (4) are subject to the same errors, since equation (4) was derived from equation (2); these errors cancel each other in the calculation of  $p_0$ .

#### 8. Relation between the Heat conducted from the Heater by Gas Molecules for a Constant Temperature Difference, and the Gas Pressure.

In some experiments measurements were made of the current flowing through the heater coil, from which the

rate at which energy was generated in the heater could be found. In order to determine that portion of the heat conducted away by the surrounding gas measurements were made to find the heat lost by radiation and conduction through the leads for various temperature differences between the heater and its surrounding at the lowest pressure obtainable.

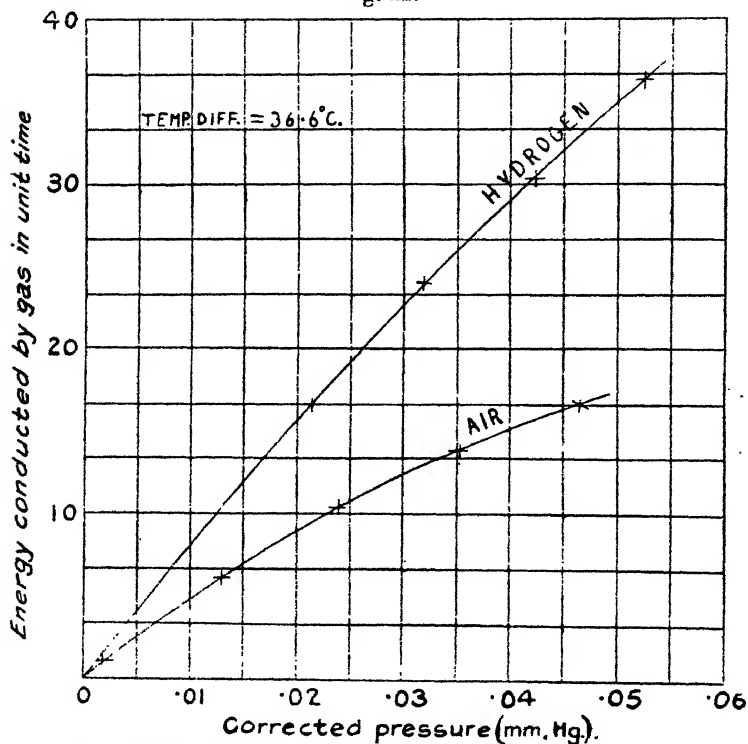
The method adopted was to exhaust the apparatus to as low a pressure as possible, shut off the pumps and take resistance, current, temperature, and time readings. The heat generated in the heater per unit-time at the instant when the pumps were cut off was obtained by extrapolation, and was, of course, equal to the heat lost by radiation and conduction through the leads. The rate of energy loss from the heater *in vacuo* was taken to be  $C^2R$ ,  $C$  being the current and  $R$  the resistance of the heating coil—i. e.,  $R_2$  less the resistance of the leads. A curve was drawn showing the relation between  $C^2R$  and  $R_2 - R_1$ , and it was found to be very nearly a straight line, as might be expected. To determine the heat conducted by gas under any given conditions the heat lost by radiation and conduction through the leads in absence of gas was obtained from the curve and subtracted from the total heat lost.

The heat conducted by the gas at various pressures having been found for air and hydrogen, the values were reduced to a common temperature difference, and curves were drawn showing the relation between the heat conducted by the gas and the pressure (fig. 11). In this calculation it is assumed that the heat conducted by the gas at a given pressure is proportional to the temperature difference. The pressure readings were corrected for the presence of vapours in the apparatus in a manner similar to that already described.

The number of molecules striking the heater per unit-area per second is  $\frac{NC}{\sqrt{6\pi}}$ , where  $N$  is the number of molecules per c.c. and  $C$  is the R.M.S. speed. The mass of gas striking unit-area per second is  $\frac{mNC}{\sqrt{6\pi}}$ ,  $m$  being the mass of a single molecule. But the pressure of the gas,  $p$ , is  $\frac{1}{3} NmC^2$ , and therefore the mass of gas striking unit-

area per second is  $\frac{3p}{\sqrt{6\pi C}}$ . At very low pressures the impinging molecules will be "cold" and will take from the heater energy proportional to  $\theta_2 - \theta_1$ , but at higher pressures the impinging molecules will be "warmed" by previous collisions with "hot" molecules rebounding from the heater, and the average amount of heat taken from the heater, and the average amount of heat taken from the heater by each molecule striking it will be reduced.

Fig. 11.



To convert energy conducted in unit time to ergs per sec., multiply by  $5.37 \times 10^3$ .

At low pressures, therefore, the heat conducted is proportional to the pressure, as can be seen from fig. 11, whilst at higher pressures the heat conducted increases more and more slowly with pressure until it becomes practically constant. The slope of each of the curves of fig. 11 as it passes through the origin has been determined, the values being as follows:—

Gas.	Rate at which energy is conducted by gas.	Temp. of surroundings.
Air.....	$2.73 \times 10^3$ ergs per second per .001 mm. Hg.	17.5° C.
Hydrogen	4.40 " " " " " "	16.4° C.

These values correspond to a temperature difference between heater and surroundings of  $36.6^{\circ}\text{C}$ .

$$.001 \text{ mm. Hg.} = \frac{13.6 \times 981}{10^4} \text{ dynes per cm.}^2$$

C (mean for  $\text{O}_2$  and  $\text{N}_2$  in air at  $17.5^{\circ}\text{C}$ .)  $5.02 \times 10^4 \text{ cm./sec.}$

C (for  $\text{H}_2$  at  $16.4^{\circ}\text{C}$ .) . . . . .  $18.9 \times 10^4 \text{ cm./sec.}$

Specific heat of air at constant volume. 0.170.

Specific heat of hydrogen at constant  
volume . . . . . 2.360.

Knowing that the mass of gas striking unit-area in unit-time is  $\frac{3p}{\sqrt{6\pi}C}$ , and assuming that the air molecules have

the same temperature as the heater on leaving, we find by making use of the above values that the energy taken from unit-area of the heater per second is  $4.78 \times 10^3$  ergs for a pressure of .001 mm. Hg,

$$\begin{aligned} \therefore \text{the effective area of the heater} &= \frac{2.73 \times 10^2}{4.78 \times 10^3} \text{ sq. cm.} \\ &= 57.2 \text{ sq. mm.} \end{aligned}$$

This value is considerably greater than that obtained by measurement (21.0 sq. mm.), and this is probably due to irregularities on the surface of the heater enabling more impacts to take place than is indicated by the simple theory used. The area of the heater available for molecular impacts is difficult to measure at all accurately, owing to the presence of the wire.

In the case of hydrogen it cannot be assumed that the molecules rebounding have the same temperature as the heater, but if  $\theta$  is the average temperature of the molecules striking the surface,  $\theta_1$  the temperature of the surface, and  $\theta_2$  the average temperature of the molecules leaving, then

$$\theta_2 - \theta = a(\theta_1 - \theta),$$

where  $a$  is the accommodation constant of Knudsen.

Using the value for the effective area of the heater already obtained,  $a$  can be found as follows:—

In a similar manner to that used for air, but using the appropriate values for hydrogen, the energy conducted per second from the heater for a pressure of .001 mm. is found to be  $10.08 \times 10^3 \times a$  ergs.

But the heat conducted per second was found by measurement to be  $4.40 \times 10^3$  ergs.

$$\therefore a = 437.$$

This value for  $a$  is intermediate between the values obtained with hydrogen by Knudsen for polished platinum and platinum slightly coated with platinum black.

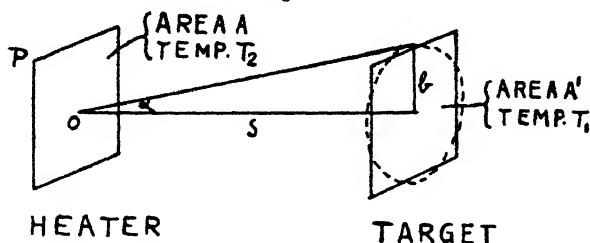
9. *Determination of the Force between two Small, Parallel Plates, due to a Temperature-Difference between them at Very Low Pressures.*

Assuming that the molecules are specularly reflected from the heater surface (fig. 12), the number of molecules reflected per second at an angle between  $\theta$  and  $\theta + d\theta$  with the normal to the surface is

$$dn = \frac{2NAC_1}{\sqrt{6\pi}} \sin \theta \cos \theta d\theta,$$

where  $N$  is the number of molecules per c.c. and  $C_1$  the R.M.S. speed of the molecules striking the heater.

Fig. 12.



The total number of molecules from the heater surface striking the target per second, supposing the pressure to be so low that none of these molecules collide with "cold" molecules on their way to the target, is

$$\begin{aligned} n &= \frac{2NAC_1}{\sqrt{6\pi}} \int_0^a \sin \theta \cos \theta d\theta \\ &= \frac{NAC_1}{\sqrt{6\pi}} \sin^2 \alpha = \frac{NAC_1}{\sqrt{6\pi}} \cdot \frac{b^2}{s^2}, \end{aligned}$$

if  $b$  is small compared with  $s$  ( $b$  is the radius of a circle having an area equal to that of target),

$$\therefore n = \frac{NAC_1}{\sqrt{6\pi}} \cdot \frac{A'}{\pi s^2}.$$

If these molecules have a mean speed  $\bar{c}_2$ , appropriate to the temperature of the heater,  $T_2$ , then, since they all strike the target nearly normally, the force on the target due to their impact is

$$\frac{NAA'C_1}{\sqrt{6\pi} \cdot \pi s^2} \cdot m\bar{c}_2 = \frac{mNAA'C_1C_2}{\sqrt{6\pi} \cdot \pi s^2} \cdot \sqrt{\frac{8}{3\pi}}$$

$$= \frac{2}{3} \frac{mNAA'C_1C_2}{\pi^2 s^2},$$

and the deflecting force on the target, due to the extra energy imparted to the molecules by the heater, is

$$\frac{2}{3} \frac{AA'mNC_1^2}{\pi^2 s^2} \left( \frac{C_2 - C_1}{C_1} \right),$$

provided that the "hot" molecules give up all excess energy to the target on impact—i. e., the temperature of these molecules on leaving the target is  $T_1$ .

Now 
$$\frac{C_2 - C_1}{C_1} = \frac{T_2 - T_1}{2T_1}$$

approximately, if  $T_2 - T_1$  is small compared with  $T_1$ , so that the deflecting force acting on the target is

$$K = \frac{pAA'}{\pi^2 s^2} \left( \frac{T_2 - T_1}{T_1} \right). \quad . \quad . \quad . \quad (8)$$

$p$  being the gas pressure in the apparatus.

Equation (8) is approximately correct for air, but in the case of hydrogen allowance must be made for the fact that in general hydrogen molecules rebounding from a surface have a mean temperature different from that of the surface. Thus, hydrogen molecules rebounding from the heater will have a mean velocity corresponding to a temperature less than  $T_2$  (say  $T_2'$ ), and the "hot" molecules rebounding from the target will have a mean velocity corresponding to a temperature higher than  $T_1$  (say  $T_1'$ ),

where 
$$T_2' - T_1 = a(T_2 - T_1)$$

and 
$$T_2' - T_1' = a(T_2' - T_1),$$

$a$  being the coefficient of accommodation of Knudsen,

$$\begin{aligned} \therefore T_1' - T_1 &= a(T_2 - T_2') \\ &= a\{T_2 - T_1 - a(T_2 - T_1)\} \\ &= a(1 - a)(T_2 - T_1). \end{aligned}$$

If the "hot" molecules rebound normally from the target, then the deflecting force due to this rebound is

$$\frac{NAA'C_1'}{\sqrt{6\pi} \cdot \pi s^2} \cdot m(\bar{c}_1' - \bar{c}_1),$$

where  $c_1'$  and  $\bar{c}_1$  are the mean speeds corresponding to the temperatures  $T_1'$  and  $T_1$ .

This force

$$\begin{aligned} &= \frac{NAA'C_1'^2}{\sqrt{6\pi} \cdot \pi s^2} \cdot m \left( \frac{C_1' - C_1}{C_1} \right) \sqrt{\frac{8}{3\pi}} \\ &= \frac{pAA'}{\pi^2 s^2} \cdot \left( \frac{T_1' - T_1}{T_1} \right) = a(1-a) \cdot \frac{pAA'}{\pi^2 s^2} \left( \frac{T_2 - T_1}{T_1} \right). \end{aligned}$$

The deflecting force due to impact is

$$\frac{pAA'}{\pi^2 s^2} \cdot \left( \frac{T_2' - T_1}{T_1} \right) = a \cdot \frac{pAA'}{\pi^2 s^2} \cdot \left( \frac{T_2 - T_1}{T_1} \right);$$

therefore the total deflecting force is

$$K = a(2-a) \cdot \frac{pAA'}{\pi^2 s^2} \left( \frac{T_2 - T_1}{T_1} \right). \quad . \quad . \quad . \quad (9)$$

Under the conditions of these experiments  $a$  has been found to be .437 for hydrogen from measurements of energy conducted from heater by bombarding molecules, and substituting this value we obtain from (9)

$$K = .683 \frac{pAA'}{\pi^2 s^2} \left( \frac{T_2 - T_1}{T_1} \right). \quad . \quad . \quad . \quad (9a)$$

This work will now be repeated assuming the molecules to be reflected from the heater surface according to the cosine law.

The number of molecules reflected from the heater surface (fig. 12), at an angle between  $\theta$  and  $\theta + d\theta$  with the normal to the surface, is

$$\frac{NAC_1}{\sqrt{6\pi}} \cos \theta d\theta.$$

The total number reflected between 0 and  $\alpha$  is

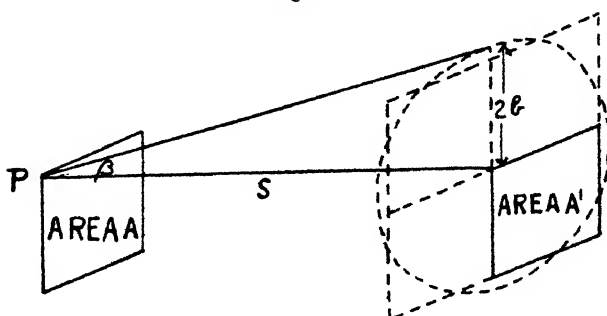
$$\begin{aligned} \frac{NAC_1}{\sqrt{6\pi}} \int_0^\alpha \cos \theta d\theta &= \frac{NAC_1}{\sqrt{6\pi}} \sin \alpha \\ &= \frac{NAC_1}{\sqrt{6\pi}} \cdot \frac{b}{s}, \end{aligned}$$



$b$  being the radius of a circle equal in area to the target and being small compared with  $s$ . This number would be correct if the molecules rebounding from the heater surface left the surface only from  $O$ ; if, however, all the molecules left from one corner of the heater surface (assumed to be a perfect square, roughly equal in area to the target), such as  $P$  (fig. 13), then the number of molecules intercepted by the target would be

$$\frac{1}{4} \frac{NAC_1}{\sqrt{6\pi}} \int_0^\beta \cos \theta d\theta = \frac{1}{4} \frac{NAC_1}{\sqrt{6\pi}} \sin \beta = \frac{NAC_1}{\sqrt{6\pi}} \cdot \frac{b}{2s}.$$

Fig. 13.



Taking the mean of these extreme values, we have approximately that the number of molecules from the heater surface intercepted by the target is

$$\frac{3}{4} \cdot \frac{NAC_1}{\sqrt{6\pi}} \cdot \frac{b}{s}.$$

Proceeding as before, the deflecting force due to the impact of these molecules is found to be

$$K = \frac{3}{4} \cdot \frac{pAb}{\pi s} \cdot \left( \frac{T_2 - T_1}{T_1} \right) \quad . \quad . \quad . \quad (10)$$

In the case of hydrogen the accommodation coefficient must be introduced as before. If we have gas at a uniform temperature contained in a vessel ( $N$  molecules per c.c. and R.M.S. speed  $C$ ), then molecules will be leaving unit-area of the surface at the rate of  $\frac{NC}{\sqrt{6\pi}}$  per second, and the pressure produced normal to the surface, due to their departure, will be  $\frac{NmC^2}{6}$ ,  $m$  being the mass of a molecule.

The mean force due to the departure (or impact) of a single molecule, therefore, is  $\sqrt{\frac{\pi}{6}} mC$ .

Assuming this relation to hold for the "hot" molecules rebounding from the target, the deflecting force produced is

$$\begin{aligned} \frac{3}{4} \frac{NAC_1}{\sqrt{6\pi}} \cdot \frac{b}{s} \sqrt{\frac{\pi}{6}} \cdot m(C_1' - C_1) &= \frac{3}{16} \frac{pAb}{s} \cdot \left( \frac{T_1' - T_1}{T_1} \right) \\ &= \frac{3}{16} a(1-a) \frac{pAb}{s} \cdot \left( \frac{T_2 - T_1}{T_1} \right). \end{aligned}$$

TABLE II.

$p = 1$  dyne per sq. cm.       $T_2 - T_1 = 36^\circ.6$  C.

*Air.*

No. of Expt.	s. cm.	T <sub>1</sub> °K.	Deflecting force in dynes.		
			Observed.	Calculated from equations (8) & (10).	
				Specular reflexion.	Cosine law.
3.....	.568	291	$9.87 \times 10^{-5}$	$7.61 \times 10^{-5}$	$25.8 \times 10^{-5}$
4.....	.568	291	$9.87 \times 10^{-5}$	$7.61 \times 10^{-5}$	$25.8 \times 10^{-5}$
5.....	.546	291	$10.6 \times 10^{-5}$	$8.23 \times 10^{-5}$	$26.8 \times 10^{-5}$
6.....	.764	291	$5.75 \times 10^{-5}$	$4.20 \times 10^{-5}$	$19.2 \times 10^{-5}$
7.....	.820	290	$5.79 \times 10^{-5}$	$3.66 \times 10^{-5}$	$17.8 \times 10^{-5}$
<i>Hydrogen.</i>			Calculated from equations (9a) & (11).		
1.....	.578	292	$7.61 \times 10^{-5}$	$5.00 \times 10^{-5}$	$15.9 \times 10^{-5}$
2.....	.531	291	$9.05 \times 10^{-5}$	$5.94 \times 10^{-5}$	$17.4 \times 10^{-5}$
3.....	.831	291	$4.53 \times 10^{-5}$	$2.43 \times 10^{-5}$	$11.1 \times 10^{-5}$

The deflecting force due to impact is from (10)

$$K = \frac{3}{4} \cdot \frac{pAb}{\pi s} \left( \frac{T_2 - T_1}{T_1} \right) \times a,$$

and the total deflecting force, after putting  $a = .437$ , is

$$K = .630 \times \frac{3}{4} \cdot \frac{pAb}{\pi s} \cdot \left( \frac{T_2 - T_1}{T_1} \right). \quad . \quad . \quad . \quad (11)$$

A comparison between the observed and calculated values of the deflecting force for air and hydrogen is given in Table II. Each observed value is obtained from the slope of the appropriate  $F-p$  curve at the origin. It will be seen that the assumption of specular reflexion gives

results which are too low, whereas, assuming that the molecules are reflected according to the cosine law, we obtain values which are too high. It would seem probable that reflexion is mainly specular, the low results being due to the underestimation of the number of molecules striking the heater surface per second. This effect was commented on when the heat conducted from the heater by gas molecules at low pressures was calculated.

### 10. Calculation of Mean Free Paths.

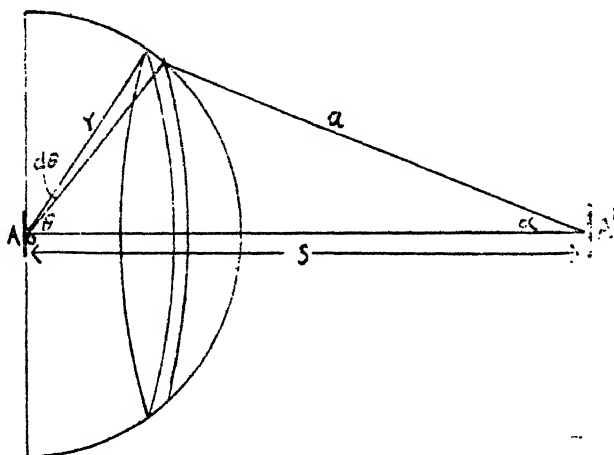
Measurements of the force between heater and target at very low pressures give no idea of the molecular mean free path, since collisions between molecules are rare in comparison with collisions between molecules and the target or heater. At higher pressures collisions between molecules become more frequent, and the deflecting force can be considered as the resultant of two forces :—

- (1) a direct force due to molecules travelling direct from heater surface to target ;
- (2) an indirect force due to the communication of extra energy to " cold " molecules, which subsequently reach the target by collision with " hot " molecules.

Whatever the law of reflexion obeyed by the molecules reflected from the heater surface, the direct deflecting force is proportional to  $pe^{-\frac{s}{L}}$ , where  $L$  is the mean free path of the gas molecules. At very low pressures  $e^{-\frac{s}{L}} = 1$ , and the deflecting force is proportional to the pressure, as already shown. Now  $pe^{-\frac{s}{L}}$  has a maximum value when  $L=s$ , and if the indirect force could be made negligible it would only be necessary to find the pressure for which the deflecting force had a maximal value, to determine the mean free path at this pressure. It was on these lines that experiments were started, but it was not found possible to realise the desired conditions. It is therefore necessary to attempt to calculate the indirect force under various conditions, although an exact analysis is not possible. It will be assumed that the molecules rebounding from the heater surface are specularly reflected, as this assumption

low pressures. Only molecules from the heater A (fig. 14) which collide with other molecules at a distance from A less than  $s$ , and their partners in these collisions, will be considered, as conditions are deliberately chosen so that the effect on A' of molecules colliding at a distance greater than  $s$  will be small. Molecules from A colliding with other molecules more than once before reaching A' and their partners in these collisions will also be ignored, as their effect will be insignificant.

Fig. 14.



The number of molecules reflected from A per second, making an angle between  $\theta$  and  $\theta + d\theta$  with a normal to the surface, is

$$\frac{2NAC_1}{\sqrt{6\pi}} \cdot \sin \theta \cos \theta d\theta,$$

$C_1$  being the R.M.S. speed of the molecules striking A. To simplify matters the molecules leaving A are regarded as leaving O, the geometrical centre of A.

The number of these molecules which collide with other molecules at a distance between  $r$  and  $r + dr$  from A per second is

$$\frac{2NAC_1}{\sqrt{6\pi}} \cdot \sin \theta \cos \theta d\theta e^{-\frac{r}{L}} \cdot \frac{dr}{L},$$

$L$  being the mean free path. (In the case of air the oxygen and nitrogen molecules are assumed to have equal mean free paths.)

The majority of molecules leaving A will collide with molecules moving in the opposite direction, and we may assume, with no great error, that after collision all directions of motion are equally likely for the colliding molecules, so that, owing to the molecules leaving A at an angle between  $\theta$  and  $\theta + d\theta$  with the normal, which collide at a distance between  $r$  and  $r + dr$ ,

$$\frac{4N\Delta C_1}{\sqrt{6\pi}} \sin \theta \cos \theta d\theta e^{-\frac{r}{L}} \frac{dr}{L} \cdot \frac{A' \cos \alpha}{4\pi u^2}$$

molecules with a R.M.S. speed  $\frac{C_1 + C_2}{2}$  will strike A' per second,  $C_2$  being the R.M.S. speed of the molecules leaving A, and it being assumed that on the average a "hot" molecule colliding with a "cold" molecule gives half of its excess energy to the latter. As previously stated, it is assumed that few of these molecules (partners in the first collision) will again collide on their way to the target, and this will be the case provided that  $L$  is not less than  $\frac{s}{2}$ .

If the average force on the target due to the impact of a molecule with R.M.S. speed

$$\frac{C_1 + C_2}{2} \text{ is taken to be } \frac{m(C_1 + C_2)}{2} \cdot \sqrt{\frac{\pi}{6}},$$

as previously explained, the force on the target due to the molecules striking with this speed is

$$\begin{aligned} & \frac{NAA'C_1 \cos \alpha}{\sqrt{6\pi} \pi a^2 L} \cdot \sin \theta \cos \theta d\theta e^{-\frac{r}{L}} \frac{dr}{L} \cdot m \left( \frac{C_1 + C_2}{2} \right) \sqrt{\frac{\pi}{6}} \\ &= \frac{pAA' \cos \alpha}{4\pi a^2 L} \cdot \sin \theta \cos \theta d\theta e^{-\frac{r}{L}} \frac{dr}{L} \left( \frac{C_1 + C_2}{C_1} \right), \end{aligned}$$

and the deflecting force is

$$\begin{aligned} & \frac{pAA' \cos \alpha}{4\pi a^2 L} \sin \theta \cos \theta d\theta e^{-\frac{r}{L}} \frac{dr}{L} \left( \frac{C_2 - C_1}{C_1} \right) \\ &= \frac{pAA' \cos \alpha}{8\pi a^2 L} \sin \theta \cos \theta d\theta e^{-\frac{r}{L}} \frac{dr}{L} \left( \frac{T_2 - T_1}{T_1} \right). \end{aligned}$$

The impulse due to the recoil of these molecules will not contribute to the deflecting force, provided that the

impinging molecules acquire the temperature of the target before leaving. In the case of hydrogen an extra deflecting force must be allowed for, but with air this force is small and will be neglected.

The total deflecting force due to all the molecules which leave the heater surface and collide at a distance from O between  $r$  and  $r+dr$  is

$$dK = \frac{pAA'}{8\pi L} e^{-\frac{r}{L}} dr \left( \frac{T_2 - T_1}{T_1} \right) \int_0^{\frac{\pi}{2}} \sin \theta \cos \theta \cdot \frac{\cos \alpha}{a^2} d\theta.$$

$$\text{But } \cos \alpha = \frac{s - r \cos \theta}{a} \quad \text{and} \quad a^2 = s^2 + r^2 - 2sr \cos \theta,$$

$$\therefore s - r \cos \theta = \frac{s^2 - (r^2 - a^2)}{2s} \quad \text{and} \quad a da = sr \sin \theta d\theta.$$

Hence

$$\begin{aligned} \int_0^{\frac{\pi}{2}} \sin \theta \cos \theta \cdot \frac{\cos \alpha}{a^2} d\theta &= \int_{s-r}^{\sqrt{s^2+r^2}} \left\{ \frac{a da}{sr} \cdot \frac{(s^2 + r^2 - a^2)}{2sr} \right. \\ &\quad \left. \cdot \frac{(s^2 - r^2 + a^2)}{2sa^3} \right\} \\ &= \frac{1}{4s^3 r^2} \int_{s-r}^{\sqrt{s^2+r^2}} \left( \frac{s^4 - r^4 - a^4 + 2a^2 r^2}{a^2} \right) da \\ &= \frac{1}{4s^3 r^2} \left[ \frac{\sqrt{s^2+r^2}}{3} \left( \frac{r^4 - s^4}{a} \right) - \frac{1}{3} a^3 + 2r^2 a \right]. \end{aligned}$$

If we put  $r = sx$ , we obtain

$$\begin{aligned} \frac{1}{4x^2 s^2} &\left[ (1-x)^4 \left\{ \frac{1}{(1-x)} - \frac{1}{\sqrt{1+x^2}} \right\} - \frac{1}{3} \{ (1+x^2)^{\frac{3}{2}} \right. \\ &\quad \left. - (1-x)^3 \} + 2x^2 \{ \sqrt{1+x^2} - (1-x) \} \right] \\ &= \frac{1}{3x^2 s^2} [(1+2x^3) + \sqrt{1+x^2}(2x^2-1)]. \\ dK &= \frac{pAA'}{24\pi Ls} e^{-\frac{sx}{L}} \left( \frac{T_2 - T_1}{T_1} \right) \left[ \left( 2x + \frac{1}{x^2} \right) \right. \\ &\quad \left. + \sqrt{1+x^2} \left( 2 - \frac{1}{x^2} \right) \right] dx. \end{aligned}$$

The expression

$$\left(2x + \frac{1}{x^2}\right) + \sqrt{1+x^2} \left(2 - \frac{1}{x^2}\right)$$

can be replaced by  $\left(\frac{4}{3} + 3x\right)$  with very little error, and making this substitution we have

$$\begin{aligned} K &= \frac{pAA'}{24\pi Ls} \left(\frac{T_2 - T_1}{T_1}\right) \int_0^1 \left(\frac{4}{3} + 3x\right) e^{-\frac{s}{L}x} dx \\ &= \frac{pAA'}{12\pi s^2} \left(\frac{T_2 - T_1}{T_1}\right) \left[\frac{9L}{s} \left(1 - e^{-\frac{s}{L}}\right) + 4 - 13e^{-\frac{s}{L}}\right]. \quad (12) \end{aligned}$$

Equation (12) will probably give values of  $K$  lower than those observed, since from measurements of heat conducted from the heater it was found that the number of impacts per unit-area of the heater was greater than simple theory indicated. To allow for this we may put

$$K = kp \left(\frac{T_2 - T_1}{T_1}\right) \left[\frac{9L}{s} \left(1 - e^{-\frac{s}{L}}\right) + 4 - 13e^{-\frac{s}{L}}\right],$$

$k$  being constant for any given experiment.

Similarly we can put for the direct force

$$k_1 p \left(\frac{T_2 - T_1}{T_1}\right) e^{-\frac{s}{L}},$$

$k_1$  also being constant, so that the total deflecting force is

$$K = kp \left(\frac{T_2 - T_1}{T_1}\right) \left[\frac{9L}{s} \left(1 - e^{-\frac{s}{L}}\right) + 4 - e^{-\frac{s}{L}} \left(13 - \frac{k_1}{k}\right)\right]. \quad (13)$$

Equation (13) is found to agree with the experimentally determined  $F-p$  curves when  $\frac{k_1}{k} = 9$ . The equation then becomes

$$K = kp \left(\frac{T_2 - T_1}{T_1}\right) \left(1 - e^{-\frac{s}{L}}\right) \left(\frac{9L}{s} + 4\right).$$

If, now, the pressure is doubled,  $L$  will be halved, and if  $K_1$  is the new value of the deflecting force, then

$$K_1 = 2kp \left(\frac{T_2 - T_1}{T_1}\right) \left(1 - e^{-\frac{2s}{L}}\right) \left(\frac{9L}{2s} + 4\right).$$

$$\therefore \frac{K_1}{K} = \frac{\left(1 + e^{-\frac{s}{L}}\right) \left(\frac{9L}{s} + 8\right)}{\left(\frac{9L}{s} + 4\right)} = \frac{F_1}{F},$$

$F_1$  and  $F$  being obtained from the appropriate  $F-p$  curve.

If  $L=s$  at the pressure  $p$ , we have

$$\frac{F_1}{F} = \frac{(1 + e^{-1}) \times 17}{13} = 1.79.$$

The value of  $p$  satisfying this condition can be found from the  $F-p$  curve.

If  $L=\frac{s}{2}$  at the pressure  $p$ ,

$$\frac{F_1}{F} = \frac{(1 + e^{-2}) \times 12.5}{8.5} = 1.67.$$

TABLE III.

<i>Air.</i>						
No. of Expt.	$F$ .	$F_1$ .	$\frac{F_1}{F}$ .	$p$ .	$s$ .	$L$ at .01 mm.
				mm.	mm.	mm.
3.....	.775	1.39	1.79	.0075	5.68	4.26
3.....	1.15	1.92	1.67	.012	5.68	3.41
6.....	.415	.742	1.79	.0070	7.64	5.35
6.....	.742	1.24	1.67	.014	7.64	5.35
7.....	.54	.90	1.67	.010	8.20	4.10
<i>Hydrogen.</i>						
1.....	1.065	1.91	1.79	.014	5.78	8.09
2.....	1.36	2.43	1.79	.015	5.31	7.97
3.....	.696	1.16	1.67	.016	8.31	6.65
3.....	.464	.830	1.79	.010	8.31	8.31

The value of  $p$  satisfying this equation can similarly be found.

The value of  $L$  being known at one pressure, it can be found at any other, since  $p \times L$  is constant.

Values of  $L$  calculated in the manner indicated are given in Table III.

The variation in the values obtained for  $L$  is partly due to limitations of the theory, and partly due to the fact that small errors in the determination of  $F$  lead to large errors in the values of  $L$ .

In the case of hydrogen, both direct and indirect forces have to be multiplied by  $a(2-a)$ ,  $a$  being the accommodation coefficient, but the method used for air to determine  $L$  can be used without alteration.



11. *Summary.*

An apparatus for measuring the force between two small, plane, parallel plates, due to a difference of temperature between them at low pressures, is described. It is found that the force is proportional to the temperature difference, other factors remaining constant, and inversely proportional to the square of the distance between the plates, provided that the distance is large compared with the linear dimensions of the plates. Both with air and hydrogen the force is found to increase linearly with the pressure at low pressures, other factors remaining constant, and under these conditions the calculated values of the deflecting force are found to agree with the observed values, allowing for some uncertainty as to the manner in which impinging molecules are reflected from the two plates. At higher pressures the deflecting force increases less rapidly than the linear relation requires, and exhibits a maximum value at about  $\cdot 07$  mm. in the case of air, thereafter slowly declining with increasing pressure. With hydrogen no maximum is obtained, although had measurements been continued at still higher pressures there is no doubt that the deflecting force would have reached a maximum value at about  $\cdot 13$  mm. From the deviations from a linear relation the mean free paths of air and hydrogen molecules at a given pressure have been calculated, and the values obtained agree with the values obtained by other methods as well as can be expected, considering the uncertainties involved in the calculation. Theoretical reasoning is adduced to explain the observed variation of the deflecting force with pressure.

The material of this publication is largely taken from a Thesis approved for the Degree of Doctor of Philosophy in the University of London.

In conclusion, the author would like to thank Professor J. R. Partington for his interest in the work.

Chemistry Department,  
East London College,  
University of London.

XIII. *Studies in Coordination.* Part I.—*Ion Hydrates.*  
By F. J. GARRICK\*.

1. *Introduction.*

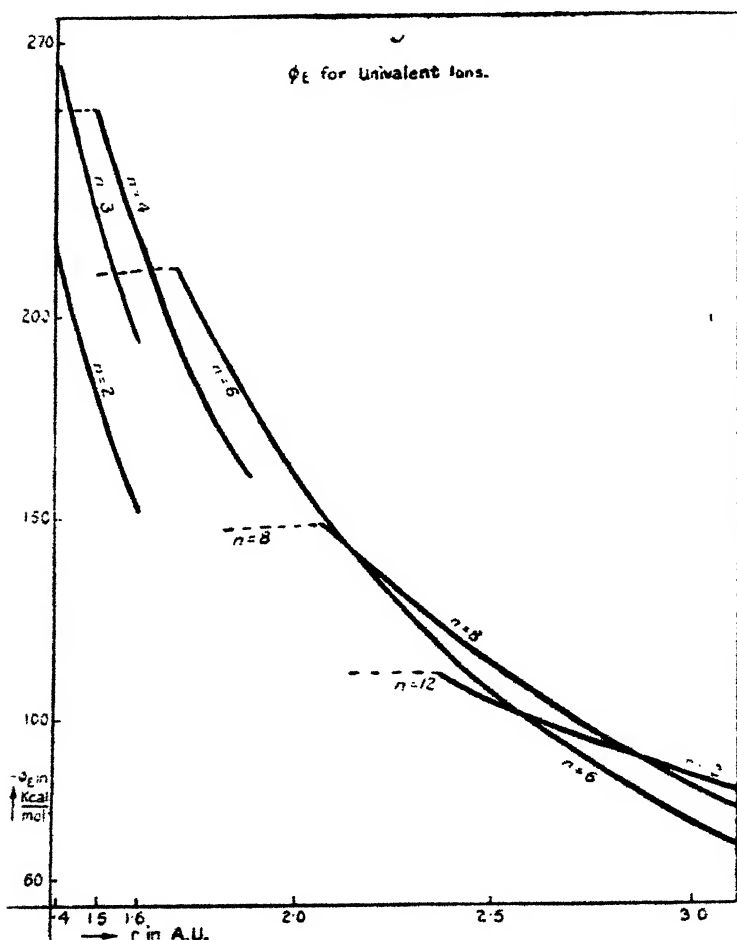
**T**HERE are at present two distinct theories of the formation of such molecular compounds as ammino- and hydrato-complex ions. On the one hand, there is Sidgwick's Coordination Covalency Theory, which is remarkably successful as representing a vast number of chemical phenomena, but which cannot well be applied quantitatively, since nothing is known about the mechanism of this coordinate electron-sharing link. Thus this theory affords little indication as to why the coordination number should have the values actually observed

On the other hand, it is held by many that the mechanism of this type of complex formation is purely electrostatic, depending on the dipole moment and polarizability of the water or ammonia molecule. This view has the advantage of introducing no new concepts, and of being readily susceptible to quantitative investigation. In the present paper an attempt is made by means of such quantitative investigation to show that the theory affords an adequate representation of the observed phenomena.

A qualitative consideration shows that, as is observed, the coordination number should be larger for large ions, but the complex less stable. For, if we consider a number of dipoles, each having its axis radial to a central charge, it is clear that, while all are attracted by the latter, they repel one another, and this repulsion increases with the number of dipoles present. At a particular distance from the central ion it may happen that with six dipoles the attractive force is greater than the repulsive, while with eight the reverse is the case. On increasing the distance, however, the attraction falls off as the inverse cube, the repulsion as the inverse fourth power of the distance, so that at a sufficient distance, even with eight dipoles, the attractive force will exceed the repulsive. Also, if the water or ammonia molecules are considered as impenetrable spheres of fixed radius, for any given coordination number there exists a lower limit to the distance from the centre, when the molecules touch one another but not the central ion. Thus for a small ion when six water molecules are present, they can approach the central ion more closely than when eight are present, and

\* Communicated by the Author.

thus the smaller number may correspond to a greater energy of formation. Both these effects can be seen on the figure, which represents the electrostatic energy of a univalent hydrato-complex ion (calculated according to the method to be described) for various coordination numbers and distances from the central ion. This figure shows how, if the complex having the maximum formation energy is assumed to be



most stable, the coordination number increases with the size of the central ion. A number of other factors must also be considered. First, the molecules are not impenetrable spheres but exert repulsive forces falling off inversely as a high power of the distance. Then, as the above-mentioned lower limits are approached, the potential energy corresponding to these repulsive forces increases rapidly. Also,

the molecules are held in an equilibrium position by the electrostatic forces and the intrinsic repulsive forces between ion and molecules and between the molecules themselves. Thus for a given ion the equilibrium distance is greater, the more molecules are present. All these factors work in the same direction, namely, in favour of a smaller coordination number.

This line of argument will now be treated quantitatively by calculating the energy of formation of various complex ions.

## 2. The Electrostatic Energy.

This may be written

$$\phi_E = \phi_A + \phi_{ER} + \phi_P.$$

Here  $\phi_A$  refers to the attraction between charge and dipoles,  $\phi_{ER}$  to the mutual repulsions of the dipoles, and  $\phi_P$  to the quasi-elastic energy of polarization.

If  $z$  be the valency of the ion, and  $ze$  its charge, and if there be  $n$  molecules, each having the electric moment  $p$ , and each having its axis radial to the ion, and at a distance  $r$ , we have

$$\phi_A = -npze r^{-2} \dots \dots \dots (1)$$

Again, if  $p'$  be the induced part of the dipole moment of each molecule (so that  $p = p' + P$ , where  $P$  is the permanent dipole moment), and if  $\alpha$  be the polarizability, we have

$$p' = \alpha E,$$

where  $E$  is the field strength, and thus

$$\phi_P = np'^2/2\alpha \dots \dots \dots (2)$$

$\phi_{ER}$  is the sum of a number of terms of the form

$$\frac{p^2}{s^3} (\sin \theta_1 \sin \theta_2 - 2 \cos \theta_1 \cos \theta_2).$$

This is the mutual potential energy of two dipoles at a distance  $s$  making angles  $\theta_1$  and  $\theta_2$  with their axes. We only consider cases where the dipoles are arranged radially and symmetrically, so that

$$\theta_1 = 180^\circ - \theta_2.$$

We may write

$$\phi_{ER} = \sum_{k=1}^{k=\frac{n(n-1)}{2}} \frac{p^2}{s_k^3} (1 + \cos^2 \theta_k) \dots \dots \dots (3)$$

The following cases are considered:—

1.  $n=2$ . Here  $s=2r$ ;  $\theta=0^\circ$ .

2.  $n=3$  (equilateral triangle).

$$s_1=s_2=s_3=r\sqrt{3}; \theta_1=\theta_2=\theta_3=30^\circ.$$

3.  $n=4$  (regular tetrahedron).

$$s_1=s_2=\dots=s_6=2r\frac{\sqrt{2}}{\sqrt{3}}; \theta_1=\theta_2=\dots=\theta_6=35^\circ.77.$$

4.  $n=6$  (regular octahedron).

$$s_1=s_2=\dots=s_{12}=r\sqrt{2}; \theta_1=\theta_2=\dots=\theta_{12}=45^\circ.$$

$$s_{13}=s_{14}=s_{15}=2r; \theta_{13}=\theta_{14}=\theta_{15}=0^\circ.$$

5.  $n=8$  (cube).

$$s_1=s_2=\dots=s_{12}=\frac{2r}{\sqrt{3}}; \theta_1=\theta_2=\dots=\theta_{12}=\cos^{-1}\frac{1}{\sqrt{3}};$$

$$s_{13}=s_{14}=\dots=s_{24}=\frac{2\sqrt{2}}{\sqrt{3}}.r; \theta_{13}=\theta_{14}=\dots=\theta_{24}=\cos^{-1}\frac{\sqrt{2}}{\sqrt{3}};$$

$$s_{25}=s_{26}=s_{27}=s_{28}=2r; \theta_{25}=\theta_{26}=\theta_{27}=\theta_{28}=0^\circ.$$

6.  $n=12$  (regular icosahedron).

$$s_1=s_2=\dots=s_{30}=1.052r; \theta_1=\theta_2=\dots=\theta_{30}=\cos^{-1}0.526;$$

$$s_{31}=s_{32}=\dots=s_{60}=1.702r; \theta_{31}=\theta_{32}=\dots=\theta_{60}=\cos^{-1}0.851;$$

$$s_{61}=s_{62}=\dots=s_{66}=2r; \theta_{61}=\theta_{62}=\dots=\theta_{66}=0^\circ.$$

In these equations  $p$  depends on  $z$ ,  $r$ , and  $n$ , as follows. We have, as above,

$$p' = \alpha F. \quad . \quad . \quad . \quad . \quad . \quad . \quad (5)$$

The field strength  $E$  at a point representing the position of one of the molecules is the vector sum of components due to the central ion and to the other dipoles. We need only consider the components along the line joining the molecule in question to the central ion, since from symmetry the components at right angles to this neutralize one another. The component of the field strength due to the central ion is  $ze/r^2$ . That due to the other dipoles is

$$-E_d = \frac{dV_d}{dr},$$

where  $V_d$  is the potential at the point in question due to the other dipoles.

We have

$$V_d = \sum_{k=1}^{k=(n-1)} \frac{p}{s_k^2} \cos \theta_k ;$$

$$d\theta_k = \frac{dr}{s_k} \sin \theta_k ; \quad ds_k = dr \cdot \cos \theta_k.$$

$$\therefore E_d = -\frac{dV_d}{dr} = \sum_{k=1}^{k=(n-1)} \frac{p}{s_k^3} (1 + \cos^2 \theta_k). \quad (6)$$

Then

$$E = \frac{ze}{r^2} - E_d, \quad \text{and} \quad p = p' + P.$$

$$\therefore p = P + \alpha E = \frac{P + \frac{\alpha ze}{r^2}}{1 + \sum_{k=1}^{k=(n-1)} \frac{\alpha}{s_k^3} (1 + \cos^2 \theta_k)}. \quad (7)$$

In equations (6) and (7),  $s_k$  and  $\theta_k$  are as given below.

$$\text{When } n=2, \quad s=2r ; \quad \theta=0^\circ.$$

$$,, \quad n=3, \quad s_1=s_2=r\sqrt{3} ; \quad \theta_1=\theta_2=30^\circ.$$

$$,, \quad n=4, \quad s_1=s_2=s_3=\frac{2\sqrt{2}}{\sqrt{3}} r ;$$

$$\theta_1=\theta_2=\theta_3=35^\circ 77.$$

$$,, \quad n=6, \quad s_1=s_2=\dots=s_4=r\sqrt{2} ;$$

$$\theta_1=\theta_2=\dots=\theta_4=45^\circ ;$$

$$s_5=2r ; \quad \theta_5=0^\circ.$$

$$,, \quad n=8, \quad s_1=s_2=s_3=\frac{2r}{\sqrt{3}} ;$$

$$\theta_1=\theta_2=\theta_3=\cos^{-1} \frac{1}{\sqrt{3}} ;$$

$$s_4=s_5=s_6=\frac{2\sqrt{2}}{\sqrt{3}} r ;$$

$$\theta_4=\theta_5=\theta_6=\cos^{-1} \frac{\sqrt{2}}{\sqrt{3}} ;$$

$$s_7=2r ; \quad \theta_7=0^\circ.$$

$$,, \quad n=12, \quad s_1=s_2=\dots=s_5=1.052 r ;$$

$$\theta_1=\theta_2=\dots=\theta_5=\cos^{-1} 0.526 ;$$

$$s_6=s_7=\dots=s_{10}=1.702 r ;$$

$$\theta_6=\theta_7=\dots=\theta_{10}=\cos^{-1} 0.851 ;$$

$$s_{11}=2r ; \quad \theta_{11}=0^\circ.$$

In applying these equations we consider the case of a hydrate-complex. Then  $P$  is  $1.75 \times 10^{-18}$  E.S.U., this being the mean of the two latest determinations—1.70 (Williams, *Z. Phys.* xxix. p. 683, 1928) and 1.79 (Stuart, *Z. Phys.* li. p. 490, 1928); while  $\alpha$  is given by  $\alpha = 3R/4\pi N$ , where  $R$  is the Lorentz retraction constant for water ( $=3.71$ ), and  $N$  is the Avogadro number ( $=6.06 \times 10^{23}$ ). This gives  $\alpha = 1.46 \times 10^{-24}$ .  $e$ , the electronic charge, is taken as  $4.774 \times 10^{-10}$ .

By means of the equations given above the electrostatic part  $\phi_E$  of the energy of a complex ion of given valency and coordination number can be calculated for various values of  $r$ , and the results for univalent ions are shown in the figure, where the ordinates represent  $-\phi_E$  in k. cal./mol. and the abscissæ  $r$  in A.U. The horizontal dotted lines show the energies corresponding to the lower limits of  $r$  in various cases, when the water molecule is regarded as an impenetrable sphere of radius about 1.2 A.U. These energies are therefore maxima for the corresponding coordination numbers.

The curves for divalent complexes are not shown, as the relations are closely similar, except that the energies are much greater. From these results alone, and neglecting the other factors mentioned above, it is possible to draw some interesting conclusions, since the other energy terms are for the most part not more than about 15 per cent. of  $\phi_E$ , as will appear later.

First,  $-\phi_E$  is less for  $n=2$  or 3 than for  $n=4$ , when  $r$  is greater than 1.4. Since the effective radius of a water molecule is about 1.2 A.U., and assuming that the stable complex is that having the maximum energy of formation, this means that for all ordinary ions the maximum coordination number is 4 or more. Then for  $r$  greater than 1.65,  $-\phi_E$  is greater for  $n=6$  than for  $n=4$ . Thus for ions of radius greater than about 0.5 A.U. the coordination number is 6 or more. The only ordinary ions smaller than this are  $H^+$ ,  $Be^{2+}$ , and possibly  $Li^+$ . For the other ions, then, it is enough to consider only  $n=6, 8$ , or 12 (*cp.* data for  $Na^+$  in Table III.).

The  $H^+$  ion is probably incapable of free existence and in solution is thought to be present as  $H_3O^+$ . For  $Be^{2+}$  (radius 0.3 A.U.) and possibly  $Li^+$  (radius 0.6 A.U.) the consideration of  $\phi_E$  alone implies that the coordination number is probably 4, but no more definite conclusions than this can be reached, since in the absence of information as to their force constants the more detailed treatment to be described for the other ions cannot be applied to them.

### 3. The Determination of the Total Energy in Particular Cases.

To determine the total energy it is necessary first to find the equilibrium distance for each ion (for, as was pointed out above, this will in general be different for different hydrates of the same ion), and second to estimate the non-electrostatic energy corresponding to the intrinsic repulsive fields. To attain these ends it is necessary to estimate the force laws of the ions and the water molecules. No direct information is available as to the applicability of spherically symmetric fields to a water molecule, nor as to the values of the force constants. But it is at least reasonable to suppose that the force law can be approximately represented by an expression of the type  $\lambda r^{-\nu}$ , and in the absence of any more definite data the values of  $\lambda$  and  $\nu$  will be deduced by means of certain more or less plausible assumptions.

The repulsive force fields of a number of ions of inert-gas type have been investigated by Lennard-Jones\*. In determining the force constants it is assumed that the "generalized diameters" are proportional to the radii of the outer electron orbits, and it seems reasonable to suppose that they are proportional to the effective radii as measured by any one appropriate method. Now the water molecule may be regarded as a pseudo-atom of the Ne type: that is, the protons are buried inside the electron shell of the oxide ion†. It will be assumed that the resulting electron structure is sufficiently like that of the ions of the Ne type that the same force index (namely, 11) may be applied, and that the generalized diameter of the water molecule is to that of a Ne atom in the ratio of their kinetic theory diameters, that is, according to Landolt-Börnstein, as 1.3 to 1.15.

Then using the notation of Lennard-Jones (except that  $\nu$  is written instead of  $n$  for the index), we have

$$\sigma_{\text{H}_2\text{O}}^{(\nu)} = \sigma_{\text{Ne}}^{(\nu)} \cdot \frac{1.3}{1.15}, \quad \dots \dots \dots (8)$$

$\sigma^{(\nu)}$  is, of course, a function of  $\nu$ . For the values of  $\nu$  we use those given by Lennard-Jones for the Ne group, namely 11 for two ions of this type or one of this type and one of Xe type, or 10 for an ion of this type and one of Ar or Kr type.

\* Lennard-Jones, Proc. Roy. Soc. A, cix. p. 584 (1925); Lennard, Jones and Taylor, *ibid.* p. 476.

† Knorr, Z. Anorg. Chem. cxxix. p. 109 (1923); Paneth and Rabino-witsch, Ber. d. D. Chem. Ges. lviii. p. 1138 (1925); Grimm, Z. Elektro-chem. xxxi. p. 476 (1925). See also Garrick, Phil. Mag. 1929, p. 102.



(The term ion in this connexion, of course, includes neutral atoms, and is here extended to the pseudo-atom  $\text{H}_2\text{O}$ .) Table I. shows the values of  $\sigma_{\text{H}_2\text{O}}^{(\nu)}$  for  $\nu=10$  and  $\nu=11$ . Here the values of  $\sigma_{\text{Ne}}^{(\nu)}$  are taken from Lennard-Jones (*loc. cit.*), and those of  $\sigma_{\text{H}_2\text{O}}^{(\nu)}$  are derived from them by equation (8).

TABLE I.

$\nu$ .	$\sigma_{\text{Ne}}^{(\nu)}$ .	$\sigma_{\text{H}_2\text{O}}^{(\nu)}$ .
10 .....	4.63	5.24
11 .....	4.30	4.86

Then to calculate the force constant for an ion and a water molecule, we use the relations

$$\sigma_{12}^{(\nu)} = \frac{(\sigma_{11}^{(\nu)} + \sigma_{22}^{(\nu)})}{2} \quad \text{and} \quad \sigma^{(\nu)} = \left( \frac{\lambda^{(\nu)}}{2.06 \times 10^{-16} \cdot (\nu-1)} \right)^{\frac{1}{\nu-1}}$$

TABLE II.

Ion.		$\nu$ .	$10^8 \cdot \sigma_{\text{ion}}^{(\nu)}$ .	$\frac{1}{2} \cdot 10^8 \cdot (\sigma_{\text{ion}}^{(\nu)} + \sigma_{\text{H}_2\text{O}}^{(\nu)})$ .	$\lambda_{\text{ion-H}_2\text{O}}^{(\nu)}$ .
Na <sup>+</sup> .....	11		4.03	4.44	0.612
K <sup>+</sup> .....	10		5.93	5.58	0.972
Rb <sup>+</sup> .....	10		6.41	5.82	1.42
Cs <sup>+</sup> .....	11		6.50	5.68	7.20
Mg <sup>++</sup> .....	11		3.51	4.19	0.344
Ca <sup>++</sup> .....	10		5.45	5.34	0.655
Sr <sup>++</sup> .....	10		5.98	5.61	1.02
Ba <sup>++</sup> .....	11		6.01	5.43	4.59

(Lennard-Jones and Taylor, *loc. cit.* pp. 482 and 483). The force constants so obtained are shown in Table II.  $\lambda$  is given in such units that when  $r$  is in A.U. the force is in dynes. The values of  $\sigma_{\text{ion}}^{(\nu)}$  are taken from Lennard-Jones, *loc. cit.* tab. viii.

These constants when substituted in the expression  $\lambda r^{-\nu}$  give as a function of  $r$  the repulsive force between the above ions and a water molecule. For an ion of known valency and for a particular number of water molecules the net electrostatic force on each water molecule can also be plotted as a function of  $r$ , and hence by graphical solution the equilibrium distances for the various systems in question can be obtained. The electrostatic attraction on each molecule, in the line joining it to the central ion, is

$$F_E = p \cdot \frac{dE}{dr}.$$

But

$$E = \frac{ze}{r^2} - \sum_{k=1}^{k=(n-1)} \frac{p}{s_k^3} (1 + \cos^2 \theta_k). \quad (6)$$

Whence

$$F_E = p \cdot \frac{dE}{dr} = -\frac{2ze p}{r^3} + \sum_{k=1}^{k=(n-1)} \frac{p^2}{s_k^4} (5 + \cos^2 \theta_k) \cos \theta_k.$$

In these equations  $s_k$  and  $\theta_k$  have the values given above for equation (7). In many cases, when the lower limits mentioned above are approached, the mutual intrinsic repulsions of the water molecules must be allowed for. Only the nearest neighbours of each molecule exert an appreciable repulsion. If  $x$  be the number of such neighbours, and  $s$  and  $\theta$  the appropriate values of  $s_k$  and  $\theta_k$ , the repulsion due to them is  $x \cdot 1.515 s^{-11} \cos \theta$ . Here 1.515 is, of course, the force constant for two water molecules. All the necessary data are now available for the calculation of the equilibrium distances. By substitution of these and the appropriate values of  $p$  (from (7)) in (1), (2), and (3), the electrostatic energy  $\phi_E$  is determined. The total energy  $\phi$  includes two other terms due to the intrinsic repulsions between ion and molecules and between the molecules themselves. These are

$$\phi_{R_1} = \frac{n\lambda}{\nu-1} r^{-(\nu-1)} \quad \text{and} \quad \phi_{R_2} = \frac{nx}{2} \cdot \frac{1.515}{10} s^{-10}.$$

Then

$$\phi = \phi_E + \phi_{R_1} + \phi_{R_2}.$$

The results are shown in Table III.  $-\phi_{(n=12)}$  is only given for the two largest ions,  $\text{Cs}^+$  and  $\text{Ba}^{2+}$ . It is always less than  $-\phi_{(n=8)}$ , and, of course, the difference is greater for the smaller ions. The numbers for  $\text{Na}^+_{(n=4)}$  are given in order to illustrate the conclusions of Sect. 2. In the table  $r$  is in A.U., and  $-\phi$  in k.cal./mol.

TABLE III.

Ion.	<i>n</i> .	<i>r</i> .	$-\phi_R$ .	$\phi_{R_1}$ .	$\phi_{R_2}$ .	$-\phi$ .
Na <sup>+</sup> .....	{ 4	2.05	132	26	4	102
	{ 6	2.22	135	18	3	114
	{ 8	2.53	112	7	8	97
K <sup>+</sup> .....	{ 6	2.58	102	18	1	83
	{ 8	2.83	95	11	3	81
Rb <sup>+</sup> .....	{ 6	2.71	93	15	0	78
	{ 8	2.92	90	10	2	78
Cs <sup>+</sup> .....	{ 6	2.92	81	14	0	67
	{ 8	3.09	82	10	1	71
	{ 12	3.6	70	3	1	66
Mg <sup>++</sup> .....	{ 6	1.81	586	75	22	489
	{ 8	2.08	473	14	42	417
Ca <sup>++</sup> .....	{ 6	2.08	441	99	5	340
	{ 8	2.28	400	51	17	332
Sr <sup>++</sup> .....	{ 6	2.20	390	86	3	301
	{ 8	2.35	369	54	11	304
Ba <sup>++</sup> .....	{ 6	2.37	332	66	1	265
	{ 8	2.53	320	33	6	290
	{ 12	2.8	313	19	13	281

## 4. Discussion of Results.

As regards the accuracy of the results the actual values of  $\phi$  are very doubtful, since  $P$  is far from certainly known, while it is highly improbable that  $\alpha$  remains constant for extreme polarizations. Moreover, the procedure used to determine the force constants may be very unsound, but this does not make much difference since large changes in  $\lambda$  only affect  $r$  slightly, while  $\phi_R$ , and  $\phi_{R_2}$  are small terms.

On the other hand, it seems likely that for the same ion with different values of  $n$ , the relative magnitudes of  $\phi$  are not far from the truth, since the errors should produce much the same effect in both cases. Since for our present purpose of determining the coordination numbers we need only the relative magnitudes of  $\phi$  for various hydrates of the same ion, it seems that the numbers may be used with fair confidence. Assuming, then, that the most stable hydrate is that for which  $-\phi$  is a maximum, we find:—

The coordination number is six for

Na<sup>+</sup>, K<sup>+</sup>, Mg<sup>++</sup>, and Ca<sup>++</sup>.

The coordination number is *eight* for

$\text{Cs}^+$ ,  $\text{Sr}^{++}$ , and  $\text{Ba}^{++}$

(for  $\text{Rb}^+$  the hexa- and octo-hydrates are about equally stable).

The coordination number is *four or six* for

$\text{Li}^+$  and  $\text{Be}^{++}$ .

The coordination number *twelve* is never found.

These results may be compared with Sidgwick's covalency rule ('The Electronic Theory of Valency', p. 152 : Oxford, 1927), "The maximum covalency (coordination number) is . . . . for the elements of the first short period 4, for the second short and first long periods 6, and for the heavier elements (Rb to U) 8."

It appears, then, that the electrostatic mechanism agrees satisfactorily with observation in the case of hydrates. It is hoped in later papers to apply the theory to other types of complex, and it may become possible to test it more stringently by direct comparison of theoretical and experimental energy quantities.

The author's thanks are due to Professor Lennard-Jones for kindly criticism and advice.

Inorganic Chemistry Dept.,  
The University,  
Leeds.

#### XIV. *The Kirchhoff Formula extended to a Moving Surface.*

By W. R. MORGANS, M.Sc., late Garrod Thomas Fellow of the University College of Wales, Aberystwyth; Commonwealth Fellow, California Institute of Technology, Pasadena\*.

##### 1. *The Kirchhoff Formula*

IT is well known that if  $\phi$  be a function which satisfies the wave equation

$$\nabla^2 \phi = \frac{1}{c^2} \frac{\partial^2 \phi}{\partial t^2}$$

within a volume  $\Omega$ , bounded by a fixed surface  $\sigma$ , and if  $\phi$  and its first derivatives are continuous and finite within that

\* Communicated by Prof. G. A. Schott, F.R.S.

volume, while the second derivatives exist and are finite, then the value of the function  $\phi$  at time  $t_0$  at a point  $P(\xi \eta \zeta)$  within the volume is given by a surface integral extended to the fixed surface  $\sigma$  of the form

$$\phi_P(t_0) = \frac{1}{4\pi} \int_{\sigma} \left\{ \frac{1}{r} \left[ \frac{\partial \phi}{\partial n} \right] - [\phi] \frac{\partial}{\partial n} \left( \frac{1}{r} \right) + \frac{1}{cr} \frac{\partial r}{\partial n} \left[ \frac{\partial \phi}{\partial t} \right] \right\} d\sigma. \quad \dots (1)$$

The square brackets mean that the enclosed functions of the time are to be taken for a time  $t$  given in terms of the time  $t_0$  by the equation

$$t = t_0 - r/c,$$

where  $r$  is the distance from the field point  $P(\xi \eta \zeta)$  to an element  $d\sigma$  of the surface, and  $n$  is the outward normal.

To assume that the surface  $\sigma$  is fixed is an unnecessary limitation on the generality of the solution, and it has been noticed that in a number of physical problems a similar type of solution is required, but one which is applicable to a moving surface  $S$ . In such cases the formula given by Kirchhoff for a fixed surface is not applicable. We shall, therefore, present a solution of the wave equation in the form of a surface integral extended to a moving surface  $S$  bounding a volume  $\Omega$ , in which the function  $\phi$  and its derivatives satisfy the conditions of finiteness and continuity as mentioned above. The method followed will be that of Kirchhoff, and the final result will show that the Kirchhoff formula is a particular case of the extended formula when the normal velocity of the surface is equated to zero.

In the following discussion we shall denote a fixed surface by  $\sigma$ , a moving surface by  $S$ , a volume integral by  $\int_{\Omega} d\Omega$ , a surface integral by  $\int_{\Omega} dS$ , and the outward normal to the surface by  $n$ .

## 2. The Kirchhoff Formula extended to a Moving Surface.

Let  $\phi$  and  $\chi$  be two functions which satisfy the equations

$$\nabla^2 \phi = \frac{1}{c^2} \frac{\partial^2 \phi}{\partial t^2}; \quad \nabla^2 \chi = \frac{1}{c^2} \frac{\partial^2 \chi}{\partial t^2} \quad \dots (2)$$

within a volume  $\Omega$  and such that they and their first derivatives are finite and continuous, while the second derivatives

exist and are finite within  $\Omega$ . Then Green's Theorem gives for a volume bounded by a surface, moving or fixed, the expression

$$\int_{\Omega} (\phi \nabla^2 \chi - \chi \nabla^2 \phi) d\Omega = \int_S \left( \phi \frac{\partial \chi}{\partial n} - \chi \frac{\partial \phi}{\partial n} \right) dS.$$

If the point P,  $r=0$ , within the volume  $\Omega$  be surrounded by a fixed infinitesimal sphere  $\sigma$ , and if we notice that

$$\phi \nabla^2 \chi - \chi \nabla^2 \phi = \frac{1}{c^2} \frac{\partial}{\partial t} \left( \phi \frac{\partial \chi}{\partial t} - \chi \frac{\partial \phi}{\partial t} \right),$$

the above becomes

$$\begin{aligned} & \frac{1}{c^2} \int_{\Omega} \frac{\partial}{\partial t} \left( \phi \frac{\partial \chi}{\partial t} - \chi \frac{\partial \phi}{\partial t} \right) d\Omega \\ &= \int_S \left( \phi \frac{\partial \chi}{\partial n} - \chi \frac{\partial \phi}{\partial n} \right) dS + \int_{\sigma} \left( \phi \frac{\partial \chi}{\partial n} - \chi \frac{\partial \phi}{\partial n} \right) d\sigma. \quad (3) \end{aligned}$$

It is known that if the volume  $\Omega$ , bounded by a surface S with normal velocity  $v$ , is a function of the time, the following expression holds :

$$\frac{\partial}{\partial t} \int_{\Omega} f d\Omega = \int_{\Omega} \frac{\partial f}{\partial t} d\Omega + \int_S v f dS,$$

where  $f$  is any function of  $x, y, z, t$ .

Applying this to (3) we obtain

$$\begin{aligned} & \frac{1}{c^2} \frac{\partial}{\partial t} \int_{\Omega} \left( \phi \frac{\partial \chi}{\partial t} - \chi \frac{\partial \phi}{\partial t} \right) d\Omega \\ &= \frac{1}{c^2} \int_S v \left( \phi \frac{\partial \chi}{\partial t} - \chi \frac{\partial \phi}{\partial t} \right) dS + \int_S \left( \phi \frac{\partial \chi}{\partial n} - \chi \frac{\partial \phi}{\partial n} \right) dS \\ & \quad + \int_{\sigma} \left( \phi \frac{\partial \chi}{\partial n} - \chi \frac{\partial \phi}{\partial n} \right) d\sigma. \quad (4) \end{aligned}$$

No other surface integral arises from  $\sigma$  due to its having zero normal velocity. If (2) holds for all values of  $t$ , we may integrate between two values of  $t$ ,  $-t_1$  and  $t_2$ , where  $t_1$  and  $t_2$  are both positive and such that for the most distant parts of S,

$$-t_1 - t_0 + r/c < 0, \quad t_2 - t_0 + r/c > 0.$$

We obtain

$$\begin{aligned} \frac{1}{c^2} \int_{-t_1}^{t_2} dt \int_S v \left( \phi \frac{\partial \chi}{\partial t} - \chi \frac{\partial \phi}{\partial t} \right) dS + \int_{-t_1}^{t_2} dt \int_S \left( \phi \frac{\partial \chi}{\partial n} - \chi \frac{\partial \phi}{\partial n} \right) dS \\ = \frac{1}{c^2} \left| \int_{\Omega} \left( \phi \frac{\partial \chi}{\partial t} - \chi \frac{\partial \phi}{\partial t} \right) d\Omega \right|_{-t_1}^{t_2} \\ - \int_{-t_1}^{t_2} dt \int_{\sigma} \left( \phi \frac{\partial \chi}{\partial n} - \chi \frac{\partial \phi}{\partial n} \right) d\sigma. \quad (5) \end{aligned}$$

We are going to particularize the function  $\chi$  from being any solution of the wave equation to one of the form  $F(ct - ct_0 + r)/r$ , where  $F(\zeta)$  vanishes for  $\zeta = \pm \infty$ , is appreciable only for  $\zeta = 0$ , and is such that

$$\int_{-\infty}^{\infty} F(\zeta) d\zeta = 1.$$

That such a function exists may be seen by taking

$$F(\zeta) = \text{Lt}_{a \rightarrow 0} \pi(\zeta^2 + a^2)^{-a}.$$

In fact,  $F(\zeta)$  can be made to differ from zero outside the arbitrary small interval  $+\delta, -\delta$ , ( $\delta > 0$ ) by as small a quantity as we please. By such a choice of  $F(\zeta)$  it is seen

that  $\chi$  and  $\frac{\partial \chi}{\partial t}$  vanish at both limits  $-t_1$  and  $t_2$ , so that the

volume integral in (5) vanishes at both limits. Moreover, as  $\sigma$  is a fixed surface independent of  $t$ , the limits of the surface integral are independent of  $t$ , so that the order of integration can be changed. Therefore

$$\begin{aligned} c \int_{-t_1}^{t_2} dt \int_{\sigma} \left( \phi \frac{\partial \chi}{\partial n} - \chi \frac{\partial \phi}{\partial n} \right) d\sigma \\ = \int_{\sigma} d\sigma \int_{-t_1}^{t_2} \left( \phi \frac{\partial \chi}{\partial n} - \chi \frac{\partial \phi}{\partial n} \right) c dt. \end{aligned}$$

Due to the change of order of integration and the choice of the function  $\chi$ , the integral can be evaluated. With Kirchhoff\*, its value as the sphere  $\sigma$  tends to zero becomes

\* Kirchhoff, 'Zur Theorie der Lichtstrahlen,' 1882.

$4\pi\phi_P(t_0)$ . Then a rearrangement of (5) gives, after multiplication by  $c$ ,

$$4\pi\phi_P(t_0) = \int_{-t_1}^{t_2} c dt \int_S \left\{ \chi \left( \frac{\partial\phi}{\partial n} + \frac{r}{c} \frac{\partial\phi}{\partial t} \right) - \phi \left( \frac{\partial\chi}{\partial n} + \frac{v}{c} \frac{\partial\chi}{\partial t} \right) \right\} dS. \quad (6)$$

Here, however, the change of order of integration is not permissible owing to the fact that the limits of the surface integration are functions of the time. To overcome the difficulty of the time integration we shall introduce three curvilinear coordinates  $u, v, w$ . The regular surface  $S^*$  can be represented by equations of the form

$$x = f(uv), \quad y = p(uv), \quad z = q(uv),$$

where we shall assume that the variables  $u, v$  are independent of  $ct$  and that  $w$  alone is a function of  $ct$ . The element of area will become in the new system of coordinates

$$dS = \sqrt{EG - F^2} \cdot du dv = H du dv, \quad \dots \quad (7)$$

where

$$E = \left( \frac{\partial x}{\partial u} \right)^2 + \left( \frac{\partial y}{\partial u} \right)^2 + \left( \frac{\partial z}{\partial u} \right)^2,$$

$$F = \frac{\partial x}{\partial u} \frac{\partial x}{\partial v} + \frac{\partial y}{\partial u} \frac{\partial y}{\partial v} + \frac{\partial z}{\partial u} \frac{\partial z}{\partial v},$$

$$G = \left( \frac{\partial x}{\partial v} \right)^2 + \left( \frac{\partial y}{\partial v} \right)^2 + \left( \frac{\partial z}{\partial v} \right)^2.$$

As  $u$  and  $v$  are both independent of  $t$ , the limits of integration in the surface integral, after replacing  $dS$  by  $H du dv$ , will also be independent of  $t$ . Consequently, a change in the order of integration is permissible. From (6) we have

$$4\pi\phi_P(t_0) = \int_S du dv \int_{-t_1}^{t_2} \left\{ \chi \left( \frac{\partial\phi}{\partial n} + \frac{v}{c} \frac{\partial\phi}{\partial t} \right) - \phi \left( \frac{\partial\chi}{\partial n} + \frac{r}{c} \frac{\partial\chi}{\partial t} \right) \right\} H c dt, \quad (8)$$

a form capable of integration.

\* We shall assume the conditions given in Goursat-Hedrick, 'Mathematical Analysis,' § 131, to hold.



Again,

$$\begin{aligned}\chi &= F(ct - ct_0 + r)/r, \\ \frac{\partial \chi}{c \partial t} &= F'/r; \quad F' = \left[ \frac{d}{d\zeta} F(\zeta) \right]_{\zeta = ct - ct_0 + r}, \\ \frac{\partial \chi}{\partial n} &= \left( -\frac{\chi}{r} + \frac{\partial \chi}{c \partial t} \right) \frac{\partial r}{\partial n}, \\ \frac{d\chi}{cdt} &= \frac{\partial \chi}{c \partial t} + \frac{\partial \chi}{\partial r} \frac{\partial r}{c \partial t}, \\ &= \left( 1 + \frac{\dot{r}}{c} \right) \frac{\partial \chi}{c \partial t} - \frac{\chi \dot{r}}{cr},\end{aligned}$$

whence

$$\begin{aligned}\frac{\partial \chi}{c \partial t} &= \left( \frac{d\chi}{cdt} + \frac{\chi \dot{r}}{cr} \right) / \left( 1 + \dot{r}/c \right), \\ \frac{\partial \chi}{\partial n} &= \left( \frac{d\chi}{cdt} - \frac{\chi}{r} \right) \frac{\partial r}{\partial n} / \left( 1 + \dot{r}/c \right), \\ \frac{\partial \chi}{\partial n} + \frac{r}{c} \frac{\partial \chi}{c \partial t} &= \frac{\partial r}{\partial n} + \frac{r}{c} \frac{d\chi}{cdt} - \frac{\partial r}{\partial n} - \frac{rr}{1 + \dot{r}/c} \frac{\chi}{r}.\end{aligned}$$

The integral (8) becomes

$$\begin{aligned}4\pi\phi_P(t_0) &= \int_s du dr \Big|_{-t_1}^t \left\{ \chi \left( \frac{\partial \phi}{\partial n} + \frac{v}{c} \frac{\partial \phi}{\partial t} + \frac{\frac{\partial r}{\partial n} - \frac{rr}{c^2}}{1 + \dot{r}/c} \phi \right) \right. \\ &\quad \left. - \frac{\frac{\partial r}{\partial n} + \frac{r}{c}}{1 + \dot{r}/c} \phi \frac{d\chi}{cdt} \right\} H c dt. \quad (9)\end{aligned}$$

Let us consider any integral of the form  $\int_{-t_1}^{t_2} \chi \mu c dt$ , where  $\mu$  is any function of  $x, y, z, ct$  denoted by  $\mu(ct)$ . With

$$\zeta = ct - ct_0 + r, \quad d\zeta = dt(c + \dot{r}),$$

the integral transforms into

$$\begin{aligned}\int_{-t_1}^{t_2} \chi \mu c dt &= \int_{-t_1}^{t_2} \frac{F(ct - ct_0 + r)}{r} \mu(ct) c dt \\ &= \int_{-\zeta_1}^{\zeta_2} \frac{F(\zeta)}{r} \frac{\mu(\zeta + ct_0 - r)}{(1 + \dot{r}/c)} d\zeta \quad \zeta_1 > 0, \zeta_2 > 0.\end{aligned}$$

Due to the choice of  $F(\xi)$  the contribution is obtained only in the neighbourhood of  $\xi=0$ , which leads to the value given by

$$\int_{-t_1}^{t_2} \chi \mu c dt = \frac{\mu(ct_0 - r)}{r(1 + \dot{r}/c)},$$

where  $\mu$  must be taken at time  $t_0 - r/c$ .

The first part of the integral (9) will give the contribution

$$\int_S du dv \left\{ \frac{H}{r(1 + \dot{r}/c)} \left( \frac{\partial \phi}{\partial n} + \frac{v}{c} \frac{\partial \phi}{\partial t} + \frac{\frac{\partial r}{\partial n} - \frac{\dot{r}v}{c^2}}{1 + \dot{r}/c} \frac{\phi}{r} \right) \right\}_{t=t_0 - r/c}.$$

Let us consider an integral of the form

$$\int_{-t_1}^{t_2} \mu \frac{d\chi}{c dt} c dt.$$

We have

$$\int_{-t_1}^{t_2} \mu \frac{d\chi}{c dt} c dt = \mu \chi \Big|_{-t_1}^{t_2} - \int_{-t_1}^{t_2} \chi \frac{d\mu}{c dt} c dt.$$

The former portion vanishes by the choice of  $\chi$ ; the latter is in the previous integrable form. The remaining part of the integral (9) will therefore give a contribution

$$\int_S du dv \frac{1}{r(1 + \dot{r}/c)} \frac{d}{c dt} \left( \frac{\partial r}{\partial n} + \frac{v}{c} \phi H \right)_{t=t_0 - r/c}.$$

The complete expression for (9) can be written as

$$\begin{aligned} 4\pi\phi_P(t_0) &= \int_S \frac{du dv}{r(1 + \dot{r}/c)} \left[ \left( \frac{\partial \phi}{\partial n} + \frac{v}{c} \frac{\partial \phi}{\partial t} + \frac{\frac{\partial r}{\partial n} - \frac{\dot{r}v}{c^2}}{1 + \dot{r}/c} \frac{\phi}{r} \right) H \right. \\ &\quad \left. + \frac{d}{c dt} \left( \frac{\frac{\partial r}{\partial n} + \frac{v}{c}}{1 + \dot{r}/c} \phi H \right) \right]_{t=t_0 - r/c} \\ &= \int_S \frac{dS}{r(1 + \dot{r}/c)} \left[ \frac{\partial \phi}{\partial n} + \frac{v}{c} \frac{\partial \phi}{\partial t} + \frac{\frac{\partial r}{\partial n} - \frac{\dot{r}v}{c^2}}{1 + \dot{r}/c} \frac{\phi}{r} \right. \\ &\quad \left. + \frac{1}{H} \frac{d}{c dt} \left( \frac{\frac{\partial r}{\partial n} + \frac{v}{c}}{1 + \dot{r}/c} \phi H \right) \right]_{t=t_0 - r/c}, \end{aligned}$$

which gives the value of  $\phi$  at time  $t_0$  at a point P. For any time  $t$  the expression can be written as

$$4\pi\phi_P(t) = \int_S \frac{dS}{r(1+\dot{r}/c)} \left[ \frac{\partial\phi}{\partial n} + \frac{r}{c} \frac{\partial\phi}{\partial t} + \frac{\frac{\partial r}{\partial n} - \frac{\dot{r}v}{c^2}}{1+\dot{r}/c} \frac{\phi}{r} \right. \\ \left. + \frac{1}{H} \frac{d}{dt} \left( \frac{\frac{\partial r}{\partial n} + \frac{v}{c}}{1+\dot{r}/c} \phi H \right) \right]_{r=t-r/c}.$$

In this it must be noticed that  $dS$  denotes the element of the moving surface whose velocity in the direction of the outward normal is  $v$ .

### 3. Verification of the Solution.

a. Its reduction to the Kirchhoff Form.

When the surface is fixed,  $\dot{r}=0$ ,  $v=0$ ,  $H$  and  $\frac{\partial r}{\partial n}$  are both independent of the time, and  $\frac{d}{dt} = \frac{\partial}{\partial t}$ . With these values the integral becomes

$$4\pi\phi_P(t_0) = \int_S \frac{dS}{r} \left[ \frac{\partial\phi}{\partial n} + \frac{\partial r}{\partial n} \frac{\phi}{r} + \frac{1}{c} \frac{\partial r}{\partial n} \frac{\partial\phi}{\partial t} \right]_{t=t_0-r/c} \\ = \int_S \left\{ \frac{1}{r} \left[ \frac{\partial\phi}{\partial n} \right] - [\phi] \frac{\partial}{\partial n} \left( \frac{1}{r} \right) + \frac{1}{cr} \frac{\partial r}{\partial n} \left[ \frac{\partial\phi}{\partial t} \right] \right\},$$

which on comparison with (1) is seen to be the Kirchhoff form.

b. Its reduction to the Poisson Formula.

As the Poisson formula is only a particular case of the Kirchhoff formula when the surface  $S$  is a sphere, centre the point P, the more general solution will reduce to the Poisson form in the same particular case.

### 4. The Form taken by the Extended Formula when the Surface $S$ is a Sphere of Radius $\rho=ct$ .

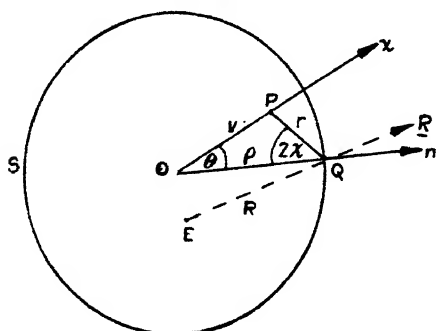
When the surface  $S$  is a sphere expanding with a radial velocity equal to that of light, the expression takes a comparatively simple form. In this case the following curvilinear coordinates may be used:—

$$u = \mu = \cos \theta; \quad v = \psi; \quad w = \rho = ct;$$

$\theta$  = angle between  $x$ -axis and the vector  $R$ ;

$\psi$  = angle between the plane PQO and the  $xy$ -plane (see fig. 1).

Fig. 1.



Then

$$du dv = d\mu d\psi; \quad H = \rho^2; \quad dS = \rho^2 d\mu d\psi; \quad v = \dot{\rho} = c;$$

$$\frac{\partial r}{\partial n} = \frac{\partial r}{\partial \rho} = \cos 2\chi; \quad \dot{r} = \dot{\rho} \cos 2\chi = c \cos 2\chi;$$

$$\frac{\partial r}{\partial n} + \frac{v}{c} = 1 + \cos 2\chi = 1 + \dot{r}/c;$$

$$\frac{\partial r}{\partial n} - \frac{\dot{r}v}{c^2} = \cos 2\chi - \cos 2\chi = 0.$$

Substituting these values the extended formula becomes

$$4\pi\phi_P(t_0)$$

$$\begin{aligned} &= \int_S \frac{d\mu d\psi}{r(1 + \cos 2\chi)} \left[ \rho^2 \left( \frac{\partial \phi}{\partial \rho} + \frac{\partial \phi}{c \partial t} \right) + \frac{d}{c dt} (\rho^2 \phi) \right]_{t=t_0-r/c} \\ &= \int_S \frac{2\rho d\mu d\psi}{r(1 + \cos 2\chi)} \left[ \rho \left( \frac{\partial \phi}{\partial \rho} + \frac{\partial \phi}{c \partial t} \right) + \phi \right]_{t=t_0-r/c} \\ &= \int_S \frac{2\rho d\mu d\psi}{r(1 + \cos 2\chi)} \left[ \frac{d}{c dt} (\rho \phi) \right]_{t=t_0-r/c} \dots \dots \dots (10) \end{aligned}$$

As remarked previously, the function  $\phi$  is continuous within the surface  $S$ . If  $\phi$  has, within  $S$ , a number of singularities,

they must be surrounded by surfaces  $\sigma$ , moving or fixed, to each of which the extended integral must be applied. Should these surfaces be chosen as fixed, then, according to 3a, the extended form reduces to the Kirchhoff form. In the periphractic region, bounded within by the surfaces surrounding the singularities and on the outside by the sphere  $S$ , the function is continuous. Consequently, the value of  $\phi$  at the point  $P$  at time  $t_0$  will be given by the modified Kirchhoff formula extended to the expanding sphere together with the integrals extended to the boundaries surrounding the singularities, due precaution being taken to the sign of the outward normal.

In the succeeding case this expanding sphere can be conveniently taken as a boundary, and the only singularity will be a simple one to be excluded by a fixed sphere. Hence two integrals will occur: the integral (10) applied to the expanding sphere, and a Kirchhoff integral extended to this fixed sphere surrounding the singularity.

5. *A Wave Function  $\phi$  which has a Singularity moving along a Curve.*

If we take for  $\phi$  \* the expression

$$\phi = f(\tau)/KR,$$

where

$$R^2 = [x - \xi(\tau)]^2 + [y - \eta(\tau)]^2 + [z - \zeta(\tau)]^2 = c^2(t - \tau)^2, \quad (11)$$

$$K = 1 - \frac{[x - \xi(\tau)]\dot{\xi}(\tau) + [y - \eta(\tau)]\dot{\eta}(\tau) + [z - \zeta(\tau)]\dot{\zeta}(\tau)}{cR},$$

and  $f(\tau)$  is any function of the variable  $\tau$  which is a solution of (11), then  $\phi$  will be a solution of the wave equation which has a singularity moving along a curve  $\Gamma$  given by

$$x = \xi(\tau), \quad y = \eta(\tau), \quad z = \zeta(\tau).$$

Here the function  $\phi$  is a function of  $\tau$  as well as of  $x, y, z$  explicitly. We shall also denote by  $\rho$  the quantity

$$\rho^2 = x^2 + y^2 + z^2.$$

If this singularity be taken as an electron, the variable  $\tau$  will denote the proper time,  $\xi(\tau), \eta(\tau), \zeta(\tau)$  its coordinates,  $x, y, z$  a field-point, and  $\phi$  a retarded potential. If, further, we

\* Proc. Lond. Math. Soc. [2] i. p. 164 (1903).

suppose that this electron be at rest at the origin  $O$ ,  $\rho=0$ , prior to the time  $\tau=0$ , and if at the instant  $\tau=0$  it be set in motion along the curve  $\Gamma$ , then electromagnetic waves emanate from the electron into the surrounding medium with velocity  $c$ , the wave boundary being an expanding sphere of radius  $\rho=ct$ . The electron at time  $\tau$  will occupy a position  $E$  given by  $R=0$  and the wave boundary will correspond to the sphere  $\rho=ct$  mentioned in § 4.

## 6. Application of the Formula to the Wave Function

$$\phi = f(\tau)/KR.$$

In order to apply the extended formula to the function  $\phi$  and thus obtain a further verification of the formula by identifying the value  $\phi_P(t_0)$  with the value obtained from the integral, we shall take as the expanding surface  $S$  the wave boundary  $\rho=ct$ , and as the boundary surrounding the electron a fixed sphere  $\sigma$ , centred at the origin  $\rho=0$ . Between the two spheres the function  $\phi$  is continuous. Therefore we have

$4\pi\phi_P(t_0)$

$$\begin{aligned}
I_2 = & \int_{\Sigma} \frac{2\rho d\mu d\psi}{8\pi(1+\cos^2\chi)} \left[ \left[ \rho \left( \frac{\partial\phi}{\partial\rho} + \frac{\partial\phi}{c\partial t} \right) + \phi \right]_{r=t-R/c} \right]_{t=t_0-r/c} \\
& + \int_{\Sigma} \frac{d\sigma}{r} \left[ \left[ \frac{\partial\phi}{\partial u} + \frac{\partial\phi}{c\partial t} \frac{\partial r}{\partial u} + \frac{\phi}{r} \frac{\partial r}{\partial n} \right]_{r=t-R/c} \right]_{t=t_0-r/c}. \quad (12) \\
= & I_1 + I_2.
\end{aligned}$$

The inner square brackets mean that the enclosed functions of the time must be calculated before  $\tau$  is given the value  $t - R/c$ . After performing the differentiations in the enclosed functions,  $\tau$  is set equal to  $t - R/c$ . The function then becomes a function of  $t$  in which we must set  $t = t_0 - r/c$ .

For the evaluation of these integrals a number of relations are required. They can be easily evaluated and are as follows\* :—

$$1/K = \frac{\partial \tau}{\partial t}, \quad . \quad . \quad . \quad . \quad . \quad . \quad . \quad . \quad (13)$$

$$K = \frac{\partial t}{\partial \tau} = 1 + \frac{1}{c} \frac{\partial R}{\partial \tau} = 1 - \frac{(\mathbf{v} \mathbf{R}_1)}{c}, \quad . \quad . \quad (14)$$

\* Schott, 'Electromagnetic Radiation,' chap. III.

where  $\mathbf{R}_1$  is the unit vector in the direction of the vector  $\mathbf{R}$ , and  $(\nabla \mathbf{R}_1)$  is a scalar product.\*

$$\frac{\partial \tau}{\partial x} = -\frac{x-\xi}{cR\mathbf{K}},$$

$$\frac{\partial \tau}{\partial \rho} = \sum_{x,y,z} \frac{x}{\rho} \frac{\partial \tau}{\partial x} = -\frac{1}{c\mathbf{K}} \sum_{x,y,z} \frac{x-\xi}{R} \frac{x}{\rho}, \quad (15)$$

$$\frac{\partial}{\partial x} (\mathbf{K}\mathbf{R})_{\tau=\text{const.}} = \frac{x-\xi}{R} - \frac{\xi}{c},$$

$$\sum_{x,y,z} \frac{x}{\rho} \frac{\partial}{\partial x} (\mathbf{K}\mathbf{R})_{\tau=\text{const.}} = \sum_{x,y,z} \left( \frac{x}{\rho} \frac{x-\xi}{R} - \frac{x}{\rho} \frac{\xi}{c} \right), \quad (16)$$

$$\frac{\partial}{c \partial \tau} (\mathbf{K}\mathbf{R}) = \mathbf{K} - k^2 - \frac{(\nabla \mathbf{R})}{c^2}, \quad (17)$$

$$k^2 = 1 - \frac{v^2}{c^2} = 1 - \beta^2.$$

### 7. The Integral $I_1$ extended to the Expanding Sphere $\rho=ct$ vanishes.

It is known that  $\tau=t-R/c$  always, and as the wave boundary corresponds to the proper time  $\tau=0$ , we find that  $R=ct$ . But as  $\rho=ct$ , then  $R=\rho$ . It has been stated, however, that we cannot put  $\tau=0$  and the consequent values  $R=\rho$ ,  $\xi=\eta=\zeta=0$  before differentiation, but rather we must differentiate first and afterwards set  $R=\rho$ , and  $\xi=\eta=\zeta=0$  (see fig. 1).

Now as  $\rho$  is the outward normal, we have

$$\begin{aligned} \frac{\partial \phi}{\partial n} &= \frac{\partial \phi}{\partial \rho} = \sum_{xyz} \frac{x}{\rho} \left( \frac{\partial \phi}{\partial x} \right)_{\tau=\text{const.}} + \left( \frac{\partial \phi}{\partial \tau} \frac{\partial \tau}{\partial \rho} \right)_{t=\text{const.}} \\ &= -\frac{f(\tau)}{K^2 R^2} \sum_{xyz} \frac{x}{\rho} \frac{\partial}{\partial x} (\mathbf{K}\mathbf{R})_{\tau=\text{const.}} + \frac{\partial \phi}{\partial \tau} \sum_{xyz} \frac{x}{\rho} \frac{\partial \tau}{\partial x}. \end{aligned}$$

Using expressions (15) and (16) it becomes

$$= -\frac{f(\tau)}{K^2 R^2} \sum_{xyz} \left( \frac{x}{\rho} \frac{x-\xi}{R} - \frac{x}{\rho} \frac{\xi}{c} \right) - \frac{1}{c\mathbf{K}} \frac{\partial \phi}{\partial \tau} \sum_{xyz} \frac{x-\xi}{R} \frac{x}{\rho}.$$

Again,

$$\frac{\partial \phi}{c \partial t} = \frac{\partial \phi}{c \partial \tau} \frac{\partial \tau}{\partial t}.$$

Using (13) we obtain

$$\frac{\partial \phi}{c \partial t} = \frac{1}{cK} \frac{\partial \phi}{\partial \tau}.$$

Consequently,

$$\rho \left( \frac{\partial \phi}{\partial \rho} + \frac{\partial \phi}{c \partial t} \right) + \phi = \frac{f(\tau)}{KR} \left[ 1 - \frac{\rho}{KR} \sum_{xyz} \left( \frac{x}{\rho} \frac{x-\xi}{R} - \frac{x}{\rho} \frac{\xi}{c} \right) \right] \\ + \frac{\rho}{K} \frac{\partial \phi}{c \partial \tau} \left[ 1 - \sum_{xyz} \frac{x-\xi}{R} \frac{x}{\rho} \right].$$

We may now put  $R=\rho$ ,  $\xi=\eta=\zeta=0$ , and the expression, if we take account of (14), is seen to vanish.

Thus we have the result that when the expanding surface  $S$  is a sphere whose radial velocity is equal to that of light and when the function  $\phi$  is a solution of the wave equation corresponding to an isotropic wave expanding outwards from the origin, the extended formula applied to this surface vanishes. The value of  $\phi$  will depend solely upon the singularities of  $\phi$  within  $S$ .

In this particular case it is a simple singularity and we are left to determine the integral  $I_2$ .

### 8. The Kirchhoff Integral $I_2$ .

To effect this latter integration we shall suppose that  $P$  is a point within the expanding sphere  $S$  such that it tends towards the surface  $R=ct_0$ . As  $P$  tends towards this sphere we can then assume that the fixed sphere  $\sigma$ , of radius  $\rho$ , tends simultaneously towards a limiting sphere at the origin  $O$ . For this purpose it is necessary that  $ct_0 = \nu + 2\rho$ , where  $\nu$  is the distance from the origin  $O$  to the field-point  $P$ . Then as  $\nu \rightarrow ct_0$ ,  $\rho \rightarrow \text{zero}$ .

Again, every element  $d\sigma$ , though contributing towards the integral, corresponds to different times  $t$ . Various elements lying at different distances  $r$  from  $P$  will correspond to different times  $t=t_0-r/c$ , which can equally well be represented by  $t=\tau+R/c$ , i. e., to different times  $\tau$  of the electron. Therefore the electron has, for an element  $d\sigma$  of the surface, a position  $E$  at time  $\tau$  such that the contribution taken in the integral at time  $t$  comes from the electron at  $E$  at time  $\tau$ . The outward normal has the direction of the inward drawn radius  $-\rho$  (see fig. 2).





From (20), (21), (22) we find that

$$\begin{aligned} \frac{\partial \phi}{\partial n} + \frac{\partial \phi}{c \partial t} \frac{\partial r}{\partial n} + \frac{\phi}{r} \frac{\partial r}{\partial n} \\ = \frac{f(\tau)}{K^2 R^2} [\cos(\rho R) - \beta \cos(v\rho)] \\ - \frac{f(\tau)}{K^3 R^2} [\cos(\rho R) - \cos(r\rho)] \frac{\partial}{c \partial \tau} (KR) \\ - \frac{f(\tau)}{KRr} \cos(r\rho) + \frac{f'(\tau)}{c K^2 R} [\cos(\rho R) - \cos(r\rho)], \quad (23) \end{aligned}$$

where we have used the simplified notation

$$\cos(\rho R) = \sum_{xyz} \frac{x}{\rho} \frac{x - \xi}{R}, \text{ etc.}$$

Substituting (17) in this expression, the integral becomes

$$\begin{aligned} I_2 = \int \frac{d\sigma}{r} \left[ \frac{f(\tau)}{K^2 R^2} \{ \cos(r\rho) - \beta \cos(v\rho) \} \right. \\ + \frac{K^2 f(\tau)}{K^3 R^2} \{ \cos(\rho R) - \cos(r\rho) \} \\ + \frac{f(\tau)}{K^3 R^2} \frac{(\dot{v}R)}{c^2} \{ \cos(\rho R) - \cos(r\rho) \} \\ \left. - \frac{f(\tau)}{KRr} \cos(r\rho) + \frac{f'(\tau)}{c K^2 R} \{ \cos(\rho R) - \cos(r\rho) \} \right]. \end{aligned}$$

Neglecting higher powers of  $\rho$  and  $c\tau$  than squares and products, we have

$$\begin{aligned} r &= (v^2 + \rho^2 - 2v\rho\mu)^{1/2} \quad \mu = \cos \theta \\ &= v - \rho\mu, \end{aligned}$$

$$ct_0 = v + 2\rho \quad \text{or} \quad c\tau = (2 + \mu)\rho - R.$$

Hence

$$\begin{aligned} R^2 &= \{c\tau - (2 + \mu)\rho\}^2 \\ &= \rho^2 - 2\rho(\xi \cos \theta + \eta \sin \theta \cos \psi + \zeta \sin \theta \sin \psi) \\ &\quad + \xi^2 + \eta^2 + \zeta^2, \quad (24) \end{aligned}$$

$\cos \theta$ ,  $\sin \theta \cos \psi$ ,  $\sin \theta \sin \psi$  being the direction cosines of OQ, and  $R = EQ$ .

By the choice of axes we may write

$$\begin{aligned}\xi(\tau) &= \dot{\xi}_0\tau + \frac{1}{2}\ddot{\xi}_0\tau^2 + \dots, \\ \eta(\tau) &= \dot{\eta}_0\tau + \frac{1}{2}\ddot{\eta}_0\tau^2 + \dots, \\ \zeta(\tau) &= \frac{1}{2}\ddot{\zeta}_0\tau^2 + \dots \quad \dot{\zeta}_0 = 0, \\ f(\tau) &= f(0) + f'(0)\tau + \dots\end{aligned}$$

To the same order of approximation we find

$$\left. \begin{aligned}\xi \cos \theta + \eta \sin \theta \cos \psi + \zeta \sin \theta \sin \psi \\ &= (\dot{\xi}_0 \cos \theta + \dot{\eta}_0 \sin \theta \cos \psi) \tau \\ &= c\tau\beta \cos(v\rho) \\ &= c\tau\beta \cos \chi \\ &= c\tau(1-K).\end{aligned}\right\} \quad (25)$$

If we substitute these values in (24), by a rearrangement we see that

$$k^2c^2\tau^2 - 2c\tau\rho(1+\mu+K) + \rho^2[(2+\mu)^2 - 1] = 0.$$

Both roots are positive for  $|\mu| < 1$  and  $|K| < 1$  and are given by

$$k^2c\tau = \rho(1+\mu+K \mp S), \quad \dots \quad (26)$$

where

$$\begin{aligned}S^2 &= (1+\mu+K)^2 - k^2[(2+\mu)^2 - 1] \\ &= [(2+\mu)\beta - \cos \chi]^2 + k^2 \sin^2 \chi > 0.\end{aligned}$$

Assuming the square root to have the positive sign, the negative sign must be taken in the expression (26) in order to make  $R$  positive, for

$$\begin{aligned}k^2R &= k^2[(2+\mu)\rho - c\tau] \\ &= \rho[S + \beta \cos \chi - \beta^2(2+\mu)]\end{aligned}$$

by the equations (25), (26).

Again by the equations (25) and (26),

$$\begin{aligned}KR &= R - [(x-\xi)\dot{\xi} + (y-\eta)\dot{\eta} + (z-\zeta)\dot{\zeta}]/c \\ &\rightarrow R - \rho\beta \cos \chi + \beta^2c\tau.\end{aligned}$$

As  $\rho \rightarrow \text{zero}$ ,  $\cos(r\rho) \rightarrow -\mu$ ,  $R \cos(R\rho) = \rho - c\tau\beta \cos \chi$ .

Therefore that part of the integrand

$$f(\tau) \left[ \frac{\cos(r\rho) - \beta \cos(v\rho)}{K^2 R^3} + k^2 \frac{\cos(\rho R) - \cos(r\rho)}{K^3 R^3} \right]$$

will tend to the value

$$\begin{aligned} & f(0) \left[ -\frac{\mu + \beta \cos \chi}{\rho^3 S^3} + \frac{k^2(\rho - c\tau\beta \cos \chi) + k^2\mu R}{\rho^3 S^3} \right] \\ &= f(0) \left[ -\frac{\mu + \beta \cos \chi}{\rho^3 S^3} + \frac{k^2 + (\mu + \beta \cos \chi)S - \beta^2\mu(2 + \mu)}{\rho^3 S^3} \right] \\ &= f(0) \frac{K^2 - \beta^2(1 + \mu)^2}{\rho^3 S^3} \dots \dots \dots (27) \end{aligned}$$

Moreover, the remaining terms of the integrand, when taken in conjunction with the element  $d\sigma$ , are going to give terms of the order  $\rho$  which will vanish as  $\rho$  tends to zero. The principal part of the integral may be written, therefore, as

$$I_2 = \frac{f(0)}{\nu} \int_{\mu=-1}^{+1} \int_{\psi=0}^{2\pi} \frac{K^2 - \beta^2(1 + \mu)^2}{S^3} d\mu d\psi. \quad (28)$$

Let

$$s = 1 + \mu = 1 + \cos \theta; \quad \beta = \cos j,$$

$$\nu = \cos \theta \cos \alpha + \sin \theta \sin \alpha \cos \psi = \cos \omega.$$

We know that

$$K = 1 - \beta \cos \theta \cos \alpha - \beta \sin \theta \sin \alpha \cos \psi$$

$$= 1 - \beta \cos \omega$$

$$= 1 - \nu \cos j,$$

$\alpha$  = angle which electron makes with OP,

$$S^2 = \cos^2 j [(\sec j - \nu)^2 + 2s(1 - \nu \sec j) + s^2].$$

We have

$$\sin \omega d\omega = \sin \theta \sin \alpha \sin \psi d\psi \quad \text{when } \theta \text{ is kept constant.}$$

Also

$$\sin^2 \theta \sin^2 \alpha \sin^2 \psi$$

$$= \sin^2 \theta \sin^2 \alpha - (\cos \omega - \cos \theta \cos \alpha)^2$$

$$= 1 - \cos^2 \theta - \cos^2 \omega - \cos^2 \alpha + 2 \cos \theta \cos \omega \cos \alpha.$$

The integral to be evaluated is

$$I_2 = \frac{f(0)}{\nu} \int_0^\pi \sin \theta d\theta \int_0^{2\pi} d\psi \frac{K^2 - \beta^2 s^2}{S^3}$$

$$= \frac{2f(0)}{\nu} \int_0^\pi \sin \theta d\theta \int_{|\theta-\alpha|}^{\theta+\alpha} \frac{K^2 - \beta^2 s^2}{S^3}$$

$$\times \frac{\sin \omega d\omega}{\sqrt{1 - \cos^2 \theta - \cos^2 \omega - \cos^2 \alpha + 2 \cos \theta \cos \omega \cos \alpha}}.$$

Now

$$\frac{\pi}{2} \sum_0^\infty (2n+1) P_n(\cos \alpha) P_n(\cos \theta) P_n(\cos \omega)$$

$$= 1/\sqrt{1 - \cos^2 \theta - \cos^2 \omega - \cos^2 \alpha + 2 \cos \theta \cos \omega \cos \alpha},$$

if the quantity under the square root is positive, and is zero when the quantity under the square root is negative.

Hence

$$I_2 = \frac{\pi f(0)}{\nu} \int_0^\pi \sin \theta d\theta \int_0^\pi \sin \omega d\omega \frac{K^2 - \beta^2 s^2}{S^3}$$

$$\sum_{n=0}^\infty (2n+1) P_n(\cos \alpha) P_n(\cos \theta) P_n(\cos \omega)$$

$$= \frac{\pi f(0)}{\nu \beta} \int_{-1}^1 \int_{-1}^1 d\mu d\nu (\sec j - \nu)^{-1} \frac{(1-x^2)}{(1-2x \cos \chi + x^2)^{3/2}}$$

$$\times \sum (2n+1) P_n(\cos \alpha) P_n(\cos \theta) P_n(\cos \omega),$$

where

$$\cos \chi = \frac{\nu \sec j - 1}{\sec j - \nu}; \quad x = \frac{s}{\sec j - \nu}.$$

Now

$$\frac{1-x^2}{(1-2x \cos \chi + x^2)^{3/2}} = \sum_{m=0}^\infty (2m+1) x^m P_m(\cos \chi)$$

and

$$\int_{-1}^1 x^m P_n(\mu) d\mu = \frac{1}{(\tau - \nu)^m} \int_{-1}^1 (1 + \mu)^m P_n(\mu) d\mu,$$

where

$$\tau = \sec j.$$

But

$$\int_{-1}^1 (1 + \mu)^m P_n(\mu) d\mu = \frac{2^{m+1}}{m-n} \frac{|m|}{|m+n+1|} \quad m \geq n,$$

so that

$$I_2 = \frac{\pi f(0)}{\nu \beta} \int_{-1}^1 d\nu \sum_{n=0}^{\infty} \sum_{m=n}^{\infty} \frac{1}{(\tau - \nu)^{m+1}} P_m \left( \frac{\nu \tau - 1}{\tau - \nu} \right) \\ \times 2^{m+1} \frac{(2n+1)(2m+1)}{|m-n| |m+n+1|} \frac{|m|}{|n|} P_n(\cos \alpha) P_n(\nu).$$

Now we also have the equation

$$\frac{1}{(\tau - \nu)^{m+1}} P_m \left( \frac{\nu \tau - 1}{\tau - \nu} \right) = \sum_{p=m}^{\infty} \frac{1}{2^m} \frac{p+m}{|p-m|} \frac{(2p+1)}{|m|} Q_p(\tau) P_p(\nu),$$

where

$$Q_n(\tau) = \frac{1}{2^{n+1}} \int_{-1}^1 (1-t^2)^n (\tau - t)^{-n-1} dt,$$

and we have  $p \geq m \geq n$ , while

$$\int_{-1}^1 P_n(\nu) P_p(\nu) d\nu = 0 \quad p > n.$$

The only terms which survive are those for which  $p = m = n$ . Thus we obtain, finally,

$$I_2 = \frac{4\pi f(0)}{\nu \beta} \sum_{n=0}^{\infty} \frac{(2n+1)^2}{|2n+1|} \frac{2n}{|2n+1|} Q_n(\tau) P_n(\cos \alpha) \\ = \frac{4\pi f(0)}{\nu \beta} \sum_{n=0}^{\infty} (2n+1) Q_n \left( \frac{1}{\beta} \right) P_n(\cos \alpha) \\ = \frac{4\pi f(0)}{\nu(1 - \beta \cos \alpha)}.$$

This, moreover, is the expression for the complete integral. It is identified immediately with the value of  $4\pi\phi_P(t_0)$ , if we put for the field-point P,  $R = \nu$  and  $\theta = 0$  in the expression

$$K = 1 - \beta \cos \theta \cos \alpha - \sin \theta \sin \alpha \cos \psi.$$

We must also take the value  $\tau = 0$  to correspond to the time  $t_0$ .

### 9. Particular Cases of the Function $\phi = f(\tau)/KR$ .

a. If we denote by  $f(\tau)$  the component velocities of the electron, the functions obtained give the components of the retarded vector potential

$$\mathbf{a} = \frac{\mathbf{v}}{[KR]}.$$

b. If we set  $f(\tau)=1$ , the function

$$\phi = 1/[KR]$$

gives the scalar retarded potential.

c. If we assume that the electron is static, at rest at the origin  $\rho=0$ , so that

$$\xi = \eta = \zeta = 0, \quad \dot{\xi} = \dot{\eta} = \dot{\zeta} = 0, \quad \text{and} \quad \rho = R,$$

then

$$K = 1,$$

$$R^2 = x^2 + y^2 + z^2,$$

$$f(\tau) = f(t - R/c),$$

and the function  $\phi$  becomes

$$\phi = \frac{(t - R/c)}{R}.$$

If this form of the function  $\phi$  is used in the extended formula, it is noticed that an easy verification is obtained.

### 10. Summary.

It has been shown that if  $\phi$  be a function which satisfies the wave equation within a volume  $\Omega$  bounded by a moving surface  $S$  and is subject to the conditions of continuity as mentioned in § 2, then the value of  $\phi$  determined at an internal point  $P$  at a time  $t$  is given by the expression

$$4\pi\phi_P(t) = \int_S \frac{dS}{r(1+\dot{r}/c)} \left[ \frac{\partial\phi}{\partial n} + \frac{v}{c} \frac{\partial\phi}{\partial t} + \frac{\frac{\partial r}{\partial n} - \frac{\dot{r}v}{c^2}}{1+\dot{r}/c} \phi \right. \\ \left. + \frac{1}{H} \frac{d}{cdt} \left( \frac{\frac{\partial r}{\partial n} + \frac{v}{c}}{1+\dot{r}/c} \phi_H \right) \right]_{r=t-r/c},$$

where  $v$  is the velocity of the element  $dS$  in the direction of the outward normal.

When the outward normal velocity of the surface is zero the extended formula reduces to the Kirchhoff form.

When the moving surface  $S$  is an expanding sphere, centre the origin  $\rho=0$ , whose outward normal velocity is equal to that of light, and when the function  $\phi$  corresponds to an isotropic wave expanding outwards from the origin, the integral extended to  $S$  vanishes, so that the value of  $\phi$

at P is due entirely to the singularities of  $\phi$  within the sphere S.

Use is made of this expanding sphere to obtain further verifications of the extended Formula by identifying the value of  $\phi$  at a point P at time  $t_0$  with that obtained from the surface integrals in which the boundary values of  $\phi$  and its derivatives are inserted. Its application to the function  $f(\tau)/[KR]$ , which includes, as particular cases, the scalar and vector retarded potentials and the function  $f(ct - R)/R$ , gives the desired values, which afford strong evidence that the formula deduced can be taken as the Kirchhoff formula extended to a moving surface.

In conclusion, I wish to express my thanks to Prof. G. A. Schott, F.R.S., Head of the Mathematics Department in the University College of Wales, Aberystwyth, for suggesting this problem, and for his assistance and advice while the work was in progress, and to H. Bateman, F.R.S., Professor of Mathematics, Theoretical Physics and Aeronautics at the California Institute of Technology, Pasadena, for the evaluation of integral (28).

Norman Bridge Laboratory of Physics,  
California Institute,  
Pasadena, California,  
April 8, 1929.

---

XV. *Some Hydrodynamical Inertia Coefficients.* By J. LOCKWOOD TAYLOR, D.Sc., *Munitions Committee Research Fellow, University of Liverpool* \*.

THE question of the "virtual inertia" of a body immersed in fluid has acquired some additional interest from the influence which it appears to have on the natural frequency of vibration of a ship †, and most of the results which follow have been obtained with this problem in view. Part I. gives solutions for motion in two dimensions due to the translation of cylinders having various cross-sections, and discusses the application of the results to the ship problem. The results can be applied immediately to the case of vertical

\* Communicated by the Author.

† Nicholls, *Trans. Inst. of Naval Architects*, p. 141 (1924); Moullin, *Proc. Cambridge Phil. Soc.* xxiv. p. 400 (1927-28).

*Phil. Mag.* S. 7. Vol. 9. No. 55. Jan. 1930.

M



vibrations, since the special boundary condition appropriate to the free surface is automatically fulfilled at an axis of symmetry perpendicular to the direction of motion. The free surface condition for the case of horizontal vibration requires special consideration (Part II.). Part III. deals with the effect of rigid boundaries, *e.g.*, as in shallow water or canals, and Part IV. the effect of the abandonment of the restriction to two-dimensional motion, and of compressibility of the fluid in a particular case—that of the circular cylinder. The inertia is generally less, in the two-dimensional case, for motion parallel to the free surface than for motion in a perpendicular direction, when the breadth of the cylinder is greater than the depth; a rigid boundary increases the inertia, as also does compressibility to a small extent, but freedom of the fluid to move in three dimensions naturally has the effect of reducing the energy.

### PART I.

The problem of fluid motion due to the translation in a direction perpendicular to the generators of cylinders having the following sections is considered.

Sections symmetrical about two perpendicular axes, bounded by :—

- (1) Two circular arcs intersecting at any angle.
- (2) Two parabolic arcs intersecting orthogonally.
- (3) Four equal straight lines.
- (4) Four semicircles.
- (5) A circle with projecting laminæ.
- (6) A square with rounded corners.

#### (1) *Section bounded by Circular Arcs.*

In terms of complex variables,  $z$ ,  $w$ , and an intermediate variable,  $t$ , the equations

$$\begin{aligned} z &= \cot t, \\ w_1 &= in \cot nt, \\ w_2 &= n \operatorname{cosec} nt, \end{aligned}$$

represent a uniform stream of unit velocity flowing past a section as described, in a direction parallel and perpendicular to the common chord, respectively. The correspondence of the various planes is as in fig. 1, the exterior angle of intersection of the arcs being  $2\pi/n$ ,  $n$  being positive and greater than unity but not necessarily integral (the case of  $n$  integral

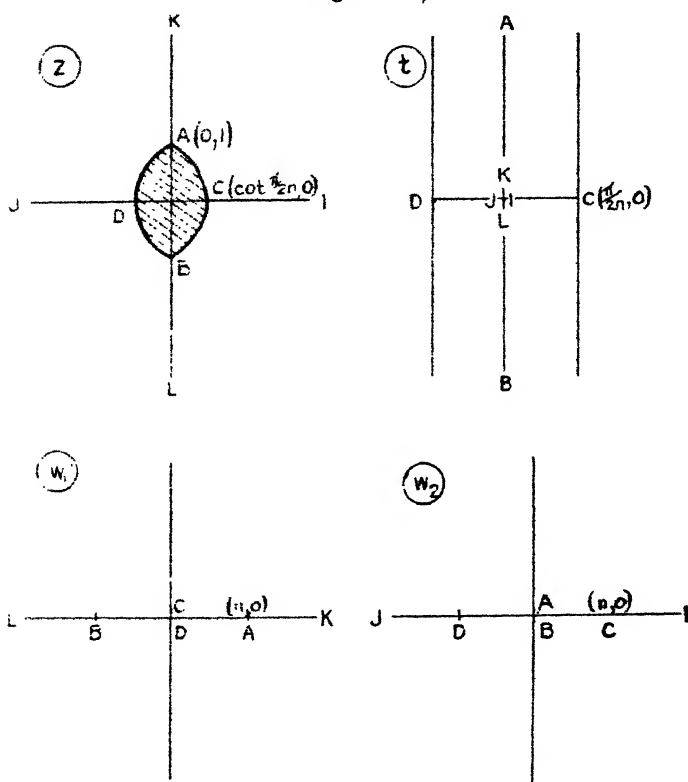
can be solved by the method of images). Expanding the trigonometrical functions, we have, when  $z, w$  are large,

$$w = iz + \frac{1}{iz} \frac{(n^2 - 1)}{3} + \dots,$$

and

$$w = z + \frac{1}{z} \frac{(n^2 + 2)}{6} + \dots$$

Fig. 1.



If  $A$  is the area of the section, and  $C$  the "entrained area," corresponding to the kinetic energy of the fluid ( $1/2 \rho C \cdot U^2$  for density  $\rho$ , and velocity  $U$ ) when the uniform stream is annulled,

$$(A + C_1) = \frac{2\pi}{3} (n^2 - 1),$$

$$(A + C_2) = \frac{\pi}{3} (n^2 + 2),$$

by a result of Leathem's\*. Also

$$A = 2 \left\{ \left( \pi - \frac{\pi}{n} \right) \cdot \operatorname{cosec}^2 \frac{\pi}{n} + \cot \frac{\pi}{n} \right\},$$

so that  $C_1, C_2$  may be found by subtraction. The table shows the values of  $C, b$  (the width of the section measured perpendicular to the direction of motion), and  $C/b^2$ . It is seen that the latter coefficient does not vary very greatly, the extreme values being  $2/\pi$  and  $\pi/2(\pi^2/6-1)$ , or 0.636 and 1.013 respectively. The latter value corresponds to the limiting case of  $w_2$  when  $n$  is large, i.e., for two circles in contact, moving perpendicular to the common tangent. The solution for this case may be written alternatively

$$w_2 = \pi \operatorname{cosec} \pi/z.$$

Similarly,

$$w_1 = i\pi \cot \pi/z,$$

$$C/b^2 = \pi/8(\pi^2/3-1) = .900$$

represents motion parallel to the common tangent, or may be regarded as the solution for a single circle, of unit radius, in contact with a plane boundary. The cases  $n=1, 2$  correspond to the known solutions for the lamina and circle respectively.

$n$ .....	1	6/3	4/3	3/2	2	3	4	5	6
$2\pi/n$ .....	$360^\circ$	300	270	240	180	120	90	60	0
Radius .....	$\infty$	2	1.41	1.15	1	1.15	1.41	2	$\infty$
Width, $b_1$ ...	0	.536	.828	1.15	2	3.46	4.83	7.46	$\infty$
„ $b_2$ ...	2	2	2	2	2	2.31	2.83	4	$\infty$
$C_1$ .....	0	.197	.488	.980	3.14	10.0	20.0	48.0	$\infty$
$C_2$ .....	3.14	2.88	2.82	2.81	3.14	4.78	7.42	15.4	$\infty$
$C_1/b_1^2$ .....	(.636)	.685	.709	.735	.785	.835	.857	.878	(.900)
$C_2/b_2^2$ .....	.785	.719	.704	.703	.785	.896	.928	.962	(1.01)

## (2) Section bounded by Parabolic Arcs.

For motion parallel to the chord (fig. 2),

$$z = \left(\frac{t}{2}\right)^2, \quad t = \int^w (w^2-1)^{-\frac{1}{2}} dw.$$

When  $w, z$  are large, this gives

$$z = w - 1/6 w + \dots,$$

$$(A + C) = \pi/3.$$

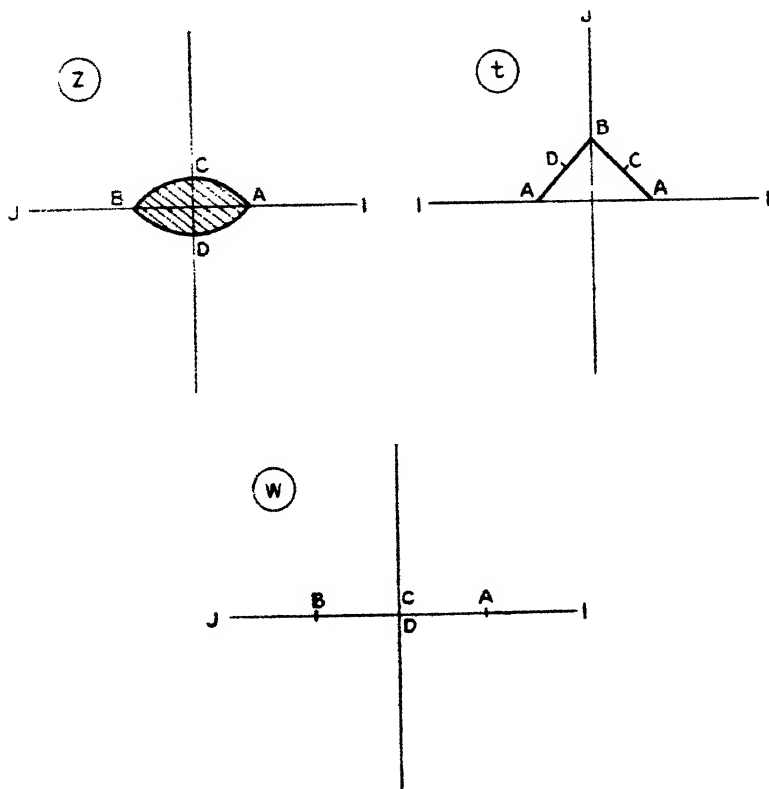
\* Leathem, Phil. Trans. A, ccxv. p. 453 (1915).

The length of the chord is

$$1/4 \left\{ \int_{-1}^1 (1-w^2)^{-\frac{1}{2}} \cdot dw \right\}^2 = \pi^2/2 \cdot K^2,$$

$K$  being the complete elliptic integral of modulus  $1/\sqrt{2}$ .

Fig. 2.



Hence

$$A = \left( \frac{\pi^2}{2K^2} \times \frac{\pi^2}{4K^2} \times \frac{2}{3} \right) = \pi^4/12 \cdot K^4 = 0.687,$$

$$C = \pi/3 - 0.687 = 0.360.$$

$$C/b^2 = 0.360 \div 0.515 = 0.698.$$

For motion perpendicular to the chord (fig. 3),

$$z = \left( \frac{t}{2} \right)^2, \quad t = \int^w \left( \frac{w}{w^2-1} \right)^{\frac{1}{2}} \cdot dw,$$

giving

$$z = w - 1/3 \cdot w + \dots,$$

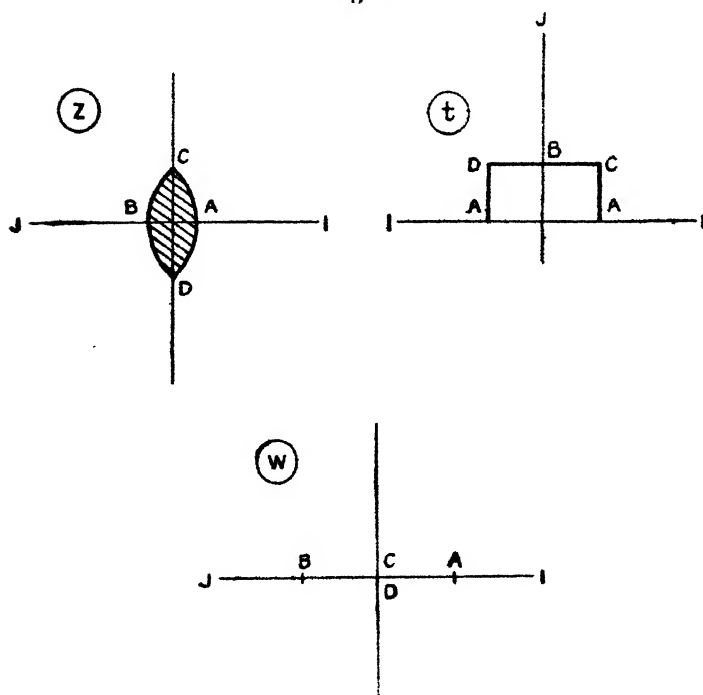
$$(A + C) = 2\pi/3,$$

$$C = 2\pi/3 - 0.687 = 1.407,$$

$$C/b^2 = 1.407 \div 2.061 = 0.683.$$

The coefficients  $C/b^2$  agree fairly closely with those for the section consisting of orthogonally intersecting circular

Fig. 3.



arcs, viz. 0.709 and 0.704 respectively, as would be anticipated.

### (3) *Quadrilateral with equal sides.*

The angle between the side and the diagonal parallel to the direction of motion being  $n \cdot \pi$ , Schwarz's method gives (fig. 4)

$$z = \int^w \left( \frac{w^2}{w^2 - 1} \right)^n \cdot dw,$$

whence

$$z = w - n/w + \dots$$

when  $z, w$  are large, so that

$$(A+C)=2 \cdot \pi \cdot n.$$

The length of a side of the quadrilateral is given by

$$s = \int_0^1 \left( \frac{w^2}{1-w^2} \right)^n \cdot dw = \frac{\Gamma(1/2+n) \cdot \Gamma(1-n)}{2\Gamma(3/2)},$$

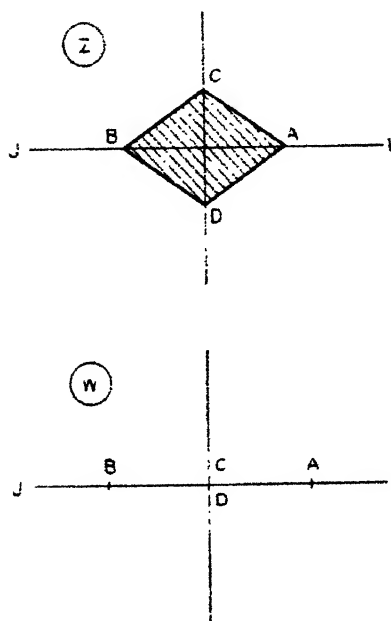
and

$$A = s^2 \cdot \sin 2 \cdot n\pi,$$

so that

$$C = 2 \cdot n\pi - s^2 \cdot \sin 2 \cdot n\pi.$$

Fig. 4.



The values of the coefficient  $C/b^2$  are tabulated below for several values of the angle  $n \cdot \pi$  :—

$n\pi$ .....	$90^\circ$	60	45	30	$\rightarrow 0$
$C/b^2$ .....	785	650	594	543	441

The value for  $n \rightarrow 0$  is obtained as follows :

$$\Gamma(1/2+n) = \sqrt{\pi}(1-n(\gamma + \log 4)),$$

$$\Gamma(1-n) = (1+n \cdot \gamma),$$

to the first order, when  $n$  is small,  $\gamma$  being Euler's constant.

Hence

$$\begin{aligned}s &= (1 - n \cdot \log 4), \\ A &= 2 \cdot n\pi(1 - 2 \cdot n \log 4), \\ C &= 4 \cdot n^2\pi \log 4.\end{aligned}$$

Also

$$\begin{aligned}b &= 2 \cdot n\pi, \\ C/b^2 &= \frac{1}{\pi} \cdot \log 4 = 0.441.\end{aligned}$$

For the particular case of the square ( $n = 1/4$ ), the entrained area is obviously the same for two directions at right angles and is therefore the same for motion in any direction. The present result is therefore directly comparable with the particular case of Riabouchinsky's solution \* for a rectangle moving parallel to a side, viz.,

$$C = \frac{\pi}{2} - (2 \cdot E - K)^2 = \frac{\pi}{2} - \frac{\pi^2}{4 \cdot K^2}$$

by Legendre's relation  $E, K$  being complete elliptic integrals of modulus  $1/\sqrt{2}$ . This is to be compared with

$$C = \frac{\pi}{2} - \left\{ \frac{[\Gamma(3/4)]^2}{2\Gamma(3/2)} \right\},$$

giving

$$K = \frac{\pi \cdot \Gamma(3/2)}{\{\Gamma(3/4)\}^2}.$$

a known relation.

#### (4) *Section bounded by Four Semicircles.*

The solution is derived from the representation of the interior of a square on that of a circle, viz.,

$$\xi = \int_0^t \frac{dt}{(1-t^4)^{\frac{1}{4}}},$$

by putting

$$\begin{aligned}z &= 1/\xi, \\ w &= t + 1/t.\end{aligned}\quad (\text{fig. 5.})$$

Hence, when  $w, z$  are large and  $\xi, t$  small,

$$\begin{aligned}\xi &= t + (t^3) + \dots, \\ z &= 1/t - (1/t^3) + \dots, \\ w &= z + 1/z + \dots,\end{aligned}$$

$$(A + C) = 2 \cdot \pi.$$

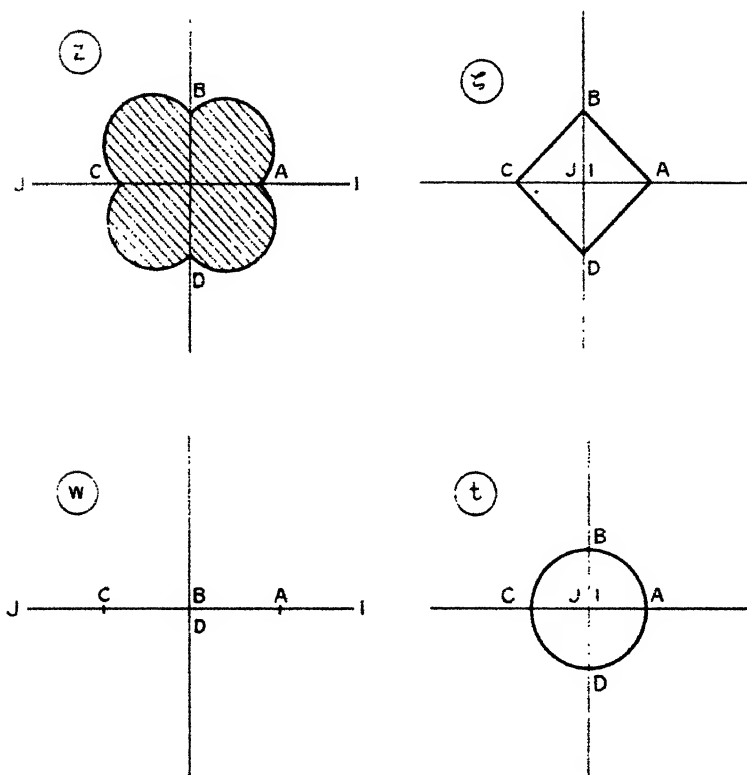
\* Internat. Congress of Math., Strasbourg, p. 568 (1920).

In the plane of  $\zeta$ ,

$$IA = \int_0^1 \frac{dt}{(1-t^4)^{\frac{1}{2}}} = K/\sqrt{2},$$

so that the half-diagonal of the square ABCD in the

Fig. 5.



$z$ -plane is  $\sqrt{2}/K$ . This gives as the total area of the section  $(1 + \pi/2) \cdot 4/K^2 = 2.99$ , so that

$$C = 2 \cdot \pi - 2.99 = 3.29 = 0.968b^2,$$

where  $b$  is the extreme width of the section  $\frac{2 + \sqrt{2}}{K}$ . Since the entrained area,  $C$ , is the same for motion in the perpendicular direction, it may also be expressed in terms of the diagonal  $4/K = b$  say, viz.,  $C = 0.707 b^2$ , corresponding to the case of motion at  $45^\circ$  to the axes.



(5) *Circle with Projecting Laminae.*

The solution is derived from that for a single lamina,

$$z = \sqrt{(w^2 - c^2)},$$

by adding a second similar term, so that

$$z = 1/2(\sqrt{(w^2 - c^2)} + \sqrt{(w^2 - 4 - c^2)})$$

represents the flow past a circle of unit radius with a lamina projecting at either extremity of the diameter perpendicular to the direction of flow, the total width  $2b$  being given by

$$c = (b^2 - 1)/b.$$

When  $w$  is large, expansion gives

$$z = w - \frac{(1 + c^2/2)}{w} + \dots$$

Hence

$$(A + C) = \pi(2 + c^2),$$

$$C = \pi(1 + c^2) = \pi \frac{(b^4 - b^2 + 1)}{b^2},$$

$$C/4b^2 = \pi/4(1 - 1/b^2 + 1/b^4).$$

The coefficient is equal to  $\pi/4$  when  $b=1$ , and also when  $b$  is large, as would be anticipated, since the influence of the circle of unit radius is then negligible. The minimum value, for  $b = \sqrt{2}$ , is  $3\pi/16$  or 0.589.

(6) *Square with rounded corners.*

By adding, in a similar manner to the above, two terms corresponding to the flow past rectangles of different proportions, the resulting section is a rectangle with the corners rounded off. Riabouchinsky \* has given the solution for a single rectangle, which may be somewhat more simply expressed as

$$z = \int \sqrt{\frac{w^2 - \cos^2 \alpha}{w^2 - 1}} \cdot dw.$$

This gives

$$(A + C) = \pi \sin^2 \alpha,$$

$$A = b \times d,$$

$$= 4(E - \cos^2 \alpha \cdot K)(E' - \sin^2 \alpha \cdot K'),$$

$E, K$  being the elliptic integrals of modulus  $\sin \alpha$ , and  $E', K'$  those of the complementary modulus  $\cos \alpha$ . The

effect of writing  $\sin \alpha$  for  $\cos \alpha$  is to interchange the breadth and depth of the rectangle so that the addition of two terms

$$2z = \int \frac{\{(\sqrt{w^2 - \cos^2 \alpha}) + (\sqrt{w^2 - \sin^2 \alpha})\} \cdot dw}{\sqrt{w^2 - 1}}$$

gives a square of side  $1/2(b+d)$ , the sides being connected by an arc of length

$$\begin{aligned} \int ds &= \int_{\sin \alpha}^{\cos \alpha} \left\{ \left( \frac{dx}{dw} \right)^2 + \left( \frac{dy}{dw} \right)^2 \right\}^{\frac{1}{2}} \cdot dw \\ &= \frac{1}{2} \int_{\sin \alpha}^{\cos \alpha} \frac{(\cos^2 \alpha - w^2 + w^2 - \sin^2 \alpha)^{\frac{1}{2}}}{(1 - w^2)^{\frac{1}{2}}} \cdot dw. \end{aligned}$$

This gives

$$s = \frac{1}{2} \sqrt{\cos 2\alpha} (\pi/2 - 2\alpha).$$

The exact area of the section may be calculated by quadrature, but if  $\alpha$  is not less than say  $\pi/6$ , it is given very nearly by

$$A = \frac{(b+d)^2}{4} - 16/30 \cdot s^2.$$

Also  $(A + C) = \pi/2(\sin^2 \alpha + \cos^2 \alpha) = \pi/2.$

For  $\alpha = \pi/6$ ,

$$b = 2(1.468 - 0.75 \times 1.686) = 0.2035 \times 2,$$

$$d = 2(1.211 - 0.25 \times 2.157) = 0.672 \times 2,$$

$$s = 1/2 \sqrt{2} \times \pi/6 = 0.185,$$

$$A = (0.8755)^2 - 0.018 = 0.749,$$

$$C = \pi/2 - 0.749 = 0.822 = 1.07 b^2,$$

$b$  being the width of the section, *i.e.*, the side of the square. Comparing this with the corresponding figure for a complete square, 1.188, it appears that the reduction of the area, by rounding off the corners, by about  $2\frac{1}{2}$  per cent. has reduced the entrained area by 10 per cent.

#### *Application of the above results.*

If  $\phi \cos \sigma t$  is the velocity potential of a fluid motion due to the simple-harmonic vibrations of an immersed body, the usual condition at a free surface is

$$\sigma^2 \phi = g \cdot \frac{\partial \phi}{\partial n}.$$

If the frequency is sufficiently large,  $\frac{g}{\sigma^2} \cdot \frac{\partial \phi}{\partial n}$  is evidently small, and the condition reduces to  $\phi=0$  \*. The order of the neglected term is  $g \cdot v/\sigma^2$ , where  $v$  is the maximum velocity of the vibration, while  $\phi$  in the vicinity of the section is of the order  $(b \cdot v)$ ,  $b$  being one of the dimensions of the vibrating body. The ratio,  $g/b\sigma^2$  or  $g \cdot T^2/4\pi^2 \cdot b$ , is very small for periods ( $T$ ) of less than one second, as in practice,  $b$  being of the order of, say, 50 feet.

The condition  $\phi=0$  is evidently fulfilled at an axis of symmetry perpendicular to the direction of motion, *e.g.*, the  $y$ -axis in all the foregoing examples, which may therefore be regarded as a free surface. Conversely, for any given section partly immersed, the section is to be completed by adding its reflexion in the free surface, and the problem solved for the section so formed. When the boundary of the section cuts the free surface at an acute angle the velocity becomes infinite at the corner, so that the approximation to the fulfilment of the surface condition is locally inadequate, but the effect on the motion as a whole is probably small. The fact that the theoretically infinite velocity at a sharp corner does not affect the practical applicability of the results appears to have been established by Moullin † in the case of a totally submerged section. He finds that for a rectangular section of breadth twice the depth, an approximation to the entrained area is that of the circumscribing circle, *i.e.*,  $5\pi/16 \cdot b^2$  or  $0.98 b^2$ , while interpolation between Riabouchinsky's results ‡ gives  $1.05 b^2$  in fair agreement. For deeper sections the approximation does not hold; thus for a square (corresponding to a partly immersed section of depth equal to half the breadth) the respective figures are  $1.57 b^2$  and  $1.188 b^2$ .

It appears more reasonable to base the approximation on the maximum width, making some allowance for the shape of section, and while no empirical formula is likely to give very accurate results for a great variety of sections, the expression  $(b^2 \times A/b \cdot d)$  or  $(A \times b/d)$  is reasonably accurate for sections (1), (2), (4), and (6), and is exact for an ellipse. The area for a partly immersed section, vibrating vertically, becomes  $(A' \times b/2d')$  where  $A'$  and  $d'$  are the actual area and depth respectively, but this makes no allowance for any departure from two-dimensional motion (Part IV.).

\* Cf. Rayleigh, 'Collected Papers,' ii. p. 208.

† *Loc. cit.*

‡ *Loc. cit.*

## PART II.

When the free surface is parallel to the direction of motion the fulfilment of the condition  $\phi=0$  is not quite so easy, but a solution can be obtained for a semi-elliptical section with the axis in the free surface.

Putting

$$x+iy = \sinh(\xi+i\eta),$$

the boundary condition,

$$\psi - c = y = \cosh \xi \sin \eta \quad \xi = \xi_0,$$

can be fulfilled for values of  $\eta$  between 0 and  $\pi$  by

$$\psi = \cosh \xi_0 \sum_1^{\infty} A_n \cdot e^{-2n(\xi-\xi_0)} \cos 2n\eta,$$

where

$$A = \frac{4}{\pi(4n^2-1)}.$$

The corresponding value of  $\phi$  is

$$\phi = \cosh \xi_0 \sum_1^{\infty} A_n \cdot e^{-2n(\xi-\xi_0)} \cdot \sin 2n\eta,$$

and when  $\xi = \xi_0$ ,

$$\phi = \phi_0 = \cosh \xi_0 \sum_1^{\infty} A_n \cdot \sin 2n\eta.$$

The entrained area is given by

$$\begin{aligned} \int_0^{\pi} \phi_0 \left( \frac{dy}{d\eta} \right)_0 d\eta &= \cosh^2 \xi_0 \sum_1^{\infty} A_n \int_0^{\pi} \sin 2n\eta \cdot \cos \eta d\eta \\ &= \cosh^2 \xi_0 \sum_1^{\infty} \frac{16 \cdot n}{\pi(4n^2-1)^2} \\ &= (2/\pi) \cosh^2 \xi_0 \\ &= (2/\pi) b^2, \end{aligned}$$

since  $\cosh \xi_0 = b$ , the major semi-axis, perpendicular to the direction of motion and to the free surface. The result is the same when motion takes place parallel to the major axis, and the semicircle and lamina are particular cases. The comparative figure for the semicircle moving perpendicularly to the surface is  $(\pi/2)b^2$ , so that the virtual inertia for horizontal motion is only  $(4/\pi^2)$  times that for vertical motion. For other sections the ratio depends, of course, on the ratio of the axes.

Moullin \* carried out experiments on a flat bar, the most direct comparison possible being that for the bar  $\frac{1}{4}$  in. thick

\* *Loc. cit.*

with its edge submerged  $2\frac{3}{4}$  in. From the ratio of the frequency in this condition to that in air, it is possible to calculate that the added mass of water is about  $0.58b^2$  per unit length as against  $0.636$ , as calculated for a lamina.

A solution can also be obtained for the case of a circular cylinder, with horizontal axis, submerged to any depth below the surface. Employing the coordinates

$$z = x + iy = \cot 1/2(\xi + i\eta) = \frac{\sin \xi - i \sinh \eta}{\cosh \eta - \cos \xi},$$

we may take  $y = \eta = 0$  as the free surface and  $\eta = \alpha$  as the boundary of the circular section, of radius  $\text{cosech } \alpha$ , the centre being at a depth  $\text{coth } \alpha$  below the surface.

The boundary condition  $\psi = -y + \text{constant}$ , for  $\eta = \alpha$ , can be satisfied by

$$\psi = 2 \sum_1^{\infty} \frac{e^{-n\alpha}}{\cosh n\alpha} \cos n\xi \cdot \cosh n\eta,$$

which makes

$$\phi = 2 \sum_1^{\infty} \frac{e^{-n\alpha}}{\cosh n\alpha} \sin n\xi \cdot \sinh n\eta,$$

and this vanishes at the free surface  $\eta = 0$ .

The kinetic energy integral

$$\begin{aligned} - \int \phi \frac{d\phi}{dn} ds &= \int_{-\pi}^{\pi} \phi \frac{dy}{d\xi} d\xi \quad (\eta = \alpha) \\ &= 2 \sum_1^{\infty} e^{-n\alpha} \cdot \tanh n\alpha \cdot \sinh \alpha \int_{-\pi}^{\pi} \frac{\sin n\xi \cdot \sin \xi d\xi}{(\cosh \alpha - \cos \xi)^2} \\ &= 4\pi \sum_1^{\infty} n \cdot e^{-2n\alpha} \cdot \tanh n\alpha. \end{aligned}$$

When  $\alpha$  is large the series converges rapidly, and expansion of the first three terms gives

$$4\pi \{e^{-2\alpha} + (e^{-6\alpha}) + \dots\}.$$

Expressing this in terms of

$$r = \text{cosech } \alpha = 2e^{-\alpha}(1 + e^{-2\alpha} \dots),$$

we have

$$\begin{aligned} &\pi r^2(1 - 2e^{-2\alpha} + \dots) \\ &= \pi r^2(1 - r^2/2c^2) \end{aligned}$$

to this order, putting  $c = \text{coth } \alpha = 1$  nearly, for the depth of immersion to the centre of the circle. The factor  $(1 - r^2/2c^2)$  shows the reduction in the kinetic energy due to the free surface, when the ratio  $r/c$  is fairly small.

When  $\alpha$  is small we have the integral

$$\int_0^\alpha n \cdot e^{-2na} \cdot \tanh n\alpha \cdot dn$$

whose value is  $1/4\alpha^2(\pi^2/6-1)$ , so that the entrained area is  $\pi\alpha^2(\pi^2/6-1)$  or  $\pi r^2(\pi^2/6-1)$ ,  $r$  being equal to  $1/\alpha$ . This result, corresponding to the case of relatively small immersion, agrees with the result of Part I. (1) for motion *perpendicular* to the surface ( $y=0$ ), i.e., the common tangent to the two circles in the example quoted. The solution just given can in fact be adapted to this case, the expression for the entrained area being identical, which shows that the direction of motion is immaterial.

### PART III.—EFFECT OF RIGID BOUNDARIES.

#### (1) *Circle with Plane Boundary.*

With the same coordinates as in the last example, the expression

$$\psi = 2 \sum_1^\infty \frac{e^{-n\alpha}}{\sinh n\alpha} \cos n\xi \sinh n\eta$$

satisfies the boundary condition  $\psi = -y + \text{constant}$  for  $\eta = \alpha$ , and also makes  $\psi = 0$  for  $\eta = 0$ , as is required for a boundary at  $y = \eta = 0$ . The expression for the entrained area

$$\begin{aligned} - \int \phi \frac{d\phi}{dn} \cdot ds &= - \int_{-\pi}^{\pi} \phi \frac{d\phi}{d\eta} \cdot d\xi \\ &= 2 \sum_1^\infty e^{-n\alpha} \coth n\alpha \int_{-\pi}^{\pi} \frac{\sin n\xi \sin \xi \sinh \alpha}{(\cosh \alpha - \cos \xi)^2} \cdot d\xi \\ &= 4\pi \sum_1^\infty n \cdot e^{-2n\alpha} \cdot \coth n\alpha. \end{aligned}$$

In the same way as before this gives, for  $\alpha$  large,

$$- \int \phi \frac{d\phi}{dn} \cdot ds = \pi r^2 \left( 1 + \frac{r^2}{2c^2} \right),$$

indicating the effect of a distant boundary, and for  $\alpha$  small,

$$- \int \phi \frac{d\phi}{dn} \cdot ds = \pi r^2 \left( \frac{\pi^2}{3} - 1 \right),$$

which again agrees with the example (1) of Part I. It can be shown that the direction of motion is immaterial in this case also.

(2) *Semicircle with Boundary and Free Surface.*

The example just considered, while of interest as giving a comparison with the results in Part II., does not satisfy the condition  $\phi=0$  at a plane through the axis of the cylinder, parallel to the fixed boundary, as would be required for a cylinder of semicircular section in a limited depth of water.

Putting  $w = C \cdot \operatorname{cosec} z/2$ ,

$$\phi = 2C \cdot \frac{\sin x/2 \cdot \cosh y/2}{\cosh y - \cos x},$$

$$\psi = 2C \cdot \frac{\cos x/2 \cdot \sinh y/2}{\cosh y - \cos x}$$

represents a doublet at the origin, with axis  $Ox$ , (with boundaries  $\psi=0$  at  $x=\pm\pi$ , and may also be regarded as representing the motion due to a small circle at the origin, moving in the direction  $Ox$ . If the velocity is unity, the condition

$$y=0, \quad \frac{d\phi}{dx} = C \cdot \frac{\cos x/2}{1 - \cos x} = 1$$

gives

$$C = \frac{1 - \cos x}{\cos x/2} = x^2/2 + x^4/48 + \dots,$$

$x$  being small, which expresses  $C$  in terms of the radius of the circle  $a$  on putting  $x=a$ . Similarly,

$$x=0, \quad \psi = C/\sinh y/2 = y, \quad C = y^2/2 + y^4/48 + \dots$$

verifies, on putting  $y=a$ , that to this order the circular shape holds.

In the vicinity of the origin, more generally, on expanding

$$\begin{aligned} \phi &= 2C \left\{ \frac{(x/2 - x^3/48 + \dots)(1 + y^2/8 \dots)}{y^2/2 + x^2/2 + y^4/384 - x^4/384 + \dots} \right\} \\ &= 2C \cdot x/r^2 (1 + \text{terms in } r^2), \end{aligned}$$

$$\frac{d\phi}{dr} = -2C \cdot \frac{\cos \theta}{r} (1 + \text{terms in } r^2).$$

Hence

$$\begin{aligned} - \int \phi \frac{d\phi}{dr} \cdot r \cdot d\theta &= 4C \cdot \left( \frac{\pi}{r^2} + \text{terms in } r^2 \right) \\ &= \frac{\pi}{r^2} (r^4 + r^6/12) \end{aligned}$$

to this order.

When  $r=a$ , this is the kinetic energy integral, the value being  $\pi a^2(1+a^2/12)$ . This applies to the case of a boundary at distance  $\pi$  from the centre of the circle, and generalization for any distance of boundary  $c$  (large in relation to  $a$ ) gives  $\pi a^2(1+a^2\pi^2/12c^2)$ .

In a very similar manner  $w=C \cdot \coth z/2^*$  represents a small circle midway between two plane boundaries at distance  $\pm\pi$ , moving parallel to the boundaries, the entrained area being  $\pi a^2(1+a^2\pi^2/6c^2)$ . In each case the plane through the centre perpendicular to the direction of motion may be regarded as a free surface, the entrained area for the semi-circle being, of course, half the above.

### (3) Lamina between two Plane Boundaries.

Applying Lamb's solution †,  $\cosh w = \mu \cosh z$ , which applies to the motion of a lamina of width  $2 \cdot \cos^{-1}(1/\mu)$  midway between two plane boundaries distance  $\pi$  apart, and moving in a direction parallel to the boundaries. At the surface of the lamina,

$$x = 0, \quad y < \cos^{-1}(1/\mu), \quad \psi = 0,$$

and

$$\phi = \cosh^{-1}(\mu \cos y), \quad \frac{d\phi}{dn} = -1,$$

so that

$$\begin{aligned} - \int \phi \frac{d\phi}{dn} ds &= 4 \int_0^{\sec^{-1} \mu} \cosh^{-1}(\mu \cos y) dy \\ &= 2\pi \log \mu \\ &= 2\pi \log \sec b, \end{aligned}$$

if  $b = \cos^{-1}(1/\mu)$  is the half width of the lamina. This gives, on expansion,

$$\begin{aligned} - \int \phi \frac{d\phi}{dn} ds &= 2\pi(b^3/2 + b^4/12 + \dots) \\ &= \pi b^3(1 + b^2/6 \dots). \end{aligned}$$

This applies to the case when the width of the lamina is moderately small in relation to the distance between the boundaries, and may be generalized for boundaries at a distance  $c$  from the centre of the lamina as  $\pi b^3 \left(1 + \frac{\pi^2 b^2}{24c^2}\right)$ .

\* Lamb, 'Hydrodynamica,' p. 68 (5th ed.).

† Loc. cit. p. 508.



The factor may be compared with that for a circle of radius  $b$  in the corresponding case considered in (2) above.

(4) *Circle completely surrounded by Rigid Boundary.*

The first order correction to the inertia coefficient for a circle enclosed by a rigid boundary, corresponding to the three-dimensional problem of an infinite circular cylinder enclosed by a fixed cylinder of any cross-section, can be readily obtained, provided a solution is known for the fluid motion due to the translation of a cylinder whose section is the inverse of that of the fixed cylinder, with respect to an internal point, namely the centre of the circle.

Taking this point as the origin, and superposing a uniform stream on the known solution, inversion gives a doublet at the origin, which may therefore be supposed to be the centre of a small circle, moving inside the fixed boundary.

In terms of  $z'$ , which is equal to  $1/z$ , we have, when  $z'$  is large, a solution of form

$$w = z' + a/z' + \dots,$$

and, accordingly, when  $z$  is small,

$$w = 1/z + az + \dots$$

$$\phi = \cos \theta / r + ar \cos \theta + \dots,$$

$$\frac{d\phi}{dr} = -\cos \theta / r^2 + a \cos \theta + \dots,$$

neglecting terms of higher degree in  $r$ .

Putting  $r=b$ , this corresponds to the case of a small circle of radius  $b$  moving in the direction  $Ox$  with velocity  $(1/b^2 - a)$ .

$$\begin{aligned} - \int \phi \frac{d\phi}{dn} ds &= - \int_0^{2\pi} \phi \frac{d\phi}{dr} b \cdot d\theta \quad (r=b) \\ &= \pi(1/b^3 - a^2 b^3). \end{aligned}$$

Correcting this for unit velocity, since the kinetic energy varies as the square of the velocity, the entrained area is

$$\begin{aligned} &\pi \frac{(1/b^2 - a^2 b^2)}{(1/b^2 - a)^2} \\ &= \pi b^2 (1 + 2ab^2) \end{aligned}$$

to this order in  $b$ .

Thus, it is only necessary to know the coefficient  $a$  in the original solution in order to determine the first order

correction to the inertia. If the boundary is a circle of unit radius which inverts into itself,  $a=1$ , giving  $\pi b^2(1+2b^2)$  or more generally when the radius of the outer circle is  $c$ ,  $\pi b^2(1+2b^2/c^2)$  in agreement, for the case of  $(b/c)$  small, with the exact solution, which in this case may readily be shown to be  $\pi b^2 \left( \frac{c^2+b^2}{c^2-b^2} \right)$ .

When the outer boundary is a square the solution of Part I. (4) may be applied.  $a=1$ , giving  $\pi b^2(1+2b^2/c^2)$  in this case also, the side of the square being  $K=1.854$ . Generalizing the solution for a square of side  $2c$  gives  $\pi b^2(1+K^2b^2/2c^2)$  or  $\pi b^2(1+1.72b^2/c^2)$ , slightly less, as would be anticipated, than for a circle of radius  $c$ .

#### PART IV.—MOTIONS IN THREE DIMENSIONS.

##### (1) *Infinite Circular Cylinder.*

If a cylinder of radius  $a$  be supposed to execute flexural vibrations of small amplitude, the velocity being given by  $b \cdot \cos kz$ ,  $z$  being measured along the axis, the appropriate solution for the motion of the external fluid is

$$\phi = C \cdot K_1(kr) \cdot \cos \theta \cdot \cos kz$$

with a suitable time-factor,  $K_1$  being Bessel's function of order unity of the second kind (and "of imaginary argument"), which is selected so as to make the motion vanish at infinity. The motion is parallel to the plane  $zx$ , and the constant  $C$  is determined by the boundary condition

$$\frac{d\phi}{dr} = -b \cdot \cos kz \cdot \cos \theta \quad (r=a)$$

$$= C \cdot k \cdot K_1'(ka) \cos \theta \cdot \cos kz,$$

$$C = b / \{ k \cdot K_1'(ka) \},$$

$$\begin{aligned} - \int_0^{2\pi} \phi \frac{d\phi}{dr} \cdot a \cdot d\theta \\ = -C^2 \cdot (ka) \cos^2 kz \cdot K_1(ka) \cdot K_1'(ka) \int_0^{2\pi} \cos^2 \theta d\theta \\ = \pi a^2 \left( \frac{1}{ka \cdot K_1'(ka)} \right) \cdot b^2 \cos^2 kz. \end{aligned}$$

If the fluid were constrained by a series of planes perpendicular to  $Oz$ , so that the motion took place in two dimensions only, the corresponding expression would be  $\pi \cdot b^2 \cdot a^2 \cdot \cos^2 kz$ ,

so that the expression in brackets, which is always less than unity, indicates the ratio in which the energy is reduced, as compared with the two-dimensional case. Its value  $R$  in terms of  $a/\lambda$  or  $ka/2\pi$ ,  $\lambda$  being the wave-length of the vibration, is given below:—

$a/\lambda$ .....	$1/4\pi$	$1/2\pi$	$3/4\pi$	$1/\pi$
$R$ .....	0.781	0.588	0.464	0.360

If, instead of seeking a solution of Laplace's equation, we had used the equation  $(\nabla^2 + k_1^2)\phi = 0$ , appropriate to a compressible fluid,  $2\pi/k_1$  being the length of the compression wave of the same frequency as the vibration, the same form of solution would have applied, provided  $k > k_1$ ,  $(k^2 - k_1^2)^{1/2}$  being substituted for  $k$ . This has the effect of increasing slightly the kinetic energy.

## (2) *Ellipsoid.*

A solution can be obtained which fulfils the boundary condition for what is practically a two-node flexural vibration of a prolate ellipsoid of revolution.

In terms of the usual coordinates \*

$$x = k\mu\zeta; \quad y = k(1 - \mu^2)^{1/2}(\zeta^2 - 1)^{1/2} \cos \omega;$$

$$z = k(1 - \mu^2)^{1/2}(\zeta^2 - 1)^{1/2} \sin \omega$$

appropriate to a prolate ellipsoid, the foci of the meridian being the points  $(\pm k, 0, 0)$ ,

$$\phi = C \cdot P_3'(\mu) \cdot Q_3'(\zeta) \cdot \cos \omega$$

is a known solution of Laplace's equation :

$$P_3'(\mu) = (1 - \mu^2)^{1/2} \cdot 1/2 \cdot (15\mu^2 - 3),$$

$$Q_3'(\zeta) = (\zeta^2 - 1)^{1/2} \cdot \left\{ \frac{1}{4} (15\zeta^2 - 3) \log \frac{\zeta + 1}{\zeta - 1} - \frac{1}{2} \left( 15\zeta + \frac{2\zeta}{\zeta^2 - 1} \right) \right\},$$

$$\frac{\partial Q_3'(\zeta)}{\partial \zeta} = (\zeta^2 - 1)^{-1/2} \cdot \left\{ \left( \frac{45}{4} \zeta^2 - \frac{33}{4} \zeta \right) \log \frac{\zeta + 1}{\zeta - 1} - \frac{45}{2} \zeta^2 + 9 + \frac{1}{\zeta^2 - 1} \right\}.$$

\* Lamb, p 130.

The velocity potential can be made to satisfy the boundary condition

$$\frac{\partial \phi}{\partial \zeta} = (a^2 - x^2) \frac{\partial y}{\partial \zeta} + 2xy \frac{\partial x}{\partial \zeta} \quad (\zeta = \zeta_0)$$

by adjusting suitably the values of  $C$  and  $a$ . Since

$$\begin{aligned} (a^2 - x^2) \frac{\partial y}{\partial \zeta} + 2xy \frac{\partial x}{\partial \zeta} \\ = \{k\zeta(a^2 - k^2\mu^2\zeta^2) + 2k^2\mu^2\zeta(\zeta^2 - 1)\}(\zeta^2 - 1)^{-\frac{1}{2}}(1 - \mu^2)^{\frac{1}{2}} \cos \omega, \end{aligned}$$

this gives

$$a^2 = \frac{k^2(2 - \zeta_0^2)}{5},$$

$$C = k \cdot a^2 \zeta_0 \div \left\{ 3/2(\zeta_0^2 - 1)^{\frac{1}{2}} \cdot \frac{\partial Q_2'(\zeta)}{\partial \zeta} \right\} \quad (\zeta = \zeta_0),$$

$$\begin{aligned} 2T &= - \iint \phi \frac{d\phi}{dn} \cdot dS \\ &= - \int_{-1}^1 d\mu \cdot \frac{\delta s}{\delta \mu} \Big|_0^{2\pi} \phi \cdot \frac{\partial \phi}{\partial \zeta} \cdot \frac{\delta \zeta}{\delta n} \cdot k(1 - \mu^2)^{\frac{1}{2}}(\zeta^2 - 1)^{\frac{1}{2}} \cdot d\omega \\ &= - \int_{-1}^1 d\mu \cdot \int_0^{2\pi} \phi \cdot \frac{\partial \phi}{\partial \zeta} \cdot k \left( \frac{\zeta^2 - \mu^2}{1 - \mu^2} \right)^{\frac{1}{2}} \\ &\quad \cdot \frac{1}{k} \left( \frac{\zeta^2 - 1}{\zeta^2 - \mu^2} \right)^{\frac{1}{2}} \cdot k(1 - \mu^2)^{\frac{1}{2}} \cdot (\zeta^2 - 1)^{\frac{1}{2}} d\omega \\ &= -k \int_{-1}^1 d\mu (\zeta^2 - 1) \int_0^{2\pi} \phi \frac{\partial \phi}{\partial \zeta} d\omega \\ &= -\pi k \cdot (\zeta^2 - 1) \cdot C^2 \cdot Q_2'(\zeta) \\ &\quad \cdot \left\{ \frac{\partial Q_2'(\zeta)}{\partial \zeta} \right\} \int_{-1}^1 (1 - \mu^2) \left( \frac{15\mu^2 - 3}{2} \right)^{\frac{1}{2}} d\mu \\ &= \frac{32\pi k^3}{21\zeta_0} \cdot a^4 \cdot \zeta^2 \left\{ \frac{-Q_2'(\zeta)}{\frac{\partial Q_2'(\zeta)}{\partial \zeta}} \right\} \quad (\zeta = \zeta_0). \end{aligned}$$

The assumed boundary condition (1) above corresponds to an approximate type of flexural vibration in which the amplitude is proportional to  $(a^2 - x^2)$ , the positions of the "nodes" being given by

$$x = \pm a = \pm k \frac{\sqrt{2 - \zeta_0^2}}{\sqrt{5}}.$$

For a slender ellipsoid,  $\zeta_0$  is very little different from unity, so that the nodes are approximately  $\pm \sqrt{1/5}$  of the major semi-axis ( $k\zeta_0$ ) from the centre of the ellipsoid. This agrees fairly closely with the actual positions for a beam having the same mass distribution as an ellipsoid of uniform density. The effect of the departure of the actual amplitude curve from the parabolic shape is probably unimportant, but as the primary object of the investigation is to compare the inertia of the water with that of the ellipsoid itself, this may be allowed for by calculating the kinetic energy of the ellipsoid for a hypothetical vibration in which the amplitude is proportional to  $(a^2 - x^2)$  as the basis of comparison.

The area of the circular section of the ellipsoid being

$$\pi k^2(1 - \mu^2)(\zeta_0^2 - 1) \quad \text{or} \quad \frac{\pi(\zeta_0^2 - 1)}{\zeta_0^2} (k^2\zeta_0^2 - x^2),$$

the kinetic energy, assuming unity density, and velocity proportional to  $(a^2 - x^2)$  is given by

$$\begin{aligned} 2T_1 &= \frac{\pi(\zeta_0^2 - 1)}{\zeta_0^2} \int_{-k\zeta_0}^{k\zeta_0} (a^2 - x^2)^2 \cdot (k^2\zeta_0^2 - x^2) \cdot dx \\ &= \frac{16\pi}{525} k^7 \zeta_0 (\zeta_0^2 - 1) (7 - 14\zeta_0^2 + 2\zeta_0^4). \end{aligned}$$

The ratio

$$\begin{aligned} T/T_1 &= \frac{2(2 - \zeta_0^2)^2}{(7 - 14\zeta_0^2 + 2\zeta_0^4)} \\ &\cdot \left\{ \begin{aligned} &30\zeta_0^2 + 4 + 4/(\zeta_0^2 - 1) - \zeta_0(15\zeta_0^2 - 3) \log \frac{\zeta_0 + 1}{\zeta_0 - 1} \\ &- 90\zeta_0^2 + 36 + 4/(\zeta_0^2 - 1) + 3\zeta_0(15\zeta_0^2 - 11) \log \frac{\zeta_0 + 1}{\zeta_0 - 1} \end{aligned} \right\}. \end{aligned}$$

This tends to the value unity as  $\zeta_0$  tends to unity, i. e., as the ellipsoid becomes indefinitely small in diameter, the length remaining constant. The fluid motion is then practically two-dimensional. The value for various ratios of the axes  $c/b$  is given below, the value of  $\zeta_0$  being  $1/\sqrt{1 - c^2/b^2}$  :—

$c/b$ .....	0.045	0.10	0.141	0.201
$T/T_1$ .....	0.946	0.825	0.729	0.615

The rotatory inertia of the ellipsoid has been neglected, since in any practical application of the results the effect of this factor would be separately estimated, if it were necessary to take it into account. It can readily be shown

that for an ellipsoid of uniform density the rotatory inertia is given by

$$R = 8/5 \frac{(\xi_0^2 - 1)}{\xi_0^2} \cdot \left( \frac{2}{7 - 14\xi_0^2 + 9\xi_0^4} \right) \cdot T_1,$$

from which the corrected ratio  $T/(T_1 + R)$  may be obtained.

The results given above, both for the ellipsoid and for the infinite cylinder, show that, even when the diameter is moderately small in relation to the wave-length of the vibration, the three-dimensional character of the fluid motion cannot be ignored. In the case of the cylinder, the *distribution* of the pressure due to the fluid inertia is, however, identical with that when the motion is confined to two dimensions, being proportional to  $\cos \theta \cdot \cos kz$ . A similar result holds in the case of the ellipsoid as regards the amount of the normal pressure on the surface, but a small correction has to be applied to the component in the direction of motion towards the ends of the ellipsoid on account of the inclination of the surface to the axis.

In applying the results obtained to bodies of other forms—for instance, the hull of a ship,—reasonable accuracy should be obtained by assuming a distribution of the “added mass” of water according to the empirical formula given at the end of Part I. above, and correcting the total amount in accordance with the ratio found for an ellipsoid of similar proportions. This applies to vibrations in a vertical plane, but for horizontal motion the correction factor will be much nearer unity, since the fluid motion, as indicated in the examples of Part II., is more local in the two-dimensional case.

The author is indebted to Professor J. Proudman for some valuable suggestions in the preparation of this paper.

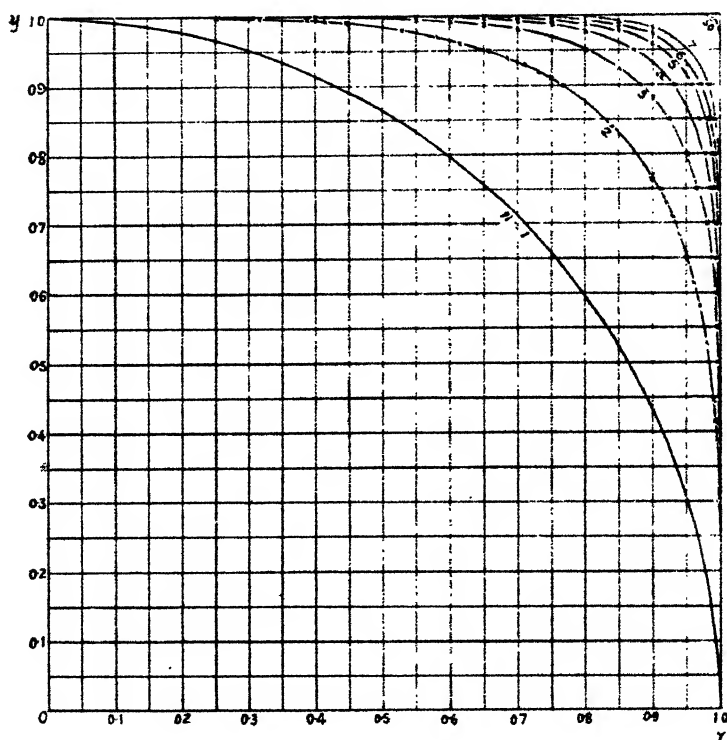
*Author's note.*—While this paper has been in the press, Prof. H. M. Lewis has published (Amer. Soc. of Nav. Arch., Nov. 1929) a solution corresponding to Part I., example (3). He also treats the case of an ellipsoid (Part IV. (2)), but neglects the term in  $\frac{\partial^2}{\partial \xi^2}$  in the boundary conditions, and arrives at different results in consequence.]

XVI. *On some Closed Algebraic Curves and their Application to Dynamical Problems.*—Part I. By SEIICHI HIGUCHI\*.

§ 1. *Introduction.*

**T**HOUGH the conception of "Closed curve of the higher order" is not new for mathematicians, so far as the

Fig. 1, a.



author is aware, no study with reference to its physical application has yet been published.

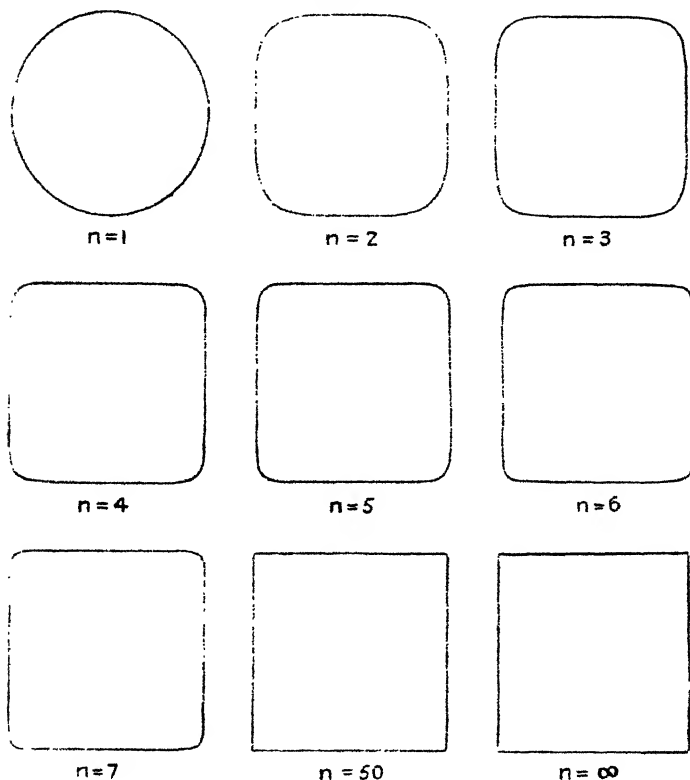
In this paper it is proposed first to deal with some closed algebraic curves, say circles of the higher order, their main properties being mentioned, omitting the proofs, and figures of groups of them are calculated and graphed; and, secondly, a few applications to the dynamical problems, *i. e.*, the area included by the curve, volume of revolution, and radius of gyration about an axis are calculated and tabulated.

\* Communicated by the Author.

However, the most important and useful application of the proposition would be no other than the discovery of the family of equipotential curves of the above; but, unfortunately, the present writer did not obtain any satisfactory results in regard to this subject.

Further applications to the physical problems will be published in the second part of this paper.

Fig. 1, b.



## § 2. Proposition of the Curve and its Characteristic Properties.

Let us consider the following system of closed algebraic curves\* :

$$x^{2n} + y^{2n} = c, \quad . \quad . \quad . \quad . \quad . \quad . \quad . \quad (1)$$

\* The orthogonal trajectories of the curves are easily found, as

$$x^{-(2n-2)} - y^{-(2n-2)} = b,$$

where  $b$  is a real number.



where  $n$  is a positive integer,  $c$  a real number, and  $x$  and  $y$  lie in the interval  $(-c, +c)$ .

Then we obtain a group of curves by changing the value of  $n$ , i. e.,  $n=1, 2, 3, 4, 5, \dots$ , including the circle for the special case when  $n=1$ .

Now we shall first study the characteristic properties of the curve, taking  $c$  as unity for the sake of simplicity.

(1) For the case where  $n$  is finite, the equation

$$y = f(x) = (1 - x^{2n})^{\frac{1}{2n}}$$

is continuous in the interval of  $x$  ( $-1 \leq x \leq +1$ ), but when  $n$  is infinite, it is discontinuous at the upper and lower limits of  $x$ , i. e.,  $x = \pm 1$ .

(2) The given curve is symmetrical with respect to the axes  $x, y$ , and also to the bisecting line  $y=x$ .

(3) The distance between the origin and the intersecting point of the curve and the bisecting line  $y=x$  is the maximum radial distance.

TABLE I.

Relation between the above Maximum Radial Distance  $r$  and the Power  $n$  in the equation (1).

$n$ .	$x$ or $y$ .	$r$ .
1 .....	0.7071	1
2 .....	0.8409	1.1892
3 .....	0.8909	1.2599
4 .....	0.9170	1.2968
...	.....	.....
50 .....	0.9931	1.4044
...	.....	.....
$\infty$ .....	1.0000	$\sqrt{2}=1.4142$

Now, based on the above proposition, we wish to propose the next expression for groups of an ellipse of a higher order, of a sphere of a higher order, of an ellipsoid of a higher order, respectively, but the discussion of these groups is here omitted,

$$\left. \begin{aligned} \left(\frac{x}{a}\right)^{2n} + \left(\frac{y}{b}\right)^{2n} &= 1, \\ x^{2n} + y^{2n} + z^{2n} &= C, \\ \left(\frac{x}{a}\right)^{2n} + \left(\frac{y}{b}\right)^{2n} + \left(\frac{z}{c}\right)^{2n} &= 1. \end{aligned} \right\}$$

## § 3. Graphical Representation of the given Curve

$$x^{2n} + y^{2n} = 1.$$

In fig. 1 (pp. 184, 185) the curves are graphed, taking the values of  $n$  as  $n=1, 2, 3, 4, 5, 6, 7, 50$  respectively, and these

TABLE II.

The Numerical Values of the Solution of  $x^{2n} + y^{2n} = 1$ .

y.	x.				y.	x.		
	n=2.	n=3.	n=4.	n=5.		n=6.	n=7.	n=50.
0.8409	0.8409				0.9438	0.9438		
0.8908	...	0.8908			0.95	0.9372		
0.90	0.7657	0.8814			0.9517	...	0.9517	
0.91	0.7487	0.8695			0.96	0.9239	0.9423	
0.9170	...	...	0.9170		0.97	0.9060	0.9272	
0.92	0.7297	0.8561	0.9139		0.98	0.8798	...	
0.93	0.7085	0.8407	0.9025		0.99	0.8342	0.8656	
0.9330	...	...	...	0.9930	0.992	0.8196	0.8521	
0.94	0.6843	0.8227	0.8891	0.9255	0.9931	...	...	0.9931
0.95	0.6563	0.8014	0.8725	0.9127	0.994	0.8009	0.8355	0.9921
0.96	0.6145	0.7753	0.8524	0.8964	0.996	0.7750	0.8124	0.9890
0.97	0.5820	0.7421	0.8275	0.8748	0.998	0.7322	0.7739	0.9831
0.98	0.5278	0.6966	0.7884	0.8438	0.999	0.6915	0.7368	
0.99	0.4455	0.6231	0.7261	0.7909	0.9992	0.6788	0.7253	0.9747
0.992	0.4217	0.6008	0.7065	0.7740	0.9994	0.6627	0.7106	0.9720
0.994	...	0.5731	0.6824	0.7529	0.9996	0.6407	0.6932	0.9681
0.998	0.2988	...	0.5959	0.6757	0.9998	0.6049	0.6571	0.9615
0.999	0.2527	0.4261	...	0.6307	0.9999	0.5713	0.6232	0.9549
0.9998	...	...	0.4500		0.99992	...	0.6158	0.9528
0.9999	...	...	...	0.5000	0.99994	...	0.6030	0.9501
					0.99996	...	0.5860	0.9465
					0.99998	...	0.5575	0.9397
1.0000	0.0	0	0.0	0.0	1.00000	0.0	0.0	0.0

numerical values are tabulated in Table II., where these calculations are made in the range of  $x$  and  $y$  covering one octant by § 2 (2).

§ 4. *Applications of our Proposition to Dynamical Problems.*

A few applications to dynamical problems are obtained as follows:—

1. Area included by the curve  $x^{2n} + y^{2n} = 1$ .

The expression of the area is

$$A = 4 \int_0^1 (1 - x^{2n})^{\frac{1}{2n}} dx,$$

and this integral is reducible to Euler's integral as :

$$\begin{aligned} \text{For } n=1, \quad A &= 4 \int_0^1 (1-x^2)^{\frac{1}{2}} dx \\ &= 4 \left[ \frac{x^2}{2} (1-x^2)^{\frac{1}{2}} + \frac{1}{2} \sin^{-1} x \right]_0^1, \end{aligned}$$

$$\text{or} \quad A = 2B\left(\frac{1}{2}, \frac{3}{2}\right) = 2\Gamma\left(\frac{1}{2}\right) \cdot \Gamma\left(\frac{3}{2}\right) = 4\Pi^2\left(\frac{1}{2}\right),$$

$$n=2, \quad A = 4 \int_0^1 (1-x^4)^{\frac{1}{4}} dx = B\left(\frac{1}{4}, \frac{5}{4}\right) = 4 \frac{\Pi^2\left(\frac{1}{4}\right)}{\Pi\left(\frac{1}{2}\right)},$$

$$n=3, \quad A = 4 \int_0^1 (1-x^6)^{\frac{1}{6}} dx = \frac{2}{3} B\left(\frac{1}{6}, \frac{7}{6}\right) = 4 \frac{\Pi^2\left(\frac{1}{6}\right)}{\Pi\left(\frac{1}{3}\right)},$$

$$n=4, \quad A = 4 \int_0^1 (1-x^8)^{\frac{1}{8}} dx = \frac{1}{2} B\left(\frac{1}{8}, \frac{9}{8}\right) = 4 \frac{\Pi^2\left(\frac{1}{8}\right)}{\Pi\left(\frac{1}{4}\right)},$$

$$n=5, \quad A = 4 \int_0^1 (1-x^{10})^{\frac{1}{10}} dx = \frac{2}{5} B\left(\frac{1}{10}, \frac{11}{10}\right) = 4 \frac{\Pi^2\left(\frac{1}{10}\right)}{\Pi\left(\frac{1}{5}\right)},$$

.....

$$\begin{aligned} n=50, \quad A &= 4 \int_0^1 (1-x^{100})^{\frac{1}{100}} dx = \frac{1}{25} B\left(\frac{1}{100}, \frac{101}{100}\right) \\ &= 4 \frac{\Pi^2\left(\frac{1}{100}\right)}{\Pi\left(\frac{1}{50}\right)}, \end{aligned}$$

.....

$$n=\infty, \quad A=4,$$

where B,  $\Gamma$ ,  $\Pi$  denote Beta, Gamma, and Gauss functions respectively.

These numerical values are tabulated in Table III.

TABLE III \*.  
A, Q, and R<sup>2</sup>.

n.	A.	Q.	R <sup>2</sup> .
1 .....	$\pi$	$\frac{1}{2}\pi$	$\frac{1}{2}$
2 .....	0.92703 73 $\times 4$	0.87401 92 $\times 2\pi$	0.89860 52 $\times \frac{1}{2}$
3 .....	0.96382 72 $\times 4$	0.93481 32 $\times 2\pi$	0.94492 99 $\times \frac{1}{2}$
4 .....	0.97849 48 $\times 4$	0.96027 50 $\times 2\pi$	0.96538 73 $\times \frac{1}{2}$
5 .....	0.98573 20 $\times 4$	0.97329 14 $\times 2\pi$	0.97622 59 $\times \frac{1}{2}$
6 .....	0.98987 68 $\times 4$	0.98085 31 $\times 2\pi$	0.98264 18 $\times \frac{1}{2}$
7 .....	0.99242 85 $\times 4$	0.98557 39 $\times 2\pi$	0.98679 04 $\times \frac{1}{2}$
...	...	...	...
50 .....	0.99983 79 $\times 4$	0.99967 81 $\times 2\pi$	0.99968 27 $\times \frac{1}{2}$
...	...	...	...
$\infty$ .....	4	$2\pi$	$\frac{1}{2}$

2. Volume of revolution about the axis  $x$  or  $y$ .

The general expression is

$$Q = 2\pi \int_0^1 (1-x^{2n})^{\frac{1}{2}} dx,$$

and these integrals are also reducible to Euler's integral, as shown below:

$$\text{For } n=1, \quad Q = 2\pi \int_0^1 (1-x^2) dx = 2\pi \left[ x - \frac{x^3}{3} \right]_0^1,$$

$$\text{or} \quad Q = \pi B\left(\frac{1}{2}, 2\right) = 2\pi \frac{\Gamma(\frac{1}{2})}{\Gamma(\frac{3}{2})},$$

$$n=2, \quad Q = 2\pi \int_0^1 (1-x^4)^{\frac{1}{2}} dx = 2\pi \frac{\Gamma(\frac{1}{4})\Gamma(\frac{1}{2})}{\Gamma(\frac{3}{4})},$$

$$n=3, \quad Q = 2\pi \int_0^1 (1-x^6)^{\frac{1}{2}} dx = 2\pi \frac{\Gamma(\frac{1}{6})\Gamma(\frac{1}{2})}{\Gamma(\frac{2}{3})},$$

$$n=4, \quad Q = 2\pi \int_0^1 (1-x^8)^{\frac{1}{2}} dx = 2\pi \frac{\Gamma(\frac{1}{8})\Gamma(\frac{1}{2})}{\Gamma(\frac{5}{8})},$$

$$n=5, \quad Q = 2\pi \int_0^1 (1-x^{10})^{\frac{1}{2}} dx = 2\pi \frac{\Gamma(\frac{1}{10})\Gamma(\frac{1}{2})}{\Gamma(\frac{3}{2})},$$

.....

\* These calculations are performed by using "The logarithmic table of Gamma function" (Gauss, Ges. W. iii. S. 161).

$$n=50, \quad Q=2\pi \int_0^1 (1-x^{100})^{\frac{1}{100}} dx = 2\pi \frac{\Pi(\frac{1}{100})\Pi(\frac{1}{50})}{\Pi(\frac{3}{100})},$$

.....

$$n=\infty, \quad Q=2\pi.$$

### 3. Radius of gyration about the axis $x$ or $y$ .

The value as generally expressed is

$$R^2 = \frac{1}{3} \frac{\int_0^1 (1-x^{2n})^{\frac{3}{2}} dx}{\int_0^1 (1-x^{2n})^{\frac{1}{2}} dx}.$$

and the calculations are shown below :

$$\begin{aligned} \text{For } n=1, \quad R^2 &= \frac{1}{3} \frac{\int_0^1 (1-x^2)^{\frac{3}{2}} dx}{\int_0^1 (1-x^2)^{\frac{1}{2}} dx} \\ &= \frac{1}{3} \frac{\left[ \frac{5-2x^2}{8} x \sqrt{1-x^2} + \frac{3}{8} \sin^{-1} x \right]_0^1}{\left[ \frac{x}{2} (1-x^2)^{\frac{1}{2}} + \frac{1}{2} \sin^{-1} x \right]_0^1}, \end{aligned}$$

$$\text{or} \quad R^2 = \frac{1}{3} \frac{B(\frac{1}{2}, \frac{5}{2})}{B(\frac{1}{2}, \frac{3}{2})} = \frac{1}{3} \frac{\Pi(\frac{3}{2})}{\Pi(2)\Pi(\frac{1}{2})},$$

$$n=2, \quad R^2 = \frac{1}{3} \frac{B(\frac{1}{4}, \frac{7}{4})}{B(\frac{1}{4}, \frac{5}{4})} = \frac{1}{3} \frac{\Pi(\frac{3}{4})\Pi(\frac{1}{2})}{\Pi(\frac{1}{4})},$$

$$n=3, \quad R^2 = \frac{1}{3} \frac{B(\frac{1}{6}, \frac{3}{2})}{B(\frac{1}{6}, \frac{7}{6})} = \frac{1}{3} \frac{\Pi(\frac{3}{6})\Pi(\frac{1}{3})}{\Pi(\frac{2}{3})\Pi(\frac{1}{6})},$$

$$n=4, \quad R^2 = \frac{1}{3} \frac{B(\frac{1}{8}, \frac{11}{8})}{B(\frac{1}{8}, \frac{9}{8})} = \frac{1}{3} \frac{\Pi(\frac{3}{8})\Pi(\frac{1}{4})}{\Pi(\frac{5}{8})\Pi(\frac{1}{8})},$$

$$n=5, \quad R^2 = \frac{1}{3} \frac{B(\frac{1}{10}, \frac{13}{10})}{B(\frac{3}{10}, \frac{11}{10})} = \frac{1}{3} \frac{\Pi(\frac{3}{10})\Pi(\frac{1}{5})}{\Pi(\frac{2}{5})\Pi(\frac{1}{10})},$$

.....

$$n=50, \quad R^2 = \frac{1}{3} \frac{B(\frac{1}{100}, \frac{101}{100})}{B(\frac{1}{100}, \frac{101}{100})} = \frac{1}{3} \frac{\Pi(\frac{3}{100})\Pi(\frac{1}{50})}{\Pi(\frac{2}{50})\Pi(\frac{1}{100})}$$

.....

$$n=\infty \quad R^2 = \frac{1}{3}.$$

XVII. *Notices respecting New Books*

*Operational Circuit Analysis.* By V. BUSH, Eng.D. (Chapman & Hall, Ltd., 11 Henrietta St., Covent Garden, W.C.2. Price 22s. 6d. net.)

**A**FTER many years of neglect and lack of appreciation, renewed interest has been taken in the operational calculus introduced by Heaviside. Numerous contributions are being made towards the extension and development of this branch of mathematics, the operational method of solving the differential equations arising in physical problems, chiefly in connexion with electrical networks. By the application of the theory of functions of a complex variable, Bromwich established the validity of the method for systems with a finite number of degrees of freedom and also developed a method for continuous systems.

The author has here brought together all the important results, and, for the first time, has set them out in systematic form. Whilst recognizing that too much attention can be paid to questions of rigour, the author gives an introductory account of contour integration, the evaluation of residues, and the derivation of the expansion theorem—the “partial fraction rule”—by contour integrals. This symbolic method has been extended by Carson and Bromwich: recently B. B. Baker has generalized the theorem, and has given a formula which includes the foregoing as particular cases. Prof. N. Wiener contributes a chapter on Fourier analysis and Asymptotic series and a useful table of operational formulæ is given in an appendix.

“The monumental nature of Heaviside’s work has not always and everywhere been appreciated,” but Dr. Bush and others, “by insisting upon a due measure of appreciation of his genius, have done much to make his work used, as well as useful.”

*La Nouvelle Mécanique de Quanta.* Par G. BIRTWISTLE. Traduit par MM. Y. ROCARD et M. PONTE. (Paris: Librairie Scientifique Albert Blanchard, 3 et 3 bis, Place de la Sorbonne. 1929.)

THE New Quantum Mechanics of the late G. Birtwistle, published only two years after his Quantum Theory of the Atom, presents a clear and comprehensive summary of the theories of Heisenberg, Dirac and Schrödinger. This book has the further merit of rousing the interest of the student in modern problems of atomic structure, and with this additional equipment enabling him to keep abreast with the developments of the recent past and to undertake the study of researches which are following one another in quick succession. It is for these reasons that the New Quantum

Mechanics has been translated by MM. Rocard and Ponte. Although it is little more than a year since the Cambridge University Press issued this book, many notable memoirs have appeared during this short period: the translators have endeavoured to incorporate the latest results by summarizing a number of contributions which have been made since the publication of the English edition. These include papers by P. Ehrenfest on the validity of the classical mechanics in wave mechanics, F. Madelung on the quantum theory in hydrodynamic form, further papers by P. Dirac and C. G. Darwin, and the work of Kretschmann, Sommerfeld, and Houston on the electron theory of metals.

It would have been an advantage if the author index had been retained, even if this required revision.

*Vorlesungen über Theoretische Physik.* Band IV. *Die Relativitätstheorie für gleichförmige Translationen.* Von Prof. H. A. LORENTZ. 1929. Geb. R.M. 13.80. (Akademische Verlagsgesellschaft, m.b.H., Leipzig.)

THE lectures on the Special Relativity theory given by Prof. H. A. Lorentz during the years 1910-12 have been revised by Dr. A. D. Fokker. Lorentz made many important contributions to the development of the principle, and provided the basis of the theory by the enunciation of the well-known Lorentz transformation. To him, in large measure, the restricted theory of relativity owes its origin. Nevertheless, his name does not appear in the text—only in one or two footnotes and in the bibliography. The chapter describing the researches on the variation of mass of an electron with velocity has been enlarged by the addition of later experimental results. These include the researches of Neumann, who, following Bucherer, used  $\beta$ -rays from radium as the source of cathode rays: the data gave a reliable value of the electron charge and confirmed the relation of dependence of mass upon velocity. A detailed account is also given of the work of Guye and Lavanchy on the experimental verification of the Lorentz formula for high-velocity cathode rays. References to original memoirs dealing with the topics in the various chapters are collected together in the Bibliography.

[*The Editors do not hold themselves responsible for the views expressed by their correspondents.*]







THE  
LONDON, EDINBURGH, AND DUBLIN  
PHILOSOPHICAL MAGAZINE  
AND  
JOURNAL OF SCIENCE.

---

[SEVENTH SERIES.]

FEBRUARY 1930.

XVIII.—*The Amplitude of Vibration of Ions in the Crystals NaCl, NaF, LiF, and KCl.* By G. W. BRINDLEY, M.Sc.,  
*Assistant Lecturer in Physics, University of Leeds* \*.

(1) *Introduction.*

THE intensity with which a beam of X-rays is reflected from a crystal depends on many factors, but of these two are of special importance, namely, the distribution of charge in the atoms or ions<sup>†</sup> composing the crystal and their thermal agitation. The amplitude of a reflected X-ray beam is a function of the angle of scattering,  $2\theta$ ,  $\theta$  being the glancing angle of incidence, and of the wavelength,  $\lambda$ . Considered classically, the decrease of the reflected amplitude as  $\theta$  increases is due to interference occurring between waves scattered from different parts of the vibrating atoms. Now, if an atom in a crystal can be regarded as a spatial distribution of charge surrounding a nucleus which vibrates as a whole or almost so—and evidence tends to show that this is approximately true<sup>(1)</sup>, then the effect of the thermal agitation may be distinguished from the effect of the space charge distribution, and the two be considered separately.

\* Communicated by Prof. R. Whiddington, F.R.S.

† Hereinafter "atoms" will include "ions."

The effect of the space charge distribution is conveniently expressed by  $F_0$ , a function of  $\theta$  and  $\lambda$ , which has been defined <sup>(2)</sup> as the ratio of the coherent radiation scattered by an atom *at rest* in a direction  $\theta$  to the amplitude which would be scattered in the same direction according to the classical theory by the same number of electrons as the atom contains considered as coincident point charges. This definition leads to a simple expression for  $F_0$  for atoms having spherical symmetry :—

$$F_0 = \int_0^\infty U(r) \frac{\sin \phi}{\phi} \cdot dr, \quad . . . . (1)$$

where  $\phi = \frac{4\pi}{\lambda} \cdot r \sin \theta$ ,

$U(r)$  being the radial density of charge at distance  $r$  from the nucleus, expressed in terms of the electron as unit. In applying equation (1) to atoms in a crystal a number of assumptions are made, some of which it is worth while to discuss briefly.

Firstly, the assumption that the classical formula for the scattering of X-rays by a free electron due to J. J. Thomson is applicable to the electrons in an atom has been considered by I. Waller in two papers, in the first of which <sup>(3)</sup> he shows that for an atom having one electron in a field of charge  $Ze$  the classical formula is still approximately valid from the point of view of quantum mechanics, and in the second <sup>(4)</sup> he extends this result to a many-electron atom, the condition to be satisfied being that the frequency of the radiation must be essentially higher than the K-absorption frequency of the scattering atom. This question is also discussed in a later paper by Waller and Hartree <sup>(5)</sup> on the total scattering of X-rays.

Secondly, it is generally assumed in comparing  $F$  curves obtained from experimental data with theoretical  $F$  curves based on calculated charge distributions that atoms in crystals are approximately spherical in shape, so that equation (1) can be applied to the theoretical charge distribution,  $U(r)$ . The justification for this is that any lack of spherical symmetry will be mainly confined to the outer parts of the atoms where  $U(r)$  is small and,  $r$  being large,  $(\sin \phi)/\phi$  also small—that is to say, deviations from spherical symmetry will be appreciable only in those parts of an atom which make very small contributions to the  $F$

function. This is very clearly shown by a number of curves given by James, Waller, and Hartree<sup>(2)</sup> for the function  $U(r) \sin \phi / \phi$  for  $\text{Cl}^-$  for different values of the parameter  $(\sin \theta) / \lambda$ . For crystals of the rock-salt type considered in this paper the assumption is certainly justified, for the spacing of the atoms in these crystals is so large that there is very little "overlapping" or "interpenetration" of neighbouring atoms; this is seen in fig. 3.

The effect of the thermal vibration of atoms in crystals on the amplitude of a reflected X-ray beam has been considered by Debye<sup>(6)</sup>, and also by Waller<sup>(6)</sup>, who has modified slightly the expression originally given by Debye. Experiments by James, Firth<sup>(6)</sup> and the present writer<sup>(7)</sup> on the reflexion of X-rays from rock-salt and sylvine over a wide range of temperature have shown that Waller's modification of Debye's formula represents very closely the variation of the intensity of reflexion with temperature from the temperature of liquid air,  $86^\circ \text{ Abs.}$ , to about  $500^\circ \text{ Abs.}$  The Debye-Waller formula may be expressed as follows<sup>(8)</sup> :—

$$F_T = F_0 e^{-M}, \quad . . . . . (2)$$

where 
$$M = 8\pi^2 \cdot \overline{u_x^2} \left( \frac{\sin \theta}{\lambda} \right)^2,$$

$\overline{u_x^2}$  being the mean square displacement of an atom in an arbitrary direction  $x$ . For a crystal of the rock-salt type,  $u^2 = 3\overline{u_x^2}$ ,  $\overline{u^2}$  being the mean square of the total displacement. Hence (2) becomes

$$F_T = F_0 e^{-\alpha (\sin^2 \theta / \lambda^2)}, \quad . . . . . (3)$$

where 
$$\alpha = \frac{8\pi^2}{3} \cdot \overline{u^2};$$

$\sqrt{\overline{u^2}}$  may be regarded as the mean amplitude of vibration at temperature  $T$ .  $F_T$  and  $F_0$  are respectively values of the  $F$  function for an atom vibrating at temperature  $T$  and for an atom *at rest*.

$F_T$  has been obtained experimentally for the following crystals of the rock-salt type:— $\text{NaCl}$  and  $\text{KCl}$  by James, Firth<sup>(6)</sup>, and Brindley<sup>(7)</sup>,  $\text{NaCl}$ ,  $\text{NaF}$ , and  $\text{LiF}$  by Havighurst<sup>(9)</sup>.  $F_0$  has been calculated by means of equation (1) for the ions  $\text{Na}^+$ ,  $\text{K}^+$ ,  $\text{Li}^+$ ,  $\text{Cl}^-$  and  $\text{F}^-$  composing these crystals from theoretical charge distributions. From this data, using equation (3),  $\sqrt{\overline{u^2}}$  may be

derived for each ion in these crystals at the temperature  $T$  at which the experimental measurements were made, i. e., about  $290^\circ$  Abs.

It seems desirable here to compare the present method of obtaining  $\sqrt{u^2}$  with that used by James and his co-workers. They make use of the following expression derived by Waller<sup>(9)</sup>:—

$$\overline{u^2} = \alpha + \beta T + \gamma/T + \delta/T^3 + \dots \quad (4)$$

in which  $\alpha$  is zero if zero-point energy having Planck's value is assumed, and  $\gamma$  and  $\delta$  can be calculated with sufficient accuracy.  $\beta$  is obtained *experimentally* by making measurements of  $F_T$  at two temperatures,  $86^\circ$  Abs. and  $290^\circ$  Abs. In this way  $\sqrt{u^2}$  is obtained without any reference to theoretical charge distributions. However, when  $F_0$  is calculated from purely experimental data, it is found to agree quite closely with  $F_0$  deduced from the charge distributions obtained theoretically by the method due to Hartree<sup>(10)</sup>. This result is of considerable importance because, apart from being powerful evidence for the existence of zero-point energy, it shows that  $F_0$  may be calculated with a fair degree of certainty\* from the theoretical charge distributions, and that the two assumptions described briefly above relating to the use of equation (1) are justified.

## (2) Theoretical Values of the Function $F_0$ .

The distributions of charge in the ions considered have been obtained by Hartree's method<sup>(10)</sup>. With the exception of  $F^-$ , these distributions had already been calculated,  $Li^+$  †,  $Na^+$ , and  $Cl^-$  by Hartree<sup>(10)</sup>, and  $K^+$  by James and the writer<sup>(7)</sup>. The distribution in  $F^-$  has been worked out by the "self-consistent field" method, using values of the initial field estimated by Hartree, and the results are given below in Table I.

In Table I.  $r$  is given in terms of the atomic unit of length ( $=a_H=0.532$  Å.U.) and  $U(r)$  is in electrons per atomic unit of length.

Values of  $F_0$  obtained from these charge distributions are given in Table II.

\* This point is considered again later.

I am indebted to Prof. Hartree for permission to use his results for  $Li^+$  previous to their publication, and also for an estimate of the "initial" field of  $F^-$  used in calculating the charge distribution.

TABLE I.

Radial Distribution of Charge in Fluorine<sup>-</sup> ion.

$r$ in atomic units.	$U(r)$ .	$r$ in atomic units.	$U(r)$ .
0	0	1.2	4.32
.02	1.58	1.4	3.37
.04	4.39	1.6	2.58
.06	6.99	1.8	1.98
.08	8.68	2.0	1.52
.10	9.59	2.2	1.18
.12	9.75	2.4	0.92
.14	9.41	2.6	0.73
.16	8.80	2.8	0.58
.18	7.99	3.0	0.46
.20	7.14		
		3.5	0.28
.25	5.34	4.0	0.17
.30	4.16	4.5	0.11
.35	3.75	5.0	0.07
.40	3.83	5.5	0.045
		6.0	0.03
.5	4.60	6.5	0.02
.6	5.30	7.0	0.01
.7	5.81	7.5	0.005
.8	5.88	8.0	0.00
.9	5.67		
1.0	5.29		

TABLE II.

Theoretical Values of the Function  $F_c$ .

$\left(\frac{\sin \theta}{\lambda}\right) \cdot 10^{-2}$	Li <sup>+</sup> .	F <sup>-</sup> .	Na <sup>+</sup> .	Cl <sup>-</sup> .	K <sup>+</sup> .
0	2.00	10.00	10.00	18.00	18.00
.05	1.99	9.49	9.87	17.11	17.72
.10	1.96	8.65	9.50	15.23	16.46
.15	1.88	7.72	8.92	13.19	14.82
.20	1.76	6.74	8.21	11.50	13.31
.25	1.64	5.70	7.45	10.23	12.00
.3	1.52	4.79	6.68	9.30	10.78
.4	1.28	3.54	5.23	8.06	8.83
.5	1.04	2.75	4.07	7.23	7.77
.6	0.82	2.20	3.22	6.49	7.05
.7	0.64	1.92	2.63	5.77	6.44
.8	0.50	1.72	2.23	5.06	5.90
.9	0.40	1.57	1.96	4.41	5.32
1.0	0.33	1.48	1.75	3.84	4.79
1.1	0.26	1.36	1.59	3.33	4.22

## (3) Calculation of the Amplitudes of Vibration.

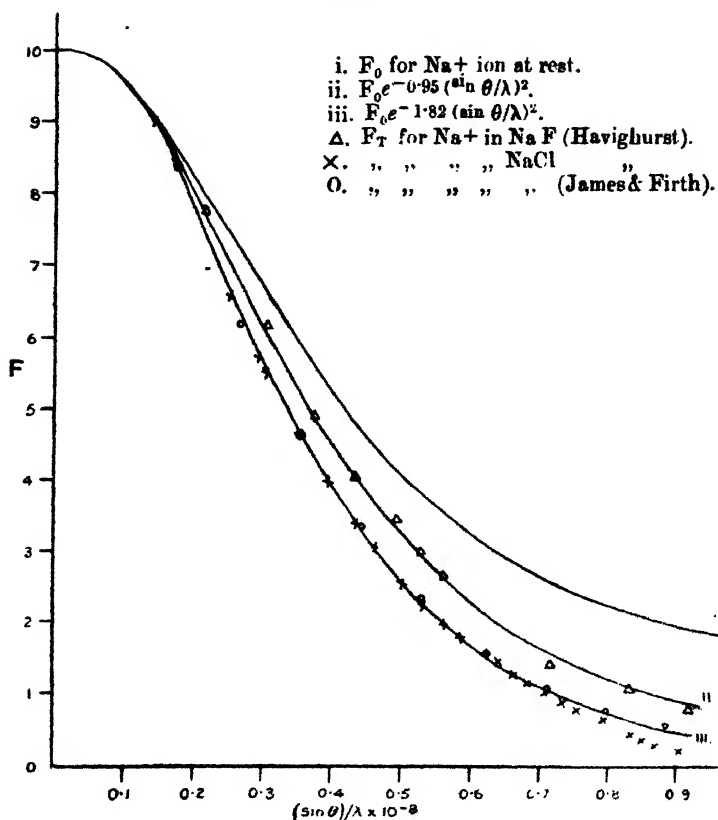
From equation (3)

$$\overline{u^2} = (3/8\pi^2)\alpha$$

and

$$\alpha = \frac{\log_e (F_0/F_T)}{(\sin \theta/\lambda)^2} \quad . \quad . \quad . \quad . \quad . \quad (5)$$

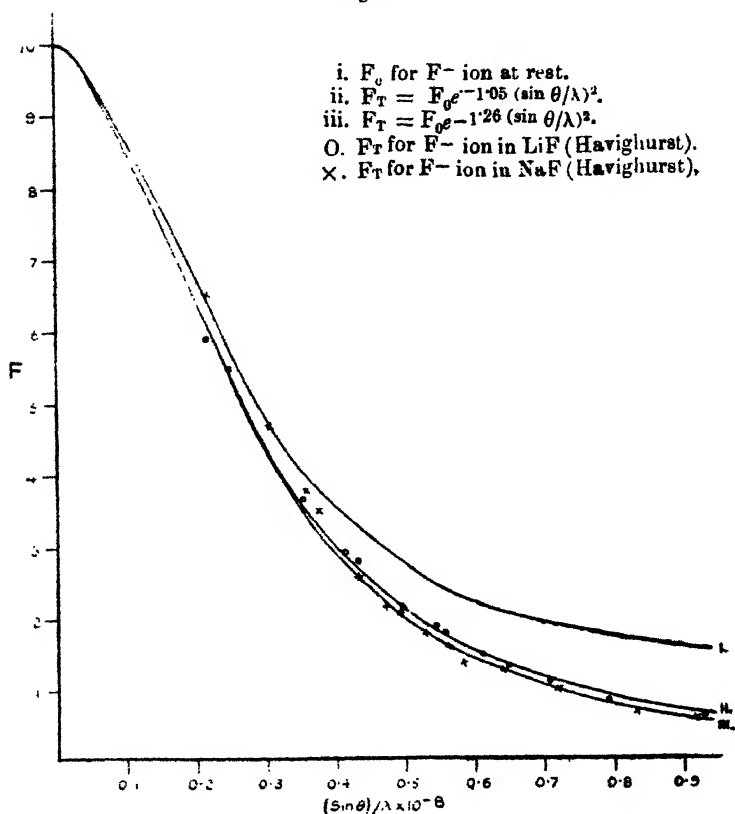
Fig. 1.

F Curves for  $\text{Na}^+$  ion.

A direct application of (5) to the  $F_0$  and  $F_T$  curves for each ion enabled a series of values of  $\alpha$  to be obtained for various values of  $\sin \theta/\lambda$  which were found to be approximately constant.  $\sqrt{\overline{u^2}}$  was then calculated from a mean value of  $\alpha$ . Further, as a check,  $F_T$  was calculated from equation (3), using the mean value obtained for  $\alpha$ , and compared with the experimental data.

In figs. 1 and 2 the results are shown for the  $\text{Na}^+$  ion in  $\text{NaCl}$  and  $\text{NaF}$  and for the  $\text{F}^-$  ion in  $\text{NaF}$  and  $\text{LiF}$ . For the  $\text{Na}^+$  ion in  $\text{NaCl}$ , the experimental results are shown obtained both by Havighurst and by James and Miss Firth. It is of interest to note that there is a close agreement between the two sets of experimental data for all values of  $(\sin \theta)/\lambda$  except beyond 0.8, where the powder method used by Havighurst appears to give results which

Fig. 2.

F Curves for  $\text{F}^-$  ion.

are too small, while the single crystal method used by James and Miss Firth gives results in better agreement with the theoretical curve. For all the ions considered—with, perhaps, the exception of  $\text{Li}^+$ , for which it is difficult to get an experimental F curve—the values of  $F_T$  given by Havighurst for *small* values of  $(\sin \theta)/\lambda$  fit quite well onto



the theoretical curves, a result which is in agreement with Havighurst's conclusion that the fine powder method eliminates the uncertainty at small angles due to secondary extinction. For average values of  $(\sin \theta)/\lambda$ , between 0.2 and 0.8, when  $\alpha$  is rightly chosen there is a very close agreement between the experimental  $F_T$  values and the theoretical  $F_0 e^{-\alpha(\sin^2 \theta / \lambda^2)}$  curve.

In Table III. values are given of  $\alpha$  and  $\sqrt{u^2}$  obtained from Havighurst's data and also values obtained by James <sup>(7) (9)</sup> using a different method.

In the experiments on sylvine, KCl, by James and the writer <sup>(7)</sup> it was not possible to obtain separate F curves

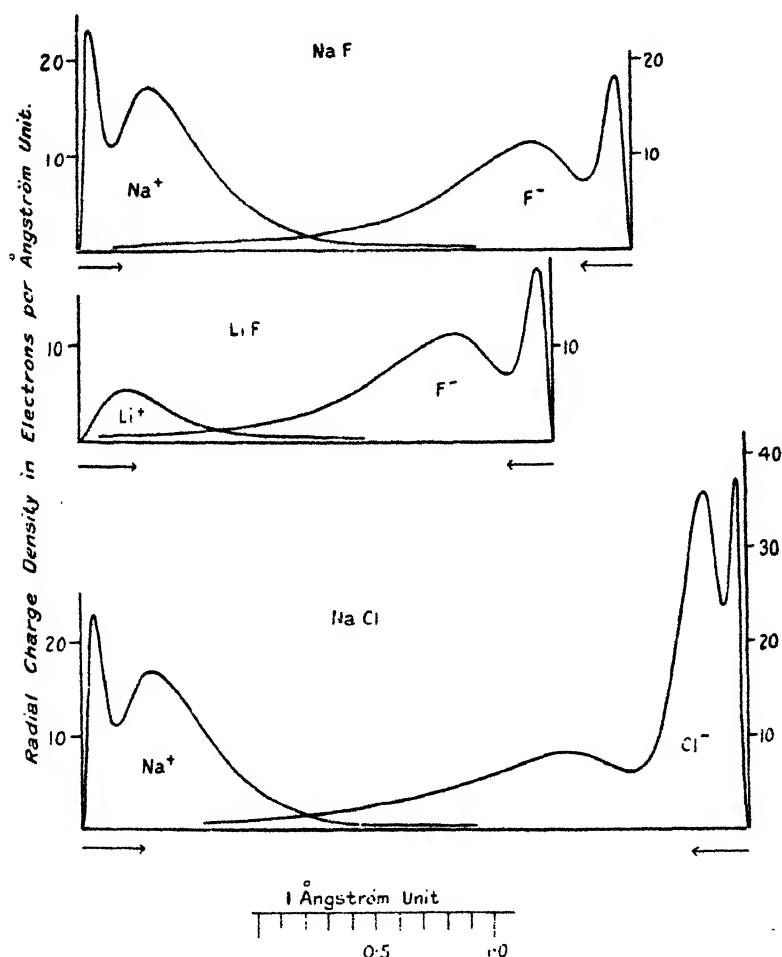
TABLE III.

Ion.	From Havighurst's data.		$\sqrt{u^2}$ , in A.U.
	$\alpha$ , in A.U. <sup>2</sup>	$\sqrt{u^2}$ , in A.U.	
{ Na <sup>+</sup> in NaCl ...	1.82	0.26 <sub>9</sub>	0.242 <sup>7</sup> Waller & James, 0.217 <sup>9</sup> <i>loc. cit.</i>
{ Cl <sup>-</sup> in NaCl ...	1.60	0.24 <sub>7</sub>	
{ Na <sup>+</sup> in NaF ...	0.95	0.19 <sub>0</sub>	0.255 { James & Brind- ley, <i>loc. cit.</i>
{ F <sup>-</sup> in NaF ...	1.26	0.21 <sub>9</sub>	
{ Li <sup>+</sup> in LiF.....	1.50	0.23 <sub>9</sub>	
{ F <sup>-</sup> in LiF.....	1.05	0.20 <sub>0</sub>	
{ K <sup>+</sup> in KCl.....	—	—	}
{ Cl <sup>-</sup> in KCl.....	—	—	

experimentally for K<sup>+</sup> and Cl<sup>-</sup>, for, since the diffracting powers of these two ions are so nearly equal, spectra of type [K—Cl] are too weak to be measured. Hence it was only possible to obtain a *mean* value of  $\sqrt{u^2}$  for the two ions. There is some data available for other crystals than those given in Table III. Results for aluminium have recently been published, by James, Brindley, and Wood <sup>(11)</sup>. Results have also been obtained for fluorite, CaF<sub>2</sub>, by Havighurst and by James and Randall, and many results have also been obtained for several specimens of this crystal by the writer and R. G. Wood, but the investigation is not yet complete. It seems better therefore to restrict the present paper to crystals of the rock-salt type, and to leave the consideration of aluminium, fluorite, and possibly of other crystals to a later paper.

To enable the results obtained for  $\sqrt{u^2}$  to be visualized easily in their relation to the sizes of the ions and the spacings of the crystal lattices fig. 3 was drawn. It shows the theoretical *radial* charge distributions for the ions (considered at rest) in NaF, LiF, and NaCl set at a

Fig. 3.



The arrows show the magnitude of the mean amplitudes of vibration of the ions at room-temperature.

distance apart equal to half the (1.0.0) spacings, *i. e.*, at the distance of closest approach. The arrows give the magnitude of the mean amplitudes of vibration at room-temperature.

It is evident that the thermal vibrations in the crystals considered are all approximately of the same magnitude—in fact, they are so nearly alike that it would be rash at present to attempt to attach any great significance to the differences between them. Since the “size” of an ion is so vague a quantity it is hardly worth while to consider a possible connexion between size and amplitude of vibration. But it is perhaps significant that in LiF and NaCl, where one ion is *much* smaller than the other, the smaller ion has the larger amplitude of vibration. In NaF, however, the reverse appears to be true, but in this crystal the sizes are more nearly equal. In LiF the vibrations are definitely smaller than in NaCl and KCl, a result which may be related to the LiF lattice being much smaller than the NaCl and KCl lattices.

Lastly, Table III. shows that the values of  $\sqrt{u^2}$  obtained by Waller and James<sup>9</sup> for  $\text{Na}^+$  and  $\text{Cl}^-$  in NaCl are smaller than the corresponding values obtained by the present method using Havighurst's data, a result which at first sight is somewhat surprising, since the experimental results of Havighurst agree well with those used by Waller and James. Though the differences are small absolutely, they are larger than can be attributed to the small differences between the two sets of experimental results. A little consideration shows that the differences arise mainly from the two methods of obtaining  $\sqrt{u^2}$ . A careful examination of the experimental and theoretical F curves given by James, Waller, and Hartree (*loc. cit.* p. 343) reveals that the theoretical curves come slightly above the experimental curves in the region between  $\sin \theta/\lambda = 0.4$  and  $0.8$ . Thus in choosing  $\alpha$  so that  $F_T$  and  $F_0 e^{-\alpha(\sin^2 \theta/\lambda^2)}$  fit most closely, the values of  $\alpha$  so obtained are, from the point of view of James's method, slightly too large; this explains the discrepancy. Which of the two methods gives the more accurate result is not clear; in the method used by Waller and James it is assumed that the temperature factor determined experimentally between  $86^\circ$  Abs. and  $290^\circ$  Abs. holds between  $0^\circ$  Abs. and  $86^\circ$  Abs., while the present method assumes, among other things, that the process of obtaining  $F_0$  from the theoretical charge distribution by equation (1) is justified. However, the results obtained by either method are probably consistent among themselves.

Finally, I would like to express my thanks to Prof. Hartree for estimating the initial field of the fluorine ion,  $F^-$ , and also to Mr. F. Tyler, B.Sc., for assistance in the calculation of the charge distribution for this ion.

#### (4) Summary.

A brief account is given of the dependence of the intensity of reflexion of X-rays on the thermal vibration and charge distribution of the scattering centres (atoms or ions) in a crystal. It is pointed out that the experimental work of James and others justifies the assumption that the charge distribution in an ion *at rest* in a crystal is given approximately by Hartree's method for the charge distribution in a free ion. By comparing X-ray scattering curves (F curves) obtained experimentally for a number of ions at room-temperature with the corresponding theoretical curves for the ions at rest an estimate has been made of the amplitude of vibration of the ions at room-temperature.

#### References.

- (1) See papers by R. W. James and others, to which references are given below.
- (2) James, Waller, and Hartree, Proc. Roy. Soc. A, cxviii. p. 334 (1928).
- (3) I. Waller, Phil. Mag. iv. p. 1228 (1927).
- (4) I. Waller, *Zeit. f. Phys.* li. p. 213 (1928).
- (5) Waller and Hartree, Proc. Roy. Soc. A, cxxiv. p. 119 (1929).
- (6) James and Firth, Proc. Roy. Soc. A, cxvii. p. 62 (1927). This paper contains references to the work of Debye and Waller on the effect of temperature on the intensity of X-ray reflexion.
- (7) James and Brindley, Proc. Roy. Soc. A, cxxi. p. 155 (1928).
- (8) Waller and James, Proc. Roy. Soc. A, cxvii. p. 214 (1927).
- (9) R. J. Havighurst, Phys. Rev. xxviii. p. 869 (1926).
- (10) D. R. Hartree, Proc. Camb. Phil. Soc. xxiv. pp. 89, 111 (1928).
- (11) James, Brindley, and Wood, Proc. Roy. Soc. A, cxxv. p. 401 (1929).

Physics Department,  
University of Leeds,  
Dec. 17th, 1929.

XIX. *A Note on the Scattering Power of the Carbon Atom in Diamond for X-Rays.* By G. W. BRINDLEY, M.Sc., Assistant Lecturer in Physics, University of Leeds \*.

A SHORT time ago the writer† calculated from an approximate model of the carbon atom its scattering power for X-rays. The results were expressed in terms of  $F$ , a function of  $\theta$  and  $\lambda$  which measures the scattering power of an atom for radiation of wave-length  $\lambda$  in a direction  $\theta$ . The theoretical  $F$  curve was found to differ considerably from an experimental  $F$  curve obtained by M. Ponte‡ for the carbon atom in diamond. Recently an entirely new experimental investigation has been made by Miss A. H. Armstrong§, who obtains values of  $F$  markedly different from those of Ponte. The purpose of this note is to point out briefly that there is a moderately good agreement between Miss Armstrong's results and the theoretical results.

The method previously used for calculating  $F$  was as follows:—Schrödinger's equation for  $\psi$  for an electron in a central Coulomb field of charge  $Z'e$  can be solved explicitly||, and its radial charge density  $U(r)=4\pi r^2 \cdot \psi\psi$  can be calculated. It was assumed that each electron in the carbon atom could be considered to be in a central Coulomb field,  $Z'$  being an effective nuclear charge equal to  $(Z-s)$ ,  $Z$  being the actual nuclear charge, 6, and  $s$  a screening constant.

Reasons were given for considering  $s$  to be small for the K electrons of carbon and of the order of 2 for the L electrons.  $U(r)$  was calculated for a  $1_1$  electron with  $Z'=6.0$ , and for a  $2_1$  and a  $2_2$  electron with  $Z'=4.0$ . Then, using the equation¶:—

$$F = \int_0^{\infty} U(r) \frac{\sin \phi}{\phi} dr \dots \dots \dots (1)$$

where  $\phi = \frac{4\pi}{\lambda} r \cdot \sin \theta,$

$F$  was calculated for each of these electrons.

\* Communicated by Prof. R. Whiddington, F.R.S.

† G. W. Brindley, Proc. Leeds Phil. Soc. i. p. 402 (1929).

‡ M. Ponte, Phil. Mag. iii. p. 195 (1927); iv. p. 232 (1927).

§ A. H. Armstrong, Phys. Rev. xxxiv. p. 1115 (Oct. 1929).

E. Schrödinger, Ann. d. Phys. lxxix. p. 361 (1926).

¶ Vide James, Waller, and Hartree, Proc. Roy. Soc. A, cxviii. p. 334 (1928).

Despite the roughness of the method, one important conclusion was obtained, namely, that for values of  $\sin \theta > 0.3$  the contribution of the L electrons to the F curve for carbon is negligibly small. This is clearly seen in the text-figure.

Now the K electron distribution in carbon will be determined mainly by the central nucleus, and the influence of the L electrons will be comparatively small; thus the K distribution will be spherically symmetrical, or almost so, and the field will be practically of the Coulomb type, so that the assumptions involved in the simple theory given above are justified for the K electrons. From the text-fig. it is seen that with only two exceptions all the experimental values of F occur at values of  $\sin \theta > 0.3$ , so that in comparing the theoretical curve with the experimental results it is only the K electrons which are involved. The L electrons, the charge distribution of which is so doubtful, only contribute appreciably to the F curve at small values of  $\sin \theta$  where there are practically no experimental data.

In the previous paper  $Z'$  was taken equal to 6.0 for the K electrons mainly for reasons of convenience; it was quite obvious that a small change of  $Z'$  for the K electrons could not possibly explain the low values of F obtained by Ponte. Since Miss Armstrong's values of F are considerably higher than Ponte's, it seems worth while to reconsider the value of  $s$  for the K electrons. A value 0.4 has been chosen, based on the following considerations:—the most accurate method which we have at present for calculating the charge distribution in a many-electron atom is that given by Hartree\*. By comparing charge distributions obtained by Hartree's method with hydrogen-like distributions,  $Z'$  can be found. For K electrons  $s = (Z - Z')$  does not vary rapidly with  $Z$ , and may therefore be obtained fairly accurately for any atom by interpolation. A small error in  $s$  of the order of 0.05 will have no appreciable effect on the F curve.

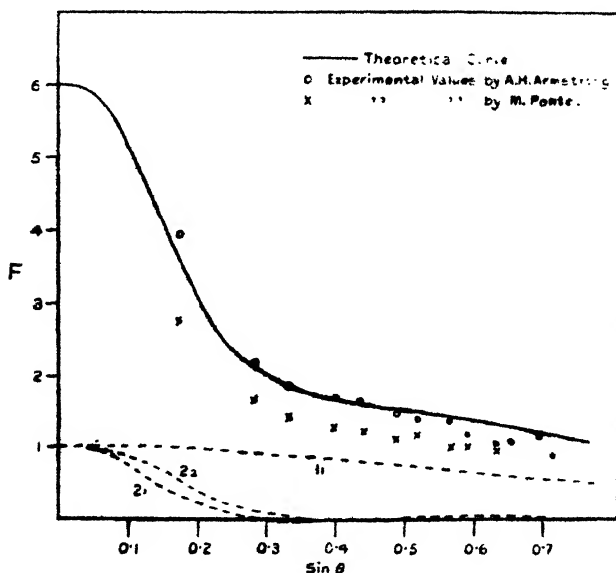
In the above table values are given of F for a  $1_1$  electron with  $Z' = 5.6$ , and for a  $2_1$  and a  $2_2$  electron with  $Z' = 4.0$ . These results are shown graphically in the text-fig. The full-line curve is the theoretical F curve for the carbon atom (assuming two  $2_1$  and two  $2_2$  electrons), the corresponding values being given in column five of the table. The circles

\* D. R. Hartree, Proc. Camb. Phil. Soc. xxiv, pp. 89, 111 (1928).

show the experimental values obtained by Miss Armstrong, and the crosses the values obtained by Ponte.

### Calculated Values of F.

Sin $\theta$ for $\lambda=0.71 \text{ \AA.U.}$	Values of F.			F for Carbon Atom.
	$1_1$ $Z'=5.6.$	$2_1$ $Z'=4.0.$	$2_2$ $Z'=4.0.$	
0.000	1.00	1.00	1.00	6.00
0.066	0.99	0.91	0.97	5.74
0.133	0.98	0.50	0.73	4.42
0.199	0.95	0.21	0.38	3.08
0.267	0.91	0.03	0.16	2.20
0.332	0.87	-0.01	0.06	1.84
0.400	0.81	-0.01	0.01	1.62
0.467	0.76	0.01	0.00	1.54
0.534	0.70	0.03	-0.01	1.44
0.667	0.58	0.04	-0.01	1.22
0.800	0.47	0.03	-0.01	0.98



The agreement between the calculated curve and the more recent experimental values is as good as can be expected. At large values of  $\sin \theta$  the experimental values tend to fall below the theoretical curve. A number of reasons may explain this. Firstly, any vibration of the

atoms in the lattice will affect the higher order spectra much more than the lower order spectra. The effect of atomic vibration on the scattering of X-rays has been considered in particular by James and his co-workers and by Waller\*. If  $F_0$  is the  $F$  function for an atom at rest, then we can write

$$F = F_0 e^{-M},$$

where

$$M = 8\pi^2 \sin^2 \theta \cdot \bar{u}_x^2 / \lambda^2,$$

where  $\bar{u}_x^2$  is the mean square displacement in an arbitrary direction  $x$ . In diamond the atoms are very closely packed. The hardness of the crystal, its very high characteristic temperature †, 1830° C., and other physical properties support the view that the atomic vibrations in diamond are very small. Further, experiments on the reflexion of X-rays over a wide range of temperature have failed to detect any change of intensity with temperature ‡. All evidence tends to show, therefore, that the atomic vibrations in diamond are very small, and if they exist at all that they are probably not large enough to explain the observed difference.

A second possible explanation is that measurements of the scattering factor  $F$  using powdered crystals appear to give results which are low at large values of  $\sin \theta$  compared with theoretical results, and also low compared with results from single crystals. This is referred to in the preceding paper by the writer on the amplitude of vibration of ions in a number of crystals of the rock-salt type.

Another possible explanation, but one which it is difficult to consider quantitatively, is this: the existence of the (222) spectrum is strong evidence for the distortion of the L electron shell of the carbon atom in diamond, and it may be that between the atomic planes there is a sufficient density of charge to scatter radiation of an appreciable amount out of phase with that scattered by the charge near the planes §. The irregularity of the  $F$  values at large  $\sin \theta$ , if not due to experimental causes, is in agreement qualitatively with this point of view.

\* *Vide* Waller and James, *Proc. Roy. Soc. A*, cxvii, p. 214 (1927), where references are given to other work.

† *Cf.* P. Debye, *Ann. d. Phys.* xliii, p. 88 (1914).

‡ I. Backhurst, *Proc. Roy. Soc. A*, cii, p. 340 (1922). Ehrenberg, Ewald, and Mark, *Zeit. f. Krist.* lxvi, p. 547 (1928).

§ *Cf.* W. H. Bragg, *Proc. Lond. Phys. Soc.* xxxiii, p. 304 (1921).



To summarize : a theoretical F curve is calculated for carbon which, beyond  $\sin \theta = 0.3$ , depends almost entirely on the K electrons for which the simple theory is adequate. There is a satisfactory agreement between the calculated curve and recent experimental data. Possible explanations are suggested for the tendency of the experimental values to fall slightly below the curve at large values of  $\sin \theta$ .

Physical Laboratories,  
University of Leeds,  
Dec. 10th, 1929.

## XX. On the Principle of Inaccessibility of the Absolute Zero.

By N. A. KOLOSSOWSKY, D.Sc., Professor of Physical Chemistry and of Thermodynamics, University of Leningrad\*.

ONE generally attributes the first idea concerning the principle of inaccessibility of the temperature of the absolute zero to Nernst †, who in a paper published in 1912, had enounced this principle and, in addition, had attempted to intimately bind it with his new heat-theorem ‡. Nevertheless, this opinion does not in any way correspond with the historic reality.

Indeed, E. Hoppe has recently indicated in his 'History of Physics' §, that analogical ideas had been enunciated already in 1874 by Koppe ||. But Hoppe is incorrect in

\* Communicated by the Author.

† See, e. g., P. Pawlowitsch, *Journ. Russ. Phys.-Chem. Soc.*, Phys. pt. xlv. (2) p. 253 (1913). H. A. Lorentz, *Chem. Weekbl.* x. p. 621 (1913); and *Journ. Russ. Phys.-Chem. Soc.*, Phys. pt. xlvi. p. 4 (1914). P. Czukor, *Verhandl. deut. phys. Ges.* xvi. p. 486 (1914); M. Polanyi, *Verhandl. deut. phys. Ges.* xvi. p. 333 (1914), and xvii. p. 350 (1915). A. Einstein, 'Rapports et discussions du 2me Conseil de physique de l'Institut, Solvay, Paris, pp. 293-298. Article of K. Bannwitz in the *Handbuch der Physik*, herausgegeben von Geiger und Scheel, ix. p. 172 (1926). W. Meissner, *ZS. f. Phys.* xxxvi. p. 325 (1926). A. Schidlof, *Journ. chim. phys.* xxiii. p. 814 (1926). W. Jazyna, *ZS. f. Phys.* xli. p. 211 (1927). F. Simon, *ZS. f. Phys.* xli. p. 806 (1927). H. Mache, *Ber. Wien. Akad. Wiss. Abt. II a.* cxxxvi. p. 75 (1927).

‡ W. Nernst, *Ber. Preuss. Akad. Wiss.* S. 134 (1912); see also W. Nernst, 'Die theoretischen und experimentellen Grundlagen des neuen Wärmesatzes,' 2te Aufl. S. 72 (1924).

§ E. Hoppe, 'Geschichte der Physik. Braunschweig' (1926) (Kinetische Gastheorie).

|| Koppe, Pogg. *Ann. cli.* p. 643 (1874).

stating that Koppe had been the pioneer in this way, for in reality already in 1862 R. Clausius \* had given the first formulation of this principle which was expressed by him in a perfectly clear manner and without any ambiguity. It is strange enough that nobody has up to date mentioned this circumstance, so much the more that, if one occupies oneself in researches in the domain of these questions, a deep study of Clausius's classical works is absolutely indispensable.

Clausius even gives a demonstration of the inaccessibility of the absolute zero, obviously deriving from the second law and particularly from the following formula :

$$Z - Z_0 = m \cdot c \cdot \ln \cdot \frac{T_0}{T},$$

where  $m$  represents the mass,  $c$  the true heat capacity †, and finally  $Z - Z_0$  the variation of disgregation ‡, *i. e.* of the degree of division of the substance corresponding to a change of temperature from  $T_0$  to  $T$ . This formula allowed Clausius to draw the following inference. "If one should wish to bring a body to the absolute zero of temperature the change of disgregation would become infinitely great, because in this case one would put  $T=0$  into the foregoing formula. This proves on principle that it is impossible to produce by means of any changes of state of a body such a cold that one could attain the absolute zero of temperature."

One obviously may discuss the objective value of Clausius's demonstration, as well as of all the other more recent ones, concerning the inaccessibility of the absolute zero, but at any rate, as regards the idea itself of this principle, one is indubitably obliged to agree, that in Clausius's statement it is as clear and precise as in the well-known one of Nernst.

\* R. Clausius, *Vierteljahrschrift Ges. Naturwiss. Zürich*, vii. p. 48 (1862); *Pogg. Ann.* cxvi. p. 73 (1862); *Phil. Mag.* (4) xxiv. pp. 81, 201 (1862); *Journ. de Liouville* (2) vii. p. 209 (1862); 'Théorie mécanique de la chaleur.' trad. par F. Folie, Paris, Lacroix, Première partie, pp. 291-293 (1868-69).

† It is here the question of heat capacities  $c$  and  $c'$  defined by the equations

$$c = c_v - AT \int \left( \frac{\partial^2 p}{\partial T^2} \right) dv \quad \text{and} \quad c' = c_p + AT \int \left( \frac{\partial^2 v}{\partial T^2} \right)_p dp.$$

These heat capacities are independent of the temperature, as well as of the state of aggregation of the substance.

‡ Conception, having a certain analogy with the modern conception introduced into the science by G. N. Lewis under the denomination of fugacity.

It is precisely to this historic fact that we wish to draw the attention of physicists, as it incontestably refers to a very important and actual problem.

Laboratory of Physical Chemistry  
of the Geological Committee,  
Leningrad (St. Petersburg).

XXI. *Effect of a Circular Hole on the Stress Distribution in a Beam under Uniform Bending Moment.* By ZIRÔ TUZI, Research Fellow, the Institute of Physical and Chemical Research, Tokyô\*.

[Plate II.]

# I. INTRODUCTION.

THE effect of a circular hole on the stress distribution in a plate under uniform *tension* has been studied by several authors both theoretically and experimentally; on the other hand, the case of *bending*, which is more important for various practical purposes, has been but little studied †, so far as the author is aware. The object of the present paper is to give full details of the experimental investigation of the stress distribution in a beam having a circular hole of various diameters on the neutral axis and subjected to a uniform bending moment, and to compare the results with the theoretical solution, which is also worked out in this paper. The experimental results are obtained by means of photo-elasticity, using a new material, "Phenolite" ‡, which is optically five times more sensitive than xylonite; and the values of stresses are measured directly, counting the numbers of interference fringes secured on photographic plates by means of monochromatic light 5461 Å. from an intense mercury lamp, so that practically no personal error can possibly enter. A uniform bending moment is applied on a beam AB, as shown in fig. 1, and photographs of its

\* Communicated by Mr. Uzumi Doi.

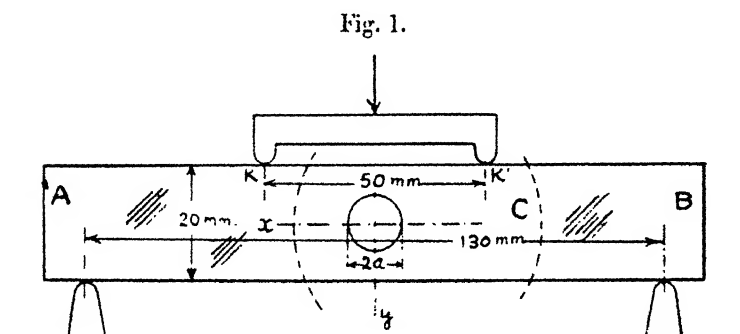
† E. G. Coker, 'Engineering,' March 8th, 1912. T. Fukuhara, Journ. Soc. Mech. Engr. (Tokyo), xxxi. no. 133, p. 169 (1928).

‡ Z. Tuzi, Sci. Pap. Inst. Phys.-Chem. Res. (Tokyo), vii. nos. 112-114, pp. 79-120 (1927).

central portion C are taken by the polarized light passing through it: a few of them are reproduced in Pl. II. There are so many fringes revealed sharp and clear, as will be seen in the reproduced examples, that it is easy to draw an accurate contour of stresses from the corresponding negative plates.

## II. THEORY.

From the photograph (Pl. II.), the tangential distribution along the periphery of the hole is obtained, as shown in fig. 2. The diagram suggests that the stress function is likely an odd one, and the following solution is worked out, for which the author wishes to express his indebtedness to Prof. N. Yamaguti, whose kind guidance facilitated the



solution. In the solution the plate of the specimen is assumed to extend infinitely, and a circular hole of the radius  $a$  is made with its centre falling on an origin arbitrarily taken through which axes of  $x$  and  $y$  are drawn. It is also assumed that the uniform bending-moment is so applied that everywhere the stress distributions are given, in the case where there is no hole, by  $\widehat{xx} = Ay$  and  $\widehat{yy} = \widehat{xy} = 0$ , in which  $\widehat{xx}$  and  $\widehat{yy}$  are the normal stresses,  $\widehat{xy}$  the shear stress, and  $A$  is a constant.

Denoting by  $\chi$  the stress function, and using the usual notations, in  $x$ - $y$  coordinates, we have

$$\nabla^2 \nabla^2 \chi = 0, \quad \text{where } \nabla^2 = \frac{\partial^2}{\partial x^2} + \frac{\partial^2}{\partial y^2}$$

and

$$\widehat{xx} = \frac{\partial^2 \chi}{\partial y^2}, \quad \widehat{yy} = \frac{\partial^2 \chi}{\partial x^2}, \quad \widehat{xy} = -\frac{\partial^2 \chi}{\partial x \partial y}.$$

Expressed in  $x$ - $y$  coordinates,

$$\chi = Aa^3 \left\{ \left[ \frac{a}{2(x^2+y^2)} - \frac{a^3}{4(x^2+y^2)^2} \right] y + \left[ \frac{1}{6a^3} - \frac{a}{2(x^2+y^2)^2} + \frac{a^3}{3(x^2+y^2)^3} \right] y^3 \right\};$$

$$\left\{ \begin{aligned} \widehat{x\bar{x}} &= Aa^4 y \left\{ \frac{1}{a^4} - \frac{1}{(x^2+y^2)^2} \left[ 6 - \frac{5a^2}{x^2+y^2} \right] \right. \\ &\quad + \frac{2}{(x^2+y^2)^3} \left[ 9 - \frac{10a^2}{x^2+y^2} \right] y^2 \\ &\quad \left. + \frac{4}{(x^2+y^2)^4} \left[ -3 + \frac{4a^2}{x^2+y^2} \right] y^4 \right\}, \\ \widehat{y\bar{y}} &= Aa^4 y \left\{ \frac{1}{(x^2+y^2)^2} \left[ -1 + \frac{a^2+4x^2}{x^2+y^2} - \frac{6a^2x^2}{(x^2+y^2)^2} \right] \right. \\ &\quad \left. + \frac{2}{(x^2+y^2)^3} \left[ 1 - \frac{6x^2+a^2}{x^2+y^2} + \frac{8a^2x^2}{(x^2+y^2)^2} \right] y^2 \right\}, \\ \widehat{x\bar{y}} &= -Aa^4 x \left\{ \frac{1}{(x^2+y^2)^2} \left[ -1 + \frac{a^2}{x^2+y^2} \right] \right. \\ &\quad + \frac{2}{(x^2+y^2)^3} \left[ 5 - \frac{6a^2}{x^2+y^2} \right] y^2 \\ &\quad \left. - \frac{4}{(x^2+y^2)^4} \left[ 3 - \frac{4a^2}{x^2+y^2} \right] y^4 \right\}. \end{aligned} \right.$$

At  $x=0$ :  $\widehat{x\bar{y}}=0$ ,

$$\widehat{x\bar{x}} = A \left( y + \frac{a^6}{y^5} \right), \quad \widehat{y\bar{y}} = Aa^4 \left( \frac{1}{y^3} - \frac{a^2}{y^5} \right).$$

At  $y=0$ :  $\widehat{x\bar{x}} = \widehat{y\bar{y}} = 0$

$$\text{and } \widehat{x\bar{y}} = Aa^4 \left( \frac{1}{x^3} - \frac{a^2}{x^5} \right),$$

so that  $\widehat{x\bar{y}}$  is maximum at  $x = \pm 1.29 a$ .

The case when the centre of the hole is shifted from the neutral axis can readily be worked out by superposing these results with that of the well-known solution for uniform tension.

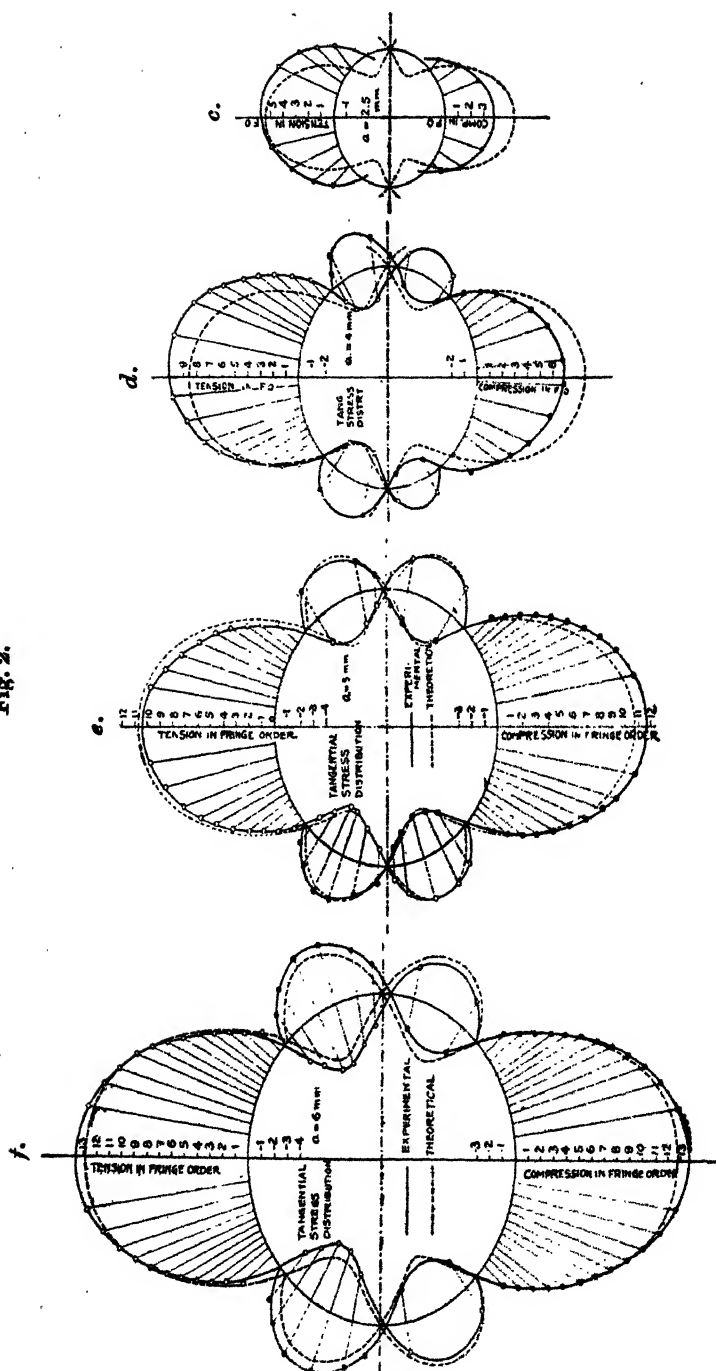
## EXPERIMENTS.

The test beams of phenolite were of 20 mm. breadth and 6 mm. thickness, with the span-length of 130 mm., each having a circular hole of diameter 0 mm., 3 mm., 5 mm., 8 mm., 10 mm., and 12 mm. (specimen *a, b, c, d, e, f*) respectively. At the centre of the two symmetrical loading points *K, K'* in fig. 1, 37.88 kg. weight was applied, that is, on each point *K, K'* 18.94 kg., for which it was ascertained that even with the weakest specimen, with the hole of the diameter  $2a=12$  mm., the maximum fibre stress-intensity did not exceed the elastic limit of the material. All the specimens had been annealed under quite the same conditions to eliminate the initial stresses, and the free boundaries, straight or circular, were filed off carefully just before the experiment, so as to attain the uniform darkness when illuminated without load. The photographs were taken\* immediately after the load was applied, and the exposure of  $\frac{1}{2}$  second was quite enough with a mercury green filter, so that they were free from the time-effect of the optical creep. As they are seen in Pl. II., sufficient numbers of sharp and clear fringes were displayed, and they are not only permanent and sure records, but are affected with little personal error indeed. The so-called "compensator," which was a small tension test-piece made from the same material as the main specimen, was used simply for the purpose of ascertaining the sense of the stresses.

First of all, the tangential stress-distributions along the periphery of the hole, where  $r=a$ , were thus obtained, and are shown in fig. 2, *f, e, d*, and *c*, and also in Table I. In the figures broken lines are drawn in accordance with the theoretical values calculated by the equations above mentioned. The value of the constant *A* was obtained from the photograph of the specimen *a*, in which  $r=0$  mm., and also verified with another specimen at sections away from the hole so as to be free from its effect, and the value was found to be  $A=1.075 \frac{\text{fringe order}}{\text{mm.}}$ . In solving the differential equations, we assumed that the plate of the specimen extended infinitely, so that both the experimental

\* The description of the experimental method is abridged in the present paper as it is quite the same as mentioned in the preceding paper of the author: "Photographic and Kinematographic Method for Photo-elasticity," Sci. Pap. Inst. Phys. Chem. Res. (Tokyo), viii. no. 149, pp. 247-267 (1928).

Fig. 2.



*Remark.*—In the following tables stresses are given in fringe order (f. o.).

TABLE I.

Specimen *f*.  $a = 6$  mm.

First quadrant.		Second quadrant.		Third quadrant.		Fourth quadrant.	
$\theta\theta$ in f. o.	Angle in degrees.	$\theta\theta$ in f. o.	Angle in degrees.	$\theta\theta$ in f. o.	Angle in degrees.	$\theta\theta$ in f. o.	Angle in degrees.
-2	4.0	-2	175.0	2	-168.5	2	-13.2
-3	11.0	-3	168.0	2	-140.0	2	-36.2
-4	20.5	-4	158.0	-2	-129.5	-2	-49.7
-4	29.0	-4	148.8	-3	-126.5	-3	-53.0
-3	37.2	-3	141.2	-4	-124.0	-4	-56.0
-2	42.3	-2	135.8	-5	-121.4	-5	-58.5
2	49.6	3	126.4	-6	-119.0	-6	-60.8
3	53.7	4	123.0	-7	-116.2	-7	-62.9
4	56.4	5	120.7	-8	-113.4	-8	-65.6
5	59.2	6	118.2	-9	-110.7	-9	-67.8
6	61.3	7	116.0	-10	-112.8	-10	-70.8
7	64.0	8	113.6	-11	-105.0	-11	-73.4
8	66.5	9	111.2	-12	-101.6	-12	-77.0
9	68.8	10	108.5	-13	-97.4	-13	-81.6
10	71.2	11	105.7				
11	74.7	12	102.2				
12	77.8	13	98.0				
13	81.8						

Specimen *e*.  $a = 5$  mm.

First quadrant.		Second quadrant.		Third quadrant.		Fourth quadrant.	
$\theta\theta$ in f. o.	Angle in degrees.	$\theta\theta$ in f. o.	Angle in degrees.	$\theta\theta$ in f. o.	Angle in degrees.	$\theta\theta$ in f. o.	Angle in degrees.
-1	5.8	-1	175.4	1	-176.8	1	-2.8
-2	13.2	-2	165.8	2	-171.2	2	-11.6
-2	38.2	-3	157.0	3	-161.0	2	-36.2
2	52.8	-3	150.6	3	-150.8	-2	-50.4
3	56.8	-2	142.6	2	-143.4	-3	-53.7



TABLE I. (*cont.*).Specimen *e*.  $a=5$  mm. (*cont.*).

First quadrant.		Second quadrant.		Third quadrant.		Fourth quadrant.	
$\theta\theta$ in f. o.	Angle in degrees.	$\theta\theta$ in f. o.	Angle in degrees.	$\theta\theta$ in f. o.	Angle in degrees.	$\theta\theta$ in f. o.	Angle in degrees.
4	59.7	-1	136.7	-2	-128.7	-4	-56.4
5	63.0	1	131.0	-3	-125.8	-5	-59.3
6	66.0	2	127.4	-4	-123.0	-6	-62.4
7	70.0	3	123.7	-5	-120.3	-7	-65.4
8	74.2	4	121.0	-6	-117.0	-8	-68.5
9	78.2	5	117.7	-7	-114.0	-9	-72.0
10	82.2	6	114.3	-8	-111.0	-10	-75.8
		7	111.2	-9	-112.5	-11	-81.0
		8	107.3	-10	-104.5		
		9	102.2	-11	-99.3		
		10	96.7				

Specimen *d*.  $a=4$  mm.

First quadrant.		Second quadrant.		Third quadrant.		Fourth quadrant.	
$\theta\theta$ in f. o.	Angle in degrees.	$\theta\theta$ in f. o.	Angle in degrees.	$\theta\theta$ in f. o.	Angle in degrees.	$\theta\theta$ in f. o.	Angle in degrees.
-2	10.0	-2	167.8	1	-174.5	-1	-1.7
-2	31.0	-2	143.6	1	-152.4	1	-12.4
-1	34.3	2	129.0	-2	-132.5	1	-39.5
2	44.8	3	124.3	-3	-121.6	-1	-49.0
3	49.7	4	120.4	-4	-117.0	-2	-54.2
4	53.8	5	116.8	-5	-110.6	-3	-58.8
5	57.7	6	112.5	-6	-101.0	-4	-64.0
6	61.0	7	109.6	-7	-92.0	-5	-70.0
7	65.8	8	105.7			-6	-75.8
8	68.8	9	100.0			-7	-85.5
9	73.0	10	94.5				
10	81.0						

TABLE I. (*cont.*).Specimen *c.*  $a=2.5$  mm.

First quadrant.		Second quadrant.		Third quadrant.		Fourth quadrant.	
$\theta\theta$ in f. o.	Angle in degrees.	$\theta\theta$ in f. o.	Angle in degrees.	$\theta\theta$ in f. o.	Angle in degrees.	$\theta\theta$ in f. o.	Angle in degrees.
2	43.0	2	133.5	-1	-129.6	-1	-45.6
3	51.8	3	123.2	-2	-118.3	-2	-58.0
4	59.2	4	112.2	-3	-104.8	-3	-70.8
5	69.3	5	100.8				

Theoretical values of  $\theta\theta$  at  $r=a$ .

Angle in degrees.	$\theta\theta$ in fringe order.			
	$a=6$ mm.	$a=5$ mm.	$a=4$ mm.	$a=2.5$ mm.
0 .....	0	0	0	0
10 .....	-2.10	-1.76	-1.40	-0.88
20 .....	-3.36	-2.81	-2.24	-1.40
30 .....	-3.22	-2.69	-2.15	-1.34
40 .....	-1.42	-1.19	-0.95	-0.59
45 .....	0	0	0	0
50 .....	1.77	1.47	1.18	0.74
60 .....	5.54	4.63	3.70	2.32
70 .....	9.30	7.75	6.21	3.88
80 .....	12.00	10.00	8.02	5.00
90 .....	12.90	10.77	8.62	5.88

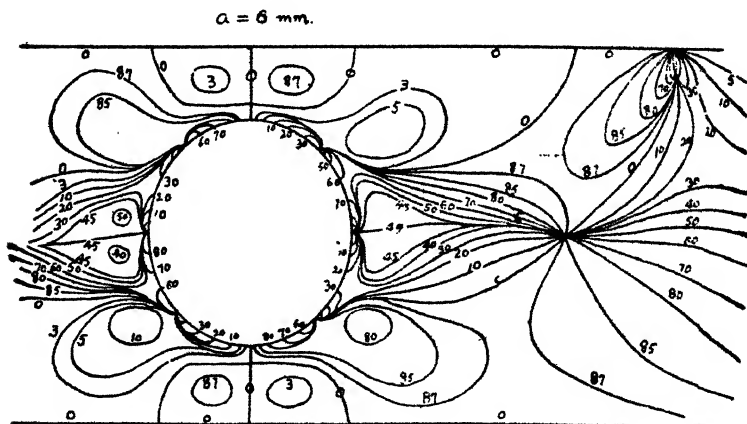
and theoretical values should agree better in the case of a smaller hole than in that of a larger. But, as is clear from fig. 2, the results are contrary to our expectation. It seems that some imperfections in our loading apparatus may be responsible for it. As is shown in fig. 1, the two load points  $K K'$  are connected rigidly to each other; consequently there might have been generated some tangential force (tension) along  $K K'$  when the specimens were deformed, and such force, if any, should act as subtractive against the fibre stress, which was compression in this case. Any unfavourable effect will be shown more conspicuously at a portion

where the fringe order is not high, and the author is of the opinion that the distinct deviation of the experimental values from the theoretical curve in cases of the specimens *d* and *c* is due to this effect.

The locations of the isoclinic lines are at times very ambiguous, as the lines are apt to appear in wide bands, especially with a thick specimen and also when the fringes of higher order are revealed. The author tried with three kinds of specimens—phenolite, xylonite, and glass, all of them being prepared in quite the same dimensions except the thickness.

It was ascertained that the locations of black lines are also quite the same for the three materials, being independent of

Fig. 3.



the thickness, and, moreover, that they were manifested most sharply by the glass specimen. Accordingly, in our cases the diagrams of isoclinic lines were studied by the aid of glass specimens, and one of them (specimen *f*) is shown in fig. 3. The orthogonal trajectories showing the directions of principal stresses were worked out, and are shown in fig. 4.

At the section  $x=0$ , each of the two stress components is calculated out graphically from the experimental data of  $p-q$  by means of the purely optical method for the symmetrical case, using the formula \*

$$p = p_0 - \Delta\phi \int_0^A \frac{p-q}{\Delta y} ds_1.$$

\* L. N. G. Filon and E. G. Coker, Brit. Assoc. Rep. 1914, p. 201; 1922, p. 350.

In the one which is shown in fig. 5 and Table II., the experimental values of  $\bar{x}\bar{x}$  and  $\bar{y}\bar{y}$  for the specimen *f* show

Fig. 4.

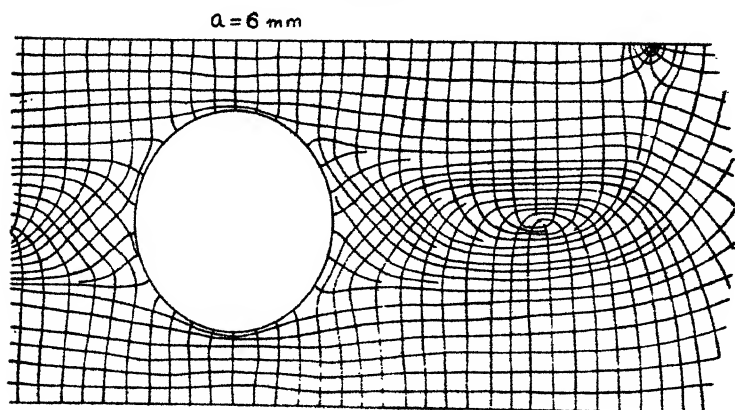
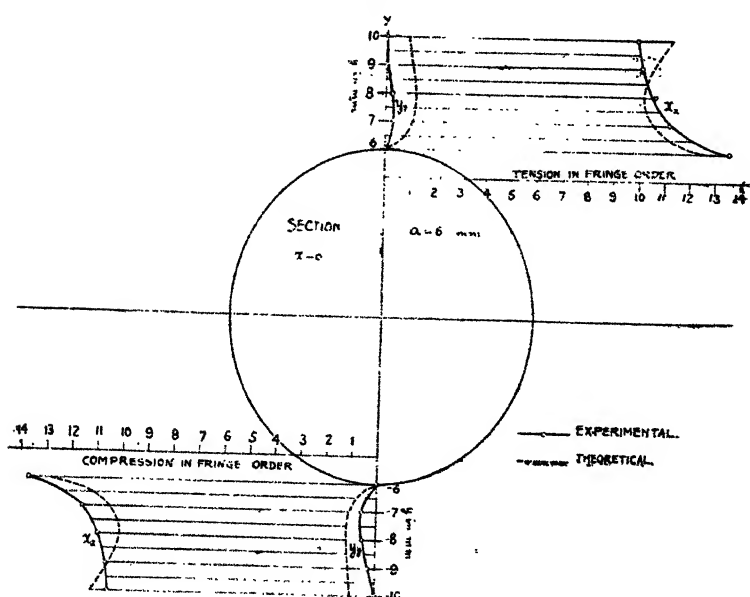


Fig. 5.



considerable deviation from the theoretical, but in this case the deviations are quite plausible, inasmuch as the effect of

the straight boundaries, which had not been taken into consideration in the solution, may act more or less, especially for the specimens of larger holes. On the other hand, however, it is a delicate problem to measure the distances of two adjacent isoclinic lines,  $\Delta y$ , as they are, at least in this section, very critical and not very distinct, so that a slight ambiguity might be the source of considerable errors. Hence the author dares not to set forth, with a firm confidence, the respective values of  $\widehat{xx}$  and  $\widehat{yy}$ , though he

TABLE II.

Stresses of  $\widehat{xx}$  and  $\widehat{yy}$  at the section  $x=0$  mm.

$a=6$  mm.

$y$ in mm.	Experimental.		Theoretical.	
	$\widehat{xx}$ in f. o.	$\widehat{yy}$ in f. o.	$\widehat{xx}$ in f. o.	$\widehat{yy}$ in f. o.
10 .....	9.90	0	11.25	0.89
9 .....	10.05	0	10.52	1.06
8 .....	10.60	0.25	10.12	1.19
7 .....	11.30	0.30	10.52	1.08
6 .....	13.50	0	12.90	0
- 6 .....	-13.70	0	-12.90	0
- 7 .....	-11.60	-0.60	-10.52	-1.08
- 8 .....	-11.00	-0.55	-10.12	-1.19
- 9 .....	-10.65	-0.30	-10.52	-1.06
-10 .....	-10.60	0	-11.25	-0.89

could not find any more reliable device to separate each stress component out of the values of  $p-q$ . At any rate, it is clear in this case that  $\widehat{yy}$  is very small compared with  $\widehat{xx}$ , and it seems to be less important to work out accurately the values of  $\widehat{yy}$  except for academic interest.

The other purely optical method preferred by Prof. L. N. G. Filon \* is based upon the following formulas :

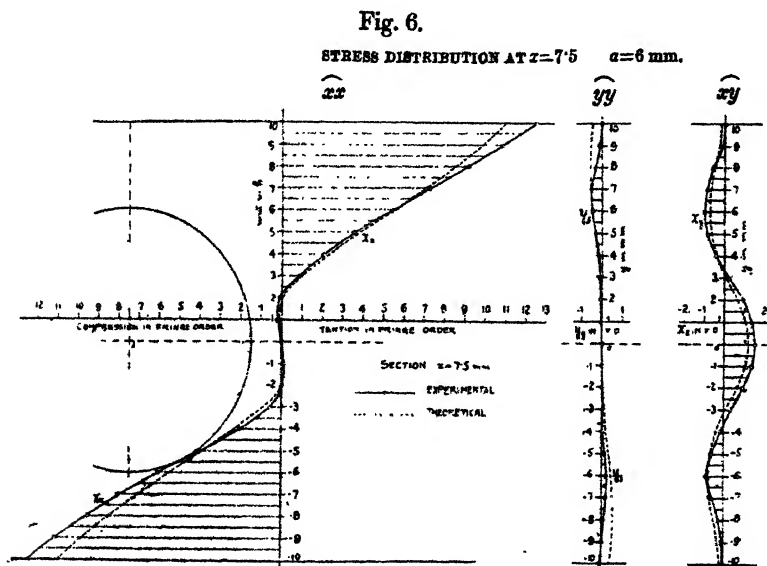
$$\widehat{xx} - \widehat{xx}_0 = - \int_{x_0}^x \frac{\partial \widehat{xy}}{\partial y} dx,$$

$$\widehat{yy} - \widehat{yy}_0 = - \int_{y_0}^y \frac{\partial \widehat{xy}}{\partial x} dy.$$

\* *Loc. cit.*

With the specimen  $f$ ,  $a=6$  mm., the stress distribution at the section  $x=7.5$  mm. was studied by this method,  $\delta x$  being taken as 2 mm.; two more sections,  $x=8.5$  mm. and  $x=6.5$  mm., were studied to work out the values of  $\frac{\delta xy}{\delta x}$ .

In this case every state was very favourable for the graphical integration, and without any remarkable ambiguities the stress components were worked out as they are shown in fig. 6 and Table III. The theoretical values



are also represented by broken lines in the figure, all of which show rather fair agreement with the experimental values.

### SUMMARY.

(1) A beam of uniform rectangular section having a circular hole of radius  $a$  on its centre line was subjected to a uniform bending moment, and its stress distribution was studied by photo-elasticity by means of the photographic method.

(2) From one of the results the form of the stress function was assumed, and a theoretical solution was worked out under the assumption of an infinitely extended plane.

(3) At several sections and boundaries the experimental values were worked out and compared with the theoretical

224 *The Effect of a Circular Hole on Stress Distribution.*

ones. The author is of the opinion that his solution serves satisfactorily enough for practical purposes, and also that the photographic method is rather preferable, being as free from errors as one can hope in such an experiment.

TABLE III.

Stresses  $\widehat{xy}$ ,  $\widehat{yy}$ , and  $\widehat{xx}$  at the section  $x=7.5$  mm.

$a=6$  mm.

$y$ in mm.	Experimental values.			Theoretical values.		
	$\widehat{xy}$ in f. o.	$\widehat{yy}$ in f. o.	$\widehat{xx}$ in f. o.	$\widehat{xy}$ in f. o.	$\widehat{yy}$ in f. o.	$\widehat{xx}$ in f. o.
10 .....	0	0	12.50	-0.20	-0.45	10.92
9 .....	-0.04	-0.13	10.86			
8 .....	-0.58	-0.36	9.17	-0.49	-0.58	8.50
7 .....	-0.90	-0.52	7.27			
6 .....	-1.01	-0.48	5.38	-0.72	-0.48	5.52
5 .....	-0.85	-0.31	3.53			
4 .....	-0.40	-0.15	2.06	-0.39	-0.21	2.31
3 .....	-0.07	-0.10	0.89			
2 .....	0.97	-0.09	-0.09	0.65	-0.09	0.04
1 .....	1.37	-0.05	-0.14	...	...	-0.09
0 .....	1.56	0	0	1.19	0	0
-1 .....	1.37	0.01	0.08	...	...	0.09
-2 .....	0.93	0.01	0.02	0.65	0.09	-0.04
-3 .....	0.33	0.05	-0.58			
-4 .....	-0.17	0.04	-2.01	-0.39	0.21	-2.31
-5 .....	-0.58	0.12	-3.94			
-6 .....	-0.83	0.28	-6.05	-0.72	0.48	-5.52
-7 .....	-0.55	0.25	-8.02			
-8 .....	-0.24	0.10	-9.48	-0.49	0.58	-8.50
-9 .....	-0.02	-0.03	-11.13			
-10 .....	0	-0.05	-13.15	-0.20	0.45	-10.92

In conclusion, the author wishes to express his hearty thanks to Viscount Prof. M. Ōkōchi and to Prof. M. Masima, who gave the author valuable suggestions throughout the course of the experiments.

**XXII. The Critical Frequency in an Ionized Medium. Steady Magnetic Force Present.** By T. L. ECKERSLEY, M.A.\*  
(Marconi's Wireless Telegraph Co., Ltd., Research Department.)

§ 1.

**I**N a recent analysis of the transmission of electromagnetic waves of frequency  $\nu$  through an ionized medium the well-known critical frequency given by

$$\nu_0^2 = \frac{Ne^2c^2}{\pi m}$$

( $N$ =no. of electrons per c.c.;  $e$ =charge of electron;  $m$ =mass of electron) was examined.

It was shown that as  $\nu$ , the frequency of the waves, approached  $\nu_0$ , the group velocity  $\rightarrow 0$ , and that physically this slowing-down of the group velocity was occasioned by the momentum given to the ions. The momentum of the wave travelling, say, in the  $x$  direction was transferred to the  $x$  momentum of the ions, and at the critical frequency the demand for momentum by the ions is equal to the supply from the wave, and this is therefore brought to a standstill. If a magnetic field is present the critical frequency is altered, and it is the purpose of the present note to show that the altered motion of the ions results in an altered critical frequency, but that the momentum balance is the same as in the previous case, and that the waves are brought to a standstill for the same reason, *i.e.* the transference of the wave momentum to the ions.

For the purpose of this analysis we require the motion of the ions in the field of the electric wave.

As in the previous case, it will not do to neglect action of the magnetic force in the wave, for it is this alone which provides the necessary forward momentum to the ions. The movement of the ions, if this be neglected, is wholly in the plane perpendicular to the ray and the balance of momentum cannot be maintained.

The simplest case to consider is that in which the magnetic force is parallel to the ray. In such a case the wave splits

\* Communicated by the Author.

† T. L. Eckersley, "Transmission of Electric Waves through an Ionized Medium," *Phil. Mag.* iv. (July 1927).



up into two circularly-polarized components, each of which travels with its appropriate group and phase velocity. Each component can be dealt with separately.

Suppose, therefore, that the wave is circularly polarized in the right-hand direction, we shall put

$$Y = Z_0 \cos pt, \quad X = 0,$$

$$Z = Z_0 \sin pt.$$

The magnetic forces  $\beta$  and  $\gamma$  are

$$\beta = H_0 \sin pt, \quad (H \text{ and } Z \text{ the same dimensionally.})$$

$$\gamma = -H_0 \cos pt.$$

The equations of motion for the ions are then

$$\begin{aligned} m \frac{\partial v_z}{\partial t} &= \frac{eH_0}{c} v_z \sin pt + \frac{eH_0}{c} v_y \cos pt \\ &= \frac{eH_0}{c} \chi_1, \quad . . . . . (1, 1) \end{aligned}$$

where  $\chi_1$  is an abbreviation for

$$v_z \sin pt + v_y \cos pt.$$

Let  $R$  be the steady magnetic field directed along  $x$ .

Similarly we have

$$m \frac{dv_y}{dt} = eZ_0 \cos pt - \frac{eRv_z}{c} - \frac{eH_0}{c} v_z \cos pt, \quad . (1, 2)$$

$$m \frac{dv_z}{dt} = eZ_0 \sin pt + \frac{eRv_y}{c} - \frac{eH_0}{c} v_z \sin pt. \quad . (1, 3)$$

Let

$$\frac{eR}{mc} = p_1 = 2\pi\nu_1,$$

where  $\nu_1$  is the resonant frequency of the electrons in the magnetic field.

By multiplying (1, 2) by  $\sin pt$  and (1, 3) by  $\cos pt$  and subtracting and denoting  $(v_y \sin pt - v_z \cos pt)$  by  $\chi_2$ , we get the equation

$$\frac{d\chi_2}{dt} = + (p - p_1) \chi_1. \quad . . . . . (1, 4)$$

Similarly, by multiplying (1, 2) by  $\cos pt$  and (1, 3) by  $\sin pt$  and adding, we get the equation

$$\frac{d\chi_1}{dt} = \frac{eZ_0}{m} + (p_1 - p)\chi_1 - \frac{eH_0}{mc}v_x; \quad \dots (1, 5)$$

the three equations are therefore

$$\left. \begin{aligned} \frac{dv_x}{dt} &= \frac{eH_0}{mc}\chi_1, \\ \frac{d\chi_2}{dt} &= (p - p_1)\chi_1, \\ \frac{d\chi_1}{dt} &= \frac{eZ_0}{m} - (p - p_1)\chi_2 - \frac{eH_0}{mc}v_x. \end{aligned} \right\} \dots (1, 6)$$

Eliminating  $v_x$  and  $\chi_2$ , we get the following vibrational differential equation for  $\chi_1$ :

$$\frac{d^2\chi_1}{dt^2} = (p - p_1)^2\chi_1 - \frac{e^2H_0^2}{m^2c^2}\chi_1. \quad \dots (1, 7)$$

*Initial Conditions.*

Inverting the equations for  $\chi_1$  and  $\chi_2$ , we get

$$\left. \begin{aligned} v_y &= \chi_1 \cos pt + \chi_2 \sin pt, \\ v_x &= \chi_1 \sin pt - \chi_2 \cos pt, \end{aligned} \right\} \dots (1, 8)$$

so that

$$\left. \begin{aligned} (v_y)_{t=0} &= (\chi_1)_{t=0}, \\ (v_x)_{t=0} &= (\chi_2)_{t=0}. \end{aligned} \right\} \dots (1, 9)$$

We will suppose that the electron starts from rest at the time  $t=0$ , so that

$$\begin{aligned} \chi_1 &= 0, & t &= 0, \\ \chi_2 &= 0, & t &= 0. \end{aligned}$$

The appropriate solution for  $\chi_1$  is then

$$\chi_1 = P \sin \bar{p}t, \quad \text{where } \bar{p}^2 = (p - p_1)^2 + \frac{e^2H_0^2}{m^2c^2}; \quad (1, 10)$$

now

$$\frac{\partial v_x}{\partial t} = \frac{eH_0}{mc}\chi_1 = \frac{eH_0}{mc}P \sin \bar{p}t$$

and

$$v_x = \frac{eH_0}{mc} \frac{P}{\bar{p}} (1 - \cos \bar{p}t), \quad \dots (1, 11)$$

since  $v_x=0$  when  $t=0$ . Similarly

$$\chi_2 = (p-p_1) \frac{P}{\bar{p}} (1 - \cos \bar{p}t); \quad \dots (1, 11)'$$

substituting in (1, 5), we get the relation

$$eZ_0 = \frac{(p-p_1)^2}{\bar{p}} P + \left( \frac{eH_0}{mc} \right)^2 P, \quad \dots (1, 12)$$

which determines

$$P = \frac{\bar{p}eZ_0/m}{(p-p_1)^2 + \frac{e^2H_0^2}{m^2c^2}} = \frac{eZ_0/m}{\left\{ (p-p_1)^2 + \frac{e^2H_0^2}{m^2c^2} \right\}^{1/2}}.$$

Now the mean forward velocity of the electrons

$$\bar{v} = \frac{eH_0}{mc} \frac{P}{\bar{p}},$$

*i. e.*

$$= \frac{e^2H_0Z_0}{m^2c} \frac{1}{\left\{ (p-p_1)^2 + \frac{e^2H_0^2}{m^2c^2} \right\}}, \quad \dots (1, 13)$$

which gives the mean forward momentum supplied to the ions.

This is

$$\begin{aligned} Nmv_x &= \frac{Ne^2H_0Z_0}{mc} \frac{1}{\left\{ (p-p_1)^2 + \frac{e^2H_0^2}{m^2c^2} \right\}} \\ &= \frac{\pi H_0Z_0}{c^3} \frac{\nu_0^2}{\left\{ (p-p_1)^2 + \frac{e^2H_0^2}{m^2c^2} \right\}}, \quad (1, 14) \end{aligned}$$

where  $N$  is the number of electrons or ions of mass  $m$  and charge  $e$  per c.c.

It will be observed that to a first approximation (neglecting  $\frac{e^2H_0^2}{m^2c^2}$  compared with  $(p-p_1)^2$ ) the ionic momentum produced is a definite fraction of the wave momentum supplied, *i. e.*  $H_0Z_0$ , a fraction which only depends on the critical frequency  $\nu_0$ , the resonant frequency  $\nu_1$ , and the actual frequency  $\nu$ .

A similar analysis may be made for the case where the

circular polarization is opposite. This is equivalent to reversing  $R$ , and we get

$$Nm\bar{v}_x = \frac{\pi H_0 Z_0}{c^3} \frac{\nu_0^2}{\left\{ (p+p_1)^2 + \frac{e^2 H_0^2}{m^2 c^2} \right\}} \quad (1, 15)$$

It might be thought that the result depended on rather arbitrary initial conditions.

In fact, by specifying  $t=0$  as the time of arrival of the waves at the electrons, we have fixed  $Y=0, Z=Z_0$  at this time.

If at  $t=0$ ,  $Y$  and  $Z$  had been arbitrarily phased, say

$$Y_x = Z_0 \cos(pt + \phi), \quad Z = Z_0 \sin(pt + \phi),$$

so that

$$Y = Z_0 \cos \phi \cos pt - Z_0 \sin \phi \sin pt,$$

$$Z = Z_0 \sin \phi \cos pt + Z_0 \cos \phi \sin pt.$$

Then referred to axes rotated about  $x$ , for an angle  $\phi$ ,

$$\left. \begin{aligned} Y_1 &= Y \cos \phi + Z \sin \phi = Z_0 \cos pt, \\ Z_1 &= -Y \sin \phi + Z \cos \phi = Z_0 \sin pt, \end{aligned} \right\}$$

as before, and, as the choice of axes is arbitrary, we may take  $Y_1$  and  $Z_1$  instead of  $Y$  and  $Z$ , and get exactly the same results as previously.

## § 2. Balance of Momentum.

As in the previous paper, we find that the momentum supplied per unit area is  $\frac{Z_0 H_0}{2\pi c}$ . The rate of increase of momentum at the head of the wave is  $\frac{Z_0 H_0}{2\pi c} \frac{U}{c}$ , where  $U$  is the group velocity, since  $\frac{Z_0 H_0}{2\pi c^2}$  is the momentum density and the head of the wave travels with the velocity  $U$ .

The head of the wave is only a sharply-defined surface moving forward with the velocity  $U$  when  $U$  does not differ largely from  $c$ ; also in this case the departure from linearity of the equations is small. For these reasons the momentum conditions can only be simply calculated when  $U$  and  $c$  do not differ much. The condition where  $U \rightarrow 0$  near the critical frequency cannot be considered without going into a great deal more detail in calculating the exact distribution of the wave-energy and the consequent ionic movements.

We therefore restrict ourselves to the case where  $U$  does not differ largely from  $c$ , or where  $\frac{v_0^2}{v(v \pm v_1)}$  is small (these two conditions being equivalent, as we shall see).

In the first place we must calculate the group velocity.

As is well known, the phase velocity in these conditions is

$$v = \frac{c}{\sqrt{1 - \frac{v_0^2}{v(v \pm v_1)}}}, \quad \dots \quad (2, 1)$$

where the symbols have their previous meanings, and where the  $+$  or  $-$  sign is taken according as the wave is circularly polarized in a right-hand or left-hand direction. The group velocity is given in general, as is well known, by the relation

$$U = \frac{dv}{d\frac{v}{v}} \quad \dots \quad (2, 2)$$

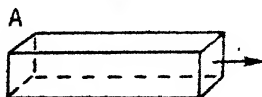
Using the above value of  $v$ , we get for the group velocity

$$U = c \sqrt{1 - \frac{v_0^2}{v(v \pm v_1)}} / \left\{ 1 \mp \frac{1}{2} \frac{v_0^2 v_1}{v(v \pm v_1)^2} \right\}. \quad (2, 3)$$

It is to be noted that  $Uv \neq c^2$  in this case.

Consider a column of radiation 1 sq. cm. in section extended along the direction of transmission.

Fig. 1.



Head end of wave moving with velocity  $U$ .

The rate of supply of æthereal momentum at  $A$  is  $\frac{Z_0 H_0}{2\pi c}$ ; at the head end of the wave the rate of gain of æthereal momentum is  $\frac{Z_0 H_0}{2\pi c} \frac{U}{c}$ , and the deficit in æthereal momentum is

$$\frac{Z_0 H_0}{2\pi c} (1 - U/c); \quad \dots \quad (2, 4)$$

the gain in ionic momentum is

$$Nmv_z = \frac{Z_0 H_0}{4\pi c} \frac{\nu_0^2}{\left\{ (\nu \pm \nu_1)^2 + \frac{e^2 H_0^2}{4\pi^2 m^2 c^2} \right\}}. \quad (1, 14,) \text{ \& } (1, 15)$$

Now by (2, 3), when

$$\frac{\nu_0^2}{\nu(\nu \pm \nu_1)} \text{ and } \frac{\nu_0^2 \nu_1}{\nu(\nu \pm \nu_1)^2}$$

are small,  $(1 - U/c)$  is

$$(a) \quad 1 - \left\{ \left(1 - \frac{1}{2} \nu_0^2 / \nu(\nu - \nu_1)\right) / \left(1 + \frac{1}{2} \nu_0^2 \nu_1 / \nu(\nu - \nu_1)^2\right) \right\}, \quad (2, 5)$$

$$(b) \quad 1 - \left\{ \left(1 - \frac{1}{2} \nu_0^2 / \nu(\nu + \nu_1)\right) / \left(1 - \frac{1}{2} \nu_0^2 \nu_1 / \nu(\nu + \nu_1)^2\right) \right\}; \quad (2, 6)$$

i. e.

$$\left. \begin{aligned} (a) \quad & \frac{1}{2} \frac{\nu_0^2}{(\nu - \nu_1)^2}, \\ (b) \quad & \frac{1}{2} \frac{\nu_0^2}{(\nu + \nu_1)^2}, \end{aligned} \right\} \dots \dots \dots (2, 7)$$

so that the deficit in æthereal momentum is to the first approximation,

$$\frac{Z_0 H_0}{4\pi c} \frac{\nu_0^2}{(\nu \pm \nu_1)^2},$$

and, except for the negligible term  $\frac{e^2 H_0^2}{4\pi^2 m^2 c^2}$ , is identical with the gain in the ionic momentum.

Extending these results to the case where  $U \rightarrow 0$ , we may conclude that the group velocity of the wave  $\rightarrow 0$  on account of the demand for momentum of the ions which tend to rob the wave of all its momentum (in the neighbourhood of  $\nu = \text{initial frequency}$ ) so that the wave can travel no further. This investigation is important from the point of view of the transmission of waves in an over-dense medium.

In the absence of a magnetic field the medium ceases to be transparent if  $N$ , the ionic density, is so great that  $\nu_0 > \nu$ . The medium may be said to be over dense in such a case.

If in such a medium a sufficiently strong magnetic field is introduced that  $\frac{\nu_0}{\nu(\nu + \nu_1)}$  is small, the medium becomes transparent (for a suitably circularly-polarized ray). The physical reason for this transparency is now clear, for whereas when no magnetic field is present the amount of

$x$  momentum produced by the waves, i. e.  $\frac{Z_0 H_0}{4\pi c} \frac{v_1^2}{v^2}$ , is greater than can be supplied by the wave, the ionic movement is so altered in the presence of the magnetic field that the forward ionic momentum is reduced in the ratio  $\frac{v^2}{(v+v_1)^2}$ . By increasing  $v_1$  the demand for  $x$  momentum by the ions can be made so small that the momentum of the wave is not appreciably reduced.

It can therefore travel through the over-dense ionized medium when a sufficiently strong magnetic field is introduced.

These results have only been deduced for the particular case where the ray direction is actually along the direction of the steady magnetic field.

#### *Transmission at any Angle $\theta$ with the Ray.*

When the ray direction makes an angle  $\theta$  with the direction of  $R$  the analysis is more complex, but it is possible to show that, but for the exceptional case where  $v_1 \doteq v_0 \doteq v$ , the above is not unique.

Thus examining the phase-velocity equation, we find that the phase velocity, group velocity  $X$ ,  $Y$ , and  $Z$  all vary continuously in the neighbourhood  $\theta=0$ , and therefore it follows that the transparency is maintained over a finite region near  $\theta=0$ , the physical reason for this transparency being that stated above, i. e. the modification of the ionic motions by the magnetic field in such a way that the demand for momentum of the ions is decreased below what can be supplied by the wave.

It seems to me to follow quite definitely that the application of a sufficiently intense magnetic field to an over-dense medium will make the latter transparent for a finite range of angles in accordance with the dictates of the phase-velocity equations.

This result has an important application in the case of the transmission of waves over the earth's surface, for in the case of waves  $>100$  m. we know that the layer is over-dense, i. e.,  $N \geq 10^6$  electrons per c.c. Although longer waves generated on the earth's surface would be wholly confined to the region between the earth and Heaviside layer in the absence of a magnetic field, sufficiently long waves can penetrate the layer when the earth's magnetic field is taken into account.

**XXIII. *The Electronic Theory of Valency.*—Part VII. *The Etch-Figures of Sylvine.* By Professor T. M. LOWRY, F.R.S., and M. A. VERNON, B.A.\***

[Plates III. & IV.]

UNTIL Bragg published the results of the X-ray analysis of rock-salt it was generally believed that the alkali halides crystallized in hemihedral forms of the cubic system. This conclusion was based on the observation that the etch-figures were not symmetrical, but were rotated in a definite direction with respect to the planes of symmetry of the crystal. The structure deduced from X-ray analysis, however, consists of two interpenetrating face-centred cubic lattices which have a complete holohedral symmetry. In the same way crystallographers had concluded from observations on twinned crystals of diamond that the crystals had a hemihedral symmetry, whereas X-ray analysis indicated that the lattice was holohedral. These observations were of importance in that they suggested the possible existence of a fine structure, which was not disclosed by X-ray analysis of the crystal-lattice, although it might be detected by the traditional methods used by crystallographers in order to determine the symmetry of crystals.

In order to resolve this apparent contradiction Herzfeld and Hettich, in 1926 †, made experiments on the etch-figures of sylvine. As a result of their experiments they suggested that the lack of symmetry of the etch-figures was not due to a lack of symmetry in the crystal structure, but to the presence of optically active impurities in the etching solution, which formed crystallographically unsymmetrical adsorption compounds on the surface of the salt. Thus, when specially purified water was used, their etch-figures were all perfectly symmetrical; but, when traces of optically-active impurities were introduced, a large number of unsymmetrical etch-figures were observed. These conclusions were questioned by J. P. Valetone ‡, but were confirmed by the more detailed report of Hettich §. The matter seemed, however, to be sufficiently important to

\* Communicated by the Faraday Society.

† *Z. Physik*, p. 38 (1926).

‡ *Ibid.* xxxix. p. 60.

§ *Z. Krist.* lxiv. p. 265 (1926).



call for further independent evidence, and the present work was undertaken for this purpose.

Experiments were first made with natural crystals of sylvine. The material was by no means perfect, and the results obtained were rather irregular. As recommended by Hettich, the water was purified by distillation from alkaline permanganate, and the glass vessels were cleansed with chromic acid and rinsed with purified water. The crystals were etched with a saturated solution of pure potassium chloride to which a few drops of purified water were added. It was observed that solutions which had been saturated by boiling with the solid salt were much less satisfactory for etching than those made by shaking with the salt in the cold, but we cannot give any explanation of this difference of behaviour. The crystal was placed on a watch-glass on the stage of a microscope, covered with the solution, and the etching process watched. Since the etch-figures of sylvine are usually convex and not concave, an oblique illumination was used in order to show up the pyramidal prominences. In one isolated instance, however, when natural sylvine was etched in presence of amyl alcohol one or two pyramidal pits were observed.

In order to get the best results it is necessary to use a fresh and perfect cleavage, and this was very difficult to obtain with the imperfect natural material. Some trouble was also caused by the tendency of the solution to deposit crystals on the surface, perhaps as a result of the large number of nuclei of crystallization provided by the irregularities on the cleavage-face. It was found, however, that nearly all the pyramids were symmetrically placed with respect to the cleavage-edges. Occasionally a few of the pyramids appeared to be twisted, but there was considerable variation in the angle of rotation of these unsymmetrical pyramids, even on the same crystal-face. A possible explanation of this anomaly is provided by the very significant fact that in some cases pyramids were seen to detach themselves bodily from the crystal, and to float a little distance before finally coming to rest in an unsymmetrical position. This was only observed when natural crystals were used, and was probably due to the presence of cleavage-cracks below these particular pyramids.

Traces of a series of optically active alcohols and esters

were next introduced into the etching solution. No appreciable alteration was observed, except perhaps a slight increase in the number of etch-figures in a given area. Specimen counts were made of the numbers of symmetrical and rotated pyramids in the field of view, and some of the results are given below. These results show clearly that the etch-figures of natural sylvine are in general perfectly symmetrical.

Impurity.	Number of Pyramids.		
	Symmetrical.	Rotated Left.	Rotated Right.
None.....	40	0	1
„ .....	30	0	1
„ .....	50	1	2
<i>t</i> -Amyl alcohol (natural) .....	45	3	3
<i>d</i> - $\gamma$ -Nonyl formate .....	60	0	1
<i>d</i> - <i>n</i> -Butyl-vinyl-carbinol .....	60	0	3
<i>l</i> - <i>n</i> -Butyl-vinyl-carbinol .....	60	2	1
<i>l</i> - <i>n</i> -Butyl-vinyl-carbinol formate .....	50	0	1
<i>l</i> -Ethyl $\beta$ -phenethyl propionate .....	50	0	1

Experiments were then made with artificial crystals. For this purpose potassium chloride was purified by repeated recrystallization from water, dried and pulverized. It was placed in a clean platinum dish and fused in a muffle-furnace. When the fused salt had been allowed to cool the top layer was a clear transparent mass, whilst below it was an agglomeration of tiny crystals. Pieces of the top layer were detached, using a carefully cleaned knife-blade and tweezers. Small cubical fragments were thus obtained, the surfaces of which were formed by exceedingly good and well-marked cleavages. The difficulties arising in the previous case from crystallization on the surface and from the floating away of pyramidal hillocks were now entirely absent, and very good etch-figures were obtained, but perhaps less rapidly than with the natural crystals. Although a large number of experiments were performed, both with and without impurities in the etching solution, *not a single unsymmetrical pyramid was observed.*

Photographs, taken with a Zeiss camera attachment to the microscope, illustrate the results obtained. In

Pl. III., where *l*-asparagine was added to the etching solution, a large number of well-developed pyramids are seen, which are all oriented alike. The cleavage-edge does not come into the field of view, which was in the centre of the crystal face, but the cleavage was found to be parallel to the square edges of the pyramids. In the experiments illustrated in Pl. IV. the impurities were (a) and (b) none, (c) and (d) amyl alcohol, (e) ethyl tartrate, and (f) *l*-asparagine. In some cases the edge of the crystal fragment is seen, instead of a cleavage-edge; but the true direction of the cleavage can be deduced from cleavage-cracks in the field of view, and this direction has been marked by a horizontal line on each photograph.

The evidence now adduced is of a different character from that of Hertzfeld and Hettich, since in our experiments we were unable to develop unsymmetrical etch-figures, whereas they were only able to get rid of them by taking special precautions. In spite of this difference, however, the two series of experiments lead to the same conclusion, namely, that crystals of sylvine do not contain any structural element which leads to the regular development of unsymmetrical etch-figures, and that when these are observed they are of a fortuitous character, which does not justify the conclusion that the crystal-lattice of the salt is unsymmetrical.

In this connexion it is desirable to emphasize the fortuitous way in which etch-figures are necessarily developed. Thus, in his recent '*Leçons de Cristallographie*' Friedel, who has made an exceptionally thorough study of the subject, finds it necessary to issue a warning in reference to the pitfalls which are associated with this method of investigating crystal-symmetry. In particular, whilst it has generally been held that the occasional appearance of unsymmetrical pitting must outweigh any number of observations in which symmetrical pits are seen, Professor Friedel insists that symmetrical pitting can only be expected on surfaces that are accurately oriented, and that, even in the case of calcite, the true cleavage-planes are interrupted by small conchoidal sections on which the etching is necessarily unsymmetrical.

The matter can, however, be carried one stage further, since on a perfectly homogeneous face there would be no irregularities from which either pitting or the development of hillocks could start, and the etch-figures would only be

of molecular dimensions. Thus, even in their purest synthetic crystals Herzfeld and Hettich found that pyramidal hillocks were only formed at points where there were minute specks of ferric oxide to check the initial action of the etch-liquid on the soluble salt. This fact would not invalidate the evidence derived from a lower order of symmetry in the etch-figures, if this could be shown to be a constant property of the crystal, but our own experiments agree with those of Herzfeld and Hettich in showing that this is not the case. We therefore conclude that the higher symmetry established by X-ray analysis cannot be challenged on the basis of data provided by the study of etch-figures.

In the case of rock-salt, then, there is at present no trustworthy crystallographic evidence which can be used to prove the presence of real molecules in the crystal. The properties of the highly-conducting liquid are also in harmony with the conception of an ionic aggregate, differing only from the solid in being mobile and disordered, instead of rigid and orderly. On the other hand, measurements of conductivity show that liquid water contains only one pair of ions for every 550 million molecules, and even this small proportion diminishes as the temperature falls. There is therefore no analogous justification for supposing that ice is "a packing of charged ions  $O^{-}$ ,  $H^{+}$ "\*, since this implies that the molecules, which make up practically the whole content of liquid water, disappear completely in the act of crystallization. Physico-chemical evidence, on the contrary, indicates that the formation of ice is accompanied by a process of polymerization, which is already in progress in the liquid state, and provides an obvious explanation of the very exceptional phenomenon of maximum density. The conclusion that ice is formed from water by polymerization rather than by ionization is also in harmony with the crystallographic evidence, since the open lattice, which is disclosed by X-ray analysis, is much more compatible with a network of bonds than with an aggregation of close-packed ions, such as is postulated in a crystal of fluor spar. Since, however, an increase in the valency of oxygen is always accompanied by the development of a positive charge, as in the formation of oxonium ions,  $OH_2 \rightarrow OH_3^{+} \rightarrow O^{++}H_4$ , it appears probable

\* Gibbs, Proc. R. S., A. cxiii. p. 361 (1926).

that, if the atoms of oxygen and hydrogen in ice are electrically charged, the quadrivalent oxygen must carry a positive charge and the bivalent hydrogen a negative charge, in place of the charges of opposite sign which would normally be carried by free ions of these elements\*.

The crystal-structure of quartz presents an analogous problem. Gibbs† has assigned to it an ionic structure, which can be justified by the fact that silicon (unlike hydrogen) does in fact possess some of the properties of a metal. The contrast between this ionic structure and the molecular structure of carbon dioxide serves, moreover, to explain the wide differences between the physical properties of the two oxides, as illustrated by the rise from a sublimation-point at  $-78^{\circ}$  to a boiling-point at  $+2600^{\circ}$  C., which occurs on passing from carbon dioxide to silicon dioxide. Nevertheless it is almost as difficult to believe that the bonds of the silicate ion disappear completely in silicic anhydride as to believe that the bonds of the water-molecule disappear completely in ice. This difficulty can, however, again be avoided by making use of Thomson's conception of intramolecular ionization‡, which was discussed somewhat fully in the first paper of the present series§. In the case of carbon dioxide the formation of a covalent molecule with non-polar double bonds between carbon and oxygen is comparatively easy; but G. N. Lewis has pointed out that "the ability to form multiple bonds is almost entirely, if not entirely, confined to elements of the first period of eight, and especially to carbon, nitrogen, and oxygen"||. This conclusion has been confirmed by the recent experiments of Professor F. S. Kipping on "The Carbon-Silicon Binding"¶, in reference to which he says that "Fresh evidence is continually being obtained . . . that an ethylenic binding between carbon and silicon is either impossible or can

\* Sugden (J. Chem. Soc. 1929, p. 316) has recently suggested a scheme in which the atoms of ice are all neutral. This depends on reducing the bonds between the atoms to *one* shared electron, instead of the *two* electrons postulated by Lewis's theory of covalency. The scheme therefore involves a novel point of view for which no sufficient experimental evidence is yet available.

† Gibbs, Proc. R. S., A. cxiii. p. 361 (1926).

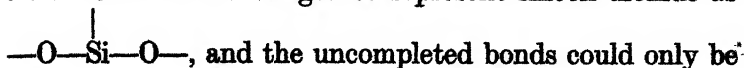
‡ Phil. Mag. [6] xxvii. p. 757 (1914).

§ Phil. Mag. xlv. p. 1105 (1923).

|| 'Valence,' p. 94 (1923).

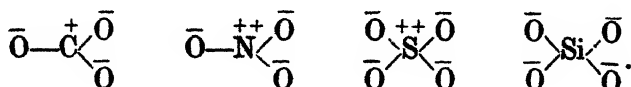
¶ J. Chem. Soc. p. 104 (1927).

only be produced under exceptional conditions. Those reactions which lead to the formation of an olefine seem to be quite inapplicable to the production of the group  $\text{>C:Si<}$ ." There is therefore a direct experimental justification for adopting Lewis's suggestion that "if silicon is incapable of sharing a double bond with oxygen . . . we should be obliged to represent silicon dioxide as

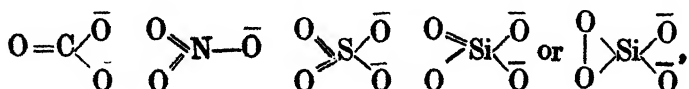


completed by union with other molecules." From this point of view the molecule of silica, with its four free bonds, resembles the atom of carbon, and should give rise to a network of the same general type as that of diamond or graphite. It would be interesting to know whether this network of bonds is compatible with the crystal structures assigned to silica in its various forms, since it appears *a priori* that such a network would be far more likely than a mere aggregate of ions to give rise to the complex polymorphism which is actually observed.

In conclusion, attention may be redirected to the formulæ assigned in the first paper of this series to the carbonate, nitrate, sulphate, and silicate ions



These formulæ, in which charged atoms are united by bonds, have the merit of satisfying the conditions of crystal-symmetry better than the traditional chemical formulæ



although the latter may perhaps represent more accurately the structure of the ions in solution when removed from the influence of the symmetrically-placed kations of the crystal. At the same time they avoid the difficulties, both chemical and physical, which arise from the attempt

to represent all these anions as metallic kations,  $\text{C}^{++++}$   
 $\text{N}^{++++}$   $\text{S}^{++++}$  and  $\text{Si}^{++++}$ , surrounded by a surplus of  
oxide ions  $\text{O}^-$ . In particular, the formulæ for the nitrate

and carbonate ions, whilst conforming strictly to the crystal-symmetry of calcite and of sodium nitrate, enable us to avoid the illogical conclusion that the real bonds of carbonic anhydride and of the oxides of nitrogen disappear completely in the carbonates and nitrates.

### *Summary.*

On etching natural crystals of sylvine with a strong solution of potassium chloride unsymmetrical pyramids were sometimes formed by the flotation of detached fragments, but on artificial crystals the etch-figures were always symmetrical, even in presence of optically-active impurities. There are therefore no trustworthy crystallographic data which can be used as evidence of a lower order of symmetry than that deduced from X-ray analysis, or as a proof of the existence of bonds between individual atoms of potassium and of chlorine. The ionic structure assigned to sylvine is also in harmony with the high conductivity of the fused salt.

On the other hand, objection is taken to the view that crystals of ice and quartz, and the anions of oxygenated acids in crystals such as calcite and barytes, are mere aggregates of oxide ions  $\bar{\bar{O}}$  with kations such as  $\overset{+}{H}$ ,  $\overset{++++}{C}$ ,  $\overset{++++}{Si}$ ,  $\overset{++++}{N}$ , and  $\overset{+++++}{S}$ . Thus the formation of ice is more likely to be a process of polymerization in which additional bonds are formed than a process of ionization in which all the bonds between the atoms are destroyed: a network of single bonds between quadrivalent oxygen and bivalent hydrogen is therefore postulated. In the same way it is suggested that the oxygen atoms in the carbonate, nitrate, sulphate, and silicate ions are linked to the central atom by single bonds, and therefore carry only single negative charges. A network of single bonds is also postulated in quartz, but in this case the atoms of quadrivalent silicon and bivalent oxygen would be electrically neutral.

One of us (M. A. V.) is indebted to the London County Council for a scholarship held during the period in which this work was carried out.

University Chemical Laboratory,  
Cambridge.

XXIV. *Some Problems in the Conduction of Heat.* By  
 GEORGE GREEN, D.Sc., *Lecturer in Physics in the Applied  
 Physics Department of the University of Glasgow* \*.

IN two previous communications † relating to the subject of heat conduction illustrations have been given of the method of solving problems by means of wave-trains. In these earlier papers the main purpose in view was to develop the fundamental solutions which generally form the basis from which we derive or build up the solution of particular problems, the application of the method to important or difficult problems being left to a later opportunity. The method is useful in all cases of plane, spherical, or cylindrical heat distributions, and it has the advantage that the mathematical solutions are arrived at by direct application of the familiar physical ideas associated with the transmission of a wave-train across a boundary or with its reflexion from the boundary. In addition, the normal coordinates, which are in general required for the solution of problems in which the conduction of heat in a limited portion of matter is under consideration, and are obtained usually by a separate investigation, are derived in the natural course of application of this method. The particular form which they take in each special case becomes evident when the boundary conditions are applied to each constituent wave-train of a given frequency, as we shall see in the special cases treated below. In the present paper the main purpose in view is to demonstrate the suitability of the method and to show its power in the treatment of problems of considerable interest and difficulty. The problems chosen for this purpose have in most cases, though not in all, been solved already by other methods, so that the relative values of the two methods of solution of heat-conduction problems can be readily determined.

The equation of heat conduction in a uniform medium may be written in the form

$$\frac{\partial v}{\partial t} = \kappa \nabla^2(v), \quad \dots \dots \dots (1)$$

where  $\kappa = K/c\rho$ ;  $v$ ,  $K$ ,  $c$ ,  $\rho$  being temperature, conductivity, specific heat, and density respectively. This equation, in one form or other, together with equations representing

\* Communicated by the Author.

† *Phil. Mag.* iii. Suppl. pp. 784-800 (April 1927): pp. 701-720 (April 1928).



special boundary conditions, has to be satisfied in all cases to be considered. As the first problem to be examined we take that of determining the temperature in a finite rod of length  $a$ , having an initial temperature distribution given by  $f(x)$ , and under a condition at the boundaries  $x=0$  and  $x=a$ , which may be that radiation takes place there to a medium at zero temperature, or that the temperature there is maintained at zero, or any similar condition. To solve this problem we start from the solution representing a plane periodic heat source  $qe^{ikx}$  situated at plane  $x=x_1$  within the medium, given in the usual notation by

$$v = \frac{q}{2K\sqrt{\frac{ik}{\kappa}}} e^{ikt-(x-x_1)\sqrt{\frac{ik}{\kappa}}} \quad \text{for } x > x_1, \quad (2)$$

$$v = \frac{q}{2K\sqrt{\frac{ik}{\kappa}}} e^{ikt-(x_1-x)\sqrt{\frac{ik}{\kappa}}} \quad \text{for } x_1 > x. \quad (2')$$

The first represents a positive wave-train supplying  $\frac{1}{2}qe^{ikt}$  heat units per unit area at  $x=x_1$  in the positive direction of  $x$  from  $x_1$ , and the second represents a negative wave-train supplying an equal amount in the negative direction from  $x_1$ . Follow now the positive train alone. At  $x=a$  some boundary condition (such as  $v=0$ ) has to be fulfilled, and as the above train alone violates this condition, it must give rise to a reflected wave-train, so that, instead of a single positive train (2), we require

$$v = \rho e^{ikt-(x-x_1)\sqrt{\frac{ik}{\kappa}}} + A\rho e^{ikt-(2a-x_1-x)\sqrt{\frac{ik}{\kappa}}}, \quad \dots \quad (3)$$

in which we have written  $\rho$  instead of  $\frac{q}{2K\sqrt{\frac{ik}{\kappa}}}$ , and  $i\lambda$  instead of  $\sqrt{\frac{ik}{\kappa}}$ . The additional term now appearing

represents the negative wave-train reflected from boundary  $x=a$ ,  $A$  being an operator or boundary coefficient whose value remains to be determined by the special boundary condition chosen. The reflected wave-train is also to be regarded as the continuation within the medium of the original wave-train as modified and redirected by the boundary. The negative wave-train introduced above in turn fails to satisfy the required boundary condition at  $x=0$ , and in turn gives rise to a reflected wave-train in the positive

direction of  $x$ . To include the effect of this second reflexion, the original positive train is now to be accompanied by two wave-trains, which are its continuations within the medium, so that from (3) we pass to

$$v = \rho e^{ikt-(x-x_1)i\lambda} + A\rho e^{ikt-(2a-x_1-x)i\lambda} + A^2\rho e^{ikt-(2a-x_1+x)i\lambda}. \quad (4)$$

The phase of each wave-train agrees with the phase of the corresponding reflected wave-train at the boundary at which reflexion takes place; thus in the above cases we have

$$x-x_1 = 2a-x_1-x \quad \text{at } x=a,$$

and

$$2a-x_1-x = 2a-x_1+x \quad \text{at } x=0.$$

At each boundary a continuing wave-train arises, and an additional term is required to represent its effect within the medium. The complete wave-system arising from the original positive wave-train by successive reflexions at boundaries  $x=a$  and  $x=0$  respectively is represented by

$$\begin{aligned} v_1 = & \rho e^{ikt-(x-x_1)i\lambda} \{1 + A^2 e^{-2a i\lambda} + A^4 e^{-4a i\lambda} + A^6 e^{-6a i\lambda} + \text{etc.}\} \\ & + A\rho e^{ikt-(2a-x_1-x)i\lambda} \{1 + A^2 e^{-2a i\lambda} + A^4 e^{-4a i\lambda} + A^6 e^{-6a i\lambda} + \text{etc.}\}. \end{aligned} \quad (5)$$

In a similar manner we find that the complete wave-system arising from the original negative wave-train by successive reflexions at boundaries  $x=0$  and  $x=a$  respectively is represented by

$$v_2 = \{\rho e^{ikt-(x_1-x)i\lambda} + A\rho e^{ikt-(x_1+x)i\lambda}\} \left\{ \frac{1}{1-A^2 e^{-2a i\lambda}} \right\}, \quad (6)$$

in which we have inserted the sum of the geometric series appearing in (5). The sum of the two expressions contained in (5) and (6) represents the temperature at any point  $x$  at instant  $t$  due to a periodic source  $qe^{ikt}$  situated at  $x_1$ , the boundaries  $x=0$  and  $x=a$  being subject to some definite condition which determines the value of the coefficient  $A$ . The temperature at time  $t$  at any point  $x$  due to an instantaneous surface source  $q$  initially at  $x_1$ , subject to the same boundary conditions, is obtained directly from the above results by an integration indicated by

$$v = \frac{1}{\pi} \int_0^\infty dk (v_1 + v_2). \quad (7)$$

When we make use of the transformation

$$\sqrt{\frac{ik}{\kappa}} = i\lambda$$

throughout, and combine corresponding terms in  $v_1$  and  $v_2$ , it will readily be found that (7) becomes

$$v = \frac{q\kappa}{K\pi} \int_0^\infty d\lambda e^{-\kappa\lambda z} \{ \cos(x-x_1)\lambda + Ae^{-ai\lambda} \cos(a-x-x_1)\lambda \} \\ \times \frac{1}{1-A^2e^{-2ai\lambda}} \quad \dots \quad (8)$$

This is essentially the solution we require in integral form, including all possible values of  $A$ . The evaluation of the integral appearing in (8) can most directly be carried out by contour integration, the path of integration with respect to  $\lambda$  being along axes inclined at  $45^\circ$  to the real axis of  $\lambda$ , and along two circular arcs connecting these axes at infinity.

We have now to assign definite values to  $A$  in accordance with the particular conditions of reflexion of each wave-train at the boundaries of the medium. If the wave-trains are reflected under the condition that at the boundaries the temperature is maintained at zero ( $v=0$  at  $x=0$  and  $x=a$ ), then  $A=-1$ : and the positive roots of  $1-e^{-2ai\lambda}=0$  are at the values of  $\lambda$  given by  $a\lambda=0, \pi, 2\pi, 3\pi$ , etc. For all such values of  $\lambda$  we have also

$$\frac{d}{d\lambda} \{1-e^{-2ai\lambda}\} = 2ai,$$

and accordingly, by means of the theorem of residues, the evaluation of (8) is given by

$$v = \frac{q\kappa}{Ka} \sum_1^\infty e^{-\kappa\lambda z} \{ \cos(x-x_1)\lambda - \cos(x+x_1)\lambda \} \\ \text{where } a\lambda=0, \pi, 2\pi, \text{ etc.} \\ = \frac{2q\kappa}{Ka} \sum_1^\infty e^{-\kappa\left(\frac{n\pi}{a}\right)z} \sin \frac{n\pi}{a} x \sin \frac{n\pi}{a} x_1, \quad \dots \quad (9)$$

the summation extending to all values of  $n$ , in agreement with the well-known result. If, on the other hand, the wave-trains are reflected at the boundaries under the condition that radiation takes place there into a medium at zero temperature

$$\left\{ -K \frac{\partial v}{\partial x} = hv \right\},$$

then

$$A = \frac{iK\lambda - h}{iK\lambda + h},$$

and the roots of the equation

$$1-A^2e^{-2ai\lambda} = 0$$

are identical with the roots of the equation

$$\tan a\lambda = \frac{2K\lambda}{K^2\lambda^2 - h^2} \cdot \cdot \cdot \cdot \cdot \quad (10)$$

Moreover, corresponding to each value of  $\lambda$  given by the roots of (10), we have

$$\frac{d}{d\lambda} \{e^{a\lambda} - A\} = - \frac{i\{a(K^2\lambda^2 + h^2) + 2Kh\}}{(iK\lambda + h)^2}, \quad \cdot \quad (11)$$

and we can find readily from these results, by applying the residue theorem, that the evaluation of (8) is now given by

$$v = \frac{q\kappa}{K} \sum e^{-\kappa\lambda^2 t} \{ \cos(x - x_1)\lambda + \cos(a - x - x_1)\lambda \} \\ \times \frac{K^2\lambda^2 + h^2}{a(K^2\lambda^2 + h^2) + 2Kh}, \quad \cdot \quad (12)$$

the summation extending to all the roots of (10) above. Since we can put

$$\cos a\lambda = \frac{K^2\lambda^2 - h^2}{K^2\lambda^2 + h^2} \quad \text{and} \quad \sin a\lambda = \frac{2Kh\lambda}{K^2\lambda^2 + h^2},$$

it can easily be verified that the above result is equivalent to

$$v = \frac{2q\kappa}{K} \sum_1^\infty e^{-\kappa\lambda^2 t} \\ \times \frac{(K\lambda \cos x\lambda + h \sin x\lambda)(K\lambda \cos x_1\lambda + h \sin x_1\lambda)}{a(K^2\lambda^2 + h^2) + 2Kh}, \quad (13)$$

which is also in agreement with a known result. If in the above results we put  $q=1$ , these solutions, (9) and (13), then are Green's Functions corresponding each to a special boundary condition. From the above treatment it is evident that the method employed is perfectly general, being applicable to any arbitrary boundary conditions. To return to the problem stated at the outset, we have merely to replace  $q$  in (9) and (13) by  $f(x_1) dx_1$ , and integrate with respect to  $x_1$  from  $x_1=0$  to  $x_1=a$ , and so obtain the temperature at  $x$  at instant  $t$  due to an initial arbitrary heat distribution in the material.

Consider next the problem of determining the temperature at any point within a sphere of radius  $a$ , having an initial temperature distribution represented by  $v=f(r)$ , and subject to a boundary condition at surface  $r=a$  which can be specified later. The investigation proceeds along exactly

the same lines as in the problem treated above. That is, we start from the solution representing a periodic heat source  $qe^{ikt}$  per unit area, situated at any surface  $r=r_1$  within the sphere, namely,

$$v = \frac{qr_1}{2Kr\sqrt{\frac{ik}{\kappa}}} e^{ikt-(r-r_1)\sqrt{\frac{ik}{\kappa}}} = \rho e^{ikt-(r-r_1)i\lambda} \quad r > r_1, \quad (14)$$

$$v = \rho e^{ikt-(r_1-r)i\lambda} \quad \dots \dots \dots r < r_1. \quad (14')$$

The first part of the solution represents a positive wave-train supplying  $\frac{1}{2}qe^{ikt}$  heat units per unit of area at  $r_1$ , and the second part represents a negative wave-train supplying an equal quantity of heat in the opposite direction from  $r_1$ . Consider the positive train alone. After one reflexion at the boundary  $r=a$ , the effect of the original train and its continuation is given by

$$\rho e^{ikt-(r-r_1)i\lambda} + A\rho e^{ikt-(2a-r_1-r)i\lambda}, \quad \dots \quad (15)$$

the additional train being the negative wave-train reflected from the boundary  $r=a$ , and agreeing in phase with the original wave-train at  $r=a$ . As we have pointed out in an earlier paper, each negative wave-train must, after passing through the origin, continue as a positive train; hence from (15) we pass to

$$\rho e^{ikt-(r-r_1)i\lambda} + A\rho e^{ikt-(2a-r_1-r)i\lambda} - A\rho e^{ikt-(2a-r_1+r)i\lambda}, \quad (16)$$

in which the new wave-train appearing is a positive train. The process is repeated by each successive positive train, so that we can write down at once the wave-system within the sphere arising from the original positive wave-train in the form

$$\rho e^{ikt+r_1i\lambda} \{e^{-r_1i\lambda} + 2i \sin \lambda r \cdot A e^{-2ai\lambda} (1 - A e^{-2ai\lambda} + A^2 e^{-4ai\lambda} - \text{etc.})\}. \quad \dots \quad (17)$$

The corresponding expression for the complete wave-system arising from the original negative wave-train is given by

$$v_2 = 2i \sin \lambda r \rho e^{ikt-r_1i\lambda} \{1 - A e^{-2ai\lambda} + A^2 e^{-4ai\lambda} - \text{etc.}\}. \quad (18)$$

In these, (17) and (18), it is evident that the trains are arranged in pairs according to powers of  $A$ , a positive and a negative together, in order to fulfil the conditions required at the origin that the temperature there is finite. The original positive train alone, represented by the first term of

(17), violates this condition, and we have accordingly to bring this term into conformity with the condition by introducing the corresponding negative train. This means that instead of (17), which is incomplete, we write the complete wave-system arising from the original positive wave-train in the form

$$v_1 = -2i \sin \lambda r \rho e^{i k t + r_1 i \lambda} \cdot \frac{1}{1 + A e^{-2 a i \lambda}} \cdot \cdot \cdot \quad (19)$$

Just as we found in the previous problem, the sum of the two expressions contained in (18) and (19) represents the temperature at  $r$  at instant  $t$  due to a periodic source  $q e^{i k t}$  per unit area situated at  $r_1$ : and from this, by an integration with respect to  $k$ , indicated by (7) above, we find the temperature at  $r$  at instant  $t$  due to an instantaneous surface source  $q$  per unit area situated at  $r = r_1$  in the form

$$v = \frac{4 q \kappa r_1}{K r \pi} \int_0^{\infty} d\lambda e^{-\kappa \lambda^2 t} \frac{\sin \lambda r \sin \lambda r_1}{1 + A e^{-2 a i \lambda}} \cdot \cdot \cdot \quad (20)$$

Taking  $A = -1$ , as before, corresponding to the condition that the surface of the sphere  $r = a$  is maintained at zero, we find that the poles of the integrand are again given by  $a \lambda = 0, \pi, 2\pi, \dots n\pi$ , etc. The evaluation of the integral required is again effected by contour integration along the path, consisting of the two axes inclined to the real axis of  $\lambda$  at angles of  $45^\circ$ , connected by a circular arc at infinity. The result obtained by means of the Residue theorem is

$$v = \frac{2 q \kappa r_1}{K r} \sum_1^{\infty} e^{-\kappa \lambda^2 t} \sin \lambda r \sin \lambda r_1, \cdot \cdot \cdot \quad (21)$$

where  $\lambda = n\pi/a$ , and the summation extends to all values of  $n$ .

Taking

$$A = \left\{ i\lambda - \left( \frac{1}{a} + \frac{h}{K} \right) \right\} / \left\{ i\lambda - \left( \frac{1}{a} - \frac{h}{K} \right) \right\},$$

corresponding to the condition that radiation takes place at surface  $r = a$  into a medium at zero temperature, we find that the poles of the integrand are at values of  $\lambda$  given by the roots of the equation

$$\tan 2a\lambda = - \frac{2\lambda \left( \frac{h}{K} - \frac{1}{a} \right)}{\left\{ \left( \frac{h}{K} - \frac{1}{a} \right)^2 - \lambda^2 \right\}} \quad \text{or} \quad \tan a\lambda = - \frac{\lambda}{\left( \frac{h}{K} - \frac{1}{a} \right)} \cdot \cdot \cdot \quad (22)$$

At each value of  $\lambda$  given by (22) we find that

$$\frac{d}{d\lambda} \{e^{2i\lambda} + A\} = i \left[ 2a \left\{ \lambda^2 + \left( \frac{h}{K} - \frac{1}{a} \right)^2 \right\} + 2 \left( \frac{h}{K} - \frac{1}{a} \right) \right] / \left\{ i\lambda + \left( \frac{h}{K} - \frac{1}{a} \right) \right\}^2, \quad \dots (23)$$

and accordingly, by means of the theorem of Residues, we find that the evaluation of (20) is given by

$$v = \frac{2q\kappa r_1}{Kra} \sum_1^{\infty} e^{-\kappa\lambda^2 t} \sin \lambda r \sin \lambda r_1 \times \frac{K^2 a^2 \lambda^2 + (ah - K)^2}{\{K^2 a^2 \lambda^2 + (ah - K)^2 + Ka(ah - K)\}}, \quad (24)$$

the summation extending to all the roots of (22) above. It will be seen that the results arrived at in (21) and (24) are in agreement with known results. To obtain the solution corresponding to an initial heat distribution throughout the sphere, we have merely to replace  $q$  by  $f(r_1)dr_1$  and integrate with respect to  $r_1$  from 0 to  $a$ .

As a further application of the same method we take the case of a sphere of one material enclosed within another material bounded also by a concentric spherical surface, the whole having an initial temperature distribution  $f(r)$ , and, as before, subject to any specified condition at the outer boundary of the outer material. We take  $K_1, \kappa_1$  to refer to the inner material bounded by the surface  $r=a$ , and  $K_2, \kappa_2$  to refer to the outer material bounded by the surfaces  $r=a$  and  $r=b$ . The complete solution aimed at consists of four parts. Starting with a periodic heat source  $qe^{ikt}$  situated at  $r_1$  within medium 1, we require the temperature at each instant ( $a$ ) at any point  $r$  within medium 1, and ( $b$ ) at any point  $r$  within medium 2. Similarly, starting with a periodic heat source  $q'e^{ikt}$  situated at  $r_1$  within medium 2, we require the temperature at each instant ( $a$ ) at any point  $r$  within medium 2, and ( $b$ ) at any point  $r$  within medium 1. Taking first the case of a source at  $r_1$  in medium 1, we build up our solution from two initial wave-trains corresponding exactly to (14) and (14') above. If we introduce the necessary modifications in our notation indicated by

$$\left. \begin{aligned} \rho_1 &= \frac{r_1}{2K_1 r} \sqrt{\frac{ik}{\kappa_1}}; & \rho_2 &= \frac{r_1}{2K_2 r} \sqrt{\frac{ik}{\kappa_2}}; \\ i\lambda &= \sqrt{\frac{ik}{\kappa_1}}; & \mu i\lambda &= \sqrt{\frac{ik}{\kappa_2}}, \end{aligned} \right\} \quad (25)$$

the expression representing the wave-system which arises from the two fundamental wave-trains within medium 1 by successive reflexions at the boundary  $r=a$  is identical with the sum of (18) and (19) above, already included in (20), namely,

$$v_1 = 4q\rho_1 e^{ikt} \sin \lambda r \sin \lambda r_1 \frac{1}{1 + A e^{-2a\lambda}} \quad \dots (26)$$

This gives the primary effect of the source at  $r_1$  at any point  $r$  within medium 1 itself.

### *First Effects Transmitted into Medium 2.*

This effect is produced, as we have seen, by the group of positive trains

$$q\rho_1 e^{ikt} \{e^{-(r-r_1)\lambda} - e^{-(r+r_1)\lambda}\} \frac{1}{1 + A e^{-2a\lambda}}, \quad \dots (27)$$

accompanied by the corresponding group of negative trains reflected from boundary  $r=a$ . Each of these positive wave-trains transmits a continuing wave-train into medium 2. For example, let

$$v_1 = q\rho_1 e^{ikt-(r-r_1)\lambda} + A q\rho_1 e^{ikt-(2a-r_1-r)\lambda} \quad \dots (28)$$

represent a positive train and the reflected train at boundary  $r=a$ , and let

$$v_2 = A' q\rho_2 e^{ikt-(a-r_1)\lambda-\mu(r-a)\lambda} \quad \dots (29)$$

represent the corresponding continuing wave-train transmitted into medium 2, then the two boundary coefficients  $A$  and  $A'$  are to be determined by the conditions

$$v_1 = v_2 \quad \text{and} \quad K_1 \frac{\partial v_1}{\partial r} = K_2 \frac{\partial v_2}{\partial r} \quad \text{at} \quad r = a. \quad \dots (30)$$

Their values will be given later. Meantime we see from the above that the first group of wave-trains transmitted from medium 1 into medium 2 is represented by

$$\left. \begin{aligned} & A' q\rho_2 e^{ikt-\mu(r-a)\lambda} \{e^{-(a-r_1)\lambda} - e^{-(a+r_1)\lambda}\} \frac{1}{1 + A e^{-2a\lambda}} \\ \text{or} & \quad \alpha' e^{-\mu(r-a)\lambda} \end{aligned} \right\} \quad (31)$$

This group of wave-trains, being positive, first undergoes reflexion at  $r=b$ , and then is partly reflected and partly transmitted into medium 1 at boundary  $r=a$ . Through successive reflexions at boundaries  $b$  and  $a$  the wave-system



in medium 2 is built up. Taking the boundary coefficient for reflexion at  $b$  as  $B$ , and that for reflexion at  $a$  as  $C'$ , we can represent the original wave-group in medium 2 and its continuations by

$$\left. \begin{array}{ll} \alpha' e^{-\mu(r-a)i\lambda} & \text{followed by} \quad B \alpha' e^{-\mu(2b-a-r)i\lambda}, \\ BC' \alpha' e^{-\mu(2b-3a+r)i\lambda} & ,, ,, \quad B^2 C' \alpha' e^{-\mu(4b-3a-r)i\lambda}, \\ B^2 C'^2 \alpha' e^{-\mu(4b-5a+r)i\lambda} & ,, ,, \quad B^3 C'^2 \alpha' e^{-\mu(6b-5a-r)i\lambda}, \end{array} \right\} (32)$$

and so on, the successive positive waves being given in the left-hand column and the successive negative waves in the right-hand column. The summations of the positive and negative waves are given by

$$\alpha' e^{-\mu(r-a)i\lambda} / (1 - BC' e^{-2\mu(b-a)i\lambda}) \dots (33)$$

and

$$B \alpha' e^{-\mu(2b-a-r)i\lambda} / (1 - BC' e^{-2\mu(b-a)i\lambda}) \dots (33')$$

respectively. By combining these we obtain the complete effect at  $r$  in medium 2 of the first transmission into medium 2 from medium 1 in the form

$$V_1 = 2iq\rho_2 e^{ikt - \{a + \mu(b-a)\}i\lambda} \sin \lambda r_1 \{e^{\mu(b-r)i\lambda} + B e^{-\mu(b-r)i\lambda}\} \cdot A' S_1 S_2, \quad (34)$$

where

$$S_1 = 1/\{1 + A e^{-2ai\lambda}\} \quad \text{and} \quad S_2 = 1/\{1 - BC' e^{-2\mu(b-a)i\lambda}\}. \quad (35)$$

### *First Effects Retransmitted into Medium 1.*

Consider now the group of negative wave-trains (33') forming part of the wave-system (34) in medium 2. Each negative wave-train, on reaching boundary  $r=a$ , transmits a negative train into medium 1. For example, with  $C$  as boundary coefficient for transmission from medium 2 into medium 1, the negative train  $\rho_2 e^{-\mu(2b-a-r)i\lambda}$  in medium 2 continues into medium 1 as the train represented by

$$C \rho_1 e^{-\mu(2b-2a)i\lambda - (a-r)i\lambda}.$$

We accordingly represent the first negative wave-system returning into medium 1 by

$$q \rho_1 e^{ikt - 2\{a + \mu(b-a)\}i\lambda + r_1 i\lambda} \{e^{r_1 i\lambda} - e^{-r_1 i\lambda}\} \cdot A' BC S_1 S_2. \quad (36)$$

These trains, being negative, continue their course through the origin, and thereafter become positive trains represented by

$$-q \rho_1 e^{ikt - 2\{a + \mu(b-a)\}i\lambda - r_1 i\lambda} \{e^{r_1 i\lambda} - e^{-r_1 i\lambda}\} \cdot A' BC S_1 S_2, \quad (37)$$

and as they continue their course by multiple reflexions at boundary  $r=a$ , in exactly the manner worked out in the case of the original positive train (14), they build up within medium 1 the system

$$v_2 = -4q\rho_1 e^{ikt} \sin \lambda r \sin \lambda r_1 \cdot e^{-2\{a+\mu(b-a)\}i\lambda} \cdot A'BC S_1^2 S_2, \quad (38)$$

which represents the first secondary effect of the source at  $r_1$  at any point  $r$  within medium 1 itself, the primary effect being given by  $v_1$  in (26) above. We can evidently rewrite (38) in the form

$$v_2 = -\alpha v_1, \quad \text{where } \alpha = e^{-2\{a+\mu(b-a)\}i\lambda} \cdot A'BC S_1 S_2. \quad (39)$$

The process described above for the trains represented by  $v_1$  is now repeated by the trains represented by  $v_2$ . The positive trains included in  $v_2$ , given in (38), again transmit wave-trains into medium 2, where they in turn build up a wave-system whose total effect is given by  $V_2$ , where  $V_2 = -\alpha V_1$ ,  $V_1$  being given by (34). The corresponding return wave-system contributes the second secondary effect, or the third actual effect, of the source at  $r_1$  to the total effect at any point  $r$  in medium 1. Denoting this by  $v_3$ , we have

$$\left. \begin{aligned} \text{and similarly} \quad v_3 &= -\alpha v_2 = \alpha^2 v_1, \\ V_3 &= -\alpha V_2 = \alpha^2 V_1, \\ &\text{and so on.} \end{aligned} \right\} \quad \cdot \cdot \cdot \quad (40)$$

The coefficient  $\alpha$  can be used, like the other coefficients, simply as an operator. The summation of all the terms  $v_1, v_2, v_3$ , etc. (and also that of the terms  $V_1, V_2, V_3$ , etc.) is now a simple matter. If we put

$$S = 1 - \alpha + \alpha^2 - \alpha^3 + \text{etc.},$$

we can now write down the total effect at  $r$  in medium 1 due to a source  $qe^{ikt}$  situated at  $r_1$  in medium 1 in the form

$$v = 4q\rho_1 e^{ikt} \sin \lambda r \sin \lambda r_1 S_1 S, \quad S = 1/(1+\alpha), \quad (41)$$

and the total effect at  $r$  in medium 2, due to the same source at  $r_1$  in medium 1, in the form

$$v = 2iq\rho_2 e^{ikt - \{a+\mu(b-a)\}i\lambda} \sin \lambda r_1 \{e^{\mu(b-r)i\lambda} + B e^{-\mu(b-r)i\lambda}\} A' S_1 S_2 S. \quad \cdot \cdot \cdot \quad (42)$$

These results contain the solutions required in the case of a periodic source  $qe^{ikt}$  situated at  $r_1$  in medium 1. The corresponding results representing the effects of a periodic source  $q'e^{ikt}$  situated at  $r_1$  in medium 2 can be obtained by exactly the same process from the initial trains

$$q'\rho_2 e^{-\mu(r-r_1)i\lambda} \quad \text{and} \quad q'\rho_2 e^{ikt-\mu(r_1-r)i\lambda}. \quad (43)$$

These wave-trains are to be regarded as continuing after reflexions at boundaries  $r=b$  and  $r=a$  respectively. The original trains and their first three or four continuations in medium 2 are indicated in order in the vertical columns:—

$$\left\{ \begin{array}{l} q'\rho_2 e^{ikt-\mu(r-r_1)i\lambda}, \\ Bq'\rho_2 e^{ikt-\mu(2b-r_1-r)i\lambda}, \\ BC'q'\rho_2 e^{ikt-\mu(2b-2a-r_1+r)i\lambda}, \\ B^2C'q'\rho_2 e^{ikt-\mu(4b-2a-r_1-r)i\lambda}, \end{array} \right\} \quad \left\{ \begin{array}{l} q'\rho_2 e^{ikt-\mu(r_1-r)i\lambda}, \\ C'q'\rho_2 e^{ikt-\mu r_1+(r-2a)i\lambda}, \\ BC'q'\rho_2 e^{ikt-\mu(2b-2a+r_1-r)i\lambda}, \\ BC'^2q'\rho_2 e^{ikt-\mu(2b-4a+r_1+r)i\lambda}, \end{array} \right\} \quad (44)$$

and so on, B being boundary coefficient determined by the conditions to be fulfilled at  $r=b$ , and C' being boundary coefficient for wave-trains reflected into medium 2 at  $r=a$ . Each positive wave-train in the above system, after reaching boundary  $r=b$ , continues as a negative train; hence the above wave-trains occur in pairs, each pair consisting of a positive followed by a negative wave-train, which together satisfy the boundary condition at  $r=b$ . The original negative wave-train  $q'\rho_2 e^{ikt-\mu(r_1-r)i\lambda}$  alone violates this condition. As before, in the case of the first term of (17), to bring the anomalous term into conformity with the condition required at  $r=b$ , the corresponding positive term must therefore be introduced at the top of the right-hand column above, namely,

$$\frac{q'\rho_2}{B} e^{ikt+\mu(2b-r_1-r)i\lambda}.$$

The summation of the above terms then gives the complete primary effect produced in medium 2 by a periodic source situated at  $r_1$  in medium 2, the result obtained being given by

$$q'\rho_2 e^{ikt} \{ e^{-\mu(b-r_1)i\lambda} + (1/B)e^{\mu(b-r_1)i\lambda} \} \{ e^{\mu(b-r)i\lambda} + Be^{-\mu(b-r)i\lambda} \} S_2. \quad (45)$$

Each negative wave-train contained in the above wave-system transmits a wave-train into medium 1, and secondary

effects are produced in medium 2 by wave-trains retransmitted from medium 1. The process has been explained above, and we need only write down here the final result, representing the complete effect at  $r$  in medium 2, due to a periodic source  $q'e^{ikt}$  situated at  $r_1$  in medium 2, in the form

$$v = q' \rho_2 e^{ikt} \{ e^{-\mu(b-r_1)i\lambda} + (1/B) e^{\mu(b-r_1)i\lambda} \} \{ e^{\mu(b-r)i\lambda} + B e^{-\mu(b-r)i\lambda} \} S_2 S_1 \quad (46)$$

Similarly the complete effect at  $r$  in medium 1, due to a periodic source  $q'e^{ikt}$  situated at  $r_1$  in medium 2, may be written in the form

$$v = 2iq' \rho_1 e^{ikt} \{ a + \mu(b-a)i\lambda \sin \lambda r \{ e^{\mu(b-r_1)i\lambda} + B e^{-\mu(b-r_1)i\lambda} \} C S_1 S_2 S_1 \quad (47)$$

where  $C$  is the boundary coefficient for wave-trains transmitted from medium 2 into medium 1 at  $r=a$ . To determine  $C$  and  $C'$ , we put

$$v_2 = q' \rho_2 e^{ikt - \mu(r_1-r)i\lambda} + C' q' \rho_2 e^{ikt - (r_1+r-2a)i\lambda} \quad (48)$$

to represent a negative train and its continuation by reflexion at  $r=a$  in medium 2, and

$$v_1 = C q' \rho_1 e^{ikt - \mu(r_1-a)i\lambda - (a-r)i\lambda} \quad (49)$$

to represent its continuation into medium 1, and apply to  $v_1$  and  $v_2$  the conditions expressed in (30) above: the same conditions used to determine  $A$  and  $A'$ . The expression (47) and the earlier expression (42) are reciprocal, as we shall see from the evaluations of the constants  $C$  and  $A$  given later. Each expression is converted into the other by the simple interchange of  $r_1$  and  $r$ , excepting, of course, where  $r_1$  and  $r$  appear in  $\rho_1$  and  $\rho_2$ .

Our system of results contained in (41), (42), (46), (47) is now complete so far as periodic sources in medium 1 and medium 2, enclosed within finite boundaries, are concerned. To arrive at the corresponding results for instantaneous sources  $q_1$  and  $q'$ , we have to evaluate two integrals of the

form  $\frac{1}{\pi} \int_0^\infty dk v$  for any point  $r$  in medium 1, and two corresponding integrals for any point  $r$  in medium 2. For the effect at  $r$  in medium 1 of an instantaneous source  $q$  per unit area at surface  $r=r_1$  also in medium 1, we have from (41) above,

$$v = \frac{4q\kappa_1 r_1}{\pi K_1 r} \int_0^\infty d\lambda \sin \lambda r_1 \sin \lambda r e^{-\kappa_1 \lambda^2} \cdot \frac{1 - BC'e^{-2\mu(b-a)i\lambda}}{D} \quad (50)$$

For the effect at  $r$  in medium 1 of an instantaneous source  $q'$  per unit area at surface  $r=r_1$  in medium 2, we find from (47)

$$v = \frac{2iq'\kappa_1 r_1}{\pi K_1 r} \int_0^\infty d\lambda \sin \lambda r e^{-\kappa_1 \lambda^2 t - \{a + \mu(b-a)\}i\lambda} \cdot \{e^{\mu(b-r_1)i\lambda} + B e^{-\mu(b-r_1)i\lambda}\} \cdot \frac{C}{D}. \quad (51)$$

For the effect at  $r$  in medium 2 of an instantaneous source  $q'$  per unit area at surface  $r=r_1$  also in medium 2, we find from (46)

$$v = \frac{4q'\kappa_2 r_1 \mu}{\pi K_2 r} \int_0^\infty d\lambda e^{-\kappa_1 \lambda^2 t} \{ (1/B) e^{\mu(b-r_1)i\lambda} + e^{-\mu(b-r_1)i\lambda} \} \cdot \{ e^{\mu(b-r)i\lambda} + B e^{-\mu(b-r)i\lambda} \} \frac{1 + A e^{-2ai\lambda}}{D}, \quad (52)$$

and for the effect at  $r$  in medium 2 of an instantaneous source  $q$  per unit area at surface  $r=r_1$  in medium 1, we find from (42)

$$v = \frac{2iq\kappa_2 r_1 \mu}{\pi K_2 r} \int_0^\infty d\lambda \sin \lambda r_1 e^{-\kappa_1 \lambda^2 t - \{a + \mu(b-a)\}i\lambda} \cdot \{ e^{\mu(b-r)i\lambda} + B e^{-\mu(b-r)i\lambda} \} \cdot \frac{A'}{D}. \quad (53)$$

In each of the above integrals the value of  $D$  is given by

$$D = (1 + A e^{-2ai\lambda}) (1 - B C' e^{-2\mu(b-a)i\lambda}) + A' B C e^{-2\{a + \mu(b-a)\}i\lambda} \\ = \frac{1}{S_1 S_2 S}. \quad (54)$$

The conditions determining the four coefficients  $A, A', C, C'$ , have already been given. The four integrals (50), (51), (52), (53) contain the solutions to a number of different problems according to the values assigned to the boundary coefficient  $B$ . When  $B$  has the value  $-1$ , the solutions apply to the case where an initial heat source exists at  $r_1$ , either in medium 1 or medium 2, while the boundary  $r=b$  is maintained at zero temperature. When  $B$  is given the value

$$\frac{a\lambda + \left(\frac{1}{b} - \frac{h}{K_2}\right)}{i\mu\lambda - \left(\frac{1}{b} - \frac{h}{K_2}\right)},$$

the solutions apply to the case where an initial heat source occurs at  $r_1$ , while radiation takes place at boundary  $r=b$  into a medium kept at zero-temperature. When we put  $B=0$ , and make  $b$  infinitely large, the solutions above can be modified to apply to the case of a sphere of radius  $a$  surrounded by a medium of different material extending to infinity, but in this case the solutions are more readily obtained by a direct application of the method employed in the present paper, particularly in the case corresponding to (52), where the initial source is in the outer medium. The solutions for the case of an initial source at  $r_1$  in medium 1, the outer medium extending to infinity, are obtained from (50) and (53) above by simply putting  $B=0$  in both.

To enable us to carry out the evaluation of the four main integrals constituting the solutions of certain problems, we require now the values of the various boundary coefficients and of the expressions depending upon them contained in the integrals. If for convenience we write

$$\left\{ K_1\sqrt{\kappa_2} + K_2\sqrt{\kappa_1} - \frac{\sqrt{\kappa_2}}{ai\lambda}(K_1 - K_2) \right\} = d,$$

we find that

$$\left. \begin{aligned} A &= \frac{\left\{ K_1\sqrt{\kappa_2} - K_2\sqrt{\kappa_1} + \frac{\sqrt{\kappa_2}}{ai\lambda}(K_1 - K_2) \right\}}{d}, \\ A' &= \frac{2K_2\sqrt{\kappa_1}}{d}, \\ C &= \frac{2K_1\sqrt{\kappa_2}}{d}, \\ C' &= \frac{\left\{ K_1\sqrt{\kappa_2} - K_2\sqrt{\kappa_1} - \frac{\sqrt{\kappa_2}}{ai\lambda}(K_1 - K_2) \right\}}{d}; \end{aligned} \right\} \quad (55)$$

so that

$$A = C - 1 \quad \text{and} \quad A' = C' + 1,$$

and

$$1 + Ae^{-2ai\lambda} = 2e^{-ai\lambda} \left\{ K_1\sqrt{\kappa_2} \cos a\lambda - \frac{\sqrt{\kappa_2}}{a\lambda}(K_1 - K_2) \sin a\lambda + iK_2\sqrt{\kappa_1} \sin a\lambda \right\} / d. \quad (56)$$

Other values required depend on the particular value chosen for  $B$ , and in what follows we have taken

$$B = \frac{i\mu\lambda + \left(\frac{1}{b} - \frac{h}{K_2}\right)}{i\mu\lambda - \left(\frac{1}{b} - \frac{h}{K_2}\right)} \quad \text{or} \quad \frac{i\mu\lambda + \left(\frac{1}{b} - \frac{h}{K_2}\right)}{d'} \dots (57)$$

Corresponding to this value of  $B$  we find that

$$D = 4ie^{-\{a+\mu(b-a)\}i\lambda} \left[ \mu\lambda f_1(\lambda) - \left(\frac{1}{b} - \frac{h}{K_2}\right) f_2(\lambda) \right] / dd', \quad (58)$$

where

$$\begin{aligned} f_1(\lambda) = & K_1\sqrt{\kappa_2} \cos a\lambda \cos \mu(b-a)\lambda \\ & - K_2\sqrt{\kappa_1} \sin a\lambda \sin \mu(b-a)\lambda \\ & - \frac{\sqrt{\kappa_2}}{a\lambda} (K_1 - K_2) \sin a\lambda \cos \mu(b-a)\lambda, \quad (59) \end{aligned}$$

$$\begin{aligned} f_2(\lambda) = & K_1\sqrt{\kappa_2} \cos a\lambda \sin \mu(b-a)\lambda \\ & + K_2\sqrt{\kappa_1} \sin a\lambda \cos \mu(b-a)\lambda \\ & - \frac{\sqrt{\kappa_2}}{a\lambda} (K_1 - K_2) \sin a\lambda \sin \mu(b-a)\lambda, \quad (60) \end{aligned}$$

$$1 - BU'e^{-2\mu(b-a)i\lambda}$$

$$\begin{aligned} = & 2e^{-\mu(b-a)i\lambda} \left[ i\mu\lambda \left\{ \left( K_1\sqrt{\kappa_2} - \frac{\sqrt{\kappa_2}}{ia\lambda} (K_1 - K_2) \right) \right. \right. \\ & \times \cos \mu(b-a)\lambda + iK_2\sqrt{\kappa_1} \sin \mu(b-a)\lambda \Big\} \\ & - \left( \frac{1}{b} - \frac{h}{K_2} \right) \left\{ K_2\sqrt{\kappa_1} \cos \mu(b-a)\lambda \right. \\ & \left. \left. + i \left( K_1\sqrt{\kappa_2} - \frac{\sqrt{\kappa_2}}{ai\lambda} (K_1 - K_2) \right) \sin \mu(b-a)\lambda \right\} \right] / dd', \quad (61) \end{aligned}$$

$$e^{-\{a+\mu(b-a)\}i\lambda} \{ e^{\mu(b-r_1)i\lambda} + Be^{-\mu(b-r_1)i\lambda} \} / D$$

$$\begin{aligned} = & \frac{\left\{ \mu\lambda \cos \mu(b-r_1)\lambda - \left( \frac{1}{b} - \frac{h}{K_2} \right) \sin \mu(b-r_1)\lambda \right\} K_1\sqrt{\kappa_2}}{\left\{ \mu\lambda f_1(\lambda) - \left( \frac{1}{b} - \frac{h}{K_2} \right) f_2(\lambda) \right\}} \dots (62) \end{aligned}$$

The evaluation of the integrals with which we are concerned can most directly be effected by contour integration, as in previous problems, along a path consisting of two axes inclined at  $45^\circ$  to the real axis of  $\lambda$ , and the circular arcs joining them at infinity. It is evident, therefore, that the solutions (50) ... (53) then consist of an infinite series of terms, the value of each term being determined by a value of  $\lambda$  which is a root of the equation

$$\mu\lambda f_1(\lambda) - \left(\frac{1}{b} - \frac{h}{K_2}\right) f_2(\lambda) = 0. \quad (63)$$

When we make use of this equation the expressions required can be greatly simplified. Corresponding to each value of  $\lambda$  given by a root of (63), we find that we can write

$$\frac{1 - BC'e^{-2\mu(b-a)\lambda}}{D} = \frac{-\mu\lambda K_1 \sqrt{\kappa_2} \cos \mu(b-a)\lambda + \left(\frac{1}{b} - \frac{h}{K_2}\right) \sin \mu(b-a)\lambda}{2i \left\{ \mu\lambda f_1(\lambda) - \left(\frac{1}{b} - \frac{h}{K_2}\right) f_2(\lambda) \right\} \sin a\lambda}, \quad (64)$$

$$\frac{1 + Ae^{-2ai\lambda}}{D} = \frac{\{f_1(\lambda) + if_2(\lambda)\} d'}{2i \left\{ \mu\lambda f_1(\lambda) - \left(\frac{1}{b} - \frac{h}{K_2}\right) f_2(\lambda) \right\}} \quad (65)$$

These results facilitate the evaluation of the integrals above by the residue theorem, for the value of  $B$  chosen above. The same results may still be made use of when  $B$  is given the value  $-1$ , for if in (57) we omit  $\mu\lambda$  throughout, the expression reduces to  $B = -1$ . Similarly the evaluations of the various terms apply to the case where  $B = -1$ , when terms containing  $\mu\lambda$  as a multiplier are omitted. Thus, instead of (63), we have now simply

$$f_2(\lambda) = 0 \quad (66)$$

as the equation whose roots are required for the evaluation of the integrals (50) ... (53), when  $B$  has the value  $-1$ .

The two equations (63) and (66) are particular cases of the more general equation  $D=0$ , where  $D$  is given by (54) above. Another case of interest is that in which  $B=0$  and  $b$  is infinitely large, corresponding to a finite sphere enclosed



within an infinite medium. The equation whose roots are required is then

$$(1 + Ae^{-2a\lambda}) = 0,$$

or its equivalent given in (56). A detailed investigation of the nature of the roots of equation  $D=0$  in all its various forms would of course be required in order to determine completely worked-out expressions for all the solutions contained in the integrals given above, but this is beyond the scope and intention of the present paper. We accordingly conclude this demonstration of the value of the method we have employed by completing the evaluations required in the special case in which  $B=-1$ . These evaluations are contained in

$$v = \sum_1^{\infty} \frac{2q\kappa_1 r_1}{K_1 r} \frac{\sin \lambda r \sin \lambda r_1 e^{-\kappa_1 \lambda^2 t}}{f_2'(\lambda)} \times -K_1 \sqrt{\kappa_2} \frac{\sin \mu(b-a)\lambda}{\sin a\lambda}, \quad (67)$$

$$v = \sum_1^{\infty} -\frac{2q'\kappa_1 r_1}{K_1 r} \frac{\sin \lambda r \sin \mu(b-r_1)\lambda e^{-\kappa_1 \lambda^2 t}}{f_2'(\lambda)} K_1 \sqrt{\kappa_2}, \quad (68)$$

$$v = \sum_1^{\infty} \frac{2q'\kappa_2 \mu r_1}{K_2 r} \frac{\sin \mu(b-r)\lambda \sin \mu(b-r_1)\lambda e^{-\kappa_1 \lambda^2 t}}{f_2'(\lambda)} \times -K_2 \sqrt{\kappa_1} \frac{\sin a\lambda}{\sin \mu(b-a)\lambda}, \quad (69)$$

$$v = \sum_1^{\infty} -\frac{2q\kappa_2 \mu r_1}{K_2 r} \frac{\sin \lambda r_1 \sin \mu(b-r)\lambda e^{-\kappa_1 \lambda^2 t}}{f_2'(\lambda)} K_2 \sqrt{\kappa_1}, \quad (70)$$

in which the summations extend to all the roots of equation (66) above. These represent respectively, in the order given,

- (1) the temperature at  $r$  in medium 1 due to an instantaneous source  $q$  per unit area at  $r_1$  in medium 1 ;
- (2) the temperature at  $r$  in medium 1 due to an instantaneous source  $q'$  per unit area at  $r_1$  in medium 2 ;
- (3) the temperature at  $r$  in medium 2 due to an instantaneous source  $q'$  per unit area at  $r_1$  in medium 2 ;
- (4) the temperature at  $r$  in medium 2 due to an instantaneous source  $q$  per unit area at  $r_1$  in medium 1.

The solutions are the equivalents of Green's Functions corresponding to a special boundary condition, namely, that the temperature is maintained at value zero at boundary

$r=b$ ; and they are fundamental solutions from which solutions to any problem of arbitrary initial heat distribution within the two media may be obtained. If we suppose, for example, that initially both media are at a uniform temperature  $\tau$ , throughout, we have merely to replace  $q$  by  $\frac{K_1}{\kappa_1} v_0 dr_1$  in medium 1, and  $q'$  by  $\frac{K_2}{\kappa_2} v_0 dr_1$  in medium 2, and integrate the four expressions given above, (67) ... (70), with respect to  $r_1$ , from 0 to  $a$  in medium 1 and from  $a$  to  $b$  in medium 2. The sum of the integrations performed on (67) and (68) gives the temperature at any point  $r$  in medium 1 at any instant  $t$ . It will readily be verified that, in virtue of equation (66) above, the expression for the sum of the integration reduces to

$$v = \sum \frac{2v_0 b K_2 \sqrt{\kappa_1}}{\lambda r} \frac{\sin a\lambda \sin \mu(b-a)\lambda \sin r\lambda e^{-\kappa_1 \lambda^2 t}}{F(\lambda)}, \quad (71)$$

where

$$F(\lambda) = K_1 \sqrt{\kappa_2} a \sin^2 \mu(b-a)\lambda + K_2 \sqrt{\kappa_1} \mu(b-a) \sin^2 a\lambda \\ - \frac{\sqrt{\kappa_2}}{a\lambda^2} (K_1 - K_2) \sin^2 a\lambda \sin^2 \mu(b-a)\lambda, \quad (72)$$

the summation extending to all the roots of (66). Similarly the sum of the integrations with respect to  $r_1$  performed on (69) and (70) above gives the temperature at  $r$  in medium 2 at any instant  $t$ : and, as in the case preceding, in virtue of equation (66) above, the expression for the sum of the integrations reduces to

$$v = \sum \frac{2v_0 b K_2 \sqrt{\kappa_1}}{\lambda r} \frac{\sin^2 a\lambda \sin \mu(b-r)\lambda e^{-\kappa_1 \lambda^2 t}}{F(\lambda)}, \quad (73)$$

the summation extending to all the roots of (66) as before. These two results contained in (71) and (73) will be found to be in agreement with the solutions of this problem given by Prof. Carslaw in *Proc. Cam. Phil. Soc.* xx. pp. 400-410 (1920-1).

The problem of determining the temperature at any point in the case where radiation occurs at the outer boundary of the outer material is one of considerable interest, for which the solution has not yet been published. The essential form of the solution is contained in the above paper, but the

problem is worthy of being worked out in full detail, including the two special cases in which the outer material is of greater and of less conductivity respectively than the inner. In like manner the problem of heat conduction in an inner sphere enclosed in a different material extending to infinity requires to be more fully discussed. It would be interesting also, and it would extend the usefulness of the method employed in the present paper to more general problems, to obtain by means of it the solution representing the temperature at any point within a sphere due to a point-source situated at any point within the sphere, the boundary being subject to any specified condition.

I desire to thank James F. Shearer, M.A., B.Sc., of this University for the interest he has taken in the work of this paper.

---

XXV. *The Propagation of Flame in Gaseous Explosions.*  
By Prof. W. M. THORNTON, D.Sc., D.Eng., *Armstrong College, Newcastle-on-Tyne* \*.

I. *Introduction.*

THE slow movement of flame in a gaseous explosion distinct from detonation proceeds by activation of gas immediately beyond the wave-front by some emanation from it. As to the nature of this activation, there is at present no general agreement. It can only occur in one of two ways, either by direct ionization from contact with the burning gas, or by changes of energy level in the unburnt molecules. Fifteen years ago the nature of the latter kind of activation had not been worked out, and though there was conclusive evidence that the ignition of gases depended more on the electrical than on the thermal properties of igniting sparks†, theories of ignition had not advanced beyond the conception of this electrical activation as some form of ionization. The proof of change of

\* Communicated by the Author.

† "The Electrical Ignition of Gaseous Mixtures," Roy. Soc. Proc. A, xc. p. 272 (1914).

energy levels in atoms and molecules has made possible the view that the activation of gases accompanying ignition either by sparks or flames may not require the pioneering formation of ions, but rather the absorption of radiation in such a manner that their electrical energy is raised, at least for the time necessary to start chemical change. On the other hand Finch and Cowan \* have shown recently that in certain modes of ignition by unidirectional discharges in gases at lowered pressures the results are proportional to the magnitude of the current, that is, to the rate of passage of ions: but in their work there is the further possibility that in the formation and recombination of ions there is radiation, which may be the active cause in starting the chemical reaction of which flame is evidence.

H. B. Dixon † found that transverse magnetic fields had no influence on the speed of flame in tubes, but the fields used, 10,000 gauss, though technically high, have been regarded since as insufficient to change the movements of ions in the explosion wave-front. Certain experiments by Lindemann and by G. N. Lewis have shown that radiation does not activate molecules over a wide range of frequencies within which it might be expected to occur. The position on this evidence is, then, a deadlock. Two methods of escape seemed possible: on the one hand to test the ionization hypothesis further by experiments in an electric field about the action of which there should be no uncertainty, or to examine the records of flame propagation for evidence which might reveal the mechanism of the process. In his Presidential Address ‡ to Section B of the British Association at Glasgow, Baly discussed very fully the manner in which radiation could enter into chemical reactions, with special reference to photoluminescence. Lenard and Klatt define two "instantaneous" states characteristic of each emission band. "In the upper state, which has a very small temperature range immediately below the upper temperature limit, the stability of the

\* S. L. Finch and L. G. Cowan, "Gaseous Combustion in Electrical Discharges. Part II.—The Ignition of Electrolytic Gas by Direct-current Discharge." Roy. Soc. Proc. A, cxvi. p. 529 (1927).

† "Explosion in the Magnetic Field," Roy. Soc. Proc. A, xc. pp. 506-11 (Aug. 1914).

‡ British Association Report, Glasgow, p. 41.

activated state is so small that the whole of the phosphorescent emission takes place within a fraction of a second after activation has ceased." The transfer of energy discussed by Baly is by the formation of complexes formed "not between any two molecules, but only between two which satisfy the conditions, the criterion being that a molecule of one compound, possibly by loss of rotational energy, can give to the molecule of another compound energy equal to the critical quantum of activation of that molecule. A complex of this type may be denoted by the symbol  $A^-B^+$ , where B has gained its critical quantum of activation at the expense of the rotational energy of A." Now the most characteristic feature of the combination of molecules in a gaseous explosion is the momentary excess of rotational energy. Evidence for this is the so-called "missing pressure" of explosion\*, the percentage of † energy radiated, and the widening of lines in the spectrum of explosions. There is therefore reason for the view that the conditions necessary for the transmission of flame by such an exchange of radiation between members of a complex are all present in the wave-front. There can be no doubt that the action is very limited in space or time, or the velocity of flame, in a tube with an open end for instance, would be much greater, having regard to the normal velocity of molecular movement in gases.

## 2. Explosions in an Electric Field of Force.

Before examining the relation between velocity of explosion and radiation, it may be of interest to give the result of measurements of the velocity of flame in an electric field of force. The influence of a moderate electric field on a steady flame has been examined by Becker ‡. A voltage of 3000 across poles 44 millimetres apart, between which flames of various kinds were maintained, though not making contact with them, has no apparent influence in distorting the flame until metallic salts are introduced.

\* "The Lost Pressure in Gaseous Explosions," *Phil. Mag.*, July 1914, p. 18.

† "The Total Radiation from a Gaseous Explosion," *Phil. Mag.*, Sept. 1915, p. 383

‡ A. Becker, "Die Electricischen Eigenschaften der Flamme," *Wien-Harms. Handbuch der Exp. Physik*, xiii. t. 1, p. 117, fig. 1, c and d.

These are driven by the field towards one pole or the other in a manner shown by the movement of the luminous part of the flame.

The ions which give to flame its electrical conductivity are probably a consequence, and not a cause, of combustion, but they are sufficient partially to short-circuit electrodes between which a strong electric field is applied. It is necessary in such a case to interpose a non-conducting barrier between the two metallic surfaces which form the poles, so that, though it has little influence on the electric gradient, it may prevent a discharge through the gas.

TABLE I.

Upward velocity of flame in 7 per cent. methane in air, central electrode in tube, mean field 10,000 volts per centimetre.

Abs. press., cm. Hg.	Velocity, cm./sec.		Ratio.
	Field on.	Field off.	
74	130	113	1.15
64	130	111	1.17
54	162	132	1.22
44	91	83	1.096
37.5	88	75	1.175
30	61	44	1.38
20	60	44	1.36

A glass tube a metre long and 3 centimetres diameter was surrounded for the middle 80 centimetres with a metal sheath, leaving a space 5 mm. wide through which to observe the passage of the flame. A metal rod 8 mm. diameter, which passed through stoppers at each end, formed the inner pole. Between this and the outer sheath a unidirectional pressure of 10,000 volts was maintained, measured by an electrostatic voltmeter. When the tube was dry, higher pressure could be used, but to avoid any risk of pilot sparks it was kept at the above value. The tube being exhausted and filled with the mixture, which had been standing over water, ignition was made by a spark

at the bottom, and the flame travelled upwards at a uniform rate.

Working with a 9.5 per cent. mixture of methane and air at atmospheric pressure, the lower end of the tube being opened after ignition, no difference in the velocity of the flame could be observed with and without the strongest fields. This observation was made immediately after the publication of Dixon's work, and was held to confirm his conclusions. On repeating this recently with a weaker mixture a transverse electric field was found to have a marked accelerating influence on the speed of the flame.

The velocities are the means of 10 to 20 determinations in each case.

The results are conclusive that at all pressures at and below atmospheric flame travels faster in a transverse electric field.

If the pioneering activation from a wave-front were ionic, the electric field used should have perceptible influence on its rate of transmission, for the velocity of an ion in a field of 10,000 v./cm. is about one-half of the velocity of agitation at normal temperature and pressure. Such a movement as this could not fail to have marked retarding effect on the advance of slow flames if it were solely one of sweeping ions from the wave-front. The observed acceleration by a field may be a consequence of the increase of kinetic energy of the gas, either in or just beyond the wave-front, due to the ionic velocity added by the field, which has the same result as raising the temperature; or, from another point of view, the flame, being a partial conductor, may be drawn up into the field.

The influence of an electric field on radiation from a flame is the widening of the lines of the spectrum in the Stark effect caused by a change of energy of the elliptical orbits of electrons of the vibrating atoms. The Stark effect has the same cause as the transverse Zeeman effect—a modification of the spin of the electrons in the orbit. This change of energy of spin may be the added energy of rotation required by Baly's complex for absorption of radiant energy from combining atoms by atoms of the same kind which are within range. As a possible cause of the accelerating influence of the field this should not be overlooked.

### 3. Evidence of Activation by Radiation from Flame.

Analysis of the slow movement of flame in tubes leads to the view that, when the diameter of the tubes is eliminated from the results, the velocity of transmission is directly proportional to the fourth power of the temperature of the flame. The most general expression for velocity of this uniform slow movement is that of Mallard and Le Chatelier who give \*

$$V = \frac{L}{c} \frac{(T - t)}{(t - \theta)} f(T, t), \dots \dots \dots (1)$$

where  $T$  is the temperature of combustion,

$t$  the ignition temperature of the mixture,

$\theta$  the initial temperature,

$L$  the thermal conductivity of the unburnt gas,

$c$  the mean specific heat of the burning or just burnt gas, and

$f(T, t)$  a constant, for a given tube.

This expression has been confirmed by Mason and Wheeler\*. Usually  $\theta$  is atmospheric temperature, and for a given mixture  $t$  is constant, so that we may write

$$V = k_1(T - t), \dots \dots \dots (2)$$

where  $k_1$  depends on the size of the tube.

When a flame is advancing with constant speed in a tube each element of the wave-front burns an equal volume of gas in the same time. The area of an annular element of the flame is  $2\pi y \delta s$ , where  $y$  is the distance of the boundary from the axis and  $\delta s$  an element of length along the curve. When the gases are perfectly mixed the rate of supply of gas to the flame is uniform over its area projected on to the cross-section of the tube. The projected area of the element is  $2\pi y \delta y$ , and if  $h$  is the heat generated per unit area and thickness of this cross-section, the rate of generation of heat in the element is

$$\frac{d}{dt} (2\pi h y dy).$$

\* See Bone and Townend, 'Flame and Combustion in Gases,' p. 106.

† Trans. Chem. Soc. iii. pp. 1044-1057 (1917).



The velocity of the flame  $\frac{dx}{dt}$  is proportional to this, so that

$$\frac{d}{dt}(2\pi h y dy) = k \frac{dx}{dt},$$

$$\text{or } y = \frac{dy}{dx} = \frac{k}{2\pi h}, \text{ a constant. . . . . (3)}$$

The curve for which the subnormal is constant is a parabola, and the flame should therefore assume a parabolic section, as, in fact, it is seen to do, each part moving with the same velocity.

The area of surface of such a flame is

$$\pi \left( \frac{D^3}{3a} + 2aD + \frac{4a^3}{D} \right),$$

where  $a$  is the semi-latus rectum. Since these flames are pointed,  $a$  is much smaller than  $D$ , and the total area is nearly proportional to  $D^3$ . Thus the mean heat generated by combustion per unit area and movement of the flame is inversely proportional to the diameter of the tube, for

$$H = \frac{\pi}{4} D^2 h / \pi \left( \frac{D^3}{3a} + 2aD + \frac{4a^3}{D} \right) \simeq \frac{3ah}{4D} \quad . \quad . \quad (4)$$

The corresponding rise of temperature is proportional not only to the mean heat of combustion over the surface of the flame of unit thickness, but to the rate at which the mixture is fed to the flame, that is, to the latter's velocity. Thus  $T-t = k_2 V/D$ , where  $k_2$  is a constant including  $3ah/4$  and other factors from eqn. (1).

Hence

$$D = k_2 V / (T-t) \quad . \quad . \quad . \quad . \quad . \quad (5)$$

is the working relation between  $D$ ,  $V$ , and  $(T-t)$ , the mean temperature of the flame being proportional to the ratio of velocity to diameter.

To carry this further, it is necessary to have recourse to observed values of  $V$  in tubes of different diameters. Burgess and Wheeler \* found the following velocities in a mixture of methane and air giving perfect combustion.

\* See Bone and Townend, *loc. cit.* p. 111, fig. 21.

TABLE II.

Diameter of Tube, D.	Velocity of flame, V.	$V/D^{\frac{1}{4}}$ .
2.5 cm.	70 cm./sec.	54
5.0	95	55
9.0	105	50
30.5	165	53
96.5	255	55.5
Mean....		53.5

It follows from their observations that the velocity of uniform motion of flame in tubes is proportional to the *cube root of the diameter of the tube*. The reason for this remarkable result, which seems to have been overlooked, is as follows.

Writing  $V = k_3 D^{\frac{1}{4}}$ , and taking, as above,  $V = k_1(T-t)$  we have

$$D = k_4(T-t)^3. \quad . \quad . \quad . \quad . \quad . \quad (6)$$

But  $D = \frac{k_2 V}{T-t}$ , so that  $V = \frac{k_4}{k_2}(T-t)^4$ , or, nearly,  $V = KT^4$ .

Thus, when the diameter of the tube is eliminated from the experimental results, the velocity of flame is found to be proportional to the fourth power of its temperature. If this were not so, Burgess and Wheeler's results would not hold.

This, then, is strong evidence that the activation by which the flame travels is radiation according to Stefan's law. The salient facts of the transmission of flame in open tubes are : (i.) it is not retarded by magnetic fields or (ii.) by electric fields, (iii.) the velocity of uniform motion is proportional to the fourth power of the temperature. It is difficult to resist the conclusion that the sole cause of the pioneering activation from flame is electromagnetic radiation.

In the Report of the National Physical Laboratory, 1927, p. 62, evidence is given that flame is in thermal equilibrium with the surrounding vapour according to

black-body radiation. Mallard and Le Chatelier's results show that the velocity of flame is proportional to the total heat generated. The present conclusion is that of this heat only that in the form of radiation is effective in the transmission of flame. For both of these to be true the energy of radiation must bear a constant ratio to the total heat of combustion, and this is known to be the case.

#### 4. *Radiation from Combining Molecules.*

The researches of Hopkinson and David \* proved that the heat of combustion radiated to the walls of an explosion vessel was nearly 22 per cent. of the whole. A reason for this figure has been given † as a consequence of the necessary spinning action of two molecules colliding at oblique incidence and cohering. Evidence of such a spinning action is important in the physics of wave-front activation, and since it could only be obtained by spectroscopy, an attempt was made to observe it directly in this manner, the argument being that rotation must, as in other well-known spectroscopic effects, result in widening of lines or bands. A long steel tube was fitted with thick glass windows at each end, with rubber cushions to avoid initial strains. The tube was filled with electrolytic gas, and this ignited by sparking-plugs placed out of sight in T pieces at each end. The flame, as seen through a spectroscope, presented marked differences when advancing towards it or receding. Lines were doubled when seen from the front, but were single, though blurred, when seen from the back, *i.e.*, with the wave-front receding. This observation, it was found later, had been made long ago by Liveing ‡, who attributed the doubling to reversal by absorption of the radiation by the undisturbed atoms of molecules between the wave-front and the window. But the lines are not merely reversed—they are doubled and widened. The so-called "steam lines" in radiation from explosion of undried gases, or from steady flames, have a

\* Roy. Soc. Proc. A, lxxxiv. pp. 155-172 (1910), or Hopkinson's Collected Papers.

† "The Lost Pressure in Gaseous Explosions," Phil. Mag., July 1914, p. 18.

‡ "Spectroscopic Studies in Gaseous Explosions," Roy. Soc. Proc. A, xxxvi. pp. 471-78.

similar appearance\*. The two chief "steam lines" are nearly equal in intensity, but are widely spaced. The constant occurrence of "reversed" lines in explosion spectra must at least be considered as caused by molecular spin when elements having high translational energy, as all have in gases, collide and combine. It is then necessary to examine the spacing of the steam lines†. From rescarches on explosion at high pressures Bone concludes that steam is formed at flame temperatures. The temperature of an oxyhydrogen flame is about 2400° C., and the corresponding velocity of hydrogen molecules  $6.25 \cdot 10^5$  centimetres per second. The oxygen molecule may be taken to have a diameter of  $3 \cdot 10^{-8}$  cm., the hydrogen molecule  $2.4 \cdot 10^{-8}$ . When collision takes place, in the accepted planetary manner, and the molecules cohere at contact, the maximum angular velocity of spin given to the resulting steam molecule is:—

$$\omega = 6.25 \cdot 10^5 \left( \frac{3 + 2.4}{2} \right) \cdot 10^{-8} = 2.3 \cdot 10^{13} \text{ radians per second,}$$

in effect about the centre of the oxygen molecule. Such a spinning system, carrying its atomic electrons, if at right angles to the line of observation, would give rise to a displacement  $\delta\lambda$  of a line of wave-length  $\lambda$ , which is to the left of the spin is one way, to the right if reversed.

Orbits otherwise orientated show the effect less, and, if in the line of vision, not at all. This displacement is comparable with the Zeeman effect, and may be tested in the same way. In that case

$$\frac{e}{4\pi mc^2} = \frac{\delta\lambda}{H\lambda^2}, \text{ and } \frac{eH}{2mc} = \frac{\delta\lambda}{\lambda^2} \cdot 2\pi c = \omega \quad . \quad (5)$$

In the spectra of explosions the steam lines appear at 3064 Å.U. Taking the value of  $\omega = 2.3 \cdot 10^{13}$ , the displacement  $\delta\lambda$  of the lines from a central position is  $\omega\lambda^2/2\pi c$ , or  $11.3 \cdot 10^{-8}$  cm. The total distance between steam lines produced in this manner should be  $22.6 \cdot 10^{-8}$  cm.

Measurements of the distance apart of the lines taken from Bone and Townend's photographs are not capable of high accuracy, but they are, on an average, a little more

\* See Bone and Townend, *loc. cit.* Cp. Pts. xxiv. to xxvii.

† W. A. Bone and others, "Gaseous Combustion at High Pressure," Phil. Trans. Roy. Soc. A, cciv. p. 304.

than a millimetre apart, and 1 millimetre corresponds to  $25.6 \cdot 10^{-8}$  cm. These values are so near, having regard to the approximate measurements, that the possibility of the steam lines being formed in this way must be seriously considered. There are no lines in the oxygen or hydrogen spectra at this wave-length, and the origin or cause of the lines, and the reason for their always being found in pairs, very strong and too widely spaced to be simply atomic, as in the case of the sodium lines, has been hitherto unknown. The explanation now suggested is that they are caused by the spin induced by combining collisions of hydrogen and oxygen molecules which lead to the formation of steam, the action being that of skaters approaching at high speed who suddenly link arms. Such a collision, if the bodies were of unequal mass, would give rise to strong oscillations as well as spin, but the translational energy, and therefore the pressure, in the case of a gaseous explosion in which many millions of such combinations occur simultaneously, would certainly be for the moment reduced.

It is possible that the doubled appearance of other than steam lines in the spectra of burning gases may be caused by this mechanical action, which must occur in gases where combining molecules are moving at high speeds before union. The other evidence for such an effect is that the observed pressure of explosion is about one-half of that calculated on the assumption that there is equipartition of energy; and further, that the total radiation agrees with that which should be available if such a spinning combination took place \*. In the calculation of explosion pressures and speeds it is necessary to use specific heats in excess of those found in steady states, but direct evidence for the molecular or atomic movement by which the energy is absorbed is still to be desired. The position is that energy radiated from a flame in a given mixture is a nearly constant proportion of the whole heat of combination; that the spectroscopic evidence indicates excessive spin in the wave-front; that the pressure is undoubtedly less than can be accounted for by any thermal exchange without considering the mechanics of the process; and finally, that by such consideration these facts can be reconciled. An inflammable mixture at the point of ignition can be regarded as a sensitive detector of radiation.

\* "The Total Radiation from a Gaseous Explosion," *loc. cit.*, p. 383.

### 5. Compression and Ignition.

Inflammable mixtures heated by sudden compression do not detonate. Flame starts at one point and spreads as from a spark. In Baly's analysis of the conditions under which radiation might become a cause of molecular activation, the excess of vibrational energy required was considered to be available at the expense of the rotational component.

But in ignition by sudden compression there is for a moment an excess of translational energy, and just as it is legitimate to consider "lost" pressure to be a momentary out of balance of equipartition of energy, so in compression the excess pressure can be considered available for such a transfer of vibrational energy in a complex of a reactant molecule and a catalyst, which in the case of gaseous explosions is most generally water-vapour, without which, as H.B. Dixon showed, explosion does not generally occur in gases.

The moment that flame appears, combination proceeds with increasing velocity, and the speed of flame driven forward by the increase of pressure around the source of ignition should be exponential, at least in a closed tube, for each element burnt adds the pressure of its products to force the flame onwards. The records of flame in gases ignited by sparks at the centre of a tube show in every case\* a velocity increasing at first exponentially, then reaching a uniform state, and so passing to the end of the tube. To take the case of plate xxii., *loc. cit.*, p. 159, the distances of the flame along the tube from the central point of ignition, at equal arbitrary intervals of time, are expressed by  $y=1.242 e^t$ , as shown in Table III.

The velocity  $dy/dt$  of the flame at any point  $y$  is  $ty$ , and the acceleration of the flame from the source is proportional to  $y$ , the distance travelled, that is, to *the volume of gas burnt*. This explains the high velocities of explosions in coal-mines, or galleries with a closed end.

Applying this to the spread of flame from a point in a vessel such as the cylinder of an internal combustion engine containing a uniform or turbulent mixture ignited by compression, spark, or hot spot, the acceleration of the flame should be proportional to the cube of the distance from the point at which ignition begins, and the velocity

\* See Bone and Townend, plates xi., xii., and xiii.

of flame proportional to the square of the distance moved, until the flame reaches the walls and ends and reflexions occur. In the movement of flame in closed tubes there is, following the period of acceleration, one of uniform velocity. (plates xi. and xii., *supra*); but at the point where the latter begins there is in every case evidence of a wave reflected back to the centre, shown by a line of more intense radiation. The distance at which this first occurs is just beyond half the length from the centre to the closed ends. With open ends this stage is not found. It is caused by compression of the unburnt gas by the expanding products of combustion, and at the transition point the pressures are for the moment equal on both sides of the wave-front.

TABLE III.

<i>t.</i>	<i>et.</i>	<i>η</i> .		Velocity of flame in arbitrary units.
		cal.	obs.	
0.5	1.648	2.04	2.0	1.0
1.0	2.718	3.35	3.5	3.5
1.5	4.481	5.55	5.5	8.25
2.0	7.389	9.17	9.0	18.0
2.5	12.182	15.1	15.0	37.5
3.0	20.08	24.9	25.0	75.0

Taking  $V_0$  as the volume of the mixture in half the tube, ignition being at the centre, and  $V$  that of the unburnt gas,  $p(V_0 - V)^{\gamma_1} = pV^{\gamma_2}$ , where  $\gamma_1$  is about 1.28 for  $\text{CO}_2$ ,  $\text{N}_2$ , and  $\text{OH}_2$ ,  $\gamma_2 = 1.35$  for  $\text{CH}_4$ ,  $\text{N}_2$ ,  $\text{O}_2$ . At equal pressures

$$(V_0 - V)^{1.28} = V^{1.35}, \quad \dots \quad (19)$$

from which  $V = 0.53V_0$ , or, with these values of  $\gamma$ , the pressures should be equal a little beyond half the distance between the centre and the end. From plate xi., when there is no initial lag, that is, taking the last two figures,  $V/V_0 = 0.55$ . The striæ in photographs of flame are, of course, lines of equal pressure in reflected waves. In the uniform speed stage of explosion there is no acceleration; but pressure equilibrium in the spaces on the two sides of the wave-front.

XXVI. *On the Scattering of  $\alpha$ -particles by Light Atoms.* By A. C. BANERJI, M.Sc.(Cal.), M.A.(Cantab.), Head of the Department of Mathematics, Allahabad University\*.

**I**N a recent Royal Society discussion† on the “Structure of Atomic Nuclei” Prof. Sir Ernest Rutherford sketched out a picture of the gradual building up of atomic nuclei out of protons and electrons. If we suppose that these two are the only primordial elements, we have to find out the fundamental principles underlying the formation of complex nuclei with all their isotopes out of these two. Attempt to achieve this end is being made from several directions:—

(i.) From the experiments of Aston‡ on the packing fraction of atoms, which give us, in conjunction with Einstein’s principle  $E = \Delta mc^2$ , the amount of energy set free when protons and electrons combine in any way to form atomic nuclei.

(ii.) From study of the origin of  $\gamma$ -rays (Meitner and Ellis) §.

(iii.) From the study of the scattering of  $\alpha$ -particles by light atoms (Rutherford, Chadwick) ||.

The last method is especially interesting. It may be remembered that it was the results of large-angle scattering of  $\alpha$ -particles which gave us the nuclear theory of the atom. We give a brief recapitulation of the results.

Let  $Ze$  be the central charge,  $(M, 2e)$  be the mass and charge of the  $\alpha$ -particle,  $v_0$  is its velocity of projection,  $p$ =perpendicular distance of the nucleus from the line of projection. The law of force is supposed to be that of inverse square distance.

Then it is found that when the nucleus is heavy the  $\alpha$ -particle describes an hyperbola, with the nucleus as the outer focus. The angle of deviation is  $\pi - 2\theta$ ,

$$\text{where} \quad \theta = \tan^{-1} \frac{p}{q}, \quad . . . . . (1)$$

$$\text{where} \quad q = \frac{2Ze^2}{Mv_0^2}. \quad . . . . . (2)$$

\* Communicated by Prof. M. N. Saha, D.Sc., F.R.S.

† Proc. Roy. Soc. cxxiii. p. 373.

‡ *Ibid.* p. 383.

§ Meitner, *Zs. f. Physik*, xxvi. p. 169; also *Handbuch der Physik*, xxii. chap. ii. D. Ellis, see recent discussion in Proc. Roy. Soc. cxxiii. p. 385.

|| Phil. Mag. iv. p. 605 (1927); also xlii. (1921); i. (1925).



The least distance of approach

$$d = q(1 + \sec \theta). \quad \dots \dots (3)$$

When

$$p = 0, \quad d = 2q.$$

In actual experiment we are concerned with the total number of particles scattered at an angle  $\theta$  with the primary beam, and incident upon unit surface placed normally.

The probability of scattering is found to be

$$\frac{1}{r^2} \left( \frac{e^2 Z}{M v_0^2} \right)^2 \frac{1}{\sin^4 \frac{\theta}{2}} = \frac{1}{r^2} \frac{(e^2 Z)^2}{4 E^2} \frac{1}{\sin^4 \frac{\theta}{2}}, \quad \dots (4)$$

where  $E$  = energy of the bombarding  $\alpha$ -particle.

If we take an element with the charge  $Ze$ , the nearest distance of approach for  $\alpha$ -rays of velocity  $2 \times 10^9$  cm. from  $\text{ThC}' = 1.71 \times 10^{-14} \cdot Z$  cm. for straight collisions, i. e., when  $\theta = 0^\circ$ .

The following are the values for a few typical elements for nearest distance of approach for straight collisions :—

$$\text{U (92)} = 1.56 \times 10^{-13} \text{ cm.}$$

$$\text{Cu (29)} = 5.0 \times 10^{-13} \text{ cm.}$$

$$\text{Mg (12)} = 2.05 \times 10^{-13} \text{ cm.}$$

$$\text{He (2)} = 3.4 \times 10^{-14} \text{ cm.}$$

It is found that up to copper results of scattering experiments are quite in accord with the formulæ given above; but marked abnormalities occur in the scattering experiments with light elements. Four elements have been studied in detail, viz., Mg, Al, He, and H. The cases of H and He are a bit more complicated, as a large part of the velocity of bombarding  $\alpha$ -particles are communicated to these nuclei. In Al and Mg this factor (communication of velocity to their nuclei) is practically negligible.

The results of these experiments (scattering of  $\alpha$ -particles by Al and Mg) have been expressed by Bieler, Chadwick, and Rutherford in the two observed curves (—O—O—O) represented at the end of this paper (figs. 3 and 4, *vide supra*). The ordinate represents the ratio of the observed number of  $\alpha$ -particles scattered to the number calculated according to the inverse square law. The abscissa represents the angle of scattering.

Bieler tried to explain these anomalies by assuming that the law of force (repulsive) very close to the nuclei is not given exactly by the inverse square distance, but, in addition, an attractive force comes into play. Bieler assumed that

this attractive force varies as the fourth power of distance, viz. :—

$$F = \frac{2Ze^2}{r^2} \left( 1 + \frac{r_0}{r^2} \right). \quad . \quad . \quad . \quad . \quad . \quad (5)$$

It should be emphasized that the attractive force is operative only when  $r$  is extremely small ( $< 4 \times 10^{-13}$  cm.). In heavy atoms up to Cu the least distance of approach is  $\geq 5.0 \times 10^{-13}$  cm., hence the classical formulæ hold; but in light atoms (*e.g.*, H, He) it may be as low as  $2 \times 10^{-14}$  cm., hence the attractive forces make themselves felt.

Working out by means of classical mechanics Bieler\* found that if the attractive force varies as the inverse fourth power of the distance, either curve (for Al or Mg) has a horizontal tangent at  $\theta = 0^\circ$ . Thus an inverse fourth-power term in the law of force has no effect on scattering at very small angles. On the other hand, he found that an inverse cube term in the law of force will make itself felt in the scattering no matter how small  $\theta$  is. But we shall see later on, working out by means of wave-mechanics, that the additional inverse cube force will have also no effect on scattering at very small angles, and that for large angles results obtained from calculations by taking the additional inverse cube force are in good agreement with observed data in the case of Al and Mg.

Debye and Hardemeier† later assumed that the attractive force varied as the inverse fifth power. They argued that as the  $\alpha$ -particle approaches the nucleus the intense forces thus arising distort or polarize the constituents of the nucleus. This gives rise to an attractive force on the colliding  $\alpha$ -particle, which varies inversely as the fifth power of distance.

Hardemeier‡ worked out in detail the path of the  $\alpha$ -particle under such a law, and also the probability of scattering. He found that with certain assumptions the law can very well explain the experimental results of Bieler. But, as Rutherford§ points out, the assumptions are a bit artificial, as the  $\alpha$ -particle is supposed to be a point-charge and the nucleus a sphere.

It has recently been supposed that the nucleus has got a spin and a finite magnetic moment. Hence the additional attractive forces are of magnetic origin. The suggestion has not yet been fully worked out.

\* Proc. Camb. Phil. Soc. xxi. p. 686 (1923).

† Phys. Zs. xxvii. p. 181 (1926).

‡ Loc. cit.

§ Discussion, Proc. Roy. Soc. cxxiii. p. 377.

*Application of Wave-mechanics.*

In recent years the idea has grown up that in the treatment of all atomic phenomena the particle should be replaced by its matter-wave. Born\* was the first to apply wave-mechanics to collision problems in general, which includes scattering as a particular case. The  $\alpha$ - or  $\beta$ -particle is considered as a de Broglie wave passing through the atom and of length  $\lambda = \frac{h}{Mv}$ . The velocity of the wave is modified on entering the atom, according to de Broglie's† hypothesis, and scattering of the  $\psi$ -function is worked out in very much the same way as diffraction problems are studied in wave-optics. Of the many interesting applications of Born's ideas (*e.g.*, to elastic and non-elastic collisions of electrons with atoms, Ramsauer effect‡, etc.) we confine our attention only to results obtained in the scattering of  $\alpha$ -particles. This was first worked out by Wentzel§ assuming the law of inverse square. He obtained a result identical with that obtained in classical mechanics. Sommerfeld|| has given a different method for calculating the potential inside atoms. He considers that all the outer electrons are assembled in the K-shell, and electricity is distributed according to the law

$$\rho = \frac{eZ^4}{\pi a^3} e^{-2r\frac{Z}{a}} \dots \dots \dots (6)$$

The distribution is the same as we find by calculating the  $\psi$ -function of the fundamental orbit of the H-atom according to Schrödinger's theory, and then interpreting the result as a continuous distribution of electricity (*vide* Schrödinger, *Ann. der Phys.* lxxix.). Then  $V$  is calculated to be

$$V = 2e^2Z\left(\frac{1}{r} + \frac{Z}{a}\right)e^{-\frac{2rZ}{a}}, \dots \dots \dots (7)$$

where  $a$  is the radius of the hydrogen atom, and the probability of scattering is found to be

$$\frac{1}{r^2} \left( \frac{e^2Z}{Mv^2} \right) \frac{1}{\left( \sin^2 \frac{\theta}{2} + \alpha^2 \right)^2}, \dots \dots \dots (4')$$

\* *Zs. f. Phys.* xxxvii. p. 863 (1926); xxxviii. p. 803 (1926).

† For modification of the theory see Dirac, *Zs. f. Phys.* xliiv.

‡ See Faxen and Holtmark, *Zs. f. Phys.* xlv. p. 307. Further papers by Holtmark in *Zs. f. Physik*.

§ Wentzel, *Zs. f. Phys.* xl. p. 590.

|| Sommerfeld, *Wellen mechanische Ergänzung*, p. 226.

where 
$$\alpha = \frac{h}{Mva} \cdot \frac{Z}{2\pi}.$$

As  $\alpha \propto 10^{-3}$ , its square can be neglected.

Thus Wentzel and Sommerfeld's formula is no improvement upon the classical formula as far as treatment of anomalous scattering is concerned. This is quite apparent if we critically examine Sommerfeld's basic assumption. The extra  $\alpha^2$ -term owes its origin to outer ring of electrons which, as far as large angle scattering is concerned, are without effect on the scattering phenomena. The same criticism may be held against another formula by Mitchell\*, who calculates the potential by an interesting method due to Fermi†. Sommerfeld himself admits in a footnote that the cases of anomalous scattering are rather to be ascribed to some peculiarity in the nuclear structure.

It will be seen that no attempt has as yet been made to account for the abnormal scattering of  $\alpha$ -particles by light atoms with the aid of wave-mechanics. This has been made in the present paper. The first difficulty which was felt was about the choice of a law of force. It was found that if either the inverse fourth-power or the fifth-power law be assumed, the Schrödinger wave-equation for the motion of any charged particle round the nucleus has no solution in polynomials with finite number of terms, giving discrete energy-values. But it is quite certain that such discrete values must exist, as otherwise it will not be possible to explain the origin of the  $\gamma$ -ray spectrum, which, according to the investigations of Meitner‡, Ellis§, and Kuhn§, arise from the transition of the  $\alpha$ -particle between levels having discrete energy-values. Again, for the scattering the Schrödinger equation gives us a solution when the attractive force varies inversely as the cube of the distance. For the inverse fourth-power law or the fifth-power law the solution will depend on the integral  $\int_0^\infty \frac{e^{bx}}{x} dx$  ( $b$  being a constant), which does not converge.

I have therefore worked out the scattering formula by wave-mechanics by assuming the inverse cube law.

The path of the  $\alpha$ -particle round the nucleus has been worked out by means of classical mechanics. In a second

\* Mitchell, Proc. Nat. Acad. Sci. Washington (1929).

† Fermi, *Zs. f. Phys.* xlviii. p. 73.

‡ *Loc. cit.*; also Proc. Camb. Phil. Soc. xxii. p. 844 (1925).

§ *Zs. f. Phys.* xliii. p. 56; xlv. p. 32.

paper I have worked out the theory of the  $\gamma$ -ray spectrum on the basis of the inverse cube law.

Path of the  $\alpha$ -particle round the nucleus worked according to the law of force

$$F = \frac{2e^2Z}{r^2} \left(1 - \frac{r_0}{r}\right), \quad \dots \dots \dots (5')$$

where  $r_0$  is the distance at which force changes in sign, i.e., where its value is zero.

Let  $v_0$  be the velocity of projection at infinity, and  $p$  be the perpendicular from the origin on the asymptote, then the equation to find the orbit is

$$\frac{d^2u}{d\theta^2} + u \left(1 - \frac{2Ze^2r_0}{Mv_0^2p^2}\right) = \frac{-2Ze^2}{Mv_0^2p^2}, \quad \dots \dots (8)$$

where 
$$u = \frac{1}{r}.$$

Put 
$$q \cdot Mv_0^2 = 2Ze^2;$$

we get

$$\frac{d^2u}{d\theta^2} + u \left(1 - \frac{qr_0}{p^2}\right) = -\frac{q}{p^2}. \quad \dots \dots \dots (8')$$

We shall measure  $\theta$  from the line of minimum (apsidal) distance. Let  $x$  be the angle which the asymptote makes with the initial line.

*Case I. (vide fig. 1) :*

When  $p^2 > qr_0$ ,  
put

$$n^2 = 1 - \frac{qr_0}{p^2};$$

we get

$$\tan nx = \frac{pn}{q},$$

and

$$\frac{1}{r} = -\frac{q}{p^2 - qr_0} + \frac{\sqrt{p^2 + q^2 - qr_0}}{p^2 - qr_0} \cos n\theta.$$

Minimum distance  $d$  is given by

$$d = \frac{p^2 - qr_0}{\sqrt{q^2 + p^2 - qr_0 - q}}.$$

} . . . (9 A)

*Case II. :*

When  $p^2 < qr_0$ ,  
put

$$n^2 = \frac{qr_0}{p^2} - 1;$$

we get

$$\tanh n'x = \frac{pn'}{q},$$

and

$$\frac{1}{r} = \frac{q}{qr_0 - p^2} - \frac{\sqrt{q^2 - (qr_0 - p^2)}}{qr_0 - p^2} \cosh n'\theta,$$

and

$$d = \frac{qr_0 - p^2}{q - \sqrt{q^2 - (qr_0 - p^2)}}.$$

(9 B)

In order that  $d$  shall be real

$$q^2 > qr_0 - p^2,$$

or

$$p^2 > qr_0 - q^2.$$

This condition is also necessary that  $\tanh n'x < 1$ , i. e.,  $x$  may be real.

Case III.:

When  $p^2 = qr_0$ .

The equation to the orbit is

$$\frac{1}{r} = \frac{1}{2q} - \frac{\theta^2}{2r_0},$$

also

$$x = \frac{r_0}{p} = \sqrt{\frac{r_0}{q}},$$

$$d = 2q.$$

(9 c)

Case IV.:

When  $p^2 \leq qr_0 - q^2$  and  $r_0 > q$ .

No real values of  $d$  and  $x$  are possible, and the  $\alpha$ -particle falls into the nucleus.

In this case, taking the initial line parallel to the asymptote or the initial direction of motion, the equation to the orbit is

$$\frac{1}{r} = \frac{q}{qr_0 - p^2} (1 - \cosh n'\theta) - \frac{1}{pn'} \sinh n'\theta \} \dots (9 d)$$

If  $\frac{\pi}{2} > x > 0$ , the  $\alpha$ -particle describes an asymptotic curve proceeding back to infinity without going round the nucleus—the deflexion is given by  $\pi - 2x$ .

If  $\pi > x > \frac{\pi}{2}$ , the particle goes round the nucleus and proceeds back to infinity—the deflexion is given by  $2x - \pi$ .

For the region  $p^2 > qr_0$ ,  $x$  has a *minimum* value  $x_m$  at  $p = p_m$ , where  $p_m$  satisfies the equation

$$\tan \frac{p_m^2 \sqrt{p_m^2 - r_0}}{r_0(q^2 + p_m^2 - qr_0)} = \frac{\sqrt{p_m^2 - qr_0}}{q}. \quad (10 A)$$

This gives a *maximum* deflexion.

For the region  $p^2 < qr_0$ ,  $x$  has a *maximum* value  $x_n$  at  $p = p_n$ , where  $p_n$  satisfies the equation

$$\tanh \frac{p_n^2 \sqrt{qr_0 - p_n^2}}{r_0(q^2 + p_n^2 - pr_0)} = \frac{\sqrt{qr_0 - p_n^2}}{q}. \quad (10 B)$$

This also gives a *maximum* deflexion.

We have seen that when  $p^2 = qr_0$ ,

$$x = x_0 = \sqrt{\frac{r_0}{q}};$$

at this value of  $p$ ,  $x$  decreases as  $p$  increases, and *vice versa*.

**Case A.:**

$$\pi > x_0 > \frac{\pi}{2}.$$

For the region  $p > p_1$ , where  $p_1 > \sqrt{qr_0}$  and  $p_1$  is given by

$$\tan \sqrt{p_1^2 - qr_0} \cdot \frac{\pi}{2p_1} = \frac{1}{q} \sqrt{p_1^2 - qr_0}, \quad (11 A)$$

the  $\alpha$ -particle returns back to infinity without going round the nucleus.

For the region  $p < p_1$ , provided  $r_0 \leq q$ , otherwise for the region  $\sqrt{qr_0 - q^2} < p < p_1$ , provided  $r_0 < q$ , the  $\alpha$ -particle goes round the nucleus and returns back to infinity.

For the region  $p \leq \sqrt{qr_0 - q^2}$ , provided  $r_0 > q$ , the  $\alpha$ -particle falls into the nucleus.

**Case B.:**

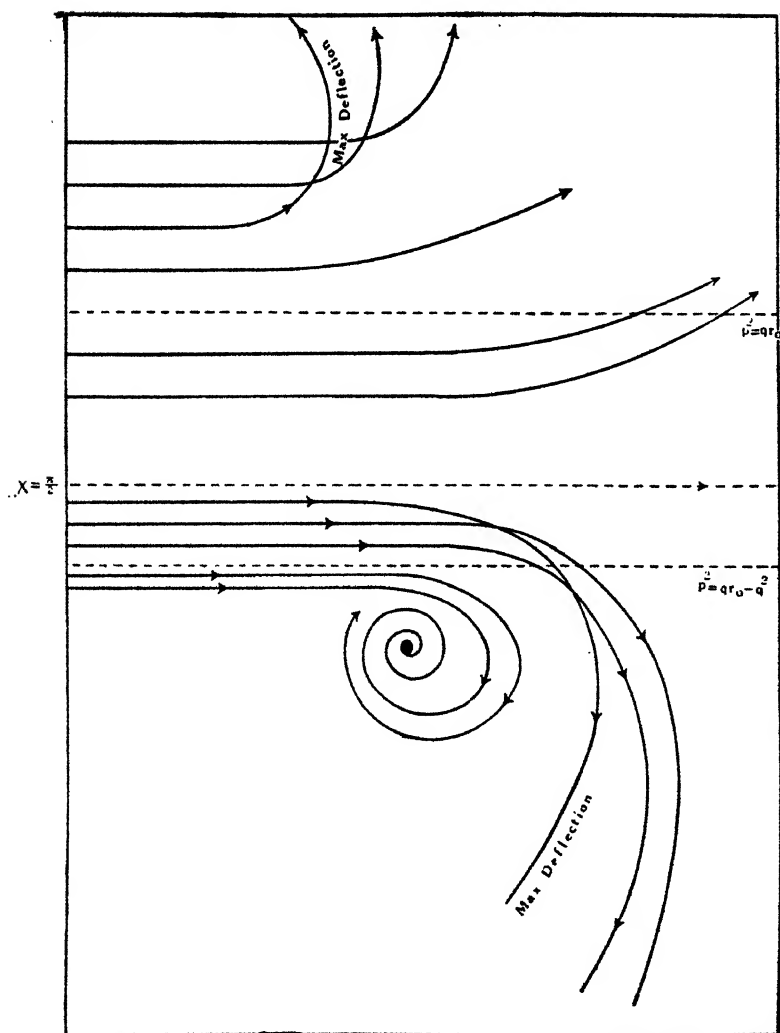
$$0 < x_0 < \frac{\pi}{2}.$$

For the region  $p > p_2$ , where  $p_2 < \sqrt{qr_0}$ , and  $p_2$  is given by

$$\tanh \sqrt{qr_0 - p_2^2} \cdot \frac{\pi}{2p_2} = \frac{1}{q} \sqrt{qr_0 - p_2^2}, \quad (11 B)$$

provided  $x_n > \frac{\pi}{2}$ , the  $\alpha$ -particle returns back to infinity without going round the nucleus.

Fig. 1.



Actual diagram of orbits calculated according to the law

$$F = \frac{2Ze^2}{r^2} \left(1 - \frac{r_0}{r}\right).$$

The figures have been drawn for the case  $r_0 = 2q$ , where  $q = \frac{2Ze^2}{Mv_0^2}$ . The three regions, (1)  $p^2 > qr_0$ , (2)  $p^2 < qr_0$  but  $> qr_0 - q^2$ , are shown by the two dotted lines. The intermediate dotted line, with arrow, is the line of demarcation between orbits going round the nucleus and orbits not going round the nucleus. The spirals inside  $p^2 = qr_0 - q^2$  show the path taken by the  $\alpha$ -particle as it approaches the nucleus (shown by the heavy dot), and causes artificial disintegration by ultimately falling into it.



For the region  $p < p_2$ , provided  $r_0 \leq q$ , otherwise for the region  $\sqrt{qr_0 - q^2} < p < p_2$ , provided  $r_0 > q$  and  $p_2 > \sqrt{qr_0 - q^2}$ , the  $\alpha$ -particle goes round the nucleus and returns back to infinity.

As before, for the region  $p \leq \sqrt{qr_0 - q^2}$ , where  $r_0 > q$ , the  $\alpha$ -particle falls into the nucleus.

If  $x_n < \frac{\pi}{2}$ , or if  $p_2 < \sqrt{qr_0 - q^2}$ , the  $\alpha$ -particle never goes round the nucleus.

It is to be noticed that  $q \propto Z$  the atomic number. If we also suppose that the attractive inverse cube-law force has magnetic origin, then  $r_0$  varies as  $\frac{1}{Z}$  roughly, because the resultant magnetic moment of the nucleus will be the vector sum of the individual magnetic moments of the constituent particles. For artificial disintegration of the nucleus the  $\alpha$ -particle must fall into the nucleus and shatter it. For this  $r_0$  must be  $> q$ . So we find that the lighter atoms for which  $r_0 > q$  can only be artificially disintegrated.

Protons are released from the nucleus both in the forward and backward directions. It has been suggested by Rutherford and Andrade \* that, when the release is in the forward direction, the  $\alpha$ -particle does not go round the nucleus, but when the release is in the backward direction the  $\alpha$ -particle goes round the nucleus. This is in agreement with the mathematical result obtained above.

We now treat the problem of scattering by wave-mechanics, taking the potential to be given by

$$V = 2e^2Z \left( \frac{1}{r} - \frac{\beta}{r^2} \right) e^{-\frac{2rZ}{a}}, \quad \dots \quad (7')$$

where  $\beta = \frac{r_0}{2}$ , which is small, and, we shall see later, is of the order  $10^{-14}$  cm., and " $a$ ," the radius of the hydrogen atom, is of the order  $10^{-8}$  cm.

Potential vanishes at

$$r = \beta.$$

The law deviates appreciably from that of inverse square law when  $r$  is of the order  $10^{-13}$  cm. or less,  $Z$  can never be larger than 100. Therefore the exponential factor is at most of the order  $e^{-1/1000}$ , which differs little from unity.

Outside the atomic radius the potential falls rapidly, and ultimately  $V$  will be negligible.

\* Andrade, 'The Structure of Atoms,' p. 99.

We follow Born's method, using Sommerfeld's notation.  
The wave equation for the total system is

$$\nabla^2 \psi + \frac{8\pi^2 M}{h^2} (E - V) \psi = 0. \quad \dots (12)$$

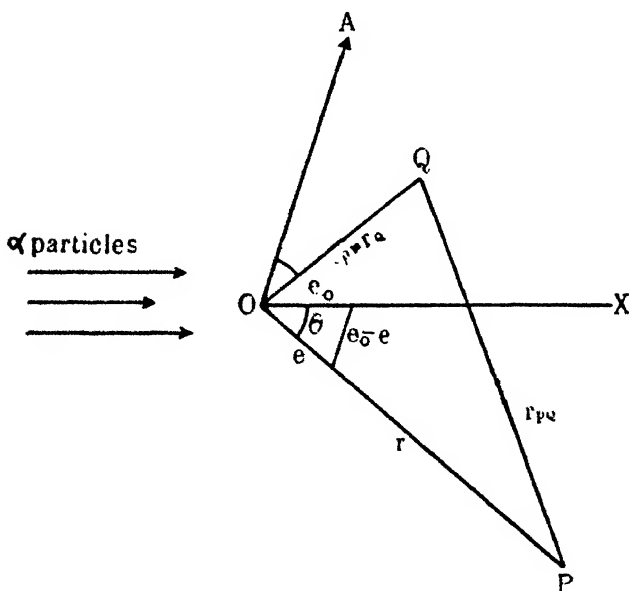
Put  $k^2 = \frac{8\pi^2 ME}{h^2},$

and write  $\psi = \psi_0 + \psi_1, \dots (13)$

where  $\psi_0$  is due to the on-coming plane wave of  $\alpha$ -particles, and  $\psi_1$  is due to scattering and has the spherical wave-form.

$\psi_1$  is small compared with  $\psi_0$ , and also  $V\psi_0$  is small in comparison with  $\psi_0$  and  $\nabla^2 \psi_0$ .

Fig. 2.



We get the two equations

$$\left. \begin{aligned} \nabla^2 \psi_0 + k^2 \psi_0 &= 0, \\ \nabla^2 \psi_1 + k^2 \psi_1 &= \frac{k^2 V}{E} \psi_0. \end{aligned} \right\} \dots (12A)$$

We obtain the solution

$$\left. \begin{aligned} \psi_0 &= e^{ikx_Q}, \\ \psi_1 &= -\frac{k^2}{4\pi E} \int V(r_Q) \frac{e^{ikr_{PQ}}}{r_{PQ}} e^{ikx_Q} d\tau; \end{aligned} \right\} \dots (14)$$

where "O" is the centre of the atom, the element of volume  $d\tau$  is situated at Q at a distance  $r_Q$  from "O", scattering is observed at P at a distance  $r$  from "O".

OX is drawn parallel to the motion of the on-coming  $\alpha$ -particles.

Take  $e$  and  $e_0$  as unit vectors in the directions of  $r$  and  $x$ ,  $r$  is large compared with  $r_Q$ , which is of the order of atomic radius.

As a first approximation,

$$r_{PQ} = r - (e, r_Q),$$

$$x_Q = (e_0, r_Q).$$

Hence

$$\psi_1 = -\frac{k^2}{4\pi E} \frac{e^{ikr}}{r} \int V(r_Q) \left\{ 1 + \frac{(e, r_Q)}{r} \right\} e^{ik(e_0 - e, r_Q)} d\tau. \quad (15)$$

Now take  $r_Q = \rho$ , and also we have

$$(e_0 - e, r_Q) = 2\rho \sin \frac{\theta}{2} \cos \phi,$$

$$(e, r_Q) = \rho \sin \left( \phi - \frac{\theta}{2} \right),$$

where

$$\angle XOP = \theta \quad \text{and} \quad \angle AOQ = \phi,$$

OA being drawn parallel to vector  $e_0 - e$ .

$$\begin{aligned} \therefore \psi_1 = & -\frac{k^2}{4\pi E} \frac{e^{ikr}}{r} \int V(r_Q) \\ & \times \left\{ 1 + \frac{\rho}{r} \sin \left( \phi - \frac{\theta}{2} \right) \right\} e^{i2k\rho \sin \frac{\theta}{2} \cos \phi} d\tau. \end{aligned}$$

Take  $\rho, \phi, \chi$  as polar coordinates.

As potential becomes practically negligible at a distance greater than the atomic radius, the integral can be taken throughout all space without any serious error.

Substituting the value of  $V(r_Q)$  and putting  $r_Q = \rho$ , we get

$$\begin{aligned} \psi_1 = & -\frac{k^2 e^2 Z}{2\pi E} \frac{e^{ikr}}{r} \int_0^{2\pi} \int_0^\pi \int_0^\infty \left( \frac{1}{\rho} - \frac{\beta}{\rho^2} \right) \\ & \times \left\{ 1 + \frac{\rho}{r} \sin \left( \phi - \frac{\theta}{2} \right) \right\} e^{-\frac{2Z}{a}\rho + i2k \sin \frac{\theta}{2} \cos \phi \cdot \rho} \cdot \rho^2 \sin \phi d\rho d\phi d\chi. \end{aligned}$$

Put  $c = \frac{2Z}{a}, \quad d = 2k \sin \frac{\theta}{2}.$

Then

$$\psi_1 = \frac{-k^2 e^2 Z}{E} \cdot \frac{e^{ikr}}{r} \int_0^\pi \sin \phi \, d\phi \int_0^\infty (\rho - \beta) \times \left\{ 1 + \frac{\rho}{r} \sin \left( \phi - \frac{\theta}{2} \right) \right\} e^{-(e - id \cos \phi) \cdot \rho} \cdot d\rho.$$

Integrating, we get after some work and putting

$$k = \frac{2\pi}{\lambda}, \quad \lambda = \frac{h}{MV}, \quad \alpha = \frac{\lambda}{a} \frac{Z}{2\pi},$$

and remembering that

$\lambda$  is of the order  $10^{-13}$  cm.,

$\alpha$  is of the order  $10^{-3}$ ,

$\beta$  is of the order  $10^{-13}$  cm.,

$r$  is finite,

$$\psi_1 = \frac{-e^2 Z}{2E} \cdot \frac{e^{i \frac{2\pi}{\lambda} r}}{r} \left[ \frac{1}{\sin^2 \frac{\theta}{2}} - \frac{4\pi\beta}{\lambda} \frac{\tan^{-1} \left( \frac{2a\pi}{Z\lambda} \sin \frac{\theta}{2} \right)}{\sin \frac{\theta}{2}} \right] \quad (15A)$$

$$\therefore |\psi_1| = \left( \frac{e^2 Z}{2Er} \right) \left| \frac{1}{\sin^2 \frac{\theta}{2}} - \frac{4\pi\beta}{\lambda} \frac{\tan^{-1} \left( \frac{2a\pi}{Z\lambda} \sin \frac{\theta}{2} \right)}{\sin \frac{\theta}{2}} \right|.$$

Also

$$|\psi_0| = 1.$$

If  $W$  is the probability of scattering, then

$$W = \left| \frac{\psi_1}{\psi_0} \right|^2 = \left( \frac{e^2 Z}{2Er} \right)^2 \left\{ \frac{1}{\sin^2 \frac{\theta}{2}} - \frac{4\pi\beta}{\lambda} \frac{\tan^{-1} \left( \frac{2a\pi}{Z\lambda} \sin \frac{\theta}{2} \right)}{\sin \frac{\theta}{2}} \right\}^2. \quad (16)$$

Let  $W_0$  be the probability of scattering according to the inverse square law, then

$$W_0 = \left( \frac{e^2 Z}{2Er} \right)^2 \frac{1}{\sin^4 \frac{\theta}{2}}.$$

$$\therefore \frac{W}{W_0} = \left\{ 1 - \frac{4\pi\beta}{\lambda} \tan^{-1} \left( \frac{2\pi a}{\lambda Z} \sin \frac{\theta}{2} \right) \cdot \sin \frac{\theta}{2} \right\}^2. \quad (17)$$

We draw a curve, taking  $\frac{W}{W_0}$  as ordinate and  $\theta$  as abscissa.

It is clear that at  $\theta=0^\circ$  the curve has the horizontal tangent  $\frac{W}{W_0}=1$ . So we find that the additional inverse cube power term in the law of force has practically no effect on the scattering at very small angles, contrary to what Bieler thought.

Now

$$\frac{2\pi a}{\lambda Z} > \frac{2\pi \times 2.4 \times 10^{-8}}{6 \times 10^{-13} \times 10^2} > 2.5 \times 10^8,$$

as  $Z$  is never greater than 100.

So if  $\theta$  is not very small ( $> 3^\circ$ ), we have

$$\tan^{-1} \left( \frac{2\pi a}{\lambda Z} \sin \frac{\theta}{2} \right) = \frac{\pi}{2}, \quad \text{approx. } (> 89^\circ).$$

We can write

$$\frac{W}{W_0} = \left( 1 - \frac{2\pi^2\beta}{\lambda} \sin \frac{\theta}{2} \right)^2. \quad \dots (17A)$$

#### *Scattering of $\alpha$ -particles by Aluminium\*.*

$\alpha$ -particles from radium C of mean range 6.6 cm. were made to bombard aluminium nucleus. The curve obtained by Bieler from experimental data may approximately be represented by

$$\frac{W}{W_0} = \left( 1 - .25 \sin \frac{\theta}{2} \right)^2. \quad \dots (17B)$$

The curves given by the above formula, as well as the curve obtained from actual data by Bieler, are drawn together for the sake of comparison. We give below some of the calculated values obtained from the formula:—

$$\begin{array}{ll} \theta = 100^\circ, & \frac{W}{W_0} = .66; \quad \theta = 70^\circ, \quad \frac{W}{W_0} = .74; \\ \theta = 90^\circ, & \frac{W}{W_0} = .68; \quad \theta = 60^\circ, \quad \frac{W}{W_0} = .77; \\ \theta = 80^\circ, & \frac{W}{W_0} = .705; \quad \theta = 40^\circ, \quad \frac{W}{W_0} = .84. \end{array}$$

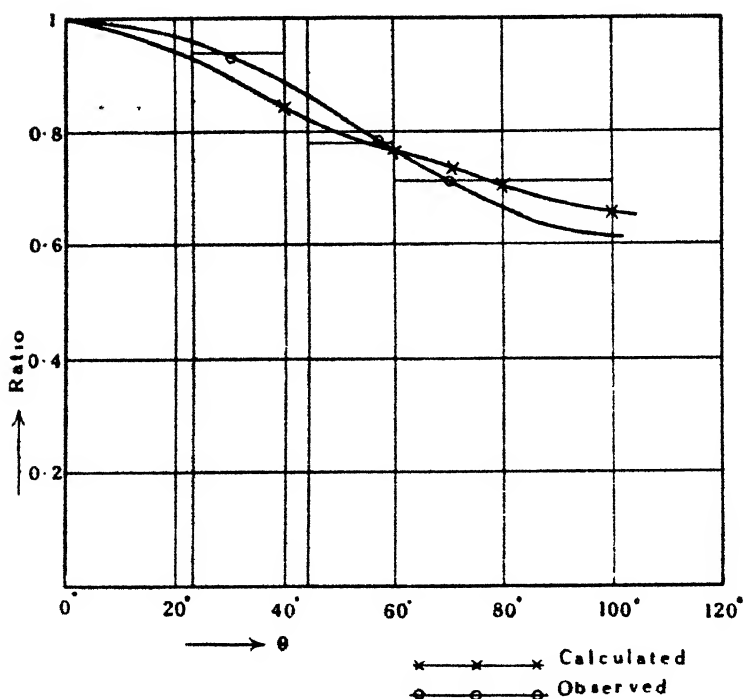
\* For observed data see Bieler, Proc. Roy. Soc. cv. p. 445 (1924).

Now for range 6.6 cm. the velocity is  $1.89 \times 10^9$  cm.

$$\therefore \lambda = \frac{h}{Mv} = \frac{6.55 \times 10^{-27}}{6.56 \times 10^{-24} \times 1.89 \times 10^9} \text{ cm.} = 5.3 \times 10^{-13} \text{ cm.}$$

$$r_0 = 2\beta = \frac{2 \times 127 \lambda}{\pi^2} = 1.4 \times 10^{-14} \text{ cm.}$$

Fig. 3.



### Scattering by Aluminium.

The ordinate represents the ratio  $\frac{W}{W_0}$ ,  $W$  = observed or calculated scattering,  $W_0$  = scattering calculated according to inverse square law.

This seems to be of the right order in dimension. The effect of the attractive force will be appreciable at 10 times or 20 times this distance. This force may have magnetic origin. At distance  $10r_0$  it will be  $1/10$  of the electrostatic force and at distance  $20r_0$  it will be  $1/20$  of the electrostatic force, and so on; if this additional attractive

force has magnetic origin, then  $\beta Z$  will be constant—i. e.,  
 $r_0 \propto \frac{1}{Z}$ .

Moreover,  $\beta$  or  $r_0$  should also vary with the velocity of the bombarding  $\alpha$ -particle.

*Scattering of  $\alpha$ -particles by Magnesium\*.*

$\alpha$ -particles from Ra C of mean range 6.2 cm. are made to bombard on magnesium. The curve obtained may be approximately represented by

$$\frac{W}{W_0} = \left(1 - .26 \sin \frac{\theta}{2}\right)^2. \quad . \quad . \quad (17c)$$

The curve given by the above formula, as well as the curve obtained by Bieler from actual data, are drawn together for the sake of comparison.

We give below some of the calculated values:—

$$\theta = 100^\circ, \quad \frac{W}{W_0} = .64; \quad \theta = 70^\circ, \quad \frac{W}{W_0} = .73;$$

$$\theta = 90^\circ, \quad \frac{W}{W_0} = .67; \quad \theta = 60^\circ, \quad \frac{W}{W_0} = .76;$$

$$\theta = 80^\circ, \quad \frac{W}{W_0} = .71; \quad \theta = 40^\circ, \quad \frac{W}{W_0} = .83.$$

Now for range 6.2 cm.  $v = 1.84 \times 10^9$  cm.

$$\therefore \lambda = \frac{6.55 \times 10^{-27}}{6.56 \times 10^{-24} \times 1.84 \times 10^9} \text{ cm.} = 5.4 \times 10^{-13} \text{ cm.}$$

$$\therefore r_0 = 2\beta = \frac{2 \times .13\lambda}{\pi^2} = 1.5 \times 10^{-14} \text{ cm.}$$

Both in the case of magnesium and aluminium we have neglected the motion of the nucleus, as even for such a large angle of scattering as  $100^\circ$  the correction for this is only 1.5 per cent. This is considerably less than the experimental error involved.

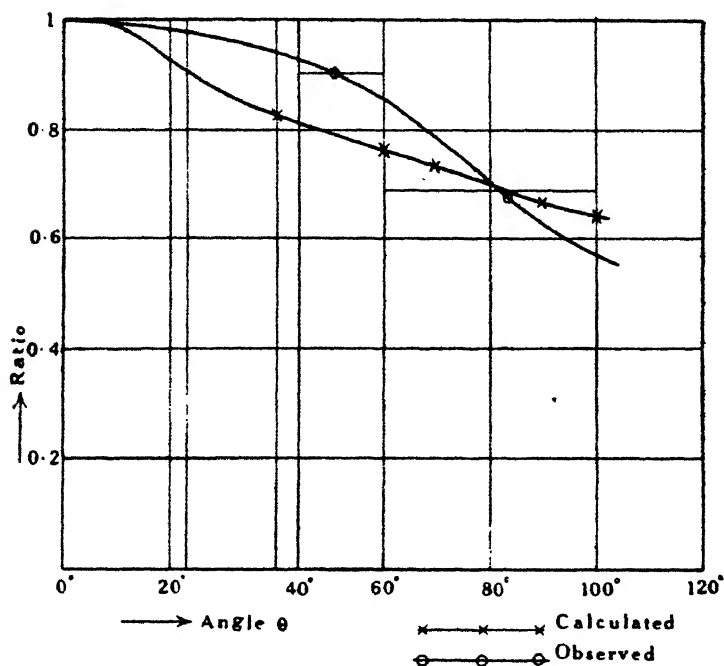
Bieler's data for aluminium and magnesium do not seem to be quite satisfactory. For  $\alpha$ -particles of mean range 6.6 cm.

bombarding aluminium nucleus the ratio  $\frac{W}{W_0}$  between  $23^\circ$  and

\* For observed data see Bieler, Proc. Roy Soc. cv. p. 445 (1924).

and  $44^{\circ}2$  was found to be  $0.94 \pm 0.02$ , and this ratio between  $43^{\circ}9$  and  $59^{\circ}7$  was found to be  $0.78 \pm 0.02$ . So that at  $44^{\circ}$  it is not clear whether this ratio has the value  $0.92$  or  $0.8$ . Again, for  $\alpha$ -particles of mean range  $3.0$  cm. bombarding magnesium nucleus the ratio  $\frac{W}{W_0}$  between  $43^{\circ}9$  and  $59^{\circ}7$

Fig. 4.



## Scattering by Magnesium.

The ordinate represents the ratio  $\frac{W}{W_0}$ ,  $W$  = observed or calculated scattering,  $W_0$  = scattering calculated according to inverse square law.

has the value  $1.05 \pm 0.06$ , whereas between  $60^{\circ}3$  and  $99^{\circ}5$  this ratio has the value  $0.79 \pm 0.08$ . It seems therefore that the decrease in the value of  $\frac{W}{W_0}$  at  $60^{\circ}$  is too abrupt.

It seems desirable that the experiments should be repeated



There is some experimental evidence that  $r_0$  varies as the velocity of bombarding  $\alpha$ -particles.

$\alpha$ -particles from polonium of mean range 3 cm. are made to bombard magnesium nucleus. In this case our curve can be roughly represented by

$$\frac{W}{W_0} = \left(1 - .18 \sin \frac{\theta}{2}\right)^2 \quad \dots \quad (17 D)$$

We write some calculated values :

$$\theta = 90^\circ, \quad \frac{W}{W_0} = .76 ;$$

$$\theta = 80^\circ, \quad \frac{W}{W_0} = .79.$$

For range 3.0 cm.  $v = 1.45 \times 10^9$  cm.

$$\therefore \lambda = \frac{6.55 \times 10^{-27}}{6.56 \times 10^{-24} \times 1.45 \times 10^9} \text{ cm.} = 6.9 \times 10^{-13} \text{ cm.}$$

$$\therefore r_0 = 2\beta = \frac{.18\lambda}{\pi^2} = \frac{.18 \times 6.9 \times 10^{-13}}{9.93} = 1.251 \times 10^{-14} \text{ cm.}$$

$$\therefore \frac{(r_0)_{3 \text{ cm. range}}}{(r_0)_{6.2 \text{ cm. range}}} = \frac{1.25}{1.5} = .83.$$

$$\text{Also} \quad \frac{(v_0)_{3 \text{ cm. range}}}{(v_0)_{6.2 \text{ cm. range}}} = \frac{1.45}{1.84} = .79.$$

$\therefore r_0$  varies roughly as  $v$  for the same element.

This may be taken as some experimental evidence for the magnetic origin of the forces, because the ponderomotive force on a charged particle in a magnetic field varies as the velocity of the particle.

Scattering as a function of energy of  $\alpha$ -particles :

In fig. 5 is represented the curves in which  $\frac{W}{W_0}$  is plotted against  $\frac{1}{E}$  for aluminium and magnesium, for a given angle of scattering ( $\theta = 135^\circ$ ). Our formula can now be re-written as a function of  $\frac{1}{E}$ . We get

$$\frac{W}{W_0} = \left(1 - \frac{C}{x^{\frac{1}{2}}}\right)^2, \quad \dots \quad (17 E)$$

where

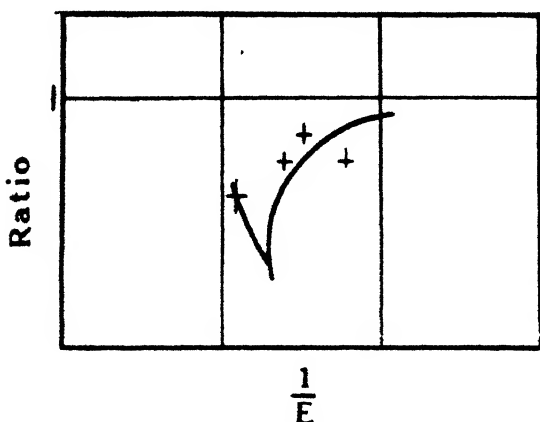
$$x = \frac{1}{E},$$

and

$$C = \frac{2\pi^2\beta}{h} \sqrt{2M}.$$

The formula can be made to represent the curve on either side of the minimum, but there is discrepancy near about the minimum. The minimum value, according to formula, of  $\frac{W}{W_0}$  is 0, whereas according to experimental results the minimum is about .3.

Fig 5.



It is impossible to remove this discrepancy with whatever law of force we may work, since  $\left| \frac{\psi_1}{\psi_0} \right|^2$  will always occur as a square and will have the minimum value zero. Hence the discrepancy is to be ascribed to our use of the Schrödinger electron.

It is now admitted that since the Schrödinger form of the wave-equation of the electron does not give the proper relativity correction, and fails also to take into account the magnetic properties of the electron (rotating electron), it should be replaced by a better model. At the present time Dirac's model of the electron and wave-equation is holding the field. One of the features of this theory is the introduction of four  $\psi$ -functions in place of one, and in normalizing we have to take the sum of their squares instead of the

square of a single  $\psi$ . The Dirac equation for the  $\alpha$ -particle or any positive particle has not yet been framed. Attempts are being made in this direction.

The cases of hydrogen and helium have to be treated differently in a separate paper. In the case of hydrogen nucleus we observed the disintegrated hydrogen particles instead of scattered  $\alpha$ -particles, and in the case of helium we observe both the protons from helium nucleus as well as scattered  $\alpha$ -particles. Moreover, in these two cases we cannot neglect the motion of the nucleus.

I have great pleasure in thanking my colleague, Prof. M. N. Saha, F.R.S., of Allahabad University, for much help and many valuable suggestions in preparing this paper.

Mathematics Department,  
University of Allahabad,  
November 20, 1929

XXVII. *The Ionization-Formula and the New Statistics.*  
By S. CHANDRASEKHAR\*.

(1) *Introduction.*

THE derivation of the formula

$$\frac{n_+ \cdot n_-}{n} = \frac{1}{h^3} (2\pi m k T)^{3/2} \cdot e^{-\chi/kT} \cdot \sigma.$$

( $n_+$  = the number of ionized atoms,

$n_-$  = the number of electrons,

$n$  = the number of neutral atoms)

has attracted much attention after its first derivation by Saha. The rigorous way of deriving the above equation has been successfully attempted by Fowler†; but no attention has so far been given to modifying the above formula on the new statistics of Fermi-Dirac. Obviously it will be of no practical importance if in the application of the new statistics we treat all the constituents—the atoms of both kinds and

\* Communicated by the Author.

† R. H. Fowler, *Phil. Mag.* xlv. p. 1 (1923); also Fowler and Milne, 'Monthly Notices,' R. A. S. lxxxiii. p. 407 (1923). A simple way of deriving the equation (1) has been given by W. F. G. Swann, *Journ. of Frank. Inst.* cc. p. 591 (1925).

the electrons—as degenerate, because the ionization formula, being most applied to the thermodynamics of a star, would not justify our assumption as to the degeneracy of the atoms themselves. But the electrons, even at that high temperature, if the pressure is sufficiently high, will be a degenerate system \*. Thus Sommerfeld's † condition of degeneracy,

$$\frac{nh^3}{2} \cdot \frac{1}{(2\pi mkT)^{3/2}} > 1 \quad \dots \quad (2)$$

gives, if the number of electrons per c.c. is  $10^{30}$ , the system to be degenerate up to temperatures below  $3 \cdot 5^\circ \times 10^9$ , and if  $n = 10^{27}$  the system will be degenerate even up to a temperature of  $3^6 \times 10^7$ .

The object of this paper is to modify the ionization formula on the Fermi-Dirac statistics for the degeneracy of the electrons. But, before dealing with that problem, the case of complete degeneracy will be discussed. The modified formula when the degeneracy of the electrons alone is considered will follow naturally from the case of complete degeneracy.

## (2) General Relation between $n_+$ , $n$ , and $n_-$ .

According to the new statistics of Fermi-Dirac, the entropy of a system is given by ‡

$$S = nk \left[ \frac{5}{2} \frac{U_{3/2}}{U_{1/2}} - \log A \right], \quad \dots \quad (3)$$

where  $U_{3/2}$  and  $U_{1/2}$  are the special cases of the general Sommerfeld § integral

$$U_\rho = \frac{1}{\Gamma(\rho+1)} \int_0^\infty \frac{u^\rho du}{\frac{1}{A} e^u + 1} \quad \dots \quad (4)$$

For a mixture of gases the entropy is given by

$$S = \sum kn_v \left[ \frac{5}{2} \frac{U_{3/2}}{U_{1/2}} - \log A_v \right]. \quad \dots \quad (5)$$

In the case under consideration, that of a monatomic gas dissociating into positive ions and electrons, the summation comprises these terms.

\* In this connexion, see an interesting contribution by Dr. E. C. Stoner, *Phil. Mag.* vii. p. 63 (1929).

Sommerfeld, *Zeits. f. Phys.* xlvii. p. 1 (1928).

† Fermi, *Zeits. f. Phys.* xxxvi. p. 902 (1926).

§ Sommerfeld, *Zeits. f. Phys.* xlvii. p. 1 (1928).

If  $\delta n$  represents an arbitrary change in the number of neutral atoms,  $\delta n_+$  and  $\delta n_-$  the corresponding changes for the positive ions and the electrons, the corresponding change in the entropy is given by

$$\begin{aligned}\delta S &= \Sigma \frac{\partial}{\partial n} \left[ nk \left\{ \frac{5}{2} \frac{U_{3/2}}{U_{1/2}} - \log A \right\} \right] \\ &= \Sigma \left\{ k \left[ \frac{5}{2} \frac{U_{3/2}}{U_{1/2}} - \log A \right] \right. \\ &\quad \left. + nk \frac{\partial}{\partial A} \left[ \frac{5}{2} \frac{U_{3/2}}{U_{1/2}} - \log A \right] \times \frac{\partial A}{\partial n} \right\} \delta n. \quad (6)\end{aligned}$$

Now

$$\frac{\partial}{\partial A} \left[ \frac{5}{2} \frac{U_{3/2}}{U_{1/2}} - \log A \right] = \left\{ \frac{5}{2} \left[ \frac{U'_{3/2}}{U_{1/2}} - \frac{U_{3/2} \cdot U'_{1/2}}{U_{1/2}^2} \right] - \frac{1}{A} \right\}. \quad (7)$$

Now

$$\begin{aligned}U_{\rho}' &= \frac{1}{\Gamma(\rho+1)} \int_0^{\infty} \frac{1}{A^2} \cdot \frac{u^{\rho} du}{\left( \frac{1}{A} e^u + 1 \right)^2} \\ &= -\frac{1}{\Gamma(\rho+1)} \int_0^{\infty} \frac{1}{A} u^{\rho} \cdot \frac{\partial}{\partial u} \left( \frac{1}{\frac{1}{A} e^u + 1} \right) du \\ &= \frac{1}{A} U_{\rho-1}. \quad \dots \dots \dots (8)\end{aligned}$$

Using relation (8), we get for

$$\begin{aligned}\delta S &= \Sigma \left\{ k \left[ \frac{5}{2} \frac{U_{3/2}}{U_{1/2}} - \log A \right] \right. \\ &\quad \left. + \frac{nk}{A} \left[ \frac{3}{2} - \frac{5}{2} \frac{U_{3/2} \cdot U_{-1/2}}{U_{1/2}^2} \right] \frac{\partial A}{\partial n} \right\} \delta n. \quad (9)\end{aligned}$$

If  $Q$  is the heat absorbed due to the ionization of  $\delta n$  atoms,

$$\delta S = \frac{Q}{T} = \frac{-\chi \delta n + \Sigma \frac{\partial E}{\partial n} \cdot \delta n}{T} \quad \dots \dots (10)$$

Now  $E$  is given in the new statistics by the expression

$$E = \frac{3}{2} \frac{VGkT}{h^3} \cdot (2\pi mkT)^{3/2} \cdot U_{3/2}. \quad \dots (11)$$

Then

$$\frac{\partial E}{\partial n} = \frac{3}{2} \frac{VGkT}{h^3} \cdot (2\pi mkT)^{3/2} \frac{1}{A} U_{1/2} \cdot \frac{\partial A}{\partial n} \dots (12)$$

Hence we get, using relation (12),

$$\delta S = \frac{\chi}{T} \delta n + \sum \frac{3}{2} V k \beta_v \cdot \frac{1}{A} U_{1/2} \frac{\partial A}{\partial n} \delta n, \dots \quad (10a)$$

where we put

$$\beta_v = \frac{(2\pi m_v k T)^{3/2}}{h^3} \cdot G. \dots \quad (10b)$$

Equating (9) and (10a), we get the general relation applicable to the new as well as the classical statistics,

$$\begin{aligned} \sum k \left[ \frac{5}{2} \frac{U_{3/2}}{U_{1/2}} - \log A \right] + \sum \frac{n k}{A} \left[ \frac{3}{2} - \frac{5}{2} \cdot \frac{U_{3/2} \cdot U_{-1/2}}{U_{1/2}^2} \right] \frac{\partial A}{\partial n} \\ = -\frac{\chi}{T} + \frac{3}{2} \sum V k \beta \cdot \frac{1}{A} \frac{\partial A}{\partial n} \cdot U_{1/2}. \dots \quad (13) \end{aligned}$$

### (3) The Classical Ionization Formula.

With the help of relation (13) we will arrive at the classical result (1) already quoted. The classical statistics correspond to a non-degenerate system, where in the distribution function  $A \ll 1$ .

In that case

$$U_p = U_{p-1} = \dots = U_{3/2} = U_{1/2} = U_{-1/2} = A \quad (14)$$

$$\begin{aligned} \text{and} \quad A &= \frac{n h^3}{V G} \cdot (2\pi m k T)^{-3/2} \\ &= \frac{n}{V \beta} \dots \dots \dots \quad (15) \end{aligned}$$

Substituting relations (14) and (15) in (13), we get

$$-k \sum \log A_v = -\frac{\chi}{T}, \dots \dots \quad (16)$$

$$-\log \frac{n}{V \beta} + \log \frac{n_+}{V \beta_+} + \log \frac{n_-}{V \beta_-} = -\frac{\chi^*}{k T}. \quad (16a)$$

Substituting values for  $\beta$ , we get at once the classical dissociation formula

$$\frac{n_+ n_-}{n} = \frac{V}{h^3} \cdot (2\pi m k T)^{3/2} \cdot G e^{-\chi/k T}, \dots \quad (17)$$

which is identical with equation (1). In the application of

\* The positive sign is given to  $\log n_+$  and  $\log n_-$  because we have taken  $\delta n$  as an increase in the neutral atoms, and therefore  $\delta n_+$  and  $\delta n_-$  are negative. Also

$$\delta n = \delta n_+ = \delta n_-.$$

this formula  $G$  can be omitted ( $G = 2$ , corresponding to spin statistical weight).

(4) *A Completely Degenerate System.*

For this we start again with the fundamental equation (13). In this case the values for  $U_\rho$  and  $A$  are completely different, and, as it will be seen, this complicates the ionization formula. Now

$$U_\rho = \frac{u_0^{\rho+1}}{\Gamma(\rho+2)} \times \left[ 1 + 2 \left\{ \frac{(\rho+1)\rho \cdot c_2}{u_0^2} + \frac{(\rho+1)\rho \cdot (\rho-1)(\rho-2) c_4}{u_0^4}, \dots \right\} \right], \quad (18)$$

where

$$u_0 = \log A, \quad \dots \quad (18a)$$

and

$$c_\nu = 1 - \frac{1}{2^\nu} + \frac{1}{3^\nu} - \frac{1}{4^\nu}, \quad \dots \quad (19)$$

giving in the special case for  $\nu = 2$  the value  $\pi^2/12$ . The value for  $A$  in the case of degeneracy is also given by

$$\log A_\nu = \frac{h^2}{2m_\nu kT} \left( \frac{3n_\nu}{4\pi G} \right)^{2/3} \quad \dots \quad (20)$$

$$= \frac{\alpha n^{2/3}}{mkT} \quad \dots \quad (21)$$

Equation (13) modified by the substitution of the values for  $U_{3/2}$ ,  $U_{1/2}$ , and  $U_{-1/2}$  in the following manner:

$$\begin{aligned} \Sigma \frac{k\pi^2}{2} (\log A_\nu)^{-1} - \Sigma \frac{nk\pi^2}{2} (\log A_\nu)^{-2} \cdot \frac{1}{A_\nu} \frac{\partial A_\nu}{\partial n} \\ = -\frac{\chi}{T} + \frac{3}{2} \Sigma V k \beta_\nu \cdot \frac{4}{3} \sqrt{\pi} (\log A_\nu)^{3/2} \\ \times \left[ 1 + \frac{\pi^2}{8 (\log A_\nu)^2} \dots \right] \frac{1}{A_\nu} \frac{\partial A_\nu}{\partial n} \quad \dots \quad (22) \end{aligned}$$

Relation (21) gives

$$\frac{1}{A} \frac{\partial A}{\partial n} = \frac{2}{3} \frac{\alpha n^{-1/3}}{mkT} \quad \dots \quad (23)$$

Making all the necessary simplifications, we get

$$\begin{aligned} \Sigma \frac{k\pi^2}{6} \frac{mkT}{\alpha n^{2/3}} - \Sigma \frac{2^{7/2} \cdot \pi^2 V \alpha^{5/2} G}{3h^3 mT} \cdot n^{2/3} \\ - \Sigma \frac{\pi^4 V}{6h^3} \cdot \frac{2^{3/2} k^2 \alpha^{1/2} mTG}{n^{2/3}} = -\frac{\chi}{T} \quad \dots \quad (24) \end{aligned}$$

Taking the volume as unity, we get our final ionization formula,

$$\frac{k^2\pi^2T}{6} \left[ \frac{1}{\alpha} - \frac{G\pi^2 2^{3/2} \alpha^{1/2}}{h^3} \right] \left[ m \left( \frac{1}{n_+^{2/3}} - \frac{1}{n_+^{2/3}} \right) - \frac{m_-}{n_-^{2/3}} \right] - \frac{2^{7/2} \pi^2 \alpha^{5/2} G}{3h^3 T} \left[ \frac{1}{m} (n_+^{2/3} - n_+^{2/3}) - \frac{n_-^{2/3}}{m_-} \right] = -\frac{\chi}{T}. \quad (25)$$

(5) *Ionization Formula for the Degeneracy of the Electrons only.*

As has been pointed out, a modification of the ionization formula will be useful only if the electrons alone are treated as degenerate. This can easily be done, if in summing up the entropy of the system in equation (5), we use for the atoms the classical values for  $U_{3/2}$ ,  $U_{1/2}$ ,  $U_{-1/2}$ , and  $A$ , and the corresponding values in the case for degeneracy for the electrons. Using relations (16) and (24), we get our ionization formula, taking into consideration the degeneracy of the electrons alone :

$$k \log \frac{n_+}{n} - \frac{k^2\pi^2T}{6} \left[ \frac{1}{\alpha} - \frac{G\pi^2 2^{3/2} \alpha^{1/2}}{h^3} \right] m_- n_-^{-2/3} + \frac{2^{7/2} \pi^2 \alpha^{5/2}}{3h^3 T} \cdot \frac{n_-^{2/3}}{m_-} = -\frac{\chi}{T}. \quad (26)$$

Equation (26) can be put in the more convenient form

$$\log \frac{n_+}{n} = -\frac{\chi}{kT} + \Phi n^{-2/3} T - \Theta n^{2/3} T^{-1}, \quad (27)$$

where  $\Phi$  and  $\Theta$  have the obvious equivalents, which can be seen by comparison with equation (26). Finally, we get

$$\frac{n_+}{n} = e^{\Phi n^{-2/3} T - \Theta n^{2/3} T^{-1} - \chi/kT}. \quad (28)$$

(6) *Numerical Calculations and Discussion with Reference to the Theory of Dwarf Stars.*

Formulæ (17) and (28) are the classical and the modified ionization formulæ connecting the ionization potential, electron-density, and the temperature. If  $x$  is the degree of ionization, we get, on substituting the known numerical values for  $\Phi$  and  $\Theta$ , the final numerical formula in the two cases as

$$\log \frac{1-x}{x} = \frac{\chi}{kT} + \frac{3.34 \times 10^{10} \times T}{n^{2/3}} + \frac{2.1 \times n^{2/3}}{10^{10} \times T}, \quad (29)$$

and 
$$\frac{1-x}{x} = \frac{n \times 4.1 \times 10^{-16}}{T^{3/2}} e^{\chi/kT}. \quad (30)$$



The condition of degeneracy gives that the electrons are degenerate at a temperature of  $10^9$  Å. when the density is  $10^{30}$ . Now we will calculate the degree of dissociation for various temperatures on both the formulæ for an ionization potential corresponding to  $\lambda = 1.22$  Å. The results are tabulated below :—

Electron density =  $10^{30}$  per c.c.,  $\lambda = 1.22$  Å.

Temperature.	$x$ by the classical formula	$x$ by the modified formula (29).
A.	%.	%.
$10^9$	6.4	0
$2 \times 10^9$	17	0
$3 \times 10^9$	28	0
$4 \times 10^9$	38	0
$5 \times 10^9$	45	0

It is very interesting to note that our formula, including the degeneracy of the electrons, gives uniformly 0 per cent. ionization, while the classical formula gives varying degrees. As a matter of fact, it gives 0 per cent. up to a temperature above which the application of the formula itself becomes invalid, due to the Sommerfeld degeneracy condition not being satisfied. The degree of dissociation given by the classical formula has no significance, because the conditions on which the formula has been derived do not hold good at such high pressures.

Our theory predicting zero per cent. ionization goes against the fundamental assumption of Fowler, Stoner, and others in the theory of dwarf stars, where the first postulate is to take for granted the complete ionization in it. The temperature and density we have taken for our calculation of the table roughly correspond to the centre of the Companion of Sirius, and there our formula predicts no ionization.

If that is the case, one may be tempted to question the validity of the fundamental assumption in the theory of dwarf stars. But for all purposes of calculation we can take the electrons as free, if we define a free electron as one which is not under the influence of *one and the same* nucleus for any finite time. Then obviously the electrons at that pressure are free electrons. The "bound electrons" are changing partners continually, and go about knocking, thus really

travelling the whole of the phase-space, just what a "free electron" is expected to do. But, none the less, the statement that *every electron* is under the influence of one or other of the nuclei at any arbitrarily chosen time remains valid. In other words, the ionization is zero, a result predicted by our theory. Thus the paradoxical statement results that the electrons, though all of them bound, are free.

### (7) *Summary.*

In this paper the ionization formula is considered afresh on the Fermi-Dirac statistics. The modified formula where the degeneracy of the electrons is considered gives, under the conditions existing in the interior of a dwarf star, a degree of ionization = 0 per cent. This result is discussed with reference to the theory of dwarf stars, where complete ionization is usually assumed.

The Presidency College,  
Madras, India,  
23rd May, 1929.

XXVIII. *The Raman-Effect in the Proximity of the Critical Point.* By S. L. ZIEMECKI, Ph.D., M.Sc., Lecturer in Physics, High School of Agriculture, Warsaw, and K. NARKIEWICZ-JODKO \*.

### 1. *The Aim of this Work.*

EXPERIMENTING with liquids, we find that some of them give easily strong sharp Raman lines, whilst others require long exposures to obtain Raman spectra consisting of faint badly defined bands. We give below some figures concerning the relative scattering powers of liquids †.

#### *Relative Scattering Powers of Liquids.*

Ethyl-ether . . . . .	1.00
Water . . . . .	0.21
Acetic Acid . . . . .	1.19
Benzene . . . . .	3.15
Paraxylene . . . . .	4.61
Carbon disulphide . . . . .	13.0

\* Communicated by the Authors. Read at the meeting of the Polish Physical Society on October 21st, 1929.

† See J. Cabannes, 'La diffusion moléculaire de la lumière,' Paris, 1929, p. 188.

Certainly it is remarkable that water, which has the smallest scattering power, is also one of the liquids giving the faintest Raman bands, while benzene and its derivatives and carbon disulphide, having great scattering power, give strong Raman spectra. This suggestion has a purely qualitative character, but shows that it would not be quite unreasonable to look for a certain connexion between the Raman effect and classical light scattering.

If we admit that such a connexion exists, we would expect a considerable increase in the intensity of the Raman effect in the proximity of the critical point, where the intensity of classical scattering is increasing hundreds or even thousands of times, causing the phenomenon of critical opalescence. This question was recognized by Raman \* himself to be of fundamental importance. Raman experimented with  $\text{CO}_2$  and further with a mixture of carbon disulphide and methyl-alcohol. In both those cases he found *an increase* of the new radiation in the proximity of the critical point. L. A. Ramdas † repeated the experiment with  $\text{CO}_2$ , and also observed an increased intensity of the effect. The question was taken up by A. Bogros and Y. Rocard ‡, and also by W. H. Martin §. These authors, working with a critical mixture of phenol and water (64 per cent. of water), obtained *absolutely negative* results; they observed no Raman spectra even after an exposure of *three hours*.

So far the problem remained unsolved. Raman himself considered his results as preliminary; he admitted that deeper research would be necessary, because he limited himself to the method of complementary light filters, and did not obtain photographs of the spectra. On the other hand, the experiments of Martin and Bogros-Rocard seemed indecisive: phenol mixtures quickly become coloured, and one could think the negative results were due to the absorption of the new radiation. Whatever it may have been, the above authors should have obtained in their photographs at least the diffused Raman bands of water, because the Raman effect is strictly additive, and with pure water one easily obtains the Raman spectrum

\* Indian Journ. of Physics, ii. pt. 3, p. 387 (1928).

† Ind. Journ. of Physics, iii. pt. 1, p. 131 (1928).

‡ *Comptes Rendus*, clxxxvi. p. 1712 (1928).

§ 'Nature,' October 6, 1928, p. 506.

with an exposure of  $1\frac{1}{2}$  hours. To elucidate the problem, the authors undertook a new line of investigation. The results obtained seem to give a decisive answer to the question, and explain also why the former scientists obtained contradictory results.

## 2. *Experimental Arrangement.*

We used in our experiments isobutyric acid, which with water gives a mixture having the critical temperature at about  $24^{\circ}\text{C}$ .; the mixture contains at the critical point 36.3 per cent. (weight) parts of acid. The isobutyric acid was obtained from Kahlbaum. The preparation, having been in continual use for many months, remained absolutely colourless and possessed the same optical properties as a new sample manufactured by Kahlbaum-Schering.

For a source of light we used a mercury-vapour lamp of a special type\*. The arc was formed in quartz tube of 2 cm. diameter, its length was 20 cm. The anode was cooled by a quick water stream. Thus heavy currents could be used, amounting to 10 amp. in our experiments. The lamp was continuously connected with a mercury diffusion pump.

The light of the lamp was concentrated at the axis of a cylindrical vessel R (see figs. 1-3) by means of a condenser of 16 cm. in diameter. The vessel had flat ends; the end turning to the collimator of the spectrograph was made from a plane-parallel plate fused in a glass tube. Sibor glass was used. The cylindrical part of the vessel R was half-silvered; this silver mirror increased the intensity of the light. To keep a steady temperature the vessel R was immersed in a metal tank filled with water of 14 litres capacity. The water was made to circulate by means of the stirrers S, moved by a motor. The heating of the water-bath was effected by means of the chromium-nickel spiral P. The temperature was easily kept constant to  $0.1^{\circ}\text{C}$ . A Leiss glass-spectrograph, model A, was used. In the green-blue part of the spectrum we had  $50\text{ \AA}$  for 1 mm. The error of the wave-length determinations should not exceed  $2\text{--}3\text{ \AA}$  units. We used Ilford Iso-Zenith plates.

\* The model of this lamp was constructed by Prof. S. Pienkowski at the Institute for Experimental Physics at the Warsaw University. We are glad to express here our best thanks to Prof. Pienkowski for his kind permission to adapt his model.

Fig. 1.

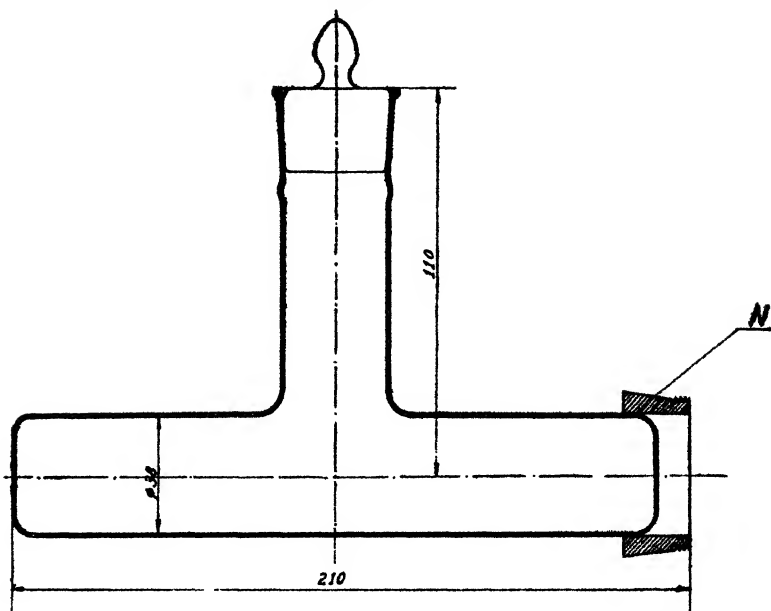
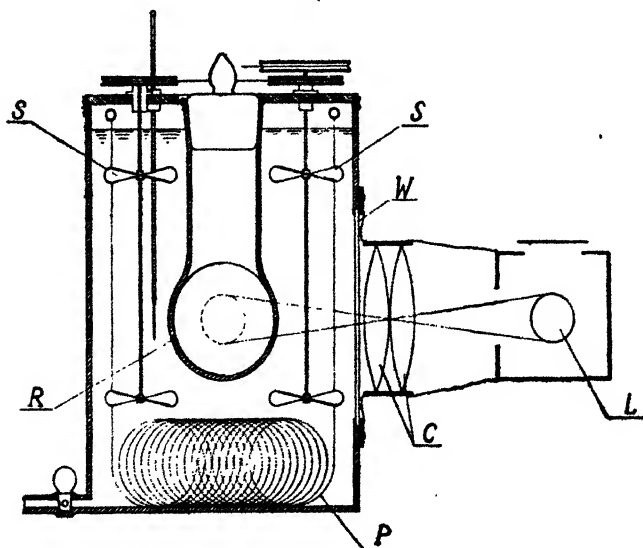


Fig. 2.



Explanation of lettering on figs. 1-3.

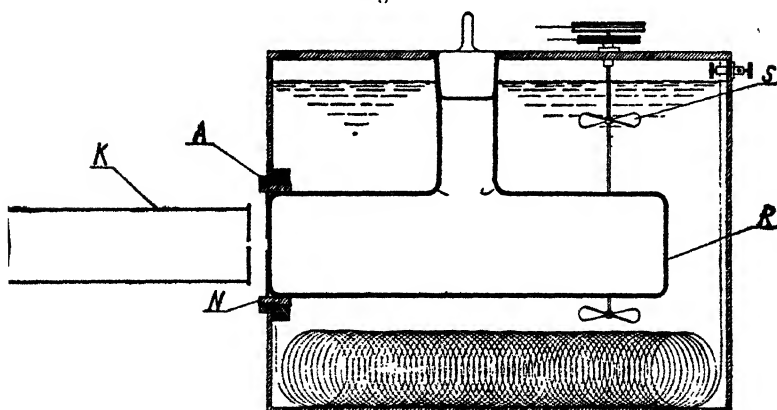
N is a brass cone which fits into the cone A (fig. 3). S denotes the vanes of the stirrers. It denotes the glass vessel containing the liquid examined. W is a glass window. L the mercury lamp, whose image is projected by the condenser lenses C. P is the heating spiral. K the collimator of the spectrograph.

(H. & D. 700). For the photographs taken during the opalescence it was found advantageous to apply anti-halo plates, the principal mercury lines being then strongly superexposed. We chose Gevaert's SSS (Super Sensima Special) plates, which gave very satisfactory photographs of the spectra.

### 3. Results.

Our experiments were conducted in the following way. We photographed the Raman spectrum some degrees over the critical point, when no distinct opalescence was yet seen. Then, allowing the liquid to cool down, we repeated the experiment, applying the same time of exposure, while

fig. 3.



the opalescence was increasing in strength. We aimed not to reach the point at which the liquid would look like diluted milk, because then the absorption of the radiation would have been too strong. The first photographs taken soon showed that the opalescence was accompanied by the appearance of many new lines which were not visible at higher temperatures. Relatively faint characteristic Raman lines of isobutyric acid also appeared, but these were more diffused than the same lines obtained with pure acid. The attempts to obtain more intense phenomena by prolonging the time of exposure did not bring expected results. The lines disappeared altogether, and a reason for their disappearance was easily found. The spectrum of the mercury-arc lamp has a weak continuous background. In ordinary conditions this continuous spectrum does not

appear on photographs, because the scattered light amounts to only a small fraction of the light incident. At the critical opalescence that fraction grows considerably, and the background becomes relatively important. In cases of long exposure the continuous spectrum totally masks the weak Raman lines. In view of the above the following method of observation was adopted. We shortened the length of exposure to the length of time necessary to obtain on the plate the strongest broad Raman-lines of isobutyric acid only —  $4605 \text{ \AA}$  and  $4661 \text{ \AA}$ . Fifteen minutes' exposure was found sufficient for this purpose. Under these conditions the continuous background was relatively harmless. Lowering the temperature and approaching the critical point, the time of the exposure remaining unchanged, we took a series of spectrum photographs. These photographs showed very clearly that the intensity of the Raman lines changed but very little, whereas the intensity of the classical scattering increased manyfold. It is true that at intense opalescence the Raman lines appeared somewhat stronger than without opalescence, but at the same time the continuous background was darker. For an approximate estimation of the strengthening of the lines we diminished the time of exposure; the temperature and the degree of opalescence remained the same. It was thus found that the strengthening of the Raman lines at maximum opalescence in our experiments did not exceed 30–40 per cent. However, we do not think that it was a real increase in the intensity of the lines, but consider it rather to be the effect of the simultaneous action on the plate of both the Raman light and also the continuous spectrum of increased intensity. At the same time the intensity of the scattered light increased approximately about 500 per cent. This effect could not be appreciated with the principal mercury lines, because they appeared on the plates much overexposed, but it was perceptible with the weak ones like  $4916 \text{ \AA}$ . It was said that there appeared at the opalescence many new lines, which we thought at the beginning to be new Raman lines. A more exhaustive study showed, however, that these new lines were but very feeble mercury lines, like 4826, 4882, 4960, 5121,  $5365 \text{ \AA}$ . They do not appear in the spectra of scattered light when the temperature is kept some degrees above the critical point, their intensity being too weak to

impress the photographic plate. The opalescence increases their intensity in the scattered light. It was possible for us to obtain the same "new lines," using instead of the critical mixture a plate of milky glass put in the vessel R (see fig. 2), which was filled with distilled water. A three minutes' exposure was then sufficient to obtain on the plate the lines mentioned.

#### 4. Conclusion.

From these experiments we infer that the Raman spectrum exists at the critical point, and its intensity remains unchanged by the critical opalescence.

The results of the investigations of Bogros-Rocard \* and Martini† are easily explained. The fact that these scientists did not obtain Raman spectra in their photographs resulted from the continuous background of the mercury spectrum, which, becoming predominant at the opalescence, masks totally the weak Raman lines. Apart from this, in the case of phenol the liquid becomes red-coloured and the absorption has a harmful effect upon the intensity of the Raman light.

The positive effect of Raman and Ramdas is accounted for if we consider that it is impossible to obtain ideal light-filters. Their blue filter transmitted also a certain percentage of green and yellow light : the amount of light transmitted was too small to be observed in ordinary conditions of light scattering. At the critical opalescence the scattering increased considerably, and the light transmitted appeared suddenly, thus giving the impression of strengthened Raman radiation.

It follows from our work that there exists a fundamental difference between Raman effect and scattered radiation, and that, on an *experimental basis*, we may call the new radiation incoherent, whereas the classical scattering is a coherent one.

A part of the expense for this study was covered by the Mianowski Foundation.

Warsaw, Physical Laboratory of  
the State High Technical School,  
founded by H. Wawelberg and S. Rotwand,  
November 3rd, 1920.

\* *Loc. cit.*

† *Loc. cit.*



XXIX. *The Theory of the Pianoforte String struck by a Hard Hammer.*—Part I. By Dr. KULESH CHANDRA KAR and MOHINIMOHON GHOSH\*.

*Introduction.*

THE theoretical inquiries into the problem of the pianoforte string are generally divided into the two following classes :—(1) those developed by Helmholtz †, Delemer ‡, and Lamb § ; (2) those advanced by Kaufmann ||, Love ¶, and Das \*\*. It is generally thought that the two classes of theories are fundamentally different, the first class being based on some assumed law of pressure between the hammer and the string, the second class giving a rigorous functional solution of the problem. It is proposed in this paper to develop a new theory of the pianoforte string, extending Rayleigh's theory of loaded string †† in the light of the theory of motion of dynamical systems under intermittent impulse as developed by one of the writers ‡‡ on different occasions, and to discuss the present theory in relation to the other theories of class (2).

Before entering into discussions about the present theory and its relation to the other existing theories it seems advisable to state briefly the results of Kaufmann's investigation §§ on the subject. According to Kaufmann, the differential equation of motion of the hammer when it strikes very near the end of the string is given by

$$m \cdot \frac{d^2y}{dt^2} + \frac{T_1}{c} \cdot \frac{dy}{dt} + \frac{T_1}{a} y = 0, \quad . . . . (1)$$

where  $y$  is the displacement of the hammer,  $t$  the time,  $m$  the effective mass of the hammer,  $T_1$  the tension of the string,  $c$  the velocity of the wave along the string, and  $a$

\* Communicated by the Authors.

† Helmholtz, 'Sensations of Tone,' Translated by Ellis.

‡ Delemer, *Ann. Soc. Sci. de Bruxelles*, pts. 3-4, pp. 219-314.

§ Lamb, 'The Dynamical Theory of Sound,' p. 74.

|| Kaufmann, *Ann. d. Phys.* liv. p. 675.

¶ Love, 'The Theory of Elasticity,' 4th Edition, Art. 281.

\*\* Das, *Proc. Ind. Assoc. etc.* vii. p. 13 (1921). *et seq.*

†† Rayleigh, 'Theory of Sound,' i. p. 204.

‡‡ K. C. Kar, *Phys. Zeit.* xxiv. p. 63 (1923); *Phys. Rev.* xxi. p. 695 (1923); Phil. Mag. (to be published) Kar and Ghosh; *Phys. Zeit.* xxix. p. 143 (1928); M. Ghosh, *Phys. Zeit.* (to be published).

§§ Kaufmann, *loc. cit.* Notations used in this paper are generally taken from Rayleigh's 'Theory of Sound.'

the shorter segment into which the string is divided by the hammer. It may be noted that the above equation holds during the time  $0 < ct < 2a$ . Now on solving the above equation one gets

$$y = \frac{v_0}{\sqrt{\frac{T_1}{ma} - \frac{T_1^2}{4m^2c^2}}} \cdot e^{-\frac{T_1}{2mc}t} \sin \left\{ t \sqrt{\frac{T_1}{ma} - \frac{T_1^2}{4m^2c^2}} \right\}, \quad (2a)$$

$0 < ct < 2a,$

or

$$y = \frac{v_0}{c \sqrt{\frac{\rho}{ma} - \frac{\rho^2}{4m^2}}} \cdot e^{-\frac{\rho c}{2m}t} \sin ct \left\{ \frac{\rho}{ma} - \frac{\rho^2}{4m^2} \right\}^{\frac{1}{2}}, \quad (2b)$$

or again,

$$y = \frac{v_0 \theta}{\sqrt{\frac{m'}{m} \left( \frac{4l}{a} - \frac{m'}{m} \right)}} \cdot e^{-\frac{m'}{m} \cdot \frac{t}{\theta}} \sin \left\{ \frac{t}{\theta} \sqrt{\frac{m'}{m} \left( \frac{4l}{a} - \frac{m'}{m} \right)} \right\}, \quad (2c)$$

where  $\rho$  is the linear density of the string,  $\theta$  the period of vibration,  $v_0$  the initial velocity of the struck point,  $l$  and  $m$  is length and mass respectively. Thus from (2c) the duration of contact is given by

$$\frac{\phi}{\theta} = \frac{\pi}{\sqrt{\frac{m'}{m} \left( \frac{4l}{a} - \frac{m'}{m} \right)}}. \quad (3)$$

The next case considered by Kaufmann is that of a hammer striking at the centre of the string. In this case the differential equation of motion of the hammer is given by

$$m \frac{d^2 y}{dt^2} = -2T_1 \cdot \frac{dy}{dx}, \quad (4)$$

where  $m$  and  $T_1$  are symbols already explained and  $x$  is taken along the string. The solution of the above equation in the first epoch, i.e.,  $0 < ct < l$ , is

$$y = \frac{v_0 mc}{2T_1} (1 - e^{-\frac{2T_1}{mc}t}), \quad (5a)$$

or,

$$y = \frac{mv_0}{2\rho c} (1 - e^{-\frac{2\rho c}{m}t}), \quad (5b)$$

which may also be written as

$$y = \frac{v_0 \theta m}{4m'} (1 - e^{-\frac{4m'}{m} \cdot \frac{t}{\theta}}), \quad \dots \quad (5 a)$$

where the symbols have the same meaning as in (2). In the second epoch the solution of equation (4) becomes

$$y = \frac{v_0}{c} \left\{ e^{-\frac{2T_1}{mc} \cdot t} \left[ 2e^{\frac{4T_1 a}{mc}} \left( ct - 2a + \frac{mc^2}{2T_1} \right) - \frac{mc^2}{2T_1} \right] - \frac{mc^2}{2T_1} \right\}, \quad (6 a)$$

or,

$$y = \frac{mv_0}{2\rho c} \left[ e^{-\frac{2\rho c}{m} t} \cdot \frac{2\rho}{m} \left\{ 2e^{\frac{4\rho a}{m}} \left( ct - 2a + \frac{m}{2\rho} \right) - \frac{m}{2\rho} \right\} - 1 \right], \quad (6 b)$$

or, in the alternative form,

$$y = v_0 \theta \left\{ e^{-\frac{4m'}{m} \cdot \frac{t}{\theta}} \left[ 2e^{\frac{2m'}{m}} \left( \frac{t}{\theta} - \frac{1}{2} + \frac{m}{4m'} \right) - \frac{m}{4m'} \right] - \frac{m}{4m'} \right\}. \quad (6 c)$$

Now, on equating  $\frac{d^2 y}{dt^2}$  from (6) to zero, the duration of contact of the hammer, if it leaves the string in the second epoch, can be easily obtained. It is, according to Kaufmann,

$$\frac{\phi}{\theta} = \frac{1}{2} + \frac{1}{4} \cdot \frac{m}{m'} \left( 1 + \frac{1}{2} e^{-\frac{2m'}{m}} \right). \quad \dots \quad (7)$$

One other case discussed by Kaufmann in his paper referred to above is that of an infinite string struck at its centre. The solution for this case is exactly the same as equation (5) for the first epoch for a finite string, for reasons which are quite obvious. It may be noted before concluding this section that Kaufmann's method for a finite string struck at its centre can be easily extended to higher epochs. The displacement in the third epoch may conveniently be given below,

$$y = \frac{mv_0}{2\rho c} \left[ 1 - e^{-\frac{2\rho c}{m} t} + 2e^{-\frac{2\rho}{m}(ct-2a)} \cdot \frac{2\rho}{m} \left( ct - 2a + \frac{m}{2\rho} \right) - 2e^{-\frac{2\rho}{m}(ct-4a)} \cdot \frac{2\rho}{m} \left\{ (ct-4a) + \frac{2\rho}{m} (ct-4a)^2 + \frac{m}{2\rho} \right\} \right]. \quad (8)$$

The above is a brief summary of Kaufmann's theory of the pianoforte string.

In the following section A we shall develop the new theory of the pianoforte string, and shall show that it gives all the results given above in a very simple way. In section B will be discussed the relations of the theories of

Love and Das with that of Kaufmann, while in section C will be given discussions about the different expressions for the duration of contact obtained from the different theories.

### SECTION A.

In all the existing theories of the pianoforte string the effect of damping has been neglected. In the present paper we shall also neglect the damping effect, which will, however, be considered in a later communication. Now, it has been shown by one of the writers \* that if the vibration of the pianoforte string during the time the hammer is in contact is taken as that of a loaded string, the load being considered as a part of the string during this time, then the equation of motion of the load or the loaded point of the string is given by

$$y = \frac{2v_0}{c\lambda} \sin c\lambda t \cdot \frac{1}{\rho \left( \frac{a}{\sin^2 \lambda a} + \frac{b}{\sin^2 \lambda b} \right) + 1}, \quad (9)$$

where  $v_0$  is the velocity of the hammer just before contact,  $c$  the velocity of the wave along the string,  $\rho$  the linear density of the string,  $m$  the mass of the hammer,  $a$  and  $b$  are the segments into which the string is divided by the hammer, and  $\lambda$  is given by the frequency equation

$$m\lambda \sin \lambda a \sin \lambda b = \rho \sin \lambda l, \quad (10)$$

$l$  being the total length of the string.

*Near the End.*

Now, if the hammer strikes the string very near its end, i. e., if  $a \ll b$  and therefore  $b = l$  approximately, we have then from equation (10), by taking  $\sin \lambda a = \lambda a$  and  $\sin \lambda b = \sin \lambda l$ ,

$$\lambda = \sqrt{\frac{\rho}{ma}} = \frac{1}{c} \sqrt{\frac{T_1}{ma}}. \quad (11)$$

Thus equation (9) becomes

$$y = \frac{2v_0}{\sqrt{\frac{T_1}{ma}}} \cdot \sin \sqrt{\frac{T_1}{ma}} \cdot t \times P, \quad (12)$$

\* K. C. Kar, Phil. Mag. p. 278 (August 1928). The value of  $y$  is not taken here as a series. This is what I pointed out in my paper referred to above.—K. C. K.

where 
$$P = \frac{1}{\frac{\rho}{m} \left( \frac{a}{\sin^2 \lambda a} + \frac{b}{\sin^2 \lambda b} \right) + 1} \dots \dots (13)$$

Now, from equation (11) we have  $\lambda$  is very small. If, however, it is so small that  $\sin \lambda a = \lambda a$  and  $\sin \lambda b = \lambda b$ , then  $\rho$  can be easily evaluated from (13). Thus we have

$$P = \frac{1}{\frac{1}{\lambda^2} \cdot \frac{\rho}{m} \left( \frac{1}{a} + \frac{1}{b} \right) + 1} \dots \dots (14)$$

Or, substituting the value of  $\lambda$  from (11), and remembering that  $b=l$  approximately, we have from (14)  $P = \frac{1}{2}$ . Thus equation (12) reduces to

$$y = \frac{r_0}{\sqrt{\frac{T_1}{ma}}} \cdot \sin \sqrt{\frac{T_1}{ma}} \cdot t \dots \dots (15)$$

It is not difficult to see that up to a first approximation, the above equation is the same as Kaufmann's equation (2). Let us now proceed to find the value of  $y$  up to a higher approximation\*.

Now, using the relation  $l = a + b$ , we have from the frequency equation (10)

$$\lambda \left( \lambda a - \frac{\lambda^3 a^3}{6} \right) = \frac{\rho}{m} \left[ \cos \lambda a + \frac{\sin \lambda a \cos \lambda b}{\sin \lambda b} \right], \dots (16)$$

neglecting higher terms.

Now, as  $\lambda$  is very small (shown before),  $\sin \lambda a$ ,  $\sin \lambda b$ , and  $\cos \lambda b$  may be taken as  $\lambda a$ ,  $\lambda b$ , and 1 respectively. Thus equation (16) reduces to

$$\lambda \left( \lambda a - \frac{\lambda^3 a^3}{6} \right) = \frac{\rho}{m} \left( \cos \lambda a - \frac{a}{b} \right) \dots \dots (17)$$

Now,  $\frac{a}{b}$  being very small compared with  $\cos \lambda a$ , which is very nearly equal to 1, we have from (17)

$$\lambda^2 a \left( 1 - \frac{\lambda^2 a^2}{6} \right) = \frac{\rho}{m} \left( 1 - \frac{\lambda^2 a^2}{2} \right) \dots \dots (18)$$

\* An alternative proof will be given in Appendix (A).

Or we have on transformation

$$\lambda^2 a(1 + \frac{1}{3}\lambda^2 a^2) = \frac{\rho}{m} \dots \dots \dots (19)$$

Solving the above quadratic equation in  $\lambda^2$ , we get

$$\lambda = \sqrt{\frac{\rho}{ma} - \frac{1}{3} \cdot \frac{\rho^2}{m^2}}, \dots \dots \dots (20)$$

up to a second approximation. Thus instead of equation (15) we have

$$y = \frac{v_0}{c \sqrt{\frac{\rho}{ma} - \frac{1}{3} \frac{\rho^2}{m^2}}} \cdot \sin \left\{ ct \sqrt{\frac{\rho}{ma} - \frac{1}{3} \frac{\rho^2}{m^2}} \right\} \dots (21)$$

If we, however, suppose the term  $\frac{1}{3} \cdot \frac{\rho^2 c^2}{m^2}$  under the square root in the above equation to be due to some term in the differential equation of motion corresponding to the damping term (as in Kaufmann), then the equation (21) may be written as

$$y = \frac{v_0}{c \sqrt{\frac{\rho}{ma} - \frac{\rho^2}{3m^2}}} \cdot e^{-\frac{1 \cdot 15 \cdot \rho c}{2m} t} \cdot \sin \left\{ ct \sqrt{\frac{\rho}{ma} - \frac{1}{3} \frac{\rho^2}{m^2}} \right\}, \dots (22)$$

which very closely agrees with Kaufmann's equation (2b). The small difference may be explained as being due to the fact that Kaufmann has taken the smaller segment to be a rigid rod, which, however, is not so actually.

#### At Midpoint (First Epoch).

In considering the general case of equation of motion of a loaded string, Lord Rayleigh has considered the force to be of the form  $e^{ipt}$ . It can be easily seen, however, that during the first epoch, i.e., before the time the reflected wave comes back to the load, the force will be of the form  $e^{-qt}$ . Thus the equation of motion of the load becomes (*vide* Rayleigh, *loc. cit.*)

$$T_1 \cdot \Delta \left( \frac{dy}{dx} \right) + F e^{-qt} = 0, \dots \dots \dots (23)$$

where  $T_1$  is the tension and  $c$  the velocity of the wave along the string. Thus from (23) the displacement of the load at any time is given by

$$y_1 = \gamma e^{-qt}, \dots \dots \dots (24)$$

where  $\gamma$  is a constant. Now at  $t=0$  we have  $y_0=\gamma$ . If we, however, suppose the displacement of the load to be zero at  $t=0$ , that is to say, if we measure the displacement from  $y_1=y_0$ , the above equation (24) becomes

$$y=\gamma(e^{-qt}-1) \quad \dots \quad (25)$$

Now, the velocity of the load just before contact with the string is  $\left(\frac{dy}{dt}\right)_{t=0}=v_0$ , and hence we get from (25)  $\gamma=-\frac{v_0}{q}$ , and thus we have

$$y=\frac{v}{q}(1-e^{-qt}). \quad \dots \quad (26)$$

It may be noted here that as we have taken the force in the first epoch to be of the form  $e^{-qt}$ , the frequency equation (10) will be (*vide* Rayleigh, Theory of Sound, *loc. cit.*)

$$m\lambda \sin \lambda a \sin \lambda b = -\rho \sin \lambda l. \quad \dots \quad (27)$$

Now at the centre  $a=b=\frac{l}{2}$ , and thus we have

$$\lambda = -\frac{2\rho}{m} \frac{\cos \lambda a}{\sin \lambda a} \quad \dots \quad (28)$$

Or, substituting the exponential values of  $\cos \lambda a$  and  $\sin \lambda a$ , we get

$$\lambda = -i \cdot \frac{2\rho}{m} \cdot \frac{e^{i\lambda a} + e^{-i\lambda a}}{e^{i\lambda a} - e^{-i\lambda a}} \quad \dots \quad (29)$$

Or again, by putting  $p=\lambda c$  (*vide* Rayleigh, *loc. cit.*), we have

$$p = -i \cdot \frac{2\rho c}{m} \cdot \frac{e^{ipa/c} + e^{-ipa/c}}{e^{ipa/c} - e^{-ipa/c}} \quad \dots \quad (30)$$

It has been shown above that in the present case  $p=iq$ . Thus we have from (30)

$$q = -\frac{2\rho c}{m} \cdot \frac{e^{-qa/c} + e^{qa/c}}{e^{-qa/c} - e^{qa/c}} \quad \dots \quad (31)$$

We have already pointed out in the introduction that the solution for a finite string during the first epoch will be exactly the same as that for an infinite string. Thus the value of  $q$  becomes on putting  $l=\infty$ , i. e.,  $a=\infty$ ,

$$q = \frac{2\rho c}{m} = \frac{2T}{mc} \quad \dots \quad (32)$$

Hence equation (26) becomes

$$y = \frac{v_0 mc}{2T} (1 - e^{-\frac{2T}{mc}t}), \quad . . . \quad (33)$$

which is Kaufmann's equation (5 a) for the first epoch or for an infinite string. We might point out here that the differential equation corresponding to (33) during this time is (*vide* also Kaufmann, *loc. cit.*)

$$m \cdot \frac{d^2y}{dt^2} + \frac{2T}{c} \cdot \frac{dy}{dt} = 0. \quad . . . \quad (34)$$

### Second and Higher Epochs.

In calculating the displacement of the hammer during the second epoch, Kaufmann has adopted the method known as the method of variation of integration constant or Saint Venant's method. Love has also used the same method of Saint Venant to find the solution during the second epoch for a rod struck at an end. It will be shown in section B that both the equations of Kaufmann and Love, though apparently of different form, are really the same. In the present section we shall, however, use Kar's theory of intermittent action which has found application\* in different branches of Physics to get very easily the displacement of the hammer during the second or subsequent epoch.

We suppose, now, that during the time it is in contact with the string the hammer moves on, imparting and thus getting back impulses at regular intervals of time  $= \frac{2a}{c}$ , being the time taken by the wave to start from the hammer or the load and come back to it after reflexion from fixed ends. The magnitude of these sudden increases of impulsive force or pressure at the centre, as taken by Kaufmann and Das, are  $2\rho rc$ ,  $4\rho rc$ ,  $4\rho rc$ ,..... etc. at  $t=0$ ,  $\frac{2a}{c}$ ,  $\frac{4a}{c}$ , ... etc.

Thus the motion of the load or the hammer during any epoch is given by the differential equation (34) with the above conditions of impulsive pressure. Now it follows from the theory of intermittent action, that if a pressure  $2\rho rc$  acts momentarily at  $t=0$ , on a system given by the equation (34), the displacement at any time  $t$  is given by (33) †. Then again, if the momentary increases of

\* *Loc. cit.* (Introduction).

† See Appendix B for proof.



pressure  $2\rho v c$  and  $4\rho v c$  take place at  $t=0$  and  $\frac{2a}{c}$ , the displacement at any time during the second epoch, i. e., between  $\frac{2a}{c}$  and  $\frac{4a}{c}$ , is given by

$$y_{\frac{2a}{c}+T} = \frac{mv_0}{2c\rho} \left[ \left\{ 1 - e^{-\frac{2c\rho}{m} \left( \frac{2a}{c} + T \right)} \right\} - 2 \left( 1 - e^{-\frac{2c\rho}{m} \cdot T} \right) \right]. \quad (35)$$

Or on simplifying we get

$$y_{\frac{2a}{c}+T} = \frac{mv_0}{2c\rho} \left\{ e^{-\frac{2c\rho}{m} \cdot T} (2 - e^{-\frac{4a\rho}{m}}) - 1 \right\}. \quad (36)$$

It may be noted here that  $T$  in the above equation is the time measured from the end of the first epoch. Thus, putting  $t = \frac{2a}{c} + T$  in Kaufmann's equation (6b) we get, after some transformation,

$$y = \frac{mv_0}{2c\rho} \left[ 2e^{-\frac{2\rho c}{m} \cdot T} \cdot \frac{2\rho}{m} \left( cT + \frac{m}{2\rho} \right) - e^{-\frac{2\rho}{m} (cT + 2a)} - 1 \right]. \quad (37)$$

Now it can be easily seen that if in the above equation  $cT$  is neglected compared with  $\frac{m}{2\rho}$ , the equation (37) becomes identical with equation (36). We may also note in this connexion that  $cT$  will generally be negligible in comparison with  $\frac{m}{2\rho}$ . Thus there is very good agreement between the present theory and that of Kaufmann. The small difference between the expressions obtained from the two theories is due to the fact that in Saint Venant's method the pressure between the hammer and the string has a sudden increase at the end of each epoch, and then it exponentially decreases, whereas according to the present theory the sudden increase of pressure takes place momentarily at the end of every epoch. This point, it may be remarked here, will be thoroughly discussed in Part II.\*

The displacement of the load or the hammer during the third epoch can be easily obtained as before. Now we have in the third epoch,

$$y_{\frac{4a}{c}+T} = \frac{mv_0}{2\rho c} \left[ \left\{ 1 - e^{-\frac{2\rho c}{m} \left( T + \frac{4a}{c} \right)} \right\} - 2 \left\{ 1 - e^{-\frac{2\rho c}{m} \left( T + \frac{2a}{c} \right)} \right\} + 2 \left\{ 1 - e^{-\frac{2\rho c}{m} \cdot T} \right\} \right]. \quad (38)$$

\* See p. 321 infra.

On simplifying, we get

$$y_{\frac{4a}{c}+T} = \frac{mv_0}{2\rho c} \left[ 1 - e^{-\frac{2\rho c}{m}T} - 2e^{-\frac{4\rho c}{m}T} + e^{-\frac{8\rho c}{m}T} \right]. \quad (39)$$

Now, on substituting  $t = \frac{4a}{c} + T$ , the corresponding equation (8) of Kaufmann reduces to

$$\begin{aligned} y_{\frac{4a}{c}+T} = \frac{mv_0}{2\rho c} & \left[ 1 - e^{-\frac{2\rho}{m}(cT+4a)} + \frac{4\rho}{m} e^{-\frac{2\rho}{m}(cT+2a)} \right. \\ & \times \left\{ (cT+2a) + \frac{m}{2\rho} \right\} - 4e^{-\frac{2\rho c}{m}T} \cdot \frac{\rho}{m} \\ & \left. \times \left\{ cT + \frac{2\rho}{m}c^2T^2 + \frac{m}{2\rho} \right\} \right]. \quad (40) \end{aligned}$$

If, as before, we assume  $cT$  as small compared with  $\frac{m}{2\rho}$ , the above equation (40) becomes exactly the same as (39) deduced from the theory of intermittent action. It may not be too much to claim at this stage that Kar's theory of intermittent action gives quite easily a value of the displacement of the hammer during any epoch which very closely approximates to the corresponding value obtained by a long process based on Saint Venant's method of variation of integration constant.

## SECTION B.

### *Love's Theory.*

As has been already pointed out, Love, in his book on Elasticity, has discussed the case of a rod struck by a load or hammer at one of its ends, the other end being fixed. The time during which the hammer is in contact with the rod is divided into a number of equal intervals, each being equal to  $\frac{2a}{c}$ , where  $a$  and  $c$  are respectively the length of the rod and the velocity of propagation of a wave along it. And the displacements for the first, the second, and the third epoch when expressed in the notations used in this paper, are :

first epoch,

$$y_{0 < t < \frac{2a}{c}} = \frac{mv_0}{\rho c} \left( 1 - e^{-\frac{\rho c}{m}t} \right); \quad (41)$$

316 Dr. K. C. Kar and Mr. M. Ghosh on the Theory  
second epoch,

$$y_{\frac{2a}{c} < t < \frac{2a}{c}} = \frac{mv_0}{\rho c} \left[ e^{-\frac{\rho}{m}t} \cdot \frac{\rho}{m} \left\{ 2e^{-\frac{2\rho a}{m}} \left( ct - 2a + \frac{m}{\rho} \right) - \frac{m}{\rho} \right\} - 1 \right]; \quad (42)$$

third epoch,

$$y_{\frac{4a}{c} < t < \frac{4a}{c}} = \frac{mv_0}{\rho c} \left[ 1 - e^{-\frac{\rho c}{m}t} + 2e^{-\frac{\rho}{m}(ct-2a)} \left\{ 1 + \frac{\rho}{m}(ct-2a) \right\} - 2e^{-\frac{\rho}{m}(ct-4a)} \left\{ 1 + \frac{\rho}{m}(ct-4a) + \frac{\rho^2}{m^2}(ct-4a)^2 \right\} \right]. \quad (43)$$

Now it is quite evident that, by putting  $\frac{m}{2}$  for  $m$  in equations (41), (42), and (43), we get the corresponding equations (5 b), (6 b), and (8) of Kaufmann for the hammer struck at the centre of the string. This is not at all surprising in view of the fact that both Kaufmann and Love have used the same method of variation of integration constant.

### *P. Das's Theory.*

In developing his theory of the pianoforte string P. Das \* has assumed that at the end of every epoch two similar waves are set up, and immediately they are formed they start from the struck point in two opposite directions. Now, to evaluate the unknown function representing the two similar waves produced, Das falls back on the well-known method of variation of integration constant adopted before by Kaufmann and Love. So, we think, Das's theory is fundamentally the same as that of Kaufmann and Love.

It is interesting to note here that, in his papers referred to above, Das has not considered the string struck at its centre. He has, however, discussed the case of a hammer striking a string at a finite distance from one end A, and at an infinite distance from the other end B. Thus he neglects reflexions from the end B and gives the expression for pressure ( $P_A$ ) between the hammer and the string at different epochs. It can be easily seen that if the hammer strikes at the centre of a finite string there will be reflexions

\* Das, *loc. cit.*

from both ends, and  $(P_A)$  will be equal to  $(P_B)$ . And so Das's expression for  $(P_A)$  when B is at an infinite distance from the hammer can be used to find out the pressures at any epoch when the hammer is at the centre. On integrating these expressions for pressure twice with respect to time, the corresponding expressions for the displacements can be easily obtained. On evaluating the expressions for "y" in this way, we find that during the first and the second epoch they are in agreement with those obtained by Kaufmann and Love. During the third epoch, however, the displacement found in this way is different from that of Kaufmann or Love. The acceleration during the third epoch, according to Das (*vide* P. Das, first paper), will be

$$\ddot{y} = -\frac{2\rho v c}{m} \left[ e^{-\frac{2\rho c t}{m}} + 2e^{-\frac{2\rho}{m}(ct-2a)} \left\{ 1 - \frac{2\rho}{m}(ct-2a) \right\} + 2e^{-\frac{2\rho}{m}(ct-4a)} \left\{ 1 - \frac{4\rho}{m}(ct-4a) + \frac{2\rho^2}{m^2}(ct-4a)^2 \right\} \right]. \quad (44)$$

Thus on integrating the above equation the displacement becomes

$$y = \frac{mv}{2\rho c} \left[ 2e^{-\frac{2\rho}{m}(ct-2a)} \left\{ 1 + \frac{2\rho}{m}(ct-2a) \right\} - e^{-\frac{2\rho c}{m}t} - 1 - \frac{4\rho^2}{m^2}(ct-4a)^2 e^{-\frac{2\rho}{m}(ct-4a)^2} \right], \quad \dots \quad (45)$$

which is different from the corresponding equation (8) of Kaufmann or Love. It may be remarked here, in conclusion, that neglecting  $ct$  compared with  $\frac{2\rho}{m}$ , Das's equation (45) approximates to our equation (40).

### SECTION C.

If the string is struck very near its end, the duration of contact between the hammer and the string as obtained from our equation (21) or (22), is

$$\frac{\phi}{\theta} = \frac{\pi}{\sqrt{\frac{m'}{m} \left( \frac{4l}{a} - \frac{4m'}{3m} \right)}}, \quad \dots \quad (46)$$

where  $\phi$  is the duration of contact, and  $\theta$  the time-period of vibration. The above equation, it may be noted, is very nearly the same as Kaufmann's expression (3).

Now if the hammer strikes at the centre of the string, the duration of contact, if the hammer leaves the string during the second epoch, can be obtained from our theory in the following way. We have from equation (36)

$$\frac{d^2y}{dT^2} = \frac{2\rho vc}{m} e^{-\frac{2\rho c}{m} \cdot T} (2 - e^{-\frac{4ap}{m}}). \quad \dots (47)$$

Thus neglecting higher terms the time at which  $\frac{d^2y}{dT^2} = 0$  is given by  $T = \frac{m}{2\rho c}$ . Thus we have

$$\frac{\phi}{\theta} = \frac{1}{2} + \frac{1}{4} \cdot \frac{m}{m'}, \quad \dots (48)$$

where  $\phi$  is the duration of contact and  $\theta$  the time-period of vibration of the string. It may be pointed out that the above equation (48) is the same as Kaufmann-Love's equation (7) \* without the factor  $1 + \frac{1}{2} e^{-\frac{2m'}{m}}$ , which is nearly equal to 1. Thus the present theory gives an approximate value of the duration of contact when the hammer leaves the centre of the string during the second epoch.

### Conclusion and Discussion.

In this paper we have confined ourselves to the approximate solution of the problem of the pianoforte string. The more rigorous solution by the same method on the assumption that after the sudden increase the impulses decrease continuously and exponentially, will be given in the second part of this paper. It is perhaps needless to remark here that the method of intermittent action adopted throughout this paper is far more simple than the lengthy and cumbrous method of variation of integration constant followed by Kaufmann, Love, and Das. Moreover, in view of the fact that the same method of intermittent action has found wide application in many problems of quantum physics, the present theory, which may perhaps be called the quantum theory of the pianoforte string, is of great interest even in molecular physics.

\* Das's theory gives the same value of the duration of contact (second epoch) as that of Kaufmann and Love.

# APPENDIX A.

Instead of supposing, like Kaufmann, that the shorter part of the string ( $a$  cm.) is rigid, we suppose it to have a linear density  $\rho_1$ , far greater than the linear density  $\rho_2$  of the other part ( $b$  cm.) In that case, the frequency equation becomes (*vide* Rayleigh, 'Theory of Sound,' i.).

$$T_1 \lambda_1 \frac{\cos \lambda_1 a}{\sin \lambda_1 a} + T_1 \lambda_2 \frac{\cos \lambda_2 b}{\sin \lambda_2 b} = p^2 m. \quad . \quad . \quad (I.)$$

It is quite evident that if the linear density of the string is the same on the two parts, *i. e.*, if  $\lambda_1 = \lambda_2$ , the above equation (I.) leads to the frequency equation (10). Now on substituting  $\lambda_1 = \frac{p}{c_1}$  and  $\lambda_2 = \frac{p}{c_2}$  where  $c_1$  and  $c_2$  are the velocities of a wave along the two portions, we have from the above equation (I.)

$$\frac{T_1}{m} \left[ \frac{1}{c_1} \cdot \frac{\cos \lambda_1 a}{\sin \lambda_1 a} + \frac{1}{c_2} \frac{\cos \lambda_2 b}{\sin \lambda_2 b} \right] = p. \quad . \quad . \quad (II.)$$

Again,  $\rho_1$  being very great compared with  $\rho_2$ ,  $c_1$  will be very small compared with  $c_2$ , and hence the above equation approximates to

$$\frac{T_1}{m c_1} \cdot \frac{\cos \lambda_1 a}{\sin \lambda_1 a} = p. \quad . \quad . \quad . \quad (III.)$$

Or, putting  $p = \lambda_1 c_1$  and  $T_1 = c_1^2 \rho_1$ , we have

$$\frac{\rho_1}{m} = \frac{\lambda_1 \sin \lambda_1 a}{\cos \lambda_1 a} \quad . \quad . \quad . \quad (IV.)$$

Thus we have, to a first approximation,

$$\lambda_1 = \sqrt{\frac{\rho_1}{m a}}, \quad . \quad . \quad . \quad (V.)$$

and to a second approximation

$$\left. \begin{aligned} \frac{\rho_1}{m} &= \frac{\lambda_1 \left( \lambda_1 a - \frac{\lambda_1^3 a^3}{6} \right)}{1 - \frac{\lambda_1^2 a^2}{2}} \\ &= \lambda_1^2 a \left( 1 + \frac{1}{3} \lambda_1^2 a^2 \right) \end{aligned} \right\}, \quad . \quad . \quad (VI.)$$

and hence, finally, we have

$$\lambda_1 = \sqrt{\frac{\rho_1}{ma} - \frac{1}{3} \cdot \frac{\rho_1^2}{m^2}}. \quad \dots \quad (\text{VII.})$$

#### APPENDIX B.

Let the differential equation of motion of a particle be

$$\ddot{x} + 2b\dot{x} + n^2x = 0. \quad \dots \quad (\text{I.})$$

Its solution in terms of initial displacement and initial velocity is

$$x_t = e^{-bt} \left\{ \dot{x}_0 \frac{\sin pt}{p} + x_0 \left( \cos pt + \frac{b}{p} \sin pt \right) \right\}, \quad (\text{II.})$$

where

$$p^2 = n^2 - b^2.$$

The solution may also be given in terms of initial displacement and initial pressure or acceleration, as

$$x_t = e^{-bt} \left\{ x_0 \left( \frac{b^2 - p^2}{2pb} \sin pt + \cos pt \right) - \frac{1}{2pb} \ddot{x}_0 \sin pt \right\}. \quad (\text{III.})$$

Thus, if the moment is excited by only pressure or acceleration acting for a moment at time  $t$ , then for the displacement at any time  $t'$ , we have from (III.)

$$x_{t'} = -e^{-b(t-t')} \cdot \frac{1}{2pb} (\ddot{x})_t \sin p(t-t'). \quad \dots \quad (\text{IV.})$$

If, now,  $n=0$ , we have  $p=ib$ , and hence equation (IV.) reduces to

$$x = \frac{(\ddot{x})_{t'}}{4b^2} \left\{ 1 - e^{-2b(t-t')} \right\}. \quad \dots \quad (\text{V.})$$

Thus, if

$$b = \frac{T_1}{mc} = \frac{c\rho}{m}, \quad (\ddot{x})_{t'} = \frac{2\rho mc}{m}, \quad \text{and } t'=0.$$

we have

$$x_t = \frac{mv}{2\rho c} (1 - e^{-\frac{2T_1}{mc}t}). \quad \dots \quad (\text{VI.})$$

XXX. *The Theory of the Pianoforte String struck by a Hard Hammer.*—Part II. By Dr. K. C. KAR and M. GHOSH\*.

**I**N Part I. of this paper (p. 306) we have assumed that intermittent impulses are imparted by the hammer at the centre of the string, momentarily, at regular intervals of time, each equal to  $\frac{2a}{c}$ , where  $a$  is half the length of the string and  $c$  the velocity of the wave along the string. On the above assumption we have derived equations for the first, second, and the third epoch, at the centre, which approximately agree with those of Kaufmann and Love. The object of the present paper is to deduce the exact equation of Kaufmann and Love, assuming that the impulses come at regular intervals of time, *i. e.* at  $t=0, \frac{2a}{c}, \frac{4a}{c}, \dots$ , as before, but instead of acting momentarily they act suddenly and then decrease exponentially with time.

It has been shown in the previous paper that the differential equation of motion of the hammer when it strikes the string at its centre is

$$\frac{d^2y}{dt^2} + \frac{2\rho c}{m} \cdot \frac{dy}{dt} = 0, \quad \dots \dots \dots (1)$$

where  $m$  is the mass of the hammer,  $\rho$  the linear density of the string, and  $c$  the velocity of the wave along it. It has also been shown in Part I. that if an impulsive pressure  $\frac{2\rho v_0 c}{m}$  acts momentarily, thus imparting a velocity  $v_0$  to the dynamical system given by the above equation, the displacement at any time  $t$  is given by

$$y_t = \frac{v_0 m}{2\rho c} \left( 1 - e^{-\frac{2\rho c}{m} t} \right), \quad \dots \dots \dots (2)$$

which is Kaufmann's equation of the hammer during the first epoch, *i. e.*  $0 < t < \frac{2a}{c}$ . Just at the end of the first epoch  $\left( t = \frac{2a}{c} \right)$ , *i. e.* just at the moment when the reflected waves starting from the hammer come back to it after

\* Communicated by the Authors.



reflexion from both the ends, the second impulsive pressure  $\frac{4\rho v_0 c}{m}$  begins to act on the hammer. As, however, the waves produced during the first epoch give rise to the force acting on the hammer at any time during the second epoch, i. e. at  $t = \frac{2a}{c} + T$ , where  $0 < T < \frac{2a}{c}$ , the pressure imparted will be  $-\frac{4\rho v_0 c}{m} e^{-\frac{2\rho c}{m} \cdot T}$ , being equal to  $2\ddot{y}$  obtained from equation (2).

Now, if a force  $-\frac{4\rho v_0 c}{m} e^{-\frac{2\rho c}{m} t'}$  acts on a dynamical system given by equation (1) at time  $t'$  for a short time  $dt'$ , it will impart to it a velocity  $-\frac{4\rho v_0 c}{m} e^{-\frac{2\rho c}{m} t'} dt'$ . Substituting the above value of the velocity in equation (2), we get for the displacement at any time measured from the beginning of the second epoch,

$$y_T = -2v_0 e^{-\frac{2\rho c}{m} t'} \left\{ 1 - e^{-\frac{2\rho c}{m} (T-t')} \right\} dt'. \quad (3)$$

As, however, the force is acting continuously on the system, we have

$$y_T = -2v_0 \int_0^T e^{-\frac{2\rho c}{m} t'} \left\{ 1 - e^{-\frac{2\rho c}{m} (T-t')} \right\} dt'. \quad (4)$$

On integrating, we get

$$y_T = -\frac{mv_0}{2\rho c} \left[ 2 \left( 1 - e^{-\frac{2\rho c}{m} \cdot T} \right) - \frac{4\rho}{m} e^{-\frac{2\rho c}{m} \cdot T} \cdot cT \right]. \quad (5)$$

On putting  $cT = ct - 2a$ , where  $t$  is the time measured from the beginning of the first epoch, we get

$$y_T = -\frac{mv_0}{2\rho c} \left[ 2 \left\{ 1 - e^{-\frac{2\rho}{m} (ct-2a)} \right\} - \frac{4\rho}{m} e^{-\frac{2\rho}{m} (ct-2a)} \cdot (ct-2a) \right]. \quad (6)$$

Thus the resultant displacement at any time during the second epoch is (from equations (2) and (6))

$$y_t = \frac{mv_0}{2\rho c} \left[ \left( 1 - e^{-\frac{2\rho c}{m} t} \right) - 2 \left\{ 1 - e^{-\frac{2\rho}{m} (ct-2a)} \right\} + \frac{4\rho}{m} e^{-\frac{2\rho}{m} (ct-2a)} \cdot (ct-2a) \right]. \quad (7)$$

Or we have, on simplifying,

$$y_t = \frac{mv_0}{2\rho c} \left[ 2e^{-\frac{2\rho}{m}(ct-2a)} \left\{ 1 + \frac{2\rho}{m}(ct-2a) \right\} - e^{-\frac{2\rho c}{m} \cdot t} - 1 \right]. \quad (8)$$

On differentiating twice with respect of time we get from equation (5)

$$\ddot{y}_T = -\frac{4\rho vc}{m} e^{-\frac{2\rho c}{m} T} \left( 1 - \frac{2\rho c}{m} T \right). \quad . \quad . \quad . \quad (9)$$

The above equation, therefore, gives the pressure imparted during the third epoch. Thus the displacement of the hammer during the third epoch due to the above-mentioned pressure can be obtained as before from equation (2). It is given by

$$y_T = -2v_0 \int_0^T \left\{ 1 - e^{-\frac{2\rho c}{m}(T-t')} \right\} e^{-\frac{2\rho c}{m} t'} \left( 1 - \frac{2\rho c}{m} t' \right) dt'. \quad (10)$$

On integrating the above equation, we get

$$y_T = -\frac{mv_0}{2\rho c} \left( \frac{2\rho c T}{m} \right)^2 e^{-\frac{2\rho c}{m} T}. \quad . \quad . \quad . \quad (11)$$

Putting  $cT = ct - 4a$ , where  $t$  is the time measured from the beginning of the first epoch, we get

$$y_T = -\frac{mv_0}{2\rho c} \left( \frac{2\rho}{m} \right)^2 (ct - 4a)^2 e^{-\frac{2\rho}{m}(ct-4a)}. \quad . \quad . \quad (12)$$

Thus the resultant displacement at any time during the third epoch is (*vide* equations (8) and (11))

$$y_t = \frac{mv}{2\rho c} \left[ 2e^{-\frac{2\rho}{m}(ct-2a)} \left\{ 1 + \frac{2\rho}{m}(ct-2a) \right\} - e^{-\frac{2\rho c}{m} t} - 1 - \frac{4\rho^2}{m^2} (ct-4a)^2 e^{-\frac{2\rho}{m}(ct-4a)} \right], \quad (13)$$

which is Das's equation for displacement calculated for the third epoch (*vide* equation (46), Part I.).

If, however, we take the pressure imparted at the beginning of the third epoch to be

$$\ddot{y}_T = -\frac{4\rho v_0 c}{m} e^{-\frac{2\rho c}{m} T} \left( 1 - \frac{4\rho c}{m} T \right), \quad . \quad . \quad (9')$$

we get in the same way as above Kaufmann and Love's equation for displacement during the third epoch (*vide* equation (8), Part I.).

It may be noted in conclusion that the assumption underlying the present method is that sudden impulses are given to the hammer at equal intervals of time, each equal to  $\frac{2a}{c}$ .

These impulses are evidently given by the waves striking the hammer after reflexion from the ends. It is perhaps useless to emphasize at this stage that the idea of impulses being given intermittently does not follow from Kaufmann-Love-Das's mathematics, as Das and Datta seem to think in their recent note in *Phil. Mag.*, Aug. 1928. Lastly, we venture to claim that our method, based on Kar's theory of intermittent action, though equally rigid, is far more simple than the tedious method of variation of integration constant followed by Kaufmann, Love, and Das.

Physical Laboratory,  
Presidency College, Calcutta,  
July 1929.

### XXXI. *Critical Stress for Tubular Struts.*

*To the Editors of the Philosophical Magazine.*

GENTLEMEN,—

IN the Supplement to your June issue Dr. Carrington (on "Critical Stresses for Tubular Struts") criticizes certain statements of mine about Southwell's formula for the collapse of tubular struts through elastic instability. There is in Dr. Carrington's paper no reference to my statement that I was dealing with "conditions which are most likely to occur in practice," or to the passage in which I pointed out that Southwell had omitted to investigate the case of failure in lobes of short wave-length. I do, however, readily admit that I ought not to have used "incorrect" in reference to Southwell's formula, but, rather, "incomplete." Moreover, I was not aware that Southwell's approximate equation for the wave-length gave such excellent results for short wave-lengths as is shown by Dr. Carrington's calculations.

May I trespass further on your space and state what I consider to be the present position of this problem? Southwell's investigation includes two types of failure: we are concerned only with the lobed type. His analysis reduces to an equation involving  $\frac{p}{E}$  the ratio of collapsing

load per square inch to Young's modulus,  $t/a$  the ratio of the half-thickness to the radius,  $K$  the number of lobes, and

$q = \frac{2\pi a}{\lambda}$  where  $a$  = the radius and  $\lambda$  the wave-length of a lobe. In any practicable material  $\frac{P}{E}$  is small, and therefore

certain terms may be neglected. If the wave-length is long certain other terms may also be neglected, and Southwell deduced a formula for the wave-length and the collapsing load which applies in these special circumstances: in the only practical application of his work with which I was acquainted, I considered that failure with a long wave-length was impossible, and I investigated the terms in his equation which could be neglected if the wave-length was assumed to be short.

Some of the practical points which influenced me may be conveniently discussed by reference to Dr. Carrington's Tables I. and II. In the first place, a solid drawn tube with a value of  $t/a = 0.001$  is not a practicable one; so far as I know, the lightest tubes yet produced have  $t/a$  about 0.016. Dr. Carrington's particular example, 1 inch diameter and .001 inch thick, is not a practicable tube to make (even by machining) in any length—let alone the several feet required to obtain failure in a few lobes; the lightest practicable tube, 1 inch diameter of any length, would be 1/50 inch thick. Dr. Carrington's other example in his Table II. refers to a tube having  $t/R = 0.04$ : this is a practicable tube to make, but, unfortunately, no materials with which an engineer is acquainted will stand stresses of several hundreds of tons per square inch and remain elastic.

Even supposing long tubes which would fail by elastic instability could be made, I consider it almost impossible to test them so as to make them fail in two or three lobes; to do this would require that the ends should be fixed in direction, and this is a very difficult condition to fulfil. Before completing my paper I examined some methods of making a thin tube long enough to fail in a few lobes, and decided that they were quite impracticable.

The practical cases I had in mind as cases to which Southwell's results might apply were a portion of an oval tube with a large radius of curvature (*e.g.*, an interplane strut of an aeroplane) and the flanges of a spar of an aeroplane. In both of these cases there is only a relatively narrow strip of tube, held at its side either by the sharply curved ends in the case of the strut, or by the webs in the case of the spar.

Leaving out of account any consideration of practical applications, Dr. Carrington's calculations are of interest in that they show that the approximate equation which Southwell gave for the long wave-lengths also gives a remarkably good approximation for short wave-lengths.

One further point of interest may be noted. If it should ever become possible to make long tubes having such values of  $t/R$  that failure by elastic instability is possible, then Southwell's approximate equation may be used to calculate the distance of the stiffeners which will be necessary to ensure that failure shall not occur at the low values corresponding to long wave-lengths.

Yours faithfully,

ANDREW ROBERTSON.

## XXXII. *Proceedings of Learned Societies.*

### GEOLOGICAL SOCIETY.

[Continued from vol. viii. p. 780.]

October 23rd, 1929.—Prof. J. W. Gregory, LL.D., D.Sc.,  
F.R.S., President, in the Chair.

THE following communications were read:—

1. 'The Carnmenellis Granite: its Petrology, Metamorphism, and Tectonics.' By P. K. Ghosh, Ph.D., D.I.C.

The paper deals with the petrology and tectonics of the Carnmenellis granite-mass and its metamorphic aureole. The granite, which occupies an area of some 50 square miles between Falmouth and Camborne (Cornwall), was divided by the Geological Survey into (1) an earlier coarse variety and (2) a later fine variety. In this paper the coarse granite of the Survey has been subdivided into three types, which, from evidence in the field as well as in the laboratory, prove to be three distinct intrusions. The petrological characters of the granites and their differentiates are described and discussed, while twelve especially made analyses illustrate the composition of the rocks and minerals of the granitic series. Twelve analyses have also been made of the associated metamorphic rocks. These latter consist of 'greenstones', slates, and schists of various types, as well as inclusions of country-rock within the granite. Special attention has been paid to the chemical nature of the alteration-products.

The structure of the area has also been investigated, and an attempt has been made to correlate the features exhibited by the granite with those of the metamorphic aureole.

2. 'Historic Changes of Level in the Delta of the Rhone.'  
By Richard Dixon Oldham, F.R.S., F.G.S.

The history of the Rhone delta may be summarized as follows:—

(1) At the opening of the Pleistocene Period the whole area, together with large tracts surrounding it, was covered by a deposit of gravel and well-rounded boulders, over which the Rhone and its tributaries wandered, with no fixed bed and with a velocity of current that gave them a torrential character.

(2) A period of subsidence followed, the gradient and the speed of current were diminished, and an alluvial delta built up, which was at least as extensive as that of the present day. Two stages can be recognized in this deposit:—the lower one is prevailingly arenaceous, and small flat pebbles are found scattered through some of the beds of sand; argillaceous beds are also represented, and occasionally a stiff tenacious clay is found. The upper stage indicates a further check in the velocity of current; the deposits are of the ordinary type of deltaic alluvium, composed of fine-grained impure sand or sandy silt. Throughout both stages marine shells, of species still living, are found, and also beds of peat, the latter having been formed above, the former below sea-level.

(3) A period of uplift then set in, and the land rose, not less than 14 metres, above the level to which it had sunk, the deposits laid down were exposed to denudation, and an undulating surface of erosion was developed. The date of this uplift cannot be defined in centuries, but it must have been long prehistoric in date, for it is on the weathered surface thus carved out of the alluvium that the settlements and structures of the Romans were erected.

(4) Finally came another period of subsidence, which was not regular and continuous, but took place at intervals, alternating with others, of longer duration, during which no material change took place. One of these periods of subsidence was earlier than the establishment of Roman dominion in Provence, and, although there is no direct evidence by which it can be dated, analogy with later events suggests that it probably took place between the years 1000 and 1500 B.C. The next change took place in the course of the 8th and 9th centuries; it amounted to about 5 metres of vertical displacement, and resulted in great geographical changes both at the time and during the succeeding centuries. Large areas of what had been dry land were submerged, and the silting-up of these spreads of shallow water led to a rapid extension of the land, and repeated changes in the course of the river. Finally, there was a fresh movement of subsidence, of shorter duration and smaller amount, for it seems to have been practically

completed during the latter half of the 18th century, and to have amounted to little more than a metre, if so much. The total amount of these movements of subsidence was about 10 metres, and at the end of them the land still stands about 4 metres, or more, above the lowest level reached before the period of uplift set in.

November 6th, 1929.—Prof. J. W. Gregory, LL.D., D.Sc.,  
F.R.S., President, in the Chair.

The following communication was read :—

‘On the Glaciation of Clun Forest, Radnor Forest, and some Adjoining Districts.’ By Major Arthur Richard Dwerryhouse, T.D., D.Sc., M.R.I.A., F.G.S., and A. Austin Miller, M.Sc.

The district described comprises the county of Radnor and parts of Montgomeryshire, Shropshire, Brecknockshire, Herefordshire, and Worcestershire, and is some 1000 square miles in area.

The ice, derived originally from the highlands of Central Wales, filled first the depression now occupied by the valleys of the Rivers Ithon and Irfon to the west of the great line of escarpment extending from Kerry Hill on the north, by Radnor Forest and Aberedw Hill, to Mynydd Epynt on the south side of the Wye Gorge.

As the ice accumulated in the depression, it first found escape by the valleys of the Severn and the Mule on the north, and by the Wye Gorge on the south.

Gradually the level of the ice rose, until it overtopped the escarpment throughout its whole length, with, perhaps, the exception of the highest parts of Radnor Forest.

The courses of the various glaciers which were thus formed in the valleys of the dip-slope are traced, and their effects, both temporary and permanent, on the drainage of the area are discussed.

The eastern boundary of the Welsh ice has been traced from Chirbury to Hereford, and the date of its culmination is shown from evidence collected in the neighbourhood of Marrington Dingle to have been subsequent to the maximum extension of the Irish-Sea Ice on the Shropshire Plain, and to belong to the period of Lake Lapworth, but not to that of the earlier and more elevated Lake Buildwas.

The principal permanent deflexion of drainage described is that of the River Teme from its pre-Glacial course from Leintwardine by way of Wigmore, Aymestry, Mortimer's Cross, and Weobley to the Wye, into its present channel by way of Downton and Ludlow gorges to Woolferton, and thence by Tenbury across the Malvern Axis to the Severn.

---

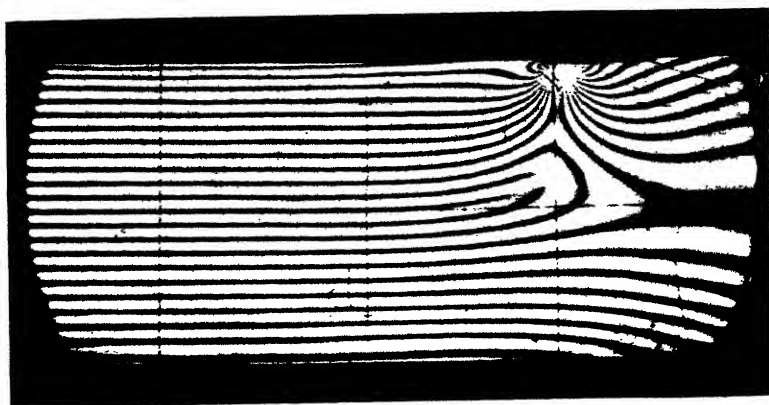
*[The Editors do not hold themselves responsible for the views expressed by their correspondents.]*





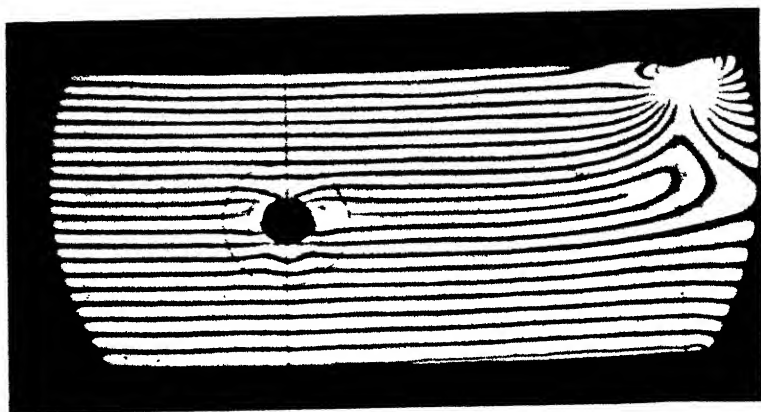
a.

$a = 0$  mm.



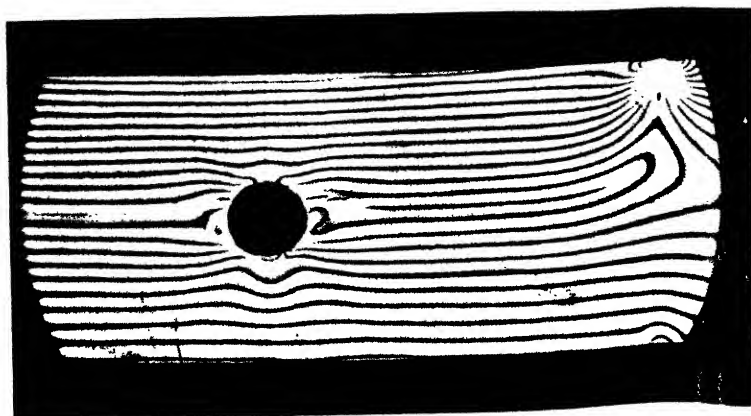
b.

$a = 1.5$  mm.



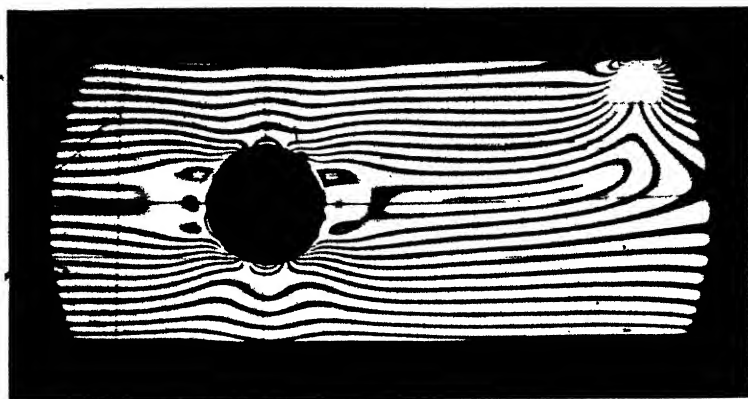
c.

$a = 2.5$  mm.



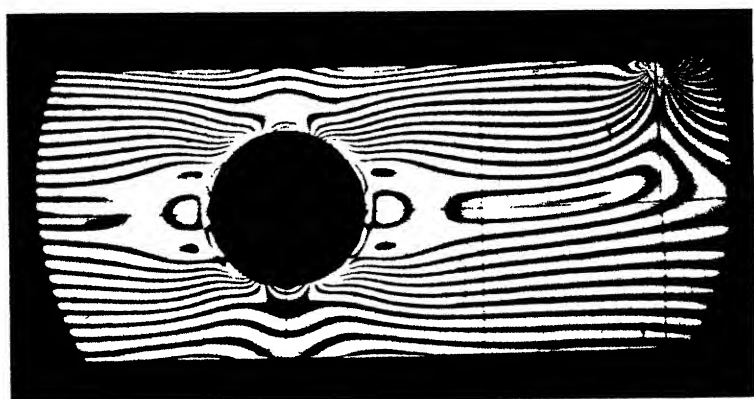
d.

$a = 4$  mm.



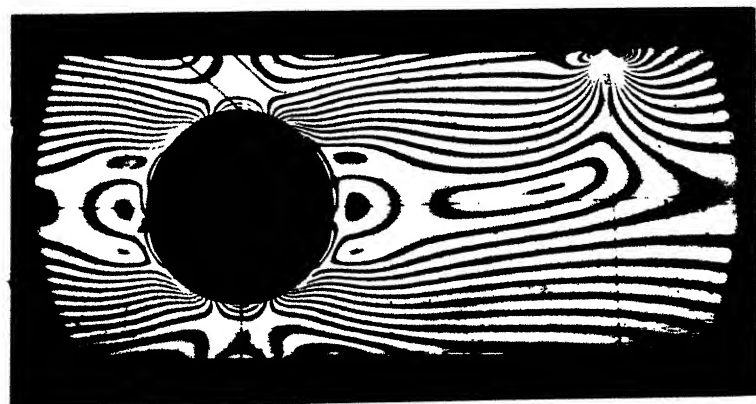
e.

$a = 5$  mm.

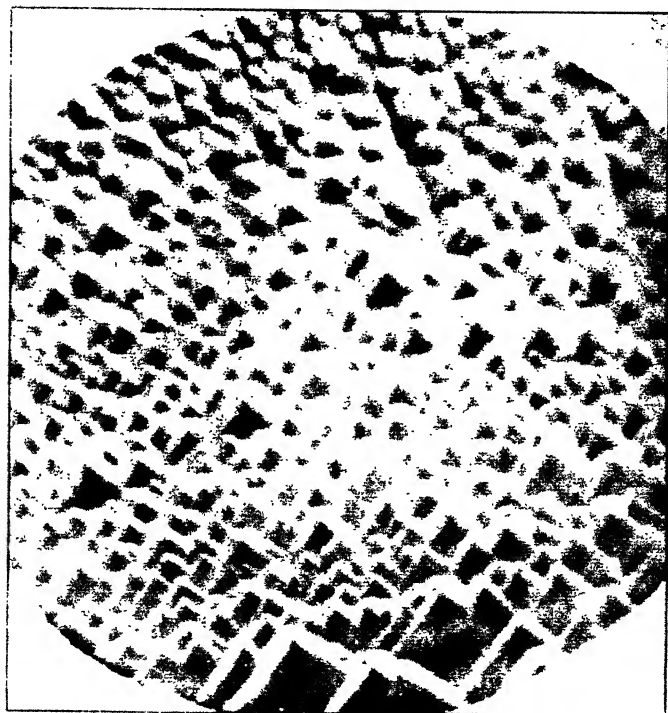


f.

$a = 6$  mm.







Etch-figures of Sylvine.



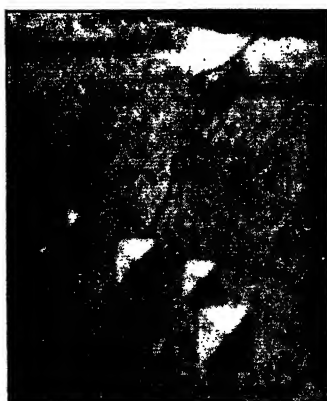
(a)



(c)



(e)



Etch-figures of Sylvine.



THE  
LONDON EDINBURGH AND DUBLIN  
PHILOSOPHICAL MAGAZINE  
AND  
JOURNAL OF SCIENCE.

---

[SEVENTH SERIES.]

---

MARCH 1930.

---

XXXIII. *Vibrations damped by Solid Friction.* By SYDNEY THOMAS, M.Sc., Lecturer in Engineering, University College, Cardiff\*.

VIBRATIONS with solid friction as the sole or principal damping agent are of common occurrence, and the solution, when friction is regarded as a force of constant magnitude reversing in direction at each semi-oscillation, presents no difficulty and little, if any, novelty. A variation having a considerable range of application arises, however, when the two bodies between which friction may exist have, on the average, a relative velocity, and its solution differs in certain respects from that of the simpler case; in particular it may be shown, analytically and experimentally, that vibrations, initiated in any manner, tend to persist within a certain maximum amplitude without any impressed disturbing force other than that provided by the relative motion of the bodies. The necessary conditions are frequently met in practice, and it appears possible that the continued vibrations maintained may be responsible, in some measure, for the production of sound by bodies in rubbing contact.

In general, both bodies may vibrate or have local vibrations within them, but for simplicity it will here be assumed that one only may oscillate, the other being regarded as rigid. The conditions are then readily visualized by considering a

\* Communicated by Prof. W. Norman Thomas, M.A., D.Phil.  
*Phil. Mag.* S. 7. Vol. 9. No. 57. March 1930.



mass  $M$  held under elastic control upon a rigid plane which moves at constant velocity  $V$ , or, alternatively, they may be found in a brake-shoe pressed upon a stiff revolving wheel of considerable mass or in a turning pair one of the elements of which is relatively inelastic. In that case, of course, moments of inertia, couples, and angular velocities may be substituted as necessary for masses, forces, and linear velocities in what follows.

*Solid friction only.*

Whilst a relative motion exists between body and plane, the equation of motion is

$$M\ddot{x} = \pm F - Rx, \quad . \quad . \quad . \quad (1)$$

$R$  being the restoring force per unit displacement from the position of zero elastic stresses and  $F$  the limiting kinetic frictional resistance. The solution is

$$x = \pm F/R + A \cos(pt + \epsilon), \quad . \quad . \quad . \quad (2)$$

and

$$\dot{x} = -pA \sin(pt + \epsilon), \quad . \quad . \quad . \quad (3)$$

where  $p = \sqrt{R/M}$  and where the sign of  $F$  is similar to that of the relative velocity  $(V - \dot{x})$  if both  $V$  and  $x$  are regarded as positive when measured in the same direction.

$F$  is a limiting value, and equation (1) ceases to apply when both  $(V - \dot{x})$  is zero and  $x$  is not numerically greater than  $F/R$ , or, perhaps more accurately,  $F_s/R$ , where  $F_s$  is the limiting static friction. In those circumstances the frictional resistance called into play is that sufficient to balance the restoring force  $Rx$ , the acceleration  $\ddot{x}$  is zero, and  $\dot{x}$  is equal to  $V$ .

The constants in equation (2) depend upon initial conditions, and if it be assumed that the vibrating mass is given an initial maximum positive displacement which ensures that at the outset  $\dot{x}$ , being zero, is not equal to  $V$ , and that the equation therefore applies, then, calling the displacement  $d_1$ , and taking zero-time at the instant of release,  $\epsilon_1 = 0$ ,  $A_1 = (d_1 - F/R)$ , and, until  $\dot{x} = V$ ,

$$x = F/R + A_1 \cos pt. \quad . \quad . \quad . \quad (4)$$

The motion is harmonic, and the space-time curve may be derived from the projections  $(x - F/R)$  of a radius of length  $A_1$  rotating at angular velocity  $p$  about a centre  $C_1$  which is distant  $F/R$  from the centre of elastic forces  $O$  (see fig. 1).

Now

$$\dot{x}/p = -A_1 \sin pt, \quad . \quad . \quad . \quad (5)$$

and if displacements are derived from vertical projections of the rotating radius, as shown in fig. 1, horizontal projections of the same radius lead to values of  $-\dot{x}/p$ .

A point of discontinuity is reached, and friction undergoes reversal when

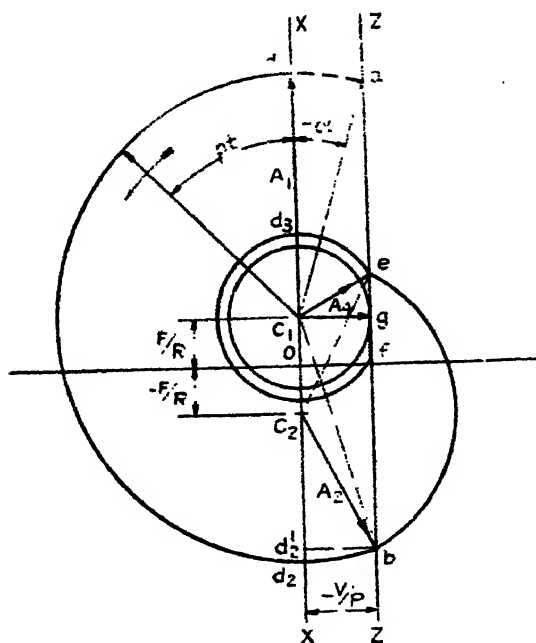
$$\dot{x} = V = -pA_1 \sin pt,$$

i. e., when  $\sin pt = -V/pA_1,$

or  $pt = -\alpha$  or  $\pi + \alpha,$

$\alpha$  being  $\sin^{-1} V/pA_1$ . In the diagram these conditions are

Fig. 1.



realized at the points  $a$  and  $b$  at which the circular locus of the extremity of  $A_1$  intersects the vertical  $ZZ$ , which is at a distance  $-V/p$  from the centre line  $XX$ , and the corresponding displacements are  $F/R \pm A_1 \cos \alpha$ .

For values of  $pt$  greater than  $(\pi + \alpha)$ , and until  $\dot{x}$  again becomes equal to  $V$ , displacements and velocities are given by

$$x = -F/R + A_2 \cos (pt + \epsilon_2), \quad . . . (6)$$

$$\dot{x} = -pA_2 \sin (pt + \epsilon_2), \quad . . . (7)$$

the values of the constants being adjusted to meet the altered conditions. At the instant of friction reversal both sets of equations must be satisfied simultaneously, and if the original time-origin be preserved, so that reversal occurs at  $t = (\pi + \alpha)/p$ ,

$$x = F/R + A_1 \cos(\pi + \alpha) = -F/R + A_2 \cos(\pi + \alpha + \epsilon_2),$$

$$\dot{x} = -pA_1 \sin(\pi + \alpha) = -pA_2 \sin(\pi + \alpha + \epsilon_2),$$

whence

$$A_2 \cos(\pi + \alpha + \epsilon_2) = A_1 \cos(\pi + \alpha) + 2F/R = C_2 d_2' \text{ (fig. 1),}$$

$$A_2 \sin(\pi + \alpha + \epsilon_2) = A_1 \sin(\pi + \alpha) = b d_2' \text{ (fig. 1).}$$

Thus  $A_2 = C_2 b$  and  $(\pi + \alpha + \epsilon_2) = \tan^{-1} b d_2' / C_2 d_2'$ , which is the exterior angle  $d_1 C_2 b$ ,  $OC_2$  being  $-F/R$ .

Alternatively, commencing anew at the point of discontinuity and transferring the origin of the time-space curve to  $(\pi + \alpha)/p$ , so that now  $t = 0$  at the instant represented by the point  $b$ ,

$$A_2 \cos \epsilon_2 = A_1 \cos(\pi + \alpha) + 2F/R = C_2 d_2',$$

$$A_2 \sin \epsilon_2 = A_1 \sin(\pi + \alpha) = b d_2',$$

whence  $A_2 = C_2 b$  and  $\epsilon_2$  is the exterior angle  $d_1 C_2 b$ .

Thus, whichever method be adopted, the continuation of the space-time curve may be derived from vertical projections of the radius  $C_2 b$  revolving at angular velocity  $p$  about  $C_2$ , additional angular displacements being measured from  $C_2 b$ . Horizontal projections, as before, give values of  $-\dot{x}/p$ .

At  $e$ , where  $\dot{x}$  again becomes equal to  $V$ , the original frictional conditions are restored, and

$$x = F/R + A_3 \cos(pt + \epsilon_3), \quad \dots \quad (8)$$

$$\dot{x} = -pA_3 \sin(pt + \epsilon_3), \quad \dots \quad (9)$$

From equations (6), (7), (8), and (9) it may readily be shown, by methods similar to those used for the determination of  $A_2$ , that  $A_3 = C_1 e$ , and that additional angular displacements should be measured from  $C_1 e$ .

The construction may thus be continued, the centre of oscillation being transferred from  $C_1$  to  $C_2$  or conversely as points of intersection of the locus of the extremities of the rotating radii with the vertical  $ZZ$  are attained. In the figure as given, those portions of the construction which lie to the left of  $ZZ$  are drawn with  $C_1$  as centre, those to the right of  $ZZ$  are taken about  $C_2$ .

The construction ceases to apply when  $\dot{x}$  becomes equal to  $V$  at a displacement which lies between  $\pm F/R$ , i.e., when the projection of a point of intersection with  $ZZ$ , such as  $f$ , lies within the region  $C_1C_2$ . As already pointed out, the frictional resistance is then less than its limiting value, and the acceleration is zero; the vibrating mass accordingly moves awhile in unison with the plane until limiting frictional conditions are restored, when elastic vibrations are resumed, and persist in a manner which is considered later.

It was assumed that the initial displacement was a maximum displacement for which  $\dot{x} = 0$ , and in those circumstances the diagram begins at a point in the centre line  $XX$  such as  $d_1$  in fig. 1. This assumption, of course, is not essential, and should oscillations commence under any other conditions of displacement and velocity, the construction may be commenced from the appropriate point on the circular curve. For example, if the plane, initially at rest, is set in motion at velocity  $V$ , the mass is held in contact with it until  $x = F_0/R$ : at the instant of release  $\dot{x} = V$ , and the initial conditions are represented by a point on  $ZZ$  at a height  $F_0/R$  above the horizontal axis  $OT$ . Expressions for  $x$  and  $\dot{x}$  differ from those of equations (4) and (5) only in that  $\epsilon_1 = \tan^{-1} - VR/p(F_0 - F)$ , and the validity of the construction is in no way impaired.

Whilst discontinuities in the expression for  $x$  and transfers between the two centres of oscillation are involved, the time-interval between successive maximum displacements is not uniform, and the motion is not truly periodic. A semi-oscillation such as  $d_1d_2$ , during which the mass moves in a direction opposed to that of the motion of the plane, occupies an interval of  $\pi/p$ , or half the natural period of oscillation, but the return swing is of longer duration, and requires a time-interval of

$$\frac{1}{p} \text{ (the sum of the angles } d_2C_1b, bC_2c, \text{ and } cC_1d_1).$$

The transfer of the centre of oscillation from  $C_1$  to  $C_2$  has the effect not only of changing the length of the rotating radius in the continuation of the construction but also of advancing its angular displacement, whilst the transfer from  $C_2$  to  $C_1$  retards it. The time-interval which elapses between the successive maximum positive displacements represented by  $d_1$  and  $d_3$  is thus

$$\frac{1}{p} (2\pi + \widehat{C_1c_2} - \widehat{C_1bC_2}),$$

a value which is not independent of the initial displacement, and which is always greater than the natural period of oscillation  $2\pi/p$ .

*Particular cases.*—When  $V$  is zero,  $ZZ$  coincides with  $XX$ , the diagram reduces to a series of semicircles about  $C_1$  and  $C_2$  in succession, and the construction is identical with that given by Mr. H. S. Rowell (*Phil. Mag.*, July 1922, p. 284). As pointed out by Mr. C. E. Wright (*Phil. Mag.*, November 1922, p. 1063), this aspect of the problem had also previously been treated analytically by Routh, 'Dynamics of a Particle' (1895 ed.), p. 65.

The time-interval between successive maximum displacements in the same direction is in this case the natural period of oscillation  $2\pi/p$ ; at each change of centre the length of the rotating radius is reduced by  $2F/R$ , each positive or negative extreme displacement is numerically less than the immediately preceding by  $2F/R$ , and the mass finally comes to rest within the stable region when the radius has been decreased to a value equal to or less than  $2F/R$ , or  $(F + F_s)/R$  if distinction is drawn between kinetic and static limiting frictions. Mr. Wright has given an expression from which the number of semi-oscillations performed may be estimated when the limiting friction is regarded as constant, or they and the final position of the mass may be determined as follows. If  $d_1$  is the numerical value of an initial position of zero velocity, the radius during the  $n$ th semi-oscillation is

$$(d_1 - F/R) - (n-1)2F/R = \{d_1 - (n - \frac{1}{2})2F/R\},$$

and for the final semi-oscillation this = or  $< (F + F_s)/R$ , whilst the radius for the preceding semi-oscillation  $\{d_1 - (n - \frac{3}{2})2F/R\}$  = or  $< (F + F_s)/R$ ; thus  $d_1$  cannot exceed  $(2Fn/R + F_s/R)$  or be less than  $(2Fn/R + F_s/R - 2F/R)$ , i.e.,  $n$  is an integer lying between  $(d_1 R/2F - F_s/2F)$  and  $(d_1 R/2F - F_s/2F + 1)$ . When  $F_s = F$  these limits become  $(d_1 R/2F \mp \frac{1}{2})$ .

Writing  $n = d_1 R/2F + k$ , the final position is given by

$$\begin{aligned} d_f &= \pm F/R \mp \{d_1 - (n - \frac{1}{2})2F/R\} = \mp (d_1 - 2nF/R) \\ &= \mp (d_1 - d_1 - 2Fk/R) = \pm 2Fk/R, \end{aligned}$$

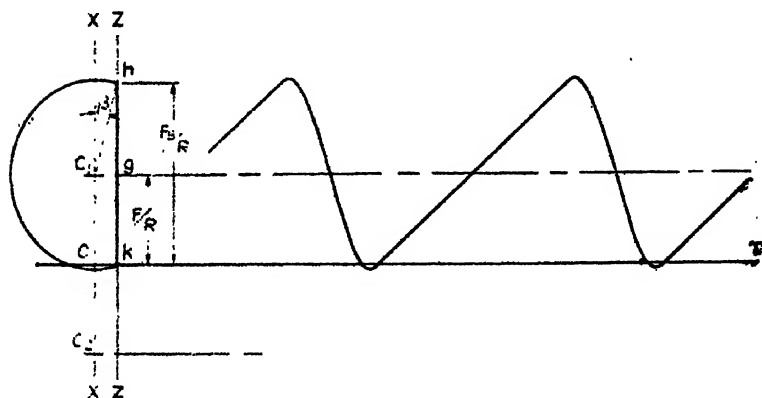
the positive sign applying if the last half-swing is about  $C_1$ , the negative if it is about  $C_2$ .

When the velocity of the moving plane is such that  $V/p$  is not less than  $(d_1 - F/R)$ , the rotating radius does not intersect or is tangential to  $ZZ$ ,  $\dot{x}$  cannot exceed  $V$ , friction

is unidirectional, and the diagram becomes merely a circle about centre  $C_1$ ; the motion is truly harmonic and, in effect, undamped, the periodic time is that of free vibration, and the sole effect of friction—apart from absorption of energy from the moving system—is to transfer the centre of oscillation from the centre of elastic forces to the position of running equilibrium when vibrations are absent. This case is of interest, for it immediately suggests that, when the bodies concerned have an average relative velocity, solid friction alone is incapable of damping out completely any vibrations which may be set up.

Returning to the more general case, when the vibrating mass attains a velocity  $V$  whilst within the region  $C_1C_2$ , as already shown, it retains that velocity, and is carried with

Fig. 2.



the plane until released at  $x=F/R$ , i.e., at the point  $g$  (fig. 1), if  $F$  is assumed to be constant. Vibrations of constant amplitude  $V/p$  thereafter continue about centre  $C_1$  for reasons which have just been considered. If, as is more likely to occur in practice, the limiting value of static friction exceeds that of kinetic friction, release does not occur until  $X=F_s/R$ . The "dead" region is thus extended, but since kinetic friction still obtains during the subsequent relative motion between mass and plane, the centre of oscillation remains at  $C_1$  as before.

The graphical construction for such conditions, together with a derived space-time curve, are illustrated in fig. 2; the mass is released at a displacement represented by  $h$ , performs an oscillatory movement about  $C_1$ , acquires again the velocity of the plane at  $k$ , and thence moves with it to  $h$ ,

where it is once more released. The increase of frictional resistance under static conditions thus provides a stimulus sufficient to maintain vibrations in spite of other damping influences if these are not enough to reduce the rotating radius to a value less than  $V/p$  in one oscillation (see also below).

All vibrations now concerned are similar and the motion is truly periodic, though the frequency is not that of the free vibrations. Each complete swing is composed in part of harmonic motion which occupies an interval of  $\frac{1}{p}(\pi + 2\beta)$ , where  $\beta$  is  $\cot^{-1}(F_s - F)p/VR$ , and in part of uniform motion at velocity  $V$  over a displacement  $2(F_s - F)/R$ , which involves a time-interval of  $2(F_s - F)/VR$  or  $2\cot\beta/p$ . If  $V$  is small whilst  $p(F_s - F)$  is relatively large, the distortion of the resulting wave-form becomes marked; this is illustrated in fig. 2, and it may be worth while noting that the wave-form there shown bears some resemblance to that representing the vibrations of a violin string.

In fig. 2 it is assumed that  $F_s$  is not so far in excess of  $F$  as to lead to oscillation about  $C_2$  as well as about  $C_1$ , but if it be so, the construction falls within the scope of fig. 1; and since release always occurs at the same displacement  $F_s/R$ , movements of the vibrating mass must be repeated at regular intervals.

### *Combined Solid and Fluid Friction.*

Mr. Rowell (Phil. Mag., November 1922, p. 951) has considered the effect of fluid friction, proportional to the velocity, in conjunction with solid friction regarded as a constant force reversing at the end of each semi-oscillation, and Professors Jenkin and Thomas (Phil. Mag., February 1924, p. 303) extended Mr. Rowell's solid friction spiral construction to include that case. The investigation may be made still more general by an extension of the methods which have here been described.

Assuming, as before, that solid friction is provided through the agency of a rigid plane moving at velocity  $V$ , and assuming also, to include all cases, that the bulk of the fluid which provides the fluid friction has a velocity  $v$ , the equation of motion is

$$M\ddot{x} = \pm F - R\dot{x} + c(v - \dot{x}). \quad (10)$$

Writing  $p = \sqrt{R/M}$  and  $n = \sqrt{p^2 - c^2/4M^2}$ , when fluid





by the lengths of perpendicular projectors (such as AB in fig. 3) from the extremity of the rotating arm to the line YY, which is inclined at  $-\phi$  to the vertical. When the spiral curve intersects YY the velocity of the vibrating mass is zero, the tangent to the spiral curve is horizontal, and the projections of such points of intersection give extreme displacements of the mass in one direction or the other. In general, the tangent to the curve is inclined at  $(\pi/2 - \phi)$  to the rotating arm. The centres of oscillation are interchanged at  $\dot{x} = V$ , i. e., at points such as  $a$  and  $b$ , where the spiral intersects the straight line ZZ parallel to YY and at a distance  $-V/p$  therefrom.

Initial conditions, of course, determine the values of the constants  $A$  and  $\epsilon$ ; e. g., assuming an initial maximum displacement  $\delta_1$ , for which  $\dot{x}$  is zero,

$$\text{from (12): } A_1 \sin(\epsilon_1 + \phi) = 0, \text{ whence } \epsilon_1 = -\phi : \quad (13)$$

from (11) and (13) :

$$A_1 \cos(-\phi) = \delta_1 - F/R - cv/R. \quad (14)$$

Thus, in fig. 3,  $A_1$  is represented by  $C_1 d_1$ , where  $d_1$  lies in YY and where the vertical projection of  $Od_1$  is the initial displacement. The time-interval  $nt$  is taken from  $C_1 Y$ , and

$$x = F/R + cv/R + A_1 e^{-\frac{ct}{2M}} \cos(nt - \phi), \quad (15)$$

$$\dot{x} = -p A_1 e^{-\frac{ct}{2M}} \sin nt. \quad (16)$$

The sign of  $F/R$  undergoes reversal at  $\dot{x} = V$ , i. e., at  $b$ , and changing the constants to meet the altered conditions we have

$$x = -F/R + cv/R + A_2 e^{-\frac{ct}{2M}} \cos(nt + \epsilon_2). \quad (17)$$

$$\dot{x} = -p A_2 e^{-\frac{ct}{2M}} \sin(nt + \epsilon_2 + \phi). \quad (18)$$

At the instant  $t_1$  of reversal of dry friction both sets of equations (15), (16) and (17), (18) must be satisfied, and

$$A_2 e^{-\frac{ct_1}{2M}} \cos(nt_1 + \epsilon_2) = 2F/R + A_1 e^{-\frac{ct_1}{2M}} \cos(nt_1 + \epsilon_1),$$

$$A_2 e^{-\frac{ct_1}{2M}} \sin(nt_1 + \epsilon_2 + \phi) = A_1 e^{-\frac{ct_1}{2M}} \sin nt_1.$$

These requirements are met if  $A_2 e^{-\frac{ct_1}{2M}}$  is represented by  $C_2 b$ ,  $(nt_1 + \epsilon_2)$  is the exterior angle  $X_2 C_2 b$ , and  $(\epsilon_2 - \epsilon_1)$  is the angle  $C_1 b C_2$ .

The construction may thus be continued by a logarithmic spiral about  $C_2$ , additional angular displacements being

measured from  $C_2b$ . In similar fashion it follows that, if this curve in turn intersects  $ZZ$  outside the region  $g_1g_2$ , as defined below, the centre of oscillation is retransferred to  $C_1$ , and the construction is carried on therefrom as before.

In the equation of motion (10) it has so far been assumed that  $F$  is a limiting value of friction and is constant, but whilst  $\dot{x}=V$ , solid friction may have any value between  $\pm F$  provided that  $x$  lies between  $\pm F/R + c(v-V)/R$ . In these circumstances solid friction naturally adjusts itself to balance the elastic force and fluid resistance, and  $\ddot{x}$  is zero. If, therefore, the spiral curve intersects  $ZZ$  within these values of  $x$ , the mass moves in unison with the plane to the limit of the region  $\pm F/R + c(v-V)/R$ , when, neglecting differences between static and kinetic limiting frictions, it is released; vibrations are resumed and the spiral construction may be continued. Substituting the values of  $x$  and  $\dot{x}$  at release in equations (11) and (12), and assuming, for present purposes,  $t=0$  at that instant, the constants in the equations of subsequent motion may be derived from

$$F/R + c(v-V)/R = F/R + cv/R + A \cos \epsilon,$$

$$\text{whence} \quad A \cos \epsilon = -cV/R. \quad \dots \dots (19)$$

$$\text{and, from (12).} \quad V = -pA \sin(\epsilon + \phi). \quad \dots \dots (20)$$

Expanding and inserting values of the trigonometrical functions of  $\phi$ , it is readily shown that  $A=V/n=(V \sec \phi)/p$ , and that  $\cos \epsilon = -\sin 2\phi$ . These conditions are satisfied if, in fig. 3,  $A$  is represented by  $C_1g_1$  inclined to  $ZZ$  at  $(\pi/2 - \phi)$  and  $\epsilon$  by the angle  $X_1C_1g_1 = -(\pi/2 + 2\phi)$ ; it follows, therefore, that  $ZZ$  is tangential to the spiral curve at the point of release, and, since  $C_2g_2$  is parallel to  $C_1g_1$ , the region  $g_1g_2$  is defined.

The progressive decrease in the length of the rotating arm makes it impossible that  $\dot{x}$  shall again attain the value  $V$ ; further interchange between centres of oscillation does not occur, and vibrations continue about  $C_1$  (if  $V$  is positive) until damped out of existence. Solid friction is now unidirectional, and it serves merely to displace the centre of oscillation and ultimate position of rest to the extent of  $F/R$ .

It may be noted that unless the damping fluid moves with the plane, so that  $v=V$ ,  $g_1g_2$  is not symmetrical about the elastic centre  $O$ , nor is it defined by horizontals through  $C_1$  and  $C_2$  unless  $V=0$ . When  $V$  is zero the construction reduces to a series of spirals about  $C_1$  and  $C_2$  in succession, each of which commences at the point of intersection of the

preceding curve with YY, and the diagram is complete when a spiral meets YY within the region  $C_1C_2$ , when the mass comes to rest, since  $x$  then lies between  $\pm F/R + cv/R$ ,  $Rx$  lies between  $\pm F + cv$ , and a value of friction numerically less than the ultimate is sufficient to maintain equilibrium. When  $V$  is not zero the mass cannot cease oscillating at any displacement other than those corresponding with  $C_1$  and  $C_2$ , according as  $V$  is positive or negative. When both  $v$  and  $V$  are zero the diagram is similar to that given by Professors Jenkin and Thomas.

If no distinction exists between the limiting values of static and kinetic frictions the least degree of fluid damping serves to bring the mass to rest eventually at  $C_1$  or  $C_2$  unless  $V$  is zero, but when  $F_s$  exceeds  $F$  vibration may be continuous. After a period of motion in contact with the plane at velocity  $V$ , release is delayed to some such point as  $h$  for which  $x = \{F_s + c(v - V)\}/R$ , and, if the relative values of  $F_s$ ,  $F$ ,  $c$ , and  $V$  are such that a velocity  $V$  is again attained during the subsequent vibration, or the spiral meets ZZ (probably within the region  $g_1g_2$ ), the cycle of uniform motion followed by oscillation is repeated indefinitely. That this may be brought about it is necessary that  $C_1h \times e^{-\frac{ct}{2M}} \geq V/n$ ,  $t$  being  $\frac{1}{n}$  (the exterior angle  $hC_1g_1$ ). Small velocity  $V$ , small fluid damping coefficient  $c$ , and appreciable difference between  $F_s$  and  $F$  are all favourable to such continued vibrations.

Where fluid damping is heavy and  $c^2/4M^2 \geq p$ , the motion is non-oscillatory, and the space-time curve is logarithmic and asymptotic to one of the lines  $x = cv/R \pm F/R$ , according as the initial displacement is positive or negative.

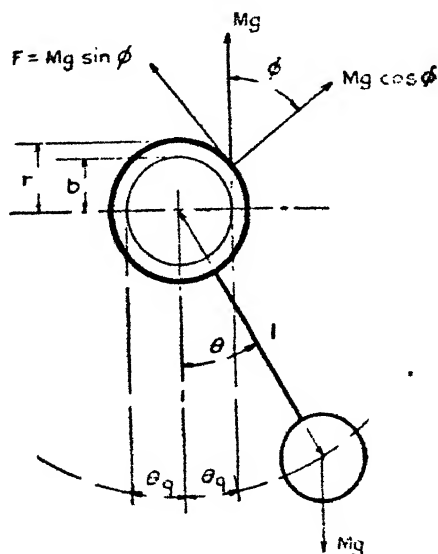
#### *Experimental. Solid friction only.*

Observations were made upon the oscillations of a pendulum of relatively small dimensions but appreciable moment of inertia, consisting of a rectangular sectioned steel bar about six inches long, weighted at its lower end. The head of the bar, which was somewhat broader than the body, was bored just large enough to form a "running" fit upon a steel journal one inch diameter. Actually the head of the pendulum was slotted from bore outwards, and fitted with a set screw for the purpose of providing a varying degree of "pinch" of the bearing upon the journal, but the arrangement proved fierce, and was employed only to ensure absence of slack at the bearing. Pressures were thus those due to

the weight of the pendulum alone, apart from small additional pressures arising from centrifugal action. The journal was allowed to remain in the chuck-jaws of the fairly heavy lathe in which it was turned, the pendulum was mounted upon it and records were taken of oscillations with both stationary and rotating unlubricated journal. Movements were recorded by a light scribe mounted on the pendulum, which bore gently upon an endless band of smoked paper stretched between two revolving parallel drums.

Photographic prints of some of these records taken from the originals by direct-contact exposure are here reproduced, and though the oscillations of the pendulum were too large

Fig. 4.



to be considered as "simple harmonic," the principal features of the damped vibrations as already enunciated are not seriously affected, and are well borne out by the numerous records obtained.

The resultant pressures and forces involved whilst motion exists between pendulum and journal are as illustrated in fig. 4, and if  $I (= Mk^2)$  is the moment of inertia of the pendulum about its centre of oscillation,  $M$  its mass,  $l$  the distance of its mass-centre from the centre of oscillation,  $F$  the ultimate tangential frictional resistance between journal and bearing, and  $r$  the radius of the journal, the equation of motion is

$$I\ddot{\theta} = \pm Fr - Mgl \sin \theta, \quad \dots \dots (21)$$

whence

$$\begin{aligned}\theta^2 &= (2g/k^2)(\pm Fr\theta/Mg + l \cos \theta) + C \\ &= a(l \cos \theta \pm b\theta) + C. \quad \dots \quad (22)\end{aligned}$$

The sign of  $F$  or  $b$  is that of  $(\Omega - \dot{\theta})$ , where  $\Omega$  is the angular velocity of the journal, and much as in the case of equation (1), equations (21) and (22) cease to apply when  $(\Omega - \dot{\theta})$  is zero, and at the same time  $\sin \theta$  is not numerically greater than  $Fr/Mgl$  or  $F_s r/Mgl$ , if static friction is taken into account.  $\theta_s = \pm \sin^{-1} Fr/Mgl$  clearly represents the positions of running equilibrium when the pendulum rides, without oscillation, on the rotating journal, and the verticals through the centre of mass are then tangential to the friction circle of radius  $b$  or  $Fr/Mg$ . Generally, whilst  $F$  has its limiting value, the line of action of the resultant pressure of the journal upon the bearing is tangential to that circle, as shown in fig. 4: the normal pressure is  $Mg \cos \phi$ , the tangential force  $F$  is  $Mg \sin \phi$ , and the eccentricity of the resultant is  $b = r \sin \phi = Fr/Mg$ . When, as in the experiments performed, the only pressures concerned are those arising from the weight of the pendulum itself, and if small additional pressures due to centrifugal action are ignored,  $F = Mg \sin \phi = \mu Mg \cos \phi$  and  $\tan \phi = \mu$ .

In applying equation (22) three cases arise as before:—

- (1) Rapidly moving journal,  $\Omega$  positive and always greater than  $\dot{\theta}$ .

Here friction is uni-directional and, throughout the motion,

$$\theta^2 = a(b\theta + l \cos \theta) + \text{const.}$$

Hence, if  $\theta_1$  is an initial maximum displacement, subsequent maximum displacements are given by

$$\cos \theta = \frac{b}{l}(\theta_1 - \theta) + \cos \theta_1,$$

*i. e.*, the pendulum eventually returns, after a complete swing, to its initial position  $\theta$ , and oscillations are continuous (see figs. 5 and 6). During a semi-oscillation from  $\theta_1$  to  $\theta_2$ , the mean position  $(\theta_1 + \theta_2)/2$  follows from

$$l(\cos \theta_2 - \cos \theta_1) = b(\theta_1 - \theta_2)$$

or

$$\sin \frac{\theta_1 + \theta_2}{2} = \frac{b(\theta_1 - \theta_2)}{l} \bigg/ \sin \left( \frac{\theta_1 - \theta_2}{2} \right),$$

and it is thus not coincident with the position of maximum velocity  $\theta_0$ , but approximates thereto.

(2) Stationary journal,  $\Omega=0$ .

Friction reverses with reversal of velocity at each semi-oscillation, and for successive maximum positions  $\theta_1, \theta_2, \theta_3$ , etc., in either direction,

$$l(\cos \theta_2 - \cos \theta_1) = b(\theta_1 - \theta_2),$$

$$l(\cos \theta_3 - \cos \theta_2) = -b(\theta_2 - \theta_3), \text{ etc.,}$$

i. e., in the first semi-oscillation the pendulum swings from one extreme to the next, equally placed on the opposite side

Fig. 5.

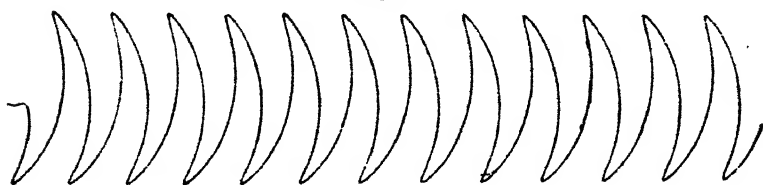


Fig. 6.

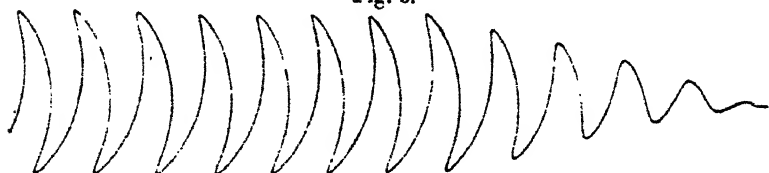
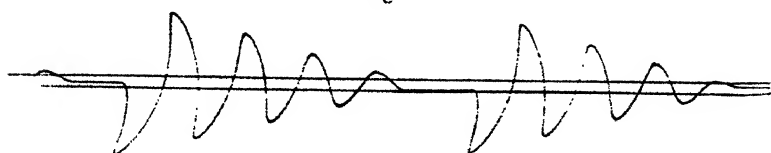


Fig. 7.



of a mean position determined by

$$\sin\left(\frac{\theta_1 + \theta_2}{2}\right) = \frac{b}{l} \left(\frac{\theta_1 - \theta_2}{2}\right) / \sin\left(\frac{\theta_1 - \theta_2}{2}\right),$$

whilst on the return swing the mean position is given by

$$\sin\left(\frac{\theta_2 + \theta_3}{2}\right) = -\frac{b}{l} \left(\frac{\theta_2 - \theta_3}{2}\right) / \sin\left(\frac{\theta_2 - \theta_3}{2}\right).$$

The mean position is thus transferred successively from one side of the central vertical position to the other, and amplitudes are diminished until  $\theta$  becomes zero within the stable region  $\pm \theta_c$ , when motion ceases (see fig. 7).

(3) Slowly rotating journal,  $\Omega$  positive but not always greater than  $\dot{\theta}$ .

From an initial maximum displacement  $\theta_1$ ,  $F$  is positive until  $\dot{\theta} = \Omega$ , when, if  $\theta$  is numerically greater than  $\theta_q$ , reversal of sign occurs. The mean position, derived as before from  $a(l \cos \theta \pm b\theta)$  a constant, thus changes from one side of the central vertical position to the other, and amplitudes are diminished until eventually  $\dot{\theta}$  becomes equal to  $\Omega$  whilst  $\theta$  is less than  $\theta_q$ . The pendulum then turns with the journal until released at  $\theta = \theta_q$ , if the difference between static and kinetic limiting frictions is negligible, and oscillations continue as in case (1) (see figs. 8 and 9).

Fig. 8.

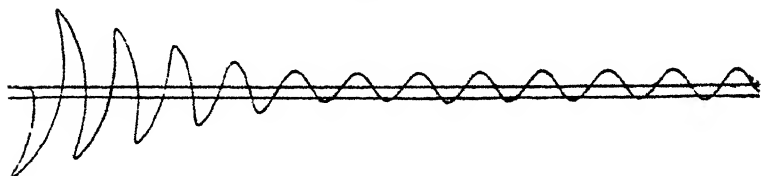
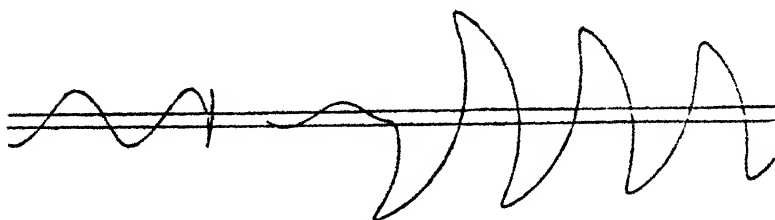


Fig. 9.



If  $F_s$  is appreciably greater than  $F$ , release is delayed until a somewhat greater value of  $\theta$  is attained; subsequent oscillations include each a period of uniform angular velocity, and the effect is continuous.

Of the records here reproduced, figs. 5 and 6 show the beginning and end of a series of oscillations following an initial displacement given to the pendulum when riding upon a rapidly revolving journal (126 rev. per min.), and it will be seen that amplitudes were undiminished until the lathe was stopped, when, as shown at the end of fig. 6, oscillations were rapidly damped out of existence. Fig. 7 is taken from the record of a series of oscillations with stationary journal. The two parallel lines shown in this and in the subsequent figures were recorded with the

pendulum at rest and drawn aside to one or other of its extreme positions of equilibrium, and they define, as nearly as could be obtained, the region of stability. The record illustrates the rapid damping effect of even small values of friction, the approximate equality of angular displacements about the limiting stable positions in succession, and the final cessation of oscillatory motion at different positions within the stable region. Figs. 8 and 9 are portions of records of oscillations performed upon a slowly revolving journal. In the former, the rapid initial damping followed by continuous oscillation when a certain amplitude had been attained is clearly shown, and the latter really portrays the same effect, for the oscillations shown to the left of the record are the continuation of the initial oscillations shown to the right after extending completely around the recording band, a length of about 20 inches.

On each record a circle, not here shown, was described by revolving the pendulum about its centre of rotation with the recording apparatus at rest, and in this fashion the radius and centre of the circular path of the scribe were determined. Using a specially constructed celluloid protractor, on which a circle of similar radius was inscribed, it was possible, by laying the zero line of the protractor along the locus of the centre of oscillation on the record, and noting the angle at which the circle intersected various parts of the oscillatory curve, to determine angular displacements from any chosen datum and to plot the records to rectangular axes. In this manner the double amplitudes of final oscillations in figs. 8 and 9 were determined and compared, and in each of the several records taken it was found that these values were approximately in proportion to the speeds of the journal: *e.g.*, in the records here reproduced the double amplitudes concerned were respectively about  $12.5^\circ$  and  $23^\circ$ , whilst the journal speeds were approximately 8 and 14 rev. per min. The ratio of amplitudes is thus 0.54 and of speeds 0.57.

The means available for driving the recording apparatus did not ensure perfect uniformity of speed during an observation, and the records are probably not quite reliable in respect of time-intervals. For this reason the curves, too, may be slightly distorted from their true forms, but the values of extreme displacements and the general characteristics of the oscillations are not affected. The records fulfil the purpose for which they were intended, that of supporting experimentally the principal deductions previously made analytically, and it is from that standpoint that they are presented.



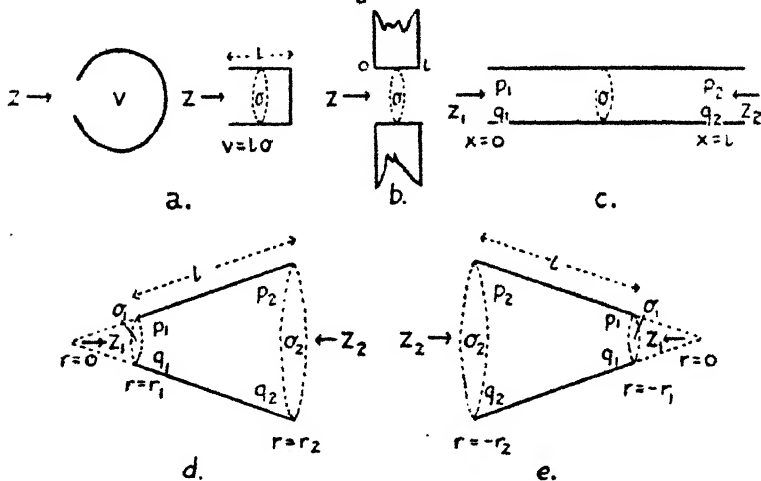
XXXIV. *On the Free Periods of Resonators.*

By ERIC J. IRONS, Ph.D.\*

## § 1. INTRODUCTION.

IN a former paper<sup>(1)</sup> use was made of the principles of "acoustical impedance" to calculate the free periods of a number of different forms of resonator, and to account for some results obtained by experiments with a Kundt's tube apparatus. In the present note the argument is presented in more detail, and is extended to include resonators having a conical horn as a component part.

Fig. 1.



Webster<sup>(2)</sup> confined his attention to plane waves in horns of narrow cross-section, and wrote

$$-\frac{dq}{dx} = -\frac{1}{\sigma} \frac{d}{dx} (q\sigma),$$

where  $\sigma$  is the area of cross-section and  $x$  is a measure of the distance along the horn. It is here shown that with conical horns Webster's differential equation is obtained without restriction as to cross-section if *spherical waves* are postulated †.

\* Communicated by the Author.

† Stewart (Phys. Rev. xvi. p. 322, 1920) states that Webster was aware of this result but did not publish it.

Immediate applications of the formulæ to be established are shown to yield more readily results which have been previously obtained by other methods.

In the earlier paper by the present writer<sup>(1)</sup> the electrical analogy of Stewart<sup>(2)</sup> was employed, and impedance was defined as  $p / \frac{dX}{dt}$ , where  $p$  represents excess pressure, and  $X$  is volume displacement. In this note Webster's practice of defining impedance by  $p/X$  is followed—as the formulæ to be established are thereby simplified—and the whole argument is made more general.

## § 2. CALCULATION OF THE IMPEDANCES OF VARIOUS UNITS.

Let us denote displacement, pressure, elasticity, condensation, frequency, and impedance by  $q$ ,  $p$ ,  $e$ ,  $s$ ,  $n$ , and  $Z$  respectively, and define  $\omega = 2\pi n$ ,  $k = \omega/a$ , and  $\beta = \rho a^2 k$ , where  $a$  is the velocity of sound and  $\rho$  is the density of the medium.

The usual assumptions that the fluid in the immediate neighbourhood of an orifice is incompressible, and that the condensation throughout a reservoir is uniform, will be made.

### (1) Reservoir. (Fig. 1, a.)

If an excess pressure  $p$  gives rise to a volume displacement  $X$  in a reservoir of volume  $v$ , then

$$p = e \cdot s = a^2 \rho (X/v),$$

and the impedance

$$Z = p/X = a^2 \rho / v. \quad \dots \dots (1.1)$$

### (2) Orifice. (Fig. 1, b.)

The equation of motion of a mass of fluid  $m$  situated in an orifice of length  $l$  and area of cross-section  $\sigma$ , when subjected to an alternating pressure  $p (= P \exp. i\omega t)$ , is

$$m\ddot{q} = \sigma P \exp. i\omega t.$$

Integrating twice gives

$$mq = (\sigma P \exp. i\omega t) / (-\omega^2),$$

and, as  $m = \rho l \sigma$  and  $X = q\sigma$ ,

$$Z = p/X = -\omega^2 \rho / c, \quad \dots \dots (1.2)$$

where  $c$  is the conductance of the orifice.

## (3) Tube. (Fig. 1, c.)

In his paper, Webster<sup>(2)</sup> gave a general method for determining the impedances of horns (of which the cylindrical tube is a special case); the present note being concerned solely with tubes and conical horns, the required formulæ may be established more directly in the following manner.

Assuming  $q$  to vary as  $\exp. i\omega t$ , we may write

$$\dot{q} = i\omega q \quad \text{and} \quad \ddot{q} = -\omega^2 q.$$

Substituting this result in the general equation of motion,

$$\rho \frac{d^2 q}{dt^2} + \frac{dp}{dx} = 0,$$

it follows that

$$\omega^2 q = \frac{1}{\rho} \frac{dp}{dx},$$

$$i. e., \quad \beta k q = \frac{dp}{dx} \quad \text{or} \quad \beta q = \frac{dp}{d(kx)} \quad \dots \quad (2)$$

For plane waves in a cylindrical tube

$$a^2 \frac{d^2 q}{dx^2} = \frac{d^2 q}{dt^2} = -\omega^2 q \quad \text{or} \quad a^2 \frac{d^2}{dx^2} \left( \frac{dq}{dx} \right) = -\omega^2 \left( \frac{dq}{dx} \right),$$

which, since

$$p = e \left( -\frac{dq}{dx} \right),$$

leads to

$$\frac{d^2 p}{dx^2} + k^2 p = 0. \quad \dots \quad (2.1)$$

the solution of this equation is

$$p = A \cos kx + B \sin kx, \quad \dots \quad (2.2)$$

and, using the result of (2), we may write

$$\beta q = -A \sin kx + B \cos kx. \quad \dots \quad (2.3)$$

Denoting values at the two ends of the tube at  $x=0$  and  $x=l$  by the subscripts 1 and 2 respectively, and writing  $\sigma$  for the cross-sectional area of the tube, we have

$$\begin{aligned} p_1 &= A, & \beta q_1 &= B, \\ p_2 &= A \cos kl + B \sin kl, & \beta q_2 &= -A \sin kl + B \cos kl, \end{aligned}$$

\* This assumes that the excess pressure  $p$  is so small that  $\rho$  may be taken as constant.

whence

$$\begin{aligned} Z_2 = p_2/X_2 &= \frac{\beta}{\sigma} \cdot \frac{p_2}{\beta q_2} = \frac{\beta}{\sigma} \cdot \frac{(p_1/\sigma q_1) \cos kl + (\beta/\sigma) \sin kl}{(-p_1/\sigma q_1) \sin kl + (\beta/\sigma) \cos kl} \\ &= \frac{\beta}{\sigma} \cdot \frac{Z_1 \cos kl + (\beta/\sigma) \sin kl}{-Z_1 \sin kl + (\beta/\sigma) \cos kl}. \quad (3.1) \end{aligned}$$

Similarly,

$$Z_1 = \frac{\beta}{\sigma} \cdot \frac{Z_2 \cos kl - (\beta/\sigma) \sin kl}{Z_2 \sin kl + (\beta/\sigma) \cos kl}. \quad (3.2)$$

These results correspond to equation (28) of Webster's paper <sup>(2)</sup>.

#### (4) Conical Horn. (Fig. 1, d.)

For spherical waves we have <sup>(4)</sup>

$$\frac{d^2(r \cdot s)}{dt^2} = a^2 \frac{d^2(r \cdot s)}{dr^2} \quad \dots \quad (4)$$

(the symbols having their usual significance), and, since  $p = e \cdot s$ ,

$$r \frac{d^2 p}{dt^2} = a^2 \frac{d^2(r \cdot p)}{dr^2}.$$

Further, if  $p$  varies as  $\exp. i\omega t$ , then

$$\ddot{p} = -\omega^2 p,$$

so that finally

$$\frac{d^2 p}{dr^2} + \frac{2}{r} \frac{dp}{dr} + k^2 p = 0. \quad \dots \quad (4.1)$$

The solution of this equation is

$$p = \frac{A \cos kr}{kr} + \frac{B \sin kr}{kr}. \quad \dots \quad (4.2)$$

Differentiating with respect to  $kr$ , we have, by virtue of (2),

$$\beta q = A \left\{ -\frac{\sin kr}{kr} - \frac{\cos kr}{k^2 r^2} \right\} + B \left\{ \frac{\cos kr}{kr} - \frac{\sin kr}{k^2 r^2} \right\}. \quad \dots \quad (4.3)$$

Considering the propagation of spherical waves in a conical horn, the smaller and larger ends of which are situated at distances  $r=r_1$ , and  $r=r_2$  from the vertex of the cone at  $r=0$ , and again denoting the values of  $p$ ,  $\sigma$ , and  $X$  at these ends by the subscripts 1 and 2 respectively, equations for  $p_1$ ,  $p_2$ ,  $\beta q_1$ , and  $\beta q_2$  may be written down. Solving for  $A$  and  $B$  between the equations for  $p_1$  and  $\beta q_1$ , and substituting the values obtained in the equations for  $p_2$  and  $\beta q_2$ , gives  $p$

and  $\beta q_2$  respectively in terms of  $p_1$  and  $\beta q_1$ . After some reduction, we have

$$\begin{aligned} Z_2 = p_2/X_2 &= \frac{p_2}{\beta q_2} \cdot \frac{\beta}{\sigma_2} \\ &= -\frac{\beta}{\sigma_2} \cdot \frac{Z_1 \sin k(l + \epsilon_1)/\sin k\epsilon_1 + (\beta/\sigma_1) \sin kl}{Z_1 \sin k(l + \epsilon_1 - \epsilon_2)/\sin k\epsilon_1 \cdot \sin k\epsilon_2 + (\beta/\sigma_1) \sin k(l - \epsilon_2)/\sin k\epsilon_2} \end{aligned} \quad (5.1)$$

where  $l = (r_2 - r_1)$  and  $\epsilon_1$  and  $\epsilon_2$  are defined by  $\tan k\epsilon_1 = kr_1$  and  $\tan k\epsilon_2 = kr_2$ .

In a similar manner it may be shown that

$$\begin{aligned} Z_1 = -\frac{\beta}{\sigma_1} \cdot \frac{Z_2 \sin k(l - \epsilon_2)/\sin k\epsilon_2 + (\beta/\sigma_2) \sin kl}{Z_2 \sin k(l + \epsilon_1 - \epsilon_2)/\sin k\epsilon_1 \cdot \sin k\epsilon_2 + (\beta/\sigma_2) \sin k(l + \epsilon_1)/\sin k\epsilon_1} \end{aligned} \quad (5.2)$$

These results correspond to equation (32) of Webster's paper <sup>(2)</sup>.

### § 3. NOTES ON THE FORMULÆ.

Throughout the paper the "length" of a pipe or cone with a *completely open* end is to be interpreted as the sum of its geometrical length and the appropriate end-correction, and the quantities involved are as shown on the respective diagrams. Terms involving friction are neglected as small compared with the terms retained, so that for resonance in any system the total impedance may be equated to zero.

The formulæ so far obtained yield immediately the following well-known results for:—

(1) *Resonance in Tubes* (using equation (3.2)).

a. Tube open at both ends.  $Z_1 = Z_2 = 0$ .

$$\therefore -(\beta/\sigma) \cdot \tan kl = 0;$$

$$\therefore kl = m\pi \quad \text{and} \quad l = m\lambda/2,$$

where  $m$  is any integer and  $\lambda$  is a wave-length.

b. Tube closed at one end.  $Z_1 = 0$ ,  $Z_2 = \infty$ .

$$\therefore (\beta/\sigma) \cot kl = 0 \quad \text{and} \quad l = [(2m + 1)/2] \cdot [\lambda/2].$$

c. Tube closed at both ends.  $Z_1 = Z_2 = \infty$ .

$$\therefore (\sigma/\beta) \tan kl = 0 \quad \text{and} \quad l = m\lambda/2.$$

Similar results are obtained using equation (3.1).

(2) *Resonance in Cones* (using equations (5.1) and (5.2)).

a. Cone open at both ends.  $Z_1 = Z_2 = 0$ .

By (5.1),

$$(-\beta/\sigma_2) \sin kl \cdot \sin k\epsilon_2 / \sin k(l - \epsilon_2) = 0,$$

and by (5.2),

$$(-\beta/\sigma_1) \sin kl \cdot \sin k\epsilon_1 / \sin k(l + \epsilon_1) = 0.$$

The only reasonable solution of both these equations is

$$\sin kl = 0 \quad \text{leading to} \quad m\lambda/2 = (r_2 - r_1),$$

with the usual notation (*cf.* Rayleigh<sup>(5)</sup>).

b. Cone closed at

(i.) Smaller end.  $Z_1 = \infty$ ,  $Z_2 = 0$ .

By (5.1),

$$(-\beta/\sigma_2) \sin k(l + \epsilon_1) \cdot \sin k\epsilon_2 / \sin k(l + \epsilon_1 - \epsilon_2) = 0,$$

and by (5.2),

$$(-\beta/\sigma_1) \sin kl \cdot \sin k\epsilon_1 / \sin k(l + \epsilon_1) = \infty.$$

Hence in both instances

$$\sin k(l + \epsilon_1) = 0 \quad \text{or} \quad \tan kl + kr_1 = 0,$$

(*cf.* Paris<sup>(6)</sup>, eqn. 44).

(ii.) Larger end.  $Z_1 = 0$ ,  $Z_2 = \infty$ .

By (5.1),

$$(-\beta/\sigma_2) \sin kl \cdot \sin k\epsilon_2 / \sin k(l - \epsilon_2) = \infty,$$

and by (5.2),

$$(-\beta/\sigma_1) \sin k(l - \epsilon_2) \sin k\epsilon_1 / \sin k(l + \epsilon_1 - \epsilon_2) = 0.$$

Hence in both instances

$$\sin k(l - \epsilon_2) = 0 \quad \text{or} \quad \tan kl = kr_2$$

(*cf.* Aldis<sup>(7)</sup>). Further, if the cone be continued to the vertex,

$$l = r_2 \quad \text{and} \quad \tan kl = k$$

(*cf.* Rayleigh, *loc. cit.*).

c. Cone closed at both ends.  $Z_1 = Z_2 = \infty$ .

By (5.1),

$$(-\beta/\sigma_2) \sin k(l + \epsilon_1) \sin k\epsilon_2 / \sin k(l + \epsilon_1 - \epsilon_2) = \infty,$$

and by (5.2),

$$(-\beta/\sigma_1) \sin k(l - \epsilon_2) \sin k\epsilon_1 / \sin k(l + \epsilon_1 - \epsilon_2) = \infty.$$

Hence in both instances

$$\sin k(l + \epsilon_1 - \epsilon_2) = 0 \quad \text{or} \quad \tan^{-1} kr_1 - kr_1 = \tan^{-1} kr_2 - kr_2$$

(cf. Rayleigh, *loc. cit.*). If the cone be continued to the vertex so that  $r_1 = 0$  and  $r_2 = l$ , then, as in the last paragraph,

$$\tan kl = kl.$$

When dealing with a system of resonators, distances will, for consistency, be measured in the direction of  $x$  positive, and the impedances of the systems to sound incident in the same direction will be calculated. This will necessitate an alteration in the formula for the impedance at the larger end of a cone. Putting  $r_1$ ,  $r_2$ , and  $l$  negative, so that  $-l = -(r_2 - r_1)$  (fig. 1, *e*), and substituting in (5.1), leads to

$$Z_2 = -\frac{\beta}{\sigma_2} \frac{Z_1 \sin k(l + \epsilon_1) / \sin k\epsilon_1 - (\beta/\sigma_1) \sin kl}{-Z_1 \sin k(l + \epsilon_1 - \epsilon_2) / \sin k\epsilon_1 \cdot \sin k\epsilon_2 + (\beta/\sigma_1) \sin k(l - \epsilon_2) / \sin k\epsilon_2} \quad (5.3)$$

It may be noted that if  $-l$  be substituted for  $l$  in (3.1), then the formulæ (3.1) and (3.2) for a tube become identical.

Moreover, if we make  $r_1 \rightarrow \infty$  and  $r_2 \rightarrow \infty$  in such a manner that  $(r_2 - r_1)$  remains finite and equal to  $l$ , then the cone becomes equivalent to a tube with  $\sigma_1 = \sigma_2 = \sigma$  (the cross-sectional area of the tube) and the values of both  $Z_1$  given by (5.2) and  $Z_2$  given by (5.3) become identical with that of  $Z_1$  for a tube (3.2).

Further, if the tube be short (so that  $kl$  may be substituted for  $\tan kl$ ) and closed ( $Z_2 = \infty$ ), then the formula for  $Z_1$  (3.2) reduces to  $a^2\rho/v$  (cf. fig. 1, *a*), which is the value for a reservoir. Similarly, if the tube be short and open ( $Z_2 = 0$ ), then the formula for  $Z_1$  becomes  $-\omega^2\rho/c$ , which is the value for an orifice.

It may also be noted that the formula for  $Z_2$  for a cone given in (5.1) reduces to that for  $Z_2$  for a tube given in (3.1) under the appropriate conditions.

#### § 4. APPLICATION OF FORMULÆ TO SOME COMPOUND SYSTEMS.

As a preliminary it may be noted that the impedance of a component part consisting of an orifice leading to a reservoir is, by virtue of (1.1) and (1.2), given by

$$-\omega^2\rho/c + a^2\rho/r.$$

For resonance this quantity must be equated to zero and, if  $n_1$  represents the natural frequency of such a resonator, then

$$n_1 = a/2\pi \cdot \sqrt{c/v},$$

the well-known formula for a Helmholtz resonator. The impedance of the system to a note of frequency  $n$  may therefore be written as

$$-(2\pi n)^2 \cdot \rho/c + (2\pi n_1)^2 \cdot \rho/c \quad \text{or} \quad -(4\pi^2 \rho n n_1/c) \cdot \left( \frac{n}{n_1} - \frac{n_1}{n} \right) \quad (1.3)$$

by substituting for  $a^2/v$  in terms of  $n_1$ .

All the formulæ to obtain results previously given by Paris (*loc. cit.*), Aldis (*loc. cit.*), Rayleigh (*loc. cit.*), and by Lees<sup>(8)</sup> have now been established. Some of these results have, subject to an implied but unnecessary assumption, already been obtained on impedance principles<sup>(1)</sup> but are included here for the sake of completeness.

(1) *Stopped Pipe with Helmholtz Resonator at the End.*  
(Boys' Resonator.) (Fig. 2.)

For resonance,  $Z_1$ , as determined by (3.2), must be zero, i. e.,

$$Z_2 \cos kL - (\beta/\sigma) \sin kL = 0,$$

where  $Z_2$  has the value given by (1.3). It follows that

$$\tan kL = - \frac{2\pi\sigma n_1}{ac_1} \left( \frac{n}{n_1} - \frac{n_1}{n} \right), \quad \dots \quad (6)$$

which is the same as the result of Paris (Ref. 6, eqn. 1).

(2) *Stopped Pipe with Helmholtz Resonator on the Side.*  
(Fig. 3.)

The impedance at  $x=l$  of the closed tube of length  $(L-l)$  is  $(\beta/\sigma) \cdot \cot k(L-l)$ . When a displacement passing from  $x=0$  to  $x=l$  reaches  $x=l$ , it may be propagated either through the orifice into the reservoir or into the tube of length  $(L-l)$ ; the impedances of these components must therefore be considered in parallel, so that

$$1/Z_2 = 1/(\beta/\sigma) \cot k(L-l) - 1/(4\pi^2 \rho n n_1/c_1) \cdot (n/n_1 - n_1/n),$$

$Z_1$  having the value given by (3.2), for resonance,

$$Z_2 \cos kl - (\beta/\sigma) \sin kl = 0,$$



whence

$$\frac{1}{\cot kl - \tan k(L-l)} = -\frac{2\pi\sigma n_1}{ac_1} \left( \frac{n}{n_1} - \frac{n_1}{n} \right) \quad (7)$$

(cf. Ref. 6, eqn. 10).

(3) *Stopped Pipe with Two Helmholtz Resonators on the Side.* (Fig. 4.)

The impedance at  $x=l_1+\delta$  (where  $\delta$  is small) is, by application of the formulæ and principles evoked in the last example, equal to

$$\frac{\beta}{\sigma} \frac{Z_0 \cos k(l_2-l_1) - (\beta/\sigma) \sin k(l_2-l_1)}{Z_0 \sin k(l_2-l_1) + (\beta/\sigma) \cos k(l_2-l_1)},$$

where

$$1/Z_0 = 1/(\beta/\sigma) \cot k(L-l_2) - 1/(4\pi\rho n n_2/c_2) \cdot (n/n_2 - n_2/n).$$

The impedance at  $x=l_1-\delta$ ,  $Z_2$ , is equal to the sum in parallel of this quantity and  $-(4\pi\rho n n_1/c_1) \cdot (n/n_1 - n_1/n)$ . Finally, for resonance, the impedance at  $x=0$ ,  $Z_1$ , is zero, so that

$$Z_2 \cos kl_1 - (\beta/\sigma) \sin kl_1 = 0.$$

After some reduction this gives

$$\frac{\cot kl_2 + T_2 \cot k(L-l_2)}{1 - S_2 \cot k(L-l_2)} = \frac{1 + S_1 \cot kl_1}{S_1 - \cot kl_1}, \quad (8)$$

where, following Paris (Ref. 6, eqns. 12, 27, and 28), we write

$$\begin{aligned} S_1 &= \cot kl_1 + \cot k\gamma_1, & T_2 &= 1 - \cot k\gamma_2 \cdot \cot kl_2, \\ S_2 &= \cot kl_2 + \cot k\gamma_2, & \tan k\gamma_s &= (2\pi\sigma n_s/ac_s) \cdot (n/n_s - n_s/n). \end{aligned}$$

(4) *Conical Horn fitted with Helmholtz Resonator at the Smaller End.* (Fig. 5.)

Substituting the value of  $Z_1$  from (1.3) in the formula (5.3) for  $Z_2$ , and equating to zero for resonance, gives

$$\begin{aligned} &-(4\pi\rho n n_1/c_1) \cdot (n/n_1 - n_1/n) [\sin k(L+\epsilon_1)/\sin k\epsilon_1] \\ &\quad - (\beta/\sigma_1) \sin kL = 0; \end{aligned}$$

whence, writing  $\Omega R_0^2$  for  $\sigma_1$ , where  $\Omega$  is the solid angle of the cone, and remembering that  $\cot k\epsilon_1 = 1/kR_0$ , we have

$$\frac{1}{(a/2\pi n R_0) + \cot(2\pi n L/a)} = -\frac{2\pi\Omega R_0^2 n_1}{ac_1} \left( \frac{n}{n_1} - \frac{n_1}{n} \right), \quad (9)$$

which is the result obtained by Paris (Ref. 6, eqn. 43).

(5) Cone Closed at Smaller End with Helmholtz Resonator on the Side. (Fig. 6.)

At the closed end of the cone  $Z_0 = \infty$ , so that the impedance due to this unit at the large end of the cone  $R_0 R_1$

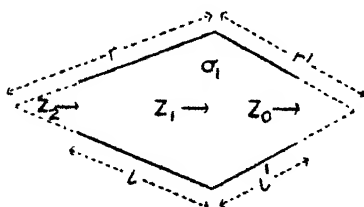
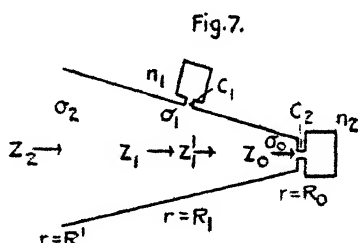
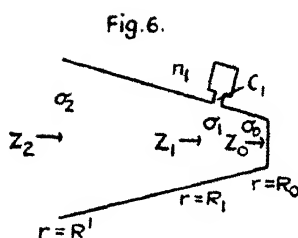
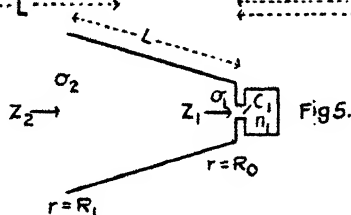
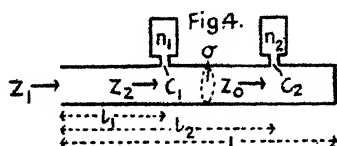
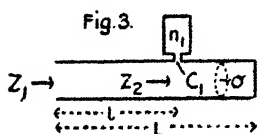
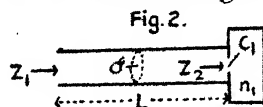
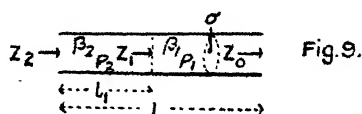


Fig. 8.

$$\tan \kappa \epsilon_1 = \kappa r; \tan \kappa \epsilon'_1 = \kappa r'.$$



is, by substitution of the relevant quantities in (5.3), equal to

$$(\beta/\sigma_1) \cdot [\sin k(R_1 - R_0 + \epsilon_0) \cdot \sin \kappa \epsilon_1 / \sin k(R_1 - R_0 + \epsilon_0 - \epsilon_1)] = Z'_1 \text{ (say).}$$

The effective impedance at  $R_1$ ,  $Z_1$ , is found by adding in parallel the impedance of the cone  $R_0R_1$  and the orifice and reservoir—thus

$$1/Z_1 = 1/Z_1' - 1/(4\pi^2\rho n n_1/c_1) \cdot (n/n_1 - n_1/n).$$

Finally, equating the value of  $Z_2$  given by (5.3) to zero,

$$Z_1 \sin k(R' - R_1 + \epsilon_1)/\sin k\epsilon_1 - (\beta/\sigma_1) \sin k(R' - R_1) = 0,$$

and substituting the value of  $Z_1$  leads to

$$\frac{1}{\cot k(R' - R_1) - \tan k(R_1 - R_0 - \rho_0)} = \frac{-2\pi\Omega R_1^2 n_1}{a c_1} \left( \frac{n}{n_1} - \frac{n_1}{n} \right), \quad (10)$$

where, as in Paris's notation,  $\rho_0$  is defined by

$$\cot k\rho_0 = kR_0$$

(cf. Ref. 6, eqn. 50).

(6) *Cone fitted with One Helmholtz Resonator at the Smaller End and Another on the Side.* (Fig. 7.)

At the smaller end of the cone

$$Z_0 = -(4\pi^2\rho n n_2/c_2) \cdot (n/n_2 - n_2/n).$$

The impedance at  $R_1$  ( $=Z_1'$ , say) of the system  $R_1R_0$  is given by

$$Z_1' = -\frac{\beta}{\sigma_1} \cdot \frac{Z_0 \sin k(R_1 - R_0 + \epsilon_0)/\sin k\epsilon_0 - (\beta/\sigma_0) \sin k(R_1 - R_0)}{Z_0 \sin k(R_1 - R_0 + \epsilon_0 - \epsilon_1)/\sin k\epsilon_0 \cdot \sin k\epsilon_1 + (\beta/\sigma_0) \sin k(R_1 - R_0 - \epsilon_1)/\sin k\epsilon_1},$$

so that the total impedance at  $R_1$  ( $Z_1$ ) is such that

$$1/Z_1 = 1/Z_1' - 1/(4\pi^2\rho n n_1/c_1) \cdot (n/n_1 - n_1/n).$$

Finally, equating the impedance at  $R'$  ( $=Z_2$ ) to zero for resonance, we obtain

$$Z_1 \sin k(R' - R_1 + \epsilon_1)/\sin k\epsilon_1 = (\beta/\sigma_1) \sin k(R' - R_1).$$

Following Paris<sup>(6)</sup>, and defining

$$\cot k\gamma = \frac{c_2}{1 - (n_2^2/n^2)} \cdot \frac{1}{k\Omega R_0^2}$$

and

$$\cot kK = \frac{kR_0 (\cot kR_0 - \cot k\gamma) - 1}{kR_0 + \cot kR_0 + kR_0 \cdot \cot kR_0 \cdot \cot k\gamma},$$

\* There is a mistake in sign in the revised form of Paris's eqn. 55.

we obtain his result,

$$\frac{1}{\cot k(R' - R_1) - \tan k(R_1 - K)} = \frac{-2\pi\Omega R_1^2 n_1}{ac_1} \left( \frac{n}{n_1} - \frac{n_1}{n} \right),$$

. . . (11)

for the resonant tones.

(7) *Two Open Cones joined at their Larger Ends.*  
(Fig. 8.)

As  $Z_0=0$ , then

$$Z_1 = (\beta/\sigma_1) \sin kl' \cdot \sin k\epsilon_1' / \sin k(l' - \epsilon_1')$$

by (5.3). For resonance  $Z_2=0$ , i. e.,

$$-(\beta/\sigma_2) [Z_1 \sin k(l - \epsilon_1) / \sin k\epsilon_1 + (\beta/\sigma_1) \sin kl] = 0$$

by (5.2), or

$$\sin kl' \cdot \sin k(l - \epsilon_1) \cdot \sin k\epsilon_1' = -\sin kl \cdot \sin k(l' - \epsilon_1') \cdot \sin k\epsilon_1,$$

or

$$\sin kl \cdot \sin kl' (1/r + 1/r') = k \sin k(l + l'), \quad . . . (12)$$

which is the result given by Aldis (*loc. cit.*).

(8) *A Composite Column of Gas.* (Fig. 9.)

Prof. Lees<sup>(8)</sup> has recently derived equations giving the free periods of a composite column consisting of two gases: his results may be obtained by impedance methods and, as an example, the formula for the instance in which both ends of the column are antinodes is derived below.

As  $Z_0=0$ , the impedance at  $x=l_1$  of the column of length  $(L-l_1)$  containing the first gas to a note of frequency  $n$  is

$$Z_1 = -(\beta_1/\sigma) \tan k_1(L-l_1),$$

where  $\beta_1 = \rho_1 a_1^2 k$  and  $k_1 = 2\pi n/a_1$ , and the subscripts refer to the constants of the first gas. Again, as  $Z_2=0$ , then by (3.2),

$$Z_1 \cos k_2 l_1 - (\beta_2/\sigma) \sin k_2 l_1 = 0,$$

where  $\beta_2 = \rho_2 a_2^2 k_2$  and  $k_2 = 2\pi n/a_2$ . Now if the period of the column when filled with the first constituent is  $n_1$ , then

$$2Lm_1 = a_1 = \sqrt{(F_1/\rho_1)}, \quad k_1 = (\pi/L)(n/n_1),$$

and

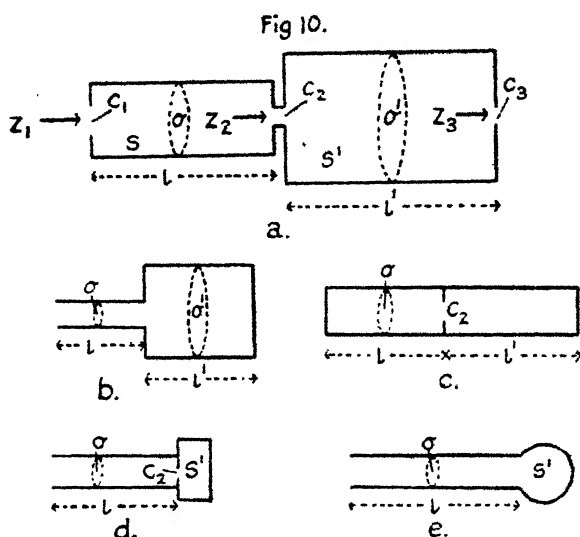
$$\beta_1 = F_1(\pi/L)(n/n_1),$$

where  $F_1$  is the modulus of adiabatic elasticity of this constituent. By writing down the equations which hold when

the second constituent fills the column similar values for  $k_2$  and  $\beta_2$  are obtained, so that finally

$$(n_2/F_2) \cot \frac{\pi}{L} \cdot \frac{n}{n_2} \cdot l_1 = -(n_1/F_1) \cot \frac{\pi}{L} \cdot \frac{n}{n_1} (L - l_1), \quad (13)$$

which is Lees' equation (7.3).



(9) *Two Coaxial Tubes with Orifices communicating with the Outer Atmosphere and with each other.*

As a final example, the resonant frequencies of the system shown in fig. 10, a will be calculated.

From equations (1.2) and (3.2) we have:—

$$Z_3 = -\omega^2 \rho / c_3,$$

$$Z_2 = \frac{\beta}{\sigma'} \left[ \frac{(-\omega^2 \rho / c_3) \cos kl' - (\beta / \sigma') \sin kl'}{(-\omega^2 \rho / c_3) \sin kl' + (\beta / \sigma') \cos kl'} \right] - \omega^2 \rho / c_2$$

$$Z_1 = \frac{\beta}{\sigma} \left[ \frac{Z_2 \cos kl - (\beta / \sigma) \sin kl}{Z_2 \sin kl + (\beta / \sigma) \cos kl} \right] - \omega^2 \rho / c_1 = 0,$$

for resonance. Whence, substituting for  $Z_2$  and  $\beta$ ,

$$\left[ \frac{\omega^2 / c_3 + (a\omega / \sigma') \tan kl'}{1 - (\sigma' \omega / ac_3) \tan kl'} \right] + \left[ \frac{\omega^2 / c_1 + (a\omega / \sigma) \tan kl}{1 - (\sigma \omega / ac_1) \tan kl} \right] + \frac{\omega^2}{c_2} = 0. \quad (14)$$

This may be regarded as the general equation for resonance

in a "series" system, and from it the following results are obtained on substituting the appropriate conditions:—

a. "Bottle-Pipe" Resonator. (Fig. 10, *b*.)

$$c_3 = 0, \quad c_1 = c_2 = \infty, \quad \text{and} \quad \tan kl \cdot \tan kl' = \sigma/\sigma', \quad \dots (14.1)$$

where  $l$  has now to be interpreted as the length of the pipe, together with the end correction as ordinarily understood (*cf.* Ref. 7).

b. Tube Closed at Both Ends and fitted with a Coaxial Diaphragm. (Fig. 10, *c*.)

$$\sigma' = \sigma, \quad c_1 = c_3 = 0, \quad \text{and} \quad \cot kl' + \cot kl = \omega\sigma/ac_2 \quad \dots (14.2)$$

(*cf.* Ref. 1, eqn. 6, and Part II. for experimental verification.)

c. Boys Resonator. (Fig. 10, *d*.)

If  $l'$  is small—which is tantamount to assuming that the condensation within the volume  $S'$  is sensibly uniform— $\tan kl'$  may be replaced by  $kl'$ , and the "pipe" becomes a reservoir. With the additional conditions  $c_1 = \infty$ ,  $c_3 = 0$ , and remembering  $l'\sigma' = S'$ , and that  $l$  now includes the end correction, it follows that

$$\tan kl = \frac{-2\pi\sigma n_1}{ac_3} \left( \frac{n}{n_1} - \frac{n_1}{n} \right), \quad \dots (14.3)$$

where  $n_1$  has its former significance (*cf.* equation (6)).

d. Pipe near its Closed End expanding into a Bulb of Small Capacity. (Fig. 10, *e*.)

As in the previous example,  $\tan kl'$  will be replaced by  $kl'$ , and, as the shape of the bulb is immaterial, it will be considered that  $S' = \sigma'l'$ : in addition,  $c_1 = c_2 = \infty$  and  $c_3 = 0$ . Substituting in (14) yields

$$\tan kl = \sigma/kS \quad \dots (14.4)$$

(*cf.* Ref. 5, p. 209).

e. Rayleigh Double Resonator.

In this resonator the pipes of fig. 10, *a* are replaced by reservoirs, and, as before, we shall write  $kl$  and  $kl'$  for  $\tan kl$  and  $\tan kl'$  respectively in (14), so that

$$\left[ \frac{1/c_3 + l'/\sigma'}{1 - \omega^2 S'/a^2 c_3} \right] + \left[ \frac{1/c_1 + l/\sigma}{1 - \omega^2 S/a^2 c_1} \right] + \frac{1}{c_2} = 0,$$

taking the volumes of the reservoirs  $S$  and  $S'$  to be  $\sigma l$  and  $\sigma' l'$  respectively. It is to be noted that the expression  $1/c_3 + l'/\sigma'$  represents the "resistance" of the orifice, together with the "resistance" of the short tube or reservoir. If, following Rayleigh, we neglect the effect of inertia in the interior of the reservoir, and assume that the  $l/\sigma$  terms are small compared with the  $1/c$  terms, then

$$\omega^4 - \omega^2 a^2 \left[ \frac{c_1 + c_2}{S} + \frac{c_3 + c_2}{S'} \right] + \frac{a^4}{SS'} [c_1 c_3 + c_2 (c_1 + c_3)] = 0, \quad \dots (14.5)$$

which is the result obtained by Rayleigh (Ref. 5, p. 190). Equation (14) would yield information concerning the overtones of this system, assuming the reservoirs to be of the form shown in fig. 10, *a*.

For a general discussion of the results obtained in this paragraph the reader is referred to the sources cited.

## § 5. CONCLUSION.

Examples of resonator problems to which the methods of this paper afford an easy solution could be multiplied, but it is hoped that the above will serve both to illustrate the principles involved and to show their general applicability. It should be noted that the method will also yield solutions to other elastic problems in which the counterparts of the general equations of § 2 obtain.

The application of the method to the theory of certain "wind" instruments is reserved for a further paper.

The author has pleasure in recording his appreciation of the kindly interest Professor Lees and Dr. E. T. Paris have shown in the present work.

## *References.*

- (1) Irons, *Phil. Mag.* vii. p. 873 (1929).
- (2) Webster, *Proc. Nat. Acad. Sci.* v. p. 275 (1919).
- (3) Stewart, *Phys. Rev.* xx. p. 528 (1922) *et seq.*
- (4) See, *e. g.*, Barton, 'Text-Book of Sound,' p. 220. (Macmillan & Co.)
- (5) Rayleigh, 'Theory of Sound,' ii. p. 114. (Macmillan & Co.)
- (6) Paris, *Phil. Mag.* xlviii. p. 769 (1924).
- (7) Aldis, 'Nature,' cxiv. p. 309 (1924).
- (8) Lees, *Proc. Phys. Soc.* xli. p. 204 (1929).

**XXXV. The Paramagnetic Rotatory Dispersion of Aqueous Solutions of Cobalt Sulphate in the Visible and Ultra-Violet Regions of The Spectrum.** By R. W. ROBERTS, *M.Sc., The University, Liverpool* \*.

**I. Introduction.**

**I**N two previous investigations † on the magnetic rotatory dispersion of certain cobalt salts in aqueous solution it was found that the magneto-optical dispersions of these solutions do not follow the laws holding for diamagnetic substances. Also it was found that the  $\text{Co}^{++}$  ion, like the ions  $\text{Fe}^{++}$  and  $\text{Fe}^{+++}$ , is capable of exerting a negative rotation of the plane of polarization. This negative rotation of the  $\text{Co}^{++}$  ion was found in solutions of the sulphate, chlorate, acetate, nitrate, and ammonium sulphate. In the case of solutions of cobalt chloride and cobalt bromide the negative rotation of the  $\text{Co}^{++}$  ion was found to be overpowered by the diamagnetic rotation due to the chlorine and bromine ions respectively. In view of these results, and others which were mentioned in the introduction to paper II., it was pointed out that the study of the Faraday effect in paramagnetic substances is capable of yielding information which cannot be obtained from ordinary dispersion data. Since the appearance of these papers Ladenburg ‡, in an outstanding work, has shown, contrary to what was usually supposed, that there are two types of magnetic rotation of the plane of polarization, the usual diamagnetic rotation found in all transparent substances, and the paramagnetic rotation which arises from paramagnetic atoms. Ladenburg has deduced a formula for this paramagnetic rotation, and also from quantum considerations given a rule governing the occurrence of negative rotations, which could not in any way be explained on classical grounds.

Recently the Ladenburg formula has been brilliantly verified by Becquerel and de Haas § for the paramagnetic

\* Communicated by Prof. L. R. Wilberforce, M.A.

† R. W. Roberts, J. H. Smith, and S. S. Richardson, *Phil. Mag.* xliv. p. 917 (1922); R. W. Roberts, *Phil. Mag.* xlix. p. 397 (1925). (Referred to as Papers I. and II. respectively.)

‡ *ZS. f. Phys.* xxxiv. p. 898 (1925).

§ *Journ. de Phys.* x. p. 283 (1925).



rotatory dispersion of the rare earth crystals tysonite and parisite at very low temperatures.

In view of these advances in our knowledge of paramagnetic rotation, it was thought that a further study of the magnetic rotatory dispersion of cobalt solutions would be of experimental and theoretical interest.

Cobalt sulphate solutions were chosen as suitable, because the diamagnetic effect due to the  $\text{SO}_4^{--}$  ion is small compared with that due to most anions.

A graph exhibiting the rotatory dispersion of a solution of  $\text{CoSO}_4$  in water has already been given in paper I.

## II. The Solutions.

Measurements of the natural and magnetic rotatory dispersions have been made on five solutions denoted by

TABLE I.

Solution.	W.	$d_1^{25}$ .	$d_4^{25}$ .
A	4.33	1.04249	1.04112
B	6.45	1.06524	1.06362
C	10.23	1.10664	1.10500
D	19.14	1.21308	1.21101
E	22.26	1.25525	1.25313
F	25.00	—	1.29465

A, B, C, D, and E. The solutions were prepared from a reagent quality of cobalt sulphate, stated to be nickel and iron free, and distilled water. The cobalt sulphate was recrystallized from distilled water several times before use. The strengths, expressed in Table I. as W grams of  $\text{CoSO}_4$  in 100 grams of solution, have been determined from the weights of the components on the assumption that the crystals had the composition  $\text{CoSO}_4 \cdot 7\text{H}_2\text{O}$ . The strength of E ( $W_E$ ), owing to error, had to be corrected by setting up, using the data for solutions B, C, D, and F (an extra solution made up for this purpose), an interpolation formula expressing W as a function of  $d_1^{25} - d_w^{25}$ ,  $d_4^{25}$  and  $d_w^{25}$  denoting the densities at  $25^\circ \text{C}$ . of the solutions and water respectively. Inserting the density of E in this formula,  $W_E$  was found to be equal to 22.28. Another determination, using the interpolation formula for a solution obtained

by diluting E, gave  $W_k=22.24$ . The mean value 22.26 has been taken throughout the work as the strength of E. The densities were determined at temperatures in the neighbourhood of 20° C. and 25° C., and reduced to 20°C. and 25° C. by linear interpolation. Owing to the small capacity of the pycknometer, the values of the densities are uncertain to about four units in the fifth decimal place.

TABLE II.

$d_4^{25}$ .	W—Manchot.	W—Interpolation.
1.1131	10.98	10.96
1.2218	20.00	19.98

Manchot, Zahrstorfer, and Zepter \* give the densities and strengths of two cobalt sulphate solutions at 25° C. For the sake of comparison their strengths and the strengths calculated by using the interpolation formula are given in Table II. It will be seen that the agreement between the two values is quite satisfactory.

### III. *Magnetic Rotation Measurements.*

PART 1. *Measurements in the Visual Spectrum (with A. Weale).*—As the apparatus used in the present investigation is different from that employed in the earlier work a brief description of it will be given.

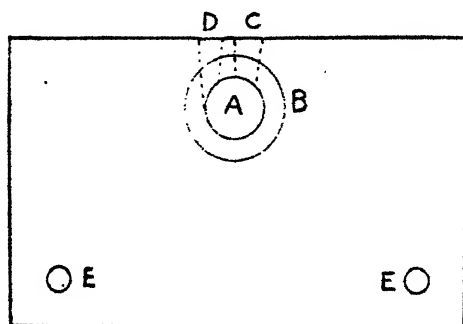
The electromagnet was a large Du Bois model which was water-cooled. The gap between the pole-pieces was kept fixed throughout the work at a distance of about 1.5 cm. Preliminary investigations by Dr. A. V. Moses and one of us (R. W. R.) with a search-coil and flux-meter showed that the field in the gap was not uniform, there being, owing to the existence of the borings, two maxima, symmetrically placed with respect to the centre of the gap. Lack of uniformity of the field is of no disadvantage in the present investigation so long as the cell holding the solution under test is always replaced in the same position. The cell was placed almost symmetrically between the pole-pieces. This adjustment need not be rigorously exact, owing to the symmetrical nature of the field.

\* *Zs. Anorg. Ch.* 141, p. 50 (1924).

The magnet was excited with a current of 10.50 amperes taken from the city mains. The current was kept constant by pressure control of a carbon resistance in series with an open wire resistance. When no loads were being taken from the mains the current was kept constant to about  $\pm 0.01$  ampere.

The cell containing the solution under test was made from a piece of plate glass whose approximate dimensions were 6.7 cm. by 11.2 cm. by 1.2 cm. A cylindrical boring A (fig. 1) 1.5 cm. in diameter was made through the plate glass perpendicular to the largest pair of faces, the axis of the boring being 1.7 cm. from the upper face of the plate. This boring was closed by cementing two plates B, about  $\frac{1}{4}$  mm. thick, of left-handed and right quartz cut perpendicular to the optic axis.

Fig. 1.



A conical boring C provided with a ground stopper served for filling purposes. A second conical boring D was fitted with a ground stopper containing a thermo-junction of copper-constantan. The base of this stopper was ground very thin and projected slightly into A. To prevent any evaporation of the solution during the observations the ground stoppers fitting C and D were waxed at the top of the conical holes.

The cell was fixed to a holder screwed into the base of the magnet by means of two screws passing through the clearance holes E drilled into the glass plate. The holder could be rotated about horizontal and vertical axes, for the purpose of setting the cell normal to the axis of the electromagnet.

The second thermo-junction was kept inside a transparent Dewar vessel containing water, stirrer, and thermometer. The thermo-junctions were in series with a moving coil galvanometer, which could be read by the observer watching the ammeter at a considerable distance away from the electromagnet.

The polarizer and analyser were mounted in bronze tubes fitting into the conical borings of the Du Bois electromagnet. This arrangement is of great convenience in securing a fixed alignment of the optical parts. The polarizer was a two-part Lippich with variable half shadow angle. The horizontal dividing line of the Lippich was very fine, and practically vanished when the setting for equal intensities in the two parts of the polarizer field was made. The polarizer tube also carried a condensing lens, by means of which an image of the source of light could be focussed centrally on the analyser diaphragm.

The analyser was a Thompson Glan glycerine-cemented prism with an opening of 10 mm. This analyser was also used for the ultra-violet work described later. Both the polarizer and analyser were provided with suitable diaphragms, so that the correct polarimetric conditions for the path of the light rays were obtained. The analyser rotated with a graduated circle provided with two opposite fixed verniers reading to  $\cdot 01^\circ$ .

The axis of rotation of the circle was set parallel to the axis of the electromagnet. The dividing line of the polarizer was focussed on the slit of a constant deviation spectroscope by means of an achromatic lens of about 20 cm. focal length. This was mounted on the analysing circle, and rotated with it.

Two sources of light were mainly used—a quartz mercury vapour lamp and a carbon arc. The chief advantages of the mercury vapour lamp arise from its great and steady intensity, which is only slightly influenced by the reversal of the current through the electromagnet. The carbon arc, although capable of giving great intensity, is not easy to maintain constant and centred, particularly when it is fed with metallic salts.

The rotations for each line have been deduced from the mean of at least ten settings of the analyser (in many cases from much more than ten), the current being reversed after every five settings. As the intensities of the lines for which readings were taken differ widely, partly

TABLE III.—Observed Rotations.

Upper line : rotations in degrees.

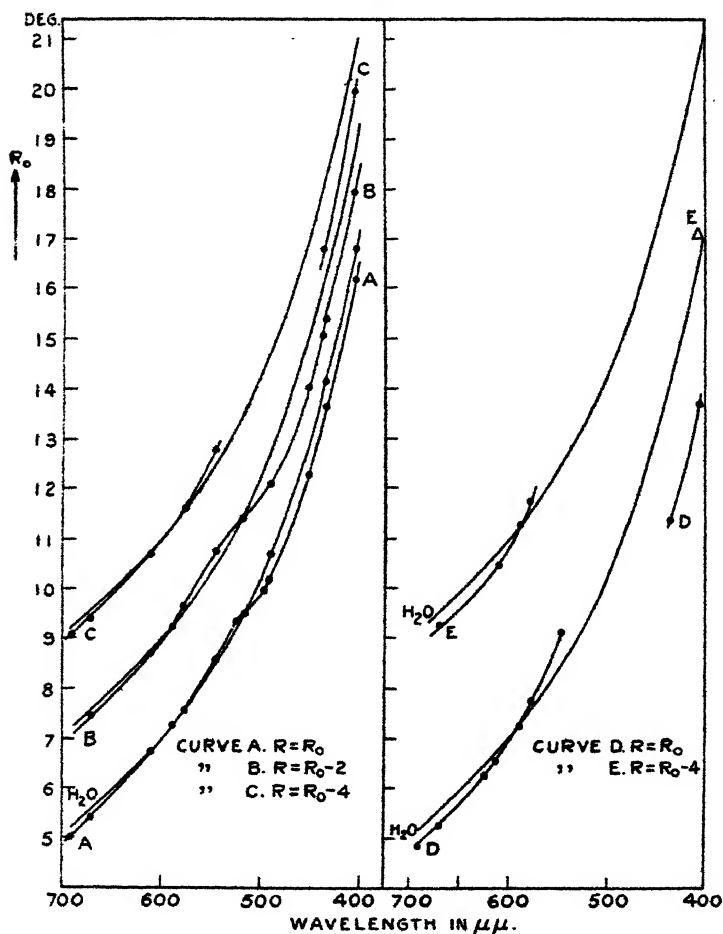
Lower line : temperature in ° C.

$\lambda$ in A.U.	H <sub>2</sub> O.	A.	B.	C.	D.	E.
6908	.....	5.01 $\pm$ .030 18.8	.....	5.07 $\pm$ .020 18.8	4.86 $\pm$ .011 15.5	
6708	5.537 $\pm$ .0089 18.7	5.46 $\pm$ .011 19.0	5.447 $\pm$ .0083 16.7	5.410 $\pm$ .0096 16.9	5.25 $\pm$ .023 18.9	5.29 $\pm$ .012 19.2
6104	6.760 $\pm$ .0046 18.7	6.736 $\pm$ .0077 19.0	6.698 $\pm$ .0073 16.7	6.70 $\pm$ .012 16.6	6.57 $\pm$ .011 17.9	6.48 $\pm$ .012 19.2
5893	7.265 $\pm$ .0027 18.7	7.289 $\pm$ .0045 18.5	7.252 $\pm$ .0086 16.7	7.208 $\pm$ .0076 16.8	7.27 $\pm$ .010 15.1	7.281 $\pm$ .0082 19.3
5780	7.519 $\pm$ .0047	7.548 $\pm$ .0035 16.9	7.658 $\pm$ .0057 16.7	7.610 $\pm$ .0037 17.2	7.746 $\pm$ .0052 15.5	7.739 $\pm$ .0052 19.3
5461	8.464 $\pm$ .0013	8.594 $\pm$ .0050 17.9	8.748 $\pm$ .0045 16.7	8.75 $\pm$ .012 19.8	9.13 $\pm$ .058	absorption.
4916	10.669 $\pm$ .0058	10.18 $\pm$ .068 19.5	10.09 $\pm$ .023*			
6234	.....	.....	.....	.....	6.24 $\pm$ .022 17.0	
5682	.....	.....	.....	7.94 $\pm$ .013 16.9		
5230	.....	9.36 $\pm$ .013				
5194	.....	.....	9.40 $\pm$ .022			
5167	.....	9.515 $\pm$ .031				
4958	.....	10.04 $\pm$ .087				
4529	.....	12.24 $\pm$ .640	12.02 $\pm$ .024			
4384	.....	.....	13.05 $\pm$ .033			

\*  $\lambda$  4910.†  $\lambda$  4527.

on account of the differences in the intensities of the lines emitted by the source, and partly on account of the unequal absorption of the lines by the solutions, I have recorded in Table III. with each rotation the mean probable error. In order to follow the course of the dispersion of the

Fig. 2.



rotation on the graph shown in fig. 2 the radii of the open circles representing the rotations have been taken equal to  $.04^\circ$ .

For the sake of clearness the rotation graphs for each solution have been drawn displaced with reference to the ordinate axis. The necessary correction in order to

obtain the observed rotation from the scale reading is indicated for each curve.

The readings in the red region of the spectrum were found to be rather trying, owing to the low intensities of the available sources, the low sensitivity of the eye in the red, and the disturbing influence due to the light scattered from the surfaces of the spectroscope lenses and prism. For the denser solutions this scattered light was considerably cut down, owing to the presence of the strong absorption band in the green.

The half-shadow angle was varied to suit the intensity of the particular line under observation. It varied from  $15^\circ$  in the red to  $1\frac{1}{2}^\circ$  for the bright lines.

TABLE IV.

Verdet's Constants.

$\lambda$ in A.U.	H <sub>2</sub> O.	A.	B.	C.	D.
6908	...	-00955	...	-00961	-00875
6708	-00998	-00983	-00981	-00989	-00975
6104	-01218	-01213	-01206	-01206	-01191
5893	-01309	-01313	-01306	-01298	-01309
5780	-01355	-01360	-01381	-01372	-01398
5461	-01534	-01549	-01577	-01578	-01649
4916	-01934	-01830	-01813*	...	...
6234	...	...	...	...	-01124
5682	...	...	...	-01432	...
5230	...	-01685	...	...	...
5194	...	...	-01692	...	...
5167	...	-01723	...	...	...
4958	...	-01830	...	...	...
4529	...	-02261	-02163†	...	...
4384	...	...	-02345	...	...

\*  $\lambda$  4910.†  $\lambda$  4527.

The observed values of the rotation, corrected for the rotation due to the end-plates (determined directly), have been reduced to give Verdet constants, which are recorded in Table IV. To this end the rotation due to the cell, filled with water, was determined for the Na line 5893 at  $18.7^\circ$  C. from forty settings of the analyser. Using the formula given by Rodger and Watson\* for Verdet's constant  $V_t$  for water at  $t^\circ$  C. (D line),

$$V_t = 0.01311' (1 - 0.04305t - 0.00305t^2), \quad 3 < t < 98,$$

\* Phil. Trans. A, clxxvi. p. 621 (1895).

the change of magnetic potential on reversal of the field with a current of 10.50 amperes was found to be 31,953 cm. gauss.

No corrections have been made for the rotation due to more than one passage of the light through the solutions, as the reflected light, owing to the want of parallelism of the plates, did not enter the slit of the spectroscope. The cell was adjusted by an autocollimation method using the analysing lens, so that the plane bisecting the angle between the faces was perpendicular to the axis of the apparatus.

From fig. 2 it will be seen that the rotations of all the solutions are less than that of water in the red, and become greater than the rotations of water on approaching the 5100 A.U. band\*. On the violet side of this band the rotation curves for the solutions are again below the water curve. An attempt was made to obtain more values of the rotation in the neighbourhood of the absorption band, using the continuous radiation from a carbon arc passing a current of about 17 amperes. The curves obtained by plotting the simultaneous readings of the drum of the constant deviation spectroscope, giving the wave-length for which matching of intensity occurred, against the readings of the analyser circle showed a similar course to those in fig. 2. both for a magnetizing current of 10.5 and 14.5 amperes.

The negative rotation due to cobalt sulphate has been previously noticed. Ingersoll † finds that, for an aqueous solution of cobalt sulphate of density 1.322 at 23° C., the rotation for  $\lambda = .8\mu$  is less than that of water by 5 parts in 70. At the Na line 5893 Wachsmuth ‡ finds that the rotation for a solution of density 1.1378 is less than that of water by 7 parts in 10,000.

PART 2. *Measurements in the Violet and Ultra-Violet.*—As visual observations in the violet region of the spectrum could not be made with ease and certainty, the rotations for the lines Hg 4358 and Hg 4047 A.U. were obtained photographically.

\* "Absorption Measurements according to Houstoun," Proc. Roy. Soc. Edinb. xxi, pp. 521, 530, 547 (1911).

† J. O. S. A. vi. p. 663 (1922).

‡ Wied. Ann. xlv. p. 377 (1801).



For the ultra-violet beyond 3300 A.U. the polarizer was replaced by a modified Jellett prism of fixed half-shadow angle equal to about  $5\frac{1}{2}^{\circ}$ . The glass condensing lens used for the visual work was replaced by a quartz-fluorite achromatic combination of 32 cm. focal length. The quartz-mercury vapour lamp, suitably housed and screened, was placed at the focus of this achromat, as with the Jellett polarizer it is necessary to use parallel light. The glass achromat mounted on the divided circle was also replaced by a second quartz-fluorite achromatic lens of about 32 cm. focal length. This lens formed an image of the horizontal dividing line of the Jellett prism on the slit of a small quartz spectrograph.

A large number of plates were taken (in conjunction with Mr. A. Weale) for each solution, using the iron arc as source. The method of burning the arc recommended by Lowry \* was adopted, and was found to give remarkable steadiness. In spite of this, some of the plates gave rather erratic values for the rotation, which indicated that the arc could not always have been symmetrically placed with respect to the axis of the apparatus. The arc was kept on the axis by hand control, so that its image, cast by a lens placed on the side of the arc remote from the apparatus, always fell on a small area marked out on the room-wall. The centre of the lens and the centre of the area were arranged to be on the axis of the apparatus.

The method adopted, when using the iron arc, was to determine the wave-length of the spectral line for which a match in intensity in its upper and lower halves was attained for a known analyser setting. Owing to the varying intensities of the lines in the iron arc spectrum, it was difficult in some cases to fix the wave-length of the match-point within narrow limits.

On account of these disadvantages in using the iron arc for magneto-optical polarimetry it was replaced by a quartz-mercury vapour lamp. This lamp was mounted geometrically on the plan of the hole, slot, and plane device. With this lamp the rotations were determined by finding the setting on the analyser circle which gave equal intensity in the upper and lower parts of the spectral line. As emphasized by Landau† and Darmois‡, for success in this

Phil. Trans. A, cccxvi. p. 391 (1927).

† *Phys. Zeit.* ix. p. 417 (1908).

‡ *Ann. de Chim. et Phys.* xxii. (8) p. 247 (1911).

method it is necessary to obtain the correct time of exposure for each line.

Settings were made for the nine lines

Hg 4358, 4047, 3663, 3341, 3131, 2805, 2655, 2537,  
2482 A.U.

TABLE V.

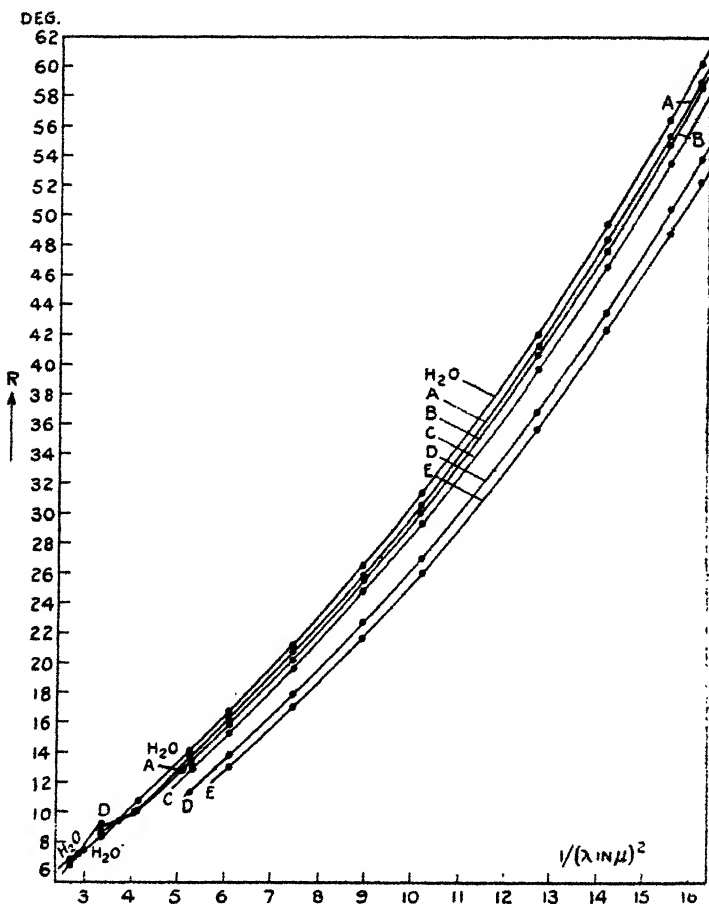
1st line. Difference of analyser readings in degrees.  
2nd „ Sum „ „ „  
3rd „ Temp. in ° C. „ „ „

λ.	H <sub>2</sub> O.	A.	B.	C.	D.	E.	Z.
4358	14.13	13.67	13.40	12.79	absorpn.	absorpn.	210.50
	210.53	210.57	210.45	210.45			
	18.4	15.9	17.8	18.8			
4047	16.80	16.19	15.95	15.35	13.72	13.02	
	210.55	210.45	210.45	210.39	210.48	210.42	210.46
	18.4	15.9	17.8	16.9	17.3	18.3	
3665	21.20	20.70	20.20	19.58	17.86	17.00	
	210.30	210.40	210.40	210.36	210.40	210.40	210.38
	20.5	16.3	17.8	17.2	17.5	17.2	
	26.53	25.80	25.49	24.75	22.70	21.75	
3341	210.23	210.24	210.25	210.33	210.24	210.15	210.24
	18.2	17.3	17.6	17.5	17.3	17.3	
	31.28	30.48	30.04	29.25	26.92	25.90	
3131	210.22	210.02	209.90	210.09	210.12	210.00	210.08
	19.6	18.4	17.9	16.6	18.0	16.8	
	42.00	41.13	40.62	39.57	36.80	35.67	
2805	209.90	209.97	209.84	209.85	209.84	209.93	209.91
	18.8	17.7	18.1	18.0	17.0	18.4	
	49.45	48.33	47.62	46.60	43.60	42.40	
2655	209.65	209.93	209.82	209.74	209.66	209.60	209.70
	19.1	18.2	17.6	19.0	18.3	18.4	
	56.50	55.37	54.86	53.56	50.34	48.96	
2537	209.60	209.53	209.50	209.50	209.60	209.60	209.55
	19.5	18.8	18.3	15.9	18.6	19.2	
	60.35	59.02	58.72	57.29	53.92	52.30	
2482	209.55	209.45	209.28	209.36	209.58	209.40	209.44
	18.3	19.5	19.2	17.4	19.0	18.9	
Av. Temp.	19.6	18.0	18.6	18.1	18.4	18.6	

for each of the five solutions (with the exception of 4358 for solutions D and E). In most cases the settings of the analyser were made at intervals of .1°. For the lines 4358, 4047, and 3663, settings were made at intervals of .05°. On each plate usually thirty exposures were made, the time of exposure varying from 1 second to 1½ minutes

(for 2482). The magnetizing current was reversed after every five exposures. It was arranged, at the expense of some repetition, that a reversal of the intensities in the upper and lower halves of a spectral line occurred for both senses of the magnetizing current, so that the rotation for

Fig. 3.



the line in question could be obtained from the one plate. As the field of the polarizer is not normal, it is necessary to match for equality of intensity just in the neighbourhood of the dividing line.

To facilitate the timing of the exposure an electromagnetically-operated steel ball was bifilarly suspended

in front of the slit of the spectroscope. This was controlled by the observer reading the ammeter.

Only settings in one region of the divided circle have been carried out, as it was found that rotation of the circle through  $180^\circ$  did not give any change in the rotation of water for  $\lambda$  3131 A.U. within the limits of experimental error. Interpolation between the settings of the analyser has been used to the extent of one-third of the interval  $1^\circ$ .

In Table V. will be found recorded with each wave-length, the difference between the analyser match-point settings for the passage of the current in both senses through the magnet, the sum of these settings, and the mean temperature of the solution during the taking of the photograph.

TABLE VI.

Verdet's Constants (min. per. cm. Gauss).

$\lambda$ in A.U.	H <sub>2</sub> O.	A.	B.	C.	D.	E.
4358	-0252	-0245	-0240	-0229	-0202	absorpn.
4047	-0301	-0292	-0286	-0275	-0244	-0231
3665	-0382	-0372	-0363	-0352	-0319	-0303
3341	-0477	-0464	-0458	-0444	-0405	-0388
3131	-0565	-0548	-0540	-0525	-0481	-0461
2805	-0756	-0739	-0730	-0710	-0658	-0637
2655	-0890	-0869	-0855	-0836	-0780	-0757
2537	-1017	-0996	-0986	-0960	-0901	-0876
2482	-1086	-1061	-1056	-1029	-0965	-0935
Av. Temp. in $^\circ$ C.	19.6	18.0	18.6	18.1	18.4	18.6

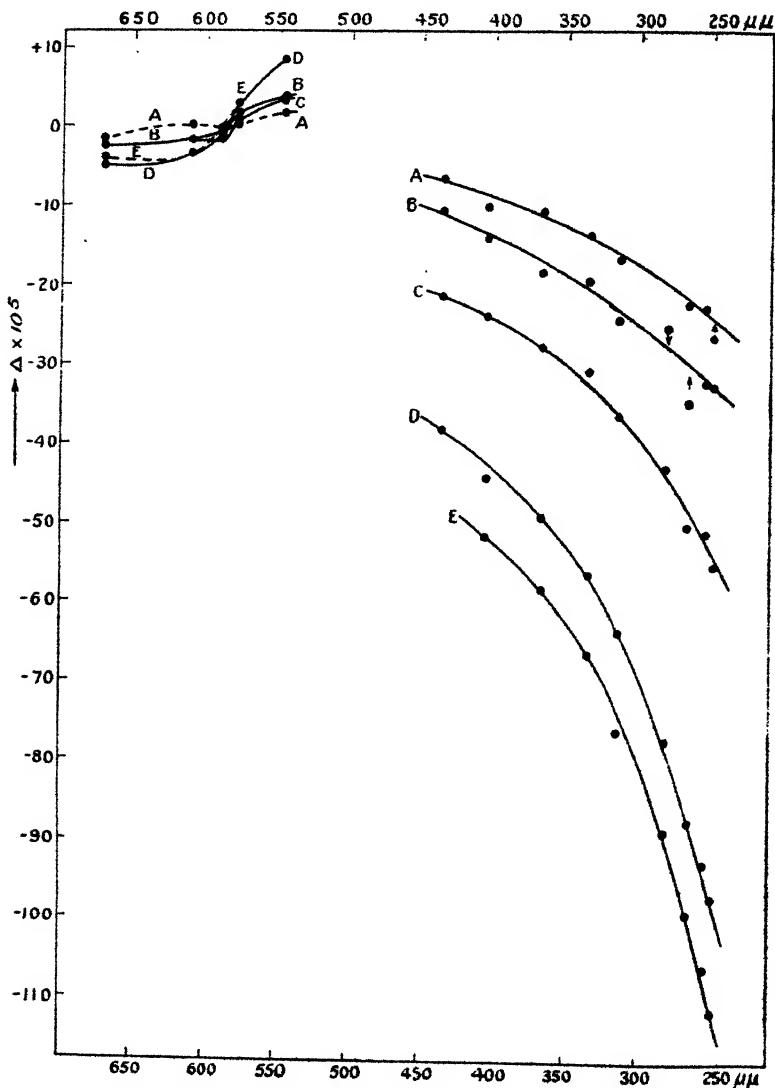
The sum of the analyser settings should be constant for a given wave-length for all the solutions, provided the zero of the apparatus does not alter. The constant values vary with the wave-length, owing to the natural rotation of the end-plates not being quite compensated. This variation with the wave-length can be readily obtained by plotting the average value of the sum of the readings (last column of Table V.) against the wave-length. The rotations due to the end-plates have been determined directly.

The observed rotations are plotted against the inverse square of the wave-length in fig. 3.

Table VI. gives the Verdet constants for the violet and

ultra-violet lines. These constants have been calculated in the same way as described for the visual work.

Fig. 4



#### IV. Natural Dispersion Measurements.

In order to apply Ladenburg's formula to the foregoing observations, the refractive indices of the solutions and water must be determined. For the purpose of obtaining

the rotation due to the salt  $\text{CoSO}_4$  in solution, a knowledge of the refractive indices to three places of decimals for a number of wave-lengths throughout the spectrum suffices. When it is desired, however, to make estimations of the frequencies of vibration of the electrons controlling the dispersion and refraction of the solutions, the refractive indices must be determined with an exactness amounting to several units in the fifth decimal place. As far as I am aware the only measurements of the ultra-violet dispersion of solutions which have been made are those of Heydweiller \* and his co-workers. In their work they used a method similar to that of Hallwachs, and obtained the differences between the refractive indices of water and the solutions directly. Their apparatus necessitated calibration by other methods.

It was thought, at first, that the method of normal incidence used by Simon † for measurements of the ultra-violet dispersion of liquids would be very convenient and of sufficient accuracy for the present work. This method, however, was found not suitable, because the two quartz-fluorite combinations used with the spectrometer were not sufficiently achromatic to permit of autocollimation adjustments with the visible light to be of value in the ultra-violet.

Also, as the axis of rotation of the telescope did not coincide with the axis of rotation of the spectrometer table, the method of setting for perpendicular incidence described by Feussner ‡ could not be adopted. After some further trials Martens' § method was used. This method, although time consuming, possesses the advantage that all the necessary measurements, with the exception of those relating to the angle of the prism, can be obtained from the photographic plate. The spectrometer, which was kindly lent to me by Prof. Baly, had a divided circle 10 inches in diameter, which could be read to 1 second of an arc by means of two microscopes provided with micrometer eyepieces.

The glass lenses provided with the instrument were replaced by the two quartz-fluorite achromatic combinations used for the magnetic dispersion work. Instead of

\* *Phys. Zeit.* xxvi. p. 526 (1925) (Summary).

† *Ann. der Phys.* lili. p. 542 (1894).

‡ *ZS. f. Phys.* xlv. p. 689 (1927).

§ *Ann. der Phys.* vi. p. 603 (1901).

the eyepiece a light aluminium frame was screwed to the telescope tube. This frame supported a metal plate-holder carrying plates 6 cm. by 4.5 cm. This holder could be raised or lowered by means of two friction rollers without any appreciable strain on the telescope mounting.

The spectrometer adjustments were carried out in the usual way. For the setting of the axis of the telescope and collimator perpendicular to the axis of rotation of the telescope Lebedeff's method \* was found very convenient.

Three positions of the draw-tube carrying the slit were used at intervals of 2 mm. in order to obtain light sufficiently parallel to cover the region 7068-2378 A.U. These positions, together with the corresponding positions of the draw-tube supporting the plate-holder, were found by Cornu's method †.

In order to deduce the angular deviation of the spectral lines on the plate, three direct slit images were recorded on each plate, with the telescope set in the direct position, and at azimuths  $\pm 1^\circ$  (sometimes  $45'$ ) with respect to this position. The angle of incidence was obtained by taking two exposures of the slit images reflected from the first prism face, with the telescope in such an azimuth that the reflected slit images were recorded on the plate in suitable positions. The mean angle of the incidence obtained by means of these two reflected images was adopted.

As all the angular deviations were small, these deviations were obtained by linear interpolations from the screw readings.

Most of the plates have been read four times, following the procedure given by Cornu ‡. This was necessary in order to eliminate errors arising from imperfections of the screw of the measuring instrument, and errors of reading arising from the lack of sharpness of the lines due to the presence of spherical aberration.

As it was necessary to remove the prism table (to which the prism was rigidly attached) from the spectrometer in order to photograph the direct slit image, the setting of the prism table had to be controlled. This was done by autocollimation with the aid of a telescope fitted with a Gauss eyepiece. To this end a mirror was attached to the side of the prism opposite the refracting edge.

\* Journ. Scient. Instr. iv. p. 100 (1926).

† Journ. de Phys. v. p. 341 (1886).

‡ Loc. cit.

The solutions were contained in a 30° hollow prism, which was closed by means of two plane parallel quartz plates (7.5 mm. thick) cut parallel to the optic axis. These plates were cemented to the prism. The prism was provided with a filling-hole into which fitted a thermometer graduated in tenths of a degree, so that estimations to hundredths of a degree could be made. The thermometer, which was the same as used in the density determinations, was calibrated against a standard thermometer provided with a recent certificate.

Most of the plates have been taken at temperatures in the neighbourhood of 21° C. In order to reduce the observations to a standard temperature taken to be 20° C., it is necessary to know the temperature coefficients of the refractive indices. In the case of water Flatow's values \*

for  $\frac{dn}{dt}$  have been used. For the solutions the values of  $\frac{dn}{di}$

have been obtained by finding the shift of the spectral lines on gradually heating the room through about 5° C. Exposures were made before heating and during the heating when the temperature became sufficiently steady. In order to distinguish between the lines of the two spectra obtained, the first spectrum was taken with a long slit and the second with a short slit.

Table VII. gives a summary of the work.

The omissions arise partly through the obscuring of some of the lines by the superposition on the spectrum of either the direct slit images or the reflected slit images and partly through absorption. No attempt has been made to follow the course of the dispersion through the absorption band, as this would require an entirely different experimental method.

In the literature † there appear considerable discrepancies among the values of the refractive indices of water in the ultra-violet. I find, on correcting for temperature and wave-length differences, that the tabulated results for water lie nearer to Gifford's ‡ results than to those of other observers.

Table VIII. gives the values of the molecular refraction  $R$  of  $\text{CoSO}_4$  at 20° C. which have been deduced from the

\* *Ann. der Phys.* xii. p. 85 (1903).

† See Duclaux and Jeantet, *Journ. de Phys.* v. p. 92 (1924).

‡ *Proc. Roy. Soc. A*, lxxviii. p. 406 (1907).



TABLE VII.

Refractive Indices at 20° C.

$\lambda$ in A.U.	H <sub>2</sub> O.	A.	B.	C.	D.	E.
7065 He	1.33003	1.33796	...	...	1.36708	1.37400
6678 "	1.33087	1.33882	1.34284	1.35016	1.36802	1.37498
6563 H <sub>a</sub>	1.33115	1.33913	1.34312	...	1.36834	
5876 He	1.33305	1.34106	1.34509	1.35241	1.37044	1.37743
5461 Hg	1.33440	1.34254	1.34666	1.35382		
4471 He	1.33945	1.34762	1.35173			
4358 Hg	1.34027	1.34845	1.35258	...	1.37841	
4047 "	1.34284	1.35108	1.35518	1.36254	1.38128	1.38839
3886 He	1.34432	1.35263	1.35678	1.36422	1.38291	1.39013
3341 Hg	1.35165	1.36015	1.36436	1.37193	1.39106	1.39834
3187 He	...	1.36317	1.36745	...	1.39426	1.40169
3131 Hg	1.35567	1.36435	1.36860	1.37632	1.39556	1.40293
2893 "	1.36168	1.37050	1.37478	1.38254	1.40220	1.40968
2805 "	1.36442	1.37334	1.37779	1.38543	...	...
2576 "	1.37338	1.38247	1.38698	1.39482	1.41506	1.42276
2482 "	1.37809	1.38732	...	1.39977	...	1.42803
2378 "	1.38434	1.39366	1.39827	1.40627	1.42705	1.43496

refractive indices of Table VII. by means of the well-known formula

$$\frac{1}{d_4^{20}} \frac{n^2 - 1}{n^2 + 2} = \frac{1}{d_w^{20}} \left( 1 - \frac{W}{100} \right) \frac{n_w^2 - 1}{n_w^2 + 2} + \frac{W R}{100 M}, \quad (1)$$

where  $n_w$  = refractive index of water at 20° C.,

$n$  = " " " " solution at 20° C.,

$R$  = molecular refraction of  $\text{CoSO}_4$ ,

$M$  = molecular weight of  $\text{CoSO}_4$  (155.1).

The extrapolations given under  $W=0$  for zero concentration have been obtained from the molecular refractivities of the five solutions by using the method of Least Squares. It was assumed with Fontell\*:

(1) that the molecular refraction is a linear function of the concentration,

(2) that the error in the molecular refraction arising from the observations is inversely proportional to the concentration.

\* Soc. Scient. Fenn., Comm. Phys.-Math. iv. no. 8 (1927).

On determining the linear function it appears that the molecular refraction increases with increasing concentration—that is, in the opposite direction to the behaviour of the majority of salts. This indicates that in  $\text{CoSO}_4$  the molecular refractivity in the crystalline state (100 per cent. solution) is greater than in the ionic state at infinite dilution. It is noteworthy that certain fluorides, in which  $\text{F}^-$ , like  $\text{SO}_4^{--}$ , has only a small dispersive effect, behave in a similar way.

TABLE VIII.

Molecular Refraction of  $\text{CoSO}_4$  at  $20^\circ \text{C}$ . ( $M=155.1$ ).

$\frac{W}{\lambda}$	0.	4.33.	6.45.	10.23.	19.14.	22.26.	Mean (obs.).
7065	...	15.86	...	...	16.09	16.05	16.00
6678	16.00	15.90	15.90	16.09	16.12	16.08 <sup>s</sup>	16.02
6563	...	15.96	15.90	...	16.14	...	16.00
5876	16.07	16.02	15.98	16.14	16.21	16.17	16.10
5461	...	16.23 <sup>s</sup>	16.23	16.17	...	...	16.21
4471	...	16.25	16.22	...	...	...	16.24
4358	...	16.26	16.25	...	16.46	...	16.32
4047	16.42	16.27	16.26	16.32 <sup>s</sup>	16.56	16.49 <sup>s</sup>	16.38
3886	16.43	16.47	16.40	16.46 <sup>s</sup>	16.62	16.56	16.50
3341	16.72	16.76	16.65	16.70	16.92	16.81	16.77
3131	16.98	17.06	16.89	16.95	17.04	16.96 <sup>s</sup>	16.98
2893	17.10	17.27	17.04	17.07	17.27	17.17	17.16
2576	17.60	17.66	17.54	17.55 <sup>s</sup>	17.61	17.55	17.58
2482	17.63	17.82	...	17.55	17.74	17.68	17.70
2378	17.77	17.98	17.82	17.69	17.93	17.85	17.85

*Calculation of the Characteristic Frequencies of the Electrons in  $\text{CoSO}_4$ .*

Heydweiller\* has shown how one can calculate, on the basis of Drude's theory of dispersion, the characteristic frequencies of the electrons responsible for the refraction and dispersion of electrolytes. He points out that the effect on the dispersion due to the kation is small, and that the dispersion is mainly governed by the comparatively loosely bound valency electrons associated with the anion. The remaining electrons in the molecule are assumed to have a common frequency which is very much greater than that of the valency electrons.

\* *Loc. cit.*

Let  $\nu_1$  = the frequency of the valency electrons in  $10^{-15}$  sec.,

$\nu_2$  = " " " remaining electrons in  $10^{-15}$  sec.,

$p_1$  = the number of valency electrons in 1 molecule,

$p_2$  = " " " electrons in 1 molecule less  $p_1$ .

Then, according to Heydweiller, the molecular refraction  $R_\nu^0$  at infinite dilution for light of frequency  $\nu$  is given by the formula

$$R_\nu^0 = 16 \cdot 286 C_\nu,$$

$$\text{where } C_\nu = \frac{p_1}{\nu_1^2 - \nu^2} + \frac{p_2}{\nu_2^2 - \nu^2} \quad \dots \quad (2)$$

The values of  $\nu_1^2$ ,  $\nu_2^2$  can therefore be determined from the values of  $C_\nu$  for two different frequencies.

TABLE IX.

$\lambda$ (vac.).	$R_\nu^0$ calc. -- $R_\nu^0$ obs. $\nu_1^2 = 6 \cdot 198, \nu_2^2 = 112 \cdot 6.$	$R_\nu^0$ calc. -- $R_\nu^0$ obs. $\nu_1^2 = 6 \cdot 140, \nu_2^2 = 112 \cdot 6.$
6680	0	-5
5877	-1	-5
4048	-6	-1
3890	-1	-5
3342	-5	-2
3133	-18	-11
2894	-9	-2
2577	-8	-11
2483	-4	-4
2379	0	-9

Applying this formula to the values  $R_\nu^0$  of  $\text{CoSO}_4$  for the lines 6678 and 2738 A.U., we find, taking  $p_1 = 2$ ,  $p_2 = 73$ , that  $\nu_1^2 = 6 \cdot 20$ , and  $\nu_2^2 = 112 \cdot 6$ . On forming the difference between the values of  $R_\nu$  calculated by means of (2) using these values of  $\nu_1^2$  and  $\nu_2^2$  and the observed values, it will be seen from the second column of Table IX. that the deviations (in units of the second decimal place) are large and lie in the same direction. A slightly better distribution of these differences is obtained by taking as  $\nu_1^2$  the mean of the values  $\nu_1^2$  obtained from the value of  $R_\nu^0$  for each line, keeping  $\nu_2^2 (= 112 \cdot 6)$  constant. This process gives a mean value of  $\nu_1^2 = 6 \cdot 14$ . The differences between the values of  $R_\nu^0$  calculated by using  $\nu_1^2 = 6 \cdot 14$  and  $\nu_2^2 = 112 \cdot 5$  in equation (2) and the observed values are given in the third column of Table IX. The

maximum deviation does not exceed 7 per 1000. In the formula we have neglected the effect of the absorption band at 5100 A.U., as the effect on the dispersion due to this band is very small.

The value  $\nu_1^2 = 6.14$  agrees well with Heydweiller's\* value  $\nu_1^2 = 6.15$  for  $\text{SO}_4^{--}$  in  $\text{Li}_2\text{SO}_4$ . The method of extrapolating for zero concentration employed by Heydweiller is, however, entirely different from the one used here. For  $\text{Li}_2\text{SO}_4$  Heydweiller obtains  $\nu_2^2 = 100.4$ . The higher value  $\nu_2^2 = 112.6$  for  $\text{CoSO}_4$  may arise through the more rigid binding of the electrons in  $\text{CoSO}_4$  than in  $\text{Li}_2\text{SO}_4$ , owing to the higher nuclear charge in the former salt.

### V. *The Application of Ladenburg's Magnetic Dispersion Formula to the Magnetic Observations.*

Ladenburg† gives the following formula for the magnetic rotation of a paramagnetic substance :

$$\chi = \sum_i \left[ \frac{(n^2 + 2)\omega}{3(\omega_i^2 - \omega^2)} \right]^2 \frac{\rho_i l \omega_L}{cn} \left\{ 1 \pm \frac{\mu_i H}{3kT} \frac{\omega_i^2 - \omega^2}{\omega_i \omega_L} \right\}, \quad (3)$$

where  $l$  is the length of path traversed;  $c = 3 \cdot 10^{10}$ ,  $\omega = 2\pi c/\lambda$ ,  $\omega_i$  the characteristic frequency of the electrons giving rise to the  $i$ th band,  $\omega_L = -eH/2mc$ ,  $\rho_i = 4\pi N_i e^2/m$ ,  $N_i$  being the number of classical dispersion electrons of type  $i$  per unit volume,  $\mu_i$  their magnetic moment,  $k$  the Boltzmann constant, and  $T$  the absolute temperature.

In order to apply this formula to a dissolved salt it is necessary to correct for the rotation due to the solvent. It is clear from the formula that it is not  $\chi$  which is additive, but the quantity  $\frac{n}{(n^2 + 2)^2} \chi$ ,  $d$  being the density of the substance.

To facilitate reference to the experimental results, we shall consider the Verdet constant  $V$  instead of  $\chi$ ,  $\chi/H$  being equal to  $\pi V/60 \times 180$ . By analogous considerations to those employed in the deduction of formula (1) we may regard the difference

$$\Delta \equiv \frac{n}{(n^2 + 2)^2} \frac{V_s}{d_s} - \frac{n_r}{(n_r^2 + 2)} \frac{100 - W}{100} \frac{V_r}{d_r}$$

as a quantity characteristic of the rotation of the dissolved

\* *Loc. cit.*

‡ *ZS. f. Phys.* xlv. p. 168 (1927). See also C. G. Darwin and W. R. Watson, *Proc. Roy. Soc. A*, cxiv. p. 474 (1927).

salt,  $V_s$  and  $V_w$  being the Verdet constants for the solution and water respectively.

Table X. gives the values of  $\Delta$  and  $\Delta/W$ , and fig. 4 a graphical representation of the values of  $\Delta$ . The paramagnetic character of the rotation due to  $\text{CoSO}_4$  is clearly

TABLE X.

Upper line :  $\Delta \times 10^3$ .  
Lower „ :  $\Delta/W \times 10^3$ .

$\lambda$ .	A.	B.	C.	D.	E.	Weighted Mean.
6708	-1.61	-2.48	...	-4.99	-4.10	
	- .37	- .38	...	- .26	- .18	- .25
6104	+ .02	-1.75	-1.87	-3.52	-3.79	
	+ .00 <sup>s</sup>	- .27	- .18	- .18	- .17	- .17 <sup>s</sup>
5893	- .46	- .94	-1.79	- .92	- .36	
	- .11	- .15	- .18	- .05	- .02	- .07
5780	+ .11	-1.60	- .64	+ 2.71	+ 2.84	
	+ .02 <sup>s</sup>	+ .25	+ .06	+ .14	+ .13	+ .13
5461	+ 1.50	+ 3.60	+ 3.05	+ 8.32	absorpn.	
	+ .35	+ .56	+ .30	+ .43 <sup>s</sup>	...	+ .41
4358	- 6.7	-10.7	-21.4	-38.2		
	- 1.55	- 1.66	- 2.09	- 2.00	absorpn.	-1.92
4047	-10.2	-14.1	-23.9	-44.4	-51.7	
	- 2.36	- 2.18	- 2.33	- 2.32	- 2.32	-2.33
3665	-10.7	-18.5	-27.8	-49.2	-58.4	
	- 2.47	- 2.87	- 2.72	- 2.57	- 2.62	-2.64
3341	-13.6	-19.6	-31.0	-56.6	-66.6	
	- 3.15	- 3.04	- 3.03	- 2.96	- 2.99	-3.01
3131	-16.8	-24.4	-36.4	-63.8	-76.3	
	- 3.92	- 3.78	- 3.56	- 3.34	- 3.43	-3.50
2805	-18.2	-25.4	-43.1	-77.5	-88.8	
	- 4.20	- 3.94	- 4.21	- 4.08	- 3.99	-4.06
2655	-22.4	-34.8	-50.5	-87.7	-99.3	
	- 5.18	- 5.39	- 4.93	- 4.58	- 4.46	-4.73
2537	-22.9	-32.4	-51.2	-93.0	-106.2	
	- 5.29	- 5.02	- 5.00	- 4.86	- 4.77	-4.91
2482	-26.8	-32.9	-55.3	-97.0	-113.8	
	- 6.19	- 5.10	- 5.40	- 5.08	- 5.11	-5.23

put in evidence, as we have an asymmetrical behaviour with respect to the two sides of the 5100 A.U. band, and a negative rotation, which increases with decreasing wavelength.

On evaluating the diamagnetic and paramagnetic parts of formula (3) we find,

$$\Delta' \equiv \frac{\pi}{180} \frac{\Delta}{60 W f} = \sum p_i (D_i \pm P), \quad \dots \quad (4)$$

where

$$f \equiv \frac{2\pi e^2}{9m^2 c^2} \frac{1}{M_{NH}},$$

$m_H$  being the mass of the hydrogen atom,

$$\left. \begin{aligned} D_i &\equiv \frac{\omega^2}{\omega_i^2 - \omega^2} = 2.815 \cdot 10^{-33} \frac{\lambda^{13}}{(\lambda^2/\lambda_i^2 - 1)^2} \\ P_i &\equiv \frac{\mu_i H}{3kT} \frac{\omega^2}{\omega_i^2 - \omega^2} \frac{1}{\omega_i \rho_L} = x_i 4.478 \cdot 10^{-31} \frac{\lambda_i'}{(\lambda^2/\lambda_i^2 - 1)} \end{aligned} \right\}, \quad (5)$$

where  $\lambda' = 10^5 \lambda$ ,  $\lambda$  being in cm.,  $x_i$  is the number of Bohr magnetons associated with the  $i$ th paramagnetic band, and  $p_i$  is the number of electrons associated with the  $i$ th band.  $T$  has been taken equal to 291.

In order to obtain the frequency of the absorption band giving rise to the negative rotation, we must eliminate the diamagnetic rotation due to the bands which account for the natural dispersion of  $\text{CoSO}_4$ . The wave-lengths of these bands are

$\lambda_1 = 1.217 \cdot 10^{-5} (\nu_1^2 = 6.14)$ ,  $\lambda_2 = .283 \cdot 10^{-5} (\nu_2^2 = 112.6)$ , and  $\lambda_0 = 5.100 \cdot 10^5$ .

The relative contribution due to these bands to the value  $\Delta'$  may be obtained by inspection of Table XI., which gives the  $D$  and  $P$  terms for a few wave-lengths. For the  $P$  terms  $x$  has been taken equal to unity for convenience. Table XII. gives the values of  $\Delta'$  for solutions D and E. Also in the second column of this Table is given the weighted mean value of  $\Delta'$  for all the solutions, the weight being taken proportional to  $W$ .

Taking, as before,  $p_1 = 2$  and  $p_2 = 73$ , we see that the valency electrons will give rise to a large diamagnetic rotation, whereas the high frequency electrons will only give rise to a comparatively small rotation. The valency electrons cannot be paramagnetically active, as the  $P$  values for  $\lambda_1 = 1.217 \cdot 10^{-5}$  are 100 times (approx.) the  $D$  values, which are of the same order of magnitude as the observed  $\Delta'$  values. We can also exclude the possibility of a paramagnetic effect due to the valency electrons on another ground. For in the case of  $\text{CoCl}_2$  and  $\text{CoBr}_2$ , where the frequencies of the valency electrons are not so high as in  $\text{CoSO}_4$ , the diamagnetic rotation overpowers the paramagnetic rotation giving rise to a positive rotation in the ultra-violet.

The 5100 A.U. band will also contribute to the diamagnetic rotation, but at present we do not know the corresponding value  $p_0$ . As more observations have been

TABLE XI.  
D and P Values.

$\lambda$ in A.U.	$\lambda_0 \quad 5.100 \times 10^{-6}$		$\lambda_1 \quad 1.217 \times 10^{-6}$		$\lambda_2 \quad .283 \times 10^{-6}$	
	$D_0$	$P_0$	$D_1$	$P_1$	$D_2$	$P_2$
6708	$\pm 2.38 \times 10^{-31}$	$\pm 3.13 \times 10^{-30}$	$\pm 1.44 \times 10^{-34}$	$1.83 \times 10^{-32}$	$\pm 4.01 \times 10^{-37}$	$\pm 2.25 \times 10^{-34}$
5789	$\pm 11.54$	$\pm 8.25$	$\pm 1.98$	$\pm 2.49$	$\pm 5.40$	$\pm 3.04$
4358	$\pm 7.34$	$\pm 8.73$	$\pm 3.74$	$\pm 4.53$	$\pm 9.54$	$\pm 5.35$
2805	$\pm .46$	$\pm 3.38$	$\pm 11.01$	$\pm 12.41$	$\pm 23.22$	$\pm 12.90$
2482	$\pm .30$	$\pm 3.08$	$\pm 16.90$	$\pm 16.93$	$\pm 29.95$	$\pm 16.71$

carried out on solution D than on solution E, we shall confine the working to this solution, and compare the calculated results with the observed results recorded in Table XII.

On subtracting  $2D_1 + 73D_2$  from the values of  $\Delta'$  for solution D, we obtain the joint contribution due to the paramagnetic and diamagnetic terms of the 5100 band and the ultra-violet paramagnetic bands. The results are given in the last column of Table XII.

To eliminate the effect due to the 5100 band we observe that for wave-lengths less than 3341 A.U.  $P_0 + D_0$  is approximately constant, the variation occurring in the second decimal place. We may therefore, as a first approximation, take the effect of this band as constant ( $=C_0$ ) for these wave-lengths. Assuming that there is only one effective paramagnetic band in the ultra-violet, we have for the three wave-lengths 3341, 2805, and 2482 A.U.,

$$-3.685 \cdot 10^{-33} = \frac{a_-}{11.16 \cdot 10^{-10} - \lambda_-} + C_0,$$

$$-5.41 \cdot 10^{-33} = \frac{a_-}{7.87 \cdot 10^{-10} - \lambda_-} + C_0,$$

$$-7.25 \cdot 10^{-33} = \frac{a_-}{6.16 \cdot 10^{-10} \lambda_-^2} + C_0,$$

$\lambda_-$  being the wave-length of the active band giving rise to the negative rotation, and  $a_-$  a constant.

The equations give

$$C_0 = .351 \cdot 10^{-33},$$

$$a_- = 32.23 \cdot 10^{-43},$$

$$\lambda_- = 1.221 \cdot 10^{-2}.$$

Having obtained an approximate value for  $a_-$  and  $\lambda_-$ , we can obtain the effect of the 5100 band by evaluating  $\frac{a_-}{\lambda_-^2 - \lambda_-^2}$

for all the wave-lengths, and subtracting these values from the last column of Table XII. If we represent the effect due to the 5100 band by  $p_0(D_0 + x_0 P_0)$ , we find for the pair of wave-lengths 5780 and 4358

$$+.68 \cdot 10^{-33} = 1.15 \cdot 10^{-30} p_0 + 8.25 \cdot 10^{-30} p_0 x_0$$

$$-.40 \cdot 10^{-33} = .73 \cdot 10^{-30} p_0 - 8.73 \cdot 10^{-30} p_0 x_0,$$

which give

$$p_0 = 1.62 \cdot 10^{-4},$$

$$p_0 x_0 = .60 \cdot 10^{-4}.$$



TABLE XII.

Values of  $\Delta'$ , etc.

$\lambda$ in A.U.	Weighted Mean.	F.	D.	$\Delta'$ calc. $\lambda_1=1187.$	$\Delta'$ calc. $\lambda_1=1046.$	$\Delta'_{-2D, -73D_2}$ $\lambda'=1187.$
6708	-18 $\times 10^{-33}$	-13 $\times 10^{-33}$	-19 $\times 10^{-33}$	-22 $\times 10^{-33}$	-24 $\times 10^{-33}$	-50 $\times 10^{-33}$
6104	-13 "	-12 "	-13 "	-12 "	-14 "	-52 "
5893	-05 "	-01 "	-04 "	-00 <sup>s</sup> "	+01 "	-45 "
5780	+09 "	+09 "	+10 "	...	...	-33 "
5461	+30 "	absorpt.	+31 "	+1.07 "	+1.06 "	-18 "
4358	-130 "	"	-1.44 "	...	...	-2.26 "
4047	-1.68 "	-1.67 $\times 10^{-33}$	-1.67 "	-1.57 "	-1.68 "	-2.64 "
3605	-1.90 "	-1.89 "	-1.85 "	-1.81 "	-1.82 "	-3.08 "
3341	-2.17 "	-2.15 "	-2.13 "	-2.07 "	-2.11 "	-3.68 <sup>s</sup> "
3131	-2.52 "	-2.47 "	-2.46 "	-2.37 "	-2.38 "	-4.30 <sup>s</sup> "
2805	-2.92 "	-2.87 "	-2.91 "	-2.90 "	-2.89 "	-5.41 "
2655	-3.40 "	-3.21 "	-3.30 "	-3.24 "	-3.20 "	-6.20 "
2537	-3.53 "	-3.43 "	-3.50 "	-3.50 "	-3.50 "	-6.86 "
2482	-3.76 "	-3.68 "	-3.65 "	-3.64 "	-3.65 "	-7.25 "

From these values we can calculate the contribution to  $\Delta'$  due to the 5100 band, and thence obtain a better value for  $a_-$  and  $\lambda_-$ .

These were found to be  $a_- = 33.76 \cdot 10^{-43}$ , and  $\lambda_- = 1.187 \cdot 10^{-5}$ . With these improved values for  $a_-$  and  $\lambda_-$  we can obtain improved values for  $p_0$  and  $p_0 x_0$ . On carrying out the calculation, we find

$$p_0 = 2.18 \cdot 10^{-4}, \quad p_0 x_0 = .57 \cdot 10^{-4}.$$

Using these constants, the values of  $\Delta'$  have been calculated, and are given in the fifth column of Table XII. The agreement between the observed and calculated values of  $\Delta$  for the different lines is as good as one can expect, with the exception of  $\lambda$  5461.

Formula (4), for solution D, thus becomes

$$\Delta' = 2D_1 + 73D_2 + p_0(D_0 + x_0 P_0) + \frac{a_-}{\lambda^2 - \lambda_-^2}.$$

where

$$\begin{aligned} p_0 &= 2.18 \cdot 10^{-4}, \\ p_0 x_0 &= .57 \cdot 10^{-4}, \\ a_- &= -33.76 \cdot 10^{-43}, \\ \lambda_- &= 1.187 \cdot 10^{-5}, \end{aligned}$$

and P and D are defined by (5).

The number of Bohr magnetons associated with the 5100 A.U. band is  $x_0 = .27$ .

In the above calculations we have assumed that the values of the frequencies of the diamagnetic bands obtained from dispersion measurements will serve for the purpose of magnetic calculations. In the case of diamagnetic salts with highly dispersive anions there appears, according to Heydweiller, good agreement between the values of the characteristic frequencies of the electrons calculated from dispersion and magnetic measurements. Also the values of these frequencies depend very little on the kation. For the more rigidly bound valency electrons such as occur in  $\text{SO}_4^{--}$  there is a much larger difference between the frequencies calculated from dispersion and magnetic observations.

According to Heydweiller the value of  $\nu_1^2$  for  $\text{Li}_2\text{SO}_4$  is about 6.9 from magnetic measurements, whereas from dispersion data the value  $\nu_1^2 = 6.15$  is obtained. Let us assume that this value of  $\nu_1^2 = 6.9$  is the value to be used for the purpose of calculating the diamagnetic rotation

in  $\text{CoSO}_4$  due to the valency electrons, on the grounds that the dispersion frequencies of  $\text{CoSO}_4$  and  $\text{Li}_2\text{SO}_4$  are nearly the same.

I have carried out a similar method to that described above, using the value  $\nu_1^2 = 6.90$  instead of  $\nu_1^2 = 6.14$  as above. In this case the new constants are found to be

$$\begin{aligned} p_0 &= 2.16 \cdot 10^{-4}, \\ p_0 r_0 &= .57 \cdot 10^{-4}, \\ a_- &= -31.36 \cdot 10^{-45}, \\ \lambda_- &= 1.046 \cdot 10^{-5}, \end{aligned}$$

and the number of Bohr magnetons for the 5100 band is .26. The values of  $A'$  calculated by means of these constants are given in the sixth column of Table XII.

The question naturally arises, what physical significance have these constants?

The value  $p_0$  is proportional to the strength of 5100 band. From absorption data Houstoun\* calculates that the number of electrons per molecule causing the 5100 band in cobalt salts is  $1.2 \cdot 10^{-4}$ .

From the magnetic data we have found  $p_0 = 2.2 \cdot 10^{-4}$ . It must be borne in mind that this value has been obtained by applying equation (3), which has been obtained by neglecting damping. This neglect of damping is shown in the small observed value for  $\lambda$  5461 A.U. in comparison with the calculated value for this wave-length.

From the value of  $a_-$  we can calculate the product of the magnetic moment of the paramagnetic band and number of electrons per molecule responsible for this band. We find from equation (5)

$$\begin{aligned} a_- &= 4.478 \cdot 10^{-45} \lambda_-^2 (p_- r_-), \\ \text{giving for } \lambda_- &= 1.187 \cdot 10^{-5}, p_- r_- = .046, \\ \text{and for } \lambda_- &= 1.046 \cdot 10^{-5}, p_- r_- = .061. \end{aligned}$$

In the case of tysonite Becquerel and de Haas† find that there is exactly one Bohr magneton associated with the active band, in spite of the much larger magneton value of the magnetic susceptibility of the crystal. If we assume that in the case of  $\text{CoSO}_4$  the moment of the active band is 1 magneton, then the number of electrons per molecule is .046 for  $\lambda = 1.187 \cdot 10^{-5}$  and .061 for  $\lambda = 1.046 \cdot 10^{-5}$ .

We know, however, from susceptibility measurements that in solution the salts of cobalt possess ionic carriers of

\* Proc. Roy. Soc. Edinb. xxxi. p. 547 (1911).

† Loc. cit.

moment equal to about four Bohr magnetons. If we suppose, which is very probable, that the magnetic moment determining the main paramagnetic rotation has the same value as that of the ionic carriers, then the strength of the ultra-violet paramagnetic band will be equal to about  $\cdot 01$ .

We have neglected the diamagnetic rotation arising from the paramagnetic band in all the calculations. For a strength equal to  $\cdot 01$ , the maximum diamagnetic contribution to  $\Delta'$  will not exceed 2 units in the second decimal place for the wave-lengths investigated. Neglecting the term for the diamagnetic rotation of the paramagnetic band will therefore not affect the results materially.

The 5100 A.U. band has been treated throughout as paramagnetic. It may be thought that the increase in the rotation on approaching this band from the red side can be accounted for by means of a single diamagnetic term in the dispersion formula. This would require, however, a much greater strength of the absorption band than is actually found from absorption measurements. Further, unless we treat this band as paramagnetic we do not obtain consistent values of  $\lambda_{\text{max}}$  from the ultra-violet observations.

The conclusion that the 5100 A.U. band is paramagnetic is in agreement with Ladenburg's\* considerations concerning paramagnetism and colour, as it is to the presence of this band that cobalt solutions owe their red colour.

Further experiments, particularly at low temperatures, are necessary in order to fix more definitely the magnetic moment determining the paramagnetic rotation of cobalt salts. In this connexion one must point out that the use of low temperatures for the investigation of paramagnetic rotation phenomena has long ago been introduced by J. Becquerel. Experiments on the magnetic circular dichroism of the 5100 A.U. band are also required in order to fix more definitely the dispersion constants and magnetic moment of this band. Experiments on these lines are contemplated.

#### *Summary.*

(1) The magnetic rotations of five solutions of cobalt sulphate in water have been investigated in the visible and ultra-violet regions at room-temperatures.

\* *ZS. f. Elektrochem.*, xxvi. p. 270 (1920).

(2) The results indicate that the rotation of  $\text{CoSO}_4$  is negative in the red and ultra-violet regions, becoming positive on approaching the 5100 A.U. band.

(3) The refractive indices of the same solutions have been determined in the same spectral regions.

(4) The molecular refractivities of  $\text{CoSO}_4$  for different wave-lengths have been calculated.

(5) The characteristic frequencies of the electrons controlling the dispersion of  $\text{CoSO}_4$  in water have been calculated.

(6) Ladenburg's rotatory dispersion formula has been used to obtain

(i.) the frequency of the ultra-violet paramagnetic band,

(ii.) the number of electrons per molecule causing the 5100 A.U. band and the moment of this band.

I wish to express my best thanks to Prof. Wilberforce for the interest he has taken in the work, and for the facilities and the apparatus placed at my disposal; to Prof. E. C. C. Baly for his kindness in lending me the spectrometer and accessories; to Mr. A. Weale, for his collaboration during the Session 1927-28; to Mr. W. Band for his assistance during the magnetic measurements in the ultra-violet; and to Dr. A. V. Moses for his assistance in some preliminary work.

The George Holt Physics Laboratory,  
The University, Liverpool,  
Dec. 19th, 1929.

---

XXXVI. *Luminosity in Gaseous Combustion.* By W. T. DAVID, *Sc.D., M.Inst.C.E.*, and W. DAVIES, *B.Sc.\**

[Plates V.-VIII.]

FOR some time past we have been taking continuous photographic records of the ultra-violet and luminous radiation emitted during the explosion and subsequent cooling of inflammable gaseous mixtures contained in closed vessels, and correlating them with continuous records of pressure variation. A typical experiment was described

\* Communicated by the Authors.

in a communication to Section G of the British Association in 1927 \*. Since then we have carried out similar experiments on a gas-engine designed to give the well-known Clerk zigzag diagram.

We had hoped, among other things, to be able to infer from these experiments when combustion became complete in a gaseous explosion and in a gas-engine, but serious difficulties arose when we attempted to interpret our results on the hypothesis that luminosity results from chemical combination. We found that the intensity of the luminous radiation at any instant was dominated by the temperature of the gaseous medium (as inferred from its pressure), and that it appeared to be hardly influenced at all by the amount of chemical combination taking place at that instant. Indeed, luminosity was manifest long after chemical union was generally supposed to have been complete, and convincing confirmation of this was afforded by the gas-engine experiments.

It was not possible, however, to explain the results on a purely thermal basis, for the more permanent gases remain dark when heated to higher temperatures than those sufficient to produce luminosity in our experiments, and we are therefore led to believe that chemical combination results in the formation of molecules (probably of  $\text{CO}_2$  and  $\text{H}_2\text{O}$ ) which are in an abnormal condition, and that in this condition the vibrations which give rise to luminous radiation are excited by much softer collisions than would be required to produce the same effect in normal  $\text{CO}_2$  and  $\text{H}_2\text{O}$  molecules.

A hypothesis of this kind serves to explain our results only if we assume that the abnormal condition of the molecules can persist for many seconds when combination takes place in the gaseous phase.

We discuss this in some detail later in this paper, and suggest that the overall process of combustion may be analysed broadly into two stages:—(i.) chemical combination resulting in the formation of abnormal molecules, and (ii.) the change from the abnormal to the normal molecular state.

The second stage we believe to be a long drawn out process (except in the case of surface combustion), and in a subsequent paper we shall describe experiments which

\* 'Engineering,' Aug. 1927.

suggest that it involves an appreciable amount of energy, and is therefore of practical importance.

*Description of Apparatus and Experimental Procedure.*

Two explosion vessels cylindrical in shape were employed in these experiments. One of these was of dimensions 12 inches in diameter by 12 inches in length, and the other 6 inches by 6 inches. The pressure indicators used were generally of the piston type, but in some experiments a diaphragm indicator was employed. They were fitted with moving mirror systems for optical recording on a revolving photographic film. The indicators were calibrated in position by admitting air under pressure into the explosion vessels and balancing the pressures against a column of mercury in a compound gauge on which readings were taken to half a millimetre.

The light emitted during the explosion, after passing through a small quartz window in the end cover, illuminated a narrow slit which was focussed on the film with its length perpendicular to the direction of motion of the film and in alignment with the reflected beam of light from the indicator mirror, so that a pressure-time curve and a simultaneous photographic record of the luminosity were obtained.

The gaseous mixtures were prepared by exhausting the explosion vessel and refilling several times with one of the constituents of the mixture to be used until all traces of the products of combustion from the previous experiment had been eliminated, and then admitting the gases from storage cylinders in the required proportion. The whole mixture was then thoroughly mixed by means of a fan mounted on a spindle passing through a gland in the end-cover. This fan was also used to produce turbulence during explosion in certain experiments which are described in the paper.

The explosions were initiated by an electric spark at the centre of the vessel from an induction coil, the primary circuit of which was closed at the proper time by a travelling contact on the revolving spindle carrying the film-drum.

The films used were Eastman Super Speed, H & D 500. Great care was exercised in developing them equally under conditions which were kept as uniform as possible.

*Results of Experiments.*

A typical record from an explosion of 30 per cent. carbon monoxide and air in the 6 in. cylinder is shown in fig. 1 (Pl. V.). In this experiment the initial pressure, represented by the zero-line of the indicator diagram, was 1 atmosphere, and the rise of pressure at any time during the explosion is shown by the height of the diagram above this line \*. The horizontal band immediately below the pressure-curve is a continuous record of the luminous radiation emitted by the gaseous mixture after ignition at the centre of the vessel by the electric spark, which was recorded on the film at the point A. During the interval between the passage of the spark and the beginning of the rise of pressure the luminosity was comparatively small, but it increased rapidly with rise of pressure to a maximum value in the neighbourhood of the maximum pressure, and afterwards decreased slowly as the products of combustion cooled. An examination of this record shows that during the actual explosion period the luminous radiation emitted was of no greater intensity than that emitted immediately after the moment of maximum pressure, although, of course, the bulk of chemical combination took place during that period. As the gases cooled the luminosity gradually decreased, but remained sufficiently intense to mark the film for a considerable time after maximum pressure. Indeed, even after this we noticed in all our experiments that the products remained incandescent for some seconds, and therefore long after the cessation of all chemical combination of the original gases as well as of any dissociated molecules.

These facts appear to be at variance with the theory that luminous emission during gaseous explosion results solely and directly from chemical combination. The record rather suggests that the intensity of the luminosity during the actual period of explosion, as well as afterwards, is entirely dependent upon the temperature of the gaseous medium as inferred from its pressure. Subsequent experiments which are now to be described definitely confirm these conclusions.

Figs. 2 to 5 (Pl. V.) show how the intensity and amount of luminous radiation emitted during explosion increased

\* The scale against the pressure-curve gives the mean gas temperature as inferred from the pressure.



as the maximum temperature was raised by substituting diluent gases of lower specific heats in mixtures containing the same amount and proportion of combustible gases. Figs. 2 and 3 (Pl. V.) were obtained with 20 per cent.  $H_2$  + 10 per cent.  $O_2$  + 70 per cent.  $N_2$ , and 20 per cent.  $H_2$  + 10 per cent.  $O_2$  + 70 per cent. Ar mixtures respectively. The chemical energy was therefore the same in both cases, but, on account of the lower heat capacity of the argon mixture, the maximum temperature developed was about  $500^\circ C.$  higher than in the nitrogen mixture, and, as will be seen, the luminous radiation was much more intense. The substitution of nitrogen for carbon dioxide as a diluent in a given mixture of carbon monoxide and oxygen also produced a similar result. This is shown in figs. 4 and 5 (Pl. V.), which were obtained with 26 per cent. CO + 30 per cent.  $O_2$  + 44 per cent.  $CO_2$ , and 26 per cent. CO + 30 per cent.  $O_2$  + 44 per cent.  $N_2$  mixtures respectively, with the fan running at 1500 r.p.m. In the former the maximum temperature reached was about  $400^\circ C.$  less than in the latter.

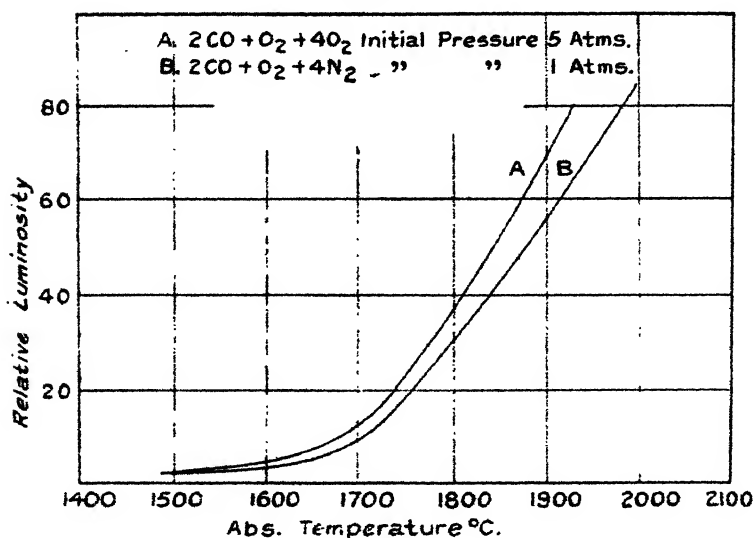
It is a well-established experimental fact that the ratio of the maximum pressure to the initial pressure, and hence the maximum temperature attained in the explosion of an inflammable gaseous mixture of any given composition, increases with the density of the mixture. This is due in the main to more effective combustion in a medium of high density. If radiation was emitted in virtue of chemiluminescence alone it would therefore be expected that the duration of emission after maximum pressure would become less as the density increased. This, however, is far from being the case, as is shown by the records in figs. 6, 7, 8 and 9 (Pl. VI.), which were obtained in experiments in the 6 in. vessel with a mixture of 28 per cent. CO and air at initial pressures varying from  $\frac{3}{4}$  to 3 atmospheres\*. Indeed, as will be noted, the duration of emission after the moment of maximum pressure in these experiments increased with the density, and this seems to be wholly due to the fact that cooling proceeded more slowly in the denser mixtures, for the temperature at which the luminosity ceased to be recorded by the films was the same at all densities. Further proof of this is given by the photometric

\* In these records the pressure-scales are different because stronger springs had to be used in the indicator at the higher pressures.

measurements recorded in fig. 10 \*. These relate to two mixtures, the one  $2\text{CO} + \text{O}_2 + 4\text{N}_2$  at atmospheric density, and the other  $2\text{CO} + \text{O}_2 + 4\text{O}_2$  at five atmospheres density. It will be noted that, in spite of the much slower cooling in the denser mixture, the relationship between the luminosity and the temperature is much the same in the two mixtures. We hope to investigate this relationship in a subsequent paper.

Similar experiments were carried out with mixtures of composition  $2\text{CO} + \text{O}_2 + 4\text{CO}$ , in which dissociation would be largely suppressed. The results were in every way similar to those obtained with CO-air mixtures.

Fig. 10.



We have also made two series of experiments in the large vessel with the mixtures  $2\text{CO} + \text{O}_2 + n\text{CO}$  at atmospheric density in which  $n$  was varied from 2 to 7. In the first series the mixtures were fired in the stagnant condition, and in the second they were put in turbulent motion by means of a fan. They can, perhaps, best be summarized in the manner shown in the Table on p. 396. It will be noted that the temperature at which luminosity reached a certain intensity, namely, that at which it became just

\* We wish to express our indebtedness to the late Mr. S. R. Pyke and to Mr. J. Tylor, who very kindly made the photometric measurements for us in Professor Whiddington's laboratory.

too weak to mark the film, was practically the same (about  $1150^{\circ}\text{C}.$ ) in all cases, although the time taken after explosion to reach this temperature varied greatly (from .26 sec. to .64 sec.), and consequently the chemical condition of the gaseous mixture varied considerably.

Although the luminosity at a temperature of  $1150^{\circ}\text{C}.$  was on the point of becoming too weak to mark the photographic film, luminosity visible to the eye continued to be manifest for some seconds afterwards, until, indeed, the temperature had fallen to  $300^{\circ}\text{C}.$  as nearly as we could judge.

Gaseous mixture.	Condition during explosion.	Time to max. press. (secs.)	Max. gas temp. $^{\circ}\text{C}.$	Duration of luminous record on film after max. press. (secs.)	Gas temp. at termination of luminous record. $^{\circ}\text{C}.$
$2\text{CO}-\text{O}_2+2\text{CO}$	Fan at work	.07	3080	.64	1150
3CO		.08	2780	.55	1190
4CO		.095	2570	.52	1170
5CO		.12	2200	.47	1180
6CO		.155	2030	.44	1170
7CO		.28	1710	.34	1160
$2\text{CO}+\text{O}_2+2\text{CO}$	Fan running	.03	3110	.47	1140
3CO		.04	2860	.41	1170
4CO		.045	2680	.35	1160
5CO		.055	2340	.33	1150
6CO		.065	2140	.29	1160
7CO		.08	1930	.26	1130

These results make it clear that the amount of radiation emitted in any given explosion depends entirely on the time integral of some function of the temperature during the explosion and the cooling period, and further confirmation of this may be obtained from an examination of the records given in figs. 11, 12, and 13 (Pl. VII.). In these figures are shown the effects of a more rapid explosion and an increased rate of cooling when this is caused by turbulence produced by a fan in the explosion vessel. Similar results are shown in figs. 14 and 15 (Pl. VII.), in which the explosion period and cooling-rate were varied by the addition of water vapour to CO-air mixtures.

#### *Gas-Engine Experiments.*

For these experiments the engine was designed to give the Clerk "zigzag" indicator diagram, which is obtained

by closing the valves automatically at the end of a suction-stroke, so that after the explosion has taken place the products of combustion are retained in the cylinder and are subjected to alternate compression and expansion, while the engine continues to run under its own momentum. From the moment of the tripping of the valves a continuous indicator diagram was recorded on a revolving photographic film by means of an optical indicator which had previously been calibrated in its working position against a standard gauge tester. The film was carried by a drum which was driven from the crank-shaft of the engine, so that the indicator diagram was recorded on a base representing angular displacements of the crank.

The results confirmed those obtained in the closed vessel, and they also show that when the products of combustion are re-heated by adiabatic compression immediately after cooling they again become highly luminous.

A typical record is shown in fig. 16 (Pl. VIII.). At the point A the piston was at the commencement of the compression-stroke with a fresh charge in the cylinder, and the valves disengaged from their cams; towards the end of compression at B ignition took place, and soon afterwards the pressure increased almost instantaneously to a maximum value at C. Immediately above the indicator diagram is the record of the luminous radiation emitted during the explosion and the expansion-stroke. The products of combustion cooled more rapidly in this case than in the closed vessel experiments on account of expansion, and they reached the temperature at which the luminosity ceased to mark the film about the middle of the stroke. At the end of the explosion-expansion stroke it is generally believed that combination is complete, for the analysis of the exhaust gas from gas-engines in normal running invariably indicates complete combination; but nevertheless the heating of the products of combustion during the subsequent compression-stroke caused them to become vividly luminous again, as shown in the record at E. The temperature reached at the end of this stroke was about  $1550^{\circ}\text{C}$ .

Owing to the continual loss of heat from the gas to the piston and the cylinder-walls the temperature reached at the end of successive compressions gradually became less, and during the next compression-stroke the temperature did not rise high enough to produce luminosity of sufficient

intensity to mark the film; but it was clearly visible to the eye at this point, and even at the end of three or four compressions afterwards, at which time the temperature was of the order of  $300^{\circ}\text{C}$ .

The record shown in fig. 17 (Pl. VIII.) was obtained by retarding the ignition until the piston had moved forward some distance on the expansion-stroke, with the result that the gases were raised to a higher temperature at the end of the first compression than was obtained during the actual explosion, and the record shows that the luminosity at this point was actually greater than during the period of chemical combination. The temperature reached at the end of the second compression in this case, viz.,  $1180^{\circ}\text{C}$ ., was also just high enough to give rise to a luminosity just sufficiently powerful to produce a faint impression on the film, as shown at G.

#### *Discussion.*

The photographic method is now extensively employed in this and other countries in investigating combustion phenomena in gaseous mixtures. The basic idea underlying this work is that luminosity results from chemical activity, and therefore that the existence of luminosity at any instant is an indication that such activity is proceeding at that instant. Pringsheim, who had made many unsuccessful attempts to make the more permanent gases luminous by direct heating to the highest temperatures he could command, was also of this opinion, but he believed that, as long as chemical activity was proceeding, the temperature of the medium in which it was taking place had a great influence upon the intensity of the luminosity. Many recent workers, however, do not appear to attach much importance to the temperature factor\*.

Our experiments appear to put beyond doubt the overwhelming influence of temperature upon the intensity of the luminous emission. The only question that arises is the part played by chemical activity†. The experiments

\* See, for example, 'Gaseous Combustion at High Pressures,' by Bone, Neuitt, & Townend. (Longmans, Green & Co., 1929, p. 202.)

† Ionization seems to have little influence on the luminous emission. Garner (Trans. Faraday Soc. vol. xxii. Oct. 1926, p. 334) has shown that the addition of a small quantity of lead tetra-ethyl suppressed ionization during explosion to a large extent, but the addition of lead tetra-ethyl to our gaseous mixture did not affect the luminosity to any measurable extent.

at once show that the intensity of luminosity at any moment is little influenced by the volume of *chemical combination* taking place at that instant, and, indeed, luminosity is manifest in our exploded gases long after the moment when chemical combination appears to have been completed. In proof of this may be urged the fact that luminosity is manifest for some time (suitably measured in seconds) after explosion, during the greater part of which time chemical analysis fails to suggest the presence of uncombined gas. Furthermore, in our gas-engine experiments it will be remembered that a series of rapid compressions of the working fluid subsequent to the explosion-expansion stroke reproduced luminosity, although, as has been frequently shown, chemical analysis of the exhaust gases of a gas-engine in normal running always suggests that combination is practically complete at the end of the explosion-expansion stroke. We think, too, that it is a safe inference from our experiments that, had we used a larger explosion vessel so that cooling took place more slowly, luminosity would have been manifest for a longer time than we observed in our vessel \*. Similarly, had our gas-engine been larger so that cooling would have been slower, re-illumination in the working fluid would have been observable over a large number of compressions.

It seems safe, therefore, to assume that luminosity may be manifest in exploded gaseous mixtures long after combination is complete : and in view of the fact that the more permanent gases cannot be rendered luminous by direct heating to temperatures at which luminosity is manifest in our experiments, it is reasonable to suggest that chemical combination results in the formation of abnormal molecules which persist for some time and only slowly pass into normal molecules †.

In a subsequent paper we describe experiments which seem to indicate that a considerable amount of energy is associated with these abnormal molecules, *i. e.*, that the energy they contain is in excess of that which would be

\* This has since been confirmed. During the explosion of a 30 per cent. CO-air mixture at three atmospheres density in an 18-inch silver-plated spherical vessel, luminosity was manifest for at least 14 seconds after maximum pressure.

† This applies only to combustion in the gaseous phase. The process seems to be enormously speeded up in contact with a hot body. This we will deal with in our next paper. (See p. 402.)

possessed by normal molecules of  $\text{CO}_2$  and  $\text{H}_2\text{O}$  constituting a gas of the same temperature. At first sight the theory that in the act of combination the heat of combustion first passes, either wholly or in part, into the form of rotational and vibratory energy of the newly formed molecules might be accepted as affording a satisfactory explanation. But the long life-history possessed by these abnormal molecules (in the absence of a disturbing cause, such as contact with a hot surface) introduces a very real difficulty, for partitioning would doubtless be effected very rapidly at explosion temperatures, and proof of this seems to be furnished by the fact that the energy in the vibrations corresponding to luminous radiation, as well as that in the vibrations corresponding to infra-red radiation\*, is always in equilibrium with the temperature (translational energy). Another explanation that might be offered is that complex molecules are formed during combination. This seems possible as a stage in the combination process, but again unlikely that they could possess a long life-history, for disintegration at explosion temperatures would probably be rapid.

We think that a possible explanation may be found in the suggestion that combination results in the formation of molecules of abnormal molecular *structure*, and that these molecules pass gradually into molecules possessing the normal structure, the process being an exothermic one. The overall process of combustion would thus be analysed broadly into two stages:—

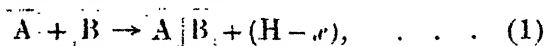
- (i.) chemical combination resulting in the formation of molecules of abnormal molecular structure, and
- (ii.) the passage (requiring time when combustion takes place in the gaseous phase) of these molecules into molecules possessing normal structure.

Our experiments, of course, offer no information as to the type of structure possessed by the abnormal molecules, but it is interesting to speculate as to possible types. Let us confine the attention to carbon-monoxide-oxygen combination. It is conceivable that the abnormal  $\text{CO}_2$  first resulting from this combination may consist of an atom of oxygen with its distinctive electron atmosphere attached as a whole to a more or less normal CO molecule,

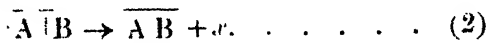
\* David, Phil. Trans. A, vol. cxi. p. 386.

which we will suppose consists of two atomic nuclei surrounded by a more or less common electron atmosphere. The passage to the normal type of  $\text{CO}_2$  may then be represented by the assimilation of the oxygen atom into the system producing a molecule consisting of three nuclei surrounded by a common electron atmosphere. It may be that the very considerable stability which we have to postulate for the abnormal type of molecule in order to account for our results is apparent rather than real, and that the apparent stability is due to continual dissociation and recombination brought about by collision or by continual interchange of partners with neighbouring molecules.

Summarizing, we suggest that the first stage in the overall process of combustion may be represented thus:—



where H is the heat of combustion, and that the second stage is indicated by



It has always been our view that the process of combination (the first stage indicated above) in any given thin layer of gas is by no means an instantaneous process, and although our present experiments offer no information on this point we are still of this opinion in view of some earlier experiments by one of us\*. We feel, however, that they do show that the second stage is a very long drawn out process in the gaseous phase, and in our next paper we describe experiments which suggest that the energy released in this stage, viz.,  $x$ , is an appreciable fraction of the heat of combustion.

We think that our experiments show that flame photographs, while they give invaluable information in regard to flame propagation in inflammable mixtures, yield no information as to the chemical condition of the gases behind the flame-front, but merely indicate their temperature.

We wish to express our indebtedness to Mr. S. G. Richardson, who made the experiments on the gas-engine and gave us great assistance in the earlier stages of the closed-vessel experiments.

\* Proc. Roy. Soc. A. vol. xcvi. p. 313 (1920).



XXXVII. *Temperature Measurements in Gaseous Combustion.* By W. T. DAVID, Sc.D., M.Inst.C.E., and W. DAVIES, B.Sc.\*

[Plate IX.]

**I**N this paper experiments are described in which the temperatures of thin platinum-rhodium wires immersed in inflammable gaseous mixtures during their explosion and subsequent cooling in closed vessels were recorded continuously and compared with the gas temperatures as inferred from the pressures.

Our results differ markedly from those of other investigators who have made similar experiments, and consequently, in order to ensure the correctness of our work, we made a large number of experiments under as widely different conditions as possible.

Briefly, they indicate that, in whatever position the wire is placed within the explosion vessel, its temperature is several hundred degrees (often  $500^{\circ}$  C. or more) higher than that of the gas (as inferred from its pressure), not only during the explosion, but also for some seconds afterwards. We found this to be the case, even when the gaseous mixtures were fired in a state of violent turbulence so that the temperature distribution subsequent to the explosion was reasonably uniform.

Similar experiments were also made in the cylinder of a gas-engine designed to give the Clerk "zigzag" indicator diagram, and the results fully confirmed those obtained in the closed vessels.

We believe that these experiments lend support to the views put forward in a previous paper on the emission of luminous radiation by gaseous mixtures during and after explosion, and they further indicate that considerable energy is associated with the abnormal molecules which are formed as a result of chemical combination in the gaseous phase.

*Experimental Procedure.*

The experiments were carried out in the explosion vessels and in the cylinder of the gas-engine described in the previous paper, and the general arrangement of the

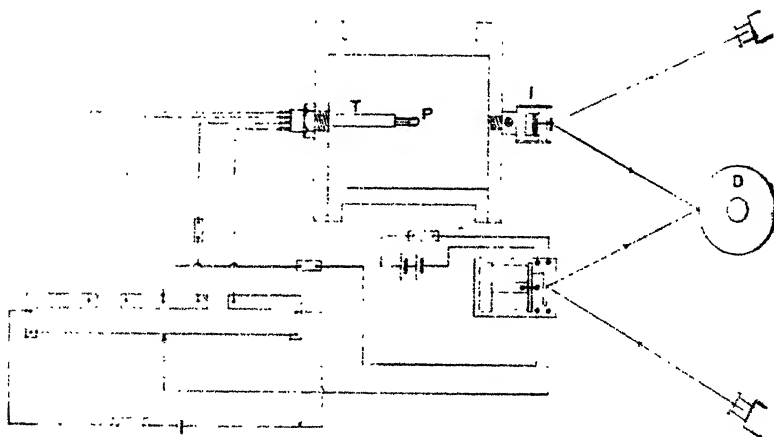
\* Communicated by the Authors.

apparatus for recording the temperature of the wire is shown in fig. 1.

The platinum-rhodium wire P was  $\cdot 001$  inch in diameter\* and  $\frac{3}{4}$  inch long and was connected to one arm of a slide-wire bridge by thick copper leads which passed into the explosion chamber through a sealed metal tube T. This tube could be adjusted to bring the wire into any desired position within the explosion chamber.

Callendar's method of compensating for the change of resistance in the leads and for their cooling effect at the junctions of the wire was adopted by connecting a short length of the same wire through a similar pair of leads to the opposite arm of the bridge and adding sufficient

Fig. 1.



external resistance to bring the point of balance to the middle of the slide wire at room temperature.

The galvanometer used in the experiments was of the Torsion String type with a natural period of  $1/50$  of a second, so that it recorded very acutely the rapid change

\* We made several experiments with wires of different diameters ranging from  $\cdot 003$  to  $\cdot 0005$  inch, and found that a wire of  $\cdot 001$  inch diameter followed the most rapid temperature changes without an appreciable lag, and this size was used in all the experiments described in the paper.

As a further check on our work we made a number of experiments in which the temperatures were measured by thermocouples consisting of platinum-rhodium and platinum-iridium wires of  $\cdot 01$  inch diameter, the results of which were found to be in complete agreement with those obtained by the resistance method.

of temperatures in the wire during an explosion. Its deflexions were recorded on a photographic film mounted on a revolving drum D, and at the same time a continuous record of the pressure was obtained on the same film by means of the optical indicator I. The calibration of the temperature scale for the wire was obtained directly by recording the deflexions of the galvanometer when the wire was placed in an electric furnace at different temperatures up to a maximum of  $1100^{\circ}\text{C}$ . This calibration was made for every new wire used in the experiments, and the extrapolation of the calibration curve to higher temperatures was verified by recording the deflexions of the galvanometer when the wire was placed in a Bunsen flame, and finally, after the completion of a series of experiments, when the wire reached its fusing point in an explosion of a strong gaseous mixture. The relationship between the temperature of the wire and the galvanometer deflexion above  $800^{\circ}\text{C}$ . was practically linear, and therefore intermediate points between the maximum furnace temperature and the melting-point of platinum rhodium could be determined with a fair degree of accuracy.

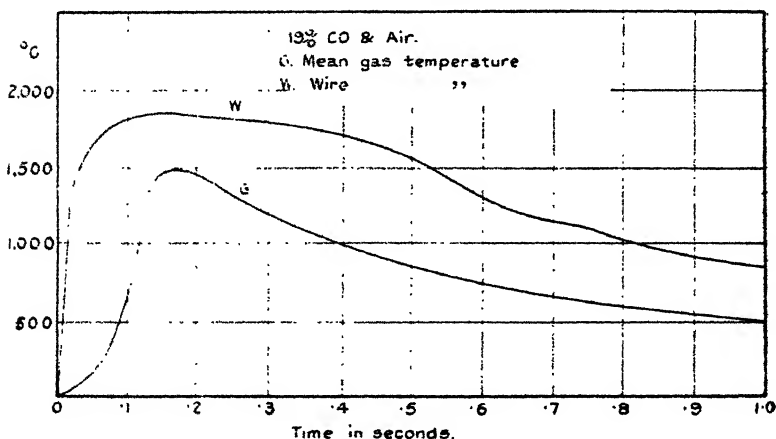
#### *Result of Closed Vessel Experiments.*

A typical record is shown in fig. 2 (Pl. IX.), in which G is the pressure record and W the curve traced by the galvanometer. The spark passed at the point A, and the temperature of the wire increased very rapidly as soon as the flame passed over it before any appreciable rise of pressure had taken place. A further and slower rise of temperature occurred in the wire after this, due to the adiabatic compression of the inflamed gases at the centre of the vessel while combustion was proceeding in the outer layers, and the wire reached its maximum temperature at the moment of maximum pressure. But after this it will be noted that the wire did not cool at the same rate as the gas.

This record was obtained with a mixture of 19 per cent. CO and air in the 6-inch vessel when the wire was placed on the axis of the cylinder at a distance of one inch from the centre. The mean gas temperature (curve G) calculated from the pressure curve and the corresponding temperature of the wire (curve W) for a period of one second after ignition are shown in fig. 3.

It will be seen that the temperature of the wire was some hundreds of degrees above that of the mean gas temperature (as inferred from the pressure), both during explosion and for more than a second afterwards. It is well known that in a stagnant mixture fired centrally the temperature of the mixture in the centre is well above the mean gas temperature; but this could hardly be to the extent shown by this experiment, and no explanation in terms of temperature variation in the gaseous mixture during the cooling period could possibly be adequate to account for the very large difference between the wire and gas temperature (of the order of  $500^{\circ}\text{C}$ . or more) during this period.

Fig. 3.



This view is confirmed by the results shown in fig. 4. These were obtained with a mixture of 17 per cent. hydrogen and air, first when the fan was at rest and then when it was running at a speed of 1500 revolutions per minute. The violent turbulence produced under these conditions practically eliminated any temperature differences in the gas, but nevertheless, as will be seen, the large temperature difference between wire and gas was maintained throughout explosion and subsequent cooling.

Moreover, we found that the temperature of the wire in any given explosion differed very little when it was placed in different positions within the 6-inch vessel. The results shown in fig. 5 were obtained with a mixture of 6.5 per cent. methane and air, first when the wire was

placed near the centre and then when it was placed near the end cover of the vessel. In the latter position it will be seen that a small increase of temperature (about  $80^{\circ}\text{C}$ . in this case) occurred in the wire before the flame reached it, due to the adiabatic compression of the unburnt gases

Fig. 4.

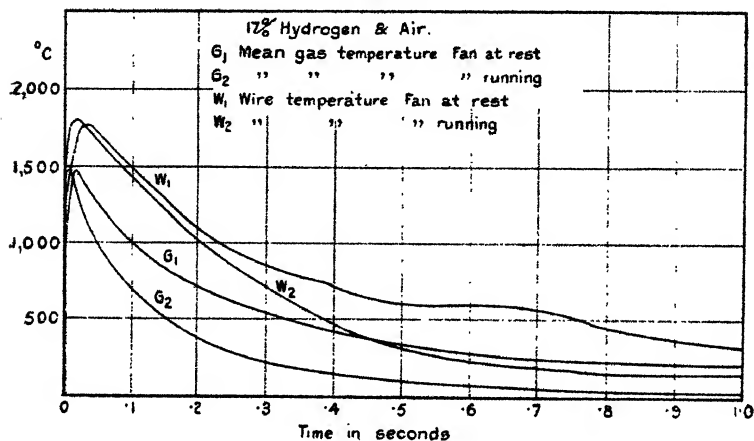
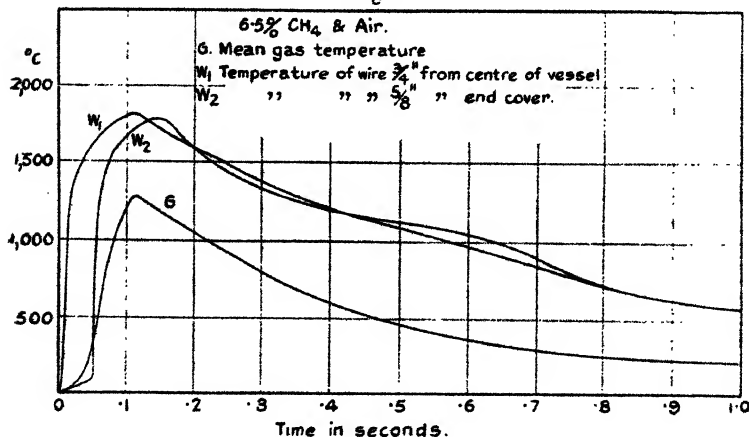


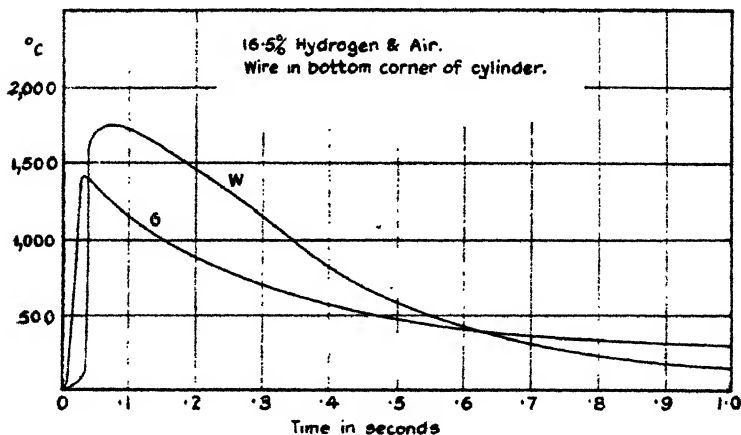
Fig. 5.



while the flame was moving outwards from the centre. We found that this initial rise of temperature in the wire agreed very closely with the calculated temperature of the unburnt gases, assuming true adiabatic compression before ignition. At the moment of maximum pressure the temperature reached by the wire in the two positions was

practically the same and about  $500^{\circ}\text{C}$ . higher than the maximum mean gas temperature. The subsequent rate of cooling was also very nearly the same in both cases. When, however, the wire was placed in the bottom corner of the cylinder about half an inch away from the walls and the end cover, its temperature, while well maintained above the mean gas temperature for a considerable portion of the cooling period, fell eventually below the mean gas temperature. This is clearly shown on fig. 6, which was obtained with a mixture of 16.5 per cent. hydrogen and air when the wire was in this position. But it is very probable that even here the temperature of the wire was at all times

Fig. 6.



far above that of the gas actually in contact with it, because, owing to very rapid cooling in the corner of the vessel, the temperature of the gas there was well below the mean gas temperature; and this view is supported by the fact that with turbulence the temperature of the wire in the same position did not at any time fall below the mean gas temperature.

The rate of explosion and the maximum gas temperature developed in a given mixture may be varied very considerably without producing any appreciable change in the rate of heating of the wire or in the maximum temperature reached by it; thus, when the explosion of dry mixtures of carbon monoxide and oxygen is accelerated by the addition of a small amount of hydrogen, the maximum mean gas temperature is considerably increased, but the

results given in fig. 7 show that, even when the gas temperature is raised by nearly  $400^{\circ}\text{C}$ . in this way, no appreciable change is produced in the rate of heating of the wire or in the maximum temperature attained by it. A similar

Fig. 7.

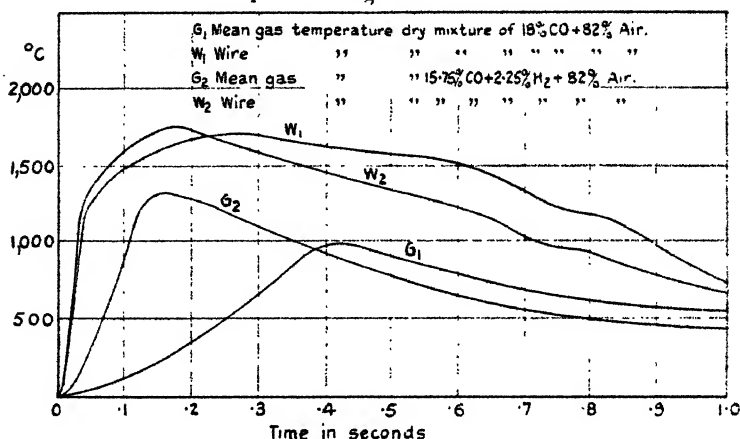
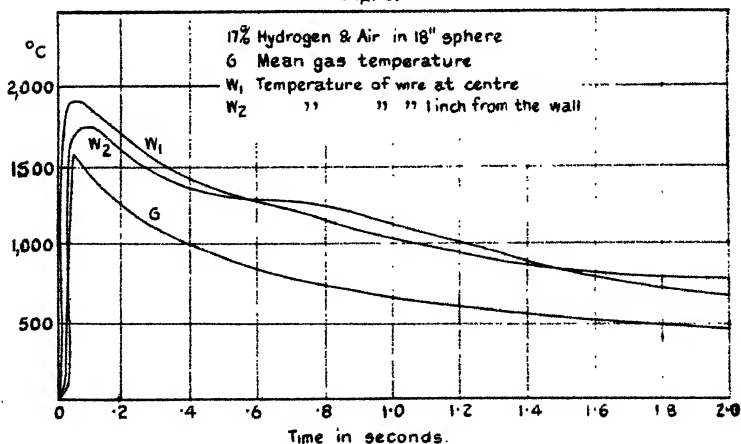


Fig. 8.



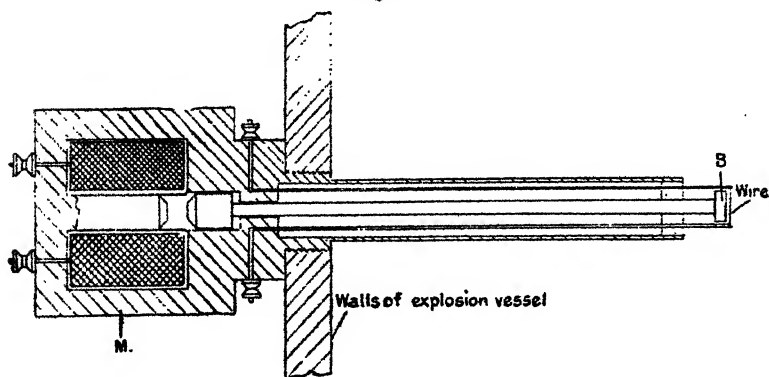
result was also obtained when water-vapour was added to the same mixture instead of hydrogen.

Similar experiments were made in a larger vessel—an 18-inch sphere. Typical results are shown in fig. 8. They relate to a mixture of 17 per cent. hydrogen and air centrally fired, and show the wire temperature in two positions—the one central and the other near the walls

—for a period of 2 seconds after ignition. They appear to confirm in every way our experiments with the smaller vessel, except that there is a rather greater difference in the maximum wire temperatures in the two positions in the larger vessel.

In all the experiments to which reference has been made, the wire was completely exposed to the gas throughout the period of explosion, and therefore only comparatively weak mixtures which would not cause the wire to fuse could be used. In order to investigate the conditions in stronger mixtures, the apparatus shown diagrammatically in fig. 9 was designed to shield the wire until it could be safely exposed at some instant during the cooling period.

Fig. 9.



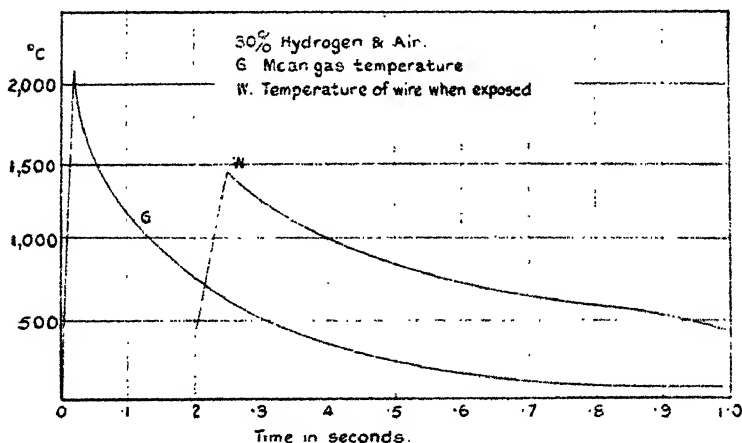
Its action depended on the shielding effect of the mass of metal B due to its proximity to the wire until, at the proper moment, it was pulled away from the wire by the electromagnet M when the circuit of the solenoid was closed by a switch automatically operated by a cam on the spindle of the film-drum. The result of an experiment with a mixture of 30 per cent. hydrogen and air in the smaller vessel is shown in fig. 10. The wire was exposed when the gases had cooled to about  $700^{\circ}\text{C}.$ , as inferred from the pressure, and its temperature was immediately raised to about  $1400^{\circ}\text{C}.$  From this point the wire remained fully exposed while the products of combustion cooled down to the temperature of the room. By exposing the wire at different times during the cooling period



in the explosion of any particular mixture, we found that its subsequent cooling curve was the same whether it was exposed early or late, so that the wire always reached the same temperature relative to that of the gas at any given instant after maximum pressure, whether it approached this temperature from above or from below.

In a later form of the apparatus the wire was completely shielded from contact with the gas until the proper time for exposure, but this modification of the apparatus did not produce any change in the results, provided no obstruction was offered to the free circulation of the gas in the vertical plane of the wire. In its original form the

Fig. 10.

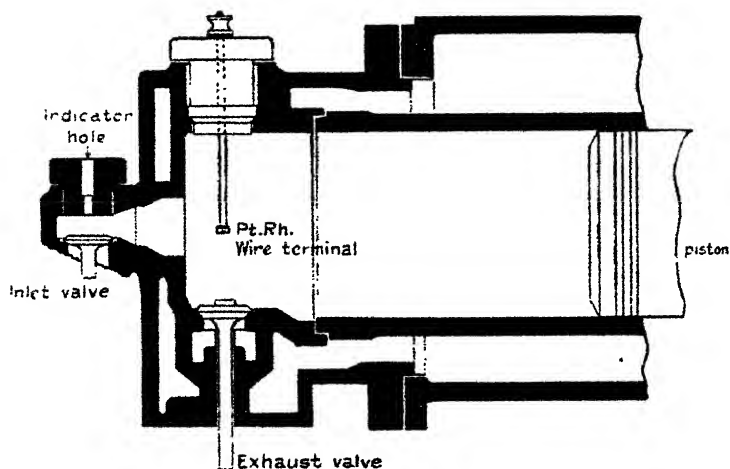


modified shield consisted of a cylinder of  $\frac{1}{8}$  inch external diameter divided along its axis into two halves which fitted closely over the wire, and when released by the magnet the two parts moved upwards and downwards respectively a total distance of about 1 inch from the wire. With the shield in this position the wire recorded a temperature of about  $300^{\circ}\text{C}$ . to  $400^{\circ}\text{C}$ . less than when fully exposed, but when the shield was made to open horizontally through an equal distance from the wire, its presence had no measurable effect upon the temperature of the wire. This fact is of considerable interest in that it shows the existence of vertical currents of hot gases at the centre of the vessel, even when the fan is running during the explosion.

*Gas-engine Experiments.*

The wire was fixed on the ends of thick brass terminals projecting into the combustion chamber as shown in fig. 11, and the recording of its temperature was carried out in the same manner as in the closed vessel experiments. At the end of the suction stroke its temperature was about  $60^{\circ}\text{C}.$ , and its rise of temperature during the compression stroke agreed very closely with the gas temperature inferred from the indicator diagram; but after ignition and during the greater part of the expansion stroke its temperature exceeded that of the gas by about  $500^{\circ}\text{C}.$ , as in the closed vessel experiments.

Fig. 11.

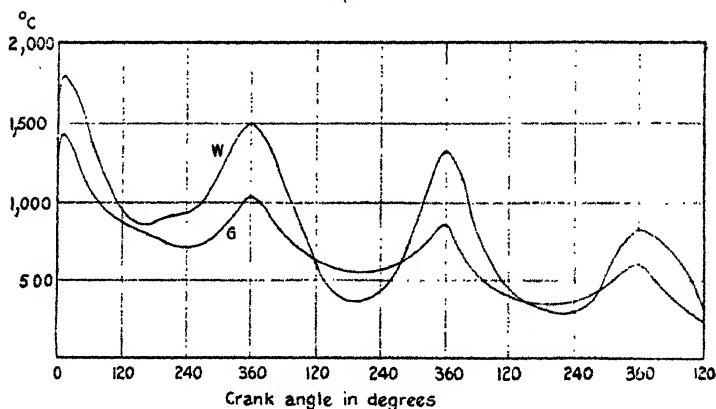


NOTE.—The platinum-rhodium wire was  $\cdot 001$  inch diameter and  $\frac{3}{4}$  inch long, mounted with its length perpendicular to the axis of the cylinder.

The results shown in fig. 12 were obtained during three revolutions of the crank after an explosion had taken place and the valves had been tripped so that the products of combustion were retained in the cylinder and alternately expanded and compressed while the engine was running under its own momentum. The temperature cycles of the wire are shown by the upper curve, and the corresponding gas temperatures as inferred from the indicator diagram are shown by the lower curve. Owing to its position in the cylinder, the wire was exposed to the

relatively small amount of cold gas emerging from the valve pocket towards the end of the expansion stroke, and after the first expansion it was cooled below the mean gas temperature during this part of the cycle. It is very probable, however, that even at this time the wire was much hotter than the gas actually in contact with it, and this is strongly suggested by the fact that it was very quickly heated above the mean gas temperature again during the early part of the next compression stroke before the hottest part of the gas came into contact with it. The extreme range of temperature variation in the wire was thus greater in this experiment than would have been the case had it not been influenced by the small quantity of

Fig 12.



cold pocket gas, as, for example, had it been moving with the piston so that it was always in the general body of the gas in the cylinder. There seems little doubt that in that case the wire would always have remained at a much higher temperature than the gas throughout the period of the experiment.

Just before tripping the valves in this experiment the engine was running at a speed of 230 r.p.m., which remained sensibly constant during the following three revolutions, so that the total time taken to perform the three cycles shown was about 0.8 second.

We take pleasure in thanking our research mechanic, Mr. H. Marvel, for assistance in the design of our apparatus and for making suggestions of value from time to time.

*Discussion.*

Our experiments are in agreement with those of Hopkinson\* in showing that the temperature of the wire as the flame passes over it almost instantaneously rises to its maximum value (apart from a small subsequent rise resulting from the adiabatic compression of the gas surrounding the wire). Harrison and Baxter †, on the other hand, found that the rise of wire temperature takes an interval of time which for any given mixture was of the order of the time of explosion of that mixture in their vessel. We are unable to reconcile their results with our own or with those of Hopkinson, though a possible explanation is that they may have had a mass of metal somewhere near the wire which may have affected the gas in its neighbourhood; and in this connexion we draw attention to the difficulties we experienced in designing our apparatus so as to secure consistent results (see p. 410).

Hopkinson inferred from his experiments that combustion was completed in any given thin layer of gas almost instantaneously after inflammation. This view did not accord with that deduced from calorimetric measurements made by one of us ‡, and it was suggested that the rapid rise of temperature of the wire was in a large measure due to combustion on the surface of the hot wire §. Our present experiments appear to confirm that suggestion.

In one important respect our work differs entirely from Hopkinson's. We found that at the moment of maximum pressure the temperature of the wires did not vary much with their position in the explosion vessel and that their temperature was always many hundreds of degrees above that of the mean gas temperature as inferred from the pressure. Hopkinson, however, found that his wires showed a wide temperature variation in the exploded gases at this moment which seemed to be rational in the light of an examination of the explosion process. He found, for example, that the temperature of the hot core of a centrally-fired mixture was at this moment much above that of the mean gas temperature as inferred from the pressure, but that as the wire was moved outwards towards the walls of the explosion vessel the temperature

\* Proc. Roy. Soc. A, lxxvii. pp. 389 & 399 (1906).

† Phil. Mag. pp. 37-41, Jan. 1927.

‡ Proc. Roy. Soc. A, xcviii. p. 310 (1920).

§ Trans. Faraday Soc. xxii. p. 343 (Oct. 1926).

fell away and became much less than the mean gas temperature \*. The wire temperature averaged over a large number of positions would thus, according to Hopkinson, be equal to the mean gas temperature (translational energy). We think that a large error must have crept into the calibration of his wire temperature recording system for wires other than the central wire, which had a separate recording system; and, indeed, Hopkinson himself does not claim great accuracy for the former recording system †.

Our experiments further show that the large difference which exists between the wire temperature and the gas temperature (translational energy) at maximum pressure continues for some seconds afterwards, and therefore long after chemical combination has been completed. The gas-engine experiments also lead to the same conclusion. We believe that the explanation is the same as that offered to account for the luminosity experiments ‡, namely, that combination in the gaseous phase results in the formation of long-lived abnormal molecules, and that considerable energy is associated with these molecules which can be unloaded upon the surface of a hot wire when they come in contact with it.

Reference may be made to the discussion in our previous paper for a fuller account of our views. We should add that in interpreting the results in the present paper it is convenient to regard the temperature of the wire as being equal to the temperature of the gas (translational energy) *plus* an amount corresponding to the excess internal energy unloaded upon it by the abnormal molecules.

We hope to be able to obtain an estimate of the magnitude of the energy associated with the abnormal molecules by calorimetric methods both in closed vessel explosions and also in a gas-engine.

Many of the curious results obtained by workers who have used platinum wires to measure the cyclical changes of temperature of the working fluid of internal-combustion engines and the temperature of the exhaust gases become understandable in the light of these experiments. A discussion of them is reserved for another paper.

\* *Loc. cit.* p. 390.

† *Loc. cit.* pp. 397-8.

‡ Ionization seems to have no influence upon the temperature of our wires as inferred from their resistance, for the addition of lead tetraethyl to our gaseous mixtures made no difference to the wire temperatures (see footnote, p. 398).

### XXXVIII. *Some Experiments with Carbon Line Resistances.*

By J. B. SETH, *M.A. (Cambridge), Professor of Physics, Government College, Lahore*, CHETAN ANAND, *M.A.*, and GIRDHARI LAL PURI, *M.Sc. (Punjab)\**.

IN a paper † from this laboratory it has already been announced how the resistance of carbon (pencil) lines drawn on ebonite or waxed ground-glass surface, when subjected to moist air of different humidities, changes in a regular manner with the relative humidity to which it is exposed; and a suggestion was made that this behaviour of carbon lines may be utilized for hygrometric purposes. The experiments described in the present paper were undertaken to study the properties of such resistances in greater detail before arriving at any suitable form of hygrometer or hygrometry based on these principles. The pencil lines for the present work were mainly those drawn on ebonite, although a number of experiments were also performed on lines on ground-glass plates, the free surface having been waxed. Lines drawn on other insulators such as sulphur and sealing-wax (blocks of which were obtained by pouring the molten materials in a wooden mould and allowing it to solidify) have also been tried, and these were found to behave in a manner similar to those drawn on ebonite. The lines which were to be subjected to humid atmospheres were drawn rather broad, several millimetres wide, in order to have a fairly large exposed surface. Their resistances were usually of the order of a tenth of a megohm.

The present experiments can be divided into two main classes, namely: (1) observing the behaviour of a line enclosed in a tube containing (a) air at low pressures, (b) nitrogen; and (2) subjecting the line to humid air in a variety of ways. The line was exposed to the humid air either by passing a continuous current of moist air over it or by placing it in a chamber containing air of a definite humidity. We may call the former the dynamical and the latter the statical method of exposure.

\* Communicated by the Authors.

† "The Effect of Moist Air on the Resistance of Pencil Lines," by J. B. Seth, Chetan Anand, and Gian Chand. *Proc. Phys. Soc. Lond.* xli, pp. 29-35 (Dec. 15, 1928).

For the dynamical mode of the experiment a current of ordinary air from the room was, to begin with, dried by making it first pass through calcium-chloride tubes and then bubble through concentrated sulphuric acid. It then passed through a pair of wash-bottles containing a solution of sulphuric acid and water of suitable strength, where it took up the desired humidity. There were a number of such pairs of wash-bottles arranged in parallel, different pairs containing solutions of different strengths, so that the dry air could be made to pass through any one of these pairs by merely turning off and on suitable stop-cocks. A current of air of the definite humidity so acquired was then passed over the pencil line, an aspirator being used to draw the air-current, and a couple of calcium-chloride tubes and a wash-bottle containing concentrated sulphuric acid having been placed between the aspirator and the glass tube containing the line. Or the air could be first stored in large bottles under pressure and then forced through the whole arrangement just described.

To obtain the static conditions the line was placed in a fairly large rectangular glass trough, which contained a dish in which sulphuric acid-water mixture of the required strength could be placed. The chamber also contained a tiny fan worked by a small motor to circulate air-currents throughout the chamber in order to make the humidity of the air inside the trough everywhere uniform. The chamber could be covered by a wooden lid, and the whole arrangement could be made air-tight by suitable means \*.

The results of various experiments are given below —

1. A line drawn on ebonite was placed in a suitably wide glass tube connected on one side to an exhaust-pump and on the other to a closed-end mercury manometer. The electrical connexions with the ends of the line were made through side-tubes with platinum wires sealed in. The only sources of leak were thus a few necessary connecting glass stopcocks, and there was only a very small leak through these ; but by occasional working of the pump the exhaustion was maintained for fairly long periods. The line was thus exposed to rarefied air at a pressure of a few

\* For details of this method of getting the so-called static state, see Proc. Phys. Soc. xxxiv. "Discussion on Hygrometry," p. 11.

millimetres. The resistance was found at first to decrease when the tube was first exhausted; but afterwards a slow increase set in, the rate of increase being greater in the beginning. Thus it was 7 in 1000 during the first week and only 2 in 1000 during the third week.

2. Another line, also on ebonite, was kept in an atmosphere of nitrogen for a period of about four weeks. Here also there was an abrupt fall of resistance during the first 24 hours, after which there was a gradual increase, the rate of increase being much greater than in the previous case. It was of the order of 1 in 14 during the first 5 days and 1 in 24 during the last 5 days.

The nitrogen was prepared by gently heating a mixture of solutions of potassium dichromate, sodium nitrite, and ammonium chloride, and was purified by being passed through potash bulbs, wash-bottles containing strong sulphuric acid, and calcium-chloride tubes containing plugs of glass-wool. It was introduced into the chamber containing the line by alternate exhaustion and filling, the process being carried out several times.

In both these experiments, *i. e.* the pencil line in vacuum and in nitrogen, the resistance fell during the night and rose during the day. This is apparently a temperature effect.

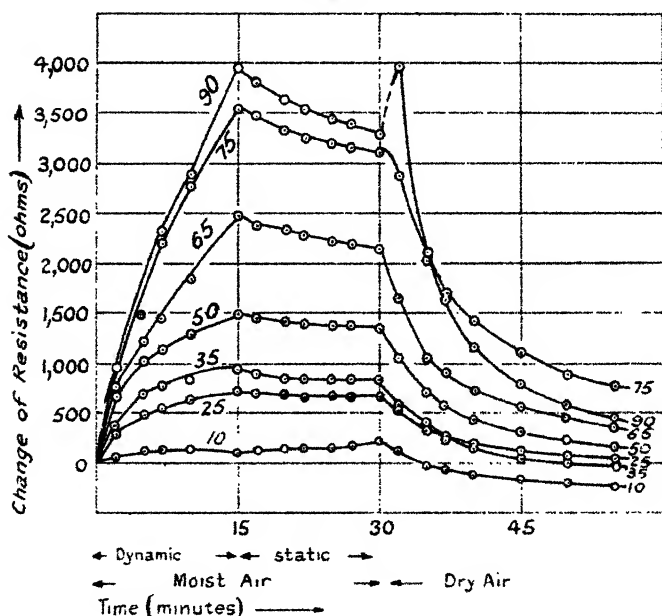
3. A previously dried (by means of a current of dry air) pencil line, on ebonite as well as on waxed ground-glass, was subjected to a current of moist air of a definite known humidity and afterwards to a current of dry air. Values of the resistance were found every few minutes. In these as well as in the experiments described below the relative humidities of the moist air to which the lines were exposed were 10, 25, 35, 50, 65, 75, and 90 per cent. The curves between resistance and time for different humidities, plotted from these observations, were of the same type as those given in the previous paper. Generally the increase of resistance with time increased with the relative humidity. In the case of 90 per cent. humidity, however, the changes in resistance were rather erratic. Sometimes the final resistance, after passing 90 per cent. humid air for, say, 15 minutes, was greater than that for 75 per cent. humidity, and sometimes it was even less than that for still lower humidities. Also, in the case of 10 per cent. humidity,



the resistance did not increase uniformly with time. Quite often, on passing moist air of this humidity, there was a fall of resistance after an initial increase, and sometimes even this initial increase was absent. Now and again, however, it increased, slowly but uniformly, throughout the period that the air of this humidity was being passed over the line.

It must also be mentioned that the changes in resistance with any particular humidity were not always the same when the same line was subjected to this humidity again

Fig. 1.



and again for the same length of time. This would seem to preclude the use of carbon lines for hygrometric purposes; but from later experiments it became evident that the changes depended not only on the relative humidity of the moist air, but also on the rate at which the current of the moist air passed over the line. More details about this matter are given later in section 7 below.

4. If, after subjecting a previously dried line to the current of moist air, say, for 15 minutes, and before passing the current of dry air over it, the moist air current is

stopped and the line allowed to remain in this humid atmosphere (giving a static state of affairs, as it were), the resistance does not remain quite steady, but changes slightly, generally increasing for lower humidities, but decreasing for the higher humidities, the decrease being more marked with increasing humidities. This is illustrated in fig. 1. where the numbers given against each curve represent the relative humidity of the moist air.

5. If a cycle of operations is performed on a previously dried line, that is to say, a current of air of 10 per cent. relative humidity passed over the line for, say, 20 minutes, then a current of higher humidity for the same length of time, and so on, till we get up to the 90 per cent. humidity, and after this air-currents of decreasing humidities are passed, coming back to the 10 per cent. humidity, then the resistance gradually increases (except that in the case of the 10 per cent. at the beginning of the cycle, there is first a slight fall of resistance), reaches a maximum, and then decreases, more or less following the cycle of humidities. In the case of the line on waxed ground glass the resistance, in our experiments, reached its maximum at the maximum humidity, but the final resistance after one complete cycle was considerably less than what it was at the beginning. For the line on ebonite the resistance attained its maximum value *after* the maximum humidity had been passed, namely at about 75 per cent. relative humidity on the descending half of the humidity cycle; but the final resistance after the complete cycle was nearly the same as, or only very slightly less than, that in the beginning.

In all cases mentioned in 3, 4, and 5 the changes are most marked in the first few minutes, the rate of change decreasing with time.

6. When experiments of the types 3, 4, and 5 are performed on lines with humidity conditions being static, the changes in resistance are not at all as regular as in the dynamic state. With the line on waxed ground-glass the changes in resistance were very erratic, and the various types of experiments were therefore confined to the line on ebonite. But here also the curves between resistance and time for different humidities were not at all regular and were more or less jumbled up.

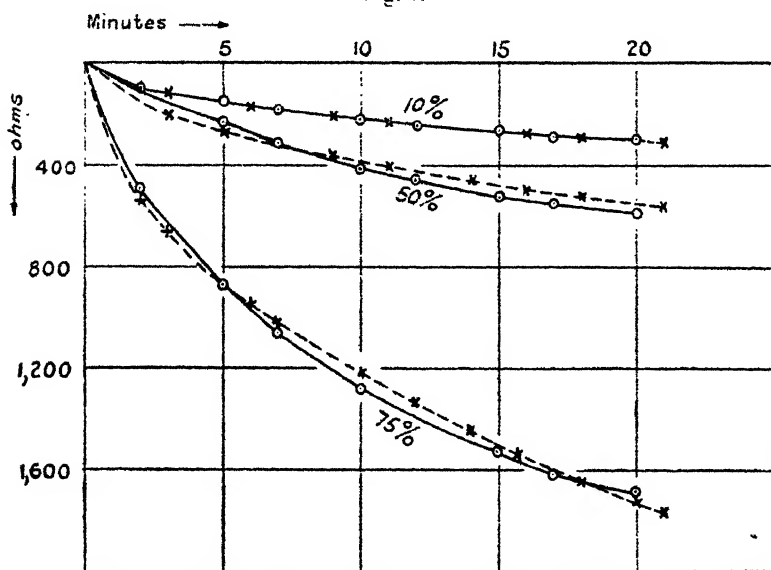
7. If we study the drying part of the curves obtained in the dynamic experiments, some rather interesting conclusions follow. For this purpose we replot the drying parts of the curves for various humidities by shifting the initial resistance (namely the resistance which the line had when the current of dry air was commenced after the line had been exposed to the moist air) to the same origin. We now find in the first place that these curves vary in much more regular manner than the curves obtained for the condition when the moist air was being passed. The anomalous behaviour for 10 and 90 per cent. humidities, previously mentioned, disappears for these curves. Thus in fig. 1, although the curves for 75 and 90 per cent. cross each other and so do those for 25 and 35 per cent., when the drying parts are drawn by shifting the initial resistance to the same origin, the curves fall in a regular manner. Secondly, it appeared as though these drying curves were parabolic, the change in resistance after a certain time (and after the line had been previously subjected to the certain humidity) being proportional to the square root of the time.

It was while studying these curves that it appeared that their size depended upon the rate at which the dry air was being passed over the pencil line. Special experiments were therefore performed to find the change in resistance with time when a previously dried line, after being exposed to currents of air of different humidities, was subjected to a current of dry air, keeping the rate at which this current was passed fixed and determinable. The rate of passage of the air was measured in terms of the fall in the level of water in the aspirator in a given time, or by collecting the air forced over the resistance in a cylinder over water. From this study it was found (1) that for a fixed humidity,  $H$ , and a fixed rate of flow of the dry air,  $F$ , the curves between the change in resistance,  $R$ , and the square root of time,  $t$ , were straight lines passing through the origin; and (2) that for a fixed humidity and a constant time the curves between  $R$  and  $F$  were also straight lines passing through the origin. Thus  $R^2 = kF^2t$ , where  $k$  is a constant, would give the equations of the drying curves: that is to say, they are parabolic. The constant  $k$  depends on the relative humidity and seems to be rather a complicated function of  $H$ . The relation between  $R$  and  $H$  appears to be nearly but not quite an exponential one. Further

experiments are needed to determine the exact relationship between these two variables, *i. e.* to find the value of the constant  $k$  in terms of the relative humidity.

The values of this constant for 10, 50, and 75 per cent. humidities turned out to be  $(5.6)^2$ ,  $(11.0)^2$ , and  $(30.8)^2$  respectively, as determined from the curves giving the results of the present experiments. In fig. 2 are given the drying curves, between change in resistance and time, for 10, 50, and 75 per cent. humidities, the rate of flow having been respectively 12.1, 11.2, and 12.5 cm. of fall of water

Fig. 2.



column in 20 minutes in the cylinder in which the issuing air was collected. The circles represent points experimentally determined, and the full lines the curves passing through these. The broken lines are parabolas with the values of parameters as given above, the crosses representing the points calculated for these parabolas. It will be seen that the fit between the experimental and calculated curves is so close for 10 per cent. humidity that the two are indistinguishable from each other on the scale of the figure. The fit for the 50 and 75 per cent. curves is not so good. But it is expected that this will become closer by improving the method of maintaining a constant rate of flow.

Presumably, the increase in the resistance when a dried line is exposed to a current of moist air would also depend on the rate at which the current of the moist air is passed over it. This would account for the behaviour of the lines remarked at the end of section 3. From the fact, however, that the drying curves are more regular and vary in a more uniform manner with the humidities to which the lines have been subjected previous to the drying process than the "wetting" curves, it would appear that if a pencil line is to be used for hygrometric purposes, it would be more profitable to study the drying curves for the line and utilize this for the purpose of measuring humidities. Moreover, from the nature of things, one may not always be able to regulate the rate of the "wetting" of a carbon line when exposed to an atmosphere of which the relative humidity is to be determined: but one can easily regulate the drying process, and from the fall of resistance during a certain time one may compute the required humidity.

XXXIX. *The Effect of a Permanent Electrical Dipole on the Internal Latent Heat of Vaporization of a Liquid.* By A. R. MARTIN, Ph.D.\*

IN the light of modern views of the electrical structure of matter the internal latent heat of vaporization of a liquid can be regarded as the work required to separate the molecules of the liquid to an infinite distance from each other against the attractive forces due to the electric field surrounding each molecule. The work of vaporizing a single molecule is, therefore, neglecting electrical saturation effects, the change in the energy in the medium resulting from the transfer of the molecule to a vacuum from a medium of dielectric constant equal to that of the liquid. In so far as the molecule may be regarded entirely as a permanent electrical dipole, this energy change is given by the expression deduced previously †,

$$\frac{\mu^2}{3a^3} \left(1 - \frac{1}{D}\right),$$

\* Communicated by Prof. J. C. Philip, F.R.S.

† Martin, Phil. Mag. viii. p. 547 (1929).

where  $\mu$  = the moment of the dipole,  
 $a$  = the radius of the molecule,  
 $D$  = the dielectric constant of the liquid.

This expression should therefore give the effect of a permanent electrical dipole on the internal latent heat of vaporization of a liquid. It can be expected to yield good results only when the molecule can with a fair degree of truth be treated as a single permanent dipole at the centre of a sphere.

In applying this idea, that part of the latent heat which is not due to the dipole (but which nevertheless is probably of electrical origin) has been allowed for in organic compounds by subtracting from the total latent heat values for the alkyl and phenyl groups derived from the latent heats of the parent hydrocarbons. Thus the value of the methyl group has been taken as one-half that of ethane, of the ethyl group five-sixths that of ethane, of the propyl group seven-eighths that of propane, of the butyl group nine-tenths that of butane, of the iso-amyl group eleven-twelfths that of iso-pentane, and of the phenyl group five-sixths that of benzene. This treatment is only approximate, especially as the data for the hydrocarbons are usually not for the same temperature as those for their derivatives. And further, it may not be justifiable to treat the external field of a weakly dipolar bond as entirely due to the dipole.

The values of  $a$  required to give the observed effect of a dipole on the internal latent heats of vaporization of twenty-one liquids are tabulated below. The latent heats have been taken from 'International Critical Tables,' vol. v., the dielectric constants at the boiling points from Grimm and Patrick\*, and at other temperatures from Landolt-Börnstein's 'Tabellen,' and the dipole moments from the table given by Højendahl†, with the exception of the dipole moment of acetonitrile, which was taken from Werner‡. The internal latent heats are given in joules per mole and are denoted by  $\lambda_i$ , and that portion of them due to the dipole by  $\Delta\lambda_i$ .

The values of the molecular radii are of the correct order of magnitude. They are smaller than those calculated from gaseous viscosities, the values obtained by this method for water, sulphur dioxide, and ammonia being respectively

\* Grimm and Patrick, J. Amer. Chem. Soc. xlv. p. 2794 (1923).

† Højendahl, 'Thesis,' Copenhagen (1928).

‡ Werner (O.), Z. physikal. Chem. iv. p. 382 (1929).

1.25\*, 1.73†, and 1.43‡ Å.U. The radius of gyration of the ammonia molecule found by Robertson and Fox § from its infra-red absorption spectrum is 0.82 Å.U.

Liquid.	Temp. °C.	D.	$\mu$ , $\times 10^{18}$	$\lambda_i$	$\Delta\lambda_i$	$\bar{a}$ , Å.U.
Water .....	25	78	1.8	41330	—	1.16
Sulphur dioxide .....	20	14	1.75	20090	—	1.42
Ammonia .....	-33	22	1.49	21290	—	1.26
Ethane .....	0	—	—	7150	—	—
Methyl iodide .....	42	6.48	1.66	24690	21115	1.30
Methyl alcohol.....	20	31.2	1.64	35020	31445	1.19
Acetaldehyde .....	21	14.8	2.72	22660	19085	1.94
Acetone.....	56	17.68	2.76	27470	20320	1.93
Acetonitrile .....	80	26.2	3.11	26870	23295	2.00
Nitromethane .....	100	27.75	3.42	31380	27805	2.01
Ethyl bromide .....	38	8.81	1.97	24775	18815	1.55
Ethyl alcohol .....	78	17.30	1.33	36440	30480	1.22
Ethyl ether .....	35	4.11	1.22	23420	11500	1.26
Ethylamine .....	15	6.2	1.33	25110	19150	1.16
<i>n</i> -Propane .....	20	—	—	12920	—	—
<i>n</i> -Propyl alcohol .....	97	11.83	1.65	38210	26910	1.23
<i>n</i> -Butane .....	20	—	—	18795	—	—
<i>n</i> -Butyl alcohol .....	117	8.19	1.65	40510	23600	1.27
Iso-pentane .....	13	—	—	24332	—	—
Iso-amyl alcohol .....	130	5.82	1.80	40750	18450	1.43
Benzene .....	80	—	—	27880	—	—
Chlorobenzene .....	131	4.20	1.59	33230	10030	1.57
Nitrobenzene .....	210	15.61	3.85	36740	13540	2.75
Aniline .....	183	4.54	1.51	36560	13360	1.39
Toluene .....	110	2.17	0.44	30120	3345	0.86
Pyridine .....	114	9.38	2.11	32250	9050	2.07

For substances in which the dipole is at one end of a large molecule the values of  $a$  are too small. The reason is that in such cases the medium approaches closely to one of the poles,

\* Smith, Proc. Roy. Soc. A, cvi. p. 83 (1924).

† Smith, Phil. Mag. xlv. p. 508 (1922).

‡ Rankine and Smith, Phil. Mag. xlii. p. 601 (1921).

§ Robertson and Fox, Proc. Roy. Soc. A, cxx. p. 206 (1928).

where the field is strong, and hence the filling of space at a fairly great distance from the other pole, where the field is much weaker, has comparatively little effect. Thus in the homologous series of alcohols  $\alpha$  does not increase as rapidly as might be expected. However, the increment is larger than usual in passing from *n*-butyl to iso-amyl alcohol, where the paraffin chain is branched and the molecule less unsymmetrical about the dipole than it would be in *n*-amyl alcohol. For benzene derivatives  $\alpha$  probably corresponds rather to the volume of the substituent than to that of the whole molecule, and might therefore be a measure of the steric hindrance effects exerted by the substituent. The order  $\text{NO}_2 > \text{Cl} > \text{CH}_3$  is the same as that given by the work of Victor Meyer and his followers\* on steric hindrance effects in the catalytic esterification of carboxylic acids.

Since the expression

$$\frac{\mu^2}{3a^3} \left( \frac{1}{D_1} - \frac{1}{D_2} \right)$$

does not consider the thermal energy and is for a hypothetical absolute zero, it gives the change in both free energy and the heat content in transferring the dipole from a medium of dielectric constant  $D_1$  to one of dielectric constant  $D_2$ . It might therefore be possible to calculate partition coefficients in the same way in which Bjerrum and Larsson † used Born's expression,

$$\frac{z^2 e^2}{2r} \left( \frac{1}{D_1} - \frac{1}{D_2} \right),$$

to calculate ionic partition coefficients. However, the calculation leads in many cases to absurd results, and even to negative radii. The disturbing factor is probably dipole association. Dipole association, which is a form of electrical saturation, does not affect the calculation of the latent heat of vaporization, because a dipole which is about to be vaporized is already a simple molecule, and in its interaction with the rest of the liquid the polarization is at least approximately proportional to the field-strength.

34 Sandy Lane,  
Teddington, Middlesex.  
9th November, 1929.

\* Werner (A.), 'Lehrbuch d. Stereochemie,' p. 385 *et seq.* (1904).

† Bjerrum and Larsson, *Z. physikal. Chem.* cxxvii. p. 358 (1927).



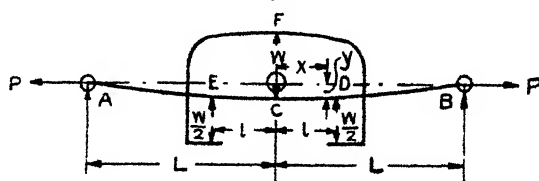
**XL. Problems of determining Initial and Maximum Stresses in Ties and Struts under Elastic or Rigid End Constraints.—**  
**Part II. By W. H. BROOKS, B.Sc., Ph.D.(Eng.) Lond.\***

**I**N the foregoing cases † the results are largely dependent upon the degrees of flexing constraints imposed by the terminal conditions. Equations obtained by the following methods will be seen to be less dependent upon terminal conditions, and practically independent of them when  $nL > \text{about } 3$ .

**Method 2 A :—**

In this method, instead of applying a central load  $W$  independently, a flexing bridge EFD is applied centrally to the pin-jointed tie, as shown in fig. 8, by means of which

Fig. 8.



$W$  is applied at  $C$  by hydraulic or mechanical means, and the resulting change in total deflexion at  $C$  or, alternatively, the slope at  $D$  is measured.

Taking an origin as shown, and remembering that  $y$  is of negative sign, in accordance with the mathematical convention of signs adopted, and that  $M_x$  is discontinuous at  $D$ , equations for the deflexion  $\delta$  at  $C$  and the slope  $\theta$  at  $D$  are established thus :—

Between  $C$  and  $D$ .

$$M_x = W(l-x)/2 + P \cdot y = EI d^2 y / dx^2. \quad (20)$$

$$\therefore d^2 y / dx^2 - n^2 y = Wl/2EI - Wx/2EI \quad (21)$$

where  $n^2 = P/EI$ .

The general solution to equation (21) is

$$y = A \cosh nx + B \sinh nx + Wx/2P - Wl/2P, \quad (22)$$

where  $A$  and  $B$  are constants.

\* Communicated by the Author.

† See Part I., Phil. Mag. (7) viii. p. 943 (1929).

Between D and B.

$$M_x = P \cdot y - EI d^2y/dx^2; \quad . \quad . \quad . \quad (23)$$

$$\therefore d^2y/dx^2 - n^2y = 0. \quad . \quad . \quad . \quad (24)$$

The general solution to equation (24) is

$$y = C \cosh nx + D \sinh nx, \quad . \quad . \quad . \quad (25)$$

where C and D are other constants to be found.

Now it follows from equations (22) and (25) that

$$y = Wx/2P - WL/2P + (W/2Pn) \cdot \cosh nx \cdot K \\ - (W/2Pn) \cdot \sinh nx, \quad (26)$$

where  $K = \sinh nl - \cosh nl \cdot \tanh nL + \tanh nL$ .

Equation (26) gives the deflexion from the axis of P at all points between C and D. When  $x = 0$ , i. e., at C,

$$y_0 = -WL/2P + (W/2Pn) \cdot K. \quad . \quad . \quad . \quad (27)$$

i. e.,

$$\delta \text{ or } -y_0 = WL/2P - W \cdot K/2Pn = W(l - K/n)/2P. \quad (28)$$

Thus

$$\delta/W = [l - \{\sinh nl - \tanh nL(\cosh nl - 1)\}/2n^2EI, \quad (29) \\ = (\text{Tie equation } G_0)$$

When  $nL > \text{about } 3$ ,

$$\delta/W \doteq \{l - (\sinh nl - \cosh nl + 1)/n\}/2n^2EI, \quad . \quad (30)$$

$$\text{i. e.,} \quad 2n^2EI\alpha \doteq \{l - \frac{1}{n_a} (\sinh n_a l - \cosh n_a l + 1)\}, \quad . \quad (31)$$

where "a" = the initial value of  $\delta/W = 0/0$ , as described in the General Procedure.

Graphical solutions to equation (29) are given by typical "G" curves in Chart III. for an instrument constant  $l = 10$  units. For values of  $L > 20$  units the dotted curve plotted from equation (31) obtains. To use this Chart, the curves plotted from generating equation G (equation (29)) are used. Having first determined the initial  $W \cdot \delta$  derivative =  $\alpha$ , the value of  $EI \cdot \alpha$  is next located up the ordinate along which polar values of  $EI \cdot \alpha$  are plotted, and a polar ray drawn to the origin. The intersection of this ray with the appropriate "G" curve of  $L$  ( $L$  is the half-length of the pin-jointed tie) locates a point vertically above the solution to  $n^2$  on the abscissa.

Thus  $P \text{ sought} = n^2EI$ .

*Method 2 A. Alternatively :—*

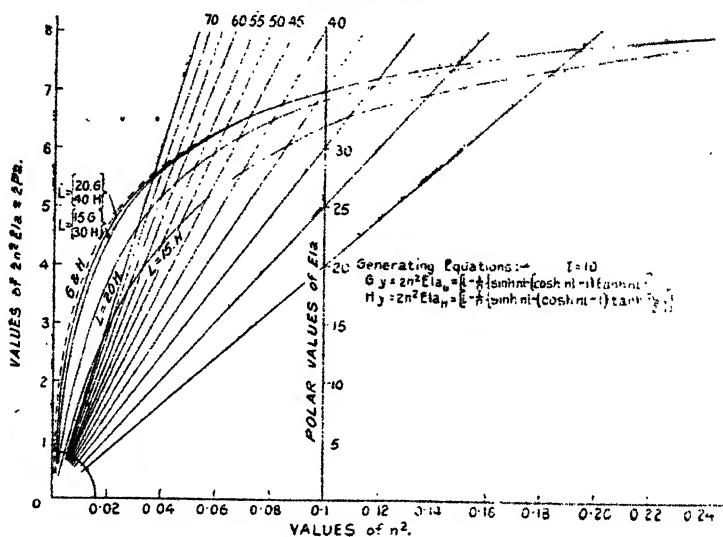
It follows from the foregoing equations that the slope  $\theta$  at D

$$= W(\cosh nl - 1)(\cosh nl - \sinh nl \cdot \tanh nl) / 2P, \quad (32)$$

and  $= (1 - \operatorname{sech} nL) / 2P$  when  $l = L$ , as in Method 1. Initially, therefore, this Method gives

$$\begin{aligned} "a" &= (\cosh n_a l - 1)(\cosh n_a l - \sinh n_a l \cdot \tanh n_a L_a) / 2n_a^2 EI. \\ &= (\text{Tie equation } G_0) \end{aligned} \quad (33)$$

CHART III.



Stress Chart for Ties G and H by deflexion.

Here " $a$ " = the  $W. \theta$  derivative, and when  $n_a L_a > \text{about } 4$ ,

$$"a" = (\cosh n_a l - 1)(\cosh n_a l - \sinh n_a l) / 2n_a^2 EI, \quad (34)$$

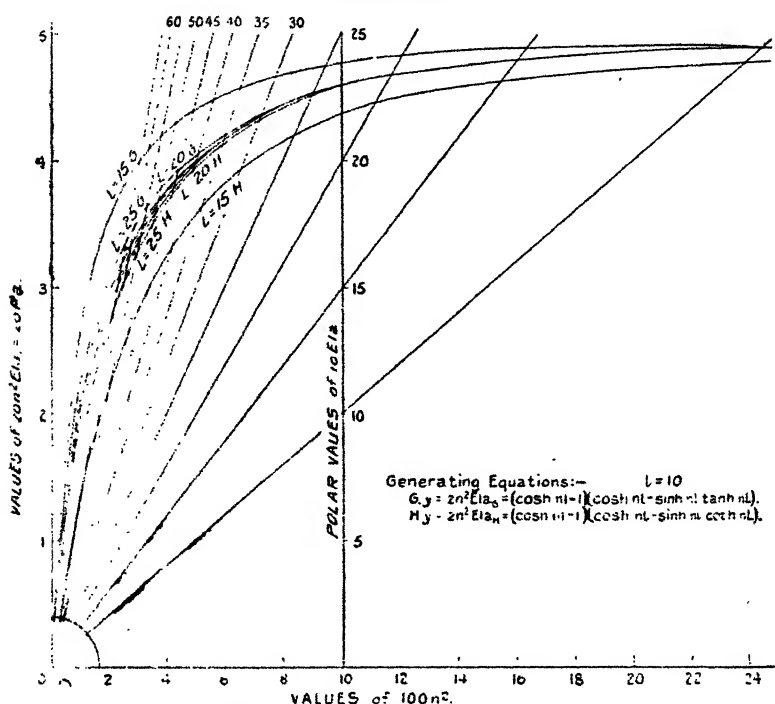
which may be used as a first approximation in the absence of a Stress Chart.

Graphical solutions to equation (33) may be obtained from the typical " $G$ " curves for low values of  $L$  and instrument constant = 10 units on Chart IV. For values of  $L > \text{about } 25$  units the dotted curve obtains, and yields solutions to equation (34).

To obtain a solution from Chart IV., the polar value of  $10EIa$  is first interpolated up the ordinate lined in where

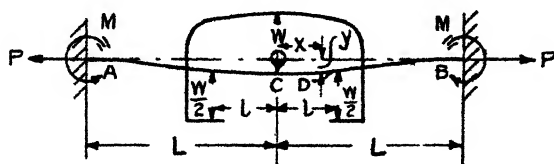
$100n^2 = 10$ , or interpolated up an intermediate ordinate for values of  $10EIa > 25$  and a polar ray drawn. The vertical projection of the point of intersection of this ray with the correct "L" curve yields solutions to  $100n^2$ , and hence to the value of  $P = n^2EI$ .

CHART IV.



Stress Chart for Ties G and H by slope.

Fig. 9.



Method 2 B:—

This method is similar to Method 2 A, but is applicable to a tie having fixed ends, i.e., the conditions are as in Method 2 A, but the ends of the tie are constrained in the line of action of  $P$  by reaction couples  $M$  at  $A$  and  $B$ , as shown in fig. 9.

Between C and D.

$$M_x = W(l-x)/2 + P \cdot y - M = EI d^2 y / dx^2, \quad (35)$$

or 
$$d^2 y / dx^2 - n^2 y = Wl/2EI - Wx/2EI - M/EI. \quad (36)$$

The general solution to equation (36), giving the deflexion at all points between C and D, is

$$y = A \cosh nx + B \sinh nx + Wx/2P - Wl/2P + M/P. \quad (37)$$

Between D and B.

$$M_x = P \cdot y - M = EI d^2 y / dx^2, \quad (38)$$

i. e., 
$$d^2 y / dx^2 - n^2 y = -M/EI, \quad (39)$$

of which the general solution, giving the deflexion at all points between D and B, is

$$y = C \cosh nx + D \sinh nx + M/P. \quad (40)$$

From the foregoing equations it follows that the conditions are satisfied when

$$M = W(\cosh nl - 1)/2n \cdot \sinh nL.$$

Also when  $x = 0$  at C, the deflexion numerically =  $\delta$ , say

$$= W[l - \{\sinh nl - \tanh nL/2 \cdot (\cosh nl - 1)\}/n]/2P. \quad (41)$$

=(Tie equation  $H_5$ )

In this case

$$\delta/W = "a" \quad \text{when} \quad n = n_a.$$

The result given in equation (41) may be checked by making the substitution  $l = L$  of Method 1 B. Thus, making this substitution, and simplifying,

$$\delta W = (L - 2/n \cdot \tanh nL/2)/2P, \text{ as in Method 1 B.}$$

Comparing equation (41) with the corresponding equation (29) of Method 2 A, it is seen that the only difference lies in the occurrence of  $\tanh nL/2$  in the former in place of  $\tanh nL$  in the latter, so that when  $nL/2 > \text{about } 4$ —a quite probable value for a long slight tie under a moderate stress—the equations become practically identical and initially equal to equation (31) given in Method 2 A. This is clearly shown in Chart III., in which the typical H curves plotted yield solutions to equation (41) for an instrument span = 20 units.

The procedure to be followed in using Chart III. here is similar to that described under Method 2 A, but using curves such as those marked H instead of using curves marked G.

The merging of the G and H curves on Chart III. into the one common dotted curve plotted from equation (31), which is independent of  $L$ , the half-length of the tie, clearly shows the negligible effect of the end constraints on the value of " $a$ ," except for low values of  $nL$ . This being so, the further deduction follows, and is fully analytically investigated in the complete Thesis, that for the higher values of  $nL$  which usually obtain in practice, it is immaterial whether the flexing bridge used in testing is applied centrally or non-centrally to the tie, or whether the tie be jointed or unjointed at any point of its length.

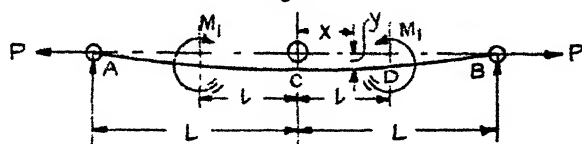
*Method 2 B. Alternatively by measurement of the slope  $\theta$  at D :—*

From the foregoing equations it follows that

$$\theta = W(\cosh nl - 1)(\cosh nl - \sinh nl \cdot \coth nL)/2P. \quad (42)$$

Typical graphical solutions to this equation are given by the H curves of Chart IV., the use of which is described under Method 2 A. Alternatively.

Fig. 10.



Comparing equations (42) and (32), it is seen that they will become identical when  $\coth nL = \tanh nL$ , and this is practically so when  $nL > \text{about } 3$ . An inspection of Chart IV. also clearly shows that for  $l = 10$  units, coincidence practically obtains when  $L > 25$  units. Thus variations in end conditions or in the length of a member above a minimum length of about 25 units do not greatly affect the difference of deflexion at C or of the slope at D, as given by the use of a flexing bridge, the slope being the least affected in all cases, but practically unaffected by terminal conditions when

$$L(P/EI)^{\frac{1}{2}} > 4, \quad \text{i.e., when } L/K \cdot (f_d/E)^{\frac{1}{2}} > 4.$$

*Tie. Method 3 A :—*

In this method a tie AB of length  $2L$ , having assumed frictionless pin-joints at A and B, is flexed by the application of equal and opposite couples  $M_1$  and  $M_1$ , applied by mechanical or hydraulic means, with axis distance  $= 2l$  apart, as shown in fig. 10.

Between C and D.

$$M_x = M_1 + P \cdot y = EI \cdot d^2y/dx^2 ;$$

$$\therefore d^2y/dx^2 - n^2y = M_1/EI. \quad . \quad . \quad . \quad (43)$$

The general solution to equation (43) is

$$y = A \cosh nx + B \sinh nx - M_1/P, \quad . \quad . \quad (44)$$

where A and B are constants to be found, and giving the deflexion at all points between C and D.

Between D and B.

$$M_x = P \cdot y = EI d^2y/dx^2 ;$$

$$\therefore d^2y/dx^2 - n^2y = 0,$$

$$\text{and} \quad y = C \cosh nx + D \sinh nx,$$

where C and D are other constants to be determined.

Now it follows from the above equations that the constant A in equation (44) =  $M_1(\cosh nl - \sinh nl \tanh nL)/P$  and the constant B = 0, in conformity with terminal conditions. Substituting these constant values in equation (44) yields, when  $x = 0$ ,

$$y_0 = M_1(\cosh nl - \sinh nl \tanh nL - 1)/P, \quad . \quad . \quad (46)$$

i. e., the numerical value of the deflexion at C

$$= \delta, \quad \text{say} \quad -y_0 = M_1(1 - \cosh nl + \sinh nl \tanh nL)/P, \quad . \quad . \quad . \quad (47)$$

$$\text{or} \quad \delta/M_1 = (1 - \cosh nl + \sinh nl \tanh nL)/P, \quad . \quad (48)$$

$$\text{and} \quad \delta \doteq (1 - \cosh nl + \sinh nl)/P,$$

for values of  $nL > \text{about } 4$ .

When  $l = L$ ,

$$\delta/M_1 = (1 - \operatorname{sech} nL)/P. \quad . \quad . \quad . \quad (49)$$

Initially, when both  $\delta$  and  $M_1 = 0$ , equation (48) becomes

$$n_a^2 EI a = 1 - \cosh n_a l + \sinh n_a l \tanh n_a L_a, \quad . \quad (50)$$

(The equation 1δ)

$$\text{which} \quad \delta \doteq 1 - \cosh n_a l + \sinh n_a l, \quad . \quad . \quad . \quad (51)$$

and equation (49) becomes

$$n_a^2 EI a = 1 - \operatorname{sech} n_a L_a, \quad . \quad . \quad . \quad (52)$$

where " $a$ " here = the  $M_1\delta$  derivative, and is determined as described in the General Procedure, substituting  $\delta$  for  $Y$  and  $M_1$  for  $X$ .

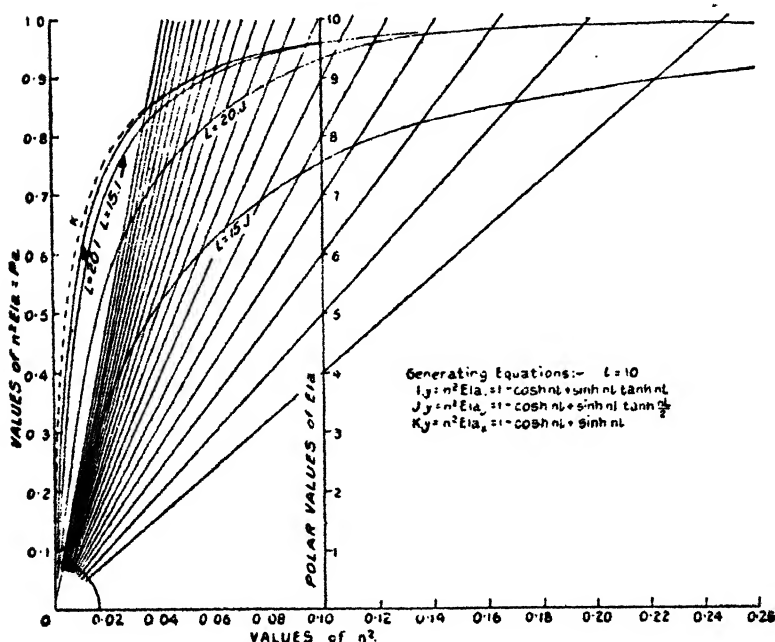
When  $nL > \text{about } 6$ , equation (49) becomes

$$"a" \doteq 1/P_a, \quad \dots \dots \dots (53)$$

since  $\text{sech } nL$  then becomes a very small fraction,

i. e.,  $P_a = 1/a = \text{reciprocal of initial } d\delta/dM_1$ .

(CHART V.



Stress Chart for Ties I, J, and K by deflexion.

In the general case of  $l < L$ , equation (51) could be used as a first approximation in solving for  $n_a$ , and equation (50) applied when  $n_a L_a$  is found to be  $< \text{about } 4$ .

The right-hand sides of the expressions (50) and (51) are the generating equations used in plotting the full-line curves I and the dotted curve K respectively, of Chart V. (*q.v.*), from which  $n_a^2$  may be found by interpolation for an instrument constant  $l = 10$  units. This Chart also clearly shows the degree of approximation introduced by using equation (51) instead of equation (50).



To obtain a solution from this Chart, the product  $EIa$  is first determined, and the corresponding polar ray drawn (by the aid of the scale and rays shown) through the origin. The intersection of this ray with the appropriate I or K curve is then interpolated and projected on to the abscissa which gives the value of  $n_a^2$ , and hence the solution to  $P_a = n_a^2 EI$  sought. (Herein the suffix "a" is suppressed for simplicity.)

*Tie. Method 3A. Alternatively by measurement of the slope  $\theta$  at D:—*

From the foregoing equations it follows that

$$\theta/M_1 = n \sinh nl (\cosh nl - \sinh nl \tanh nL)/P, \quad (54)$$

(Tie equation I<sub>9</sub>)

and for values of  $nL > \text{about } 4$  may be written

$$\theta/M_1 = n \sinh nl (\cosh nl - \sinh nl)/P;$$

$$\text{i. e.,} \quad \theta/M_1 = \sinh nl (\cosh nl - \sinh nl)/n \cdot EI, \quad (55)$$

which, in the absence of a Stress Chart, may be used for a first approximation to indicate the probable value of  $n$  and hence of  $nL$ . If  $nL$  is seen to be  $> \text{about } 4$ , no further approximation will be necessary, since  $\tanh nL$  is then very nearly equal to unity and equation (55) practically = equation (54). When  $nL < \text{about } 4$ , the exact expression (54) should be used.

In any case, the initial value of "a," which is here the  $M_1\theta$  derivative, may be found by substituting  $M_1$  for  $X$  and  $\theta$  for  $Y$ , as shown in the General Procedure.

When "a" is known, equation (54) may be written

$$an_a \cdot EI = \sinh n_al (\cosh n_al - \sinh n_al \tanh n_aL_a), \quad (56)$$

and equation (55) may be written

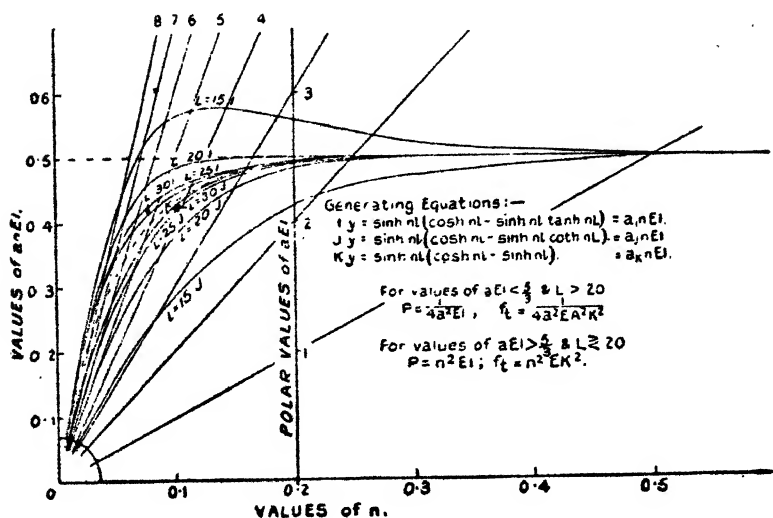
$$an_a \cdot EI = \sinh n_al (\cosh n_al - \sinh n_al). \quad (57)$$

The right-hand side of expression (56) is the expression used in plotting the I curves of Chart VI., in which also the dotted curve K is obtained by plotting the right-hand side of expression (57). This Chart shows clearly how the former expression approximates to the latter as  $L$  increases.

Having measured "a" by the above method, and computed the value of  $a \cdot EI$ , a solution to  $P_a$  is obtained from Chart VI., by locating the point of intersection of the corresponding polar ray with the appropriate I or K curve. Projecting

from the point so found on to the abscissa determines  $n_a$ , and hence  $P_a = n_a^2 \cdot EI$ .

CHART VI.



Stress Chart for Ties I, J, and K by slope.

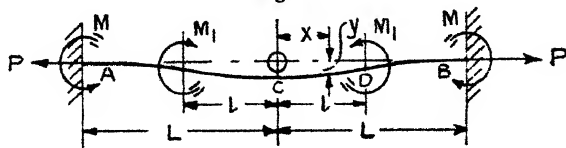
$l = 10$  units.

Distance between couples = 20 units.

*Tie. Method 3 B :-*

Here a tie AB of length  $2L$ , having its ends constrained in the direction of AB by fixing couples  $M$  and  $M$ , as shown in fig. 11, is flexed as in Method 3 A.

Fig. 11.



Between C and D.

$$M_x = M_1 + P \cdot y - M = EI \cdot d^2 y / dx^2;$$

$$\therefore d^2 y / dx^2 - P \cdot y / EI = (M_1 - M) / EI = d^2 y / dx^2 - n^2 y. \quad (58)$$

The general solution to equation (58) is

$$y = A \cosh nx + B \sinh nx - (M_1 - M) / P, \quad (59)$$

where A and B are constants to be determined.

$$M_x = P.y - M = EI.d^2y/dx^2;$$

$$\therefore d^2y/dx^2 - n^2y = -M/EI. \quad \dots (60)$$

The solution to equation (60) is

$$y = C \cosh nx + D \sinh nx + M/P, \quad \dots (61)$$

where C and D are constants to be determined.

On evaluating the constants in the above equations, substituting and reducing, it is seen that

$$M = M_1 \sinh nl / \sinh nL.$$

It also follows that

$$y = M_1 \sinh nl (\sinh nL \coth nl - \cosh nL) \cosh nx / P \sinh nL \\ - M_1 (1 - \sinh nl / \sinh nL) / P,$$

and when  $x = 0$ , the numerical value of the deflexion  $y_0$  at  $C = \delta$ , say  $= M_1 (1 - \cosh nl + \sinh nl \tanh (nL/2)) / P$ , (62)

or the deflexion per unit couple

$$= \delta / M_1 = \left( 1 - \cosh nl + \sinh nl \cdot \tanh \frac{nL}{2} \right) / P \quad (63)$$

(Tie equation  $J_\delta$ )

= the  $M_1 \delta$  derivative when  $P = P_a$ . (See General Procedure.)

When  $nL > \text{about } 8$ , equation (63) becomes

$$"a" = (1 - \cosh nal + \sinh nal) / n_a^2 EI, \quad \dots (64)$$

which is the same as equation (51) in Method 3 A.

Graphical solutions to equation (63) may be rapidly obtained by interpolation from curves such as those lettered J in Chart V., which curves approximate to the dotted curve K for higher values of L, as was also seen in Method 3 A.

*Tie. Method 3 B. Alternatively by measurement of the slope  $\theta$  at D :—*

It follows from the foregoing equations that

$$\theta / M_1 = \sinh nl (\cosh nl - \sinh nl \cdot \coth nL) / n \cdot EI, \quad (65)$$

or initially, when  $P = P_a$ ,

$$"a" = \sinh n_a l (\cosh n_a l - \sinh n_a l \cdot \coth n_a L_a) / n_a \cdot EI, \quad (66)$$

(Tie equation  $J_\theta$ )

and when  $n_a L_a > \text{about } 4$ ,  $\coth n_a L_a$  practically = unity, and equation (66) may then be written

$$a \cdot n_a \cdot EI = \sinh n_a l (\cosh n_a l - \sinh n_a l), \quad (67)$$

which is the same expression as obtains for the same tie with assumed frictionless hinges, as may be seen by comparing this equation with equation (57) of Method 3 A.

Graphical solutions to equations (66) and (67) may be readily obtained by the aid of Chart VI., which also clearly indicates the approximation of the former expression to the latter expression as  $L_a$  or  $n_a L_a$  increases.

While it is experimentally possible in practice to secure the frictionless hinged results (see paragraph under Method 1 A), it is very improbable that constraints, however rigid they may appear, will provide the exact conditions assumed in the foregoing case, and, in general, it should be assumed that the actual cases arising in practice will fall somewhere between these two ideal conditions. In other words, when a tie is pin-jointed at the ends through elastic constraints, friction couples will be set up at the ends directly flexing is attempted, of the same order as but smaller in magnitude than those set up by yielding clamps which allow the extremities of the tie to take up a slight unknown slope. This combination of conditions is discussed fully in the Thesis under "Case K," in which unknown couples,  $M$  and  $M$ , are assumed to constrain the ends of the tie at an unknown slope varying with  $M$ .

In the Thesis it is theoretically established that under these latter conditions the equation which obtains is

$$\theta/M_1 = \frac{n}{P} \cdot \sinh nl \{ (\cosh nl - \sinh nl \cdot \tanh nL) - M \cdot \operatorname{sech} nL/M_1 \}, \quad \dots \quad (68)$$

which agrees with equation (54) when  $M = 0$ .

Now when  $nL$  in equation (68)  $> \text{about } 4$ , which would generally be the case for a tie of fair length under a moderate stress,  $\tanh nL$  and  $\coth nL$  approach very nearly to unity. For example, in a tie rod 1 in. diameter and 20 feet long under an initial axial stress ( $f_t$ ) of only 5000 lb. per square inch, and  $E = 30 \times 10^6$  lb per in.<sup>2</sup>  $nL$ , i. e.,  $\frac{L}{K} \cdot \sqrt{f_t/E}$  (where

$K$  is the radius of gyration of the cross-section about a diameter at right angles to the plane of bending =  $d/4$ ),  $= 120/\frac{1}{4} \cdot (5000/30 \times 10^6)^{\frac{1}{2}} = 6.2$ , and  $\tanh nL = \coth nL = 1$ .

(Here and in the following, the suffix "a" is suppressed for clarity.) For a tie of the same dimensions as the above, under half the above stress,

$$nL = 480/100 \cdot (2.5/3)^{\frac{1}{2}} = 4.380,$$

$$\tanh nL = 0.99969, \text{ and } \coth nL = 1.0003.$$

Hence, in expression (68),  $\tanh nL$  may be taken = 1.

Again, for the 1-in. diameter tie-rod taken above, when  $f_t = 5000$  lb. per sq. in.,  $\text{sech } nL = 1/201.7156$ , and when  $f_t = 2500$  lb. per sq. in.,  $\text{sech } nL = 1/39.9253$ . Consider, therefore, the term  $M \cdot \text{sech } nL / M_1$  in equation (68).  $M$  will have its greatest value when the ends of the tie are rigidly clamped, and then  $= M_1 \cdot \sinh nl / \sinh nL$ , which, substituted in the term under consideration, reduces it to  $\sinh nl \cdot \text{sech } nL / \sinh nL$ , which when  $f_t = 5000$  lb. per sq. in.  $= \sinh nl / 201.7156 \times 201.713$ , a negligible fraction of  $\sinh nl$ .

When  $f_t = 2500$  lb. per sq. in. only, the term reduces to  $\sinh nl / 39.9253 \times 39.9128$ , again a negligible fraction of  $\sinh nl$ .

Hence a very near approximation to equation (68) is

$$\theta / M_1 = n \sinh nl (\cosh nl - \sinh nl) / P,$$

or initially, when  $P = P_a$ , for  $\theta = 0$  and  $M_1 = 0$ ,

$$"a" = \sinh nl (\cosh nl - \sinh nl) / n \cdot EI, \dots (69)$$

where "a" is the  $M_1 \theta$  derivative. (See General Procedure.)

Graphical solutions to this general expression may be quickly obtained by using the dotted curve K in Chart VI.

It therefore appears that the slope of the tie at the axis of the couple  $M_1$  applied at D is practically independent of the manner in which the tie has its ends constrained, and the expression (69) is general for values of  $nL$  greater than about 4. Experimental verification of this deduction is given fully in the Thesis.

When  $nL < \text{about } 4$ , it is instructive to investigate what percentage error will be introduced by using the approximate expression (69) instead of the exact expression (68), or by using the equivalent expression (66), to which expression (68) reduces when the greatest value of  $M = M_1 \cdot \sinh nl / \sinh nL$  is substituted therein. Taking this latter approximation, the difference consists in using  $(\cosh nl - \sinh nl)$  instead of the exact quantity

$$(\cosh nl - \sinh nl \cdot \coth nL).$$

Considering again, therefore, the tie-rod in which  $L = 120$  in.,  $l = 20$  in., diameter = 1 in.,  $E = 30 \times 10^6$  lb. per sq. inch, and assuming that the direct tensile stress has been lowered to only 500 lb. per sq. inch from various causes unforeseen when designing the member,

$$nL = L/K \cdot (f/E)^{\frac{1}{2}} = 120/\frac{1}{4} \cdot (500/30 \times 10^6)^{\frac{1}{2}} = 1.96,$$

$$nl = l/K \cdot (f/E)^{\frac{1}{2}} = 0.3264,$$

$$\sinh nl = 0.33181; \cosh nl = 1.05361; \text{ and } \coth nL = 1.04050$$

$$\therefore \cosh nl - \sinh nl = 0.72180,$$

and

$$\cosh nl - \sinh nl \cdot \coth nL = 1.05361 - 0.34500 = 0.70861.$$

The error, therefore, is 0.01319 in 0.70861, or only 1.862 per cent. for this very low stress, and will clearly become less as  $\coth nL$  approaches unity with increase of stress in the same member.

Hence the expression

$$“a” = \sinh nl \cdot (\cosh nl - \sinh nl) / n \cdot EI$$

may be applied to all but perhaps very short and stout tie-rods flexed as discussed in Methods 3 A and 3 B, when the ends are constrained in any manner and the length is unknown. Thus, having found “a” experimentally, the above equation may be solved for  $n$  by the aid of Chart VI. Then initially,  $P$  (really  $P_a$ ) =  $n^2 \cdot EI$ , and the direct stress in the tie when the readings were taken to determine “a”

$$= f_a = n^2 EK^2,$$

where  $K$  is the radius of gyration of the uniform cross-section of the tie about an axis at right angles to the plane of flexing.

When discussing Methods 2 A and 2 B applicable to ties, further theoretical investigations were made in the Thesis to ascertain whether the equations which were obtained in the centrally loaded cases held for non-central loading also. The conclusions were there found to be affirmative. Similar further investigations into Methods 3 A and 3 B were also made, and the conclusions obtained were likewise found to be affirmative, and were experimentally verified.

(To be continued.)

**XLI. Thermionic Emission and Electrical Conductivity of Oxide Cathodes.** By A. L. REIMANN and R. MURGOOI\*.

(Communication from the Staff of the Research Laboratories of the General Electric Co., Ltd., Wembley.)

**ABSTRACT.**

THE following observations were made :—

(1) The electrical conductivity,  $c$ , of a "formed" alkaline earth oxide varies with the temperature,  $T$ , according to a law of the form

$$c = \alpha e^{-\frac{\beta}{T}},$$

where  $\alpha$  and  $\beta$  are constants.

(2) During the process of forming, both the thermionic emission and the conductivity grow similarly, and after its completion both are "poisoned" similarly by exposure of the oxide to

- (a) oxygen,
- (b) a discharge in carbon monoxide, and
- (c) a discharge in hydrogen.

Complete recovery of the formed condition by re-forming is possible only a few times in succession after poisonings by (a) and (b), but any number of times after poisoning by (c).

(3) At current densities comparable with those in the coatings of oxide cathodes from which saturated thermionic space current is being taken, the current conducted through an oxide powder between two electrodes, embedded therein, also saturates.

On the basis of these observations, together with the results of related work by other investigators, we have formulated the following theory of the action of oxide cathodes :—

(1) The coating conducts the space current, which, of necessity, passes through it, electrolytically. Practically only the metallic ions are mobile, the oxygen ions playing no active part in the electrolysis.

Communicated by C. C. Paterson, Director.

(2) The whole surface of each crystal of oxide of a formed cathode is covered with a mobile monatomic layer of alkaline earth metal. The passage of space current is accompanied by a continual circulation of this metal, which diffuses outward along the surfaces of the crystals and inward through the crystals in the form of electrolytic ions.

(3) At the usual operating temperatures of oxide cathodes the average life of alkaline earth metal particles on the emitting surface is of the order of  $10^{-3}$  second, and the rate of flow of this metal over the surface of an idealized independent unit of barium circulation in the form of a cube of side  $l$  would be of the order of  $300 l$  per second.

(4) The coating is probably in very imperfect contact with the core metal, so that the space current passes from core metal to coating mainly in the form of thermionically emitted electrons. Sufficiently copious electron emission of the core metal at the low temperatures of operation of these cathodes would be made possible by a contamination of its surface with adsorbed barium or with barium and oxygen.

Explanations are suggested for

- (1) the eventual "life-failure" of oxide cathodes,
- (2) the observed phenomena relating to poisoning,
- (3) the considerable variation in the published values of the thermionic constants of oxide cathodes.

---

## INTRODUCTION.

IT is well known that before an alkaline earth oxide cathode will give its characteristically high thermionic emission it has to be "activated" or "formed." The forming process may consist in merely heating the cathode to bright redness in a good vacuum<sup>(1,2)</sup> but activation is much more rapid and a higher final emission is generally obtained if, whilst the cathode is being heated, electrons are drawn from it<sup>(3,4)</sup>. In the latter case, the growth of emission is accompanied by a considerable evolution of gas<sup>(3,4)</sup>, which has been shown to be oxygen<sup>(5)</sup>. The electron emission is increased some thousandfold by the forming operation, but it is at once destroyed, or "poisoned," if the cathode is exposed to certain electro-



negative gases, such as oxygen <sup>(1, 3, 4, 6)</sup>. Considerable de-activation also results from prolonged heating of the cathode at a high temperature, which is, however, insufficient to bring about appreciable loss of coating by evaporation <sup>(1, 2, 3, 4)</sup>.

The study of these phenomena has led to the formulation of the theory that the high electron emissivity of a formed cathode is due to the presence of free alkaline earth metal at the emitting surface. If the cathode is activated by the first method the free metal is supposed to be formed from the oxide by thermal dissociation, if by the second mainly by the electrolytic action of the space current on the oxide through which it passes <sup>(1, 2, 3, 4)</sup>. To overcome the difficulty arising from the fact that at the usual operating temperatures of these cathodes ( $\sim 1000^\circ \text{K.}$ ) the vapour pressures of the alkaline earth metals are of the order of some centimetres of mercury, Schottky and Rothe <sup>(7)</sup> have suggested that the metal forms an adsorbed film at the surface of the oxide only a single atom in thickness, and so has a vapour pressure of a much lower order than that characteristic of the metal in bulk, as in the case of an adsorbed monatomic film of thorium <sup>(8)</sup> or of caesium <sup>(9, 10, 11, 12)</sup> on tungsten.

Now the theory that the passage of the space current through the coating electrolyses it, although apparently demanded by the experimental facts <sup>(3, 4, 5)</sup>, involves certain difficulties. It may readily be calculated what quantity of electricity, passing electrolytically through a coating of known weight, will completely break it up into its chemical constituents. On the assumption that the products of electrolysis escape from the cathode as they are liberated from the coating, we may thus determine for how long any given space current may be passed before all the coating will have disappeared. It is found, however, that normally the "life" of an oxide cathode, *i. e.*, the time during which it retains its high electron emissivity, is of the order of  $10^5$  or  $10^6$  times as long as it could possibly be if the above assumptions (electrolytic conduction, escape without recombination of electrolysed material) were correct, and that at the end of life there is no important diminution in the quantity of coating present. Also it is not clear why, if the evolution of gas which accompanies forming is due to electrolysis, it does not continue to be evolved after activation is complete.

In the hope of finding a solution of these difficulties we have carried out an investigation of the electrical conductivity of the coatings of oxide cathodes. There have been two previous investigations of the conductivity of alkaline earth oxides, by Horton <sup>(13)</sup> and by Spanner <sup>(14)</sup>, both of whom found that the conductivity,  $c$ , varies with temperature according to an exponential law of the form

$$c = \alpha e^{-\frac{\beta}{T}} \dots \dots \dots (1)$$

Their measurements were not, however, made under electron-emitting conditions, but with the oxides exposed to air. They could not therefore hope to discover any changes in conductivity accompanying thermionic activation, the observation of which might throw some light on the cessation of the evolution of gas upon the completion of activation and on the problem of the long life of oxide cathodes.

#### EXPERIMENTAL ARRANGEMENTS.

All our measurements were made with diode valves, whose cathodes consisted of two filaments, each of length 1.5 cm. and diameter 0.04 mm., which, after having been provided with a coating of oxide, made adherent by sintering at a red heat, had 0.5 cm. of their central portions twisted together. Another coating of oxide was then applied to the twisted portion of the cathode, in order to provide a substantial bridge of oxide between the wires. Finally the free ends were de-coated by being immersed in weak nitric acid. With this arrangement it was found that when the cathode was heated in vacuo by passing a current through the wires, the central coated portion had a very uniform temperature distribution.

The coating consisted of equal proportions by weight of barium and strontium oxides. The core-wires were usually of nickel, but in some cases they were of Pt-10 per cent. Rh alloy. The central, twisted portion of the cathode formed the axis of a cylindrical anode of nickel, of length 0.3 cm. and diameter 1.0 cm. One or more small "getter" disks of previously out-gassed nickel, carrying small pieces of magnesium, were also provided. The whole was mounted on a pinch and sealed into a small glass bulb provided with a length of glass tubing for attachment to the pump.

For heating the cathode and measuring the current conducted between the two filaments through the oxide a specially designed motor-driven commutator was utilized, capable of being run at either 50 or 100 revolutions per second. Connexion to the cathode-heating and conductivity-measuring circuits could be made in such a way that when the commutator was run these circuits were completed during alternate equal periods of time, separated from one another by short intervals to provide against accidental overlapping. The contacts, which were of tungsten, were of the "make and break" type, each controlled by an adjustable spring, and actuated by an eccentric cam (stroke  $1/50$  in.) and lever. During the cathode-heating phase the heating current was passed through the two filaments in series. This current was measured by a milliammeter, the conduction current by a microammeter with universal shunt, and the potential across the coating by a voltmeter. In calculating the conductivity from the readings of the two last-named instruments, the resistance of the microammeter and shunt was allowed for. The factor by which the readings of the instruments had to be multiplied to give the true intermittent values of the quantities they were designed to measure was readily calculated from the "make and break factor" of the commutator. It was found that when the cathode had the dimensions given the resistance of the hot nickel filament-wires involved in the conductivity-measuring circuit was negligible in comparison with that of the oxide.

The procedure up to the point of sealing off a valve from the pump was as follows:—

After having baked the valve on the pump at  $400^{\circ}\text{C}.$ , the cathode was heated to bright redness and the anode raised to a red heat by high-frequency induction. Finally, magnesium getter was dispersed from one of the disks, also by induction heating, whereupon the valve was sealed off.

## EXPERIMENTAL RESULTS.

### 1. *Forming.*

During the process of thermionic forming the conductivity of the oxide increases about a thousandfold. The conductivity may also be made to grow to its maximum

value by passing a current through the oxide between the two filaments instead of between both filaments together and the anode. It is then necessary, in order for complete "conductivity forming" to take place, that about the same quantity of electricity should be passed through the oxide, and this at about the same temperature as in the case of thermionic forming. "Conductivity forming" is accompanied by thermionic activation in the same way as thermionic forming is accompanied by growth in conductivity. This is, perhaps, not surprising, for so far as the oxide itself is concerned the only thing that physically differentiates the two kinds of forming from one another is the path taken by the forming current. The maximum values attained by the emission and the conductivity sometimes, however, differ slightly according to the direction in which the forming current is passed. The value of either quantity is then up to 20 per cent. greater when this direction is that in which the current passes in the measurement of the quantity in question than when it is not. Also, if one quantity has been formed to its maximum value by passing the current in the more favourable direction, its value may be decreased by anything up to about 20 per cent. upon thereafter passing the current in the less favourable direction. In these cases the formed condition is thus slightly directional.

## *2. Poisoning.*

Not only are conductivity and thermionic emission formed together, they are also poisoned together.

Our first experiments on poisoning were made with oxygen, obtained by heating a small grain of potassium permanganate contained in a glass tube attached to the valve. After the coating of the cathode had been formed a little oxygen was introduced into the valve, which was thereupon immediately re-gettered from another disk in order to make sure of the removal of any trace of oxygen not absorbed by the first deposit of getter. The short exposure of the cold cathode to oxygen was found to poison completely both the emission and the conductivity. A certain degree of recovery of both occurs on re-forming, i. e., heating the cathode to a suitable temperature whilst a current is passed through the oxide. This recovery is, however, not often complete, and invariably takes place

very slowly. The extent to which recovery is possible becomes progressively less after successive oxygen poisonings.

Oxide cathodes may also be poisoned by exposure to an electric discharge in carbon monoxide. A bulb containing a nickel spiral was attached to the valve. The nickel spiral, when heated by a current, gave off a mixture of carbon monoxide and hydrogen. The hydrogen could readily be diffused out through an attached palladium tube heated in the extreme oxidizing tip of a blowpipe-flame. By this means the whole system, consisting of valve, bulb containing nickel spiral, palladium tube, and Pirani gauge, could be filled several successive times with CO to a pressure of the order of 1/100 mm.

When a discharge is passed between cathode and anode the carbon monoxide is cleaned up on to the getter. In the course of this clean-up both the emission and the conductivity of the oxide become partially poisoned, being reduced to about one-tenth and one-quarter respectively of their initial values. Re-forming at first completely restores the initial values, but after CO has been cleaned up a few times in succession recovery by re-forming is no longer possible or occurs only to a very slight extent.

In other experiments hydrogen was admitted through a palladium tube and cleaned up on to the magnesium getter by passing a discharge. Poisoning was observed qualitatively similar to that brought about by a discharge in CO, but quantitatively it was much less, and after each poisoning it was found possible to recover completely by re-forming both the emission and the conductivity.

### 3. *Temperature-Dependence of Conductivity.*

No means were provided in the construction of these valves for accurate temperature measurement. Nevertheless from the known law of variation of thermionic emission with temperature, and the measured relationship between conductivity and thermionic emission at different (unknown but reproducible) temperatures, we have been able to confirm the result of Horton<sup>(13)</sup> and Spanner<sup>(14)</sup> that the conductivity varies with temperature according to an exponential law of the form

$$c = \alpha e^{-\frac{\beta}{T}} \dots \dots \dots (1)$$

Although, strictly speaking, the law of variation of emission with temperature is of the form

$$i = aT^2 e^{-\frac{b}{T}}, \quad \dots \dots \dots (2)$$

over a restricted range of temperatures a practically equally good empirical formula is

$$i = A e^{-\frac{B}{T}}, \quad \dots \dots \dots (3)$$

in which

$$A = aT_m^2, \quad B = b + 2T_m^*. \quad \dots \dots \dots (4)$$

where  $T_m$  represents the mean temperature of the range in question. The test for the validity of formula (3) is the rectilinearity of the curve connecting  $\log i$  with  $\frac{1}{T}$ .

In order for the departure from strict rectilinearity of this curve to be detected when the temperatures at which readings are taken extend over a range of only a few hundreds of degrees, it would be necessary for temperatures in the region in question (here of the order of 1000° K.) to be measurable with a possible error not exceeding a small fraction of a degree. For all practical purposes, then, we may take formula (3) as representing sufficiently accurately the dependence of emission on temperature.

Eliminating  $T$  between formulæ (1) and (3), we have

$$B(\log c - \log \alpha) = \beta(\log i - \log A). \quad \dots \dots (5)$$

Therefore, by plotting  $\log c$  against  $\log i$  we should, if formula (1) is a true representation of the temperature dependence of conductivity, obtain a straight line, whose slope is  $\beta/B$ . From fig. 1, in which a few typical plots of  $\log c$  against  $\log i$  are shown, it is seen that the relationship between the two quantities is indeed linear. We may therefore conclude that formula (1) represents the law of temperature dependence of conductivity to the same order of accuracy as formula (3) represents that of emission.

In the case of a few valves the rate of increase of conductivity with temperature was apparently abnormally low at relatively low temperatures (shown dotted in two

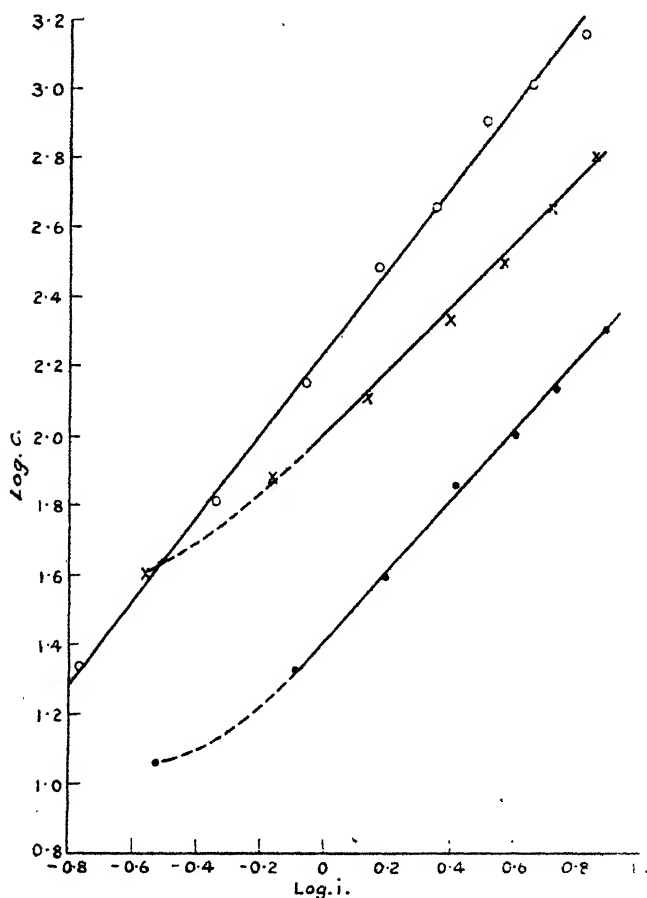
---

\* The relationships between the constants in (2) and (3) are best obtained by equating the expressions for  $\log i$  in the two formulæ and differentiating with respect to  $T$ .

of the curves of fig. 1). We cannot suggest any plausible explanation for this.

The slopes of the straight lines connecting  $\log c$  with  $\log i$  vary about a mean value of approximately  $45^\circ$ . The mean of sixteen measurements of  $\beta/B$  is 0.99, and the

Fig. 1.

Relationship between  $\log c$  and  $\log i$ .

spread is from 0.83 to 1.20. The variations are too great to be due to experimental error and must be attributed to real differences in the condition of the oxides. No special theoretical significance is therefore to be attached to the fact that the mean of several determinations happens to come out to almost exactly 1.

It is interesting to compare these results with those obtained by Horton <sup>(13)</sup> and Spanner <sup>(14)</sup> in the case of single oxides under conditions different from those obtaining in our experiments. The value of  $\beta$  obtained from Horton's measurements on CaO is  $2.16 \times 10^4$  deg. The value of B for CaO, according to the recent very careful measurements of Espe <sup>(4)</sup>, is  $2.3 \times 10^4$  deg. From these two determinations we obtain for  $\beta/B$  the value 0.94. From Spanner's measurements the following values are obtained :—

	$\beta$ .	B.	$\beta/B$ .
CaO .....	$1.68 \times 10^4$	$2.85 \times 10^4$	0.59
SrO .....	$1.53 \times 10^4$	$2.55 \times 10^4$	0.60
BaO .....	$1.29 \times 10^4$	$2.20 \times 10^4$	0.59

In view of our observations on the effects of oxygen poisoning, it may seem surprising that the values of  $\beta$  obtained from the measurements of Horton and Spanner, whose specimens of oxide were exposed to air, are of the same order as those obtained by us when the conductivity was measured in a good vacuum. It must be remembered, however, that we have not made any measurements of the *temperature dependence* of the conductivity of a poisoned oxide coating, and therefore know nothing of the effects of poisoning on  $\beta$ .

#### 4. Saturation of Conduction Current.

In the foregoing the conductivity was measured by the slope of the straight line which connects the conduction current with the voltage between the two wires when both of these quantities are small. At current densities comparable with those existing when saturated thermionic space current is being taken the current-voltage relationship ceases to be linear, showing incipient current-saturation. Examples of such curves, two of which have been taken far enough to show the effect, are given in fig. 2.

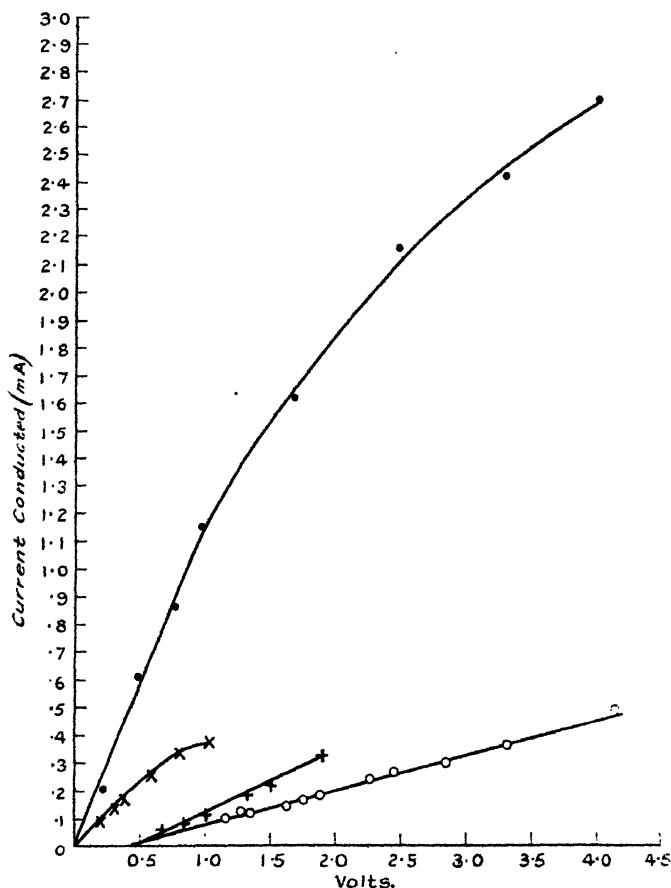
#### 5. Polarization.

The conduction current-voltage curves to which we have just referred generally, but not always, pass through the origin. In those cases where they do not, the intercept on the voltage axis may be taken to be a measure of the back E.M.F. due to polarization.



Another method by which we attempted to measure polarization was, by means of a change-over switch, suddenly to substitute a galvanometer or a microammeter for the conductivity-measuring circuit in the non-heating phase of the commutator. A deflexion was then observed on the instrument which corresponded in sign with the

Fig. 2.



Relationship between Conduction Current and Voltage.

intercept of the current-voltage curve on the voltage axis. From the magnitude of this deflexion and the known resistance of the coating and galvanometer the polarization E.M.F. could then be calculated.

The results given by the two methods agree in order of magnitude, but that is all that can be said. Relatively

few valves showed polarization at all. When a back E.M.F. was observed it was usually of the order of  $\frac{1}{2}$  volt. Two valves, with which polarization was at first observed, failed to show any polarization later. They had in the meantime been used for other experiments.

We have not been able to discover any general law which determines under what conditions polarization is to be observed. We were prevented from pursuing our work on polarization by the fact that the time which one of us (R. M.) was able to devote to the investigation was limited. Further work is now in progress in these Laboratories.

## DISCUSSION.

### 1. *Preliminary Remarks.*

The similarity of the phenomena exhibited by the conduction current and the thermionic current as regards forming, poisoning, and saturation is very striking, and might lead one to suspect that what has been measured as conductivity is, perhaps, merely some manifestation of the thermionic properties of the oxide, bearing little or no relationship to the true electrical conductivity of the oxide crystals.

The following considerations, however, make this view untenable. Conductivities were always measured by the slopes of the rectilinear lower portions of the conduction current-voltage curves. Now, if these were essentially thermionic space-current curves, and the fall of potential in the oxide powder were located mainly in the spaces separating adjacent crystals from one another, the lower infra-saturation parts of the current-voltage curves would be the same, or almost the same, at all temperatures. As we have seen, however, the rate of change of current with voltage in this region increases with temperature according to the exponential law (1). The falls of potential across the spaces between the crystals must therefore, in this infra-saturation region, be small in comparison with those across the crystals themselves. The slopes of the lower portions of the current-voltage curves are therefore a measure of the true conductivity of the crystals. On the other hand, the saturation of the conduction current at high current densities is probably a thermionic phenomenon. We shall discuss this in Section 6.

## 2. *Nature of the Conductivity.*

The fact that the oxides are dielectrics and that the law connecting conductivity with temperature is of the form (1) is, as we shall see, strong evidence pointing to the conclusion that the oxides conduct electrolytically, and not, as Horton<sup>(13)</sup> and Spanner<sup>(14)</sup> supposed, electronically.

The only cases of which we are aware in which electronic conduction in dielectric crystals has been observed are those in which an enhanced conductivity has been induced by photoelectric means. Such photoelectrically induced conductivity has been studied by Röntgen, Joffé<sup>(15, 16)</sup>, and others, and Lukirsky<sup>(17)</sup> has been able to show conclusively that the carriers of the enhanced current are electrons. Where, as in the case of rock-salt, observations have been made of the temperature coefficient of this electronic conductivity, it has been found to be negligibly small<sup>(18)</sup>.

On the other hand, Tubandt and Lorenz<sup>(19)</sup>, Lukirsky, Shukareff, and Trapesnikoff<sup>(20)</sup>, and Joffé<sup>(21)</sup>, in investigations of the normal (*i. e.* not photoelectrically induced) conductivity of a large number of transparent dielectric crystals, have shown that, without exception, the conductivity is electrolytic, accurately obeying Faraday's law. Joffé and Kirpitchewa<sup>(22)</sup> and others have furthermore found that the conductivity of such crystals increases with temperature according to an exponential law of precisely the form (1) which Horton<sup>(13)</sup>, Spanner<sup>(14)</sup>, and we have found to apply in the case of alkaline earth oxides.

The behaviour of oxide cathodes during the early stages of "forming" also favours the view that their coatings conduct electrolytically, at least initially. Horton<sup>(13)</sup> has actually found that the rate of evolution of gas in the initial stages of forming is within 8 per cent. of that required by Faraday's law. The fact that gas is no longer evolved by a completely formed cathode means either :

(1) that some new material has appeared in the coating through which the current is now conducted electronically instead of through the electrolytically conducting oxide; or

(2) that the change which accompanies forming is of such a nature as thereafter to prevent the escape of the products of electrolysis, and to make possible their recombination.

The objection to the former of these alternatives is that the temperature dependence of the conductivity of formed

coatings is that characteristic of electrolytes. The latter alternative requires that either one or both of the products of electrolysis shall be capable of diffusing through the coating in the direction opposite to that in which the corresponding ions move in electrolysis, and that this diffusion shall not be accompanied by any appreciable evaporation. Espe<sup>(4)</sup> has already suggested that the barium\* liberated electrolytically at the boundary between coating and core-metal diffuses outward to the emitting surface.

### 3. *Barium Circulation.*

Now it has been shown by Tubandt and Lorenz<sup>(19)</sup> and by Lukirsky, Shukareff, and Trapesnikoff<sup>(20)</sup> that generally, in the electrolysis of solid dielectrics, practically only one kind of ion (usually the positive one) is mobile. Let us suppose that the alkaline earth oxides are no exception to this general rule, and that the  $Ba^{++}$  ions are mobile, the  $O^{--}$  practically immobile. In the coating of an oxide cathode, then, a given atom of barium must be capable of functioning as an ion in electrolysis at least  $10^5$ – $10^6$  times. In the steady state there can be no progressive change in the number of ions inside a crystal. Therefore, corresponding to every ion arriving and being neutralized at the electrolytic cathode, there must on the average be one ion separated from a surface layer at the electrolytic anode. We thus see that the electrolytic theory of the conductivity of oxide coatings, together with the assumption that, as in most solid dielectrics, practically only the positive ion is mobile, leads necessarily to the conclusion that there must be uncombined barium at the thermionically emitting anode side of the coating. This conclusion is in striking agreement with the "free barium" theory of the thermionic emission of oxide cathodes<sup>(1, 2, 3, 4)</sup>. The question as to the precise condition of this surface barium may be left open for the present.

The diffusion of barium in a direction opposite to that of the drift of the electrolytic ions may take place in either of two ways—through the bodies of the crystals or along their surfaces. In either case, of course, the mechanism of the diffusion is one of thermal agitation, and the rate of transport of barium by it must equal that associated

\* We shall, for the sake of brevity, write barium where we mean barium and/or strontium and/or calcium.

with the ionic drift taking place under the directional action of the field. The mobility (using the word now in its wider meaning) of atoms inside the crystals must be considerably less than that of the ions, on account of the greater size of the former, and in the case of a "volume" diffusion the relative sluggishness of their motion could only be compensated for if their concentration greatly exceeded that of the ions. On the basis of this picture it is difficult to imagine why mere exposure of the cold formed oxide to oxygen, affecting as it does only the surfaces of the crystals, should so completely poison the conductivity. If, on the other hand, it is supposed that the barium diffuses along the surfaces of the crystals, such poisoning becomes quite understandable, for the surface barium, being oxidized, is no longer available for the formation of fresh barium ions to take the place of those being removed by electrolysis. Such surface diffusion would be analogous to the case of thoriated tungsten, in which, as Clausning<sup>(23)</sup> has conclusively shown, the thorium diffuses to the surface of the cathode during the process of thermionic activation along the tungsten grain boundaries, and not through the actual crystals. Thus we may conclude that the diffusing barium almost certainly constitutes a mobile adsorbed layer of atomic thickness, or a quasi-two-dimensional gas, on the surfaces of the crystals.

It is interesting to consider some of the quantitative requirements of the theory of barium circulation. The emission obtainable from a well-formed oxide cathode at its normal operating temperature is usually of the order of  $\frac{1}{2}$  ampere per cm.<sup>2</sup>, or  $2 \times 10^{18}$  electrons per cm.<sup>2</sup> per sec. Assuming that the electrolytic ions are doubly charged, we see that  $10^{18}$  ions will be formed from surface barium per second from each square centimetre of emitting crystal surface. In a closely packed barium layer there will be roughly  $10^{15}$  atoms per square centimetre. Therefore the average life of an adsorbed particle (atom, or ion associated with two electrons) of barium on the emitting surface must be of the order of  $10^{-3}$  second. This result is in excellent agreement with the value (also  $10^{-3}$  second) calculated by Schottky<sup>(24)</sup> from Johnson's<sup>(25)</sup> measurements of the "flicker" effect of oxide cathodes. Incidentally it is plain that Schottky's result, when considered in conjunction with the great length of life of oxide cathodes, constitutes independent evidence in support of an

essential part of our theory, viz., the repeated appearance of the same particles of barium at the emitting crystal surfaces.

The rate at which barium must diffuse along the surface of the oxide in an independent unit of barium circulation in order to maintain the supply of electrolytic ions at its anode depends, of course, both upon the size of the unit and upon the current passing through it. Let us imagine an idealized independent unit of barium circulation in the form of a cube of side  $l$ . If the temperature is such that the emission density has the above value of  $\frac{1}{2}$  ampere per  $\text{cm.}^2$ , then, roughly, each thousandth of a second it is necessary for the barium particles on the emitting face to be replaced by fresh ones diffusing over the four adjacent faces. The average distance over which the latter will have to move in order to take the place of those which have disappeared from the emitting face is roughly  $0.3\ l$ . The rate of flow of the two-dimensional barium gas will therefore be of the order of  $300\ l$  per second. The approximately independent units of barium circulation will not have linear dimensions of a greater order than the thickness of the coating, but, as we shall see later, they may be much less. Thus, in the case of a coating of thickness  $1/100\ \text{mm.}$ , the rate of barium diffusion during the passage of saturated space current would certainly not have to be greater than about  $3\ \text{mm.}$  per second.

#### *4. Thermionic Emission from Adsorbed Barium.*

The two-dimensional gas adsorbed on the surfaces of the crystals is the source from which are drawn not only the electrolytic  $\text{Ba}^{++}$  ions, but also the thermionically emitted electrons. Now, if the surface layer consisted of ordinary barium atoms the work-function of an oxide cathode, as measured by the temperature-dependence of the emission, would be of the same order of magnitude as the second ionization potential of the metallic constituent of its coating, for each atom would have to part with both its valence electrons in becoming converted into an electrolytic ion. These second ionization potentials are 9.95, 11.0, and 11.8 volts respectively for Ba, Sr, and Ca. However, the thermionic work-functions of the corresponding oxides, according to the more recent published data, range only from about 1 to about 2 volts. It follows therefore that in the two-dimensional gas the barium

must be at least very nearly in the ionized condition, owing, no doubt, to the electrical forces exerted on it by the underlying oxide. We have thus to regard the surface layer as consisting of a mixture of  $\text{Ba}^{++}$  ions and electrons in some kind of loose association with one another, and together forming an electrically neutral system—a partial two-dimensional analogue of an ordinary three-dimensional mass of metal containing its “free” electrons\*.

It should be pointed out here that the thermionic emission from such a two-dimensional gas adsorbed on the surface of an insulator differs in several important respects from that of a metal whose surface is covered by a monatomic layer of foreign atoms or ions, such as thoriated or caesium tungsten. In the latter case the emitted electrons originate from underneath the electrical double layer due to the adsorbed film, and must pass through it on their way out. It has been shown that if the effects of the forces exerted laterally on one another by the adsorbed particles (atoms or ions) on the double layer may be neglected the work-function varies linearly with the concentration of the adsorbed particles<sup>(8, 26)</sup>. In the case we are considering, however, the electrons do not pass through the double layer, but originate from its outer portion. There does not therefore appear to be any reason why the work-function should vary linearly with the concentration of the two-dimensional gas.

In the case of metallic cathodes an appreciable fraction of the work function is due to the forces of attraction exerted on the escaping electrons by their electrical images in the conductor<sup>(27, 28)</sup>. In the case of oxide cathodes, however, the image force contribution to the work-function must be considerably smaller, owing to the fact that the electrons are ejected from the surface of a dielectric instead of from that of a metal.

Finally, whereas in the case of metallic cathodes with adsorbed films, the latter are not affected in any way by the electrons which pass through them, the taking of space current from an oxide cathode involves a continuous removal of the constituents of the adsorbed film, one barium ion passing into an oxide crystal for every two electrons escaping. The concentration of the film

\* We are indebted to Mr. R. H. Fowler for this picture of the surface layer.

is therefore determined, in any given case, by the requirement of statistical equilibrium between the rate of removal of the two-dimensional gas from the emitting surface (determined by the magnitude of the space current) and the rate of its replenishment by diffusion.

### 5. *Forming and Poisoning.*

On the basis of the theory of barium circulation it is easy to explain the forming and poisoning of the conductivity under conditions in which the thermionic emission is also formed or poisoned, as the case may be. If barium has not yet appeared at the anode surfaces of the units of barium circulation, or if it has been removed or combined with, fresh barium ions are not available to take the place of those being removed by electrolysis, the concentration of the barium ions inside the crystals falls below its surface barium conditioned value, *i. e.*, below that of the immobile oxygen ions, and the conductivity, which at a given temperature is proportional to the concentration of the mobile ions, also falls. Conductivity and emission are formed and poisoned together, simply because they both depend on the same thing, *viz.*, the presence of uncombined barium at the surfaces of the crystals.

In the process of forming or recovery from poisoning (which is essentially the same thing) the movement under the action of the field of the barium ions which are constantly being formed by temperature dissociation, and their recapture by immobile oxygen ions at positions in the crystal lattices nearer the cathode than the points of their birth by dissociation, results in the gradual appearance of oxygen at the electrolytic anode, whence it evaporates. This oxygen is then removed, either by the pump or by the getter. After a time the barium in the system is in excess of the oxygen by a sufficient amount to cover the surface of each crystal of oxide with a monatomic layer. Evolution of oxygen then ceases, and the forming is complete.

### 6. *Condition of the Surface of the Core-Metal and of the Coating. Effects of Ageing and Poisoning.*

The appearance of saturation of the conduction current at about the same current density as corresponds to the  
*Phil. Mag.* S. 7. Vol. 9. No. 57. March 1930. 2 H



passage of saturated thermionic space current suggests that there is some thermionic limitation to the conduction current. Such limitation may occur either at the boundary between core-metal and coating or within the coating itself. Wherever the limitation exists there must be imperfection of contacts, so that the current passes from core-metal to coating, or from one crystal of oxide to the next, as the case may be, mainly in the form of electrons, emitted by the one and collected by the other. On the whole, perhaps, such imperfection of contacts may be expected to occur rather at the boundary between the dissimilar core-metal and coating than between the crystals of the oxide. It is, of course, possible that the contacts are imperfect in both cases. Whatever may be the condition of the coating, however, it is probable that the electrons pass from the core-metal to the coating thermionically. It is obviously impossible that they should do this if the surface of the core-metal remained clean. It is, however, not to be expected that the core-metal should remain uncontaminated during the process of forming. We have already supposed that in this process the crystals of oxide become covered with a mobile monatomic layer of barium. Extending slightly the theory of activation already developed, we may suppose that the barium covering the crystals of oxide adjacent to the core-metal is able to flow across such contacts as exist between oxide crystals and metal, and to spread over the surface of the latter. Oxygen may also reach the core-metal during the forming process, when, as we have seen, it is evolved from the oxide. Now it has been observed that if oxygen and barium are supplied to hot tungsten two monatomic layers are, in general, formed on its surface, the inner one being of oxygen and the outer one of barium. This will be so, irrespectively of the order in which the oxygen and barium are supplied to the hot tungsten, since barium on oxygen on tungsten is more stable than oxygen on barium on tungsten. There is evidence that the same thing is true when other metals take the place of tungsten. Now the thermionic properties of monatomic layers of barium on tungsten and of barium and oxygen on tungsten have been very exhaustively studied by Ryde and Harris \* in these Laboratories, who have found that

\* A series of papers on this work is in course of preparation.

the emission obtainable from them is of the same order as that given by ordinary oxide-coated cathodes at the same temperature. Thus it appears entirely plausible that the thermionic activation of oxide cathodes is accompanied by the contamination of the surface of the core-metal by a monatomic layer of barium or by a double atomic layer of barium and oxygen, and that, in either case, the core-metal thereby acquires an extraordinarily high electron emissivity. If, as we have supposed, the core-metal and coating are only imperfectly in contact with one another, these electrons must be collected by the coating and re-emitted from its outer surface. If, in addition, the crystals of coating are in poor contact with one another, each crystal must be supposed to collect electrons on its inner surface and re-emit them from its outer. If this is the case, the linear dimensions of the independent units of barium circulation may be of a much lower order than the thickness of the coating.

Assuming that, as we have supposed, electrons pass from the core-metal to the coating mainly thermionically, it is seen that it is *a priori* by no means certain whether the Richardson straight line represents the thermionic properties of the contaminated core-metal or those of the coating. Either the core-metal emits electrons at a greater rate than the coating can re-emit them, in which case a fraction of the electrons emitted by the core-metal returns to it, or else the coating emits more electrons than it receives from the core-metal, so that it re-absorbs a fraction of them. In other words, the thermionic emission of the cathode as a whole is limited either by the coating or by the core-metal, whichever of the two systems in series has the lesser thermionic emissivity.

It appears that, at least in certain cases, it is the contaminated core-metal, and not the coating, by which the emission is limited. Since, according to our assumption, the coating receives as many electrons from the space that separates it from the core-metal as it permanently loses, by re-emission, from its outer surface, there can be no net heat loss from the coating, and the only cooling that the cathode will suffer by its electron emission will be that due to the evaporation of electrons from the contaminated core-metal. The work-function of the cathode, calculated from the latent heat of evaporation of electrons, will therefore in any case be that of the contaminated core-metal.

Occasional comparisons have been made, *e.g.*, by Davisson and Germer<sup>(29)</sup>, between the work-function measured in this way and that determined from the slope of the Richardson straight line, and the two determinations have been found to be in good agreement. But we have already seen that the slope of the Richardson straight line corresponds to the work-function of whichever of the two systems (core-metal or coating) has the lesser emissivity. Thus in those cases where there is agreement between the work-functions determined by the two methods we may conclude that, if the coating is indeed in poor contact with the core-metal, it is the core-metal which limits the emission. This conclusion accords well with the fact of experience that the nature of the core-metal has a considerable influence on the thermionic properties of coated cathodes.

On the other hand, however, it would appear that if only the units of barium circulation in the coating could be made large enough, the emission of the cathode should no longer be limited by the core-metal, but by the coating. The rate of disappearance of barium from the thermionically emitting surface of such a unit is proportional to the space current, and in the steady state the rate of replenishment by surface diffusion must be equal to the rate of disappearance. The rate of flow of the two-dimensional barium gas must be proportional to the surface concentration gradient. There is an upper limit to the concentration of the monatomic layer of barium (which concentration will be greatest at the cathode end of the unit), determined by the underlying oxide crystal lattice. Thus it is seen that, with a given space current, the greater the linear dimensions of the units of barium circulation, the less will be the concentration of barium at their thermionically emitting anode surfaces. Now the electron emissivity of the oxide must certainly diminish with decreasing concentration of the barium adsorbed on its surface, so that we may say that the larger the units of barium circulation the smaller will be the electron emissivity of the oxide.

The gradual formation of large units in which barium has to circulate, *e.g.*, by crystal growth, may possibly be responsible for the deterioration in the emissive properties of coated cathodes that occurs in life. The initial emission of a cathode that has deteriorated in this way cannot be restored by any thermal or electrical treatment (such as

re-forming) or by any improvement in the vacuum. It would appear, then, that the loss in thermionic activity is due to some change in the coating. It is difficult to imagine any such change other than one of size or mutual relationship of the crystals.

The permanence of the poisoned condition of a filament which has been exposed, when formed, to oxygen, may perhaps be explained in a similar manner. An unformed cathode suffers no harm when it is exposed, cold, to oxygen. The only thing that differentiates a formed from an unformed crystal is the presence on the surface of the former of a monatomic layer of adsorbed barium. On exposure of such a formed crystal to oxygen the adsorbed barium will be oxidized and the crystal will increase in size by one layer of oxide molecules. Whatever may be the condition of the coating, such a growth of its component crystals will tend to increase the size of the barium circulation units. If, as a result of re-crystallization having occurred when the cathode was first heated, the coating is in the form of a compact mass, with crystals in good contact with each other, the barium must be supposed to diffuse to the outer surface of the coating along the grain boundaries. These, however, would in time be filled up by the oxidation of their contained barium. On the other hand, if the crystals are originally in poor contact with one another, each must be regarded as an almost independent barium circulation unit. The crystals will, however, not be entirely independent units, for there must be some contacts between adjacent crystals. It is quite conceivable that the growth of each crystal by a molecular thickness will increase the areas of contact many times, and thus, by reducing the degree of independence of the separate crystals, increase the effective sizes of the units of barium circulation.

Exposure of a formed oxide cathode to a discharge in CO also results in progressive poisoning, which presently becomes permanent. It has been shown by Hogness and Harkness<sup>(30)</sup> that oxygen is one of the products of the disintegration of CO molecules by an electric discharge. The effect of exposing an oxide cathode to such a discharge is therefore probably the same as that of exposure to oxygen.

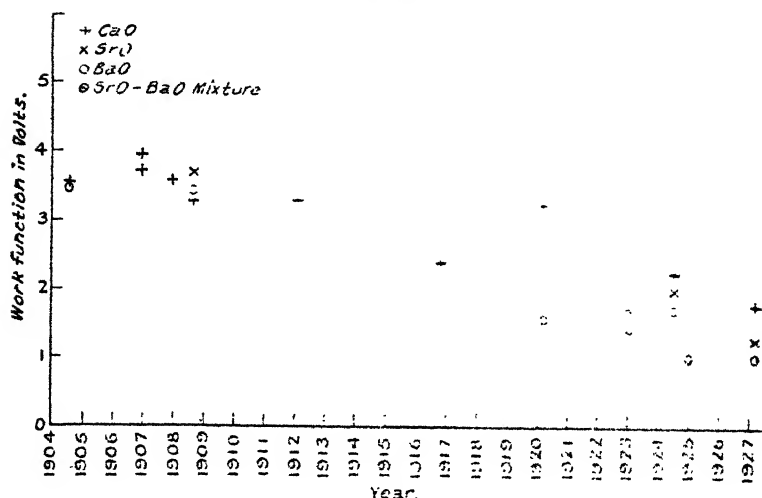
If a formed oxide is made the cathode of a discharge in hydrogen presumably the only possible effect of the

discharge on the coating is the removal of the adsorbed barium. There is then nothing to prevent the adsorbed layers from being re-formed on the crystals in the same manner as they were formed originally. Mere removal of barium cannot increase the areas of contact between the crystals. Hydrogen poisoning is therefore not permanent.

### 7. Variability of Emission from Oxide Cathodes.

Published values of the thermionic constants of oxide cathodes are much less in agreement with one another than

Fig. 3.



Published Values of Work-functions of Oxide Cathodes.

are those of any other kind of thermionic emitter. A good idea of the poorness of the agreement may be formed by plotting the values of one of these constants (*e. g.*, the work-functions) against the times of their publication. This has been done in fig. 3\*. Uncertainty of temperature measurement, although probably a contributory cause, seems alone to be hardly adequate to account for the whole

\* The papers from which these values have been taken are Nos. 2, 6, 8, 12, 15, and 17 of Arnold's<sup>(6)</sup> Bibliography, and Nos. 1, 3, 4, 6, 14, and 19 of our own.

of this variation. We must therefore look for other causes.

Let us first consider the case where the condition of the coating is so unfavourable that it is the coating, and not the contaminated core-metal, by which the emission is limited. We do not know in what manner the thermionic constants of a formed oxide depend upon the surface concentration of adsorbed barium. Probably all that it is safe to say is that the concentration and the emission increase and decrease together. We have already seen that at each temperature the surface concentration of barium is determined by the condition that there must be equilibrium between the removal of barium by its conversion into electrolytic ions and the arrival of fresh barium by diffusion. The coefficient of diffusion may itself vary violently with the temperature, in the same kind of way as does the emission. This will, for example, be the case if, in diffusing, the particles of barium move in "jumps" between neighbouring positions of equilibrium in relation to the underlying crystal lattice. Thus the temperature variation of the emission may not be a measure of the true work function at all, the surface concentration of barium being different at each temperature. The relative importance of this falsification of the work-function measurements will depend upon the size of the units of barium circulation.

If, on the other hand, the units of barium circulation in the coating are so small that it is the core-metal which limits the emission, certain variations in thermionic properties may still occur. That different contaminated core-metals should have different thermionic properties is, of course, quite natural. But even when the core-metal is not changed, some variation in these properties may still occur as a result of gas contaminations. Such variation is more particularly to be expected in the case of metals which are only with difficulty out-gassed, such as, for example, platinum. The thermionic behaviour even of uncoated platinum is notoriously erratic. Unfortunately platinum is the metal which has generally been used hitherto as the core-material of coated cathodes.

Further work on oxide cathodes is in progress in these Laboratories, by means of which it is hoped that more precise information may be obtained concerning several points with regard to which uncertainty still exists.

## References.

- (1) L. R. Koller, *Phys. Rev.* xxv. p. 671 (1925).
- (2) M. S. Glass, *Phys. Rev.* xxviii. p. 521 (1926).
- (3) H. Rothe, *ZS. f. Phys.* xxxvi. p. 737 (1926).
- (4) W. Eape, *Wiss. Veröff. d. Sienn. Konz.* v. pp. 29, 46 (1927).
- (5) F. Detels, *Jahrb. d. drahtl. Telegr.* xxx. pp. 10, 52 (1927).
- (6) H. D. Arnold, *Phys. Rev.* xvi. p. 70 (1920).
- (7) W. Schottky and H. Rothe, *Handb. d. Experimentalphysik*, vol. xiii. pt. ii. p. 221.
- (8) I. Langmuir, *Phys. Rev.* xxii. p. 357 (1923).
- (9) I. Langmuir and K. H. Kingdon, 'Science,' pp. 57, 58 (1923).
- (10) K. H. Kingdon, *Phys. Rev.* xxiv. p. 510 (1924).
- (11) I. Langmuir and K. H. Kingdon, *Proc. Roy. Soc.* cvii. A, p. 61 (1925).
- (12) J. A. Becker, *Phys. Rev.* xxviii. p. 341 (1926).
- (13) F. Horton, *Phil. Mag.* xi. p. 505 (1906).
- (14) H. J. Spanner, *Ann. d. Phys.* lxxv. p. 609 (1924).
- (15) W. C. Röntgen and A. Joffé, *Ann. d. Phys.* xli. p. 449 (1913).
- (16) W. C. Röntgen and A. Joffé, *Ann. d. Phys.* lxiv. p. 1 (1921).
- (17) P. Lukirsky, *Journ. Russ. Phys. Chem. Soc.* (1916). A. Joffé, 'The Physics of Crystals,' p. 129.
- (18) P. Lukirsky, *Rep. Phys. Tech. Inst.* p. 174 (1926). A. Joffé, 'The Physics of Crystals,' p. 129.
- (19) C. Tubandt and F. Lorenz, *ZS. f. Phys. Chem.* lxxxvii. pp. 513, 543 (1914).
- (20) P. Lukirsky, S. Shukareff, and O. Trapeznikoff, *ZS. f. Phys.* xxxi. p. 524 (1925).
- (21) A. Joffé, 'The Physics of Crystals,' p. 92.
- (22) A. Joffé and M. Kirpichewa, *Journ. Russ. Phys. Chem. Soc.* xlviii. (1916). A. Joffé, 'The Physics of Crystals,' p. 87.
- (23) P. Clausen, 'Physica,' vii. p. 193 (1927).
- (24) W. Schottky, *Phys. Rev.* xxviii. p. 74 (1926).
- (25) J. B. Johnson, *Phys. Rev.* xxvi. p. 71 (1925).
- (26) W. Schottky and H. Rothe, *Handb. d. Experimentalphysik*, vol. xiii. pt. ii. p. 163.
- (27) P. Debye, *Ann. d. Phys.* xxxiii. p. 441 (1910).
- (28) W. Schottky, *ZS. f. Phys.* xiv. p. 63 (1923).
- (29) C. Davisson and L. H. Germer, *Phys. Rev.* xxi. p. 208 (1923); and xxiv. p. 666 (1924).
- (30) T. R. Hogness and R. W. Harkness, *Phys. Rev.* xxxii. p. 936 (1928).

XLII. *Effect of Occluded Gases and Moisture on the Resistance of Air Condensers at Radio Frequencies.* By HAZEL M. FLETCHER, Instructor in Physics, Wellesley College, Wellesley, Mass.\*

## Introduction.

IN some work done in this laboratory, Department of Physics, Indiana University, on the resistance of air

\* Communicated by Prof. R. R. Ramsey, Ph.D.

condensers, Mr. B. D. Morris \* thought that he had discovered evidence that the radio-frequency current was pulling out gas from the plates of the condenser. This was given as the explanation of the fact that the two bulbs of the differential thermometer used in the experiment cooled at different rates. To avoid the effect that this liberation of gas might have on the equilibrium pressure, Morris substituted a thermojunction method in which a number of junctions were connected so that a galvanometer in the circuit registered a deflexion which was proportional to the difference of temperature of the two bulbs. The final equilibrium temperature was then independent of

Fig. 1.

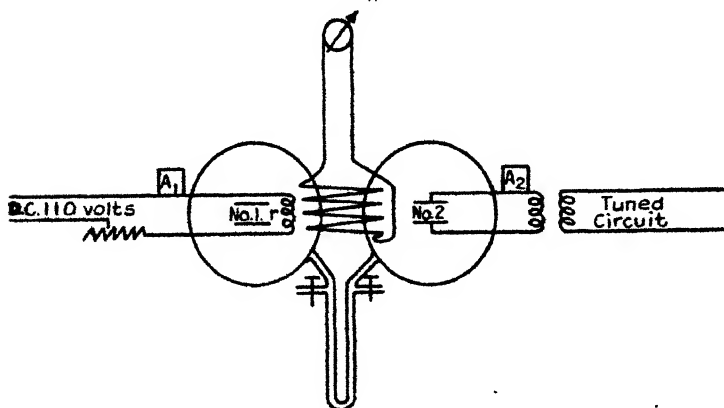


Diagram of apparatus.

liberation of gas, which was not true if a U-tube filled with water were used.

To investigate this supposed gas effect was the primary purpose of this investigation.

#### *Apparatus and Method of taking Data.*

The apparatus used in this experiment was similar to that used by Ramsey and Morris. However, in this experiment both a water manometer and thermocouple were used.

The diagram of the apparatus is shown in fig. 1. Two air-tight bulbs were formed by sealing with beeswax two 1.5 litre pyrex-glass beakers on to photographic glass plates. In each bulb was placed a radio-frequency condenser of the same size and kind. Condenser No. 2

\* Phys. Rev. xxxiii. p. 1076 (1929).



was connected with a variable inductance which was coupled to a vacuum-tube oscillator circuit; condenser No. 1 was placed in the other bulb in order to maintain the same thermal capacity. The resistance wire  $r$  was connected in series with a variable resistance and the 110-volt mains. The water manometer measured the differential pressure in the two bulbs, and the difference in temperature was indicated by the D'Arsonval galvanometer in the thermocouple circuit, which consisted of eight iron advance-junctions in opposition series.

Three sets of condensers were used in this experiment, and three separate sets of apparatus were assembled. Readings were taken on a brass condenser of capacity .000265 M.F., an aluminium condenser, No. 1, of capacity .0002678 M.F., and another aluminium condenser, No. 2, of capacity .0002 M.F.

Suppose  $i$  is the direct current in the resistance wire registered by the D.C. milliammeter ( $A_1$ ),  $I$  is the radio-frequency current in condenser No. 2 registered by the hot-wire ammeter ( $A_2$ ),  $r$  is the resistance of the resistance wire, and  $R$  is the resistance of condenser No. 2. Now, if the heating effects are balanced,  $I^2R = i^2r$ . All quantities in this equation are known except  $R$ .

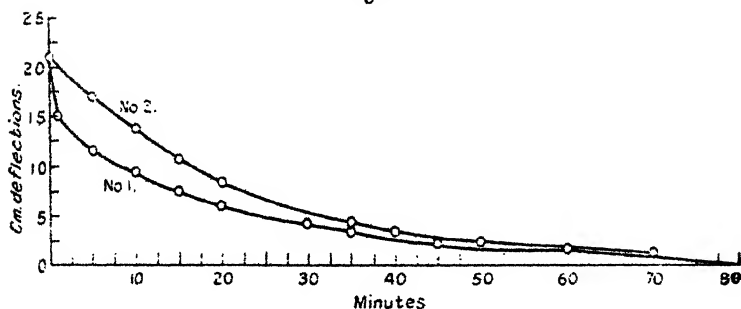
Before taking measurements the bulbs must be at the same temperature, which will be shown if there is no deflexion of the galvanometer. The screw stopcocks were opened to make sure that the bulbs were at atmospheric pressure, and then closed. Tests were made before and after runs to make sure that there were no leaks. The primary circuit was closed, and the capacity of the variable condenser in the primary or oscillator circuit and the inductance in the secondary circuit were varied until the desired current and wave-length were obtained. The direct current was then varied until the heating effect of the resistance wire was balanced by the heating effect of condenser No. 2. The equilibrium was shown when the galvanometer showed no deflexion and the pressures as shown by the manometer were the same.

### *Results and Discussion on Occluded Gas.*

The fact that the condenser heated by the radio-frequency current always was slower in heating and cooling led Morris to think that gas was being driven out. Fig. 2

is a typical curve showing the heating and cooling of the condensers. In preliminary experiments with the aluminium condensers a direct current of .5 ampere was found to balance a radio-frequency current of 2 amperes. These currents were turned on at the same time, and readings were taken of time in minutes, temperature in centimetres of deflexion of the galvanometer, and differential pressure in centimetres of water. After the currents had been running for 65 minutes the bulbs were at thermal equilibrium, and the circuits were opened and readings taken while the condensers cooled. During the time of heating it was thought that the radio-frequency current was pulling out occluded gas from the plates of the condenser. Part of the heat energy would be used, and

Fig. 2.



(Cooling curves for brass condensers.

Direct current .335 ampere.

Radio-frequency current 2.1 amperes.

Wave-length 170 m.

No. 1, cooling curve for brass condenser heated with direct current.

No. 2, cooling curve for brass condenser heated with radio-frequency current.

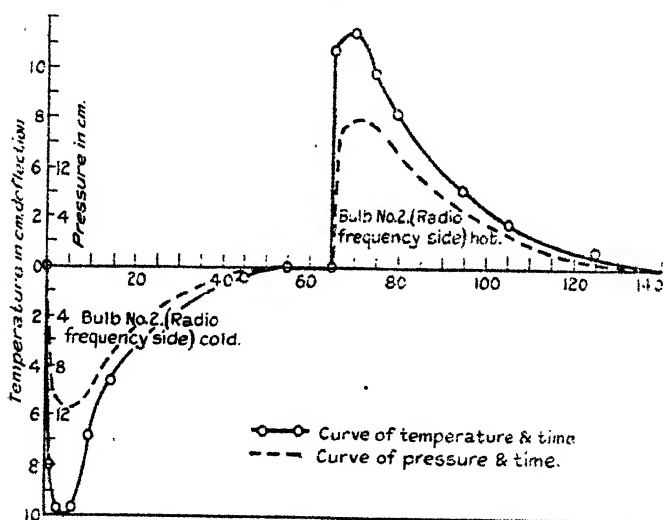
this would cause a slower rate of heating for condenser No. 2. During the cooling period it was thought that the gas was readsorbed on the plates, and the heat of adsorption was given out which would cause slower cooling of condenser No. 2.

If occluded gas were driven out, the pressure in bulb No. 2 would be greater than in No. 1 when the galvanometer indicated thermal equilibrium. In many runs the final pressures were often the same; but usually the final pressure in bulb No. 1 was slightly greater than in

No. 2, and there were a few runs in which the final pressure in No. 2 was the greater.

Calculations were made from cooling curves to see if the volume of gas could be determined. Fig. 3 shows the cooling curves for the brass condensers. In preliminary experiments it had been found that the heating effect of a direct current of .335 ampere just balanced that of a radio-frequency current of 2.1 amperes. Curve No. 1 was obtained by heating condenser No. 1 with .335 ampere without any radio-frequency current flowing. After an hour and a quarter the current was turned off, and readings

Fig. 3.



Differential heating and cooling curves for aluminium condenser No. 1.

Radio-frequency current 2 amperes.

D.C. current .5 ampere.

Wave-length 120 metres.

Current turned off at 65 min.

were taken of the time and deflexions. Curve No. 2 is the cooling curve of the brass condenser heated with the radio-frequency current.

Let  $\theta$  be the excess of the temperature of the bulbs above the temperature of the room,  $T$  the time in seconds, and  $R$  the radiation constant of the two condensers, assuming Newton's law of cooling. At thermal equilibrium both condensers are radiating heat as fast as they

are being supplied, and  $R\theta = \frac{i^2 r}{4 \cdot 2}$ . The heat given out by either condenser can be calculated by the relation  $H = \theta RT$ . Then the difference in the amount of heat given out by the two condensers is  $\Delta H = \int R\theta dT$ . But  $\int \theta dT = A$  is proportional to the area between the two curves. Therefore  $\Delta H = RA$ . Now, if this difference in the amount of heat given out is due to the heat of adsorption of gas,  $\Delta H$  must be equal to the heat of adsorption of the occluded gas. Let  $C$  represent the number of calories of heat given out when 1 c.c. of gas is adsorbed and  $V$  the volume of occluded gas driven out. Then  $CV = RA$ . Data from the cooling curves gave a result of 47 calories. Heat of adsorption tables showed that a value of 1 to  $\frac{1}{2}$  calorie per 1 c.c. of adsorbed gas would be reasonable to assume for  $C$ . Then  $V$  would equal from 50 to 100 c.c. of gas. Larger results were calculated from the cooling curves of the aluminium condenser. These results are unreasonable when the difference of pressure as measured by the U-tube is considered.

This gas effect was also tested by placing the condenser in an exhausted air-chamber and noting the change of pressure when radio-frequency current flowed in the condenser. There was no noticeable change in pressure.

These different rates of heating and cooling cannot be due to occluded gases, but are due to an unequal heat distribution in the two bulbs. Between the 55- and 65-minute interval on the curve in fig. 2 the condensers are radiating heat at the same rate as they are receiving heat. The source of heat in bulb No. 2 is inside the condenser, while the source of heat in bulb No. 1 is a small wire outside the condenser. Even though the thermojunctions in both bulbs are at the same temperature, condenser No. 2 is at a higher average temperature than No. 1, since the heat must be conducted from the inside to the outside of condenser No. 2.

#### *Resistance of Condensers.*

It was soon noticed that the measured resistance varied from time to time, and it was suspected that this might be due to moisture. At first measurements were taken without any attempt being made to vary the amount of

moisture. Later the air was saturated and measurements were repeated. Then the bulbs were opened, the condensers dried out by heating, and some  $P_2O_5$  put in the bulbs to take up any moisture. It was difficult to check these resistances with those found before when saturated vapour was in the bulbs. It was thought that there might be moisture in the bulbs from the water in the U-tube. The water in the manometer was then

TABLE I.

Brass Condenser, capacity .000265 M.F.

		Wave-length.	$R_0$ .	$R_s$ .	Ratios of $R_0$ .
(1) ...	Air not	70 m.	.076 ohm.	.044 ohm.	(2) ÷ (1) = 2.34
(2) ...	saturated.	170	.178	.043	
(3) ...	Air	70	.173	.101	(4) ÷ (3) = 2.31
(4) ...	saturated.	170	.400	.096	
(5) ...	$P_2O_5$ in	70	.125	.073	(6) ÷ (5) = 2.04
(6) ...	jars.	170	.255	.061	
(7) ...	$P_2O_5$ in jars,	70	.070	.040	(8) ÷ (7) = 2.06
(8) ...	cymene in	170	.144	.035	
(9) ...	manometer.	350	.329	.038	(9) ÷ (8) = 2.28

Ratios of resistances ( $R_0$ ) when air is saturated and when not saturated :

70 m.	170 m.
(3) ÷ (1) = 2.28	(4) ÷ (2) = 2.25
(3) ÷ (5) = 1.38	(4) ÷ (6) = 1.57
(3) ÷ (7) = 2.47	(4) ÷ (8) = 2.78

replaced by cymene, which has a specific gravity of 0.856 and boils at 175° C

The results are given in the column marked  $R_0$  in Tables I., II., and III. Morris has found that the resistance of a condenser can be reduced to "standard values" by the empirical formula,

$$R_s = R_0(300/\lambda_0) (C_0/0.001)^{3.2}.$$

The brass condenser obeys the law,

$$R_s = R_0 \left( \frac{\lambda_s}{\lambda_0} \right) \left( \frac{C_0}{C_s} \right)^{3/2},$$

and both the aluminium condensers obey the law,

$$R_s = R_0 \left( \frac{\lambda_s}{\lambda_0} \right)^{1/2} \left( \frac{C_0}{C_s} \right)^{3/2},$$

TABLE II.

Aluminium Condenser No. 1, capacity .0002678 M.F.

		Wave-length.	$R_0$ .	$R_s$ .	Ratios of $R_0$ .
(1) ...	Air not	70 m.	.226 ohm.	.064 ohm.	(2) ÷ (1) = 1.05
(2) ...	saturated.	170	.237	.043	
(3) ...	Air	70	.274	.077	(4) ÷ (3) = 1.19
(4) ...	saturated.	170	.326	.059	
(5) ...	P <sub>2</sub> O <sub>5</sub> in	70	.171	.048	(6) ÷ (5) = 1.04
(6) ...	jars.	170	.178	.032	
(7) ...	P <sub>2</sub> O <sub>5</sub> in jars.	70	.205	.058	(8) ÷ (7) = 1.25
(8) ...	cymene in	170	.256	.046	
(9) ...	manometer.	350	.325	.041	(9) ÷ (8) = 1.27

Ratios of resistance ( $R_0$ ) when air is saturated and when not saturated :

70 m.	170 m.
(3) ÷ (1) = 1.21	(4) ÷ (2) = 1.37
(3) ÷ (5) = 1.60	(4) ÷ (6) = 1.83
(3) ÷ (7) = 1.33	(4) ÷ (8) = 1.27

rather closely.  $R$ ,  $\lambda_s$ , and  $C_s$  are standard resistance, wave-length, and capacity; and  $R_0$ ,  $\lambda_0$ , and  $C_0$  are the measured values. Since the resistance of a condenser consists of metallic resistance and dielectric resistance, the relative amounts of which vary with the condenser, it cannot be expected that the same formula will apply to all condensers. Tables I., II., and III. give the average results of the three condensers with various amounts of

moisture.  $R_s$  is the calculated value using the empirical formula,

$$R_s = R_0 \left( \frac{300}{\lambda_0} \right) \left( \frac{C_0}{.001} \right)^{3/2}$$

for the brass condenser, and

$$R_s = R_0 \left( \frac{300}{\lambda_0} \right)^{1/2} \left( \frac{C_0}{.001} \right)^{3/2}$$

for the aluminium condensers.

TABLE III.

Aluminium Condenser No. 2, capacity .0002 M.F.

		Wave-length.	$R_0$ .	$R_s$ .	Ratios of $R_0$ .
(1) ...	Air not	70 m.	.058 ohm.	.010 ohm.	(2) ÷ (1) = 1.15
(2) ...	saturated.	170	.064	.007	
(3) ...	Air	70	.100	.018	(4) ÷ (3) = 1.67
(4) ...	saturated.	170	.167	.019	
(5) ...	P <sub>2</sub> O <sub>5</sub> in	70	.034	.006	(6) ÷ (5) = 1.23
(6) ...	jars.	170	.042	.005	
(7) ...	P <sub>2</sub> O <sub>5</sub> in jars,	70	.030	.005	(8) ÷ (7) = 1.03
(8) ...	cymex in	170	.031	.003	
(9) ...	manometer.	350	.041	.003	(9) ÷ (8) = 1.32

Ratios of resistances ( $R_0$ ) when air is saturated and when not saturated:

70 m.	170 m.
(3) ÷ (1) = 1.72	(4) ÷ (2) = 2.00
(3) ÷ (5) = 2.94	(4) ÷ (6) = 3.98
(3) ÷ (7) = 3.34	(4) ÷ (8) = 5.38

The resistance of each condenser increases with the amount of moisture present. The ratios of  $R_0$  when the air is saturated and when not saturated, except one (ratios 1.33 and 1.27 for aluminium condenser No. 1), increase with wave-length. These ratios show that the dielectric losses are larger than the metallic losses in aluminum condenser No. 2, and that the dielectric losses are relatively smaller in aluminium condenser No. 1.

The ratios of the resistance ( $R_0$ ) given in the last columns of the tables show that the resistance increases with wave-length. Since the metallic resistance decreases and the dielectric losses increase with wave-length, these ratios show that the dielectric losses are greater than the metallic resistance. The metallic resistance of the brass condenser is greater than that of the two aluminium condensers, for the ratios for the aluminium condensers are approximately 1.1, and for the brass 2.2. The resistance of aluminium No. 1 and the brass condenser are comparable, but the resistance of aluminium condenser No. 2 is much lower. An appreciable amount of the resistance of the first two must be due to metallic resistance since the plates of aluminium condenser No. 2 were larger in area and much thicker.

In conclusion, radio-frequency currents do not pull out an appreciable amount of adsorbed gas from the metal plates of condensers. The resistance of condensers varies with the amount of moisture present. These variations are considerable, and probably this accounts for the fact that the results obtained by different experimenters for resistance of condensers do not check very closely. The dielectric losses and the metallic resistance vary with wave-length, and the ratio of these resistances is not the same in all condensers. The dielectric losses of the three condensers tested in this experiment were greater than the metallic resistance.

This investigation was made under the direction of Dr. R. R. Ramsey, Professor of Physics of Indiana University. The writer is indebted to him for whatever merits this paper may possess.

### *Bibliography.*

- Bureau of Standards, Circular No. 74.  
C. N. Weyl and S. Harris, *Institute of Radio Engineers*, xiii. p. 109, Feb. 1925.  
E. Offerman, *Zeit. für Hochfreq.* xxvi. p. 152 (1925).  
C. D. Callis, *Phil. Mag.* i. p. 428 (1926).  
R. R. Ramsey, *Phil. Mag.* ii. p. 1213 (1926).  
S. L. Brown, C. F. Weibusch, and M. Y. Colby, *Phys. Rev.* xxix. p. 887 (1927).  
D. W. Dye, *Proc. Phys. Soc.* xl. p. 285 (1928).  
R. W. Wilmotte, *Journ. Sci. Instruments*, xii. p. 369 (1928).  
G. W. Sutton, *Proc. Phys. Soc.* xli. p. 126 (1929).



**XLIII. On an Anomalous After-Effect of Dielectrics for their Apparent Resistivity.** By Prof. H. SAEGUSA and S. SHIMIZU, *Physical Institute of Tohoku Imperial University, Sendai* \*.

§ I. *Introduction.*

THAT the electrical conductivity of quartz is greatly affected by a previously applied potential is discussed in A. F. Joffé's book†. This is an interesting and important phenomenon from the point of studying the electrical conduction in dielectrics. For the past several years the conductivity of dielectrics has been studied in our institute as one of the main topics for dielectrics, and during the course of studying we found independently the fact that the electrical conductivity of quartz is greatly affected by a previously applied potential, and that there is an anomalous after-effect with respect to its recovery time duration.

The present investigation was undertaken for the purpose of studying systematically the anomalous after-effect of dielectrics, and the results for quartz plate cut perpendicular to its optical axis are given in this paper.

§ II. *Apparatus and some Precautions for the Experiment.*

The main part of the present apparatus is shown in fig. 1. The constancy of temperature of the interior part of the metallic box which contains the main part of the apparatus is ensured by means of the following devices.

Both sides of the metallic box are covered with asbestos paper, and this box is covered with a wooden box the outside of which is also covered with a thick felt. The electric heaters, made of nichrome wire, are fixed on the upper and the bottom sides of the inside of the wooden box. The copper-constantan thermo-junction is placed near the specimen in the interior of the metallic box for measuring the temperature of the specimen, this thermo-junction

\* Communicated by the Authors. An abstract of this paper was published in 'Nature,' vol. cxxiii. p. 713 (1929), under the title "Anomalous After-effect with Quartz," and was read before the annual meeting of the Math. Phys. Soc. Japan, July 24 (1929).

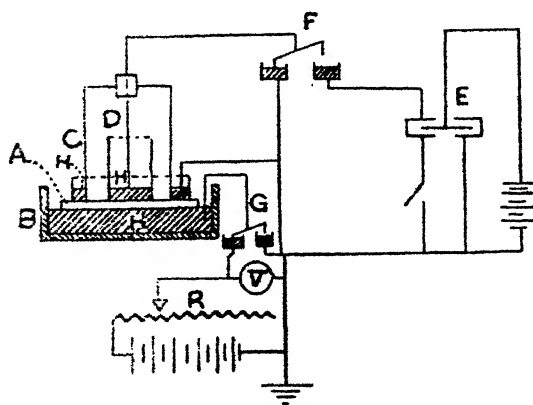
† A. F. Joffé, 'The Physics of Crystals' (1928).

being made by connecting copper and costantan wires, fifteen each in series ; and an ordinary thermometer is also put in the interior of the metallic box. By adjusting the heating current, the temperature of the interior of the metallic box is kept constant within  $\frac{1}{10}^{\circ}$  during 2 hours at least near the room-temperature.

The interior of the metallic box is maintained in as dry a state as possible, using  $P_2O_5$  and circulating perfectly dried air through the box ; thus, the humidity in the interior of the box is kept always below 5 per cent. of the relative humidity at the temperature  $10^{\circ} C$ .

The leakage-rate of electricity through the apparatus is taken before the beginning of the experiment, and the

Fig. 1.



The symbols in the figure are as follows:—

- A. Specimen, thin circular plate which is floating on the surface of mercury H.
- B. Circular vessel made of ebonite.
- C. Concentric cylinder made of iron, and the mercury between the outside walls is earthed.
- D. Open circular cylinder made of iron which is situated at the centre of the specimen.
- E. Dolezalek's quadrant electrometer.
- F. Mercury locker for connecting the inside part of D to one pair of quadrants of the electrometer or to the earth.
- G. Mercury locker for connecting the mercury between A and B to the potential source or to the earth.
- H. Mercury.
- R. Reducing resistance.
- V. Precision voltmeter for measuring the applied voltage.

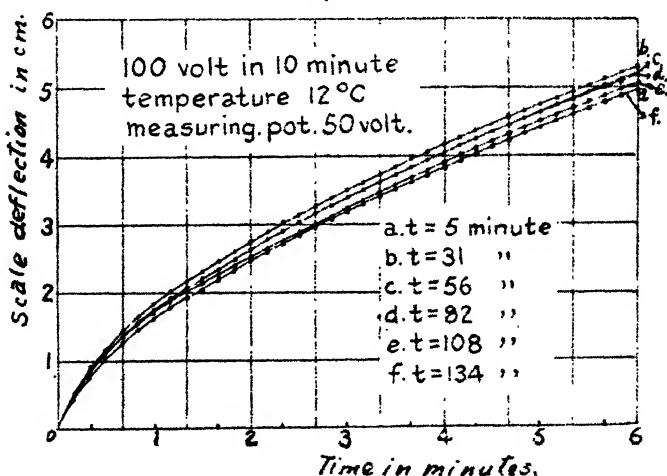
correction for it is made in the results of the experiment if necessary.

The specimen used in the present experiment is well-polished quartz circular plate cut perpendicular to its optical axis and 0.85 mm. thick.

### § III. Method of Experiment.

We put a known potential to the mercury on which the specimen floats during a certain constant time (always 10 minutes in the present experiment, except in some special

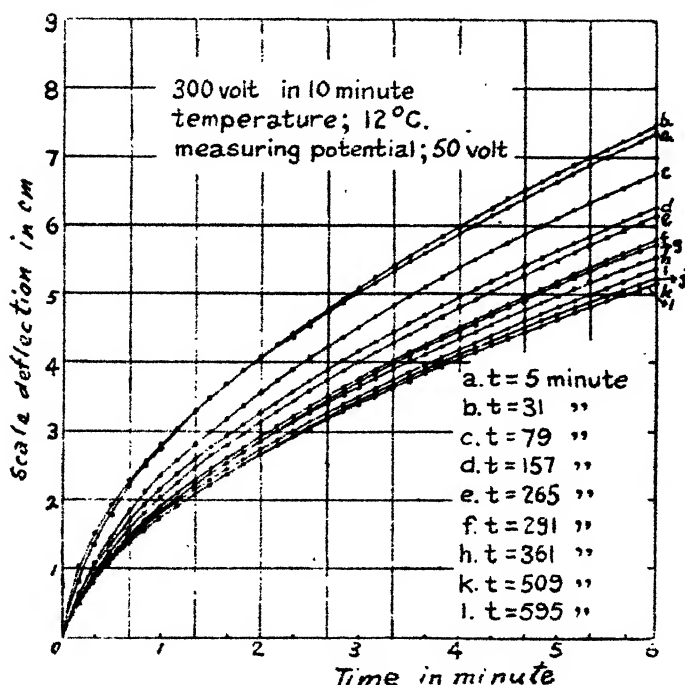
Fig. 2.



cases); during this time interval the opposite side of the specimen is kept in connexion with the earth; thus, the electricity is conducted freely to the earth through the specimen, and we call this previously applied potential "A potential" for convenience. Then the other side of the specimen is also connected to the earth during a known time, and it is then disconnected from the earth and connected to the potential source of a constant potential. The opposite side of it, *i. e.*, the mercury inside cylinder D, is also disconnected from the earth and connected to the electrometer, the deflection of which is observed with time up to several minutes (always 6 minutes, except in some special cases). Next, both sides of the specimen are earthed until the residual charge and the time effect due to

the latter measuring potential have almost disappeared, and then the observation, as before, is made under the same external condition as above during the same time interval, and then both sides of the specimen are again earthed. These processes of the observation are repeated till the rate of accumulation of the electric charge becomes almost the same as in the neutral state of the specimen, *i. e.*, till the effect of A potential on the apparent resistivity of the specimen has completely disappeared.

Fig. 3.



The correction of the residual charge due to A potential is made for the observed value.

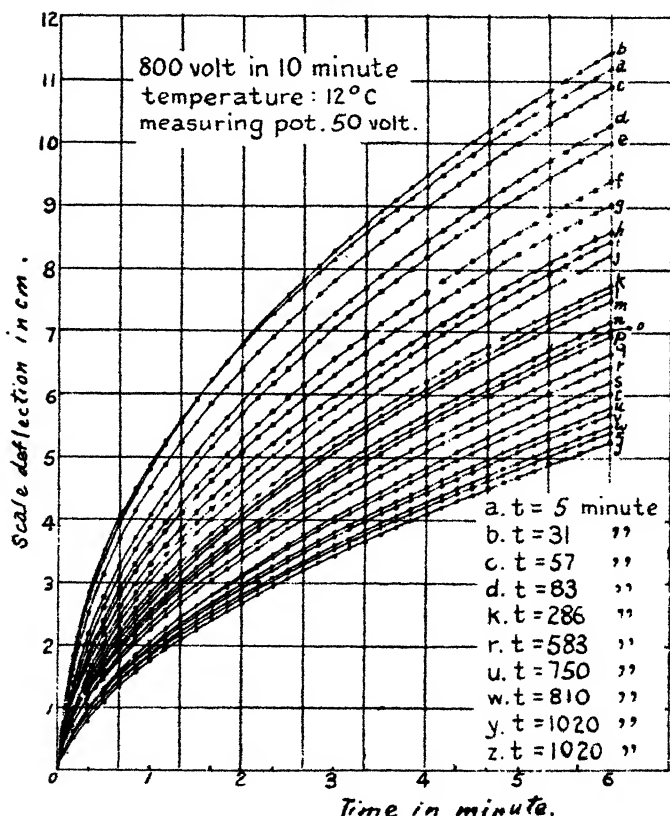
The apparent resistivities for every earthing time from the initial are calculated from the ratio of the measuring potential (always 50 volts, except in some special cases) to the initial tangent of every accumulating curve as

$$R = \frac{V}{\frac{dQ}{dt}}, \quad \dots \dots \dots (1)$$

This is the same expression as equation (16) in the former paper \* by one of the writers. And it gives correctly the apparent resistivity at given time from initial, and here we state that Curtis's equation

$$V = Ri + \frac{1}{c} \int_0^t i dt$$

Fig. 4.



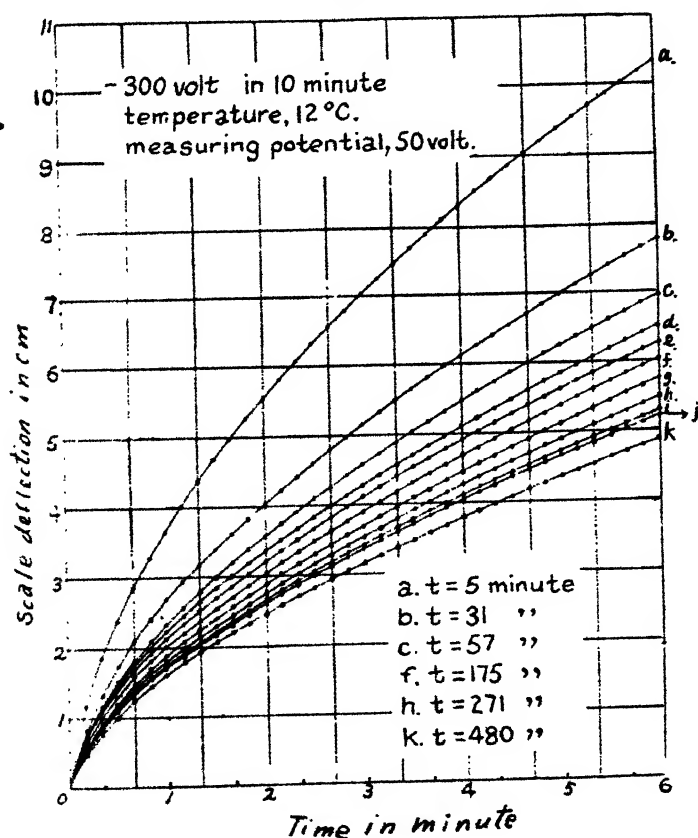
though used in the former paper above referred to, is not generally applicable to the calculation of the apparent resistivity at any time. Thus, equations (14), (15) in the same former paper give also nothing accurate as to apparent resistivity, but equation (16) gives the accurate value at  $t=0$  as above stated.

\* H. Saegusa and K. Saeki, Sci. Rep. Tohoku, xviii. p. 231 (1929).

## § IV. Anomalous After-Effect with Quartz.

(1) *The relation between A potential and the recovery time.*—Some experimental results of the accumulating curves for various A potentials and for various earthing times as graphically given in figs. 2-4 and fig. 5 show the

Fig. 5.

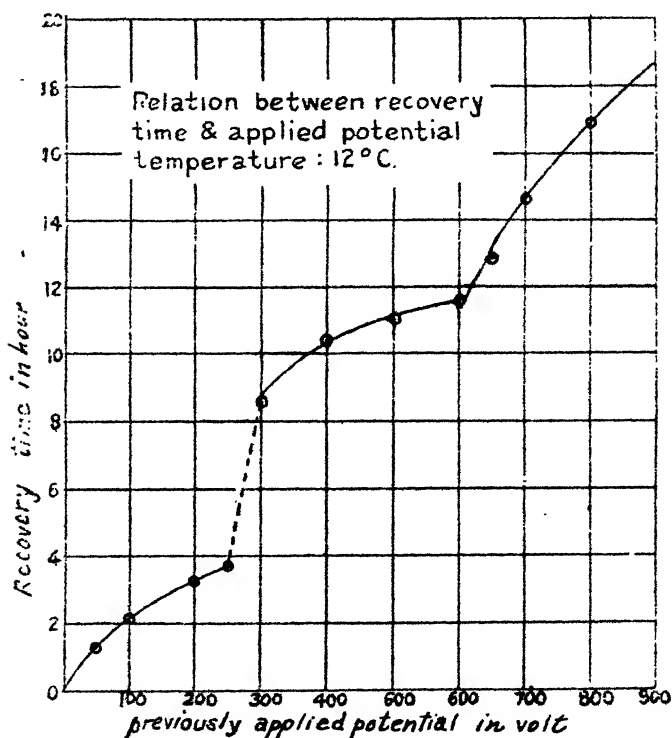


typical one of the experimental results for negative A potential. The letters *a, b, c, . . .* in these curves show that *a* is the curve at 5 minutes' earthing (the first earthing) from the instant A potential is earthed, *b* the curve at 20 minutes after the observation of a curve is finished (the observation of *a* curve continues 6 minutes and then the side which is connected to the electrometer is earthed till the beginning of the observation of *b* curve), i. e., at

31 minutes from the initial, and so also in the same way the curves *c, d, . . .* (the time intervals for these curves are written in these figures). But for the cases when *A* potential is comparatively large, the time interval of earthing between each two successive observations is made longer and longer as the accumulation curve approaches the neutral state.

As seen from these curves, the initial inclination is much larger than that of the neutral state, and it becomes smaller

Fig. 6.



as the earthing time increases and gradually tends to that of the neutral state. Thus from equation (1) the apparent resistivity will be much smaller than that of the neutral state, and it gradually becomes equal to the latter.

Fig. 6 and Table I. show the relation between *A* potential and the recovery time of the after-effect, *i. e.*, the time interval between the instant of the first earthing and the

final state ; during this time interval the after-effect of A potential continues. As seen from fig. 6, the recovery time of the after-effect is considerably long, and it becomes gradually longer as A potential increases, and at the potential between 250–300 volts (about 300–350 volts per mm. thick) it discontinuously becomes long, and again the increase rises slowly up to 600 volts (700 volts per mm. thick), and after that the time interval increases rapidly with the potential and tends gradually to a saturation value. It is a noticeable fact that the variation of the recovery time with A potential is exactly the same for both cases whether A potential is positive or negative.

In a paper\* by one of the writers it was concluded that the limit potential is most important for several dielectric

TABLE I.

A potential in volts.	Recovery time in minutes.	A potential in volts.	Recovery time in minutes.
50	70	500	663
100	134	500	695
200	200	650	770
250	223	700	882
300	509	800	1020
400	620		

phenomena—for example, the so-called stationary dielectric hysteresis appears for larger applied potential than the limit potential, and an anomaly for the residual charge is also observed at this potential. And the limit potential for quartz plate cut perpendicular to its optical axis is equal to 324 volts per mm. thickness as the mean value from the residual charge and the time effect.

Hence the discontinuous increase of the recovery time occurs at about the limit potential ; thus, we should like to call this discontinuous change of the after-effect “the anomalous after-effect for resistivity of dielectrics,” and we conclude that it appears at the limit potential of dielectrics.

It seems to be a noticeable fact that the increase of the recovery time from 600 volts is due also to the same cause

\* H. Saegusa, Sci. Rep. vol. x. p. 101 (1921).



to which the increase of the stationary values of the residual charge and the time effect with respect to the applied potential from about 600 volts is due, as shown in the paper above referred to.

(2) *Variation of the apparent resistivity.*—The relation between the ratio of the apparent resistivity at 5 minutes

Fig. 7.

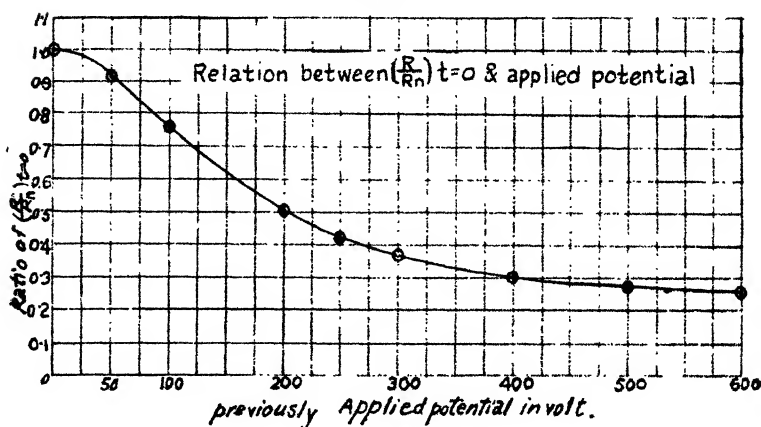


TABLE II.

A potential in volts.	$\frac{R}{R_n}$	A potential in volts.	$\frac{R}{R_n}$
0	1.000	300	0.371
50	0.910	400	0.301
100	0.773	500	0.280
200	0.503	600	0.260
250	0.418		

after the beginning of the first earthing (calculated from initial tangent of a curve using equation (1)) to that of the neutral state and A potential is shown in fig. 7 and Table II. As seen from this figure the apparent resistivity decreases rapidly as A potential increases, and from about 300 volts of A potential the decrease of the resistivity gradually becomes small and the resistivity tends to a stationary value. These features are quite

similar for both cases where A potential is either positive or negative.

Figs. 8-11 show that the ratio of the apparent resistivity at neutral state to that of every earthing time (they are calculated from every initial tangent of  $a, b, c, \dots$  curves using equation (1)) decreases as the time interval from the beginning of the first earthing increases and gradually tends to unity. This variation shows that the apparent resistivity recovers gradually as the time elapses,

Fig. 8.

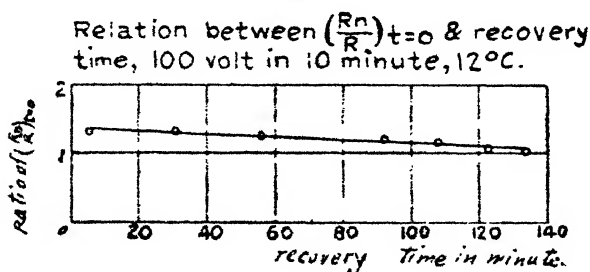
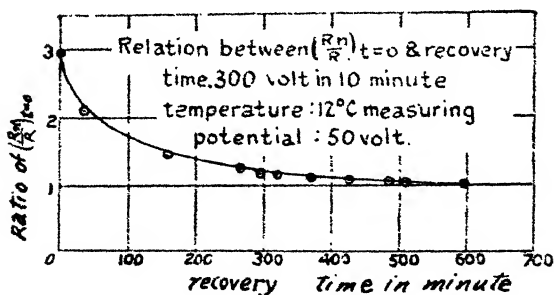


Fig. 9.



and tends to that of the neutral state. The recovery of the apparent resistivity is also quite similar for both cases, namely, when A potential is either positive or negative.

The correction of the residual charge of A potential is mainly made for the point from  $a$  curves in figs. 2-5. When A potential is small the points near the origin in figs. 8-11 are not so affected by the residual charge of A potential as in the cases when A potential becomes large. Thus, as A potential becomes large several points near the

origin except the initial point from a curve are omitted to avoid much effort for the correction of the residual charge. These points are not very necessary to show the general feature of the recovery of the apparent resistivity.

Fig. 10.

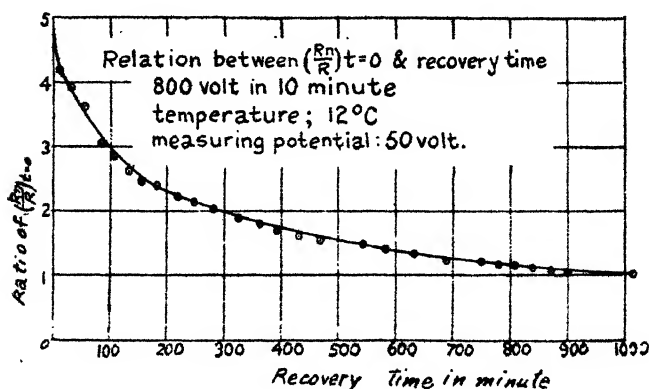
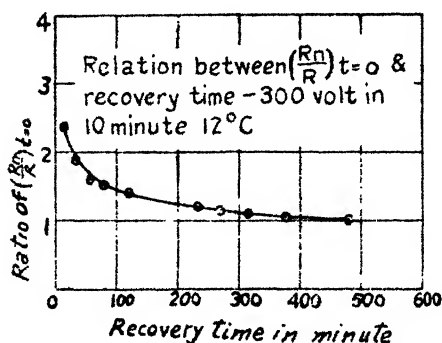


Fig. 11.



### § V. Various Experiments for the After-Effect.

For the purpose of studying thoroughly the nature of the after-effect for the apparent resistivity, the following experiments were made:—

- (1) The case when A potential is smaller than the measuring potential:

The boundary conditions for the experiment are the same as in § IV., but in this case A potential is constant and

equal to 300 volts, and we take the measuring potentials 400, 500, and 600 volts, and every observing time, 1 minute.

Figs. 12-14 show the results of the experiment. In this case the ratio of the apparent resistivity at the neutral

Fig. 12.

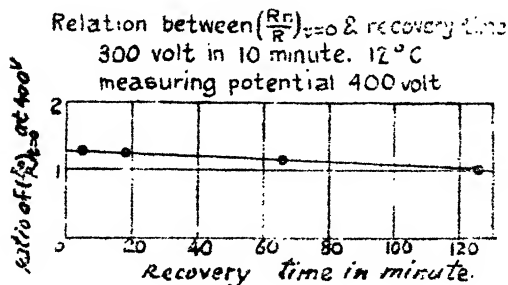


Fig. 13.

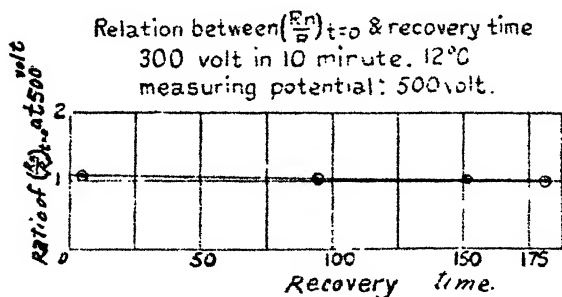
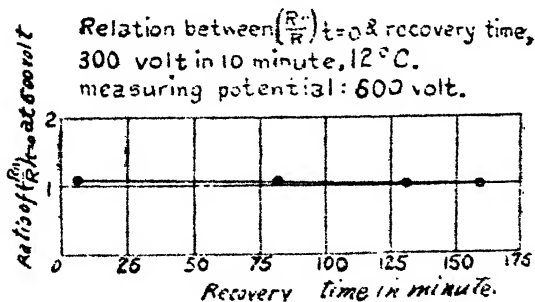


Fig. 14.



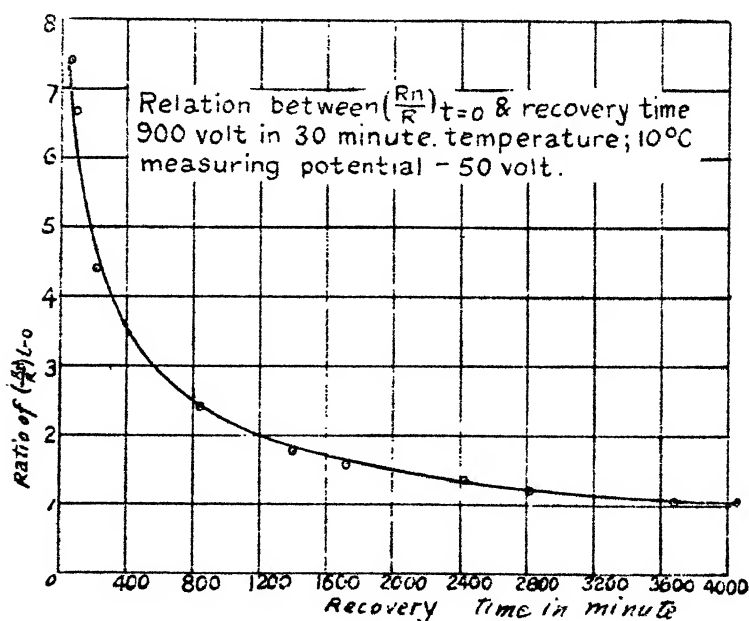
state to that at various times from the beginning of the first earthing is much smaller than that of the case when A potential is larger than the measuring potential, and the recovery time duration is also much less. This variation

becomes small as the measuring potential increases. Thus, the after-effect due to A potential, which is smaller than the measuring potential, is small, and there appears no after-effect where A potential is negligible with respect to the measuring potential.

- (2) The case when the applied time interval of A potential is much longer than the case in § IV. :

Fig 15 shows the decrease of the ratio of the apparent resistivity at the neutral state to that at various observing

Fig. 15.



times with respect to the recovery time. In this case A potential is 900 volts, and its applied time interval 30 minutes, and the measuring potential -50 volts. The after-effect becomes large in comparison with that in § IV.

Fig. 16 shows a similar relation when the measuring potential is +50 volts. In this case, however, the recovery time is smaller than in the case when the measuring potential is negative.

Fig. 17 shows a similar relation to the above, but in this case as A potential 900 volts is first applied during 30 minutes, and after 3 minutes -900 volts is then applied

during 30 minutes, and then the observation is made as in the cases in § IV. In this case the ratio of the apparent resistivity at the neutral state to that at various times up to the neutral state varies similarly with the above case, but the recovery time is nearly equal to the case when fig. 15 is obtained.

Fig. 16.

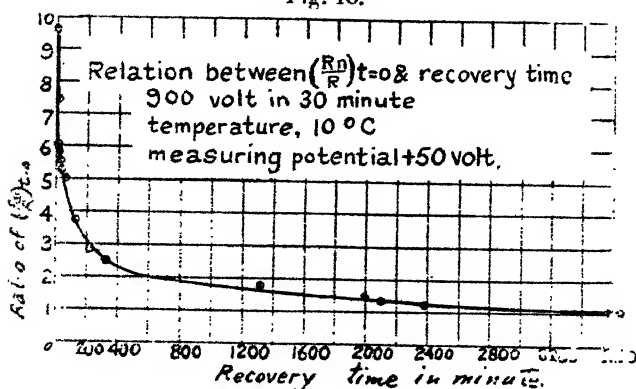
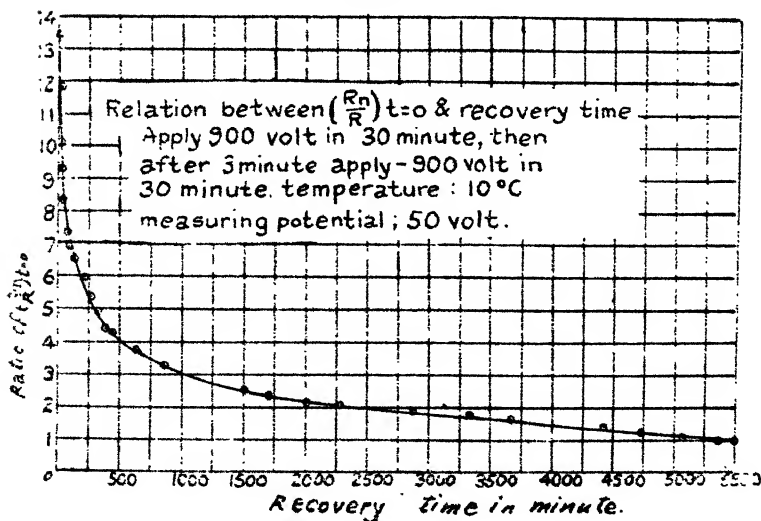


Fig. 17.



No result is shown in this paper, but a cyclic application of A potential between positive and negative was made. And from these results we may state here that the after-effect due to the cyclic application of A potential becomes larger and larger as the number of applications increases,

and gradually tends to a saturated state. And we state here that the after-effect becomes large with applied time interval of A potential, and gradually tends to a saturated state.

### § VI. *Concluding Remarks.*

The anomalous after-effect for the apparent resistivity is one of the interesting and important characteristics of dielectrics for the problem of electrical conduction in dielectrics, and it is a new characteristic of non-metallic crystals.

It is a remarkable fact the the anomalous after-effect appears at the limit potential. Thus, it seems to us that there will be a close connexion among the after-effect, the residual charge, and other dielectric phenomena, such as dielectric hysteresis, etc.

As shown in the present experiment, the recovery time of the after-effect is as long as several hours or more; hence the apparent resistivity of a dielectric is not so easily determined except in the case when the dielectric is in its neutral state. Thus, the apparent resistivity must be defined not only by the charging time, as shown in the former paper, but also by its history of charging.

The anomalous after-effect for the apparent resistivity is exactly the same for both cases when the previously applied potential is either positive or negative; hence the after-effect depends simply on the absolute value of the applied potential, so that it is likely to be due to some nature of the atomic lattice of crystalline dielectrics.

It seems that the after-effect increases rapidly with the time interval of the previously applied potential, and then gradually tends to a stationary value. And by cyclic application of the previously applied potential between positive and negative it also increases and tends to a stationary value.

The after-effect due to a previously applied potential which is smaller than the measuring one is comparatively small, and it becomes smaller and smaller as the former potential becomes smaller and smaller than the latter potential.

In conclusion, we are sincerely thankful to the Saito Gratitude Foundation in Sendai for the financial aid given us for these experiments.

**XLIV. On the Vortex System in the Wake of a Cylinder in a Fluid.** By Prof. H. LEVY and S. G. HOOKER, A.R.C.S., B.Sc.\*

**I**N an investigation of the stability of two parallel rows of rectilinear vortex filaments as they would be originated in the wake of a cylindrical obstacle in unbounded fluid, Karman has found theoretically † that, if  $h$  = distance between the parallel rows, and  $a$  = distance between consecutive vortices of the same row, then the spacing of the stable system, in alternate arrangement, is such that

$$\frac{h}{a} = 0.281.$$

From momentum considerations, moreover, he deduced that the resistance  $D$  of the body giving rise to the system is

$$D = \rho V(2.828 - 1.12 U_0) U_0 h,$$

where  $\rho$  = density of the fluid,

$V$  = velocity of the body,

and  $U_0$  = velocity of the vortex system relative to the obstacle.

In its application to real liquids the assumption was made, of course, that while the fluid was viscous enough to enable the vortices to be generated, it was not so viscous that their strength would decay appreciably during the time taken to establish a fairly long street.

In this formula for resistance the ratios  $\frac{U_0}{V}$  and  $\frac{h}{b}$  ( $b$  being a characteristic linear dimension of the body) were not found by analysis, but required to be determined experimentally. This arose from the fact that Karman's theory did not connect up the established vortex street with the conditions at the obstacle which gave rise to it.

In an extension of the theory, Heisenberg ‡ sought to evaluate these two ratios for the case of a flat plate, from the two following assumptions :—

- (a) A discontinuous surface springs from the edge of the obstacle, and all the vorticity so produced passes down the wake as individual vortices.

\* Communicated by the Authors.

† Karman and Rubach, *Phys. Zeit.* xiii. (1912).

‡ *Phys. Zeit.* xxiii. (1922).



- (b) The amount of fluid swept forward by the plate in its forward motion is equal in volume to the amount of fluid streaming back between the parallel rows.

These lead to the values

$$\frac{U_0}{V} = 0.2295, \quad \frac{h}{b} = 1.54,$$

and therefore

$$k_D = \frac{D}{b\rho V^2} = 0.909.$$

These compare with Karman's experimentally determined values of

$$\frac{U_0}{V} = 0.20, \quad \frac{h}{b} = 1.545, \quad k_D = 0.805.$$

It is important to notice that Heisenberg's assumptions lead to a rate of generation of vorticity  $R = \frac{1}{2}V^2$  at the edge of the plate.

In its experimental application to a wind-channel the effect of the walls on the state of motion and on the resistance has to be considered. This has been dealt with by Glauert \* on the following assumptions:—

(1) In any practical application the breadth  $h$  of the vortex street will not exceed one-sixth of the breadth  $H$  of the channel.

(2) The increase of the suction in the dead-water region behind the body, due to the constraint of the channel walls, is equal to the drop in pressure outside the vortex street far behind the body.

(3) The values of  $K$ ,  $\sqrt{R}$ ,  $\sqrt{S}$ , which are proportional to  $V$  in an unlimited fluid, are assumed to be proportional to a certain effective velocity in the channel, which is the arithmetic mean of the velocities far in front of and far behind the body.

Broadly speaking, the main justification that Glauert advances for the validity of these assumptions is that they are not essentially unreasonable and that they lead to values of  $D'$  and  $k_D'$  which are verified experimentally. He then obtains the following formulæ:

$$\frac{U_0'}{U_0} = 1 - \frac{2\sqrt{2}\frac{U_0}{V}}{1 - \frac{2U_0}{V}} \cdot \left(\frac{U_0 h}{Vb}\right) \cdot \frac{b}{H}, \quad \dots \quad (1)$$

\* Proc. Roy. Soc. A, vol. cxx. p. 34 (1928).

$$\frac{K'}{K} = 1 + \sqrt{2} \cdot \left( \frac{U_0 h}{Vb} \right) \cdot \frac{b}{H}, \quad \dots \quad (2)$$

$$\frac{h'}{h} = \frac{a'}{a} = 1 + \frac{\sqrt{2}}{1 - \frac{2U_0}{V}} \left( \frac{U_0 h}{Vb} \right) \frac{b}{H}, \quad \dots \quad (3)$$

$$k_D' = k_D + 16 \left( \frac{U_0 h}{Vb} \right)^2 \cdot \frac{b}{H}, \quad \dots \quad (4)$$

where  $b$  = breadth of plate,

$H$  = breadth of channel;

the accented letters denote values in the channel, and unaccented ones values in the infinite fluid.

Apart from the difficulty of perceiving adequate physical reasons why precisely these assumptions, and these only, should lead to experimentally verified results, there are one or two criticisms that might legitimately be raised.

Glauert's assumptions lead to the conclusion that  $R$ , the rate of discharge of vorticity at the edge of the obstacle, is given by  $R = V^2$ . In checking his formulæ (1), (2), (3), (4) against experiment, however, he has made use of Heisenberg's values for  $\frac{U_0}{V}$ ,  $\frac{h}{b}$ , and  $k_D$ , which themselves

have been derived on the basis that  $R = \frac{1}{2}V^2$ . This, however, while it throws doubt on the effectiveness of his check, does not in itself affect the validity of the argument leading to the above formulæ.

In actual fact it can easily be shown \* that Heisenberg's assumption (3) applied to Glauert's case would lead directly to  $K = K'$ , a result quite inconsistent with equation (2). It is clear that the two treatments, Heisenberg's and Glauert's, cannot possibly be consistently combined.

Moreover, even if Heisenberg's final results are taken to check Glauert's conclusions, the values obtained from direct experiment by Fage and Johansen for certain other quantities not used by Glauert in illustration, do not provide such happy agreement, as the following table shows:—

$$* \frac{Kh}{a} = V_0 b, \quad \text{and} \quad \frac{K'h'}{a'} = V_0 b. \quad \therefore \quad \frac{Kh}{a} = \frac{K'h'}{a'}.$$

If  $h'/a' = h/a$ , then  $K = K'$ .

Quantity.	Fage and Johansen.	Glauert.
$\frac{h'}{a'}$ .....	$\left\{ \begin{array}{l} (x/b=5.0, 10.0, 20.0) \\ 0.248, 0.381, 0.525 \end{array} \right\}$	0.281
$\frac{K'}{a'V}$ .....	0.74	0.628
$\frac{W-U_0'}{V}$ .....	0.767	0.847
$\frac{a' \dagger}{b}$ .....	5.25	5.84
$\frac{R' \dagger}{\sqrt{a}}$ .....	1.10	1.07
$\frac{k' \dagger}{D}$ .....	1.065	1.052
$\frac{b}{a'} \frac{W-U_0'}{V} \dagger$ .....	0.146	0.146

† Shown by Glauert in illustration.

The above experimental values were obtained by Fage and Johansen from their experiments on a flat plate in a wind-channel, fourteen times the width of the plate. While these values in the cases checked by Glauert appear to provide good agreement, serious divergencies occur in other cases, notably in such fundamental values as the spacing of the vortices and the strength of the vorticity.

Before drawing any hard and fast conclusions therefrom, it is necessary to consider more closely the possible accuracy of some of the experimental values. A detailed examination of the work of Fage and Johansen makes it certain that their values of the drag coefficient  $k_p'$ ,  $f$ , the frequency of the vortices, and therefore the longitudinal spacing, are accurate. Difficulties however arise, as the experimenters themselves indicated, in connexion with the lateral spacing  $h'$  of the two rows, for this involves the specification of the centre of each moving vortex. For this purpose the experimenters determined the positions of maximum and minimum velocity outside and inside the street respectively, taking a point midway between these positions as the centre. While the position of the maximum was very definite, the same could not be said for the position of the minimum, where a fair margin of error might result. This means that quantities in the above table, depending for their value directly on the lateral spacing, are subject to possible inaccuracy. One vital point, however, appears to be certain—that Fage and Johansen\*, working over a range of twenty diameters in the wake of the obstacle, find that the

\* Roy. Soc. Proc. A, cxvi. p. 170 (1927).

Karman ratio  $\frac{h}{a}$  specifying the spacing is, with one exception, much greater than 0.281; the difference is too great for this to be accounted for by an error in the measurement of  $h$ . Moreover, it cannot be traced to the image effect of the channel walls, for L. Rosenhead\*, who has given a complete investigation of the stability of the double row in the channel, finds that the stability ratio  $h/a$  is given by

$$\frac{h}{a} = 0.281 - 0.090 (a/H)^6,$$

where  $2H$  is the breadth of the channel, and in the presence of walls is therefore always less than 0.281. As long as the values of  $h/a$  stand, viz. 0.248, 0.381, 0.525 at distances of 5, 10, and 20 diameters respectively behind the body, deductions as regards resistance drawn from an assumed constant arrangement specified by 0.281 can hardly be reliable. *Between 5 and 20 diameters the spacing ratio increases by over 100 per cent.*

These experimental results then, if they are to be accepted, seem to suggest that the vortex street does not in fact behave stably in the wake of a body in a channel, in spite of the mathematical theory.

It becomes of some interest therefore to examine whether the assumptions made in establishing the stability of the vortex street in these circumstances are sufficiently valid for the purposes in hand. These assumptions are comparatively simple, and may be detailed as follows:—

(1) The viscosity of the fluid is presumed to be sufficient to allow of the origin of the vortex street, but not sufficient to effect any appreciable decay.

(2) The vortices are presumed concentrated throughout the whole process as filaments, so that no spread under viscous action takes place.

(3) The distribution of basic velocity, *i.e.*, the flow upon which the vortex effect is superposed, is presumed constant across the channel.

The experimental work of Fage and Johansen, and their efforts to determine the centres of the vortices by measuring their radii, are sufficient to show that the assumptions (1) and (2) are not realized in practice. Whether this is sufficient to invalidate the theory is a matter for examination.

\* Phil. Trans. A, ccxxviii. pp. 275-329.

Assumption (3), on the other hand, may be seen almost from the beginning to involve a possible serious error. In a uniform channel in which there is no obstacle there is no doubt that over a wide portion of the section the mean velocity distribution is fairly constant, although it drops to zero at the walls; but it is not at all clear that when an obstacle is inserted the full distribution of velocity can everywhere in the wake be completely analysed into two simple constituents, viz. :—

- (a) A uniform distribution throughout,
- (b) That due to the idealized vortex street.

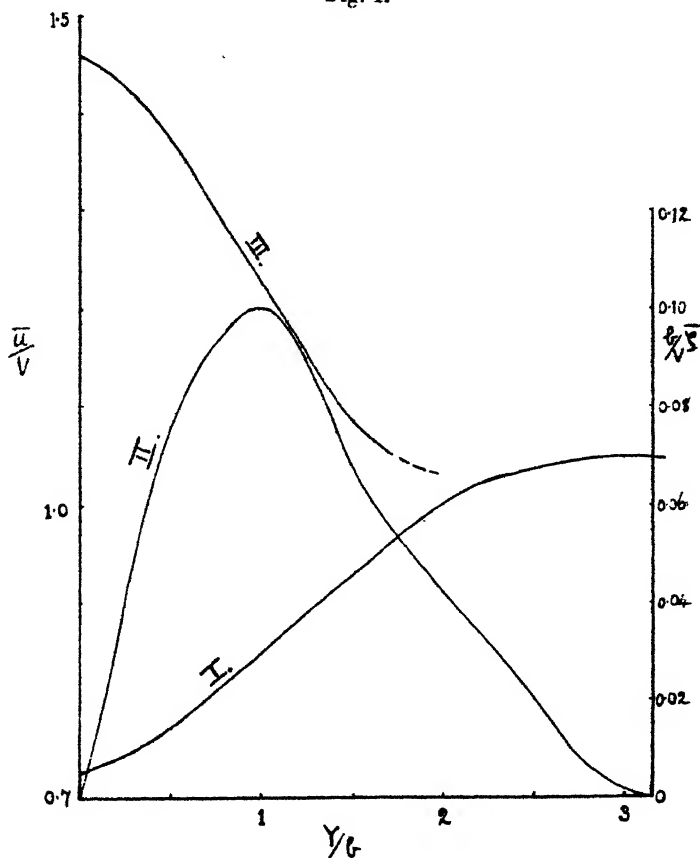
The point has, apparently, not been dealt with by any of the writers on this subject. In a very wide channel, where the *body* is in motion along the axis, there appears no reason to suspect the contrary, and, in fact, Karman and others appear to have found his arrangement verified\*. In the normal case of a wind-tunnel test, on the other hand, where the *fluid* moves past the stationary body at a speed corresponding to a Reynolds' number well above the critical value for the channel, conditions are very different. Along the walls it is known that there develops a boundary layer whose depth increases down wind, and, if turbulent, may spread well into the centre of the channel. Although the walls, regarded as completely replaced by images, may have little direct influence on the arrangement of the vortices shed behind a body in such a channel, as Glauert and Rosenhead have shown, the vortices themselves may have a considerable effect on the spreading boundary layer by drawing out the vorticity in that layer until it intermingles with that concentrated in the individual eddies that have sprung from the edge of the body. Thus the eddies of positive sign shed from one edge of the body may be expected to be swept along in a milieu of negative vorticity drawn from the boundary layer, and the negative eddies from the opposite edge in one of positive vorticity. Such a state of affairs may make a considerable difference to the conclusion as regards stability, since the vortices would be in motion in a field in which a velocity gradient existed. From the experimental work of Fage and Johansen† it is, in fact, quite simple to examine whether such a basic velocity gradient actually exists.

\* It is to be expected nevertheless that the Karman spacing would be a function of Reynolds's number, but this does not appear to have been examined experimentally.

† Fage and Johansen, p. 194.

In fig. 1, Curve I.\* is the mean velocity at various points across a section of the channel in the rear of a flat plate at a down-stream distance of ten breadths of the plate. Curve II., obtained from Curve I. by graphical differentiation, and verified by integration back to it, gives the mean vorticity across the same section. It will be seen that the

Fig. 1.



general shape is similar to that of a skew frequency curve. According to Fage and Johansen the centre of the vortex is situated at  $Y/b=1.0$ , and its inner and outer boundaries lie at  $Y/b=0$  and  $Y/b=2.0$ .

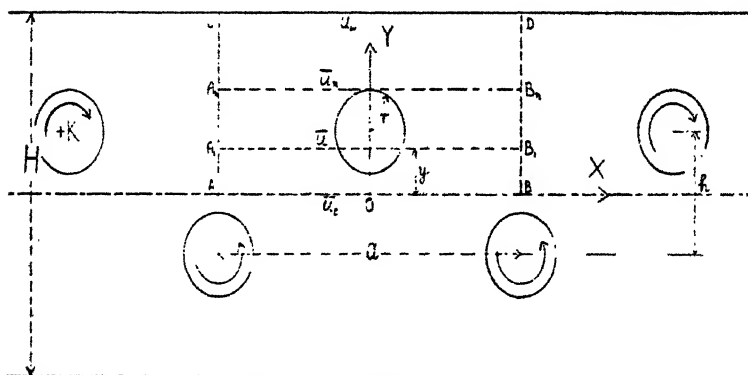
The validity of the assumption that the whole vortex may be regarded as concentrated at one position ( $Y/b=1.0$ )

\* *Loc. cit.* p. 188.

becomes doubtful if the spread and asymmetry of this curve are noted. This distribution of vorticity and the corresponding distribution on the other half of the channel will correspond to an equivalent gradient in velocity. We have to examine whether this can be wholly accounted for by the individually concentrated vortices assumed in the simplified analysis. It may be remarked that the total vorticity as determined from this curve amounts to 0.32, whereas the strength adopted for the concentrated vortices was 0.74, indicating a strong basic field of negative vorticity.

Since it is the mean velocity which is measured experimentally at points in a wind-channel, let us seek in the first place the mean distribution, across the channel, of the

Fig. 2.



velocity due to a street of eddies of finite circular areas with constant vorticity  $\omega$ . Fage and Johansen have found that the diameter of these eddies is approximately equal to the width of the street. At a distance of ten diameters down-stream neighbouring vortices appear to be at least three diameters apart; but it is clear that since the diameter (as seen in fig. 1, Curve II.) is not very clearly defined, the effect of neighbouring vortices on each other's sectional shape will not be as pronounced as if they were entirely confined to the circular regions here assumed. At any rate, we shall assume as a rough approximation that they can move forward as a system without change of shape.

In fig. 2,  $CD$  represents a period lengthwise along the channel. From symmetry the flow across  $AC$  and  $BD$  is everywhere at right angles to these lines. If  $A_n B_n$  does

not intersect an eddy, then, taking the circulation round  $A_n B_n D C A_n$ , we have

$$I(A_n B_n' D C A_n) = 0,$$

$$i. e., \quad \int_{A_n B_n} u \, dx = \int_{C D} u \, dx,$$

$$\text{or} \quad \bar{u}_n = u_w,$$

where  $\bar{u}_n$  and  $u_w$  are respectively the mean velocities along  $A_n B_n$  and the sides of the channel.

Thus the mean horizontal velocity at all points outside the street due to the vortex system is constant, and equal to that at the channel wall. We shall see in a moment that, in fact, this is zero.

Again,

$$I(ABDCA) = -K = -\pi r^2 \omega$$

where  $K$  is the total vorticity in the eddy,

$$\int_{AB} u \, dx - \int_{CD} u \, dx = -K,$$

$$i. e., \quad u_c - u_w = -K/a,$$

where  $u_c$  is the mean velocity along the centre of the channel.

Now it is easily demonstrated that the mean back flow along the centre of the channel is  $K/a$ , *i. e.*,

$$u_c = -K/a.$$

Hence also

$$\bar{u}_n = u_w = 0.$$

Thus the mean effect on the fluid outside the street is zero, while between the rows the vortices continue to pump the fluid back towards the obstacle. We note incidentally that the mean slip due to the vortices of the fluid at the boundary is zero.

Considering a circuit such as  $(A_1 B_1 D C A_1)$  we find immediately

$$ua = -(\text{Area of circle enclosed in the circuit}) \times \omega$$

$$= -\omega \left\{ \pi r^2 - r^2 \cos^{-1} \left( \frac{h/2 - y}{r} \right) \right.$$

$$\left. + \left( \frac{h}{2} - y \right) \sqrt{r^2 - \left( \frac{h}{2} - y \right)^2} \right\}.$$



At points removed from the street the circular vortices are equivalent to line vortices of strength  $K$  where

$$K = \omega \pi r^2,$$

$$u = -\frac{K}{\pi a} \left\{ \pi - \cos^{-1} \left( \frac{h-2y}{2r} \right) + \left( \frac{h-2y}{2r} \right) \sqrt{1 - \left( \frac{h-2y}{2r} \right)^2} \right\}.$$

This is the expression for the mean down-stream velocity due to the street, and holds for positive values of  $y$  between  $\frac{h}{2} - r$  and  $h$ . Fage and Johansen found experimentally that the diameter of the vortices was approximately equal to the distance between the rows, i. e.,

$$r = \frac{h}{2}.$$

In this case, if  $Y = y/h$ ,

$$\bar{u} = -\frac{K}{\pi a} \left\{ \pi - \cos^{-1} (1-2Y) + (1-2Y) \sqrt{1 - (1-2Y)^2} \right\},$$

when  $0 < Y < 1$ ,

and  $\bar{u} = 0$ , when  $1 < Y < \frac{H}{2h}$ .

At a distance of ten breadths behind the plate the following experimental values were obtained :

$$\frac{K}{aV} = 0.74, \quad \frac{h}{b} = 2.0,$$

where  $b$  = breadth of the plate, and

$V$  = undisturbed velocity at a distance in front of the plate.

Substituting these values in the above formulæ for the mean velocity distribution, this can be plotted across the channel. Subtracting this from the experimentally determined mean velocity distribution, we obtain the basic flow which is given by fig. 1, Curve III. This curve indicates that there is a distinct gradient of velocity over the region where the vortex trail exists, and this must be assumed to arise from that vorticity which exists in the fluid and has not been accounted for in the concentrated vortices of the Karman street. Where the centres of the vortex exist this basic velocity (fig. 1, Curve III.) would appear to have a gradient of approximately  $-0.3$ .

The stability analysis must therefore be considered *de novo* without the assumption made by Glauert and others that there is a uniform distribution of velocity across a section. It will, in point of fact, be seen that with a basic distribution of the type we have derived from the analysis of the experimental results of Fage and Johansen the system is no longer stable.

Another point to be noticed is that the assumption that the vortices are circular eddies of constant velocity is by no means necessary in determining the basic flow, but was adopted here by reason of its simplicity. Any type of vortex could have been similarly dealt with, and so long as its area was such that it did not extend for any considerable distance over the centre of the channel the gradient in velocity would not be affected to any material extent. In any case which is at all consistent with the experimental results this gradient will be negative, and will persist of the same magnitude for a great distance down the channel, though ultimately damped out by the viscous action.

Returning to the stability investigation of a vortex street in a bounded fluid, we consider only that case which arises in practice, *i. e.*, the case when the street is confined to the more central portions of the channel. Under these circumstances the effect of the images on the arrangement has been shown by Glauert and Rosenhead to be negligible, and the following discussion will therefore deal only with the effect of the basic velocity in the channel upon the stability of the vortex street.

Take the axis of  $X$  down channel and the axis of  $Y$  in the plane of the motion at right angles to this. Assume that the basic velocity is steady and is given by

$$u = V_0 f(y/H).$$

The vortices are presumed to be moving down-stream in parallel rows situated along the lines  $y = \pm h/2$ . Then the fluid along these lines will be moving with velocity

$$u = V_0 f\left(\frac{h}{2H}\right),$$

due to the basic flow, and the vortices will be travelling down-stream with velocity

$$V_0 f\left(\frac{h}{2H}\right) - u_0,$$

where  $u_0$  = velocity due to the mutual interaction of the

vortices, which is dependent upon their individual strength and the dimensions of the street.

If a vortex in the upper row receives a displacement  $\beta$  in the  $y$  direction, its velocity due to the general motion in the channel will be

$$u + \delta u = V_0 f\left(\frac{(h/2 + \beta)}{H}\right) = V_0 f\left(\frac{h}{2H}\right) + \frac{\beta V_0}{H} f'\left(\frac{h}{2H}\right)$$

to first order in  $\beta$ .

The equations of motion of the displaced system of vortices, as found by Karman \*, are :

$$\frac{2\pi\alpha^2}{K} \frac{d\alpha}{dt} = -A\beta - B\alpha' - C\beta',$$

$$\frac{2\pi\alpha^2}{K} \frac{d\beta}{dt} = -A\alpha - (A' + B)\beta',$$

where

$$A = \frac{1}{2}\phi(2\pi - \phi) - \frac{\pi^2}{\cosh^2 k\pi},$$

$$B = \text{pure imaginary}$$

$$0 < \phi < 2\pi, k = h/a,$$

$$C = \frac{\pi^2 \cosh k\phi}{\cosh^2 k\pi} - \frac{\pi\phi \cosh k(\pi - \phi)}{\cosh k\pi}.$$

Following the usual method we see that, when a basic velocity distribution is taken into account, to the first of the above equations of motion, a term,

$$-\frac{2\pi\alpha^2}{K} \frac{V}{H} f'\left(\frac{h}{2H}\right)\beta,$$

must be added, due to the basic flow. This is negative, because the velocity producing the vortices is in the opposite direction to  $\frac{d\alpha}{dt}$ . Thus the equations of motion of the system

in a bounded fluid, neglecting the image effects, become

$$\frac{2\pi\alpha^2}{K} \frac{d\alpha}{dt} = -A\beta - B\alpha' - C\beta' - \frac{2\pi\alpha^2}{K} \frac{V}{H} f'\left(\frac{h}{2H}\right)\beta,$$

$$\frac{2\pi\alpha^2}{K} \frac{d\beta}{dt} = -A\alpha - (A' + B)\beta'.$$

For convenience, write

$$\theta = \frac{2\pi\alpha^2}{K} \frac{V}{H}, \quad \text{and} \quad f'\left(\frac{h}{2H}\right) = S.$$

\* *Loc. cit.*

Hence  $\theta^2$  is a positive non-dimensional quantity, and  $\frac{VS}{H}$  is the gradient of velocity across the lines  $Y = \pm \frac{h}{2}$ .

The previous equations can now be written

$$\frac{2\pi a^2}{K} \frac{d\alpha}{dt} = -(A + \theta^2 S)\beta - B\alpha' - C\beta',$$

$$\frac{2\pi a^2}{K} \frac{d\beta}{dt} = -A\alpha - C\alpha' + B\beta'.$$

These have two types of solution :

$$(i.) \quad \alpha = \alpha', \quad \beta = -\beta',$$

$$(ii.) \quad \alpha = -\alpha', \quad \beta = \beta',$$

and exponentials  $e^{\lambda t}$  are involved, the corresponding values of  $\lambda$  being

$$\frac{2\pi a^2}{K} \lambda_1 = -B \pm \sqrt{(A+C)(A-C+\theta^2 S)},$$

$$\frac{2\pi a^2}{K} \lambda_2 = B \pm \sqrt{(A-C)(A+C+\theta^2 S)}.$$

The coefficient  $B$  being purely imaginary, it follows that for stability both quantities under the root sign must be negative, i. e.,

$$\begin{aligned} (A+C)(A-C+\theta^2 S) &\leq 0, \\ (A-C)(A+C+\theta^2 S) &\leq 0. \end{aligned} \quad 0 < \phi < 2\pi$$

These are the conditions for stability, and are analogous to Karman's single condition

$$A^2 - C^2 \leq 0, \quad 0 < \phi < 2\pi.$$

Now, when  $\phi$  is small,

$$A \doteq \pi\phi - \frac{\pi^2}{\cosh^2 k\pi},$$

$$C \doteq -\pi\phi + \frac{\pi^2}{\cosh^2 k\pi}.$$

Hence the condition

$$(A-C)(A+C+\theta^2 S) < 0$$

becomes

$$-\frac{2\pi^2}{\cosh^2 k\pi} \theta^2 S \leq 0.$$

But since  $S$ , the measure of the basic velocity gradient, is negative, the condition for stability is violated. It appears therefore that when the velocity gradient is negative there is no stable arrangement of the vortex street in the region remote from the walls. It may be remarked, however, that if the vortex street were wide enough, the effect of the images on the motion arising from any displacement of the original system would be, in a sense, contrary to that of the velocity gradient. Thus a possible stable arrangement may exist in which  $h$  is only slightly less than  $H$ , but this does not correspond to the practical case.

The instability of the vortex street in a channel in which the fluid is in motion past a fixed obstacle is, in fact, borne out by the measurements of Fage and Johansen, who at 5, 10, and 20 diameters behind the obstacle find spacing ratios  $h/a$  of 0.248, 0.381, 0.525, indicating a systematic spread of the vortex street.

In the light of the foregoing discussion it appears clear that the theoretical results obtained by Glauert and others on the assumption that the Karman arrangement is maintained stably and unimpaired in a flowing channel do not possess a valid physical basis.

The experiments of Karman and Rubach, on the other hand, were concerned with the motion of a body along a channel in which the fluid was at rest. In these, of course, the calculated arrangement was substantially verified at the particular value of Reynolds's number for their experiments.

#### XLV. *On the Damping of a Pendulum by Viscous Media (Aniline).* By F. E. HOARE, M.Sc., A.R.C.S.\*

##### *Introduction.*

**I**N a former paper † the equation

$$\log \frac{a_0}{a_1} = K_1 \sqrt{\frac{\eta T}{r^2 \rho}} + K_2 \cdot \frac{T^2}{x r^{3/2}} \frac{a_0 - a_1}{\log \frac{a_0}{a_1}}$$

was deduced to represent the damping of the oscillation of a simple pendulum when the bob was immersed in water

\* Communicated by Prof. F. H. Newman, D.Sc.

† Phil. Mag. ser. 7, viii. p. 899.

where the notation is as previously. The extent to which this equation is theoretically justified is difficult to estimate, but it represents the experimentally observed facts with a fair degree of accuracy, giving mean values for the viscosity  $\eta$  within a few per cent. of the correct value when the constants  $K_1$  and  $K_2$  have been found from the results obtained with one pendulum, and these values then used in conjunction with the results from other pendulums. It was suggested\* that the physical meaning of  $K_1$  and  $K_2$  might be found from further experiments, using different liquids, and with that objective in view the following experiments have been made.

### *Experimental.*

The experimental procedure followed was the same as that formerly employed. Three spheres,  $1\frac{1}{2}$  in.,  $1\frac{3}{4}$  in., and 2 in. diameter, suspended by fine wires, were allowed to oscillate in aniline (kindly loaned by Messrs. Baird and Tatlock, London), this liquid being chosen as it has a comparatively high viscosity and can be obtained in a fairly pure condition. Each pendulum was allowed to oscillate first with a short period and then with a long period, the amplitude being observed after a few swings had been made ( $a_0$ ) and then again after ten complete vibrations ( $a_1$ ) for each value of the period. The method employed in reading the amplitudes with a telescope having proved very satisfactory in the previous experiments, it was again used in the present work.

Unfortunately, it was impossible to use such large quantities of aniline as of water, and consequently a much smaller containing vessel was used. The dimensions of this were 9 inches deep and 7 inches in diameter, the aniline nearly filling the vessel. These dimensions may be sufficiently small to necessitate a correction for enclosed space such as has been deduced by Stokes†; as, however, the correction of Stokes is obtained from the theory which starts from the assumption that the decay of amplitude is proportional to the velocity, and this assumption has been shown to be erroneous by the previous experiments, it was considered that there would be little justification in employing such a correction.

\* *Loc. cit.*

† Stokes, Camb. Phil. Soc. ix. p. 8.

At the conclusion of the experiments the viscosity of the aniline was determined by the flow-tube, method using the Poiseuille formula. The result was in very good agreement with the value generally accepted \*, and from this and a determination of the density at 11.3° C. it was concluded that the aniline was sufficiently pure to give results which should agree with the values already mentioned.

### *Results.*

The method of testing the application of the equation is the same as in the previous work. Any two results were selected, actually in this case being the first observed result for the 2 in. sphere when vibrating with a long and short period, and these were used to calculate the values of  $K_1$  and  $K_2$  by substituting the correct values for  $\eta$  and the observed values of  $a_0$  and  $a_1$ . Using these values for  $K_1$  and  $K_2$ , the value of  $\eta$  for each of the results obtained with the different spheres was computed.

The values of the constants thus obtained are

$$K_1 = 5.81,$$

$$K_2 = 6.41,$$

the amplitude being measured in cms.

The density as determined at 11.3° C. was 1.02, grs. per c.c., and this value has been used throughout in the calculations.

The following table gives the mean value of the viscosity as determined, using the different spheres :—

Sphere.	T, secs.	Number of Observa- tions.	Temp. ° C.	Mean value for $\eta$ c.g.s.	True value for $\eta$ c.g.s.
1½ in.....	2.56	6	14° C.	.0558	.0551
1½ „ .....	3.64	6	10.4° C.	.0604	.0637
1¾ „ .....	2.558	6	12.9° C.	.0585	.0575
1¾ „ .....	3.656	6	10.8° C.	.0600	.0627
2 „ .....	2.57	6	12.7° C.	.0624	.0581
2 „ .....	3.644	6	10.2° C.	.0637	.0645

\* Kaye and Laby, 'Physical and Chemical Constants,' p. 30.

The values in the last column are obtained by interpolation from the values in Kaye and Laby's book of Constants.

### *Discussion of Results.*

From these results it will be seen that in the case of each sphere the short-period observations give values for the viscosity which are too high, and the long-period observations values which are too low. This systematic variation from the true result can, perhaps, be attributed to three causes. The first and most obvious is some defect in the proposed equation which was not apparent when dealing with water. The second cause may be that aniline is hygroscopic and that during the course of the experiments the viscosity gradually decreased. As all the short-period results were taken first this would account in part for the systematic error, but it would probably be of a smaller magnitude than that indicated. Lastly, there is the neglect of any correction for the enclosed space; and this might be some function of the time of swing.

The values of the constants  $K_1$  and  $K_2$  obtained in the case of water and in the case of aniline do not suggest any simple relation connecting them with other properties of the liquid which might have been expected, and until the mathematical theory is rigorously developed to take into account the term which represents the damping due to the square of the velocity more experimental work will be of little use.

### *XLVI. Positive and Negative Photophoresis of Colloidal Particles in Aqueous Solutions. By WILFRED W. BARKAS, M.Sc.\**

**I**N a previous paper (Phil. Mag. vol. ii. pp. 1019-26, 1926) experiments are described which seem to show the phenomenon of photophoresis in aqueous solutions. If suspensions of copper, silver, gold, or gamboge, set up in a rectangular glass cell (some 10 cm. square and 1 cm. thick) are allowed to settle in the dark for

\* Communicated by Prof. A. W. Porter, F.R.S.



several hours, the falling particles (if of sufficient size to settle out) form a horizontal cloud surface some few millimetres below the surface of the liquid. When the cell is illuminated through one of its edges and viewed through the flat faces, it is found after a time that the cloud surface is no longer horizontal, the particles appearing to drift towards the source of light and to heap themselves up on the light side of the cell. The cloud surface takes up a characteristic formation, while the boundary to the cloud in the suspending medium becomes very sharply defined.

The present paper divides itself into two sections ; the first deals with further experiments similar to those described in the former paper with modifications of the apparatus, the second with observations made on separate particles in the ultramicroscope.

### I. CLOUD-DRIFT EXPERIMENTS.

The glass cell chosen was smaller than before, being about 4 cm. square and 0.8 cm. in thickness. The top of the cell was closed by means of a glass plate, held in place by a tightly-fitting cap of celluloid, enabling the cell to be totally immersed in a thermostat tank. The tank was of plate glass about  $20 \times 6$  cm. and 16 cm. deep. The cell was placed cross-wise in the tank so that it could be illuminated through only 1 cm. of water, and viewed from one end of the tank. Instead of a lamp heater, a coil of resistance wire (immersed in a thin test-tube full of paraffin oil) was used, and the control and stirrer were designed so as not to obstruct the view of the cell. It was found that the temperature could be kept constant to  $0.3^\circ$  C. in the neighbourhood of  $18^\circ$  to  $25^\circ$  C. The whole tank was placed in a light-tight box about 25 cm. cube made with square openings in its four faces into which could be fitted opaque stops to control the illumination of the cell. The stirrer and control leads entered through a hole in the lid of the box, the stirrer not being connected with the table in any way, so that vibrations of the motor were avoided.

The source of illumination was, as before, a pointolite placed about one metre away, the beam being focussed (after passing through a thick cooling cell) by means of an achromatic lens. This part of the apparatus was mounted

so that it could be easily moved from one side of the tank to the other.

With these precautions it was considered that extraneous disturbances such as temperature changes and vibrations would be eliminated. Under these conditions the former experiments on suspensions of gold, silver, and gamboge were repeated with results identical with those described before.

The following tests were made to determine if the effect was due to convection currents in the liquid.

(A) Removing the cooling cell and concentrating the beam of light into the body of the suspension usually set up true convection currents. These always took up a spiral formation, there being usually more than one centre of convection. The cloud, which was previously horizontal, became churned up and very irregular in optical density. The final condition of the suspension was one of complete mixing, *i. e.* there was no tendency, once convection had occurred, for the cloud to take up the stable and characteristic form described before.

(B) A test was made on a cloud of true solution. The cell was filled with water and a few crystals of potassium permanganate were dropped into it. This was set up in the thermostat and allowed to stand until the permanganate solution had diffused up as a horizontal cloud of decreasing density but of fairly sharp upper boundary. On illuminating the cell in the usual way, no sign of movement of the cloud could be observed after two hours' exposure. On removing the cooling cell and concentrating the beam, convection currents were observed as described in the previous section.

(C) On varying the thickness of the cooling cell, no change in the speed of cloud formation could be observed unless true convection currents occurred.

Further, it should be noticed that the phenomenon was first observed in the case of a suspension set up in a room containing several windows which were illuminated in turn in the course of the day. The cloud always followed the brightest window, though no sunlight fell on the cell itself at any time. It seems unlikely that there could be sufficient temperature gradient across the cell, in this case, to affect the particles.

It would seem therefore, from the results of the above tests, that convection is not the primary cause of the phenomenon.

### *Intensity of Illumination.*

On reducing the intensity of the light on the cell, a point is reached where no photophoresis occurs, even after prolonged exposure. At this stage the photophoretic effect is completely masked by the brownian diffusion of the particles. It is this diffusion which causes the cloud to reassume its former horizontal form after the light has been extinguished.

### *Colour of Illumination.*

No very satisfactory results could be obtained for the drifting of particles under monochromatic illumination, either by the use of filters or by selecting a band of wavelengths from the spectrum. Presumably the intensity of such a selected beam was not sufficient to overcome the diffusion of the particles. In one instance, however, with a purple gold sol, very slow cloud-drift was obtained with both red and green filters, the direction being negative on Ehrenhaft's convention in each case\*. The filters were judged (visually) to be of approximately equal optical density. Thinner filters produced more rapid cloud formation.

Ultra-violet light from a mercury arc was also used. No definite results could be obtained, however, even when the cell was removed from the thermostat tank to avoid absorption by the water. Since photophoresis occurs under X-ray illumination, we may suppose that an insufficient intensity of light was the cause of the null results.

It is hoped to undertake further work in this connexion.

### *Positive Photophoresis in Liquids.*

In the sols so far tried, namely gold, silver, copper, and gamboge, the photophoresis is in each case negative, *i.e.* the motion is towards the source of light. It was found, however, that an oil suspension (prepared by stirring a solution of paraffin oil in alcohol into a large volume of

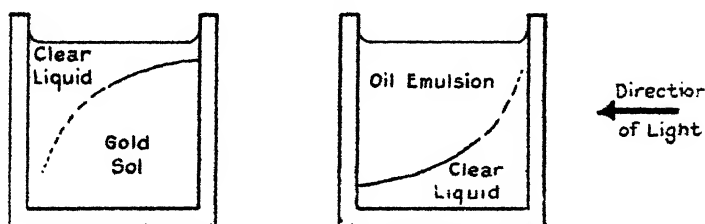
\* *Phys. Zeits.* xviii. pp. 352-368 (1917); *Ann. d. Phys.* no. 10, pp. 81-132 (1918).

water) showed equally marked positive photophoresis, the cloud drifting away from the source of light. This is the only instance so far observed of positive photophoresis in aqueous suspensions. The oil particles being lighter than water, rise upwards from the bottom of the cell and, on illumination, move over to the top corner away from the source of light. Owing to the white colour of the suspension it is not possible to photograph the cloud, but the formation is exactly similar to the case of negative drift reversed, of course, in direction (fig. 1).

## II. MICROSCOPIC OBSERVATIONS.

In order to observe the drift in separate particles, a modification of the Zsigmondy ultramicroscope was first used (fig. 2). Light from the slit was concentrated through the second lens, in the usual way, and reflected down

Fig. 1.



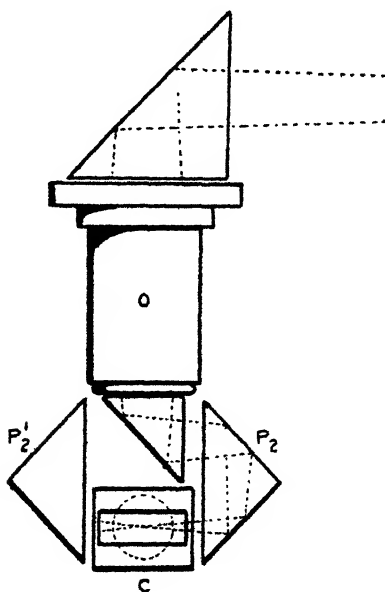
Cloud formation after action of light.

vertically into a low-power condensing objective (O) which brought the light to a focus some 3 cm. distant from the front face. On the front lens was fixed a small silvered right-angled prism which turned the light-beam horizontal. The objective and the prism could be rotated through  $180^\circ$  about a vertical axis, thus sending the beam either right or left as desired. The cell (C) was a one-piece glass trough 1 cm. in length with optical glass ends. This was placed vertically below O and was illuminated by means of the two prisms ( $P_2$  and  $P_2'$ ) placed one on each side of (C) as shown in fig. 2. The cell was viewed through the microscope placed with its axis horizontal, the focus of the light being coincident with the axis of the microscope. (The microscope objective is indicated by a dotted circle in the figure.) The prisms  $P_2$  and  $P_2'$  were mounted on the stage of the microscope, whose usual adjustments allowed for the necessary centring of the light-beam, while

the cell was mounted on a bracket passing back through the centre of the stage and connected to the condenser mount of the substage. By these means it was possible to change the direction of the light by a simple rotation of the objective "O" through  $180^\circ$ , no re-focussing being necessary. The whole of this portion of the apparatus was heavily lagged with cotton-wool to shield it from external temperature changes.

The eyepiece contained a squared graticule placed so that one set of lines was parallel to the light-beam.

Fig. 2.



First method of illumination.

The suspensions used were of the same materials as before, but were not identical with the former ones, for the following reasons:—First, the concentrations suitable for viewing in the ultramicroscope were necessarily much lower than those used in section I. As a result the solution was not sufficiently concentrated for the cloud to be seen with the naked eye, and hence no estimate could be made of the distance below the free cloud surface at which the observations were made. Secondly, owing to the somewhat delicate adjustments required for setting up a

solution for viewing, it was not practicable to use a suspension which settled out under gravity. Hence only such suspensions were used as remained indefinitely in suspension, or whose rates of sedimentation were extremely slow. In the case of the large-scale experiments, it was found that no free cloud surface was formed on illuminating a suspension of non-settling particles. This does not mean, however, that no motion of the particles would take place along the path of a restricted beam of light, as an equal and opposite motion would be possible, by diffusion, in the un-illuminated parts of the cell, tending to equalize the distribution throughout the solution. In the microscope the illumination is restricted to a narrow beam in the centre of the cell, so that the motion, if observed, would be due to the action of the light, as the back diffusion would take place outside the field of view.

Owing to the rapid brownian movement of the particles, no general drift can be observed in the microscope, and it becomes necessary to follow a large number of particles and average the results.

The first method adopted was to observe the time taken by any particle to move one square up or down the light-beam. The light was changed in direction after every three or four observations to avoid any tendency to static equilibrium of the cloud under the action of the light.

Preliminary tests on silver particles gave, in general, a larger number going upstream (negative photophoresis) than in the opposite direction, while the average velocity of both groups of particles was very nearly equal. In quantitative measurements the following results may be cited as typical :—

TABLE I.

Sol.	No. of particles moving one square.		Velocity in cm./sec. $\times 10^4$ .		Ratio of numbers.	Ratio of velocities.
	+ve.	-ve.	+ve.	-ve.		
Gold .....	124	148	1.26	1.41	1.19 -ve	1.12 -ve
Paraffin oil ...	42	39	3.0	3.52	1.07 +ve	1.11 +ve

In many cases, however, the ratio of the numbers and the velocities were not both of a sign corresponding to

the large-scale experiments, and it soon became apparent that there were several disadvantages in this method of measurement. These were:—(1) The average velocity of the cloud as a whole, apart from the brownian motion, could not be calculated because, unless the time of observation is the same for all particles, the probable distance moved under the molecular bombardment alone will not be the same for all particles. (2) There is no direct means of obtaining a measure of the radius of the particles observed. (3) The time taken for a particle to cross one square in the eyepiece is, in some cases, several minutes, which makes the observation of large numbers of particles very tedious. Larger magnifications could not conveniently be used. Finally (4), owing to the size of the cell required for transverse illumination, the possibility of small convection currents could not be overlooked.

For these reasons the method of observation was changed, and at the same time the apparatus was modified to the use of a Zeiss dark-ground cardioid condenser, the microscope this time being vertical.

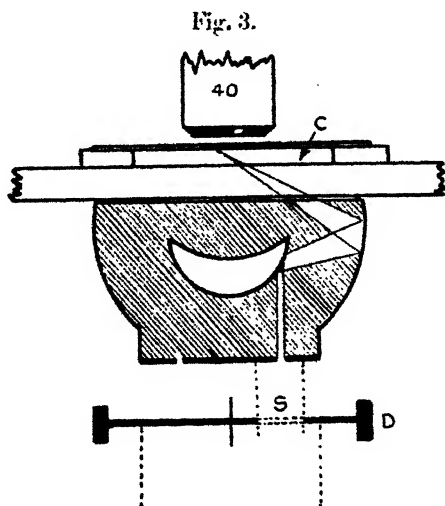
The light from the arc was rendered accurately parallel by means of the usual two bench lenses of the ultramicroscope. It issued as a horizontal beam of about 1.5 cm. diameter, and was reflected through a right angle on to the underside of the cardioid (fig. 3), giving the usual dark-ground illumination in a cell (C) about 0.2 mm. deep placed on the microscope stage. The walls of this cell were made of strips of cover-slip mounted on the slide in the form of a square about 1 cm. side. These were smeared with vaseline and the cell filled with the solution. It was sealed by a full-sized cover-slip pressed down lightly from above to remove the excess liquid. The horizontal position of the cell and its extreme thinness assured a minimum of convection currents in the liquid.

Since the cardioid condenser gives a flat cone of illumination, a particle, viewed along the axis of the cone, is equally illuminated on all sides. In order to introduce unidirectional illumination, a circular diaphragm (D) having a single radial slit (S) about 1 mm. wide was placed in the position of the usual iris diaphragm, under the cardioid, on the substage of the microscope. When in position, a small segment only of the annular aperture of the cardioid was illuminated, and, by rotating the stop, the ray could be made to enter the cell from any desired

direction. The substage could be swung out when full illumination was desired.

The ray actually enters the cell at an angle of  $40^\circ$  to the horizontal, but, by racking the microscope, any portion of the ray in the field of view could be brought into focus.

All observations were made at a height of 0.1 mm. above the bottom of the cell, or, more accurately, each observation was begun at this point, though the subsequent movement of the particle necessitated constant focussing. In order to ensure that the apex of the light-cone should be at this point, it was necessary to be able to rack the cardioid slightly without breaking the film of immersion oil between



Second method of illumination. Cross-section of cardioid condenser with stop for unidirectional illumination.

it and the slide. As the usual cedar-wood oil becomes very viscous on prolonged exposure, it was replaced in these experiments by santal oil (index of refraction 1.506), which was found to remain mobile indefinitely.

A  $30^\circ$  thermometer was mounted with its bulb as near as possible to the cell, and the whole lagged round with cotton-wool.

In order to facilitate timing, a small square of glass was mounted on the top lens of the eyepiece at  $45^\circ$  to the axis, while the stop-watch was placed some 50 cm. away in such a position that it could be seen as a faint "Pepper's Ghost" superimposed on the image of the



particles. The light falling on the watch could be controlled.

A Zeiss 40 objective and a  $\times 12$  eyepiece were used, one side of the eyepiece squares being equivalent to  $8.33 \times 10^{-4}$  cm., the microscope tube being considerably extended to facilitate viewing.

With this apparatus a particle could be viewed for any desired time. The time chosen throughout the experiments was half a minute. Focussing the microscope to 0.1 mm. above the bottom of the cell, the stop-watch was started at an instant when any particle happened to be under a cross in the eyepiece, and at the end of half a minute its position relative to the cross in question was recorded on squared paper. The direction of the light was reversed after every three or four observations, separate records being taken of the movements of particles under these two directions of illumination. The X axis was taken parallel to the light-beam, the positive direction being that of the light.

From these records the following calculations were made :—

### *Radius of the Particles.*

The radius ( $a$ ) of a particle moving under molecular bombardment is connected with the average square of the distance moved  $\bar{S}^2$  in time  $t$  secs. by the equation of Einstein and Smoluchowski :

$$a = \frac{RT}{3\pi N\eta \bar{S}^2},$$

where  $\eta$  = the viscosity of the suspending medium,  $T$  = the absolute temperature, while  $N$  and  $R$  have their usual significance.

In the case of full illumination, the displacements may be taken parallel to any coordinates. In the case of uni-directional illumination, the displacements at right angles to the light-beam only were taken ( $Y^2$ ).

### *Cloud Velocity.*

Neglecting for the moment the brownian movement and any possible drifting of the solution as a whole, due to convection currents, we take the displacements parallel to the light-beam, making the sign of the displacement correspond to the direction of the light.

Suppose  $n_+$  particles move, in the positive direction, an average distance  $x_+$ , and  $n_-$  particles move, in the negative direction, an average distance  $x_-$ , then the distance moved by the cloud of particles as a whole will be given by the displacement of an imaginary partition in the cloud which moves such that the average concentration of particles either side of it remains equal. If we take  $\bar{X}$  to be this displacement, we have that

$$n_+(x_+ - \bar{X}) = n_-(x_- + \bar{X}).$$

Since  $\bar{X}$  is the distance moved in  $t$  secs., the velocity of the cloud,  $V_x$ , relative to the light is given by  $V_x = \bar{X}/t$ .

(Since the motion perpendicular to the light-beam is supposed to be independent of the light, we need only consider the linear distribution of the particles along the  $X$  axis.)

The brownian motion of the particles, being independent of the light, should, on the average, give no displacement of the cloud as a whole, while any convection drift should be eliminated, provided an equal number of observations are made for each direction of the light. No static equilibrium of the cloud is to be expected when the direction of the light is constantly changed. We may, however, calculate the velocity of the cloud, parallel to the coordinate axes, due to accidental convection currents, by use of the above analysis, provided we take the sign of the displacements relative to the cell and not relative to the direction of the light. These results are also entered in Table II. It will be seen that these velocities are in every case very much less than the photophoretic velocity, except in the case of paraffin oil, where it is about one-half.

### *Force acting on the Particles.*

Since the force ( $F$ ) required to impart a velocity ( $v$ ) on a particle of radius ( $a$ ) moving in a fluid of viscosity ( $\eta$ ) is given by

$$F = 6\pi\eta av,$$

we may obtain this force from the calculated values of " $a$ " and  $V$  as given above, or directly from the observations of  $Y$  and  $\bar{X}$  giving

$$F = \frac{2RTX}{N\bar{Y}^2},$$

which is independent of the viscosity of the liquid.

Since, however, the light-beam enters the cell at an angle of  $40^\circ$  to the focal plane of the microscope, the values of the force given above must be multiplied by secant  $40^\circ$  (1.307) to give the force acting along the light-beam necessary to produce the observed velocity in the focal plane.

*Pressure acting.*

Assuming that the force acts parallel to the light-beam, we may obtain the pressure acting as

$$P = F/\pi a^2.$$

In terms of the actual observations made, this is  $P = 6\eta v/a$ , or

$$P = \frac{18\pi N\eta^2}{RT} \cdot \frac{X}{t} \cdot \frac{Y^2}{t}.$$

$P$  being proportional to  $\eta^2$ , any error in the measurement of the temperature will cause a large error in the value of the pressure.

RESULTS.

The results are tabulated in Table II.

Columns 3 and 4 give the number of particles observed and their average velocities in positive and negative directions. The velocities are given in squares per half minute.

Column 5 gives the velocities of the cloud in cm./sec.  $\times 10^6$ , the sign being relative to the direction of the light.

Columns 6 and 7 give the velocities of the cloud along the X and Y axes respectively in cm./sec.  $\times 10^6$  relative to the cell and independent of the direction of the light. These are the convection velocities.

Column 8 gives the mean square of the displacements in half a minute (in terms of the eyepiece scale) perpendicular to the light.

Column 9 shows the average value of the radius of the particles (in cm.  $\times 10^5$ ) calculated from these displacements or by other means.

Columns 10 and 11 give the force (in dynes  $\times 10^{11}$ ) and the pressure respectively.

In the first experiments A, B, and C the method of recording did not permit of obtaining the convection-

TABLE II.

1.	2.	3.	4.	5.	6.	7.	8.	9.	10.	11.
	Number of particles.	$\pi^+$	$\pi^-$	$\pi^+$	Convection along X axis (cm./sec. $\times 10^6$ ).	Convection along Y axis (cm./sec. $\times 10^6$ ).	Mean square of displacement (Y axis).	Mean radius, cm. $\times 10^6$ .	Force acting, dynes $\times 10^{11}$ .	Pressure, dynes/sq. cm.
(A) Gamboge uncentrifuged.	55	0.459		23	0.566	32	0.35	1.91	-3.22	-0.281
(B) Silver .....	78	0.631		33	0.674	45	0.498	1.34	-2.09	-0.361
(C) Gold No. 2 ..	60	0.592		25	0.548	35	0.331	1.26	-1.15	-0.232
Ditto .. ....	52	0.562		21	0.490	31	0.405	1.69	-1.42	-0.137
(D) Gold No. 1 ..	130	0.358		62	0.418	68	0.336	1.49	-0.917	-0.0075
(E) Gamboge centrifuged.	105	0.707		43	0.703	62	0.731	2.68	-2.28	-0.111
Ditto, with full illumination to test size only .....							0.689	2.82		
Ditto, size given by method of fractional centrifuging .....							approx. 2.64			
(F) Paraffin oil ...	84	0.737	51	0.725	33	1.89 (left)	0.734	2.65	+2.26	+0.141
Ditto, with full illumination to test size only .....						2.86 (up)				
Ditto (fresh sample) ..	82	0.715	48	0.742	34	0.17 (right)	0.883	2.26	+1.75	+0.0093
Ditto, with full illumination to test size only .....						2.70 (up)	0.782	2.49		
							0.855	2.45		

current velocities. This was remedied in the later experiments.

*Expt. E.*—A centrifuged suspension of gamboge was used and the values of the radius compared. From the centrifuge the radius should be in the neighbourhood of  $2.64 \times 10^{-5}$  cm.

*Expt. F.*—Two samples of the same suspension. The results show the positive photophoresis in paraffin oil.

These results all confirm the indications given in the large-scale experiments in section I. and in the previous paper \*, and show that, on the average, migration of the particles does in fact take place under the action of the light. The actual velocities of the cloud appear, however, to be much less than those calculated in the previous paper. On the other hand, the velocity of cloud-drift, in the large-scale experiments calculated from the motion of the upper surface of the cloud, is a maximum value, and must vary from this value near the surface of the cloud down to zero for points near the bottom of the cell.

Comparing these results with those found by Ehrenhaft for photophoresis in gases, we see that in the case of gold and silver the motion in water is opposite to that in air. In a particular case among his results † silver particles of radius  $1.36 \times 10^{-5}$  cm. are used, and these are sufficiently close to those given in Expt. B above to afford a comparison. Owing to the different viscosities of nitrogen and water, we should not expect the same velocities in the two cases, but for the forces acting we have :—

Silver particles.	Radius.	Force.
In nitrogen (Ehrenhaft) .....	$1.39 \times 10^{-5}$ cm.	$19.83 \times 10^{-11}$ dynes
In water (Barkas).....	$1.34 \times 10^{-5}$ cm.	$2.09 \times 10^{-11}$ dyne.

Making allowances for the smaller intensity of illumination from the cardioid condenser as compared with that of the true ultramicroscope as used by Ehrenhaft, we may say that the forces involved in the two cases are of the same order of magnitude, though of opposite sign.

\* *Loc. cit.*

† *Phys. Zeits.* xviii. p. 353 (1917).

The aim of the present paper, however, is principally to show that both positive and negative photophoresis occur in liquids, and to support the view that the observed motions are not due to convection currents in the suspending liquid as a whole. The number of particles observed in the experiments of section II. is not sufficient to yield very accurate quantitative values of the radius of the particles, but even on this number the *direction* of the cloud-drift is quite definite.

My thanks are due to Professor A. W. Porter, F.R.S., and to Professor E. N. da C. Andrade, D.Sc., for their assistance in connexion with the above work.

Carey Foster Laboratories,  
University of London.  
University College,  
Nov. 1929.

---

XLVII.—*The Band Spectra of Cadmium and Bismuth.* By  
S. BARRATT and A. R. BONAR. *Department of Chemistry,*  
*University College, London* \*.

THE difficulties often encountered in discovering the nature of the molecule responsible for a new band spectrum are well evidenced by the frequent controversies to be found in spectroscopic literature over problems of this type. To the list of spectra of elusive origin must certainly be added the absorption-band spectra which are developed in the vapour of cadmium metal when the specimen is of the usual grade of purity. These bands, which have several times been employed in the calculation of the heat of formation of the cadmium molecule, etc., were first described by Mohler and Moore (J. Opt. Soc. Amer. xv, p. 74, 1927), who distinguished several band groups in the spectrum, and attributed them all (with a reservation in respect of two) to a cadmium molecule of the type Cd<sub>2</sub>. In a subsequent paper (J. M. Walter and S. Barratt, Proc. Roy. Soc., A, cxxii. p. 201, 1929) experiments were described which indicated that six of the seven groups were due to the presence of impurities, only Group I. of Mohler and Moore at  $\lambda$  2212 being a true cadmium

\* Communicated by the Authors.

spectrum. This conclusion was reached as the result of two series of observations :—

(1) Specimens of cadmium from different sources show large variations in the relative intensities of the band groups, while it is possible to suppress all the spectra (except Group I.) by adding to the cadmium vapour a trace of an alkali metal, the addition leaving unaffected both Group I. and the atomic absorption. The alkali metal presumably combines in a preferential way with the impurities, yielding compounds which are either non-volatile or possess no absorption in the regions under examination.

(2) The various groups of bands can be individually intensified by adding to the vapour further quantities of certain impurities.

As the result of such experiments Groups III., IV., and V. of Mohler and Moore (lying between  $\lambda$  3181 and  $\lambda$  3018) were attributed to a compound of cadmium and chlorine, probably the subchloride  $\text{CdCl}$ . This conclusion has been amply confirmed in this laboratory by further work, which will shortly be ready for publication, on the cadmium subhalide spectra. Groups VI. and VII. (between  $\lambda$  3323 and  $\lambda$  3182) were attributed to the absorption of thallous chloride vapour, present as an impurity in the cadmium. At that time this spectrum was otherwise unknown, but it has since been very fully examined (as the thallous chloride spectrum) by K. Burkow (*Zeitschrift für Physik*, lviii. p. 232, 1929), and we now have ourselves many plates of the spectrum, recorded from pure thallous chloride vapour, showing no trace of cadmium absorption\*. It would therefore seem that the origins suggested in the previous paper for Groups III. to VII. are no longer open to serious question.

Group II. of Mohler and Moore ( $\lambda$  2856– $\lambda$  2644) is of greater interest, but we believe that the new facts concerning this spectrum, which are detailed below, fix its origin

\* R. K. Waring (*Phys. Rev.* xxxii. p. 435, 1928) has described this same spectrum as the mercury-thallium spectrum, as he observed it in the absorption spectrum of the vapours of a mercury thallium mixture. Thallium metal, unless specially treated, always contains traces of chlorine, which are quite sufficient to account for this observation. The agreement between his measurements on the bands and those of the authors quoted above is quite satisfactory.

with a reasonable degree of certainty. The origin previously suggested for this spectrum (Walter and Barratt, *loc. cit.*) was the molecule of a cadmium-oxygen compound, not the normal oxide, but possibly one of the type  $\text{Cd}_2\text{O}$ . The experimental evidence for this suggestion was the enhancement of the spectrum caused by the addition of cadmium oxide to the metal in the furnace-tube. It was never found possible, even so, to obtain this band group in the intense development reached by the others (*e. g.*, the  $\text{CdCl}$  bands) on addition of appropriate impurities. This, it was thought at the time, might indicate instability of the suboxide molecule, but it is now realized that the facts have a far more simple explanation. The same spectrum was ascribed by A. Jablonski (*Bull. Acad. Pol.* p. 163, 1928, and *C. R. Soc. Pol. de Phys.* iii. p. 357, 1928) to the same origin as that which had been assigned to it by Mohler and Moore, namely the  $\text{Cd}_2$  molecule, and this conclusion he has recently reaffirmed (*Z. Physik*, lvii. p. 692, 1929). He observed the spectrum both in absorption and in fluorescence. It may also be mentioned that this same spectrum has been described by R. K. Waring (*loc. cit.*) as the spectrum of an indium-cadmium molecule. The conclusion is obviously erroneous, as the spectrum has been obtained by three other workers without the intervention of indium; but the observation is not without interest in view of the results described below. The wave-length comparison in the table leaves no doubt of the identity of Waring's spectrum with that under discussion.

While we had satisfied ourselves, by the experiments described in the previous paper, that this band system was not due to a cadmium molecule, irregularities in the enhancement caused by addition of the oxide to the vapours finally led us to suspect that the hypothesis of a cadmium suboxide molecule was in error. It seemed that the spectrum must be caused by some unsuspected impurity in the cadmium, which was also present, but probably in greater concentration, in the cadmium oxide which we had been using. We made many attempts to produce this spectrum in absorption along the lines suggested by this view, and we finally obtained it from the vapour of a specimen of elementary arsenic in the total absence of cadmium. The same plates, however, also showed the line absorption of bismuth, and, following up



this indication, we were naturally led to examine the behaviour of pure bismuth itself. The vapour of this metal at above  $800^{\circ}\text{C}$ . gave the spectrum in such great intensity that it was evident that its real origin had at last been traced. There was no record whatever of the

Table of Wave-lengths in the  $\text{Bi}_{\infty}$  Spectrum  
(or " $\text{Cd}_2$ " Spectrum).

Mohler & Moore. ( $\text{Cd}_2$ ).	Jablonski. $\text{Cd}_2$ .	Waring. In-Cd.	(W. & B. $\text{Cd} + \text{O}$ ). B. & B. $\text{Bi}_{\infty}$ .	Narayan & Rao. $\text{Bi}_{\infty}$ .
—	—	—	2856	2859.9
—	—	—	2844	2842.9
—	2825	—	2825	2828.2
—	2810	—	2810	2813.5
—	2795	2800.2	2797	2799.8
2781	2781	2787.9	2783	2785.0
2767	2767	2776.3	2769	2772.7
2756	2755	2753.0	2756	2759.6
2745	2745	2741.1	2745	2744.8
2736	2736	2739.7	2732	2732.6
2726	2727	2729.8	2721	2722.0
2709	2708	2712.4	2710	2712.3
2701	2700	2705.5	2699	2701.9
2694	2694	2694.2	2690	2693.2
2680	2678	2684.2	2679	2681.5
2673	2672	2672.1	2673	2670.0
2659	2659	2661.4	2660	—
2653	2654	2652.8	2652	—
—	2646	—	2644	—

sensitive cadmium line  $\lambda$  3261 on these photographs. We next re-examined all the plates obtained in the earlier experiments which recorded the bands in question, and upon each one was found the bismuth atomic absorption line  $\lambda$  3067. Further, fortunately the bismuth band spectra have been previously described, so that immediate confirmatory evidence of our conclusion was available. The ultra-violet absorption bands of bismuth, as listed by

Narayan and Rao (Phil. Mag. l. p. 645, 1925), agree quite well with the measurements on this elusive spectrum made by all the authors mentioned above. We have reproduced the individual wave-length estimates in the following table in order that the identity of the spectra may not be in doubt. If the diffuse nature of the bands be taken into consideration, the agreement between the various observers is most satisfactory.

The wave-length lists are almost complete in each case, except that Jablonski has recorded several additional bands on the short wave-length side, which have not otherwise been measured, and therefore do not assist the comparison.

Our experimental conclusion in respect of these bands may be summarized as follows \* :—

(1) Conditions can be maintained under which the bands do not appear in dense cadmium vapour.

(2) When the bands are recorded from cadmium vapour so is the bismuth absorption line  $\lambda$  3067.

(3) The bands are developed at great intensity in the absorption spectra of bismuth vapour when the sensitive cadmium line  $\lambda$  3261 is absent.

It is only possible to infer that the bands arise from a molecule of bismuth itself or of a bismuth compound. We have examined the behaviour of several specimens of bismuth, and the effects of atmospheres of argon and hydrogen on the spectrum, and also the effect of addition of small quantities of potassium to the absorbing vapours, without detecting any anomaly in the relative intensities of the bands and of the atomic bismuth lines. While the past history of the spectrum inclines one to caution in stating any opinion as to its origin, we believe on the above grounds that it is a true bismuth molecular spectrum. The complexity of the molecule is a more uncertain matter, but having due regard to the very low partial pressures of bismuth at which the bands are observable, it is a reasonable hypothesis that the molecule is  $\text{Bi}_2$ . There is a second extensive absorption-band system of bismuth. It

\* We have thought it unnecessary to give any account of the apparatus used in our experiments, as it remained unchanged from that which has been described in the earlier paper from this laboratory.

is situated in the visible region, and only develops at much higher temperatures than does the system under discussion. These visible bands may possibly be due to a bismuth molecule of greater molecular weight which only appears at higher vapour pressures.

The enhancement of the bands which we found to follow upon additions of cadmium oxide was evidently purely accidental in nature, and was due to the presence of bismuth as impurity in the specimen of cadmium oxide upon which we drew.

The band system, as an inspection of the frequency differences shows, converges towards a short wave-length limit. This convergence limit is given by Jablonski, who has measured the spectrum further in this direction than any of the other observers, as  $\lambda$  2561. If we assume (1) that the molecule from which the bands originate is  $\text{Bi}_2$ , and (2) that on dissociation the molecule breaks up into one normal atom and one in the excited state associated with the "raie ultime" of bismuth,  $\lambda$  3067, then we can calculate in a simple fashion the heat of formation of the molecule. The numerical value so obtained is 0.80 volt or 18.5 Kg. cal. per gm. mol., which is quite a probable figure for a molecule of this type.

Two of the other spectra discussed in the earlier paper (Walter and Barratt, *loc. cit.*) were assigned to associations of oxygen with zinc and mercury respectively. In view of the present results it would seem not improbable that these spectra also are really due to traces of impurities which have not as yet been recognized. We have continued our attempts to identify them, but so far unsuccessfully, and the spectra would certainly repay further examination. The present investigation will suffice to show that the ultimate conclusions may be quite unexpected ones.

#### SUMMARY.

(1) A band spectrum hitherto assumed to be that of a cadmium molecule is shown to be due to bismuth.

(2) On certain assumptions as to the nature of the bismuth molecule its heat of formation is estimated at 18.5 Kg. cal.

XLVIII. *Precision Measurements of X-Ray Reflexions  
from Crystal Powders.*

*To the Editors of the Philosophical Magazine.*

GENTLEMEN,—

I AM greatly obliged to Mr. M. Luther Fuller for his letter in the October number of the *Philosophical Magazine* \*, where he communicates the result of a new determination of the lattice spacing of cadmium oxide by Pierre van Dyck, which agrees closely with the value given by Adamson and myself †, when we proposed cadmium oxide as a standardizing substance for X-ray powder measurements. When determining the lattice constant we investigated whether the difference between our value 4.683 and the result of the previous determinations by Davey and Hoffmann ‡, and by Scherrer §, both giving 4.72, could be attributed to impurities. Records taken with specimens from different sources and with different degree of purity agreed within the limits of error, and it is very gratifying to find that the new determination by van Dyck with extremely pure cadmium oxide prepared from vacuum distilled cadmium gives 4.681, which again agrees with our value within the limits of error. Mr. Fuller mentions that a determination by van Dyck with pure commercial cadmium oxide gave the same value too.

Mr. van Dyck used a standard Davey apparatus with a powder rod, while we used the focussing method described by one of us ‖, and the main object of Mr. Luther Fuller's letter is to point to the agreement between the results, in order to show that the methods are equally precise. I fully agree with him in believing that there is no case for claiming the general superiority of one or the other arrangement. On the other hand, the comparison of particular results offers but a limited opportunity for comparing the merits of different methods. In fact, the

\* M. Luther Fuller, *Phil. Mag.* viii. p. 585 (1929).

† J. Brentano and J. Adamson, *Phil. Mag.* vii. p. 507 (1929).

‡ W. P. Davey and E. C. Hoffmann, *Phys. Rev.* xv. p. 333 (1920).

§ P. Scherrer, *Zeits. f. Kryst.* lvii. p. 196 (1922).

‖ J. Brentano, *Proc. Phys. Soc. Lond.* xxxvii. p. 184 (1925).

precision attained will largely depend on the particular experimental conditions, unless an attempt is made to obtain the greatest possible accuracy, which was not done here. The practical purpose of determining whether one or the other arrangement is better suited in any definite case may therefore be served by indicating some points which lead to a certain differentiation.

The features and merits of the simple arrangement possible with a powder rod, giving at one time a record over the greatest angular range and requiring a very small quantity of powder, are well known.

The focussing method, on the other hand, has been developed to meet definite requirements, for which other methods are not so well adapted; namely, the quantitative measurement of intensities and the exact evaluation of angles of deflexion, in particular, in the region of smaller angles. For quantitative intensity measurements it introduces such relations that the evaluation of relative intensities or different reflexions becomes independent of the dimensions and of the absorption coefficient of the particular powder specimen\*. For the measurement of angles very sharp symmetric lines can be obtained with wide incident beams for any angle of deflexion, and in particular, by placing the photographic film further away from the powder than the entrance slit of the camera, the distance of the recording film can be increased without too great a loss of intensity. This leads to a reduction of the times of exposure, where the evaluation can be derived from the record of a small angular range; for instance, in determining the lattice constant of cadmium oxide the diameter of the beam falling on the powder was 6 mm., corresponding to an angular width of  $2.8^\circ$ , and the lines measured, viz., 400, 331, 420, 422, 333 for cadmium oxide, and 422, 333, 442, 440, 531, 600, 620 for sodium chloride, were comprised within a range of glancing angles  $\theta$  of  $19^\circ$  for  $\text{Cu K}\alpha$  radiation. Again, we can avail ourselves of the focussing condition in order to stress the accuracy of the measurements in the region of small angles of deflexion, the advantage being that the simpler pattern of lines generally found for smaller angles and smaller indices is better adapted for identification than the more complex pattern at

\* J. Brentano, *Phil. Mag.* vi. p. 178 (1928).

larger angles ; for instance, in determining the spacing and the rhombohedral angle of carbonates \*, the measurements were carried out in an angular range which comprised the first reflexions and did not extend to angles greater than  $\theta=47^\circ$ . The determination of the rhombohedral angle depends on small changes in the relative position of individual lines, and it would not have been easy to obtain the necessary accuracy for small angles without recurring to focussing. Here the identification of lines at large angles was difficult when several carbonates were present as impurities.

In the second part of his letter Mr. Luther Fuller endorses our proposal of using cadmium oxide as standardizing substance, and says that he had found that cadmium oxide lines were particularly sharp, sharper than the lines from sodium chloride. Our own finding was that the lines from cadmium oxide were slightly, but distinctly, broadened. This diversity may depend on the particular state of the specimens, although in our experiments the broadening has appeared to be a feature of all specimens examined, and Mr. Luther Fuller has certainly experimented with samples from different sources too. It may also depend on the characteristics of the methods we have outlined above : the practical application of the powder-rod method leading to derive a determination from the measurement of a great number of reflexions and to lay less stress on obtaining great sharpness of the individual line ; the application of the focussing method giving more prominence to the exact record of each single reflexion.

We have pointed out that the broadening of the cadmium oxide lines may actually appear to be a certain handicap in making exact measurements, and I wish, therefore, to explain that a condition which we desired to be implicitly satisfied in selecting a standardizing substance was that it should not only be serviceable as a reference substance for the measurement of angles but also of intensities. This requires that the particles should be so small as to reduce the size of the crystal units sufficiently to make extinction effects negligible, or, at least, that the powder should be sufficiently fine to obtain a uniform average of any residual extinction effect. This restricts the number

\* J. Brentano and W. E. Dawson, *Phil. Mag.* iii. p. 411 (1927); and J. Brentano and J. Adamson, *loc. cit.*

of substances which appear suitable, in particular for substances containing elements of greater atomic weight, where the limit at which primary extinction becomes appreciable can be put at about 100 crystal planes, while much larger units are permissible for crystals constituted of light elements. The limited number of regularly spaced crystal planes reduces the resolving power, and accordingly the sharpness of the lines. It is in this way that cadmium oxide seemed to be best suited among the substances we have investigated with the aim of finding a standardizing substance with great volume absorption and volume scattering.

In the case of sodium chloride, although a very imperfect crystal, extinction effects are by no means negligible, and it has been shown that the ordinary process of grinding will not remove a certain amount of primary extinction \*. Considering the relatively small atomic numbers of its constituents, this corresponds to fairly large crystal units consisting on an average of several thousand layers. Accordingly, sodium chloride lines are practically sharp. This was also found to be the case in our experiments.

These points have a certain bearing on the choice of a standardizing substance. A substance of the type of cadmium oxide covers a wide range of requirements, and, apart from the use for intensity measurements, the fact that it is largely constituted of small crystal units giving little extinction enhances the intensity of the reflexions, a point which has also been noted by Mr. Luther Fuller. On the other hand, it must be recognized that, in order to obtain very sharp lines for the most exact angular measurements, a substance with sufficiently large crystal units must be chosen. This involves considerable extinction, and reduction of intensity in particular, with substances consisting of elements with high atomic numbers.

Paris, 31 Dec., 1929.

J. BRENTANO.

\* Bragg, James, and Bosanquet, *Phil. Mag.* xli, p. 309 (1921); xlii, p. 1 (1921); xlii, p. 433 (1922). R. J. Havighurst, *Phys. Rev.* xxix, p. 882 (1926). J. Brentano, *Phil. Mag.* iv, p. 620 (1927).

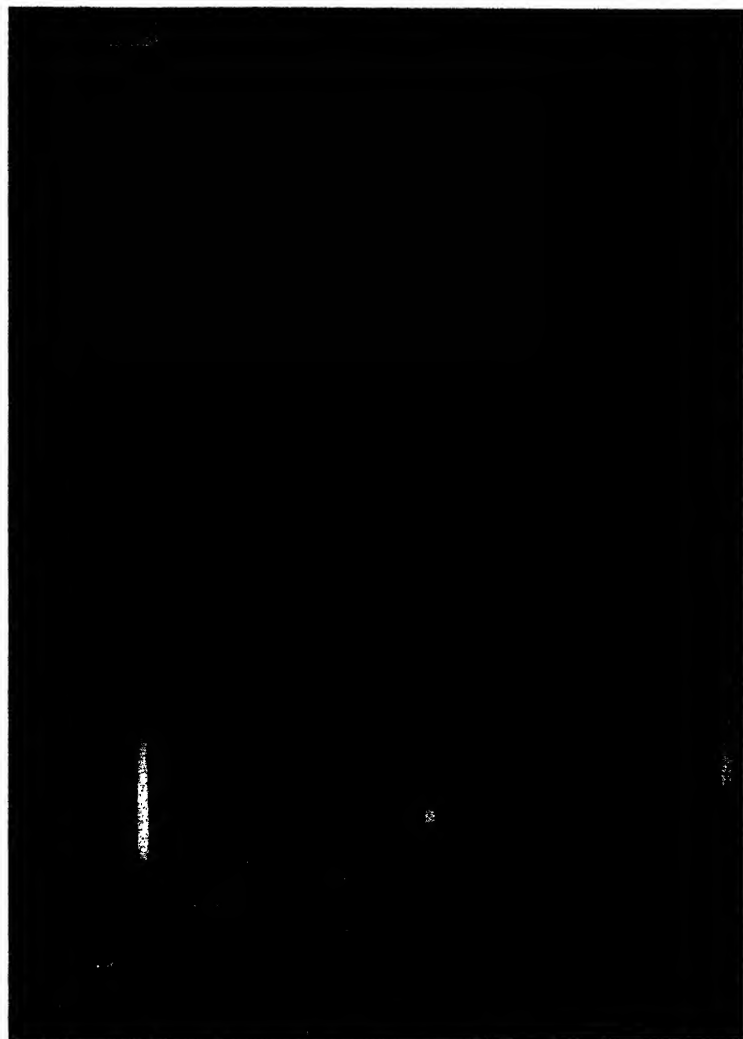
FIG. 1.

FIG. 2.

FIG. 3.

FIG. 4.

FIG. 5.



1.—30 % CO + 70 % Air.	Initial pressure 1 atmosphere.	Fan at rest
2.—20 % H <sub>2</sub> + 10 % O <sub>2</sub> + 70 % N <sub>2</sub> .	"	"
3.—20 % H <sub>2</sub> + 10 % O <sub>2</sub> + 70 % Ar.	"	"
4.—26 % CO + 30 % O <sub>2</sub> + 44 % CO <sub>2</sub> .	"	Fan running at 1500 r.p.m.
5.—26 % CO + 30 % O <sub>2</sub> + 44 % N <sub>2</sub> .	"	"

Speed of film 1 revolution per second in each case.



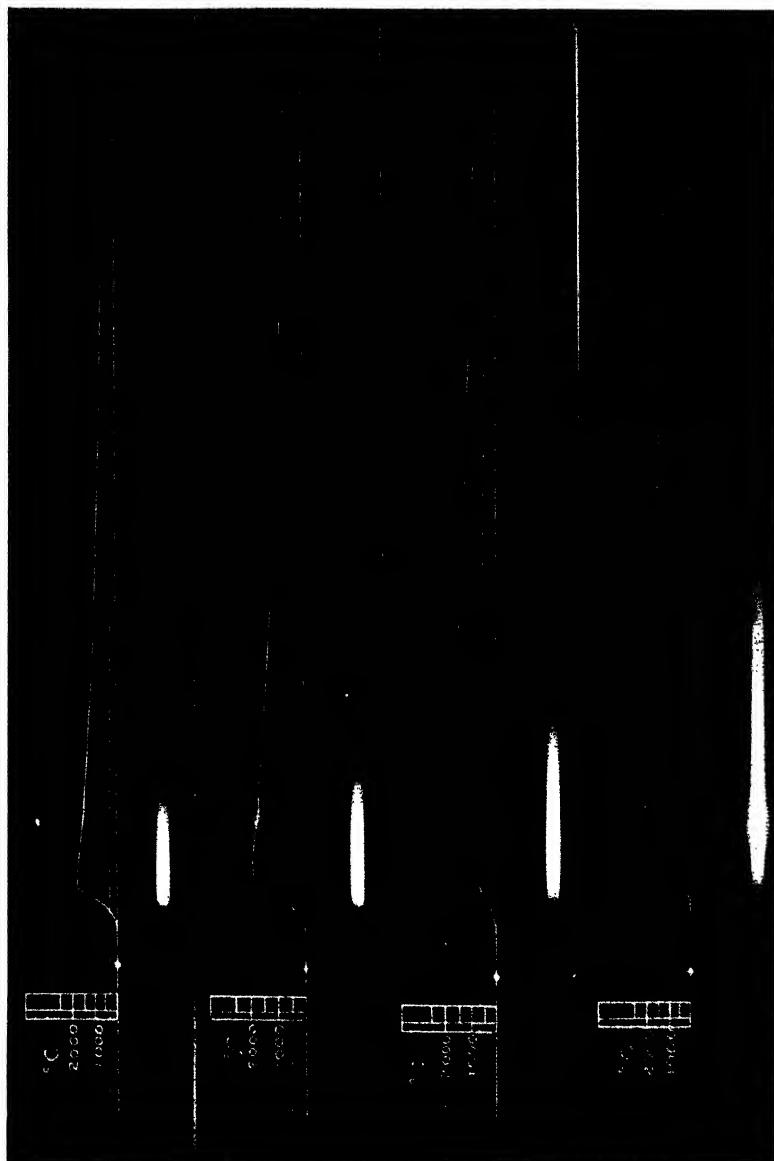


FIG. 6.

FIG. 7.

FIG. 8.

FIG. 9.



- 6.—28% CO+72% Air. Initial pressure  $\frac{3}{4}$  atmosphere. Fan at rest.  
 7.— " " " 1 " "  
 8.— " " " 2 atmospheres. "  
 9.— " " " 3 " "

Speed of film 1 revolution per second in each case.



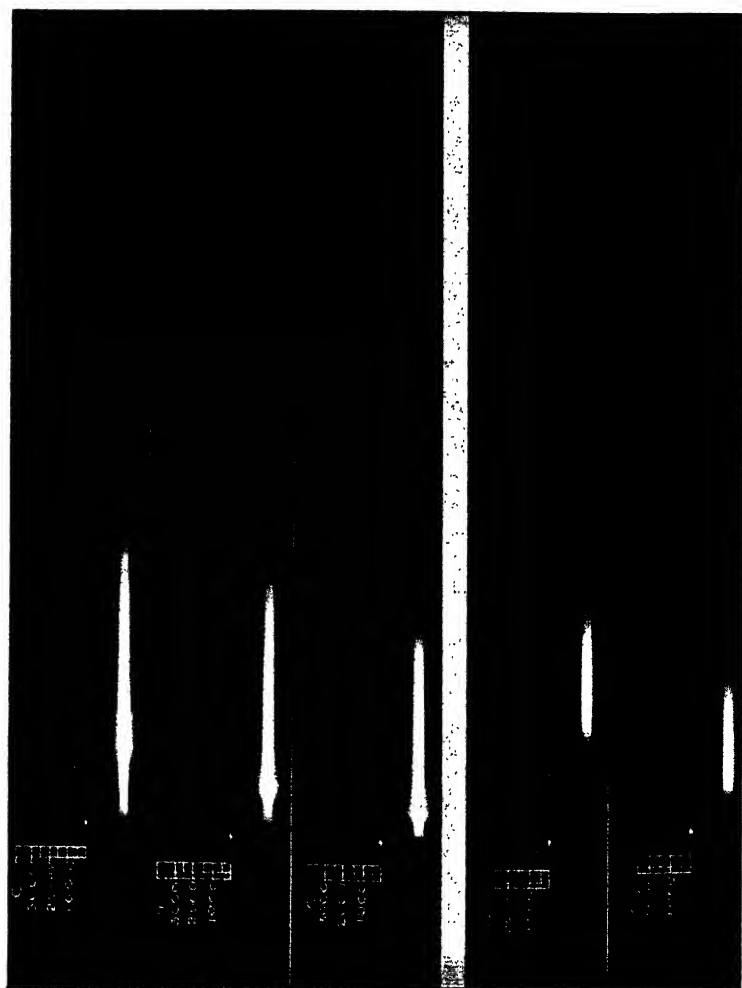
FIG. 11.

FIG. 12.

FIG. 13.

FIG. 14.

FIG. 15.



11. -50% CO + 25% O<sub>2</sub> + 25% CO<sub>2</sub>. Initial pressure 1 atmosphere. Fan at rest.
12. " " " " " Fan running at 1500 r.p.m.
13. — " " " " " 2800 .
14. -35% CO + 65% Air (partially dried). " " Fan at rest.
15. — " " (saturated with water-vapour at 15° C. " " "

Speed of film 1 revolution per second in each case.



FIG. 16.

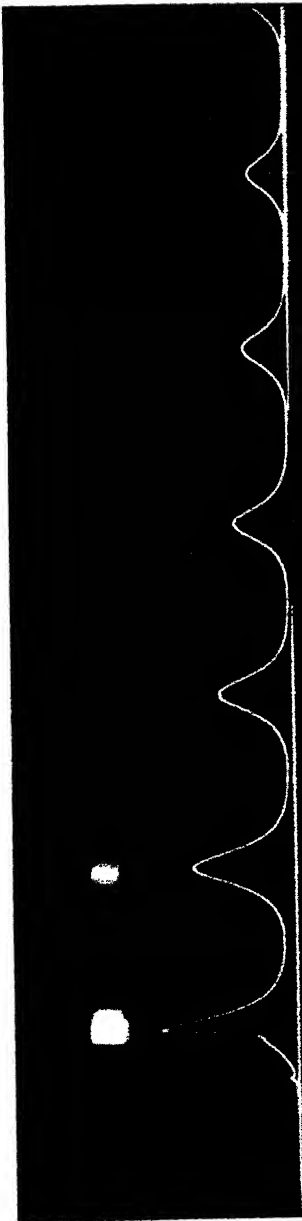


FIG. 17.

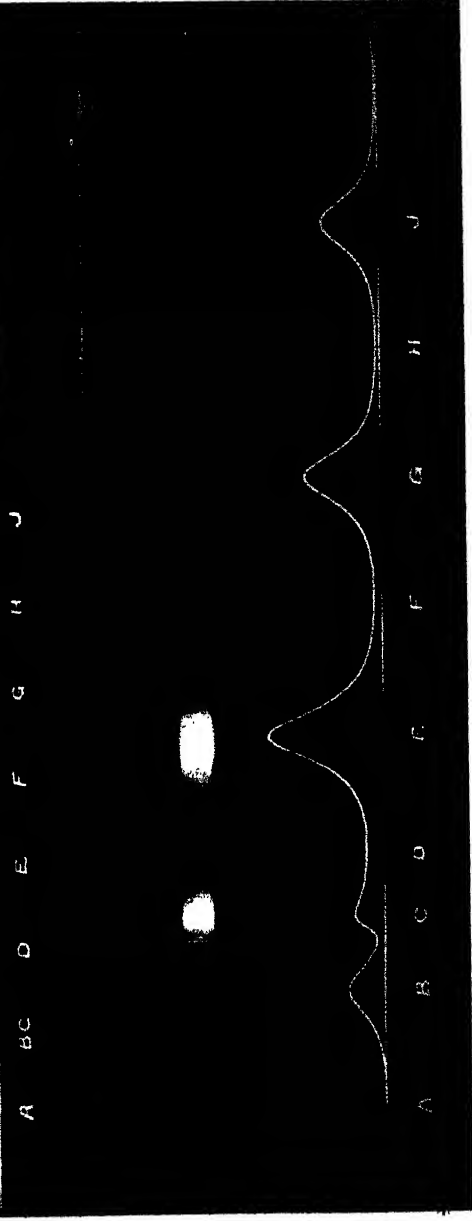
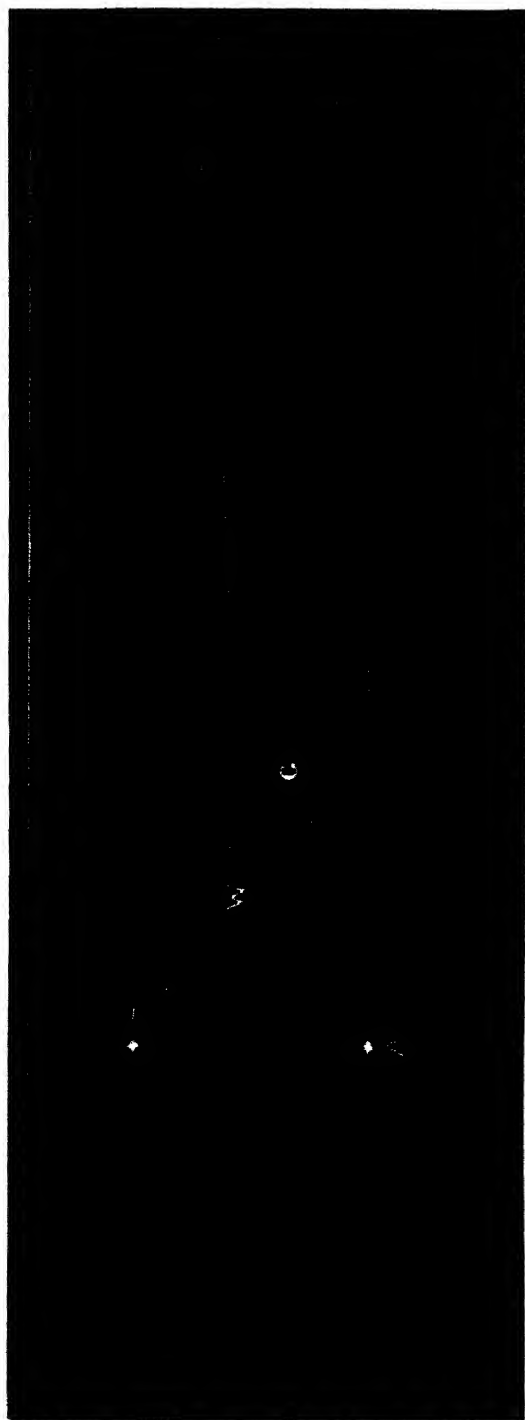




FIG. 2.







THE  
LONDON, EDINBURGH, AND DUBLIN  
PHILOSOPHICAL MAGAZINE  
AND  
JOURNAL OF SCIENCE.

---

[SEVENTH SERIES.]

---

APRIL 1930.

---

XLIX. *On the Cathode Dark Space in the Geissler Discharge.* By E. C. CHILDS, B.Sc.\*

SERIOUS investigation of the cathode (or Crookes's) dark space in the Geissler discharge seems first to have been begun by Aston <sup>(1)</sup> in 1911. As is well known, when a current of electricity is passed between metal electrodes in gases at low pressure, we have, going from the anode to the cathode, the positive glow or column, the Faraday dark space, the negative glow, the Crookes's dark space, and, in a few gases, a very thin region next to the cathode known as the primary dark space. As the pressure of gas decreases, these glows and dark spaces move towards the anode, and at pressures of the order of a millimetre of mercury the positive column and Faraday dark space disappear. It was this type of discharge that was studied by Aston. It was pointed out that for reasons which differ from those commonly accepted nowadays, the distribution of potential and electric field in the region of the cathode dark space cannot be ascertained with any degree of reliability by any method which depends on the introduction of a probe into the discharge. In consequence, a method was devised in which a stream of cathode rays, generated in a side tube, was projected across the main

\* Communicated by Prof. E. V. Appleton, F.R.S.

tube, the deflexion of the spot on a willemite screen being a measure of the electric intensity at right angles to the path of the beam (*i. e.* along the main tube). The conclusion drawn from the results of this experiment was that in such a discharge the fall of potential along the tube is entirely localized in the cathode dark space, the negative glow being wholly at anode potential.

This work led to perhaps a more important investigation <sup>(2)</sup> of the relations holding between the current density, the potential difference across the cathode dark space (and incidentally across the tube), the length of the dark space, and the pressure of gas in a discharge-tube, using various active and inert gases. It was found that the active gases obeyed, to a fair degree of accuracy, the empirical equations :

$$D = A P + B/C^{\frac{1}{2}}, \quad . \quad . \quad . \quad . \quad . \quad . \quad (1)$$

$$V = E + F C^{\frac{1}{2}}/P, \quad . \quad . \quad . \quad . \quad . \quad . \quad (2)$$

in which A, B, E, and F are constants. Throughout this paper the length of the cathode dark space will be represented by D, the potential difference between the electrodes by V, the current density by C, and the pressure of gas in the tube by P.

The behaviour of the inert gases deviated slightly from that of the active gases, and it was found that they obeyed more closely an equation derived by eliminating P between (1) and (2), *i. e.*

$$V - G = K D C^{\frac{1}{2}}, \quad . \quad . \quad . \quad . \quad . \quad . \quad (3)$$

G and K being constants containing A, B, E. and F. These experiments were conducted with a discharge-tube containing a cathode surrounded by a guard-ring, but it was assumed that the current density was uniform over a large proportion of the total area. It will be shown in this paper that this assumption is not valid.

In the light of modern work on space-charge and the current across ionic sheaths, the cathode dark space assumes a new significance. Langmuir <sup>(3)</sup> has shown, both theoretically and practically, that a probe introduced into a gas discharge becomes surrounded by a sheath of electrons or positive ions, according to whether the probe is at a positive or negative potential respectively with respect to the space potential. The potential difference between the probe and the region of the discharge into which it is



rods served to clamp the rings to the plate. The underside of the plate was well waxed to render the assembly air-tight, the leads to the split cathode being soldered to the ends of the rods.

A glass bell-jar was ground onto the base-plate and waxed down, provision for the anode rod and pumping being made at the top by means of a brass cap fitted with two tubes. This tube was constructed by Mr. N. L. Harris, now of the General Electric Company. When it was in use the air was first pumped out by a Cenco Hyvac pump, and then hydrogen was admitted from a coal-gas flame by means of a palladium tube, the gas-pressure being measured by a McLeod gauge, a liquid-air

TABLE I.

Ring.	Inner diameter.	Outer diameter.	Area.
1 .....	0 cm.	2.315 cm.	4.20 sq. cm.
2 .....	2.355 cm.	4.115 cm.	8.95 sq. cm.
3 .....	4.215 cm.	6.075 cm.	15.04 sq. cm.
4 .....	6.150 cm.	7.940 cm.	19.80 sq. cm.
5 .....	8.000 cm.	9.740 cm.	24.25 sq. cm.

trap ensuring that no mercury vapour passed into the experimental tube.

The electrical connexions are shown in fig. 1, in which A is a milliammeter indicating the total current through the tube produced by the battery  $B_1$  and regulated by the saturated diode D. The tube voltage is indicated by the voltmeter V. Each of the cathode rings C is connected to one of a system of mercury cups M, provided with interchangeable links, in one of which is a galvanometer  $a$  and potential divider P fed from a second battery of lead accumulators  $B_2$ .

It will at once be apparent from this that not only can the current to any one ring be measured, but also the potential of any ring with respect to the others can be varied at will.

With this tube the current densities at five different distances from the centre of the cathode were measured. The mean current density over a ring was taken to be the

same as that at a distance from the centre equal to the arithmetic mean of the inner and outer radii. It was found that at the lower pressures, *i. e.* pressures less than about .8 mm. of mercury, the current density was reasonably uniform over all but the outermost of the five rings, but at higher pressures considerably more current passed to the outer rings than to the inner. Such a case is shown in fig. 2, drawn from the data in Table II.

Fig. 1.

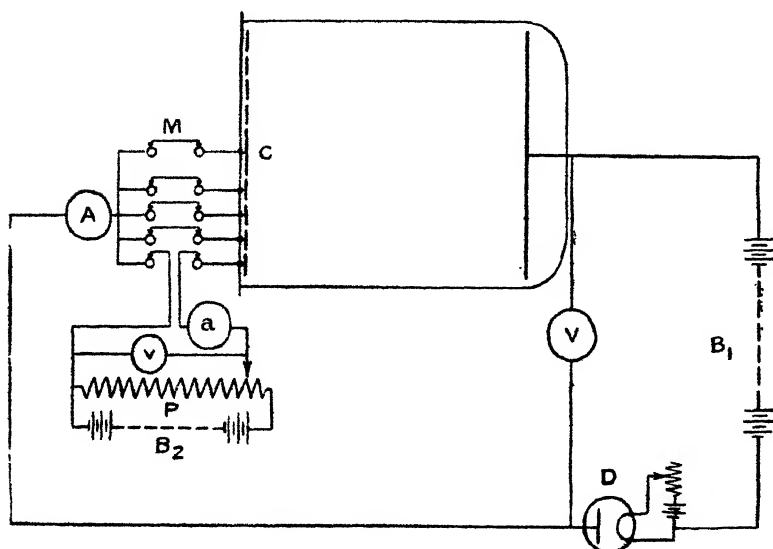


TABLE II.

Gas-pressure = 1.24 mm. Hg.

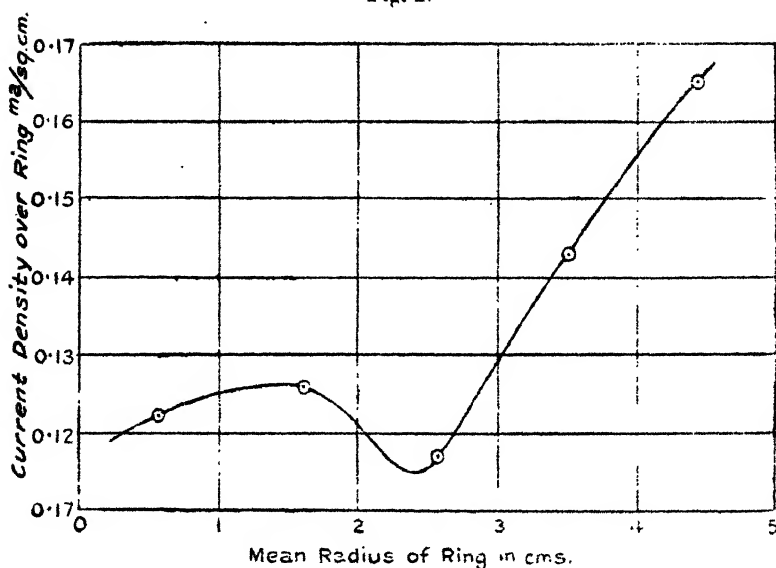
Tube voltage = 240.

Tube current = 10 m.a.

Ring.	Mean distance from centre.	Current density.
1 .....	0.58 cm.	0.122 m.a./sq. cm.
2 .....	1.62 cm.	0.126 m.a./sq. cm.
3 .....	2.57 cm.	0.117 m.a./sq. cm.
4 .....	3.52 cm.	0.143 m.a./sq. cm.
5 .....	4.44 cm.	0.165 m.a./sq. cm.

It must be understood that only those cases have been considered in which the tube current is sufficiently large for the glow to cover the cathode, a condition which has been called the abnormal cathode fall. With low pressures and *small* currents, the current density may fall off to zero at the outer zones of the cathode, but as in such cases the utility of a guard-ring is questionable, we are not concerned with these conditions. With higher pressures and small currents through the tube the glow may disappear, not from the outer edges of the cathode, but from one side, and consequently the current density to the outer rings again

Fig. 2.



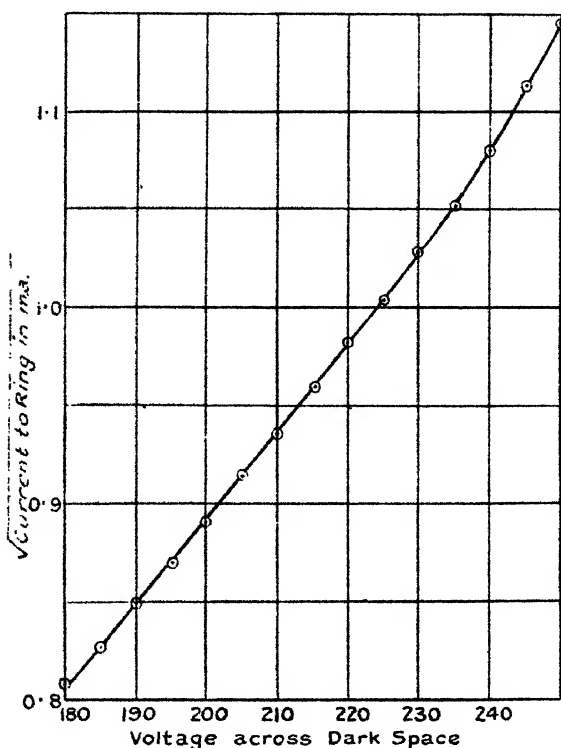
*appears* to decrease, although actually it may really increase.

With the information gained from these experiments, it was decided to construct the new tube with a cathode of radius about 1.5 cm. surrounded by a guard-ring of diameter 7.0 cm.

While the split-cathode tube was in use, it was decided to conduct some experiments to find out in what way the current to any ring depended upon the potential difference between that ring and the negative glow boundary of the cathode dark space. It was hoped that by keeping all the rings but one at a constant potential, the thickness of

the dark-space would be unaffected by the variation of the potential of the one, and thus the dependence of current on the P.D. across the dark-space alone would be ascertained. Each ring in turn was made more and more positive with respect to the remainder of the cathode, and as any possible change in dark-space thickness would have been an increase, it was impossible to observe through the glow over the other rings whether or not any such change took place.

Fig. 3.



This experiment is admittedly open to very strong criticism, but the results, taken in conjunction with more reliable evidence, may be regarded as having some weight. At the lower pressures, the current-voltage relation was found to approximate to Aston's law (equation 3). Fig. 3, drawn from Table III. is a curve obtained by plotting the square root of the current to ring No. 3 against the potential difference across the dark-space. This example was taken at random from the low-pressure curves,



since they all exhibited the same characteristics. As will be seen, the curve is very nearly a straight line over the greater part of its range. This range could not be extended owing to arcing taking place between the ring and its neighbour when the potential difference between them was large.

Whatever law the voltage-current curve obeyed at high pressures, it was certainly not Aston's law, but seemed to involve an even lower power of  $C$ .

TABLE III.

Gas-pressure = 53 mm. Hg.

Tube voltage = 250.

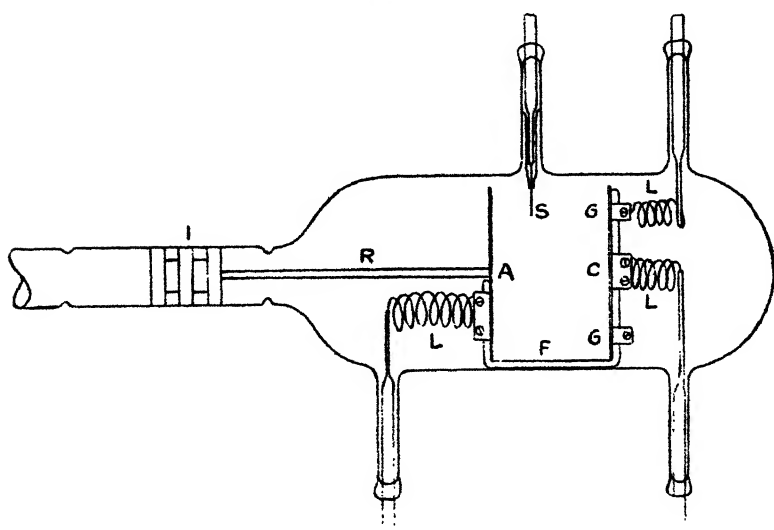
Tube current = 6.0 m.a.

P.D. between ring and cathode. (v.)	P.D. across dark-space. (250 - v.)	Current to ring. (C.)	$\sqrt{C}$ (m.a.) <sup>1/2</sup> .
0 volts.	250 volts.	1.312 m.a.	1.145
5 "	245 "	1.242 m.a.	1.113
10 "	240 "	1.172 m.a.	1.081
15 "	235 "	1.112 m.a.	1.051
20 "	230 "	1.059 m.a.	1.029
25 "	225 "	1.011 m.a.	1.003
30 "	220 "	0.964 m.a.	0.982
35 "	215 "	0.921 m.a.	0.959
40 "	210 "	0.876 m.a.	0.936
45 "	205 "	0.836 m.a.	0.914
50 "	200 "	0.796 m.a.	0.891
55 "	195 "	0.759 m.a.	0.870
60 "	190 "	0.721 m.a.	0.849
65 "	185 "	0.686 m.a.	0.827
70 "	180 "	0.651 m.a.	0.807

This may be due to the fact that the thickness of the dark-space is small at the higher pressures and current densities, and consequently any alteration in thickness would have a greater relative effect on the current passing to the ring. One very curious phenomenon observed at a pressure of 1.24 mm. Hg. was the manner in which the central disk was affected by changes of potential of its neighbour. A marked discontinuity was found in the voltage-current curve for ring No. 2, the current

suddenly falling to a very small amount. It was observed that at this discontinuity, which occurred when the P.D. between the ring and the remainder of the cathode was about 8 volts, the glow disappeared, not only from above ring No. 2, but also from above the central disk, or ring No. 1. The tube current in this case was again 10 m.a. Similar effects were observed when the split electrode was the anode of the discharge-tube.

Fig. 4.



#### *Construction of Experimental Discharge-tube.*

Having found from the preliminary experiment the relative sizes of cathode and guard-ring necessary to make such an arrangement effective, an electrode system was designed and constructed as shown in fig. 4.

An anode of nickel A, 7 cm. in diameter, was separated from the cathode C (diameter 2.98 cm.) and guard-ring G (external diameter 7 cm.) by a glass framework F, the fastenings being small nickel clips silver-soldered to the electrodes and clamped to the glass rods. The distance between the anode and cathode was 5.1 cm. A nickel rod R was riveted to the centre of the anode, the other end being screwed into an iron armature I, provision thus being made for moving the electrode system as a whole by means

of an external electromagnet. The armature was designed to slide in a glass tube, which it fitted fairly well, its movement being restricted by constrictions in the tube. This was necessary to prevent the whole system falling into the discharge-tube and causing damage there. Grooves were turned round the circumference of the iron and along its length, so that air might be pumped out past it. These grooves were important, not so much from the point of view of pumping speed, as from the fact that if the tube was exhausted too rapidly, a solid armature was found to act like a piston, being driven along the tube with sufficient force to crack the glass. Electrical connexion to these three electrodes was effected by means of flexible spirals of enamelled copper wire, L, clamped under nuts on the electrode clips at one end and soldered to strips of copper foil at the other. Phosphor-bronze wire could not be obtained, and as the copper wire was soft, longer and consequently less self-supporting spirals had to be used. No sealing-wax was used in the tube, all seals being made by fusing the strips of copper foil into the ends of the side-arms.

Before proceeding with the practical details of the experiment, it would be advisable to give a brief summary of the theory underlying the methods used<sup>(7)</sup>. We may assume, as a working hypothesis, that in any particular region of a Geissler tube the energy of the discharge is distributed among the electrons and ions according to the Maxwell-Boltzmann law, corresponding to a space potential  $v_s$  with respect to the anode. If a probe or sounding electrode is inserted into this region and is maintained at a potential  $v$  with respect to the anode, then a current will flow to the probe and will change as  $v$  is varied. Owing to the mobility of the electrons being much greater than that of the positive ions, the condition that  $v=v_s$  is not in general satisfied when the current to the sound electrode is zero. If we vary  $v$  and plot a current-voltage curve, the resulting "characteristic" may be split up into three sections. When the sound is very strongly negative with respect to the space potential, the current is carried by positive ions alone, practically all the electrons being rejected. When the sound is but slightly negative, positive ions are still accelerated to the collector, but also the faster electrons are not retarded sufficiently to prevent them from contributing to the total current. As  $v$

approaches the value  $v_s$ , the positive-ion current becomes negligible compared with the electron current, although the latter is still carried by retarded electrons. Finally, when  $v$  is positive with respect to  $v_s$ , the electrons are accelerated, and the current becomes so large that the main discharge is affected, the energy distribution no longer being truly Maxwellian.

The first part of the curve is of importance in this experiment, only in so far as it allows us to make a correction for the positive-ion current to the second part, thus giving us the true electron current. If  $i_+$  is the current due to accelerated positive ions, the first part of the curve is of the form :

$$i_+^2 \propto 1 + ve/kT, \quad . \quad . \quad . \quad . \quad . \quad (4)$$

in which  $e$  is the charge on the ion,  $k$  is the Boltzmann constant, and  $T$  is the temperature corresponding to the energy of the ions. This equation only holds good when the radius of the probe wire is small compared with that of the sheath of positive ions which is formed round it. The straight line obtained by plotting  $i_+^2$  against  $v$  may be extrapolated to correct the second part of the characteristic, as mentioned above.

It may be shown that the retarded electron current varies with  $v$  according to the law :

$$i_- = IAe^{\frac{(v-v_s)e}{kT}}, \quad . \quad . \quad . \quad . \quad . \quad (6)$$

where  $I$  is the electron current density in the discharge, and  $A$  is the area of the sound electrode;  $e$  and  $T$  have their previous significance, but this time they refer to electrons and not to positive ions. From this equation we can derive the form :

$$\log i_- = \text{constant} + \frac{(v-v_s)e}{kT} \quad . \quad . \quad . \quad . \quad . \quad (7)$$

and if  $\log i$  is plotted against  $v$ , the result should be a straight line of slope  $e/kT$ . This is born out in practice, which justifies the original assumption as to the distribution of energy between the electrons.

The third part of the characteristic, dealing with the accelerated electrons, again obeys a law of the form given by (5). Consequently, if the logarithm of the corrected electron current is plotted against the potential of the

sound electrode the result is a curve which departs from a straight line at the space potential. This is a very convenient method, which is used in the experiment described here to find the space potential at the negative glow boundary of the cathode dark-space. Applied as a correction to the tube voltage, this gives the difference of potential existing across the dark space.

The dimensions of the sound electrode (S in fig. 4) were arrived at from the following considerations. The plane electrode is particularly good as a sound, as the "kink" at the space potential in the semi-log curve is well defined. Since, however, a very small region was investigated in this experiment, such an electrode was obviously ruled out. For this reason, among others, the sphere was also rejected. By process of elimination the cylindrical form was chosen, the probe being molybdenum wire, .015 cm. in diameter. Wire of this small size was chosen because when a cylinder of large radius is used the accelerated positive-ion current is not limited by orbital motion, but by space-charge, and equation (5) no longer holds good. This means, of course, that the sound-current cannot be corrected for the positive-ion contribution in order to get the true electron current. There is also, of course, the same objection to a cylinder of large radius as there is to a plane.

A short length of molybdenum wire was pinched into the end of a short copper rod, which was in turn silver-soldered to a strip of copper foil for sealing-in purposes. The whole was sheathed in a glass tube which was drawn down to a small bore at one end, through which 1.28 cm. of the molybdenum wire was allowed to protrude. Care was taken that the wire did not touch the glass at the point where it emerged from the sheath.

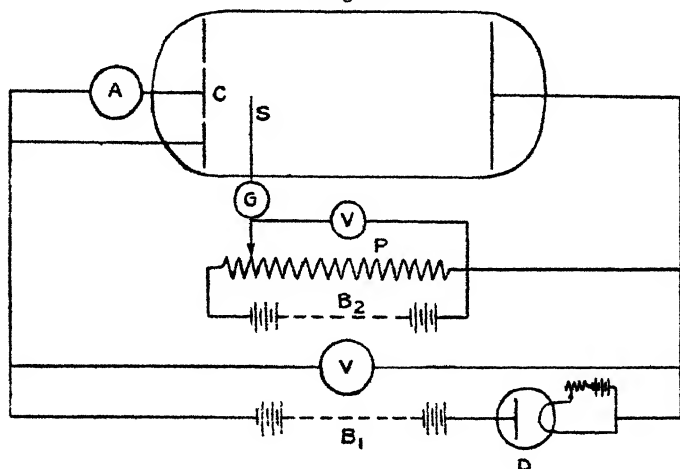
The electrical connexions were as shown in fig. 5. The discharge was maintained by a large battery of lead storage cells,  $B_1$ , the current being regulated by a saturated diode D. This arrangement has the great advantage that, provided the diode is of the bright emitter type, the current it passes is independent of slight fluctuations in the battery voltage, and may readily be varied by adjusting the filament current by means of a rheostat. The current to the cathode C produced by a potential difference  $V$  was measured by a milliammeter A. A varying potential  $v$  was applied to the sound by means of another battery  $B_2$ , and a potentiometer P, the resulting current being

measured by a shunted galvanometer G. Before the apparatus was used, the insulation between the guard-ring and the cathode was tested to ensure that the currents to them did not mix before they were measured.

In order to find the thickness of the dark-space, an accurate sighting tube as used by Aston was employed. At the eye end was a pinhole, the object end being fitted with a pointer. This tube was mounted on a base which slid along a scale mounted parallel to the discharge-tube.

A Gaede annular jet mercury-vapour pump, backed by a Cenco Hyvac pump, served to exhaust the tube to a pressure immeasurable by a large McLeod gauge (at the

Fig. 5.



most  $10^{-5}$  mm. Hg.). Owing to the copper-to-glass seals it was unsafe to bake out the tube, and it was necessary to rinse it out several times with the gas to be used to ensure purity. The first gas used was hydrogen, admitted by a hot palladium tube, but the dark-space was found to be so ill-defined that it was soon abandoned. Neon was then tried, the purest specimen obtainable having a composition of 98 per cent. neon and 2 per cent. helium. Although the boundary of the dark-space was still somewhat diffuse under certain conditions of pressure and current density, yet its colour was bluish as distinct from the pink of the negative glow, and its thickness could generally be measured by the sighter to within 2 per cent.

The gas was stored in a reservoir over water, and was admitted to the discharge-tube by sharing a volume at

high pressure, contained in the space between two taps sealed close together, with a large evacuated bulb. A small portion of the gas in the bulb was then shared in a similar manner with the discharge-tube, final adjustment being effected by pumping.

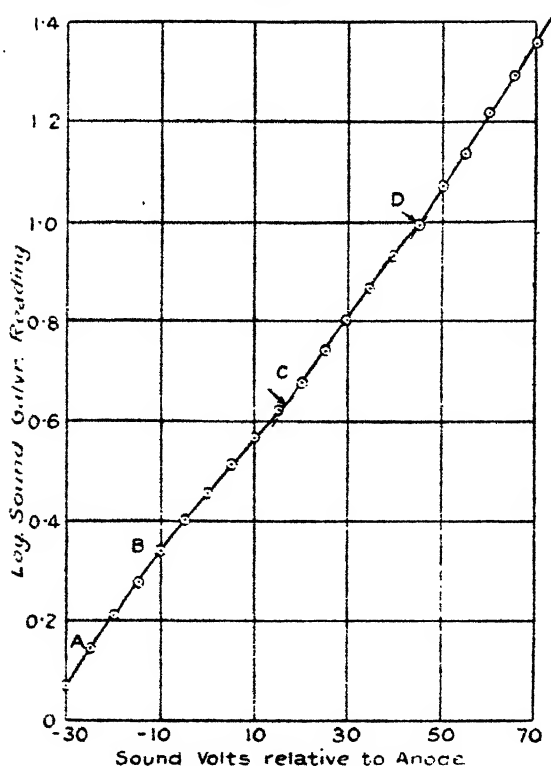
The use of liquid-air traps between the discharge-tube and the rest of the apparatus effectually prevented the entry of mercury vapour from the McLeod gauge and the pump.

The procedure adopted during the taking of a set of readings was as follows. A suitable pressure of neon and value of tube current having been obtained in the tube, the sighting-tube was laid on the probe, and by careful manipulation of an electromagnet the electrode system was shifted along the discharge-tube until the boundary of the dark-space coincided with the sound in the field of view. A current-voltage characteristic was then taken, and the space potential of the boundary was found and applied to the tube voltage as a correction. The sighting-tube was next laid on the cathode, the difference of the two readings giving the thickness of the dark-space. In this way the four quantities necessary to test Aston's law were obtained, viz. gas-pressure, current density, thickness of the dark-space, and the potential difference across it.

Unfortunately, it was found that the positive-ion current to the sound-electrode in the region investigated did not obey the law expressed in equation 5, and as a consequence the true electron current was an unknown quantity. The logarithm of the total current was plotted against the potential of the probe, and fortunately the electron current was sufficiently in excess of the positive-ion contribution to nullify the effect of the latter on the straightness of the line obtained over the greater part of the curve, as will be seen by reference to fig. 6. This is a typical "semi-log" curve, and it will be noticed that the affected part of the curve is satisfactorily distant from the kink indicating the space potential (C). In the neighbourhood of the dark-space the curves exhibit an upward tendency after the space potential has been reached, as is shown by the section CD. The rapid increase of current beyond the point D is due to ionization by collision taking place in the electron sheath surrounding the sound electrode, a state of affairs which seemed to set in gradually at low

pressures and current densities, and taking the form of violent arcing at the higher pressures. The curve shown in fig. 6 is of the type to be expected in the neighbourhood of the cathode dark-space. Normally the "semi-log" curve becomes more horizontal after the space potential has been reached, but Emeléus<sup>(8)</sup> found an upward tendency after the "kink," as shown at C (fig. 6) when the exploring electrode was near the dark-space.

Fig. 6.



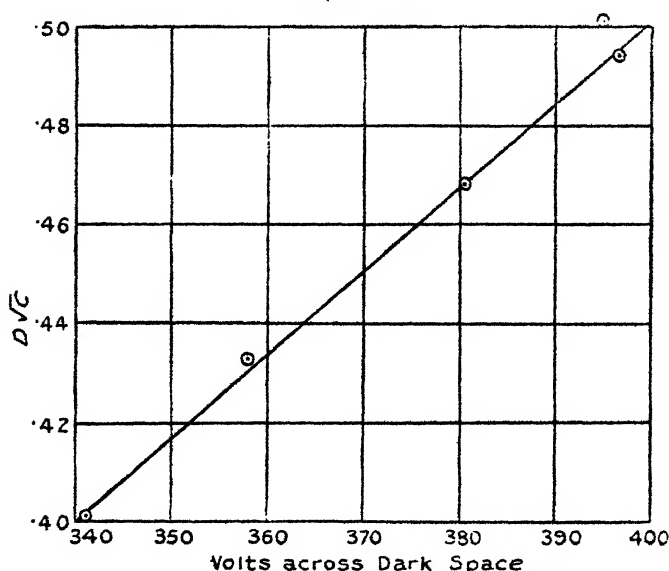
At the point D it was noticed that a faint red glow appeared at the top of the sound-wire where it emerged from the glass sheath, and as the potential was increased this glow gradually spread and increased in brightness. The space potential, it will be observed, is 16 volts *positive* with respect to the anode. This indicates that the electron concentration gradient was sufficiently great to allow a drift current to flow against the electric field in the negative glow. Here we differ from Aston, who would



have assumed in this case that the potential difference between the cathode and the boundary of the dark-space was the same as the tube voltage, viz. 345 volts, whereas it was actually 361 volts, a difference of 3 per cent. This should not be a sufficiently large error to cause any material difference between the results of the present investigation and those of Aston's original experiments, and actually very little difference was observed.

Several pressures of neon were tried in an attempt to obtain an extensive range of tube currents, for, as a rule, the low current densities were productive of curved and diffuse dark-space boundaries, and large currents were

Fig. 7.



accompanied by the striking of the discharge to the back of the cathode. The former type of discharge, not entirely covering the cathode, probably rendered the guard-ring inoperative, and the latter type was entirely useless. When suitable discharges were obtained, the results of the experiments were plotted in the manner shown in fig. 7 and Table IV. The abscissa is the P.D. across the dark-space, while the product of the dark-space thickness and the square root of the current to the cathode is the ordinate.

The one bad point was the result of a discharge which appeared to be extremely unstable, although when tested

with a wavemeter and also with a detector circuit coupled to a coil in the anode lead, no trace of oscillatory current was found.

The straight line fits in very well with (3), and the constant  $G$  has a value of 113 volts. This is about 25 volts in excess of Aston's value, but the discrepancy is doubtless due to the correction for the potential of the dark-space boundary, in the present work.

TABLE IV.

Gas-pressure = 33 mm. Hg.

Tube volts. V.	Boundary potential. $v_s$ .	P.D. across dark-space.	Dark-space thickness. D.	Current to cathode. C.	$D\sqrt{C}$ .
380	16.5 v.	396.5 v.	0.9 cm.	0.3 m.a.	.494
370	25.0 v.	395.0 v.	1.02 cm.	0.25 m.a.	.509
358	22.5 v.	380.5 v.	1.06 cm.	0.195 m.a.	.468
345	13.0 v.	358.0 v.	1.12 cm.	0.15 m.a.	.433
327	14.0 v.	341.0 v.	1.27 cm.	0.10 m.a.	.401

### Discussion of Results.

Whenever definite evidence has been forthcoming to help us to decide between Aston's law and the Langmuir space-charge law, the decision has always been in favour of the former. This, perhaps, is not surprising, for the space-charge theory was developed for the case of electron emission in high vacuum, no allowance being made for collisions between the electrons and gas molecules. McCurdy<sup>(9)</sup> has extended this simple theory to cover the case of an electron making so many collisions that it reaches a limiting velocity. The current in this case is still proportional to  $V^{3/2}$ . It is probable that of these extremes of condition neither are to be found in the cathode dark-space.

Compton<sup>(10)</sup> has shown that the assumption of space-charge limitation is more defensible with the abnormal cathode fall than in the case of the normal, for which he has developed a new theory. That the current in the former type of discharge is not so limited has been shown in this paper. It is possible that the primary dark space<sup>(11)</sup>

discovered by Aston in certain gases is a sheath of space-charge of the type discussed above, as its thickness is so small that a current carrier would have little opportunity of making a collision in its journey across; but the knowledge of this possibility does little to solve the problem of the mechanism of conduction of electricity across the Crookes's dark-space.

It may be remarked here that the visual measurement of the dark-space thickness is contrary to the opinions of Seeliger and Lindow<sup>(12)</sup>, who have pointed out that the eye estimates the region of maximum light-intensity gradient to be the boundary of the dark-space, the thickness thus measured being perhaps as little as 50 per cent. of the distance from the cathode to the region of maximum light-intensity. There would seem to be little reason for defining the dark-space on the latter basis, but rather to define the boundary as the region of minimum electric field<sup>(10)</sup>. This region has been found by some workers in this field<sup>(6)</sup> to correspond at least approximately to the visual boundary, and certainly would not yield a dark-space thickness in excess of that observed by means of the sighter.

The work was carried out while the author was in receipt of a grant from the Department of Scientific and Industrial Research.

The writer would like to take this opportunity of acknowledging his indebtedness to Professor E. V. Appleton for his continued help and discussion during the progress of the work, and to Dr. K. G. Emeléus for his useful criticism of the manuscript.

### *References.*

- (1) Aston, *Proc. Roy. Soc. A*, lxxxiv. p. 526.
- (2) Aston, *Proc. Roy. Soc. A*, lxxxvi. p. 168.
- (3) Langmuir and Mott-Smith, *Gen. Elec. Rev.* xxvii. p. 449 (1924).
- (4) Langmuir, *Phys. Rev.* ii. p. 450 (1913).
- (5) Ryde, *Phil. Mag.* xlv. p. 1149 (1923).
- (6) Emeléus and Harris, *Phil. Mag.* iv. p. 49 (1927).
- (7) See (3) above,
- (8) Emeléus, *Proc. Camb. Phil. Soc.* xxiii. p. 531 (1926).
- (9) McCurdy, *Phys. Rev.* xxvii. p. 157 (1926).
- (10) Compton and Morse, *Phys. Rev.* xxx. p. 305 (1927).
- (11) Emeléus and Carmichael, *Phil. Mag.* v. p. 1039 (1928).
- (12) Seeliger and Lindow, *Phys. Zeit.* xxvi. p. 393 (1925).

*L. The Hall Effect, Electrical Conductivity, and Thermo-electric Power of the Lead-Antimony Series of Alloys.*  
By EMLYN STEPHENS, M.Sc., Physics Department,  
University College of Swansea \*.

*Introduction.*

**T**HERE is no satisfactory theoretical explanation of electrical conduction and the galvanomagnetic effects in metals and alloys, and further knowledge of the various phenomena is still necessary. A great deal of the earlier experimental work has been carried out with impure materials, and it is well known that some physical properties are found to show large variations with a slight trace of impurity.

In two previous papers † the variation of electrical properties with composition of two series of alloys in which compounds are formed have been discussed. The object of the present work was to study the variation of the Hall effect, electrical conductivity, temperature coefficient of resistance, and thermoelectric power with composition of a series of alloys which shows no extreme variation of crystal structure over a large range of composition. The examination of the properties of this series is important from a theoretical standpoint, and in a further paper the electrical properties of the three series will be discussed in relation to theory. According to the equilibrium diagram‡ of the Pb-Sb alloys, a solid solution of Sb in Pb is formed up to about 2 per cent. by weight of Sb, but all other alloys consist of a eutectic mixture of this solid solution and Sb crystals.

The determinations of the electrical resistivity, temperature coefficient of resistance, thermoelectric power, and Hall coefficient have been made for the same specimen. The alloys required annealing, as their electrical properties depend on their physical state. In the present experiments the electrical resistivity was determined for the alloys after preparation, and was afterwards redetermined for each alloy after annealing at a suitable temperature.

\* Communicated by Prof. E. J. Evans, University College of Swansea.

† Stephens and Evans, *Phil. Mag.* vii. Jan. 1929; Stephens, *Phil. Mag.* viii. Sept. 1929.

‡ International Critical Tables, ii.

This was repeated until further annealing produced no change in the resistivity. The other properties were then determined for the alloys in this final state.

Matthiessen\* and Smith† have determined the electrical conductivity curve of the Pb-Sb system of alloys, and the latter investigator also measured the thermal conductivities of these alloys and discussed his results in relation to the Wiedmann-Franz law. The curve connecting thermoelectric power and composition of the alloy was determined by Rudolfi‡, and measurements of the electrical conductivity and thermoelectric power of annealed specimens of these alloys were made by Broniewski and Sliowski§, who were engaged in a study of the equilibrium diagram of the Pb-Sb system.

### *Experimental Arrangement.*

The experimental arrangements used in the present work have been described in an earlier paper||, so that a brief description here will be sufficient.

The alloys were made from very pure metals, the lead and antimony containing .0043 per cent. and .084 per cent. impurities respectively. The impurities in the lead were: silver .0005 per cent., antimony .0005 per cent., copper .0003 per cent., bismuth .0015 per cent., iron .0012 per cent., and zinc, .0003 per cent., while the impurities in the antimony were: iron .041 per cent., lead .025 per cent., copper .012 per cent., sulphur .003 per cent., and arsenic .003 per cent. The alloys were chill cast in the form of plates, some in a graphite mould 15 cm. long, 2.0 cm. wide, and .4 cm. thick, and the others in an iron mould 15 cm. long, 3.0 cm. wide, and .4 cm. thick. The antimony plate cast in the iron mould was composed of small crystals, and in order to study the possible effect of crystal size on the Hall coefficient a second plate, consisting of large crystals, was made by allowing the molten metal to cool in a hot sand mould.

Altogether 10 plates were cast, of the following percentage composition by weight:—(1) 100 per cent. Pb; (2) 96 per cent. Pb, 4 per cent. Sb; (3) 90 per cent. Pb,

\* Pogg. Ann. cx. p. 28 (1860).

† Phys. Rev. xxiii. p. 307 (1924).

‡ Zeit. Anorg. Chem. lxvii. p. 65 (1910).

§ Rev. de Met. xxv. p. 397 (1928).

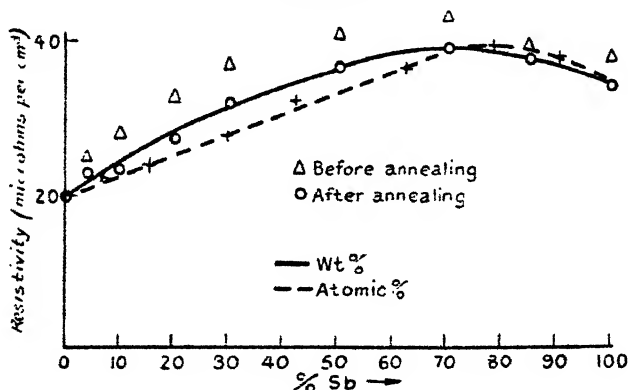
|| Stephens, loc. cit.

10 per cent. Sb ; (4) 80 per cent. Pb, 20 per cent. Sb ; (5) 70 per cent. Pb, 30 per cent. Sb ; (6) 50 per cent. Pb, 50 per cent. Sb ; (7) 30 per cent. Pb, 70 per cent. Sb ; (8) 15 per cent. Pb, 85 per cent. Sb ; (9) and (10) 100 per cent. Sb.

(a) *Electrical Resistivities and Temperature Coefficients of Resistance of the Alloys.*

The electrical resistivity was determined by fixing a plate of the alloy across two knife-edges, and determining the resistance of a known length by means of the Kelvin Bridge. The determinations before and after annealing were made at 0° C., and the values of the resistivities in

GRAPH I.



the initial and final states of the alloy are given in Table I. and Graph I.

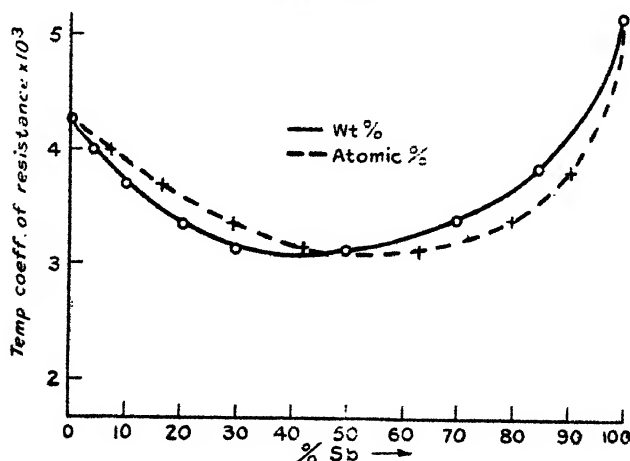
The mean temperature coefficient of resistance over the range of temperature between 0° C. and 100° C. was determined for each alloy in its final state only, and these results are given in Table I. and Graph II. The resistance of a length of plate of these alloys could be determined with an accuracy of about 1 in 800, but as the determination of the resistivity also involved measurements of the thickness and width, the accuracy of the resistivity determinations is about  $\frac{1}{3}$  of one per cent. The determination of the temperature coefficients did not involve any measurements of the dimensions of the plates, and it is considered that the temperature coefficients are also accurate to within about  $\frac{1}{3}$  per cent.

TABLE I.

Composition of alloy by weight.	Resistivity before annealing, in microhms per cm. <sup>3</sup>	Resistivity after annealing, in microhms per cm. <sup>3</sup>	Mean temp. coeff. of resistance between 0° C. and 100° C. $\times 10^4$ .
100 % Pb .....	19.6	19.6	42.7
*96 % Pb, 4 % Sb ...	24.95	22.73	40.2
90 % Pb, 10 % Sb ...	27.8	23.82	37.1
80 % Pb, 20 % Sb (a)	33.0	27.4	33.6
*80 % Pb, 20 % Sb (b)	33.1	27.7	—
70 % Pb, 30 % Sb ...	37.1	32.3	31.4
50 % Pb, 50 % Sb ...	41.0	36.7	31.3
30 % Pb, 70 % Sb ...	43.3	39.4	33.8
*15 % Pb, 85 % Sb ...	39.7	38.3	38.2
100 % Sb ...	38.5	35.3	51.4

\* Annealed in vacuum.

GRAPH II.



## (b) Thermoelectric Power of the Alloys.

The thermoelectric powers of the alloys were determined with copper leads soldered to the ends of the plates. One junction was enclosed in steam while the other was kept at the temperature of running tap-water. The thermo-E.M.F. over this range of temperature was

determined by means of a Tinsley vernier potentiometer, and the values of the thermoelectric powers in microvolts per degree centigrade with respect to both copper and lead are given in Table II. and Graph III. Repeated determinations of the thermoelectric power of the copper-alloy couples made when the temperature of the cold junction was varied over a range of several degrees were in good agreement, so that the relation between E.M.F. and temperature was probably linear between room-temperature and 100° C.

TABLE II.

Composition of alloy by weight	Thermoelectric power with respect to Cu, in microvolts per degree centigrade.	Thermoelectric power with respect to Pb, in microvolts per degree centigrade.
100 % Pb .....	-3.16	0
96 % Pb, 4 % Sb .....	-2.67	+ .49
90 % Pb, 10 % Sb .....	-2.30	+ .86
80 % Pb, 20 % Sb .....	- .62	+ 2.54
70 % Pb, 30 % Sb .....	+1.15	+ 4.31
50 % Pb, 50 % Sb .....	+3.21	+ 6.37
30 % Pb, 70 % Sb .....	+2.20	+ 5.36
15 % Pb, 85 % Sb .....	+2.46	+ 5.62
100 % Sb .....	+38.0	+41.16

(c) *Hall Effect of the Alloys.*

A transverse magnetic field produces a rotation of the equipotential lines in a plate carrying an electric current, so that a difference of potential is set up between the edges of the plate. This transverse galvanomagnetic potential difference, *E*, is given in abs. units by the formula

$$E = \frac{RHI}{d},$$

where *H* is the magnetic field in gauss, *I* the current in abs. units, *d* the thickness of the plate in cm., and *R* the Hall coefficient.

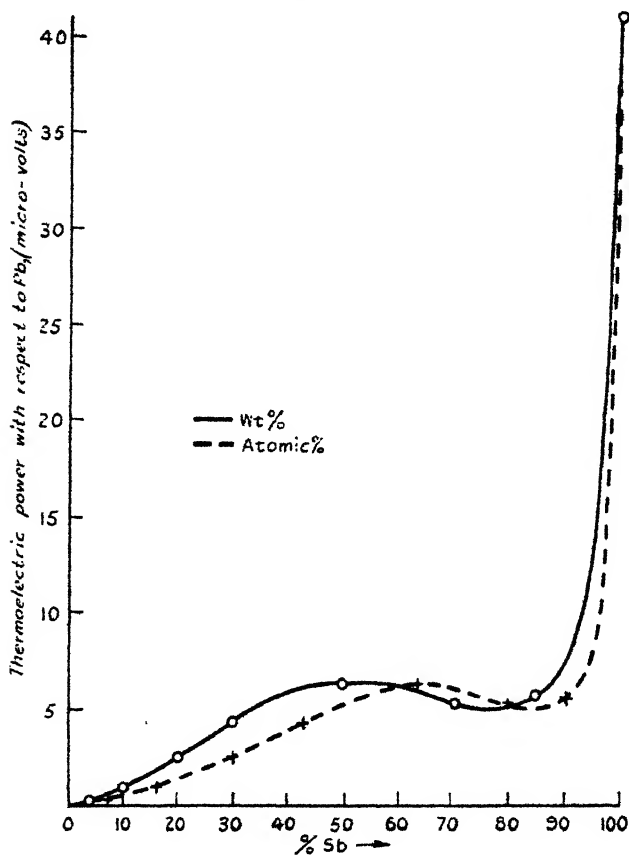
This coefficient *R*, which depends on the temperature and, also, for some metals, on the intensity of the magnetic



field, has different signs in various metals. The Hall coefficient is +ve for both antimony and lead, the value for lead being about .05 per cent. that for antimony.

Although the Hall effect for antimony is very large, it is small for some of the Pb-Sb alloys, and a very sensitive galvanometer was required to measure the P.D. The

GRAPH III.



delicate Paschen galvanometer used in the present experiments was mounted on a stone pillar at a distance of  $7\frac{1}{2}$  metres from a large circular electromagnet which had been rotated into such a position that its effect on the galvanometer was a minimum. Magnetic fields ranging from 3088 gauss to 8468 gauss could be obtained in the 1.5 cm. air-gap between the pole-pieces when the electromagnet was excited by currents varying from 1 ampere to 6 amperes.

The alloy plate under investigation was rigidly fixed in a vertical position in the magnetic field by two brass clamps which also served as leads for the primary current. These clamps were fixed to a wooden frame which also supported the secondary electrodes, consisting of spring copper contacts carried by bars of ebonite. These electrodes, which could be moved vertically along the edges of the plate by means of a screw arrangement, were connected to the galvanometer by long, well insulated, flexible wires. These wires were pulled taut so as to eliminate the effects of vibration as far as possible.

In a determination of the Hall coefficient, the secondary electrodes were adjusted on an equipotential line. Then, with the secondary circuit closed, no deflexion is produced in the galvanometer when the primary current is reversed, but on applying the magnetic field, and again reversing the current, with the secondary circuit closed, a deflexion due to the Hall P.D. between the edges of the plate is produced in the galvanometer. The Hall P.D. was determined for several values of the magnetic field up to 8500 gauss, and a graph drawn showing the relation between the P.D. and magnetic field. The value of

$E$  determined from this graph was then used to calculate  $H$  the Hall coefficient from the equation  $R = \frac{Ed}{HI}$ .

The primary current (4 amps.) passing through the plates of high lead content could be read on a Weston ammeter with an accuracy of about 1 in 1200, and the minimum current (1 ampere) used for the antimony plate and the alloys of high antimony content could be read with an accuracy of about 1 in 300. This ammeter was periodically calibrated by comparison with a large Weston Standard Ammeter.

The magnetic fields corresponding to various currents passing through the electromagnet were determined by means of a Grassot fluxmeter with an accuracy of about 1 in 250. The fluxmeter and search-coil were calibrated by means of a delicate ballistic galvanometer and a search-coil of known mean area.

The Hall effect was determined at room-temperature, the exact temperature being observed by a thermometer suspended with its bulb in contact with the plate.

The experimental results for the Hall coefficients are given in Table III. and Graph IV.

In addition to the Hall potential difference, a transverse galvanomagnetic temperature difference is set up between the edges of the plate. This is the Ettingshausen effect, and the difference of temperature,  $\Delta T$ , is given by

$$\Delta T = \frac{P \cdot H \cdot I}{d},$$

where  $H$  is the magnetic field in gauss,  $I$  the current in absolute units,  $d$  the thickness of the plate in cm., and  $P$  the Ettingshausen coefficient.

TABLE III.

Composition of alloy by weight	Hall coefficient.	Temperature ° C.
100 % Pb .....	+·00009*	20·0
96 % Pb, 4 % Sb...	+·000997	19·6
90 % Pb, 10 % Sb...	+·00324	17·4
80 % Pb, 20 % Sb...	+·00429	18·7
70 % Pb, 30 % Sb...	+·00530	20·1
50 % Pb, 50 % Sb...	+·0112	20·3
30 % Pb, 70 % Sb...	+·0333	20·3
15 % Pb, 85 % Sb...	+·0876	17·8
100 % Sb...	+·213	17·8

\* Campbell, 'Galvanomagnetic and Thermomagnetic Effects.'

If the secondary electrodes in the Hall-effect determinations are not made of the same material as the plate itself, the Ettingshausen temperature difference  $\Delta T$  set up between the edges of the plate will result in a thermo-E.M.F.  $\theta \cdot \Delta T$  in the secondary circuit, where  $\theta$  is the thermoelectric power of the electrode with respect to the plate. Therefore the total potential difference as measured by the galvanometer in the Hall-effect determination is given by

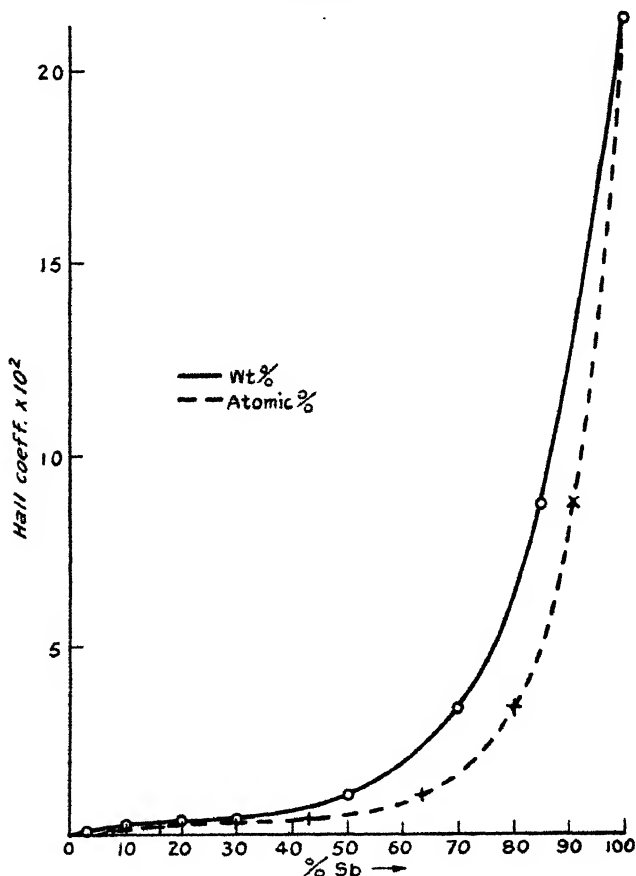
$$E = E_H \pm \theta \cdot \Delta T,$$

where  $E_H$  is the true Hall P.D., and the Hall coefficient becomes

$$R = \frac{E \times d}{H \times I} \pm P \cdot \theta.$$

As a result of special experiments, it was found that the Ettingshausen effect for the alloys was inappreciable, and the Hall coefficients have been determined within 1 per cent. In the case of antimony, the use of copper electrodes made accurate measurements of the Hall coefficient rather difficult, owing to the heat generated

GRAPH IV.



by the magnet and the large thermoelectric power of copper with respect to antimony. This difficulty was overcome by employing antimony electrodes, and in addition the Ettingshausen effect was practically eliminated.

All the alloys were annealed at the same temperature,  $232^\circ \text{C.}$ , in an electric furnace, an atmosphere of coal-gas being used to prevent oxidation. A few alloys were

annealed with the furnace evacuated to about  $\frac{1}{10}$  mm. pressure, and the results are in agreement with those obtained for the alloys annealed in coal-gas. The annealing was performed in periods of 15 hours, and the furnace was allowed to cool before removing the alloy.

### *Discussion of Results.*

The curves showing the relation between the resistivity, temperature coefficient of resistance, thermoelectric power, Hall effect and the concentration of Sb in the alloy are all continuous, and furnish no irregularities or singular points. These curves, as would be expected, are in distinct contrast to those obtained for a series of alloys in which compounds are formed.

If the alloys were purely mixtures of lead and antimony, the electrical resistivity would be expected to vary uniformly with the composition by volume. The resistivity of the alloy formed by the addition of lead to pure antimony is greater than that for the pure antimony, although lead is a better conductor than antimony. The alloy of maximum resistivity has a composition of about 28 per cent. by weight of lead, but a further increase in the lead content of the alloy produces a regular diminution in the resistivity. Broniewski and Sliwowski\* also find a maximum corresponding to 28 per cent. by weight of lead in their resistivity-composition curve, but the value of the resistivity determined by them is about 5 per cent. higher. The resistivity of the antimony used in the present experiments was 2 per cent. lower than that determined by Broniewski and Sliwowski.

The temperature coefficient of resistance of pure antimony is very large, being about 25 per cent. greater than that for lead. The purer the metal, the greater is its temperature coefficient of resistance, and for many metals the addition of only a trace of foreign metal diminishes the temperature coefficient considerably. Probably in this case the diminution in the temperature coefficient is caused by the introduced metal forming a solid solution with the pure metal. With the addition of pure lead to antimony the temperature coefficient of resistance at first diminishes rapidly, and 3 atoms per cent. of lead is sufficient to

\* *Ioc. cit.*

diminish it by about 17 per cent. The minimum temperature coefficient ( $31.0 \times 10^{-4}$ ), is obtained for an alloy having a composition of about 47 atoms per cent. lead. The value of the temperature coefficient does not differ much from this minimum value over the range of composition from 38 atoms per cent. Pb to about 54 atoms per cent. Pb. This minimum temperature coefficient for the Pb-Sb alloys is much greater than the minimum obtained for the Cu-Sb\* and Cu-Sn† series of alloys, in which there are extreme changes of crystal structure, and it seems as if the temperature coefficient of resistance is intimately connected with the structure.

An examination of the four graphs given in the present paper does not indicate any close connexion between the phenomena. The addition of a small quantity of lead to antimony diminishes the thermoelectric power by a far greater amount than the Hall effect, and further addition of lead does not produce similar variations in these effects. The addition of 5 atoms per cent. of lead is sufficient to diminish the thermoelectric power of antimony by about  $\frac{1}{5}$ ths of its initial value, but the Hall coefficient for this alloy is about 75 per cent. of that for pure antimony. This decrease in the thermoelectric power caused by the addition of lead is maintained until the composition of about 15 atoms per cent. of lead is reached. Further addition of lead produces an increase in thermoelectric power until a maximum is attained corresponding to the composition of 35 atoms per cent. of lead, which is followed by a gradual diminution in thermoelectric power. The form of this thermoelectric power-composition curve is similar to that obtained by Broniewski and Sliwowski‡.

Graph IV., showing the relation between the Hall coefficient and composition of the alloy, is very interesting. The addition of antimony to lead produces a small increase in the Hall coefficient until the composition of 20 atoms per cent. of antimony is reached. Between compositions of 20 and 50 atoms per cent. of Sb, a very small increase in Hall coefficient which is practically proportional to the change in composition is obtained. With further addition of antimony the Hall coefficient increases more rapidly, being about half that of antimony for an alloy containing

\* Stephens and Evans, *loc. cit.*

† Stephens, *loc. cit.*

‡ *Loc. cit.*

6 atoms per cent. of lead. In alloys of high antimony content, practically all the antimony in the alloy is present as pure crystals, and so the Hall coefficient for an alloy of, say, 50 atoms per cent. of Sb would be expected to be about half that of pure antimony. This alloy has a Hall coefficient of only  $2\frac{1}{2}$  per cent. of that of pure antimony, and it seems as if there is some inter-crystal force opposing the effect of magnetism.

According to the magnetic susceptibility-composition curve for the Pb-Sb alloys determined by Honda and Endo \*, the addition of about 5 per cent. of lead to antimony reduces the susceptibility of antimony to about one-half its original value. With further addition of lead the susceptibility diminishes linearly to the value for pure lead. Although the Hall coefficient-composition curve is somewhat similar in form to the susceptibility curve, there does not seem to be any intimate relation between them.

TABLE IV.

Magnetic field ...	3088	4632	5789	6833	7704	8468
Hall coefficient...	+·232	+·232	+·234	+·232	+·229	+·217

Mean temperature=16·3° C.

The Hall coefficients for all the alloys examined did not vary with change of magnetic field from 3088 to 8468 gauss. The coefficients for the alloys were also examined over a range of temperature of about 5° C., but no change in the Hall coefficient was observed.

Two plates of pure antimony were examined, the crystals of one being very much larger than those of the other, due to the different methods of preparation. The Hall coefficient for the plate of large crystals was found to be 9 per cent. greater than that for the small crystals. It was constant for each plate for magnetic fields up to about 7000 gauss, but diminished for larger fields. The variation of the Hall coefficient with magnetic field for the plate of large crystals is shown in Table IV. and Graph V.

Heaps † found that the Hall coefficient for antimony diminished from +·220, corresponding to a magnetic field of 1700 gauss, to +·204, corresponding to a magnetic

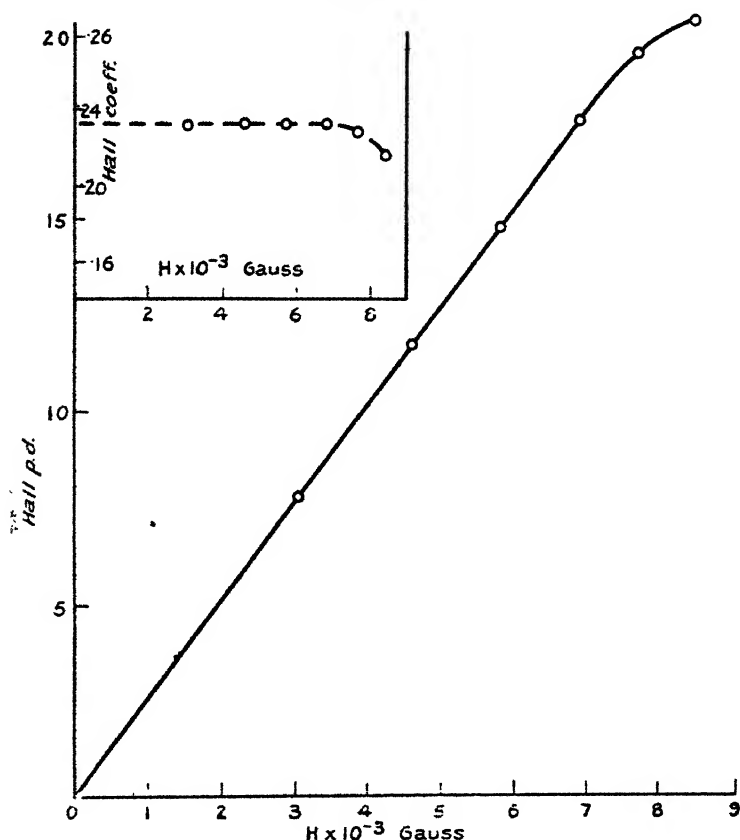
\* Journ. Inst. Met. xxxvii. p. 29 (1927).

† Heaps, Phil. Mag. vol. I. Nov. 1925.

field of 3600 gauss, and that further increase in the magnetic field produced only a small diminution in the Hall coefficient.

The effect of annealing, as shown in Table I. and Graph I., was to produce a diminution in resistivity of all the alloys.

GRAPH V.



### Summary.

(a) The Hall effect, electrical resistivity, temperature coefficient of resistance and thermoelectric power of the lead-antimony series of alloys have been determined. The alloys were chill cast, and the electrical resistivity at  $0^{\circ}\text{C}.$  was determined in this state. The resistivity was redetermined after the alloys had been annealed, and the annealing was continued until the resistivity showed no further variation. The temperature coefficient of resist-



ance, thermoelectric power, and Hall effect were then determined for the alloys in this final state.

(b) Each of the curves showing the relation between Hall effect, electrical resistivity, temperature coefficient of resistance, thermoelectric power, and the concentration of one metal in the alloy is continuous and no irregularities are obtained, but there is no indication of any close connexion between any of the phenomena.

(c) The effect of annealing was to produce a diminution in resistivity of all the alloys.

In conclusion, I wish to express my gratitude to Professor E. J. Evans, D.Sc., for his valuable help and advice.

December 1929.

LI. *The Behaviour of Electrons in Magnetic Fields.* By V. A. BAILEY, M.A., D.Phil.(Oxon.), F.Inst.P., Associate Professor of Physics, University of Sydney\*.

1. **T**HE best method for the determination of the drift-velocity  $W$  of electrons in gases in uniform electric fields is that originally used by J. S. Townsend and H. T. Tizard†, which depends on the principle that a uniform magnetic field, of intensity  $H$  and perpendicular to the electric field of intensity  $Z$ , deflects the stream of electrons through an angle  $\theta$ , where  $\tan \theta = HW/Z$ .

It has been used with accuracy over a wide range of conditions in many kinds of gases, and has helped in obtaining definite information about the effects of collisions between electrons and molecules which has not been possible otherwise.

There are two effects which may, however, make its application difficult in certain circumstances, namely, the remarkable divergence of electronic streams in gases like argon and neon, and the formation of large numbers of negative ions in gases like hydrogen chloride, ammonia, nitric oxide, and nitrous oxide.

With the first it is possible to use large gas-pressures  $p$  and large electric intensities  $Z$  to reduce the divergence

\* Communicated by Prof. J. S. Townsend, F.R.S.

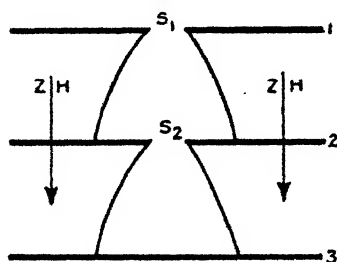
† J. S. Townsend, 'Motion of Electrons in Gases,' p. 21, or 'Electricity in Gases,' p. 121.

conveniently for a given value of  $Z/p$ ; but with the second even the use of small pressures and electric intensities may not always suffice to overcome the difficulties.

Another method for determining  $W$  has therefore been devised which provides a means of measuring the velocities of electrons in the presence of negative ions. It is not as simple as the one mentioned above, but it involves the same general principles.

The velocities for electrons in hydrogen obtained by the two methods are in good agreement, which is further evidence in support of these methods of investigation. The attack \* on experiments of this kind (depending on statistical effects), made by the advocates of theories proposed by J. Franck, has no scientific foundation †.

Fig. 1.



## 2. Theoretical Principle.

The new method makes use of the reduction of the divergence of an electronic stream which occurs when a uniform magnetic field is applied in the *same* direction as the electric field, and is illustrated by the diagram in fig. 1.

When the stream issues from the slit  $S_1$  the diffusion of the electrons causes it to diverge, which divergence is generally measured by means of the fraction  $R$  of the whole stream which passes through the second slit  $S_2$  (or which arrives on a metallic strip) situated at a distance  $c$ . For given dimensions of the slits, and with no magnetic field, this fraction  $R$  can be expressed ‡ as a known function  $R(Z/kc)$  of the ratio  $Z/kc$ , where  $k$  is the mean energy of agitation of the electrons in terms of the mean energy of

\* R. Atkinson, Proc. Roy. Soc. A, cxix. p. 335.

† J. S. Townsend, Proc. Roy. Soc. A, cxx. p. 511 (1928).

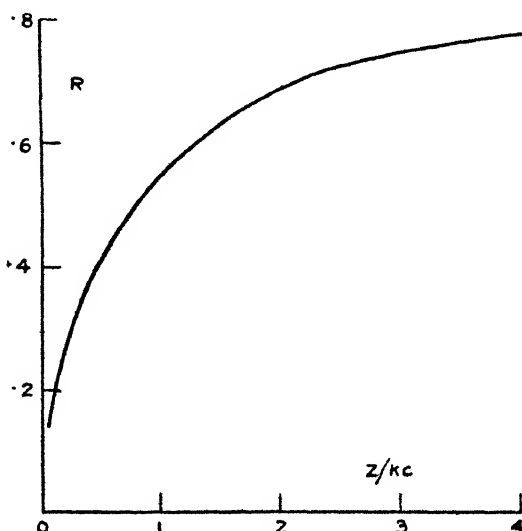
‡ Vide J. S. Townsend, 'Motion of Electrons in Gases,' pp. 7-9, and V. A. Bailey and J. D. McGee, Phil. Mag., Dec. 1928, p. 1076.

agitation of any molecule at 15° C. The fraction  $R$  is given in terms of the quantity  $Z/kc$  by the curve in fig. 2 when the slits are 4 mm. wide.

It will now be shown that the presence of the magnetic field reduces the divergence of the stream and affects the distribution ratio  $R$  as if the ratio  $Z/kc$  were replaced by  $Z\sigma/kc$ , where

$$\sigma = 1 + \left( \frac{HW}{Z} \right)^2 \dots \dots \dots (1)^*$$

Fig. 2.



The equations of motion † are

$$nu = -K_h \frac{\partial n}{\partial x},$$

$$nv = -K_h \frac{\partial n}{\partial y},$$

$$nw = -K \frac{\partial n}{\partial z} + nW,$$

\* In e.m.u.

† J. S. Townsend, 'Electricity in Gases,' p. 101, where

$$\omega T = \frac{He}{m} T = \frac{HW}{Z}.$$

The  $y$ -axis is taken parallel to the slits, and the  $z$ -axis parallel to  $Z$  and  $H$ .

where  $n$  is the number of electrons per c. c. at a point  $(x, y, z)$ ,  $nu$ ,  $nv$ ,  $nw$  are the net rates of flow of electrons across unit areas normal to the axes of coordinates, and  $K$ ,  $K_\perp$  are the coefficients of diffusion of electrons respectively along and perpendicular to the magnetic field; these coefficients are related by the formula

$$K_\perp = K/\sigma.$$

The equation of continuity for the steady state is

$$\frac{\partial(nu)}{\partial x} + \frac{\partial(nv)}{\partial y} + \frac{\partial(nw)}{\partial z} = 0,$$

so, on eliminating  $nu$ ,  $nv$ ,  $nw$  by substitution from the equations of motion, the following is obtained:

$$\frac{1}{\sigma} \left( \frac{\partial^2 n}{\partial x^2} + \frac{\partial^2 n}{\partial y^2} \right) + \frac{\partial^2 n}{\partial z^2} = \frac{W}{K} \cdot \frac{\partial n}{\partial z}.$$

This can be simplified by integrating each term with respect to  $y$ , and taking as limits of integration points on the side-boundary, since in the actual instrument these points are too distant for any of the electrons to reach them, and so there

$$n = 0, \quad \frac{\partial n}{\partial y} = 0.$$

The result is

$$\frac{1}{\sigma} \frac{\partial^2 q}{\partial x^2} + \frac{\partial^2 q}{\partial z^2} = \frac{W}{K} \cdot \frac{\partial q}{\partial z},$$

where  $q = \int n dy$  with the limits mentioned. On using Townsend's well-known relation

$$\frac{W}{K} = 41 \frac{Z}{k},$$

and making the substitution  $z = c\zeta$ , this in turn becomes

$$\frac{\partial^2 q}{\partial x^2} = 41 \left( \frac{Z\sigma}{kc} \right) \frac{\partial q}{\partial \zeta} - \frac{\sigma}{c^2} \frac{\partial^2 q}{\partial \zeta^2}. \quad \dots (2)^*$$

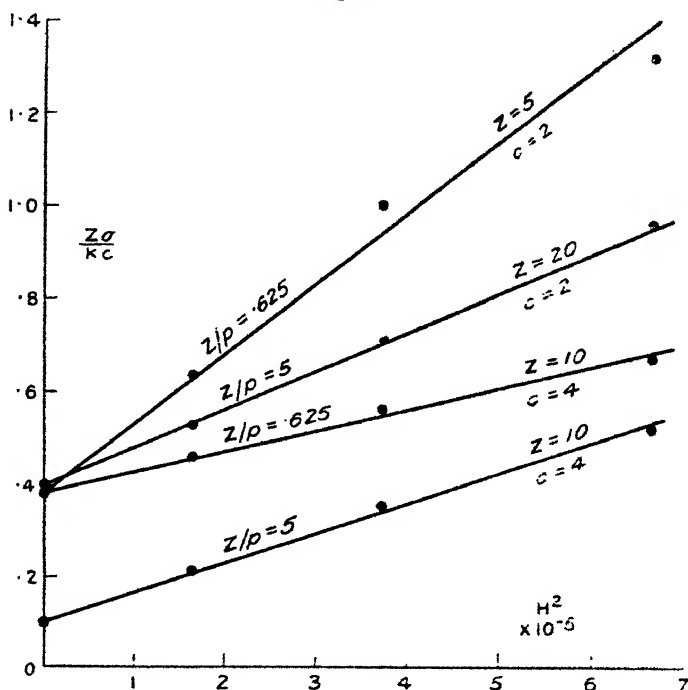
If the quantity  $Zc/k$  be not too small, the second term on the right may be neglected in comparison with the first, which gives

$$\frac{\partial^2 q}{\partial x^2} = 41 \left( \frac{Z\sigma}{kc} \right) \frac{\partial q}{\partial \zeta}.$$

\*  $Z$  is in volts per centimetre.

Since  $\zeta$  is a pure number with limiting values 0 and 1, and in the diffusion instrument only dimensions in the direction of the  $z$ -axis can be varied, the ratio  $R$  depends on the quantity  $Z\sigma/kc$  alone; this quantity becomes  $Z/kc$  when the magnetic field is absent, so the assertion made about the divergence of an electronic stream in a magnetic field is now established\*.

Fig. 8.



### 3. Experimental Verification.

Before considering the way in which this principle may be applied to the determination of the drift-velocity  $W$ , some experiments with hydrogen may be described which were made† with the purpose of testing its truth.

In each set of observations the pressure  $p$ , the electric intensity  $Z$ , and the spacing  $c$  of the slits were maintained constant, and the ratio  $R$  was determined for magnetic fields

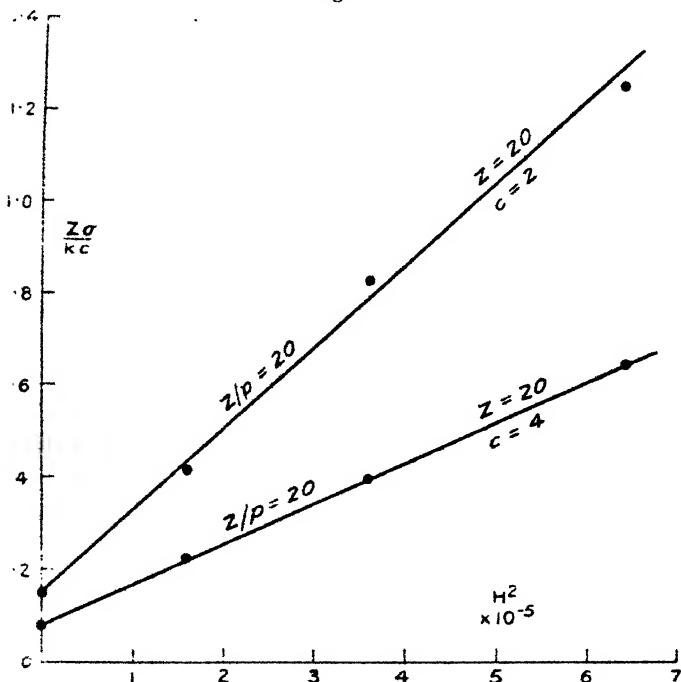
\* A more rigorous, but less useful, statement is that the magnetic field affects the ratio  $R$  as if the dimensions of the instrument in the  $x$ -direction were increased by the factor  $\sqrt{\sigma}$ ; this follows on making the substitution  $x = \xi/\sqrt{\sigma}$  in the accurate differential equation.

† I am indebted to Mr. W. E. Duncanson, B.Sc., for most of them.

of different intensities. These intensities were 0, 408, 612, and 816 gauss. The values of  $Z\sigma/kc$ , corresponding to the values of  $R$ , were then obtained by means of the curve in fig. 2, and the points, with abscissæ  $x=H^2$  and ordinates  $y=Z\sigma/kc$ , were plotted as in figs. 3 and 4.

Six sets of observations were thus made with the forces, pressures, and spacings given in the columns  $Z$ ,  $p$ , and  $c$  of Table I. In each set the points  $(x, y)$ , corresponding to the four values of  $H$ , were found to lie on a straight line

Fig. 4.



(within limits of experimental error), as may be seen in the figs. 3 and 4\*.

This is in agreement with the relation (1), for it may be written as

$$y = 10^{-16} \left( \frac{W^2}{Zkc} \right) x + \frac{Z}{kc},$$

and  $Z$ ,  $c$ ,  $k$ , and  $W$  are constants in each set of experiments.

Additional tests of the theory are provided by the slopes

\* The points in fig. 4 correspond to the magnetic intensities 0, 400, 600, and 800.

$dy/dx$  of the straight lines, for these enable the values of the velocity  $W$  to be calculated by means of the formula

$$W = \sqrt{Zkc \cdot dy/dx} \times 10^8,$$

and a comparison to be made with the values  $W_T$  obtained by means of Townsend's method.

This is shown in Table I., where  $Z$  is in volts/cm.,  $p$  in mm. of mercury,  $c$  in centimetres, and  $W$  in centimetres/sec.

Thus the preliminary experiments give results in accordance with the theory, as is indicated by the agreement between the numbers in the last two columns.

TABLE I.

$Z/p$ .	$Z$ .	$p$ .	$c$ .	$W \times 10^{-5}$ .	$W_T \times 10^{-5}$ .
625	5	8	2	9.9	9.9
	10	16	4	10.9	
5	10	2	4	26	25.5
	20	4	2	29.5	
20	20	1	2	74.5	70
	20	1	4	74.5	

#### 4. Experimental Procedure.

In practice the velocity  $W$  is more conveniently determined by means of the following method, which is based on the same principle, for, in general, with a given set of values of  $Z$ ,  $p$ , and  $c$ , the value of  $k$  has to be determined as well as that of  $W$ . If, then,  $k$  be known,  $W$  is easily obtained by observing what value of  $H$  will make the divergence of the stream (measured by  $R(Z\sigma/kc)$ ) identical with that of a stream composed entirely of negative ions (measured by  $R(Z/c)$ ). For, if this value be denoted by  $H_0$ , then

$$R\left(\frac{Z\sigma}{kc}\right) = R\left(\frac{Z}{c}\right).$$

Therefore  $k = \sigma = 1 + (H_0 W/Z)^2$ ,

and so  $W = \frac{Z}{H_0} \sqrt{k-1} \times 10^8$ . . . . . (3)

from which  $W$  may be determined.

This method has been applied to hydrogen, with the results shown in Table II. The values of  $W$  in the fifth column have been calculated by means of equation (3), and are seen to agree well with the values  $W_T$  obtained by means of Townsend's method.

TABLE II.

$c=4$  cm.,  $Z=4$  volts/cm.,  $R(Z/c)=.555$ .

$Z/p$ .	$k$ .	$p$ .	$H_0$ .	$W \times 10^{-5}$ .	$W_T \times 10^{-5}$ .	$186 Z^2/H_0^2 \times 10^4$ .	$\lambda \times 10^4$ .
.625	6.5	6.4	950	9.86	9.9		
5	26	.8	760	26.3	25.5	51	46
20	78	.2	500	70.2	70	118	117

In connexion with this method it is interesting to observe that, by making the electrons appear to behave like negative ions, the effects of the latter (when present) on the divergence have been completely eliminated. It follows that, even when large numbers of negative ions are present, this method is still applicable, and so enables reliable values of  $W$  to be obtained when the values of  $k$  have been determined, as for example, in the recent work on Ammonia\*.

A remarkable consequence of the method is that for values of  $k$  greater than 20 the values of  $\lambda$ , the fraction of its own energy lost by an electron in a collision, are given by the simple formula

$$\lambda = 186 Z^2/H_0^2, \quad . . . . . (4)^\dagger$$

which involves only the electric and magnetic intensities. This follows from the relations

$$\lambda = 2.46 W^2/u^2, \quad u = 1.15 \sqrt{k} \times 10^7, \quad \text{and (3),}$$

where  $u$  is the velocity of agitation of an electron, when  $1/k$  is negligible compared with unity, and is illustrated by the numbers in the last two columns of Table II.

Experiments for the determination of  $\alpha/p$ ,  $k$ , and  $W$  in ammonia and hydrogen chloride are now in progress, and the results will be published in the near future. These results will make possible reliable estimates of  $h$ , the probability of attachment of an electron which collides with a molecule.

\* V. A. Bailey and J. D. McGee, *loc. cit.*

†  $Z$  is in volts/cm.



LIII. *Hamilton's Principle and the Field Equations of Radiation.* By D. MEKSYN\*.

§ 1. *Summary.*

THE problem of finding from Hamilton's Principle the most general field laws for an antisymmetric tensor of the second rank in five dimensions is solved.

The tensor has 10 (6 + 4) components four of which are complex, and two scalar functions are introduced as a result of the variational problem ; in all there are sixteen functions. The sixteen equations obtained are those of radiation.

For the case of free motion and, to the first approximation, for an external electromagnetic field these sixteen equations can be combined into eight (C. G. Darwin's equations)†. For the case of an electromagnetic field these equations are presented in a general tensor form, and the well-known operators

$$p_1 = \frac{h}{2\pi i} \frac{\partial}{\partial x} + \frac{e}{c} A_1 \dots$$

appear quite naturally as terms in contravariant differentiation.

It appears that the five-dimensional continuum represents a natural system of reference for radiation phenomena.

§ 2. *The Method of Solution.*

We have to solve the problem of finding the most general field equations for a particular tensor in space, which follow from Hamilton's Principle.

The method of solution is purely formal, and is equally well applied to 3, 4, and 5 dimensions.

We describe the field in all cases by an antisymmetric tensor of the second rank. For 3, 4, and 5 dimensions we obtain the electrostatic, electromagnetic, and the radiation field equations.

We solve the problem for an antisymmetric tensor of the second rank, because we know that for 3 and 4 dimensions this tensor represents some existing physical state, and, hence, it is natural to inquire whether this is also the case for 5 dimensions. The equations obtained represent a formal generalization of Maxwell's ones.

\* Communicated by the Author.

† Proc. Roy. Soc. A, cxviii. p. 654.

In so far as the solution of the least action problem is concerned, we have to bear in mind the following: if the quantities in the Hamiltonian are differentials, the variational problem can be solved directly (as in dynamics), otherwise these quantities ought to be represented by means of differential coefficients of some other quantities, because without such representation the variational method cannot be applied.

Of course the equations obtained depend, to some extent, upon the form of this representation. We try therefore to find the most general form of representation of an anti-symmetric tensor of the second rank, with the only limitations that these expressions must not conflict with the law of transformation of the particular space.

### § 3. *Application to Three Dimensions.*

In order to make these considerations clear we give here the solution of this problem for the case of three dimensions.

The field is described by a three-vector  $E(E_x, E_y, E_z)$ . The Hamiltonian is

$$W = \frac{1}{2} \int E^2 dx dy dz. \quad . \quad . \quad . \quad (1)$$

Now Stokes has proved\* that a three-vector can be represented by means of scalar and vector potentials  $\phi$ ,  $V(V_x, V_y, V_z)$  as follows:—

$$E = \text{grad } \phi + \text{rot } V, \quad . \quad . \quad . \quad (2)$$

under the condition that

$$\text{div } V = 0. \quad . \quad . \quad . \quad (3)$$

As a matter of fact  $\phi$  and  $V$  are found from

$$\nabla^2 \phi = \text{div } E; \quad \nabla^2 V = -\text{rot } E.$$

The field equations are obtained from  $\delta W = 0$ , using (2) and (3).

We have

$$\int \left( \delta \frac{E^2}{2} + \mu \delta \text{div } V \right) dx dy dz = 0. \quad . \quad . \quad (4)$$

Using (2), and integrating by parts, we easily find that (4) is equivalent to

$$-\int \{ \text{div } E \cdot \delta \phi + ([\text{grad } \mu - \text{rot } E] \cdot \delta V) \} dx dy dz = 0,$$

\* A. E. H. Love, 'A Treatise on the Mathematical Theory of Elasticity,' p. 47 (1920).

and the field equations are

$$\left. \begin{aligned} \operatorname{div} \mathbf{E} &= 0, \\ \operatorname{rot} \mathbf{E} &= \operatorname{grad} \mu. \end{aligned} \right\} \dots \dots \dots (5)$$

It can be shown that all four quantities  $\mathbf{E}$  and  $\mu$  satisfy Laplace's equation.

In (5) there appear, except for the electrostatic vector  $\mathbf{E}$ , also a new quantity  $\mu$ . It will be shown in a separate paper that this quantity represents the potential of a hydrostatic pressure, which is necessary for stability of an electron.

#### § 4. *Some Metrical Properties of Five-dimensional Space.*

We give here for convenience' sake a few well-known laws of the five-dimensional space\*.

The transformations for the space-time coordinates do not depend upon the fifth dimension, and are the same as in the theory of Relativity. The transformation of the fifth dimension is merely

$$x_5' = x_5. \dots \dots \dots (6)$$

If we apply these rules to an antisymmetric tensor of the second rank

$$T_{\mu\nu}' = \frac{\partial x_\mu'}{\partial x_\alpha} \frac{\partial x_\nu'}{\partial x_\beta} T_{\alpha\beta}, \dots \dots \dots (7)$$

we find that the six space-time components are transformed as an antisymmetric tensor of the second rank in the Theory of Relativity, and the four components associated with the fifth dimension

$$T_{\nu\mu 5}' = \frac{\partial x_\mu'}{\partial x_\alpha} \frac{\partial x_5'}{\partial x_\beta} T_{\alpha\beta} = \frac{\partial x_\mu'}{\partial x_\alpha} T_{\alpha 5} \dots \dots (8)$$

are transformed as a four-vector.

The fundamental tensor is

$$\left. \begin{aligned} \gamma^{ik} &= g^{ik}, & \gamma^{i5} &= -\beta\phi^i, & \gamma^{55} &= 1 + \beta^2\phi_k\phi^k, \\ \gamma_{ik} &= g_{ik} + \beta^2\phi_i\phi_k, & \gamma_{i5} &= \beta\phi_i, & \gamma_{55} &= 1 - (i, k = 1, 2, 3, 4), \end{aligned} \right\} \dots \dots (9)$$

where  $g_{ik}$  is the gravitational tensor and  $\phi_i$  is the vector-potential of an external electromagnetic field.

\* O. Klein, *Zeits. f. Phys.* xlv. p. 189 (1928).

For  $\beta$  we take the value

$$\beta = \frac{e}{imc^2}. \quad . \quad . \quad . \quad . \quad . \quad (10)$$

For this value of  $\beta$  the track of an electron becomes, as Fock\* and Fisher have shown, a null geodesic, and Schrödinger's wave equation appears to be the usual wave equation in this space.

### § 5. Representation of an Antisymmetric Tensor of the Second Rank by means of Two Vectors.

The method of derivation of the field equations in the case of five dimensions is similar to the classical one, and is based upon representation of an antisymmetric tensor of the second rank by means of differential coefficients of two five-vectors. As we have pointed out, such representation is necessary in order to solve the variational problem.

Let us find out under what conditions this is possible.

Let  $F_{\alpha\beta}$  be an antisymmetric tensor,  $k_1 \dots k_5$  and  $l_1 \dots l_5$  two five-vectors.  $F_{\alpha\beta}$  can be expressed as follows:—

$$F_{\alpha\beta} = \frac{\partial k_\alpha}{\partial x_\beta} - \frac{\partial k_\beta}{\partial x_\alpha} + \frac{\partial l_\delta}{\partial x_\gamma} - \frac{\partial l_\gamma}{\partial x_\delta}, \quad . \quad . \quad . \quad (11)$$

$$\alpha\beta\gamma\delta = (1, 2, 3, 4).$$

The signs in the six equations (11) correspond to an odd number of permutations in the series  $\alpha\beta\gamma\delta$ . Also

$$F_{\alpha 5} = \frac{\partial k_\alpha}{\partial x_5} - \frac{\partial k_5}{\partial x_\alpha}; \quad G_{\alpha 5} = \frac{\partial l_\alpha}{\partial x_5} - \frac{\partial l_5}{\partial x_\alpha}, \quad . \quad (11a)$$

$$\alpha = (1, 2, 3, 4).$$

It appears that, except for  $F_{\alpha\beta}$ , new quantities  $G_{15} \dots G_{45}$  have to be introduced; we can thus consider the fifth dimensional components of  $F_{\alpha\beta}$  as complex.

The origin of these quantities is as follows:—In order to justify our form of representation of the tensor  $F_{\alpha\beta}$  by means of two vectors  $k$  and  $l$ , we have to prove that from a given tensor  $F_{\alpha\beta}$  we can always discover the vectors  $k, l$  (see equations (12)).

In the case of 3 and 4 dimensions  $k$  and  $l$  satisfy the usual wave equation, and we may expect that this will hold good for the present case.

\* *Zeits. f. Phys.* xxxix. p. 22 (1926); J. K. Fisher, *Proc. Roy. Soc. A*, cxxiii. p. 489 (1929).

From the simple algebra of evaluating the equations (12) it follows that, unless we make use of additional quantities  $G_{15}\dots$ , we are unable to obtain the required equations for  $k$  and  $l$ .

We have now to prove that if  $F_{\alpha\beta}$  and  $G_{15}\dots$  are given, the two vectors  $k$  and  $l$  can be found.

The following expressions are easily obtained :—

$$\left. \begin{aligned} \frac{\partial F_{\alpha\beta}}{\partial x_\gamma} + \frac{\partial F_{\beta\gamma}}{\partial x_\alpha} + \frac{\partial F_{\gamma\alpha}}{\partial x_\beta} + \frac{\partial G_{\delta\beta}}{\partial x_\delta} &= \square^2 l_\delta - \frac{\partial L}{\partial x_\delta}, \\ \frac{\partial G_{\alpha\delta}}{\partial x_\alpha} &= -\square^2 l_\delta + \frac{\partial L}{\partial x_\delta}, \\ \alpha\beta\gamma\delta &= (1, 2, 3, 4). \end{aligned} \right\} \quad (12)$$

The law of composition of the four equations which follow from the first expression in (12) is simple ; the values  $\alpha, \beta, \gamma$  are any three from 1, 2, 3, 4 taken in order ; the sign in (12) corresponding to an even number of permutations in the series  $\alpha\beta\gamma\delta$ . Also

$$\frac{\partial F_{\alpha\beta}}{\partial x_\beta} = \square^2 k_\alpha - \frac{\partial K}{\partial x_\alpha}, \quad \dots \dots (12a)$$

$$\alpha, \beta = 1, 2, 3, 4, 5.$$

In all the equations the expression must be summed with respect to those indices which occur twice.

In the equations (12) and (12a)

$$\left. \begin{aligned} K &= \text{div } k, \\ L &= \text{div } l, \\ \square^2 &= \frac{\partial^2}{\partial x_1^2} + \frac{\partial^2}{\partial x_2^2} + \frac{\partial^2}{\partial x_3^2} + \frac{\partial^2}{\partial x_4^2} + \frac{\partial^2}{\partial x_5^2}. \end{aligned} \right\} \quad (13)$$

We assume

$$K=0, \quad L=0, \quad \dots \dots (14)$$

and the two vectors  $k_1\dots k_5$ ,  $l_1\dots l_5$  can be evaluated from (12) and (12a).

It is clear that not all components of the tensors  $F$  and  $G$  are independent; the two antisymmetric tensors have fourteen components, whereas we have only eight independent quantities to express them. Hence the components of the antisymmetric tensor must satisfy six additional conditions. They are easily found, and are given later (equations (19)).

§ 6. *The Variational Problem and the Field Equations.*

The Hamiltonian has in this case the following expression:—

$$W = \frac{1}{2} \int (F_{14}^2 + F_{24}^2 + F_{34}^2 + F_{23}^2 + F_{31}^2 + F_{12}^2 + F_{15}^2 + F_{25}^2 + F_{35}^2 + F_{45}^2 + G_{15}^2 + G_{25}^2 + G_{35}^2 + G_{45}^2) dx_1 dx_2 dx_3 dx_4 dx_5. \quad (15)$$

The field equations are obtained from the condition

$$\delta W = 0. \quad (16)$$

In the evaluation of (16) we have to make use of the equations (11), (11a), and (14) after the latter have been multiplied by indeterminate factors  $\mu$  and  $\lambda$  respectively; the Hamiltonian becomes

$$\int \delta \left( \frac{F_{14}^2 + \dots + G_{45}^2}{2} \right) + \mu \delta K + \lambda \delta L) dx_1 \dots dx_5 = 0. \quad (16a)$$

Integrating by parts (16a) we easily find the required equations. They are as follows:—

$$\frac{\partial F^{\alpha\beta}}{\partial x_\beta} + \frac{\partial \mu}{\partial x_\alpha} = 0, \quad (17)$$

$$\alpha, \beta = 1, 2, 3, 4, 5;$$

also

$$\left. \begin{aligned} \frac{\partial F^{\alpha\beta}}{\partial x_\gamma} + \frac{\partial F^{\beta\gamma}}{\partial x_\alpha} + \frac{\partial F^{\gamma\alpha}}{\partial x_\beta} + \frac{\partial G^{\beta\delta}}{\partial x_5} + \frac{\partial \lambda}{\partial x_6} &= 0, \\ \alpha\beta\gamma\delta &= (1, 2, 3, 4), \\ \frac{\partial G^{5i}}{\partial x_i} + \frac{\partial \lambda}{\partial x_5} &= 0, \quad i = 1, 2, 3, 4, 5. \end{aligned} \right\} \quad (18)$$

The first expression in (18) comprises four equations; the signs correspond to an even number of permutations in the series  $\alpha\beta\gamma\delta$ .

As we have pointed out, there are six additional conditions to be imposed upon the components of the antisymmetric tensor. It is easily verified from (11) and (11a) that these conditions are

$$\frac{\partial F_{\alpha\delta}}{\partial x_\beta} - \frac{\partial F_{\beta\delta}}{\partial x_\alpha} + \frac{\partial F_{\delta\gamma}}{\partial x_\gamma} - \frac{\partial F_{\gamma\delta}}{\partial x_\delta} - \frac{\partial F_{\alpha\beta}}{\partial x_5} = 0, \quad (19)$$

$$\alpha, \beta, \gamma, \delta = (1, 2, 3, 4).$$

These are six equations, and the signs in (19) correspond to an odd number of permutations in the series  $\alpha\beta\gamma\delta$ .

In order to eliminate imaginary quantities from the equations (17–19), and bring them into the same form as

Maxwell's equations, we have merely to bear in mind that the following quantities are purely imaginary :—

$$x_4, F_{15}, F_{25}, F_{35}, G_{45}, F_{12}, F_{31}, F_{23}, \mu. \quad (20)$$

The equations obtained (17–19) can be easily brought into J. M. Whittaker's equations \*; his six-vector and two four-vectors correspond to our antisymmetric tensor with fourteen components. Whittaker's way of deriving these equations is different from ours. He assumes eight equations, as given, and derives the other eight ones from Hamilton's principle.

§ 7. We show now that the system of sixteen equations (17–19) can be easily brought into C. G. Darwin's form of Dirac's equations.

We consider the case when there is no electromagnetic or gravitational field. For that case we need not distinguish between covariant and contravariant tensors.

We combine the first three equations of (17) with (19) (for  $F_{14}, F_{24}, F_{34}$ ) multiplied by  $i = \sqrt{-1}$  respectively, and combine the fourth with the fifth equations (17) multiplied also by  $i$ ; the same procedure we adopt with respect to equations (18) and (19) (for  $F_{23}, F_{13}, F_{12}$ ). The result is

$$\left. \begin{aligned} & \left( \frac{\partial}{\partial x_4} + i \frac{\partial}{\partial x_5} \right) (F_{14} - iF_{15}) + \frac{\partial}{\partial x_2} (F_{12} - iG_{35}) \\ & \quad - \frac{\partial}{\partial x_3} (F_{31} - iG_{25}) + \frac{\partial}{\partial x_1} (\mu + iF_{45}) = 0, \\ & \left( \frac{\partial}{\partial x_4} + i \frac{\partial}{\partial x_5} \right) (F_{24} - iF_{25}) - \frac{\partial}{\partial x_1} (F_{12} - iG_{35}) \\ & \quad + \frac{\partial}{\partial x_3} (F_{23} - iG_{15}) + \frac{\partial}{\partial x_2} (\mu + iF_{45}) = 0, \\ & \left( \frac{\partial}{\partial x_4} + i \frac{\partial}{\partial x_5} \right) (F_{34} - iF_{35}) + \frac{\partial}{\partial x_1} (F_{31} - iG_{25}) \\ & \quad - \frac{\partial}{\partial x_2} (F_{23} - iG_{15}) + \frac{\partial}{\partial x_2} (\mu + iF_{45}) = 0, \\ & \left( \frac{\partial}{\partial x_4} - i \frac{\partial}{\partial x_5} \right) (\mu + iF_{45}) - \frac{\partial}{\partial x_1} (F_{14} - iF_{15}) \\ & \quad - \frac{\partial}{\partial x_2} (F_{24} - iF_{25}) - \frac{\partial}{\partial x_3} (F_{34} - iF_{35}) = 0. \end{aligned} \right\} \quad (21)$$

These are exactly Dirac's equations in Darwin's form.

\* Proc. Roy. Soc. A, cxxi. p. 543.

To obtain the terms  $mc$  we have merely to suppose that the fifth coordinate enters in the functions in the following dependence :—

$$e^{\frac{2\pi i}{h} m c x_s} \cdot \cdot \cdot \cdot \cdot \cdot \cdot \cdot (22)$$

### § 8. The Field Equations for an External Electromagnetic Field.

To determine the field equations for the case of an external electromagnetic field we have to represent our equations in general tensor form\*.

The equations (17) are easily written out in a tensor form. They are

$$F^{\alpha\beta}{}_{\beta} + \mu^{\alpha} = 0, \quad . \quad . \quad . \quad . \quad . \quad (23)$$

$$\alpha, \beta = (1-5),$$

where  $\mu^a$  represents a contravariant differentiation with respect to  $x^a$ , or

$$\mu^a = \gamma^{a\sigma} \mu_\sigma. \quad . \quad . \quad . \quad . \quad . \quad . \quad (24)$$

We transform in (23) the terms  $F^{a\bar{b}}_b$ . We have, for instance,

$$F^{15} = \gamma^{1\alpha} \gamma^{5\beta} F_{\alpha\beta} = \gamma^{11} \gamma^{52} F_{12} + \gamma^{11} \gamma^{53} F_{13} + \gamma^{11} \gamma^{54} F_{14} + \gamma^{11} \gamma^{55} F_{15} \\ + \gamma^{15} \gamma^{15} F_{51} + \gamma^{15} \gamma^{52} F_{52} + \gamma^{15} \gamma^{53} F_{53} + \gamma^{15} \gamma^{54} F_{54}. \quad (25)$$

If we insert in (25) the values (9) of the fundamental tensor for the case when there is no gravitation, we easily find

$$F^{15} = F_{15} + \gamma^{52} F^{12} + \gamma^{53} F^{13} + \gamma^{54} F^{14}, \quad . \quad (26)$$

and hence the first equation (23) takes the form

$$F^{12}_2 + \gamma^{52} F^{12}_5 + F^{13}_3 + \gamma^{53} F^{13}_5 + F^{14}_4 + \gamma^{54} F^{14}_5 + F_{15,5} + \mu^1 = 0,$$

or finally the first set of equations (23) becomes

$$\left. \begin{aligned} F^{12, 2} + F^{13, 3} + F^{14, 4} + F_{15, 5} + \mu^1 &= 0, \\ . &. \\ F^{41, 1} + F^{42, 2} + F^{43, 3} + F_{45, 5} + \mu^4 &= 0, \\ F_{51, 1} + F_{52, 2} + F_{53, 3} + F_{54, 4} + \mu_5 &= 0. \end{aligned} \right\} \cdot \quad (27)$$



These appear to be equations between quantities not of the same variance, but it is to be noted that this results from the removal of the gravitational field so that there is no distinction between the two types of variance.

We have to bear in mind that a contravariant differentiation with respect to  $x_k$  ( $k=1, 2, 3, 4$ ) is, to the first approximation, equivalent to the operator  $\frac{h}{2\pi i} \cdot \frac{\partial}{\partial x_k} + \frac{e}{c} \phi_k$ .

We see that this operator appears quite naturally in our equations.

To present (18) in a tensor form we make use of the same procedure as in the case of the second set of Maxwell's equations in the Special Theory of Relativity. We introduce, instead of the tensor  $F^{\alpha\beta}$ , a new one in the following manner:—

$$\left. \begin{array}{l} \text{Instead of } F^{43}, F^{24}, F^{32}, F^{41}, F^{13}, F^{21}, \\ \text{we take } G^{12}, G^{13}, G^{14}, G^{23}, G^{24}, G^{34}. \end{array} \right\} \quad (28)$$

We complete thus the missing terms of the tensor  $G^{\alpha\beta}$ . To find the covariant components of  $G^{ik}$  we make use of the six equations

$$\gamma^{4\alpha}\gamma^{3\beta}F_{\alpha\beta} = \gamma^{1\alpha}\gamma^{2\beta}G_{\alpha\beta}, \quad . \quad . \quad . \quad (29)$$

and four equations

$$G^{i5} = \gamma^{i\alpha}\gamma^{5\beta}G_{\alpha\beta}. \quad . \quad . \quad . \quad (30)$$

From (29) and (30) we easily find the covariant tensor  $G_{\alpha\beta}$ . So, for instance,

$$G^{15} = G_{15} + \gamma^{52}F_{43} + \gamma^{53}F_{24} + \gamma^{54}F_{32}.$$

Now the equations (18) become

$$\begin{aligned} G^{\alpha\beta}{}_{,\beta} + \lambda^{\alpha} &= 0, \quad . \quad . \quad . \quad (31) \\ \alpha, \beta &= (1-5), \end{aligned}$$

and the five equations (31) can be represented in the same form as (27).

We transform the set of equations (19). The simplest assumption would be for the first equation (19)

$$F_{15,2} - F_{25,1} + G_{45,3} - G_{35,4} - F_{12,5} = 0. \quad . \quad (32)$$

If we express  $F_{12}$  by means of  $F^{12}$ , when the gravitational field is absent,

$$F^{12} = F_{12} + \gamma^{15}F_{52} + \gamma^{25}F_{15},$$

and combining this expression with (32), we obtain

$$F_{15}^2 - F_{25}^1 + G_{45,3} - G_{35,4} - F_{15}^{12} = 0,$$

or the equations are not symmetric with respect to the functions  $G_{k5}$  and  $F_{35}$ ; they do not agree to the first approximation with Dirac's equations.

We assume, therefore, the following form for our equations:—

$$(F^{\alpha}_{\beta})^{\beta} - (F^{\beta}_{\beta})^{\alpha} + (G^{\delta}_{\beta})^{\gamma} - (G^{\gamma}_{\beta})^{\delta} - F^{\alpha\beta}_{\beta} = 0, \quad (33)$$

$$\alpha, \beta, \gamma, \delta = (1, 2, 3, 4).$$

The signs in the six equations (33) correspond to an odd number of permutations in the series  $\alpha\beta\gamma\delta$ . Here  $(F^{\alpha}_{\beta})^{\beta}$  means the contravariant differentiation of  $F^{\alpha}_{\beta}$  with respect to  $x_{\gamma}$ .

For the case when there is no gravitation

$$F^1_{\beta} = \gamma^{1\alpha} F_{\alpha\beta} = F_{1\beta},$$

or the operators are performed upon the same functions as in (27) and (31).

The field equations for the general case of an electromagnetic and gravitational force are (23), (28), (31), and (33).

Wheatstone Laboratory,  
King's College, London.

LIII. *Frictional Electricity.* By Professor P. E. SHAW,  
M.A., D.Sc., University College, Nottingham \*.

**T**HIS subject is far the oldest branch of electricity, and it provides far the easiest way of raising electric charges. There can be no easier experiment than that of rubbing one's fountain-pen on a coat-sleeve and using the excited pen to raise a small scrap of paper.

It is all the more remarkable that, after a century of great advance in the theory and application of electricity, and after a generation of unparalleled progress in its fundamentals, our knowledge of frictional (or tribo-) electricity is still meagre. Writers of text-books and

\* Communicated by the Author.

reference books allot a mere page or two of qualitative information, and then, after brief and guarded statements on the subject, seem glad to leave it for safer and more matured topics, such as, say, voltaic or thermo-electricity. However, it is possible after the progress made in tribo-electricity in the last fifteen years to bring together many new salient facts. Closer study of this subject, so simple-seeming, has revealed complications apparently unsuspected by the earlier workers. We will indicate some experimental results and some principles which are only found in recent research, or are revealed now for the first time.

I.—The time-honoured method of discharging an excited body is to pass it through a flame. This process is unnecessarily drastic ; for the ionized zone above and around a flame acts quite well. But the flame method is definitely bad, since it not only discharges the body but may, as we shall see in the next section, modify its surface profoundly. How often has a teacher, using the flame method, found his experiment go all wrong, and then had to take refuge in the traditional excuse that frictional electricity is a fickle, "fortuitous" subject on account of atmospheric moisture ! To discharge a rod we do not use the flame method, but its surrounding zone.

II.—When a glass rod which rubs *positive* to silk is placed, even for a second or two, in a flame, it is then found to rub *negative* to the silk, and, further, the friction between the glass and silk has now increased considerably. But on continuing the rubbing with vigour the glass returns to its positive state, and friction is again low. This reversible process, which is quite dependable, was investigated by the writer \* ; but its physical significance has only just been revealed. We can rub glass from the negative to the positive state by ordinary silk, flannel, or felt ; but when these fabrics have been exhaustively cleansed of fats, waxes, etc. by purest benzene or chloroform, the glass is persistently negative. Now, if on the cleansed fabric any one of many solid organic compounds of low melting-point be placed, the glass will after persistent rubbing become positive. The choice of organic material is very great ; fatty, bibasic, or aromatic acids, esters or

\* Shaw, Proc. Phys. Soc., April 1915 ; Proc. Roy. Soc. A, xciv. (1917).

ketones, all operate well. It is clear, then, that an organic film, with good polish, is formed on the glass and is removed at once by a flame, or, alternatively, by raising its temperature to  $300^{\circ}\text{C}$ . Thus in the well-known experiment of rubbing glass positive with silk, the surface rubbed is not glass at all, but an organic film; but when clean fabric is rubbed on clean glass the charge on the latter is invariably negative. Sir W. B. Hardy\* in his investigations on boundary lubrication, found such films to have very low friction, and to be very tenacious. He considered them very thin, possibly monomolecular.

Recent work has shown that these organic films form more or less readily not only on glass but on various metals, ebonite, etc., and as with glass, and by their presence, change these surfaces from a negative to a positive one when rubbed with, say, filter paper or clean silk.

III.—Faraday and others have observed that apparently identical solids, say two like feathers, become charged when rubbed together. This effect has now been investigated †. Excellent material for the purpose is ebonite. Two pieces of it cut from the same rod and rubbed will, in general, give charges of an irregular kind. To make these charges regular anneal the rods by raising them to  $100^{\circ}$  in boiling water. Dry them and allow to cool. Then, laying one rod (*a*) across the other (*b*), stroke the latter with the former. At once (*a*) becomes negative, (*b*) positive. This electric separation is not due to any difference in the rods, for when the rods are changed, so that (*b*) is rubbed on (*a*), (*b*) becomes negative and (*a*) positive. On continuing the rubbing of (*b*) on (*a*) the charges gradually decrease, vanish, and finally reverse signs, so that (*b*) is now positive.

These effects are attributable to the different strains arising on the rods where they rub one another. The two surfaces being equally hard must both become strained in rubbing. But the upper rod (*b*) bears throughout a stroke on one spot, so that at that spot the effect is concentrated, and the strain grows quickly; the other rod (*a*) is rubbed along a whole generating line, so the strain is distributed over a large area, and no part of it becomes greatly strained until after many strokes.

\* Proc. Roy. Soc. A, cviii. (1925).

† Shaw, Proc. Phys. Soc., August 1927.

The upshot is that the acting parts of (*b*) and (*a*), being strained in different degree, the rods, though *chemically* identical, differ *physically*. They therefore act tribo-electrically as different bodies, and become charged negative and positive respectively.

To pursue the argument : since the energy spent on each rod is the same, the smaller area of (*b*) becomes hotter than the larger area of (*a*), and being hotter recovers more quickly from the strain. So in the end the strain on (*a*) becomes greater than that on (*b*), and the sign of the charge reverses, as we have seen. The rule is that the more strained surface is negative to the less strained. Other materials, *e. g.*, amberite, celluloid, and metals, show the same effects. It has been observed by Beilby \* that two wires of identical metal, one strained, the other annealed, show the thermo-electric effect when placed in contact. Thus we have independent support for the statement that strain changes the physical nature of a surface.

IV.—Rubbing is the usual way of exciting charges, but normal impact of the two surfaces serves quite well, as shown by Richards † and by others. On consideration one sees that in normal impact, while most of the force is expended in direct compression of the two surfaces, these will in general experience a certain amount of tangential or sliding movement, the only purely normal contact occurring in the ideal case when two perfectly plane surfaces meet, in normal contact.

Thus the word “frictional” in its usual sense is not strictly applicable to this subject, since triboelectricity arises without rubbing or friction.

An interesting effect occurs in this connexion. Let two rods of ebonite or other good insulator be struck together violently with a glancing blow so as to meet in oblique, not normal, impact. If the two rods be then together brought near a gold-leaf electroscope there will generally be found on them a net *negative* charge of considerable amount. Faraday’s law states that the charges on the two surfaces produced by rubbing are equal and opposite, *i. e.*, the net charge is nil. This is true for *rubbing* where the surfaces

\* Beilby, ‘Aggregation and Flow of Solids,’ Macmillan & Co.

† Richards, *Phys. Rev.* 1920, p. 290.

remain in contact for much longer time than in the process of oblique *impact*. But the law fails, as we see, for violent oblique impact. We have failed to find it in cases of normal impact. In the case of a glancing blow the surfaces separate more quickly.

In the circumstances we cannot conceive that negative electricity is generated by the impact; so the only conclusion is that one or both of the rods has lost some *positive* charge to the air. To explain this one supposes that something like an explosion occurs on one or both of the surfaces, the ejectamenta to the surrounding air having net positive charge. We know from Hertz's theory of elastic deformation that the force per unit area at the centre of the contact area in impact may amount to many thousands of atmospheres, and when the two surfaces recoil after the blow is delivered some material may be shot out of the surfaces. If the positive surface loses more than the negative one, the above effect would be produced.

V.—The results of an impact experiment of a different kind lends support to the principle just enunciated. Rudge\* showed that certain powders, when blown from a vessel by a blast of air, attain charges. The writer † has investigated this effect with sand blown through a sand-tube and with a variety of metal filings blown through metal tubes. In each case the filings and tube are of the same material, so there is similarity between this case and the impact of two like insulators, as in the last section. The charge is measured for filings, tube, and emerging air, and the result for all the cases tried is that the filings, the tube, and the air each attain charges which, within experimental errors, are regular. So here again oblique impact between like materials gives rise to a net charge for the two solid materials used and an equal and opposite net charge for the air. It may be observed in passing that this affords an explanation of several meteorological phenomena, such as lightning discharges in volcanic eruptions, electrical sand-storms in deserts, and electrical snow-storms sometimes observed in the Antarctic.

\* Rudge, Roy. Soc. Proc. A, May 1914.

† Shaw, Roy. Soc. Proc. A, cxvii. (1929).

VI.—We have seen in Section II. that organic films on a surface profoundly affect its triboelectric behaviour. There are three other kinds of film \* which have a definite influence on results:—(1) Adsorbed water films condense from the air on many surfaces, particularly glass; these act in a negative way. (2) alkaline films or surfaces also act negatively due to the formation when rubbed of  $-(OH)$  ions. (3) acid films act positively, on account of the production of  $+(H)$  ions. These effects, which are pitfalls for the unwary, demonstrate the futility of seeking data from solids of uncertain composition or surface purity. Many acids and alkalies are extraordinarily tenacious on neutral surfaces like glass; so that, after they have been applied to a surface, abrasion by a hard solid is the only way to move their residual films.

VII. A comprehensive theory to embrace all the known effects of triboelectricity cannot be produced till the subject has been more fully investigated quantitatively. Many physicists have been content to borrow the Volta contact potential principle, so well established for metals, to explain the charges arising triboelectrically when surfaces, whether of metals or non-metals, rub together. Now, we have seen that film effects may play a large part in the nature of triboelectric charges, and allowance for these films must be most carefully made.

But even allowing that such films are adventitious, and should be removed before the real triboelectric effects are observed, we still have to reckon with two factors other than a mere contact effect. These only come into being because of the relative *motion* of the surfaces, and therefore cannot arise in the Volta contact potential, which is purely a statical phenomenon.

These two factors are (1) strain of surfaces, and (2) rise of temperature, both caused by the rubbing; and we have seen that results are fundamentally affected by them.

Riecke † and others ‡ have established formulae for the charge arising when two insulators are rubbed together. In the equation

$$Q = \frac{a}{b} (1 - e^{-bv}),$$

\* Shaw & Jex, Roy. Soc. Proc. A, cxviii. (1928).

† Wied. Ann. 1787, p. 414.

‡ French, Phys. Rev., Feb. 1917.

$Q$  = charge attained,  $w$  = total work done,  $a$ ,  $b$  are constants for the surfaces depending on their specific excitability and leakage. But such simple expressions take no account of the two dynamical factors mentioned above.

Another fundamental objection to a simple volta contact theory is that, whereas in this theory the potential difference arises when the metals are in contact, in triboelectricity the charge is only seen after separation. Some experiments have been made to demonstrate that charges really do exist between insulators when in contact, but they seem most inconclusive. Even if they are allowed to stand as proof on the point, it must be remembered that in triboelectricity the charges are invariably observed *after the surfaces separate*. Is it to be assumed that the process of separating linked molecules does not of itself cause charging?

It will surely be difficult, or impossible, to appraise the influence of these two dynamical factors, so that the charges can be calculated when any given pure substances of known figure are rubbed together with a known expenditure of work. The utmost attainable outcome may be an empirical equation, which, of course, is always a formulated confession of ignorance.

There is a large and promising field of research in this subject. Triboelectricity, which deals with the rough clash of solid surfaces, proves to be a very involved subject. Solid surfaces are more complex than are liquid surfaces, but in recent years much light has been shed on their composition by many different lines of reasoning, notably: the theory of the lattice electrical structure of crystals: the Debye theory of the dipole nature of dielectric molecules: the double electric layer of Helmholtz: Hardy's theory of boundary lubrication: and the Langmuir-Adam work on the monomolecular solid films on water.

The theory of the polar structure of atoms and molecules, and their resultant orientation in suitable fields, should prove as powerful in triboelectricity as in other fields of research.



LIV. *On new Methods in Statistical Mechanics.* By MEGHNAD SAHA, D.Sc., F.R.S., and RAMESH CHANDRA MAJUMDAR, M.Sc., Allahabad University\*.

AT the present time a number of new methods are being developed in statistical mechanics, and it is difficult to see the connexion amongst them. In this essay an attempt is made to review these methods and supply the link amongst the different theories.

Almost all the old (Planck) and new methods (Bose-Einstein<sup>(1)</sup>, Fermi-Dirac<sup>(2)</sup>) start with Boltzmann's theorem

$$S = k \log W,$$

and with Planck's definition of  $W$ , viz. :—

$W$  = Thermodynamical Probability.

There is an alternative function  $G$  due to Boltzmann<sup>(3)</sup> and Gibbs<sup>(4)</sup> which may be described as the total phase volume described by a thermodynamical system. Ehrenfest and Trkal<sup>(5)</sup> treat problems of chemical equilibrium etc. with the aid of this function (they called it  $\{\gamma\}$ ), and find their method superior to Planck's. There is a certain amount of ambiguity in Planck's definition of  $W$ ; according to him  $W$  is a whole number, but Ehrenfest and Trkal have shown that Planck's expression for  $W$  has to be divided by  $N!$  to get the correct expression for  $S$ . The need for this operation is not clear. Planck<sup>(6)</sup> has apparently admitted the soundness of this criticism, and in a recent paper puts a new interpretation on  $W$ . He defines  $W$  as the maximum number of probable states which can give rise to the total energy  $E$ . Planck shows that, with this definition,

$$W = \frac{G}{h^{3N} N!} \dots \dots \dots (1)$$

The same conclusion has been reached independently and simultaneously by Saha and Sur<sup>(7)</sup> from different conceptions. They emphasize the necessity for laying down a unit of probability. At absolute zero  $S = 0$  and  $W = 1$ , and the total phase-volume described  $= h^{3N} N!$  in the simplest case (*i. e.*, a perfect monatomic gas). Denoting this by  $G_0$ , and the corresponding probability by unity, the mathematical value of probability at any temperature

$$W = \frac{G}{G_0} = \frac{G}{h^{3N} N!}.$$

\* Communicated by the Authors.

The conceptions of Planck and Saha and Sur, though apparently different, are in essence identical.

We shall therefore start with the theorem (1) and calculate  $W$ , introducing (1) classical conceptions, (2) the Fermi-Dirac condition, (3) the Bose-Einstein condition.

Let us suppose the assembly to be distributed in equi-energy layers with the energy-interval  $(\epsilon_s, \epsilon_s + d\epsilon_s)$  for each particle, and let  $N_s$  be the number of particles in this interval. The phase-volume occupied by each particle

$$g_s = 2\pi V (2m)^{3/2} \epsilon_s^{1/2} d\epsilon_s. \quad (2)$$

Then, according to Ehrenfest and Trkal,

$$G = \frac{N!}{\prod N_s!} \prod g_s^{N_s}. \quad (3)$$

This theorem has been given by Ehrenfest and Trkal without proof, though to many it may not be so self-evident. We are therefore supplying a proof. Let  $G_N$  denote the phase-space described by  $N$ -particles, and  $G_{N-1}$  the phase-space described by  $N-1$ -particles, the remaining particle being assigned to the region  $(dx dy dz dp_x dp_y dp_z)$ . We have

$$G_N = \frac{V^N (2\pi m)^{\frac{3N}{2}} E^{\frac{3N}{2}}}{\Gamma\left(\frac{3N}{2} + 1\right)}. \quad (3')$$

Now we have <sup>(8)</sup>

$$\frac{G_{N-1}}{G_N} = \frac{dw}{d\tau}, \quad (4)$$

where  $dw$  is the probability that the particle is to be found in the phase-volume considered. We have therefore

$$dw = \frac{N_s}{N},$$

and  $d\tau$  the phase-volume of the particle under question  $= g_s$ . Thus

$$G_N = G_{N-1} \cdot \frac{g_s}{(N_s/N)}.$$

Then by successive application of the same theorem

$$G_N = G_{N-N_s} \left( N \frac{g_s}{N_s} \right)^{N_s},$$

and finally, taking all the energy-layers,

$$\begin{aligned} G_N &= \prod_s g_s^{N_s} \left( \frac{N}{N_s} \right)^{N_s} \\ &= \frac{N!}{\prod_s N_s!} \prod_s g_s^{N_s}. \quad \dots \dots \dots (3) \end{aligned}$$

We have thus reduced the calculation of the phase-volume from the  $6N$  dimensional space to one of 6 dimensions. We shall now show that the classical expression for entropy is easily obtained from this value of  $G$ . We have

$$W = \frac{1}{\prod_s N_s!} \prod_s \left( \frac{g_s}{h^3} \right)^{N_s}.$$

Let  $\frac{g_s}{h^3}$  be denoted by  $a_s$ ;

$$\begin{aligned} \text{then } S &= K \log W \\ &= K \left\{ \sum_s N_s \log a_s - \sum_s N_s (\log N_s - 1) \right\} \\ &= K \sum_s N_s \log \frac{a_s}{N_s} + KN. \quad \dots \dots \dots (4) \end{aligned}$$

$$\begin{aligned} \text{Now } \left. \begin{aligned} E &= \sum_s N_s \epsilon_s \\ N &= \sum_s N_s \end{aligned} \right\} \dots \dots \dots (5) \end{aligned}$$

Hence, applying the variation-principle,

$$\left. \begin{aligned} \delta S &= \sum_s \delta N_s (\log a_s - \log N_s) \\ \delta N &= \sum_s \delta N_s \\ \delta E &= \sum_s \delta N_s \epsilon_s \end{aligned} \right\} \dots \dots \dots (6)$$

$$\text{Therefore } \log a - \log N + \lambda \epsilon_s + \mu = 0$$

$$\text{or } N_s = \alpha a_s e^{\beta \epsilon_s}. \quad \dots \dots \dots (7)$$

It can now be easily proved in the usual way that

$$\beta = -\frac{1}{kT}, \quad \text{and} \quad \frac{1}{\alpha} = \frac{V}{Nh^3} (2\pi mkT)^{3/2}, \quad \dots \dots (8)$$

and substituting these values, we can easily show that  $S$  gets the classical value, viz.,

$$NK \log \left\{ \frac{V}{Nh^3} (2\pi mkT)^{3/2} e^{5/2} \right\}. \quad \dots \dots \dots (9)$$

Now we shall show how the Fermi-Dirac expression can be obtained from the definition of  $W$ .

The phase-volume of the assembly

$$G = \frac{N!}{\prod_s N_s!} \prod_s g_s^{N_s}$$

has been calculated on the supposition that the phase-volume occupied by each individual particle is infinitely small compared with the total phase-volume at its disposal, viz.,  $g_s$ . Let us now give up this assumption, and suppose it occupies a finite phase-volume " $a$ ." Then

$$G = \frac{N!}{\prod_s N_s!} \prod_s g_s(g_s - a) \dots (g_s - \overline{N_s - 1}a). \quad (10)$$

The argument is just the same as that which we introduce in the calculation of the van der Waals's correction " $b$ " from probability consideration. When each particle occupies negligible volume we have

$$W \propto V^N;$$

but when the volume " $\beta$ " cannot be neglected,

$$W \propto \prod_{\gamma=1}^N (V - \gamma - 1\beta).$$

In the above method we have introduced the phase-volume  $g_s$  instead of the space-volume  $V$ , and calculated  $G_N$ . Now

$$\begin{aligned} W &= \frac{G}{h^{3N} N!} \\ &= \frac{1}{\prod_s N_s!} \prod_s \left( \frac{g_s}{h^3} \right) \dots \left( \frac{g_s}{h^3} - \overline{N_s - 1}a \right) \\ &= \frac{1}{\prod_s N_s!} \prod_s a_s(a_s - \epsilon) \dots (a_s - \epsilon \cdot \overline{N_s - 1}), \end{aligned}$$

where  $\epsilon = \frac{a}{h^3},$

$$= \prod_s \frac{a_s!}{N_s! (a_s - \epsilon N_s)!} \dots \dots \dots (11)$$

If we put  $\epsilon=1$ , we get the Fermi-Dirac expression for  $W$ ; when  $\epsilon=-1$  we have

$$W = \prod_s \frac{a_s + \overline{N_s - 1}!}{(a_s - 1)! N_s!}, \quad (12)$$

which is the Bose-Einstein expression for  $W$ .

It may be mentioned here that the above discussion was originally inspired by an article of L. Brillouin (*Ann. d. Phys.* vii. 1927). But in spite of apparent resemblance, the method given here differs in essential points from Brillouin's. Firstly, Brillouin follows Bose-Einstein and Fermi-Dirac closely in calculating probability by making use of  $a$ , (which is Brillouin's  $g_s$ ) as the number of degrees of freedom which a particle can have when its energy lies between  $\epsilon_s$  and  $\epsilon_s + d\epsilon_s$ . It may be easily shown that though we obtain the various values of  $N_s$  by subjecting Brillouin's expressions for  $W$  to the usual variational process in the three different cases (equations 21), they do not give us absolute values of entropy unless some assumption is made regarding the value of  $A$  or  $G$  in equation (21) of Brillouin. We have to make

$\frac{G}{a} = N$  in order to get the correct value of  $S$ . The justifi-

cation for this assumption is not clear, and Brillouin has made no attempt to calculate the absolute value of  $S$ . He devotes a good deal of discussion over the origin of the

permutability factors  $\frac{N!}{\prod_s N_s!}$ , which is quite unnecessary.

The factor comes out automatically when we calculate the total phase-volume of the ensemble not in  $6N$  dimensions, but in 6 dimensions.

The above method has therefore the merit of giving a deduction for the absolute value of  $S$  on the three views from a unitary standpoint. The classical statistics and Fermi-statistics are easily understandable, and probably in the case of Fermi-Dirac statistics it affords a clearer physical view of the case than Fermi's original method. There may be many who share with us the difficulty in understanding the extension of the Pauli Principle, which has been shown to be the guiding principle in the formation of atoms out of protons and electrons, to the case of an ensemble of  $N$  independent particles possessing only translatory motion (*e. g.*, Hall, *Proc. Nat. Acad. Sci.* 1928). The deduction given here follows exactly the same lines as the deduction of the van der Waals's correction for finite volumes, and is therefore physically more comprehensible.

Of greater difficulty is the comprehension of the Bose-Einstein statistics. Here " $a$ ," the phase-volume of any particle, has to be put negative ( $-h^3$ ). These statistics have therefore to be definitely ruled out in the case of material particles. But as it is found to be correct in the statistics

of light-particles, we have to assume that when a photon enters a phase-space, the space expands, since the total phase-volume is increased by the phase-volume of the photon. A discussion will be found in Brillouin's paper above referred to.

### References.

- (1) Bose, *Zeits. f. phys.* xxvii. p. 384 (1924). Einstein, *Sitz. Preuss. Akad.* p. 261 (1924); p. 3 (1925).
- (2) Fermi, *Zeits. f. phys.* xxxvi. p. 902 (1926). Dirac, *Proc. Roy. Soc. A*, cxii. p. 661 (1926).
- (3) Boltzmann, "Über die Eigenschaften Monozyklischer System." *Wien. Ber.* xc. (1884); *Wiss. Abhandl.* iii. Nr. 73, S. 132 ff.
- (4) Gibbs, 'Statistical Mechanics.'
- (5) Ehrenfest and Trkal, *Proc. Amst. Acad.* xxiii. (1920).
- (6) Planck, *Zeits. f. phys.* xxxv. p. 155 (1925).
- (7) Saha and Sur, *Phil. Mag.* i. p. 280 (1926).
- (8) Jeans, 'Dynamical Theory of Gases,' 2nd ed. chap. iv. pp. 58 62. Wassmuth, *Statistische Mechanik*.

## LV. Application of the Photoelectric Cell to the Measurement of Small Displacements. By J. A. C. TEEGAN, M.Sc., Lecturer in Physics, and K. G. KRISHNAN, B.Sc., Demonstrator in Physics, University College, Rangoon\*.

1. **A**N ingenious method of recording small displacement by means of a photoelectric cell is described by Cristescu†. The rays from a source of light rendered parallel by a collimator fall on two gratings mounted parallel, the one behind the other. The front grating is connected to the body the displacement of which is to be measured. When the spaces of the gratings coincide the light passes through and is focussed on the cell, the current being recorded on a sensitive galvanometer. A displacement of the front grating reduces the light, and the galvanometer deflexion is reduced. With gratings of only 5 lines per mm. a displacement of .1 mm. produces a deflexion of 10 galvanometer divisions.

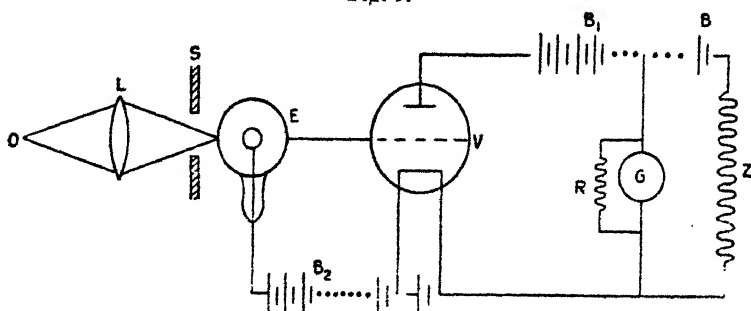
2. A method based on somewhat similar principles is described in this paper. Fig. 1 illustrates the general arrangement. Light from a "pointolite" source is focussed by the lens L on the photoelectric cell E

\* Communicated by the Authors.

† Cristescu, *Phys. Zeits.* xxx. pp. 24-27 (1929).

(potassium vacuum type). A slit  $S$  is placed in the path of the beam just in front of the cell. The width of the slit is variable, and can be adjusted by means of a micrometer screw device reading to  $\cdot 1$  mm. The quantity of light entering the cell is proportional to the area, and hence to the width of the slit. Assuming a linear relation between the photoelectric current and the illumination, the current is a linear function of the width of the slit if the slit when fully open (5 mm.) is uniformly illuminated (the attainment of this condition requires careful adjustment). The photoelectric current is amplified as shown, the valve being operated on the linear portion of its "characteristic." For small values of the photoelectric current the amplification is uniform, and the anode current is proportional to the width of the slit.

Fig. 1.

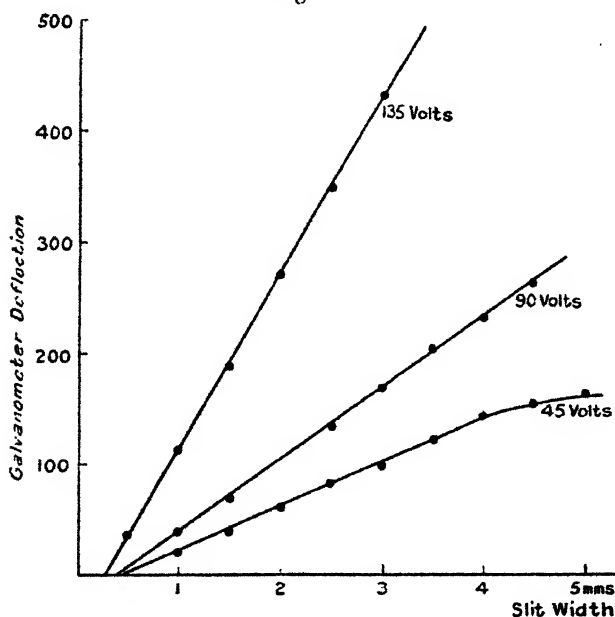


Initially, with slit closed the anode current is balanced by means of the potential compensating device  $ZB$ . If  $C$  is any value of the anode current a current  $\frac{Z}{Z+G} (C-C_0)$  will flow through the galvanometer  $G$ , and for values of  $C$  close to  $C_0$  a sensitive galvanometer can be used to measure  $C$ . This balancing device has the additional advantage of eliminating errors due to any "dark current" in the photoelectric cell.

3. In fig. 2 the variation of the anode current (galvanometer deflexion) with "slit width" is illustrated for different values of the photoelectric potential. In each case the deflexion is a linear function of the slit width, the sensitivity diminishing as the voltage on the cell is decreased. For a voltage of 135 volts a change in width of 1 mm. corresponds to a deflexion of 120 scale-divisions

(1 division =  $\cdot 15$  microamp.). A movement of 1 mm. produces therefore an anode current variation of 17 microamps. On a unipivot Paul galvanometer this produces a deflexion of about 35 scale-divisions, and movements of  $\cdot 1$  mm. can be determined with accuracy. Under these conditions extremely steady conditions have been obtained. On a sensitive mirror galvanometer (1 division =  $10^{-9}$  amp.) a movement of 1 mm. would correspond to a galvanometer deflexion of 17,000 divisions.

Fig. 2.



4. In practice it has not been found possible to obtain such extremely high sensitivity, owing to unsteadiness. The unsteadiness is associated with

- (1) Fluctuation in high-tension and low-tension batteries.
- (2) External high frequency disturbances in the laboratory.
- (3) Fluctuation in the intensity of the light source.

The unsteadiness due to batteries can be reduced to a practical minimum by employing batteries of large capacity in perfect condition. A battery built up of small accumulator-cells is suitable for the high-tension source



of voltage ; it is also an advantage to tap off two or four volts from the anode battery B for use in the balancing circuit BZ. High frequency effects can be eliminated by careful screening, and the apparatus is being redesigned in a more compact form with a view to removing this source of disturbance. With a sensitive galvanometer shunted 10, we have obtained steady readings except for the slight and continual drift of the zero. One of the authors has investigated the possibility of eliminating this "zero drift" effect in a thermionic valve experiment of this type dealing with the measurement of air-stream velocities \*. It arises from the falling off in the discharge rate of the batteries with time, and can be very successfully eliminated by using the current from a second thermionic valve to balance the main anode current instead of the battery B, both valves being supplied by the same H.T. and L.T. batteries. The incorporation of such a device in the present apparatus, however, considerably complicates the arrangement, and it is better to seek sensitivity by other means (see below).

5. The method of employing the present apparatus for recording small displacement is obvious. The movable portion of the slit is attached to the object the displacement of which is to be determined, the difference in the galvanometer deflexion before and after being a measure of the displacement. Except in experiments where the continual variation of a displacement is required, the "zero-drift" error is not of importance, as the zero can be redetermined each time an observation is made.

6. The possibility of increasing the sensitivity of the instrument is now being investigated, with a view to developing an ultra-micrometer on these principles. Very high and uniform amplification can be obtained by using a dull-emitter four-electrode valve † as an amplifier, and it is hoped in this way (using a more sensitive photoelectric cell) to increase the practical sensitivity to a great extent. The application of the method to that employed by Cristescu is also under investigation.

Physics Department,  
University College,  
Rangoon, Burma.  
11th September 1929.

\* Teegan, *Phil. Mag.*, May 1926, pp. 1117-1121.

† D. T. Harris, *Journ. Scientific Inst.*, Jan. 1929.

LVI. *Theory of Collision of Spheres of Soft Metals.*  
 By J. P. ANDREWS, M.Sc., F.Inst.P. (East London College)\*.

ABSTRACT.

BEGINNING with the fact that when two spheres of soft metal collide, permanent deformation is produced when the velocity of approach exceeds a definite critical value; and with the aid of the assumption that over the permanently deformed region the pressure remains constant at all points, a theory of collision is worked out. This theory is found capable of accounting for the variation with the velocity of approach  $v$ , of

- (a) The duration of contact  $t$  of the spheres,
- (b) the diameters  $d$  of the permanent deformations, and
- (c) the coefficient of restitution  $e$ .

The detailed character of the experimental results is explained.

At high speeds of approach, the duration of contact and the quantity  $e^2v^2$  are linear functions of  $\frac{1}{v}$  and of  $v$  respectively; while it appears that a definite quantity of energy is required per unit mass of the material apparently removed during deformation. A latent heat of deformation for a number of substances is calculated.

Finally, the influence of viscous resistance and of time-effects, such as the elastic after-effect etc., is considered.

IN a recent paper †, I have shown that when two exactly similar spheres are allowed to collide at different velocities  $v$ , the duration of their contact is calculable from an empirical formula of the type

$$t = t_0 + a/v^n,$$

where  $t$  is the duration of contact and  $t_0$ ,  $a$ , and  $n$  are constants. The diameters of the permanent deformations produced on the spheres when the velocity exceeds a value  $v_0$  are represented by the following formula:

$$d = b(v - v_0)^m,$$

\* Communicated by the Author.

† Phil. Mag. viii. p. 781 (1929).

$b$  and  $m$  being constants characteristic of the material and the size of the spheres.

Further experiment upon imperfectly elastic spheres is available in the work of C. V. Raman\* at low velocities of approach. By a photographic method the variation of the coefficient of restitution was investigated, and found to approach unity at very low speeds. The curves published by Raman are of the type shown in fig. 6.

A theory of collision, to be sufficient, must explain and correlate these results.

As a preliminary explanation and justification of the ideas involved in this theory, consider the hypothetical case of the impact of a pair of ideally plastic spheres; that is, spheres which remain permanently deformed whenever they come into contact. Whilst in contact these spheres will have a common plane of contact, touching each of the spheres in a circle of radius  $r$  (the circle of contact). The fundamental assumption of the present theory is that the pressure is the same,  $p_0$ , at all points over this circular area of contact, and is independent of  $r$ .

The total force at any instant tending to separate the spheres is therefore  $\pi r^2 p_0$ . But if the distance between the centres of the spheres is  $2R - 2S$ ,  $R$  being the radius of the spheres,  $RS = r^2$ , by Hertz's theory, so that the force is  $\pi R p_0 S$ .

The axis of  $S$  is the line joining the centres. Choose the origin as the point of intersection of the plane of contact with this axis; then, since the distance between the centres is  $2R - 2S$ , the coordinate of the centre of one of them is  $R - S$ , and we may write, if  $M$  is the mass of one sphere,

$$M \frac{d^2}{dt^2} (R - S) = \pi R p_0 S,$$

and if  $n^2 = \frac{\pi R p_0}{M}$ , the solution is  $S = A \sin nt$ , provided  $S = 0$

when  $t = 0$ . Consequently  $\frac{ds}{dt} = 0$ , when  $\cos nt = 0$ , or  $nt = \frac{\pi}{2}$ ; that, is when

$$t = \frac{\pi}{2} \sqrt{\frac{M}{\pi R p_0}} \quad \dots \dots \dots (1)$$

Now allow the plastic spheres to be endowed with a very small elastic reaction, otherwise negligible, which will,

\* C. V. Raman, *Phys. Rev.* xii. p. 442 (1918).

however, be just sufficient to separate the spheres after the relative velocity has been annulled. Then equation (1) gives the duration of the contact, and it will be observed that the velocity of approach does not affect its constant value.

The actual cases under consideration approximate to this state at very high speeds of approach; the duration of contact, therefore, should tend to a constant value as  $v$  becomes large. This agrees with experimental evidence.

From equation (1) we have the relation

$$p_0 t_0^2 = \frac{\pi M}{4R}.$$

Now  $p_1$ , the least pressure required to initiate permanent deformation, may be calculated from Hertz's theory of perfectly elastic collision and the value  $v_0$  of the velocity at which deformation was first produced. This may be compared with  $p_0$  calculated from the last relation, using the value of  $t_0$  derived from the experiments. The numbers are compared in Table I. (The calculation of  $p_1$  differs from that in the former paper in that  $S_0$ , the critical value of  $S$ , was calculated from the formula  $5.984 S_0/v_0 = t_1$ , where  $t_1$  is the duration when  $v = v_0$ .  $t_1$  was taken from the experimental curves.)

TABLE I.

Substance.	$p_0$ (dynes/cm. <sup>2</sup> ).	$p_1$ (dynes/cm. <sup>2</sup> ).
Aluminium .....	$2 \times 10^9$	$3.4 \times 10^9$
Tin .....	$1.2 \times 10^9$	$2.1 \times 10^9$
Babbitt .....	$2.6 \times 10^9$	$1.1 \times 10^9$
Lead-Tin .....	$4.8 \times 10^9$	$1.1 \times 10^9$
Brass .....	$2.2 \times 10^{10}$	about $5 \times 10^9$

Considering that

- (1)  $p_1$  depends on  $v_0$ , which can only be measured by extrapolation, sometimes rough;
- (2) the calculation of  $p_1$  requires the knowledge of elastic constants whose values could not be obtained very accurately in some cases,

the agreement justifies us in identifying  $p_0$  and  $p_1$ . The idea of a constant pressure  $p_0$  is supported by the work of J. H. Vincent\*, in which steel balls produced indentations in lead plates.

\* J. H. Vincent, Proc. Camb. Phil. Soc. 1898-1900.

## DEVELOPMENT OF THE THEORY.

I. *Duration of Contact.*

We will assume that when  $v$  is less than  $v_0$ , the velocity of approach at which permanent deformation commences, the spheres are perfectly elastic. The conditions are then exactly those visualized in Hertz's original theory, which may be taken over unchanged; and this leads to the following formula for the duration of contact:

$$t = 5.886 \left[ \frac{5M}{16k} \right]^{2/5} \cdot \frac{1}{v^{1/5}}, \quad \dots \quad (2)$$

where  $k = \frac{\pi E}{3} \sqrt{R}$ .  $E$  is an elastic modulus.

For velocities of approach exceeding the critical value  $v_0$ , we may divide the process of collision into three periods:—

(a) *The elastic period.*

Until the stress at the centre of the circle of contact attains the value  $p_0$ , all the retarding forces will be perfectly elastic. The time required to attain this stress will, however, depend on  $v$ , and we may call it  $t_a$ .

(b) *The plastic period.*

The spheres attain the stress  $p_0$  while moving with a definite velocity which depends on  $v$ . Subsequently they are brought to zero relative velocity under the combined action of two forces: (1) due to the pressure  $p_0$  evenly distributed over the central plastic area, and (2) an elastic force due to the strained annulus enclosed between the plastic circle and the circumference of the circle of contact. A time  $t_b$  will be required to reduce the spheres to zero relative velocity.

(c) *The return period.*

Instantly following the attainment of relative rest, the spheres begin to move apart. The accelerating forces are now everywhere elastic, since the stress within the plastic circle immediately falls to less than  $p_0$ . The time required from zero relative velocity until the spheres finally separate is  $t_c$ .

The complete duration of contact is therefore

$$t = t_a + t_b + t_c.$$

The detailed calculation of these periods now follows, and we shall make continual use of two formulæ taken from Hertz's theory \*, viz. :—

(a) The stress at any point within the circle of contact of radius  $r_0$  at which the pressure  $p_0$  is not yet attained is given by

$$\frac{E \sqrt{r_0^2 - r^2}}{2R},$$

where

$$E = \frac{4g}{\pi(1-\sigma^2)} \cdot \quad \begin{array}{l} (g = \text{Young's Modulus} \\ \sigma = \text{Poisson's Ratio}). \end{array}$$

(b) By integration, before any portion of the area in contact has attained the pressure  $p_0$ , the total force tending to separate the spheres is

$$K = \frac{\pi E}{3R} (RS)^{3/2},$$

where  $2R-2S$  is the distance between the centres of the spheres.

(a) *The calculation of  $t_a$ .*

Let the axis of  $S$  be the line joining the centres, and let the intersection of this with the plane of contact be the origin. If the distance between the centres after contact is  $2R-2S$ , the coordinate of the centre of one of them is  $R-S$ . The retarding force is, as quoted above,

$$K = kS^{3/2},$$

where

$$k = \frac{\sqrt{R}\pi E}{3}.$$

Hence, if  $M$  is the mass of one sphere,

$$M \frac{d^2}{dt^2} (R-S) = kS^{3/2}$$

or

$$\frac{d^2 S}{dt^2} + \frac{k}{M} \cdot S^{3/2} = 0.$$

Multiplying by  $\frac{ds}{dt}$  and integrating,

$$\frac{1}{2} \left( \frac{ds}{dt} \right)^2 + \frac{2}{5} \frac{k}{M} S^{5/2} = \text{const.} \quad . \quad . \quad . \quad (3)$$

\* *Vide Love, 'Elasticity.'*

Since, now,  $\frac{ds}{dt} = v/2$  when  $S = 0$ , we have

$$\frac{ds}{dt} = \sqrt{\frac{v^2}{4} - \frac{4}{5} \frac{k}{M} S^{5/2}},$$

and the time  $t_a$

$$= \int_0^{S_0} \frac{ds}{\left[ \frac{v^2}{4} - \frac{4}{5} \frac{k}{M} S^{5/2} \right]^{1/2}},$$

where  $S_0$  is the value of  $S$  at the moment  $p_0$  is attained. Let  $\psi$  be the maximum value of  $S$ , which would have been reached had perfect elasticity reigned throughout. Then

$$\psi = \left[ \frac{5}{16} \frac{M}{k} v^2 \right]^{1/5}.$$

$t_a$  may then be reduced to

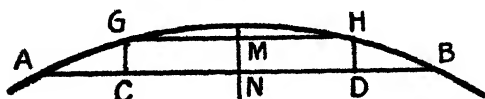
$$t_a = \frac{2\psi}{v} \int_0^{S_0/\psi} \frac{dx}{(1-x^{5/2})^{1/2}} \dots \dots \dots (4)$$

Now  $S_0 < \psi$ , so that the integral has to be computed for values of  $\frac{S_0}{\psi}$  between 0 and 1. This was done numerically without difficulty.

(b) *The calculation of  $t_b$ .*

Let fig. 1 represent the portion of a sphere concerned in

Fig. 1.



a collision. Let  $AB = 2r_0$  be a diameter of a circle of contact, and let  $CD = 2r_1$  be a diameter of the plastic circle. Stress at E, as before,

$$= \frac{E}{2R} \sqrt{r_0^2 - r^2}.$$

Force due to elastic annulus AC

$$= \int_{r_1}^{r_0} \frac{2\pi r E}{2R} \sqrt{r_0^2 - r^2} dr = \frac{E\pi}{3R} (r_0^3 - r_1^3)^{3/2}.$$

But as the pressure at C =  $p_0$ , this force may be written

$$\frac{8 \pi R^2 p_0^3}{3 E^2}.$$

It is noteworthy that this is constant, independent of the velocity of approach.

The force inside the annulus, due to the plastic circle, is  $\pi r_1^2 p_0$ , and as

$$r_1^2 = RS - p_0^3 \frac{4R^2}{E^2},$$

the total force is

$$\frac{8 \pi R^2 p_0^3}{3 E^2} + R p_0 \pi S - p_0^3 \frac{4 \pi R^2}{E^2} = R p_0 \pi S - \frac{4 \pi R^2 p_0^3}{3 E^2}.$$

The equation of motion is consequently

$$M \frac{d^2 S}{dt^2} = - \left[ R p_0 \pi S - \frac{4 \pi R^2 p_0^3}{3 E^2} \right],$$

or, writing  $\beta$  for  $S - \frac{4 R p_0^3}{3 E^2}$ ,

$$\frac{d^2 \beta}{dt^2} + \frac{\pi R p_0}{M} \beta = 0.$$

And since (1)  $S = S_0$  when  $t = 0$ ,

(2)  $\frac{ds}{dt} = v_1$  when  $t = 0$ ,

the solution is

$$\beta = A \sin (nt + \delta), \quad n^2 = \frac{\pi R p_0}{M}, \quad (5)$$

where

$$\tan \delta = \frac{1}{v_1} \frac{8 R p_0^3}{3 E^2} \sqrt{\frac{\pi R p_0}{M}}$$

and

$$A^2 = \frac{M}{4 \pi R p_0} v^2 + \frac{64 R^2 p_0^4}{9 E^4} - \frac{4}{5} \frac{k}{\pi R p_0} S_0^{5/2}.$$

The velocity  $v_1$ , at which the sphere enters on this stage, may be calculated from equation (3) thus :

$$v_1^2 = \frac{v^2}{4} - \frac{4}{5} \frac{k}{M} S_0^{5/2}.$$



From equation (5),  $\frac{ds}{dt} = 0$  when  $t = \frac{1}{u} \left( \frac{\pi}{2} - \delta \right)$ .

So that

$$t_b = \sqrt{\frac{M}{\pi R p_0}} \left\{ \frac{\pi}{2} - \delta \right\}. \quad (6)$$

As a check, when  $v$  is very large,  $\delta$  approaches zero, and  $t_b$  approaches the value

$$\frac{\pi}{2} \sqrt{\frac{M}{\pi R p_0}},$$

as in equation (1).

(c) *The calculation of  $t_c$ .*

We imagine that on release the part CD rises to GH (fig. 1) and stops there. This is an approximation of the same order as the others implicit in this theory. GH will then be the diameter of the permanent deformation. Let us suppose then that the diameter of the circle of contact at any instant is  $r_0$ , and that  $CN = GM = r_1$ , the radius of the plastic circle.

The force due to the elastic annulus is, as before,  $\frac{E\pi}{3R} (r_0^2 - r_1^2)^{3/2}$ . If  $p$  is the stress at the edge of the plastic circle at any moment,  $p$  is also the pressure at all points within that circle, according to our previous notions.  $r_1$  will remain constant.

The force due to the plastic circle, now non-plastic, is

$$\frac{\pi r_1^2 E}{2R} \sqrt{r_0^2 - r_1^2}.$$

Hence the total force

$$F = \frac{E\pi}{R} \left[ \frac{(r_0^2 - r_1^2)^{3/2}}{3} + \frac{r_1^2}{2} (r_0^2 - r_1^2)^{1/2} \right].$$

If, then, we write  $u = r_0^2 - r_1^2$ , so that  $\pi u$  represents the area of the annulus, we may write the equation of motion

$$M \frac{d^2 u}{dt^2} = - E\pi \left[ \frac{u^{3/2}}{3} + \frac{r_1^2}{2} u^{1/2} \right],$$

remembering that  $r_0^2 = RS$ .

Multiplying by  $\frac{du}{dt}$  and integrating, we have, if  $\frac{du}{dt} = 0$  when  $u = u_0$ ,

$$\left(\frac{du}{dt}\right)^2 = \frac{2\pi E}{M} \left[ \frac{2}{15} (u_0^{5/2} - u^{5/2}) + \frac{r_1^2}{3} (u_0^{3/2} - u^{3/2}) \right], \quad (7)$$

and 
$$t = \int_{u_0}^u \frac{du}{\left(\frac{du}{dt}\right)}.$$

If we write  $\frac{u}{u_0} = x$ , this is reducible to

$$t_c = \sqrt{\frac{M}{2\pi E}} \cdot u_0^{1/4} \int_0^1 \frac{dx}{\sqrt{\frac{2}{15} u_0 (1 - x^{5/2}) + \frac{r_1^2}{2} (1 - x^{3/2})}}. \quad (8)$$

This integral has to be calculated graphically for each value of  $r_1^2$ ; that is, for each value of the velocity of approach, since  $r_1$  is a function of  $v$ .

From the fact that the pressure at G is  $p_0$  at the instant of greatest compression, we derive that

$$u_0 = r_0^2 - r_1^2 = \frac{4p_0^2 R^2}{E^2},$$

a constant quantity, independent of the velocity of approach. From this result and the maximum value of  $S$ , derived from equation (5), it is easy to show that

$$r_1^2 = R \sqrt{\frac{M}{4\pi R p_0} v^2 + \gamma} - \frac{8}{3} \frac{R^2 p_0^2}{E^2}, \quad \dots \quad (9)$$

where

$$\gamma = \frac{64}{9} \frac{R^2 p_0^4}{E^4} - \frac{4}{5} \frac{k S_0^{5/2}}{\pi R p_0}.$$

The complete duration of contact is now calculable from the three equations (4), (6), and (8).

## II. The Diameters of the Permanent Deformations.

$r_1$  is the radius of deformation. Consequently equation (9) gives the variation of this quantity with velocity of approach.

III. The Coefficient of Restitution  $e$ .

The velocity of separation  $\frac{1}{R} \frac{du}{dt} = \left( \frac{ds}{dt} \right)$  may be obtained from equation (7) by putting  $u = 0$ ; for at that instant when  $r_0 = r_1$ , we are imagining the spheres to separate.

$$\left( \frac{du}{dt} \right)^2 = \frac{2\pi E}{M} \left[ \frac{2}{15} u_0^{5/2} + \frac{r_1^2}{3} u_0^2 \right], \quad \dots \quad (10)$$

the value of  $r_1^2$  coming from (9).

The ratio of the velocity of separation to the velocity of approach gives  $e$ .

## NUMERICAL ILLUSTRATION.

In order to bring out the salient features of the theory, all the required quantities were computed for a typical case invented for the purpose, for which the following are the data :—

$$\begin{aligned} p_0 &= 5.5 \times 10^9 \text{ dynes/cm.}^2, \\ \text{Young's Mod. } \dots \quad q &= 5.85 \times 10^{11} \text{ dynes/cm.}^2, \\ \text{Poisson's Ratio } \dots \quad \sigma &= 0.3, \\ R &= 4 \text{ cm.}, \\ M &= 660 \text{ gm.} \end{aligned}$$

This is an example approximating to the actual case of Aluminium in my experiments. An attempt at exact comparison is, however, out of the question, because  $r_0$ , which plays such an important part in the theory, could only be determined approximately, and a small variation in its value has an important influence in the calculations. From these values we derive

$$\begin{aligned} E &= 8.20 \times 10^{11} \text{ dynes/cm.}^2, \\ k &= 1.72 \times 10^{12}. \end{aligned}$$

The critical velocity  $v_0$ , at which permanent deformation commences

$$\begin{aligned} v_0 &= 10.75 \text{ cm./sec.}, \\ u_0 &= 2.88 \times 10^{-3} \text{ cm.}^2, \\ \gamma &= -4.4 \times 10^{-8}. \end{aligned}$$

From these all the other useful quantities may be obtained.

The computations required for the integrals were performed graphically and may be left undescribed. Their results are summarized below.

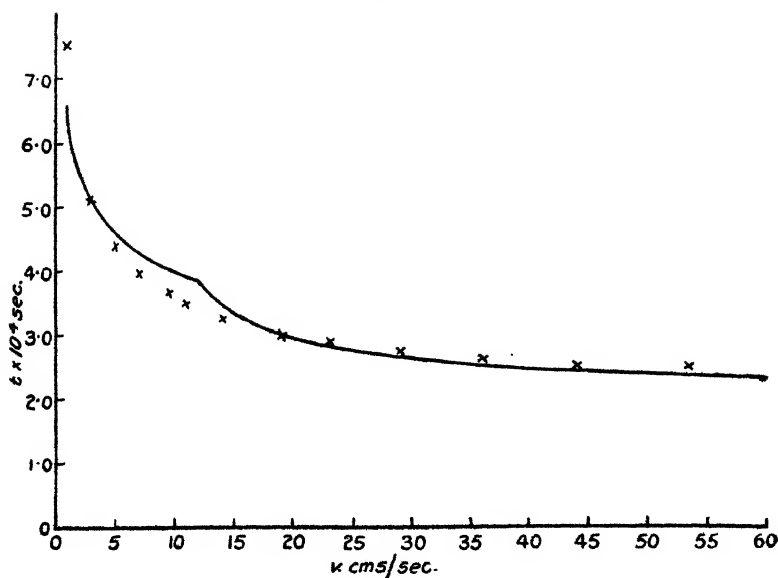
## I. The Duration of Contact.

TABLE II.

$v$ cm./sec.	$t_a$ $\times 10^4$ .	$t_b$ $\times 10^4$ .	$t_c$ $\times 10^4$ .	Total sec. $\times 10^4$ .
1.0	—	—	—	6.34
2.0	—	—	—	5.52
4.0	—	—	—	4.81
6.0	—	—	—	4.43
8.0	—	—	—	4.18
10.0	—	—	—	4.00
12.0	1.48	0.49	1.78	3.75
15.0	1.06	0.80	1.47	3.33
19.0	0.805	0.99	1.21	3.005
24.0	0.62	1.12	1.07	2.81
30.0	0.48	1.21	0.96	2.65
37.0	0.40	1.27	0.84	2.51
45.0	0.325	1.32	0.76	2.405
60.0	0.25	1.37	0.65	2.27

These results are represented by the full curve of fig. 2.

Fig. 2.



The outstanding features of the curve are :

- (1) Its evident tendency to a constant value  $t = t_0$  ;
- (2) the pronounced alteration in direction at  $v = v_0$ .

This last appeared at first sight to be a new prediction ; but I find that my experimental results practically all show such a tendency. In the account of these experiments no explanation was forthcoming, and I had assumed that experimental error must have entered to a greater extent than I could account for, since attempts to "improve" the curve by more careful observation did not succeed. In fig. 3

Fig. 3.

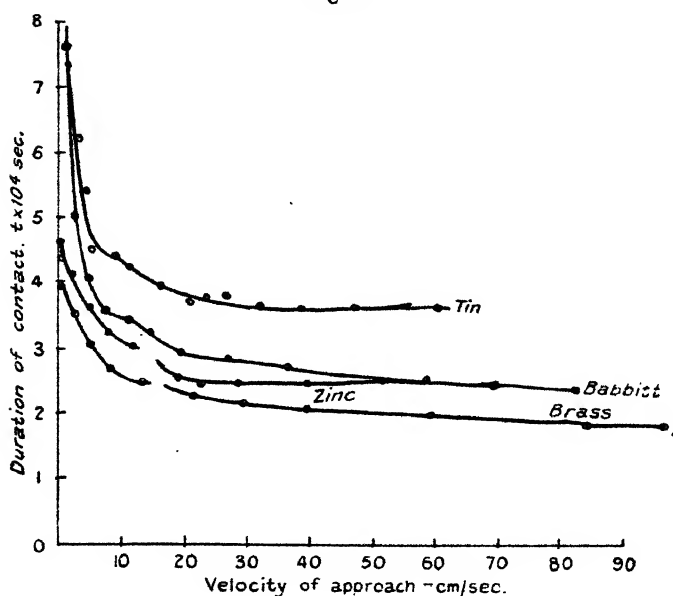


TABLE III.

Substance.	$(v_0)_1$ cm./sec.	$(v_0)_2$ cm./sec.
Aluminium .....	About 12	About 8
Tin (2) .....	2.5	5 to 7
„ (3) .....	3 to 7	8
Babbitt .....	10.0	10.0
Zinc .....	9 to 10	12
Lead-Tin .....	0 to 4	Cannot be detected.
Brass .....	8.0	(c.) 15

are re-drawn some experimental curves exhibiting the effect to a greater or less degree. Table III. shows the values of

$v_0$  derivable from the two methods,  $(v_0)_1$  being obtained from the measured diameters of the deformations, and  $(v_0)_2$  from the effect just described. The table will also serve to indicate to what extent the value of  $v_0$  so obtained may be relied on.

An explanation of the constants in the empirical equation  $t = t_0 + a/v^n$  may now be sought.  $t_0$  appears quite clearly

to be the value  $\frac{\pi}{2} \sqrt{\frac{M}{\pi R p_0}}$  of equation (1).

To interpret the remaining part, the curve of fig. 2 was subjected to the same process as the experimental curves of fig. 3, namely an empirical equation of the required type

was fitted to it, employing  $t_0 = \frac{\pi}{2} \sqrt{\frac{M}{\pi R p_0}} = 1.535 \times 10^{-4}$ .

This gave, as a reasonably fair fit,

$$t = 1.535 \times 10^{-4} + \frac{6.03 \times 10^{-4}}{v^{0.47}},$$

the curve for this equation smoothing over the characteristic bend at  $v_0$ . The crosses in fig. 2 are calculated from this equation. The agreement is similar to that given by similar equations with the experimental results. It is clear, then, that  $a$  and  $n$  have no special significance, and their values cannot yield any useful information after the manner of  $t_0$ . The fact that the first part of the curve represents perfectly elastic collision is obscured by this formula.

## II. The Diameters of the Permanent Deformations.

In fig. 4 are plotted the calculated values of the diameters  $d$  and the velocities of approach. The crosses are values from an empirical formula derived from these calculated results,  $d = 2.938 \times 10^{-2}(v - v_0)^{0.487}$ . It will be remarked how closely the theory accounts for the empirical equation. In the example worked out it is possible to say definitely that the index 0.487 is not 0.500, although so close. Reference to my previous paper will show that this agrees completely with experiment.

## III. The Coefficient of Restitution.

Fig. 5 shows the variation of the coefficient of restitution as the velocity of approach varies. Fig. 6 gives for comparison some curves from C. V. Raman's results. The

general similarity is evident, and the portion on the experimental curves indicating a coefficient of restitution equal to unity is reproduced by the theory.

Fig. 4.

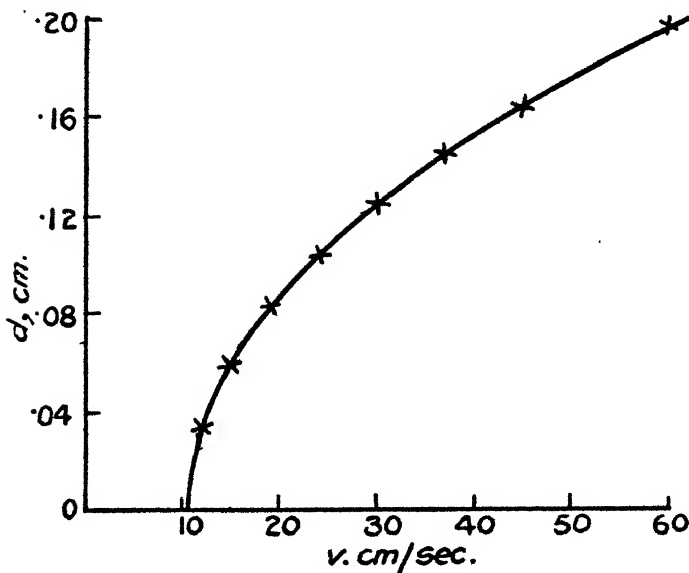
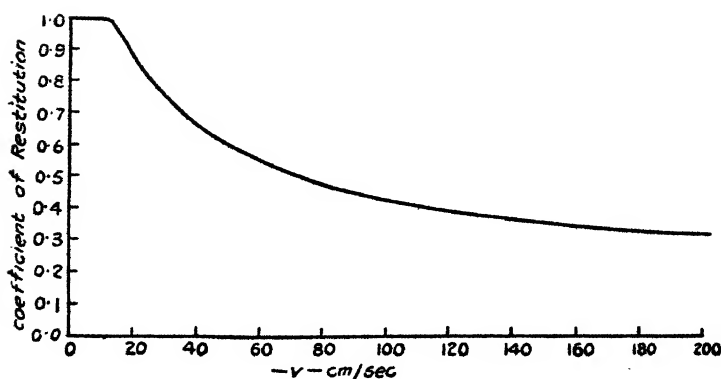


Fig. 5.



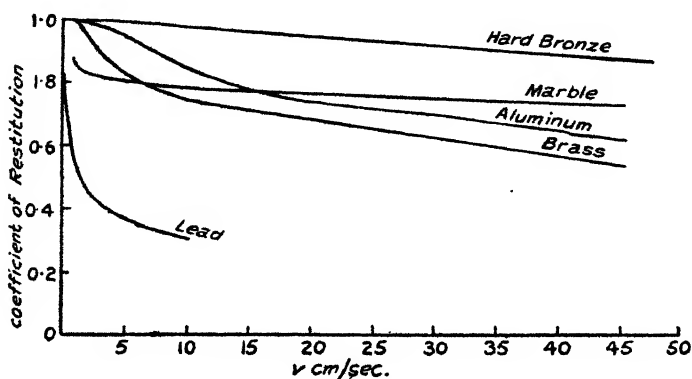
### DISCUSSION OF THE THEORY.

The success with which the theory accounts for a number of different experimental results tends to justify the otherwise rather arbitrary assumption of perfect elasticity when the

velocity of approach is less than  $v_0$ . It is a fact that the first few of my observations, that is, at low velocities, are the least accurate, and special experiments are in progress to test the hypothesis at such speeds. Nevertheless, in most cases the inverse fifth-power law for the duration of contact is approximated to.

When  $v$  is large compared with  $v_0$  a number of simplifying approximations are possible, which lead to several instructive deductions. These approximate results are, for the sake of

Fig. 6.



brevity, merely summarized below. The values to which  $t_a$ ,  $t_b$ , and  $t_c$ , respectively, approach at high speeds are

$$t_a = \frac{8R}{\lambda^2} \cdot \frac{1}{v},$$

$$t_b = t_0 - \frac{16R}{3\lambda^2} \cdot \frac{1}{v},$$

$$t_c = 0;$$

the complete duration of contact is therefore approximately

$$t = t_0 + \frac{8R}{3\lambda^2} \cdot \frac{1}{v},$$

and we have the approximate relation  $(t - t_0)v = 8R/3\lambda^2$ , where  $\lambda = E/p_0$ .

For the approximate diameters of the permanent deformations at high speeds we have

$$d_1^2 = 4Rt_0v/\pi - 32R^2/3\lambda^2,$$



or, at even higher speeds,

$$d_1^2 = \frac{4R}{\pi} t_0 v.$$

From this it follows that the volume of the spherical cap apparently removed when the sphere is deformed is proportional to the kinetic energy of the approaching sphere at very high speeds. This is like the rule first laid down by J. H. Vincent for the case of steel balls dropped into lead plates.

We have

$$(\text{vol. of cap}) = \frac{1}{8p_0} \cdot (\frac{1}{2} M v^2),$$

or, mass apparently removed,  $\frac{\rho}{8p_0} (\frac{1}{2} M v^2)$ , where  $\rho$  = density.

In other words, the energy per gram measured in heat units required to remove the material—what might indeed be called the latent heat of deformation of the material,  $L$ —is

$$\frac{8p_0}{\rho \times 4.2 \times 10^7} \text{ cal. per gm.}$$

In Table IV. are tabulated the values of this quantity for the substances used in my experiments. These are to be considered as only approximate values.

TABLE IV.

Substance.	Al.	Sn.	Zn.	Babbitt.	Lead-Tin.	Brass.
L cal./gm. ....	70	16	120	34	52	About 200

It should be emphasized that the elastic constants do not enter into this matter, which evidently is a phenomenon characteristic of the plastic condition.

When  $v^2/3$  is not much larger than  $p_0^5/E^4R$ , the square of the velocity of separation has the value

$$\frac{w^2}{2} = -\frac{512}{45} \frac{\pi R^3 E}{M \lambda^5} + \frac{32 \pi E R^2}{3 M \lambda^3} \sqrt{\frac{M}{4 \pi R p_0}} \cdot v \left( 1 - \frac{64 \pi R^2 p_0}{15 \lambda^4 M v^2} \right);$$

but when  $v^2/3$  is much larger, the last term in brackets approximates to unity, and we are left with the rule that  $e^2 v^2$  is a linear function of  $v$ :

$$e^2 v^2 = av - b.$$

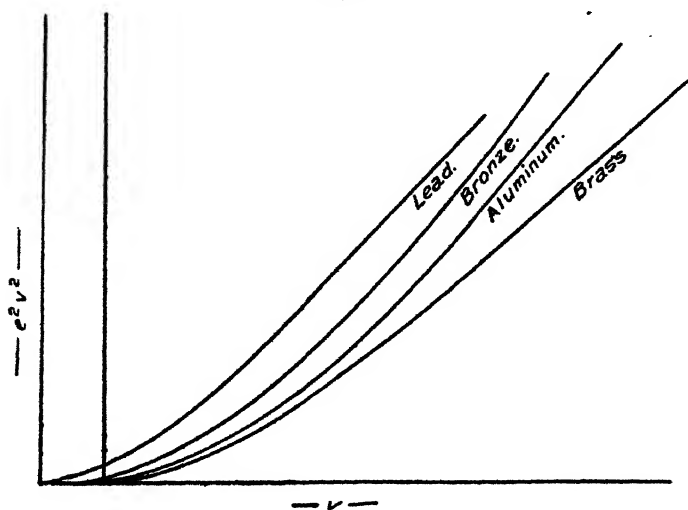
Moreover, at such speeds  $a^2/b = 5.02$  for all spheres.

In fig. 7 are plotted Raman's experimental results, using  $e^2v^2$  as ordinate and  $v$  as abscissa. The tendency to linearity at high speeds is noteworthy as confirming the theory. The ratios  $a^2/b$  are, however, in no case 5.02, but always smaller. This we should anticipate if  $v^2/3$  is not much greater than  $p_0^5/E^4R$ . It is impossible finally to decide this point, since no data are available regarding the spheres used in Raman's experiments.

#### CONCLUDING OBSERVATIONS.

The assumption, fundamental to this theory, that the pressure is constant over the plastic circle is equivalent to

Fig. 7.



saying that the material of which that circle is composed, acts like a liquid. It must, moreover, behave like a very mobile liquid, for any differences of pressure have to be equalized in about  $10^{-4}$  sec. under a pressure of a thousand atmospheres. It is almost inconceivable at first sight that the large viscous forces which must enter do not appear to have any marked final influence. That plastic material is actually moved seems more likely, in so far as a pronounced rim always surrounds the plastic circle as though material had been exuded. The key to the difficulty of this motion, and probably to that of the viscous resistances produced, appears to be the very small quantity of matter to be transported and the large pressure gradients available.

A gradient as large as  $10^8$  dynes per  $\text{cm.}^2$  per cm. from the centre of the plastic circle outwards would only mean a variation of about 1 per cent. in the value of the normal pressure  $p_0$  across this circle. The viscous effect would only tend to increase such a gradient, which, it appears, is never raised sufficiently high to interfere seriously with the constancy of the normal pressure  $p_0$ .

Finally, it is worth remarking that collision experiments are among the few in the domain of elasticity into which time-effects, such as the elastic after-effect, fatigue, etc., do not enter to any appreciable extent. It is no doubt partly due to this fact that a simple explanation such as that given in this theory is possible, while the interpretation of experiment, so complex in other elastic problems, becomes in this case much easier.

During the development of this theory I have had the benefit of Prof. Lees's criticism, and have pleasure in recording my thanks.

## LVII. *Some Phenomena of the Contact of Solids.*

By WILLIAM STONE \*.

THE publication of a paper† by G. A. Tomlinson on "Molecular Cohesion" has recalled to my memory some experiments on this subject which I made in 1922, and an account of which I gave in a lecture (unpublished) before the Royal Society of Victoria, Australia, in August, 1923. The experiments were similar to Mr. Tomlinson's but had a considerably wider scope and, in certain respects, led to conclusions different from his.

The object of the experiments was to secure preliminary data for an experimental study of "solid friction." It was hoped that light might be thrown on the questions of when and under what conditions contact of solids takes place, and of the nature and magnitude of the forces acting between bodies in, or nearly in, contact—forces over which the experimenter has no control.

\* Communicated by Sir J. J. Thomson, O.M., F.R.S.

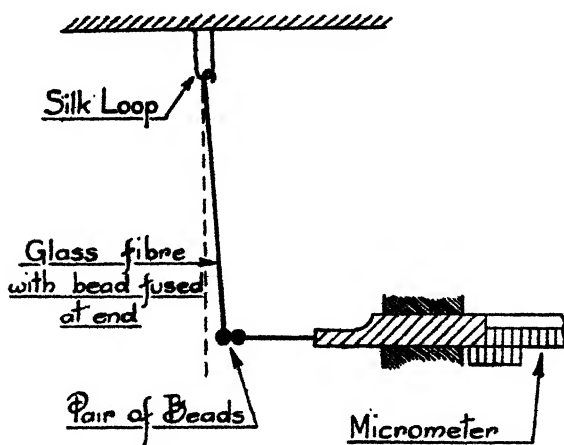
† Phil. Mag. vi. p. 695 (1928).

The principle of the method of experiment is illustrated in fig. 1.

By moving the bead attached to the micrometer, the suspended bead could be deflected, if there were adhesion between the beads, and the amount of deflexion measured. Consequently, the force tending to separate the beads could be directly estimated. For certain experiments, the bead apparatus was mounted in a chamber at the top of a specially designed electroscope as illustrated in fig. 2 and described later.

In the main series of experiments, the bodies tested for adhesion were small glass beads, one or two millimetres

Fig. 1.



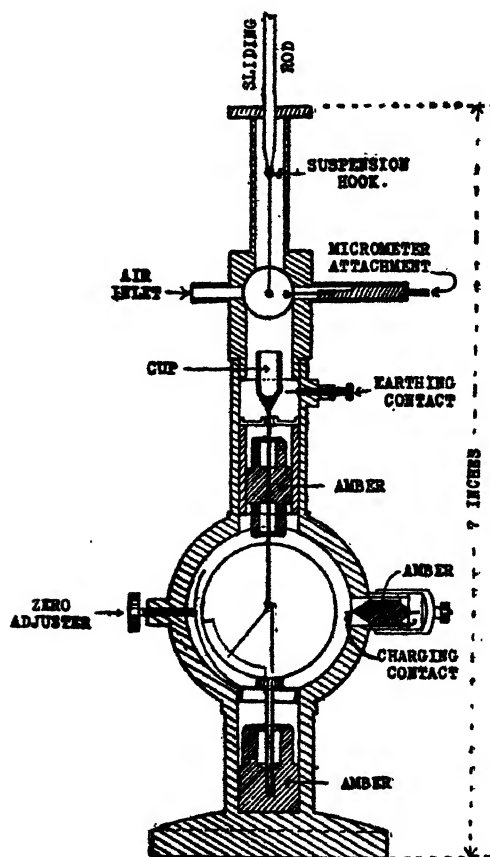
Principle of Experimental Method.

in diameter. The beads were specially made by the following process.

Glass rod was thoroughly washed, and drawn out after heating over a good Bunsen flame. The fibre so drawn out was cut, and the two ends so formed were fused into beads to constitute one pair. The beads were formed in a small blue gas flame, the oxidizing part being used. The burner consisted of glass tube drawn into a capillary and mounted horizontally, so that the glass fibre could be held approximately vertical and in the flame from the horizontal gas jet.

The fibre remote from the beads was held in steel tweezers, the points of which had just been made red hot. The fibre was then cut the desired length, and a small hook was formed on its free end if this was required to suspend the bead.

Fig. 2.



Section through axis of Electroscope.

The beads made in this way were assumed to be clean. As soon as each bead was made, it was placed in the apparatus in which it was to be tested.

Many different kinds of glass were used. Speaking generally, one type of glass gave the same results as another but there were one or two remarkable exceptions (page 619).

*Adhesion in a Natural Atmosphere.*

The earlier experiments were made in the natural atmosphere of the room. In this case, beads of each of the kinds of glass employed adhered when newly made; but lead glass beads only adhered feebly and, in a few cases, not at all.

Beads which had been contaminated by handling, or by being left exposed on the table, usually would not adhere when brought into contact. If, however, these beads were breathed on while they were in contact, strong adhesion at once took place, of the same order of magnitude and as lasting as that obtained with beads newly formed. If the beads were then forcibly separated, they would seldom adhere again until they had once more been breathed upon, or cleaned by heating or otherwise. Contaminated beads, after being made red hot, behaved like those freshly made. Clean beads, also, adhered after being breathed on in contact. Separation did not take place even though a force of from 5 to 10 per cent. of their weight tended to cause them to do so.

Any of the beads, whether (a) clean or (b) contaminated and breathed on, could be made to slide one over the surface of the other although acted on by a force tending to separate them. In most cases, as soon as the motion started the beads slid over each other in a manner which suggested that their surfaces were lubricated and that they were held together as by a force of mutual attraction. The force tending to separate them was about two-thirds of that which a first test showed would separate them.

Adhering beads which have been newly formed, and contaminated beads which have been breathed on when in contact, will continue to adhere for several days if they are protected from draughts of air by a suitable glass shade, even though the force tending to separate them is from 50 per cent. to 75 per cent. of that which will separate them.

In fine, freshly made beads (whether breathed on or not, while in contact) or contaminated beads that have been breathed on while in contact adhere, and forces of at least 10 per cent. of their weight are required to separate them.

They will sustain forces of one half to three-quarters

of this amount for indefinitely long periods—several days, at all events.

In looking for possible explanations of the phenomena observed, the following points were kept in view :—

- (a) true adhesion of uncontaminated glass with glass ;
- (b) surface tension of a film of water or other liquid between the beads ;
- (c) general electrification of the beads, or local electrification at or near the area of contact ;
- (d) adhesion due to contaminating matter not removable from the glass by recognized methods of cleaning.
- (e) gravitational forces.

A simple calculation will show that the forces found to exist far exceed the gravitational force of attraction, so that this force can only play a negligible part.

With respect to *surface tension*, an attempt was made to drive off any adsorbed liquid film between the beads by the application of heat from a gas flame. It was expected that this would also remove electrification except from the area of contact and possibly that immediately adjacent to it.

In one set of tests, newly formed soft German soda glass beads were mounted and brought into contact. The areas of contact were then subjected to tension as usual by moving the micrometer. A very small gas flame (the gas issuing from a capillary gas jet), from 2 to 3 mm. high, was then placed about 3 cm. from the glass beads and vertically below them and was kept there until it was judged that the beads had attained a steady temperature. No visible effect was produced.

The gas jet and flame were then raised in short steps at intervals of about 15 seconds, without any visible effect, until finally the faint colour of sodium flame appeared above the beads. The flame was kept in this position until the beads attained a dull red heat, whereupon instead of separating they drew together and ultimately fused into a solid mass (fig. 3).

Exactly similar effects were obtained with beads which had been contaminated and breathed upon.

Many pairs of beads (from soft German soda glass) were tested in this manner : always with the same results.

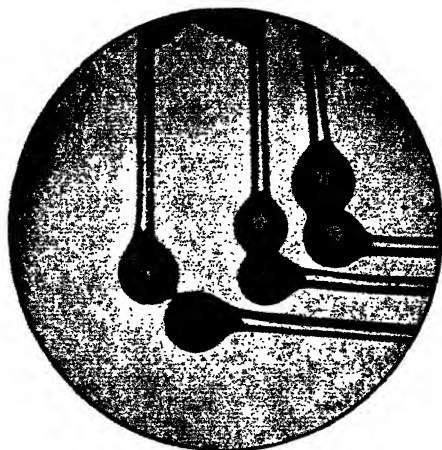
It had been anticipated that gases or vapours would be evolved at the surfaces of contact of the beads which had been breathed on and that the beads would then separate. This expectation was in no case realized.

Beads of certain kinds of glass did not fuse in the way just described until they had been breathed on and then heated more quickly.

Beads of other kinds of glass, again, did not draw together. Fine necks formed between them, which drew out and finally fused.

It must be borne in mind that, at the comparatively high temperatures of fusion, we are no longer dealing with solid bodies, but with highly viscous fluids.

Fig. 3.



As regards *electrification*, attempts were made to remove possible electrical charges from the beads by passing a Bunsen flame over them and over the glass fibres still attached to them, before bringing them into contact. The beads were then brought into contact and the flame was again passed over them. After this treatment, the phenomena were the same as those already described.

The beads and fibres were then breathed on whilst separated, and the fibres were earthed. Again no change of behaviour was observed. A gold leaf electroscope was instantly discharged when a similar piece of glass fibre, 10 to 15 cm. long, was breathed on and quickly brought into contact with the plate of the instrument.



When dried with a gentle heat, these fibres would only cause a very slow fall of the gold leaf.

*Adhesion in an Atmosphere Artificially Dried.*

It seemed desirable that more elaborate experiments should be made with a view to throwing light on

- (i.) the part possibly played by water in some form ;
- (ii.) the electrical state of the beads.

As regards (i.), the researches of Langmuir and others have clearly demonstrated the very great, indeed the almost insuperable difficulty of removing all water molecules from the surface of glass. It seemed therefore desirable that all possible precautions should be taken to ensure that the bead surfaces were as dry as they could be made.

At the same time, it was important to have facilities for testing the electrical state of the beads while the experiments were going on.

Both of these objects were secured with the help of the specially constructed piece of apparatus shown in fig. 2, comprising a chamber through which dry air could be passed and an electroscope by which a bead suspended in the chamber could be tested for electrification at any moment.

The suspended bead could be raised or lowered between limit stops by means of a balanced arm not attached to the electroscope. The horizontally mounted bead could be moved by means of a micrometer supported on an independent pillar. The air inlet, earthing plunger, sliding charging contact, and zero adjustment, are shown in the figure. The gold leaf was about 1.5 cm. long and not quite 1 mm. in width.

The deflexions of the gold leaf and distances between the two beads were measured by means of microscopes independently mounted.

The observation chamber had two opposite circular windows glazed with selected microscope cover-glass.

When the suspended bead was being tested for electrification the horizontal bead was drawn back by means of the micrometer screw and the suspended bead was lowered almost to the bottom of the cup attached to the conductor from which the gold leaf is suspended.

To charge the electroscope, the cap covering the "charging contact" was removed, and the contact wire pressed into contact with the inner chamber. The "earthing contact" was also pressed in. The charge was given from a rubbed rod of glass or ebonite until the desired initial deflexion of the gold leaf was produced. The "charging contact" was then drawn back by means of the small hook on it, the cap put on to protect the instrument from induction disturbances, and the "earthing contact" withdrawn.

The insulation by amber was fairly good. The fall of the gold leaf due to leakage was tested after the experiments herein referred to were terminated. At the end of three months the deflexion of the gold leaf was about 50 per cent. of its value at the commencement of the test.

A great many experiments were made with glass beads in the observation chamber above this electroscope. The effects looked for were:—

- (i) attraction at a distance ;
- (ii) adhesion ;
- (iii) electrification of the suspended bead.

In all cases the chamber enclosing the gold leaf was positively charged.

The radius of swing of the suspended bead was about 2.2 cm.

The capacity of the electroscope was about 4 cm.

The electroscope was roughly calibrated by using a brass sphere of 0.177 cm. radius suspended by a cocoon silk fibre. It was charged by bringing it into contact with the end of a fine wire connected to the + terminal of a few dry cells. The terminal P.D. of the battery was determined with an ordinary commercial voltmeter. The brass sphere was then put in the place of the suspended glass bead and lowered into the electroscope. Care was taken to keep other conductors at a considerable distance from the brass sphere when charging it.

The observations, in particular the deflexions of the gold leaf and the distance between the nearest points of the two beads after separation, were recorded in scale-divisions of the eyepiece micrometers used, and could of course be reduced to absolute measure. It is unnecessary to give the actual figures here.

The current of air through the chamber could be increased or decreased at will. The air on its way to the chamber was bubbled through sulphuric acid, mainly to enable its rate of flow to be checked, and then through two glass tubes, the first completely filled with freshly prepared calcium chloride for a length of 75 cm.; the second completely filled with phosphorus pentoxide for a length of 9 cm.

When taking the attraction at a distance, a scale-division line was made just to touch the suspended bead. This bead was then watched carefully and the horizontal bead was advanced to it. A movement of the suspended bead of 0.2 of a scale-division could easily be detected, corresponding to a movement of 0.003 mm., or a force of about 0.00014 of the weight of the bead. The largest suspended bead referred to in this paper was 1.72 mm. in diameter; taking the density of glass as 2.5, the weight of the bead is 0.00666 gram, and the horizontal component of the force 0.0000093 gram for a deflexion of 0.2 of a scale-division.

The general procedure with this apparatus was first, before the dry air was turned on, to bring the bead attached to the micrometer into contact with the suspended bead. Adhesion then regularly took place. Next, the dry air was turned on. When the beads had been exposed to the action of the dry air for some time, the micrometer bead could be brought up to the suspended one and drawn away again without any sign of adhesion. This condition of no adhesion could be steadily maintained so long as the current of dry air was kept going. When the dry air was turned off again, the beads at once began to show adhesion when brought together and the distance to which the suspended bead could be drawn over without losing contact with the other increased rapidly. It reached its normal value in a few minutes.

At times, a pair of adhering beads were drawn over by the micrometer so as to produce a force tending to separate them. The dry air was then turned on. The dry air caused the silk suspending loop to contract and draw the suspended bead over the surface of the other. These movements took place for some time in steps, but usually did not cause the beads to separate.

While watching the behaviour of the beads in the observation chamber, one had the distinct impression that

adhesion only occurred when there was something on the beads—say an electric charge or a water film—which could be removed or at least changed by the action of dry air.

Subsidiary experiments on the conductivity of water films, adsorbed on rods made from the same samples of glass as the beads, showed clearly that the free water on their surfaces is quickly removed by the action of dry air around them. On the other hand, no evidence of the electrification of soft German soda glass beads was detected at any time during the conduct of the experiments.

The absence of attraction at a distance, of adhesion in very dry air, and of any deflexion of the gold leaf of the electroscope, all strongly suggest that water, in some form, exercises an important influence on the adhesive properties of glass with glass.

It may be noted, however, that beads made from Jena combustion tubing showed phenomena differing widely from those observed with beads of the other samples of glass experimented with. These beads, when first put into the observation chamber, showed strong adhesion, and, after the first separation, strong electrification. When the beads were then exposed to the air of the room and the test repeated, they were found to be completely discharged, but they soon acquired a small charge of the opposite sign from before. After turning on dry air, the electrification of the suspended bead again changed sign, and it continued to increase with each contact between the beads.

#### *No Adhesion Between Beads Immersed in Water.*

A few experiments were made with glass beads immersed in water.

The beads were mounted in a vertical tube with a flat glass window. The tube and contents were mounted on a tilting table such as is used for testing level tubes.

By altering the tilt, the suspended bead was made to press against the other bead and was left in this position for some time. The tilting table was then brought very slowly to its zero position, and then a little further—far enough, if the bead were free, to cause a separation of a few hundredths of a millimetre.

*In every case the beads separated*, but in some cases intervals up to half an hour elapsed before light could be seen between the beads with the aid of a microscope.

*Absence of Mechanical Injury to Surfaces.*

Many beads were subjected to careful microscopical examination with a view to ascertaining whether they had received mechanical injury such as has been described by Hardy and others.

*So long as the only force pressing them together was their mutual adhesion*, not one case of injury to the surfaces which had been in contact was detected.

Many of these beads, after their first examination, were again caused to slide over each other, this time with some added force applied by hand. In these cases, tearing of the surfaces usually took place and the appearance of the damage, as seen by the microscope, was in all respects similar to that described by Hardy and recently by Tomlinson.

*Summary.*

The conclusions to which these experiments seem to point are these :—

(1) In the case of glass, adhesion is due to the presence of water molecules entangled in the surface layer of the glass. That the adhesion is due to water molecules seems proved by the fact that, in air which was artificially maintained in as dry a condition as possible, the adhesion phenomena practically disappeared.

(2) If water molecules once become entangled in the surface, they are difficult to remove. They can be removed by a current of dry air, so long as the beads are separate, but if the water molecules are entangled in the region of contact between two glass beads that are touching, it is extremely difficult to get rid of them by any of the ordinary means of drying, so that adhesion shows itself and persists—even though the beads be heated until they fuse together.

(3) The phenomenon of adhesion may or may not be accompanied by electrical effects. In the case of German soft soda glass it is not ; in the case of Jena combustion glass, it is.

(4) There is no adhesion between beads immersed entirely in water.

(5) Surfaces of contact are *not* injured so long as the only forces acting are those of natural adhesion.

LVIII. *On the Probability Method in the New Statistics.*

By S. CHANDRASEKHAR \*.

(1) *Introduction.*

**P**ROBLEMS in statistical mechanics can in general be treated by two methods. One is the method of the kinetics of collisions and the establishment of a H-theorem; the other is the method of counting the complexions. Both these methods have been incorporated into the quantum statistics †.

Recently, however, a new method has been developed—"a geometrical weight method"—by W. S. Kimball ‡. This method has many advantages over the two previous methods, and it seems, therefore, useful to generalize Kimball's treatment to include the new statistics.

The basis of this new treatment is the definition of a quantity called the *range*, and its equivalence with the statistical weight. For ordinary space the dimensional range is the volume occupied by the gas. This may be analysed by taking the reciprocal of the density  $\frac{1}{n}$ , which is a measure of the weight or the probability of the volume state of this particle. On the *classical theory*, if there are  $N$  mass points, all of them are equally likely to be in this volume, so that  $N$  times  $\frac{1}{n}$  is the weight. By similar reasoning, the range of a mass point at a particular place in the velocity space is the reciprocal of the number of particles included in unit length of the velocity space there. Likewise the momentum range per mass point is uniquely defined throughout the momentum space. The action range per unit particle is similarly defined as the product of the range per particle in the volume-space and the range per particle in the momentum space.

(2) *The Statistical Distribution Function.*

We consider, as usual, an assembly of  $N$  mass points which may be subjected to any exterior field of force, but

\* Communicated by R. H. Fowler, F.R.S.

† L. W. Nordheim, Proc. Phys. Soc. A, cxix, p. 689 (1928); S. Chandrasekhar, Phys. Rev. (to appear shortly); E. Fermi, *Zeits. für Physik*, xxxvi. p. 902 (1926); L. Brillouin, *Ann. de Phys.* vii. p. 315 (1927).

‡ W. S. Kimball, Jour. Phys. Chem. xxxiii. p. 1558 (1929).

interact with each other only at very small distances. The state of such an assembly is given in the usual manner by a distribution function,

$$f(x, y, z, \xi, \eta, \zeta),$$

which gives the number of particles in every infinitesimal range  $dx dy dz d\xi d\eta d\zeta$  of the given phase-space, so normalized that

$$\int f d\Omega = N, \dots \dots \dots (1)$$

where

$$\Delta\Omega = dx dy dz d\xi d\eta d\zeta.$$

It follows, therefore, that the six-dimensional range is given by

$$\frac{1}{r} = \frac{dn}{\Delta\Omega} = f(x, y, z, \xi, \eta, \zeta), \dots \dots \dots (2)$$

which is the number of mass points in unit range in the volume element  $\Delta\Omega$ . The reciprocal of the above gives the distance there is in the phase-space between successive particles.

$$r = \frac{1}{f(x, y, z, \xi, \eta, \zeta)} = r_{i+1} - r_i \dots \dots \dots (3)$$

If there are  $N$  mass points in the *classical theory*, all are equally likely to be in the range in question, independent of the number already in it, and therefore the probability that one of them will be in the specified range is  $N$  times (3). Hence the weight per particle is

$$w = \frac{N}{f(x, y, z, \xi, \eta, \zeta)} \dots \dots \dots (4)$$

On the other hand, the essential feature of the Fermi-Dirac statistics is the impossibility of more than one particle occupying one and the same phase-element (according to Pauli's exclusion principle). If, therefore, the cell is already occupied, then the weight for that particular phase-element is zero. When, however, the space is not densely packed, there is correspondingly only a reduction. The simplest possible extra-factor is therefore

$$\left(1 - \frac{f}{A}\right)^*,$$

where  $A$  is the number of quantum cells in the phase-

\* The weight would then reduce to zero when  $A = f$ , in accord with Pauli's principle.

space (for the ordinary translational motion  $A$  is, of course, equal to  $(m^3g/h^3)$ ). We have in this case

$$w = \frac{\left[ 1 - \frac{f(x, y, z, \xi, \eta, \zeta)}{A} \right]^N}{f(x, y, z, \xi, \eta, \zeta)} \quad \dots \quad (5)$$

In the Einstein-Bose statistics the weight should be *increased*, and one has therefore

$$w = \frac{\left[ 1 + \frac{f(x, y, z, \xi, \eta, \zeta)}{A} \right]^A}{f(x, y, z, \xi, \eta, \zeta)} \quad \dots \quad (6)$$

With these expressions (5) and (6), instead of (4) which Kimball uses, the new statistical formulæ could be derived. Thus the weight that measured the probability that a particle will be in the  $i$ th range, corresponding to (5) and (6), is

$$w_i = \frac{1 \pm \frac{f_i}{A_i}}{f_i} N \quad \dots \quad (7)$$

It may be necessary to distinguish between the  $A$ 's, for their masses may be different. In the case of non-degenerate systems throughout the phase-space  $f/A \ll 1$ , and we return to the classical theory. We have for the total weight, therefore,

$$W = \frac{\left( 1 \pm \frac{f_1}{A_1} \right) \left( 1 \pm \frac{f_2}{A_2} \right) \dots \left( 1 \pm \frac{f_N}{A_N} \right) N^N}{f_1 f_2 \dots f_N} \quad \dots \quad (8)$$

We will now introduce a new function  $g$  instead of  $f$ , defined by the relation

$$g = \frac{f}{1 \pm f/A}, \quad \dots \quad (9)$$

which implies no loss of generality, since the  $g$  is a single-valued function of  $f$ . Hence

$$W = \frac{N^N}{g_1 g_2 \dots g_N} \quad \dots \quad (10)$$

Now we can apply the Lagrange method for conditional maxima forming the function

$$F = W + \lambda E, \quad \dots \quad (11)$$

where  $\lambda$  is arbitrary.



Taking the partial derivatives for the  $3N$  independent-velocity variables,

$$\left. \begin{aligned} \frac{\partial F}{\partial \xi_r} &= -W \frac{d}{d\xi_r} \log g_r + \lambda m \xi_r, \\ \frac{\partial F}{\partial \eta_r} &= -W \frac{d}{d\eta_r} \log g_r + \lambda m \eta_r, \\ \frac{\partial F}{\partial \zeta_r} &= -W \frac{d}{d\zeta_r} \log g_r + \lambda m \zeta_r, \end{aligned} \right\} \dots \quad (12)$$

we easily get from these relations

$$g = B' e^{v'(\xi^2 + \eta^2 + \zeta^2)}, \quad \dots \quad (13)$$

$B'$  and  $C'$  being independent of the velocities. It follows, therefore, that

$$f = \frac{A}{e^{v'(\xi^2 + \eta^2 + \zeta^2)} / B \mp 1}, \quad \dots \quad (14)$$

i. e., the well-known Einstein or Fermi formula.

The same result can be obtained if we consider (3) and express  $W$  explicitly as a product of the successive differences of the  $v$ 's. In the classical theory (Kimball, *loc. cit.*, eq. (32) we have

$$W = N^N \prod_{i=1}^N (v_i - v_{i-1}). \quad \dots \quad (15)$$

On the other hand, in the quantum theory we have

$$W = N^N \prod_{i=1}^N \left(1 \pm \frac{f_i}{A_i}\right) (v_i - v_{i-1}). \quad \dots \quad (16)$$

If we apply, as before, the Lagrange method for conditional maxima, we get

$$\dots = \frac{\frac{\partial}{\partial v_i} \log \left(1 \pm \frac{f_i}{A_i}\right) \left(1 \pm \frac{f_{i+1}}{A_{i+1}}\right) (v_i \pm v_{i-1}) (v_{i+1} \pm v_i)}{v} = 2b. \quad (17)$$

If we introduce the approximations

$$(1 \pm f_i/A_i)(1 \pm f_{i+1}/A_{i+1}) = (1 \pm f_i/A_i). \quad \dots \quad (18a)$$

$$\text{and} \quad (v_i - v_{i-1})(v_{i+1} - v_i) = (v_i)^2. \quad \dots \quad (18b)$$

we get the same distribution formulæ as before.

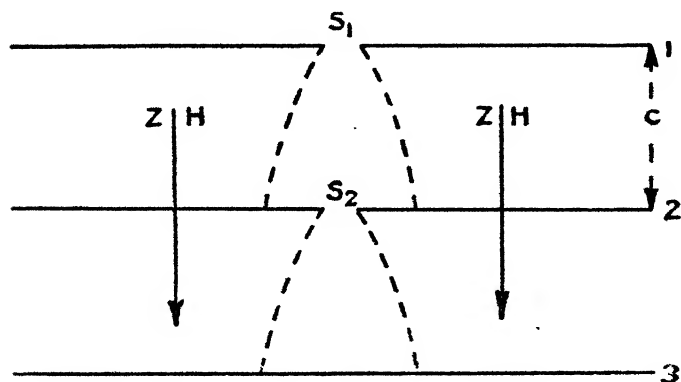
### *Summary.*

The recently developed geometrical statistical weight theory (Kimball) has been generalized to include the quantum statistics.

LIX. *The Behaviour of Electrons in Magnetic Fields.* By V. A. BAILEY, M.A., D.Phil. (Oxon.), Associate Professor of Physics, University of Sydney\*.

1. **I**N a recent communication† it has been shown how to determine the divergence of a stream of electrons which moves in a gas simultaneously under the actions of parallel electric and magnetic forces. The principle established may be illustrated by the diagram.

The stream entering at the opening  $S_1$  diverges as it approaches the electrode 2, on account of the diffusion of the electrons, and only a certain fraction  $R$  of this stream



passes through the opening  $S_2$ . If  $Z$  is the electric force,  $H$  the magnetic force,  $c$  the distance between the electrodes 1 and 2,  $k$  the mean energy of agitation of the electrons in terms of that of a molecule at  $15^\circ\text{C.}$ ; and  $W$  is the mean velocity of the stream in the direction of  $Z$ , then the fraction  $R$  is a function  $R(\zeta)$  of the ratio  $\zeta = Z\sigma/kc$  where  $\sigma = 1 + (HW/Z)^2$ .

Observations on electrons in hydrogen were found to be in complete agreement with this principle, so it was applied to the determination of the velocity  $W$  in this gas and gave values which are the same as those obtained in 1921 by means of Townsend's well-known method.

\* Communicated by the Author.

† See p. 580 of the present number.

Four other simple methods of applying this principle are given below. The first three are of particular interest, for, unlike the one already published, they do not require that the function  $R(\zeta)$  be known. The values of  $W$  obtained by means of the different methods are all in good agreement.

## 2. Second Method.

The ratio  $R$  is measured with a known set of values of the electric force  $Z$ , the gas-pressure  $p$  and the spacing  $c$ ; under these conditions  $\zeta$  has the value  $\zeta_1 = Z/kc$ . Then  $Z$  and  $p$  are diminished by the same factor  $n$  (which may have any convenient value), the magnetic force  $H$  is applied, and the ratio  $R$  is again determined; the corresponding value of  $\zeta$  is  $\zeta_n = Z\sigma/nkc$ . The force  $H$  is adjusted to make the value  $R$  equal to that in the first set of conditions; this is equivalent to making  $\zeta_n$  equal to  $\zeta_1$ . Hence  $\sigma = n$ , and so

$$W = \frac{Z}{H} \sqrt{n-1}. \quad . \quad . \quad . \quad (1)$$

## 3. Third Method.

With this the first set of conditions is the same as in the method just described, and may be represented by  $Z$ ,  $p$ , and  $c$ ; therefore  $\zeta_1 = Z/kc$ . The second set is that represented \* by  $Z$ ,  $p$ ,  $nc$ , and  $H$ , for which  $\zeta_n = Z\sigma/knc$ . The value of  $H$  is adjusted as before, which is equivalent to making  $\zeta_n$  equal to  $\zeta_1$  and leads again to the relation (1).

The following table gives an actual example of its application to electrons in hydrogen:—

$Z$ (volts/cm.).	$p$ (mm.).	$c$ (cm.).	$H$ (e.m.u.).	$R$ .
20	4	2	0	.375
20	4	4	698	.375

Since  $n = 2$  the value of  $W$  obtained by means of (1) is

$$\frac{20 \times 10^8}{698} \sqrt{2-1}, \quad i. e. \quad 28.6 \times 10^5 \text{ cm./sec.}$$

The value obtained previously by means of Townsend's method is  $25.5 \times 10^5$ .

## 4. Fourth Method.

The first set of conditions for this is again represented by  $Z$ ,  $p$ , and  $c$ , for which  $\zeta_1 = Z/kc$ . The second set is represented by  $Z/n$ ,  $p/n$ ,  $nc$ , and  $H$ ; therefore  $\zeta_n = Z\sigma/n^2kc$ . If

\* *i. e.* the only changes are an increase of the distance between the electrodes 1 and 2, and the application of the magnetic field.

H be adjusted as before, then for this value  $\zeta_n$  is equal to  $\zeta_1$ . Hence  $\sigma = n^2$ , and so

$$W = \frac{Z}{H} \sqrt{1 - \frac{1}{n^2}} \quad \dots \quad (2)$$

Its application to electrons in hydrogen is shown in the following table, where  $n = 2$  :—

Z (volts/cm.).	p (mm.).	c (cm.).	H (e.m.u.).	R.
20	4	2	0	375
10	2	4	626	375

Therefore

$$W = \frac{20 \times 10^8}{626} \sqrt{1 - \frac{1}{4}} = 27.6 \times 10^5 \text{ cm./sec.},$$

which is in agreement with the value  $25.5 \times 10^5$  referred to above.

This method is of special interest, for it can be established without neglecting any term in the complete differential equation \* for the density of the electrons at a point, and because it is also suitable when negative ions are present if the instrument † with two successive chambers be used.

With this instrument the quantity  $a = R(Z/kc)e^{-\alpha c}$  is measured, where  $\alpha$  is the probability that an electron becomes attached to a molecule per centimetre of its motion in the direction of Z. If the first set of conditions

$$Z, p, c, \text{ gives } a = Re^{-\alpha c},$$

and the second set

$$\frac{Z}{n}, \frac{p}{n}, nc, H \text{ gives } a_{nk} = R_{nk}e^{-\alpha_{nk}nc},$$

then  $a_{nk} = a$  when the value of H is such that  $\sigma = n^2$ .

For the second set  $R_{nk}$  depends on the differential equation

$$\frac{\partial^2 q}{\partial x^2} = 41 \left( \frac{Zn^2}{nkc} \right) \frac{\partial q}{\partial \zeta} - \frac{n^2}{n^2 c^2} \frac{\partial^2 q}{\partial \zeta^2},$$

which is the same as that determining R, namely,

$$\frac{\partial^2 q}{\partial x^2} = 41 \left( \frac{Z}{kc} \right) \frac{\partial q}{\partial \zeta} - \frac{1}{c^2} \frac{\partial^2 q}{\partial \zeta^2}$$

and the boundary conditions are the same too. Also

\* Number (2) in the communication cited.

† V. A. Bailey and J. D. McGee, Phil. Mag. p. 1076 (Dec. 1928).

$a/p$  depends on  $Z/p$  alone, so  $a_{nc} = ac$ , and therefore  $a_{nh} = a$ . The value of  $H$  is adjusted until this condition is satisfied, and then  $W$  may be calculated by means of the formula (2).

### 5. Fifth Method.

Under the two sets of conditions required for the third method, let the corresponding quantities  $a$  and  $a_{nh}$  be measured. By adjustment of  $H$ , the value of  $a_{nh}$  may be made equal to  $ae^{-ac(n-1)}$ , whose value is known if that of  $a$  has already been determined. Therefore,

$$R\left(\frac{Z\sigma}{knc}\right)e^{-anc} = R\left(\frac{Z}{kc}\right)e^{-ac} \times e^{-ac(n-1)}.$$

$\therefore \sigma = n$ , and so  $W$  may be determined by means of equation (1).

LX. *The Nature of Friction.* By Prof. P. E. SHAW,  
M.A., D.Sc., University College, Nottingham\*.

### I.

**T**RIBOELECTRICITY and friction are two aspects of the same event: the rupture of the combination between atoms of solid surfaces. In friction we deal with the energetics; in triboelectricity with the electric charges caught on each of the surfaces in the act of rupture. The residual charges observed are greatest when different insulators have been in contact, but it has been shown † that charges, though smaller than these, arise when identical insulators part company; and this is also the case for identical metals provided they are parted at great speed ‡. We can express these relations in symbols. It has been established that rate of charging varies as the work done in rubbing §, so

$$\frac{dq}{dt} = a \cdot \frac{dw}{dt}$$

\* Communicated by the Author.

† Proc. Phys. Soc. xxxix. p. 449 (1927).

‡ Proc. Roy. Soc. A. (1929).

§ Owen, Phil. Mag. 1909; Jones, Phil. Mag. 1925.

where

$q$  = charge,

$w$  = work,

$a$  = constant, specific for the materials used.

Similarly for leakage,

$$\frac{dq'}{dt} = b \frac{dw}{dt} \cdot Q.$$

$q'$  = leakage and re-combination,

$b$  = leakage constant, depending on charge,

$Q$  = accumulated charge ;

but

$$dQ = dq - dq' = (a - bQ)dw.$$

Hence

$$Q = \frac{a}{b}(1 - e^{-bw}).$$

Taking the three cases mentioned above. For unlike insulators,  $a$  is large,  $b$  small, therefore  $Q$  is large. For like insulators,  $a$  is small,  $b$  is small,  $Q$  is moderate. For like metals,  $a$  is small,  $b$  is large,  $Q$  is immeasurably small, unless by speedy separation of the surfaces  $b$  is made ineffective.

In the cases of like insulators and like metals  $a$  is small, not because the total electron flow is small, but because, for materials almost identical in nature, the flow each way across the interface is almost equal.

According to these views, friction is in all cases due to the breaking of electric attachments, and is directly proportional to the electric separation (if the flow of electrons both ways across the interface be added together) plus any work performed in *surface strain*.

We assume that when atoms meet, they invariably combine (unless they happen to be inert gases). This generalization is based on various facts :

(a) Adsorption. Here condensed vapour is strongly attached to the solid surface.

(b) The seizing of truly parallel clean surfaces when wrung together (*e.g.*, Johansson gauges). More convincing even than the seizing is the fact that after repeated wringing the surfaces are torn up, and their 'truth' ruined. In like manner many metals, initially smooth, become very rough when rubbed dry *in vacuo*.

(c) The cohesion invariably found between solid particles crystallizing from solution or emerging from fusion.

(d) Triboelectric charges. Whatever the solids used, such charges arise, as shown above, when separation occurs, and they denote combination of the surfaces before they separate. It is not implied that combination at cold contact of solids is as complete as, say, after fusion. Atoms of solid surfaces, being held by their neighbours, are not as free to form polar attachments as when in a fluid state. But there seems justification for the belief that *solid* combination does occur in kind, if not in full degree. The principle that solids invariably combine when brought into intimate contact may seem contrary to experience. For instance, such ordinary processes as hand-shaking or walking would be supremely difficult if great force were needed to break solid bonds when the hands separate, or the foot is raised from the ground. But, fortunately, the usual surface conditions in the cases cited are those described in impact (Section IV. of this paper) where dry surfaces of elastic solids are specified. If one surface were covered with an inelastic, plastic substance like pitch, cohesion on a large scale without repulsion would occur, and separation of the surfaces would become difficult. The strength of attachment of a solid for pitch, atom for atom, is small but the immense number of atoms which can combine, one substance being plastic, makes the total strength of attachment considerable.

## II.

Three surface effects specially concern us in connexion with friction :—

- A. Repulsion, the direct reaction to pressure normal to the surface.
- B. Cohesion of the surfaces whilst under pressure, as displayed in sliding friction.
- C. Cohesion of the surfaces, when under tension, as in rolling friction and the rebound of impact.

The relation of B to C is obscure. We might expect the interface strength to be very different according as (in B) the normal stress between the surfaces is a pressure in some cases thousands of atmospheres ; or as (in C) it is a tension, presumably of the order of the tenacity of the material, say, a thousand atmospheres, if expressed as an inverse pressure. The strength of cohesion in each case is due to some unknown

disposition of the electric and magnetic fields of the atoms, but this disposition must be very different for compression and for tension.

Employing Hertz's equations of deformation (see Prescott's 'Applied Elasticity,' p. 632) and considering the case of a sphere touching a plane,

$$a^3 = \frac{3(1-\sigma^2) \cdot W R}{2\pi E}, \quad . . . . . \text{(I.)}$$

$$p = \frac{3W}{2\pi a^3} \cdot (a^2 - r^2)^{1/2}, \quad . . . . . \text{(II.)}$$

$$d_0 = \frac{3W}{2\pi a} \cdot \frac{1-\sigma^2}{E}; \quad . . . . . \text{(III.)}$$

where

$a$  = radius of the circular area of contact between sphere and plane,

$r$  = any radius in this circle  $< a$ ,

$R$  = radius of the sphere,

$E$  = Young's modulus,

$\sigma$  = Poisson's ratio,

$p$  = pressure at any point in the circle of contact,

$d_0$  = displacement at the centre of circle,

$W$  = force between the sphere and plane.

By the law of friction

$$W = R = \frac{1}{\mu} T.$$

Where

$R$  = aggregate repulsion of all atoms bearing on one another at the interface of sphere and plane.

$T$  = aggregate cohesion of these combined atoms to resist shear.

$$\therefore R = \int_a^0 p 2\pi r dr,$$

$$T = \int_a^0 g 2\pi r dr,$$

where  $p = \nu\rho$ ,  
 $g = \nu\tau$ ;



where

$p$  = pressure per unit area at any radius  $r$  in the circular area of contact as given by (II.),

$g$  = cohesion strength per unit area at any radius,

$\nu$  = number of atoms per unit area bearing on one another across the area of contact,

$\rho$  = repulsion per atom,

$\tau$  = cohesion per atom, to resist shear

$$\therefore W = \int_a^0 \nu \rho \cdot 2\pi r dr = \frac{1}{\mu} \int_a^0 \nu \tau 2\pi r dr, \quad \text{(IV.)}$$

clearly  $\nu$  has the same values throughout on both sides of the equation, and we can apply the law of friction to the limiting case when only one atom of each surface is in contact, then

$$\rho = \frac{1}{\mu} \cdot \tau,$$

i. e., the ratio of  $\tau$  to  $\rho$  is constant throughout the area of contact.

From equations (I.) and (IV.),  $\sigma$ ,  $\Re$  and  $E$  being constant,

$$\int_a^0 \nu \rho 2\pi r \cdot dr \propto W \propto a^3,$$

$$\therefore \nu \rho \pi a^2 \propto a^3,$$

$$\therefore \nu \rho \propto a \propto W^{1/3}.$$

Thus, if  $W$  increases 8-fold, radius of area increases 2-fold, area 4-fold, and  $\nu \rho$  2-fold.  $\nu$  and  $\rho$  increase together until the limiting pressure  $\rho$  max., sustainable by the material is reached. The solid structure then gives way at the centre of pressure. Permanent strain ensues and both the law of friction and Hertz's equations fail.

It is convenient to distinguish between permanent superficial- and permanent body-strain. All actual solid surfaces are rough compared with atomic dimensions. Even polished surfaces (whose roughness is of the order of a wave-length of light) on coming into contact meet at their outstanding protuberances. As these contact areas are small, the pressure between them is great, and this causes a flattening of the protuberances until sufficient actual contact area is developed to provide total repulsion equal to the external applied force. The superficial strain thus produced extends to a small depth, say of the order of a wave-length.

## III.

Certain reactions between solid surfaces, as in impact, sliding and rolling friction, polishing, filing, and grinding are highly complex. They all bring into action on the surface atoms such large forces as to produce rupture and ionization; some of them, the last three, go further and exceed the body elastic limit. Each of the two reacting surfaces being free, has its own electrostatic and magnetic fields more complicated than in the body of the solid, where, at least in the single crystals, simplicity reigns. If further the surfaces are in contact with an atmosphere, adsorbed films and solid contamination add more factors to the equation of state. But at least we can minimize the last troubles by experimenting *in vacuo* with dry solids. We shall suppose in what follows that the reacting surfaces are dry, *i. e.*, free of even residual films.

## IV.

Before dealing with friction consider a simpler effect, impact, and suppose a sphere to be approaching a plane at normal incidence. To take the sequence of events in order :

(1) The first contact is between two atoms one on each face; these combine with loss of energy and heat is developed, as in the familiar case of the surface combination known as adsorption.

(2) The two combined atoms at the interface are now at atomic distance apart and are in equilibrium; but with the onward motion of the sphere they are forced together.

Repulsion between them—due presumably to electrostatic separation and/or electromagnetic rotation—grows as the centres of the atoms approach one another, and work, most of it reversible, is performed by the oncoming sphere in building up this repulsion.

In the end, the distance between the sphere and the plane reaches its lower limit, by which time other pairs of atoms have met and undergone similar combination followed by repulsion. The sphere has now momentarily come to rest and the contact area has attained its maximum as at PPP, fig. 1. The pressure developed is maximum at O and falls to zero at the edge PPP, according to equation (II.).

Consider fig. 2 where abscissæ and ordinates stand respectively for radii of the interface and force between opposed faces.

There is an annular zone between radii  $a'$  and  $a$  in which atoms are combined, but are separated by more than atomic distance. In this zone attraction occurs across the interface, but for radii less than  $a'$  atoms are within atomic distance and repel one another. The pressure  $W$  is sustained by the algebraical sum of the total attraction  $A$ , and total repulsion  $R$ , i. e., by the difference between the two shaded areas.

$$\therefore W = R - A.$$

The existence of the zone of attraction is undoubted when the surfaces are separating, and the area of contact diminishing; we assume its presence prior to this separation, though this is not essential to the argument. The annular space is negligibly small compared with the whole area  $\pi a^2$ , except when this area, or the curvature of the sphere, is small, so that equations (I.) and (II.), which take no account

Fig. 1.

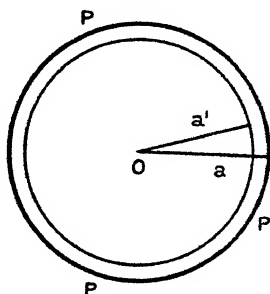
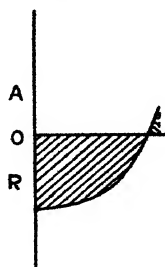


Fig. 2.



of such a zone, may for present purposes be considered valid. It is in accordance with these views that the seizing of surfaces only occurs when their curvatures are equal and opposite so that they 'fit'—flat surfaces of course being only a special case of this. In all such cases the attraction zone is relatively large, and in such an example as that quoted by G. A. Tomlinson\* for lead, the attraction zone occupies the whole contact area when the pressure is negative.

(3) When the sphere rebounds from rest on the plane, the atoms in contact across the interface are torn apart, the peeling process occurring at the extreme outer edge of the annular zone, where by supposition the atoms are at more than atomic distance apart.

\* Phil. Mag., June Suppl., 1929, p. 936.

The work required to break these bonds is done by the potential energy accumulated in the spring of the lattice structure.

When the rebounding sphere is nearly free of the plane and the contact area reduced to small dimensions, all the remaining pairs of atoms are in attraction. To break these remaining bonds absorbs energy from the sphere.

In the meeting and separation of the two surfaces in impact, there are losses due to various irreversible processes:

(1) During the meeting, on account of permanent displacement of atoms in the solid structure, and the combination of surface atoms; (2) during separation on account of the breaking of bonds still remaining when all the repulsion energy has been spent in the rebound.

The coefficient of restitution measured in impact experiments reveals these energy losses which, for instance, are small for steel and great for lead.

## V.

Now consider sliding friction. Begin with the sphere at rest on the plane under its own weight  $W$ , and the contact area as shown in fig. 1. On applying force to draw the sphere, without rotation, over the plane, the first effect is to strain the bonds attaching the interface atoms. The bonds have a measurable elastic limit as shown experimentally by Rankin\*. No rupture occurs for forces less than a critical value. When, however, sufficient tangential force  $T_s$  is applied, all the bonds formed across the interface are broken and sliding occurs. Amonton's law

$$T_s = \mu W,$$

gives the relation of the stresses to the coefficient. As sliding proceeds the bonds are continually broken and remade and, since kinetic and statical friction are equal, the total number of bonds,  $N$ , remains a statistical constant.

## VI.

Next consider the case of rolling friction and imagine the sphere as before, resting on the plane under its own weight before friction commences. The law of rolling friction is

$$T_r = \lambda W,$$

where  $T_r$  is the force applied to the centre of the sphere to

\* Phil. Mag., Oct. 1926.

roll it without slip (ignoring for the moment the O. Reynolds slip).  $\lambda$  = coefficient of rolling friction.

Imagine the force gradually applied. What first happens, as Tomlinson\* showed, is that for small angular displacement of the sphere there is an elastic limit (within which the bonds are strained but hold fast). When this angle is exceeded the bonds give way not, as with sliding, over the whole area of contact, but only on the extreme periphery of the attraction zone in the wake of the rolling sphere, and corresponding new bonds form on the extreme edge in front. All the other bonds are affected but not broken as the motion commences, those in front of the centre of the interface being relaxed, and those behind strained. It is thus clear that the force required to move the sphere unit distance is less for rolling than for sliding in proportion to the bonds broken in the two cases.

We can look at it another way and consider the forces required to break a single bond (1) by rolling and, (2) by sliding. As the sphere rolls each atom as it rises from contact in the wake of the sphere traces out a cycloid.

Let the contact point move from A to O while the contact atom rises from A to P.

Let  $S$  = movement of the centre ( $C = OP$ ),

$r$  = radius of the sphere,

$\theta$  = angle moved.

$$= \frac{S}{r}, \text{ for small angles,}$$

$$PN = r(1 - \cos \theta),$$

as  $\theta$  is small,

$$\cos \theta = 1 - \frac{\theta^2}{2} = 1 - \frac{S^2}{2r^2}.$$

$$\therefore PN = \frac{S^2}{2r}.$$

Let the distance between atoms =  $d$ , and let  $kd$  = distance the bonds stretch before breaking; if  $PN = kd$ ,

$$s = \sqrt{2kdr}.$$

Thus the centre of the sphere moves distance  $\sqrt{2kdr}$  before single rupture occurs.

Now suppose the sphere to slide, and let the distance for rupture in sliding be  $ld$ . The values of  $k$  and  $l$  may be very

\* *Loc. cit.*

different ; for in rolling, atoms are strained across empty space ; whereas in sliding the atom of the sphere in moving from one atom on the plane never moves far from other atoms. Besides, rupture occurs, in rolling, when the atomic bonds are in *tension*, whereas they are, in sliding, *pressed* together with average forces of large amount.

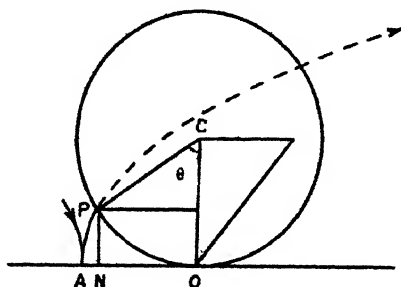
Since the coefficients  $\lambda$  and  $\mu$  are inversely proportional to the distances required for rupture in the two cases,

$$\frac{\lambda}{\mu} = \frac{ld}{\sqrt{2kdr}} = l\sqrt{\frac{d}{2kr}}.$$

Putting  $d = 2.8 \times 10^{-8}$  for steel, making  $r = 1$  cm., and noting that  $k, l$  are of the order one.

$$\frac{\lambda}{\mu} \text{ is of the order } 10^{-4}.$$

Fig. 3.



Tomlinson \* finds the ratio to be  $.5 \times 10^{-4}$  for an experiment on steel. So the results by different methods are in sufficiently close agreement.

The supposition that breaking-tension in rolling equals the breaking shear-stress in sliding is conjectural. The reasoning is employed merely to compare rolling and sliding friction on the basis that both kinds are due to the breaking of solid bonds.

## VII.

The laws of friction employed above can have only limited application. The law of sliding friction cannot apply when either surface has extremely large curvature as, for instance, when a sharp tool is drawn over a plane ; for then flow of the material occurs in the body of the solid, and if the law

\* *Loc. cit.* p. 916.

of friction were applied  $\mu$  would approach infinity. Again, the law breaks down when the sum of the curvatures of the two surfaces is very small. Thus, as already mentioned, when two approximately flat surfaces bear hard on one another, and the pressure is then removed, seizure occurs and  $\mu$  becomes infinite.

So far as we know, no severe experimental test of the law of sliding friction between dry solids has ever been made. Tomlinson, working on metals in the air\*, has obtained a most interesting relation between the coefficient of friction and the elastic constants. In his law

$$\mu = C \cdot (v_A + v_B)^{2/3},$$

the bracket term involves compressibility and rigidity of the two solids in friction;  $C$  is a constant, varying 15–25 per cent. from its mean. Considering the uncertainty in many of the elastic constants this is good agreement, especially as readings in friction never attain high percentage constancy, and some of the irregularities in  $C$  may be due to this cause. Friction of solid surfaces is a rough-and-tumble affair depending on “catch-as-catch-can” contact of rough surfaces, and cannot be expected to have the constancy of such properties as, say, weight or rigidity.

Considering the complex relation between the pressure and area of contact of the two reacting bodies, the law of friction, as generally understood, is remarkably simple, and would seem to justify the simple conclusions reached above.

#### SUMMARY.

It has already been shown that the parting of solid surfaces invariably gives rise to electric separation, even when the two materials used are identical insulators or identical metals.

Thence it is assumed that what happens in all cases of solid contact is that: solid combination takes place when contact occurs: charging of both surfaces occurs when they separate. In friction, the work done is the equivalent of the work performed in total electric separation, plus any work performed in deformation of the surface structure.

The strength of attachment of two atoms (as shown in their resistance to shearing stress) and their mutual repulsion at any point of the area of contact, both vary throughout the area, but their ratio is constant. The ratio between the

\* *Loc. cit.*

distances which the combined atoms separate before parting company in the two cases of sliding and rolling friction respectively, is estimated by the force required for separation in the two cases. The law of friction is limited in application; it becomes invalid for extreme curvatures as well as for extreme loading.

LXI. *A Skew Double-Slider-Crank Mechanism.* By P. CORMAC, M.Sc., F.R.C.Sc.I., University College, Dublin\*.

THE double-slider-crank mechanism STST—the plane mechanism of four pieces, with each piece carrying the elements of a sliding and a turning pair—is met with occasionally in machinery. It derives from the quadric crank-chain by making the links  $a, b, c, d$  of infinite length, but such that  $a$  and  $b$  have a finite difference  $\epsilon_1$ , while  $c$  and  $d$  have a finite difference  $\epsilon_2$ . A special case occurs when  $\epsilon_2$  is zero. Here one of the sliding axes is parallel to the line joining the centres of the two turning pairs. A second special case occurs when  $\epsilon_1$  is made equal to  $\epsilon_2$ . Now the line joining the centres of the turning pairs always remains equally inclined to the two sliding axes. As noted by Hearson†, in this case the mechanism has a dead centre position. In the dead centre position—that is, when the sliding axes are parallel—the chain is not closed, it becoming then simply a sliding pair. It is important to note that the normal reactions on the sliders in the neighbourhood of the dead centre position may be very great.

The existence of a skew form of the double-slider-crank chain does not appear to have been previously noticed. In the skew chain the axes of the two turning pairs are parallel, the sliding axes make equal fixed angles with the turning axes, and they are equally inclined to the plane containing the turning axes. A plan of the chain is shown in the figure.

The links are numbered 1, 2, 3, 4, the sliding pairs being 14 and 23 and the turning pairs 12 and 34. If piece 1 be fixed, 2 will rotate about centre 12, sweeping out a cone of revolution, base angle  $\alpha$ . Piece 3 maintains contact with this cone, while it may slide in the direction of the generator with which it is at the instant in contact. The locus of the

\* Communicated by the Author.

† Proc. Roy. Soc. A, clxxxvii. p. 28 (1896).

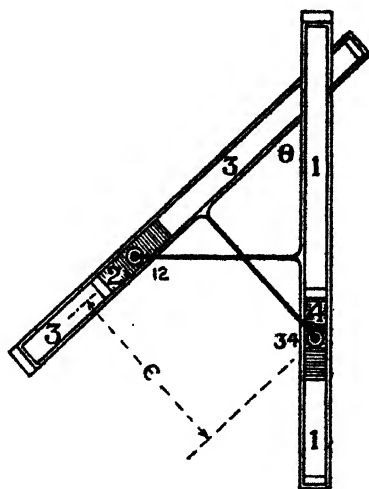


centre 34 is therefore the hyperboloid of revolution which is swept out by a generator through 34 drawn parallel to slide 3. Let slide 1 be an element of the second generation of this hyperboloid of revolution. Slide 1 will then completely constrain the path of centre 34, and will thus constrain the motion of piece 3.

The relation between the linear velocity  $v$  of the sliding pairs and the angular velocity  $\omega$  of the turning pairs is

$$v = \frac{1}{2} \omega \sec \alpha \cdot \sec^2 \frac{1}{2} \theta.$$

The skew mechanism has neither dead-centre nor change-point positions, and the normal reactions on the sliders have



always finite values. An exception, however, must be made of the particular case in which the sliding axes are perpendicular to the turning axes, the chain then becoming the special form of the plane double-slider-crank in which the sliding axes deviate by equal angles from the line through the centres of the turning pairs, a form which has been noted above.

The skew double-slider-crank chain derives from Bennett's\* skew parallelogram chain by passing two alternate vertices of the skew isogram to infinity. It may thus be classified as a special case of the skew isogram.

As the four pieces are similarly placed in the chain, the four possible inversions result in the same mechanism.

\* Proc. Lond. Math. Soc. xiii. p. 151 (1914).

LXII. *On the Scattering and Diffraction of Cathode-Rays.*  
 By PAUL WHITE, B.A. (Cantab.), Carnegie Teaching  
 Fellow in the University of Aberdeen\*.

1. *Introduction.*

WHEN a narrow pencil of electrons falls upon a thin sheet of amorphous material, its individual members suffer various deflexions by the atoms through which they pass, and the pencil as a whole is scattered. If it then falls normally on a photographic plate placed a short distance away from the scattering material, the blackening produced on development will be a maximum in the centre where the whole pencil would have fallen if no matter had been in its path, and with increasing distance from the centre will fall off symmetrically on all sides.

Recently, however, G. P. Thomson and Reid† have shown that if the film through which the electrons pass is microcrystalline, there may appear superimposed on this distribution of electrons other electrons, scattered in an alternative manner, their angles of deviation having, not the continuous range of values present in the previous case, but a number of discrete values. These are recorded on the photographic plate as rings concentric with the central spot produced by the former set of electrons.

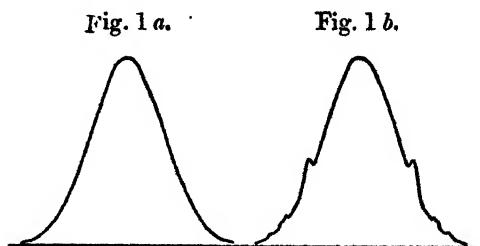
We can describe the effect quantitatively by plotting against the distance  $r$ , measured from the centre of symmetry of the photograph, the number of electrons per unit area falling on the plate at that distance  $r$  and thus obtaining what may be called an electron-distribution curve. It has long been known that when the scattering material is amorphous, the curve has the general form given by Gauss's Error Law (fig. 1*a*) for suitable incident velocities of the electrons and sufficiently great film-thicknesses. No experiments have hitherto been made to determine the curve when the scattering material is microcrystalline, but it is clear that the general form in this case will be that shown in fig. 1*b*, in which each pair of symmetrically-disposed small maxima corresponds to one ring on the photographic plate, that is, to one discrete value of the angle of deviation.

\* Communicated by Prof. G. P. Thomson.

† G. P. Thomson and A. Reid, 'Nature,' cxix. p. 890 (1927); G. P. Thomson, Proc. Roy. Soc. cxvii. p. 600 (1927).

The former type of scattering has been subjected to numerous investigations, and the results can be fairly completely described in terms of classical mechanics\*. It is only possible to give an account of the phenomenon discovered by Thomson and Reid in terms of wave-mechanics. In the one case the electron is regarded as a charged particle deflected by the electrostatic attraction of an atomic nucleus or of several atomic nuclei successively; in the other it is considered as a train of de Broglie waves diffracted by the atoms and hence reflected by suitable net-planes in the minute crystals of the scattering material as are the X-rays in a Debye-Scherrer powder experiment.

While the radii of the rings have been critically compared with the wave-length relations suggested by



General form of electron distribution curve for amorphous and micro-crystalline materials respectively: strictly diagrammatic.

wave-mechanics, the subject of intensities has been hitherto practically untouched. In particular no data have previously been given for the relative numbers of electrons occurring in the central spot and in the rings.

The aim of the present work was to determine electron-distribution curves experimentally, and hence to deduce the relative numbers of electrons falling in the central spot, in one of the rings or in the continuous background. Since the visibility of rings depends on their sharpness of resolution and high intensity relative to the background, a knowledge of the factors governing these quantities will enable us to arrange the most favourable conditions for observing rings in difficult cases.

\* W. Bothe, *Zs. f. Phys.* iv. p. 300, v. p. 63 (1921). Compare Geiger and Scheel's '*Handbuch der Physik*,' xxiv. (article by Bothe), pp. 15-18.

## 2. Experimental Method.

A photographic method was used, and the number of electrons per unit area falling in the neighbourhood of any point was deduced from the optical density of the image there. The mode of obtaining the photographs was exactly that used by Thomson and Reid (*loc. cit.*). A very fine pencil of cathode rays emerged from a discharge-tube through a cylindrical channel in the anode 6 cm. long and 0.0115 cm. in radius. The high-tension supply to the tube was derived from an induction coil with mercury-interrupter, rectifying valve, and Leyden jars, and was of the order of 30 kilovolts. G. P. Thomson has shown that electron-beams so obtained are very nearly homogeneous and have a velocity very nearly corresponding to the whole fall of potential across the tube as measured by a pair of spark-balls in parallel with it.

The pencil of cathode-rays was scattered by a film of gold of the order of  $10^{-6}$  cm. thick, placed close to the exit-aperture of the channel in the anode, and fell normally upon a photographic plate placed 32.7 cm. from the gold.

Paget process plates were used and developed in hydroquinone until the optical density was judged suitable for photometry.

Exposures varied from a few seconds to several minutes. The camera was fitted with a device for moving the plate rapidly (under gravity) without letting the vacuum down; by this means two exposures were made immediately after one another on each plate under rigorously identical conditions, except that their durations, which were measured, were in the ratio of about one to three. By this device it is possible to convert densities of the images to terms of relative numbers of electrons incident per unit area, in spite of the fact that very little is known of the photographic characteristics of plates for electrons of these velocities. (See below, pp. 645, 646.)

The optical densities of the images were measured with a microphotometer of the Lindemann type at a series of points lying on a line through the centre of the figure. The microphotometer was by the Cambridge Instrument Company.

## 3. Thickness of Gold Films.

The films were prepared by sputtering gold upon a skin of cellulose acetate and dissolving the latter away with

acetone in the manner recommended by Jolyot and developed by Thomson\* for this type of work.

Their thicknesses (order of  $10^{-6}$  cm.) were found in the following way from their opacities.

It can easily be shown that when a parallel beam of light of wave-length  $\lambda$  cm. in air falls normally upon a thin plane-parallel sheet of absorbing material of thickness  $t$  cm. and complex refractive index,  $n+ik$ , the ratio of the transmitted to the incident *intensity* is equal to

$$\frac{16(n^2+k^2)}{(n+1)^2+k^2} \cdot \frac{\exp\left(-\frac{4\pi kt}{\lambda}\right)}{1-2r\cos(2\alpha+\phi)\exp\left(-\frac{4\pi kt}{\lambda}\right)+r^2\exp\left(-\frac{8\pi kt}{\lambda}\right)},$$

where  $r$  is the reflexion-coefficient of the substance in bulk

(for *intensities*), and is equal to  $\frac{(n-1)^2+k^2}{(n+1)^2+k^2}$ ,

$$\tan \alpha = \frac{2k}{n^2+k^2-1}$$

$$\text{and} \quad \phi = \frac{2\pi}{\lambda} \cdot 2nt.$$

All these constants have been measured by Hagen and Rubens† for thin films of gold for a large range of wave-lengths, and we can accordingly deduce the thickness if the opacity is known. In order to do so rigorously we should need to use monochromatic light; but this is inconvenient experimentally, and by a fortunate accident turns out to be unnecessary in the case of gold.

For a considerable range of wave-lengths to be admissible in the light used, it is sufficient that the opacity should be sensibly the same throughout the range; for otherwise a system of weighting the wave-lengths would be necessary in working out the results, and in practice would be quite impossible to perform. Now, the photometer used for finding the opacities of the gold films (as also of the plates) acts by means of a potassium photo-cell. Accordingly the effective wave-lengths lie between the photo-electric threshold of potassium and the limit of transparency of the glass of the lenses etc.; the largest part of the response of the instrument must be caused by radiation

\* Proc. Roy. Soc. cxxv. p. 352 (1929).

† Hagen and Rubens, *Verh. d. Deut. Phys. Ges.* iv. p. 55 (1902).

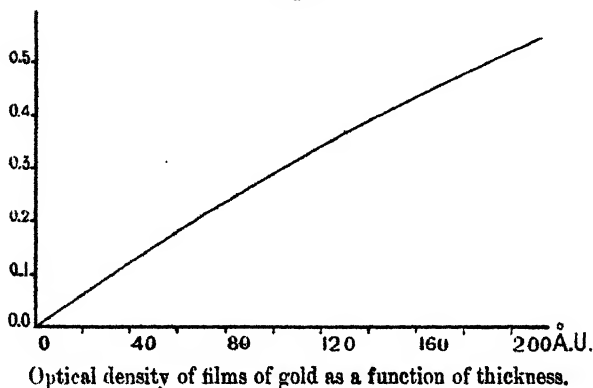
well within these wave-length limits, say, between 3750 Å.U. and 5000 Å.U. By calculating from Hagen and Rubens's data the opacity of a gold film 100 Å.U. thick for a number of wave-lengths, it can be shown that there is only a small variation in the range in question. We are accordingly able to employ white light with the same simplicity as monochromatic light, and to calculate opacities from the data for a mean wave-length.

In fig. 2 the optical density so found is plotted against thickness of gold.

The following values were assumed :—

$$\begin{aligned}\lambda &= 4500 \text{ Å.U.}, & n &= 1.53, \\ r &= 0.34, & k &= 1.73\end{aligned}$$

Fig. 2.



A small error enters on account of the convergence of the beam falling on the film in this photometer. It would be very tedious to evaluate a correction for this accurately, but a rough estimate shows that it is only of the order of 1 or 2 per cent., which is less than the macroscopic variation in thickness in a single film.

#### 4. *Measurement of Plates.*

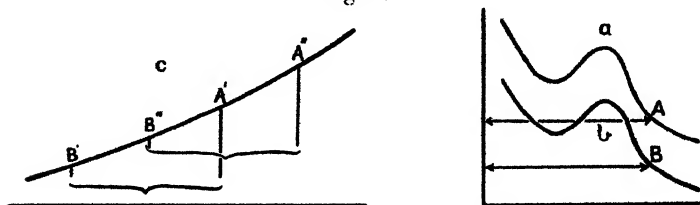
By means of the microphotometer mentioned above the distribution of optical density along a line through the centre of each image was measured, and these readings were plotted as in fig. 3, *a* and *b*.

In order to convert these readings to terms of numbers of electrons incident per unit area, it is necessary to correct for the characteristics of the photographic plate. Unfortunately, very little is known with certainty about the

behaviour of plates for electrons of these velocities. The following procedure, however, enables us to determine the characteristic curve directly and individually for each plate, and for exactly the electron-speed and conditions of development used in each case. It assumes only that the Reciprocity Law holds for electrons of these velocities; that is, that the time of exposure necessary to produce a given blackening of the plate is inversely proportional to the intensity of the electron-beam. This is known to be so from the work of Bothe\*.

This method, which may be called the method of duplicate exposures, is capable of wide application where the photographic characteristics are unknown but the Reciprocity Law holds. Two exposures whose durations were in a known ratio were made on each plate, and both images were measured on the photometer and optical

Fig. 3.



Construction of characteristic curve *c* (density against log of exposure) from a pair of photometer curves *a* and *b*.

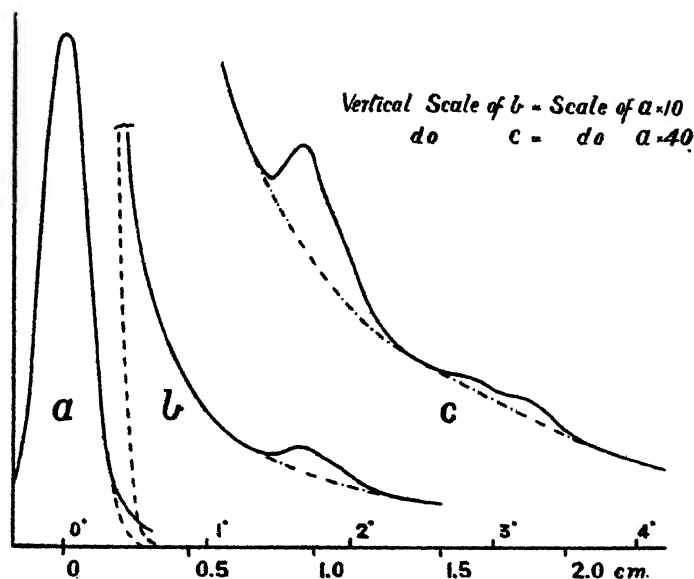
density plotted against position as in fig. 3, *a* and *b*, where the ratio of times is one to three. Now, if two points *A*, *B* are found, one on each curve, at equal distances from their respective central ordinates, they correspond to points on the plate where the intensities of electron-illumination were the same, since the conditions are the same for the two exposures, but the durations of illumination were in the ratio 3 : 1. The ordinates *A*, *B* must therefore be the ordinates (optical densities) of two points *A'*, *B'* on a characteristic curve (fig. 3, *c*) whose distance apart in abscissa (logarithm of total exposure) is  $\log_{10} 3$ . Since the zero of abscissa has no absolute significance in fig. 3, *c*, we can plot *B'* at once and *A'* from it. In the same way we can obtain an indefinite number of pairs of points (*A''*, *B''*) whose ordinates and the difference of whose abscissae

\* W. Bothe *Zs. f. Phys.* viii. p. 243 (1922); xiii. p. 106 (1923).

are known. It is necessary to choose the absolute value of their abscissæ so that one smooth curve can be passed through all the points. This is easily secured after one or two trials, and actually the result depends hardly at all on the judgment of the draughtsman, as an unskilful choice of the point A" is revealed at once by the awkward position which results for B".

When the characteristic curve has been drawn, the curves of fig. 3, *a* and *b*, can at once be replotted in terms of relative intensities of electron-illumination (*cf.* fig. 4, which is a composite curve, discussed in next paragraph).

Fig. 4.



Experimental curve of electron distribution.

Except for a multiplicative constant, the curves for the two exposures should give the same result, and in practice the discrepancy is less than the error of the individual points.

It would be possible to obtain a characteristic curve directly by making a number of exposures of known durations and measuring the density of the central spot in each case. The present method, however, enables the exposures to be completed rapidly, and so reduces the danger of failure due to small changes in the hardness of the discharge-tube. It also avoids the necessity for measuring



accurately many small intervals of time, and leads to the correction of each point on fig. 3 by data derived from itself and similarly disposed points, and hence avoids uncertainty due to local exhaustion of the developer at dense points.

### 5. *The Curves of Electron-Intensity.*

The results obtained after correction for the photographic characteristics of the plates in the manner described above (§ 4) are plotted in fig. 4, in which ordinates are numbers of electrons falling per unit area, and abscissæ either distances along the plate ( $r$ ) or angles of deviation by the film. Owing to the large range of ordinates involved, it was not possible to obtain the whole curve from one pair of exposures, and it was necessary to compile it from the results of a series of plates taken with the same electron-velocity and the same gold film (not merely with another film of the same measured thickness). The sections into which fig. 4 is divided are chosen for convenience in drawing, and do not correspond in any way to the parts measured on single plates.

Each curve consists of a central maximum and subsidiary maxima in symmetrically-disposed pairs, each pair corresponding to one ring on the plate: for the sake of clarity, only the maxima on one side of the centre are shown in the figure. The central portion agrees closely with the form given by Gauss's Error Function,  $e^{-\frac{r^2}{a^2}}$ , within a distance of about 2 mm. on each side. Further out, the experimental ordinates are greater than the Gaussian. The dashed line of fig. 4 is a prolongation of the best-fitting Gaussian curve. The chain-dotted lines are interpolations beneath the subsidiary maxima, and divide the part of the area of the curve attributed to rings (which is also very closely of Gaussian form, where resolved) from that attributed to background.

Plates were obtained corresponding to energies between 20,000 volts and 48,000 volts and thicknesses of gold between  $110 \times 10^{-8}$  cm. and  $250 \times 10^{-8}$  cm. The rings were not prominent for the lower voltages, and the slowest electrons for which it was profitable to photometer their traces were of 30,000 volts.

It may be said at once that the general scale of intensities of the rings is governed, in so far as it depends upon

the film, not only by the mean thickness, but also by some further unidentified factor or factors. Two films of the same optical density give the same ratio between the intensities of various rings (for electrons of the same speed), but, in general, different ratios between the intensities of central spot, rings, and background\*. As the nature of these other factors defining the properties of any individual film is obscure, no profitable investigation of the dependence upon film-thickness of the proportion of electrons appearing in the rings could be made; further work on this point is proceeding. Moreover, the data are only strictly comparable among themselves when drawn from a series of plates obtained with one and the same film. The films are eventually punctured by the electron beam and rendered useless. If this occurs before a whole series of satisfactory plates has been taken, the work already done on the particular film is rendered of little value except to confirm the general trend of results given by a more permanent film. Most of the data quoted in this paper have been corroborated in a general way by such fragmentary results.

#### 6. *Compensation of Instrumental Effects.*

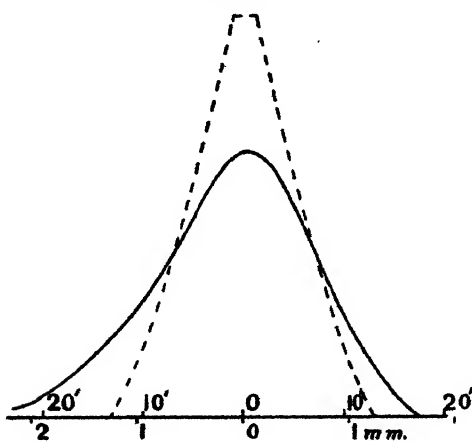
The curves obtained after correcting for the non-linearity of the photographic law certainly give the relative number of electrons per unit area falling in the neighbourhood of any point; but before any useful data of general significance can be drawn from them, it is necessary to compensate them for several effects which give rise to spurious broadening of the central spot and loss of resolution of the rings. Even in the absence of a gold film the trace obtained on the plate is not a geometrical point, but has a finite size, due to:—

- (a) Finite breadth and cross-firing of the initial beam of electrons;
- (b) their mutual repulsion while passing down the camera;
- (c) scattering by residual gas in the camera;
- (d) scattering and irradiation in the sensitized layer of the plate.

\* Cf. Rupp, *Ann. der Phys.* i. p. 773 (1929).

All these agencies affect equally well the trace obtained in the presence of a gold film, and it is necessary to estimate their total effect and to correct the results embodied in fig. 4 for it as follows. The total effect can be found experimentally by exposing a plate without inserting a gold film. In fig. 5 is shown the curve so obtained (smooth curve) with electrons of 30 kilovolts, and also the curve calculated for the effect (*a*) only (broken line). It appears that this geometrical effect is capable of explaining nearly all the finite size of the observed trace, and as it is independent of the voltage of the electrons, it is possible to

Fig. 5.



Finite breadth of unscattered beam. Full line: experimental. Broken line: geometrical effect only. The slight asymmetry in the experimental curve is probably due to a minute curvature of the channel in the anode.

consider as constant the size of the trace in the absence of gold, at least for the moderate ranges of voltage involved.

The problem of compensating for this parasitic broadening of the image, that is, of deducing from the curves of figs. 4 and 5 a curve corresponding to an ideally narrow initial beam, is dealt with in an Appendix. The solution will clearly be a curve in which the individual features are sharper than in fig. 4, but in which the relative areas of the various parts are unchanged. In the Appendix it is shown that it is legitimate to consider the several sections independently with the following results (the experimental curve of fig. 5 being taken to be Gaussian):—

(1) The central maximum remains of Gaussian form, its square-parameter being reduced from its experimental value (measured from fig. 4) by the square-parameter of the spurious broadening curve (measured from fig. 5, smooth curve).

(2) The maxima corresponding to rings also remain Gaussian, and are reduced in breadth in the same way (but retain their distance from the centre to a first approximation).

(3) The background to these subsidiary maxima, since its form cannot be represented analytically in any simple way, could only be treated numerically and at great labour. However, in the remoter parts of the field its ordinate only varies slightly in a distance equal to the whole breadth of the curve of fig. 5, and here the parasitic effects can simply be neglected.

### 7. Results. *The Central Maximum.*

The discussion of results falls naturally into three parts: the form of the central maximum with the general background; the form of the rings; and the relation between the magnitudes of the different parts of the curve.

Since the central maximum was always nearly Gaussian in form:

$$y = y_0 \exp\left(-\frac{x^2}{a^2}\right),$$

the results can be conveniently tabulated by giving values of the parameter  $a$ , which serves as a measure of the breadth of the peak and is referred to here as the "half-breadth." The quantity  $a^2$  is the "square-parameter" of the last paragraph. The half-breadth was estimated in two ways from the curves,  $a_1$  being calculated from the measured area and height of the hump in the curve ( $\text{Area} \div \text{Height} = \sqrt{\pi} \cdot a_1$ ), and  $a_2$  being obtained by halving the distance between the points at which the curve fell to  $\frac{1}{e}$  of its maximum height.

The close agreement between  $a_1$  and  $a_2$  serves to confirm that the form of the curve is Gaussian.

In Table I. the experimental half-breadths are given for those sets of conditions for which a full range of plates

was obtained. The column headed A gives the values of the half-breadths obtained by correcting for the finite size of the initial beam; we may call this quantity the "true half-breadth." The column headed  $\theta$  gives the latter expressed as angle of deflexion by the film.

The quantity K tabulated in the last column is defined as

$$\frac{A \text{ (in mm.)} \times \text{Energy (in electron-K.V.)}}{\text{Film-thickness (in \AA.U.)}}$$

This quantity is calculated for the purpose of comparison with the classical theory of scattering. It is not unreasonable to suppose in the first place that the electrons which appear in the central maximum have been scattered in the ordinary way by collision with the gold atoms of the film,

TABLE I.  
Half-breadth of Central Maximum.

Voltage.	Film thickness.	$a_1$ .	$a_2$ .	A.	$\theta$ .	K.
30 K.V.	0	1.00 mm.	1.04 mm.	0	0	—
30 "	140 A.U.	1.31 "	1.29 "	0.80 mm.	0°140	2.03
30 "	250 "	1.59 "	1.57 "	1.18 "	0°207	2.24
45 "	140 "	1.15 "	1.16 "	0.51 "	0°090	1.94

and to test this we compare K with the value predicted by theory. The calculated half-breadth depends somewhat on the radial distribution assumed for the electrons about the gold nucleus. Bothe (*loc. cit.*) has given a formula founded on a uniform volume distribution of electrons through a sphere, which leads to a value 470 for K, as against 2 from the present work. We should expect such an assumption to lead to prediction of a somewhat excessive amount of scattering, as we now know that the electron-density in an atom increases rapidly as the nucleus is approached, and the screening of the nuclear field is therefore actually greater than given by uniform distribution. The change in K produced by such a modification of the theory (*e.g.* by assuming Thomas's data \* for the atomic field) is however not large; indeed, the theory without modification agrees very satisfactorily with the only other measures of multiple scattering of

\* L. H. Thomas, Proc. Camb. Phil. Soc. xxiii. p. 542 (1927).

electrons available—those of Crowther\* for  $\beta$ -rays of 600 K.V. We are therefore led to the conclusion that the electrons forming the central spot have not been scattered in accordance with classical theory. The half-breadth calculated for electrons of 30 K.V. and films of  $10^{-6}$  cm. is of the order of 10 cm. as against 1 mm. here observed.

Two explanations of the presence of these unexpectedly lightly-scattered electrons are possible. It is not unlikely that the effect is in part due to submicroscopic non-uniformity of the film. Minute areas may be exceptionally thin, and there may actually be holes through which electrons can pass almost unscattered. It is however possible that the central maximum constitutes an interference maximum of zero order. This view is further examined below (§9). In practice both effects probably occur, but it is impossible to distinguish electrons which appear in the central spot after having passed through holes from those which passed through the full thickness but remained unscattered. The films were examined carefully under a high magnification, and only such as showed uniformity of opacity and complete absence of holes were used. Since, however, their mean thickness corresponded to only about 40 atom layers (80 if face-centring atoms are counted separately), it is very probable that gaps are present which, if they are of width of the same order as the thickness of the film, will not be visible under the microscope. The method of preparation by sputtering would certainly lead us to expect considerable irregularities; moreover, in the case of rolled films ( $\frac{1}{30}$  mm. thick), which are presumably much more compact than sputtered films, Evans and Bannister† have been led to assume the presence of cracks emerging to the surface and having a width “a few times the diameter of an iodine molecule,” i. e. say 10–20 Å.U.

Although it has been shown that some electrons escape the scattering process, others must also occur which have been scattered to the full extent required by the classical theory. These we should expect to be distributed according to a Gaussian law with half-breadth of the order of 10 cm. ( $20^\circ$ ). Unfortunately, the angles subtended by the plate at the gold film in the present apparatus are too

\* J. A. Crowther, Proc. Roy. Soc. lxxxiv. p. 226 (1910).

† U. R. Evans and L. C. Bannister, Proc. Roy. Soc. cxxv. p. 370 (1929).

small to observe any but the inner portions of such a distribution, *i. e.* up to about 3 cm. ( $6^\circ$ ) from the centre. Over a region of this size the incidence of fully-scattered electrons should thus be practically uniform, and we cannot distinguish the blackening of the plate caused by these electrons from the continuous background (if any) formed by parasitic causes such as X-rays generated in the film. In order to form an estimate of the way in which the continuous background varies at greater distances from the centre, and thus to gain some idea of what fraction of its intensity is due to extraneous causes, exposures were made with a bar-magnet fixed near the camera in a plane midway between the film and the plate. The field was sufficient to deflect the central spot several centimetres. There appeared to be a residual effect of appreciable magnitude, but very much smaller than the effect due to electrons (order of one-twentieth of the background intensity near the centre). The electronic effect varied with the distance from the centre in a way somewhat different from that required by the function  $\exp\left(-\frac{x^2}{a^2}\right)$ , falling more rapidly in the inner parts and less rapidly in the outer parts. This is in accordance with what is to be expected when the film is not of uniform thickness (a number of component Gaussian curves of different breadth giving an aggregate curve of this general form) and when multiple scattering gives place to plural scattering.

### 8. The Rings.

Maxima corresponding to reflexions from the following planes were dealt with :

(111), (200), (220), (311), (222), (331), (420),

but of these the fourth could not be resolved from the fifth, nor the sixth from the seventh. In each case the rings appear resolved to the eye, which is peculiarly sensitive to *gradients* of blackening (especially when arranged in a recognizable geometrical form), but the photometric traces were hopelessly entangled. The first and second also overlapped considerably, but by replotting on a large scale it was possible to apportion the area of the curve between them tolerably accurately.

In Table II. are given the results from a very complete series of plates which were measured in detail. All data

referring to film-thickness  $140 \text{ \AA.U.}$  were obtained from the same film, and are thus comparable *inter se*. The areas under the maxima (not including background), the heights of the maxima from the background level, and the magnitudes of the background under each ring are given in arbitrary units, the latter two being to the same

TABLE II.  
Dimensions of Rings.

Plane.	Area.	Height.	Back-ground.	N.	$a_1$ .	$a_2$ .
30,000 volts; thickness $250 \text{ \AA.U.}$						
111	11.9	7.2	10.1	23.3	0.93 mm.	0.84 mm.
200	4.1	2.9	9.4	8.2	0.80 "	0.75 "
220	3.7	2.4	7.4	10.5	0.91 "	0.87 "
311 } 222 }	4.7	2.4	6.6	16.0		
331 } 420 }	1.7	0.95	5.2	7.4		
45,000 volts; thickness $140 \text{ \AA.U.}$						
111	4.4	2.9	7.0	7.6	0.86	0.90
200	1.4	1.0	5.9	2.8	0.78	0.80
220	1.5	0.8	4.2	4.2	1.06	1.02
311 } 222 }	3.0?	1.0	3.4	10.2?		
331 } 420 }	1.25	0.5	2.0	5.4		
30,000 volts; thickness $140 \text{ \AA.U.}$						
111	7.2	3.8	11.0	12.5	1.07	1.05
200	2.1	1.5	9.2	4.2	0.80	0.79
220	0.8	0.45	5.9	2.3	1.10	1.00
311 } 222 }	1.45	0.75	4.7	4.9		
331 } 420 }	This ring very weak.					

scale, and the first to this scale multiplied by millimetres. The quantities  $a_1$ ,  $a_2$  are, as before, the parameters of the Gaussian curve to which the profile of each ring approximates and serve, as before, as a measure of the breadth of the trace; N is the relative number of particles falling into each ring, and is proportional to the product of the area under the maximum and the radius of the ring in question.



The most striking feature of this table is the approximate constancy of the half-breadth of the rings. The extreme variation in  $\alpha$  is only 35 per cent. for a simultaneous change of 50 per cent. in the energy of the rays and 80 per cent. in the thickness of the foils. A very curious result appears, however, when the mean value of  $\alpha$  (0.90 mm.) is compared with the half-breadth of the central spots given in Table I. Not only do all the central maxima have greater half-breadths than any of the rings, but also the unscattered beam shows a greater value than the majority of the rings; that is, these rings are narrower than the minimum breadth admissible on geometrical grounds. It might therefore be supposed that the half-breadths of the subsidiary maxima are being systematically underestimated. The only way in which this can occur seems to be that the background has been interpolated too high everywhere. The displacement of the chain-dotted lines in fig. 4, necessary to give the narrowest ring the minimum geometrical breadth only is, however, about 10 per cent. of the background-ordinate, and must be applied everywhere if the background is to be represented by a smooth curve. This implies that no rings whatever are resolved, and gives a very awkward and improbable form to the profile of each. The anomalous sharpness of these traces appears, therefore, to be an objective phenomenon. We may conclude that if it were not masked by the finite breadth of the initial beam, the resolving power of the gold film would be very high.

### 9. General Magnitudes. Discussion.

In order to find the total (relative) number of electrons falling within given limits of distance from the centre, the number of electrons per unit area at each distance must be multiplied by that distance and the product integrated. Fig. 6 is obtained from fig. 4 by multiplying each ordinate by the corresponding abscissa, and therefore areas in the figure so formed are proportional to total numbers of electrons. The broken curves have the same significance as before. The areas of the various portions of the figure are given in arbitrary units in Table III. for the case of film-thickness  $140 \times 10^{-8}$  cm. and electrons of 30 kilovolts.

The entry for "background within 2 cm. of centre" refers to a much larger area on the plate than any entry

above it, and it is accordingly the only one on which the spurious contribution due to X-rays etc. has any appreciable effect. Although the magnitude of the necessary correction is not known exactly, it is certainly not large (cf. end of § 7).

The radius 2 cm. within which the background is measured has no real significance. This figure is simply

Fig. 6.

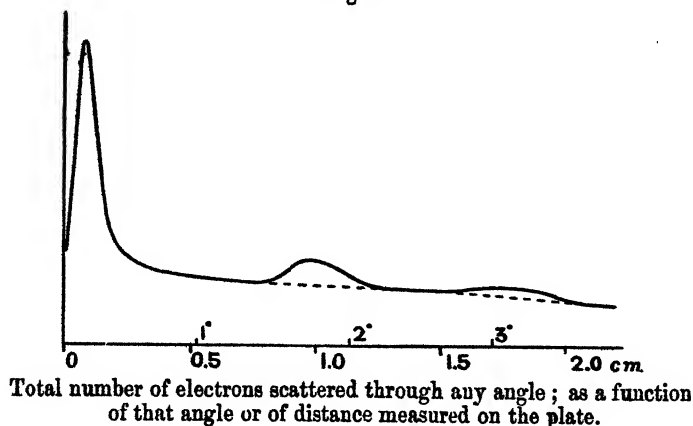


TABLE III.

Region.	Relative number of electrons.
Central maximum .....	60
Ring (111) .....	7.1
„ (200) .....	2.4
„ (220) .....	1.3
„ (311+222) .....	2.7
Background within 2 cm. of centre .....	180
Total background .....	Order of 300

quoted as an indication of the magnitude of the effect involved, because the whole background cannot be accurately measured on the present apparatus. The only data available for the intensity further out are those obtained by shifting the electron pattern to the side of the plate by means of a magnet (§ 7). This process certainly

introduces errors, but serves to give us the order of magnitude of the total effect (order of 300 units).

We have shown that the films are not uniform in thickness. For this reason it is impossible to obtain all the information we hoped for from these data, and the experiment must be regarded as a preliminary one. If we knew that all electrons passed through the same thickness of gold, we could work out from the intensities of rings and background the relative proportion of elastic and inelastic scattering. Unfortunately, when the films are not uniform, the rings are mainly due to those electrons that have passed through the thinner parts of the film, while the background is derived from all parts. We cannot draw any conclusions from the relative intensities until we know more about the variations of the film.

It might at first appear that no rings ought to be expected at all, since the conditions for multiple scattering are satisfied in the region in question for films several times thinner than the average thickness of those used in these experiments. On the other hand, even when multiple scattering occurs, there will be a finite probability that a particle will emerge having made only one serious collision. When this collision is elastic such particles appear as rings. It would be very difficult to calculate the chance that a particle should experience one collision violent enough to deflect it to form part of a ring system, and no other sufficiently serious to throw it out again; but a rough estimate based on Lennard-Jones and Woods's\* data for the distribution of electron-density in a lattice of heavy atoms indicates that the probability is very small indeed. On the other hand, the fact that rings are experimentally observed shows that it cannot be negligible in the conditions occurring in these experiments. The electrons forming rings must have passed through the thickness of gold, and cannot have been reflected from planes of atoms forming the walls of cracks in the films, since the rings have those radii which are calculated for the case in which refraction of the train of de Broglie waves on entering the metal is not considered, and the angle of incidence must therefore have been considerable.

If the conditions are such that an appreciable number of electrons make one serious collision only (deflexion of  $1^\circ$

\* J. E. Lennard-Jones and H. J. Woods, *Proc. Roy. Soc.* cxx. p. 727 (1928).

or more, say), and that one, moreover, elastic, there must be also an appreciable number which have made no serious collision at all. The wave-trains corresponding to electrons which have not been scattered, or which have been elastically scattered through very small angles, will be in phase, and will therefore interfere constructively to form part of the central spot. For slightly larger angles of scattering the phase agreement will be imperfect, and the intensity accordingly less. The central spot will therefore have a finite breadth which corresponds to the finite breadth of the spectrum of zero order in diffraction theory.

It would be interesting to know what fraction of the total number of incident electrons thus penetrates practically unscattered. But the present results will give us only an approximate estimate, as we do not know with certainty the total magnitude of background, nor to what extent the incident beam passes through holes in the film. In order to form an accurate estimate of this ratio, an apparatus is now under construction in which the angle subtended by the photographic plate at the gold film is very much larger than in the present apparatus, and in which the film can be swung out of the path of the beam without letting down the vacuum. It will, therefore, be possible in successive exposures to measure the unscattered beam and the whole of the scattered beam, and thus to obtain this ratio accurately.

#### *Summary.*

The angular distribution of electrons of about 30 K.V., after scattering by sputtered films of gold about 200 A.U. thick, has been found by measuring with a photometer photographs of the type obtained by Thomson and Reid. A method is described for calculating from the photographic densities the number of electrons falling upon unit area, even when the photographic characteristics are unknown. The relative intensities and profile of the rings, central spot, and general background have been measured. The profile of the rings is inexplicably sharp. The central spot is probably due partly to electrons which have passed through holes in the film, and partly to electrons which have passed through the thickness of the film but have remained unscattered although the conditions for multiple scattering are in this case satisfied. The general background is due to electrons which are scattered either inelastically or more than once.

I am glad to have this opportunity of expressing my gratitude to Prof. G. P. Thomson for his very stimulating advice and discussion during the progress of this work.

### *Appendix.*

If  $y=g(r)$  represents the number of electrons falling per unit area at a distance  $r$  from the centre of symmetry of the figure, when the instrumental causes of finite breadth alone act (cf. fig. 5),  $y=f(r)$  the required distribution corresponding to infinitely narrow initial beam, and  $y=F(r)$  the resultant effect which is experimentally determined (fig. 4), it is easy to see that the three functions are related by the equation :

$$F(R) = \int_0^\infty \int_0^{2\pi} f(\sqrt{r^2 + R^2 - 2Rr \cos \theta}) \cdot g(r) \cdot r d\theta dr.$$

Since this is linear in  $F$  and  $f$ , the subdivision of the area under  $F(r)$  into sections for separate consideration, as carried out in § 5, is justified.

Moreover, if  $f$  and  $g$  are Gaussian functions each symmetrical about the origin and of parameters  $a$ ,  $b$  respectively, we have :

$$\begin{aligned} F(R) &= \int_0^\infty \int_0^{2\pi} \exp\left(-\frac{r^2 + R^2 - 2Rr \cos \theta}{a^2}\right) \exp\left(-\frac{r^2}{b^2}\right) r d\theta dr \\ &= \int_0^\infty \exp\left(-\frac{r^2 + R^2}{a^2} - \frac{r^2}{b^2}\right) \cdot \sum_{t=0}^\infty \frac{2\pi}{(t!)^2} \left(\frac{R^2 r^2}{a^4}\right)^t r dr \\ &= \frac{\pi a^2 b^2}{a^2 + b^2} \exp\left(-\frac{R^2}{a^2 + b^2}\right), \end{aligned}$$

and the curve of fig. 6 is Gaussian with parameter  $\sqrt{a^2 + b^2}$ . This is the case of section (1) of § 5.

The integral corresponding to section (2) of § 5 runs :

$$\int_0^\infty \int_0^{2\pi} \exp\left(-\frac{r^2 + R^2 - 2Rr \cos \theta}{a^2} - \frac{(r-p)^2}{b^2}\right) r d\theta dr,$$

where  $p$  is the radius of the ring in question. This cannot be evaluated in finite terms. If, however, the radius  $p$  is large compared with the breadths  $a$  and  $b$ , as is always the case in practice, we may neglect the curvature and write the integral :

$$\int_0^\infty \int_0^\infty \exp\left(-\frac{(x-x')^2}{a^2} - \frac{(y-y')^2}{a^2}\right) \exp\left(-\frac{(x-p)^2}{b^2}\right) dx dy,$$

which equals

$$\frac{\pi a^2 b}{\sqrt{a^2 + b^2}} \exp\left(-\frac{(p-x')^2}{a^2 + b^2}\right),$$

again of Gaussian form with parameter  $\sqrt{a^2 + b^2}$ .

If  $f$  is a constant, the double integral is no longer a function of  $R$ , and  $F$  is a constant also.

### LXIII. *Hydrogen and Helium Lines as Standards of Wave-length.* By W. G. PENNEY, A.R.C.S.\*

IN connexion with the use of the lines of the Lyman series of hydrogen as standards of wave-length in the far ultra-violet, the question was raised by Professor A. Fowler as to the correct theoretical expression for their wave-number. From the theory it is known that these lines actually are doublets, but the resolving power of spectroscopic apparatus in the region of 1000 Å.U. is at present insufficient to reveal this fine structure, which is further obscured by the comparative breadth of the lines themselves. In the absence of any detailed information regarding this breadth, one may consider the measurements to refer to the centre of gravity of the two components in each line, and the wave-number of this may be computed since the theory furnishes us with the wave-numbers and the relative intensities of the individual components. The same remark applies to the lines of the Balmer series in spectrograms where they are unresolved, and to the lines in the spectrum of  $\text{He}^+$  which correspond to the Lyman and Balmer lines.

On the following page are given diagrams showing the origin of the various component lines in the two series. Disregarding at first the electron spin, the level with principal quantum number  $n$  consists of  $n$  component levels distinguished by the azimuthal quantum number  $l$ , which takes the values 0, 1, ...  $(n-1)$ . Taking the spin into account, each level  $l$  splits up into two component levels with total quantum number  $j = l \pm \frac{1}{2}$ , excepting the level  $l=0$ , which remains single and has the value  $j = \frac{1}{2}$ . These new levels, however, coincide again in pairs, which are bracketed together in the diagrams, excepting the level with the largest value of  $j$ . The new levels have energy values given, according to Dirac, Darwin, and Gordon †, by the original

\* Communicated by Prof. S. Chapman, F.R.S.

† P. A. M. Dirac, Proc. Roy. Soc. A, cxvii. p. 610 (1928); C. G. Darwin, Proc. Roy. Soc. A, cxviii. p. 654 (1928); W. Gordon, *Zeit. f. Phys.* xlviii. p. 11 (1928).

fine structure formula of Sommerfeld, referring to an atom with nuclear charge  $Z$  and a single electron,

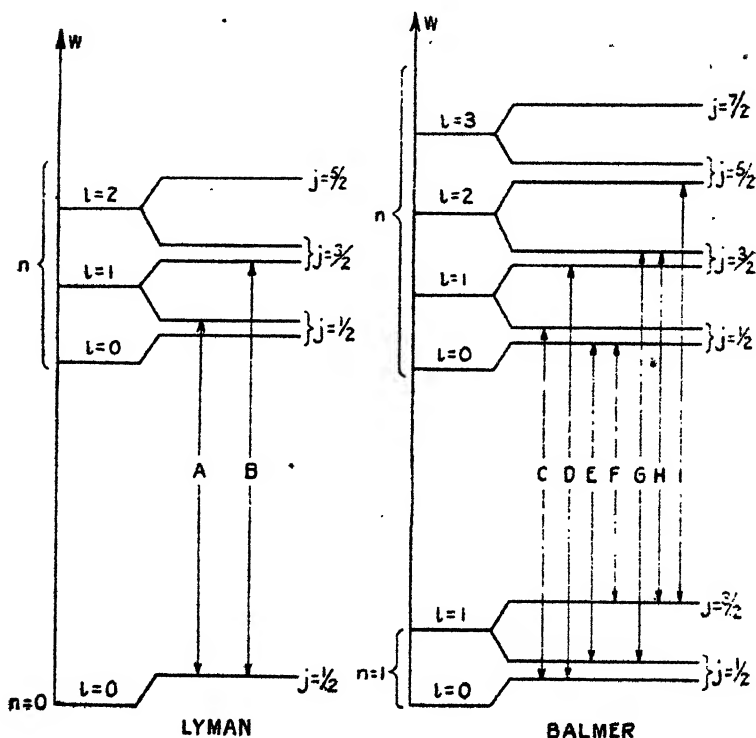
$$W = -\frac{Z^2 R c h}{n^2} \left[ 1 + \frac{Z^2 \alpha^2}{n^2} \left( \frac{n}{j + \frac{1}{2}} - \frac{3}{4} \right) \right], \quad \dots (1)$$

in which higher powers of the small quantity

$$\alpha^2 = 5.31 \times 10^{-5}$$

have been neglected, while  $R$  denotes the Rydberg constant,  $c$  the velocity of light, and  $h$  Planck's constant. The component lines are subject to the selection rules

$$\Delta l = \pm 1, \quad \Delta j = 0 \text{ or } \pm 1$$



The lines of the Lyman series are thus seen to consist of two, and those of the Balmer series of five, components, since C coincides in wave-number with E, and D with G. The relative intensities are, according to the theory\*, given by the following proportions:

$$A : B = 1 : 2 \dots \dots \dots (2)$$

\* M. V. Sugiura, *Journ. de Phys.* viii. p. 8 (1927); *Scient. Papers of the Inst. of Phys. and Chem. Res. Tokyo*, No. 193 (1929); W. Gordon, *Ann. d. Phys.* ii. p. 1081 (1927).

for the components of the Lyman lines, and

$$(C+E):(D+G):F:H:I=\left[\frac{4}{n^2}+\frac{1}{3(n^2-1)}\right]:$$

$$\left[\frac{8}{n^2}+\frac{32}{3(n^2-4)}\right]:\frac{2}{3(n^2-1)}:\frac{32}{15(n^2-4)}:\frac{96}{5(n^2-4)} \quad (3)$$

for the components of the Balmer lines.

The wave-number of the centre of gravity of the various lines may then be calculated by means of the equation

$$\nu = \frac{\sum g_i \nu_i}{\sum g_i}, \quad \dots \quad (4)$$

where the  $\nu_i$  are the wave-numbers of the components and the  $g_i$  proportional to their intensities. With the help of equations (1) to (4) there results for the wave-number of the Lyman lines

$$\nu = Z^2 R \left(1 - \frac{1}{n^2}\right) + Z^4 R \alpha^2 \left(\frac{1}{4} - \frac{2}{3n^2} + \frac{3}{4n^4}\right), \quad (5)$$

and for the Balmer lines

$$\nu = Z^2 R \left(\frac{1}{4} - \frac{1}{n^2}\right) + Z^4 R \alpha^2 \left(\frac{137n^4 - 384n^2 + 240}{192(5n^2 - 4)(3n^2 - 4)} - \frac{109n^4 - 284n^2 + 160}{15n^2(5n^2 - 4)(3n^2 - 4)} + \frac{3}{4n^4}\right). \quad (6)$$

The value of the Rydberg constant  $R$  has been very accurately determined, both for  $H$  and  $He^+$ , by Houston\* with the help of interferometric measurements of the individual components of the first two lines in the Balmer, and the first line of the Fowler series respectively. He finds

$$R_H = 109677.76 \pm 0.02,$$

$$R_{He} = 109722.40 \pm 0.02$$

with his own estimate of error. Using equations (5) and (6) and the values given for  $R$  and  $\alpha^2$ , the frequencies of the centre of gravity of the first three lines in the Lyman series and the first six lines in the Balmer series of  $H$ , as well as those of the corresponding lines in the spectrum of  $He^+$ , have been computed. The results are compiled in the Tables.

The calculated values of the centre of gravity of the lines considered here agree within the experimental error with the empirical ones determined by Curtis and Lyman† for

\* W. V. Houston, Phys. Rev. xxx. p. 608 (1927).

† See A. Fowler, 'Report on Series in Line Spectra.'



H and  $\text{He}^+$ , but excepting the Balmer lines of H these latter are not accurate enough to show if the correction of the unresolved lines for their fine structure improves the agreement or not. Work is now in progress in Professor Fowler's laboratory with the object of increasing the precision of wave-length determinations in the ultra-violet, which will necessitate taking the correction into account for these other lines as well.

## Hydrogen.

LYMAN.		BALMER.		
$\nu_{\text{vac}}$	$\lambda_{\text{vac}}$	$\nu_{\text{vac}}$	$\lambda_{\text{vac}}$	$\lambda_{\text{air}}$
82259.57	1215.664	15233.232	6564.595	6562.785
97492.71	1025.718	20564.819	4862.673	4861.319
102824.31	972.533	23032.584	4341.675	4340.459
		24373.097	4102.885	4101.731
		25181.386	3971.187	3970.068
		25705.995	3890.143	3889.045

Helium<sup>+</sup>.

$\nu_{\text{vac}}$	$\lambda_{\text{vac}}$	$\nu_{\text{vac}}$	$\lambda_{\text{vac}}$
329187.1	303.779	60960.24	1640.413
390146.0	256.314	82295.62	1215.131
411481.6	243.024	92170.88	1087.941
		97535.22	1025.271
		100769.75	992.361
		102869.07	972.109

I should like to express my thanks to Dr. R. de L. Kronig for many helpful suggestions.

Imperial College of Science,  
South Kensington, S. W. 7.  
January 30, 1930.

*Corrector's Note.*—There appeared in 'Nature,' cxxv. p. 233 (1930), measurements by Edlén and Ericson on the lines of  $\text{Li}^{++}$ ,  $\text{Be}^{+++}$  corresponding to the Balmer and Lyman series of H, but again these are not accurate enough to show if the correction for fine structure improves the agreement or not.

LXIV. *The Space-Group of the Alkaline Sulphates.* By  
Professor A. Ogg, *Physics Department, University of  
Cape Town* \*.

MY conclusion † that the space-group of the alkaline sulphates is  $V_{\lambda}16$  has been confirmed ‡ by W. Taylor and T. Boyer. Since, however, F. P. Goeder assigns § some of these sulphates to the space-group  $V_{\lambda}13$  it is necessary to reconsider the evidence. Dr. A. E. H. Tutton in a recent paper || considers that the balance of the evidence is in favour of  $V_{\lambda}16$ . It can easily be shown that in order to satisfy the symmetry of the group  $V_{\lambda}13$ , the conditions of the X-ray spacings of the group  $V_{\lambda}13$  are that

- (i.) planes of the type  $(hkl)$  have their spacings halved if  $(h+k)$  is odd ;
- (ii.) planes of the type  $(hko)$  have their spacings halved if  $(h+k)$  is odd ;
- (iii.) all other planes have normal spacings.

Since the selection of the axes relative to the elements of symmetry is arbitrary, we can say from the above conditions that two of the pinakoid spacings must be halved, while one must be normal. According to the experimental evidence, all the pinakoid spacings are halved. The space-group  $V_{\lambda}13$  is therefore untenable. The space-group  $V_{\lambda}16$  is the only group which satisfies the spacings of the X-ray reflexions.

Dr. Tutton has compared ¶ the dimensions of the crystal unit obtained by Ogg and Hopwood in the first investigations \*\* with those †† of Taylor and Boyer and finds a maximum difference of half a per cent. It is interesting to compare the experimental data with the dimensions calculated from fundamental physical constants and Tutton's values of the densities and axial ratios.

The volume of the unit is given by

$$V = abc = \frac{nMe}{\rho cF},$$

\* Communicated by the Author.

† Proc. Roy. Soc. S. Africa, July 1927 ('Nature,' cxx. p. 408, 1927); Phil. Mag. v. p. 354 (1928).

‡ Mem. and Proc. Manchester Lit. and Phil. Soc. lxxii. p. 125 (1928).

§ Proc. Nat. Acad. of Sci. of U.S.A. xiii. p. 793 (1927) and xiv. p. 766 (1928).

|| Phil. Mag. viii. no. 49, p. 195 (1929).

¶ Loc. cit.

\*\* Phil. Mag. xxxii. p. 518 (1916).

†† Loc. cit.

where  $abc$  are the sides of the unit,  $n$  the number of molecules per crystal unit = 4,  $M$  the molecular weight,  $e$  the charge on an electron =  $(4.774 \pm 0.005)10^{-10}$  e.s.u.,  $\rho$  the density,  $c$  the velocity of light =  $(2.99796 \pm 0.00004)10^{10}$  cm./sec.,  $F$  the Faraday =  $(9648.9 \pm 0.7)$  e.m.u.

A comparison of the calculated dimensions with the published experimental results shows that the results of W. Taylor and T. Boyer are in closest agreement with the calculated values, the maximum difference being 0.2 per cent.

The following table shows how close the agreement is for the two salts investigated by them :—

TABLE I.

Crystal.	Calculated dimensions.		Observed dimensions.
	Volume $10^{-24}$ c.c.	Axes $10^{-8}$ cm.	(Taylor and Boyer) Axes $10^{-8}$ cm.
$K_2SO_4$ .....	431.52	$\begin{cases} a & 5.757 \\ b & 10.056 \\ c & 7.457 \end{cases}$	
$Rb_2SO_4$ .....	487.50	$\begin{cases} a & 5.984 \\ b & 10.458 \\ c & 7.827 \end{cases}$	
$(NH_4)_2SO_4$ ...	492.26	$\begin{cases} a & 5.976 \\ b & 10.608 \\ c & 7.764 \end{cases}$	$\begin{matrix} 5.98 \\ 10.62 \\ 7.78 \end{matrix}$
$Cs_2SO_4$ .....	562.94	$\begin{cases} a & 6.248 \\ b & 10.937 \\ c & 8.237 \end{cases}$	$\begin{matrix} 6.24 \\ 10.92 \\ 8.22 \end{matrix}$

TABLE II.

	Distances between Atomic Centres.	
	From sulphates (Ogg).	Sum of atomic radii (Pauling).
K—O .....	2.71 A.	2.73 A.
Rb—O .....	2.89	2.88
Cs—O .....	3.10	3.09

Another point of interest is that the shortest distance \* between the centres of the metals and oxygen in the structure given by me is in agreement with the sum of the atomic radii calculated by Pauling from the conception of wave mechanics.

University of Cape Town,  
October 1929.

*Note by Dr. A. E. H. TUTTON, F.R.S., Cambridge.*

The further evidence now presented by Prof. Ogg, from his latest measurements, renders it clear that the space-group of the alkali sulphates is undoubtedly  $V_1 16$ . Moreover, in his paper read on July 25th at the 1929 Meeting of the British Association at Cape Town, when the writer of this note was present, Prof. Ogg gave the following as his latest and most accurate X-ray measurements of the absolute lengths in Ångström units ( $10^{-8}$  cm.) of the orthorhombic unit-cell-edges.

	a.	b.	c.
$K_2SO_4$ .....	5.76	10.05	7.46
$Rb_2SO_4$ .....	5.97	10.43	7.81
$(NH_4)_2SO_4$ ...	5.97	10.60	7.76
$Cs_2SO_4$ .....	6.24	10.93	8.23

The values for all four salts are remarkably close to the calculated values given in his present Table I.; and the values for the ammonium and caesium salts are equally close to, practically identical with, those of Taylor and Boyer. The greatest difference anywhere is only 0.02 (0.2 per cent.). Also it may be pointed out that the distances between the atomic centres of the nearest metallic and oxygen atoms given in his Table II. are further confirmed by the very similar values which have been published by Wasastjerna from optical data, and by V. M. Goldschmidt for co-ordination number [6].

These highly satisfactory later results confirm and yet more fully emphasise the conclusions published by the writer in his communication to this Magazine in August 1929 on the "Significance of X-Ray Analysis of Alkali Sulphates"†.

\* Phil. Mag. v. p. 354 (1928).

† Phil. Mag. viii. p. 195 (1929).

LXV. *Critical Stresses for Tubular Struts.**To the Editors of the Philosophical Magazine.*

GENTLEMEN,—

**R**EGARDING Professor Andrew Robertson's letter in your February issue concerning my paper on "Critical Stresses for Tubular Struts," I should like to say that no reference to practical applications is made in the paper because it is solely concerned with the interpretation of a mathematical equation.

I should also like to correct a few errors which appear on p. 1065 of the paper. Near the top of the page "The minimum value of this" should read "The minimum value of  $p$ ." Immediately following equation (11), "where  $A = \frac{1}{3} \frac{t^2}{a^2} \frac{m^2}{m^2 - 1}$ " is omitted; and lower down the page, "For instance if  $m=2$ " should read "For instance if  $k=2$ ."

The College of Technology,  
Manchester.  
February 12, 1930.

Yours faithfully,  
H. CARRINGTON.

LXVI. *Notices respecting New Books*

*Source Books in the History of the Sciences.* A Source Book in Mathematics. By DAVID EUGENE SMITH, Ph.D., LL.D., Professor Emeritus in Teachers College, Columbia University, New York City. (London: McGraw-Hill Publishing Co. Price 25s. net.)

**T**HE publishers of this series of Source Books aim at presenting the most significant passages from the work of the leading scientists of the last three or four centuries. With such a wealth of material accumulating a demand for selected sources necessarily arises. This series, indeed, breaks new ground, and puts together in an accessible form carefully selected material which in due course will cover the leading Physical and Biological Sciences.

The general editor, Professor G. D. Walcott, of Brooklyn, N. Y., began to organize the Advisory Board in 1924, and to Professor D. E. Smith was allotted the task of carrying out the general idea in the field of Mathematics.

The material in his volume covers the  $4\frac{1}{2}$  centuries closing with the year 1900. Over such a wide field the task of selection has necessarily presented many difficulties.

The field of Number starts at the logical beginning of the subject, and extends to even such a modern development as Nomography.

The field of Algebra is interpreted to cover Equations Symbolism, and Series, the early method of solving the cubic and biquadratic equations and numerical equations of higher degree and so on.

To the person interested in statistics the special section devoted to Probability is most welcome.

The field of Geometry ranges from the contributions from such 16th century writers as Fermat, Desargues, Pascal and Descartes, to a few of those who, in the 19th century, revived the study of the subject and developed various forms of modern geometry.

The fields of Calculus, Function Theory, Quaternions, and the rest of mathematics presented a formidable task, but some attention has been paid to each domain.

The student of the history of mathematics will welcome this book with avidity. Its standard of scholarship is high, and there is evidence that the difficult decisions which have at many points confronted the organizers of this work have been made with wisdom and the greatest of care.

*The Great Mathematicians.* By H. W. TURNBULL, M.A., Regius Professor of Mathematics in the University of St. Andrews. (London: Methuen & Co., Ltd. Price 3s. 6d. net. 1929.)

THIS little book will be sure of a warm welcome from all those who are interested not only in the subject matter of Mathematics, but also in its history. The inevitable drawback that mathematical study is saturated with technicalities from beginning to end, often means in practice that the student has little time or opportunity to study its history.

In this little book Professor Turnbull has been specially concerned with revealing something of the spirit of Mathematics, without unduly burdening the reader with intricate symbolism.

In view of the new significance of Mathematics as the basis of all sciences, such a task is well worth performing. The student not only of Mathematics, but also of Physics, Chemistry, and Bio-Chemistry, and, indeed, of any of the precise sciences will find the information it contains valuable and stimulating.

Professor Turnbull should be congratulated on his success in showing how a mathematician thinks, and how his imagination, as well as his reason, leads him to new aspects of the truth.

*Logic for Use.* By F. C. S. SCHILLER, Fellow of Corpus Christi College, Oxford, Fellow of the British Academy. (London: Bell & Sons, Ltd., 1929. Price 16s. net.)

IN this book Dr. Schiller outlines the new logic which systematically scraps the cardinal notions of the traditional logic—formal validity, absolute truth, logical necessity, absolute certainty, and all-inclusiveness—and replaces them by real truth, progressive knowledge, purposive connexion, probability, and relevant selection.

How far he has been successful in this task will be an open question. That there is room for such a work is undeniable.

The book is, of course, a sequel to the author's 'Formal Logic.' Most of it was actually delivered in a course of special lectures in the University of California in 1929. It has, in fact, been

planned as much for the student of the sciences as for those to whom the study of logic has been a traditional occupation.

The author is of the opinion that the study of modern logic, while still in its infancy, will be capable, possibly in the course of a few centuries, of developing into a body of knowledge.

With the author's hope and belief that this subject ought to be progressive like the sciences, one cannot but have sympathy, but it would be difficult to see in the present work a suitable foundation for such a body of knowledge.

The work is marred by the author's habit of tilting at windmills, which cannot but repulse the student who, even if he has not suffered from the alleged drawback of an Oxford education, will be more concerned to try to find a logic useful to him in his scientific work than to study the inter-relations of the author's views, at once iconoclastic and vague, and the traditional idea of logic, which, as all the world knows, belongs not to the laboratory, but to the study thick with the dust of the ages.

As a part of a general education in the art of thinking, the student with sufficient time and the necessary drive may be recommended to give this book a cursory reading.

*Handbuch der Experimental Physik.* Herausgegeben von W. WIEN und F. HARMS. Band 8, erster teil, geb. R.M. 65. Band 9, erster teil, geb. R.M. 44.60. (Akademische Verlagsgesellschaft, m.b.H., Leipzig.)

IN the first of these volumes—*Energie und Wärmeinhalt*—the editor, Prof. A. Eucken, has given a comprehensive survey of the experimental researches in this special branch of physics; so far as it is possible to keep pace with the rapid progress which has been made in recent years, this book provides a very complete and up-to-date summary of results, especially the experimental methods of thermometry and calorimetry and the experimental determination of specific heats of solids, liquids, and gases. A large amount of information is brought together on the measurement of heats of solution, dilution and combustion. Although the experimental aspect of the subject has been emphasized, the theoretical investigations of Debye and others have not been omitted.

The four sections of the second volume are devoted to the subjects of the production and measurement of high and low temperatures, the liquefaction of gases, the conduction and radiation of heat. Prof. Wien, the chief editor of this encyclopædic handbook, and Dr. Müller were responsible for the section on radiation. Soon after the completion of this work Prof. Wien died, and this volume may be regarded as a worthy memorial of one of the greatest research workers in physical science. His contributions to the theory of black body radiation, as set out in his two laws, the displacement law and the energy distribution formula, were of capital importance, and showed the way to the complete solution of this problem. A beautiful portrait of

Prof. Wien forms the frontispiece of this volume. Extensive indexes of authors and subjects and numerous references to original papers are given in both volumes: in printing, binding, and illustration a very high standard has been reached. The editors and publishers deserve the highest commendation for their enterprise in providing these valuable books of reference for workers in this branch of physics.

*Leçons de Mécanique Rationnelle, Tome deuxième.* Par FRANÇOIS BOURY. (Paris: Librairie Scientifique. Albert Blanchard, 3 et 3 bis, Place de la Sorbonne. 1929. Prix 90 frs.)

THE first volume of this work was published five years ago and provided an introductory course to the study of statics, dynamics, potential and the theory of linear vectorial functions. The application of these functions to the problems of moments of inertia and the dynamics of solid bodies generally is made in the second volume, which is devoted to the study of the dynamics of a point and of systems. The author gives a detailed account of vibrations and resonance, especially the vibrations of strings and rods, the torsional vibrations of shafts, etc., phenomena which are of increasing importance in both mechanical and physical science. The theory of vibratory movements is completed by the application of the Lagrange equations to the study of small movements about a position of stable and unstable equilibrium. The notion of the gyroscopic couple is introduced, based upon a paper contributed by the author to *L'Enseignement mathématique* about fifteen years ago. A clear and interesting treatment is also given of topics which are indispensable for the effective study of recent developments in mathematical physics. The importance of laboratory practice and manipulation in the study of theoretical mechanics are recognized by the attention given to the experimental measurement of moments of inertia, of vibrations, damped and undamped, and gyroscopic couples. A valuable feature of the book is the inclusion of numerous exercises given at the end of the chapters, some of them with fully worked-out solutions.

## LXVII. *Proceedings of Learned Societies.*

### GEOLOGICAL SOCIETY.

[Continued from p. 328.]

November 20th, 1929.—Prof. J. W. Gregory, LL.D., D.Sc., F.R.S., President, in the Chair.

‘The Upper Estuarine Series of Northamptonshire and Northern Oxfordshire.’ By Beeby Thompson, F.G.S., F.C.S.

In Northamptonshire, between the Lincolnshire Limestone and the Great Oolite Limestone in north-eastern parts of the county,



and between the Northampton Sand (or the Lower Estuarine Beds) and the Great Oolite Limestone in all other parts of the county, occurs a series of variable beds, largely variegated clays containing abundance of vegetable matter of probably freshwater origin, interspersed with brackish-water beds and with distinctly marine beds. To this aggregate J. W. Judd, in 1867, gave the name 'Upper Estuarine Series', which he then thought represented the Stonesfield Slate or Lower Zone of the Great Oolite of the more south-westerly parts of England, Oxfordshire particularly.

An addition to Judd's general description was made by the Author in 1909 ('Water-Supply of Bedfordshire & Northamptonshire') in the introduction of 'Upper Estuarine Limestone', commonly a water-bearing bed in the midst of the series, and now generally recognized. This bed actually divided the series into three parts, a division retained in this paper, but to which is added much additional information, palæontological and other, about each part.

In Northern Oxfordshire, between certain Inferior Oolite Limestones or White Sands (the time-equivalents of the Lincolnshire Limestone?), or Ferruginous Sands (the equivalents of the Variable Beds of the Northampton Sand or even of the Ironstone Series) below, and the Great Oolite Limestone above, occurs a series of beds which in various parts physically, and in others palæontologically, agree, as does the complete set in sequential position, with the Upper Estuarine Series of Northamptonshire. It is an important object of Part I of this paper to show how the Northamptonshire and Oxfordshire sections on this geological horizon may be more definitely correlated.

A type-section of the Upper Estuarine Beds of Northamptonshire is given with extended explanation. A comparison of Northamptonshire and Northern Oxfordshire sequences, as given by the Author, M. Odling, and E. Walford, is made, in an attempt to show the approximate equivalence of the Upper Estuarine Limestone of Northamptonshire with the Chipping Norton Series of Oxfordshire, making allowances for much more variability in character of the series in Oxfordshire than in Northamptonshire, and particularly, in places, the extension of marine beds into the lower part.

Part II includes a large number of illustrative sections for Northamptonshire, in which it is shown how the extended classification of beds can be used for identifying unconformities due to earth-movements developed at different times.

---

[*The Editors do not hold themselves responsible for the views expressed by their correspondents.*]

THE  
LONDON EDINBURGH AND DUBLIN  
PHILOSOPHICAL MAGAZINE  
AND  
JOURNAL OF SCIENCE.

[SEVENTH SERIES.]

SUPPLEMENT, MAY 1930.

LXVIII. *An Analysis of the Spectrum of Hg II.*  
By W. M. HICKS, F.R.S.\*

THE present paper was very largely written up when, by the kindness of Dr. Paschen, the author became acquainted with his communication to the Berlin Academy † in which he had discussed the Hg II spectrum on the basis of a new set of observations on the spectrum produced by his method of the hollow cathode, which is peculiarly suitable for this purpose. Our two results are quite different, but not mutually exclusive (saving a few allocations) except in one crucial point. While we have both taken the accepted 35104 as  $S_1^2 2$ , we have given to the  $p_{1,2}$  term in this values differing by 1363. Both cannot be correct, unless we accept the incredible supposition that the same frequency can be caused by transitions between different pairs of levels. Paschen's allocations march well with those for Zn II and Cd II given by von Salis ‡, and at a first glance seem to hold well together. At the same time those of my discussion seemed to me also to hold together, and they had led to the recognition of a new class of facts, possible but only occurring in rich spectra, indeed explaining to some extent why a spectrum like that of mercury is so rich in lines. A special examination of Paschen's

\* Communicated by the Author.

† *Sitz. Ber. preuss. Akad.* 32, 1, 28.

‡ *Ann. der Phys.* 76, 145, 25.

results therefore seemed called for, with special reference to the contradiction above referred to. The result has been to lead me to the conviction that the line  $n=35104$  does not belong to his  $S(2.m)$  system. I give the result of my discussion as Part II. of this paper. The natural procedure would have been to make it Part I., but many points of the argument could not have been followed without a previous knowledge of the result of my own analysis. It is needless to say that the general arrangement of his allocations ( $Pm$  excepted) is little affected.

My analysis has shown that the lowest  $p_2^*$  level is multiple. In other words, that to one  $P_1(m)$ ,  $S_1(2.m)$ ,  $D_1(2.m)$  several  $P_2$ ,  $S_2$ ,  $D_2$  lines appear. It has not been possible to decide whether there is one particular  $p_2$ , with, so to say, accidentals, or whether there are a definite number of equal normality. That must be left for a more complete analysis than is possible in a preliminary paper. But the more probably occupied  $p_2$  levels appear to be restricted to four. The result of this multiplicity is to produce a number of different doublet separations. As the  $d$  terms depend ultimately on the lowest  $d_2$  term, which itself is determinable in terms of these  $p$  displacements, it would follow that if the various  $p_2$  were equally normal, we should find a corresponding number of independent D series. I have made a preliminary test for these, and believe I have found definite evidence for their existence; but it will be sufficient here to give the evidence for one only, with corresponding F and G series. The general argument is given in the text, but the details, many of very great interest, are given in the notes to the different series tables.

The mercury spectrum shows evidence of the presence of the satelloidal effect, although it is not so striking and conclusive as in copper. The evidence is given in § 8, which may be read, perhaps with advantage, before the general discussion.

\* Throughout, Rydberg's notation is used. This is based directly on observed relations, as all notations should be. To base a general notation on a theory current at a special instant seems subject to two serious objections: (1) a constant change with theory most exasperating to future readers; (2) it lays too much stress on the correspondence of the last-made hypothesis to reality. As a fact, although not so originally intended, Rydberg's subscripts may be regarded as giving the order in which the different levels—such as  $p_1$ ,  $p_2$ ,  $p_3$ —are met with as we pass from outside into the nucleus.

I have recently † suggested that when the energy of a transition has been transmitted to the nucleus, the latter would emit it as a radiation of frequency given by  $E = nh\nu$ , in which  $n$  is not restricted to unity, as is usually supposed. I had originally intended to merely illustrate this by giving such examples as might have been noted in Hg II as a mere list of raw material for future consideration. But so many were found, and they threw so much light on the cause of the non-appearance of certain lines, especially in  $S_1m$ , that I have discussed them in the notes to the various series as they arose. A \* is attached to each line showing this effect. They are collected also in a single table at the end of Part I.

### PART I.

References are concisely referred to by three successive numbers. Thus 21, 105, 28 denote vol. 21, p. 105, year 1928.

W.N.=wave number. O.E.=observation error. O—C  $d\lambda$  means excess of observed wave-length over a calculated value.

Unless expressly noted,  $\lambda$  or  $n$  to three decimal places are by Stiles, and in *R.A.*, given in italics, by Eder and Valenta; also below  $\lambda=1760$  by Carroll. E. V.=Eder and Valenta. E. H.=Exner and Haschek. K. R.=Kayser and Runge. Stk.=Stark. Ly.=Lyman. S.=Stiles. Bl.=L. and E. Bloch. D.=Déjardin. Cd.=Cardaun. C.=Carroll. P.=Paschen. McL.=McLennan. W.=Wiedmann.

Series lines  $p_2-sm$ ,  $p_3-sm$ , etc., are written  $S(2.m)$ ,  $S(3.m)$ , etc. Shifts produced in a term by a one-oun displacement are indicated by a thick minus. Thus  $p_12-$  is change in the value of  $p_12$  by one oun.

1. The elements of group II. show very close correlation between the corresponding series lines in the neutral and singly ionized spectra. This fact is of considerable assistance in arriving at the constitution of the unknown Hg II series. In particular we find—

1. In all cases the first separation of the doublet is a little less than twice the first separation of the triplet.
2. The denominators of  $p_1^{s1}$  and  $p_1^{s2}$  in each sub-group are very closely in the same ratio ‡.

In the Zn-subgroup these ratios for doublet and triplet for Zn, Cd, Eu are 1.312, 1.306, 1.32. For Hg we should then expect a ratio close to 1.32. The first separation of

† "The Nucleus as Radiator," Phil. Mag. 8, 108, 29.

‡ Phil. Mag. 44, 351, 22.

the triplet in neutral Hg is  $\nu_1 = 4630.6$ . We expect then a doublet separation a little less than 9261. The denominator of  $p_1^{*1}$ , or 40141 is 1.65296. This multiplied by 1.32 should then be of the order of the denominator of  $p_1^{*2}$ . The result,  $4R/(2.1819)^2 = 92156$ , should then be within a few hundreds of the true  $p_1^{*2}$ , i.e., the limit of the  $S_1^{*2}$  series.

In his memoir of 1890, Rydberg suggested as analogues of the doublets he had found in Zn and Cd the lines (W.N. in modern measures)

2,	35104.16	9829.28	44933.4
3,	39412.27	---	---

The 39412 is now known to be a definite neutral line, but the first set have ever since been accepted as the representatives of  $S^{*2}$ . Indeed, we can take 35104 quite definitely as  $S_1^{*2}$ , for not only is it in complete step with that of the other elements, but Runge\* and Paschen have found a Zeeman pattern for it supporting this allocation. Many other instances of the 9829 separation occur in the spectrum; but although the observed region has since been much extended, no one has yet succeeded in arranging other pairs in S or D series. Carroll, who has pushed the observed region down to  $\lambda = 740$ , has proposed certain allocations. He says that he had been unable to make any progress on that basis. When writing my critical studies of spectra many years ago, I came to the same conclusion, and tried, in place of it, another very common separation of 9333 which also is much closer to the expected value, but again in vain. Carroll has used another separation value of 9122, also very common.

Let us start from the given datum of  $S_{12} = 35104$ , and examine the spectral data at about 9260 ahead. We find a bunch of very strong lines in Déjardin's Class  $E_1$ . They are reproduced here with some weaker ones for later use. The measures of Cardaun are used where available. The separations from 35104 are given in thick type, followed by ordinal numbers for reference. Of the numbers following the W.N., the first gives the intensity according to Déjardin, the second according to Cardaun, and the third, in roman numerals, gives Déjardin's

\* Astro. J. 15, 233, 02.

classification  $E_1$  . . . according to the increasing intensity of the excitation at which they first appear.

69	<b>9051.17</b>	1	44155.33	0	- iii?	$\lambda$ 2264.08
	<b>56.44</b>	2	160.60	5, 2n	i	63.76
69½	<b>86.59</b>	3	190.75	7, 3,	i	62.215
67½	<b>9121.88</b>	4	226.04	7, 3n	i	60.41
	<b>9268.89</b>	5	373.05	7, 3n	i	52.92
71	<b>9333.41</b> <sup>(1)</sup>	6	---			
35104.16 10n, 8n, i	71½	<b>71.94</b>	7	476.10	2n - i	47.70
	71½	<b>9438.72</b>	8	542.88	7 - ii	44.33
	72½	<b>9507.08</b>	9	611.24	0n - i	40.89
	72½	<b>80.6</b>	10	684.8	0 - i?	37.2
	73½	<b>9724.11</b>	11	828.27	5 - i	30.04
	74	<b>57.91</b>	12	862.07	1 - ii	28.36
	74½	<b>9829.28</b>	13	933.44	10, 3n	i 24.82
	75	<b>9903.31</b>	14	45000.6	0 - i	21.5

(<sup>1</sup>) This separation has not been observed from 35104. But it is here inserted as it will be found to be one of the most important in the series relations. No. 4 shows it back, thus 34892.26 **9333.78** 44226.04.

Confine attention first to the lines observed by Cardaun, shown in italics. They are all of the same character, and there is nothing to show which is definitely  $S_22$ , except that the separation 9829 leads to a line which Déjardin shows as much more intense than the others. Can it be that they all belong to  $S_22$ ? In other words, are there a set of independent  $p_2$  terms? If so, since all separations depend on multiple own displacements, they must all be collaterals of one another. Now if we compare the separations to Déjardin's strong lines, but taking 1 in place of 2, omitting 5, and including 9333, their successive differences are 35, 35, 211, 105, 286, 105. All these are multiples of 35, again strongly suggesting displacement. This can roughly be tested at once, since the value of  $p_1$  is known so closely, and  $p_2$  should be about 9300 ahead, or equal to about 101400. A rough calculation shows that one-own displacement shifts 30.5 in  $p_1$  and 35.5 in  $p_2$ . Now it is quite easy to find such a value of  $p_1$ , near 92156, that a suitable multiple own displacement will produce a separation of given value, say 9086.59. But it will not produce all the others correctly unless they are actually such a set of mutual collaterals. As a fact we do find this.

We get such a set by taking  $p_1=92024\cdot56$ . To allow for O.E. in the separations take this  $+\xi$  as the true  $p_1$ . Then

$$p_1^2=92024\cdot56+\xi=4R/\{2\cdot183432-11\cdot863\xi\}^2.$$

$$\text{Ratio } p^2, p^3 \text{ denominators}=1\cdot321.$$

$$\text{also } \delta=1450\cdot090 \pm \cdot009, \delta_1=362\cdot522,$$

The separations as calculated are as follows, the own multiple displacements being written on the right in terms of  $\delta$  and the observed values below with  $O-C \, d\lambda$  in ( ).

- |                                                             |                                                                |                                                         |
|-------------------------------------------------------------|----------------------------------------------------------------|---------------------------------------------------------|
| 1. $9051\cdot41 + \cdot150 \xi, 69$<br>51·17 (−01)          | 6. $9333\cdot41 + \cdot155 \xi, \beta$                         | 13. $9829\cdot74 + \cdot164 \xi, \gamma$<br>29·28 (023) |
| 3. $9086\cdot59 + \cdot152 \xi, 69\frac{1}{2}$<br>86·59 (0) | 8. $9439\cdot45 + \cdot158 \xi, 71\frac{1}{2}$<br>(38·72) (03) | (5) $9262\cdot80 + \cdot155 \xi, 70$                    |
| 4. $9121\cdot80 + \cdot154 \xi, \alpha$<br>21·38 (004)      | 11. $9723\cdot08 + \cdot162 \xi, 73\frac{1}{2}$<br>24·11 (−05) |                                                         |

The deductions according to the above method are exact within about  $\cdot02$ , and if the supposition is real, the values obtained must agree with the observed separations within their O.E. Any error in  $S_1^2$  will affect all the separations by the same amount, and can be met by a suitable value of  $\xi$ . Of the others, five are by Cardaun, with small possible errors. Taking his estimates, the O.E. in W. N. may be of the order  $\cdot2$  in (2),  $\cdot13$  in (3),  $\cdot39$  in (4),  $\cdot39$  in (5),  $\cdot40$  in (13). Lines (8), (11) are by E. H., and should be subject to errors of about  $\pm 2$ . It is thus seen that 9086·59 is by far the most reliable. All the separations are within their respective O.E., but the 9829 is closer to the maximum error than to be expected. It is  $\cdot46$  larger, and can be explained later by a satelloid effect  $y=\cdot45$ , but Paschen's two readings give 9829·50 ( $d\lambda=\cdot01$ ). If, then, the lines involved are what they appear, viz., displaced  $S_2$ , the limit  $p_1^2$  can only differ from 92024·56 by a very small amount depending only on the O.E. in  $S_1=35104$ . This makes

$$s^2=p_1^2-S_1^2=56920\cdot18=4R/\{2\cdot776246\}^2,$$

giving a value of the denominator in close march with

\* The value given in my 'Analysis' was  $1450\cdot180 \pm \cdot100$ . The above has been redetermined from recent more accurate measures.

those of the other elements of this group. A further scrutiny of the lines in the  $S_2$  region shows the existence of other separations to weak lines satisfying similar displacement conditions within O.E. They are Nos. 7, 9, 10, 12, 14 in the list above, due respectively to displacements of  $71\frac{1}{2}$ ,  $72\frac{1}{2}$ ,  $72\frac{3}{4}$ , 74, 75  $\delta$ .

Nos. 2, 5 do not conform, although they would appear to belong to the system. The relation of 2 to 1 appears to be of a "satelloidal" nature, and is discussed under that head in § 8. No. 5 *may* be of a similar nature, but another possible explanation, which would remove the line 44373 from any connexion with the S series, should not be omitted here. In a linkage map containing 35104 we find the mesh:

35104.16	9268.88	44373.02
9121.88		9121.5
44226.04	9268.5	53494.5 (1.y.)

This means that either 9121, 9268 act as links *or* we have to deal with a new term  $t$  with lines  $p_1-s_2$ ,  $p_2-s_2$ ,  $p_1-t$ ,  $p_2-t$ . In this case it is easily seen that  $t=47649.34=4 \times 11912.13$ , whilst Rydberg's table shows that 11912 is due to a denominator 3.033. As we shall see later that these various separations do as a fact enter also as  $b$ -links, also that the separation 9262 has a considerable occurrence, and as the character of 44373 is the same as that of the other  $S_2$  lines, we shall assume provisionally that it is actually related to the S series. The question of the reality of the relationship may at present be left open, as it has little bearing on the general dependence of the  $p_2$  on several independent displacements in  $p_1$ .

The question however arises, is there one normal  $p_2$  with a normal  $\Delta$  depending on a definite *own* multiple, the others being merely collaterals of this, *or* are some or all independent and different  $p_2$ ? The question does not affect their values, and actually they are quantitatively collaterals. But it has important bearings on the properties of other terms—especially the  $d$ —and on the numbers of the  $p$ -links  $a$ ,  $b$ ,  $c$ ,  $d$ ,  $e$ . If there is one normal  $p_2$  we should expect one set of  $p$ -links and one set of  $d$  terms (or at most two). If they are all independent, we should expect sets of  $p$ -links for each and corresponding  $d$  sets for each, with consequent great complexity.



We shall, however, not discuss these general links in this paper, and shall postpone the other case until we deal with the D series later.

Granting the real existence of these various  $p_2$  levels, one important inference can be drawn. A reference to the intensities given in the list shows that those of the different  $S_2$  are comparable with that of  $S_1$ , that is, that the total intensities of all the  $S_2$  lines together must very largely exceed that of  $S_1$ . In other words, the occupancy by an electron of the outer  $p_12$  level must have a much smaller probability than the occupancy of the lower congruity of  $p_22$ . We shall get some evidence later, however, to indicate that this is only apparently so, and is due to the energy of fall in any case being radiated according to the law  $E=2h\nu$  or  $3h\nu$  instead of  $h\nu$ . Indeed the majority of the  $S_1$  lines show this effect.

Having definitely settled the  $S_12$  line and the various  $S_2$ , the next step in the analysis of the spectrum is to examine it systematically for the existence of the  $p$  separations. This has been done for 9121, 9333, 9829, or  $\alpha$ ,  $\beta$ ,  $\gamma$ . The result is to show the presence of an overwhelmingly large number throughout the whole spectrum, and especially to show that, besides entering as doublet separations of S and D lines, they occur also as links. This is shown by the existence of sequences of links. Moreover, the unexpected result definitely appears that these ionized links are attached to neutral lines as well as to ionized ones. It is sufficient to mention this here, the evidence is given below (§ 9). But it is important to state one result. If  $p_1$  receives an own displacement, a given  $\Delta$  induces the same displacement in  $p_2$ , but the shifts produced are different, and the corresponding doublet separation is changed. If in any case these changed separations occur—especially if several are present—it is clear evidence that the  $p$  has been subject to the corresponding displacement (see, *e. g.*, notes to S1). The values are found at once from the difference between the own shift on  $p_1$  which is 30.557 and those on  $p_2$ . The latter can be determined from Table I., where differences of successive  $p_2$  give the own shift. The change in separation in all cases is of the order 5.

2. The mantissa for  $m=3$  must be slightly larger than for  $m=2$ , and produce a pair with a doublet separation. The only line satisfying this condition in Carroll's list, and

associated with doublet separations, is  $n=61580$ . Adopting this as  $S_1 3$ , we calculate from it and  $S_1 2$  the formula

$$sm = 4R / \{m + .835827 - .119166/m\}^2.$$

The combination  $s2 - s3 = 26473.90$  is observed at

$$1, 26473.742; 3776.259 \text{ A.U.}$$

Extrapolating for  $m=1$  we should expect a mantissa somewhat smaller than the calculated value, which gives  $S_1 1 = -54700 \pm$ . We find near two sets of strong lines which are equivalent to  $(\pm \delta_1) S_1 (\pm \delta_1)$  requiring  $S_1 = -57495.30$ . Although this has been wholly disrupted, there are two for  $S_2$  with separations respectively of 9121, 9722 ( $\alpha, 73\frac{1}{2}\delta$ ) within O.E. (see specially the notes to  $S_1$ ). Although this line is not directly observed in  $h\nu$  emission, it is very exactly so in  $3h\nu$  and possibly  $2h\nu$ . Also the corresponding  $S(3.1) = -P(1.3)$  is seen, as well as a line linked to it by the  $e$  neutral link, and the combination  $s1 - s2$ . Thus

$\frac{1}{2} \times 57495.30 = 19165.10$	obs. 1 i 19165.044
possibly $\frac{1}{2} \times \dots = 28747.65$	obs. 1, 28745.11 W. $d\lambda = .3$
$-57495.30 + 20612.06 (=e) = 36883.24$	obs. 1 i 36883.271
$s1 - s2 = 92590.46$	obs. 4, 92584. $d\lambda = .16$ on 1080.1

Against this choice of  $S_1$  it may be objected that it is out of step with the march of the corresponding series in Zn, Cd, Eu, although its mantissa is roughly in step. But no other seems acceptable. Carroll has allocated  $-60609.79120.6 - 51489.06$ , which at first sight seems admissible. But it is still more out of step, and, moreover, they seem quite possibly linked in series with the neutral line  $D_{22}^{95}$  (see Ex. I. in § 9). Also the intensities are in the ratio 30:50 instead of the normal ratio of 2:1. A. T. Williams ('Nature,' 124, 985, 29) states that 51489 is the true "raie ultime" and not 54063, usually taken as  $S'1$ .

In addition to the series  $p2 - sm = S(2.m)$  we find also corresponding  $p3 - sm = S(3.m)$  and  $p4 - sm = S(4.m)$ . We shall see later that  $P_1 3$  is 14116.93, so that  $S(3.m)$  must be a parallel series at a distance  $-14116.93 - 35104.16 = -49221.09$ . In all these sets the  $S_1$  exhibit collaterals, often symmetrical, i. e.,  $\pm$  the same displacement, whilst there are numerous observed lines for different  $S_2$ . Indeed, in several cases the collateral displacements in the same

order in the three series are similar (see notes to Table III.). Whilst direct observations in  $S_1(2.m)$  are wanting for  $m=4$  and beyond, the corresponding are observed in  $S_1(3.m)$  for  $m=4, 9, 10, 11$  and in  $S_1(4.m)$  for  $m=11$ . Also 5, 6, 7, 8 are disrupted into observed lines. For more complete discussion see the lists of S series below and the notes appended thereto, which will repay careful attention.

The apparent instability of the  $S_1$  lines may be illustrated thus. Consider an electron in an outer  $s$  orbit, say above  $s_3$ . Of those falling into the lowest  $p$  level ( $p_2$ ) they either all avoid the  $p_1$  and take, instead of  $p_1$ , displaced  $p_1$  orbits, or the energy of transition is emitted as  $2h\nu$  or  $3h\nu$ . Of those falling into the  $p_3$  levels, some may stop in  $p_13$ , but a large number choose displaced  $p_13$ . When, however, the outer  $s$  orbit is further out, the chance of falling to the  $p_13$  is larger, i.e., the line is observed. In the great majority of cases an electron must have originally occupied a displaced  $s$  orbit when it falls into a displaced  $p_1$ , and in several the displacement in each orbit is the same\*.

As a further test of the correct allocations in  $S_1$  and also as a test for the presence of neutral links to ionized lines, the  $e.S(2.m)$  have been investigated. The neutral  $e$  link is 20612.06. The result is given in Table IV. which shows a parallel set to  $S_2.2$ , repeating its general features, with satelloid indications to be expected in linkages.

3. In the discussion of the data for the various  $S_2$  lines separations due to all possible displacements between 698 and 758 were sought for (for the actual values of  $\nu$  see Table I.). The result is to show that the actual  $p_22$  are restricted to a few only. The number of occurrences in the  $S_2(2.m)$  are as follows:—

69.	$\frac{1}{4}$ .	$\frac{1}{2}$ .	$\frac{3}{4}$ .	70.	$\frac{1}{4}$ .	$\frac{1}{2}$ .	$\frac{3}{4}$ .	71.	$\frac{1}{4}$ .	$\frac{1}{2}$ .	$\frac{3}{4}$ .	72.
2	3	6	2	0	1	1	1	1	1	1?	2	0
72 $\frac{1}{2}$ .	$\frac{1}{4}$ .	$\frac{3}{4}$ .		73.	$\frac{1}{4}$ .	$\frac{1}{2}$ .	$\frac{3}{4}$ .	74.	$\frac{1}{4}$ .	$\frac{1}{2}$ .	$\frac{3}{4}$ .	75.
2	0	4		0	1	0	5	1	1	5	0	1?

---

\* If we adopt the view as to the source of emission given in a recent paper (Phil. Mag. 8, 108, 29) we are led to the conclusion that the configuration of the nucleus of heavy atoms like Hg is not a constant one, and that each modification causes resonance at slightly different frequencies.

Some of the examples may be coincidences, but the numeration quite definitely points to four  $p_2$  with separations due to  $69\frac{1}{2}(\alpha)$ ,  $72\frac{3}{4}$ ,  $73\frac{3}{4}$ ,  $74\frac{1}{2}(\gamma)$  as being, if the expression may be used, more normal than the others. In other words, the probabilities of these four levels being occupied are about equal, and much greater than that for the others. With rising orders of  $pm$  the displacements decrease in all this group, and this is indicated in Hg by a consideration of those observed in  $S(3.m)$ ,  $S(4.m)$  and  $P(m)$ , which, besides showing a general drift to lower multiples, also include examples between  $68\frac{3}{4}$  to 67. It was not until writing up the paper that this effect was noted. A further search for lower multiples in  $S(3.m)$ ,  $S(4.m)$ , and  $(Pm)$  for  $m > 3$  is desirable.

### The $P^2$ Series.

4. The true P series  $s1 - pm$  will lie in the far ultra-violet,  $m=2$  excepted, but we should expect also to find representatives of  $s2 - pm$ , where  $s2 = p_1 2 - S_1 2 = 56920.18$ . We start with  $p_1 2 = 92024.56 = 4R / \{2.183432\}^2$ . For  $p_1 3$  we expect a mantissa somewhat greater. The nearest possible line is at 14116.93, which requires  $p_1 3 = 42803.25$  and denominator 3.201495. Since  $s1 = 149519.64$ , the  $P(1.m)$  series is  $149519.64 - 56920.18 = 92599.46$  ahead of  $P(2.m)$ . The corresponding  $P_1(1.3)$  should therefore be at 106716.10, and we find it at  $106712 \pm 5$ , the  $\pm 5$  referring to equally probable values without O.E. As we shall see immediately,  $P_2$  lines are also observed. This agreement therefore not only supports the allocation of 14116, but also the allocation for  $S_1$ , with its value for  $s1$ .

The  $p_2 3$  separations will depend on displacements of the same order of magnitude as those of  $p_2$ , and we should expect to find here also the same kind of instability in the  $p_2 3$  term as in  $p_2 2$ , extending even, in analogy with the other elements of the group, to lower own multiples with increasing order. The values have been calculated both for  $p_3$  and  $p_4$ , and are given in Table I. A reference to Table V. will show that we get three representatives of  $P_2(1.3)$  in the ultra-violet and four of  $P_2(2.3)$  in the red, the latter by McLennan and Shover, only measured to 1 A.U.

Since for  $m=4$  the mantissa is slightly larger than in  $m=3$ , the line 32169 fits in for  $P_1 4$ . With this we get a

line for  $P_24$ , whose measures by Stiles and by Cardaun differ by  $dn=2.40$  (? satelloid effect). Their mean is separated 1196.48 from  $P_1$ , whilst  $67\frac{3}{4}\delta$  shifts 1196.86, the same within O.E., and corresponding to an equal one in  $P_3$ . No corresponding  $P(1.4)$  at 124768 is seen. These two allocations for  $m=3, 4$  give the series formula. The series are also supported by indications of the parallel  $P(3 . m)$  for  $m=6, 7, 8$  and also by  $p-p$  combinations.

### *The D<sup>2</sup> Series.*

5. Any predetermination of the D series must depend on the fact that the mantissa of the extreme satellite term of lowest order is an exact multiple of  $\Delta$ , i. e., of the displacement which produces the  $p$  doublet. To apply this rule with exactness requires a knowledge of the exact values of the D-limit ( $p_1$ ), of  $R$ , and of  $\Delta$ . The whole question is discussed in some detail in Chap. IX of my 'Analysis of Spectra.' It is sufficient here to say that with a good  $p_12$  and  $\Delta$ , as we have in the present case, and using the incorrect \*  $R=109678.6$  (Rydberg's value in I.A), the mantissa thus found is, as a rule, for neutral doublets at least, less than an exact multiple by a small quantity of the order 100.

In our present discussion we have the complication of the existence of a set of values of  $\Delta$ , without any indication as to which is the normal one, if a single normal one really exists. Judging from the intensities of the  $S_2^22$  lines, the  $\Delta$  producing  $\gamma$  or 9829 would appear the normal one; judging from the rule that the doublet separation is always close to  $2v_1$  of the preceding triplet series, that producing  $\alpha$  or 9122 would appear the normal. On the other hand it is possible that several act as independent normal  $\Delta$ , producing independent D and F series. If so, we shall find in the spectrum a large number of terms whose denominators differ by our multiples, and it may be

\* In all data requiring the use of  $R$ , I have used this value, so as to get a uniform system between data for elements obtained at varying dates. The uniformity is necessary when dealing with displacements, and the slight difference from its true value has no appreciable effect on the results. The verification of the multiple  $\Delta$  law for the extreme D satellite requires, however, for its exactness the use of the true  $R$ , which are slightly different for  $p$  and  $d$  terms. The error in W. N. at most only amounts to a few units, and is immaterial for the present purpose of identification of observed lines.

difficult in all cases to determine to which system of  $\Delta$  or of  $d_1, d_2$  terms they are to be ascribed. We should then make tests with the three  $\alpha, \beta, \gamma$  values in succession. This has been done with some interesting results. It will be sufficient here to confine the discussion to the case of  $\alpha$  only.

A glance at the data for the other elements of this group will show that we must expect a lowest order of  $m=1$ , a mantissa of about  $\cdot 8$  with a satellite displacement of about  $9\frac{1}{2}\delta$ . Accepting this, and applying the above rules, we expect for  $d_2 1$  a denominator  $1+8\Delta$ , and a displacement for  $d_1$  of about  $9\frac{1}{2}\delta=13776$ . Here, putting in decimal points,

$$8\Delta = \cdot 806250, \quad 8\Delta + 9\frac{1}{2}\delta = \cdot 820026.$$

Calculation then at once produces  $D_{12}1$ , and  $D_{11}1$  at lines precisely observed in the spectrum. They are:

$$8ii \quad -42463\cdot 90 \quad 2028\cdot 12 \quad 2i \quad -40435\cdot 78$$

(we anticipate by stating that corresponding F with  $d-d$  combinations are also found). The denominators of these lines are

$$D_{12} \quad 1\cdot 806130 = 1 + 8\Delta - 120 \\ \cdot 013774 = 9\frac{1}{2}d - 2.$$

$$D_{11} \quad 1\cdot 819904$$

For the corresponding  $D_{22}$  lines see Table VI. The only peculiarity is the large intensity of the  $D_{12}$  and its class E2. This may be due to the fact that the  $D1$  are negative lines, so that the transition is not from  $d$  to  $p2$ , but  $p2$  to  $d1$ , in which the electron from  $p2$  would have its more probable final level in  $s1$  rather than in  $d1$ .

The  $D_{11}2$  must have a denominator somewhat less than  $2\cdot 8199$ , and there must be a  $D_{12}$  showing the own multiple displacement. This gives the second set in the list with a satellite separation  $501\cdot 12$  due to  $8\frac{3}{4}\delta$ . The series formula is then calculated from  $m=1, 2$ . For the discussion of the succeeding lines see the lists and notes below. There is also a related  $D(3.m)$  series as well as a considerable number of  $d1-dm$  and  $d2-dm$  combinations.

The probability of transitions from upper  $d$  levels ( $d_1$ ) to upper  $p$  is seen to be abnormally low. In  $D(2.m)$ ,  $D_{12}$  lines are seen from  $m=1$  to 5, but  $D_{11}(3, 4, 5)$  are not observed. They are present in the parallel  $D(3.m)$  for  $m=4, 5$ , where  $m=3$  lies in the ultra-red region. In this

series also we find representatives of  $D_{12}$  for  $m=7, 8$ . It is noticeable that the order  $m=6$  appears to be totally disrupted in both  $D(2.6)$ ,  $D(3.6)$  as well as in  $S_6$ .

### The $F^2$ Series.

6. The constitution of the  $f$  term is not so definitely known as that of the  $d$ . The evidence, so far as it goes, tends to show that it is closely analogous to  $d$ , and that its extreme satellite term of lowest order is close to a multiple of  $\Delta$ , and that this multiple is higher than that for the  $d$ . We shall employ this to get at least approximation to the position of the lower  $F$  lines. The series depending on  $d_1$  for its limits will lie in the ultra-violet, but we should also expect to find a corresponding series with the same  $fm$  and limits depending on  $d_2$ . We will make a first attempt with denominator  $2+9\Delta$ .

Here  $2+9\Delta=2.907032$ . The respective limits are

$$d_{11}, d_{21} \quad 132460.12 + 2028.12$$

$$d_{12}, d_{22} \quad 55330.09 + 502.02$$

The  $F_1(1.m)$  and  $F_1(2.m)$  are thus separated by 77130.03. The above considerations show that we should expect  $F_{12}(1.2)$  somewhat less than 80520, and another 2028 ahead. We find such, as well as  $F_3$ , at

$$F_2 \quad 1n, \quad 80153.9 \quad 2028.9 \quad 1, \quad 82182.8 \quad d\lambda = .01 \text{ on two lines}$$

$$F_3 \quad 1, \quad 103438 \quad 2032 \quad 1, \quad 1055.0 \quad d\lambda = .04 \quad \text{,,} \quad \text{,,}$$

with denominators 2.896105, 3.892030.

Both separations are within O.E. of these high wave numbers, and the intensities really indicate strong lines. In general,  $F$  lines have much closer satellites than the  $D$ . In this sub-group  $ZnF$  shows none,  $CdF$  indicates a very close one by its diminished doublet separation,  $EuF$  gives a quite definite one, due to 11 lines. We should then expect, also, satellites in  $Hg$ , *i.e.*  $F_{11}$  larger than  $F_{12}$ , and should not be surprised, in accordance with the abnormal complexity we have found in this element, to find several.

For  $F(1.3)$  there is a possible  $F_{11}$  with a satellite separation of 107. Displacements of  $20\delta_1$ ,  $19\delta_1$ , would produce separations of 107.62, 102.26 respectively.

The  $F(2.m)$  being 77130.03 below  $F(1.m)$  places the  $F(2.3)$  about  $26368 \pm$ . This clearly settles the  $F_{12}$ ,  $F_{11}$  at the observed

$$1, \quad 26375.42 \quad 102.26 \quad 1, \quad 26177.68,$$

giving the exact  $19\delta_1$  separation. These are good measures and enable us to reconstitute to the same exactness the F(1.3) lines. Also the F(1. *m*) lines give a  $f_2 2 - f_2 3$  combination about  $23344 \pm$  which we find at  $23348.221$ . This, then, further provides a similar correction for F(1.2). The directly observed separation for F(1.3) is, however, 107—the  $20\delta_1$ —although it may be 102 within O.E. There are, then, two possible cases, viz.,  $20\delta_1$  or  $19\delta_1$  in F(1.3) with  $19\delta_1$  only in F(2.3), for the persistence of satellite separations in parallel series, although usual, is not without exception. The values thus corrected are, then,

	(107).		$d\lambda$ .	102.		$d\lambda$ .
$F_{12} 2$ .....	80151.87		—03	...157.23		06
$F_{22} 2$ .....	82180.0	<b>2028.12</b>	—04	...185.35		04
$F_{12} 3$ .....	103500.09		02	...505.45		07
$F_{11} 3$ .....	607.71	<b>107.62</b>	02	...607.71	<b>102.26</b>	02
$F_{22} 3$ .....	105528.21	<b>2028.12</b>	—02	...533.57		03

The 102 arrangement is sustained by a  $3h\nu$  effect,

$$3 \times 26719.0 = 80157$$

It remains to determine the satellites or the  $F_{11}$  for  $F_{12}(1.2)$ , which are important as giving separations for the G series. Three possible lines, marked *a*, *b*, *c* in Table VII., for F(1.2) are present, with observed separations from  $F_{12}$  of 122.2, 186.7, 296.6. The own multiples give the following:—

$$9\delta_1 = 117.68; 10\delta_1 = 130.75; 14\delta_1 = 182.80; 23\delta_1 = 299.84$$

As the observed  $\lambda$  are given to .1 or  $dn = 6.5$ , the test holds for all within O.E., and none are excluded on this basis. It may be noted that if we take the separations on the corrected  $F_{12}$  above, those on the 102 basis agree closely with  $9\delta_1$ ,  $14\delta_1$ . Again, this basis is sustained for  $\sigma = 182$  by a  $2h\nu$  effect, and for 299 by  $4h\nu$  (Table VII., *b*, *c*).

$$2 \times 40171.44 = 80342.88 \quad d\lambda = .09$$

$$4 \times 20114.50 = 80458.0 \quad d\lambda = -.06$$

For further details as to the series and *ff* combinations, see the F list and notes below.

It may be noted that as 117.68 is 182.16 behind 299.84, the four lines in  $F_1(1.2)$  may be regarded as two inde-



pendent sets of one satellite, each with the same own displacement. Thus

$F_{12}$	80157.23		$aF_{12}$	274.91	
$bF_{11}$	340.03	182.80	$cF_{11}$	457.07	182.16

of which one may belong to the  $\alpha$  system and the other to an independent one.

### *The G Series.*

7. With  $f_{12}, f_{13}$  as the limits of the G series,  $G(2.m)$  will be in the visible spectrum and  $G(3.m)$  for orders  $\geq 6$ . Any determination of the  $G(2.m)$  is rendered difficult by the complexity of the  $f_2$  satellites and the actual presence in the spectrum of numerous separations of these  $f_2$  values, and of  $d_1 d_2$  sets. The allocation given in the list must be roughly correct, but the whole region shows such evidence of linkings with  $d, f$  separations and displacements that the exact details may have to be modified with further knowledge. The discussion will be taken on the list as it stands, and afterwards some examples of complexities will be taken in illustration. This is important as evidence of complexities actually existing in the spectrum. It will then be best to begin with  $G(3.m)$  and look for  $f_{13} - g_2, f_2 3 - g_2$ , i. e., separations about 102.26. In the region for  $m=6, 7, 8$  we find the sets reproduced as raw material after Table VIII. Here the figures in brackets denote the denominators as given by Rydberg's tables. An inspection shows at once that a regular series is indicated by those marked A and by those alone. The good measures for  $m=7, 8$  are taken for the formula.

### *Satelloids.*

8. The occurrence of wave-number differences amongst S2 and other lines between the measures of apparently the same line by two observers, greater than their O.E., has been already noted. Their appearance suggests the existence of an effect similar to that exhibited in copper, which for convenience I called the satelloidal effect. In copper \* we find a very considerable number of examples of strong lines accompanied by numerous close companions,

\* Phil. Mag. 2, 196, 26.

neither true satellites nor analogues of the very close sets in complex lines. These are such that their separations from the main line are always multiples of a constant  $\cdot 57$  (or  $\cdot 54$ ). If a similar effect is found to exist in mercury we must conclude that we are in the presence of a general constructional law of spectra. Its discussion is therefore of more importance than for the analysis of the mercury spectrum alone. Examples of the effect so noted—without any special examination of the whole spectrum—are given in the following table. The first thirteen deal with measures by different observers, differences, therefore, ostensibly due to different excitations. They are chiefly between Cardaun and Stiles, both very reliable, and showing differences depending on  $2\cdot 7$ .

C., D., P., S., Ly. denote, respectively, Cardaun, Déjardin, Paschen, Stiles, Lyman.

1. S. 27711·377		12. C. 44226·04		21. S. 29827·86	
P. 16·61	$5 \times 2\cdot 761$	D. 27·60	$2\cdot 93$	S. 32·422	$10 \times 4\cdot 56$
S. 25·185		P. 28·973		22. P. 33268·64	
2. C. 30626·20		13. C. 44373·05 <sup>(1)</sup>	$2\cdot 76$	P. 74·07	$12 \times 4\cdot 52$
S. 28·900	$2\cdot 70$	D. 75·02		23. P. 25356·87 <sup>(4)</sup>	
3. S. 30971·538		P. 75·813 <sup>(2)</sup>		P. 59·14	$5 \times 4\cdot 54$
C. 73·96	$2\cdot 40$	14. P. 22034·79		24. S. 24742·604	
4. C. 31648·46		P. 37·61	$2\cdot 82$	P. 43·04	$\cdot 45$
S. 51·316	$2\cdot 86$	15. P. 30133·45		25. C. 37651·18	
5. C. 33919·24		P. 36·36	$2\cdot 91$	S. 51·637	$\cdot 46$
S. 22·003	$2\cdot 76$	16. C. 31920·28		26. S. 38803·383	
6. C. 35104·16		C. 25·731	$2 \times 2\cdot 725$	C. 03·895	$\cdot 51$
S. 06·162	$2\cdot 00$	17. C. 33687·579		27. S. 41410·261	
7. S. 35616·731		C. 88·351	$2\cdot 76$	C. 12·12	$4 \times 4\cdot 65$
P. 22·11	$2 \times 2\cdot 69$	C. 91·111		28. C. 41523·71	
8. C. 36089·49		18. C. 35229·84		S. 26·827	$7 \times 4\cdot 45$
S. 92·230	$2\cdot 74$	C. 40·65	$4 \times 2\cdot 702$	29. C. 44933·44	
9. D. 38741·49		19. C. 40023·65		D. 34·45	
P. 47·05	$2 \times 2\cdot 78$	C. 39·51	$5 \times 2\cdot 732$	P. 35·66	$5 \times 4\cdot 44$
10. C. 40112·12		20. C. 25092·883 <sup>(3)</sup>		30. D. 53490·81	
S. 14·894	$2\cdot 77$	C. 93·349	$\cdot 466$	Ly. 94·8 <sup>(1)</sup>	
11. D. 44155·33		C. 93·834	$\cdot 485$	P. 97·62 <sup>(3)</sup>	$15 \times 4\cdot 54$
C. 60·60	$3 \times 2\cdot 73$	C. 94·307	$\cdot 473$		
P. 62·94					
D. 63·52					

(1) (2) These sets are separated respectively by  $\alpha$ , viz. :—9121·8, 9121·80.

(3) P gives a single line equal the mean.

(4) S gives ... 56·863; ... 59·138. sep.  $2\cdot 275 = 5 \times 4\cdot 55$ .

It might be objected that these were due to some systematic differences, but in general these observers agree very closely, and in the above those of Stiles are sometimes in defect and sometimes in excess of those of others. Examples 14 . . . 19 deal with pairs by the same observer. Here the duplicity is evident, and the observed separations will be more exact, as free from those errors. These first two groups refer to a separation about 2.74. The satelloidal effect, however, may be due to a still smaller constant of which 2.7 is a multiple, and this is indicated by Ex. 20, containing four close, equally-spaced lines by Cardaun at a mean separation of .47, whilst  $2.7 = 6 \times .45$ . Runge and Paschen give here three close companions separated by .473, .432 or mean = .453. The last eleven examples depend on this smaller value. Multiples of this are also indicated in companions in Ex. 1, 11, 12, 13, 17. The existence of the effect must therefore be regarded as established by the large number of consonant examples found. This being accepted, Ex. 3, 6 should not be included, as differing from the 2.7 by more than the O.E. The most reliable values should be those deduced from Cardaun's readings, viz., 2.725(2), .76(1), .702(4), .732(5), the figures in brackets denoting weights. The weighted mean is 2.726. Ex. 11 by D. gives 2.730(3); 14, 15 by P. give 2.82(1), 2.91(1). For the smaller values we similarly find .475(3), .456(10), .452(12), .454(5), .45, .46, .51, .465(4), .445(7), .444(5); 454(15) weighted mean  $y = .4547$  whilst  $6 \times .4547 = 2.728$ . The agreement of the two sets is remarkable. Other examples will be found in the examples of linkages given below. The relation between the lines 1 and 2 in the list in § 1 is clearly of a satelloidal nature. The calculated separation for 69δ is 9051.41, which is 5.03 behind the strong line of 2. This is due to  $11y = 5.00$ .

From analogy with the effect as found in copper we should then expect :

(1) That a line which is affected thereby must be one which contains  $p^2$  as one of its terms, although in the present state of our knowledge, the presence of higher orders of  $p$  should not be excluded absolutely.

(2) That true link-values frequently occur between one line and a satelloid of another, which satelloid, however, is not necessarily itself observed. With good measures, if an approximate link differs little from a true one by a multiple of  $y=4547$  it should be taken, provisionally at least, as a true link thus modified. There are large numbers of these cases, some of which are noted in the next section, and also in the notes to the tables.

### Links.

9. In examining the whole spectrum for separations differing by a few units from  $\alpha$ ,  $\beta$ ,  $\gamma$  an exceedingly large number of such cases was found. Evidence was obtained that they occur also as links. This is completely in accordance with the fact that the  $\nu$  separations of  $p$  terms also serve as  $b$  links. The complete analysis of the whole spectrum would require the discussion of the linkage systems for all the recognized link values. This would be a big undertaking with such a rich spectrum as that of mercury, with its possibly complex sets of links, and is not necessary for the isolation of the normal neutral or ionized series, but some attention should be paid to the  $b$  links, if only to distinguish them from the equal doublet  $\nu$  separations.

An important new fact emerges, viz., that ionized links are attachable to neutral lines, as well as neutral links to ionized lines. Some illustrations of the first statement are given below, whilst support for the second is given by the very complete set  $e.S^2m$ , where  $e$  is the neutral  $e=20612.06$ . In the simple excitation of a neutral line an electron is raised to a higher level (say)  $i pm$ . In a more complicated excitation a second electron (that which would act for an ionized line if the first were expelled) may be raised to its corresponding  $ii p_1 2$ , and then both fall to their corresponding  $i s$  and  $ii p_2 2$  levels. It is possible that the value of the  $ii p_2$  level may be slightly affected by the presence of the far out  $i pm$ , thus modifying slightly the observed link value. If this is so we may have at our disposal a means of studying directly the interatomic actions of electrons.

All links yet recognized are calculable from series constants (the lowest  $p, s, d$  terms and the  $\nu$  separation). Their appearance in any case, the  $b=\nu$  link excepted, there-

fore definitely denotes a linkage. The separations now to be considered are all, on our initial supposition, either  $\alpha$  separations or  $b$  links. There is nothing, then, to distinguish an individual case as between the doublet separation of two bi-term lines or a link. But one distinguishing feature of linkages is that sets of successive links occur, a phenomenon which cannot happen with a normal series separation. Moreover, when the individual links appear slightly modified, the modifications in a complete chain often annul one another, and the sum of the observed is equal to the sum of the corresponding normal links. In any case a long set of such close link values amongst lines which are not crowded together will indicate their link nature. The number of such sets in this spectrum is surprisingly great. I give here a few illustrations taken almost at random, but sufficient to show that these  $\alpha$ ,  $\beta$ ,  $\gamma$  separations can appear as links. The numbers in brackets after a wave number give the separations from the next lines in the spectrum before and after, and serve as indicators of the degree of crowding in the region of the line.

## A.

1, 26621.89 (8, 20)    9120.1    2 i 3574.2 (36, 76)    9120.1    1 iii 44862.07 (34, 72).

The third line is (748)S<sub>2</sub>2, with a separation .70 ( $d\lambda = .03$ ) too small. The middle one has only been observed by B!., but it serves to indicate the double linkage. If the third is the corrected (748)S<sub>2</sub>2, the link sum is  $2 \times 9120.45 = 2\alpha - 270$ , with the large satelloid value 2.72.

## B.

1 iii	21511.164 (7, 40)	
3 i	30628.900 (130, 60)	9117.74
4 i	39752.755 (34, 11)	23.855
0 ii	48873.48 (109, 24)	20.73
1	57998.9 $\pm 1.7$ (86, 100)	25.4

## C.

S <sub>2</sub> 2	35104.16	
S <sub>2</sub> 2	44933.44	9828.29
4	54760.4 (194, 72)	27.0
3	64591.1 (67, 113)	30.7
2	74421.4 (39, 78)	30.3

B. The last line is by Ly., and the  $\pm 1.7$  refers to equally probable values. As they stand, the sum of the separations is  $4 \times 9121.93$ . Correcting the last line to ... 8.48 ( $d\lambda = .01$  on 1724.2) makes the sum exactly  $4\alpha$ . No  $\beta$  or  $\gamma$  links are found to these lines.

C. This is a chain continuing the S<sub>1</sub>2 and  $\gamma$ S<sub>2</sub>2, with the same separation. As in Ex. B, in the complete chain the

modifications are annulled, and the total separation is  $4 \times 9829.31$ . With the high W. N. the O.E. are considerable, and the 9829.3 is not necessarily exact. But the individual lines are well isolated from others, and the agreement is sufficiently close to establish the fact that 9829 behaves also as a link. The first is a genuine  $\nu$  or exact  $\gamma - y + .06$ ; the last three are  $b$  links. The multiple  $4\gamma$  requires the last line to be 1.44 greater, or  $d\lambda = -.02$  on  $\lambda = 1343.7$ .

D (four sets).

(The 98 in the 9829 and the intensities are omitted.)

10004		10591		10802		14193	
198267	<b>22.7</b>	i 20420.4	<b>29.4</b>	i 30635.96	<b>33.9</b>	ii 24022.18	<b>29.1</b>
29654.5	<b>27.8</b>	30247.32	<b>26.9</b>	ii 30466.0	<b>30</b>	33851.7	<b>29.6</b>
39487.44	<b>32.9</b>	i 40082.21	<b>34.39</b>	40291.24	<b>25.2</b>		
i 49318.76	<b>31.32</b>						
24.60							
Mean...	<b>9828.69</b>	... 30.15	<b>9830.40</b>	<b>9829.70</b>		<b>9829.35</b>	

The sets all start from ultra-red lines, the first three by McL. and the last by W. The lowest line in the first, by P. and D., show the satelloidal effect  $5.84, 13y=5.91$ . A satelloid  $-4y$  on D's would give a mean value  $9829.70$  or  $\gamma-.03$ . In the second the deviations in the mean from the normal cannot be met by O.E. on the first line. But the whole, with Ex. C., are sufficient to show that  $9829$  behaves as a link as well as a doublet separation.

**E (two sets).**

3	10802 (38, 47)		1	13216-2 (72, 24)	
1	20134-2 (19, 14)	<b>9332-2</b>	1	22548-34 (8, 11)	<b>9332-1</b>
4 ii	29469-25 (34, 12)	<b>35-0</b>	2n	31880-68 (89, 9)	<b>32-34</b>
3A	32803-895 } (23, 22) Cd.	<b>34-64</b>	2 ii	41212-2 (57, 21)	<b>31-84</b>
	383 }	<b>S. 34-13</b>	0 i	51040-98 (26, 53)	<b>9828-46</b>
		<b>9333-63. ... 46</b>			

These involve the  $\beta$  separation. The first set starts from the same line as in Ex. D, 3, the last being the arc line  $S_2^{34}$ , the two measures by Cd., S. respectively. The S. measure gives the exact mean  $\beta$ , but the Cd. as  $S_2^3$  gives the exact  $v_1, v_2$  in  $S^{34}$ .

## F.

2	26588-854 (15, 20)	9117-15	} 2, 35106-005	{	9122-26	5 i	44828-27 (73 $\frac{1}{2}$ ) S <sub>2</sub> 2
8 i	26375-26 (16, 17)	9330-74			9331-88	0 i	45037-88 (17, 38)
1	25876-847 (38, 21)	9829-16			9827-85	1 i	45533-86 (30, 17)

Several interesting points arise with these lines.

(a) The series inequality  $9829-16 + 9122-26 = \alpha + \gamma + .08$ .

(b) 44828 is  $(73\frac{1}{2}\delta)S_2 2$  and 26375 is  $F_{12}^2(2,3)$ , and the two cannot come in the same chain. S. gives two close lines 26376-818 and .79-027 separated by 2-209.

(c) Also another pair by S. 25876-847, .73-094, separated by  $3-75 = 8y + .11$ .

(d) The presence of the  $p2$  being assured by  $S_2$ , these separations can be written.

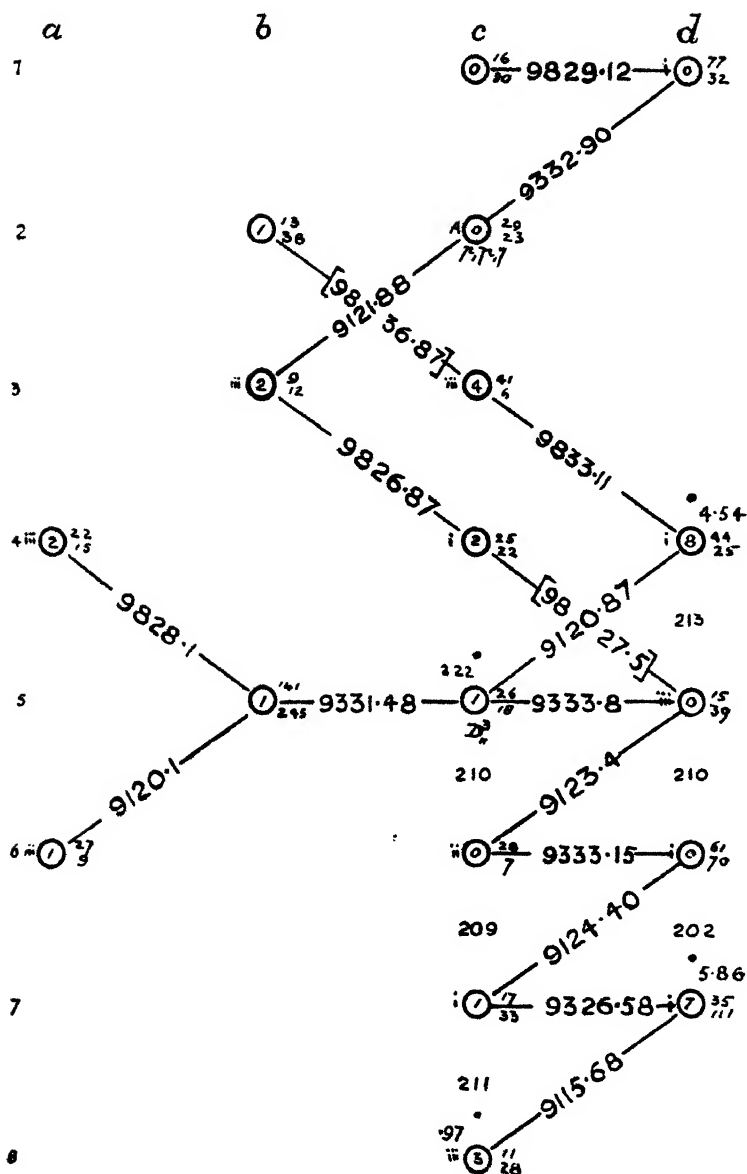
$$\begin{array}{ll}
 \alpha - 10y - .10 & \alpha + y \\
 \beta - 6y + 0 \text{ (2-72)} & \beta - 1-53 ? \\
 \gamma - y - .06 & \gamma - 4y + 0
 \end{array}$$

## G.

This is a linkage map on a more considerable scale. It doubtless contains some false—i. e., chance—links, but it affords very definite evidence for ionized links attached to neutral lines. It also illustrates an arrangement of frequent occurrence whose interpretation may be of importance.

We get direct evidence of the satelloidal effect in the lines at  $c5$ ,  $c8$ ,  $d4$ ,  $d7$  from the recent measures of Paschen. At  $d4$  P.'s measure 48695-216 is separated from D.'s by 4-54, or an exact  $10y$ . We note, also, that the links to these are  $9120-87 = \alpha - 2y - .02$  and  $9827-57 = \gamma - 2y - .26$ . We must accept the first, but the second is more doubtful with a succeeding  $9836-84 = \gamma + 16y - .08$ . At  $c5$  P. gives a line 2-22 behind it with  $5y = 2-27$ . At  $d7$ ,  $c8$ , P.'s values are  $5-86 = 13y - .05$  and  $.97 = 2y + .06$  behind those of D. Here, also, the attached links are

MAP.



a. 21419.2; 21127.3.—b. 29529.81; 29258.261; 30247.41.—  
c. 37884.02; 38380.24; 38866.65; 39085.15; 39578.89; 39789.34;  
30998.09; 40208.92.—d. 47713.14; 48699.76; 48912.7; 49122.49;  
49324.60.



$9326.58 = \beta - 6.84$  with  $15y = 6.82$  and  $9115.68 = \alpha - 6.15$  with  $13y = 5.91$ , of which the first at least may be accepted as possible.

The line at  $c5$  is quite definitely  $D_{11}^{313}$ . As we have seen, it is also linked by  $\alpha$  to a  $2y$ -satelloid of  $D$ 's  $48699.76$  at  $d4$ . The  $9333.8$  is  $\beta$  within the O.E. of the line  $48912.7$  ( $d5$ ). In other words, we find two ionized links to the neutral  $D_{11}^3$ . The  $9331.48$  back is  $\beta - 4y - 12$ . The  $b5$  is an arc line only observed by K. R. and E. V. with the considerable possible error of  $1.8$ . It has been allocated by P. to a combination  $p_2^{31} - p_2^{32}$ , in which, I think, his  $P_2^{32}$  may be doubtful. If his allocation is correct,  $9331$  must be a chance coincidence; if the link is real,  $\beta - 4y$ ,  $b7$  is  $\beta.D_{11}^3(13)$ , and not the  $pp$  combination. The back lines from it are  $\gamma$ ,  $\alpha$  within the O.E. of the lines at  $a4$ ,  $a6$ .

The line  $38380.24$  at  $c2$  is  $p_1^{31} - p_1^{37}$  with the exact  $\alpha$  back to  $b3$ . Also the two links to  $d1$ ,  $9332.90$  and  $9829.12$ , are  $\beta - 52$ ,  $\gamma - 55$ , thus forming a parallel inequality, and definitely giving  $c1$  as  $\gamma$ . ( $p_1 p_1^7$  or  $c3$ ).  $\beta$ . The set, however, cannot be linked to  $D_{11}^{13}$ , and one at least of the defective  $9826.87$ ,  $9827.5$  to  $C5$ ,  $d5$  will be false. This is indicated in the map by [ ],  $9826.87$  is  $\beta - 2.80$ , with the big satelloid  $2.72$ .

Lastly, we note the curious appearance of alternate  $-\alpha$ ,  $+\beta$  links successively from  $d4$  downwards. If  $d4$  be written  $X$ , the linking means that the other lines depend on  $\alpha.X$ ,  $\alpha.X.\beta$ ,  $2\alpha.X.\beta$ ,  $2\alpha.X.2\beta$ , ...  $4\alpha.X.3\beta$ . But the arrangement may be interpreted in another way, as sets of lines differing by an amount close to  $213$ . To illustrate, suppose for the moment  $c5$ ,  $d4$  were  $p_1^2 - t$ ,  $p_2^2 - t$ . The lines in the map would be constituted by successive displacements in the  $t$  term of the same amount. Here such displacements would be positive, and the succeeding shifts would show decreasing amounts, as, indeed, the figures in the map indicate. This appearance of large numbers of separations in special regions near those of  $d$  or  $f$  satellites is quite common in general, and indicates that normal  $D$  or  $F$  lines are in the neighbourhood. In the present case this explanation is not tenable, for  $c5$  is certainly an arc line, and almost certainly is  $D_{11}^{313}$ . To produce a shift of  $210$  in the  $d_1(13)$  would require a displacement of the denominator from  $13.9$  to  $17.8$ , and is quite out of the question.

## H.

	a.	b.	c.	d.
1.		1 iii 22649.73	9830.6	2 iii 32480.3 9121.7 0 A 41602.0
	9121.7		9334.24	
2. 0, 13528			5 A 31983.97	$D_{22}^{32}$
	9333.5		9122.41	
3.		2 i 22861.56		
	9833.0			
4. 2, 13028.5				

Here again at b1 we find a satelloidal indication. S. gives three lines, all of class E3, and E.V. two.

1 iii 22644.255			1, 22639.1
1 iii 49.733	5.478	$12y = 5.456$	1, 42.2 3.1
1 iii 60.268	10.535	$23y = 10.46$	

All the links are normal except those on c2, which is  $D_{22}^{32}$ . These may be written  $\beta + 2y - .09$  and  $\alpha + y + .13$ , but if the satelloidal effect is really present it must be due to the  $p2$  present in the links themselves. 13528 has been allocated by Paschen to  $G_1^{32}(4.9)$ . We get a parallel inequality from b1 to c1, c2, viz. :—

$$9830.6 - 9334.24 = \gamma - \beta + .10.$$

Thus, putting  $D_{22}^{32} = D$ ,

$$c1 = \beta . D . \gamma + .10, \quad d1 = \beta . D . \alpha . \gamma + 0.$$

This whole set is a very clear example of linkage to a neutral line by ionized links.

## I.

1	9121.0	2	9334.62	$D_{23}^{35}$	9830.57	10	9120.64	8	9330.1	0
				$D_{22}^{35}$	9119.62	0	9830.84	10		

The numbers in the line places are intensities.

$$D_{22}^{35} = 41658.49, \quad D_{22}^{35} = 41664.74.$$

The lines in the fifth column are 60609.7 by C. and 60615.6 by Ly., and are both of similar intensity. At first sight they might be taken as measures of the same line, but they differ by more than their average amount. The arrangement shows that one is linked to the main  $D_{22}^{35}$  and the

other to the satellite  $D_{23}5$ , in each case by series inequalities, viz. :—

$$9830\cdot57 + 9120\cdot64 = \gamma + \alpha - \cdot26 \quad d\lambda = 0$$

$$9119\cdot62 + 9830\cdot84 = \gamma + \alpha - 1 \quad d\lambda = \cdot02$$

$$\text{Also} \quad 9121\cdot0 + 9334\cdot62 = \alpha + \beta + \cdot4 \quad d\lambda = \cdot06$$

or the first chain as a whole  $= 2\alpha + \beta + \gamma + \cdot1$  with all modifications annulled.  $d5 = \cdot3776$ , so that the link modifications can be accounted for by displacements in the  $d5$  terms. Thus  $9119\cdot62$  is  $\alpha - 2\cdot21$ , and  $6\delta_1$  shifts  $2\cdot26$ ;  $9120\cdot64 = \alpha - 1\cdot20$ , and  $3\delta_1$  shifts  $1\cdot13$ . The agreement is thus very close within O.E., but, unfortunately, the evidence cannot be considered decisive, since the own shifts on  $d5$  are so small and the O.E. on the higher wave numbers are so large. Moreover, all our preconceptions, although dangerous guides, go against such strong lines being really linked to lines of order  $m=5$ . The importance of this discussion lies in the fact that 60609, 51489 (the fourth and fifth in the first row) have been allocated by Carroll to  $-S^2_1$ , an allocation accepted by Paschen.

## J.

	a.		b.		c.		d.
1.	1	9121 4	} 10 $S_1^{33}$	9832 52	4 ii	9120 96	} 1 i
2.							
3.	4	9330 9		9124 71	5	9828 77	
4.				9828 3	} 1		
5.			5	9121 3			
6.				9333 6	1 n		

Col. a. (9186·1; 8976·6) McL.—b. 18307·456; 17603·9.—c. 28139·978; 27432·173; 26725·195; 26938·5.—d. 37260·94. The numbers in line positions are intensities.

This is given to illustrate a similar arrangement with a  $S_3$  line. It can be seen that where the links are not normal they can be made so by satelloidal considerations. Stark gives a line 7·4 less than  $c_3$ . This is possibly due to an own displacement in  $s_2$ , since  $s_2 = 7\cdot04$ .

I add a few further indications excerpted from larger maps, illustrating ionized links to neutral series lines.

$$\begin{aligned} (1) \quad 9333 \cdot 34 \quad D_{11}^{24} \quad 9121 \cdot 59 \quad (3 \text{ iii}) & \quad (1) \left\{ \begin{array}{l} 9121 \cdot 27 \quad S_1^{33} \\ 9829 \cdot 75 \quad (1) \end{array} \right. \\ \quad \quad \quad D_{23}^{23} \quad 9121 \cdot 89 \quad (1 \text{ ii}) & \\ \quad \quad \quad (2 \text{ i}) \quad 9829 \cdot 7 \quad S_1^{34} & \end{aligned}$$

$$D_4 = 35659 \cdot 49; D_3 = 37672 \cdot 32; S_3 = 34548 \cdot 85; S_4 = 40571 \cdot 17.$$

The foregoing examples afford indisputable evidence that the  $\alpha$ ,  $\beta$ ,  $\gamma$  separations appear as links, and, moreover, as links attachable to neutral lines as well as to ionized. The examples given are a sample only of the very large mass of data at disposal. The attachment to neutral lines shows also that they cannot enter there as displacements in a bi-term line, and thus directly supports the supposition of § 1 that their origin is due to independent  $p_2^+$  terms.

TABLE I.

The  $p_2$  separations from  $p_1$  (2, 3, 4).

$$p_1 2 = 92024.56; p_1 2 - = 30.557.$$

$\delta$ .	$p_2$	$p_3$ .	$p_4$ .
67	.....	2721.08	1183.12
68	.....	63.67	1201.44
69	9051.41	2806.29	19.75
69½	86.59	16.95	24.33
69¾	9121.80 $\alpha$	27.62	28.91
69¾	57.03	38.28	33.50
70	92.26	48.94	38.08
70½	9227.51	59.63	42.67
70½	62.80	70.32	47.25
70¾	98.09	81.01	51.84
71	9333.41 $\beta$	91.70	56.42
71½	68.73	2902.38	61.02
71½	9404.08	13.08	65.62
71¾	39.45	23.79	70.23
72	74.84	34.51	74.81
72½	9510.30	45.21	79.42
72½	45.65	55.92	84.02
72¾	81.11	66.66	88.61
73	9616.58	77.40	93.21
73½	52.06	88.12	98.81
73½	87.56	98.84	1302.42
73¾	9723.08	3009.57	07.02
74	58.61	20.31	11.63
74½	94.17	31.04	16.24
74½	9829.74 $\gamma$	41.77	20.85
74¾	65.31	52.50	25.47
75	9900.90	63.24	30.09

TABLE II.

 $S^2(2.m).$ 

$$92024.56 - 4R/(m + .835829 - .119166/m)^2.$$

$$p_1 2 = 30.557; p_2 2 = 35.18(68\delta) \text{ to } 35.56(74\delta).$$

$sm -$ $m.$	I.	n.	v.	$d\lambda.$
63.26				
1.*		[-57495.30] <sup>(1)</sup>		
	1 i	-48371.96	<b>9123.34</b>	.06 $\alpha$
*	0 ii	-47772.65	<b>722.65</b>	-.02 73 $\frac{1}{2}$
14.865				
2.*	10 i	35104.16		
	0 iii	44155.33	<b>9051.17</b>	.01 69
*	7 i	190.755	<b>086.59</b>	0 69 $\frac{1}{2}$
	7 i	226.04	<b>121.88</b>	0 $\alpha$
?	7 i	373.05	<b>268.89</b>	?
	7 ii	542.88	<b>438.72</b>	.03 71 $\frac{1}{2}$
??	0 i	611.24	<b>507.08</b>	.16 72 $\frac{1}{2}$
	0 i	684.8	<b>580.6</b>	.03 72 $\frac{1}{2}$
	5 i	828.27	<b>724.11</b>	-.05 73 $\frac{1}{2}$
	1 ii	862.07	<b>757.91</b>	.03 74
	10 i	933.44	<b>829.28</b>	$\gamma$ $\gamma$
?	0 i	45000.6	<b>896.4</b>	-.2 75
5.8147				
3.*	1	61578.06		
	4	70671.4	<b>9091.3<sup>(2)</sup></b>	-.09 69 $\frac{1}{2}$
	1	700.05	<b>121.99</b>	.00 $\alpha$
	2	71407.86	<b>829.80</b>	.00 $\gamma$
2.865				
4.*	3n	[73030.73]		
?	3n	82447.0	<b>9416.3</b>	-.18 71 $\frac{1}{2}$
	3	877.5	<b>846.8</b>	-.2 $\gamma$
1.616				
5.		[79036.66]		
*	1n	88090.2	<b>9053.5</b>	-.02 69
	1n	160.1	<b>123.4</b>	-.02 $\alpha$
	1	292.4	<b>255.7</b>	.09 70 $\frac{1}{2}$
*	0	550.4	<b>513.7</b>	-.03 72 $\frac{1}{2}$
	1	621.1	<b>584.4</b>	-.02 72 $\frac{1}{2}$
	0	754.8	<b>718.1</b>	.06 73 $\frac{1}{2}$
*	2	865.2	<b>828.6</b>	.01 $\gamma$

$sm -$ $m.$	I.	n.	v.	$d\gamma.$
1.0045				
6.	*	[82580.04]		
	1	91734.7	<b>9153.8</b>	.04 69 $\frac{1}{2}$
	0	954.0	<b>373.1</b>	-.05 71 $\frac{1}{2}$
.665				
7.		[84848.02]		
	0	93967.3	<b>9119.3</b>	.03 $\alpha$
	1	94437.6	<b>589.6</b>	-.08 72 $\frac{1}{2}$
	1	509.0	<b>661.0</b>	.08 73 $\frac{1}{2}$
	0	562.6	<b>714.6</b>	.09 73 $\frac{1}{2}$
.153				
8.	*	[86385.98]		
	1	95483.6	<b>9097.7</b>	-.1 69 $\frac{1}{2}$
	2	96182.05	<b>796.07</b>	-.01 74 $\frac{1}{2}$
*	1	237.1	<b>851.2<sup>(3)</sup></b>	-.2 $\gamma$
.336				
9.	*	[87477.28]		
*	2	96646.4	<b>9169.1</b>	-.13 69 $\frac{1}{2}$
	1n	777.3	<b>300.0</b>	-.02 70 $\frac{1}{2}$
	1	918.0	<b>440.7</b>	-.01 71 $\frac{1}{2}$
10.		[88279.67]		
	2	97503.9	<b>9224.2</b>	.03 70 $\frac{1}{2}$
11.		[88882.86]		
	3n?	98020.0 <sup>(4)</sup>	<b>9135.1</b>	-.13 $\alpha$
	1	212.5	<b>327.6</b>	.06 $\beta$
	0?	483.4	<b>598.5</b>	-.17 72 $\frac{1}{2}$
	1?	6 <sup>(5)</sup>	<b>734.4</b>	-.12 73 $\frac{1}{2}$

(1) Disrupted to  $(\pm \delta_1) S_1(\pm \delta_1)$ .(2) Estimated from C's  $S_1 = 61550.1$ , the same observer. Paschen's intensities are 5, abs. 9, 2.(3) Or  $74\frac{1}{2} \delta_1 d\lambda = .15$ .(4) Is probably  $P^2(1.7)$ .(5) Is  $P^2(1.5)$ .\* See  $n\lambda\nu$  list.

2. 2847.83 Cd.; 2264.03 D.; (...62.215; ...60.41; ...52.92) Cd.; ...44.40 E. H.; (...40.89; ...37.2; ...30.4; ...28.36) D.; ...24.82 Cd.; ...21.5 D.—  
 3. 1623.955 P.; 1415.0; (...14.427; 00.406) P.—4. 1212.9; ...06.6.—  
 5. 1135.2; ...34.3; ...32.6; ...29.3; ...28.4; ...26.7; ...25.3.—6. 1090.1; ...87.5.—7. 1064.2; ...58.9; ...57.5.—8. 1047.3; ...39.695 P.; 39.1.—  
 9. 1037.4; ...33.3; ...31.8.—10. 1025.6.—11. 1020.2; ...18.2; ...15.4; ...14.0

## Combinations.

$s_1-s_2$	4, 1080.1	92584
$s_2-s_3$	1, 3776.259	26472.742

## Notes.

The own shifts are given in the table. The limit  $p_1$  is determined as explained in the text. The formula is determined from this and  $m=2, 3$ .

$m=1$ . The extrapolated value of the denominator for  $m=1$  is 1.716663, and we should expect a value slightly less, or  $s_1-p_2$  about 57400  $\pm$ . We find here the sets:—

Ly. ....	6 57466.4	63.1	8 57529.5
C. ....	1 58.1		4 27.5
	9829.4; ...21.1		9339.7; ...37.9
D. ....	0 47636.98 iii?		On 48189.64 ii?

The mean of Ly and C. for the first gives ... 62.2, with doublet separation 9825.2. They suggest at first sight ( $\pm\delta_1$ )  $S_1$ ; but since here the W.N. is  $s_1-p_2$  (not  $p_2-s_1$ ) this would require the  $(+\delta_1)\beta$  separation on the right and  $(-\delta_1)\gamma$  on the left, whilst the opposite is clearly indicated. The difficulty is explained by the fact that  $s_1-$  is 63.26. The conditions are then met by the double displacement  $(\pm\delta_1)/(\pm\delta_1)$  shifting 63.26—30.56=32.70, or 65.40 for the two. We then get not only the observed separation of the two sets, but also the 9333.41+4.79=9338.20 and 9829.74—5.02=9824.72 in their proper positions. We can then calculate the true  $S_1$  from the more accurately measured  $(-\delta_1)S_2(-\delta_1)=-48189.64$ . Thus

$$(-\delta_1)S_1(-\delta_1)=-48189.64-9338.20=-57527.84.$$

Also  $p_1(-\delta_1)=92024.34+30.61=92054.95$ ;

whence  $s/(-\delta_1)=149582.79=4R/\{1.712577\}^2$

$$s_1=4R/\{1.712577+362\}^2=149519.64$$

$$S_1=-57495.30.$$

While this is not seen, two corresponding  $S_2$  lines are, viz. :—those in the table. We have here a very striking example of a normal line wholly disrupted into a very common arrangement of equal—like or unlike—displacements on both terms. The above value of  $S_1$  is subject to the same O.E. as that of 48189. The value of  $(\delta_1)S_1(\delta_1)$  calculated from this  $S_1$  is 57462.45, practically the mean of Ly. and C., whilst  $(\delta_1)S_2(\delta_1)$  is  $(\quad)S_1(\quad)-9824.72=47637.73$ . The measure by D. is .75 less, or  $d\lambda=.04$  between his two lines.

Although  $S_1$  is wholly disrupted, we find a line linked to it by the neutral  $e=20612.06$ , viz., 1 i, 36883.27; separated from it by 20612.03, practically the exact  $e$  i. The corresponding  $s1-p_13=P_1(1.3)$  is also found. We get, also, a very striking illustration of the general relation  $E=n\hbar\nu$  for  $n=3$  in the observed line

$$1 \text{ i } 19165.044 \quad \text{or} \quad \frac{1}{2} S_1 - .05.$$

Also for  $S_2$

$$1, \quad 2 \times 24098.9 \text{ E.V.} \quad = 48197.8 \quad \mathbf{9297.5} \quad (70)\frac{1}{2} \delta \quad d\lambda=.01$$

$m=2$ . The following collaterals are found, comparing Stiles with Stiles (35106.16) :—

	Obs.	
$(-\delta_1)S_1(\delta_1) = 35751.58$	$\dots 54.233 - 6y + .07$	3 2848.774
$(\delta_1)S_1(-2\delta_1) = 35045.88$	$\dots 47.739 - 4y - .05$	2 i ...52.415
$? (-\delta)S_1(2\delta_1) = 35258.12$	$\dots 257.451 + y - .22$	1 ...35.448
Cd. $(-3\delta_1)S_1(3\delta_1) = 35240.44$	$\dots 240.65$	$\frac{1}{2}$ ...36.80

Further, if the  $2\hbar\nu$  effect is admitted, the additional  $S_2$  lines come in:—

1 4510.5 Stk.	$2 \times 22164.8 \pm 1 = 44329.6 \pm 2$	<b>9225.4</b>	.2	70 $\frac{1}{2}$
2 iii 4506.704	$2 \times \dots 82.964 = \dots 365.928$	<b>9261.77</b>	.1	70 $\frac{1}{2}$
1 iii 4499.8 E. V.	$2 \times \dots 217.5 \pm .5 = \dots 435.0 \pm 1$	<b>9330.84</b>	.25	71

$m=3$ . The far more accurate measures of P. have been inserted. Bl. gives two collaterals, 1,61512.0, 1,61648.5, shifted 68 on either side of  $S_1$ , whilst  $2\delta_1/-\delta_1$  shifts  $61.12 + .5.81 = 66.93$ . They are then  $(\pm 2\delta_1)S_1 3(\mp \delta_1)$ .

Also, if  $2\hbar\nu$  be admitted,

$$2 \times 35669.186 \text{ Cd.} = 71338.37 \quad \mathbf{9760.31} \quad -.07 \quad 74$$

$m=4$ . The calculated  $S_1$  shows two very doubtful  $S_2$ , and is itself disrupted; the corresponding line in  $S(3.4)$  is visible. It is emitted as  $h3\nu$ ,  $2h\nu$  however, viz.  $3 \times 24343.34$ ;  $3 \times 36525$ .

$$1 \ 1367.2 \quad 73142.2 = (-\delta)S_1(-\delta) \quad d\lambda = -.01$$

On the  $2h\nu$  basis

2 ii	2433.87 D.	$2 \times 41074.37 = 82148.74$	9118.0	.1	$\alpha$
1 iii	2424.46 D.	$2 \times 41233.78 = \dots 467.56$	9436.8	.08	$71\frac{1}{2}$
0	2421.35 D.	$2 \times \dots 286.73 = \dots 573.46$	9542.7	.09	$72\frac{1}{2}$
1 i	2417.16 D.	$2 \times \dots 358.29 = \dots 716.58$	9685.8	.05	$73\frac{1}{2}$

The first, 41074, is also  $S_2(3.9)$ .

$m=5$ . The following collaterals are noted:—

1n,	1264.7	79070.1	$(-\delta_1)S_1(+\delta_1)$	$d\lambda = -.07$
1n,	63.7	79132.7	$(-3\delta_1)S_1(3\delta_1)$	$d\lambda = .00$
1n,	64.1	78982.0	$(2\delta_1)S_1(2\delta_1)$	$d\lambda = -.05$

The  $s5$ — are now, and beyond  $m=5$ , comparable with O.E. Those given here may therefore err by one unit on  $sm$ . All the  $S_2$  are successive lines in C.'s list.

$m=6$ . This even order seems to show no collaterals except, possibly,  $(\delta)S_1(-\delta) = 82454.84$ . An observed 82447.0 may be a merge of this and  $S_24$ .

$m=7$ . Doubtful collateral

$$(-\delta)S_1(-\delta) = 84961.8 d\lambda = -.14.$$

$m=8$ . The O—C values may be partly due to formula errors. If the true  $S_1$  be that suggested by  $2 \times 43194.63$ , the formula error is 3.32,  $d\lambda = -.03$  and the separations are then more closely met.

On  $2h\nu$  basis

$$0 \text{ ii} \quad D. 2 \times 47755.07 = 95510.14 \quad 9124.2 \quad -.05 \quad \alpha$$

$m=9$ .

	Obs.	
$(\delta_1)S_1(\delta_1) = 87447.00$	$\dots 50.8$	$d\lambda = -.05$
$(2\delta)S_1(2\delta) = 87235.50$	$\dots 37.2$	$= -.02$

With these high orders the S and D lines come close together. There are several other near possible collaterals, but they may be related to D9.



TABLE III.

S(3, m).

S(4, m).

$$p_1 2 - p_1 3 = 49221 \cdot 09; p_1 3 - = 9 \cdot 6708.$$

$$p_1 3 - p_1 4 = 18052 \cdot 33; p_1 4 - = 4 \cdot 2625.$$

1, 2. See P(1.3), P(2.3).

2. See P(2.4).

5.8147

3. [12356.97]

-[5695]

1 15376.89 3019.92 .11 74

2.865

4. 1 23808.5

-.09

[5755]

[ 7.98]

? 1 26573.232 2765.25 -.2 68

1 613.0 805.0 .18 69

2 ii 624.3 816.4 .08 69½

2 A 656.782 838.80 -.07 69¾

1 677.606 869.62 .09 70½

3 ii 806.584 998.60 .03 73½

\* 1 829.4 3021.4 -.1 74

1.616

5. [29816.27-7]

5. [11763.3]

\* 1 32772.23 2955.96 -.02 72½

3 13029 1265.7 0 71½

\* 3 ii 825.16 3008.89 .06 73¾

4 900.46 084.19 .03 75½

2 922.23 105.96 .00 76

1.004

6. \* [33360±]

6. [15307.2]

1 36123.0 2763 0 68

1 i 16500 1192.8 -.2 67½

2 ii 535 227.8 -.4 α

1 i 573 265.8 .07 71½

2 ii 593 285.8 .6 72½

2 i 615 307.8 .3 73¾

.665

7. [35627.06-13]

7. [17574.60]

3 ii 38457.30 2830.24 -.17 α

3 i 18803.47 1228.87 .00 α

0 ii 500.20 873.19 -.20 70½

4 i 821.5 246.9 -.09 70½

0 ii 518.05 891.00 .05 β

1 i 834.3 259.7 -.4 71½

2 i 881.9 307.7 .2 73¾

? 1 i 903.3 328.7 .7 75

453

8. [37164.89]

8. [19112.56]

0 ii 39908 2743 -.05 67½

2 20328.6 1216.0 -.2 68¾

0 ii 981.39 816.50 .02 69½

1 415.2 1302.6 .05 73½

1 iii 40207.95 3043.06 .09 γ

2 ii 420.4 307.8 .2 73¾

2 ii 237.24 072.35 .09 75½

2 n 443.067 330.50 .10 75

.336

TABLE III. (cont.).

S(3.m).				S(4.m).			
9.	[38256.19]			9.	[20203.86]		
1 ii	38258.91	2.72=6 $\gamma$	0	2	21419.2	1215.3	-02 68 $\frac{1}{2}$
2 ii	41074.87	2818.18	-07 69 $\frac{1}{2}$	1	442.1	238.2	-02 70
2 ii	212.52	956.33	-02 72 $\frac{1}{2}$	2 $\pi$ i	445.714	241.85	-17 70 $\frac{1}{2}$
1 iii	233.78	977.59	-00 73	1	483.9	280.0	-1 72 $\frac{1}{2}$
0	286.73	3030.54	-03 74 $\frac{1}{2}$	1 iii	21511.164	307.30	-06 73 $\frac{1}{2}$
10.	[39058.58]			10.	[21006.25]		
1 ii	60.40	1.81=4 $\gamma$	-12	1 iii	226.4	220.2	-1 69
1 ii	780.35	2721.79	-06 67	1 iii	257.563	251.31	-10 70 $\frac{1}{2}$
4 i	41825.44	766.86	-1.8 68	2 ii	266.818	260.57	-10 71 $\frac{1}{2}$
0 i	847.33	788.75	-21 68 $\frac{1}{2}$	1 iii	312.716	306.47	-1 73 $\frac{1}{2}$
0 ii	861.5	803.0	-1 69				
0 i	871.69	813.11	-2 69 $\frac{1}{2}$				
1 ii	949.87	891.29	-02 $\beta$				
0 i	42039	980.4	-2 73				
11. 0 i	39663.21		-02	11. 2 $\pi$ i	21610.4		-1
1 i	42532.01	2868.80	-08 70 $\frac{1}{2}$	2 iii	22811.222	1200.8	-1 68
(4) i	620.85	957.64	-09 72 $\frac{1}{2}$	2 i	861.561	251.1	-1 70 $\frac{1}{2}$
3 i	693.84	3030.63	-02 74 $\frac{1}{2}$	1	879.5	269.1	-2 71 $\frac{1}{2}$

S(3.m). 3. 6501.47 P.—4. 4199.1; 3762.122; ...56.6; ...55.0 Stk.; ...51.737; ...47.401; ...41.7; ...29.399; ...26.3.—5. 3150.58 K. R.; ...45.56 P.; ...38.69 K. R.; ...36.68 E. H.—6. 2767.6.—7. 2599.51; (...96.61; ...95.41.—8. 2505; ...00.41; 2493.23) D.; ...86.32 P.; ...84.51.—9. 2612.99; 2433.87; ...25.71; ...24.46; ...21.25.—10. 2559.37; 2392.74) D.; ...90.16 St.; (...88.91; ...88.1; ...87.52; ...83.07; ...78) D.—11. (2520.47; 2350.45; ...45.55; ...41.54) D.

S(4.m). 5. 7673 W.—6. (6059; ...46; ...32; ...25; ...17) Bl.—7. 5316.87 W.; ...11.7; ...08.0; 5294.7; ...88.7.—8. 4917.9; 4897.1 W.; ...95.8; ...95.45 W.—9. 4667.5; ...62.6 W.; ...61.635; ...53.6 W.; ...47.452.—10. 4499.8; ...98.0; ...91.603; ...89.732; ...80.496.—11. 4626.2; 4382.580; ...72.930; ...69.6.

## Notes.

$m=3$ . If the separation is the correct 3020.21, the correct  $S_1$  should be .29 less and =12335.68. Instead of this are found two lines on either side displaced ( $\pm \delta_1$ ) S ( $\pm 2\delta_1$ ), shift = 9.67 + 11.63 = 21.30. Thus

	Obs.	
$(\delta_1)S_1(-2\delta_1)=12335.38$	...36	1, 8104
$(-\delta_1)S_1(2\delta_1)=...77.98$	...77	2, 8077

In S(2.3) were found ( $\pm 2\delta_1$ )  $S_1(\mp \delta_1)$ .

$m=4$ . The value deduced from  $S(2.4)$  is 23809.64. This gives exact  $\nu$  with the 26573. The observed is 23808.5. The value in [ ] used as  $S_1$  is the value deduced from the accurate measure of the collateral  $(2\delta_1)/(-6\delta_1)$  given below. All these are within O.E. of  $S(2.4)$ . In the neighbourhood are found

	Calc.	Obs.	
$(2\delta_1)S_1(-6\delta_1)$	= 23771.45	...71.452	1 4205.546
$(\delta_1)S_1$	= 23798.31	...98.9	1 ...00.8
$S_1$	= [23807.98]	...08.5	
$(-2\delta_1)S_1(-2\delta_1)$	= 23821.59	...21.646	2 ii 4196.684
$(-3\delta_1)S_1(\delta)$	= 23848.45	...48.367	1 i ...91.982

23771, 23821 are mutually displaced by  $(\delta)/(-\delta)$ . In  $S(2.4)$  we found  $(-\delta)/(-\delta)$ . The agreement in these very accurate measures, with such large own shifts, is remarkably close. 26646 or  $(69\frac{3}{4})S_2$  is given by Bl. as an arc line. But Steinhausen gives it as enhanced. Also E.V. and E.H. give it intensity 4 in the spark to Stiles's 2 in the arc.

$m=5$ . The  $S_1$  is taken .7 larger than that deduced from  $S(2.5)$ . The following collaterals have been noted

	Obs.	
$(-\delta_1)S_1(\delta_1)$	= 29827.56 ...27.36	$D_{11}(3.5)$ 1 3351.61
$(-2\delta_1)S_1(-2\delta_1)$	= 29832.38 ...32.42	1 iii 3351.098

They are No. 22 in the satelloid list.

$S(3.m).$

$S(4.m).$

$m=6$ .

This even order, as in  $S(3.6)$ , gives no observed line, no evident collaterals, and few  $S_2$ .

The  $S_2$  are a set of five successive lines observed by Bl. alone.

$m=7$ .

	Obs.
$(\delta_1)/(-\delta_1)$	= 35616.71 ...16.73
$(-\delta)/(\delta)$	= ...68.40 ...69.186 Cd.,

but they are No. 8 in the satelloid list. P. gives 35622.11, .5.38 larger. It may be  $2\delta$  on  $\delta$ , shift=.5.32.

The first  $S_2$  by W. ( $\lambda=5316.87$ ) is marked "i" on the supposition that it is the same as 5317.2 by Bl., which is doubtful. The last four are a successive set by E. V.

	Obs.
$(2\delta)/(\delta)$	= 17543.16 ...43.03 P.
$(5\delta_1)/0$	= .. 53.29 ...52.5 E. V.

S(3.m) (cont.).

S(4.m) (cont.).

$m=8$ .

Collaterals show that  $[S_1]$  should be about .23 less. Thus

Collaterals.

	Obs.
$(-\delta)/(-2\delta_1) = 37202.43$	...02.426
$(2\delta)/(-9\delta_1) = 37149.40$	...49.48 D.
$(10\delta_1)/(-11\delta_1) = 37129.15$	...29.33 D.

	Obs.
$(3\delta_1)/(3\delta_1) = 19101.11$	...01.6 E. V.
$(6\delta_1)/(3\delta_1) = 19088.35$	...88.1 Stk.
$(-6\delta_1)/(-3\delta_1) = 136.77$	...36.7 Stk.

The last is  $(2\delta_1)/(-2\delta_1)$  on the second, but see D(3.8).

$m=9$ .

The calc.  $S_1$  differs from the obs. by 2.72 or the persistent satelloid 6 $\mu$ . The separations are taken from [ ]. With the observed line

The last  $S_2$  has reliable measure, and corrects  $[S_1]$  by .28, and this simultaneously alters the  $d\lambda$  for the others to 0, 0, .23, -.09, 00. This excludes the 70 $\frac{1}{2}$ .

	Obs.
$(3\delta_1)/(-3\delta_1) = 38228.89$	...29 D.

$(-5\delta_1)/(-5\delta_1) = 20223.51$ (or .79)	Obs. ...23.8 E. V.
-------------------------------------------------	--------------------

$m=10$ .

If  $[S_1]$  be taken .50 less the three reliably measured lines give separations respectively with  $d\lambda = .00, -.01, -.01$ , but E. V.'s require -.2.

$m=11$ .

The intensity for the 72 $\frac{1}{2}$  is that for it and a near line combined.

The two reliable measures for the 68, 70 $\frac{1}{2}$  lines differ by 50.34 compared with 1251.84 - 1201.44 = 50.40. Accepting them as true,  $S_2$  corrects E. V.'s  $S_1$  by -.68 ( $d\lambda = .14$ ). Also reduces that for 71 $\frac{1}{2}$  to .1.

Table of Observed Collaterals in Our Multiples.

$m$ .	S(2.m).	S(3.m).	S(4.m).
1.	$\pm 1/\pm 1$		
2.	$-1/+1$ ; $\pm 1/\mp 2$ $-3/3$ ; $-4/2$		
3.	$\pm 2/\mp 1$	$\pm 1/\mp 2$	
4.	$-4/-4$	$\left. \begin{matrix} 2/-6 \\ -2/-2 \end{matrix} \right\} \text{rel } 4/-4$ $1/0$ ; $-3/1$	
5.	$-1/1$ ; $2/2$ $-3/3$	$-1/1$ ; $-2/-2$	...
6.	$4/-4$	...	...
7.	$-4/-4$	$-4/1$ ; $1/-1$	$8/1$ ; $5/0$
8.	...	$-4/-2$ $8/-9$ ; $10/-11$	$3/3$ ; $\pm 6/\pm 3$
9.	$1/1$ ; $8/8$	$3/-3$ 3 A 2	$-5/-5$

TABLE IV.— $e.S^2(2.m)$ .

$$e=20612.06.$$

m.	l.	n.	v.	dλ.					
1.	3i	-36883.272		0	6.	[61968.88]			
	1	-27795.3	9088.0	-18.69½	3	71907.86	9439.0	.01	71½
2y	2	725.185	158.09	.01 69½	1	653.8	685.0	.05	73½
	1	688.3	195.0	-.36 70	7.	[64236.0]			
	1	617.2	266.1	-.4 70½	0	73399.9	9163.9	.12	69½
	3	514.350	368.92	-.01 71½	2	458.71	222.7	.05	70½
4y	8ii	477.259	406.01	.00 71½	2	501.3	265.3	.04	70½
	1	052.3	831.0	-.2 γ		674.55	438.5	.01	71½
2.		[14492.10]			?	1 74060.30	824.3	.09	γ
	1	24545.0	9052.9	-.3 69	8.	[65773.92]			
-5y	4ii	611.783	9119.68	.03 a	0	72.2		.04	
	3	649.180	157.08	.00 69½	*	3 74861.5	9089.3	.05	69½
-2y	1	24001.339	509.24	-.02 72½	3	895.1	122.9	.01	a
	1	005.7	513.6	.3 72½	1	928.8	156.6	.00	69½
5y	1	112.735	618.67	.02 73	4	75142.8	370.6	.03	71½
3y	2ii	145.566	653.46	.01 73½	3n	386.4	614.2	.04	73
8y	1	147.635	655.53	.02 73½	3	568.6	896.4	.08	75
-3y	1	178.463	686.36	.02 73½	9.	[66865.22]			
4y	4ii	252.537	760.44	.00 74	1	76132.5	9267.3	.07	70½
3.	0iii	40968.66		-.04	1	266.0	400.8	.05	71½
	1ii	50478.29	9509.63	.02 72½	2	593.1	727.9	.08	73½
-7y	2ni	* 617.53	648.87	.00 73½	1	799.0	933.9	.04	75½
-2y	2n	690.65	722.00	0 73½	10.	[67667.61]			
4.		[52418.67]			4	69.52		.04	
	*		9830	0 γ	0	77077.2	9407.7	.03	71½
5.		* [58424.60]				106.9	437.4	.04	71½
	0	67444.5	9019.4	.06 63½	0	220.1	550.6	.08	72½
	2	755.3	330.7	.06 β	0	429.3	759.8	.02	74
	1	870.2	445.6	.1 71½					
	2	68150.0	725.4	.05 73½					
	3	222.1	797.5	.07 74½					

\* See *new* list.

1. 2710.454; 3596.8 Stk.; 3805.804; ...10.7; ...20.0 Stk.; ...33.435;  
 ...38.340; ...95.6.—2. 4246.1 Stk.; ...33.985; ...27.200; 4196.684; ...65.264;  
 ...64.6; 46.024; ...40.385; ...40.182; ...34.750; ...22.121.—3. (2440.15;  
 1980.40; ...74.95; ...72.10) D.—5. 1482.7; ...75.9; 73.4; ...67.35 McL.;  
 ...65.8.—6. 1400.406 P.; 1395.6.—7. 1362.4; ...61.307 P.; ...60.52 McL.;  
 ...57.321 P.; ...50.251 P.—8. 1520.4; 1335.8; ...35.2; ...34.6; ...30.8;  
 ...26.5; ...23.3.—9. 1313.5; ...11.2; ...05.6; ...02.1.—10. 1477.770 P.;  
 1297.8; ...96.9; ...95.4; ...91.5.—11. 1291.5.

As in the  $S(2.m)$  lines all contain the  $p^2$  term, the presence of satelloids may be not unexpected. It has been found that in Cu linkages exact link values frequently go to main-line satelloids, so that a similar effect should be looked for here. This can only be tested where we have very accurate measures. Where these have been found, the suggested  $\gamma$  multiples are entered in the first column ( $m$ ) and the residual errors in the  $d\lambda$  column.

## Notes.

$m=3$ . 40968.0 is calculated from C.'s 61580. If we use P.'s 61578.06, giving 40966.00, the observed  $d\lambda=.15$  is probably  $> O.E.$  This would seem to establish C.'s as a real value, satelloidal 2.71 to P.'s.

As  $2h\nu$  with exact  $\nu$ , without satelloids

$$1, 2 (25310.274 + .08) \quad 50620.70 \quad 9652.04 \quad .01 \quad 73\frac{1}{2}$$

$m=4$ . No representatives for  $e.S_1$  or  $e.S_2$  have been noted. But we do find  $u.S_1$  and  $e.S_1.u$ . I find the neutral  $u$  link, calculated from a possible  $s_1$  (an allocation not published), and tested on a long list of neutral lines, to be 14819.4. With this

	Obs.	
$u.S_1(4) = 73030.75 - u = 58211.3$	...06 (Ly.)	
$e.S_1(4).u = 52418.67 + u = 67338.1$	...40.1	$d\lambda = -.04$

As a possible  $2h\nu$  effect

$$2 \times 31124.47 = (62248.94) \quad \text{gives } 9830.1 \gamma \quad d\lambda = .00$$

$$\lambda = 2, 3211.98 \text{ P.} \quad 2 \text{ iii } 3212.0 \text{ BL.}$$

$m=5$ . The  $72\frac{3}{4}\delta$  line, 1467.35, is McL.'s measure ( $C = \dots 7.5$ ). This also shows 9334.4 forwards. McL. allocates this to a doubly ionized line iii  $d^3p^3$ .

$$2h\nu \ 2(29210.9 + 1.4) = e.S_1.5 \quad d\lambda = 1$$

$m=6$ . 71407 is also  $S_2.23$ .

$m=8$ . For the first  $S_2$  there is a  $2h\nu$  representative which gives nearly an exact  $\nu$ , viz.,  $2 \text{ i}, 2 \times 37428.9 = 74857.8, 9085.8$ .

$m=9$ . The first separation 9267.3 may be a representative of the 9268.7 appearing with the  $S_{1,2}$  list in §1.

TABLE V.— $P^2m$ .

$$s_1 = 149519 \cdot 64.$$

$$s_1 = 63 \cdot 26.$$

$$s_2 = 56920 \cdot 18. \quad 92599 \cdot 46. \quad s_2 = 14 \cdot 865.$$

$$s_3 = 30444 \cdot 3. \quad 26475 \cdot 9. \quad s_3 = 5 \cdot 8147.$$

$$p_1(m) = 4R/\{m + 236030 - 103608/m\}^2.$$

 $p_1 =$ 

$m.$	$l.$	$n.$	$v.$	$d\lambda.$
------	------	------	------	-------------

P(1.  $m$ ).P(2.  $m$ ).

2.

see 81.

see -82.

9-6708.

3. 1 \* 106712  $\pm$  5 [...16]

1 14116-93 0

\* 0 103928 2784 0 68 $\frac{1}{2}$ 

1 11394 2723 67

1 864 2848 0 70

1 11363 2754 67 $\frac{1}{2}$ 

2 605 3107 0 76

1 11319 2798 68 $\frac{1}{2}$ 1 11077 3040  $\gamma$ 

4-2625.

4. \* [124768]

1 i 32169-257 0

1 30971-558 } 1196-79 0 67 $\frac{1}{2}$  $\frac{1}{2}$  73-96

2-2435.

5. [133384]

1 i 49784-65 6

0 148-5 636-1 -03 69

\* 1 i 096-52 688-13 1  $\gamma$ P(3.  $m$ ).

1-3936.

6. 1 i 19101-6 3

1 ii 45550-67 } §

2 ii 18741-4 360-2 0 66 $\frac{1}{2}$ 

0 ii 606 } †

3 712-3 389-3 0 71 $\frac{1}{2}$ \* 0 ii 230-83 375-2 0 69 $\frac{1}{2}$ 

3 i 699-7 401-9 0 74

0 163-00 387-67 $\frac{1}{2}$  0 71 $\frac{1}{2}$ 1 n 678-4 423-2 -2 77 $\frac{1}{2}$ 

-8445.

7. 3 22034-79 09

\* 0 n i 48482-91 }

2 ii 21794-6 240-2 08  $\alpha$ 

\* 0 i 521-50 }

3 780-84 253-95 02 73 $\frac{1}{2}$ 0 iii 279-70 241-80 01 70 $\frac{1}{2}$ 

-5718.

8. 3 ii 23941-770 }

1 983-644,

1 n 798-9 }

P(1.  $m$ ). 3. 937-1; 962-2; 962-8; 965-2.P(2.  $m$ ). 3. 7081-96 St.; (8774; ...98; ...88-32; 9025) McL.—

4. 3107-659; 3327-840; ...7-59 Od.—5. (2451-16; ...90-0; ...93-23) D.—

6. 2194-67; ...92; 2210-19; ...13-51) D.—7. (2061-92; ...60-28; ...70-60) D.

P(3.  $m$ ). 6. 5223-8; 5334-3; ...42-6 P.; ...46-3; ...52-4.—7. 4537-01 P.; 4587-1; ...89-91 P.—8. 4175-628; ...68-837; 4200-8.

Notes.

$m=3$ .—In P(2.3) the correct  $\nu$  are 2721.03 ; 53.06 ; 95.65 ; 3041.67. The last three  $P_2$  have similar linkages, viz. :—

	9828.1	1	20905.1	9120.8	3 iii	30025.9	Bl.
1, 11077	9121.3	1 ii	20198.32	9826.6	↑	9332.02	↓
	9330.5	1 iii	20407.52	9122.82	1	29530.34	
	9829.4	1 iii	21148.01				
11319	9124	2n	20443.07	11363	9122.7	1 ii	20485.7
	9331	1 iii	20650.43				

In P(1.3) there is also a possible  $2h\nu$  representative

$$2 \times 51040.00 \text{ iii } D=103889.0 \quad 2836\gamma \quad d\lambda=.04.$$

$m=4$ . There is a long set of successive lines, only observed by Bl., and all of class E2, which fit in for various  $P_2$  lines :—

1.	1	3243.7	30820.1	1349.2	$d\lambda=-.1$	76 $\frac{1}{2}$
2.	1	43.9	843.9	25.4	0	74 $\frac{1}{2}$
3.	1	39.4	861.0	08.3	-.13	73 $\frac{1}{2}$
4.	1	38.5	869.6	1299.7	-.2	73 $\frac{1}{2}$
5.	2	35.3	900.1	69.2	.1	71 $\frac{1}{2}$
6.	2	30.7	944.1	25.2	-.1	69 $\frac{1}{2}$
7.	1	25.9	990.2	1179.1	-.06	66 $\frac{1}{2}$
8.	1	24.0	31008.4	60.0	-.07	65 $\frac{1}{2}$

with, possibly, a few others of larger multiples. The class iii points to the supposition that these are not normal lines, but accidentals formed by the high excitation. Many show similar links. Thus 1, +9123.1 ; 2, +9121.8 ; -9122.0 ; 3, +9121. ; -9823.9 ; 4, -9828.0 ; 5, -9829.4 ; 7, -9121.2, +9828.1.

The following collateral coincidences may be noted :—

	Obs.
(2 $\delta_1$ )P(1.4)(- $\delta$ )=124624.5	1 ...22.1
( $\delta$ )P(2.4)(- $\delta_1$ ) = 32105.54	1 iii ...05.8 Bl.
( $\delta_1$ )P(2.4)(- $\delta_1$ ) = 32150.13	3 iii ...49.2 Bl.



$m=5$ . The formula  $P_1(2.5)$  is 40794.58. Denoting this by (P).

		Obs.	
$[P](-\delta_1)=40785.61=X$	1 i ... 4.65 D.	$d\lambda=-.06$	
$(2\delta_1)X(-2\delta_1)=51.40$	0 iii ... 51.4 D.	$d\lambda$	0
$(-2\delta_1)X(\delta_1)=40817.58$	0 ii ... 18.29 D.	$d\lambda$	.04
$(-3\delta_1)X(-\delta_1)=27.942$	2 ii ... 27.96 D.	$d\lambda$	0

\*  $3, 2 \times 20048.2$  E. V. =  $P_2$ .

40784 has a curious linkage set, viz.,

1 ii 40784.65	9331.37	6 ii 50116.02	* $2, 2 \times 25059.006$ , exact $\beta$ .
	↓ 9832.88		
6 41286.73	9330.80	2 ii 50617.53	* $3, 2 \times 25308.9$ E. V.
	↑ 9126.22		
0 ii 41491.31	9330.80	0 i 50621.79	
	↓ 9830.48		
1 ii 41988.81	9332.8	4 i 51321.79	* $1, 2 \times 25660.733$
	↑ 9122.8		
0 42199	↑		

$m=6$ . The formula value for  $P(2.6)$  is 45578.90, which is the mean of the two bracketed lines in the list. These are separated by  $55.3 \pm$ . A displacement  $\delta/\delta$  shifts  $59.46 - 4.01 = 55.45$ . They therefore suggest  $(\pm 2\delta_1)/(\pm 2\delta_1)$ . Taking the reliable measure 45550.67 as  $(2\delta_1)P(2\delta_1)$  gives  $P=45578.39$ , which reproduces the formula value ( $d\lambda=.02$ ), but no  $P_2$  lines corresponding to this have been noted. 45163 is an arc line and  $D_{33}^3 8$ , and is probably a coincidence.

\*  $2$  iii  $2 \times 22615.5 = P_2 6$ .

The  $P(3.m)$  now come into view. The calculated  $P_1$  is  $45578.39 - 26475.90 = 19102.49$ , obs. by E.V...1.6.

$m=7$ . Again we find the formula value of 48509.14 disrupted into two, viz.,

	Obs.
$(2\delta_1)P(\delta)=48482.78$	...82.91
$(-\delta_1)P(-3\delta_1)=...521.47$	...21.50

with two  $2h\nu$ . \*  $2 \times 24241.07 = P_1$ ;  $2 \times 24261.843 = P_1$ .

The calculated for P(3.7) is 22035.24, for which we find three close lines.

1 iii 22032.698 St. 2.09 3, ...4.79 P. 2.82 2, ...7.61 P.

which appear satelloidally connected. The  $\alpha$  separation for  $p_7$  is 239.76 and  $p_2 7 = 8805$ .

$m=8$ . The formula value for P(3.8), 23957.82, is not observed, but two near lines on either side fit as collaterals:—

	Obs.
$(3\delta_1)P(2\delta_1)=23941.5$	...41.770
$(-\delta)P(\delta)=...83.3$	...83.644

These are very reliable measures with separation = 41.874. The two sets of displacements give  $(23.359 + 2.287) + (17.444 - 1.143) = 41.847$ , or  $d\lambda = .005$  on two lines, a remarkably close agreement. The 23798 may be a  $P_2$  representative to an intermediate line. The doublet separations corresponding to  $69\delta$ ,  $74\delta$  are 160.76, 172.65.

### pp Combinations.

In these tables wave numbers in the same horizontal line refer to the same  $p(2)$ ; in the same column to various  $p_2 3$  or  $p_2 4$ ; thus 55302 is  $\alpha p_2 - \gamma p_3$ ,  $\alpha p$ , etc., denoting the  $p_2$  depending on the  $69\frac{1}{2}\delta$  displacement, etc. To save space, however, a given column is not confined to the same  $p_2$ . Over each wave number are placed (1) the separation from the corresponding  $p_2$  on the left, (2) the displacement involved as a multiple of  $\delta$ , and (3) the O—E  $d\lambda$ . The  $\lambda$  are given below, each column in order. Examples for the  $(69\frac{1}{2})p_2 2$  are also given. It will be noticed that no  $p_1 2 - p_1 m$  are observed.

$p_2 \dots p_1$			
$p_2 - p_1 +$	1214.5 68 $\frac{1}{2}$	.01	
$p_1 2 [67.273.42]$	2, 66058.9		
9086.59	1217.2 69	.05	1273.7 72 .02
$(69\frac{1}{2}\delta)[76360.01]$	4, 75142.8 (1)		1, 75086.3 (2)
9121.9	1252.5 70 $\frac{1}{2}$	.01	1309.0 74 .04
$\alpha p_2 [76395.30]$	4, 75142.8 (1)		1, 75086.3 (2)
9333.4	1220.4 69	.01	
$\beta p_2 [77606.8]$	2n, 75386.4		
9833.5 (.06)			
$\gamma p_2 2, 77106.9$			
1296.9; 1513.8; 1330.8, ...1326.5; 1331.8, ...			

(1), (2) Necessarily closely the same. Also (1) is  $e. S_2 28$ .

*p2-p3.*

<i>p2-p1</i> 3	2825.99 $\alpha$ —.07	2846.86 70 —.1	2915.8 71½	.03	3051.31 74½ —.09
<i>p1</i> 2[49221.09]	1 i 46395.10	3 iii 46374.25	0 i 46305.3	0 ii 46170.78	
9086.59 69½		2870.4 70½ 0			
(69½) [58307.68]	—	3 55437.3	—	—	—
9121.9 $\alpha$	2807.2 69 .02	—	—	—	3040.6 $\gamma$ .04
$\alpha p2$ [58343.0]	1 55535.8 (1)	—	—	2 55302.4	
9333.4 $\beta$		2879.6 70½ —.06	2956.9 71½	.04	3018.7 74 .05
$\beta p2$ [58554.5]	—	7 55674.9 *	9 55597.6 (2)	1 55535.8 (1)	
9829.7 $\gamma$	—	2870.1 70½ 0	—	—	—
$\gamma p2$ [59051.8]	—	1 56181.7	—	—	—

2154.72, 1800.7; 2155.69, 1803.9, 1796.2, 1780.0; 2158.9, 1793.7; 2165.19, 1803.3, 1800.7. The lines in *R.A.* are by *Lx*.

(1) These are necessarily very close.

(2) This belongs also to a set parallel to *S1*(*HgI*), viz.:—1631.—*S1*. Also this and 55674 should probably be excluded as too intense, in spite of numerical agreement, or they may be covered by stronger lines. The latter has a  $2h\nu$  representative, but it probably belongs to some other allocation.

TABLE VI.—D<sup>2</sup>; (8Δ<sub>a</sub>).

92024·34	$p_1 2- = 30·557$	
42803·25	$p_1 3- = 9·6708$	Sep. = 49221·09
24750·92	$p_1 4- = 4·2625$	„ = 18052·33
$d_1 m = 4R / \{m + \cdot 811818 + \cdot 008086/m\}^2$ .		

$d_1 m -$ m.	I.	n.	v.	dλ.						
					D(2. m).		D(3. m).			
52768; $d_2 - = 53.99$ .										
1.	8 ii	{ -42463.90		0				{ [-91684]		
	2 i	{ -40435.78	2028.12	0	9½	1 n	-89645	2038		
	1 n	-33200.14	9263.76	.08	70½					
14246; $d_2 - = 14.439$ .										
2.	1 i	{ 36192.88		0		3		{ -13028.21		
	4 ii	{ 694.5	501.63	0	8½	1		{ -(12526.55)	501.66	
	1 i	45533.86	9340.98	β+7.57	1		-10296	2732.2	.5	67½
	4 i	632.36	9439.48	0	71½	2	-10084	2944.2	.8	72½
	0 i	46029.85	9863.97	γ+7.24	3		-9784.9	2741.6	.7	67½
					4		-9664.8	2861.7	.2	70½
					6		-9634.1	2892.4	.7	β
57307; $d_2 - = 5.795$ .										
3.	1	{ 61648.5		0				{ [12427.41]		
		{ [61873.18	224.7	0	9½			{ [12652.09]	224.6	
	1	70700.35	9051.5	.00	69	2	15330.54	2903.13	-3	71½
	0	736.4	9087.9	.02	69½					
	2	71407.86	9759.3	.02	74					
D <sub>21</sub>	0	957.2	9084.0	-.05	60½					
2.851										
4.	0	{ 72987.4				3		{ 23768.32		
		{ [73092.22]	104.8	-.02	9½	1		{ 23670.5	102.2	.1 9
	1	82182.8	9195.4	.04	70	1	26703.64	2935.32	-10	72
	4	82250.4	9263.0	.003	70½	1 ii	712.69	2944.37	-11	72½
						1	767.83	2999.51	-11	73½
1.6226										
5.	1 n	{ 78982.7				3 ii		{ 29764.23		
		{ [79043.10]	60.4	0	9½	1		{ 29827.86	63.63	.03 9½
	0	88778.4	9795.7	.02	74	1 iii	32527.8*	2763.7	0	68
						1 iii	549.0	2784.8	0	68½
						2 iii	654.3	2890.1	.1	β
						3 i	709.60	2945.4	0	72½
1.0057										
6.	*	{ [82534.86]						{ [33313.77]		
		{ [...73.22]	[38.36]		9½			{ [52.13]		
	1	91650.6	9115.7	.07	α	3 i	36195.35	2831.58	-.04	70½
						1	355.15	3041.38	.02	γ

TABLE VI.—D<sup>3</sup>; (8Δ<sub>8</sub>) (cont.).

6669	D(4. m).								
7.					7.	{ [35591.39]			
	{ [17539.1]					1 i { 616.73	-.04		
	{ [ 564.4]					2 ii 38323.04	2731.65	.00	67½
						2 i 472.99	2881.60	-.04	70½
						2 i 601.62	3010.24	-.06	73½
						1 i 631.47	3040.08	-.1	γ
					D <sub>21</sub> { 3 ii 326.98	2710.25	.01	66½	
						0 ii 518.05	2901.32	.07	71½
4648									
8.	[19097.15]				8.	2 i 37149.48			
	1 i 101.6					[ 53.49]	4.01	.01	9
	20236.4	1169.3	0	66½		1 i 39965.73	2816.25	.04	69½
	2 i 348.9	1251.7	.03	70½		1 i 998.09	2848.61	.02	70
	1 i 390.609	1293.46	.06	73		1 i 40096.52	2947.04	.00	72½
						0 ii 191.62	3042.14	-.03	γ

D(2. m). 1. 2354.216; 2472.31 D.; 3011.17 K.—2. (2762.25; ...24.4) E. H.; (2195.48; ...90.74; ...71.82) D.—3. 1622.1 Bl.; 1414.427 P.; ...13.7; ...00.416 P.; ...09.3.—4. 1370.1; 1216.8; ...15.8.—5. 1266.1; 1126.4.—6. 1091.1.

D(3. m). 1. 1115.5.—2. 7673 McL.; 7944.66 P.; (9710; 9914; 10217; 10344; 10377) McL.—3. 6521.13 P.—4. 4206.100; 4188.2 Stk.; 3743.747; ...42.480; ...34.770.—5. 3358.775; ...51.61 St.; (3073.4; ...71.4; ...61.5) Bl.; ...53.32 P.—6. 2761.971; ...49.83 P.—7. 2806.844; 2608.618; (2598.45; ...89.79; ...87.79; 2608.35; 2595.41) D.—8. (2691.03; ...01.39) D.; 2499.366; (...93.23; ...88.58; 87.33) D.

D(4. m). 8. 5233.8; 4933.0; ...13.0; ...02.853.

$m=1$  (see text). The neutral  $e$  linked line to the corrected  $D_{11}(3.1)=-89657$  is found. Thus

Obs.

-89657+20612=69045 ...46.5 2, 1448.3

The  $\alpha D_3$  should be at 33342.10. It is just possible this may be indicated by Bl.  $\lambda$ , 1 i 5994, 16678,  $d\lambda=2$  as  $2h\nu$ .

$m=2$ . For  $D_{12}$  S. gives a value 2.46 larger. The measures of E. H. are inserted because they give the exact value of  $\gamma$ , 9439.49 and also a satellite separation which is due to an exact own multiple  $8\frac{1}{2}\delta$  within O.E. calc.  $\sigma=502.03$ ,  $d\lambda=.03$ . The first and third  $\nu$  are  $17\gamma=7.70$  and  $16\gamma=7.25$  in excess, and are entered only as suggesting the presence of the satelloidal effect.

In the D(3.2) the three last entered as  $D_{21}$  are too strong. They are probably only coincidences.  $m=2, 3$  are in the infra-red, with only few observations, and none in the spark spectrum. Little weight, therefore, can be given to these allocations.

$m=3$ . No line is observed for the calculated  $D_{11}$ , but the calc. (61873) gives an exact  $9\frac{1}{2}\delta$  displacement with  $\sigma=224.78$ . Also  $d_12, d3$  combinations sustain the allocations with a  $2h\nu$  representative. Although  $D_{11}$  is not seen, the forbidden  $D_{21}$  is. The vanishing of  $D_{11}$  suggests that it has been disrupted into collaterals. One such is given by Bl. at 1, 1617.5, 61820.0 which is  $(\delta_1)D_{11}(-\delta)$ ,  $d\lambda = .005$ . For intensity comparison with the others, the intensity of 70700 is given as 1, that of Bl., instead of 9 by P., as his excitation was more comparable. In the original allocation the measures of Bl. and Ly 1414.4 and 1400.4, were used giving separations 9052.8, 9760.8. It is striking to see how, with Paschen's good measures, the practically exact values 9051.41, 9758.61 result. But they are also equally good  $S_2(2.3)$  with 9121.99, 9829.80.

$m=4$ . In D(3.4) the  $D_{12}$  calculated from D(2.4) is 2.00 too small, possibly the error is in the latter. If the observed is a one own collateral (shift=2.85), it should be .85 larger ( $d\lambda = -.1$ ) when the three  $D_2$  separations from the accurately measured lines all become exact.

The  $2h\nu$  basis affords two extra  $D_2$ , viz.,

$$2 \times 41212.52 \text{ D } 2 \text{ iii} = 82425.04 \quad 9437.6 \quad .02 \quad 71\frac{1}{2}$$

$$2 \times 41373.86 \text{ D } 1 \text{ i} = 82747.72 \quad 9760.3 \quad .02 \quad 74$$

$m=5$ . The satellite separation for  $9\frac{1}{2}\delta$  is 60.09.

The  $D_{12}(3.5)$  calculated from D(2.5) is 2.62 too large. The observed gives the exact  $D_2$  separations shown, but the calculated 29761.61 gives also close values with the following:—

Bl.	1 iii	3059.6	32674.5	2912.9	0	71 $\frac{1}{2}$
"	1 iii	53.7	37.7	2976.1	.1	73
P.	3 ii	45.56	25.16	3063.55	-.04	74 $\frac{1}{2}$

The satellite separation of 63.63 is an extra  $2\delta_1$  displacement on the D(2.5) value, i. e., it is due to  $9\frac{1}{2}\delta$ .

There is a line near  $D_{11}$  at 1, iii 29832.42, whilst Cd. gives a single line at the mean of these two. The separation is 4.56, and is possibly a satelloidal  $10\gamma$  with Cd. at  $5\gamma$ .

$$* 2 \times 16263.79 = 32527.58 = D_{22}.$$

$m=6$ . The non-observed  $D_{11}(2.6)$  is sustained by a  $2h\nu$  effect.

$$2 \times 41286.73 D., 0. = 82573.46$$

$m=7$ .—The formula value for  $D_{11}$  is 35616.23, obs. ...6.73.

### *dd Combinations.*

Obs.

$d_2 2 - d_2 3$ [25453.1]	...52.31	1, 3927.81	$d\lambda = .1$
$d_1 2 - d_2 3$ [24954.6]	...53.85	3 ii 4006.27	$d\lambda = .12$
$d_1 2 - d_1 3$ [25779.19]	...80.5	1, 3970.3	$d\lambda = .2$

No  $d2 - d(4, 5)$ .

$d1 - d2$ .

Obs.

$d_1 - d_2$ [76628.66]	...34.2 *	1, 1304.9	$d\lambda = -.09$
$d_1 - d_1$ [77130.29]	$(\pm \delta_1)/(\pm 2\delta_1)$		

The o. rved  $d_1 d_2$  shows an exact  $2h\nu$  effect, viz.,  $2 \times 38317, 2609 D$ .

There is no direct obs. for 77130, but two exact collaterals are found.

$(+\delta_1)/(2\delta_1)$  shifts  $52.77 - 28.49 = 24.28$ . Thus

Obs.

$(\delta_1) [ ] (2\delta_1)$	$= 77106.01 *$	...06.9	2, 1296.9
$(-\delta_1) [ ] (-2\delta_1)$	$= ...54.57 *$	...54.5	0, 1296.1

The mean of the two is the exact  $d_1 d_1$ . The first shows a  $2h\nu$  effect and the second a  $3h\nu$ , viz. :-

$2 \times 38555.19$	1 iii 32592.91 D.	$d\lambda = .1$	on $d_1 d_1$
$3 \times 25718.999$	1, 3887.079	$d\lambda = .02$	" "

If both these are real relations they must give within their O.E. lines which differ by an exact  $2 \times (\delta_1)/(2\delta_1)$ , or

48.56. With O.E.  $d\lambda_1 d\lambda_2$ , their W.N. are less by  $14.86 d\lambda_1$ ,  $6.60 d\lambda_2$ . The difference is therefore

$$(\dots 57.0 - 19.8 d\lambda_2) - (\dots 10.38 - 29.7 d\lambda) \\ = 46.6 + 29.7 d\lambda_1 - 19.8 d\lambda_2.$$

Thus  $29.7 d\lambda_1 - 19.8 d\lambda_2 = 2$ .

As  $d\lambda_1 = .1$ ,  $d\lambda_2 = -.05$  would produce 4, we may consider the condition met.

$$d_2 - d_2 \quad [78656.78] \quad \text{Obs.} \quad (\pm \delta_1) / (\mp 3\delta_1)$$

No direct obs., but the two collaterals named are found.

$\delta_1 / -3\delta_1$  shifts  $53.99 + 3 \times 14.439 = 97.30$ . Thus

$$\begin{array}{rcccl} & & \text{Obs.} & & \\ (\delta_1) [ ] (-3\delta_1) = 78559.48 & * & \dots 560.8 & 0, 1272.9 & d\lambda - .02 \\ (-\delta_1) [ ] (3\delta_1) = 78754.08 & & \dots 752.6 & 4, 1269.8 & d\lambda - .04 \end{array}$$

The first shows both  $2h\nu$ , and  $3h\nu$  effects, viz. :—

$$\begin{array}{rcccl} 2 \times (39279.4 \pm .8) & \text{is} & 2545.1 \text{ D.} & d\lambda = .01 & \text{on } dd \\ 3 \times 26187.199 & & 1, 3817.571 & .. -.1 & .. \end{array}$$

Here, if both are real, they must give the same value within O.E. Hence.

$$\dots 58.8 - 15.4 d\lambda_1 = \dots 61.60 - 6.85 d\lambda_2$$

$$\text{or} \quad -15.4 d\lambda_1 + 6.85 d\lambda_2 = 2.8$$

With  $d\lambda_2 = .05$  this requires  $d\lambda_1 = -.16$ , and the connexion is perhaps just possible.

$$d1 - d3.$$

We get only displaced representatives for each possible combination. As, however, the own shift on the  $d3$  is about 6, which corresponds to  $d\lambda = .06$  on these high wave numbers, we can have no certainty within about one own on  $d3$ . In the following list the calculated  $d - d$  are in [ ].

$$\begin{array}{rcccl} & & \text{Obs.} & & \\ d_1 - d_2 & (\delta_1) [102084.3] (\delta_1) = 102037.3 & * & \dots 041 & 1, 980.0 \\ & (-\delta_1) [ ] (\delta) = 102113.9 & & \dots 114 & 4, 979.3 \\ d_1 - d_1 & (-\delta_1) [102309] (-3\delta_1) = 102344 & & \dots 344 & 7, 977.1 \\ d_2 - d_2 & (2\delta_1) [104112] (2\delta_1) = 104016.1 & & \dots 015 & 1, 961.4 \\ d_2 - d_1 & (-\delta_1) [104337] (-\delta_1) = 104385.3 & * & \dots 384 & 4, 958.0 \end{array}$$



The following  $n\hbar\nu$  are found:—

$$0i \ 1958\cdot57, \ 2 \times 51040\cdot98 = 102081\cdot96 \text{ gives } d_1 - d_2$$

$$1i \ 2873\cdot243, \ 3 \times 34793\cdot693 = 104381\cdot08 \text{ gives } (-\delta_1)d_2d_1(-\delta_1)$$

TABLE VII.— $F^2$ ;  $(9\Delta\alpha)$ .

$$d_{11} = 132460\cdot12. \quad \sigma = 2028\cdot12. \quad d_1 - = 52\cdot768; \quad d_2 - = 53\cdot986.$$

$$d_{12} = 55330\cdot09. \quad \sigma = 502\cdot02. \quad d_1 - = 14\cdot246; \quad d_2 - = 14\cdot439.$$

$$d_{13} = 30151\cdot2. \quad \sigma = 224\cdot6. \quad d_1 - = 5\cdot734; \quad d_2 - = 5\cdot795.$$

$$f_2 m = 4R/\{m + \cdot887110 + \cdot015588m\}^2.$$

$F(1.m).$

$F(2.m).$

$$f_2 - = 13\cdot093; \quad af_2 - = 13\cdot048; \quad f_1 - = 13\cdot024; \quad cf - = 12\cdot983.$$

2.	2	1n *	80153·9	}	9 $\delta_1$ gives	117·68		
	a	1	276·1		122·2	10 $\delta_1$ "	130·75	
	F <sub>11</sub> b	1 *	340·6		186·7	14 $\delta_1$ "	182·80	
	c	1n *	450·5		296·6	23 $\delta_1$ "	299·84	
	1	82182·8	2028·9					
f <sub>1</sub> - = 5·365; f <sub>2</sub> - = 4·395.								
3.	1	103498		1	26375·42		0	
	2	605	107	1	477·683	102·26	19 $\delta_1$	
	1	105530	2032	1	[877·61]?	502·19	F <sub>22</sub>	
				1	980·22	502·54	F <sub>21</sub>	
f- = 2·718.								
4.				4 i	(36952·74)			
				5 i	992·23	(39·51)	0	
				3 ii	(37459·32)	(506·60)		
				1 ii ?	494·02	501·80		

$F(3.m).$

$f - = 1\cdot554.$								
5.	1 iii	17515·3	(25178·5)	3 i	42693·84			—·51
				4 i	(733·48)	(39·64)		
	2 ii	17732·788	217·5	5 i	43194·63	500·8		
$f - = 972.$								
6.	1 iii	20910·7	(25178·2)	0n i	46111 ±	[... 067·77]		1
		---	---	1 i	(148·40)	(38 ±)		
	3	21136·6	225·9	1 i	612·48	501		
$f - = 747.$								
7.	1 iii	23104·091	(23178·29)	0 iii	48379·7	[... 81·53]		—·09
	1	23228·2	224·1					
8.		[24600]		0 iii	49778·67	[... 77·83]		·03

The values of F(1.2), F(1.3), corrected as explained in the text, are :—

(107)	(102)	(107)	(102)
80151.87	...157.23 <sup>(1)</sup> *	103500.09	103505.45
269.55	...274.91	...607.71	...607.71
334.67	...340.03 <sup>(1)</sup> *	105528.21	105533.57
451.71	...457.07 <sup>(1)</sup> *		
82180.0	...185.55		

<sup>(1)</sup> These are sustained by  $3h\nu$ ,  $2h\nu$  affects :—

$3 \times 26719.0 = 80157$	1n 3742.7	$d\lambda = +0$
$2 \times 40171.44 = 80342.88$	1 ii 2488.58 D.	" = - .09
$4 \times 20114.50 = 80458.0$	1, 4970.30 W.	" = - .06

F(1.m). 2. 1247.6; ...45.7; ...44.7; ...43.0; ...16.8.—3. 966.2; ...65.2; ...47.6.

F(2.m). 3. 3790.4; ...75.697; 24.000; ...05.368.—4. 2705.358; ...02.470; 2668.77 D.; ...66.30 D.—5. (2341.54; ...39.37; ...14.39) D.—6. (2168; ...66.24; ...44.67) D.—7. 2070.60 D.—8. 2008.55 D.

F(3.m). 5. 5707.7 Bl.; 5637.710.—6. 4781.0 Stk.; ...29.9.—7. 4327.025; ...04.0.

### Notes.

$m=3$ . The line 26375 is given by both W. and Bl. as an arc line. E.V., however, give it as a spark line of intensity 8, and Steinhausen definitely states it is enhanced. The  $F_{22}$  is not observed, but the value entered in [ ] is derived from 26845.239 as  $F_{22}(-6\delta_1)$ . There is evidence of considerable disturbance in this region. In succeeding orders there seems to be disruption into a normal set (Class  $E_1$  and displaced from the calculated values), and another shifted about 39. In the table these are placed in (-). The formula is calculated from 26375 and 36992 as  $F_{12}(2.m)$  for  $m=3, 4$ . The calculated values for  $m=5, 6, 7, 8$  are 42685.09, 46087.77, 48281.53, 49777.83.

$m=4$ . As they stand in the table, the four lines appear at first sight to form an excellent F type, with the last as a forbidden  $F_{21}$ . The apparent satellite separation of 39.51, however, does not satisfy the own multiple rule— $14\delta_1$ ,  $15\delta_1$  require 38.05, 40.76—and especially it occurs in succeeding orders. They must, if admitted as F, therefore be due to a parallel series with displaced  $d2$ . Here  $3\delta_1$  on  $d_12$  shifts 42.73.  $F_{12}$  calculated from the formula based on F(1.2), F(1.3) is 36983 so close as to support 36992. There would seem to be no satellite.

$m=7, 8$ . The  $ff$  combinations seem to support the calculated values, as do also the  $F(3.m)$  distinctly.

$m=5$ . The direct 224.6 in  $F(3.m)$  does not appear. But it appears back to 1 iii, 17290.809. This, if not a coincidence, must be a linkage effect; in other words, a case where an electron falls from  $f_5$  to  $d_13$  and another raised from  $d_23$  to  $d_13$  either simultaneously or before the emission takes place.

### *ff Combinations.*

$f_22-f_23$	23348.221	3 ii	4282.781
$b f_12-f_23$	23164.650	1	4315.713
$a_1 f_22-(102)f_13$	23332.8	3 ii	4284.6 P.
$a_2 f_22-(107)f_13$	23325.56	1	4285.942
$cf_12-f_13$	23151.3	1	4818.3
$a_1 f_22-f_4$	33851.7	1 n	2953.3
$a_1 f_22-f_5$	39552.90	1 iii	2527.50 D.
$a_2 f_22-f_6$	42938.99	1 ii	2328.17 D.
$f_12-f_7$	45075.04	0 ii	2217.83 D.
$f_12-f_8$	46574.92	1 ii	2146.40

TABLE VIII.—G.

$$bf_12=52120.09. \quad cf_12=52003.05. \quad f_13=28852.59.$$

$$bf_1- = 13.024; \quad f_2- = 13.093; \quad cf_1- = 12.980; \quad f_1- = 5.365; \\ f_2- = 5.395.$$

$$g_2m = 4R/\{m + .933582 + .102144/m\}^2.$$

$$G2.m. \left\{ \begin{array}{l} b \ 23267.50 \\ c \ 23150.46 \end{array} \right\} G3.m.$$

5.092.					
3.	1	24147.635			
	2	330.580	182.94		
2.608.					
4.	1	34290.6	(23267.6)		
		(173.55)	(23150.5)		
				[11023.0]	
$G_{11}?$	[188.5]	15 (23150)	1	11038 ± 1	15
1 i	360.1	186 ±		[11125.2]	(102.2)
$G_{21}$	1 iii	484 ± 6	296 ±		
1.519.					
5.	2 i	39619.36	(23150.46)	[16468.90]	
		(802.64)	183.28	1 i	16573 ± 2
					104 ± 2

TABLE VIII.—G. (cont.).

·947.						
6.	1 ii	42938·99	(23149·2)	1 i	19789·6	
	1 i	55·04	16·05	2 i	803·1	13·3
	---			0	893·737	102·9
·633.						
7.				2	21907·99	
				2 iii ?	913·1	5·1
				1	22012·5	104·5
·444.						
8.				1 i	23371·211	
				2	473·7	102·5
·323.						
9.				2	24425·1	
				1	527·776	102·7
10.				1 n	35196·0	
				1	303·515	107·5

G(2. *m*). 3. 4140·182 W.; ...08·899.—4. 2915·5; ...25·385; ...09·5 Bl. 2899 Bl.—5. 2523·26 D.; ...11·64 D.—6. 2328·17 D; ...27·30 D.

G(3. *m*). 4. 9057 McL.—5. 6032 Bl.—6. 5051·8; ...48·4; 25·563.—7. 4563·27 P.; ...62·3; ...41·7.—8. 4277·569; ...59·0.—9. 4093·1; ...75·864.—10. 3967·9; 3950·906.

## Notes.

*m*=3. The observed should be somewhat larger than the extrapolated value of 24134. The line given satisfies this, but it is one of a complicated set of collaterals.

*m*=4. The calculated  $G_{12}(2.4)$  are  $cG=34163.9$ ,  $bG=34281.6$ . These should be the observed 34290 and a line covered by the neutral  $S_1^{34}$ , 34173. The  $G(3.4)$  are in a little observed region, and the  $G_{11}(2.4)$  in the list is very doubtful. Taking it as corresponding to  $G_{11}(3.4)$ , it gives a forbidden  $G_{22}$  of class iii.

*m*=5. (16477·07; 16579·31) for  $G(3.5)$ . The second settles the observed  $G_2$ , and the unobserved  $G_{12}$  gives the exactly observed  $G(2.5)$ ; but  $G_2(2.5)$  is covered by the neutral  $D_{11}^{3(17)}$ .

*m*=6. [19771·53.] The obs. are 18·3 ahead of the calculated, which is excessive for an order one less than that of the formulæ standards. Again they are in a complicated complex of related lines (see below).

*m*=7, 8.—These are taken as standards for the formula.

*Raw Material for G(3, 6, 7, 8).*

6.			7.			8.		
4i	19747·6	(6·94)	1n	21837·0	(7·91)	2iii	23291·49	(3·88)
3i	849·1	101·5	2ni	940·0	103·0	1n	394·72	103·23
1i	19789·8	(6·957) A	2	21907·99	(7·95) A	1	23325·55	(8·91)
0	892·74	102·9	1	22012·5	104·5	3n	428·05	102·50
1n	19808·6	(9·966)	1iii	21988·547	(7·995)	1i	23371·211	(8·94) A
2ii	911·6	103·0	1	22093·3	104·8	2	473·7	102·5
2ii	12921·5	(7·01)				3ii	23441·970	(9·05)
1ii	20025·95	104·4				1	545·0	103·0

A denotes the lines taken as representatives of G. The figures in ( ) give the denominators of *gm*.

$m=6$ . In this column not only does 19789 show a *cf* separation to G(3.6), but we also find

1n	19808·6	(23269·1)	1i	43077·74
2ii	19911·6		5	43194·63 117

This gives the *bf* separation within  $dn=1·6$  or  $d\lambda=.4$  on E. V.'s excessive measure, and perhaps the difference 23269 is a near coincidence. The set would fit, however, in the G(6) scheme as  $G_{11}$ , with a satellite separation of 18·8 ( $20\delta_1=18·94$ ), in which case 19911 would be a forbidden  $G_{21}$ , and the class ii would be explained. The corresponding  $G_{12}$  and  $G_{22}$  in the G(2.6) or 43059, 43241 have not been observed. The set would appear to fit in better in the following schemes, in which case 43077 is not a G(2.6) line. The two observed 19808 and 19789 are separated 38, 19 from the calculated  $G_{12}·6$ . The values of  $f_{13}$ — and  $g_2$ — being respectively 5·365, ·947,  $(-3\delta_1)/(3\delta_1)$  shifts 18·9. In fact, if the calculated value be taken as  $G_{16}$ , the whole set in this column may be represented in a collateral scheme as given below, in which the first column gives the collateral notation, the second the calculated W. N., and the last the observed with O—C  $d\lambda$  values. In forming this it must be remembered that an own displacement in the limits  $f_1, f_2$  alters the doublet separation by ·03. The calculated  $G_{12}·6=19771·53$  requires correction for formula error, and this is obtained from the very accurate observed 19892·737. The

separation 102.35 corrects 19789.8 to ... 90.39. This as  $(-3\delta_1)G(3\delta_1)$  gives  $G$  as 19771.46 or  $O-C \, dn = -.09$ ,  $d\lambda = .02$ .

$(5\delta_1)/(-3\delta_1)$	19747.48		4 i 19747.6		-.02
	849.59	102.11	3 i 19849.1	101.5	.1
$G_{1.6}$	$\begin{bmatrix} 19771.46 \\ 873.72 \end{bmatrix}$			102.26	
$(-3\delta_1)/(3\delta_1)$	19790.39		1 i 19789.8		.1
	892.74	102.35	0	892.737	102.9 0
$(-6\delta_1)/(6\delta_1)$	19809.32		1 n 19808.6		.1
	911.76	102.44	2 ii 19911.6	103.0	-.02
$(-2\delta)G_2(6\delta_1)$	19922.74		2 ii 19921.5		.2
$=(-27\delta_1)G_1(6\delta_1)  $	20025.73	102.99	1 ii 20025.952	104.4	-.1

The last line is directly calculated, and differs from the second of the reliable measures by  $dn = .22$ . This involves the O.E. of the other as well, say .10 or  $d\lambda = .02$  on each. It is noticeable how the displacements on the  $g$  term are all multiples of  $3\delta_1$ , and on the  $f$  with the exception of the first.

$m=7$ . In this set are observed two apparent  $bf$ ,  $G(2.m) - G(3.m)$  separations 23267.50, viz. :—

21837.0	23268.9	1 i 45105.95
21988.54	...65.43	0 i 45253.97

The first is the  $bf$  separation within O.E., but the measures in the second do not admit this, at least directly. In the first it means that 21837 must contain the term  $bf_{1.3}$  unaltered. Then the W.N. differs from 21908 ( $G_7$ ), too much to be explained on a satellite basis. If, then, the  $bf$  relation is real, the two lines must be related on a linkage basis. Their separation 71 suggests the difference of two  $p$ -links. In that case we should expect to find the singly-linked line. We find such at 31167.0, with a parallel inequality due to a  $6\delta_1$  displacement due to  $\beta$  and the  $(70\frac{1}{2}\delta)$  link 9262.80. The scheme is given thus, with  $l$  standing for this link and additional linked line.

$G$	21907.99				
	9262.80	$G.l$			$G(-6\delta_1).l$
		(31170.79)	3.79	$(6\delta_1 \equiv 3.80).1$ ,	...67.0
	9333.79		9120.45		
$\beta.G.l$	21837.0	$d\lambda = .08$		2 i 40291.24	$G(-2\delta_1).a.l$

$m=8$ . The only  $bf$  relation is a very exact one on the first :—

$$23291.491 \quad 23267.38 \quad 0 \text{ iii } 46558.87$$

both class iii lines, which excludes the set from being a normal G. Its close  $bf$  ( $d\lambda=.04$ ) settles that it belongs to the system without any displacement on the  $f_{13}$  limit. This whole region is a very puzzling one, being crowded with lines related by chains of 183, 300 separations, showing, therefore, the presence of  $f(2)$  terms, unless these  $f(2)$  separations also act as links, a supposition not to be pedantically set aside.

TABLE IX.

The  $n\nu$  sets.

In  $S_2$  &c. lines the values corrected for the exact  $\nu$  separation are placed in ( ). The  $d\lambda$  corrections in observed to meet these are placed after the wave number, and the last column gives the O—C  $d\lambda$  on these observed lines.

$S_{1,1}$	57495.30	3 (19165.044 + .05)	1 i	5216.384	.01
		2 (28745.11 + 2.5)	1	3478.00 W.	.3
$S_{2,1}$	47772.65 (.22)	2 (23885.238 + .87)	1	4185.511	.14
$S_{1,2}$	35104.16	2 (17552.5 - .4)	1	5695.7	-.1
$S_{2,2}$	44190.755	2 (22093.3 + 2.05)	1	4525.1	.4?
$S_{1,3}$	61578.06	2 (30789.7 + .7)	3 iii	3246.9 Bl.	-.08
$S_{1,4}$	73030.73	3 (24343.341 + .23)	2	4106.745	.04
		2 (36525 - .9)	1 ii	2737 Bl.	-.7
$S_{2,4}$	82877.5 (60.40)	2 (41438.2 + .55)	0 ii	2412.5 D.	.03
$S_{2,5}$	88550.4 (47.0)	4 (22136.3 + .4)	4	4576.4	.08
		3 (29516.289 - .6)	3 i	3386.991	-.07
		2 (44273 + .5)	0	2258 D.	.02
$S_{2,5}$	88865.2 (6.3)	4 (22217.5 <sup>(1)</sup> - .9)	1 iii	4499.8	-.2
$S_{1,6}$	82580.94	3 (27528.2 - 1.2)	1	3631.7 Stk.	-.1
$S_{1,8}$	86385.98	2 (43194.62 - 1.63)	5 i	2314.39 D.	-.09
$S_{1,8}$	96237 (51.3)	4 (24090.6 + 2.2)	1 u	4155.1	.4
$S_{1,9}$	87477.28	4 (21869.0 + .32)	1 iii	4571.5	.06
		2 (43739.03 <sup>(1)</sup> - .39)	0	2285.58 D.	-.02
$S_{2,9}$	96646.4 (32.4)	2 (48316.10 + .1)	0 ii	2069.04 D.	0
$S_{2,11}$	98212.5 (8.3)	3 (32737.7 + 1.7)	1 iii	3053.7 Bl.	.17
$S_{1,3.4}$	26828.81	2 (13414 + .4)	2	7453 W.	.2
$S_{1,3.5}$	32772.23	2 (16386 + 0)	2 i	6101 Bl.	0
	32825.16 (.84)	2 (16416 - 3.0)	2 i	6090 Bl.	1

TABLE IX. (cont.).

$S_1(3.6)$	33360 (59.3)	2 (16678 +1.6)	1 i 5994 Bl.	.5
$e. S_2 3$	[50620.72]	2 (25310.274 + .08)	1 3949.851	.01
$e. S_1 5$	58424.60	2 (29210.9 +1.4)	1 3422.5 Stk.	.1
$P_1(1.3)$	106716	3 (25577 -5)	1 ii 2310 Bl.	.4
$P_2(1.3)$	103928 (31.1)	2 (51963.17 +2.4)	0 iii 1923.81	.08
$P_1(1.4)$	124768	5 (24953.846 - .24)	3 ii 4006.270	-.04
$P_2(2.5)$	40096.52	2 (21048.2 + .05)	3 4986.7	.01
§	40784.65 . $\beta$	2 (25059.006 + .02)	2 3989.457	0
§	50617.53	2 (25308.9 - .13)	3 3350.2	-.04
§	51321.79	2 (25660.733 + .16)	1 3895.254	.02
$P_2(2.6)$	45230.83	2 (22615.5 - .08)	2 iii 4420.6	-.01
$P_1(2.7)$	48482.91	2 (24241.07 <sup>(2)</sup> + .38)	1 4124.071 Cd.	.06
$p_2, p_3$	55674.9	2 (27837.507 - .03)	2 n 3591.255	0
$D_2(3.5)$	32527.8	2 (16263.79 + .11)	3 6146.93 P.	.03
$D_{11}(2.6)$	82573.22	2 (41286.73 <sup>(2)</sup> - .11)	0 2421.35	.00
$d1 d2$	76634.2	2 (38317 + .1)	0 2609 D.	0
†	77106.9	2 (38535.19 -1.7)	1 iii 2592.91 D.	-.1
†	77154.5	3 (25718.999 - .13)	1 3887.079	-.02
†	78559.48	3 (26187.199 - .70)	1 3817.571	-.15 ??
		2 (39279.4 + .35)	1 ii 2545.1 D.	.02
$d1 d3$	102084.3	2 (51040.98 +1.17)	0 i 1958.57 D.	-.04
†	104385	3 (34793.693 +1.3)	1 2873.243	.1
$F_{12}(1.2)$	80157.23	3 (26719.0 + .03)	1 n 3741.7	.00
$b. F(1.2)$	80340.03	2 (40171.44 -1.33)	1 ii 2488.58 D.	-.08
$cF(1.2)$	80457.07	4 (20114.50 - .24)	1 4970.50 W.	-.06

 $2h\nu$  lines to unobserved series lines.

$S_2 1$	2 (24098.9 - .25)	48197.30	<b>9298.09</b>	$70\frac{1}{2}$	1 4148.6	-.04
$S_2 2$	2 (22164.8 +1.03)	44331.67	<b>9227.51</b>	$70\frac{1}{2}$	1 4510.5 Stk.	.2
	2 (22182.964 + .52)	44336.96	<b>9262.80</b>	$70\frac{1}{2}$	2 iii 4507.704	.1
	2 (22217.5 <sup>(4)</sup> +1.3)	44437.6	<b>9333.41</b>	$\beta$	1 iii 4499.8	.25
$S_2 3$	2 (35669.186 - .85)	71336.67	<b>9758.61</b>	74	3 2802.716 Cd.	-.06
$S_2 4$	2 (41074.37 +1.9)	82152.53	<b>9121.80</b>	$\alpha$	2 ii 2433.87 D.	.1
	2 (41233.78 +1.31)	82470.18	<b>9439.45</b>	$71\frac{1}{2}$	1 iii 2424.46 D.	.08
	2 (41286.73 <sup>(2)</sup> +1.46)	82576.38	<b>9545.65</b>	$72\frac{1}{2}$	0 2421.35 D.	.08
	2 (41358.29 + .85)	82718.29	<b>9687.56</b>	$73\frac{1}{2}$	1 2417.16 D.	.05
$S_2 8$	2 (47755.07 -1.18)	95507.88	<b>9121.80</b>	$\alpha$	0 ii 2093.35 D.	-.05
$e. S_2 4$	2 (31124.47 - .30)	62248.34	<b>9829.67</b>	$\gamma$	2 iii 3211.98	-.03

§ Of linked. See notes to P(2.5).

† Of collaterals. See notes to the  $dd$  table.



TABLE IX. (cont.).

$e. S_2 8$	2 (37428.9 + 1.35)	74860.57	<b>9086.59</b>	69½	3 i	2670.94 D.	.1
$P_2(1.3)$	2 (51940.0 - 1.14)	103877.72	<b>2838.28</b>	69½	0 iii	1924.7 D.	-.04
$D_2 4$	2 (41212.52 <sup>(1)</sup> + .9)	82426.85	<b>9439.45</b>	71½	2 ii	2425.61 D.	.05
	2 (41373.86 - .85)	82746.01	<b>9758.61</b>	74	1 i	2416.25 D.	-.05

(1) This is  $S_2 310$  with  $d\lambda = -.12$ , larger than here, but  $S_2 310$  is definitely here. The  $\frac{1}{2}S_2 9$  possibly occurs especially as  $\frac{1}{2}S_1 9$  does, but it is overlaid by this definitely are line.

(2) Observed by S., but not by Bl., and so is not classified, but Od. gives it as seen in the arc, and not in the spark.

(3) This is also  $\frac{1}{2}S_2(2.4)$  for an observed  $S_2$ , and also is a  $S_2(3.9)$ , but the latter's separation value (74½) is exceptional. The  $\frac{1}{2}D_{11}$  must be accepted at least.

(4)  $\frac{1}{2}S_2(5)$  with  $\gamma$  and  $\frac{1}{2}$  unobs.,  $S_2 2$  with  $\beta$ . The observed line is actually the mean of these two, and may be a merge.

(5) Is also a  $S_2(3.9)$ .

Perhaps the most remarkable fact emerging is that while a small proportion of the numerous  $S_2$  lines occur, all the  $S_1$  examples from  $m=1$  to 9, with the only exceptions of  $m=5, 7$ , are seen, even in the cases where  $S_1$  themselves are wanting. This systematic effect points to the relations as being real, and not mere coincidences.

It is clear from the nature of the emission that no  $n\hbar\nu$  line can show a link connexion, unless the original line is connected with an  $n$ -fold chain of the same link. For this reason I have tested each of the lines in the above list. My hand-list of wave numbers is a maze showing link connexions from the vast majority of the lines. Yet it is remarkable how all the above, with few exceptions, show none. This seems a clear indication that they are of a special nature. I do not discuss the exceptions here, but there are two which are specially important as having been used as evidence for establishment of relations in the mercury spectrum. They are two, viz., the  $3\hbar\nu$  for  $S_1 1$  and  $F_{12}(1.2)$ . In the former 19165 shows a possible back  $\alpha$  link to 10044. This is explained by the fact that 10044 is itself also a  $3\hbar\nu$  for the emission  $\hbar\nu=30133.45$ . Thus

$$\begin{array}{rcccl}
 S_1 1 & 9123.34 & S_2 1 & 9125.71 & 39246.25 & 9112.80 & 30133.45 = 3 \times 10044.46 \\
 & \alpha + 3\gamma + .18 & & \alpha + 9\gamma - .18 & & \alpha - 20\gamma + .09 \\
 & & & \text{obs.: ...44} & 2, & 9953
 \end{array}$$

The total separation is  $3\alpha - 8\gamma + .09 = 3$  (9120.68).

In  $F(1.2)$ , 26719.0 shows a back  $\gamma$  link  $= 9289.0$  to 16890, 1 i 5919 Bl. Here again 16890 appears as a  $3\hbar\nu$  to an observed line. Thus

$$3 \text{ iii } 1972.72 \quad 50674.74 = 3 \text{ (16890 + 1.58)} \quad d\lambda = .3 \text{ on } 5919$$

## PART II.

*Relation to Allocations by Paschen.*

The line  $n=35104$  has been taken, both in Part I. and by Paschen, as  $S_12$  in the two systems of allocations. In other words,

$$35104 = 92034 - s2 = 90661 - as2,$$

where, to avoid confusion, *as* stands for Paschen's *s*-term. These cannot both subsist. Either there must be some error in one of the  $p_2$  limits, or the line cannot belong to both systems. The 92034 is quite definite if the assumptions which form the basis of Part I. are sustained. They stand or fall together. The 90661 depends on the connexion between series  $p_2 - tm$  and  $p_3 - tm$ , in which the second is sufficiently numerous to give the value  $p_3$ , and only an allocation for one common order  $m$  gives a relation between  $p_2$  and  $p_3$ . Either, then, this relation must be defective, and give an erroneous value of  $p_12$ , or the line cannot belong to both series. This is the question which it is proposed to discuss in this Part II. Paschen's P and S allocations are collected together into two tables given at the end.

1. Taking the three lines for  $m=3, 4, 5$ , in Paschen's  $P_1^2(2.m)$  sets, we get the formula

$$n = 55925.33 - 4R / \{m + 180792 + 434404/m\}^2$$

The limit ( $s2$ ) is 360 larger than that given by Paschen, but the possible error in its value must be much less than this, if the set forms a real series. With this limit and the  $P_1(2.3)=16257$  there results  $p_13=39668$ . The  $S(3.m)$  series gives, using  $m=4, 5, 6$  a limit  $p_13=39297.76$ , which practically agrees with Paschen's value. These two values for  $p_13$  differ too much to be ascribable to formulæ errors, and seem to point to some error in allocation of at least one of the two sets or to the presence of collaterals.

With  $s2=55925$  the  $p_12$  term determined from  $S_1(2.2)=35106$  is  $91031.47 + \xi$ . To produce a separation of  $9121.88 + d\nu$  in this requires a displacement of

$$102335 + 10.498d\nu - 1.609\xi = 70\frac{1}{2}\delta + 104 + 10d\nu - 1.68\xi.$$

No possible values of  $d\nu$  or  $\xi$  can make this satisfy the own law; nor can the succeeding  $p_13, \dots$  be met by own

multiples without excessive and arbitrary changes in the limit. If, however, the value of  $p_1 3$  be taken from the above  $S(3.\infty) = 39297.76$ , the  $p_1 2$  deduced in a similar way is 90661, and this exactly obeys the own law, The displacement is

$$102957 + 10.507 dv - 1.625 \xi \\ = 71\{1450.099 + .148dv - .013\xi\} = 71\delta.$$

But again none of the higher order separations can be met. Expressing them in terms of order of magnitude, *i. e.*, of nearest own multiple, we find, with the limit  $s_2 = 55925$ ,

9122	3673 (3424) *	853	262	199
70½δ	99¼δ (93δ)	57½δ	41δ	37¼δ

\* See below.

The 99¼ (100¾ on the 90661 limit) is a far larger multiple than in any known case. These multiples show in some cases a steady rise with increasing order, or more generally a steady fall from the first one, but I know of no example in which there is a rise followed by a fall. The rapid fall here, however, is analogous to those in Zn ii and Cd ii as allocated by von Salis.

The  $\alpha/m$  term in the formula is positive, contrary to the usual rule for  $p$  terms, and, moreover, is very large. Indeed it is small and negative in the Zn ii, Cd ii. We should hardly expect, then, to get very accurate extrapolation for  $m=2$ , and only roughly near ones for  $m=6, 7, 8$ . The extrapolated values for these latter are 44706.42, 47562.69, 49456.21. These suggest the sets added to the P list of 44709, 47584, 49466, which agree within formula errors with the corresponding  $P_1(3.m)$  observed lines as allocated by Paschen (see the table, wherein additional lines are added, denoted by †. In extrapolation to lower orders changes in the mantissa indicated by a formula seem to be exaggerated in the observed. Here we then expect for  $m=2$  a denominator somewhat greater, or a term  $p_2$  somewhat less than the extrapolated value, here [76292.86], which gives a negative value for  $P(2.2)$ , *i. e.*, it gives  $p_1 2 - s_2 = 20367.53$ . We find near this two pairs:

2 i 4913.0	20348.9 [7.43]	(43.16)	1 i 4902.853	20390.609
	9120.3			9121.99
4 ii 3392.397	29469.252		1 3387.414	29512.602

These sets, both giving the proper 9121 separations, are clearly related to the  $P(2.2)$  of this series—either as both

collaterals of the normal P(2.2) or one as P(2.2) and the other a collateral. We note

(1) Any displacement can only occur on the  $s_2$  term, otherwise the doublet separations would be largely altered. If the 20348 be corrected from the good measure  $29469.252 - 9121.80 = 20347.45$ , the separation from the second is 43.16. The  $s_2 - = 14.476$ , so that  $3\delta_1$  shifts 43.43, and explains their relative displacement.

(2) The extrapolated  $p_1 2 = 76292.86$  is in better step with those for Zn and Cd. Thus

Zn 97892, Cd 89750, Eu ?, Hg 76292.

(3) The displacement on  $76292 + \xi$  to produce 9120.80 is  $90\frac{1}{2}\delta + 60 - 2.45\xi$ . A value of  $\xi = 25$  on a formula extrapolation is not excessive, so that the value of  $p_2 = 76317$  is in step with the other elements, and obeys the own law, although with a very excessive multiple.

2. The  $-P_1(2.2)$  or  $S_1 2$  then belonging to this series cannot be 35104. It would appear that the formula, in spite of its abnormal form, fits a regular series of some nature. The positive value of  $\alpha/m$  suggests that, if a real series, it refers to a  $d, d$ . Also the limit may be written as  $4R/\{2.800829\}^2$ , with a mantissa  $8 \times 100104$ , again suggesting a  $d_2$  term analogous to those discussed in Part I. Indeed, it is possible to make additions to the set as given by Paschen to give it the appearance of a  $dd$  series with a  $d_2$  separation of  $3423 \pm$ ; or we may arrange new lines in which this separation replaces 3673. The first case is illustrated by additional lines in the P list in ( ). On this supposition  $62\delta$  in the limit produces a separation 3424.6. The second is illustrated by additional lines, also in ( ), in the S list. On this supposition a displacement of  $93\delta$  is required to produce 3423.74 in the  $p_3$  term. The march of the new separations is now superior to that of 3673, but still remains anomalous. We may add that 3673 occurs also in connexion with  $P_1(1.2)$  or 60607, and quite out of place. The corresponding line is due to Ly., and to determine a satisfactory measure we use both of his measures. They are

But both arrangements seem to be rather examples of the danger of trusting equal separations as necessarily referring to bi-term lines, especially in very rich spectra where numerous links occur. I believe I have shown\*, for instance, that such trust vitiates the arrangement of terms in the spectrum of copper as given by both Shenstone and Sommer. In the present case it may be noted, in illustration, that  $3673 - 3424 = 249 = 7 \times 35.7$ , which suggests that the two values differ by the difference of two  $p_2$  terms (or links) due to  $m\delta_1$  and  $(m+7)\delta_1$ . Also the neutral  $c$  link is  $5481.07$  and  $9157.03 (69\frac{1}{2}\delta) - c = 3675.97$ .

3. We may further criticise the " $P(2.m)$ " lines from another quarter. They are all closely associated with the  $\alpha, \beta, \gamma$  separations, but whether as links or as themselves containing  $p_2$  terms is not at once evident. The latter would definitely exclude the set as being a  $P(2.m)$  series. If we complete the  $\alpha, \beta, \gamma$  maps, we find the lines associated with near lines showing the satelloidal effect. We have learnt in the case of copper that such lines include the  $p$  term, and possibly only the lowest  $p$  term. Again, then, we have a doubt suggested that the series in question is not a  $P(2.m)$ . It will be sufficient to illustrate this by giving the results for one only, viz., the " $P(2.3)$ ," in which the  $P_1 - 16257$ —has itself a near line separated from it by  $6.79$  with  $15y = 6.805$ . The lines adduced are all successive.

		( 3 ii	25356.863		
		2	59.138	2.27	$5y + 0$
		1	70.98 P.	11.84	$26y - .04$
9120.03		1	77.032	6.05	$13y + .15$
( $\alpha - 4y + .04$ )		8b	80.39 Cd.	3.36	not $M(y)$
16257.00					
263.79	6.79	4A	25591.284 <sup>(1)</sup>		
9334.80		4n	800 Cd.	.516	$y + .06$
( $\beta + 3y + .03$ )					
		1	26072.948		$2 \times 2.72$
		1	78.4 E. V.		$16y = 7.22$
9828.53		1 iii	85.534	12.586	$28y - .11$
( $\gamma - 3y + .18$ )					

(<sup>1</sup>) This is neutral D1(4). Here it must be chance coincidence.

\* See specially Phil. Mag. 4, 1207-9, 1929.

		3	21687.24 P.		
	<b>9118.30</b>	2	701.92 P.	<b>14.68</b>	$32y=14.518$
	( $\alpha-8y+13$ )	1 i	13.671	<b>11.75</b>	$26y=11.796$
		2	21907.99 P.		
12583.62	<b>9329.36</b> <sup>(1)</sup>	2n iii ?	13.1 E. V.	<b>5.1</b>	$11y=4.99$
	( $\beta-9y+03$ )				
		3 i	22394.7 E. V.		
		1	408.2	<b>3.5</b>	$7y=3.18$
	<b>9835.73</b>	1 iii	19.354	<b>11.1 14.6</b>	$32y=14.52$
	( $\gamma+13y+12$ )				

(<sup>1</sup>) If the line is corrected by  $11y+0$  to 21912.98.

It will be seen that these near lines show separations all very close multiples of the satelloid constant  $y$ . Whether individual examples are real cases or not the general consensus of the whole is in striking support of the existence of this effect in connexion with the lines linked to these P(2.3). The appearance of these  $\alpha$ ,  $\beta$ ,  $\gamma$  may of course be due to a concurrence of three links on the same line, but the most natural conclusion to draw is that they occur because the original lines 16257 contain the  $p_1 2$  term, and the others the respective  $p_2 2$  corresponding to  $\alpha$ ,  $\beta$ ,  $\gamma$ . If so, we should further expect to find lines corresponding to other  $p_2$  lines. An inspection gives the results for 16257.00, ... 63.79 indicated in the following list, in which the first two columns give all the successive  $\delta$  multiples and the corresponding true separations. The details for 12583 are omitted, but the existence of the effect here is indicated by attaching a † to the value in the second column. A \* indicates that the same separation occurs in the S(2. $m$ ) allocation of Part I.

The corrections to be applied to the observed separations to make them equal to the standard  $v$  in the second column are indicated on the left of the observed W.N. The figures in thick type on the right are for use later.

The greatest deviation entered is that for  $69\frac{1}{2}\delta$ , but is accepted, as the observed difference 2.74 is the persistent satelloid 2.72 effect. The others are met by small  $y$ -multiples with great exactness, as indicated on the lists. That for  $\beta$  or 718 must be excluded, since it is an arc line (Bl.), and, indeed, is D<sup>14</sup>—or, if it is covered by this, it affords no evidence for our purpose. But including it,

$\delta$	$\mu$	$\gamma$	3	16257.00	$\gamma$	795.2	.6263.76	3 ii	25490.64	613.52
69	9051.41*		3	25308.9		795.2				
69†	86.59*	-2.74	4 ii	340.846		763.21				
69†	9131.80*	-4y + .04	1	377.032		727.13				
69‡	57.03									
70	92.26	y + .04	2	440.747		654.41				
70†	9227.51									
70†	62.80*									
70‡	98.09†									
71	9333.41	3y - .03	4 A	591.284		512.87				
71†	68.73*	-2y + .09	1	624.925		579.24				
71†	9404.08†	-y + .1	1	660.733		443.44				
71‡	39.45*†									
72	74.84†									
72†	9510.30*†									
72†	45.65	4y	1	804.5		299.6				
72‡	81.11*†	y - .1	1 iii	838.460		265.70				
73	9616.58*	-y - .03	1	873.097		231.06				
73†	52.06									
73†	87.56									
73‡	6723.08*									
74	58.61*	(-3.30	2	26012.313)		091.85				
74†	94.17	2y + .19	1	051.879		052.28				
74‡	9829.71*	-3y + .18	1 iii	085.534		018.63				
74‡	65.31									

 $\beta$

a first glance shows a tendency for the representatives to appear in sets of three successive  $\nu$  with that for 748 absent. For this, however, a line 2, 26012.313, giving 9755.31, with defect 3.30, might possibly be accepted, since  $7y=3.176$ . This table seems to give decisive evidence that these lines contain the  $p_1 2$  term, and further, that as the separations are all forward,  $p_1 2$  must enter as a positive term. In that case, if a bi-term line, i. e., as  $p_1 2 - t$ , the  $t$ -term in 16257 would be

$$92024.34 - 16257.00 = 75767.34 = 4R / \{2.406300\}^2,$$

quite out of step with known terms in other elements of this group. If it is linked with  $S_{12}$  or 35104.16, the linkage value must be  $-18847.16$ . The same link attached to my allocation of  $S_{13}=61580.1$  should show a line at 42733.0, and this is found at 4 i, 42733.362. The same linkage also is found with the extrapolated value for  $m=2$  in the suggested completion of Paschen's " $P(2m)$ ," viz.,

3423.12	{	23771.452	18849.40	On ii 42620.85
		29469.25	18846.95	4 i 48316.10
		20348.33		

These repetitions give support for the reality of the linkage origin of 18847. The value is closely met by the sum of two  $p_2$  links—thus  $9051.41 + 9794.17 = 18845.58$ . The lines given in the above list would represent the intermediate one-linked lines. The separations from 35104 are given by the figures in thick type on the right (9 omitted). It must be noted, however, that on this basis only one pair can serve to unite 35104 and 16257, and the other separations shown in the list can be attached to one of the two lines only. This double linkage is clearly seen to be near that entered in italics, the links being for it, and the two next:

$$9086.59 - 6y - .02 + 9758.61 + 10y + .06 \\ = (69\frac{1}{4}) + (74) + 4y + .04,$$

$$9120.03 + 9727.13 = \alpha - 4y + .04 + (73\frac{3}{4}\delta) + 9y - .03 \\ = \alpha + (73\frac{3}{4}) + 5y + .01,$$

$$9192.26 + y + .04 + 9652.06 + 5y + .08 \\ = (70) + (73\frac{1}{4}) + 6y + .12.$$



From the nature of the case, near values of  $\nu$  must give closely similar results, so that it is not possible to definitely settle which gives the true double linkage. We shall provisionally accept the second of these, not only because it shows the smallest error ( $\cdot 01$ ), but because it involves the two separations  $\alpha$  and  $(73\frac{3}{4}\delta)$  which occur in §3 of Part I as of most frequent occurrence. A consideration of the other separations shows that nearly all the other cases are linked to 16257, and not 35104, but it is here omitted as of little interest for the present purpose. We seem, then, driven to the conclusion that the proposed  $P(2.m)$  lines are really of the form  $p_1 2 - tm$ , with linkage effects added.

4. Passing now to the proposed  $P(1.m)$  sets, 111969 is given as  $P_1(1.3)$ . It is separated 95712 from 16257 or "P(2.3)." If these allocations be accepted, this is the value of  $s_1 - s_2$ , which again is sustained by the fact that the  $S_2 - S_1 = s_1 - s_2$  has the same value, and there is no doubt but that  $S(2)$  is at least one real  $S_{1,2}$  line of Hg. If however, the doubt as to 16257 being  $P(2.3)$  is justified, it would follow that the allied 111968 set do not belong to  $P(1.3)$ , and that  $s_1 - s_2$  is not 95712. It would then follow that 60607 is also not  $P(1.2)$ . But the double appearance of 95712 as

$$S(2.2) + 60607 \cdot 6 = 95713 \cdot 7$$

and  $111968 \cdot 6 - 16257 \cdot 00 = 95711 \cdot 6$

can scarcely be a coincidence, but must indicate a relation with the  $S_2$  lines, either some change from a  $s_2$  term to some other, or this combined with a linkage. It may be significant that  $95711 \cdot 6 - 92034 \cdot 6 = 3677 \cdot 0$  close to Paschen's 3673.3. Also 60609 seems to show the same 3673 separation as the  $P(1.3)$  (see above). To these considerations may be added the following.

- (1) The example I in the link discussion of §9 shows that the 60609 has a very exact series inequality with  $D_{23}^{35}$ .
- (2) Although the intensities of 60607, 51484 are large, they make  $P_1$  much less intense than  $P_2$  instead of twice as great, the normal value. This large discrepancy can scarcely be due to extra absorption of the  $P_1$  by the vapour. It must however

be confessed that the observed absorption of 51484 by ionized vapour supports its allocation as depending on one of the lowest levels. On the other hand, the statement by Williams referred to in §2, that it is a "raie ultime" would definitely relate it to the neutral atom.

- (3) If Paschen's relations of the S. P lines be accepted,  $s_1=151268$ ,  $p_1,2=90661.9$ , and the denominators of the lines are as follows :—

	$p.$		$s.$
60707	2.201003	-60707	1.702068
111968	3.341145	35106	2.810129
$p_1,4$	4.322842	60807	3.833442

The change in mantissa between the lower two levels in both seems excessive, and in 2.201003 is in the *wrong direction*. Accepting 60707 as P1 of this system, the latter abnormality seems to me fatal against 90661 being  $p_1,2$ , i.e., against 35106, from which it is deduced, as being S2 of the same system. Also the *sm* formula determined from  $m=4, 5, 6$  is of quite normal form and has a small  $a/m$  term, so that the calculated  $s_2$  should only have a small error. The formula gives  $s_2=55077.73$ , with resulting  $-S(3.2)=P(2.3)=15780$ , instead of 16257, and not sustaining 90661 as  $p_1,2$ , or accepting 90661 as  $p_1,2$ , it gives  $S_2=35583$ . The latter as an extrapolated value to  $m=2$  agrees very satisfactorily with the observed very strong line 10, 35514.43, only observed by Paschen. He has taken this to be  $s_1-d_1^+$  where  $d_1^+$  is a  $d$  term analogous to that of the well-known  $\lambda=5105 = p_1-d^+$  in the spectrum of copper. But it, as Paschen himself has pointed out, is forbidden on two counts, as being a transition from  $d$  to  $s$  and from  $j=3$  to  $j=1$ . Forbidden lines have a way of existing in spite of legislation laid down for them, but it is hard to accept that they can be of such high intensity as Paschen has found for them. Also he has allocated 25093.6 to an analogue of the Cu line  $\lambda=5105$  as  $d_1^+-p_1,2$ . But in Cu this line is a single line of great sharpness, whereas, as we have seen in the No. 20 in the satelloid list of Part I. Cardaun has given it complex with four companions, and Runge and Paschen in 1902 gave it as triple. The Zeeman pattern is diffuse, probably

owing to the superposition of the companions. Paschen seems to accept the allocation of this 5105 as a  $-D_{11}^+$  to the 5782, 5700 as  $-D_{22}^+, -D_{12}^+$ . But the characters of the two sets are completely different, and I have attempted\* to show that this supposition cannot be sustained.

5. Paschen has noted a relation between three lines to which he has given the allocations shown herewith:—

$$60607.6 - 25093.6 = 35514$$

$$s1 - p_1 2 - (d_1^+ - p_1 2) = s1 - d_1^+$$

If, however, 35514, as suggested above, is the S2 of his system (say)  $ap_1 2 - as2$ , 25093 must be  $as2 - t$  and 60607  $ap_1 2 - t$ . The extrapolated  $as2 = 55077 + dn$  would then give

$$t = 29984 + dn = 4R / \{3.825130 - 63.8 dn\}^2.$$

To compare with this denominator we have those of Paschen's  $d3 = 3.839$  and the  $s3, d3$  of Part I., viz., 3.7961, 3.8161. In analogy with the 26473 as  $s2 - s3$  of Part I., it would seem natural to give to it the similar allocation here of  $as2 - as3$  and to 60607 that of  $ap2 - as3$ .

6. The foregoing discussion is a criticism of that part only of Paschen's allocations which involve the lowest  $p_1$  term. Indeed a part of it is based on the acceptance of the  $p3 - sm$  series as correct. It seems definitely to show that 35104 does not come into the scheme as the  $p_1 2 - s2$  of that system. The  $p3 - dm$  set also extrapolate to a  $p2 - d2$ , which is not that allocated by Carroll and by Paschen if  $p_1 2$  is 90660. Also the separation 560 corresponds to a displacement of about  $3\frac{1}{2}\delta$ , and is thus much less than in the other elements of this group instead of larger. At the same time in themselves they look a good D set, and it cannot be said that they are definitely not. If they are sustained, the 43935 must be removed from the  $S_2 2$  list of Part I.—9829.28 becomes  $p_1 2 - p_2 2 + s2 - d_1 = s_2 - d_1 - 9121.80$ , and 9829.67 is the link  $p_3(74\frac{1}{2}\delta) - p_1$ . The general argument of Part I. is not affected. We must await the determination of its Zeeman pattern.

\* Phil. Mag. 4, 1163-5, 1927.

P<sup>2</sup>.

$$55925.33 - 4R/\{m + .180792 + .434404/m\}^2.$$

$$s_2 - = 14.476.$$

P(1. m).

P(2. m).

	<i>n.</i>	<i>v.</i>			
2.	30	60607.58		1 i	-20390.609 †
	50	51484.90	<b>9122.68</b>	1	-29512.602 †
3.	10	111968.6		20	16257.00
	4	108296.3	<b>3672.3</b>	8	12583.62
	3	(530 ± 12)	<b>3439 ± 12</b>		<b>3673.38</b>
4.				8 i	32080.721
				2	31227.72
				1 n	(28658.67)
					<b>853.00</b>
					<b>3422.05</b>

P(3. m).

5.	0	14413.1	25701.8	5 i	40114.394	
				3 i	39752.755	<b>362.14</b>
				4 ii	(36694.251)	<b>3420.64</b>
6.	$\frac{1}{2}$	10912.26	25797	0	44709 ± 10 [6.4] †	
	3	18712.3			(412286.73)	<b>3423</b>
	1 n	10678.4 †	<b>233.9</b>	2 n i	44476	† <b>233</b>
7.	1	21764.3 (1) †	25798	1 i	47584.83 [62.29] †	
	1	21510.4 †	<b>153.9</b>	0 ii	431.10	† <b>153.73</b>
				1 i	( 160.60)	<b>3424.23</b>
8.	2	23060.3 †	25796.5	1 i	49466.87 [56.21] †	
				1 i	(46048.08)	<b>3148.8</b>

† Paschen's  $m=7$  is

2 21701.92

1 21542.65 **159.27**

If 14413 is correctly allocated to P(3.5), it gives  $s_2 - s_3 = 25701$ , but those for  $m=6, 7, 8$  suggest 25798—and then, also, 35106 is not in this series.

S<sup>2</sup>.

$$90661.92, p_1 2 - = 29.881; p^2 2 - = 34.502.$$

$$39297.76, p_1 3 - = 8.527; p_2 3 - = 9.750.$$

$$sm = 4R/\{m + .862651 - .080901/m\}^2.$$

*sm*—.

S(2. m).

1.	30	-60607.58	
	50 i	-51484.89	<b>9122.69</b>
			<b>14.476</b>
2.	50 i	35106.14	
	10 i	44228.979	<b>9122.84</b>

**S<sup>3</sup> (cont.).**

<b>S(2.m).</b>			<b>S(3.m).</b>		
5.636		51362			
3. 1	60807.80			[9445]	
1	69931.54	<b>9123.74</b>	0	13118	
2.801					
4.			3 ii (20840.521)	<b>3421.3</b>	—
			8 i 20588.516		
			6 24261.843	<b>3673.32</b>	
			2 ii (24022.181)	<b>3433.6</b>	
1.591					
5.			3 26172.80		
			3 ii 30136.35	<b>3673.55</b>	
			1 ii (26712.686)	<b>3423.69</b>	
.9898					
6.			2 29945.72		
			2 33613.61	<b>3667.89</b>	
			2 ii (30183.75)	<b>3429.86</b>	
<b>S(4.m).</b>					
		15800+			
7. 0	16351	...28		[32179]	
			2 i 35852.308		
8. 4 i	17867.066	...28.5		[33695.59] †	
9. 1	18950.6 †	...28.7	1 iii 34772 ± 6	[79.34] †	
2 i	19803.1 †	<b>853</b>			
10. 4 i	19747.6 †	...27	1 ii 35577 ± 6	[74.21] †	
	— — —		1 i 39246.25 †		
11. 2 i	20348.9 †	...28		[36176.32]	

W. N. in ( ) and † added by W. M. H.

**Notes.**

$m = 3$ . The extrapolated formula for P(3.3) gives  $S(3.3) < 9478.55, 13151.87$ . Wiedemann has observed 2, 7606,  $13144 \pm .8$ , with which might possibly go McJennan's 2, 10567, 9461.6 sep.  $3690 \pm 1$ . Paschen's allocation of [9445] depends on this 3673, which, if the reasoning in the text is accepted, is a doubtful  $p3$  doublet.

January 1930.

LXIX. *The Scattering of Sound-Waves by small Elastic Spheres.* By K. F. HERZFELD\*.

THE scattering of sound-waves by small spheres has been investigated by Lord Rayleigh †, but only in the case in which the sphere is either liquid or perfectly rigid. In this paper the investigation shall be extended to a solid sphere with finite elastic constants. The first attempt showed a curious difficulty which will be explained first.

The general method to solve such a problem consists in solving separately the equations of motion inside the sphere and in the surrounding liquid. These solutions appear in the form of a progressing series of zonal harmonics, the coefficients of which are functions of the radius vector, and are furthermore multiplied by an indeterminate coefficient. These numerical coefficients are then determined with the help of the surface conditions, considering the factors of each zonal harmonic separately.

In the case of a liquid sphere in another liquid we have one longitudinal wave inside the sphere and one scattered longitudinal wave outside of it (apart from the incident wave, the coefficients of which are known). Accordingly, we have for each zonal harmonic two unknown coefficients which have to be determined by two surface conditions. As such the equality of normal displacements on both sides of the surface, and the equality of normal pressures on both sides of the surface, are chosen, while no account is taken of tangential movement. This latter is justified by the neglect of internal friction. It then turns out that for a small sphere the relative order of magnitude of subsequent coefficients decreases proportionally to  $k^2 R_0^2$ , where  $R_0$  is the radius of the sphere and  $k$  is the propagation constant ( $2\pi$  divided by the wave-length). The two first coefficients are an exception in so far as they are of the same order of magnitude, both proportional to  $R_0^3$  or to the volume of the sphere.

The same holds true for a rigid sphere ‡ where the two

\* Communicated by the Author.

† Lord Rayleigh, 'Theory of Sound,' ii. 2nd ed. p. 242 (London, 1896); 'Collected Papers,' i. p. 139. See also H. Lamb, 'Hydrodynamics,' 5th ed. p. 486 (Cambridge, 1924).

‡ The effect of a rigid sphere in a viscous medium has been calculated by Sewell, Phil. Trans. A, ccx. p. 239 (1910). See also Lamb, 'Hydrodynamics,' 5th ed. p. 621.

unknown coefficients are the velocity of the sphere as a whole and the coefficient of the scattered wave. The surface conditions and the statement in respect to the order of magnitude of the coefficients are the same as for a liquid sphere. But if we want now to treat a solid sphere with finite elastic constant, we have one more unknown coefficient, namely inside the sphere the coefficients of the longitudinal and of the transversal waves, and outside the coefficient of the longitudinal wave in the liquid; accordingly we need three surface conditions. If we select then, as was attempted first, the two conditions mentioned before, namely the two recurring to the normal velocity and stress, and in addition the condition of equality of tangential stress on both sides of the surface, it is possible to solve the equations formally; but it turns out that now the second coefficient is no longer of the same order of magnitude of the first one, but subject to the general rule mentioned above, namely smaller by a factor  $k^2 R_0^2$ .

It was thought that this difficulty, namely that a general elastic sphere should give a result different from the one common to both a liquid and a rigid sphere, was due to a wrong extrapolation (wrong way of passing to the limit), and accordingly it was decided to solve the problem for the quite general case of an elastic sphere in a fluid of moderate viscosity giving now four unknown coefficients, namely the ones for longitudinal and transversal waves in the sphere as well as longitudinal and transverse waves in the liquid, and correspondingly four surface conditions, namely for the normal velocities, the normal pressures, the tangential velocities, and the tangential stresses. It is then found that the difficulty disappears, and if the extrapolation to a non-viscous fluid is performed now, one gets a result in agreement with the cases of the fluid and of the rigid sphere.

### *The Equations of Motion and their Integration.*

The equations of motion of an elastic sphere are given in Love \*. Their integration was given by Chree †, who discussed also the free vibrations of such spheres. If we

\* A. E. H. Love, 'Treatise on Elasticity,' 3rd ed. Chap. xii. (Cambridge, 1920).

† H. Lamb, Lond. Math. Soc. Proc. vol. xiii. pp. 51, 189 (1882); C. Chree, Camb. Phil. Trans. vol. xiv. p. 50 (1885), vol. xvi. p. 14 (1898).

call  $v$  the velocity, we can write the equation of motion in general in the following form :

$$-v = \frac{1}{k_1^2} \text{grad div } v + \frac{1}{k_3^2} (\Delta v - \text{grad div } v). \quad (1)$$

We get this equation from the usual equation of motion which involves the displacement instead of the velocity by assuming the displacement to be proportional to  $e^{2\pi i v t}$  and differentiating the whole equation partially in respect to  $t$ . Designating the density of the solid by  $\rho_1$  and the elastic constants by  $\lambda_1$  and  $\mu_1$  in the same sense as Love does,  $k_1$  and  $k_3$  have the following meanings :

$$k_1^2 = 4\pi^2 \nu^2 \frac{\rho_1}{\lambda_1 + 2\mu_1}, \quad . \quad . \quad . \quad (2)$$

$$k_3^2 = 4\pi^2 \nu^2 \frac{\rho_1}{\mu_1}. \quad . \quad . \quad . \quad (2')$$

$k_1$  and  $k_3$  are the propagation constants of the longitudinal (compressional) and transversal (shearing) wave. To integrate equation (1) we proceed following Love and Lamb in the following manner :—We divide the velocity into two parts,  $v = v' + v''$ . The first part will be due entirely to sources and sinks and will have a velocity potential  $\psi_1$  :

$$\psi_1 = -\frac{1}{k_1^2} \text{div } v, \quad v' = -\text{grad } \psi_1, \quad . \quad . \quad (3)$$

$$\Delta \psi_1 + k_1^2 \psi_1 = 0; \quad . \quad . \quad . \quad (4)$$

the other part will have no divergence, but is rotatory. We simplify the procedure employed in the books mentioned above by using a method common in electrodynamics\*. We introduce a vector  $\Pi_3$  which is analogous to a Hertz vector in electrodynamics. Owing to the fact that we assume symmetry around the  $z$ -axis (the axis of propagation of the plane exciting waves), we get great simplification. Step by step the reasoning is as follows : From  $\text{div } v'' = 0$  it follows for (1)

$$\Delta v'' + k_3^2 v'' = 0, \quad \text{or} \quad -\text{rot rot } v'' + k_3^2 v'' = 0.$$

We then write to guarantee the disappearance of  $\text{div } v''$  :

$$v'' = \text{rot rot } r \Pi_3. \quad . \quad . \quad . \quad (5)$$

The symmetry is insured if we assume the vector  $\Pi_3$  to have only an  $r$ -component (we are going to designate from now

\* P. P. Debye, *Ann. d. Phys.* vol. xxx. p. 57 (1909).



on this component simply by  $\Pi_3$ ), and not to depend on the geographical length  $\phi$ . It follows, then,

$$\Delta \Pi_3 + k_3^2 \Pi_3 = 0, \quad . \quad . \quad . \quad (6)$$

$$v_r'' = -\frac{1}{r} \frac{1}{\sin \theta} \frac{\partial}{\partial \theta} \sin \theta \frac{\partial \Pi_3}{\partial \theta}, \quad . \quad . \quad . \quad (7)$$

$$v_\theta'' = \frac{1}{r} \frac{\partial^2}{\partial \theta \partial r} (r \Pi_3). \quad . \quad . \quad . \quad (7')$$

If we now introduce polar coordinates into our Laplacian, and assume again independence of everything from the geographical length, the general solution of the equations (4) and (6) has the form

$$\sum_n a_n \frac{Z_{n+1/2}(kr)}{\sqrt{kr}} P_n(\cos \theta), \quad . \quad . \quad . \quad (8)$$

where  $Z_{n+1/2}(kr)$  is a general cylindrical harmonic of order  $n+1/2$  and argument  $kr$ ,  $k$  being either  $k_1$  or  $k_3$ . As the only cylindrical functions which remain finite at the origin are the Bessel functions  $J$ , we have to choose them for the inside of the sphere. We introduce the abbreviation

$$I_n(x) = \sqrt{\frac{\pi}{2}} \frac{J_{n+1/2}(x)}{\sqrt{x}}, \quad . \quad . \quad . \quad (9)$$

and write then our solution

$$\psi_1 = \sum A_n I_n(k_1 r) P_n(\cos \theta), \quad . \quad . \quad . \quad (10)$$

$$\Pi_3 = \sum B_n I_n(k_3 r) P_n(\cos \theta). \quad . \quad . \quad . \quad (11)$$

In the liquid we can write the equation of motion according to Lamb\* quite similar to (1),

$$-v = \frac{1}{k_2^2} \text{grad div } v + \frac{1}{k_4^2} (\Delta v - \text{grad div } v). \quad . \quad (12)$$

In this equation  $k_2$  and  $k_4$  are again the propagation constants of the longitudinal and transversal wave in the liquid. They are determined by the constants of the liquid in a similar manner as (2) and (2'), namely

$$k_2^2 = 4\pi^2 \nu^2 \frac{\rho_2}{\lambda_2 + 4\pi i \nu \mu_2}, \quad . \quad . \quad . \quad (13)$$

$$k_4^2 = 2\pi \nu \frac{\rho_2}{i \mu_2}. \quad . \quad . \quad . \quad (13')$$

\* H. Lamb, 'Hydrodynamics,' 5th ed. pp. 547, 611 (Cambridge, 1924).

Here  $\rho_2$  is the density of the liquid,  $\frac{1}{\lambda_2}$  the compressibility, and  $\mu_2$  the coefficient of internal friction. The only difference compared with (2) and (2') is the appearance of  $2\pi\nu\mu_2$  instead of  $\mu_2$ . This makes both propagation constants complex, but, as shown by Lamb\*, the imaginary part in  $k_2$  is very small for example, for water, while we have for  $k_4$

$$k_4 = \sqrt{2\pi\nu} \sqrt{\frac{\rho_2}{2\mu_2}} (1-i), \dots \dots (13'')$$

and accordingly a very heavy absorption for the transversal waves.

The solution of equation (12) proceeds in a quite analogous way to the solution of (1). We write  $v = v' + v''$ .  $v'$  is determined by the divergence of  $v$  and has a velocity potential  $\psi_2$ ,

$$\Delta\psi_2 + k_2^2\psi_2 = 0, \dots \dots (14)$$

$$v' = -\text{grad } \psi_2, \dots \dots (15)$$

while  $v''$  is the rotatory part deducible from a vector  $\Pi_4$ , for which we get

$$\Delta\Pi_4 + k_4^2\Pi_4 = 0, \dots \dots (16)$$

$$v_r'' = -\frac{1}{r} \frac{1}{\sin\theta} \frac{\partial}{\partial\theta} \sin\theta \frac{\partial\Pi_4}{\partial\theta}, \dots \dots (17)$$

$$v_\theta'' = \frac{1}{r} \frac{\partial^2}{\partial\theta\partial r} (r\Pi_4). \dots \dots (17')$$

The solution of (14) and (16) will again be of the form (8); but now we have not to select the Bessel function  $J$ , as the origin is outside of the region considered, but we have to use the second of the so-called Hankel functions†  $H$ , which, at large distance, corresponds to spherical waves travelling outwards. In the case of the transversal waves these will be heavily damped‡. We introduce again an abbreviation analogous to (9):

$$h_n(x) = \sqrt{\frac{\pi}{2}} \frac{H_{n+1/2}(x)}{\sqrt{x}}, \dots \dots (18)$$

and have the solutions of (14) and (16):

$$\psi_2 = \sum C_n h_n(k_2 r) P_n(\cos\theta), \dots \dots (19)$$

$$\Pi_4 = \sum D_n h_n(k_4 r) P_n(\cos\theta). \dots \dots (20)$$

\* *Loc. cit.*

† See, for example, 'H. Bateman, 'Wave-Motion,' Cambridge, p. 37 (1915).

‡ See H. Lamb, 'Hydrodynamics,' p. 586.

We will assume later that  $kR_0$  will be small compared with unity. Accordingly it will be useful to give the power development for the two first functions (9) and (18):

$$I_0(x) = 1 - \frac{x^2}{6} + \frac{x^4}{120} - \dots, \quad . \quad . \quad . \quad (9')$$

$$I_1(x) = \frac{x}{3} - \frac{x^3}{30} + \frac{x^5}{840} - \dots, \quad . \quad . \quad . \quad (9'')$$

and

$$h_0(x) = i \frac{e^{-ix}}{x} = \frac{i}{x} + 1 - \frac{i}{2}x + \dots, \quad . \quad . \quad . \quad (18')$$

$$h_1(x) = -\frac{e^{-ix}}{x} \left(1 - \frac{i}{x}\right) = -i \frac{d}{dx} \left(\frac{e^{-ix}}{x}\right) = \frac{i}{x^2} \left(1 + \frac{x^2}{2} - \dots\right). \\ . \quad . \quad . \quad (18'')$$

The impinging plane wave has finally a velocity potential

$$\psi_0 = e^{-ik_2 z} = e^{-ik_2 r \cos \theta} = \sum (-i)^n (2n+1) I_n(k_2 r) P_n(\cos \theta). \\ . \quad . \quad . \quad (21)$$

### The Surface Conditions.

The normal pressure in the solid is given in Love's book\*. We can introduce the velocity instead of the displacement by dividing through by  $2\pi i\nu$ . We find then

$$\begin{aligned} p_{rr} &= \frac{\lambda_1}{2\pi i\nu} \operatorname{div} v + \frac{2\mu_1}{2\pi i\nu} \frac{\partial v_r}{\partial r} = \frac{\lambda_1 + 2\mu_1}{2\pi i\nu} \operatorname{div} v \\ &\quad + \frac{2\mu_1}{2\pi i\nu} \left(-\operatorname{div} v + \frac{\partial v_r}{\partial r}\right) \\ &= 2\pi i\nu \rho_1 \left\{ + \frac{1}{k_1^2} \Delta \psi_1 + \frac{2}{k_3^2} \left(-\Delta \psi_1 + \frac{\partial^2 \psi_1}{\partial r^2} \right. \right. \\ &\quad \left. \left. + \frac{\partial}{\partial r} \frac{1}{r} \frac{1}{\sin \theta} \frac{\partial}{\partial \theta} \sin \theta \frac{\partial \Pi_3}{\partial \theta} \right) \right\} \\ &= -2\pi i\nu \rho_1 \left\{ \psi_1 + \frac{2}{k_3^2} \left( \frac{2}{r} \frac{\partial \psi_1}{\partial r} + \frac{1}{r^2} \frac{1}{\sin \theta} \frac{\partial}{\partial \theta} \sin \theta \frac{\partial}{\partial \theta} \psi_1 \right. \right. \\ &\quad \left. \left. - \frac{\partial}{\partial r} \frac{1}{r} \frac{1}{\sin \theta} \frac{\partial}{\partial \theta} \sin \theta \frac{\partial \Pi_3}{\partial \theta} \right) \right\}. \quad (22) \end{aligned}$$

Here repeated use has been made of (4).

\* See Love, 'Elasticity,' p. 284.

In the liquid the tensions are given in Lamb's book on p. 602. To eliminate the pressure  $p$ , we make use of the following formula:—

$$p = \frac{1}{2\pi\nu} \frac{\partial p}{\partial t} = \frac{1}{2\pi\nu} \frac{\lambda_2}{\rho_2} \frac{\partial \rho}{\partial t} = - \frac{\lambda_2}{2\pi\nu} \operatorname{div} v.$$

It then turns out that the normal tension  $p_{rr}$  takes the same form as in the solid (22), with the exception already noted in (13') that  $2\pi\nu\mu_2$  takes the place of  $\mu_1$ . Accordingly we can write after the same transformations which were performed in (22)

$$p_{rr} = -2\pi\nu\rho_2 \left\{ \psi_2 + \psi_e + \frac{2}{k_4^2} \left( \frac{2}{r} \frac{\partial(\psi_2 + \psi_e)}{\partial r} + \frac{1}{r^2} \frac{1}{\sin\theta} \frac{\partial}{\partial\theta} \sin\theta \frac{\partial(\psi_2 + \psi_e)}{\partial\theta} - \frac{\partial}{\partial r} \frac{1}{r} \frac{1}{\sin\theta} \frac{\partial}{\partial\theta} \sin\theta \frac{\partial\Pi_4}{\partial\theta} \right) \right\}. \quad (23)$$

The surface condition as to the normal pressures consists in putting (22) equal to (23).

The tangential stress in the solid is expressed in terms of the displacement, instead of which we can introduce  $\frac{v}{2\pi\nu}$ .

Then the tangential stress takes the form

$$\begin{aligned} & \frac{\mu_1}{2\pi\nu} \left( \frac{\partial v_r}{\partial\theta} + r^2 \frac{\partial}{\partial r} \frac{v_\theta}{r} \right) \\ &= - \frac{\mu_1}{2\pi\nu} \frac{\partial}{\partial\theta} \left\{ \frac{\partial\psi_1}{\partial r} + r^2 \frac{\partial}{\partial r} \frac{\psi_1}{r^2} + \frac{1}{r \sin\theta} \frac{\partial}{\partial\theta} \sin\theta \frac{\partial\Pi_3}{\partial\theta} - r^2 \frac{\partial}{\partial r} \frac{1}{r^2} \frac{\partial\Pi_3}{\partial r} \right\} \\ &= -2 \frac{\mu_1}{2\pi\nu} \frac{\partial}{\partial\theta} \left\{ r \frac{\partial}{\partial r} \left( \frac{\psi_1}{r} \right) + \frac{\partial\Pi_3}{\partial r} + \frac{\Pi_3}{r} \left( 1 + \frac{k_3^2 r^2}{2} \right) + \frac{1}{r \sin\theta} \frac{\partial}{\partial\theta} \sin\theta \frac{\partial\Pi_3}{\partial\theta} \right\}. \quad (24) \end{aligned}$$

The same formula is valid for this liquid, except for the replacement of  $\mu_1$  by  $2\pi\nu\mu_2$ . The surface condition then takes the form

$$\rho_1 k_4^2 \left( \frac{\partial v_r}{\partial\theta} + r^2 \frac{\partial}{\partial r} \frac{v_\theta}{r} \right)_{\text{solid}} = \rho_2 k_3^2 \left( \frac{\partial v_r}{\partial\theta} + r^2 \frac{\partial}{\partial r} \frac{v_\theta}{r} - r \frac{\partial \psi_e}{\partial r} \right)_{\text{liquid}} \quad (25)$$

Finally, we have the condition of equal radial velocity

$$\frac{\partial \psi_1}{\partial r} - \frac{1}{r} \frac{1}{\sin \theta} \frac{\partial}{\partial \theta} \sin \theta \frac{\partial \Pi_3}{\partial \theta} = \frac{\partial (\psi_2 + \psi_e)}{\partial r} - \frac{1}{r} \frac{1}{\sin \theta} \frac{\partial}{\partial \theta} \sin \theta \frac{\partial \Pi_4}{\partial \theta} \quad \dots (26)$$

and equal tangential velocity

$$\frac{1}{r} \frac{\partial}{\partial \theta} \psi_1 + \frac{1}{r} \frac{\partial^2}{\partial \theta \partial r} (r \Pi_3) = \frac{1}{r} \frac{\partial}{\partial \theta} (\psi_2 + \psi_e) + \frac{1}{r} \frac{\partial^2}{\partial \theta \partial r} (r \Pi_4) \quad \dots (27)$$

We introduce now the development (10), (11), (19), (20), (21), make use of the differential equation of the zonal harmonics

$$\frac{1}{\sin \theta} \frac{d}{d\theta} \sin \theta \frac{d}{d\theta} P_n = -n(n+1) P_n,$$

and equal the coefficients of each zonal harmonic. We find then, for the surface conditions, if a dash denotes differentiation in respect to the argument,

$$\begin{aligned} \frac{\rho_1}{\rho_2} A_n \left[ \left( 1 - \frac{2n(n+1)}{k_3^2 r^2} \right) I_n(k_1 r) + 4 \frac{k_1}{k_3} \frac{1}{k_3 r} I_n'(k_1 r) \right] \\ + 2 \frac{\rho_1}{\rho_2} n(n+1) B_n \frac{d}{dk_3 r} \frac{I_n(k_3 r)}{k_3 r} \\ = C_n \left[ \left( 1 - \frac{2n(n+1)}{k_4^2 r^2} \right) h_n(k_2 r) + 4 \frac{k_2}{k_4} \frac{1}{k_4 r} h_n'(k_2 r) \right] \\ + 2n(n+1) D_n \frac{d}{dk_4 r} \frac{h_n(k_4 r)}{k_4 r} \\ + (-1)^n (2n+1) \left[ \left( 1 - \frac{2n(n+1)}{k_4^2 r^2} \right) I_n(k_2 r) \right. \\ \left. + 4 \frac{k_2}{k_4} \frac{1}{k_4 r} I_n'(k_2 r) \right], \quad \dots (23') \end{aligned}$$

$$\begin{aligned} \frac{\rho_1}{\rho_2} \frac{k_4^2}{k_3^2} A_n r^2 \frac{d}{dr} \frac{I_n(k_1 r)}{r} \\ + B_n \frac{\rho_1}{\rho_2} \frac{k_4^2}{k_3^2} \left[ \frac{d}{dr} (r I_n(k_3 r)) - \left( n(n+1) - \frac{k_3^2 r^2}{2} \right) I_n(k_3 r) \right] \\ = C_n r^2 \frac{d}{dr} \left[ \frac{h_n(k_2 r)}{r} \right] + D_n \left[ \frac{d}{dr} (r h_n(k_4 r)) \right. \\ \left. - \left( n(n+1) - \frac{k_4^2 r^2}{2} \right) h_n(k_4 r) \right] \\ + (-1)^n (2n+1) r^2 \frac{d}{dr} \left( \frac{I_n(k_2 r)}{r} \right), \quad \dots (25') \end{aligned}$$

except for  $n=0$ .

$$\begin{aligned}
 k_1 A_n I_n'(k_1 r) - n(n+1) k_3 B_n \frac{I_n(k_3 r)}{k_3 r} \\
 = k_3 C_n h_n'(k_3 r) - n(n+1) D_n k_4 \frac{h_n(k_4 r)}{k_4 r} \\
 + (-1)^n (2n+1) k_2 I_n'(k_2 r), \quad . \quad . \quad (26')
 \end{aligned}$$

$$\begin{aligned}
 A_n I_n(k_1 r) - B_n \frac{d}{dr} [r I_n(k_3 r)] \\
 = C_n h_n(k_3 r) - D_n \frac{d}{dr} [r h_n(k_4 r)] \\
 + (-1)^n (2n+1) I_n(k_2 r), \quad . \quad . \quad (27')
 \end{aligned}$$

except for  $n=0$ . In all these formulas there has to be substituted  $r=R_0$ , the radius of the sphere. As the coefficients of the development (21) are all of the same order of magnitude, while for  $kR_0 < 1$  the relative order of magnitude of two consecutive functions  $I_n$  and  $I_{n+1}$  is proportional to  $kR_0$ , the relative order of magnitude of two subsequent functions  $h_n$  and  $h_{n+1}$  is proportional to  $\frac{1}{kR_0}$ . The statement made on p. 740 concerning the relative order of magnitude of consecutive coefficients can easily be verified, except in the case  $n=0$  in relation to  $n=1$ .

### The Coefficients of the Scattered Wave.

In the evaluation of the equations (25') to (27') we shall limit ourselves for the sake of simplicity to small spheres so that  $k^2 R_0^2$  will be neglected in comparison with unity. This means that for spheres of diameter 0.1 mm. radius and a frequency of 300 kilocycles (about 5 mm. wave-lengths) we make an error of about 1 per cent. An exception will be made for  $k_4 R_0$ , as this might not be small for high frequencies in water. On account of the complex character of  $k_4$  we will keep

$$e^{-i k_4 R_0} = e^{-\frac{|k_4|}{\sqrt{2}} R_0 - i \frac{|k_4|}{\sqrt{2}} R_0}$$

without making a Taylor development. We then find for  $n=0$

$$\begin{aligned}
 \frac{\rho_1}{\rho_2} A_0 \left(1 - \frac{4}{3} \frac{k_1^2}{k_2^2}\right) = \frac{C_0}{k_2 R_0} \left(1 - i k_2 R_0 - \frac{4 k_2^2}{k_4^2} \frac{1}{k_2^2 R_0^2}\right) \\
 + \left(1 - \frac{4}{3} \frac{k_3^2}{k_4^2}\right), \quad . \quad . \quad (23'')
 \end{aligned}$$

$$-k_1 A_0 \frac{k_1 R_0}{3} = -k_2 \frac{C_0}{k_2^2 R_0^2} - \frac{1}{3} k_2 \cdot k_2 R_0, \quad . \quad . \quad (26'')$$

Therefore

$$C_0 = -\frac{k_2^3 R_0^3}{3} \frac{\frac{\rho_2}{\rho_1} \frac{k_1^2}{k_2^2} - 1 + \frac{4}{3} \frac{k_1^2}{k_2^2} \left(1 - \frac{\rho_2}{\rho_1} \frac{k_3^2}{k_4^2}\right)}{1 - \frac{4}{3} \frac{k_1^2}{k_2^2} \left(1 - \frac{\rho_2}{\rho_1} \frac{k_3^2}{k_4^2}\right)} \quad (28)$$

Furthermore, we get for  $n=1$

$$\begin{aligned} & \frac{\rho_1}{\rho_2} \frac{A_1}{3} k_1 R_0 \left[1 - \frac{4}{5} \frac{k_1^2}{k_2^2}\right] - \frac{4}{15} \frac{\rho_1}{\rho_2} B_1 k_3 R_0 \\ &= \frac{C_1 \epsilon}{k_2^3 R_0^3} \left[1 - 2 \frac{k_2^2}{k_4^2} - \frac{12}{k_4^2 R_0^2}\right] \\ & \quad - \frac{12 \epsilon D_1}{k_4^2 R_0^2} e^{-\iota k_4 R_0} \left[\frac{1 + \iota k_4 R_0}{k_4^2 R_0^2} - \frac{1}{3}\right] - 3 \iota \frac{k_2 R_0}{3} \left(1 - \frac{4}{5} \frac{k_2^2}{k_4^2}\right), \\ & \quad \dots (23''') \end{aligned}$$

$$\begin{aligned} & - \frac{k_4^2}{k_2^2} \frac{\rho_1}{\rho_2} A_1 \frac{k_1^3 R_0^3}{15} + \frac{k_4^2}{k_2^2} \frac{\rho_1}{\rho_2} B_1 \frac{1}{10} k_3^3 R_0^3 \\ &= - \frac{3 C_1 \epsilon}{k_2^2 R_0^2} (1 + \frac{1}{6} k_2^2 R_0^2) \\ & \quad - \frac{3 D_1 \epsilon e^{-\iota k_4 R_0}}{k_4^2 R_0^2} (1 + \iota k_4 R_0 - \frac{1}{2} k_4^2 R_0^2) + 3 \iota \frac{k_2^3 R_0^3}{15}, \\ & \quad \dots (25''') \end{aligned}$$

$$\begin{aligned} & k_1 A_1 \left(\frac{1}{3} - \frac{k_1^2 R_0^2}{10}\right) - 2 k_3 B_1 \left(\frac{1}{3} - \frac{k_3^2 R_0^2}{30}\right) \\ &= -2 \iota \frac{k_2 C_1}{k_2^3 R_0^3} - 2 \iota \frac{D_1 k_4 e^{-\iota k_4 R_0}}{k_4^3 R_0^3} (1 + \iota k_4 R_0) \\ & \quad - 3 \iota k_2 \left(\frac{1}{3} - \frac{k_2^2 R_0^2}{10}\right), \quad \dots (26''') \end{aligned}$$

$$\begin{aligned} & A_1 k_1 R_0 \left(\frac{1}{3} - \frac{k_1^2 R_0^2}{30}\right) - 2 B_1 k_3 R_0 \left(\frac{1}{3} - \frac{k_3^2 R_0^2}{15}\right) \\ &= \frac{C_1 \epsilon}{k_2^2 R_0^2} \left(1 + \frac{k_2^2 R_0^2}{2}\right) + \frac{D_1 \epsilon}{k_4^2 R_0^2} e^{-\iota k_4 R_0} [1 + \iota k_4 R_0 - k_4^2 R_0^2] \\ & \quad - 3 \iota k_2 R_0 \left(\frac{1}{3} - \frac{k_2^2 R_0^2}{30}\right). \quad \dots (27''') \end{aligned}$$

On the right-hand side of (23''') and (25''') we had to go to the next higher power in the development of  $h_1$ , and on the left-hand side of (26'') and (26''') to the next higher power in the development of  $I_1$  on account of  $k^2 R_0^2$  in the denominator, so that the resultant formulas will be accurate within the limit stated on p. 749.

Subtracting (27''') from (26''') we find

$$\frac{3\iota}{k_2^3 R_0^3} \left\{ C_1 \left( 1 + \frac{k_2^2 R_0^2}{6} \right) + D_1 \frac{k_2^2}{k_4^2} \left( 1 + \iota k_4 R_0 - \frac{k_4^2 R_0^2}{3} \right) e^{-\iota k_4 R_0} \right\} \\ = \frac{k_2^2 R_0^2}{5} \left( \frac{k_1^3}{k_2^3} \frac{A_1}{3} + \frac{k_3^3}{k_2^3} \frac{B_1}{3} + \iota \right),$$

where higher powers in  $kR_0$  are necessary for the solution of (23''') and (25'''). Introducing this equation into (23''') and (25''') leads to

$$\frac{k_1}{k_2} \frac{A_1}{3\iota} \left[ \frac{\rho_1}{\rho_2} + \frac{4}{5} \left( \frac{k_1^2}{k_4^2} - \frac{\rho_1}{\rho_2} \frac{k_1^2}{k_3^2} \right) \right] + \frac{4}{15} \frac{k_3}{k_2} \frac{B_1}{\iota} \left( \frac{k_3^2}{k_4^2} - \frac{\rho_1}{\rho_2} \right) = \frac{C_1}{k_2^3 R_0^3} - 1, \quad (23''')$$

$$\frac{k_1}{k_2} \frac{A_1}{3\iota} \left( \frac{k_1^2}{k_4^2} - \frac{\rho_1}{\rho_2} \frac{k_1^2}{k_3^2} \right) + \frac{k_3}{k_2} \frac{B_1}{3\iota} \left( \frac{k_3^2}{k_4^2} + \frac{3}{2} \frac{\rho_1}{\rho_2} \right) = -\frac{5}{2} \frac{C_1}{k_2^3 R_0^3}. \quad (25''')$$

These, when subtracted, give

$$\frac{k_1}{k_2} \frac{A_1}{3\iota} \frac{\rho_1}{\rho_2} - 2 \frac{k_3}{k_2} \frac{B_1}{3\iota} \frac{\rho_1}{\rho_2} = 3 \frac{C_1}{k_2^3 R_0^3} - 1,$$

while the lowest order in (26''') can be written

$$\frac{k_1}{k_2} \frac{A_1}{3\iota} - 2 \frac{k_3}{k_2} \frac{B_1}{3\iota} = -1.$$

This finally leads to the solution

$$C_1 = k_2^3 R_0^3 \frac{\rho_2 - \rho_1}{3\rho_2}, \quad (29)$$

$$D_1 e^{-\iota k_4 R_0} = -k_2 k_4^2 R_0^3 \frac{\rho_2 - \rho_1}{3\rho_2} \frac{1}{1 + \iota k_4 R_0}, \quad (29')$$

with an accuracy sufficient for the calculation of the scattered wave. This is then given by

$$\psi_2 = \frac{k_2^2 R_0^3}{3} \frac{\frac{\rho_2}{\rho_1} \frac{k_1^2}{k_2^2} - 1 + \frac{4}{3} \left( \frac{k_1^2}{k_3^2} - \frac{\rho_2}{\rho_1} \frac{k_1^2}{k_4^2} \right)}{1 - \frac{4}{3} \left( \frac{k_1^2}{k_3^2} - \frac{\rho_2}{\rho_1} \frac{k_1^2}{k_4^2} \right)} \frac{e^{-\iota k_2 r}}{r} \\ + \frac{k_2^2 R_0^3}{3} \frac{\rho_2 - \rho_1}{\rho_2} \frac{e^{-\iota k_2 r}}{r} \left( 1 - \frac{\iota}{k_2 r} \right) \cos \theta. \quad (30)$$

$$\Pi_4 = -\frac{k_2 k_2 R_0^3}{1 + \iota k_4 R_0} \frac{\rho_2 - \rho_1}{\rho_1} e^{-\iota k_4 (r - R_0)} \left( 1 - \frac{\iota}{k_4 r} \right) \cos \theta. \quad (31)$$



LXX. *Propagation of Sound in Suspensions.*

By K. F. HERZFELD\*.

*Introduction.*

THE development of the sonic interferometer by Hubbard and Loomis† has made possible a very precise measurement of the velocity of sound in liquids, and this can be used to calculate with high accuracy the compressibility of liquids. The measurement of the compressibility of solids, on the other hand, which is of great importance for our knowledge of the molecular forces, needs quite an elaborate experimental equipment‡. It would be of great advantage if the same method (sonic interferometer with piezo-electric quartz as source) could be used. It was therefore thought possible to measure the velocity of sound in suspensions of small particles, the compressibility of which should be investigated, in a liquid for which the velocity of sound could be determined separately.

In fact, it had been observed previously that the pitch of a liquid column changes when a granular deposit is stirred up§, but no quantitative theory existed. In giving here the theory, we do not distinguish between adiabatic and isothermal compression. In solids the difference is small. Furthermore, we neglect any influence of a change in temperature which might occur in the suspension through conduction from the liquid which, compressed adiabatically, will undergo small periodic temperature changes.

We will assume that the particles are small spheres, and we will treat them as isotropic solids, assuming that this will be a fair average of the effect of the random orientation of anisotropic particles.

There are two methods to calculate the velocity of propagation as influenced by obstacles. We will first describe one which best gives the physical meaning, but is only suited for a first approximation, and then proceed with a method necessary for higher approximations, but less clear.

\* Communicated by the Author.

† J. C. Hubbard and A. L. Loomis, *Phil. Mag.* v. p. 1177 (1928); A. L. Loomis and J. C. Hubbard, *Journ. Amer. Opt. Soc.* xvii. p. 295 (1928).

‡ See, for example, T. W. Richards, *Carnegie Inst. Wash.* No. 76, 1907; E. Madelung und R. Fuchs, *Ann. d. Phys.* lxxv. p. 289 (1921).

§ Unpublished observation of J. C. Hubbard.

Calculation of the Velocity in Suspensions.

First Approximation.

The idea of this method is due to Lord Rayleigh\*, and consists in the following:—

If a plane wave (the primary wave) falls on a small object, this object will emit a scattered wave which, at large distances, will die out. If we have now a layer of thickness  $dz$  containing  $N$  of the obstacles per cub. cm., and extending to infinity in a plane at right angles to the direction of propagation of the primary beam ( $z$ -direction), the scattered waves from all these obstacles will compound at a large distance from the layer to two plane waves of the same frequency as the primary wave, one going in the opposite direction (reflected wave from the layer), the other going in the same direction as the primary beam. The latter, together with the primary wave, will give a resultant wave, which will have a phase difference proportional to  $dz$  compared with the primary wave. This will amount to the same thing as if the primary wave had a different velocity of propagation in the layer  $dz$ .

In the case of the first approximation, with which we are dealing now, we can describe the motion in the liquid by a velocity potential  $\psi$ , so that the velocity is given by

$$v = -\text{grad } \psi. \quad (32)$$

The primary wave will have a velocity potential equal to

$$\psi_0 = e^{2\pi i\nu \left(t - \frac{z}{V_0}\right)}. \quad (33)$$

We write now the velocity potential of the plane wave compounded from the scattered waves:

$$\psi' = A \epsilon dz e^{2\pi i\nu \left(t - \frac{z}{V}\right)}. \quad (34)$$

We want the resultant wave, the velocity potential of which will be equal to  $\psi_0 + \psi'$ , equivalent to a wave which has had a different velocity  $V$  in the layer  $dz$ , and which, therefore, has a velocity potential

$$\psi = e^{2\pi i\nu \left(t - \frac{z-dz}{V_2} - \frac{dz}{V}\right)} = e^{2\pi i\nu \left(t - \frac{z}{V_2}\right)} \left(1 + 2\pi i \left(1 - \frac{V_2}{V}\right) \frac{dz}{\lambda}\right).$$

\* Lord Rayleigh, *Phil. Mag.* (5) xlvii. p. 375 (1899); 'Collected Papers,' iv. p. 307. See also K. F. Herzfeld, *Zeit. f. Phys.* xxiii. p. 341 (1924).

where  $\lambda = \frac{V^2}{\nu}$  is the wave-length. From this it follows

$$1 - \frac{V_2}{V} = \frac{\lambda}{2\pi} A. \quad \dots \quad (35)$$

In our particular case the velocity potential of a wave scattered by a fluid sphere of density  $\rho_1$  and compressibility  $K_1$  in a liquid of density  $\rho_2$  and compressibility  $K_2$  is \* ( $R_0$  radius of the sphere):

$$\psi'' = \frac{4\pi^2 R_0^3}{3\lambda^2 r} \left( \frac{K_1 - K_2}{K_1} + 3 \frac{\rho_2 - \rho_1}{\rho_2 + 2\rho_1} \cos \theta \right) e^{2\pi i \nu \left( t - \frac{r}{V_2} \right)}. \quad (36)$$

We have to integrate this over an infinite surface in the  $xy$  plane. The first part of our expression gives directly a plane wave (containing  $z$  only in the form 2). The next member gives, besides a plane wave, additional terms with powers of  $z$  in the denominator, which therefore die out at great distances. If we introduce the abbreviation

$$\beta = N \frac{4\pi R_0^3}{3}$$

which gives the fraction of space filled by the particles, we find then from equation (35)

$$- \frac{V - V_2}{V} = \frac{\beta}{2} \left( \frac{K_1 - K_2}{K_1} + 3 \frac{\rho_1 - \rho_2}{\rho_2 + 2\rho_1} \right). \quad \dots \quad (37)$$

If we compare this with the result which we should get in a uniform medium having a compressibility  $K_2 + \beta(K_1 - K_2)$  and a uniform density  $\rho_2 + \beta(\rho_1 - \rho_2)$ , namely

$$- \frac{V - V_2}{V} = \frac{\beta}{2} \left( \frac{K_1 - K_2}{K_2} + \frac{\rho_1 - \rho_2}{\rho} \right), \quad \dots \quad (37')$$

we see that the first member is identical, while the second agrees only if the difference in density is small.

In the preceding calculation we have used only the first member in the series which gives the scattered wave.

This means that we have neglected  $\left(\frac{R_0}{\lambda}\right)^2$  compared with unity. In this case only the total volume  $\beta$  enters, not the radius explicitly. We are going to use the same approximation for solid spheres, and may hope that then the formula will be applicable also if the particles are not exactly

\* Lord Rayleigh, 'Theory of Sound,' 2nd ed. ii. p. 284 (London, 1896).

spheres, as only the total volume of the suspended material matters.

Furthermore, we have taken into account only uniform expansions of this sphere and motions of the sphere as a whole, but neglected all shearing and frictional effects. As explained in the preceding paper, we have to proceed in a different manner for a solid sphere. The introduction of (30) and (30') of the preceding paper, instead of (36) into (35) then leads to the following formula for the propagation of a sound-wave through a suspension of solid spheres:—

$$\frac{V_2 - V}{V} = \frac{\beta}{2} \left[ \frac{\rho_2 k_1^2}{\rho_1 k_2^2} \frac{1}{1 - \frac{4}{3} \frac{k_1^2}{k_2^2}} - 1 + \frac{\rho_1 - \rho_2}{\rho_2} \right]. \quad (38)$$

Here, only the longitudinal waves have been taken into account, as the transversal waves in the liquid die out so rapidly that they do not contribute to the wave-front of the secondary wave at a great distance. The absorption of energy, for which they are responsible, is taken care of in the imaginary parts of the longitudinal waves, the amplitudes of which are influenced by the presence of the transversal waves in the surface condition. In formula (38) only the real parts of the amplitudes of the longitudinal waves have been taken in, and  $\frac{k_1^2}{k_4^2}$  and  $\frac{k_2^2}{k_4^2}$  have been neglected compared with unity.

Furthermore, the mutual influence that the suspended particles have on each other has been neglected in the calculation for both liquid and solid suspension. One part of this influence could easily be taken into account\*, namely the influence of the reflected wave on preceding layers.

This would substitute for  $\frac{V - V_2}{V_2}$  the expression  $\frac{V^2 - V_2^2}{2V_2^2}$ ,

corresponding in optics to the change from  $n-1$  to  $\frac{n^2-1}{2}$ .

But we have, besides, to consider the analogy of the Lorenz-Lorentz force in optics, and to do this a more complicated method is necessary.

If we now introduce the values of  $k_1^2$  and  $k_2^2$  from (2) and (2'), introduce the cubical compressibility of the solid

$$\frac{1}{K_1} = \lambda_1 + \frac{2}{3}\mu_1,$$

\* P. P. Ewald, *Physica*, iv. p. 234 (1924).

and finally substitute for  $k_2^2$  its value (13), neglecting as before the imaginary part, the expression appearing in the bracket of (38) becomes

$$\frac{\rho_2 k_1^2}{\rho_4 k_2^2} \frac{1}{1 - \frac{4}{3} \frac{k_1^2}{k_2^2}} = \frac{\lambda_2}{\lambda_1 + 2\mu_1} \frac{1}{1 - \frac{4}{3} \frac{\mu_1}{\lambda_1 + 2\mu_1}} = \frac{\lambda_2}{\lambda_1 + \frac{2}{3}\mu_1} = \frac{K_1}{K_2},$$

and (38) takes the form

$$\frac{V_2 - V}{V} = \frac{\beta}{2} \left( \frac{K_1 - K_2}{K_2} + \frac{\rho_1 - \rho_2}{\rho_2} \right), \quad . \quad . \quad (38')$$

which is identical with (37').

### *Ewald's Method.*

#### *Outline of the Method.*

To make the rather complicated calculation which will follow a little more clear, we give first an example of Ewald's method\* in the simplest case. Assume that we have a medium filled with  $N$  oscillators per cu. cm. These oscillators shall give a scattered wave of the simplest type (spherical symmetry, as in the case of an expanding sphere). We put the velocity potential of the scattered wave equal to

$$\psi'' = a\psi_0 e^{2\pi i \nu t - i k_2 r}$$

if the velocity potential of the primary wave has the amplitude  $\psi_0$ . In this formula  $k_0$  means the "propagation constant"  $= \frac{2\pi}{\lambda_2}$ , where  $\lambda_2$  is the wave-length in the empty medium (without oscillators).

We now want to set up a state of motion in which the oscillators oscillate at a given frequency, and the phase of the oscillators proceeds in the form of a plane wave along the direction  $z$ . We call the propagation constant of this oscillator phase  $k = \frac{2\pi}{\lambda}$ , where  $\lambda$  would then be the wave-length of the oscillator phase, or the wave-length of the gross disturbance, or the quantity which we should measure as wave-length in the medium filled with oscillators.

\* P. P. Ewald, Thesis (Münich, 1912); *Ann. d. Phys.* xlix. pp. 1, 117 (1916). See also a number of papers by L. Natanson in *Bull. Acad. Sci. Crak.* C. G. Darwin, *Trans. Camb. Phil. Soc.* xxiii. p. 137 (1924).

If we are deep in the medium, the disturbance will be made up entirely from the mutual radiation of the oscillators, the primary beam having been lost in surface-layers. We know, therefore, on the one hand, that the disturbance is given by the plane wave which has, at the point  $z'$ , the velocity potential

$$\psi = \psi_0 e^{2\pi i \nu t - k z'}.$$

On the other hand, this must be made up by contributions from all oscillators, and therefore be equal to

$$\begin{aligned} \psi &= a N \psi_0 e^{2\pi i \nu t} \int \frac{e^{-i k_0 r - i k z}}{r} \cdot 2\pi r^2 dr d\theta \\ &= 2\pi N a e^{2\pi i \nu t - k z'} \int \frac{e^{-i k_0 r - i k r \cos \theta}}{r} 2\pi r^2 dr d\theta \\ &\quad (z = z' + r \cos \theta). \end{aligned}$$

This leads to the equation of dispersion

$$1 = \frac{4\pi N a}{k_0^2 - k^2},$$

defining the propagation constant  $k$  and therefore the velocity of the resultant wave in agreement with a direct calculation by the method mentioned before.

### *The Exciting Field.*

To calculate the exciting field on the surface of one particle, we have to sum up the contributions of all other particles, which we assume uniformly distributed over the medium, substituting an integration for the summation. The task would be very simple if we could assume the other particles to be present everywhere (integration over the whole space). Instead, we have to consider that the centre of no other particle can be inside a sphere of radius  $2R_0$  around the centre of the considered particle. Accordingly we have to subtract from the previous integral (which in optics is analogous to the electric field) the contributions which would come from particles contained in the sphere  $2R_0$  (this corresponds in optics to the negative Lorentz-Lorenz force, leaving finally after subtraction the exciting force).

In principle these will be contributions to the exciting field from both the longitudinal and the transversal waves; but here, too, as in the preceding paper, we shall neglect the

contributions of the transversal waves. From what we have just explained, it can be seen that only waves coming from a distance farther than  $2R_0$  to the surface of the considered sphere (that means waves which will have travelled at least the distance  $R_0$ ) will contribute to the exciting field. If we now assume that  $k_4 R_0$  is large compared with unity, as it will be for high-frequency sound-waves in water, and particles not much smaller than 0.01 mm., the absorption of the transversal waves will be sufficient to make them negligible. Accordingly, the exciting field will be calculated from the longitudinal waves alone.

We want first to show that it is possible to get the exciting velocity from an exciting potential  $\psi_e$ . We call the place where we want to calculate the velocity  $x, y, z$ , the place of the particle acting as source  $\xi, \eta, \zeta$ . If we have  $N$  particles per cm.<sup>3</sup>, the particles in  $d\xi, d\eta, d\zeta$  give a velocity in  $x, y, z$ :

$$v_x = -\frac{\partial}{\partial x} \psi_2 \cdot N d\xi d\eta d\zeta e^{-ikz},$$

as we have assumed that there is an "oscillator wave" proceeding through the medium proportional to  $e^{-ikz}$ , giving a corresponding phase-factor. In  $\psi_2$  the argument is

$$r = \sqrt{(x-\xi)^2 + (y-\eta)^2 + (z-\zeta)^2}, \quad \cos \vartheta = \frac{z-\zeta}{r}.$$

Therefore the resultant velocity is

$$v_x = -N \iiint e^{-ikz} \frac{\partial \psi_2}{\partial x} d\xi d\eta d\zeta = -\frac{\partial \psi_e}{\partial x}, \quad (39)$$

$$\psi_e = N \iiint e^{-ikz} \psi_2 d\xi d\eta d\zeta. \quad (40)$$

We then divide  $\psi_e$  into two parts,  $\psi_e'$  being calculated by integration over the whole space from which  $\psi_e''$ , the contribution of a sphere of radius  $2R_0$  around the centre of the considered particle, has to be subtracted:

$$\psi_e = \psi_e' - \psi_e''. \quad (41)$$

In the calculation of  $\psi_e'$  we introduce polar coordinates  $R, \Theta, \Phi$  around the point of observation  $x, y, z$ . We write

$$e^{-ikz} = e^{-ikz_e - ik(z-z)} = e^{-ikz_e - ikR \cos \Theta}.$$

Here we have made use of the fact that  $r=R$ , while  $\vartheta$  (the angle  $r$  makes with the  $z$ -axis measured in the place of the

particle) is  $\pi - \Theta$ , where  $\Theta$  is the angle  $r$  (or  $R$ ) makes with the  $z$ -axis in the observation point. (40) then takes the form

$$\psi_e' = N e^{-ikz} 2\pi \iint e^{-ikR \cos \Theta} \psi_2 R^2 dR \sin \Theta d\Theta.$$

In this we introduce (19) and (21), make use of the well-known formulas

$$\int P_n P_m \sin \Theta d\Theta = 0 \quad n \neq m, \quad \int P_n^2 \sin \Theta d\Theta = \frac{2}{2n+1},$$

and remember that

$$P_n(\cos \theta) = (-1)^n P_n(\cos \Theta).$$

We then find

$$\psi_e' = N e^{-ikz} \sum C_n \alpha_n(k_2 k) \quad . \quad . \quad . \quad (41)$$

with \*

$$\begin{aligned} \alpha_n(k_2, k) &= 4\pi \epsilon^n \int_0^\infty I_n(kR) h_n(k_2 R) R^2 dR \\ &= 2\pi^2 \epsilon^n \int \frac{J_{n+\frac{1}{2}}(kR) H_{n+\frac{1}{2}}(k_2 R)}{R k_2} R dR \\ &= \frac{2\pi^2 \epsilon^n}{\sqrt{k_2 k (k_2^2 - k^2)}} \left[ R \{ k_2 H_{n+\frac{1}{2}}(k_2 R) J_{n+\frac{1}{2}}(kR) \right. \\ &\quad \left. - k H_{n+\frac{1}{2}}(k_2 R) J_{n+\frac{1}{2}}(kR) \} \right]_0^\infty \\ &= -\frac{4\pi}{\sqrt{k_2 k}} \frac{1}{k_2^2 - k^2} \epsilon^{n+1} \left( \frac{k}{k_2} \right)^{n+\frac{1}{2}} = -\frac{4\pi}{k_2} \frac{\epsilon^{n+1}}{k_2^2 - k^2} \left( \frac{k}{k_2} \right)^n. \end{aligned} \quad . \quad . \quad . \quad (42)$$

Here  $\lim_{R \rightarrow \infty} e^{i(k-k_2)R}$  has to be neglected, as is the case also in Ewald's work, as otherwise the particular form of the outward boundary would play a rôle (give a diffraction pattern). Re-writing (41) we get finally for the first part of the exciting field

$$\begin{aligned} \psi_e' &= \frac{3\beta}{k_2^3 R_0^3} \frac{k_2^2 \epsilon}{k^2 - k_2^2} \sum C_n \epsilon^n \left( \frac{k}{k_2} \right)^n \\ &\quad \times \sum (-1)^m (2m+1) I_m(kR) P_m(\cos \Theta). \end{aligned} \quad (43)$$

\* See, for example, P. Schafheitlin, 'Theorie der Besselschen Funktionen,' p. 68 (Leipzig, 1908).



The calculation of  $\psi_e''$  is much more complicated on account of the finiteness of the limits in the integral. If we call, as before,  $\xi, \eta, \zeta$  the position of the source,  $x, y, z$  the point at which the potential has to be calculated,  $x_0, y_0, z_0$  the centre of the sphere for the surface of which we want to calculate the exciting radiation, we have to introduce polar coordinates around this centre :

$$R^2 = (\xi - x_0)^2 + (\eta - y_0)^2 + (\zeta - z_0)^2,$$

$$R \cos \Theta = \zeta - z_0.$$

The expressions  $r$  and  $\theta$ , which appear in the formula (19) of  $\psi_2$ , have, on the other hand, the meaning

$$r^2 = (x - \xi)^2 + (y - \eta)^2 + (z - \zeta)^2,$$

$$r \cos \theta = \zeta - z.$$

Our task is then the evaluation of

$$\begin{aligned} \psi_e'' &= N e^{-ikz_0} \int_0^{2R_0} \int_0^\pi \int_0^{2\pi} e^{-ik(\zeta - z_0)} \psi_2 d\Phi \sin \Theta d\Theta R^2 dR \\ &= \frac{3}{4\pi} \beta \frac{e^{-ikz_0}}{R_0^3} \int_0^{2R_0} \int_0^\pi \int_0^{2\pi} e^{-ik(\zeta - z_0)} [C_0 h_0(k_2 r) \\ &\quad + C_1 h_1(k_2 r) P_1(\cos \theta) \dots] R^2 dR \sin \Theta d\Theta d\Phi. \quad (44) \end{aligned}$$

As before, we restrict our calculations to members larger than  $k^2 R_0^2$ . Accordingly we develop  $h_0$  and the  $e$  power. Furthermore, we make use of the formula following from (18') and (18'') :

$$h_1(kr) \cos \theta = \frac{\partial r}{\partial z} h_1(kr) = \frac{\partial r}{\partial z} \left( -\frac{dh_0(kr)}{dkr} \right) = -\frac{\partial}{\partial kz} h_0(kr).$$

Accordingly we can re-write (44) in the following manner :

$$\begin{aligned} \psi_e'' &= \frac{3}{4\pi} \beta \frac{e^{-ikz_0}}{R_0^3} \left( C_0 - C_1 \frac{\partial}{\partial k_2 z} \right) \\ &\quad \times \int_0^{2R_0} \int_0^\pi \int_0^{2\pi} \left[ 1 - ik(\zeta - z_0) - \frac{k^2}{2} (\zeta - z_0)^2 - \dots \right] \\ &\quad \left[ \frac{1}{k_2 r} + 1 - \frac{ik_2 r}{2} + \dots \right] R^2 dR \sin \Theta d\Theta d\Phi \\ &= \frac{3}{4\pi} \beta \frac{e^{-ikz_0}}{R_0^3} \left( C_0 - C_1 \frac{\partial}{\partial k_2 z} \right) \left\{ \frac{32\pi}{3} R_0^3 + \frac{1}{k_2} \right\} \end{aligned}$$

$$\begin{aligned}
 & \times \int_0^{2R_0} \int_0^\pi \int_0^{2\pi} \frac{1}{r} [1 - ikR \cos \Theta \dots] R^2 dR \sin \Theta d\Theta d\Phi \} \\
 & + \frac{3}{4\pi} \beta \frac{e^{-ikz_0}}{R_0^3} C_1 \frac{\partial}{\partial k_2 z} \left[ \frac{ik_2}{2} \int_0^{2R_0} \int_0^\pi \int_0^{2\pi} r R^2 dR \sin \Theta d\Theta d\Phi \right. \\
 & \left. + \frac{k^2}{2k_2} \int_0^{2R_0} \int_0^\pi \int_0^{2\pi} \frac{R^2}{r} \cos^2 \Theta R^2 dR \sin \Theta d\Theta d\Phi \right] \\
 & = \frac{3}{4\pi} \beta \frac{e^{-ikz_0}}{R_0^3} \left( C_0 - C_1 \frac{\partial}{\partial k_2 z} \right) \left[ \frac{3}{2} R_0^3 + \frac{k}{k_2} \right. \\
 & \times \int_0^{2R_0} \int_0^\pi \int_0^{2\pi} \frac{1}{r} [1 - ikR \cos \Theta \dots] R^2 dR \sin \Theta d\Theta d\Phi \left. \right] \\
 & + \frac{3}{4\pi} \beta \frac{e^{-ikz_0}}{R_0^3} \frac{k}{2} C_1 \\
 & \times \int_0^{2R_0} \int_0^\pi \int_0^{2\pi} \frac{z - z_0 - R \cos \Theta}{r} R^2 dR \sin \Theta d\Theta d\Phi \\
 & + \frac{3}{4\pi} \beta \frac{e^{-ikz_0}}{R_0^3} \frac{C_1}{2} \frac{k^2}{k_2^2} \\
 & \times \frac{\partial}{\partial z} \int_0^{2R_0} \int_0^\pi \int_0^{2\pi} \frac{1}{r} R^2 \cos^2 \Theta \cdot R^2 dR \sin \Theta d\Theta d\Phi. \quad (45)
 \end{aligned}$$

In the evaluation of this integral we find integrals of the form

$$\int_0^{2R_0} \int_0^\pi \int_0^{2\pi} \frac{1}{r} R^n \cos^n \Theta R^2 dR \sin \Theta d\Theta d\Phi.$$

We remark that they represent the electrostatical potential at a point  $xyz$  inside of a sphere of radius  $2R_0$ , in which there is a positive electric density distributed according to  $R^n \cos^n \Theta$ . We therefore solve the Laplace equation

$$\Delta V = -4\pi R^n \cos^n \Theta$$

with the conditions of continuity of  $V$  and  $\frac{\partial V}{\partial R}$  on the surface

of the sphere and a vanishing potential at infinity. We get

$$\left. \begin{aligned} \int_0^{2R_0} \int_0^\pi \int_0^{2\pi} \frac{1}{r} R^2 dR \sin \Theta d\Theta d\Phi &= \frac{4\pi}{6} (12R_0^2 - R^2), \\ \int_0^{2R_0} \int_0^\pi \int_0^{2\pi} \frac{1}{r} R \cos \Theta R^2 dR \sin \Theta d\Theta d\Phi \\ &= \frac{4\pi}{10} R \cos \Theta (6R_0^2 - R^2), \\ \int_0^{2R_0} \int_0^\pi \int_0^{2\pi} \frac{1}{r} R^2 \cos^2 \Theta R^2 dR \sin \Theta d\Theta d\Phi \\ &= \frac{4\pi}{3} \left( 4R_0^4 - \frac{R^4}{20} \right) + \frac{4\pi}{3} R^2 \left( \frac{4}{15} R_0^2 - \frac{R^2}{7} \right) P_2(\cos \Theta) \\ &= 4\pi \left[ \frac{R^4}{140} - \frac{1}{14} R^2 z^2 + \frac{2}{5} R_0^2 z^2 - \frac{2}{15} R_0^2 R^2 + \frac{4}{3} R_0^4 \right]. \end{aligned} \right\} \dots (46)$$

This leads then to the following potential (45) of the "Lorentz-Lorenz force":—

$$\begin{aligned} \psi_e'' &= \frac{3}{4\pi} \frac{\beta}{R_0^3} e^{-ikz_0} \left( C_0 - C_1 \frac{\partial}{\partial k_2 z} \right) \left\{ \frac{32\pi}{3} R_0^3 \right. \\ &\quad \left. + \frac{4\pi}{k_2} \left[ \frac{4\pi}{6} (12R_0^2 - R^2) - ik \frac{4\pi}{10} R \cos \Theta (6R_0^2 - R^2) \right] \right\} \\ &\quad + \frac{3}{4\pi} \frac{\beta}{R_0^3} e^{-ikz_0} \frac{1}{2} C_1 \left[ \frac{4\pi}{6} R \cos \Theta (12R_0^2 - R^2) \right. \\ &\quad \left. - \frac{4\pi}{10} R \cos \Theta (6R_0^2 - R^2) \right] + \frac{3}{4\pi} \frac{\beta}{R_0^3} e^{-ikz_0} \frac{C_1}{2} 4\pi \frac{k^2}{k_2^2} \\ &\quad \times \frac{\partial}{\partial z} \left[ \frac{R^4}{140} - \frac{1}{14} R^2 z^2 + \frac{2}{5} R_0^2 z^2 - \frac{2}{15} R_0^2 R^2 + \frac{4}{3} R_0^4 \right] \\ &= \beta e^{-ikz_0} C_0 \left[ \frac{1}{k_2 R_0} \left( 6 - 8ik_2 R_0 - \frac{R^2}{2R_0^2} \right) \right. \\ &\quad \left. + \frac{3}{10} \frac{k}{k_2} \left( 6 \frac{R}{R_0} - \frac{R^3}{R_0^3} \right) P_1(\cos \Theta) \right] \\ &\quad + \beta e^{-ikz_0} C_1 \left\{ \frac{k}{k_2} \frac{1}{k_2 R_0} \left( \frac{R^2}{2R_0^2} - \frac{9}{5} \right) + \left[ \frac{1}{k_2^2 R_0^2} \frac{R}{R_0} \right. \right. \end{aligned}$$

$$\begin{aligned}
 & + \frac{R}{R_0} \left( \frac{21}{10} + \frac{4}{5} \frac{k^2}{k_2^2} - \frac{1}{10} \left( 1 + 3 \frac{k^2}{k_2^2} \right) \frac{R^2}{R_0^2} \right) P_1(\cos \Theta) \\
 & + \frac{2}{5} \frac{k}{k_2} \frac{1}{k_2 R_0} \frac{R^2}{R_0^2} P_2(\cos \Theta) - \frac{3}{35} \frac{k^2}{k_2^2} \frac{R^3}{R_0^3} P_3(\cos \Theta) \Big\}. \\
 & \qquad \qquad \qquad \dots \dots \dots (47)
 \end{aligned}$$

In this formula the development has been extended just to the necessary limit.

### The Surface Conditions.

The surface conditions are exactly the same as in the preceding paper, with the one exception that the normal tension due to the exciting field has to be written

$$\begin{aligned}
 p_{rr} = & -2\pi\nu\rho_2 \left[ \frac{k^2}{k_2^2} \psi_e' + \frac{2}{k_4^2} \left( \frac{2}{r} \frac{\partial \psi_e'}{\partial r} + \frac{1}{r^2} \frac{1}{\sin \theta} \frac{\partial}{\partial \theta} \sin \theta \frac{\partial \psi_e'}{\partial \theta} \right) \right. \\
 & + \frac{1}{k_2^2 r^2} \frac{\partial}{\partial r} \left( r^2 \frac{\partial \psi_e''}{\partial r} \right) - \frac{4}{k_4^2 r} \frac{\partial \psi_e''}{\partial r} \\
 & \left. + \left( \frac{1}{k_2^2} - \frac{2}{k_4^2} \right) \frac{1}{r^2} \frac{1}{\sin \theta} \frac{\partial}{\partial \theta} \sin \theta \frac{\partial \psi_e''}{\partial \theta} \right]
 \end{aligned}$$

instead of (23), because  $\psi_e'$  satisfies the equation  $\Delta\psi + k^2\psi = 0$  and not  $\Delta\psi + k_2^2\psi = 0$ . We then find for the member not depending on the angle  $\vartheta$

$$\begin{aligned}
 \frac{\rho_1}{\rho_2} A_0 \left( 1 - \frac{4k_1^2}{3k_2^2} \right) = & \iota \frac{C_0}{k_2 R_0} \left( 1 - \iota k_2 R_0 - \frac{4}{k_4^2 R_0^2} \right) \\
 & + \frac{3\beta}{k_2^3 R_0^3} \frac{k_2^2}{k^2 - k_2^2} \left( C_0 \iota - C_1 \frac{k}{k_2} \right) \left( \frac{k^2}{k_2^2} - \frac{4}{3} \frac{k^2}{k_4^2} \right) \\
 & + \frac{1}{k_2^3 R_0^3} \left( -\frac{3\iota\beta C_0}{k_2 R_0} + 3\beta C_1 \frac{k}{k_2} \frac{1}{k_2 R_0} \right) \\
 & - \frac{4}{k_4^2 R_0^2} \left( -\frac{\iota\beta C_0}{k_2 R_0} + \beta C_1 \frac{k}{k_2} \frac{1}{k_2 R_0} \right), \quad (48)
 \end{aligned}$$

$$\begin{aligned}
 -k_1 A_0 \frac{k_1 R_0}{3} = & -k_2 \frac{\iota C_0}{k_2^2 R_0^2} - \frac{3\beta}{k_2^3 R_0^3} \frac{k_2^2}{k^2 - k_2^2} \left( C_0 \iota - C_1 \frac{k}{k_2} \right) \frac{k^2 R_0}{3} \\
 & + \frac{\iota\beta C_0}{k_2 R_0^2} - \beta C_1 \frac{k}{k_2} \frac{1}{k_2 R_0^2}, \quad (49)
 \end{aligned}$$

or

$$\frac{\rho_1}{\rho_2} \frac{A_0}{3} k_2^3 R_0^3 \left(1 - \frac{4}{3} \frac{k_1^2}{k_3^2}\right) \\ \dots = \beta \left( \frac{k^2}{k^2 - k_2^2} - 1 \right) \left( C_0 - C_1 \frac{k}{k_2} \right) \left( 1 - \frac{4}{3} \frac{k_2^2}{k_4^2} \right), \quad (48')$$

$$\frac{k_1^2}{k_2^2} \frac{A_0}{3} k_2^3 R_0^3 = C_0 + \beta \left( \frac{k^2}{k^2 - k_2^2} - 1 \right) \left( C_0 - C_1 \frac{k}{k_2} \right). \quad (49')$$

The elimination of  $A_0$  leads to

$$C_0 = \beta \left( \frac{k^2}{k^2 - k_2^2} - 1 \right) \left( C_0 - C_1 \frac{k}{k_2} \right) \left\{ \frac{\rho_2 k_1^2}{\rho_1 k_2^2} \frac{1 - \frac{4}{3} \frac{k_2^2}{k_4^2}}{1 - \frac{4}{3} \frac{k_1^2}{k_3^2}} - 1 \right\}. \\ \dots \quad (50)$$

Similarly, we get for the factor of  $P_1(\cos \Theta)$  in close analogy to equations (23''') to (27''')

$$\frac{\rho_1}{\rho_2} \frac{A_1}{3} k_1 R_0 \left( 1 - \frac{4}{5} \frac{k_1^2}{k_3^2} \right) - \frac{4}{15} \frac{\rho_1}{\rho_2} B_1 k_3 R_0 \\ = \frac{C_1}{k_2^2 R_0^2} \left( 1 - 2 \frac{k_2^2}{k_4^2} - \frac{12}{k_4^2 R_0^2} \right) - \frac{12 D_1 e^{-ik_4 R_0}}{k_4^2 R_0^2} \left( \frac{1 + ik_4 R_0}{k_4^2 R_0^2} - \frac{1}{3} \right) \\ - \frac{9\beta}{k_2^3 R_0^3} \frac{k_2^2}{k^2 - k_2^2} \left( C_0 - C_1 \frac{k}{k_2} \right) \frac{k R_0}{3} \frac{k^2}{k_2^2} \left( 1 - \frac{4}{5} \frac{k_2^2}{k_4^2} \right) \\ - \frac{3\beta C_0}{k_2^2 R_0^2} \frac{k}{k_2} \left( 1 - \frac{4}{5} \frac{k_2^2}{k_4^2} \right) - \frac{\beta C_1 \eta_1}{k_2^2 R_0^2} \left( 1 + 3 \frac{k^2}{k_2^2} \right) \left( 1 - \frac{4}{5} \frac{k_2^2}{k_4^2} \right), \\ \dots \quad (51)$$

$$- \frac{k_4^2}{k_3^2} \frac{\rho_1}{\rho_2} A_1 \frac{k_1^3 R_0^3}{15} + \frac{k_4^2}{k_3^2} \frac{\rho_1}{\rho_2} \frac{B_1}{10} k_3^3 R_0^3 \\ = - \frac{3 C_1}{k_2^2 R_0^2} \left( 1 + \frac{k_2^2 R_0^2}{6} \right) - \frac{3 D_1 e^{-ik_4 R_0}}{k_4^2 R_0^2} \left( 1 + ik_4 R_0 - \frac{1}{2} k_4^2 R_0^2 \right) \\ + \frac{9\beta}{k_2^3 R_0^3} \frac{k_2^2}{k^2 - k_2^2} \left( C_0 - C_1 \frac{k}{k_2} \right) \frac{k^3 R_0^3}{15} \\ + \beta C_0 \frac{k}{k_2} \frac{3}{10} + \beta C_1 \frac{1}{10} \cdot 2 \left( 1 + 3 \frac{k^2}{k_2^2} \right), \quad \dots \quad (52)$$

$$\begin{aligned}
 & k_1 A_1 \left( \frac{1}{3} - \frac{k_1^2 R_1^2}{10} \right) - 2k_3 B_1 \left( \frac{1}{3} - \frac{k_3^2 R_0^2}{30} \right) \\
 &= -2 \frac{\iota k_2 C_1}{k_2^3 R_0^3} - 2 \frac{k_4 D_1 \iota e^{-\iota k_4 R_0}}{k_4^3 R_0^3} (1 + \iota k_4 R_0) \\
 &\quad - \frac{9\iota\beta}{k_2^3 R_0^3} \frac{k_2^2}{k^2 - k_2^2} \left( C_0 \iota - C_1 \frac{k}{k_2} \right) k \left( \frac{1}{3} - \frac{k^2 R^2}{10} \right) \\
 &\quad - \beta C_0 \frac{3}{10} \frac{k}{k_2} \frac{3k_2}{k_2 R_0} - \beta C_1 \iota k_2 \left[ \frac{1}{k_2^3 R_0^3} + \frac{1}{k_2 R_0} \left( \frac{9}{5} - \frac{1}{10} \frac{k^2}{k_2^2} \right) \right], \\
 &\quad \dots \dots (53)
 \end{aligned}$$

$$\begin{aligned}
 & A_1 k_1 R_0 \left( \frac{1}{3} - \frac{k_1^2 R_0^2}{30} \right) - 2B_1 k_3 R_0 \left( \frac{1}{3} - \frac{k_3^2 R_0^2}{15} \right) \\
 &= \frac{C_1 \iota}{k_2^2 R_0^2} \left( 1 + \frac{k_2^2 R_0^2}{2} \right) + \frac{D_1 \iota e^{-\iota k_4 R_0}}{k_4^2 R_0^2} (1 + \iota k_4 R_0 - k_4^2 R_0^2) \\
 &\quad - \frac{9\iota\beta}{k_2^3 R_0^3} \frac{k_2^2}{k^2 - k_2^2} \left( C_0 \iota - C_1 \frac{k}{k_2} \right) k R \left( \frac{1}{3} - \frac{k^2 R^2}{30} \right) \\
 &\quad - \frac{3}{2} \beta C_0 \frac{k}{k_2} - \beta \iota C_1 \left[ \frac{1}{k_2^2 R_0^2} + 2 + \frac{1}{2} \frac{k^2}{k_2^2} \right]. \quad \dots \dots (54)
 \end{aligned}$$

For the solution we follow closely the procedure of the first paper. Subtracting (54) from (53), we get

$$\begin{aligned}
 & \frac{3\iota}{k_2^2 R_0^2} \left\{ C_1 \left( 1 + \frac{k_2^2 R_0^2}{6} \right) + D_1 \frac{k_2^2}{k_4^2} e^{-\iota k_4 R_0} \left( 1 + \iota k_4 R_0 - \frac{k_4^2 R_0^2}{3} \right) \right\} \\
 &= \frac{A_1 k_1^3 R_0^3}{15} + \frac{B_1 k_3^3 R_0^3}{15} \\
 &\quad + \frac{3}{5} \iota \beta \frac{k}{k_2} \left( \frac{k^2}{k^2 - k_2^2} - 1 \right) \left( C_0 \iota - C_1 \frac{k}{k_2} \right) + \frac{\iota \beta C_1}{5}. \quad (55)
 \end{aligned}$$

We introduce this into (51) and (52), and get then from (52) an equation identical with (25'''), while (51) leads to

$$\begin{aligned}
 & \frac{k_1}{k_2} \frac{A_1}{3\iota} \left[ \frac{\rho_1}{\rho_2} + \frac{4}{5} \left( \frac{k_1^2}{k_4^2} - \frac{\rho_1}{\rho_2} \frac{k_1^2}{k_3^2} \right) \right] + \frac{4}{15} \frac{k_3}{k_2} \frac{B_1}{\iota} \left( \frac{k_3^2}{k_4^2} - \frac{\rho_1}{\rho_2} \right) \\
 &= \frac{C_1 (1 - \beta)}{k_2^3 R_0^3} - \frac{3\beta}{k_2^3 R_0^3} \frac{k}{k_2} \left( \frac{k^2}{k^2 - k_2^2} - 1 \right) \left( C_0 \iota - C_1 \frac{k}{k_2} \right).
 \end{aligned}$$

Subtracting from this (25'''), we find

$$\begin{aligned} \frac{\rho_1}{\rho_2} \left( \frac{k_1}{k_2} \frac{A_1}{3\epsilon} - \frac{k_3}{k_2} \frac{2B_1}{3\epsilon} \right) k_2^3 R_0^3 \\ = 3C_1 \left( 1 - \frac{\beta}{3} \right) - 3\beta \frac{k}{k_2} \left( \frac{k^2}{k^2 - k_2^2} - 1 \right) \left( C_0 \epsilon - C_1 \frac{k}{k_2} \right), \end{aligned}$$

which, compared with the lowest order in (54),

$$\begin{aligned} \left( \frac{k_1}{k_2} \frac{A_1}{3\epsilon} - \frac{k_3}{k_2} \frac{2B_1}{3\epsilon} \right) k_2^3 R_0^3 \\ = -\beta C_1 - 3\beta \frac{k}{k_2} \frac{k_2^2}{k^2 - k_2^2} \left( C_0 \epsilon - C_1 \frac{k}{k_2} \right), \end{aligned}$$

gives the final result

$$C_1 = \frac{\beta}{1 - \frac{\beta}{3} \frac{\rho_2 - \rho_1}{\rho_2}} \left( C_0 \epsilon - C_1 \frac{k}{k_2} \right) \frac{k}{k_2} \left[ \frac{k^3}{k^2 - k_2^2} - 1 - \frac{\rho_1}{\rho_2} \frac{k_2^2}{k^2 - k_2^2} \right] \quad (56)$$

or

$$\begin{aligned} \frac{k}{k_2} C_1 &= \frac{\beta}{1 - \frac{\beta}{3} \frac{\rho_2 - \rho_1}{\rho_2}} \left( C_0 \epsilon - C_1 \frac{k}{k_2} \right) \frac{k^2}{k_2^2} \frac{k_2^2}{k^2 - k_2^2} \left( 1 - \frac{\rho_1}{\rho_2} \right) \\ &= -\frac{\beta}{1 - \frac{\beta}{3} \frac{\rho_2 - \rho_1}{\rho_2}} \left( C_0 \epsilon - C_1 \frac{k}{k_2} \right) \left( \frac{k^2}{k^2 - k_2^2} \right) \frac{\rho_2 - \rho_1}{\rho_2}. \quad (56') \end{aligned}$$

Subtracting this from (50), we have on the left side also  $\left( C_0 \epsilon - C_1 \frac{k}{k_2} \right)$ , which can be cancelled out on both sides, leaving the expression for  $k^2$  as a condition for the solubility of the surface conditions

$$\begin{aligned} 1 &= \beta \frac{k_2^2}{k^2 - k_2^2} \left\{ \frac{\rho_2 k_1^2}{\rho_1 k_2^2} \frac{1 - \frac{4}{3} \frac{k_3^2}{k_4^2}}{1 - \frac{4}{3} \frac{k_1^2}{k_3^2}} - 1 \right\} \\ &\quad - \frac{\beta}{1 - \frac{\beta}{3} \frac{\rho_2 - \rho_1}{\rho_2}} \frac{\rho_2 - \rho_1}{\rho_2} \left( \frac{k_2^2}{k^2 - k_2^2} + 1 \right). \quad (57) \end{aligned}$$

We solve this equation for

$$\frac{k^2 - k_2^2}{k_2^2} = \frac{V_2^2 - V^2}{V^2},$$

where  $V_2$  is, as before, the velocity of propagation in the pure liquid, and  $V$  the velocity in the suspension. We get

$$\frac{V_2^2 - V^2}{V^2} = \frac{\beta}{1 - \frac{2}{3}\beta \frac{\rho_1 - \rho_2}{\rho_2}} \left\{ \left( 1 + \frac{\beta}{3} \frac{\rho_1 - \rho_2}{\rho_2} \right) \times \left[ \frac{\rho_2}{\rho_1} \frac{k_1^2}{k_2^2} \frac{1 - \frac{4}{3} \frac{k_2^2}{k_4^2}}{1 - \frac{4}{3} \frac{k_1^2}{k_3^2}} - 1 \right] + \frac{\rho_1 - \rho_2}{\rho_2} \right\}, \quad (58)$$

or, taking into account the transformations which led to (38'),

$$\frac{V_2^2 - V^2}{V^2} = \frac{\beta}{1 - \frac{2}{3}\beta \frac{\rho_1 - \rho_2}{\rho_2}} \times \left\{ \left( 1 + \frac{\beta}{3} \frac{\rho_1 - \rho_2}{\rho_2} \right) \frac{K_1 - K_2}{K_2} + \frac{\rho_1 - \rho_2}{\rho_2} \right\}. \quad (58')$$

Comparing this with (38'), we see that (58') is identical with (38') if we keep only the lowest power of  $\beta$  and take into account the fact mentioned on p. 755 that  $\frac{V_2 - V}{V}$  is approximately  $\frac{1}{2} \frac{V_2^2 - V^2}{V^2}$  for small values of  $V_2 - V$ . It is curious to note that for an equal density of sphere and liquid the only effect of taking into account the interaction of the particles is the replacement of  $\frac{V_2 - V}{V}$  by  $\frac{V_2^2 - V^2}{2V^2}$ , being due to the reflected wave from particles farther ahead (p. 755).

On the other hand, if the compressibilities are equal, (58') can be put into a form which is somewhat similar to the statement in optics that the refractivity  $\frac{n^2 - 1}{n^2 + 2}$  is proportional to the density, namely into the form

$$\frac{1 - \frac{V^2}{V_2^2}}{\frac{V^2}{V_2^2} + 2} = \frac{\beta}{3} \frac{\rho_1 - \rho_2}{\rho_2}.$$

This similarity is probably due to the fact that the optical wave as well as the acoustical waves due to density differences can be derived from dipole sources.



If we transform equation (58') to give an evaluation of the compressibility, we find

$$\frac{K_1 - K_2}{K_2} = \frac{V_2^2 - V^2}{\beta V^2} - \frac{V_2^2}{V^2} \frac{\frac{\rho_1 - \rho_2}{\rho_2}}{1 - \frac{2}{3} \beta \frac{\rho_1 - \rho_2}{\rho_2}} \quad (59)$$

To sum up the accuracy, we have neglected  $\left(\frac{2\pi R_0}{\text{wave-lengths}}\right)^2$  compared with unity. By this restriction we have accomplished that only  $\beta$ , which represents the fraction of the volume filled by the suspended particles, appears. It may be hoped, therefore, that our result will also be valid if the form of the particles deviates from spheres. Furthermore, if the particles are not isotropic, it seems probable that, due to the random orientation, they will act like particles of an isotropic solid with constants calculated according to Voigt\*, who gave formulæ for the behaviour of a microcrystalline substance built from anisotropic grains of random orientation.

We have neglected the damping of the longitudinal waves in the liquid, and the contribution of the transversal waves to the exciting field, which is justified for water if the frequency is sufficiently high; but otherwise we have not made any assumption about the smallness of  $\beta$  (the amount of suspended material). Finally, we have neglected in the equations of motion of the viscous fluid squares of the velocities, which means we have assumed that the intensity is small, and we have simply spoken of compressibility without specifying the difference between isothermal and adiabatic compressibility. In a uniform medium the latter should be taken, but here we might have heat conduction from the liquid to the solid, and as the difference between the two compressibilities is small, this will not make any difference.

### Conclusion.

Formulas for the velocity of sound in a suspension of small solid particles have been developed. These can be used to calculate the compressibility of the solid materials from measurements of the velocity of propagation. Such experiments have been started in this laboratory.

Department of Physics,  
Johns Hopkins University,  
Baltimore, Md.

---

\* W. Voigt, *Gott. Abh.* xl. (1887); *Wied. Ann. d. Phys.* xxxviii. pp. 573 (1889).

LXXI. *Investigation of the Cataphoresis of small Particles in Water.* By DOROTHY A. NEWTON, B.Sc.\*

INTRODUCTION.

IN 1808, Reuss <sup>(1)</sup> observed the fact that when a porous diaphragm separates two parts of a liquid through which an electric current is flowing, the liquid flows through the membrane sometimes towards the anode, but more often towards the cathode. This phenomenon was termed electric endosmosis. In 1861, Quinke <sup>(2)</sup> observed the fact that air bubbles in water through which an electric current was passing moved towards the anode, acting as if negatively charged. The same effect has since been observed for liquids and solid drops in water. This motion is termed cataphoresis.

Helmholtz <sup>(3)</sup> was the first to attempt to give a theoretical explanation of endosmosis and cataphoresis. He showed that both could be explained, if it was assumed that there existed an electrical double layer at the boundary of the two substances. In the case of endosmosis, it is assumed that the layer next to the diaphragm is fixed to the surface, but the layer within the liquid is free to move, so that when a P.D. is maintained between the liquid on the two sides of the diaphragm, the mobile part of the double layer moves through the pores, dragging with it, by viscous drag, the neighbouring liquid. In the case of cataphoresis, one layer resides in the surrounding liquid and the other on the surface of the particle, causing it to act as if it were charged when placed in an electric field. The velocity acquired by such a particle was calculated by Helmholtz, and is given by

$$V = \frac{x\rho d}{\eta}$$

$$= \frac{k\sigma c}{4\pi\eta} \times \text{radial voltage in double layer,}$$

where

$x$  = the electric field,

$\rho$  = surface density of charge on the particle,

$d$  = distance between two layers of electricity,

\* Communicated by Prof. J. A. Crowther, M.A., Sc.D. Thesis presented for the Degree of M.Sc. in the University of Reading.

$\eta$  = coefficient of viscosity of the liquid,

$k$  = specific inductive capacity,

$\sigma$  = specific resistance of liquid,

$c$  = current per unit area.

According to this formula,  $V$  is directly proportional to the applied electric field. This has been verified experimentally for air bubbles in water by McTaggart <sup>(4)</sup> and for oil drops in water by Mooney <sup>(5)</sup>. Also, the velocity of the drop should be independent of its size. Alty <sup>(7)</sup> has shown that this is not true for bubbles of air in water. He finds that for large air bubbles of diameter 2 mm. the velocity is small and the bubbles move as if negatively electrified. This velocity steadily increases as the diameter decreases, until the latter is reduced to about .25 mm., near which size the velocity attains a maximum and remains fairly constant until the diameter is about .15 mm. For diameters less than this the velocity decreases steadily until the bubble disappears. Mooney found that for oil drops ranging in diameter from  $.05 \times 10^{-3}$  cm. to  $4 \times 10^{-3}$  cm., in a field of 10 volts per cm. the velocity gradually decreases with the diameter. Hardy <sup>(6)</sup>, employing the U-tube method and working with a colloidal solution of globulin, found that his results were in agreement with Helmholtz's theory over a wide range of diameters, but he states that when the diameters were so large as to give a milky coloration, the velocity falls off as the size increases.

It thus appears that the theory holds for small colloidal particles, but is not adequate for microscopic particles.

When observations are made on drops or bubbles in water in a closed cell, the observed velocity neglecting gravity, when an electric field is applied, is due to the cataphoretic velocity of the bubble together with the endosmotic velocity of the water. On Helmholtz's theory the mobile part of the double layer at the walls of the cell moves when an electric field is applied, and as the cell is closed there must be a return flow along the axis of the tube. In a later part of the paper it is shown how the true cataphoretic velocity of a bubble may be determined. Both McTaggart and Alty have assumed in their work that the effect of endosmosis may be neglected except at a small distance from the wall of the cell, and have made

observations on bubbles on the axis of the cell and termed the observed velocity the cataphoretic velocity of the bubble. That their assumption is not correct is shown by results given later in this paper. To obtain the true value of the cataphoretic velocity, it would be necessary to

Fig. 1.



subtract from their value the endosmotic velocity of the water on the axis of their tube.

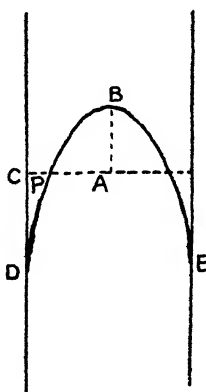
#### *Apparatus.*

In the present investigation experiments were chiefly done on oil drops in water. The form of cell used is shown in fig. 1. It consists of a glass tube 20 cm. in length

of internal diameter 0.7 cm. with a small piece of platinum carrying a platinum wire fused into one end to form the lower electrode. The upper electrode consists of a piece of platinum bearing a platinum wire passing through a rubber cork which fits closely into the upper end of the tube. To avoid distortion of the optical image of a bubble in the cell due to the curvature of the glass tube, a small hole (about 1 mm. in diameter) was bored in the tube at the centre, the glass ground flat at this place, and a small piece of cover-slip cemented on to the tube to act as a window.

The cell was cemented into a brass tube about 18 cm. long, 1 cm. in diameter, fitted with two glass windows

Fig. 2.



diametrically opposite in the centre of the tube. The cell was so placed that its small cover-slip window was opposite one of the windows of the brass tube, as shown in fig. 1. The space between the tube and the glass cell was filled with water to maintain a uniform temperature throughout the cell. The brass tube was supported in a cubical box, pierced with two holes, one in each of two opposite vertical sides. The tube was so placed that its windows faced these holes, so that light from a lamp passed through one to illuminate a bubble inside the cell, and the object-glass of a horizontal microscope placed in the other allowed the bubble to be viewed. A water cell interposed between the cell and the lamp absorbed the heat rays.

All experiments were made in a dark room, the temperature throughout being about 15° C.



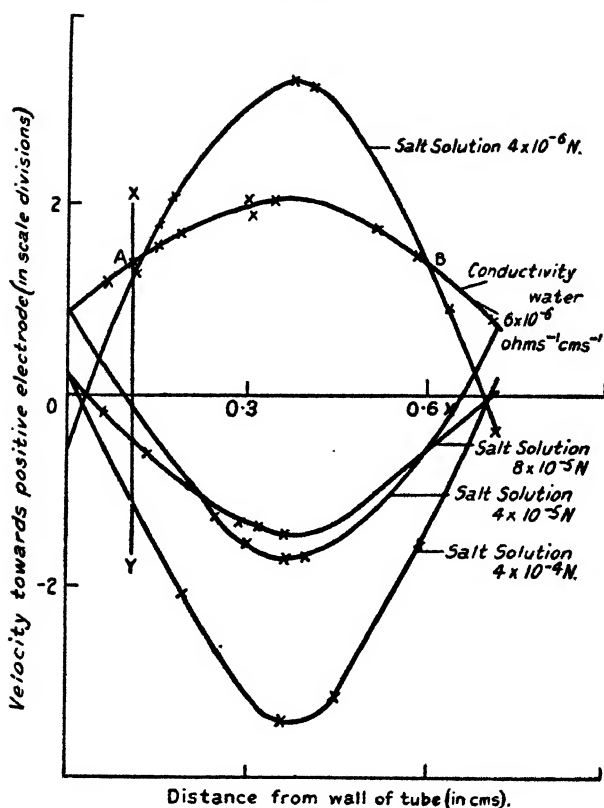
Also, since the curve is parabolic,

$$\frac{p^2}{r^2} = \frac{v_0}{v_{\infty} v_c}$$

$$= \frac{1}{2}, \text{ using equation (i.)}$$

$$p = \frac{r}{\sqrt{2}}.$$

Fig. 3.



Thus the stationary layer is at a distance  $\frac{r}{\sqrt{2}}$  from the axis.

The fact that the distribution of velocity across the tube is parabolic is shown to be experimentally correct by velocity curves given in this paper.

The observed velocity, therefore, of a drop at a distance  $\frac{r}{\sqrt{2}}$  from the axis, where  $r$  is the radius of the cell, would

be its true cataphoretic velocity, since the endosmotic velocity of the water at this point is nil.

This fact was used in the present investigation to find the true cataphoretic velocity of oil drops in water.

*Experimental Determination of Cataphoretic Velocity  
of Oil Drops in Water.*

A mixture of distilled water and a few drops of paraffin oil (density .82, viscosity .033) was well shaken in a separating funnel and allowed to stand until the larger drops of oil had risen. The fine emulsion of oil drops in water at the bottom of the vessel was allowed to run into the glass cell, the rubber stopper carrying the upper electrode was placed in position, and the cell put into the wooden box in an upright position with its cover-slip window facing the microscope. The apparatus was left for a short while to come to a steady temperature.

The microscope was moved by means of a screw until the front wall of the cell was in focus. The reading of the horizontal scale was noted. The microscope was then moved forward until a drop of a suitable diameter was sighted in the centre of the scale. Its velocity was timed with the electric field first in one direction and then in the other and the reading of the horizontal scale of the microscope noted. This was done for a number of drops across the tube. As Mooney<sup>(5)</sup> has shown that for oil drops in water the velocity is not independent of the size of the drop, throughout the experiments observations have been made only on drops of diameter equal to 1 division on the eyepiece scale, which equals  $2.4 \times 10^{-3}$  cm.

The observed velocity of the drop is due to the sum of the effects of gravity and the electric field. To find the effect of the electric field, let

$V_f$  = velocity due to field,

$V_g$  = velocity due to gravity,

$V_u$  = observed velocity of bubble when field is in one direction,

$V_p$  = observed velocity of bubble when field is in other direction (all measured in the same sense).

Then 
$$V_f = \frac{V_u - V_p}{2} \quad \dots \dots \dots \text{(ii.)}$$



The velocity of the bubble due to the field was obtained by (ii.) from observations of  $V_u$  and  $V_p$ . By this method the effect of slow convection currents which may occur in the liquid is eliminated.

A curve was then plotted between  $V_F$  and the distance of the drop from the front inner wall of the tube. The true cataphoretic velocity of the drops of diameter equal to  $2.4 \times 10^{-3}$  cm. may be read off from the curve—it is the velocity of a drop at the stationary layer, *i. e.* at a distance  $\frac{r}{\sqrt{2}} = \frac{.35}{\sqrt{2}}$  cm. from the centre of the tube. A

typical curve obtained for oil drops in water of conductivity  $6 \times 10^{-6}$  ohm $^{-1}$  cm. $^{-1}$  is AB in fig 3. The cataphoretic velocity of a bubble is given by the value at A or B on the curve—the mean of these two readings is taken as the correct value. For the curve AB of fig. 3 it is seen to be  $3.17 \times 10^{-3}$  cm./sec. The field across the tube is 10 volts/cm. The cataphoretic velocity of drops in water of conductivity  $6 \times 10^{-6}$  ohm $^{-1}$  cm. $^{-1}$  may therefore be expressed as  $3.17 \times 10^{-4}$  cm./sec./volt/cm.

It will be seen from fig. 3 that curve AB is symmetrical about the axis, thus showing that the small cover-slip window has a negligible effect on the flow of water at a small distance from the walls.

Every curve obtained was of the parabolic form of the curve represented in fig. 3, as is required by the theory of the cell given above. If, as McTaggart and Alty assumed, the effect of endosmosis may be neglected at a short distance from the walls, the observed velocity of bubbles of the same diameter at all positions across the tube, except near the walls, should be the same. This is obviously not the case, as may be seen from any of the velocity curves given in this paper. It must therefore be concluded that the assumption of McTaggart and Alty is incorrect, and that from their values of the observed velocity of the drops must be subtracted a constant depending on experimental conditions, to obtain the cataphoretic velocity of the bubbles.

If  $V_F$  = the velocity of a drop at the stationary layer,

$V_C$  = the observed velocity of a drop at the centre of the tube,

$V_W$  = the observed velocity of a drop at the wall of the tube (all measured in the same sense).

then, from the theory of the cell,

$$V_C - V_F = V_F - V_W.$$

It was found on examination of the curves that this was true within the limits of experimental error.

The value  $V_C - V_F$  = endosmotic velocity of the water at the wall of the cell for the particular experiment. Hence the endosmotic velocity of the water under observation may be found from the velocity curve. An attempt was made to obtain very small beads of the same glass as the wall of the tube to see if the endosmotic velocity in that case was equal and opposite to the cataphoretic velocity, as deduced from Helmholtz's theory. The velocity under gravity of the smallest obtainable, however, was too great for any observations to be taken, so the comparison could not be made.

*Effect of introducing small Traces of  $Th(NO_3)_4$   
into the Water.*

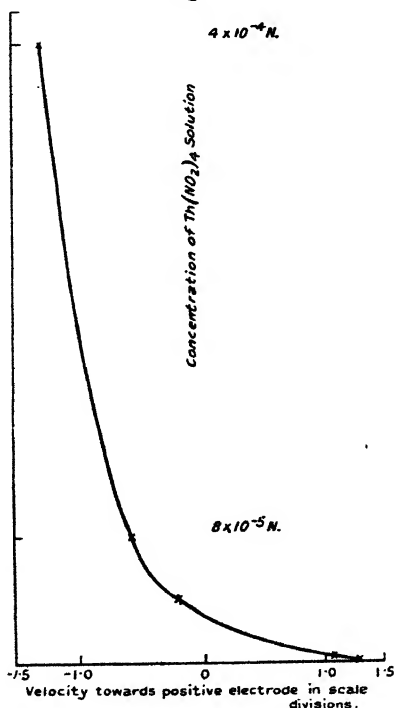
Mooney made one or two observations on oil drops in very dilute salt solution, but no very definite results were obtained. It was therefore thought worth while to investigate further to see whether the addition of salt had the same effect on oil drops as McTaggart found it to have on air bubbles, *i. e.* of decreasing the charge to zero and ultimately reversing it.

The conductivity of the water used in the present experiments was of the order of  $6 \times 10^{-6}$  ohm<sup>-1</sup> cm.<sup>-1</sup>. A standard solution of  $4 \times 10^{-4}$  Normal was made up, and from it solutions of concentration  $4 \times 10^{-4}$  N.,  $8 \times 10^{-5}$  N.,  $4 \times 10^{-5}$  N., and  $4 \times 10^{-6}$  N. were obtained. Observations were made on the velocity of oil drops in each of the four solutions and in pure water, and velocity curves plotted as described above. A solution of salt greater than  $4 \times 10^{-4}$  N. causes the conductivity of the liquid to become so great that bubbles of gas are evolved at the electrodes almost immediately the field is applied, and consequently no observations could be made. The curves obtained for these solutions are given in fig. 3. The line XY represents the position of the stationary layer, and the velocity at that point is the cataphoretic velocity of the bubbles observed. Fig. 4 shows the relationship between the cataphoretic velocity and the concentration of salt. It will be seen from this curve that the drop behaves as an

uncharged particle when the salt concentration is  $3 \times 10^{-5}$  N.

Although the cataphoretic velocity towards the positive electrode decreases steadily until for  $4 \times 10^{-4}$  N. it has a negative value, the endosmotic velocity as given by the difference between the observed velocity at the centre of the tube and the stationary layer is a little irregular. This is possibly owing to the fact that the curves were not obtained in order, and thus all traces of the salt may not

Fig. 4.



have been removed from the walls after each experiment, but it is interesting to note that the addition of salt ultimately changes the direction of movement at the walls, *i. e.* the sign of the charge of the mobile part of the double layer, in the same way as the sign of the charge on the bubble is ultimately reversed.

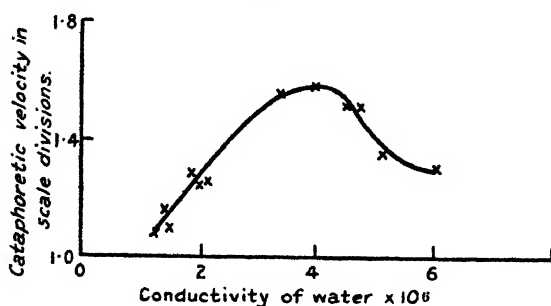
No satisfactory explanation has yet been put forward of the effect that small traces of salt have on the cataphoretic velocity of the drops or bubbles. The phenomenon has been found to be true for colloidal solutions, air

bubbles, and, by this present work, for oil drops in water. It is thought that in some manner the ions of the salt "cover" the ions in the double layer and so neutralize the effective charge on the drop.

### *Effect of the Conductivity of the Water.*

The conductivity of the water used in the previous experiments was about  $6 \times 10^{-6} \text{ ohm}^{-1} \text{ cm.}^{-1}$ . To obtain purer water than this a still similar to the one described in a paper by Bourdillon in the 'Journal of the Chemical Society,' 1913, was used. The water was collected in a hard glass flask fitted with a rubber cork into which a soda-lime tube was fitted and a siphon tube, so that the water could easily be run out without removing the rubber

Fig. 5.



stopper. Observations were made on oil drops in this purer water, and the cataphoretic velocity of the drops obtained from the velocity curves as described above. Experiments were carried out with water of conductivity ranging from  $1.3 \times 10^{-6}$  up to about  $8 \times 10^{-6} \text{ ohm}^{-1} \text{ cm.}^{-1}$ . A curve was drawn connecting the cataphoretic velocity with the conductivity of the water, and is given in fig. 5. It will be seen that there is a definite maximum cataphoretic velocity at a conductivity of  $4 \times 10^{-6} \text{ ohm}^{-1} \text{ cm.}^{-1}$ , and that the velocity decreases more rapidly at first on the higher conductivity side, but at about  $6 \times 10^{-6}$  becomes more or less constant at velocity of  $3.17 \times 10^{-3} \text{ cm./sec.}$  On the lower conductivity side the velocity drops quite rapidly until at a conductivity of  $1.3 \times 10^{-6} \text{ ohm}^{-1} \text{ cm.}^{-1}$  it is  $2.5 \times 10^{-3} \text{ cm./sec.}$  under  $\frac{2}{3}$  of its value at  $4 \times 10^{-6} \text{ ohm}^{-1} \text{ cm.}^{-1}$ .

Alty<sup>(7)</sup> describes some experiments on air bubbles in water of different conductivities. He found that the bubbles had a smaller velocity in pure water, conductivity about  $2 \times 10^{-6} \text{ ohm}^{-1} \text{ cm.}^{-1}$  than in distilled water of higher conductivity, that the velocity rose to a maximum and fell off fairly quickly at first on the higher conductivity side. The value he gives of the conductivity water at maximum velocity,  $8 \times 10^{-6} \text{ ohm}^{-1} \text{ cm.}^{-1}$ , is decidedly higher than the one obtained in the present experiments. The two results, however, cannot easily be compared, as the smallest air bubble used was 1 mm. in diameter and the cataphoretic velocity of a drop is not independent of its diameter. It does, however, seem to be quite evident in both experiments that the velocity rises to a definite maximum as the conductivity of the water is varied.

It was hoped when this set of experiments were commenced to obtain very pure water of conductivity about  $0.5 \times 10^{-6} \text{ ohm}^{-1} \text{ cm.}^{-1}$ . Bourdillon claims in his paper that, from the form of still described, water of conductivity as low as  $.1 \times 10^{-6} \text{ ohm}^{-1} \text{ cm.}^{-1}$  could be obtained. Since Reading water is contaminated with chlorine, the boiler was filled with filtered rain-water. When, however, the conductivity of the water produced was introduced into the glass vessel and measured by a reflecting moving coil galvanometer, in no case was it less than  $1 \times 10^{-6} \text{ ohm}^{-1} \text{ cm.}^{-1}$ . It was therefore not possible to discover whether the drop in very pure water ultimately had no charge.

Hardy<sup>(6)</sup>, working with colloidal solutions of globulin, found that the velocity was very much reduced in pure water, so that the results obtained in these experiments on oil drops in pure water agree with those obtained with air bubbles and some colloidal solutions.

### *Effect of adding Alcohol to Water.*

To determine whether the addition of alcohol to the water affects the cataphoretic velocity of the drops, some experiments were made on oil drops in different mixtures of water and absolute alcohol. The conductivity of the water used was about  $5 \times 10^{-6} \text{ ohm}^{-1} \text{ cm.}^{-1}$ . Observations were made on oil drops in mixtures of 10 per cent., 20 per cent., .... 100 per cent. alcohol, and the cataphoretic velocity of the drop obtained from the curves in the usual manner. A curve was then drawn connecting the cata-

phoretic velocity with the percentage of water in the liquid, and is given in fig. 6. It will be seen that the velocity steadily decreases as the percentage of water decreases, until, when the percentage of water equals about 48, the velocity is reduced to zero and remains zero for further reduction in the proportion of water. Velocity curves show that the endosmotic velocity of the water is also reduced in the same manner.

Fig. 6.

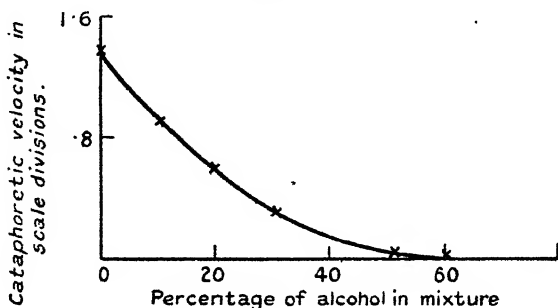
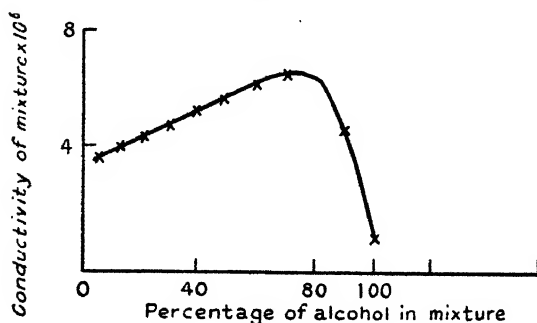


Fig. 7.



To find if the conductivity of the mixture had any bearing on this effect, the conductivity for different mixtures as measured by the moving-coil galvanometer was plotted against the percentage of water, and the result is given in fig. 7. On comparing the two curves, fig. 6 and fig. 7, there does not appear to be any obvious connexion between the conductivity and the cataphoretic velocity; in fact, the conductivity is just rising to a maximum when the cataphoretic velocity falls to zero.

By the theory developed by Helmholtz, embodied in the equation quoted in the first part of this paper, there

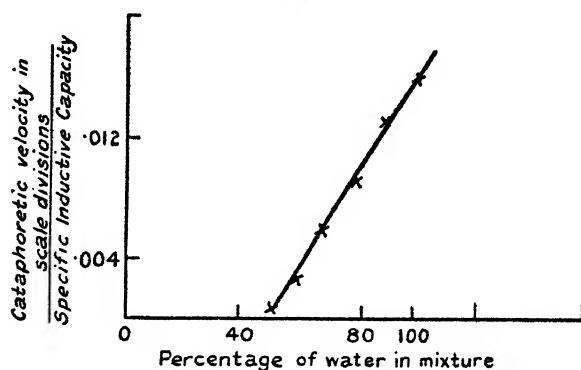
should be some relationship between the specific inductive capacity of the liquid and the cataphoretic velocity of a drop in the liquid. To test this the values of the specific inductive capacity of different mixtures of alcohol and water were obtained from the 'International Critical Tables,' and a curve drawn relating to ratio

$$\frac{\text{cataphoretic velocity of the drop}}{\text{specific inductive capacity}}$$

to the percentage of water in the mixture. The result is given in fig. 8. From this curve the relationship is seen to be linear, and may be represented by

$$\frac{V}{K} = ax - b,$$

Fig. 8.



where  $a$  and  $b$  are constants.

$V$  = cataphoretic velocity of the bubble,

$K$  = specific inductive capacity of the mixture,

$x$  = percentage of water in the mixture.

It is difficult to see just how the introduction of the alcohol into the water reduces the charge on the double layer to zero. As in the case of very pure water, we have the fact of the velocity being reduced to zero when there are still numbers of ions in the liquid. There is no indication of any reversal of the sign for further decrease in the percentage of water. The velocity remains nil, so that the effect does not appear to be similar to that

found when small traces of salt are introduced into the water, which was accounted for by supposing that the ions in the double layer were "covered" by ions of the opposite sign, and thus the charge is reduced to zero and ultimately reversed.

*Effect of other Substances in Water.*

Some very interesting results were obtained when experiments were made on substances in water other than paraffin oil. The following is a list of different substances on which observations were made :—

Bakelite.	Oil of cloves.
Aluminium.	Oil of lavender.
Barium carbonate.	Soft wax.
Copper.	Beeswax.
Starch.	Calcspar.
Zinc oxide.	Resin.
Titanic acid.	

Where possible the substance was broken up under water to avoid the possibility of there being an air film around the small particles. In no case was it found that the cataphoretic velocity was towards the negative electrode—all substances acted as if negatively charged. It appears from this set of experiments that for microscopic particles, at least, all suspensions in water act as if negatively charged. This is contrary to some results quoted in chapter vii. of Burton's book on 'Physical Properties of Colloidal Solutions.' This is probably due to the fact that in former experiments on cataphoresis the effect of endosmosis does not seem to have been considered.

It was noticed, on inspecting the results, that the cataphoretic velocity obtained for broken bits of substances was always very much less than that outlined for spheres. An attempt was therefore made to make observations on the same substance in spherical and in broken form. It was obviously not possible to do this with many substances, since the diameter of the spheres to be experimented on should be of the order of  $2.4 \times 10^{-3}$  cm. To obtain spheres of this size it was necessary to experiment with a substance which melted at a temperature below  $100^{\circ}$  C., so that it could be shaken up with boiling water into very small drops and allowed to cool. It was found that by this



method very small spheres of spermaceti, stearin, naphthalene, beeswax, resin, and soft wax could be obtained. Small bits of these substances were got by filing them under water, and experiments were made on the spherical and broken form of each in water of conductivity about  $4 \times 10^{-6}$  ohm $^{-1}$  cm. $^{-1}$ . The results are given in the following table :—

Substance.	Velocity in spherical form.	Velocity in broken form.
Spermaceti	$3.78 \times 10^{-4}$ cm./sec./volt/cm.	$1.71 \times 10^{-4}$ cm./sec./volt/cm.
Stearin ...	$3.05 \times 10^{-4}$ " " "	$2.19 \times 10^{-4}$ " " "
Naphthalene	$3.78 \times 10^{-4}$ " " "	$2.3 \times 10^{-4}$ " " "
Beeswax...	$3.9 \times 10^{-4}$ " " "	0 " " "
Resin .....	$3.9 \times 10^{-4}$ " " "	$2.19 \times 10^{-4}$ " " "
Glass .....		$2.08 \times 10^{-4}$ " " "
Soft wax...	$3.9 \times 10^{-4}$ cm./sec./volt/cm.	

From the above results it appears that the shape as well as the size of the particle have a bearing, in some manner, on the cataphoretic velocity, neither of which effects is allowed for in the Helmholtz theory. As may be seen, the velocity obtained for all spheres have about the same value,  $3.9 \times 10^{-4}$  cm./sec./volt/cm., the value obtained for oil drops in water of conductivity  $4 \times 10^{-6}$  ohm $^{-1}$  cm. $^{-1}$ . The low result of stearin in spherical form may be accounted for by the fact that the spheres were not absolutely spherical, but tended to be rather of an elliptical shape. Except for beeswax, which apparently has no charge when in broken form, all broken particles have a velocity of about  $2.2 \times 10^{-4}$  cm./sec./volt/cm.

It seems from this that the fundamental factor in determining the charge of the double layer on a drop or particle is the liquid surrounding it and the size and shape of the particle. The nature of the composition of the particle appears to have little bearing on the charge. Alty<sup>(7)</sup>, working on bubbles of different gases, found that the observed velocity was the same irrespective of the nature of the gas. If the composition of the drop has little or no effect on the charge, it would be expected that all particles should have the same sign of charge in the same liquid, as was found with all substances on which experiments were made. It thus appears, both from Alty's results and those described here, that if the charge can be

explained by ions being adsorbed on the surface, it must be assumed that all the ions are contributed by the liquid surrounding the drop, and except for its shape and size, the nature of the drop is immaterial.

*Effect of X-Rays on small Oil Drops.*

A short time ago some work was done in this laboratory to investigate the effect of X-rays on colloidal particles and it was thought worth while to extend the investigations to drops visible in a low-power microscope. The method first adopted was that of trying to keep an oil drop stationary in water by means of the application of a suitable electric field; to pass X-rays from a Shearer tube through the liquid in the neighbourhood of the drop, and by measuring its velocity before and after exposure in a field of greater strength to discover the effect, if any, of the X-rays on the drop. It was found, owing to slow convection currents in the liquid, which could not be eliminated, that it was impossible to keep the drop stationary for any length of time, and since, owing to endosmotic velocity of the water, it was only possible to compare the velocity due to cataphoresis of a bubble at different times if the drop was in the same position, it was obvious that another method would have to be employed.

The method finally adopted was that of X-raying the emulsion as a whole, and then finding the cataphoretic velocity of the drops by the method described earlier. A small, cylindrical, hard-glass dish was made to contain the emulsion to be exposed, of cross-section equal to that of the X-ray beam at a distance of about 1 cm. from the aluminium window in the X-ray tube. A little lead plate was made to hold it in position. The oil and water were shaken up as before and the glass vessel filled with the emulsion. A sample of the same emulsion was placed in another vessel to act as a standard. The X-ray tube was run for a considerable time, up to 2 hours. The current through the tube was kept at 3 milliamps., and the high potential was of the order of 60,000 volts. After the exposure the emulsion was poured into the long glass cell used in previous experiments, observations were made on drops across the tube, and the cataphoretic velocity obtained as before. The cell was then thoroughly washed out, the standard solution poured in, and the cataphoretic velocity obtained.

Although four sets of experiments, as described above, were performed on oil drops in water, the times of exposure varying from 40 minutes, up to 2 hours, in no case was there any indication of the X-rays having had any permanent effect on the drops.

In the work done on colloids in this laboratory, it was found that X-rays had no effect on any of the negatively-charged particles tried. Oil drops in water act as if they were negatively charged. If, therefore, the charge on the small microscopic drop is of the same nature as the charge on particles in a colloidal solution, the results found in these experiments would appear to substantiate those obtained earlier. As has been observed earlier in the paper, no substance could be found which was positively charged in water; thus the positive results obtained with X-rays on colloids could not be tested for oil drops. The method used here could only detect a permanent effect on the particles, and therefore it is uncertain whether or not the X-rays have a temporary effect on the drops on which experiments were made.

### *Summary.*

The chief results of this work are summarized below :—

(i.) Small traces of  $\text{Th}(\text{NO}_3)_4$  in water reduce the charge on an oil drop and eventually reverse it. Using water of conductivity  $6 \times 10^{-6} \text{ ohm}^{-1} \text{ cm.}^{-1}$ , a concentration of  $3 \times 10^{-5} \text{ N.}$  reduces the charge to nil.

(ii.) The cataphoretic velocity of an oil drop rises to a maximum of  $3.9 \times 10^{-4} \text{ cm./sec./volt/cm.}$  for water of conductivity  $4 \times 10^{-6} \text{ ohm}^{-1} \text{ cm.}^{-1}$ . In purer water the velocity is much less, falling to  $2.5 \times 10^{-4} \text{ cm./sec./volt/cm.}$  for water of conductivity  $1.3 \times 10^{-6} \text{ ohm}^{-1} \text{ cm.}^{-1}$ .

(iii.) Addition of alcohol to the water causes the velocity to be reduced to zero when 47 per cent. of the mixture is water.

(iv.) The velocity ( $V$ ) is shown to be related to the specific inductive capacity ( $K$ ) for mixtures of alcohol and water by the equation  $V = K(ax - b)$ , where  $a$  and  $b$  are constants and  $x$  the percentage of water in the liquid.

(v.) All substances tried act as if negatively charged in water.

(vi.) Spherical drops have a much higher cataphoretic velocity than broken bits of the same substance.

(vii.) Solid and liquid spherical drops of all substances tried have a velocity of  $3.9 \times 10^{-4}$  cm./sec./volt/cm. in water of  $4 \times 10^{-6}$  ohm $^{-1}$  cm. $^{-1}$  conductivity.

(viii.) X-rays have no permanent effect on the charge of oil drops in water.

### *References.*

- (1) Reuss (Wiedemann's *Electricität*).
- (2) Quinke, Pogg. *Ann.* cxiii p. 513 (1861).
- (3) Helmholtz, *Ann. der Phys.* vii. p. 337 (1879).
- (4) McTaggart, *Phil. Mag.* xxvii. (1914).
- (5) Mooney, *Physical Review*, xxiii. (1924).
- (6) Hardy, *Journal of Physiology*, xxxiii. (1905).
- (7) Alty, *Proc. Roy. Soc. A*, cvi. (1924).
- (8) McTaggart, *Phil. Mag.* xxviii. (1914).
- (9) McTaggart, *Phil. Mag.* (1922).

In conclusion I should like to express my thanks to Professor Crowther and Dr. Bond for the great interest they have shown and the help given in the progress of this work.

Department of Physics,  
University of Reading,  
Dec. 31st, 1929.

---

LXXII. *The Quantum Theory of X-Ray Exposures on Photographic Emulsions* \*. By L. SILBERSTEIN and A. P. H. TRIVELLI †.

[Plate X.]

### *Introduction.*

IN 1922 L. Silberstein<sup>(1)</sup> proposed the quantum theory of light exposure on photographic emulsions, based on the assumption that every grain becomes developable with every absorbed light quantum. An analogous case is that of  $\alpha$ -particles. Kinoshita<sup>(2)</sup>, and still more conclusively Th. Svedberg<sup>(3)</sup>, have shown that every  $\alpha$ -particle hitting a silver halide grain of a photographic emulsion makes it developable. The sensitivity of the grain is, therefore, determined by its projective area, and the probability

\* Communication No. 409 from the Kodak Research Laboratories.

† Communicated by the Authors.

that a grain (in a one-grain layer) will be made developable by exposure to  $\alpha$ -particles is given by the equation :

$$p = 1 - e^{-na}$$

where  $a$ =the projective area of the grain and  $n$ =the number of  $\alpha$ -particles per unit-area of plate. The only difference from Silberstein's quantum theory in its simplest form was that the  $\alpha$ -particle was replaced by the light dart, light being regarded as discrete in nature, and every light dart containing one quantum of energy. When using a great range of sizes of large clumps of grains the experimental investigations of A. P. H. Trivelli and F. L. Righter<sup>(4)</sup> were, in the beginning, in good agreement with the results of the quantum theory.

Independently of this theory a chemical theory of sensitivity had developed, founded by J. M. Eder<sup>(5)</sup> and supported by Lüppo-Cramer<sup>(6)</sup>, Th. Svedberg<sup>(7)</sup>, and F. F. Renwick<sup>(8)</sup>. According to this, statistical variation of sensitivity is inherent, *i. e.*, exists previously to exposure to light. It was supposed to be caused by specks or nuclei of a substance other than silver bromide. This substance was provisionally termed the photocatalyst.

In 1909 Lüppo-Cramer<sup>(6)</sup> showed that chromic acid could desensitize photographic emulsions, and suggested that it was due to destruction of ripening nuclei. In a letter to the 'British Journal of Photography'<sup>(9)</sup> it was suggested by S. E. Sheppard that certain specific desensitizing experiments might afford a means of distinguishing a pure quantum action from the sensitivity nucleus theory. The investigations of E. P. Wightman, A. P. H. Trivelli, and S. E. Sheppard<sup>(10)</sup> on the distribution of sensitivity and size of grain in photographic emulsions show that the action of a desensitizer, such as chromic acid, must be due to the destruction of pre-existing specks or nuclei, which are not silver halide, confirming Lüppo-Cramer's investigations. W. Clark<sup>(11)</sup> and F. C. Toy<sup>(12)</sup> confirmed the results obtained and added new evidence, so that there was no doubt of the existence of a sensitivity-promoting substance other than silver bromide distributed in specks among the grains. Strong evidence has been advanced by S. E. Sheppard<sup>(13)</sup> that these sensitivity centres or sensitizing specks contain silver sulphide. In the meantime it was shown by L. A. Jones and A. L. Schoen<sup>(14)</sup> that in the experiments of A. P. H. Trivelli and F. L. Righter,

which L. Silberstein used to test his equation, the number of quanta incident at  $\lambda 470 \text{ m}\mu$  was about  $4.7 \times 10^{12}$  per  $\text{cm}^2$ . This means that only a small fraction of the grain area—between 0.00001 and 0.0001—could be regarded as sensitive, if the premise is to be maintained that a grain is made developable when hit by a single light dart, absorbing one quantum. This opinion and new sets of experimental data led L. Silberstein<sup>(15)</sup> to modify the original formula. The simplest modification consists in replacing the exponent  $na$  by  $n\epsilon a$ , in which  $\epsilon$  = the fraction of the area of a silver halide grain which is vulnerable, *i. e.*, ready to become developable on being hit by a light dart. It was considered by L. Silberstein that the main results would not be greatly altered if the simple assumption is replaced by a more general one. According to this, let the sensitive part of the area of a grain, instead of being in a lump, consist of a number of separate vulnerable or sensitive spots, each of area  $\omega$ , and distributed haphazardly among the individual grains (each of area  $a$ ). The necessary and sufficient condition for a grain to be made developable will now be that at least one of its spots should be hit by at least one light dart of sufficiently short wave-length.

This theory appeared to represent, roughly at least, the observed facts. The discrepancies between the theoretical results and the experimental findings, *viz.*, the number of grains of a given size made developable by a given exposure, at that time seemed rather irregular and not seriously exceeding the limits of experimental error. But after a more detailed scrutiny the deviations of the theory from the experiment turned out to be distinctly systematic, and F. C. Toy's criticism<sup>(16)</sup> was found to be materially correct by S. E. Sheppard, A. P. H. Trivelli, and R. P. Loveland<sup>(17)</sup>. Finally, L. Silberstein<sup>(18)</sup> showed mathematically that there is no possible form of the distribution function  $f(\epsilon)$  which would give a faithful representation of the experimental findings obtained, with precision, in these laboratories with the grains of a slow process emulsion.

### *Evidence for a Quantum Theory of X-Ray Exposures.*

Th. Svedberg, O. H. Schunk, and H. Anderson<sup>(19)</sup> had suggested that developable nuclei were formed only when light quanta of sufficient energy struck the grain and were

absorbed within a certain minimum area. On the basis of Zsigmondy's<sup>(20)</sup> investigations about the deposition of gold on colloidal gold particles H. J. Vogler and W. Clark<sup>(21)</sup> estimated that about 300 silver atoms are necessary to form a developable centre.

W. Nernst and W. Noddack<sup>(22)</sup> have given evidence that the impact of one  $\alpha$ -particle in a grain produces about 50,000 free silver atoms; while for one quantum of blue-violet light (436–365  $m\mu$  wave-length) not more than one atom of silver is set free. W. Meidinger<sup>(23)</sup> found that among certain emulsions the great differences in photographic sensitivity for white light were much less for  $\alpha$ -particles. He also showed that the sensitizing and desensitizing for light by alkali and acid treatment respectively, which he obtained on certain emulsions, were absent on exposures to  $\alpha$ -particles. He suggested, further, that similar relations might be obtained for X-rays as being intermediate in energy concentration between light and  $\alpha$ -particles.

That the X-ray latent image is quite different from the latent image produced by visible radiation was mentioned in 1908 by Lüppo-Cramer<sup>(24)</sup>. In their studies on sensitivity S. E. Sheppard and A. P. H. Trivelli<sup>(25)</sup> have tested in two ways the ratio of quantum energy to sensitivity. First, a photographic emulsion was prepared with a relatively inert gelatin and also with gelatin sensitized with allyl thio-urea, the grain size distribution being the same in the two cases. Sensitometric comparisons were made with these two emulsions both for white light and for X-rays. The speed values for white light were, respectively, 30 H. and D. and 470 H. and D. There was little difference in the relative speeds (computed similarly from the inertias) of the emulsions when exposed to X-rays. The experiment indicates that no such sensitizing for X-rays is obtained by formation of nuclei containing silver sulphide as is obtainable for white light. Secondly, the same effect was found with the chromic acid treatment. There was a pronounced desensitizing effect for blue light, and this was practically negligible for X-rays. The quantum energies applied at a selected mean wave-length were:

Blue light at about 4000 Å.U. :  $h\nu = 4.92 \times 10^{-12}$ ,

X-rays at 0.275 Å.U. :  $h\nu = 7.16 \times 10^{-8}$ .

W. Nernst and W. Noddack<sup>(26)</sup> computed that an X-ray quantum of about  $0.5 \text{ \AA.U.}$  liberates about 1000 silver atoms in a silver halide grain. This is much more than is necessary to produce developability. The Compton effect is regarded as strong evidence for the discrete structure of X-ray radiation. If, therefore, every absorbed X-ray quantum produces a centre of developability independent of the sensitivity specks for the blue-violet exposure, the original simple form of Silberstein's quantum theory of exposure should hold for X-rays. The experimental investigation of this conclusion was supported by two other considerations.

In 1915 Lüppo-Cramer<sup>(27)</sup> discovered evidence of an intensification of the latent image by hydrogen peroxide. It was found by E. P. Wightman, A. P. H. Trivelli, and S. E. Sheppard<sup>(28)</sup>, in the course of a study of the action of hydrogen peroxide on photographic plates on which the silver halide grains were spread in a single layer, that the number of developed grains in unit-area affected by light followed by hydrogen peroxide treatment was greater than the sum of those developed in unit area which were acted on separately by light and hydrogen peroxide.

This work was followed by an extensive investigation of the phenomenon by E. P. Wightman and R. F. Quirk<sup>(29)</sup>, and W. C. Bray and R. S. Livingston<sup>(30)</sup> showed that hydrogen peroxide reacts with bromide and hydrogen ions to give bromine and water; the bromine can react with more peroxide to give again bromide and hydrogen ions and oxygen. Lüppo-Cramer<sup>(31)</sup> had discovered that dilute bromine solution causes latent fog on a photographic plate. E. P. Wightman<sup>(32)</sup> found that three minutes' treatment with bromine water, 1 : 200,000, caused not only slight latent fog but also a fair intensification of the latent image.

All photographic emulsions contain more or less free potassium bromide which gives bromine with hydrogen peroxide. K. C. D. Hickman<sup>(33)</sup> obtained evidence that while in bulk bromine reacts with the silver sulphide of the sensitizing speck to give silver bromide, sulphuric acid, and hydrobromic acid; on the other hand, when formed in limited quantity by the photochemical decomposition of silver bromide grains, as in a photographic exposure, it may react with silver sulphide in such a way as to give rise to metallic silver instead of silver bromide, and, possibly

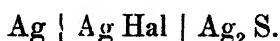


in greater proportion than one silver atom for each silver halide pair decomposed. Silver is presumed to be more effective than its equivalent of silver sulphide in producing developability. It was shown by R. H. Lambert and E. P. Wightman<sup>(34)</sup> that Hickman's hypothesis was thermodynamically plausible.

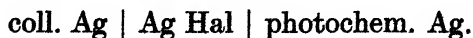
It is obvious that if the X-ray latent image is a pure silver speck of about 1000 to 2000 silver atoms, there is no possibility of an intensification of the X-ray latent image by hydrogen peroxide, provided the given reaction holds. E. P. Wightman and R. F. Quirk<sup>(35)</sup> were able to show experimentally with an Eastman speedway and with an Eastman process-plate that this prediction was correct.

The other consideration was a plausible explanation of the Luther-USchkoff phenomenon. In 1903 R. Luther and W. A. USchkoff<sup>(36)</sup> discovered that the latent image of X-rays on photographic plates can be made visible by exposing the plate to daylight if the previous X-ray exposure is sufficient, but still kept below the limits of directly detectable visibility. This phenomenon is explicable by the combination of the concentration speck theory and the quantum theory of X-ray exposure.

The concentration speck theory, as modified by Trivelli<sup>(37)</sup>, regards the sensitivity speck on the silver halide grains as an amicroscopical Becquerel cell of the structure



B. H. Carroll and D. Hubbard<sup>(38)</sup> have shown that, in addition to silver sulphide in colloidal state, colloidal silver may act as a sensitivity speck. It is well known that silver against silver in an electrolyte may show a potential difference if the constitution of both silver electrodes is different. For instance, two pieces from the same silver wire show a potential difference if one of these pieces is bent and the other left straight. The strain in one of the silver electrodes is sufficient to produce a potential difference. It is, therefore, quite possible that colloidal silver particles introduced on the surface of the silver halide grain with the photochemical liberated silver form Becquerel cells of the structure



Instead of colloidal silver it may also be a silver speck

formed by an absorbed X-ray quantum, which, after a short induction period, may form a Becquerel cell of the structure

X-ray Ag | Ag Hal | daylight Ag.

It cannot be expected that these cells will produce the same powerful concentration action as a silver sulphide electrode will, because the potential difference between the electrodes will be much smaller. After the exhaustion of the concentration action of these specks they act as weak spots in the crystal lattice of the silver halide, and continue to grow slowly by prolonged daylight exposure.

We may, therefore, in all probability regard the Luther-USchkoff effect as the result of an introduction of new sensitivity centres for daylight exposure on the silver halide crystals of a photographic emulsion by the absorbed X-ray quanta.

All these considerations together led to a renewed investigation of the quantum theory of X-ray exposure on photographic emulsions.

### *Experimental Details.*

The experimental test of the quantum-theory formula requires an investigation of both factors ( $n$  and  $\alpha$ ) of the exponent. For the choice of a suitable photographic emulsion it must be determined which factor is more important—the exposure or the size of the projective area of the grain. For one-grain-layer plates the range of available exposures is very small for X-rays. With fully developed grains X-ray exposures very soon reach high contrast values. We used a pure silver bromide emulsion, for reasons to be discussed later, with a wide range of different grain sizes. The size-frequency curve of this emulsion is given in Pl. X. fig. 1. The classification of the larger grains becomes less reliable with the applied rule method<sup>(39)</sup>. The largest grains beyond class 20, therefore, were omitted from the investigation. The classes were

Class	1=0.1–0.3 $\mu^2$ ,
„	2=0.3–0.6 $\mu^2$ ,
„	3=0.6–0.9 $\mu^2$ ,
.	.
.	.
.	.
.	.
.	.
.	.
Class	20=5.8–6.0 $\mu^2$ ,

giving a sufficient range for testing.

From this emulsion one-grain-layer plates were made and exposed to X-rays from a water-cooled Coolidge tube running at 85,000 volts, at a distance of 80 cm. between the target of the tube and the photographic plate. The exposures were made in strips on the plate in powers of 2 ratio and the time of every exposure regulated by hand, which makes  $n$  less reliable. After exposure the plates were developed for seven minutes in the following developer (4 times diluted) :

Hydroquinone . . . . .	5.5 grams.
Sodium sulphite (anhydr.) . . .	50.0 „
Sodium carbonate . . . . .	50.0 „
Potassium bromide . . . . .	0.02 „
Water . . . . .	to 1 litre.

As shown in Pl. X. fig. 2, where a photomicrograph of one of the exposures at a magnification of  $2500\times$  is reproduced, this developer develops pure silver bromide grains of the same shape and size as the original grain. This simplified the method of investigation considerably. In previous investigations we had used a method first applied by Th. Svedberg<sup>(40)</sup>, in which the original grains on a one-grain-layer plate were first counted and classified. Then a plate coated similarly was used for exposure and development; the developed grains were removed by chromic acid and sulphuric acid, and the remaining grains were counted and classified. If narrow classes of grains were required this procedure had to be repeated several times and the results averaged.

The development of pure silver bromide emulsions with a hydroquinone developer greatly simplifies this method. We are able to determine immediately, on one spot, which grains were affected and which remained intact. One plate is insufficient, and this eliminates development deviations and differences in the distribution of grains on the different plates.

In the photomicrograph Pl. X. fig. 1, which shows only undeveloped grains, there are a few black grains among the undeveloped grains. This is due to their thickness, and a distinction between these grains and the developed grains can be detected very easily on the negatives. They show an internal structure and are not entirely black.

Three different exposures were investigated. The second exposure was twice as great as the first, and the third was twice as great as the second. For every exposure 300 fields at a magnification of  $10,000\times$  were used. From a series of ten different exposures these three were microscopically the only useful fields. One of these fields was omitted because of the erratic results, which we believe to be caused by the influence of some contamination (occurring during the setting) of the gelatin of the one-grain-layer plate on a spot of that exposure region.

### *Treatment of Data.*

If the probability  $p$  of a grain of size  $a$  being affected by the exposure  $n$  is

$$p = 1 - e^{-na},$$

then the number  $k$  of grains actually affected out of a total of  $N$  grains, all of size  $a$ , is

$$k = Np \pm N \text{ (P.D.)},$$

where (P.D.), the probable deviation, is given by

$$\text{(P.D.)} = 0.477 \sqrt{\frac{2p(1-p)}{N}}.$$

Unless the deviation from the calculated data is more than 2.5 or 3 times greater than (P.D.) the agreement can be considered fairly satisfactory. All observed data falling within the limits of the probable deviation can be regarded as being in perfect agreement with the theoretical values.

For the determination of the calculated data we use, instead of the size  $a$  of the grain, the average size  $\bar{a}$  of the class of grains—that is to say, neglecting the small correction for the finite width of the classes \*, we put

$$p = 1 - e^{-n\bar{a}}.$$

This gives

$$\log (1 - p) = -n\bar{a},$$

$$\log (1 - p) = -Mn\bar{a},$$

$$\frac{-\log (1 - p)}{\bar{a}} = Mn = \text{constant} = C$$

(i. e., constant within an exposure step), where  $M=0.4343$ .

\* Formulated in a previous paper.

*Discussion of Data.*

It was found as an average for

$$\text{Step 4 : } C_4 = 0.0427,$$

$$,, \quad 3 : C_3 = 0.0832.$$

TABLE I.

Step 4.

$$C_4 = 0.0422.$$

Class.	$\bar{a}$ .	N.	$100 \frac{k}{N}$ obs.	$100 \frac{k}{N}$ calc.	$100$ (P.D.).	$100 \Delta$ .	$\frac{\Delta}{(P.D.)}$ .	C.
1 .....	0.23	4182	0.7	2.2	0.6	1.5	2.5	0.014
2 .....	0.45	3295	3.3	4.3	1.3	1.0	0.8	.032
3 .....	0.75	1821	5.0	7.0	1.8	2.0	1.1	.030
4 .....	1.05	1014	11.2	9.7	1.9	-1.5	0.8	.049
5 .....	1.35	688	17.3	12.3	2.0	-5.0	2.5	.061
6 .....	1.65	532	15.7	14.7	2.6	-0.4	0.3	—
7 .....	1.95	482	19.5	17.3	2.6	-2.2	0.8	.048
8 .....	2.25	408	16.7	19.7	3.2	2.9	0.9	—
9 .....	2.55	350	22.0	21.9	3.2	-0.1	0.03	.042
10 .....	2.85	292	23.1	24.2	3.5	1.1	0.3	.040
11 .....	3.15	252	18.9	26.4	4.2	7.5	1.8	—
12 .....	3.45	229	22.3	28.5	4.3	6.2	1.4	.032
13 .....	3.75	185	23.2	30.5	4.7	7.3	1.6	.031
14 .....	4.05	180	20.0	32.5	5.2	3.3	2.4	—
15 .....	4.35	166	30.8	34.5	4.5	6.3	1.4	.037
16 .....	4.65	159	30.8	36.4	4.6	5.5	1.2	.034
17 .....	4.95	123	41.3	38.2	4.6	-3.1	0.7	.047
18 .....	5.25	128	44.7	39.9	4.4	-4.8	1.1	.049
19 .....	5.55	107	45.8	41.7	4.7	-4.1	0.9	.048
20 .....	5.85	81	55.6	43.4	5.0	-12.2	2.4	.060

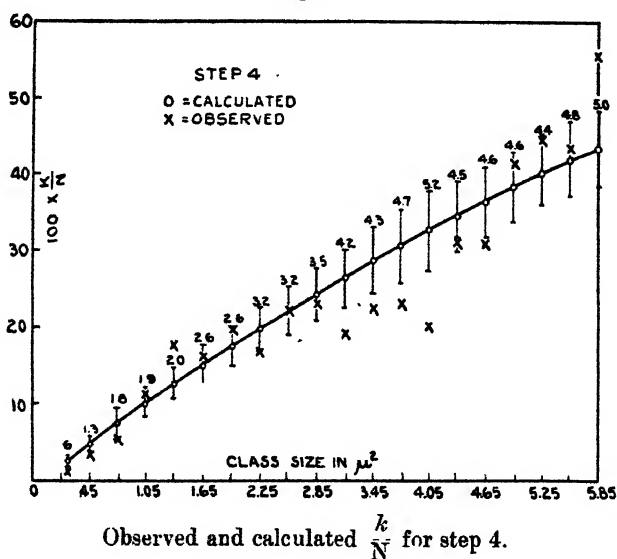
This ratio of  $C_4$  to  $C_3$  represents fairly well the ratio 1 : 2 as it should be according to the given exposure times. We choose for the calculation of the  $p$ -values the average of  $C_4$  and  $\frac{1}{2}C_3$ . Thus we take  $C_4 = 0.0422$  and  $C_3 = 0.0844$ .

In Table I. are given the observed and the calculated values for step 4. Delta represents the difference between these values, and  $\frac{\Delta}{(P.D.)}$  expresses how far we may rely on

the results of the comparison as a support of the theoretical considerations.

In fig. 1 are plotted the observed and calculated  $\frac{k}{N}$  data for step 4, with the calculated probable deviations represented by vertical strokes. We see that from the twenty data fourteen observations are in perfect agreement with the theoretical requirements; two observations are fairly well represented, and four observations show deviations 2.4-2.5 times greater than the probable deviations, and are thus still fairly satisfactory.

Fig. 1.



In Table II. are given the observed and the calculated  $\frac{k}{N}$  data of step 3. In fig. 2 are plotted these data, with the probable deviations. We see that from the twenty observations ten are in perfect agreement with the theoretical requirements, six observations are fairly satisfactory, three observations have deviations which are 2.3, 2.4, and 2.5 times larger than the probable deviation, which means that they are still satisfactory, while only one observation is far off the theoretical value.

This agreement between theory and experiment seems close enough to enable us to assert that the quantum theory of X-ray exposures on photographic plates holds.

*The Distribution of the Latent Image.*

There are many evidences for the assumption that the latent image produced by visible light on photographic emulsions lies practically on the surface of the silver halide grains <sup>(41)</sup>.

On the other hand, the absorption of X-rays in a silver bromide crystal of a photographic emulsion is negligible.

TABLE II.

Step 3.

 $C_3=0.0844$ .

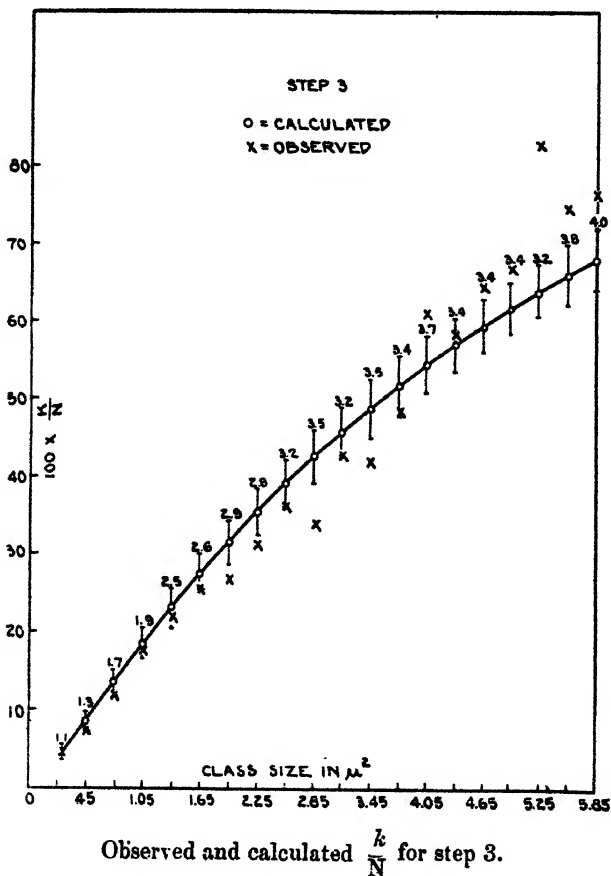
Class.	$\bar{a}$ .	N.	$\frac{k}{100 \bar{N}}$ obs.	$\frac{k}{100 \bar{N}}$ calc.	100 (P.D.).	100 $\Delta$ .	$\frac{\Delta}{(P.D.)}$ .	C.
1 .....	0.23	3379	4.4	4.4	1.1	0.0	0.0	0.084
2 .....	0.45	2621	7.3	8.4	1.3	1.1	0.8	.074
3 .....	0.75	1651	11.8	13.6	1.7	1.8	1.1	.073
4 .....	1.05	1036	17.8	18.4	1.9	0.6	0.3	.081
5 .....	1.35	612	21.9	23.1	2.5	1.2	0.5	.079
6 .....	1.65	512	25.5	27.4	2.6	1.9	0.7	.077
7 .....	1.95	428	26.7	31.5	2.9	4.8	1.7	.069
8 .....	2.25	402	32.3	35.4	2.8	3.1	1.1	.075
9 .....	2.55	291	36.2	39.1	3.2	2.9	0.9	.077
10 .....	2.85	266	33.7	42.5	3.5	8.8	2.5	—
11 .....	3.15	252	42.7	45.8	3.2	3.1	1.0	.077
12 .....	3.45	221	42.0	48.8	3.5	6.8	1.9	.069
13 .....	3.75	201	48.4	51.7	3.4	3.3	1.0	.077
14 .....	4.05	137	61.3	54.5	3.7	6.8	1.8	.102
15 .....	4.35	164	58.4	57.1	3.4	1.3	0.4	.087
16 .....	4.65	143	64.8	59.5	3.4	5.3	1.6	.098
17 .....	4.95	139	66.9	61.8	3.4	5.1	1.5	.097
18 .....	5.25	122	82.8	63.9	3.2	18.9	5.9	—
19 .....	5.55	95	74.7	66.0	3.8	8.7	2.3	.107
20 .....	5.85	81	76.5	67.9	4.0	9.5	2.4	.108

on an ordinary photographic film more than 90 per cent of the incident X-ray energy penetrates the emulsion.

Comparing the development of a one-grain-layer plate of a visible-light exposure with one of an X-ray exposure, we noticed a difference. Within a few minutes all day-light-affected grains are developed, and additional development gives development fog, which increases much more slowly than the number of developed grains. The X-ray

affected grains continue to produce developed grains with increasing time of development in gradually changing rate. This led to the conclusion that we have to regard the X-ray latent image as being distributed haphazardly through the entire silver halide grain. This explains the differences R. Wilsey<sup>(42)</sup> found in the values of the development factor  $k$  for daylight and for X-ray exposures.

Fig. 2.



### Summary.

1. Evidence is given for the validity of the quantum theory of X-ray exposure on photographic emulsions.
2. An experimental investigation was made, the observed data were compared with the calculated values, and the principle of the theoretical probable deviation was applied.



3. It was found that there is a close agreement between theory and experiment.

4. The distribution of the X-ray latent image was discussed.

Our thanks are due to Mr. E. C. Jensen for assisting us in the various calculations.

### References.

- (1) Phil. Mag. xliv. p. 257 (1922).
- (2) Proc. Roy. Soc. lxxxiii. A. p. 432 (1910).
- (3) Phot. Journ. lxii. pp. 186, 310 (1922).
- (4) Phil. Mag. xlv. p. 252 (1922).
- (5) Eder's *Handbuch*, ii., i. p. 288 (1927).
- (6) *Phot. Mitt.* p. 328 (1909).
- (7) Phot. Journ. lxii. p. 312 (1922).
- (8) Journ. Soc. Chem. Ind. xxxix. p. 156-T (1920).
- (9) Brit. Journ. Phot. lxix. p. 514 (1922).
- (10) Journ. Frank. Inst. cxciv. p. 485 (1922).
- (11) Phot. Journ. lxiv. (1924).
- (12) Phil. Mag. xlv. p. 352 (1922).
- (13) Phot. Journ. lxv. p. 380 (1925). Colloid Symposium Monograph, iii. p. 76 (1925). Brit. Journ. Phot. lxxiii. p. 33 (1926).
- (14) Journ. Opt. Soc. Amer. vii. p. 213 (1923).
- (15) Phil. Mag. xlv. p. 1063 (1923).
- (16) *Loc. cit.* xlv. p. 715 (1922).
- (17) *Loc. cit.*
- (18) *Loc. cit.* i. p. 464 (1928).
- (19) Phot. Journ. lxiv. p. 272 (1924).
- (20) *Koll.-Chem. Beihefte*, ix. p. 222 (1917).
- (21) Brit. Journ. Phot. p. 670 (1927).
- (22) *Sitz. Ber. Preuss. Akad. Wiss.* p. 110 (1923).
- (23) *Zeits. Physik. Chem.* cxiv. p. 108 (1924).
- (24) *Phot. Rund.* p. 221 (1906).
- (25) Phot. Journ. lxvi. p. 505 (1926).
- (26) *Loc. cit.*
- (27) *Phot. Korr.* lii. p. 136 (1915).
- (28) Journ. Frank. Inst. cc. p. 335 (1925).
- (29) *Loc. cit.* cciii. p. 261 (1927); cciv. p. 731 (1927).
- (30) Journ. Amer. Chem. Soc. xlv. pp. 1251, 2048 (1923); xlviii. p. 45 (1926).
- (31) *Photogr. Problème*, p. 132 (1907).
- (32) Brit. Journ. Phot. lxxiv. p. 447 (1927).
- (33) Phot. Journ. lxvii. p. 34 (1927).
- (34) Journ. Phys. Chem. xxi. p. 1249 (1927).
- (35) Proc. Seventh Int. Congress Phot. p. 235 (1929).
- (36) *Phys. Zeit.* iv. p. 866 (1903).
- (37) Journ. Frank. Inst. cciv. p. 649 (1927).
- (38) Bur. Stand Journ. Res. p. 565 (1928).
- (39) Journ. Phys. Chem. xxvii. p. 1 (1923).
- (40) *Zeits. wiss. Phot.* xx. p. 36 (1920).
- (41) Cf. Eder's *Handb.* ii. i., p. 278 (1927).
- (42) Journ. Opt. Soc. Amer. xii. p. 661 (1926).

Rochester, N.Y.

October 7th, 1929.

LXXIII. *Forced Vibrations with combined Viscous and Coulomb Damping.* By J. P. DEN HARTOG \*.

I. *Introduction.*

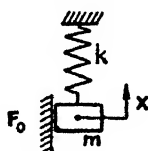
THE free vibrations of a single degree of freedom system affected by a constant friction force are determined by the pair of equations :

$$m\ddot{x} + kx \pm F_0 = 0,$$

of which the solution for any initial condition is well known. When, moreover, a sinusoidal disturbing force is acting on the mass, a steady periodic non-harmonic motion will be set up after a sufficient length of time.

It is evident that in case the friction force is small with respect to the disturbing force amplitude, the ensuing motion will be continuous, while for large values of the friction force a single cycle of the motion may consist of regions of motion

Fig. 1.



and regions of standstill. In this paper an analytical solution has been obtained for motions without standstill, *i. e.* for sufficiently small damping †. It is found that this solution is valid for such values of the friction and the frequency as are ordinarily met in engineering applications.

II. *Only Coulomb Damping.*

The differential equation (of fig. 1) is

$$m\ddot{x} + kx \pm F_0 = P_0 \cos(\omega t + \phi), \quad . . . (1)$$

where the upper (+) sign holds for upward motions ( $\dot{x} > 0$ ) and the lower (−) sign for  $\dot{x} < 0$ . The quantity  $\phi$  is a parameter as yet devoid of meaning. Introducing the notations :

$$F_0/k = x_f, \quad P_0/k = a, \quad k/m = \omega_n^2,$$

\* Communicated by R. V. Southwell, F.R.S.

† An approximate solution, based on a graphical method for values  $\omega/\omega_n < 1.1$ , including both motions with and without stops, is described by W. Eckolt, *Zt. f. techn. Physik*, vii. p. 226 (1926).

the equation for  $\dot{x} < 0$  can be written as

$$\ddot{x} + \omega_n^2(x - x_f) = a\omega_n^2 \cos(\omega t + \phi). \quad (2)$$

In order to obtain a periodic solution for the motion, the following boundary conditions are imposed:—

$$\left. \begin{aligned} t = 0, \quad x = x_0, \quad \dot{x} = 0, \\ t = \pi/\omega, \quad x = -x_0, \quad \dot{x} = 0. \end{aligned} \right\} \quad (3)$$

The motion thus defined for the downward half cycle between the maxima  $+x_0$  and  $-x_0$  has to be completed by an upward motion which is identical with the previous half except for a negative sign. This describes a motion which has the same period as the impressed force and therefore can be called a forced vibration. It is seen from (2) and (3) that  $\phi$  represents the “phase-angle” by which the force leads the motion. Since the motion is non-harmonic, it is clear that this “phase-angle” applies only to the *maxima* of force and motion, and that in general the phase between the zeros of force and motion will be different from  $\phi$ .

The general solution of (2) is

$$x = C_1 \sin \omega_n t + C_2 \cos \omega_n t + \frac{\omega_n^2}{\omega_n^2 - \omega^2} a \cos(\omega t + \phi) + x_f. \quad (4)$$

The four conditions (3) can be satisfied by assigning certain values to  $C_1$ ,  $C_2$ ,  $x_0$ , and  $\phi$ . Eliminating  $C_1$  and  $C_2$  from (4) by means of the two first conditions (3), leads to

$$\begin{aligned} x = x_0 \cos \omega_n t + x_f(1 - \cos \omega_n t) \\ + \frac{a\beta^2}{\beta^2 - 1} \left[ \cos \phi \{ \cos \omega t - \cos \omega_n t \} \right. \\ \left. + \sin \phi \left\{ \frac{\sin \omega_n t}{\beta} - \sin \omega t \right\} \right], \quad (4a) \end{aligned}$$

where

$$\beta = \omega_n / \omega.$$

Substitution of the last two conditions in this gives two equations:

$$\left. \begin{aligned} A \cos \phi + B \sin \phi + C = 0, \\ P \cos \phi + Q \sin \phi + R = 0, \end{aligned} \right\} \quad (5)$$

where

$$A = -a \cdot \frac{\beta^2}{\beta^2 - 1} (1 + \cos \beta \pi).$$

$$B = +a \frac{\beta}{\beta^2 - 1} \cdot \sin \beta \pi,$$

$$P = +a\omega_n \frac{\beta^2}{\beta^2-1} \cdot \sin \beta\pi,$$

$$Q = +a\omega_n \frac{\beta}{\beta^2-1} (1 + \cos \beta\pi),$$

$$C = +x_0(1 + \cos \beta\pi) + x_f(1 - \cos \beta\pi),$$

$$R = (x - x_0)\omega_n \sin \beta\pi.$$

From (5) we get

$$\cos \phi = \frac{BR - CQ}{AQ - PB}; \quad \sin \phi = \frac{CP - AR}{AQ - PB},$$

or, after substitution of the values for A etc.,

$$\left. \begin{aligned} \cos \phi &= \frac{x_0}{a} \cdot \frac{\beta^2 - 1}{\beta^2}, \\ \sin \phi &= -\frac{x_f}{a} \cdot \frac{\beta^2 - 1}{\beta^2} \cdot \frac{\beta \sin \beta\pi}{1 + \cos \beta\pi}. \end{aligned} \right\} \quad \cdot \quad (6)$$

Eliminating  $\phi$  and solving for the amplitude  $x_0$ , we have

$$x_0 = a \sqrt{\left(\frac{\beta^2}{\beta^2-1}\right)^2 - \left(\frac{x_f}{a}\right)^2 \cdot \left(\frac{\beta \sin \beta\pi}{1 + \cos \beta\pi}\right)^2} \quad (7)$$

Introducing the notations :

$$V = \frac{\beta^2}{\beta^2-1} = \frac{\omega_n^2}{\omega_n^2 - \omega^2} = \text{"response function,"}$$

$$U = \frac{\beta \sin \beta\pi}{1 + \cos \beta\pi} = \text{"damping function,"}$$

the results (6) and (7) can be written as

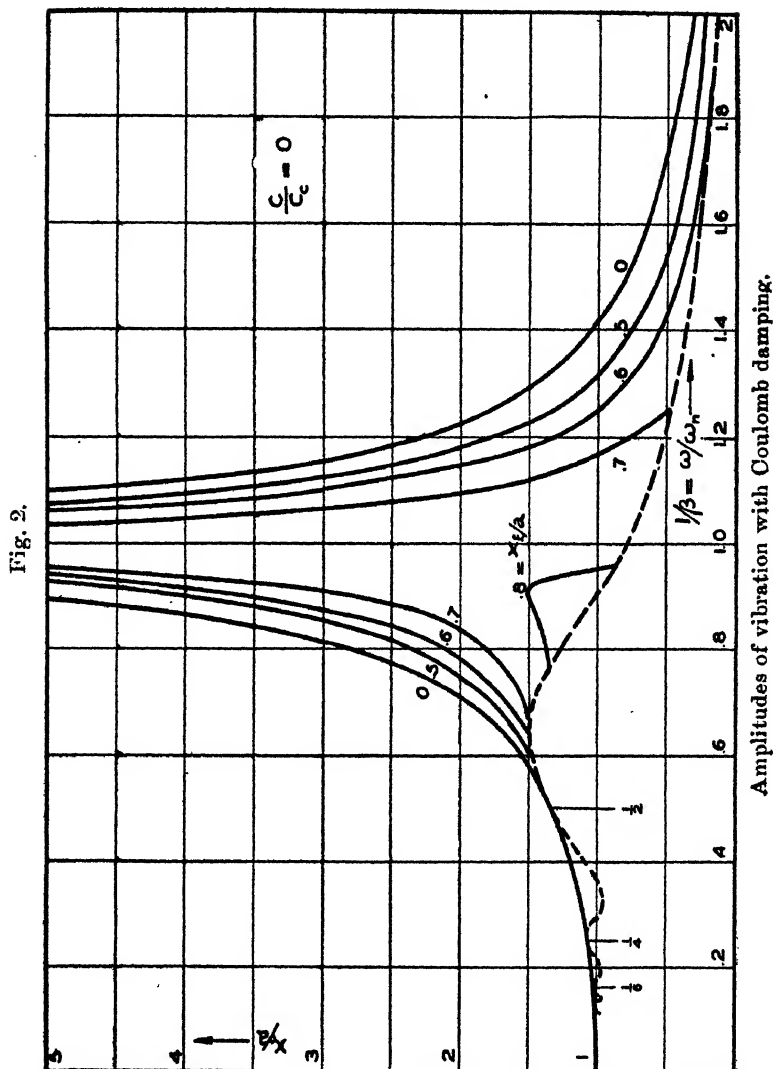
$$\sin \phi = -\frac{x_f}{a} \cdot \frac{U}{V}; \quad \cos \phi = +\frac{x_0}{a} \cdot \frac{1}{V}, \quad (6a)$$

$$x_0 = a \sqrt{V^2 - \left(\frac{x_f}{a}\right)^2 U^2} \quad (7a)$$

It is seen that the amplitude  $x_0$  is not proportional to the impressed force  $P_0 (=ak)$ . The influence of the damping appears in the formula as the ratio of the friction force to the impressed force :  $x_f/a = F_0/P_0$ .

## III. Validity of Solution.

This solution is valid only when  $\dot{x} \leq 0$  during the interval  $0 \leq t \leq \pi/\omega$ . Substituting (6a) and (7a) into (4a), and differentiating, the condition can be transformed to



$$\frac{x_0}{x_f} \geq \beta^2 \left[ \frac{\beta \sin \beta \omega t + U (\cos \omega t - \cos \beta \omega t)}{\beta^2 \sin \omega t} \right] \quad (8)$$

for  $0 \leq t \leq \pi/\omega$

or  $\frac{x_0}{x_f} \geq \beta^2 \cdot S,$

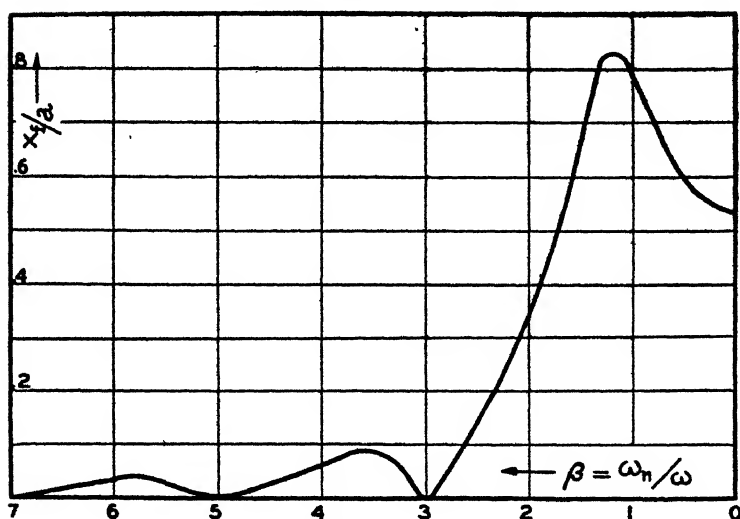
where  $S$  denotes the maximum value of the bracket during that time-interval. For  $t=0$  the bracket is equal to unity, and numerical calculations have shown that in quite many cases this is also the maximum value. From (7) and (8) we deduce

$$\frac{x_0}{a} \geq \sqrt{\frac{V^2}{1 + (U/S\beta^2)^2}} \cdot \cdot \cdot \cdot (9)$$

and

$$\frac{x_f}{a} \leq \sqrt{\frac{V^2}{(S\beta^2)^2 + U^2}} \cdot \cdot \cdot \cdot (10)$$

Fig. 3.



Damping determining boundary of non-stop motion.

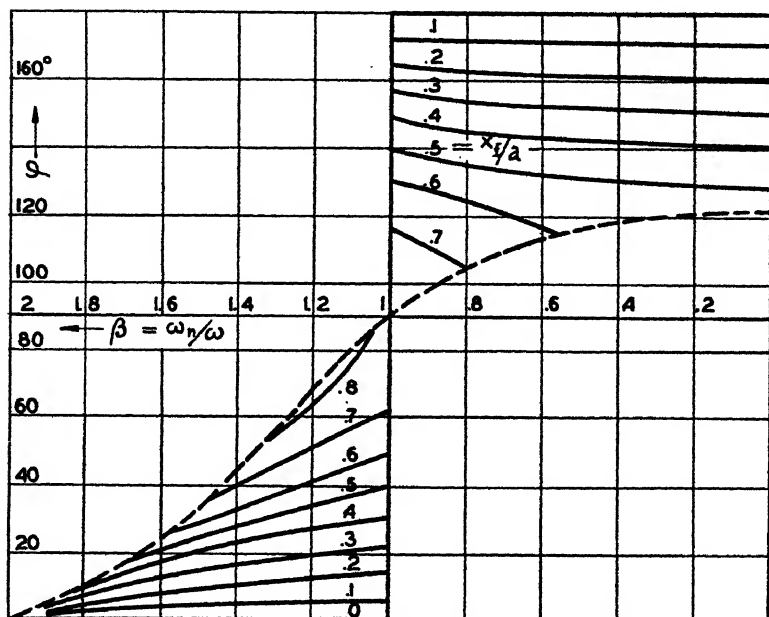
Fig. 2 shows a graphical representation of these results. The dotted line is the boundary (equation (9)), below which only motions with stops occur. It is seen that for frictions  $x_f/a < \pi/4$  the amplitude at resonance becomes infinitely large.

The relation (10) is represented by fig. 3, so that for frictions below this line the solutions (6) and (7) are valid and motions without stops can exist, while for higher frictions this is not the case. Comparing fig. 3 with the dotted boundary of fig. 2, it is seen that for even integer values of  $\beta (= \omega_n/\omega)$  the amplitude of the motion (and the phase-angle) are independent of the amount of friction up to the limit set by fig. 3. For odd integer values of  $\beta$  the

smallest friction will cause stops in the motion and a considerable decrease in the amplitude. It might be said that for odd  $\beta$  the friction is "infinitely efficient" in reducing the amplitude, while for even  $\beta$  it is "infinitely inefficient."

Fig. 4 gives the results (6a) for the phase-angle, showing the peculiarity of jumps in the angle at resonance for any friction up to  $x_f/a = \pi/4$ .

Fig. 4.



Phase-angle diagram with pure Coulomb damping.

#### IV. Combined Viscous and Coulomb Damping.

The analysis for this case is quite analogous to the previous one. The differential equations are

$$m\ddot{x} + kx + c\dot{x} \pm F_0 = P_0 \cos(\omega t + \phi), \quad . \quad . \quad (11)$$

or for the downward stroke only,

$$\ddot{x} + \omega_n^2(x - x_f) + \frac{c}{m} \dot{x} = a\omega_n^2 \cos(\omega t + \phi), \quad . \quad (11a)$$

with the boundary conditions (3).

Using the abbreviations :

$$p = \sqrt{\omega_n^2 - \frac{c^2}{4m^2}} = \omega_n \sqrt{1 - \left(\frac{c}{c_c}\right)^2},$$

$$q = \sqrt{\left(\frac{1}{V}\right)^2 + \left(\frac{2}{\beta} \cdot \frac{c}{c_c}\right)^2},$$

where

$$c_c = \text{critical damping} = 2m\omega_n,$$

the general solution of (11a) can be written

$$x = e^{-\frac{ct}{2m}} [C_1 \cos pt + C_2 \sin pt] + \frac{a}{q} \sin(\omega t + \epsilon) + x_f, \quad (12)$$

with

$$\tan(\phi - \epsilon) = \frac{c\omega}{k - m\omega^2} = \frac{2V}{\beta} \cdot \frac{c}{c_c}. \quad (12a)$$

Now  $C_1$ ,  $C_2$ ,  $x_0$ , and  $\phi$  are determined so as to satisfy the four conditions (3) in exactly the same manner as before, though the calculation becomes rather involved.

The result can be conveniently presented in the following form :—

$$\frac{x_0}{a} = -G\left(\frac{x_f}{a}\right) + \sqrt{\frac{1}{q^2} - H^2\left(\frac{x_f}{a}\right)^2}, \quad (13)$$

$$\sin \epsilon = -qH \frac{x_f}{a}; \quad \cos \epsilon = q \left[ \frac{x_0}{a} + G \cdot \frac{x_f}{a} \right], \quad (14)$$

the first of which gives the amplitude directly, while the second, in conjunction with (12a), allows of an easy numerical calculation of the phase-angle  $\phi$ .

In these expressions  $G$  and  $H$  are functions of the viscous damping  $c/c_c$  and of the frequency  $\beta$  :

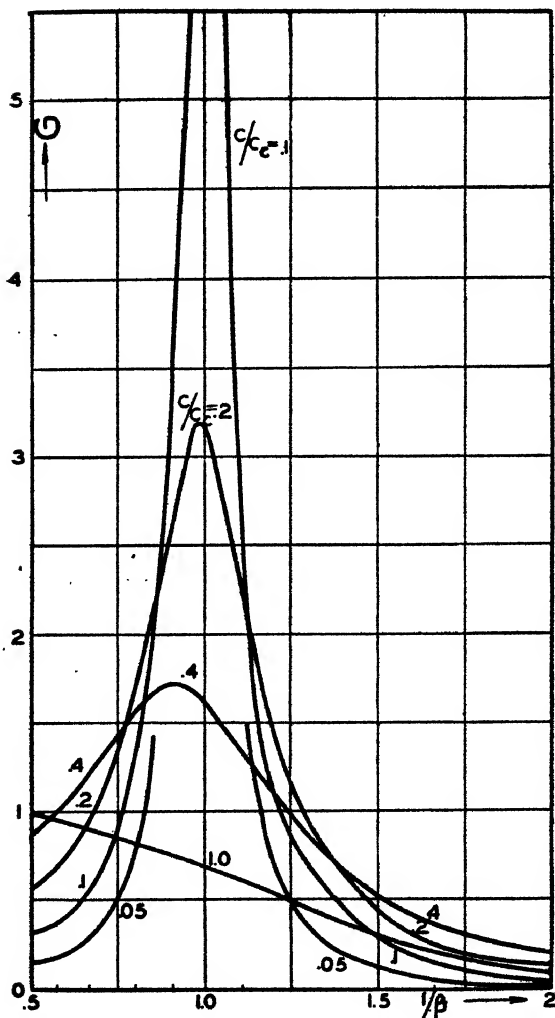
$$\left. \begin{aligned} G &= \frac{\sinh(\beta\pi c/c_c) - \frac{c/c_c}{\sqrt{1-(c/c_c)^2}} \cdot \sin \beta\pi \sqrt{1-(c/c_c)^2}}{\cosh(\beta\pi c/c_c) + \cos \beta\pi \sqrt{1-(c/c_c)^2}}, \\ H &= \frac{\beta}{\sqrt{1-(c/c_c)^2}} \cdot \frac{\sin \beta\pi \sqrt{1-(c/c_c)^2}}{\cosh(\beta\pi c/c_c) + \cos \beta\pi \sqrt{1-(c/c_c)^2}}. \end{aligned} \right\} \quad (15)$$

It is seen that in the absence of Coulomb damping, (13) reduces to  $x_0/a = 1/q$ , which is the well-known result for viscous damping only. Likewise in this case the auxiliary



angle  $\epsilon$  becomes zero, so that the phase (12a) coincides with the well-established theory.

Fig. 5.

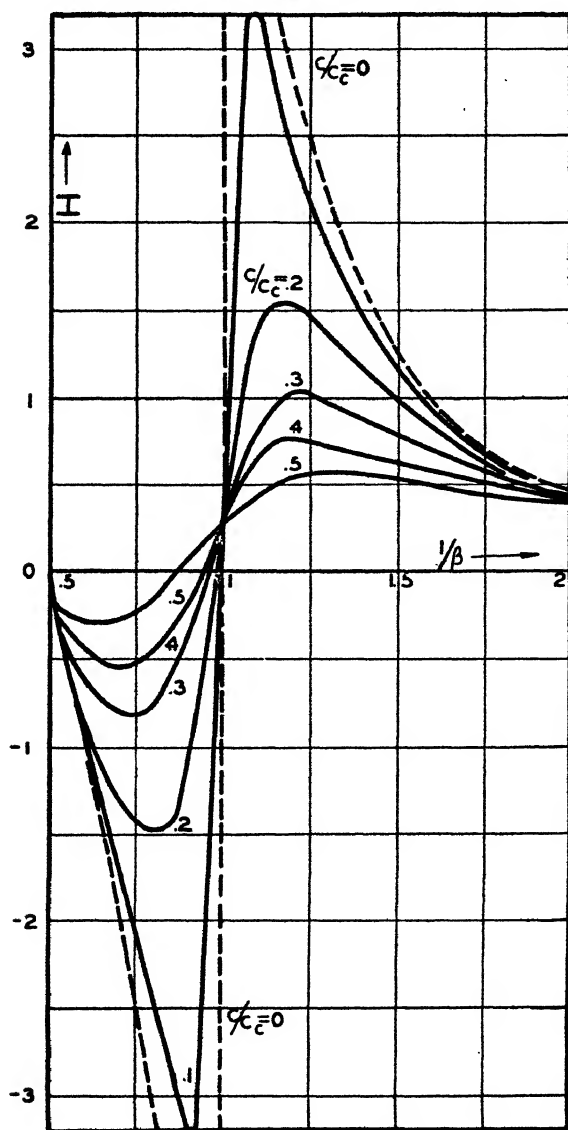


Graph of the G function.

It is of interest to note that for  $c/c_c=0$  the G function is zero for all values of  $\beta$ , except  $\beta=1$ , where G tends to infinity. The H function reduces to V for  $c/c_c=0$ . Since these two functions play an important role in the numerical

calculations, they are shown in figs. 5 and 6 for various values of  $c/c_c$ .

Fig. 6.



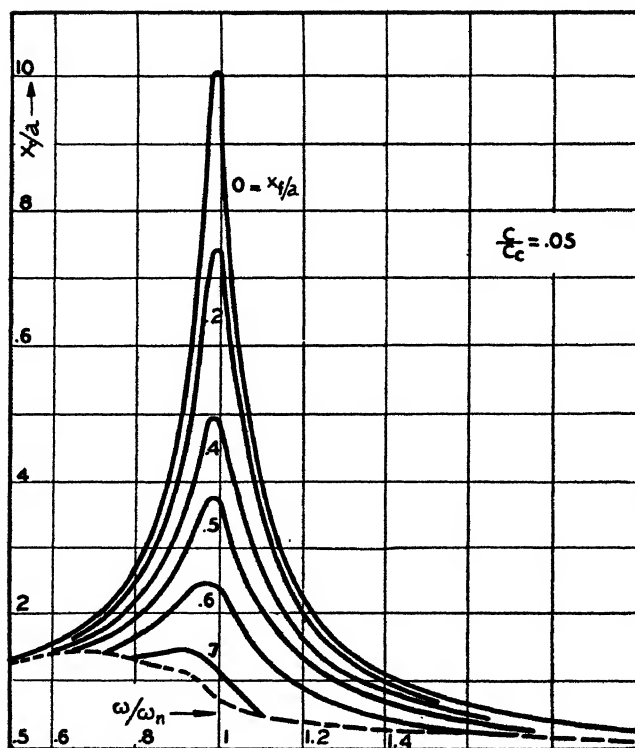
Graph of the H function.

The numerical results of the amplitudes of vibration for six values of  $c/c_c$  are represented in figs. 7 to 12. The condition of validity of the solution,  $\dot{x} \leq 0$ , becomes

$$\frac{x_0}{x_f} \geq \frac{e^{-\frac{ct}{2m}}}{\sin \omega t} \cdot \left\{ \left( \frac{p}{\omega} + \frac{c^2}{4m^2 p \omega} \right) (1+G) \sin pt \right. \\ \left. + H \left( \frac{c}{2pm} \sin pt - \cos pt \right) \right\} + H \cotg \omega t - G$$

for  $0 \leq t \leq \pi/\omega$ . . . . . (16)

Fig. 7.



Amplitudes with mixed damping.

For  $t=0$  this expression reduces to

$$\frac{x_0}{x_f} \geq -G + 2H\beta c/c_c + \beta^2(1+G), \quad . . . (17)$$

which quite often is also the maximum value of (16). In fact, for any  $\beta < 2$  this is the case. Let  $S_1$  denote the ratio

Fig. 8.

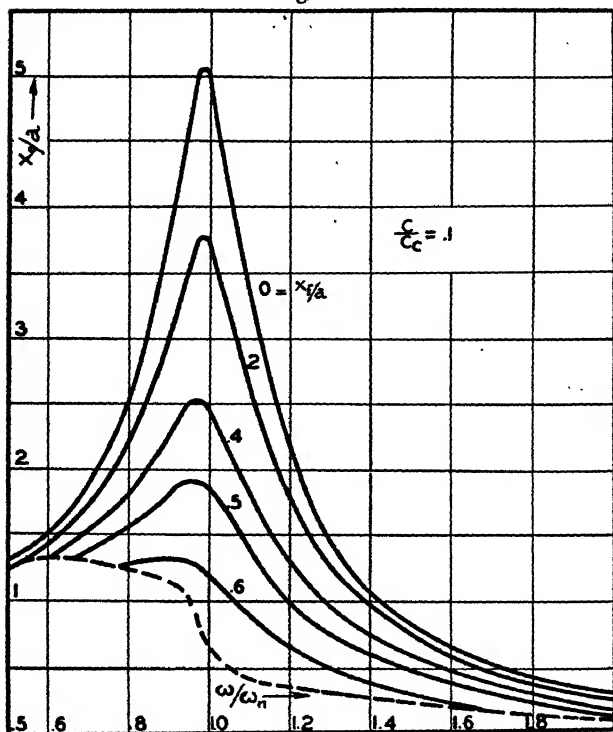


Fig. 9.

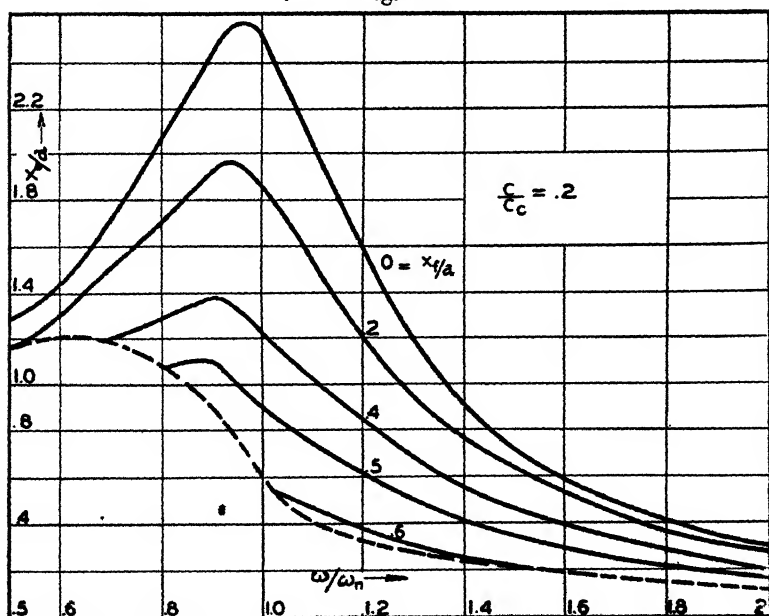


Fig. 10.

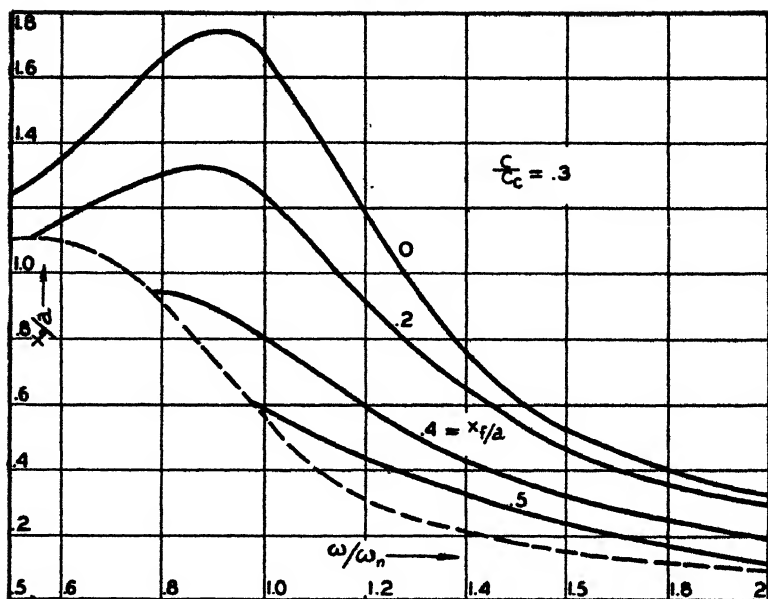
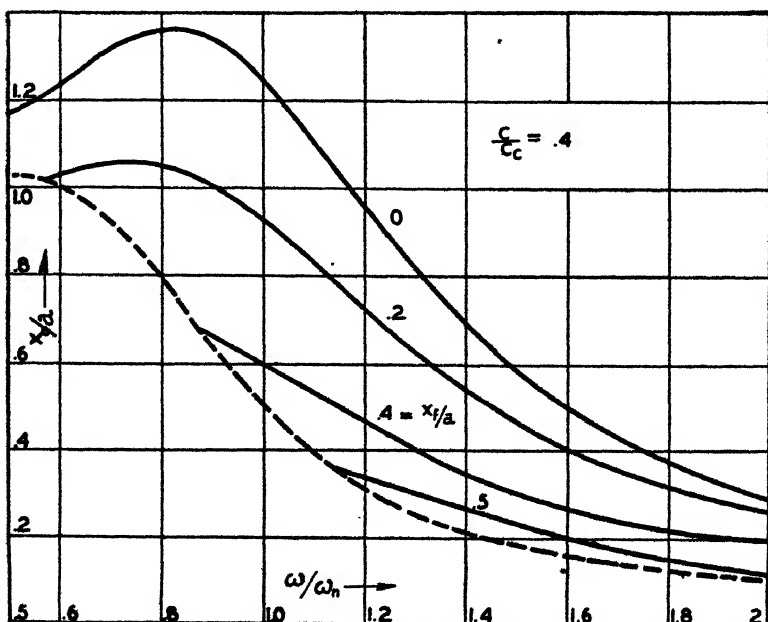


Fig. 11.

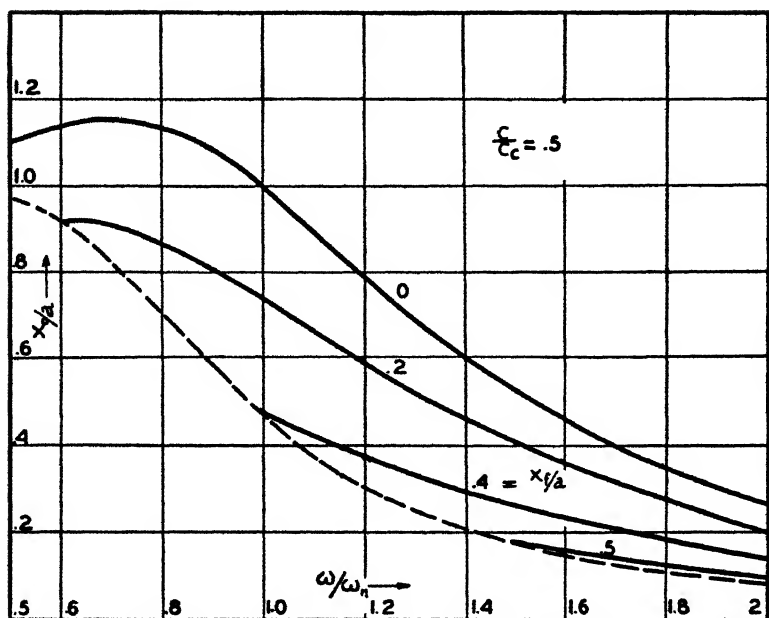


of the maximum of (16) and (17), which is equal to unity for  $\beta < 2$ . Then we have

$$\frac{x_0}{a} \geq \frac{S_1(I-G)}{q \sqrt{H^2 + \{S_1 I + (1-S_1)G\}^2}},$$

$$\frac{x_f}{a} \leq \frac{1}{q \sqrt{H^2 + \{S_1 I + (1-S_1)G\}^2}},$$

Fig. 12.



where

$$I = 2H\beta c/c_c + \beta^2(1+G).$$

With these formulæ the dotted lines in figs. 7-12 have been calculated.

The phase-angle diagram for  $c/c_c = .1$  is given in fig. 13. Since the amplitudes at resonance are finite, no discontinuity in the angle occurs. It is noted that the angle at resonance is quite near to  $90^\circ$ , while for other frequencies the phase-angle differs considerably from that of a motion with viscous damping only. The greatest difference occurs at  $\beta = 0$  or  $\omega_n = 0$ , which is of importance for engineering applications (Lanchester torsional vibration damper).

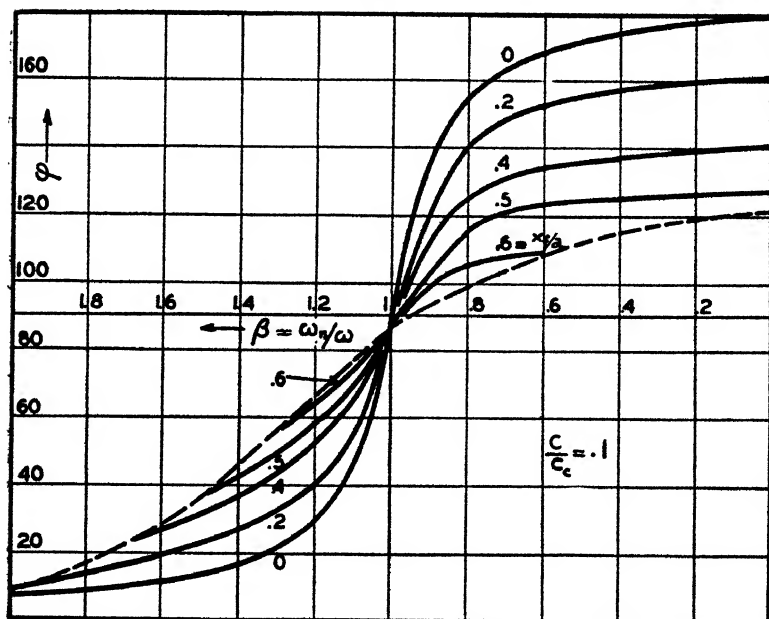
Due to the fact that  $\phi \approx 90^\circ$  at resonance, the amplitude at that point for combined damping can be calculated with a fair approximation from an energy consideration. Assuming the motion sinusoidal, the work input per cycle by the force  $P_0 \sin \omega t$  is

$$\pi P_0 x_0.$$

The friction force is  $F_0 + cx_0 \omega \sin \omega$  and its work absorption per cycle is

$$\int_0^T (F_0 + cx_0 \omega \sin \omega t) \cdot v dt = 4F_0 x_0 + c\omega x_0^2 \pi.$$

Fig. 13.



Phase-angles with mixed damping.

Equating the two, we get

$$x_0 = \frac{P_0}{c\omega} \left[ 1 - \frac{4}{\pi} \frac{F_0}{P_0} \right]. \quad \dots \quad (17)$$

The difference of this expression with the exact solution naturally increases with the amount of damping of either kind: for  $c/c_c = .5$  and  $x_f/a = .4$  it is only 3 per cent. The degree of approximation can be visualized from the fact that for  $\beta = 1$ ,  $G$  is large and  $H$  small, so that (13) reduces to

$\frac{1}{q} - G\left(\frac{x_f}{a}\right)$ . Moreover, at resonance both  $1/q$  and  $G$  are nearly proportional to  $c/c_0$ .

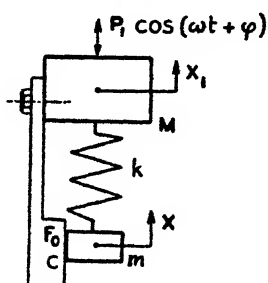
At frequencies other than resonance no simple rule for the amplitude can be given; then recourse has to be taken to figs. 7 to 12.

### V. Other Problems to which the Solution applies.

1. If in fig. 1 no external force be acting on the mass, but the upper end of the spring be moved  $a_0 \cos(\omega t + \phi)$ , it can be verified that the above solution holds for the absolute motion of the mass, when only  $a$  be replaced by  $a_0$ .

2. If in fig. 1 the rubbing wall be tied to the upper end of the spring and this end with the wall be subjected to the

Fig. 14.



motion  $a_0 \cos(\omega t + \phi)$ , the above solution holds for the relative motion between mass and wall, if only  $a$  be replaced by  $a_0/\beta^2$ .

3. Fig. 14 represents a two-mass system with relative damping and a force  $P_1 \cos(\omega t + \phi)$  acting on the mass  $M$ . It can be shown that all previous results apply to the relative motion  $x - x_1 = y$ , if only  $m$  be replaced by  $mM/(m + M)$  and  $P_0$  by  $P_1 \cdot m/(M + m)$ . The absolute motions of  $m$  and  $M$  can be found to be

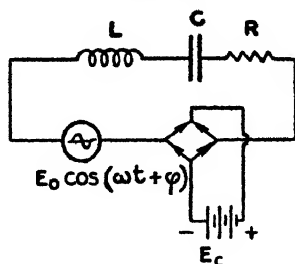
$$\left. \begin{aligned} x &= \frac{M}{M+m} y - \frac{P_1}{\omega^2(M+m)} \cos(\omega t + \phi), \\ x_1 &= -\frac{m}{M+m} y - \frac{P_1}{\omega^2(M+m)} \cos(\omega t + \phi). \end{aligned} \right\} \quad (18)$$

4. It is evident that all the above problems have torsional equivalents when masses are replaced by moments of inertia, displacements by angles, etc.



5. An electrical problem leading to the same differential equation is shown in fig. 15. The four rectifiers keep the constant battery voltage always directed against the current. The previous results hold if the velocity  $\dot{x}$  be replaced by the

Fig. 15.

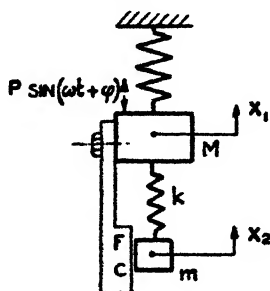


current  $i$ , the mass  $m$  by the inductance  $L$ , the spring constant  $k$  by the inverse capacity  $1/C$ , the viscous friction  $c$  by the resistance  $R$ , the constant friction  $F_0$  by the battery voltage  $E_c$ , and the force amplitude  $P_0$  by the voltage amplitude  $E_0$ .

## VI. *Systems with many Degrees of Freedom.*

The method outlined above is not restricted to systems with a single degree of freedom, but can be successfully applied to problems of greater complication. As an example

Fig. 16.



let us consider fig. 16. Two simultaneous differential equations can be written down, conveniently in the variables  $x_1$  and  $x_1 - x_2 = x_r$ . When only one-half stroke of the motion is considered, there will be no ambiguity in the sign of the Coulomb damping term. As before, a parameter  $\phi$  is written

in the expression for the disturbing force. Since the differential equations are linear and of the second order, their solution can be written down involving four constants. Let the initial conditions be

$$t=0; \quad x_1=x_{10}; \quad \dot{x}_1=\dot{x}_{10}; \quad x_r=x_{\max.}; \quad \dot{x}_r=0.$$

With these conditions the integration constants can be eliminated, and the solution appears as a function of four parameters— $x_{10}$ ,  $\dot{x}_{10}$ ,  $x_{\max.}$ , and  $\phi$ —which can be determined by four conditions at  $t=\pi/\omega$ , namely

$$x_1=-x_{10}, \quad \dot{x}_1=-\dot{x}_{10}, \quad x_r=-x_{\max.}, \quad \text{and} \quad \dot{x}_r=0.$$

The solution thus obtained is valid only if

$$x_r \leq 0 \quad \text{for} \quad 0 \leq t \leq \pi/\omega.$$

In a similar manner the steady-state solutions for systems of any number of degrees of freedom involving both viscous and Coulomb damping can be determined.

#### *Acknowledgement.*

The author's thanks are due to the University of Pittsburgh for permission to publish this work, which represents an abstract of a doctor's dissertation.

Research Laboratories,  
Westinghouse Electric & Mfg. Co.,  
East Pittsburgh, Penn.

#### LXXIV. *The Psychophysical Law.*—I. *The Sense of Vision.*

By P. A. MACDONALD, *M.Sc., Hudson Bay Fellow, and*  
JOHN F. ALLEN, *B.A., Research Assistant, Department of*  
*Physics, University of Manitoba, Winnipeg, Canada* \*.

IT has long been known that the physical intensity of a sensory stimulus may be increased by an amount so small that the increment does not cause a corresponding increase in the sensation evoked by the stimulus. Denoting the physical intensity of the stimulus by  $I$ , and the small increment by  $\delta I$ , experiment has shown that  $\delta I$  may be increased to a critical value such that a just perceptible increase in the sensation results. This value of  $\delta I$  is

\* Communicated by Prof. Frank Allen.

known as the differential threshold, and is usually denoted by  $\Delta I$ .

The variation of the magnitude of  $\Delta I$  with reference to different values of  $I$  was first seriously investigated by Weber, who concluded that a simple relation existed between these quantities, which is expressed by the equation

$$\frac{\Delta I}{I} = c,$$

where  $c$  is a constant.

Extending Weber's work, an attempt to establish a relation between the intensity of a physical stimulus and the corresponding sensation evoked was made by Fechner, who used Weber's relation as the basis of his development of the subject.

"Fechner's Law," following Parsons's treatment\*, states that "the sensation varies as the logarithm of the stimulus, *i. e.* the sensation changes in arithmetical proportion as the stimulus increases in geometrical proportion.

"Stated algebraically, if  $S$  is the measure of a sensation and  $\delta S$  the just appreciable difference,  $I$  the measure of the stimulus and  $\delta I$  a small increment, then

$$\delta S = k \frac{\delta I}{I} \quad (\text{Weber's law}),$$

where  $k$  is a constant; therefore, on the questionable assumption that it is permissible to integrate small finite quantities ( $\delta s$  etc.),

$$\begin{aligned} S &= k \int \frac{dI}{I} \\ &= k \log I + k' \quad (\text{Fechner's law}, \end{aligned}$$

where  $k'$  is another constant."

Both laws have been subjected to an immense number of experimental investigations in the various senses. It is only in the sense of vision, however, that the researches have reached a high degree of accuracy, the best work, by general consent, having been carried out by König†. As König's ability and prolonged experience in visual measurements preclude the likelihood of errors in his

\* Sir J. H. Parsons, 'Colour Vision,' 2nd ed. p. 23

† A. König, *Physiol. Optik.* 1903.

measurements, only his work will be considered in this treatment, and taken as typical of the best experimental work and procedure.

König, keeping his eyes in darkness adaptation, used as a stimulus a patch of light viewed through a suitable ocular. The upper half of the patch being maintained at a definite brightness,  $I$ , the intensity of the lower half was varied by nicol prisms until it was just perceptibly brighter than

TABLE I.  
König's Data.

$\lambda = 6700 \text{ \AA.}$		$\lambda = 5050 \text{ \AA.}$	
$I$ .	$\frac{\Delta I}{I}$ .	$I$ .	$\frac{\Delta I}{I}$ .
48950	·0215	19610	·0197
19680	·0163	9819	·0184
9844	·0158	4920	·0163
4912	·0180	1965	·0179
1967	·0169	982	·0188
983	·0172	490	·0197
490	·0206	196	·0222
196	·0224	97·6	·0250
97·1	·0300	48·7	·0258
48·1	·0391	19·4	·0306
19·1	·0465	9·64	·0375
9·35	·0701	4·76	·0513
4·54	·101	1·87	·0701
1·66	·207	0·920	·0874
·742	·347	0·454	·100
·312	·603	0·178	·124
		0·0866	·154
		0·0408	·224
		0·0150	·336
		0·00729	·372
		0·00339	·475

the upper. The difference between the physical intensities of the two patches was then determined by the relative rotations of the nicols, and taken as the value of the differential threshold  $\Delta I$ . The upper half of the field was then increased by the numerical value of  $\Delta I$  to give a new value of  $I$ , and the lower increased again until it became just perceptibly brighter. In this manner measurements were obtained throughout the whole range of intensities available for various monochromatic radiations and for white light, two series of which are reproduced in Table I. From an inspection of these data it will be seen that they are not connected by any linear relationship.

In a recent paper by Hecht \*, data from various sources relating to the Weber and Fechner laws in vision have been discussed and the following conclusion reached :—

“ There is presented a series of data, assembled from various sources, which proves that in the visual discrimination of intensity the threshold difference  $\Delta I$  bears no constant relation to the intensity  $I$ . The evidence shows unequivocally that, as the intensity rises, the ratio  $\frac{\Delta I}{I}$  first decreases and then increases.”

From the evidence available Parsons † also concludes : “ Weber’s law does not hold good for very low or very high intensities of stimuli, and is only approximate at best.”

While König’s measurements are probably beyond criticism, the interpretation of them as a valid experimental examination of the Weber law appears to be unsound for the following reasons :—

In observing the patch of light, one-half being at an intensity  $I$  and the other at a greater intensity  $I + \Delta I$ , two sensations are evoked by the stimulation of two adjoining retinal areas, whereas the Weber law deals with but a single sensation at any one time.

It has been shown by Allen ‡ that stimulation of a retinal area elicits complex neural reactions which modify the sensitivity of adjoining areas. The magnitude of the inductive reactions varies in some way with the intensity and duration of stimulation and with the wave-length of the light employed. The unequal stimulation of two adjoining areas by the same hues but of different intensities, as in König’s experiments, causes mutual inductive actions which tend to equalize the sensations. Under such conditions a value of  $\Delta I$  obtained by slowly increasing the brightness of one patch cannot accurately represent the real differential threshold, and the ratio  $\frac{\Delta I}{I}$  will

consequently be either too large or too small. It has been shown by Allen that the darkness adaptation of the unused eye further modifies the sensitivity of the receptors in the observing eye.

\* Journ. Gen. Physiol. vii. p. 265 (1924).

† Loc. cit. p. 23.

‡ Journ. Op. Soc. Am. vii. pp. 583, 913 (1923); *ibid.* ix. p. 375 (1924); *ibid.* xiii. p. 383 (1926).

One of the outstanding features of the visual mechanism is its great amplitude of adaptation, or its ability to respond accurately to stimuli varying over a wide range of intensity. It might be expected, in order for the process of adaptation to operate in the most efficient manner, that there would occur some modifications of the neural reaction processes at different ranges of intensity of stimulation. König, however, seems to have taken no precautions against the danger of concealing such possible modifications.

Consider, for example, his curve obtained with radiation of wave-length  $6700 \text{ \AA}$ . There are in it only 16 points, representing a very wide range of intensities from the least perceptible to the greatest. The extensive graphical interpolation necessitated by such widespread points would effectively conceal any alterations in the response of the receptors except those of the greatest magnitude. Such measurements, therefore, should not be interpreted as a satisfactory experimental examination of Weber's law.

Again, much work has been done with white light. It has been found by Allen \* that each spectral wave-length is a physiological stimulus with a character peculiar to itself, differing, sometimes widely, from that possessed by every other hue. Since white light may be composed of all wave-lengths in the visible spectrum, and in varying amounts depending on the nature of the source, it would contain practically an infinite number of physical variables, and in consequence would elicit a corresponding complexity of sensations. In considering the interpretation of experimental results, it should be borne in mind that the essential condition of the scientific method of experimentation is the reduction to a minimum of the number of variables observed at any one time.

These criticisms of König's method may be briefly summarised thus :—

1. Owing to the nature of the apparatus, two distinct sensations of different intensities were obtained at the same time. This is not the condition required by Fechner's interpretation of Weber's ratio.

2. The normal condition of the sensitivity of the retina was not maintained because of the presence of inductive processes.

\* Journ. Op. Soc. Am. xiii. p. 383 (1926).

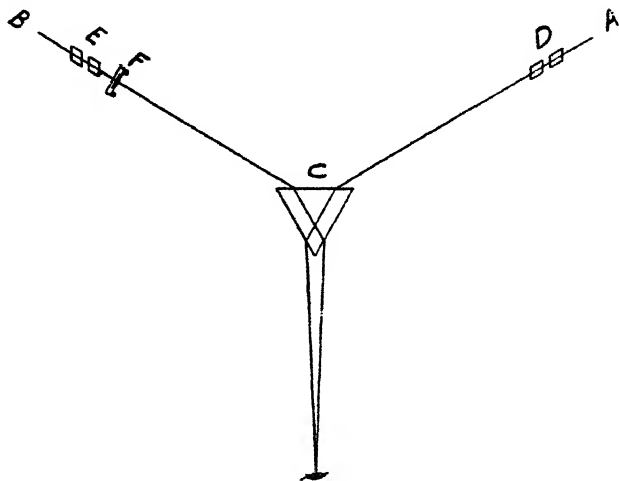
3. The method of adding the value of the differential threshold to the intensity in order to determine the next intensity at which to examine Weber's ratio, leaves a constantly widening gap between successive readings far too great for an exacting examination of the law.

4. The use of white light in examining simple visual laws introduces a confusing complexity.

*Experimental Arrangements for a New Examination of Weber's Law.*

In the present attempt to examine Weber's law and to avoid the criticisms of König's method, the arrangement of apparatus was similar in principle to the diagram in fig. 1.

Fig. 1.



Two incandescent lamps, A and B, operated from a 60-cycle alternating current of 110 volts, were the sources of radiation. The light was passed by two collimators through two refracting edges of the prism C in such a manner that radiations of the same wave-length from each source were superposed in the focal plane of the Hilger shutter eyepiece of the telescope. The actual instrument used was the tricolour spectrometer designed by Professor Frank Allen \*. The intensity of the radiation from each source was controlled by pairs of nicol prisms, D and E, placed between the sources and the slits of the collimators.

\* Journ. Op. Soc. Am. viii. p. 339 (1924).

Between the source B, the corresponding nicol prisms E, and the prism C was placed in the path of the light a camera shutter F, which was normally kept closed. By this arrangement a small patch of light of the desired wavelength of constant and measured intensity could be observed, and a measured increment of the same colour could be added uniformly over the whole of the same patch by opening the camera shutter for a brief interval of time. Thus by repeated trials the just perceptible increment could be determined with precision, and without employing a second patch of colour as a standard of comparison.

The apparatus was mounted in a room well lighted by diffused daylight, both eyes being thus adapted to the state in which they are ordinarily used. A definite intensity I of the stimulus from the source A was obtained by rotating the polarizer of the nicols D. This stimulus was received on the right eye for approximately 2 seconds when the camera shutter was opened. An increase of intensity was looked for, since the release of the shutter allowed an increment of radiation of intensity  $\Delta I$ , coming from the source B, to be superposed on the intensity I for a period of one-fifth of a second. A rest interval of 3 minutes was then allowed for the eye to resume its normal condition, after which the process was repeated, the value of the intensity  $\Delta I$  being either raised or lowered according to whether it had been noticeable or not at the previous opening of the shutter.

When the intensity had been reached at which the increment was just perceptible, its magnitude was determined by measuring the angle between the principal planes of the nicols E, the magnitude of the intensity I being likewise determined from the other pair of nicols D. No attempt was made to determine the absolute value of the Weber ratio  $\frac{\Delta I}{I}$ .

Examination of Weber's law with three different spectral colours—red, yellow, and green—of wave-lengths 6678 Å., 5875 Å., 5015 Å., was made in this manner.

The measurements are given in Table II. The intensity of the stimulus is proportional to  $\sin^2 \phi$ , where  $\phi$  is the angle between the principal planes of the nicols A, such that where  $\phi = 0$  the nicols transmit no light. Similarly,



$\sin^2 \theta$  determines the intensity of the differential threshold,  $\theta$  being the angle between the principal planes of the nicols B. No numerical relation between the intensity and the differential thresholds was determined.

The data are shown graphically in figs. 2, 3, and 4, where stimulating intensities are plotted as abscissæ and

TABLE II.

## Experimental Confirmation of Weber's Law.

Intensity =  $\sin^2 \phi$ . Differential threshold =  $\sin^2 \theta$ .

CURVE A. $\lambda = 6678 \text{ \AA.}$		CURVE B. $\lambda = 5875 \text{ \AA.}$		CURVE C. $\lambda = 5015 \text{ \AA.}$	
$\sin^2 \phi$ .	$\sin^2 \theta$ .	$\sin^2 \phi$ .	$\sin^2 \theta$ .	$\sin^2 \phi$ .	$\sin^2 \theta$ .
1.0000	0.3167	1.0000	0.1141	1.0000	0.4318
0.9700	0.3059	0.9700	0.1068	0.9700	0.4088
0.8830	0.2742	0.8830	0.0862	0.8830	0.3580
0.7550	0.2240	0.8078	0.0677	0.7550	0.2820
0.7114	0.2073	0.7550	0.0620	0.7035	0.2563
0.6712	0.1979	0.5867	0.0499	0.6545	0.2412
0.6292	0.1887	0.4134	0.0347	0.5867	0.2252
0.5867	0.1796	0.2500	0.0205	0.4134	0.1796
0.4134	0.1372	0.1170	0.0055	0.2500	0.1294
0.2500	0.0997	0.0300	0.0007	0.1786	0.1104
0.2132	0.0896			0.1170	0.0912
0.1786	0.0814			0.0669	0.0606
0.1590	0.0751			0.0300	0.0380
0.1464	0.0691				
0.1313	0.0606				
0.1170	0.0513				
0.1006	0.0403				
0.0904	0.0369				
0.0688	0.0288				
0.0467	0.0231				
0.0301	0.0181				
0.0076	0.0116				

the corresponding differential thresholds as ordinates. It will be seen that the curves obtained are all exact straight lines, there being, however, at definite values of the intensities abrupt changes in the slope similar to those obtained by Allen in his detailed experimental study of the Ferry-Porter law.

Each part of the graph, therefore, conforms to the law

$$\frac{\Delta I}{I} = C,$$

where the constant C has a different value for each part of the graph.

Fig. 2.

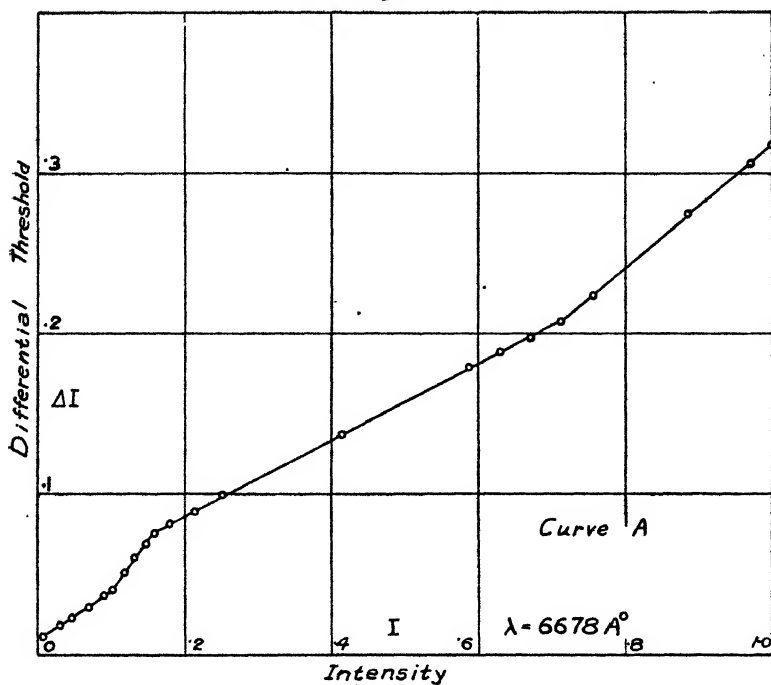
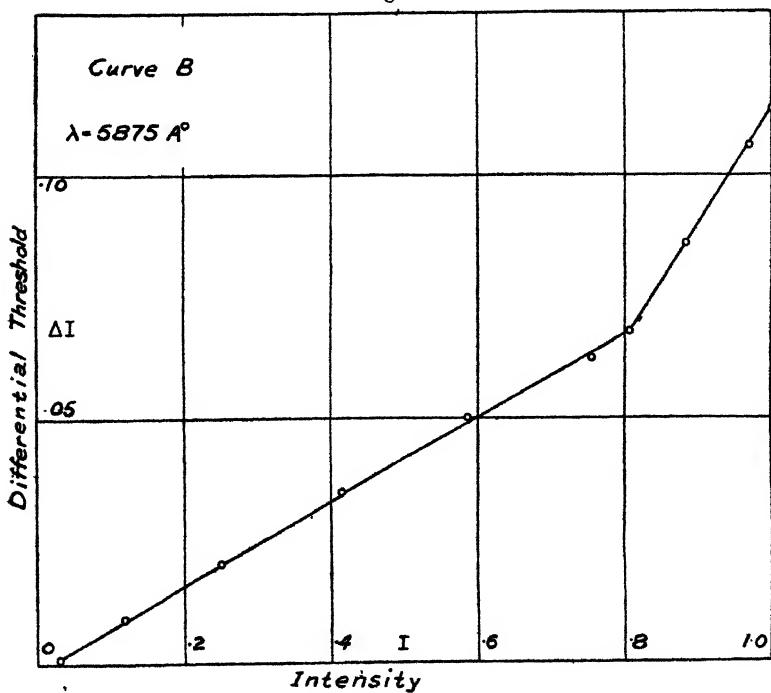
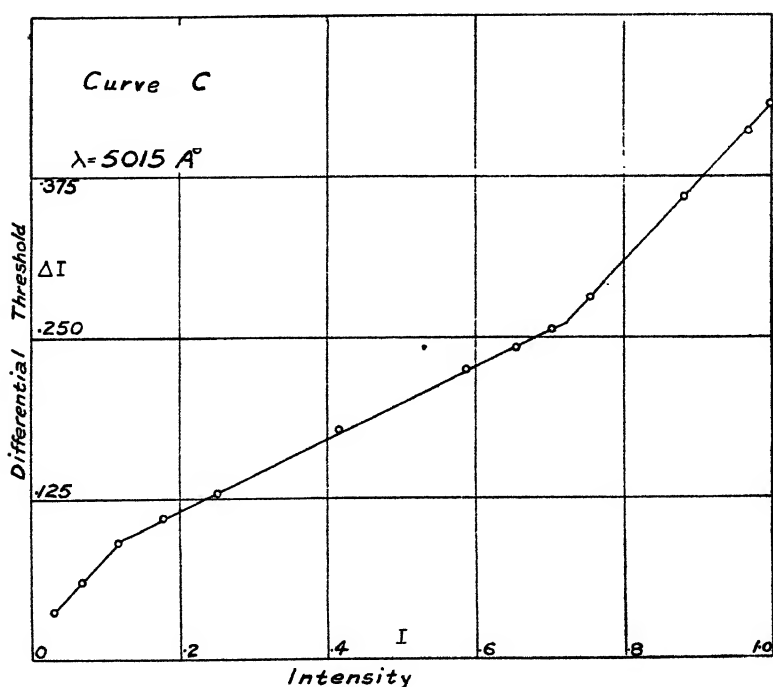


Fig. 3.



It is evident from the curves presented in this communication that for the visual sense Weber's law holds exactly over all ranges of intensity, there being, however, at definite intensities sudden changes in the value of the ratio of the differential threshold to the stimulating intensity. Previous investigators had been expecting to obtain a single constant holding for all ranges of intensity, and their failure to recognize the possibility of different

Fig. 4.



constants for different ranges of intensity has led to the conclusion that Weber's law was not true. The different numerical values for the ratio obtained by various observers would be accounted for both on this basis and on an observation which we have made that the ratio varies with the area of the surface examined.

A more detailed discussion of the results will be deferred to later parts of this communication in which experiments on other senses will be described.

In conclusion the authors desire to emphasize the fact that the purpose of this paper is to show that a definite algebraic ratio connecting the increment of intensity with the intensity of the stimulus does exist. It is not intended to be a complete quantitative investigation of the subject, for the laboratory facilities were not sufficiently extensive to permit the absolute values of the stimuli to be readily determined. Indeed, it would seem better to defer such measurements until a more detailed examination of the conditions underlying the law has been made.

We desire to express our sincere thanks to Professor Frank Allen, not only for the use of his laboratory, but for much stimulating criticism during the progress of the work. We also desire to thank the Hudson's Bay Company and the National Research Council of Canada for the substantial grants which enabled this work to be undertaken.

LXXV. *The Psychophysical Law.—II. The Sense of Audition.* By P. A. MACDONALD, M.Sc., Hudson Bay Fellow, and JOHN F. ALLEN, B.A., Research Assistant, University of Manitoba, Winnipeg, Canada\*.

IN subjecting Weber's Law to an examination in the sense of hearing, the fundamental principle and precautions followed were similar to those employed in the investigation of the same law in vision which was described in a previous communication † to this Magazine.

The source of sound of adjustable intensity and frequency was a Stern tonvariator which was sounded by a stream of air previously collected over water in a constant-pressure tank. The particular instrument first used was that formerly employed by Miss Weinberg and Professor Allen in their researches on the critical frequency of pulsation of tones ‡. The frequency chosen by the present writers was 180 D.V., which was within the limits of frequency studied by the former investigators. The intensities used in this part of the present communication were

\* Communicated by Prof. Frank Allen.

† Macdonald and J. F. Allen, "The Psychophysical Law.—I. Vision," see Part I. of this paper, p. 817.

‡ Phil. Mag. xlvii. pp. 50, 941 (1924).

selected to conform to those which had been assumed, as stated by other investigators\*, to be proportional to the blowing pressure of the air. The weights placed on the pressure tank were therefore taken as proportional to the intensities of the sound emitted by the tonvariator. Considering the small range of intensities employed, this assumption is probably quite accurately justified.

TABLE I.  
Weber's Law in Audition. Frequency 180 D.V.

I.	Log I.	$\Delta I.$	$\frac{1}{\Delta I}$	
Kilograms.		Kilogram.		
0.5	1.699	0.1575	6.349	C
1.0	0	0.1825	5.479	
1.5	0.176	0.1975	5.063	
2.0	0.301	0.2075	4.817	
2.0	0.301	0.2070	4.831	
3.0	0.477	0.2220	4.505	
3.5	0.544	0.2275	4.396	
1	0	0.182	5.495	B
3	0.477	0.222	4.505	
5	0.699	0.247	4.049	
7	0.845	0.267	3.745	
9	0.954	0.287	3.484	
11	1.041	0.297	3.367	
2	0.301	0.212	4.717	A
4	0.602	0.237	4.219	
6	0.778	0.257	3.891	
8	0.903	0.277	3.610	
10	1.000	0.292	3.425	
12	1.079	0.302	3.311	

A, readings taken Sept. 14th A.M.

B, " " " " P.M.

C, " " " " 15th A.M.

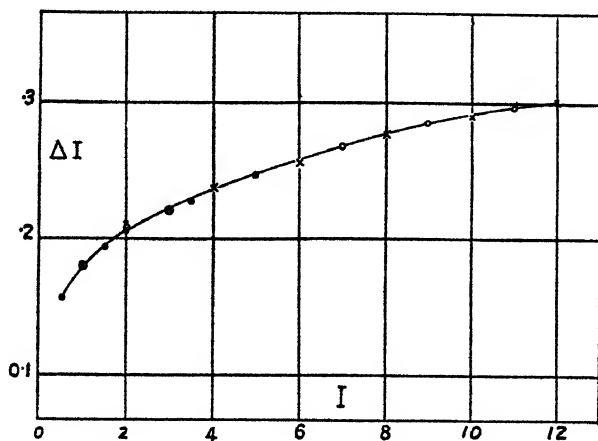
The experimental procedure was as follows:—After listening to the sound for 2 seconds, a small additional weight was lowered to the top of the tank by a lever so as to increase suddenly the intensity of the sound. By repeated trials a value of this weight was found which produced a just perceptible increment of intensity. In this manner a series of measurements was made, covering the selected range of intensities, which are given in Table I.

\* Love and Dawson, *Phys. Rev.* xiv. p. 49 (1919).

The values in this table are arranged in three groups, which were obtained, as indicated in the table, on three successive half-days. Several measurements of three intensities, it will be noticed, were found which agree extremely well.

In fig. 1, all the values of  $\Delta I$ , the just perceptible increments or differential thresholds, are plotted as ordinates with corresponding values of the intensity  $I$  as abscissæ. The points fall on a single curve which is unmistakably concave towards the horizontal axis. It is quite evident that these measurements do not even remotely conform to Weber's law, which states that the

Fig. 1.



Weber's Law. The ratio of  $\Delta I$  to  $I$  is not constant.

Group C in Table I. are denoted by solid circles.

„ B „ „ „ circles.

„ A „ „ „ 's.

ratio of  $\Delta I$  to  $I$  is a constant. For, if they did, the graph should be a straight line. The curved form of the graph suggested that possibly a logarithmic relation might exist between  $\Delta I$  and  $I$ , and consequently reciprocals of  $\Delta I$  and values of  $\log I$  were plotted in fig. 2 as ordinates and abscissæ respectively.

The resulting graph is evidently composed of two linear parts, the one to the left indicated, however, by only two points which represent the lowest intensities. The remaining points lie very close to the same straight line, though those marked with an  $\times$ , which represent group A of the measurements in Table I., may form a slightly

different straight line. The graph is represented by the equation

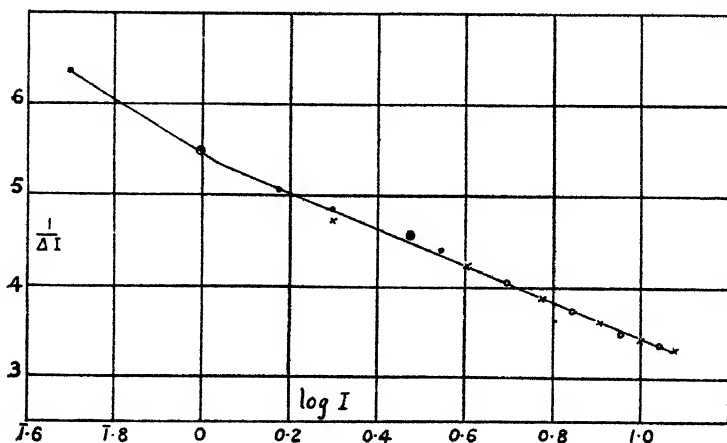
$$\frac{1}{\Delta I} = -k^2 \log I + C,$$

or, in analogy with Weber's law,

$$\frac{\frac{1}{\Delta I}}{\log I} = C_1,$$

where  $k^2$ ,  $C$ , and  $C_1$  are constants whose numerical values differ for the two parts of the graph.

Fig 2.



Weber's Law. The ratio of  $\frac{1}{\Delta I}$  to  $\log I$  is constant in each part of the graph.

Group C in Table I. are denoted by solid circles.

„ B „ „ „ circles.

„ A „ „ „ 'x'.

As some doubt was entertained whether it was justifiable to use the weights on the tank as measures of the intensity of the sound, it was decided to re-examine the relationship of the two intensities with another tonvariator of higher pitch and a greater range of intensities.

Since with different blowing pressures both the intensity and the frequency of the sound alter, it was necessary before using the instrument to calibrate both variables as functions of the blowing pressure. The two operations were carried out simultaneously by using a Rayleigh disk,

a device which has so frequently been employed that no description of it is necessary here.

The disk having been set approximately in resonance with another tonvariator at the frequency of 575 D.V. by adjusting the length of the resonance tube in which the disk was suspended, the room was vacated by the observer, who made further adjustments of the tonvariator from the adjoining room by a rod passing through a hole in the wall. In the observer's room was also placed the pressure tank, from which air was delivered to the tonvariator through a rubber tube. A definite blowing pressure was obtained by placing weights on the top of the tank, and the frequency of the tonvariator altered until the deflexion of the disk was a maximum. The tonvariator was then in exact resonance with the disk, the deflexion of which was a measure of the intensity  $I$  of the sound. The deflexion was read in centimetres by a telescope, and in no case was it greater than  $10^\circ$ .

The following procedure was adopted in making a series of measurements. A definite weight having been placed on the pressure tank, the tonvariator was adjusted to give the proper frequency, after which the sound was stopped to allow the restoration of the ear to its normal sensitivity. The observer then placed his head against a rest in order to keep it always in the same position for an observation, and, after allowing the tonvariator to sound for approximately 2 seconds, lowered by a cord a small weight to the top of the tank and listened for an increase in the intensity of the sound. Observing a rest period of 5 minutes between successive trials, the small weight was altered in magnitude until a value was found that caused a just perceptible increase in the intensity of the sound. The small weight was then taken as a measure of the magnitude of the differential threshold  $\Delta I$ . The data obtained in this manner are given in Table II. and are shown graphically in fig. 3.

It will be noticed in the table that the values of the intensity  $I$ , given by deflexions of the Rayleigh disk, are not proportional to the weights in the first column. The graph for the calibration of the intensities of the sound in centimetres of deflexion when they are plotted against the weights on the tank is therefore not a straight but a curved line. In the measurements of increments, however, the additional weights placed on the pressure tank are used

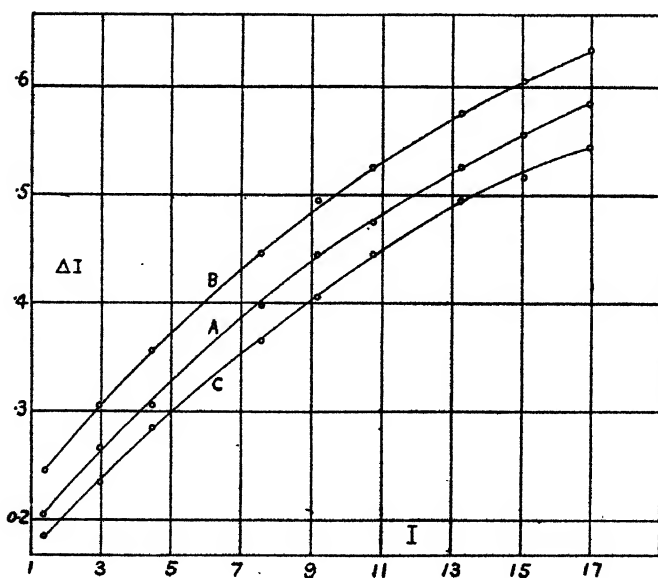


TABLE II.

Weber's Law in Audition, for different States of Aural Adaptation. Frequency 575 D.V.

W. Kilo-grams.	I. Cm.	Log I.	Normal, A.		Depression, B.		Enhancement, C.	
			$\Delta I$ .	$\frac{1}{\Delta I}$ .	$\Delta I$ .	$\frac{1}{\Delta I}$ .	$\Delta I$ .	$\frac{1}{\Delta I}$ .
			Kilo-gram.		Kilo-gram.		Kilo-gram.	
4	1.4	0.146	0.205	4.878	0.245	4.082	0.185	5.405
6	3.0	0.477	0.265	3.774	0.305	3.279	0.235	4.255
8	4.5	0.653	0.305	3.279	0.355	2.817	0.285	3.509
12	7.6	0.881	0.395	2.532	0.445	2.247	0.365	2.740
14	9.2	0.964	0.445	2.247	0.495	2.020	0.405	2.469
16	10.8	1.033	0.475	2.105	0.525	1.905	0.445	2.247
20	13.3	1.124	0.525	1.905	0.575	1.739	0.495	2.020
24	15.1	1.179	0.555	1.802	0.605	1.653	0.515	1.942
28	17.0	1.230	0.585	1.709	0.635	1.575	0.545	1.835

Fig. 8.



Weber's Law. The ratio of  $\Delta I$  to  $I$  is not constant.

Graph A is for normal sensitivity of the ear.

„ B „ depressed „ „

„ C „ enhanced „ „

as values of  $\Delta I$ , and their reciprocals are also employed for the ordinates of the graphs in both figures. This procedure does not involve any error either in the graphs themselves or in the law deduced from them, for we found that portions of the calibration curve may without appreciable error be taken as straight lines through an amount representing as much as one or even 2 kilograms. The additional weights necessary to obtain just perceptible increments of intensity varied from 0.185 to 0.635 kilogram, and are well inside the limits within which the calibration curve may be regarded as linear. Indeed, by this method increased precision of measurement is secured, for the additional deflexions of the disk by the increased weights would be only from about 0.16 to 0.3 cm., quantities so small that errors of observation would be relatively large, whereas the additional weights vary from 185 to 635 grams, in measuring which no error is involved.

In fig. 3 the values of  $\Delta I$  and  $I$  are plotted as ordinates and abscissæ respectively, as in fig. 1, to see whether the linear relation expressed by Weber's law exists between them. This graph also clearly shows that the law is not true for the sense of hearing. On plotting in fig. 4 the reciprocals of the three sets of measurements of  $\Delta I$  against the values of  $\log I$ , as in fig. 2, we obtain three graphs of unquestionably linear form, each of which consists of two parts represented by the above equations with appropriate values of the constants.

The three converging graphs represent the same number of different states of sensitivity or adaptation of the right ear of the observer, of which A is for normal, B for depressed, and C for enhanced sensitivity. The conditions under which they were obtained are described by one of the writers in the following paper in this number\*.

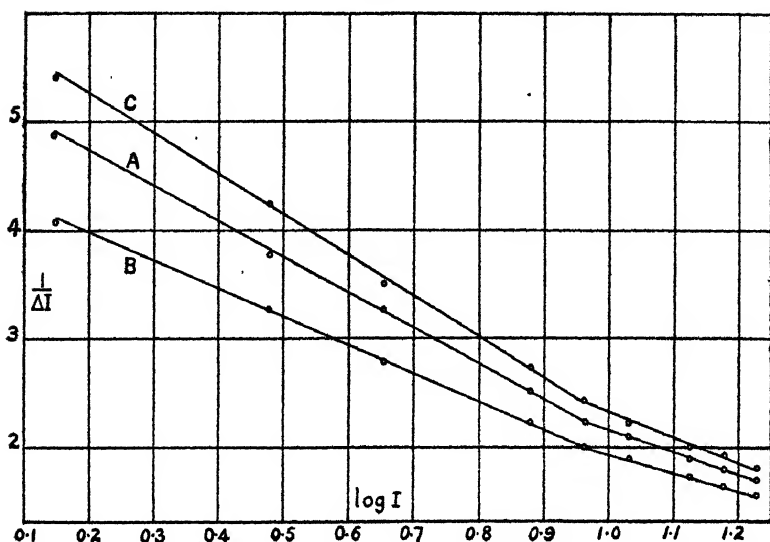
From this figure it is evident, in addition, that the new form of Weber's law for the sense of hearing applies not only to the normal state of sensitivity of the aural receptors, but to the two conditions of adaptation, depression and enhancement as well.

Owing to the importance of Weber's law and its numerous applications, arrangements are now being made

\* John F. Allen, "The Depression and Enhancement of Auditory Sensitivity," p. 834, *infra*.

to continue the investigation with experimental arrangements that will afford a much greater range of intensities, both high and low, than has been possible with the torvariators.

Fig. 4.



Weber's Law. The ratio of  $\frac{1}{\Delta I}$  to  $\log I$  is constant in each part.

Graph A is for normal sensitivity of the ear.

„ B „ depressed „ „

„ C „ enhanced „ „

LXXVI. *The Depression and Enhancement of Auditory Sensitivity.* By JOHN F. ALLEN, B.A., *Research Assistant in Physics, University of Manitoba, Winnipeg* \*.

THE investigations conducted by Prof. Frank Allen and his associates on the senses of vision †, touch ‡, taste §, temperature and pain ||, the contraction of muscles ¶,

\* Communicated by Prof. Frank Allen.

† Allen, *Journ. Op. Soc. Am.* vii. pp. 583, 913 (1923); *ibid.* ix. p. 375 (1924); *ibid.* xiii. p. 383 (1926).

‡ Allen and Hollenberg, *Quart. Journ. Exper. Physiol.* xiv. p. 351 (1924). Allen and Weinberg, *ibid.* xv. p. 377 (1925).

§ Allen and Weinberg, *ibid.* p. 385 (1925).

|| Allen and Macdonald, *ibid.* xvi. p. 321 (1927).

¶ Allen and O'Donoghue, *ibid.* xviii. p. 199 (1927).

and the secretion of glands \* have uniformly shown that depression and enhancement of sensitivity or response of the organs are produced as two of the results of stimulation, the amount and character varying with the intensity of the stimulus and the conditions under which it is applied. Very weak stimulation of  $\alpha$  intensity, as it has been termed, depresses the sensitivity of the retina, while more intense stimulation of  $\beta$ ,  $\gamma$ , etc. intensities enhances it. In the sense of taste the actions of weak and strong gustatory stimuli are similar to those in vision. In the sense of touch, and probably in that of hearing, the reverse is true, since weak tactile stimuli enhance and strong depress the sensitivity. All these induced effects, which are variously due to motor, secretory, or sensory reflex action, occur with both ipsilateral and contralateral stimulation. It has also been discovered that when the sensitivity of receptors, muscles, and glands has been disturbed by stimulation, their normal condition is restored by a series of neural oscillations of depression and enhancement—that is, of the corresponding physiological processes of inhibition and facilitation, during which the response is diminished or augmented respectively, according to the phase of the oscillation which is predominant when subsequent stimulation occurs.

In studying auditory responses by the method of the critical frequency of pulsation or flutter of tones, Miss Weinberg and Allen † did not obtain enhanced sensitivity of the receptors, though depression was found to occur. At that time the oscillatory character of the recovery of normal sensitivity had not been recognised, and consequently they were not aware of the very simple method of obtaining the anticipated enhancement which is employed in the present investigation.

This new method was developed by Macdonald and the writer ‡ for the purpose of testing the validity of Weber's law in the auditory sense, and is analogous to the method employed by them for a similar purpose in vision §.

The source of sound was a Stern tonvariator blown by air from a constant-pressure tank. The tonvariator was

\* Allen, *ibid.* xix. pp. 337, 363 (1929).

† Phil. Mag. (6) xlvii. pp. 50, 126, 141, and 941 (1924).

‡ Macdonald and J. F. Allen, "The Psychophysical Law.—II. Audition," Phil. Mag. ix. p. 827 (1930).

§ Macdonald and J. F. Allen, "The Psychophysical Law.—I. Vision," Phil. Mag. ix. p. 817 (1930).

always adjusted to give a pure tone of frequency 575 D.V., the intensity of which was measured by the deflexions of a Rayleigh disk. The tonvariator and disk were conveniently placed in a room by themselves, and the pressure tank and observer were in a room adjoining. Through a hole in the brick wall the sound came to the observer, while by means of a telescope the scale of the disk apparatus was read, and the tonvariator maintained in adjustment by a long rod.

In order to obtain depression and enhancement of sensitivity of the auditory receptors, a second tonvariator was placed in the same room with the observer. This was adjusted to the same frequency, 575 D.V., as the tonvariator with which the measurements were made.

### *The Normal Graph.*

The first measurements made were for the purpose of obtaining a graph for the normal sensitivity of the ear which should form the standard with which other graphs for different conditions of sensitivity could be compared. The method of obtaining the normal graph was described in the paper by Macdonald and Allen to which reference has been made. Briefly, it consists of a series of measurements for the whole range of intensities within the capacity of the tonvariator, each of which represents the increment of sound which, when added to the intensity of the tone previously emitted by the tonvariator, is just perceptible. The measurements of the series of just perceptible normal increments, or differential thresholds, are given in Table I., and are plotted as graph A in fig. 1, with values of the logarithms of the intensity as abscissæ and reciprocals of increments as ordinates. The graph consists of two linear parts with an abrupt change of slope, each of which conforms to the equation :

$$\frac{1}{\Delta I} = -k^2 \log I + C,$$

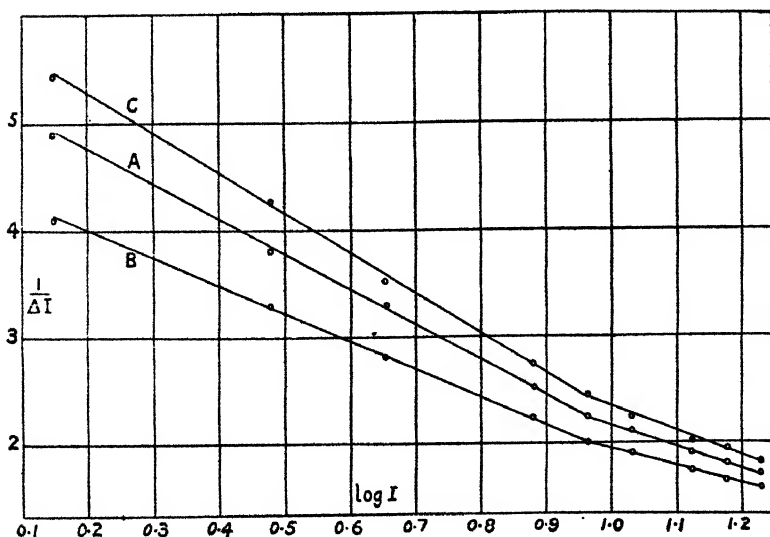
where  $I$  is the intensity of the tone, or the deflexion in centimetres of the Rayleigh disk which is proportional to it;  $\Delta I$  is the just perceptible increment of intensity, or the additional weight in kilograms placed upon the tank to give the increased intensity; and  $k^2$  and  $C$  are constants. The negative sign indicates the direction of the slope.

TABLE I.

Enhancement and Depression of Auditory Sensitivity.  
Ipsilateral Stimulation. Frequency 575 D.V.

W.	I.	Log I.	Normal, A.		Depression, B.		Enhancement, C.	
			$\Delta I.$	$\frac{1}{\Delta I}.$	$\Delta I.$	$\frac{1}{\Delta I}.$	$\Delta I.$	$\frac{1}{\Delta I}.$
Kilo-grams.	Cm.		Kilo-gram.		Kilo-gram.		Kilo-gram.	
4	1.4	0.146	0.205	4.878	0.245	4.082	0.185	5.405
6	3.0	0.477	0.265	3.774	0.305	3.279	0.235	4.255
8	4.5	0.653	0.305	3.279	0.355	2.817	0.285	3.509
12	7.6	0.881	0.395	2.532	0.445	2.247	0.365	2.740
14	9.2	0.964	0.445	2.247	0.495	2.020	0.405	2.469
16	10.8	1.033	0.475	2.105	0.525	1.905	0.445	2.247
20	13.3	1.124	0.525	1.905	0.575	1.739	0.495	2.020
24	15.1	1.179	0.555	1.802	0.605	1.653	0.515	1.942
82	17.0	1.230	0.585	1.709	0.635	1.575	0.545	1.835

Fig. 1.



Enhancement and depression of auditory sensitivity with  
ipsilateral stimulation.

A, normal sensitivity; B, depressed sensitivity; C, enhanced sensitivity.

It will be noticed in the tables, as remarked in a former paper on Weber's law to which reference has been made, that the values of the intensity  $I$ , given by deflexions of the Rayleigh disk, are not proportional to the weights in the first column. The graph for the calibration of the intensities of the sound in centimetres of deflexion when they are plotted against the weights on the tank is therefore not a straight but a curved line. In the measurements of increments of intensity, however, the additional weights placed on the pressure tank are used as values of  $\Delta I$ , and their reciprocals are also employed for the ordinates of the graphs in both figures. This procedure does not involve any error either in the graphs themselves or in the law deduced from them, for we found that portions of the calibration curve may without appreciable error be taken as straight lines through an amount representing as much as 1 or even 2 kilograms. The additional weights necessary to obtain just perceptible increments of intensity varied from 0.185 to 0.635 kilogram, and are well inside the limits within which the calibration curve may be regarded as linear. Indeed, by this method increased precision of measurement is secured, for the additional deflexions of the disk by the increased weights would be only from about 0.16 to 0.3 cm., quantities so small that errors of observation would be relatively large, whereas the additional weights vary from 185 to 635 grams, in measuring which no error is introduced.

#### *The Effect of Ipsilateral Stimulation.*

In order to study the effect of ipsilateral stimulation, the second tonvariator mentioned above was placed close to the right ear of the observer and tuned to exactly the same pitch as that of the measuring tonvariator. The intensity of the sound emitted by the stimulating tonvariator was not determined, but it was probably fifteen or twenty times as great as that of the measuring instrument.

The experimental procedure was as follows :—First, the head was placed in the head-rest and the stimulating tonvariator sounded for 1 minute. It was then silenced and an increment reading taken immediately with the measuring tonvariator. It was found that a greater increment of sound-intensity than that which was formerly sufficient had to be added before it was distinguishable.

After resting for 10 minutes, without additional stimulation, another reading was taken, when it was found that a smaller increment than the normal amount could be distinguished. A sufficient time was then allowed for the ear to recover its normal state of sensitivity, when the readings were repeated with a higher intensity.

The complete series of measurements are given in Table I., and are plotted with the normal graph in fig. 1. Graph A represents the measurements of just perceptible increments when the ear is in its normal condition of sensitivity; B represents similar measurements when the ear is depressed in sensitivity; and C the corresponding measurements when the aural sensitivity is enhanced. Each graph consists of two linear parts, which are represented by the equation given above with appropriate changes in the values of the constants.

These measurements show that immediately following somewhat intense stimulation the auditory receptors are depressed in sensitivity. The enhancing neural process then gradually rises in influence, by means of which the receptors recover their normal sensitivity. The process does not then cease, but continues its action until the sensitivity becomes much enhanced. The inhibitory process then in turn rises to predominance, during which the receptors become depressed in sensitivity. In illustration of this oscillatory character of the neural reactions, it was found that, starting with normal equilibrium, the receptor sensitivity immediately after stimulation was depressed; in 7 minutes a normal reading was obtained, which indicated the restoration of the normal state; in 10 minutes the reading showed enhancement of sensitivity as indicated in fig. 1; finally, in 15 minutes, a normal measurement was again obtained. No further readings were taken to discover whether the oscillatory process subsided at this time or again depressed the sensitivity.

It is thus clear that in the auditory sense, as in other sensory, motor, and secretory processes, equilibrium is restored by a series of neural oscillations of a pendular type with a definite amplitude and periodic time, by means of which the receptor sensitivity becomes alternately depressed and enhanced. Possibly this behaviour of the nervous system may throw some light on the physiological nature of the processes of inhibition and facilitation which are still involved in deep obscurity.



*The Effect of Contralateral Stimulation.*

Having obtained depression and enhancement of sensitivity by stimulating the right ear, contralateral effects were sought by placing the stimulation tonvariator, with the same frequency and intensity as before, close to the left ear while the right was temporarily protected by a heavy pad of wool and metal. The left ear was then stimulated for the same time, 1 minute, as before, after which the right ear was uncovered and an increment reading taken with it. This measurement showed depres-

TABLE II.

Enhancement and Depression of Auditory Sensitivity.  
Contralateral Stimulation. Frequency 575 D.V.

W.	I.	Log I.	Normal, A.		Depression, B.		Enhancement, C.	
			$\Delta I.$	$\frac{1}{\Delta I}.$	$\Delta I.$	$\frac{1}{\Delta I}.$	$\Delta I.$	$\frac{1}{\Delta I}.$
Kilo-grams.	Cm.		Kilo-gram.		Kilo-gram.		Kilo-gram.	
4	1.4	0.146	0.205	4.878	0.225	4.444	0.195	5.128
6	3.0	0.477	0.265	3.774	0.285	3.509	0.245	4.082
8	4.5	0.653	0.305	3.279	0.335	2.985	0.295	3.390
12	7.6	0.881	0.395	2.532	0.425	2.353	0.375	2.667
14	9.2	0.964	0.445	2.247	0.475	2.105	0.425	2.353
16	10.8	1.033	0.475	2.105	0.505	1.980	0.455	2.198
20	13.3	1.124	0.525	1.905	0.545	1.835	0.505	1.980
24	15.1	1.179	0.555	1.802	0.585	1.709	0.535	1.869
28	17.0	1.230	0.585	1.709	0.615	1.626	0.565	1.770

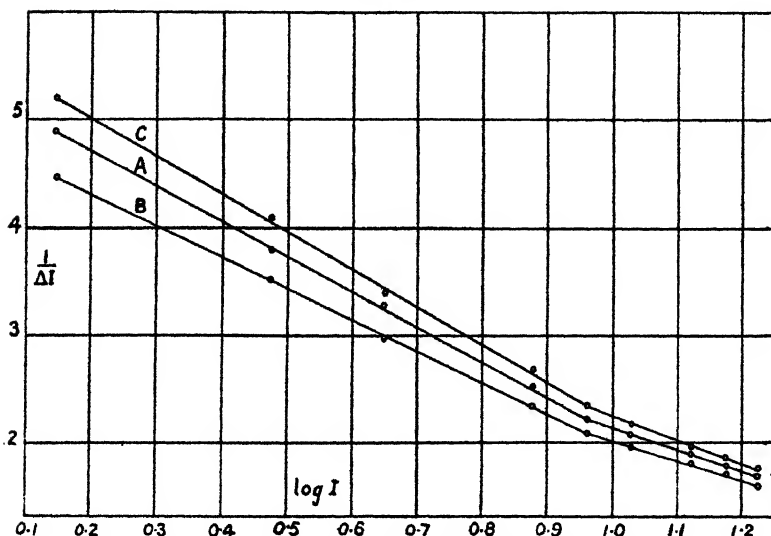
sion of sensitivity as before, but not in so marked a degree. After resting for 10 minutes a second reading was taken which showed enhancement of sensitivity, but also to a less extent than before. The measurements were similarly continued throughout the complete range of intensities. The results are plotted in fig. 2, from the data in Table II. in comparison with the same normal as before. In this figure A is the normal graph, B the graph for contralateral depression of sensitivity, and C that for contralateral enhancement. In both figures the depression graphs are below the normal and the enhancement above, since the reciprocals of increments are plotted as ordinates. The

contralateral effects are similar to the ipsilateral, except in magnitude. The linear parts of the graphs conform to the same equations as before, with suitable changes in the values of the constants.

Both groups of graphs in figs. 1 and 2 may also be represented by the equation :

$$\frac{1}{\log I} = C,$$

Fig. 2.



Enhancement and depression of auditory sensitivity with contralateral stimulation.

A, normal sensitivity ; B, depressed sensitivity ; C, enhanced sensitivity.

which has been found by Macdonald and the writer \* to denote the relationship between the just perceptible increment of intensity of a sound and the intensity, instead of Weber's law, which does not hold in the sense of hearing. The new law is thus verified in normal, depressed, and enhanced states of aural sensitivity under both ipsilateral and contralateral conditions of stimulation.

The marked convergence of both groups of graphs towards the greater values of the intensities, indicates that with high degrees of stimulation there will be no

\* "The Psychophysical Law.—II. Audition," *Phil. Mag.* ix. p. 327 (1930).

distinction between the normal, depressed, and enhanced states, since all will become merged into one.

From these investigations it is clear that the auditory sense is subject to the same conditions and exhibits the same neural characteristics as the other senses, the muscles, and the glands. It is evident also that the afferent and efferent nerves of both ears are interconnected in the auditory centres of the cortex, where the same processes of inhibition and facilitation are elicited as, for example, in the senses of vision and taste. Possibly by their means, phenomena of binaural contrast may occur analogous to those in vision and taste. It may also be the case that contralateral influences may be involved in the process of locating the direction of sound.

It is quite probable, by analogy with the sense of touch, that enhancement of sensitivity instead of depression may first be evoked by very weak stimulation of the ear, and the oscillations thus be reversed in phase. It did not occur to the writer to test this supposition at the time the apparatus was available, and its study must be left for subsequent investigation.

I desire to express my thanks to Professor Frank Allen and Mr. P. A. Macdonald, M.Sc., for many suggestions in regard to these investigations ; and also to the National Research Council of Canada for the grant by which I was enabled to act as Research Assistant to Professor Allen for the year.

---

LXXVII. *Concerning Electrical and other Dimensions.* By  
W. N. BOND, M.A., D.Sc., F.Inst.P., Lecturer in Physics  
in the University of Reading \*.

#### SUMMARY.

COMMON misconceptions concerning dimensions, which are specially noticeable where electrical and magnetic quantities are concerned, are discussed. The meaning of fractional indices in dimensional formulæ is considered, and a law is suggested for the frequency-distribution of the indices.

\* Communicated by the Author.

I. *Certain Misconceptions.*

THE first part of this paper is an attempt to point out certain common misconceptions, which are chiefly noticeable when the dimensions of electrical and magnetic quantities are discussed. I believe my treatment is in essential agreement with work of Maxwell, J. J. Thomson, and P. W. Bridgman, but to a lesser extent with writings of J. H. Jeans, R. T. Birge, G. W. C. Kaye and T. H. Laby, W. Watson, and others.

The difficulties may be indicated by a few quotations. Thus, Kaye and Laby state\* “ $v$ , the ratio of the electromagnetic to the electrostatic unit of quantity . . . is a pure number.” But J. J. Thomson† and A. Gray‡ state the ratio of the units,  $v$ , in “cm. per second.”

Again, W. Watson states § :

$$[K^{-\frac{1}{2}}\mu^{-\frac{1}{2}}] = [LT^{-1}],$$

but later says “indicating this velocity of  $v$ , we have

$$[\mu^{-\frac{1}{2}}K^{-\frac{1}{2}}]/[LT^{-1}] = v.”$$

(This is typical of statements in many text-books.)

Further, I may quote R. T. Birge || :—“These difficulties are connected with the unknown dimensions of magnetic permeability  $\mu$ , and specific inductive capacity  $\epsilon$ . . . . In the present paper we are concerned only with numerical magnitudes and no particular attention has accordingly been paid to this matter of dimensions. . . . In a number of the equations given in Table c, the two sides of the equation do not check dimensionally unless one assumes  $\mu$  and  $\epsilon$  to be dimensionless.”

These difficulties disappear if we follow Maxwell, J. J. Thomson, and P. W. Bridgman. Thus Maxwell states ¶ :—“The only systems of any scientific value are the electrostatic and the electromagnetic systems. . . .

$$[e] = [L^{\frac{3}{2}}M^{\frac{1}{2}}T^{-1}]$$

in the electrostatic system.”

Again, J. J. Thomson writes \*\*:—“On the electrostatic system of units  $K$  is of no dimensions . . . .”

\* ‘Phys. and Chem. Constants,’ 4th ed. p. 7 (1921).

† ‘Elements of Elec. and Mag.’ 4th ed. p. 479 (1909).

‡ ‘Abs. Measurements in Elec. and Mag.’ 2nd ed. p. 688 (1921).

§ ‘Text-Book of Physics,’ 7th ed. p. 788 (1920).

|| Phys. Rev., Suppl., i. no. 1, p. 66 (July 1929).

¶ ‘Elec. and Mag.’ 3rd ed. ii. p. 266 (1892).

\*\* Loc. cit. p. 466.

On the ordinary electrostatic system the dielectric constant of a vacuum is by definition unity; a dielectric constant is measured as a ratio of two forces (or of two charges) expressed in the same units and is of no dimensions, just as are angles in radians and refractive indices. A similar argument applies to the electromagnetic system. The dimensions of charge, etc., as measured in the two systems will differ, and the ratio of the units will have the same dimensions as a velocity.

Objections to the above procedure must be on the grounds either that it is inexpedient or that it is incorrect. As regards expediency, we have the statement of Maxwell quoted above, and Bridgman's opinion, given in his 'Dimensional Analysis,' that no useful purpose has been served by retention of the symbols  $[k]$  and  $[\mu]$ . We may also note that in the cases of angles and refractive indices no independent arbitrary units are preserved and used, and very little use has been found for the corresponding special dimensional symbols. Finally, we quoted above certain difficulties and contradictions resulting from the partial or inaccurate uses of other systems of units and dimensions.

People who object to the above type of procedure as being incorrect seem to forget that the dimensions of a quantity (that is measured in derived units) are but an abbreviated statement of how the derived unit was defined, telling us how the magnitude of the derived unit will be changed when we change the size of the arbitrary primary units, but make no other changes. The dimensions are the result of our method of definition and not a unique property of the thing we desire to measure\*.

Thus, Jeans † objects that if we defined the unit of mass by the gravitational equation

$$m \cdot f = m \cdot m' / r^2,$$

mass must not be said to have the dimensions  $[L^3T^{-2}]$ , as:—

"we know that mass is something entirely apart from length and time, except in so far as it is connected with them through the law of gravitation."

But the statement  $[M] = [L^3T^{-2}]$  does not tell us how mass is related to length and time, but how our proposed unit of mass will be affected by changes in the sizes of our length and time units.

I will try to explain this by other examples. In place of

\* N. E. Dorsey, *Int. Crit. Tables*, i. pp. 18-19.

† 'Elec. and Mag.' 2nd ed. par. 18 (1911).

defining unit force in the usual way, it appears to me to be just as legitimate (though less convenient) to define it by the "gravitational attraction." We should then have

$$P = m \cdot m' / r^2, \quad P = m \cdot f / G, \quad \text{and} \quad [P] = [L^{-2}M^2].$$

We cannot deduce that force is or is not "entirely apart from" time.

It may be difficult to realize that (in terms of  $[M]$ ,  $[L]$ ,  $[T]$ ), it is only as the result of *definitions* that volume has the dimensions  $[L^3]$ , velocity  $[LT^{-1}]$ , etc., so I will discuss the problem a little further. Whenever we measure a quantity in terms of units of a different kind, we make use of properties of Nature. Even the use of "cubic centimetres" implies the possibility of making cubes defined by the cm. length unit; and before we can measure a volume as the product of three lengths, we must assume that eight equal cubes can be fitted together to form one cube having double the length of side. (Presumably this can only be done exactly where there is no gravitational field\*.) Similarly, we could use properties of Nature and measure lengths in "light-seconds," and the unit of volume could be taken as the space enclosed by the "spherical" wave-front of light that had travelled in a vacuum from a point source for one second. Following the usual practice of omitting to state the details of the method of definition when we write down the dimensions, the measurements would now be said to be in "sec." and "sec.<sup>3</sup>" respectively of dimensions  $[T]$  and  $[T^3]$ . If we desire to retain as primary units the cm., gm., and sec., there is no necessity to use "light-seconds"; but for the derived unit of volume, that defined by the light wave would be a legitimate alternative to the "cubic centimetre."

Again, after the manner of measuring angles as the ratio of lengths, velocities could be measured as fractions of that of light in a vacuum. The actual measurements would result in the ratio of two times or lengths, and velocity would have no dimensions in terms of  $[M]$ ,  $[L]$ , and  $[T]$ .

I cannot, therefore, agree with Watson's statement (*loc. cit.*) that "the dimensions of any physical quantity must be independent of the particular system of units adopted"; the dimensions of permeability which Birge (*loc. cit.*) terms "unknown" seem merely arbitrary; and the dimensions of charge (as given in my quotation from Maxwell) seem no more "apparent" (Jeans, *loc. cit.*, paragraph 588) than are the dimensions usually given for area, volume, force, etc.

\* Eddington, 'Report on Relativity Theory of Gravitation,' p. 28.

II. *Fractional Indices in Dimensional Formulæ.*

Secondly, let us consider the fractional indices in the dimensional formulæ. Were an arbitrary unit of volume used, and the length unit derived from it,  $[V]^{\frac{1}{3}}$  would be used in place of  $[L]$ , and  $\frac{1}{3}$ ,  $\frac{2}{3}$ , etc., would appear as indices. Thus indices  $\frac{1}{2}$ ,  $\frac{2}{3}$  are not specially peculiar and merely correspond to our "measuring" electrical and magnetic quantities by the mechanical results of their interaction in pairs.

The likelihood of fractional indices occurring may be indicated by the following discussion (which may also have other uses). If no derived units were used, all the indices would be unity. When a small arbitrary number of arbitrary primary units replace the multiplicity of independent units, zero index is of little importance, only indicating that certain arbitrary units were not used in the particular measurement. Apart from the question of convenience,  $[L]^3$  and  $[V]$ ,  $[L]$  and  $[V]^{\frac{1}{3}}$ ,  $[L]/[T]$  and  $[T]/[L]$ ,  $[M][L]^3$  and  $[L]^3/[M]$  are equally likely. Thus a single index in a dimensional formula is equally likely to fall in any one of the ranges ( $-\infty$  to  $-1$ ), ( $-1$  to  $0$ ), ( $0$  to  $1$ ), and ( $1$  to  $\infty$ ). But only fairly simple integers or fractions are to be expected, as the number of separate measurements used together is generally small.

The Table below indicates the frequency with which the various indices occur in our ordinary measurements:—

Magnitude of index in dimensional formula.

4  $3\frac{1}{2}$  3  $2\frac{1}{2}$  2  $1\frac{1}{2}$  1  $\frac{1}{2}$  0  $-\frac{1}{2}$  -1  $-1\frac{1}{2}$  -2  $-2\frac{1}{2}$  -3  $-3\frac{1}{2}$  -4 -6

Number of occurrences in 443 cases taken at random.

1	0	11	1	36	9	128	49	—	35	93	4	46	0	25	0	4	1		
				122				113				81½				126½			

I find that the frequency-distribution of the squares of the indices is very similar to that found for "non-dimensional constants" (*e.g.*  $4\pi/3$ )\*. This is illustrated in the following Table, derived from the previous Table:—

Range of value of (index)<sup>2</sup>.

(0 to ½) (½ to 1) (1 to 2) (2 to 4) (4 to 8) (8 to 16) (16 to 32) (32 to ∞)

Number found.

84	110½	110½	54	42	38½	2½	1
----	------	------	----	----	-----	----	---

\* Bond, *Phil. Mag.* vii. pp. 719-721 (April 1929).

Number according to suggested distribution law.

110.7	110.7	110.7	55.4	27.7	13.8	6.9	6.9
-------	-------	-------	------	------	------	-----	-----

Fractional number according to suggested distribution law.

$\frac{1}{4}$	$\frac{1}{4}$	$\frac{1}{4}$	$\frac{1}{8}$	$\frac{1}{16}$	$\frac{1}{32}$	$\frac{1}{64}$	$\frac{1}{64}$
---------------	---------------	---------------	---------------	----------------	----------------	----------------	----------------

Department of Physics,  
University of Reading.  
December 18, 1929.

# LXXVIII. The Soft X-rays of Manganese.

By F. C. CHALKLIN, *Ph.D.*, *University of Sheffield* \*.

EXPERIMENTS making use of the photo-electric method have shown that for each of the elements iron, cobalt, nickel, and copper there exists, in the soft X-ray region, a considerable number of critical potentials. To account for these Professor O. W. Richardson and the writer have suggested a scheme involving the assumption that the critical potentials are due to transitions from a number of initial levels to a Rydberg series of virtual levels†. The scheme works well for iron and fairly well for cobalt and nickel, but for copper there is a large number of discontinuities for which the scheme does not account. It is clearly of interest to examine the elements which are near to iron, cobalt, nickel, and copper in the periodic table, and to ascertain whether or not the suggested scheme accounts for the critical potentials obtained.

In the present series of experiments the critical potentials of manganese have been determined by two distinct variations of the photo-electric method. The first of these methods depended on a simultaneous comparison of the photo-electric current produced by the manganese radiations with that produced by the radiations from an anticathode of which the critical potentials were known (*e. g.*, carbon).

Fig. 1 shows the soft X-ray tube used for this purpose. The tube was constructed of transparent silica in order to facilitate the de-gassing process, and the seals were made

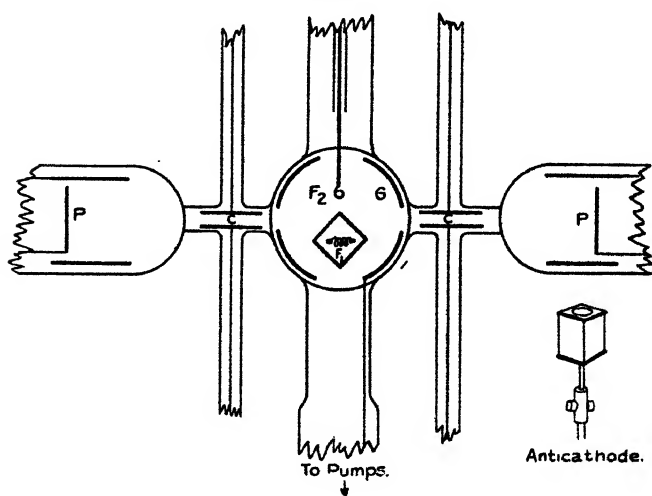
\* Communicated by Prof. O. W. Richardson, F.R.S.

† Proc. Roy. Soc. A, cxix. p. 64 (1928); A, cxxi. p. 218 (1928).



with red sealing-wax. The electrodes were, with the exceptions mentioned below, all constructed of molybdenum \*, in order to avoid as far as possible the danger of metal evaporating during the bake-out and condensing on the anticathode. The framework of the anticathode allowed four targets to be slid into position, thus surrounding a tungsten filament  $F_1$ †, from which an electronic stream could bombard the targets and de-gas them with little fear of the outer faces becoming sputtered. The targets were approximately 1.5 cm. wide and 2 cm. in height. The whole anticathode was mounted on an iron swivel, but was separated from it by a molybdenum rod, so

Fig. 1.



that the iron portions should not reach the high temperatures attained by the anticathode during bombardment. During these experiments a carbon target was exposed to one photo-electric cell, and the manganese target faced the other cell. Suitable potentials were applied to the condenser plates C and to the cylinder G to prevent ions and electrons from reaching the photo-electric plates P. A single tungsten filament  $F_2$  supplied both targets with an electron stream. A Gaede three-stage mercury vapour

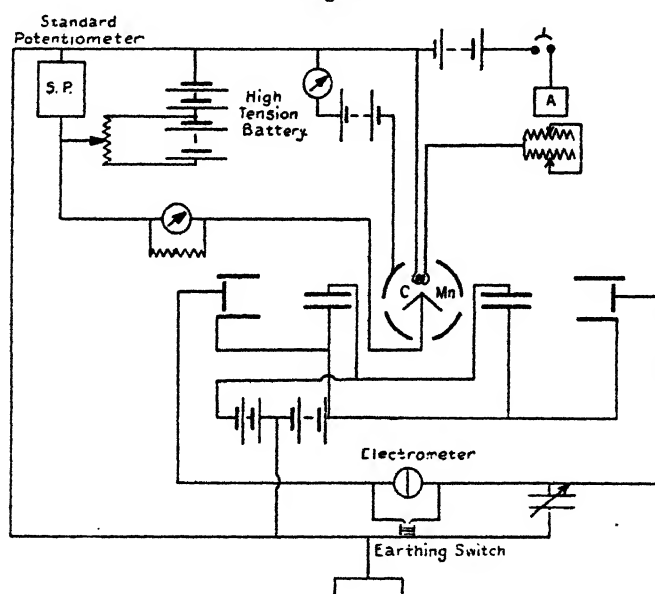
\* Very kindly supplied by Metropolitan Vickers Electrical Co., Ltd., Manchester.

† For the tungsten wire used the writer is indebted to the General Electric Co., Ltd., Wembley.

pump was used to evacuate the apparatus, and, although a narrowing was necessary at a stopcock and at two liquid air traps, 3.5 cm. tubing was used where possible in order to facilitate the pumping.

Fig. 2 shows the electrical connexions in use during the experiment. Suppose the total thermionic current from filament to anticathode to be  $I_t$ . A fraction of it,  $Ai_t$ , goes to the carbon target and a fraction,  $Bi_t$ , goes to the manganese target. The photo-electric current due to each target may be taken as approximately proportional

Fig. 2.



to the electronic current bombarding that target. Again, it is well known that the photo-electric current is approximately proportional to the bombarding voltage  $V$ . Hence the photo-electric currents due to carbon and manganese are respectively  $VMAi_t$  and  $VNBi_t$ , where  $M$  and  $N$  are constants representing the efficiency of each target in producing photo-electrons under the given conditions of geometry of tube and photo-electric plate. The ratio of the two photo-electric currents will be

$$\frac{i_{p2}}{i_{p1}} = \frac{NB}{MA} \quad \dots \dots \dots (1)$$

A and B are unlikely to vary very greatly with voltage (and certainly they should not vary discontinuously), so the ratio should remain constant as we vary the potential on the tube. However, at a critical potential of manganese,  $i_{p_2}$  will begin to differ from  $VNB_i$ , and will only be represented by that expression again at some higher voltage. Hence, if the ratio were plotted against the voltage, it would be expected that the curve would in general be parallel to the voltage axis; it would begin to leave this straight line at a critical potential; the difference would increase to a maximum and the curve would then tend to return to the original course. The magnitude of the difference should be proportional to the thermionic current.

The two photo-electric plates were connected to opposite pairs of quadrants of a Dolezalek electrometer. One of these two insulated systems was made of variable capacity by placing, in parallel with it, a variable condenser. The variable condenser could then be adjusted until the electrometer did not charge up. When this is the case,

$$\frac{i_{p_1}}{C_1} = \frac{i_{p_2}}{C_2}, \quad \frac{i_{p_2}}{i_{p_1}} = \frac{NB}{MA} = \frac{C_2}{C_1} \dots \dots (2)$$

Since, in this experiment, we were only concerned with the critical potentials, it was not necessary to make an absolute determination of the ratio  $\frac{i_{p_2}}{i_{p_1}}$  by the measurement of the capacities,  $C_1$  and  $C_2$ . After the variable condenser had been adjusted until the rate of charging up was very slow, the voltage was varied, and for each value of the voltage the rate of charging of the electrometer was observed. Discontinuities were found in the curves obtained by plotting rate of charging against voltage. This procedure avoided the calibration of the variable condenser and the troublesome business of adjusting the condenser for each voltage. Fig. 3 shows examples of the curves obtained.

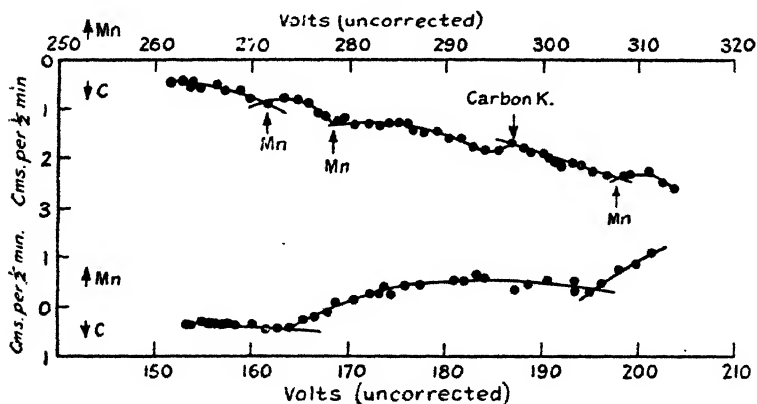
The method has the following advantages:—

- (1) It is a null method, and allows the thermionic current to be raised to a high value. This affords greater sensitiveness in the determination of the deviations from the initial value of  $\frac{i_{p_2}}{i_{p_1}}$ , and hence allows the critical potentials to be observed the more readily.

(2) As anticipated from the analysis, the deviations from the balance position are never very great, and therefore it is possible to take long curves without resetting the condenser.

(3) Equation 2 shows that the balance-point is unaffected by changes in thermionic current. (This is probably only true for small changes of  $i_t$ , for large changes would probably cause changes in A & B.) The deviations from the balance-point (measured by the deflexions of the electrometer) should be proportional to the thermionic current, but since these deviations are small it is unnecessary to correct them for the slow gradual changes in  $i_t$ . Thermionic current-readings were, however, taken from time to time during the curves.

Fig. 3.



(4) We are left with only two instruments to read—the electrometer, and the standard potentiometer with which the voltage was measured.

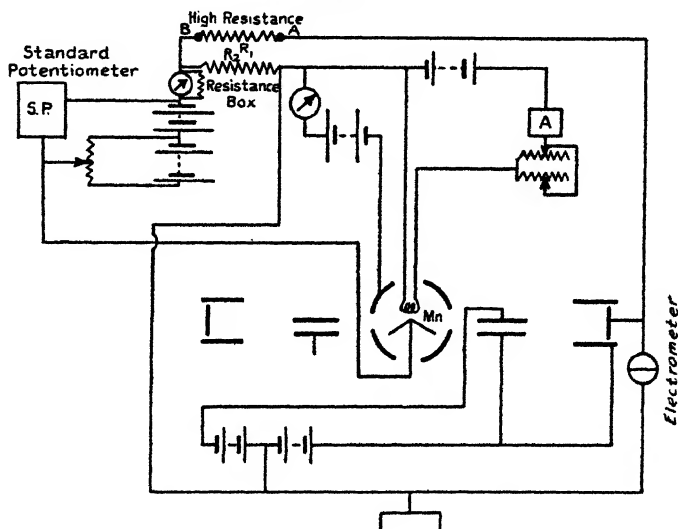
(5) This method was primarily designed to look for and measure the difference between the critical potentials of an element and its compounds. In this case one target would be made of the element and the other of the compound, the critical potentials of each could be obtained on the same curve, and small differences of voltage between the discontinuities could be measured with greater accuracy than if the two targets were examined separately.

The method has a number of disadvantages. It is necessary to know the critical potentials of one of the targets. Carbon was used as the standard target in this

experiment, as one would only expect to get the K discontinuity occurring in the range under examination, and this had been verified by a number of experimenters, who had determined the voltage of the discontinuity. During the course of our experiments, however, a letter from Richardson and Andrewes to 'Nature' announced the discovery of a large number of discontinuities whose position depended on the crystalline state of the carbon.

It is difficult, from the curves obtained by this method, to distinguish between manganese discontinuities and carbon discontinuities. For this reason manganese was subsequently examined by a steady deflexion method which

Fig. 4.



did not involve the use of a carbon target. The steady deflexion experiments indicate that, with the exception of carbon K, practically all the discontinuities obtained by the first method can be obtained from the manganese face of the anticathode. (The exceptions are 132, 248.5, 309.2, and 339.2. The first of these was, however, obtained for Mn by Andrewes, Davies, and Horton.)

The first method also involves, in an aggravated form, the difficulties encountered in using a timing method with an electrometer. If the method is to be sensitive a heavy charge must be allowed to collect on the pairs of quadrants, and leakages are therefore accentuated.

Fig. 4 shows the electrical connexions of the second

method.  $R_1$  is a high resistance constructed by depositing lampblack on a silica rod.  $R_2$  is a resistance-box. The tube used for the first method was again employed, but we now only made use of the photo-electric cell exposed to the manganese radiation. The photo-electric current from this cell flowed through  $R_1$ , so that in the steady state the p.d. between A and B would be  $i_{p_2} \cdot R_1$ . The thermionic current flows through  $R_2$ , and therefore the potential of A (measured by the electrometer) with respect to earth is  $i_{p_2} \cdot R_1 - i_t \cdot R_2$ . If this is adjusted to zero by means of the resistance-box  $R_2$ , we have,  $VNB i_t \cdot R_1 = i_t \cdot R_2$ .

As in the first method the balance-point is independent of the thermionic current. Again it was not considered convenient to adjust  $R_2$  for zero electrometer deflexion at each voltage, and, instead, the value of  $R_2$  was kept fixed during the taking of a set of readings, and the reading of the electrometer taken. This gave a measure of the quantity  $i_t \cdot R_1 \cdot B \Delta(VN)$ , where  $\Delta(VN)$  is the change in VN from its value at the balance-point. Readings of  $i_t$  were taken, but it was not deemed necessary to divide the electrometer readings, but to leave  $i_t$  in the expression as a constant unless the readings of it showed it to vary in such a way as to cause a discontinuity in the electrometer reading—voltage curves. It was deemed wise to abandon such discontinuities. Fig. 5 shows some of the curves obtained by this method.

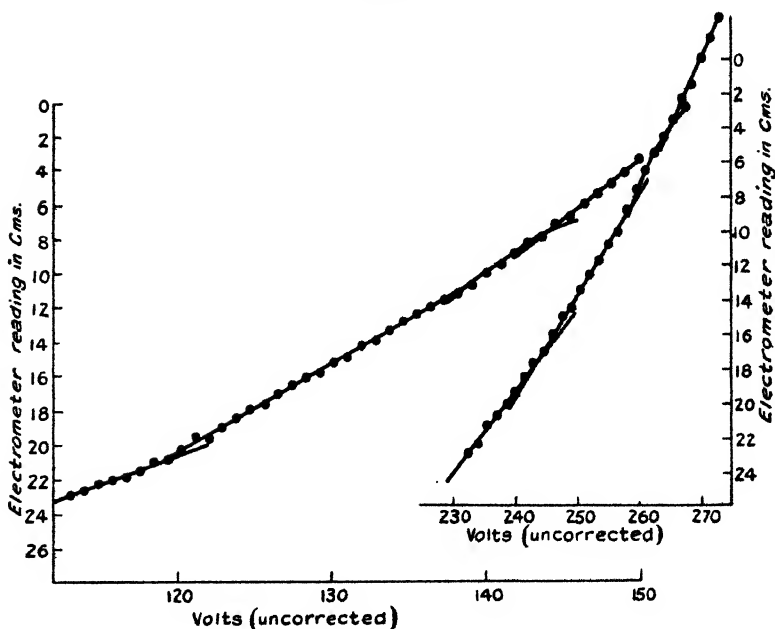
The results obtained by the two methods are shown in Table I. It was feared that the positions of the discontinuities obtained by the second method might be affected by the time-lag in the high resistance. Some curves were taken with increasing voltage and some with decreasing, and it was thought that it might be preferable to take a mean of the average value of a discontinuity on curves of ascending voltage and of the average on descending voltage. For no critical potential, however, did this value differ by more than half a volt from the mean of all the values for the critical potential. We have therefore adhered to the usual method of taking the mean.

Do series similar to those found \* for iron, nickel, cobalt, and copper also apply to the results obtained for manganese? For each of these four elements four critical potential series were found of the form  $A - b/n^2$ , the four series having different values of A, but the same value of b.

\* Richardson and Chalklin, Proc. Roy. Soc. A, cxxi. p. 233 (1928).

It was therefore concluded that for each of the elements there were four initial levels which we called  $X_0$ ,  $X_1$ ,  $X_2$ , and  $X_3$ , from which transitions took place to the same series of final levels represented by  $b/n^2$ . Whether or not the  $X$  levels are to be identified with the  $M$  levels is at present uncertain. For each of these elements critical potentials occur which appear to be due to transitions from the  $L_{II, III}$  level to  $X$  levels, and, making use of the combination principle, the  $L_{II, III}$  level was calculated. A Moseley diagram of the  $L_{II, III}$  level thus obtained for these elements

Fig. 5.



gives a straight line. An extrapolation gives the  $L_{II, III}$  level of  $Mn$  to be approximately 740 volts. Thoraëus has found the X-ray emission lines  $L_{\alpha_{1, 2}}$  and  $L_{\beta_1}$  for  $Mn$  to occur at  $19.39 \text{ \AA}$  and  $19.04 \text{ \AA}$  respectively. These values are equivalent to 637 and 648 electron volts. For the four elements mentioned the voltages corresponding to these lines were roughly equal to  $L_{II, III} - X_3$ . If this identification is made for manganese we find  $X_3 = 740 - 640$  (approx.) = 100 volts (approx.). It thus appears that the  $X_3$  level is in roughly the same position as for iron, cobalt, nickel, and copper, and that an  $X_3 \rightarrow b/n^2$  series will be

outside the range of our present experiments, which did not go below 110 volts.

A knowledge of the wave-lengths of the  $L_1$  and  $L_2$  lines would, in a similar way, enable a prediction of the  $X_1$  level, but, unfortunately, the writer has been unable to discover any measurements of these lines.

TABLE I.

Method 1.	Method 2.	Weighted mean.	Andrewes, Davies, and Horton †.
Volts.	Volts.	Volts.	Volts.
—	—	—	49
—	—	—	73
—	—	—	88
—	—	—	105
—	—	—	113
122.1	121.0	121.7	117
132.0	—	132.0	134
—	141.3	141.3	—
145.4	146.8	145.9	—
—	159.8	159.8	157
166.6	168.4	167.9	—
181.9	181.1	181.2	179
193.7	194.5	194.2	189
201.0*	200.4	200.5	—
—	211.5	211.5	—
—	218.2	218.2	—
224.9*	224.4	224.6?	—
239.0	241.3?	239.7	—
248.5	—	248.5	—
259.9	259.7	259.8	—
—	265.6	265.6?	—
273.6	273.7	273.6	—
284.4	285.3*	284.5	—
297.9(carbon K?)	298.8	298.8	—
309.2	—	309.2?	—
315.9*	315.1	315.4	—
—	323.4	323.4?	—
—	332.2	332.2?	—
339.2	—	339.2?	—
362.2*	361.8	361.9	—
368.1*	367.8	367.9	—
379.4	378.1	378.7	—
400.8	403.2	401.5	—
412.0*	411.9*	412.0	—

\* Only obtained on one occasion.

† Proc. Roy. Soc. A, cxvii. p. 649 (1928).

Two series given in Tables II. and III. have, however, been obtained, and appear to be the  $X_1$  and  $X_0$  series. They employ the value 2357 for " $b$ ," as did also the series



of cobalt and nickel (copper also had roughly the same value of  $b$ ).

The suggested series appears to give only a fair representation of the experimental results. In giving the observed value 146.8 we have neglected the results obtained for this discontinuity by Method I., in which the effect at 141.3 volts was not resolved, and in which, therefore, an effect at 146.8 might be expected to be obtained too low. Even so, the discrepancy between the observed value 146.8 obtained by Method 2 and the predicted value 149.0 is rather large. Again, the experimental values 173.8 and 179.4, which have been taken to correspond to the series values for  $n=10$  and  $n=11$ , were only obtained once, and do not therefore appear in our listed values in Table I.\*

TABLE II.

$X_1=197.3$ volts.		
$n$ .	$X_1 - \frac{b}{n^2}$ .	Observed.
4 .....	50 volts.	49 volts (A, D, and H).
5 .....	103 "	105 " (A, D, and H).
6 .....	131.8 "	132.0 " (value from Method 2).
7 .....	149.0 "	146.8 " (value from Method 2).
8 .....	160.5 "	159.8 "
9 .....	168.2 "	167.9 "
10 .....	173.7 "	173.8 " (only observed once).
11 .....	177.8 "	179.4 " (only observed once).
12 .....	180.9 "	181.2 "

(The two A, D, and H values used were beyond the range of the present experiments.)

On the other hand, it would be reasonable to expect that for such large values of  $n$  the critical potentials would be weak. The readiness with which the 181.1 break was obtained in Method 2 was probably due to its being made up of more than one unresolved effect.

The suggested series has, however, a number of virtues. There has been no necessity to change the constant  $b$  from the value used for the series of Co, Ni, and Cu. Secondly, the series accounts for all the discontinuities which we have obtained in this region except those at 141.3 and 121.9 volts, and of these the 141.3 break is accounted for below.

There appears to be evidence in favour of another series with the same value of  $b$  and with a limit approximately

\* Andrewes, Davies, and Horton have a critical potential at 179 volts.

the same as that of the  $X_0$  series for iron. This is shown in Table III.

This series seems to be quite satisfactory apart from the value for  $n=8$ , in which the observed critical potential is 3 volts from the predicted value. Again, the series has accounted, with some completeness, for the critical potentials found in the region concerned, and it will be noticed that, with the exception of the 121.7 effect and three breaks between 200 and 220 volts, the two series together account for all the critical potentials obtained by the writer below 280 volts.

The critical potential series scheme does not in its present form account for the discontinuities found for manganese above 280 volts, and for iron, cobalt, nickel, and

TABLE III.

$X_0=283.3$ volts.			
$n$ .	$X_0 - \frac{b}{n^2}$ .	Observed.	
4 .....	141.1 volts.	141.3	volts.
5 .....	194.0	194.2	"
6 .....	224.8	224.6 ?	"
7 .....	240.2	239.7	"
8 .....	251.5	248.5	"
9 .....	259.2	259.8	"
10 .....	264.7	265.6 ?	"
11 .....	268.7	—	"
12 .....	271.8		"
13 .....	274.3	273.6	"

copper there were unpredicted effects in this region. It is therefore clear that, if it is to be comprehensive, the series scheme will require extension. The data at present available do not, however, justify such an extension.

In conclusion, the writer wishes to express his gratitude to Professor O. W. Richardson for his advice and interest in the experiments; to Professor S. R. Milner, in whose department this work has been carried out, for his interest and encouragement; and he is indebted to his wife (L. P. Davies), who has rendered very valuable assistance in the carrying out of the experiments.

Thanks are due to the Government Grant Committee of the Royal Society for a grant by means of which apparatus was purchased.

LXXIX. *The Effective Temperature of a Warmed Room.*

By A. F. DUTTON, M.A., D.I.C.\*

[Plate XI.]

1. **E**XPERIENCE shows that when the walls of a room are cold a higher air-temperature is required for comfort than when the walls are warm. In a comfortably warmed room a sedentary man loses by radiation and convection some 17·5 B.Th.U. per square foot of effective surface per hour, and if normal clothing be worn, the average temperature of the surface from which this heat is lost to the room is about 75° F. Under such conditions, as has been pointed out by Dr. Hill, of the National Institute for Medical Research, changes in the humidity are immaterial so far as heat losses are concerned †.

Pending a more precise physiological standard of thermal comfort, a provisional standard has been based upon this rate of loss of heat, according to which a room is postulated to be comfortably warmed where a sizable black body at 75° F. loses heat at the rate of 17·5 B.Th.U. per sq. ft. per hour ‡.

The temperature of an environment with air and walls at different degrees is not easily specified. From the point of view of comfort it is the rate at which heat is lost from the body which is important. The effective temperature of an environment may therefore be defined as that temperature of a uniform enclosure in which, in still air, a sizable black body at 75° F. would lose heat at the same rate as in the environment.

2. An instrument has been constructed to record the effective temperature in a room. A thermostatic device tends to maintain at 75° F. the surface of the instrument, a black-painted hollow copper cylinder. The cylinder, which sits on a 28 in. wooden stool, is 22 in. high and 7½ in. in diameter, a replica of that used as an automaton § for regulating the heating of a room. It is heated electrically and the power supplied, which is controlled by the thermostat, is recorded. The power record is scaled to give the

\* Communicated by the Author.

† Medical Research Committee, Special Report, no. 32, p. 100.

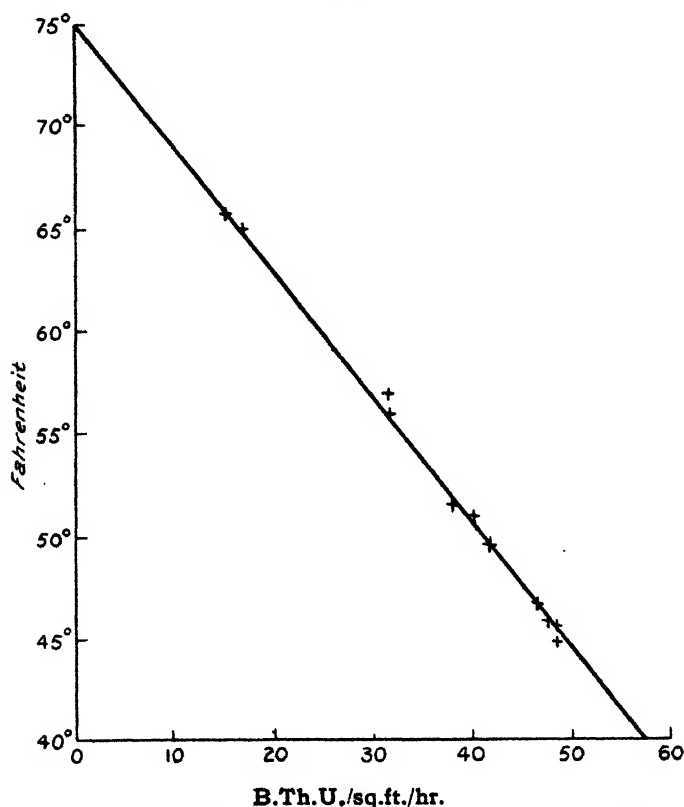
‡ Journal of Scientific Instruments, vi. p. 249 (1929).

§ "The Eupatheostat," Journal of Scientific Instruments, *loc. cit.*

rate at which the cylinder loses heat or, more conveniently, in degrees of effective temperature.

The scale of effective temperature was determined experimentally by recording the heat loss in still air in a room with air and walls at the same temperature. Corresponding values are plotted in fig. 1. An effective temperature of  $64.3^{\circ}\text{F.}$  corresponds with a heat loss of 17.5

Fig. 1.



Relation between effective temperature and the heat loss from a body at  $75^{\circ}\text{F.}$

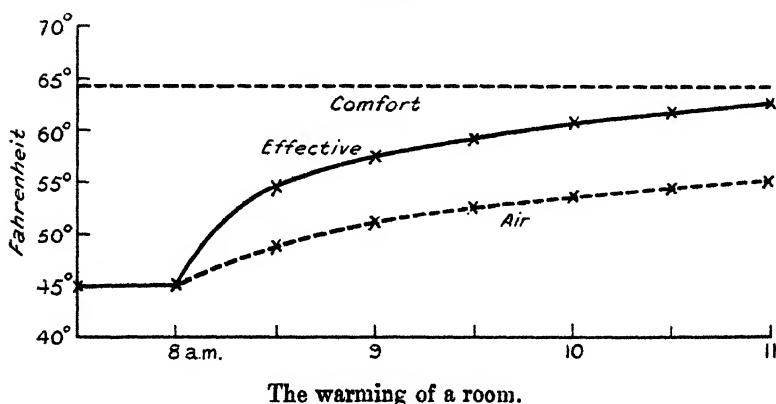
B.Th.U. per sq. ft. per hour, the provisional standard of thermal comfort.

The instrument, which it is proposed to call the Eupatheoscope, in contradistinction to the Eupatheostat, is required for the investigation of the influence of the fabric of the walls upon the rate of warming of a room.

3. Some rooms are not readily warmed and it has been demonstrated theoretically \* that, with double the rate of heating which serves to maintain warmth, the time taken to warm the surface of a 9-inch brick wall is six hours, while for a 1-inch wall of wood affording the same insulation the time is ten minutes.

Fig. 2 is a record of the warming of a small furnished room with walls of 9-inch brick plastered internally. It shows not only the slow rise of the temperature of the air but also that, even in the radiant heat 8 ft. from a gas fire burning 0.2 therm per hour, a comfortable warmth was not attained in three hours.

Fig. 2.



4. For measuring the effective temperature of a room a special kata-thermometer has also been devised. To ensure that the surface is at the same temperature as the thermometric liquid, the bulb is made of copper with a very thin lining of glass (0.4 mm.) and the thermometer is filled with mercury. The thermometer is allowed to cool from  $75\frac{1}{2}^{\circ}$  F. to  $74\frac{1}{2}^{\circ}$  F.—in a comfortably warmed room this takes one minute—and the stop-watch used for timing is graduated in degrees of effective temperature (Pl. XI.). The thermometer is readily warmed with the hands.

The kata-thermometer was compared with a eupatheoscope in the same environment. Corresponding readings are shown in the Table (p. 861).

\* Phil. Mag. iv. p. 888 (1927).

It was anticipated that some allowance would have to be made for the excessive convection loss of the thermometer, due to its small dimensions. To enable this to be effected the cooling in the same environment of a similar thermometer with a silvered bulb was observed. The experiments

Air Temperature.	Effective Temperature.	
	Eupatheoscope.	Kata-thermometer.
46° F.	46.1° F.	45.7° F.
50	50.0	50.2
53	56.6	57.1
58	53.9	63.7
61	65.8	65.6
62	67.0	66.5
65	65.0	65.2

showed, however, that the auxiliary thermometer affords no advantage and that the cooling of the black thermometer gives a sufficiently accurate measure of the effective temperature.

### LXXX. *Notices respecting New Books.*

*A Comprehensive Treatment on Inorganic and Theoretical Chemistry.*  
By J. W. MELLOR, D.Sc. Vol. IX. As, Sb, Bi, V, Cb, Ta.  
[Pp. xiv + 967.] (London: Longmans, Green & Co., Ltd., 1929. Price 63s. net.)

THE ninth of the thirteen volumes which will comprise Dr. Mellor's 'Comprehensive Treatise' is devoted to the ter-valent and quinquivalent elements, arsenic, antimony, bismuth, vanadium, columbium, and tantalum. It follows the same general lines as the preceding volumes. For each element an account is given of its history, occurrence, methods of extraction, physical and chemical properties, its uses, its atomic weight, and valency. Then follow sections devoted to the various compounds of the element. An important feature of the work is the comprehensive list of references to original sources; an examination of these indicates that the literature up to and including the year 1927 has been incorporated in the present volume.

The elements dealt with in this volume have several features of interest, as poisons, as possessing allotropic modifications, as forming colloidal solutions, and as constituents of metallic alloys. These properties are all fully dealt with.

The volume, along with the other volumes of the series, will be found invaluable for reference purposes, not only by chemists, but also by physicists and other scientific workers.

*Elementary Applications of Statistical Method.* By H. BANISTER, B.Sc., Ph.D. [Pp. vi+58.] (London: Blackie & Son, Ltd., 1929. Price 3s. 6d. net.)

THOSE who have to deal with statistical data and who possess no training in mathematics or statistics will find this small volume a suitable introduction to statistical methods. For such persons it can be followed with advantage by Fisher's 'Statistical Methods for Research Workers.' Such subjects as the tabulation of data, frequency distribution, goodness of fit, measures of dispersion, the significance of the mean and of the difference between the means of two samples and correlation, are dealt with in a very brief and elementary manner, and illustrated by simple examples. Probability tables and tables of goodness of fit are given in Appendices in a graphical form. Four figure tables of logarithms and anti-logarithms are also included; these might well have been omitted, being probably accessible in one form or another to all who will use this book.

*The Elementary Differential Geometry of Plane Curves.* By R. H. FOWLER, M.A., F.R.S. (Cambridge Tracts in Mathematics and Mathematical Physics, No. 20.) [Second Edition. Pp. ix+105.] (Cambridge: at the University Press, 1929. Price 6s. net.)

THE value of this work lies in the fact that a connected account of the elementary differential properties and geometry of plane curves was not previously available in the English language. The author does not claim that the matter is in any sense new nor that the treatment is novel. The treatment is, however, rigorous and connected, and the tract will be welcomed by those who do not possess Goursat's 'Cours d'Analyse' or some similar work.

The first edition appeared in 1920. The second edition is unaltered except for the correction of various mistakes. The author states in the preface to this edition that "I have not been in any way concerned with this subject since this tract was first published." It is to be regretted that Prof. E. H. Neville's revised theory of envelopes has not been incorporated, though the nature and scope of this is clearly explained in the preface. To have incorporated this would have necessitated a somewhat extensive revision of the work, for which presumably the author could not find time. On the principle that half a loaf is better than no bread, we must be thankful that the publishers have not permitted the tract to go out of print, and that this well-written account of the differential geometry of plane curves is still obtainable.

LXXXI. *Proceedings of Learned Societies.*

## GEOLOGICAL SOCIETY.

[Continued from p. 672.]

December 4th, 1929.—Prof. J. W. Gregory, L.L.D., D.Sc.,  
F.R.S., President, in the Chair.

THE following communication was read:—

‘Foliation in its Relation to Folding in the Mona Complex at Rhoscolyn (Anglesey).’ By Edward Greenly, D.Sc., V.P.G.S.

Further studies on the major anticline of Rhoscolyn have thrown much light on successive stages of the metamorphism.

The major, minor, and minimum foldings (with their thrustings) have each given rise to a foliation; that produced by the major folding being, on the nearly horizontal core of the great anticline, conspicuously transverse to the bedding of the massive grits of the South Stack Series. Yet it is thrown into isoclines by the minor folding, which is therefore subsequent to it. Where the cross-foliation of the major folding has been isoclinally folded, the foliation of the minimum folding runs right up to it at any angle without being itself folded in the least, whence it follows that the minimum is later than the minor structure. Thus the three foliations (major, minor, and minimum) developed in chronological order.

Thrusts often truncate the minor isoclines, and on decapitated anticlines where the beds are steep the beds above and below the thrust have been made to interdigitate. Sometimes this is carried so far as to drive long wedges of thin grits in between the laminae of the major cross-foliation. In this manner the structures usually found at a thrust-plane have often been completely obliterated, even when the thrust is considerable.

The relations of major to minor folding furnish an explanation of the fact that the major cross-foliation, unlike a slaty cleavage, fails to traverse the pelitic beds. The foliation of the plutonic intrusions, and the tremolite-schists, are products of the major movements.

In ‘The Geology of Anglesey’ the principal metamorphism was ascribed to the major and subsequent movements. Re-examination has shown, on the contrary, that this metamorphism is independent of, and older than, all three. Its foliation is developed along innumerable thrusts, but these are at angles so acute to the bedding that, especially when thrown into rapid isoclines, they easily escape notice. This is the true explanation of ‘monoplastic schists.’

The view now abandoned was based upon the aureoles of the basic intrusions, but a fresh study has revealed that their evidence gives decisive confirmation of the view now adopted. They are frequently cut by thrusts of the major series, but are never affected by the principal metamorphism. There are several lines of evidence, perhaps the most striking being the fact that the thermal minerals of the aureoles crystallize across and obliterate the planes of the



principal metamorphism, which is, therefore, anterior to the intrusions and thus to the major folding.

This early foliation is really the regional metamorphism. But the thrusting to which it is due, unlike those of the three later series, can be referred to no visible folding. Accordingly, its disentanglement goes to confirm the hypothesis that recumbent folding exists, and is the dominant structure of the Mona Complex.

These studies, carried out only on a single tectonic horizon, greatly extend the chronology of the metamorphism of the Mona Complex.

December 18th, 1929.—Prof. J. W. Gregory, LL.D., D.Sc.,  
F.R.S., President, in the Chair.

The following communication was read :—

‘The Geology of the Shiant Isles’. By Frederick Walker, M.A.,  
Ph.D., D.Sc.

The Shiant Isles form a small uninhabited archipelago in the North Minch, some 5 miles east of the Park district of Lewis. The group is made up almost entirely of crinanite sills separated by relatively thin argillaceous strata which have undergone considerable contact-alteration, but the fossil content of which (ammonites, belemnites, and one species of *Inoceramus*) assigns them to a low position in the Upper Lias. The two largest islands are each over a mile in length, and are joined by a shingle-beach. Their principal feature is a crinanite sill at least 500 feet thick, with a picrite base. The transition between the crinanite and the picrite is gradual, and the ultrabasic rock is considered to have accumulated by the gravitational settling of olivine-crystals, this hypothesis being borne out by a series of chemical analyses, modes, and specific gravities. Numerous veins of teschenitic and syenitic composition pierce the picrite, and probably represent the expulsion of residual magma at various stages during crystallization.

A third large island lies about a mile to the east of the other two, and is also to a great extent made up of a single thick sill of crinanite. East of this island, however, the crinanite passes gradually into syenite, towards the centre of the sill, the thickness of the alkaline rock being at least 60 feet. The syenite carries abundant analcite and occasional nepheline, but otherwise resembles closely the rock of Gamhnach Mor in Mull. It is riddled by veins of still more alkaline material, and cut by horizontal sheets of olivine-basalt which are chilled against it. The alkaline centre of the sill is thought to have originated through auto-intrusion caused by pressure on the crystal-mesh of the crinanite. Similar syenitic bands occur in the crinanite of the smaller islands.

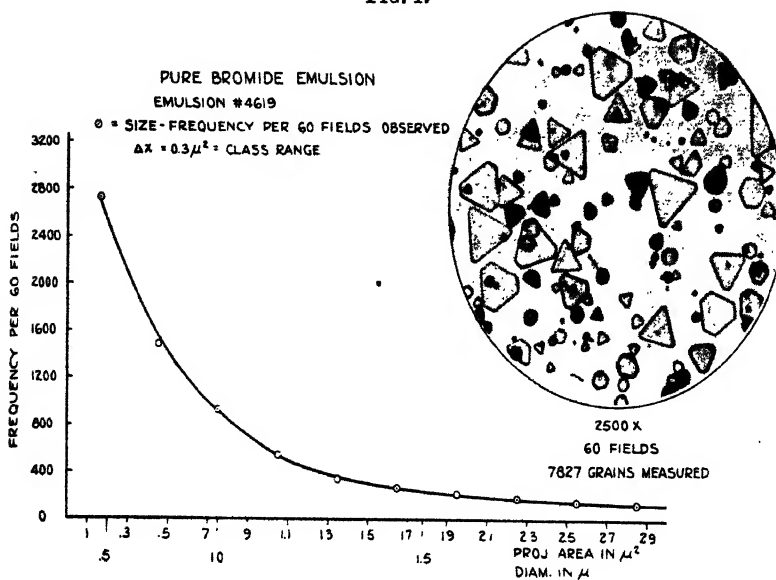
The age of the igneous activity is almost certainly Tertiary, and is probably the same as that of the Trotternish sills in Skye.

Although glacial striæ are not seen on the islands, their general aspect indicates a flow of ice from south to north during the Glacial Period.

---

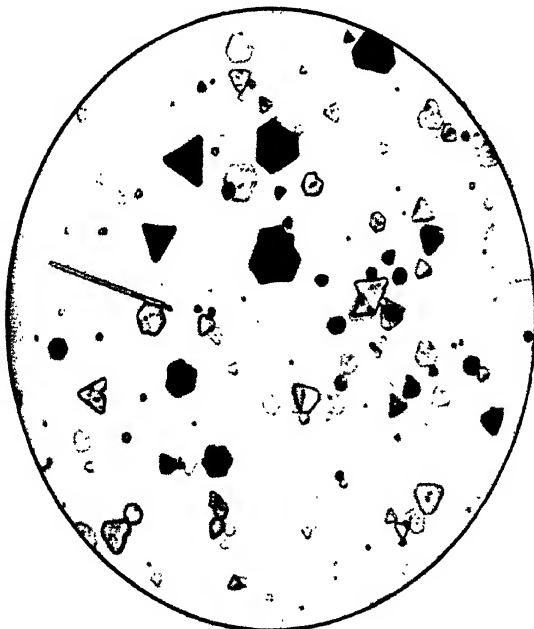
[The Editors do not hold themselves responsible for the  
views expressed by their correspondents.]

FIG. 1.



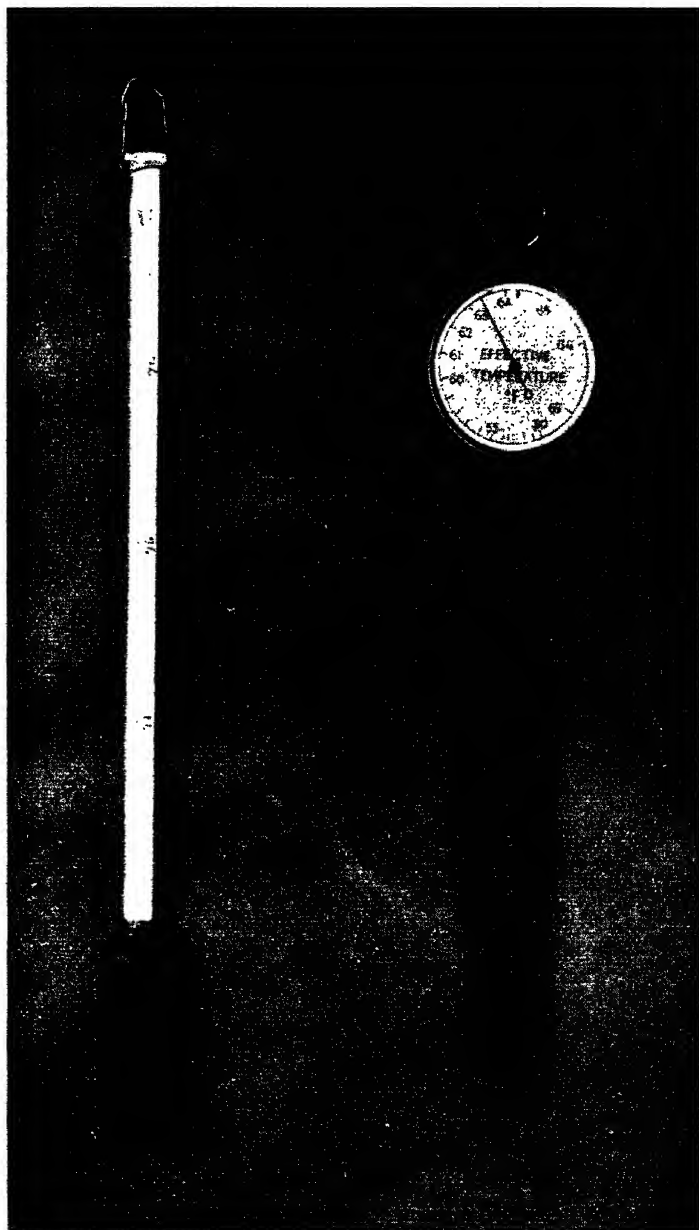
Size-frequency distribution of pure silver bromide.

FIG. 2.



X-ray exposure on pure silver bromide, developed with hydroquinone.





Effective Temperature Thermometer.



THE  
LONDON, EDINBURGH, AND DUBLIN  
PHILOSOPHICAL MAGAZINE  
AND  
JOURNAL OF SCIENCE.

[SEVENTH SERIES.]

MAY 1930.

LXXXII. *Dipoles in Relation to the Anomalous Properties of Dielectrics.* By S. WHITEHEAD, M.A., A.M.I.E.E.\*

PREFACE.

IN studying the properties of ebonite as a dielectric at various frequencies it has been observed that the losses at low stresses expressed as power factor are practically constant over a range of frequencies from power frequencies up to millions per second, but there is an anomaly in the neighbourhood of 1000 cycles, in which part of the range the power factor is decreased.

Several hypothetical explanations have been suggested and are under consideration. This report covers the application of the Dipole Theory of Debye to anomalous properties of dielectrics.

CONTENTS.

	Page
I. Introduction—The Dipole Theory .....	866
II. Anomalous Properties (including Secondary Field) .	868
III. Anomalous Effects (neglecting Secondary Field) ..	873
IV. Other Effects .....	875
V. Experimental Work .....	875
Appendix .....	876

\* Report Ref. L/T 34 received from the British Electrical and Allied Industries Research Association.

*Phil. Mag. S. 7. Vol. 9. No. 60. May 1930.*

3 L

## I. INTRODUCTION—THE DIPOLE THEORY.

THE dipole theory was first introduced by Debye in order to explain the large temperature coefficients of the specific inductive capacities of the alcohols. Previous theories, such as those of Faraday, Mossotti, and Lorentz, which involved the assumption either of conducting particles or of an actual displacement of charges within the molecule or atom, were unable to account for the large variation of this induced polarization with temperature which is observed in some cases. Debye adopted Langevin's theory of paramagnetism. He assumed that there are dipoles of fixed electric moment in the medium, just as there are molecular or atomic magnets in a paramagnetic medium. Normally these dipoles have a random distribution, so that the component of density of electric moment in any direction, *i. e.*, the polarization, cancels out, and there is no resultant field. When, however, an electric field is applied the dipoles tend to orientate themselves in the direction of the field according to Boltzmann's law, since they have a potential energy depending on orientation. They may indeed have a definite orientation under exceptional circumstances without an electric field, as, for example, if an "electret" is solidified in an electric field. The dipoles move more easily when liquid than when solid, so that they align themselves while liquid and are caught in that position when solid. On removal of the field the "electret" continues to have a polarization which may continue for some months.

Generally, however, the dipoles do not align until an electric field is applied. The proportion in any direction can then be calculated, assuming Boltzmann's law as above. To a first approximation (at not very high field strengths) this distribution is given by

$$f = A \left( 1 + \frac{\mu F}{kT} \cos \theta \right). \quad . \quad . \quad . \quad . \quad . \quad (1)$$

(See Appendix (a) (2)),

where

$f d\Omega$  = number of dipoles per c.c. pointing in direction indicated in solid angle  $d\Omega$ ,

$\mu$  = dipole moment,

$k$  = Boltzmann's constant,

$T$  = absolute temperature,

$\theta$  = angle of orientation of dipoles,

$F$  = field strength.

From this the polarization or electric moment per c.c.,  $P$ , can be calculated, since

$$P = 4\pi \int_0^\pi \mu f \cos \theta 2\pi \sin \theta d\theta, \quad . . . (2)$$

where  $N$  = number of dipoles per c.c.

Thus we obtain the expression

$$P = 4\pi\mu^2FN/3kT. \quad . . . (3)$$

$F$  is the total inducing field, that is, the external field together with that due to neighbouring molecules, so that, if  $\epsilon$  is the specific inductive capacity,

$$\frac{\epsilon - 1}{\epsilon + 2} = b + 4\pi\mu^2N/9kT. \quad . . . (4)$$

(See Appendix (a) (4)),

where  $b$  = polarization arising from other causes, *e.g.*, a separation of charges, as in Lorentz's theory, or surface charges at different layers.

The form of variation of  $\epsilon$  with temperature has been verified for a number of liquids and gases and some viscous materials. On the whole the theory has been satisfactorily verified qualitatively in those cases where dipoles might be expected. Quantitatively the theory is not so satisfactory, but the agreement is good in some instances. Certain refinements have been made to Debye's original theory, but no unquestioned improvement has resulted. The average values of the dipole moments work out of the order of  $10^{18}$  e.s.u.

In arriving at the above results it has been assumed that the dipoles are quite free to move, their directions being altered by collisions. In gases this is probably the case, but in liquids, and certainly in solids, retarding forces of a frictional nature will oppose the motion, and the movement of dipoles will result in heating, while they will not reach their most probable distribution for appreciable periods of time. Now this effect can be taken into account and brought in relation with the effective viscosity of the medium, and the following approximate equation is found for  $f$  :—

$$r \frac{\partial f}{\partial t} \frac{1}{\sin \theta} \frac{\partial}{\partial \theta} \left\{ \sin \theta \left( kT \frac{\partial f}{\partial \theta} + A\mu F \sin \theta \right) \right\} . \quad (5)$$

(See Appendix (b), equation (8)),



where

$\rho$  = frictional resistance coefficient =  $8\pi\eta a^3$  for a fluid,  
if  $\eta$  = viscosity,  $a$  = radius of molecule,

$t$  = time,

$A$  = constant depending on number of dipoles, etc.

From the presence of this frictional resistance arise :

- (1) A varying capacity current or absorption current.
- (2) An energy loss in the dielectric, that is a power loss and power factor.

## II. ANOMALOUS PROPERTIES (INCLUDING SECONDARY FIELD).

### (a) *Absorption Current.*

If  $F$  is constant, then one of the solutions of (5) is

$$f = A \left[ 1 + \frac{A\mu F \cos \theta}{kT} \left( 1 - e^{-\frac{2t kT}{\rho}} \right) \right]. \quad (6)$$

(See Appendix (c), equation (10).)

From (6) the polarization can be found from (2), whence, as in (4), the following equation is obtained :—

$$\frac{\epsilon - 1}{\epsilon + 2} = b + \frac{4\pi\mu^2 N}{9kT} \left( 1 - e^{-\frac{2t kT}{\rho}} \right), \quad (7)$$

and

$$2 + \epsilon = 3 \left[ 1 - b - a \left( 1 - e^{-\frac{2t kT}{\rho}} \right) \right], \quad (8)$$

where

$$a = \frac{4\pi\mu^2 N}{9kT}.$$

For a condenser of unit geometric capacity and unit thickness the capacity current is

$$i = F \frac{\partial \epsilon}{\partial t} \\ = F \frac{6kTa}{\rho} e^{-\frac{2t kT}{\rho}} \left\{ 1 - b - a \left( 1 - e^{-\frac{2t kT}{\rho}} \right) \right\}^2. \quad (9)$$

This gives an absorption current which decreases nearly

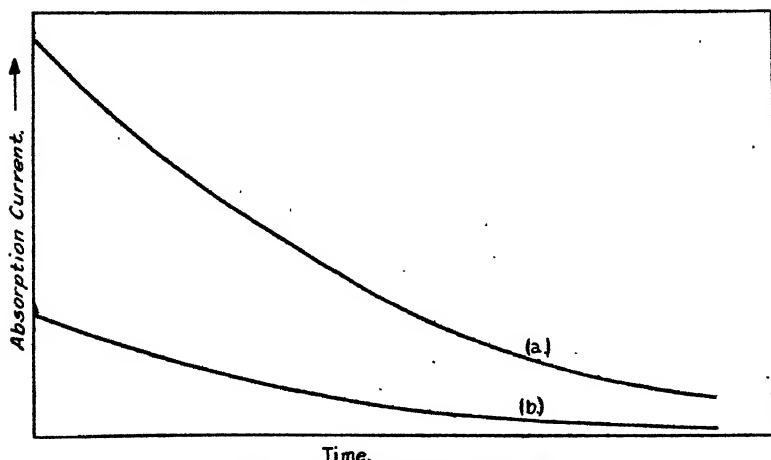
exponentially to zero with time, but not quite so rapidly (see fig. 1 (a)). The initial value is finite and given by

$$6FkTa/\rho(1-b)^2.$$

Returning to equation (6), it is seen that, after a field  $F_1$  has been applied for  $t_0$  seconds, the distribution  $f$  is given by

$$f = A \left[ 1 + \frac{\mu F_1 \cos \theta}{kT} \left( 1 - e^{-\frac{2t_0 kT}{\rho}} \right) \right].$$

Fig. 1.



Absorption current/time curves.

If now a field  $F_2$  is applied for a further  $t$  seconds a distribution which satisfies the differential equation and the conditions is given by

$$f = A \left\{ 1 + \frac{\mu F_1 \cos \theta}{kT} \left( 1 - e^{-\frac{2(t+t_0)kT}{\rho}} \right) + \frac{\mu(F_2 - F_1) \cos \theta}{kT} \left( 1 - e^{-\frac{2tkT}{\rho}} \right) \right\} \dots (10)$$

(See Appendix (d), equation (14).)

From the form of equation (10) it would appear that the absorption current due to dipoles obeys the Super-position Principle.

#### (b) Power Loss in Alternating Fields.

It is here necessary to find a solution of (5) when

$$F = F_0 e^{j\omega t},$$

where  $\omega = 2\pi$  frequency.

Such a solution is given by

$$f = A \left[ 1 + \frac{1}{\left(1 + \frac{j\rho\omega}{2kT}\right)} \frac{\mu}{kT} F \cos\theta \right]. \quad (11)$$

(See Appendix, equation (15).)

Thus

$$\frac{\epsilon - 1}{\epsilon + 2} = b + \frac{4\pi\mu^2N}{9kT\left(1 + \frac{j\rho\omega}{2kT}\right)}. \quad (12)$$

Let, as before,

$$a = \frac{4\pi\mu^2N}{9kT} \quad \text{and} \quad \frac{\rho\omega}{2kT} = x,$$

$$\begin{aligned} \epsilon &= 3 \left( 1 - b - \frac{a}{1 + jx} \right) - 2 \\ &= \frac{(1 + 2b) [(1 - b)(1 + x^2) - a] + 2a(1 - b - a) - jax}{(1 - b - a)^2 + (1 - b)^2 x^2}. \end{aligned} \quad (13)$$

The specific power loss in absolute units is given by the imaginary part of the above expression multiplied by  $\omega$ , that is

$$\frac{W_\rho}{2kT} = \frac{x^2 a}{(1 - b - a)^2 + (1 - b)^2 x^2}. \quad (14)$$

The power loss is zero at zero frequency, and then rises, as in fig. 2, and finally tends asymptotically to a maximum value at high frequencies given by

$$\frac{a2kT}{(1 - b)^2 \rho};$$

that is

$$W_{\max.} = \frac{2kT}{\rho} \frac{P(\text{due to dipoles})}{(1 - P(\text{without dipoles}))^2}. \quad (15)$$

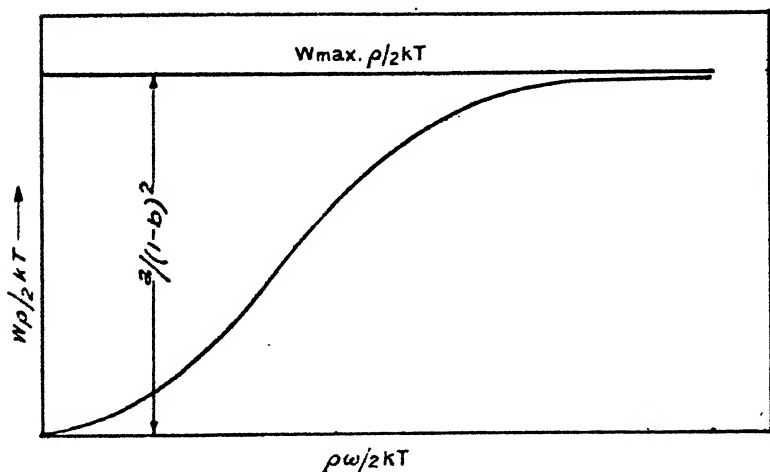
P = polarization.

Again,

$$\begin{aligned} \frac{W}{W_{\max.}} &= 1 / 1 + \left( 1 - \frac{a}{1 - b} \right)^2 \frac{1}{x^2} \\ &= 1 / 1 + \frac{1}{x^2} \left( \frac{\epsilon(\text{without dipoles}) + 2}{\epsilon(D.C.) + 2} \right)^2. \end{aligned} \quad (16)$$

Since  $a$  varies as  $1/T$ ,  $W_{\max.}$  should be independent of temperature. Since also  $W/W_{\max.}$  is a function of  $\rho\omega/2kT$ ,  $W$  should decrease with temperature if  $\rho$  is constant. It is, however, highly probable that  $\rho$  varies with temperature, particularly with solids, and if, as is to be expected,  $\rho$  decreases with temperature,  $W_{\max.}$  will increase with temperature. Owing, however, to the fact that  $\omega/T$  is a parameter in the expression for the loss, the latter will decrease with temperature for a given frequency. Such an effect is only occasionally observed, and then only over a limited range.

Fig. 2.



Variation of specific power loss with frequency.

### (c) Power Factor.

If the loss angle is small, then  $\tan \delta$  may be taken instead of  $\sin \delta$ . With this assumption the power factor becomes from (13)

$$\left. \begin{array}{l} \text{Power} \\ \text{factor} \end{array} \right\} = \tan \delta = \frac{ax}{(1+2b)[(1-b)(1+x^2)-a] + 2a(1-b-a)} \quad \dots (17)$$

Thus the power factor increases with frequency up to a maximum for the frequency given by

$$\frac{\rho\omega}{2kT} = \sqrt{\left(1 - \frac{a}{1-b}\right) \left(1 + \frac{2a}{1+2b}\right)}, \quad \dots (18)$$

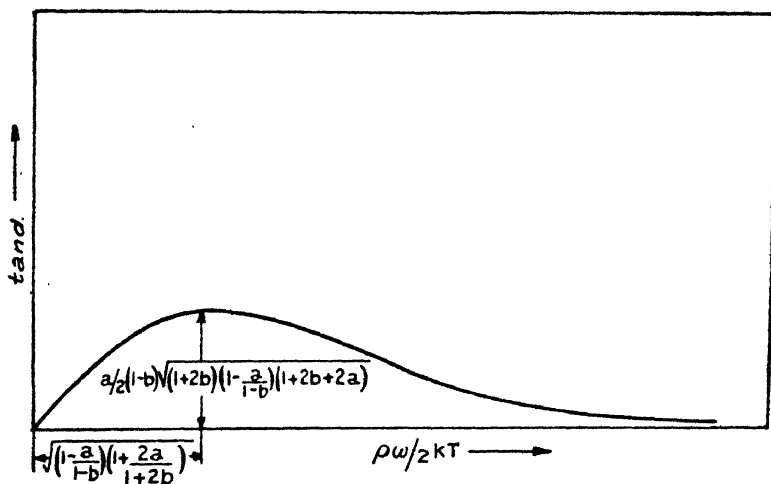
and then decreases asymptotically towards zero (see fig. 3).

The maximum value of  $\tan \delta$  is given by

$$(\tan \delta)_{\max.} = \frac{a}{2} (1-b) \sqrt{(1+2b) \left(1 - \frac{a}{1-b}\right) (1+2b+2a)} \quad \dots (19)$$

From the present result and from those concerning power loss it is probable that dipole losses occur alone only very rarely. It is nevertheless possible that the presence of a component of loss due to dipoles may account for some of the divergences from general relations such as Schweidler's laws. Maxima and minima in the power factor could be

Fig. 3.



Variation of power factor with frequency.

explained by the effect of dipoles coming into action at different frequencies. It may be noted that

$$\omega = \frac{2kT}{\rho}$$

is of the order of  $10^{10}$  for water at normal temperatures. It would be much less for solids, owing to greater viscosity.

$$b = \frac{\epsilon - 1}{\epsilon + 2} \quad (\text{when there are no dipoles}),$$

$$a = \frac{\epsilon - 1}{\epsilon + 2} \quad (\text{when only dipoles are considered});$$

$a$  and  $b$  are thus always less than unity.

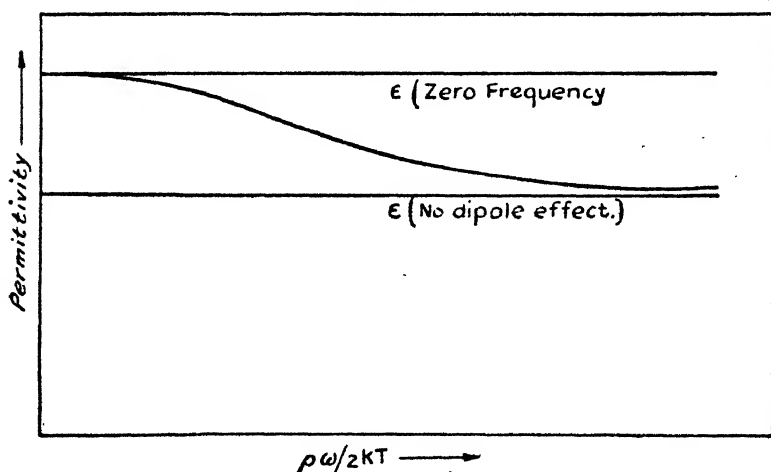
(d) *Permittivity.*

From equation (13) the following expression for the permittivity  $K$  is found:—

$$K = \frac{\sqrt{\{(1+2b)[(1-b)(1+x^2)-a]+2a(1-a-b)\}^2+a^2x^2}}{(1-a-b)^2+a^2x^2} \quad (20)$$

According to this equation the permittivity decreases with frequency from the value for the S. I. C. at zero frequency to the value when the dipoles no longer have any effect upon permittivity; the reason being that for extremely high

Fig. 4.



Variation of permittivity with frequency.

frequencies they hardly move at all during a cycle, and therefore contribute little to the capacity current. The form of variation of  $K$  is shown in fig. 4. It may be noted that for liquids little variation in frequency occurs up to the order of  $10^6$  p.p.s., but with solids, where the viscosity is much larger, variation should be observed at lower frequencies.

### III. ANOMALOUS EFFECTS (NEGLECTING SECONDARY FIELD).

Under Section I. above the field due to the induced polarization was taken into account when dealing with the field which tends to align the dipoles. The equations are

much simplified if only the impressed external field is supposed to affect the dipoles. Equation (4) becomes

$$\epsilon = 1 + b + 4\pi\mu^2 N / 9kT, \quad . \quad . \quad . \quad (21)$$

since now  $\epsilon = 1 + P/F$ .  $\epsilon$  in the above equation refers to the S. I. C. in constant fields.

(a) *Absorption Current.*

Equation (8) now becomes

$$\epsilon = 1 + b + a \left( 1 - e^{-\frac{2kT}{\rho}} \right), \quad . \quad . \quad . \quad (22)$$

and the charging current is

$$i = \frac{2akT}{\rho} e^{-\frac{2kT}{\rho}} \quad . \quad . \quad . \quad (23)$$

This is a simple exponential form, and is shown on fig. 1 *a* for comparison. The initial value is  $2akT/\rho$ , i. e.,  $1/3$  or less than the previous value.

(b) *Power Loss.*

Equation (13) becomes

$$\epsilon = 1 + b + \frac{a}{1+x^2} - \frac{jax}{1+x^2}, \quad . \quad . \quad . \quad (24)$$

Thus the specific power is given by

$$W = \frac{ax^2}{1+x^2} \frac{2kT}{\rho}, \quad . \quad . \quad . \quad (25)$$

and the same remarks as in Section II. (b) apply here also:

$$W_{\max.} = \frac{2akT}{\rho}, \quad . \quad . \quad . \quad (26)$$

$$\frac{W}{W_{\max.}} = \frac{x^2}{1+x^2} \quad . \quad . \quad . \quad (27)$$

These equations correspond to equations (15) and (16), but it now appears that  $W/W_{\max.}$  should be independent of the nature of the material except its effective viscosity towards dipole movements.

(c) *Power Factor* :

$$\tan \delta = \frac{ax}{(1+b)(1+x^2)+a}; \quad . \quad . \quad . \quad (28)$$

$\tan \delta$  increases to a maximum for

$$\frac{\rho\omega}{kT} = \sqrt{\frac{1+a+b}{1+b}} = \sqrt{\frac{\epsilon_{\text{D.C.}}}{\epsilon_{\text{without dipoles}}}},$$

$$(\tan \delta)_{\text{max.}} = a/2 \sqrt{(1+b)(1+a+b)}. \quad . \quad . \quad (29)$$

(d) *Permittivity* :

$$K = \sqrt{[(1+b)(1+x^2)+a]^2 + a^2x^2/1+x^2}. \quad . \quad (30)$$

As before, the permittivity decreases from the S. I. C. for steady fields to the value when the dipoles have no effect.

#### IV. OTHER EFFECTS.

(a) *High Field Strengths.*

At high field strengths the S. I. C. due to dipoles is no longer independent of the field strength. The S. I. C.  $\epsilon$  and the permittivity decrease with the field  $F$  according to the law

$$\epsilon = A_0 - A_1 F^2. \quad . \quad . \quad . \quad (31)$$

The power loss would increase and no longer obey the Square Law. Evidence, however, even for cases where anomalous effects may be neglected is uncertain.

(b) *Magnetic Fields.*

If the dipole has also a comparable magnetic moment then the anomalous phenomena and the S. I. C. will be altered in the presence of a magnetic field. In most cases, however, the susceptibility of dielectrics would appear too small for an effect of this particular type to be of great consequence. It is, however, known that in some cases the properties of dielectrics are affected by a magnetic field.

#### V. EXPERIMENTAL WORK.

As mentioned above, the effect of dipoles upon anomalous dispersion has for some years been known and investigated in the case of liquids. More recently the effect has been



applied to viscous dielectrics at commercial frequencies with some success (Kitchin and Muller, 'Physical Review,' pp. 979-987, xxxii. no. 6, Dec. 1928). These authors experimented with castor-oil and rosin, and obtained a variation of power factor and permittivity with temperature of a type predicted by theory.

The present paper was in manuscript form three years ago, and was received by the E. R. A. previous to the article referred to above. It is therefore felt that there is sufficient reason for issue at this date on this account, and because the treatment is slightly different from that given by the above authors. The latter take Debye's expression for the absorption coefficient  $\alpha$ , and make use of the following relation for the power factor :

$$\text{power factor} = 2\alpha/(1 - \alpha^2),$$

and find the maximum value of  $\alpha$  and the power factor in terms of the permittivity  $\epsilon$  at zero and infinity ( $\epsilon_0$  and  $\epsilon_\infty$ ).

The present paper was rather intended to show the analogies and differences between the dipole theory and other theories (*e. g.*, Pellat, Schweidler, Wagner, and Décombé) of the anomalous properties of dielectrics.

#### APPENDIX.

##### (a) *Normal Dipole Effect.*

Let

$\mu$  = dipole moment,

$f$  = number of dipoles pointing in directions  $\theta$  contained in solid angle  $d\Omega$ ,

$F$  = field strength (supposed uniform),

$P$  = polarization of medium,

$E$  = field affecting dipoles (supposed uniform),

$N$  = number of dipoles per c.c.,

$k$  = Boltzmann's constant,

$T$  = absolute temperature,

$\epsilon$  = specific inductive capacity.

Each dipole has a potential energy given by  $\mu E \cos \theta$  with reference to the field  $E$ .

Thus

$$f = Ae \frac{\mu E \cos \theta}{kT} \quad \dots \quad (1)$$

$$= A \left( 1 + \frac{\mu E \cos \theta}{kT} \right) \quad \dots \quad (2)$$

to a first approximation.

The total electric moment per c.c. in direction of  $E$  is

$$\begin{aligned} P &= 4\pi \int_0^\pi f \mu \cos \theta d\Omega \\ &= 4\pi \int_0^\pi N \left( 1 + \frac{\mu E \cos \theta}{kT} \right) \cos \theta d(\cos \theta) \\ &= 4\pi \mu^2 EN / 3kT. \quad \dots \quad (3) \end{aligned}$$

But  $E = F + P/3$  (Larmor's theory).

The total induction  $= D = F + P = \epsilon F$ .

$$\therefore P = (\epsilon - 1)F;$$

$$\therefore E = F(\epsilon + 2)/3;$$

$$\therefore P/E = 3P/F(\epsilon + 2)$$

$$= \frac{3(\epsilon - 1)}{(\epsilon + 2)}.$$

Thus

$$\left[ \frac{\epsilon - 1}{\epsilon + 2} \right] = 4\pi \mu^2 N / 9kT$$

when dipoles alone are considered.

To this must be added the polarization due to other causes, which in the present memorandum is taken, for convenience, to be independent of temperature and frequency, although in practice it will not usually be so.

Accordingly

$$\frac{\epsilon - 1}{\epsilon + 2} = b + \frac{4\pi \mu^2 N}{9kT}, \quad \dots \quad (4)$$

when all effects are considered where the additional polarization  $= bE$ :

The right-hand side of (4) may be called the specific polarization, so that

$$b = \text{specific polarization without dipoles,}$$

$$\frac{4\pi\mu^2N}{9kT} = a = \text{specific polarization due to dipoles.}$$

If the secondary field were neglected, and  $E$  taken as equal to  $F$ , then

$$\epsilon = 1 + P/F$$

$$= 1 + b + a. \quad . \quad . \quad . \quad . \quad . \quad (5)$$

(b) *Effect of Frictional Resistance.*

The moment tending to resist the motion of the dipole may be taken as

$$\rho \frac{d\theta}{dt} = M,$$

where  $\rho$  is the coefficient of internal friction. For a fluid we may put

$$\rho = 8\pi\eta a^3,$$

where  $a$  = radius of dipole,  $\eta$  = viscosity of medium.

The mean motion of the dipoles, which may be supposed as oscillating round varying positions of equilibrium, can be treated analogously with Einstein's equations for the Brownian movement, and by direct substitution in Einstein's equation it is found

$$\frac{\partial f}{\partial t} = \frac{\Delta}{4T \sin \theta} \frac{\partial}{\partial \theta} \left( \sin \theta \frac{\partial f}{\partial \theta} \right) - \frac{1}{\rho \sin \theta} \frac{\partial}{\partial \theta} f M \sin \theta, \quad (6)$$

where

$\Delta$  = mean square motion,

$T$  = elementary interval of time considered.

Again Einstein's equation for  $\Delta$  may also be adopted, which becomes in this case

$$\frac{\Delta}{T} = kT/\rho.$$

Thus, finally,

$$\rho \frac{\partial f}{\partial t} = \frac{1}{\sin \theta} \frac{\partial}{\partial \theta} \left[ \sin \theta \left( kT \frac{\partial f}{\partial \theta} - M \right) \right]. \quad . \quad . \quad (7)$$

Now the couple on the dipole due to the field  $F$  is  $\mu F \sin \theta$ . Thus, in order to find  $f$ , we may put for an average

$$f \rho \frac{d\theta}{dt} = Mf = -A\mu F \sin \theta,$$

so that

$$\rho \frac{\partial f}{\partial t} = \frac{1}{\sin \theta} \frac{\partial}{\partial \theta} \left[ \sin \theta \left( kT \frac{\partial f}{\partial \theta} + A\mu F \sin \theta \right) \right]. \quad (8)$$

(c) *Constant Fields.*

Let  $F$  be independent of  $t$ . Then (8) reduces to

$$\rho \frac{\partial f}{\partial t} = \frac{1}{\sin \theta} \frac{\partial}{\partial \theta} \left( \sin \theta kT \frac{\partial f}{\partial \theta} \right) + 2A\mu F \cos \theta. \quad (9)$$

Let

$$f = f_1 + \frac{2A\mu F \cos \theta t}{\rho}.$$

Then

$$\rho \frac{\partial f_1}{\partial t} = \frac{kT}{\sin \theta} \frac{\partial}{\partial \theta} \sin \theta \frac{\partial f_1}{\partial \theta} - \frac{4A\mu F t}{\rho} kT \cos \theta.$$

Let

$$f_1 = f_2 - \frac{4A\mu F t^2 \cos \theta}{2\rho^2}.$$

Then

$$\rho \frac{\partial f_2}{\partial t} = \frac{kT}{\sin \theta} \frac{\partial}{\partial \theta} \sin \theta \frac{\partial f_2}{\partial \theta} + \frac{8A\mu F t^2 \cos \theta (kT)^2}{2\rho^2}.$$

Thus by successive approximation it is found that

$$f = \frac{A\mu F \cos \theta}{kT} \left[ \frac{2tkT}{\rho} - \frac{1}{2!} \left( \frac{2kTt}{\rho} \right)^2 + \frac{1}{3!} \left( \frac{2kTt}{\rho} \right)^3 \dots \right].$$

We may also add  $f = A$ , which does not affect the solution obtaining.

$$f = A \left[ 1 + \frac{\mu F \cos \theta}{kT} \left( 1 - e^{-\frac{2kTt}{\rho}} \right) \right]. \quad (10)$$

On substituting in (3) and determining  $\epsilon$ , it follows that

$$\frac{\epsilon - 1}{\epsilon + 2} = b + a \left( 1 - e^{-\frac{2kTt}{\rho}} \right). \quad (11)$$

Suppose  $F = F_1$  for a period  $t_0$ , then at the end of the interval

$$f = A \left[ 1 + \frac{\mu F \cos \theta}{kT} \left( 1 - e^{-\frac{2kTt}{\rho}} \right) \right]. \quad (12)$$

If  $F_1$  is changed to  $F_2$ , then, after a further period  $t$ ,  $f$  may be assumed as made up of two parts,  $\phi$  and  $\psi$ .

$$\begin{aligned} f &= \phi + \psi \\ &= A \left[ 1 + \frac{\mu F_1 \cos \theta}{kT} \left( 1 - e^{-\frac{2(t+t_0)kT}{\rho}} \right) \right] \\ &\quad + \frac{A\mu(F_2 - F_1) \cos \theta}{kT} \left( 1 - e^{-\frac{2tkT}{\rho}} \right). \quad (13) \end{aligned}$$

On substituting in (9), it is seen that

$$\rho \frac{\partial \phi}{\partial t} = \frac{kT}{\sin \theta} \frac{\partial}{\partial \theta} \sin \theta \frac{\partial \phi}{\partial \theta} + 2A\mu F_1 \cos \theta$$

and

$$\rho \frac{\partial \psi}{\partial t} = \frac{kT}{\sin \theta} \frac{\partial}{\partial \theta} \sin \theta \frac{\partial \psi}{\partial \theta} + 2A\mu(F_2 - F_1) \cos \theta.$$

$$\therefore \rho \frac{\partial(\phi + \psi)}{\partial t} = \frac{kT}{\sin \theta} \frac{\partial}{\partial \theta} \sin \theta \frac{\partial(\phi + \psi)}{\partial \theta} + 2A\mu F_2 \cos \theta. \quad (14)$$

Thus, over the period  $t_0$  to  $t_0 + t$  expression (13) satisfies the general condition (9). Further, when  $t = 0$ ,

$$f = A \left[ 1 + \frac{\mu F_1 \cos \theta}{kT} \left( 1 - e^{-\frac{2t_0 kT}{\rho}} \right) \right],$$

so that (13) satisfies the conditions of the problem.

(d) *Alternating Fields.*

In this case  $F = F_0 e^{j\omega t}$  where  $\omega = 2\pi$  frequency. Put

$$f = A(1 + \phi e^{j\omega t})$$

in (9). Then

$$\frac{j\omega \phi}{kT} = \frac{1}{\sin \theta} \frac{d}{d\theta} \sin \theta \frac{d\phi}{d\theta} + 2\mu F_0 \cos \theta. \quad (15)$$

The solution of this is

$$\phi = \frac{1}{1 + \frac{j\rho\omega}{2kT}} \frac{\mu F_0 \cos \theta}{kT}.$$

Thus

$$f = A \left[ 1 + \frac{1}{1 + \frac{j\rho\omega}{2kT}} \frac{\mu}{kT} F_0 e^{j\omega t} \cos \theta \right]. \quad (16)$$

LXXXIII. *The Free and Forced Symmetrical Oscillations of Thin Bars, Circular Diaphragms, and Annuli.* By A. G. WARREN, M.Sc., M.I.E.E., F.Inst.P., Research Department, Woolwich\*.

THE use, within recent years, of circular diaphragms of considerable size as acoustic generators in wireless loud-speakers and in gramophones has awakened an extended interest in their operation. The case of the free edge rigid disk was investigated by Rayleigh ('Sound,' ii. p. 162 *et seq.*); recently that analysis has been extended by McLachlan (Proc. Roy. Soc. cxxii. p. 604; Phil. Mag. Suppl. June 1929, p. 1011). Such a generator is capable of excellent results over the lower portion of the musical scale, but the output falls off rapidly at high frequencies. The range of uniform reproduction may be extended by reduction of mass of the moving system, but mechanical rigidity is thereby lost, and the basic assumption of the theory is no longer applicable.

The present work arose in an attempt to extend the theory somewhat further. McLachlan has shown that over the upper portion of the musical scale the acoustic reaction is but a small percentage of the accelerational forces. It has been assumed in what follows that the acoustic reaction is negligible. The results are applicable over the whole of the audible range if the mass of the diaphragm is considerable, over a more restricted portion if the mass is small. Though the investigation is but a limited addition to the theory of the speaker, the problem is presented as one of considerable interest in itself. The case of reeds, or thin bars, is included because the equations, while bearing a general resemblance to those for diaphragms, are much simpler and are more easily followed physically. Further, it is believed that at least some of the results relating to thin bars are new.

*General Conditions of Free and Forced Oscillations.*

The periods of the natural vibrations of reeds or thin bars have been determined by Rayleigh ('Sound,' i. chap. viii.). He has also determined the natural periods of a disk clamped at its edge. The avenue of approach to the problems is here rather different. The motion of the system is determined under the action of a harmonic force. The ratio, force divided by acceleration, measured at the place of application

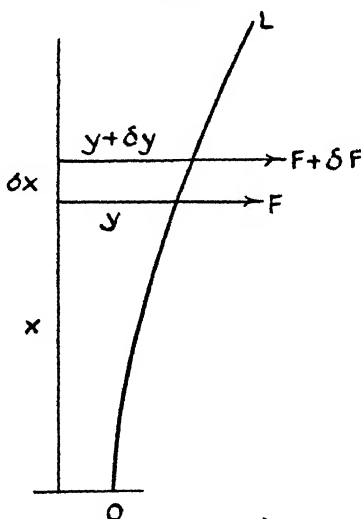
\* Communicated by the Author.

of the force, is the apparent mass of the system. This apparent mass is zero for one type of symmetrical natural vibration; it is infinite for another type. The natural oscillations are thus included as particular cases in the more general problem.

*Free and Forced Vibrations of Reed.*

Unless the bending of a vibrating reed is great, the energy of rotation is negligible. The conditions of statical equilibrium with regard to curvature are therefore applicable. At any section the curvature is proportional to the bending moment; the linear acceleration of any element of the bar

Fig. 1.



is proportional to the net force applied. Assuming a sinusoidal variation of all quantities, we have, therefore (fig. 1),

$$\frac{d^2 y}{dx^2} = \mu M \quad . \quad . \quad . \quad . \quad . \quad (1)$$

$$-\delta F = m \cdot \delta x \cdot \frac{d^2 y}{dt^2}, \quad . \quad . \quad . \quad . \quad . \quad (2)$$

where

- $M$  = bending moment at any section,
- $F$  = normal force at the section,
- $m$  = mass per unit length,
- $y$  = lateral displacement at a distance  $x$ ,
- $\mu$  = constant depending upon stiffness,
- $t$  = time.

Using  $\frac{dM}{dx} = F$  and  $\frac{d}{dt} \equiv j\omega$  (where  $j = \sqrt{-1}$  and  $\omega = 2\pi \cdot \text{frequency}$ ), equations (1) and (2) become

$$\frac{d^2y}{dx^2} = \mu F, \quad \dots \dots \dots (3)$$

$$\text{and} \quad \frac{dF}{dx} = m\omega^2 y; \quad \dots \dots \dots (4)$$

$$\left. \begin{array}{l} \text{or} \quad \frac{d^4y}{dx^4} = \mu\omega^2 my \\ \text{and} \quad \frac{d^4F}{dx^4} = \mu\omega^2 mF \end{array} \right\}; \quad \dots \dots \dots (5)$$

whence

$$y = X \cosh \gamma x + Y \sinh \gamma x + Z \cos \gamma x + W \sin \gamma x, \quad \dots (6)$$

where  $\gamma^4 = \mu\omega^2 m$ .

The constants  $Y/X$ ,  $Z/X$ ,  $W/X$  are determined by the end conditions. If the oscillating force be applied at 0, the apparent mass  $M_a$  is given by

$$M_a = \text{Lt}_{x=0} \left\{ -\frac{1}{\mu\omega^2} \frac{d^3y}{dx^3} \right\} = \frac{m}{\gamma} \cdot \frac{(W-Y)}{(X+Z)}. \quad (7)$$

The range of  $\gamma$  is of interest. If we have a steel reed 1 cm. wide and  $\frac{1}{2}$  mm. thick  $\gamma$  is approximately  $1.2 \times 10^{-2} \sqrt{\omega}$ , or  $3 \times 10^{-2} \sqrt{f}$ . If the length  $l$  is 10 cm.,  $\gamma l$  varies from 1.8 to 30 between frequencies of 36 and 10,000.

Particular cases of interest are given by:—

(a) *End L free; slope at 0 maintained unchanged.*

The constants of integration are determined by the conditions

$$\frac{d^3y}{dx^3} = 0 \quad \text{and} \quad \frac{d^2y}{dx^2} = 0 \quad \text{at} \quad x = l \quad \text{and} \quad \frac{dy}{dx} = 0 \quad \text{at} \quad x = 0,$$

giving

$$\left. \begin{array}{l} \frac{Y}{X} = -\frac{Cs + Sc}{1 + Cc + Ss} \\ \frac{W}{X} = \frac{Cs + Sc}{1 + Cc + Ss} \\ \frac{Z}{X} = \frac{1 + Cc - Ss}{1 + Cc + Ss} \end{array} \right\}, \quad \dots \dots \dots (8)$$

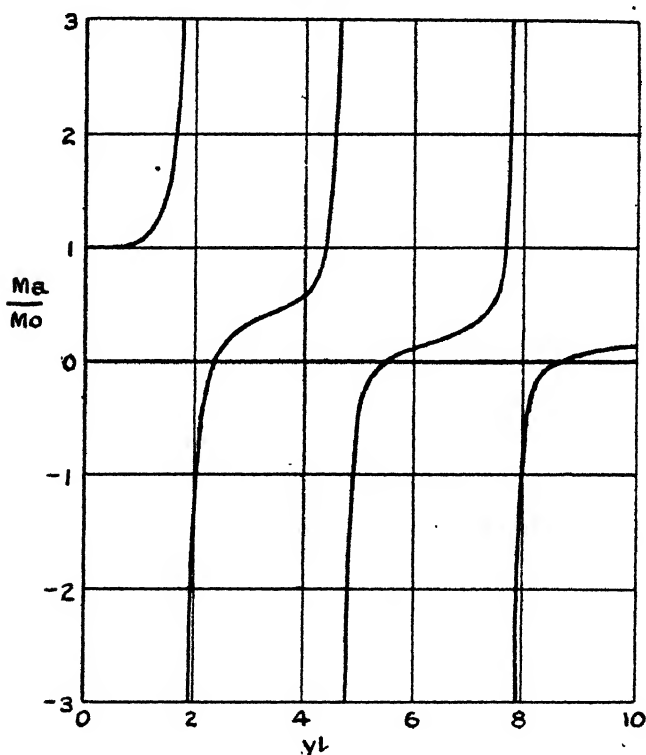


where  $C \equiv \cosh \gamma l$ ,  $S \equiv \sinh \gamma l$ ,  $c \equiv \cos \gamma l$ ,  $s \equiv \sin \gamma l$ , and the apparent mass

$$M_a = \frac{m}{\gamma} \cdot \frac{Cs + Sc}{1 + Cc} \quad . \quad . \quad . \quad (9)$$

When  $\gamma$  is very small (9) reduces to  $ml$ , the mass of the reed. Fig. 2 shows the change of apparent mass with

Fig. 2.



Showing change of apparent mass of reed with frequency.

frequency, and fig. 3 the form of the reed at various typical frequencies. The apparent mass is infinite when

$$Cc = -1 \quad . \quad . \quad . \quad (10)$$

The end 0 is then stationary, and equation (10) gives the natural frequencies of a reed clamped at one end. This condition is fulfilled by  $\gamma l = 1.875 \dots, 4.694 \dots, 7.854 \dots$ , etc.

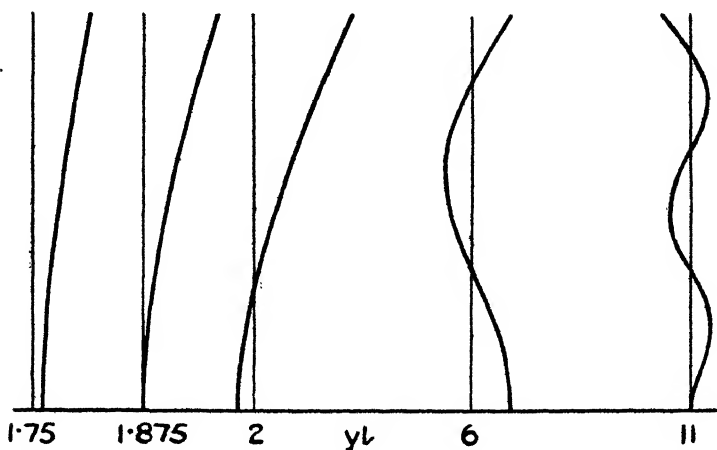
(Rayleigh, i. p. 278). It is easy to show that the displacement of the free end of the reed is then

$$y_l = \pm 2X. \quad . . . . . (11)$$

At high frequencies, when  $1/C$  becomes negligible, the apparent mass becomes

$$M_a = \frac{m}{\gamma} \cdot (1 + \tan \gamma l). \quad . . . . . (12)$$

Fig. 3.



Showing form assumed by reed at various frequencies. The first three cases illustrate the changes consequent upon passing through a frequency of natural oscillations.

The apparent mass is zero when

$$Cs + Sc = 0. \quad . . . . . (13)$$

This case is clearly that of the natural *symmetrical* vibrations of a reed  $2l$  in length, free at both ends.

(b) *Both ends free.*

The constants of integration are determined from the conditions

$$\frac{d^3 y}{dx^3} = 0 \quad \text{and} \quad \frac{d^2 y}{dx^2} = 0 \quad \text{at} \quad x = l \quad \text{and} \quad \frac{d^2 y}{dx^2} = 0 \quad \text{at} \quad x = 0,$$

giving

$$\left. \begin{aligned} \frac{Y}{X} &= \frac{-1 + Cc - Ss}{Cs - Sc} \\ \frac{W}{X} &= \frac{1 - Cc - Ss}{Cs - Sc} \\ \frac{Z}{X} &= 1 \end{aligned} \right\}, \dots \dots (14)$$

and the apparent mass

$$M_a = \frac{m}{\gamma} \cdot (1 - Cc). \dots \dots (15)$$

The natural oscillations are given by

$$Cc = +1. \dots \dots (16)$$

For a reed of length  $2l$  the natural oscillations are similarly given by

$$\text{Cosh } 2\gamma l \cdot \cos 2\gamma l = 1, \dots \dots (17)$$

which may be written

$$(Cs + Sc)(Cs - Sc) = 0. \dots \dots (18)$$

$Cs + Sc = 0$  (13) gives the symmetrical oscillations (see above).

$Cs - Sc = 0$  (19) gives the natural oscillations for which the centre of the reed is a point of inflexion. The symmetrical oscillations occur when  $2\gamma l = 4.730 \dots, 10.995 \dots, 17.278 \dots$ , etc.; the asymmetrical oscillations when  $2\gamma l = 7.853 \dots, 14.137 \dots$ , etc. (compare Rayleigh, i. pp. 277, 278).

(c) *L clamped, so that position and slope are maintained unchanged; slope at 0 maintained unchanged.*

The constants of integration are determined by the conditions

$$\frac{dy}{dx} = 0 \quad \text{and} \quad y = 0 \quad \text{at} \quad x = l; \quad \frac{dy}{dx} = 0 \quad \text{at} \quad x = 0,$$

giving

$$\left. \begin{aligned} \frac{Y}{X} &= \frac{Cs + Sc}{1 - Cc - Ss} \\ \frac{W}{X} &= -\frac{Cs + Sc}{1 - Cc - Ss} \\ \frac{Z}{X} &= \frac{1 - Cc + Ss}{1 - Cc - Ss} \end{aligned} \right\}, \dots \dots (20)$$

and the apparent mass

$$M_a = -\frac{m}{\gamma} \cdot \frac{C_s + S_c}{1 - C_c} \quad \dots \quad (21)$$

Hence the symmetrical natural vibrations of a reed of length  $2l$ , clamped at both ends, are given by

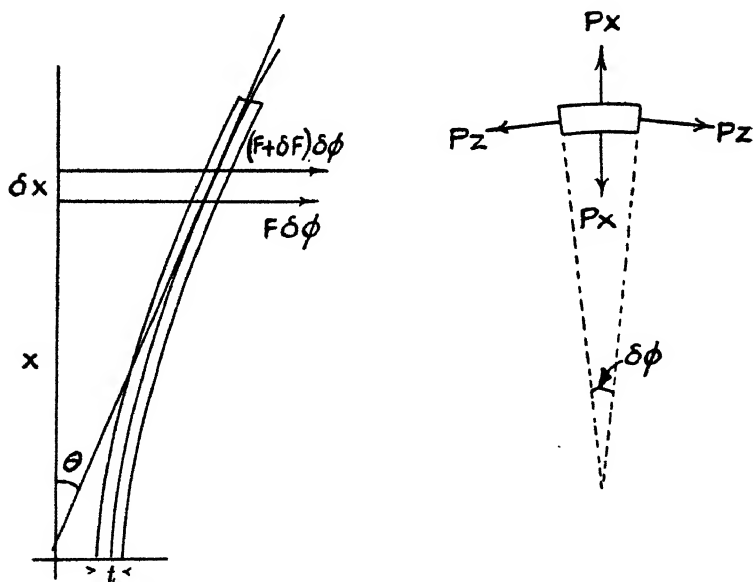
$$C_s + S_c = 0, \quad \dots \quad (22)$$

and the complete system of natural vibrations is given by

$$\text{Cosh } 2\gamma l \cdot \cos 2\gamma l = 1, \quad \dots \quad (23)$$

$$\text{or} \quad (C_s + S_c)(C_s - S_c) = 0. \quad \dots \quad (24)$$

Fig. 4.



Equations (23) and (24) are identical with (17) and (18), showing that the natural periods of a reed *free* at both ends are the same as those of the same reed *clamped* at both ends (see Rayleigh, i. p. 275).

#### *Free and Forced Vibrations of Diaphragm.*

In this case, again, the rotational energy may be neglected and the form of an element of the diaphragm may be determined from the moments acting upon it. At unit distance from the neutral surface (fig. 4) the circumferential

strain is  $\theta/x$  and the radial strain is  $d\theta/dx$ , giving the circumferential stress

$$p_z = \frac{E\sigma}{\sigma^2 - 1} \left( \sigma \frac{\theta}{x} + \frac{d\theta}{dx} \right), \quad \dots \quad (25)$$

and the radial stress

$$p_r = \frac{E\sigma}{\sigma^2 - 1} \left( \frac{\theta}{x} + \sigma \frac{d\theta}{dx} \right), \quad \dots \quad (26)$$

where  $E$  = Young's modulus.

$\sigma$  = Poisson's ratio (expressed as a number greater than unity).

The moment on the element caused by the circumferential stress is

$$\frac{1}{12} \delta x \cdot \delta \phi \cdot t^3 \cdot \frac{E\sigma}{\sigma^2 - 1} \left( \sigma \frac{\theta}{x} + \frac{d\theta}{dx} \right).$$

The bending moment at a radius  $x$  caused by the radial stress is

$$\frac{1}{12} x \cdot \delta \phi \cdot t^3 \cdot \frac{E\sigma}{\sigma^2 - 1} \left( \frac{\theta}{x} + \sigma \frac{d\theta}{dx} \right),$$

and its contribution to the turning moment on the element is

$$\frac{1}{12} \delta x \cdot \delta \phi \cdot t^3 \cdot \frac{E\sigma}{\sigma^2 - 1} \left( \frac{d\theta}{dx} + \sigma \frac{d\theta}{dx} + \sigma x \frac{d^2\theta}{dx^2} \right).$$

From the equilibrium conditions we obtain

$$\frac{F \cdot \delta \phi \cdot \delta x}{2\pi} = \frac{1}{12} \delta x \cdot \delta \phi \cdot t^3 \cdot \frac{E\sigma^2}{\sigma^2 - 1} \left( x \frac{d^2\theta}{dx^2} + \frac{d\theta}{dx} - \frac{\theta}{x} \right). \quad (27)$$

where  $F$  is the total shearing force at a radius  $x$ .

Equation (27) may be rewritten

$$x \frac{d^3y}{dx^3} + \frac{d^2y}{dx^2} - \frac{1}{x} \frac{dy}{dx} = aF, \quad \dots \quad (28)$$

$$\text{where} \quad \frac{1}{a} = \frac{\pi}{6} t^3 \frac{E\sigma^2}{\sigma^2 - 1}.$$

If  $m$  is the mass of unit area of the diaphragm, we have

$$-\delta F = 2\pi x \cdot \delta x \cdot m \cdot \frac{d^3y}{dt^2}, \quad \dots \quad (29)$$

$$\text{or} \quad \frac{dF}{dx} = 2\pi \omega^2 m x y. \quad \dots \quad (30)$$

From (28) and (30) we obtain, writing  $b \equiv 2\pi\omega^2 m$ ,

$$\frac{d^4 y}{dx^4} + \frac{2}{x} \frac{d^3 y}{dx^3} - \frac{1}{x^2} \frac{d^2 y}{dx^2} + \frac{1}{x^3} \frac{dy}{dx} - aby = 0, \quad (31)$$

which may be written

$$(\nabla^2 + k^2)(\nabla^2 - k^2)y \equiv 0, \quad (32)$$

where  $k^4 \equiv ab$

(for the same material, of the same thickness,  $k$  has almost the same value as  $\gamma$ ),

$$\text{and} \quad \nabla^2 \equiv \frac{d^2}{dx^2} + \frac{1}{x} \frac{d}{dx}.$$

This is a Bessel equation, whose solution is

$$y = AJ_0(kx) + BY_0(kx) + CI_0(kx) + DK_0(kx). \quad (33)$$

In the case of an annular ring the constants of integration may be determined from the conditions obtaining at its inner and outer edges. Generally two equations are given by the conditions at the outer edge, and a third equation by the condition imposed at the inner edge by the method of attachment of the driving mechanism. These equations may be written respectively :

$$a_1 A + b_1 B + c_1 C + d_1 D = 0, \quad (34)$$

$$a_2 A + b_2 B + c_2 C + d_2 D = 0, \quad (35)$$

$$a_3 A + b_3 B + c_3 C + d_3 D = 0. \quad (36)$$

Their solution for  $B/A$ ,  $C/A$ ,  $D/A$  completely determines the motion for any value of  $k$ . For the natural oscillations a fourth equation (usually  $F = 0$  at  $x = r$ ) is given by the extra condition postulated for the inner rim. It may be written

$$a_4 A + b_4 B + c_4 C + d_4 D = 0. \quad (37)$$

The frequencies of the natural vibrations are then given by

$$\begin{vmatrix} a_1 & b_1 & c_1 & d_1 \\ a_2 & b_2 & c_2 & d_2 \\ a_3 & b_3 & c_3 & d_3 \\ a_4 & b_4 & c_4 & d_4 \end{vmatrix} = 0. \quad (38)$$

When the annulus is driven at its inner rim the force exerted there is (from (28) )

$$F = \frac{k^3 r}{a} \{ AJ_1(kr) + BY_1(kr) + CI_1(kr) - DK_1(kr) \}, \quad (39)$$

and the acceleration is

$$\frac{d^2 y}{dt^2} = -\omega^2 y = -\omega^2 \{A J_0(kr) + B Y_0(kr) + C I_0(kr) + D K_0(kr)\}.$$

. . . . (40)

Writing  $\omega^2 a = k^4/2\pi m$ , the apparent mass then becomes

$$M_a = -\frac{2\pi m r}{k} \left\{ \frac{A J_1(kr) + B Y_1(kr) + C I_1(kr) - D K_1(kr)}{A J_0(kr) + B Y_0(kr) + C I_0(kr) + D K_0(kr)} \right\}.$$

. . . . (41)

Typical conditions which determine the coefficients in equations (34) to (36) may be considered. An edge (usually the outer) may be clamped in such a manner that its position and the slope in its neighbourhood are maintained; or an edge (usually the inner) may be driven in such a way that as  $y$  changes  $dy/dx$  remains unaltered. In these cases no difficulty arises in expressing the conditions mathematically. The case of a free edge, however, has been a matter of discussion. One condition is, of course, that  $F$  disappears; it is the other condition which is open to question. Here it is assumed that at a free edge ( $a$ ) the radial stress disappears, ( $b$ ) the expression for the radial stress given in equation (26) is applicable. Condition ( $b$ ) is open to criticism. The diaphragms employed, however, are always thin and the distance from the edge at which condition ( $b$ ) is fulfilled with practical accuracy must be but a small fraction of the radius of the disk. A similar assumption is made in connexion with the theory of beams, and then the error must be enormously greater. It seems reasonable to assume that any error introduced in the present case is negligible. We arrive, therefore, at the following equations for typical edge conditions. At radii where the displacement is zero we have

$$A J_0(kx) + B Y_0(kx) + C I_0(kx) + D K_0(kx) = 0; \quad (42)$$

where the slope is zero we have

$$A J_1(kx) + B Y_1(kx) - C I_1(kx) + D K_1(kx) = 0; \quad (43)$$

where  $F$  is zero we have

$$A J_1(kx) + B Y_1(kx) + C I_1(kx) - D K_1(kx) = 0; \quad (44)$$

and where the radial stress is zero

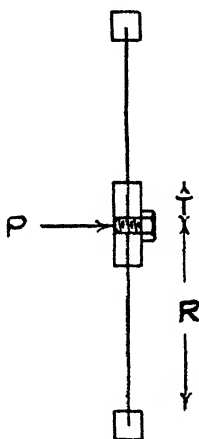
$$\frac{\sigma - 1}{\sigma \cdot kx} \{A J_1(kx) + B Y_1(kx) - C I_1(kx) + D K_1(kx)\} -$$

$$\{A J_0(kx) + B Y_0(kx) - C I_0(kx) - D K_0(kx)\} = 0. \quad (45)$$

*Free Symmetrical Vibrations of Annulus or Disk with Clamped outside Edge, the Slope being maintained at the Inner Edge.*

The particular example here considered is, in the case of the annulus, rather artificial. It has been chosen rather to illustrate the method, the equations being simpler than those of the annuli considered later, in which one or both of the edges are free. The diaphragm is supposed to be firmly clamped at its rim. The centre is clamped between two rigid plates of radius  $r$ , so that at this radius  $dy/dx$  must remain zero (fig. 5). An alternating harmonic force is applied at

Fig. 5.



the centre, and the equations of motion determined. At certain frequencies the force  $P$  disappears for finite amplitudes of vibration. These are the natural frequencies under the conditions considered. When  $r$  is made indefinitely small the natural frequencies of the disk are obtained.

The conditions for the annulus are :—

$$dy/dx = 0 \quad \text{and} \quad y = 0 \text{ at } x = R, \quad dy/dx = 0 \text{ at } x = r,$$

giving

$$AJ_1(kR) + BY_1(kR) - CI_1(kR) + DK_1(kR) = 0, \quad (34a)$$

$$AJ_0(kR) + BY_0(kR) + CI_0(kR) + DK_0(kR) = 0, \quad (35a)$$

$$AJ_1(kr) + BY_1(kr) - CI_1(kr) + DK_1(kr) = 0. \quad (36a)$$



These equations completely determine the motion at all frequencies. At those frequencies at which the annulus vibrates naturally the shearing force is zero at radius  $r$ , or

$$AJ_1(kr) + BY_1(kr) + CI_1(kr) - DK_1(kr) = 0, \quad (37a)$$

whence from (36a) and (37a)

$$\left. \begin{aligned} AJ_1(kr) + BY_1(kr) &= 0 \\ CI_1(kr) - DK_1(kr) &= 0 \end{aligned} \right\} \quad \dots \quad (46)$$

Substituting from (46) in (34a) and (35a), we obtain

$$J_1(kR) - \frac{J_1(kr)}{Y_1(kr)} Y_1(kR) - \frac{D}{A} \left\{ \frac{K_1(kr)}{I_1(kr)} I_1(kR) - K_1(kR) \right\} = 0, \quad \dots \quad (47)$$

and

$$J_0(kR) - \frac{J_1(kr)}{Y_1(kr)} Y_0(kR) + \frac{D}{A} \left\{ \frac{K_1(kr)}{I_1(kr)} I_0(kR) + K_0(kR) \right\} = 0, \quad \dots \quad (48)$$

whence

$$\begin{aligned} & \frac{J_1(kR)Y_1(kr) - J_1(kr)Y_1(kR)}{J_0(kR)Y_1(kr) - J_1(kr)Y_0(kR)} \\ & + \frac{K_1(kr)I_1(kR) - K_1(kR)I_1(kr)}{K_1(kr)I_0(kR) + K_0(kR)I_1(kr)} = 0. \end{aligned} \quad (49)$$

Equation (49) gives the natural symmetrical vibrations of the annulus under the stated conditions.

If  $r$  is made vanishingly small, (49) reduces to

$$\frac{J_1(kR)}{J_0(kR)} + \frac{I_1(kR)}{I_0(kR)} = 0. \quad \dots \quad (50)$$

(See Rayleigh, i. p. 366.)

This is the corresponding equation for the *disk*, and might have been obtained directly by putting  $r=0$  in (34a) to (37a). The gravest mode of oscillation of the disk is given by  $kR = 3.2$  approximately. Succeeding oscillations occur when  $kR$  is approximately 6.3, 9.4, 12.5 etc.

For the driven diaphragm general expressions embodying equations (34a) to (36a) may be deduced. It is, however, usually more convenient to work directly from the equations as they stand. When, however, the inner radius is very small considerable simplification is possible. Except for the free oscillations it is not permissible to consider the inner radius reduced to absolute zero, as the actuating force would

then produce an infinite stress. There is no objection, however, to considering the inner radius being made very small, the forces employed being correspondingly small. Putting equations (34a) and (35a) in the form of (34) and (35), that is, writing  $a_1 = J_1(kR)$ ,  $b_1 = Y_1(kR)$ ,  $c_1 = -I_1(kR)$ ,  $d_1 = K_1(kR)$ ;  $a_2 = J_0(kR)$ ,  $b_2 = Y_0(kR)$ ,  $c_2 = I_0(kR)$ ,  $d_2 = K_0(kR)$ , and putting  $kr = 0$  in equation (36a), we obtain

$$B = D, \quad . \quad . \quad . \quad . \quad . \quad . \quad (51)$$

$$\frac{B}{A} = \frac{D}{A} = \frac{a_2 c_1 - a_1 c_2}{c_2(b_1 + d_1) - c_1(b_2 + d_2)} \\ = - \frac{I_1 J_0 + I_0 J_1}{I_0(Y_1 + K_1) + I_1(Y_0 + K_0)}, \quad . \quad (52)$$

$$\frac{C}{A} = - \frac{a_2(b_1 + d_1) - a_1(b_2 + d_2)}{c_2(b_1 + d_1) - c_1(b_2 + d_2)} \\ = - \frac{J_0(Y_1 + K_1) - J_1(Y_0 + K_0)}{I_0(Y_1 + K_1) + I_1(Y_0 + K_0)}, \quad . \quad (53)$$

the arguments of the functions in (52) and (53) being  $kR$ . The motion of the centre of the disk is given by

$$y_0 = AJ_0(kr) + BY_0(kr) + CI_0(kr) + DK_0(kr). \quad . \quad (54)$$

In this equation two functions,  $Y_0(kr)$  and  $K_0(kr)$ , become infinite as  $r$  vanishes, but their sum is finite. An examination of the simplification effected in equation (36a) shows that the difference between  $B$  and  $D$  is of such an order that when multiplied by  $Y_0(kr)$  or  $K_0(kr)$  the product becomes vanishingly small as  $r$  approaches zero. It therefore follows that the remainder terms in

$$y_0 = AJ_0(kr) + CI_0(kr) + B\{Y_0(kr) + K_0(kr)\} \quad . \quad (55)$$

are negligible.

From (41) and (36a) we see that the apparent mass for this case is

$$M_a = - \frac{4\pi m r}{k} \left\{ \frac{AJ_1(kr) + BY_1(kr)}{AJ_0(kr) + BY_0(kr) + CI_0(kr) + DK_0(kr)} \right\}. \\ . \quad . \quad . \quad . \quad (56)$$

Putting in the limiting values,

$$J_0(kr) = 1, \quad I_0(kr) = 1,$$

$$Y_0(kr) + K_0(kr) = \log 2 - \gamma = .11593, \quad J_1(kr) = kr/2,$$

$$Y_1(kr) = -1/kr, \quad I_1(kr) = kr/2, \quad K_1(kr) = 1/kr,$$

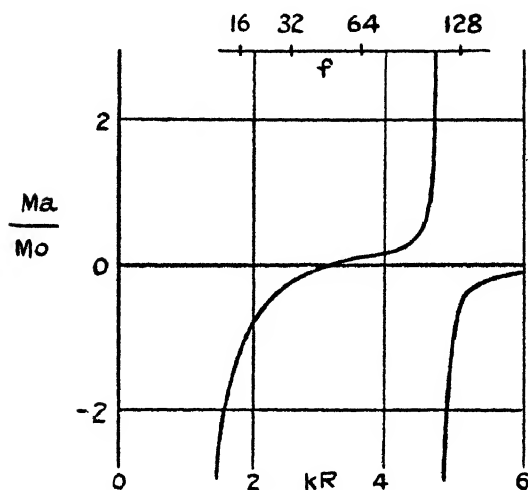
(56) reduces to

$$M_a = \frac{4\pi m}{k^2} \left\{ \frac{B}{A + 11593B + C} \right\}. \quad \dots (57)$$

The equivalent mass vanishes, and we obtain the natural oscillations, when  $B=0$  ((52) and (57)), a relation confirming equation (50). The disk may, however, vibrate with its centre fixed. The apparent mass is then infinite, and the natural frequencies of vibration are given by

$$A + 11593B + C = 0. \quad \dots (58)$$

Fig 6.



Variation of apparent mass of disk with clamped edge.

The variation of apparent mass at low frequencies, determined from (52), (53), and (57), is shown in fig. 6. (The frequency-scale shown on this and on various subsequent diagrams refers to an aluminium diaphragm having a mass of .05 gm. per sq. cm., the radius  $R$  being 10 cm. Assuming  $\sigma = 4$ , we obtain  $kR = .45\sqrt{f}$  approximately.)

*Annulus or Disk with Free Outer Edge, the Slope being maintained at the Inner Edge.*

If the outer rim of the diaphragm be free instead of clamped we approximate to the arrangement used in loud

speakers. For the diaphragm driven through a clamp at its centre equations (34) to (36) become

$$AJ_1(kR) + BY_1(kR) + CI_1(kR) - DK_1(kR) = 0, \quad (34b)$$

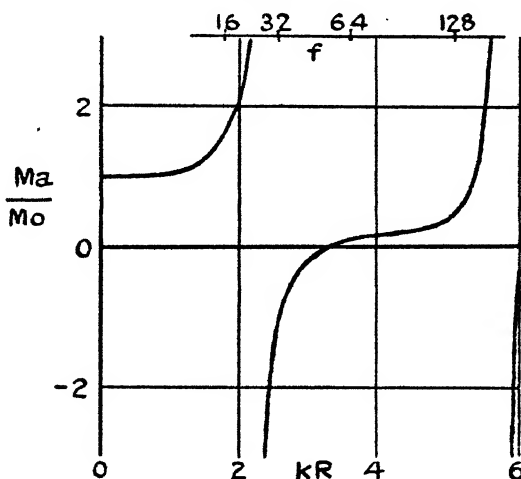
$$\frac{\sigma - 1}{\sigma \cdot kR} \{AJ_1(kR) + BY_1(kR) - CI_1(kR) + DK_1(kR)\}$$

$$- \{AJ_0(kR) + BY_0(kR) - CI_0(kR) - DK_0(kR)\} = 0, \quad (35b)$$

$$AJ_1(kr) + BY_1(kr) - CI_1(kr) + DK_1(kr) = 0. \quad (36b)$$

These three equations determine the motion completely.

Fig. 7.



Variation of apparent mass of annulus with free edge.

Equation (36b) is identical with (36a) of the previous case, and hence the apparent mass is given by (56). It is easy to show that at low frequencies

$$M_0 = \pi m(R^2 - r^2), \quad \dots \dots \dots (59)$$

the actual mass of the diaphragm. Fig. 7 has been plotted to show the variation of apparent mass of an aluminium diaphragm at low frequencies, assuming  $m = .05$ ,  $\sigma = 4$ ,  $r = 2$  cm.,  $R = 10$  cm.

When the inner radius becomes vanishingly small we obtain the case of the disk. As in the previous example,

$$B = D, \quad \dots \dots \dots (51a)$$

$$\frac{B}{A} = \frac{D}{A} = \frac{a_2 c_1 - a_1 c_2}{c_2(b_1 + d_1) - c_1(b_2 + d_2)}, \quad \dots \quad (52a)$$

$$\frac{C}{A} = -\frac{a_2(b_1 + d_1) - a_1(b_2 + d_2)}{c_2(b_1 + d_1) - c_1(b_2 + d_2)}, \quad \dots \quad (53a)$$

where

$$a_1 = J_1(kR), \quad b_1 = Y_1(kR), \quad c_1 = I_1(kR), \quad d_1 = -K_1(kR);$$

$$a_2 = \frac{2(\sigma-1)}{\sigma \cdot kR} J_1(kR) - J_0(kR), \quad b_2 = \frac{2(\sigma-1)}{\sigma \cdot kR} Y_1(kR) - Y_0(kR)$$

$$c_2 = I_0(kR), \quad d_2 = K_0(kR).$$

Hence

$$M_a = \frac{4\pi m}{k_2} \left\{ \frac{B}{A + 11593 B + C} \right\} \quad \dots \quad (57a)$$

This apparent mass has been plotted for various frequencies in fig. 8. Fig. 9 shows the form of the disk at various typical frequencies.

The natural symmetrical oscillations of the whole disk moving freely are given by  $B = 0$ , or

$$\begin{aligned} I_1(kR) \cdot J_0(kR) + I_0(kR) \cdot J_1(kR) \\ = \frac{2(\sigma-1)}{\sigma \cdot kR} J_1(kR) \cdot I_1(kR). \quad \dots \quad (60) \end{aligned}$$

The numerical values of  $kR$  fulfilling this relation depend to some extent upon the value of  $\sigma$ . When  $\sigma = 4$ , the gravest mode of oscillation is given by  $kR = 3.0$  approximately. It will be noticed that the frequencies of the gravest modes of the diaphragm with free and clamped edges are not greatly different; the free and clamped reeds were shown to have the same natural frequencies. (Equations (17), (18), (23), (24).)

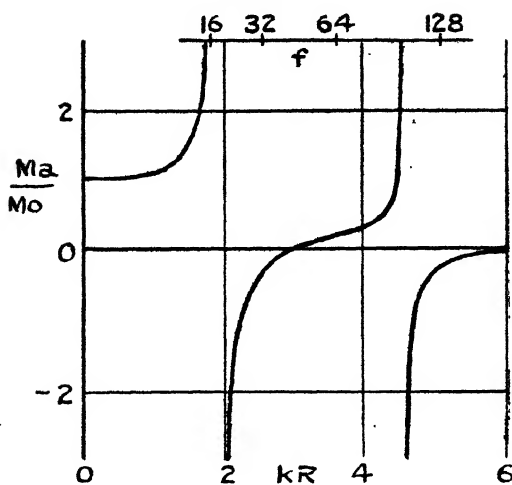
For the disk vibrating with its centre fixed the natural frequencies are given by

$$A + 11593 B + C = 0, \quad \dots \quad (59a)$$

as before. Succeeding oscillations occur when  $kR$  is approximately 1.9, 4.6, 7.9, etc.

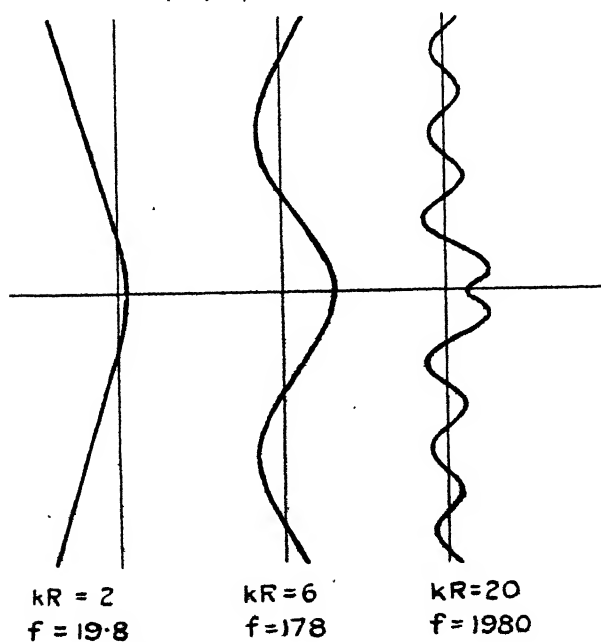
The natural oscillations with fixed centre have limited amplitudes determined by the magnitude of the applied alternating harmonic force. The amplitudes of the natural oscillations with free centre are, however, large, and are only limited by dissipation and radiation, the extent to which the limitation is operative being, of course, conditioned by the magnitude of the applied force.

Fig. 8.



Variation of apparent mass of disk with free edge.

Fig. 9.



Form of free edge disk at typical frequencies.

*Annulus or Disk with both Edges Free.*

The general equations expressing the conditions are

$$AJ_1(kR) + BY_1(kR) + CI_1(kR) - DK_1(kR) = 0, \quad (34c)$$

$$\frac{\sigma-1}{\sigma \cdot kR} \{AJ_1(kR) + BY_1(kR) - CI_1(kR) + DK_1(kR)\}$$

$$- \{AJ_0(kR) + BY_0(kR) - CI_0(kR) - DK_0(kR)\} = 0, \quad (35c)$$

$$\frac{\sigma-1}{\sigma \cdot kr} \{AJ_1(kr) + BY_1(kr) - CI_1(kr) + DK_1(kr)\}$$

$$- \{AJ_0(kr) + BY_0(kr) - CI_0(kr) - DK_0(kr)\} = 0. \quad (36c)$$

These equations completely determine the motion. For the natural vibrations we have

$$AJ_1(kr) + BY_1(kr) + CI_1(kr) - DK_1(kr) = 0. \quad (37c)$$

The frequencies may be determined from these four equations.

If  $kr$  be made very small, (36c) becomes

$$B - D = 0, \quad . \quad . \quad . \quad . \quad . \quad (61)$$

and (37c) becomes

$$B + D = 0. \quad . \quad . \quad . \quad . \quad . \quad (62)$$

Hence

$$B = D = 0. \quad . \quad . \quad . \quad . \quad . \quad (63)$$

Substituting in (34c) and (35c), we obtain

$$I_1(kR) \cdot J_0(kR) + I_0(kR) \cdot J_1(kR) = \frac{2(\sigma-1)}{\sigma \cdot kR} J_1(kR) \cdot I_1(kR),$$

$$. \quad . \quad . \quad . \quad (60a)$$

which is identical with (60). It will be noted that the assumptions involved in the two cases are fundamentally different. The identity of the results shows that the behaviour of the disk is unaltered by its being punctured at its centre, a result which is consistent with the fact that the curvature and radial stress disappear at the centre of the disk.

*Asymptotic Conditions at High Frequencies.*

Curves given so far have been plotted for values of the argument  $kR$  not exceeding 6. For the aluminium diaphragm already mentioned this corresponds to frequencies below 178 cycles per second. It is clear that for the major part of the musical scale the argument of the relevant functions, being proportional to the square of the frequency, assumes

fairly large values, and the asymptotic values of the functions themselves become applicable.

For the disk, whether free or clamped at its edge, we find approximately

$$\frac{B}{A} = \frac{D}{A} = -\frac{J_0 + J_1}{Y_0 + Y_1}, \quad \dots \quad (52b)$$

$$\text{and} \quad \frac{C}{A} = 0. \quad \dots \quad (53b)$$

The apparent mass therefore approximates to (from (57) and (57a))

$$\begin{aligned} M_a &= \frac{4\pi m}{k^2} \frac{J_0 + J_1}{-(Y_0 + Y_1) + (\log 2 - \gamma)(J_0 + J_1)} \\ &= \frac{4\pi m}{k^2} \frac{J_0 + J_1}{G_0 + G_1} = \frac{8m}{k^2} \tan kR, \quad \dots \quad (57b) \end{aligned}$$

(the argument being  $kR$ )

$$\text{whence} \quad \frac{M_a}{M_0} = \frac{8 \tan kR}{\pi k^2 R^2}. \quad \dots \quad (64)$$

At high frequencies the natural oscillations are thus given by

$$kR = n\pi, \quad \dots \quad (65)$$

and the oscillations with fixed centre by

$$kR = (n + \frac{1}{2})\pi. \quad \dots \quad (66)$$

These conditions are approached for comparatively small values of  $kR$ .

Fig. 10 shows the asymptotic variations of apparent mass over the musical scale, together with the variations at low frequency for the free edge disk. The distribution of the natural oscillations of this disk is shown on the same figure.

For parts of the disk well removed from both centre and edge the displacement equation at very high frequencies becomes

$$y = AJ_0(kx) + BY_0(kx), \quad \dots \quad (67)$$

where

$$J_0 = \sqrt{\frac{1}{\pi x}} (\cos kx + \sin kx),$$

$$Y_0 = (\log 2 - \gamma) \sqrt{\frac{1}{\pi x}} (\cos kx + \sin kx)$$

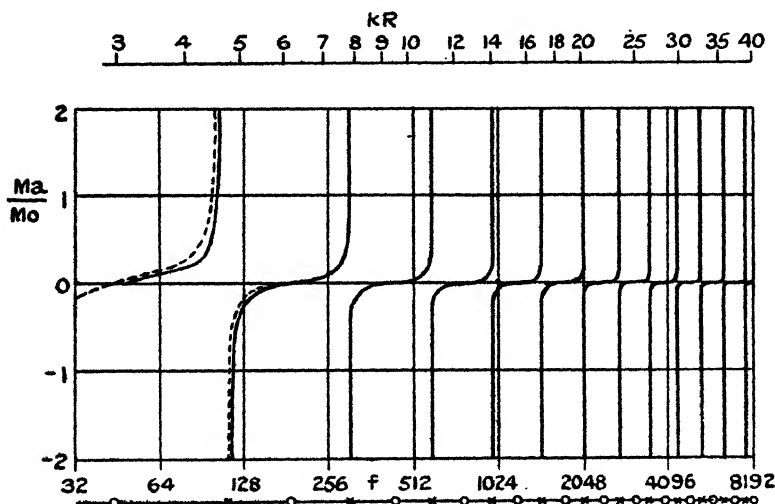
$$- \frac{1}{2} \sqrt{\frac{\pi}{x}} (\cos kx - \sin kx)$$



$$\frac{B}{A} = \frac{\tan kR}{\frac{\pi}{2} - (\log 2 - \gamma) \tan kR}$$

There is therefore a decrescent sinusoidal variation of displacement along the axis of the disk, the amplitude at any radius  $x$  being proportional to  $1/\sqrt{x}$ ; the wave-length  $\lambda$  is  $2\pi/k$ . It is towards this condition that the third curve of fig. 9 approximates.

Fig. 10.



The full curve shows the variation of the apparent mass of either a free or clamped edge disk calculated from the asymptotic values of the functions. The broken line refers to a free edge disk using the true values of the functions.

⊙ Natural oscillations, centre free; amplitude limited only by dissipation and radiation.

× Natural oscillations, centre fixed; amplitude definitely limited.

### Conclusion.

Present day practice in loud speaker design is based upon the theory of the rigid diaphragm, analysed by Rayleigh and others. It is true that to secure increased rigidity practical diaphragms are usually coned. Such a conformation affects not only the stiffness but also the acoustic output. The elastic equations of such diaphragms are different from those for flat disks. The differences, however, are not fundamental, but rather of degree. Other reasons must be sought for the

fact that in practice the reproduction of the upper portion of the musical scale is realized, although it is denied by the "rigid disk" theory. The analysis presented above cannot claim to be more than a contribution towards the more general solution of the problem. The effect of flexure of the diaphragm upon its acoustic output has not yet been examined, except roughly. But it is suggested that the "rigid disk" theory must be abandoned. It has served the useful practical purpose of securing good reproduction over the lower portion of the musical scale; in isolated cases empirical work has extended the range of quality over the greater part of the musical range. Till, however, the theory has been placed upon a sound basis design cannot be satisfactory.

That the types of vibrations suggested above actually occur is easily shown experimentally. The unsymmetrical vibrations have not been considered; they do not lend themselves so readily to analysis. But from the practical point of view they should be of little importance. They can only arise as highly damped transients or from bad design, and can be avoided. The symmetrical vibrations must occur at all frequencies; they are of importance over a considerable portion of the musical range.

---

LXXXIV. *Lag in a Thermometer when the Temperature of the External Medium is Varying.* By A. T. STARR, B.A. (Cantab.), B.Sc. (London)\*.

1. *Introduction.*

A. R. McLEOD† has discussed the lag in a thermometer with a spherical or cylindrical bulb in a medium whose temperature varies at a constant rate. Dr. Bromwich‡ has treated the same problem by the method of the Heaviside operational calculus. S. P. Owen§ has allowed for the containing glass vessel. It is here attempted to treat the problem for a more general variation of temperature of the external medium, the method being that of the operational calculus.

\* Communicated by the Author.

† Phil. Mag. i. p. 134 (1919).

‡ Phil. Mag. i. p. 407 (1919).

§ Lond. Math. Soc. (1920).

It is very difficult, if not impossible, to obtain a theoretical expression for the rate of climb of an aeroplane, and hence for its height at any given time. But it is comparatively easy to take an actual curve between height and time and find an analytical expression for the height in terms of time. It is known that the temperature of the atmosphere decreases linearly with the height from the ground for the heights that aeroplanes attain at present, and hence we have a relation between the temperature of the external medium and the time which will fit the actual case as closely as we need.

## 2. *Determination of the Temperature of the Medium as a Function of the Time.*

We take the temperature of the air (which is here the external medium) at ground-level as the standard temperature, and call it the zero temperature.

Let  $u$  be the temperature of the atmosphere at height  $Z$ , and  $t$  the time to reach the height  $Z$ .

Then we have

$$u = -\alpha Z,$$

where  $\alpha$  is a constant.

The curve connecting  $Z$  and  $t$  is given.

Let us take, as an example, the actual case of a supercharged "Liberty" engine, D.H.9.A.

The curve is fairly straight to begin with, showing a constant rate of climb, but then becomes concave downwards, showing a diminished rate of climb, as we should expect.

It is reasonable to assume that the curve can be expressed as  $Z$  in an ascending power series in  $t$ , viz. :—

$$Z = a_1 t + a_2 t^2 + a_3 t^3 + a_4 t^4 + \dots$$

We find that the coefficients decrease rapidly, and we may stop at  $a_4 t^4$ .

We have the following values of height for time :—

$t$ (in minutes) ...	0.	5.	10.	15.	20.	25.	30.	35.	40.
$Z$ (in feet) .....	0	4800	9300	14000	18500	23000	26900	30700	33500

Assuming that

$$Z = a_1 t + a_2 t^2 + a_3 t^3 + a_4 t^4, \quad \dots \quad (1)$$

and substituting for  $t = 10, 20, 30, 40$ , we get

$$a_1 = 919.25, \quad a_2 = 1.625, \quad a_3 = -.0417, \quad a_4 = -.00125.$$

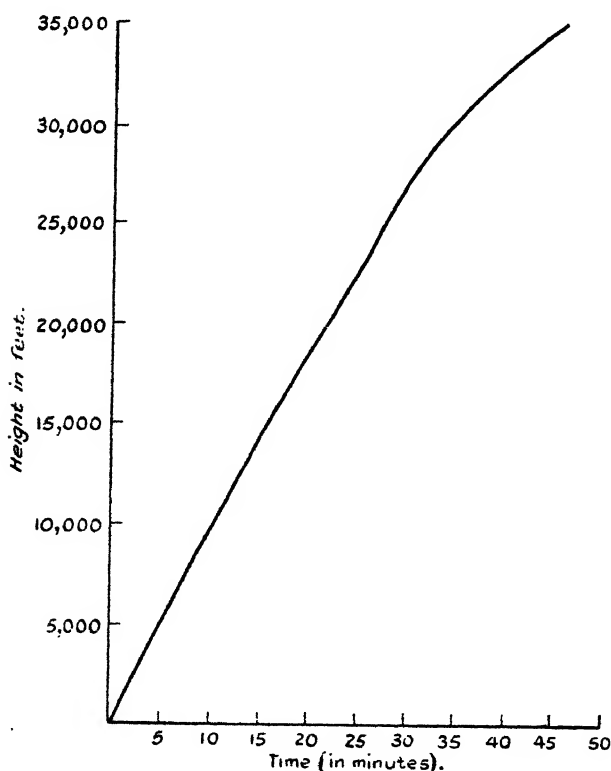
These values fit the curve almost exactly at  $t=10, 20, 30, 40$ , and give  $Z=4730, 13950, 22857$  respectively at  $t=5, 15, 25$ .

The fact that  $a_2$  is positive shows that the best rate of climb is not at the ground-level, but at some higher level.

The value of  $t$  for the best rate of climb is given by

$$\frac{d^2Z}{dt^2} = 2a_2 + 6a_3t + 12a_4t = 0,$$

giving  $t=8.6$ , corresponding to a height of about 8000 feet.



We thus have

$$\begin{aligned} u &= -(919.25t + 1.625t^2 - .0417t^3 - .00125t^4) \\ &= b_1t + b_2t^2 + b_3t^3 + b_4t^4. \end{aligned}$$

### 3. *Thermometer with a Spherical Bulb and Infinite Surface Conductivity.*

Let us consider the case of a thermometer with a spherical bulb, neglecting the effect of the containing glass vessel and



We thus get

$$rv/c = \frac{\sinh(qr/c)}{\sinh q} \int_{-\infty}^{\infty} \phi(h) e^{-ph} p H(t) dh,$$

which expresses  $v$  in operational form.

This can be translated back into ordinary form by Bromwich's method of the complex variable\*, and we obtain

$$\begin{aligned} rv/c &= \frac{1}{2\pi i} \int_L e^{pt} \frac{\sinh(qr/c)}{\sinh q} dp \int_{-\infty}^{\infty} \phi(h) e^{-ph} dh \\ &= \frac{1}{2\pi i} \int_{-\infty}^{\infty} \phi(h) dh \int_L e^{p(t-h)} \frac{\sinh(qr/c)}{\sinh q} dp, \quad (4) \end{aligned}$$

where  $p$ , in this last integral, is regarded as a complex variable,  $q$  is given by equation (2), and  $L$  is a curve from  $c - i\alpha$  to  $c + i\alpha$ , where  $c$  is positive and finite, such that all the singularities of the integrand are on the left side of the path.

In (4) the range of  $h$ , which gives a contribution to the integral, is  $0 \leq h \leq t$ .

So

$$\frac{rv}{c} = \frac{1}{2\pi i} \int_L e^{pt} \frac{\sinh(qr/c)}{\sinh q} dp \int_0^t e^{-ph} \phi(h) dh.$$

The poles of the integrand for the complex integration occur at  $q = in\pi$ ,  $n=0$  being excluded, i. e., at  $p = -n^2\pi^2\alpha^2/c^2$ . We then get for (4)

$$\frac{rv}{c} = -\frac{2\pi\alpha^2}{c^2} \sum_{n=1}^{\infty} (-1)^n n \sin \frac{n\pi r}{c} \int_0^t e^{-n^2\pi^2(t-h)/c^2} \phi(h) dh,$$

which is the expression that McLeod obtains.

The thermometer registers the average value of the temperature, viz.,

$$\bar{v} = (3/4\pi c^3) \int_0^a 4\pi r^2 v dr. \quad \dots \quad (5)$$

We can find  $\bar{v}$  from (5), as McLeod does, but it is easiest to delay the interpretation of the operational form until the final stage; for example, here we first take the average, treating operators as ordinary numbers during this process, and then we interpret. This is one of the great advantages of the operational method, and very much labour is saved in this way.

\* H. Jeffreys, *loc. cit.* p. 19, (2).

For the general case of  $u = \phi(t)$  we get

$$\begin{aligned}\bar{v} &= 3 \left( \frac{1}{q} \coth q - \frac{1}{q^2} \right) u \\ &= \frac{3}{2\pi i} \int_L e^{pt} \left( \frac{1}{q} \coth q - \frac{1}{q^2} \right) dp \int_{-\infty}^{\infty} \phi(h) e^{-ph} dh \\ &= \frac{3}{2\pi i} \int_L e^{pt} \left( \frac{1}{q} \coth q - \frac{1}{q^2} \right) dp \int_0^t \phi(h) e^{-ph} dh \\ &= 3 \int_0^t \left[ \phi(h) dh \times \text{residues of } e^{p(t-h)} \left( \frac{1}{q} \coth q - \frac{1}{q^2} \right) \right] \\ &= \frac{6a^2}{c^2} \sum_{n=1}^{\infty} \int_0^t \phi(h) e^{-\frac{n^2\pi^2 a^2}{c^2}(t-h)} dh. \quad \dots \dots \dots (6)\end{aligned}$$

This gives the average temperature for a general variation of the temperature of the external medium.

If  $\phi(t) = (Gt)$ , (6) gives

$$\bar{v} = Gt - \frac{1}{15} \frac{c^2}{a^2} G + 6G \frac{c^2}{\pi^4 a^2} \sum_{n=1}^{\infty} n^{-4} e^{-n^2\pi^2 a^2 t/c^2}, \quad \dots (7)$$

agreeing with McLeod's particular result.

The lag is thus

$$\frac{1}{15} \frac{c^2}{a^2} G - 6G \frac{c^2}{\pi^4 a^2} \sum_{n=1}^{\infty} n^{-4} e^{-n^2\pi^2 a^2 t/c^2}. \quad \dots \dots (8)$$

In our case  $u$  is easily transposable into operational form, and we have

$$u = b_1 t + b_2 t^2 + b_3 t^3 + b_4 t^4 = b_1/p + b_2 2!/p^2 + b_3 3!/p^3 + b_4 4!/p^4.$$

Hence

$$\bar{v} = 3 \left( \frac{1}{q} \coth q - \frac{1}{q^2} \right) (b_1/p + b_2 2!/p^2 + b_3 3!/p^3 + b_4 4!/p^4). \quad (9)$$

But

$$\begin{aligned}\frac{1}{q} \coth q - \frac{1}{q^2} &= 2^2 B_2/2! + 2^4 B_4 q^2/4! + 2^6 B_6 q^4/6! + \dots \text{etc.} \\ &= A_2 + A_4 q^2 + A_6 q^4 + \dots, \quad \text{say,}\end{aligned}$$

where  $B_2, B_4, \dots$  are Bernoulli's numbers. Hence

$$\left( \frac{1}{q} \coth q - \frac{1}{q^2} \right) t^n$$

has a polynomial contribution of

$$\begin{aligned}& (A_2 + A_4 p c^2/a^2 + A_6 p^2 c^4/a^4 + \dots) n! p^{-n} \\ &= A_2 t^n + A_4 n t^{n-1} c^2/a^2 + A_6 n(n-1) t^{n-2} c^4/a^4 + \dots\end{aligned}$$

Thus  $\bar{v}$  has a polynomial contribution

$$\begin{aligned}
 & 3b_1\{A_2t + A_4c^2/a^2\} + 3b_2\{A_2t^3 + A_42c^2t/a^2 + A_62c^4/a^4\} \\
 & \quad + 3b_3\{A_2t^3 + A_43c^2t^2/a^2 + A_63.2.c^4t/a^4 + A_83.2.c^6/a^6\} \\
 & \quad + 3b_4\{A_2t^4 + A_44c^2t^3/a^2 + A_64.3.c^4t^2/a^4 \\
 & \quad \quad + A_84.3.2.c^6t/a^6 + A_{10}4.3.2.c^8/a^8\} \\
 & = 3A_2(b_1t + b_2t^2 + b_3t^3 + b_4t^4) \\
 & \quad + 3A_4(c^2/a^2)[b_1 + 2b_2t + 3b_3t^2 + 4b_4t^3] \\
 & \quad + 3A_6(c^4/a^4)[2b_2 + 3.2b_3t + 4.3b_4t^2] \\
 & \quad + 3A_8(c^6/a^6)[3.2.1.b_3 + 4.3.2.b_4t] \\
 & \quad + 3A_{10}(c^8/a^8)4.3.2.1.b_4 \\
 & = 3A_2u + 3A_4c^2a^{-2}u' + 3A_6c^4a^{-4}u'' + 3A_8c^6a^{-6}u''' \\
 & \quad + 3A_{10}c^8a^{-8}u''', \quad (10)
 \end{aligned}$$

where dashes denote differentiation with respect to  $t$ . It is obvious that expression (10), continued for the requisite number of terms, would hold when  $u$  is a finite polynomial in  $t$ .

We have

$$B_2 = \frac{1}{6}, \quad B_4 = -\frac{1}{30}, \quad B_6 = \frac{1}{42}, \quad B_8 = -\frac{1}{30}, \quad B_{10} = \frac{5}{66},$$

and hence

$$A_2 = \frac{1}{3}, \quad A_4 = \frac{1}{45}, \quad A_6 = \frac{2}{945}, \quad A_8 = -\frac{1}{4725}, \quad A_{10} = \frac{2}{93555}.$$

The polynomial contribution thus found is the contribution to the general sum by the residue at  $p=0$ , which is a pole of

$$\left(\frac{1}{q} \coth q - \frac{1}{q^2}\right)p^{-m},$$

if  $m > 0$ . This is the part which predominates when  $t \rightarrow \infty$ , for then the other terms tend *exponentially* to zero. This is an example of the tendency that operators have of resembling ordinary numbers; for  $p^{-1} = t$ , and we see that the important part at  $t = \infty$  is the part obtained at  $p = 0$ .

$$\left(\frac{1}{q} \coth q - \frac{1}{q^2}\right)p^{-m}$$



has poles at  $q = in\pi$ , corresponding to  $p = n^2\pi^2 a^2 c^{-2} = \alpha_n$ , say.  
 $\bar{v}$  is  $f(p)/\Delta(p)$ , where  $f(p)$  and  $\Delta(p)$  are *polynomials* in  $p$ , given by

$$f(p) = (q \cosh q - \sinh q)/q^3,$$

and

$$\Delta(p) = p^m \sinh q/q.$$

$$f(\alpha_n) = (-1)^{n-1} n^{-2} \pi^{-2}$$

and

$$\alpha_n \Delta'(\alpha_n) = \alpha_n^{m+1} \frac{1}{q} \frac{dq}{dp} \cosh q = (-1)^n \frac{1}{2} \alpha_n^m.$$

Hence the exponential terms given by

$$\left( \frac{1}{q} \coth q - \frac{1}{q^2} \right) p^{-m}$$

are

$$(-1)^{m+1} (2a^2/c^2) \sum_{n=1}^{\infty} (n^2\pi^2 a^2/c^2)^{-m-1} e^{-n^2\pi^2 a^2 t/c^2}.$$

Thus the final expression for  $\bar{v}$  is the expression (10) plus

$$\left. \begin{aligned} & 6b_1 \frac{a^2}{c^2} \sum_{n=1}^{\infty} \left( \frac{n^2\pi^2 a^2}{c^2} \right)^{-2} e^{-n^2\pi^2 a^2 t/c^2}, \\ & -12b_2 \frac{a^2}{c^2} \sum_{n=1}^{\infty} \left( \frac{n^2\pi^2 a^2}{c^2} \right)^{-3} e^{-n^2\pi^2 a^2 t/c^2}, \\ & +36b_3 \frac{a^2}{c^2} \sum_{n=1}^{\infty} \left( \frac{n^2\pi^2 a^2}{c^2} \right)^{-4} e^{-n^2\pi^2 a^2 t/c^2}, \\ & -144b_4 \frac{a^2}{c^2} \sum_{n=1}^{\infty} \left( \frac{n^2\pi^2 a^2}{c^2} \right)^{-5} e^{-n^2\pi^2 a^2 t/c^2}. \end{aligned} \right\} \quad \cdot \cdot \quad (11)$$

The steady lag is

$$\begin{aligned} & -3\{A_4 c^2 a^{-2} u' + A_6 c^4 a^{-4} u'' + A_8 c^6 a^{-6} u''' + A_{10} c^8 a^{-8} u''''\} \\ & = \frac{1}{15} \frac{c^2}{a^2} u' - \frac{2}{315} \frac{c^4}{a^4} u'' + \frac{1}{1575} \frac{c^6}{a^6} u''' - \frac{2}{31185} \frac{c^8}{a^8} u'''' \quad (12) \end{aligned}$$

#### 4. The Sphere with Finite Conductivity at the Surface.

The surface condition is now

$$K \frac{\partial v}{\partial r} = h(u-v), \quad \text{at } r = c.$$

Substituting in  $rv = A \sinh(qr/c)$ , we obtain

$$\frac{rv}{c} = \frac{ch \sinh(qr/c)}{K(q \cosh q - \sinh q) + ch \sinh q} u.$$

This gives

$$\begin{aligned} \bar{v} &= \frac{3ch(q \cosh q - \sinh q)/q^2}{ch \sinh q + K(q \cosh q - \sinh q)} u \\ &= \frac{3\left(\frac{1}{q} \coth q - \frac{1}{q^2}\right)}{1 + \lambda q^2 \left(\frac{1}{q} \coth q - \frac{1}{q^2}\right)} u, \dots \dots \dots (13) \end{aligned}$$

where

$$\lambda = \frac{K}{ch}.$$

The operator acting on  $u$  in (13), when expanded in ascending powers of  $q^2$ , gives

$$\begin{aligned} &A_2 + q^2(A_4 - \lambda A_2^2) + q^4(A_6 - \lambda 2A_2A_4 + \lambda^2 A_2^3) \\ &\quad + q^6[A_8 - \lambda(2A_2A_6 + A_4^2) + \lambda^2 3A_2^2A_4 - \lambda^3 A_2^4] \\ &\quad + q^8[A_{10} - \lambda(2A_2A_8 + 2A_4A_6) + \lambda^2(3A_2^2A_6 + 3A_2A_4^2) \\ &\quad \quad - \lambda^3 4A_2^3A_4 + \lambda^4 A_2^5] \\ &\quad + \text{higher powers of } q \\ &= A_2 + A_4' q^2 + A_6' q^4 + A_8' q^6 + A_{10}' q^8 + \dots, \text{ say.} \end{aligned}$$

By (12) the steady lag is

$$-3\{A_4' c^2 a^{-2} u' + A_6' c^4 a^{-4} u'' + A_8' c^6 a^{-6} u''' + A_{10}' c^8 a^{-8} u'''\},$$

where

$$A_4' = -\frac{1}{45} - \frac{\lambda}{9}, \quad A_6' = \frac{2}{945} + \frac{2\lambda}{135} + \frac{\lambda^2}{27},$$

$$A_8' = -\frac{1}{4725} - \frac{8\lambda}{10125} - \frac{\lambda^2}{135} - \frac{\lambda^3}{81},$$

$$A_{10}' = \frac{2}{93555} + \frac{2\lambda}{8505} + \frac{17\lambda^2}{14175} + \frac{4\lambda^3}{1215} + \frac{\lambda^4}{243},$$

giving for the steady lag the value

$$\begin{aligned} &\left(\frac{1}{15} \frac{c^2}{a^2} u' - \frac{2}{315} \frac{c^4}{a^4} u'' + \frac{1}{1575} \frac{c^6}{a^6} u''' - \frac{2}{31185} \frac{c^8}{a^8} u'''\right) \\ &\quad + \lambda \left(\frac{1}{3} \frac{c^2}{a^2} u' - \frac{2}{45} \frac{c^4}{a^4} u'' + \frac{8}{3375} \frac{c^6}{a^6} u''' - \frac{2}{2835} \frac{c^8}{a^8} u'''\right) \end{aligned}$$

$$\begin{aligned}
& + \lambda^3 \left( -\frac{1}{9} \frac{c^4}{a^4} u'' + \frac{1}{45} \frac{c^6}{a^6} u''' - \frac{17}{4725} u'''' \right) \\
& + \lambda^3 \left( \frac{1}{27} \frac{c^6}{a^6} u''' - \frac{4}{405} \frac{c^8}{a^8} u'''' \right) - \lambda^4 \frac{1}{81} \frac{c^8}{a^8} u'''' . . . \quad (14)
\end{aligned}$$

The poles of (13) are given by

$$1 - \lambda + \lambda q \coth q = 0,$$

i. e., by  $q = i\omega$ , where  $\omega \cot \omega = 1 - 1/\lambda$ ,  $\omega$  being known to be real\*.

Considering

$$3 \left( \frac{1}{q} \coth q - \frac{1}{q^3} \right) p^{-n} / \left\{ 1 + \lambda q^2 \left( \frac{1}{q} \coth q - \frac{1}{q^3} \right) \right\},$$

we have

$$F(p) = 3(q \coth q - \sinh q)/q^3,$$

$$\Delta(p) = p^n \{ \sinh q + \lambda(q \cosh q - \sinh q) \} / q,$$

whence

$$F(\alpha)/\alpha \Delta'(\alpha) = \frac{6a^2}{c^2} \frac{1}{(1 - \lambda + \lambda^2 \omega^2) \left( -\frac{\alpha^2 \omega^2}{c^2} \right)^{n+1}}.$$

Thus the lag is expression (14) plus the following :

$$\left. \begin{aligned}
& - 6b_1 \frac{c^2}{a^2} \sum \frac{1}{(1 - \lambda + \lambda^2 \omega^2) \omega^4} e^{-\alpha^2 \omega^2 t / c^2}, \\
& + 12b_2 \frac{c^4}{a^4} \sum \frac{1}{(1 - \lambda + \lambda^2 \omega^2) \omega^6} e^{-\alpha^2 \omega^2 t / c^2}, \\
& - 36b_3 \frac{c^6}{a^6} \sum \frac{1}{(1 - \lambda + \lambda^2 \omega^2) \omega^8} e^{-\alpha^2 \omega^2 t / c^2}, \\
& + 144b_4 \frac{c^8}{a^8} \sum \frac{1}{(1 - \lambda + \lambda^2 \omega^2) \omega^{10}} e^{-\alpha^2 \omega^2 t / c^2}.
\end{aligned} \right\} . . . \quad (15)$$

### 5. Cylindrical Bulb with Infinite Surface Conductivity.

The equation of heat-conduction is now

$$\frac{1}{r} \frac{\partial}{\partial r} \left( r \frac{\partial v}{\partial r} \right) = \frac{1}{a^2} \frac{\partial v}{\partial t},$$

\* Vide Bromwich, *loc. cit.*

leading to  $I_0(qr/c)$  instead of  $\{\sinh(qr/c)/(qr/c)\}$ , where  $I_0(x)$  is the modified Bessel function  $J_0(ix)$ . We obtain

$$\bar{v} = \frac{2}{c^2} \int_0^c rv \, dr = \frac{2}{q} \frac{I_0'(q)}{I_0(q)} u. \quad (16)$$

We have

$$\frac{2}{q} \frac{I_0'(q)}{I_0(q)} = 1 + C_4 q^2 + C_6 q^4 + C_8 q^6 + \dots,$$

where

$$C_4 = -\frac{1}{2.4}, \quad C_6 = \frac{4}{2.4^2.6}, \quad C_8 = \frac{-33}{2.4^2.6^2.8},$$

$$C_{10} = \frac{1026}{2.4^2.6^2.8^2.10}.$$

Hence, as in (10), the pole  $p=0$  gives a steady lag of

$$-[C_4 c^2 a^{-2} u' + C_6 c^4 a^{-4} u'' + C_8 c^6 a^{-6} u''' + C_{10} c^8 a^{-8} u''']. \quad (17)$$

The other poles of (16) are given by

$$q = i\omega, \quad p = -a^2 \omega^2 / c^2,$$

where  $J_0(\omega) = 0$ .

$$\frac{2}{q} \frac{I_0'(q)}{I_0(q)} p^{-n} = \frac{4a^2}{c^2} \sum \left( -\frac{c^2}{a^2 \omega^2} \right)^{n+1} e^{-a^2 \omega^2 t / c^2}.$$

Hence

$$\begin{aligned} \bar{v} = u - & \frac{1}{8} \frac{c^2}{a^2} u' + \frac{4}{2.4^2.6} \frac{c^4}{a^4} u'' - \frac{33}{2.4^2.6^2.8} \frac{c^6}{a^6} u''' \\ & + \frac{1026}{2.4^2.6^2.8^2.10} \frac{c^8}{a^8} u'''' \\ & + \frac{4c^2}{a^2} b_1 \sum \frac{1}{\omega^4} e^{-a^2 \omega^2 t / c^2} - \frac{8c^4}{a^4} b_2 \sum \frac{1}{\omega^6} e^{-a^2 \omega^2 t / c^2} \\ & + 24 \frac{c^6}{a^6} b_3 \sum \frac{1}{\omega^8} e^{-a^2 \omega^2 t / c^2} - 96 \frac{c^8}{a^8} b_4 \sum \frac{1}{\omega^{10}} e^{-a^2 \omega^2 t / c^2}. \quad (18) \end{aligned}$$

## 6. Cylindrical Bulb with Finite Surface Conductivity.

Instead of equation (16), we obtain

$$\begin{aligned} \bar{v} &= \frac{2}{q} \frac{I_0'(q)}{I_0 + \lambda q I_0'(q)} u \quad (19) \\ &= \frac{\frac{2}{q} I_0'(q) / I_0(q)}{1 + \frac{1}{2} \lambda q^2 \left\{ \frac{2}{q} I_0'(q) / I_0(q) \right\}} u. \end{aligned}$$

The operator in (19) when expanded is

$$(1 + C_4' q^2 + C_6' q^4 + C_8' q^6 + C_{10}' q^8),$$

where

$$C_4' = C_4 - \frac{1}{2}\lambda, \quad C_6' = C_6 - \frac{1}{2}\lambda 2C_2C_4 + \frac{1}{4}\lambda^2,$$

$$C_8' = C_8 - \frac{1}{2}\lambda(2C_2C_6 + C_4^2) + \frac{1}{4}\lambda^2 3C_2C_4 - \frac{1}{8}\lambda^3,$$

$$C_{10}' = C_{10} - \frac{1}{2}\lambda(2C_2C_8 + 2C_4C_6) + \frac{1}{4}\lambda^2(3C_2^2C_6 + 3C_2C_4^2) \\ - \frac{1}{8}\lambda^3 4C_2^3C_4 + \frac{1}{16}\lambda^4.$$

Hence the pole  $p=0$  gives to  $\bar{v}$  the expression

$$u + C_4' c^2 a^{-2} u' + C_6' c^4 a^{-4} u'' + C_8' c^6 a^{-6} u''' + C_{10}' c^8 a^{-8} u'''. \quad (20)$$

The other poles are at

$$q = i\omega, \quad p = -a^2 \omega^2 / c^2,$$

where

$$J_0(\omega) + \lambda \omega J_0'(\omega) = 0.$$

We have

$$\left( \frac{\frac{2}{q} I_0'(q) / I_0(q)}{1 + \frac{1}{2} \lambda q^2 \left\{ \frac{2}{q} I_0'(q) / I_0(q) \right\}} \right) p^{-n} \\ = \frac{4a^2}{c^2} \sum \frac{(-c^2/a^2)^{n+1}}{(1 + \lambda^2 \omega^2) \omega^{n+1}} e^{-a^2 \omega^2 t / c^2}.$$

Hence  $\bar{v}$  = expression (20).

$$+ 4 \frac{c^2}{a^2} b_1 \sum \frac{1}{\omega^4 (1 + \lambda^2 \omega^2)} e^{-a^2 \omega^2 t / c^2} \\ - 8 \frac{c^4}{a^4} b_2 \sum \frac{1}{\omega^6 (1 + \lambda^2 \omega^2)} e^{-a^2 \omega^2 t / c^2} \\ + 24 \frac{c^6}{a^6} b_3 \sum \frac{1}{\omega^8} \frac{1}{1 + \lambda^2 \omega^2} e^{-a^2 \omega^2 t / c^2} \\ - 96 \frac{c^6}{a^6} b_4 \sum \frac{1}{\omega^{10}} \frac{1}{1 + \lambda^2 \omega^2} e^{-a^2 \omega^2 t / c^2}.$$

I wish to thank the Department of Scientific and Industrial Research for their grant, which made this work possible.

LXXXV. *A Molecular Theory of Elastic Hysteresis.* By  
G. A. TOMLINSON, B.Sc. (From The National Physical  
Laboratory.)\*.

1. **V**ARIOUS theories have been proposed to account for the phenomena of elastic hysteresis, though none has yet apparently received general acceptance, and for this reason a new theory put forward tentatively in the following paper may have some features worth consideration.

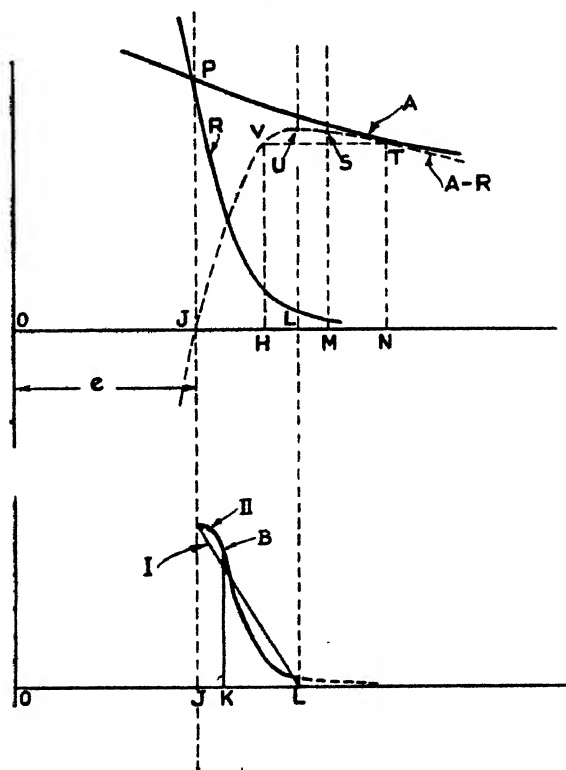
Earlier workers, and even some contemporary workers, have considered that some form of solid friction or viscosity always opposes an elastic strain, and so causes elastic hysteresis. Such an idea does not accord very well with present views regarding the nature of an elastic strain, unless it can be asserted that there is friction between two neighbouring atoms in a crystal lattice. Various recent workers are therefore inclined to attribute hysteresis to a loss of energy occurring in some way amongst the atoms at the crystal boundaries<sup>(1)</sup>. The term internal friction is still widely used, however, as the phenomena undoubtedly suggest the presence of some kind of friction.

In a previous paper<sup>(2)</sup> the writer has suggested an atomic theory of solid friction, based on the hypothesis that the atoms are subject to both an attraction and a repulsion, the latter having a considerably greater rate of change and a much smaller range than the former. It is now suggested that elastic hysteresis is due to the same atomic mechanism involving a loss of energy when a solid passes through a strain cycle. A brief *résumé* of the hypothesis advanced in the previous paper is necessary for the discussion of the present theory. It is not necessary to take into account the nature of the atomic forces, or to assume any mathematical relation between the forces and the atomic distances. It is assumed, however, that atomic equilibrium is obtained simply by the action of the two forces of attraction and repulsion, and the supposed forces are shown by the descriptive curves A and R of fig. 1, the abscissæ being the distance between the atom-centres. This distance is normally  $e$  or OJ in the unstrained material, when A and R are equal and opposite.

\* Communicated by the Author.

At this point the atoms are in highly stable equilibrium, since  $\frac{dR}{dx}$  is much greater than  $\frac{dA}{dx}$ , and on increasing the distance between them the equilibrium remains stable for some distance, but gradually changes into an unstable state at some separation OL at which  $\frac{dR}{dx} = \frac{dA}{dx}$ .

Fig. 1.



Consider a simple chain of three atoms originally in equilibrium, as shown by the point P, and suppose the outer ones to be gradually drawn away. The middle atom will remain equidistant from its neighbours in stable equilibrium so long as the separation of the atoms does not exceed OL. The atoms can be restored to their original position or beyond, or generally may go through any cycle of displacements for any number of times without loss of

energy, provided the range of stable equilibrium is not exceeded.

If we now suppose the chain of atoms to be further extended so that the separation of each pair exceeds OL, the equilibrium steadily changes from stable to unstable, and eventually the centre atom must leave its symmetrical position and attach itself to one or other of its neighbours in a condition of stable equilibrium again. Since the change in the condition of equilibrium is gradual and continuous, there is a certain probability that the centre atom may retain its symmetrical position halfway between the others for a very short distance, such as LM, beyond the point at which equilibrium is exactly neutral. It will at this point fly back to one of its attracting neighbours with additional kinetic energy or heat equal to the area LMSU, which is an irreversible stage in the cycle of displacements.

In the writer's theory of friction the surface atoms of two bodies in contact are supposed to form such chains temporarily at all points where the atoms approach close enough to come into repulsion and so support the load. On separating again the above process occurs, and results in what may be described as a plucking action of the atoms on each other, which is irreversible and involves a direct conversion of mechanical work into heat.

The same hypothesis may be applied to any phenomena in which relative motion in repeated cycles occurs amongst the atoms, such as stress-strain or magnetic cycles. The present paper is mainly concerned with the loss of energy accompanying a stress-strain cycle, and in a manner reverts to the view that elastic hysteresis is caused by internal solid friction, though only in the restricted sense in which friction has been treated in the previous paper—that is to say, it is not supposed that any gross tangential frictional forces operate on planes of slip within the solid, in the way that friction ordinarily manifests itself to the senses, but only that the process whereby individual atoms dissipate energy is identical in solid friction and in elastic hysteresis.

The hypothesis may be applied to suggest an interpretation of elastic hysteresis in the following way. It is quite improbable that the whole of the atoms of a solid are arranged throughout in the ideal condition of equilibrium corresponding to the atomic distance OJ of fig. 1.



It is far more likely to be the case that there are a large number of points at which small chains of contiguous atoms are slightly displaced either closer together or further apart than the ideal distance. Such local displacements may have any values between zero and  $JL$  in the one direction, and between zero and some indeterminate limit in the other direction, but we are only concerned for the present with the former. The magnitude of the maximum relative displacement  $JL$  which a pair of neighbour atoms may receive and yet remain in equilibrium is somewhat uncertain, but appears to be small compared with the distance between the atoms. Estimates based on the limiting elastic strain and on the limiting thermal expansion show the possible displacement to be of the order  $\frac{1}{1000}$  to  $\frac{1}{100}$  of the atomic dimensions respectively.

It appears, therefore, that it is only necessary to assume a random distribution of distortion centres involving quite minute atomic displacements as premises for the present hypothesis.

If the material is now supposed to be strained in any manner by which the stretched chains are further extended, certain atoms by our hypothesis will in turn be drawn slightly into the unstable region and will fly back with added kinetic energy. On removing the stress the chains can reform in their original condition. Thus the strain may be quite elastic, in the sense that no atom is finally displaced permanently from its original position, or the dimensions and form of the specimen are exactly recovered, and yet even with very small stresses a loss of energy can occur with every strain cycle, which is found by experiment to be the case. Thus in some experiments described later the writer has found quite a measurable loss of energy when aluminium undergoes a stress cycle of maximum value only 2 lb. per sq. inch.

2. We shall now consider to what extent the theory briefly outlined above is in agreement with certain experimental data of elastic hysteresis. It is well known that the area of the stress-strain hysteresis loop, obtained by using a sensitive extensometer, increases rapidly with the range of stress applied. There are not many data available, however, as to the exact relation between the loss of energy per cycle and the stress range. This is

probably due to the limitations of the extensometer method, as the loss of energy on reducing the stress soon becomes too small for reliable measurement in terms of stress and strain. Some experiments have therefore been made by the writer with the object of finding the relation between the maximum stress and the internal loss per cycle for a number of different materials. A torsional oscillation method was used because of its greater sensitivity, and the loss of energy was found from the rate of decay of amplitude. A ground-steel disk about 6 in. in diameter was suspended in the field of a horizontal optical projector in such a way that a fine indicating point attached to the edge of the disk was in focus on the screen. The period of oscillation was adjusted by means of the length of the suspension to be 4 secs. As the motion of the indicating point was magnified 50 times, only quite a small angular movement was required, the maximum amplitude being less than  $5^\circ$ . This, together with the long period and the smooth form of the disk led to the great advantage that the correction for loss of energy in air resistance was always small and sometimes negligible compared with the hysteresis loss. The actual air resistance of the disk at different amplitudes was fairly well known when oscillating with a period of 4 secs., having been determined experimentally some time previously in the course of some experiments on rolling friction.

The successive amplitudes of the indicating point were marked off at the screen. In some cases a definite number of oscillations were allowed between marking the amplitudes, when the hysteresis damping was small. From these measurements can be found the decrement  $\delta\theta$  per oscillation for any amplitude  $\theta$ . The loss of energy per cycle is then  $\lambda\theta \cdot \delta\theta$ , if  $\lambda$  is the torsional stiffness of the suspension. Since the system has a constant moment of inertia and a constant period,  $\lambda$  is the same for all the materials. The maximum stress in any cycle can be calculated from the equation

$$f_{\max.} = \frac{C\theta r}{l}, \quad (1)$$

where  $C$  = modulus of rigidity,

$r$  = radius of suspension wire,

$l$  = length.

This, however, involves a knowledge of  $C$  for all the materials, and the following method was actually used. If  $T$  is the twisting couple and  $J$  the polar moment of inertia of the cross-section of the wire,

$$f_{\max.} = \frac{T}{J} = \frac{\lambda \theta r}{J} = \frac{2\lambda \theta}{\pi r^3} \quad \dots \quad (2)$$

For the series of materials  $\lambda$  is constant; hence, if  $f_{\max.}$  is calculated by equation (1) for any one material such as steel having a well-established value for  $C$ , it is only necessary to know the radii of all the specimens to be able to calculate the stresses in all other cases by simple proportion from equation (2).

The results that have been obtained from such measurements show that the loss of energy per c.c. per cycle, denoted by  $h$ , is given by

$$h = k(f_{\max.})^n, \quad \dots \quad (3)$$

in which  $k$  is a constant for each material, and the index  $n$  is found to be always about 2, but in a number of metals it is rather greater than 2. In no material tested has an index less than 2 been found.

Since the strain applied is torsional the range of stress to which any element of the specimen is subjected varies from zero to the surface stress  $f_{\max.}$  It can be shown, however, that within the elastic limit the hysteresis loss under uniform shear stress for any maximum stress  $f$  is also proportional to  $(f)^n$ .

Thus, let us assume the loss per c.c. to be  $kf^n$ , then the total loss is given by

$$E = \Sigma k(f)^n \delta V,$$

if  $\delta V$  is an element of volume for which the maximum stress in the cycle is  $f$ , or

$$E = \int_0^a k(f)^n 2\pi r l dr,$$

where  $r$  is the radius of any cylindrical shell of thickness  $dr$ ,  $l$  is the length, and  $a$  the radius of the specimen.

At a radius  $r$  the stress  $f = \frac{f_{\max.}}{a} r$ . Hence

$$E = 2\pi k l \int_0^a \frac{(f_{\max.})^n}{a^n} r^{n+1} dr$$

$$= \frac{2}{n+2} k \pi a^2 l (f_{\max})^n$$

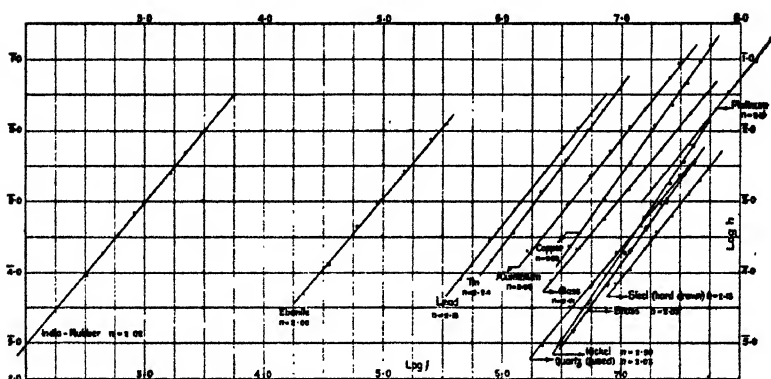
$$= \frac{2}{n+2} k V (f_{\max})^n,$$

or hysteresis loss per unit volume

$$h = \frac{2}{n+2} k (f_{\max})^n. \quad \dots \quad (4)$$

Hence, when the hysteresis loss of a torsion specimen is found to be proportional to a power of the maximum stress at the surface, it follows that the same power law applies

Fig. 2.



to the case of a uniform stress, but the constant in the latter case is greater in the ratio  $\frac{n+2}{2}$ .

The results of the measurements are shown by the curves of fig. 2. These show in c.g.s. units the hysteresis loss per unit volume of the torsion specimens plotted against maximum stress, logarithmic plotting being employed. It will be seen that all the curves are fairly closely linear, and there are slight variations in slope, the index  $n$  being given in brackets for each material. The maximum stress applied is comparatively low, and except for the platinum specimen does not exceed about 1000 lb. per sq. inch, and is as small as 140 lb. per sq. inch for the softer metals tin and lead. There is therefore little doubt that the stresses are well within the ordinary elastic range of the materials.

These results may be compared with those of Kimball and Lovell<sup>3</sup>, who give a general formula for the internal friction loss per unit volume similar to the above, but with a uniform index 2. They state, however, that the formula is not given as an exact relation, but merely as the nearest all round statement of results obtained.

Reverting to the theory, it can be shown that such a result as the above would in general be expected. In the first place the loss of energy entailed in the supposed plucking process is liable to vary considerably, as different atoms may be drawn different distances into the unstable region. A great number of atoms are involved, however, and there will be a statistical average value  $\epsilon$  for this loss of energy. The atoms to be affected first in an elastic strain are those already displaced by the maximum amount  $JL$  of fig. 1. Other atoms initially displaced by an amount such as  $JK$  will contribute to the loss of energy at a stage when the applied strain is equal to  $KL$ . Thus in any strain the total loss of energy depends on the statistical average value of  $\epsilon$  and on the numerical distribution of the initial displacements of the atoms according to the magnitude of the displacement.

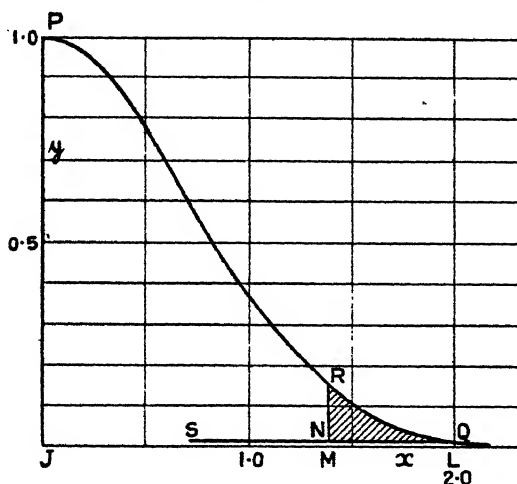
Since the normal distance between the atoms is  $e$  or  $OJ$ , corresponding to equilibrium between the repulsion and attraction, it is reasonable to suppose that of the atoms further apart than this there will be the greatest number in the neighbourhood of  $OJ$  and the least in the neighbourhood of  $OL$ . There should be none at all at greater distances than  $OL$ . If, then, the ordinate  $KB$  of the distribution curve shown at the foot of fig. 1 represents the number of atoms displaced by an amount  $JK$ , a curve having a maximum at  $J$  and approaching zero at  $L$  would be expected. If we now use the same diagram to represent the elastic displacement of the atoms due to an applied strain, taking the point  $L$  as origin and proceeding in the direction of  $J$  for an extension of the atom chain, it is clear that the amount of energy lost in a strain such as  $LK$  will be proportional to the area under the distribution curve from  $L$  to  $K$ .

Two types of distribution curve are shown in fig. 1, the first of which is linear, corresponding to a distribution in which the number of atoms having a particular displacement decreases uniformly as the displacement increases. The chief interest of this curve lies in the fact that it

evidently leads to the result that the loss of energy in a strain cycle is proportional to the square of the maximum strain or stress, as found by experiment in some materials.

As the phenomenon of hysteresis must involve very large numbers of atoms, it would appear more reasonable to expect a distribution of displacements determined by statistical considerations, and curve II. in fig. 1 therefore shows the probability curve of the type  $y=e^{-x^2}$ . This curve approaches the axis of  $x$  asymptotically, and at the same time in our hypothesis no displacements exceed  $JL$ , while the number which has the limiting value  $JL$  is supposed to approach zero, to avoid a discontinuity at

Fig. 3.



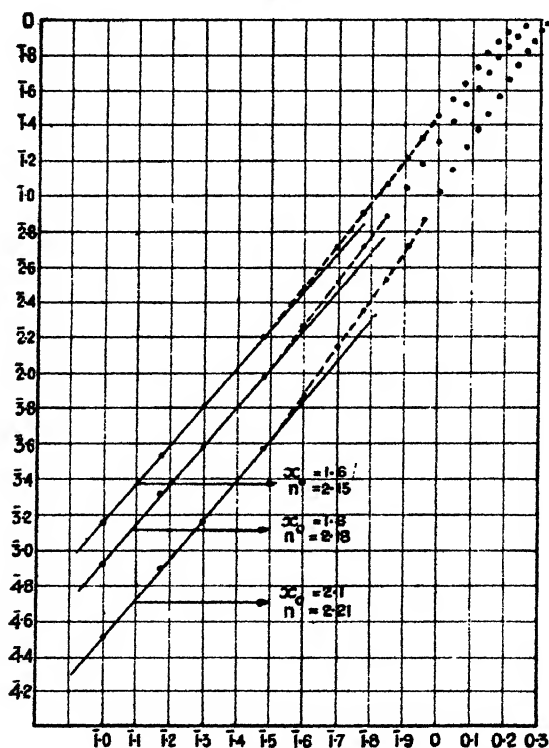
this point in the law of distribution. We shall therefore attempt to satisfy all these conditions by taking an arbitrary point such as Q in fig. 3 low down on the curve, and shall assume the ordinates of the curve, taken from the base line  $SQ$ , to represent the numerical distribution of displacements.

It is interesting that with such a distribution the theory indicates that the loss of energy in hysteresis would be given by a relation  $h=k (f_{\max})^n$ , with an exponent  $n$  having a value somewhat greater than 2, as found experimentally for various metals.

Referring to fig. 3, in which the probability curve is drawn to scale, the hysteresis loss for a strain proportional

to LM is proportional to the area RQN. Having chosen an arbitrary value for  $x_0$ , the abscissa of the point Q, the relation between the area, and the value of LM can be readily computed numerically by means of the tabulated values of the probability integral. The results of this calculation for three different positions of the point Q, corresponding to values 1.6, 1.8, and 2.1 for  $x_0$ , are shown in fig. 4. These cover the complete range of the distribu-

Fig. 4.



tion curve from Q to P, and the results are plotted logarithmically. The units employed in this diagram are quite arbitrary, and simply depend on the numerical values of the coordinates in fig. 3. It is clear that for a comparison with the hysteresis measurements of fig. 2 the lower part only of these curves need be considered, in view of the small range of strains concerned in the experiments. It will be seen in fig. 4 that the lower part of each curve is closely linear, indicating that the theory would give a

simple power law for the hysteresis loss of energy, and the values of the exponent in the three cases taken are 2.15, 2.18, and 2.21 respectively. The suggested theory, on assuming a reasonable type of distribution of displacements, thus appears to offer an explanation of the empirical power law which is well established by the experiments.

3. The theory proposed will now be considered from some other points of view. It is of some interest to notice, firstly, that the theory quite well accounts for the fact that elastic hysteresis is a process which is perfectly reversible in the elastic sense but quite irreversible thermodynamically. Thus, in passing through a strain cycle the increment of kinetic energy assumed to be gained by certain atoms is completely irreversible. On the other hand, the original arrangement of the atoms can recur exactly on removing the strain, as by this theory the production of heat energy is accounted for without having to consider any internal slip motion as taking place attended by some form of friction very similar to ordinary solid friction. The theory thus affords a satisfactory explanation of the perplexing fact, now well established, that under certain circumstances a solid can continue to dissipate energy by repetition of strain cycles apparently indefinitely, without any cumulative effect such as change in size or shape or internal structure.

The assumed mechanism by which the atom receives kinetic energy is itself irreversible, in the sense that it can only occur during a strain which causes an extension in the atomic chains. It would follow from the present theory that the instantaneous rate of loss of energy in the course of a stress-strain cycle would be very variable. Considering a symmetrical cycle, such as occurs in a torsional oscillation, as shown in fig. 5, the rate would be zero throughout the period of decreasing stress. During the period of rising stress the rate would commence at zero, increasing rather rapidly as the stress increased.

In this connexion some experiments made by Constant<sup>(4)</sup> are of much interest. In these experiments the rate of generation of heat in a magnetic hysteresis cycle was determined by a series of temperature measurements of the specimen. It was found that all the rise of temperature occurs in the stage of the cycle during





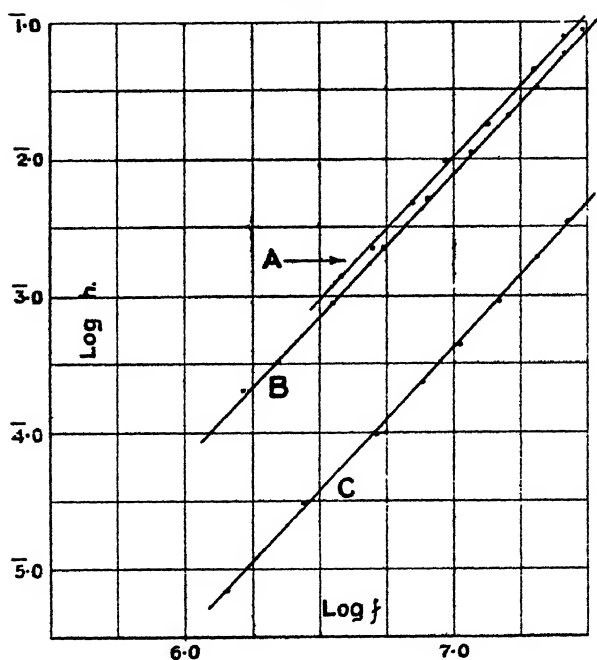
fully compatible with the observed form of the loop. It is found that when the stress is increasing from zero to the maximum, along the portion AB or CD of the cycle, the stress-strain relation is not quite linear, and the curve bends over more and more as the stress increases. On decreasing the stress the return portion BC of the cycle is found to be almost exactly linear and parallel to the initial slope of AB. The work done in straining the material along AB is represented by the area ABE, and the energy returned on coming back along the path BC is BCE, which is equal to AFG, the work that would be necessary to strain the material had the stress and strain remained proportional. Hence the path AB requires more energy than the return path BC by the amount ABC. In the theory proposed such a distinction between the condition of increasing and decreasing stress is definitely necessary, and this feature of the theory appears to be in good accordance with the form of the hysteresis loop found by the extensometer.

Since the theory indicates that a dissipation of energy occurs only in the course of a strain which involves an extension of the atom chains, it would follow that in a uniform compression, in which there can only be a compression of the chains everywhere, there should be an absence of hysteresis. It is significant that Bridgman<sup>(5)</sup> states that solids are found to behave with perfect elasticity under hydrostatic pressure even up to pressures of 12,000 atmospheres. There is not in general a strictly linear relation between stress and strain, but there is found to be no measurable departure from true elasticity on applying and removing the pressure.

The theory is found to be qualitatively in agreement with experiment as regards the effect on the hysteresis loss of overstrain and annealing. If the energy loss occurs as supposed entirely at certain points at which the atom chains are stretched by local distortion, and these points are scattered in a random way throughout the mass, it is reasonable to infer that by overstraining the material the total number of atoms displaced from the true equilibrium position would be increased. Some direct evidence of this is provided by the fact that overstraining a metal generally diminishes its density. In annealing, on the other hand, the atoms are set into more violent motion, and are then allowed to settle down slowly.

Initially some groups of atoms are nearer together than the equilibrium distance and others are further apart, and the process of annealing provides the atoms with an opportunity to re-arrange themselves slightly, aided by their own intrinsic forces, so that their final disposition is a closer approximation to the ideal formation. The hysteresis loss would therefore be expected to increase on overstraining a material and to decrease on annealing it. The above argument carries more weight if there is any reason to consider the strained atom chain to be quite an abnormal condition only occurring very sparsely

Fig. 6.



distributed. This point is discussed in a subsequent section of the paper, where reasons are given for thinking that the number of displaced atoms is only an extremely small proportion of the total number.

The above deductions are found to be well substantiated by the following experiment. An aluminium specimen was overstrained by twisting beyond its elastic limit, and the relation between hysteresis loss and maximum stress was then determined. The result obtained is shown by curve A of fig. 6 plotted logarithmically. Curve B is the

similar relation for the original material. The specimen was then annealed in a somewhat crude but effective way by passing a flame up and down its length a number of times, after which the result shown by curve C was obtained.

The three curves are closely parallel straight lines, showing that the hysteresis in each condition follows the same law  $h = k(f_{\max})^n$ , only the constant  $k$  being affected. In terms of the theory the statistical distribution of the atoms is not altered, but only the total number of displaced atoms. The difference in the latter or in the value of  $k$  is greater than appears from the logarithmic plotting. Thus the vertical distance between curves A and C is 1.4 on the logarithmic scale used—that is, the loss of energy in hysteresis after annealing is only about  $\frac{1}{2.5}$  of that found after overstraining. A similar effect was found on annealing a brass wire specimen, the hysteresis being reduced to  $\frac{1}{4}$  of the amount found in the unannealed state. Such results seem to indicate fairly definitely that hysteresis is a consequence of the presence of internal strains.

Certain results of other workers on internal friction will next be considered briefly as regards their bearing on the present theory. Kimball and Lovell<sup>(3)</sup> have quite established the fact that the energy loss per cycle is independent of the frequency of the cycles over a wide experimental range. Such a result was indicated, but not so completely confirmed, by the results of Hopkinson and Williams<sup>(4)</sup> and Rowett<sup>(7)</sup>, working actually on a different aspect of the subject. This fact is difficult to reconcile with the views of some who prefer to regard hysteresis as a viscous phenomenon of the solid state, but is, on the other hand, a result to be expected by the proposed atomic theory, at least as regards ordinary frequencies attainable by experiment.

Another experimental result found by Guye<sup>(8)</sup> is that the internal friction of metals depends on the temperature, generally decreasing considerably as the temperature is reduced. Such a result has a simple explanation in the present theory and may be regarded as a consequence of the thermal contraction of the metal. The average distance between the atoms is slightly reduced, causing a general diminution in the displacements in the strained atom chains, as a result of which the numerical scale of the

distribution curve becomes reduced, and less energy is dissipated in any given strain cycle. Such an explanation, of course, involves the assumption that the force-fields of the atom are unaffected by the temperature of an aggregation of atoms.

4. If the view that both friction and elastic hysteresis have the same origin is provisionally accepted, it becomes possible to derive some further information about the process by combining data found experimentally as to the loss of energy in rolling friction and in hysteresis. The actual amount of energy involved on the average in each atomic separation can be estimated, and from this it can be shown that only an extremely small fraction of the atoms are concerned in the hysteresis loss in a stress-strain cycle.

The following data are taken from the previous paper<sup>(2)</sup>, and concern the loss of energy in the rolling friction of a highly lapped steel cylinder rolling on a lapped steel plane surface:—

Diameter of cylinder = 0.254 cm.

Length of cylinder in rolling contact = 0.254 cm.

Load on cylinder = 300 gm. (M).

Coefficient of rolling friction = 0.000044 ( $\lambda$ ).

Width of elastic contact area between cylinder and plane =  $8.28 \times 10^{-4}$  cm. ( $2a$ ).

Mean contact stress  $f = 0.14 \times 10^{10}$  dynes per sq. cm.

Maximum contact stress  $f_m = 0.21 \times 10^{10}$  dynes per sq. cm.

In rolling through unit distance a total area of 0.254 sq. cm. comes into contact, and is subject at some moment to the maximum normal stress  $f_m$ . The loss of energy amounts to

$$E = \lambda Mg \text{ ergs,}$$

and, if we can estimate the total number  $N$  of atomic separations involved, an estimate of  $\varepsilon = \frac{E}{N}$ , the energy lost in the separation of one pair of atoms can be derived.

Unfortunately we can do no more than find two limits within which  $N$  most probably falls. An upper limit  $N_1$  may be estimated by making the simple assumption that

the contact area of 0.254 sq. cm. is packed with atoms every one of which comes into repulsive contact with a corresponding atom in the other body. If  $e$  denotes the average distance between the atoms, for which the lattice constant  $2.86 \times 10^{-8}$  cm. will be assumed as a probable value, we have approximately

$$N_1 = \frac{0.254}{e^2} = 3.1 \times 10^{14}.$$

And the loss of energy involved in one atomic separation has a lower limit  $\epsilon_1$ , given by

$$\epsilon_1 = \frac{E}{N_1} = \frac{0.000044 \times 300 \times 981}{3.1 \times 10^{14}} = 4.1 \times 10^{-14} \text{ erg.}$$

The above estimate of  $N_1$  is almost certainly too large, and it is more probable that in an elastic contact where the maximum stress has the comparatively low value  $0.21 \times 10^{10}$ , the total number of atoms under repulsion is considerably less than the maximum possible number. In the writer's opinion, as described more fully in the previous paper on friction, the range of the repulsion is so small compared even with atomic dimensions that the atoms gradually come into repulsion to an extent which adjusts itself by the elastic strain to the normal stress, at least during the range of elastic contact. If the stress is further increased a point is reached at which the metal flows, and it may be reasonably assumed that then all the possible atoms are in active repulsion and are individually exerting the maximum repulsion that the strength of the lattice permits. For hard steel this flow stress is known to be about  $7.5 \times 10^{10}$  dynes per sq. cm., from which it may be inferred that the maximum atomic repulsion is about

$$7.5 \times 10^{10} \times e^2 = 6.15 \times 10^{-5} \text{ dyne.}$$

To derive a lower limit  $N_2$  we can assume that the stress  $0.21 \times 10^{10}$  acting on the area 0.254 sq. cm. is supported by  $N_2$  atoms repelling with forces having all possible values between zero and the maximum value of  $6.15 \times 10^{-5}$  dyne. In this way we have

$$N_2 = \frac{0.21 \times 10^{10} \times 0.254}{3.07 \times 10^{-5}} \\ = 1.74 \times 10^{13}$$

$$\text{and} \quad \epsilon_2 = 7.4 \times 10^{-13} \text{ erg.}$$

This estimate  $N_2$  is almost as certainly too small as  $N_1$  is too large, since we have assumed that under a stress of only about  $\frac{1}{3.5}$  of the flow stress there is an equal probability of all values of the repulsion right up to the maximum occurring with the flow stress.

The loss of energy in elastic hysteresis for steel piano-wire was found by experiment to be as follows :—

Maximum Stress.	Hysteresis loss per cycle.
Dynes per sq. cm.	Ergs per c. c.
$5.4 \times 10^7$	3.00
4.68	2.02
3.72	1.285
2.68	0.63
1.97	0.40
1.57 <sup>5</sup>	0.212
1.19	0.113
0.84 <sup>5</sup>	0.067

Taking the first value in the Table of 3 ergs per c.c., even with the smaller estimate  $\epsilon_1$  the number of atoms involved in this loss of energy will be only

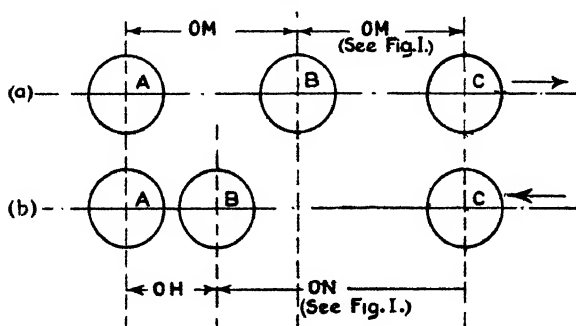
$$\frac{3}{4.15 \times 10^{-14}} = 0.725 \times 10^{14}.$$

The total number of atoms in 1 c.c. of iron is of the order  $0.8 \times 10^{23}$ ; hence, at the highest estimate only about 1 in  $10^9$  of the total atoms contributes to this loss of energy, although the whole number concerned in the hysteresis is very great, approximately  $10^{14}$ . Thus it appears probable that the conditions of locally stretched atomic chains we have assumed to exist are quite sparsely scattered throughout the metal.

5. Certain of the well-known phenomena of hysteresis can be accounted for by the present theory. We have already seen how the general shape of the stress-strain loop may be deduced from the theory, and the formation of a loop will now be considered briefly from a somewhat different standpoint. For any given strains, such as OQ

in fig. 5, the rising stress LQ is always greater than the falling stress MQ, and this can be explained by the supposition that it is only with an extending atom chain that atoms can be displaced at all into the region of unstable equilibrium. In fig. 7 three atoms are shown diagrammatically: (a) as extended slightly beyond the critical distance as C moves to the right in an elastic strain, and (b) as distributed later after B has returned to a stable position and C is returning towards A. A reference to fig. 1 shows that the net attraction A—R between the atoms in case (a) is MS, while in case (b) it will be HV between A and B and NT between B and C, these being necessarily equal. It is clear that in case (a) this force must be greater than it is in case (b). With a rising stress

Fig. 7.



there are by our hypothesis a number of atoms passing through the condition corresponding to case (a). Regarding stress as the aggregate of the atomic forces, such atoms contribute a larger element of force with rising stress than the same atoms disposed as shown by case (b) when the stress is diminishing, and we should therefore expect the rising stress to exceed the falling stress for the same strain.

It is well known that in many metals if a stress-strain cycle is repeated a large number of times the loss of energy per cycle is found to diminish fairly rapidly at first, and then more and more slowly, becoming finally approximately constant. If the stress range is not great enough to induce a condition of fatigue, the final state



of hysteresis apparently may persist indefinitely. Gough and Hanson<sup>(9)</sup>, for example, have subjected iron to no less than a hundred million cycles. This diminution in the hysteresis may be observed either by measurements of the stress-strain loop with an extensometer or by thermal measurement of the energy dissipated, a method successfully developed by Haigh. The effect is so marked that it has been suggested that there are two or even three different types of hysteresis. The initial stage, in which a rapid diminution of the lost energy occurs, has been called primary or transient hysteresis, leading to the second stage, which may be regarded as true elastic hysteresis, and is a stable condition of imperfect elasticity. If a sufficiently great stress range is employed, the second type of hysteresis gradually merges into what has been distinguished as a third type. In this there occurs a slow increase in the loss of energy, together with the development of a state of fatigue, and this phase ends in fracture of the material.

As regards the first and second types of hysteresis, a possible explanation of the observed phenomena can be given by the present theory. It may be suggested that the observed diminution in the energy dissipated per cycle from the primitive state to the final cyclic elastic condition is due to a process of auto-annealing, by which the displaced atoms are gradually enabled to adjust themselves in relation to their near neighbours, and arrive at a disposition more and more like the ideal condition of equilibrium. In a previous section the marked reduction in hysteresis produced by annealing has been attributed to a general tendency of the atoms at the strain centres to redistribute themselves more in equilibrium with their neighbours, this tendency being facilitated by the increased energy of motion imparted temporarily during annealing. It will now be shown that the momentary increase in the energy of those atoms, which by the theory give rise to the hysteresis, is itself a quantity comparable with the increased thermal energy of the atom in annealing. This leads to the view now suggested as a possibility, namely, that the hysteresis loss of energy dissipated in heat itself produces the gradual effect of internally annealing the material. The total amount of heat energy concerned is only enough to raise the whole mass very slightly in temperature, but this heat is primarily generated by only

a very small fraction of the total number of atoms, and the temporary access of energy of any atom may reasonably be supposed to assist in the tendency to a better adjustment of position in just the same way as in annealing. On this view the atoms which actually need the aid of annealing are just those which receive the extra energy in each stress-strain cycle. No appreciable accumulation of energy from one cycle to the next will occur, as the time required to disperse the heat by conduction through the minute distances concerned is very small by comparison with the interval of time elapsing between successive cycles. The supposed process recurs, however, with every cycle until as many as possible of the displaced atoms are one by one assisted to take up a more normal arrangement with their neighbours, and by minute stages the distorted local condition becomes relieved. At the same time the energy dissipated becomes less and less, and a stage is reached at which no further readjustment occurs, a stage corresponding to the elastic or second type of hysteresis.

In a previous section we have given estimates of upper and lower limits of the energy lost per atom. These estimates are  $74 \times 10^{-14}$  and  $4.15 \times 10^{-14}$  erg, and from the manner of deriving them it is probable that they are decidedly too high and too low respectively. For our present purpose we shall take the geometric mean of the two  $17.5 \times 10^{-14}$  as a probable value, thereby assuming that each limit has the same probable percentage error. The average amount of energy possessed by one atom of iron at  $15^\circ \text{C}$ . can be computed approximately from the mass of the atom and specific heat data, and is about  $10 \times 10^{-14}$  erg. Hence, if we accept  $17.5 \times 10^{-14}$  as a probable value for the average quantity of energy added, this corresponds to the energy increment of a temperature rise amounting to  $400\text{--}500^\circ \text{C}$ . Even if the estimate of  $17.5 \times 10^{-14}$  should be high for the average value, the individual increments of energy of different atoms are probably very variable, and a certain proportion of the atoms may in every cycle receive sufficient heat energy to produce in time the local annealing effect in the way suggested.

If the present view is substantially correct, it follows that there is no physical distinction at all between the first and second phases of hysteresis, and the observed

difference is merely a numerical difference in the total number of displaced atoms involved.

6. The relative behaviour as regards hysteresis of the metals and non-metals deserves a brief discussion, as it involves the important question of whether a crystal unit is liable to elastic hysteresis, to which, unfortunately, no very conclusive answer can be given at present.

It was found that in the case of all the metals, which are composed of crystal aggregates, the index  $n$  had a value exceeding 2, whereas the non-metals, glass, quartz (fused), ebonite, and indiarubber, which have an amorphous atomic structure, all give an index which is closely equal to 2. Apart from this, however, there is no difference in behaviour as regards hysteresis between the crystalline and the amorphous materials. An inspection of fig. 2 shows how completely the curves for glass and quartz fit in with those of the metals. As the atoms constituting any crystal unit are arranged in a nearly perfect geometrical lattice, it is almost certain that the groups of bonding atoms between two crystals which are differently orientated must be disposed in some irregular manner. If the view expressed in this paper concerning the minute range of the atomic repulsion force is correct, the border-line between a lattice formation and an amorphous grouping of the atoms is fairly sharply defined, and any small cluster of atoms only need extremely small displacements to disturb completely the normal condition of equilibrium and result in an amorphous arrangement. It seems probable, therefore, that this is the condition of the bonding atoms, as Rosenhain supposes for other reasons in his well-known theory of inter-crystalline cement. The occurrence of strained atom chains therefore appears likely to be much more frequent among the bonding atoms than among those forming the regular lattice of the crystal unit, and it might be expected on general grounds that the hysteresis loss under low stresses would therefore be largely or even wholly confined to the former atoms.

On the other hand, there is the experimental fact that the hysteresis of glass and fused quartz, which are amorphous throughout, is very similar to that of the group of metals, which can contain only a very small proportion of probable amorphous material. If, therefore, the

hysteresis in the crystal aggregate is confined to the bonding atoms, it would follow that the loss of energy per unit mass of amorphous material must be far greater for the metals than for the non-metals, a conclusion which is difficult to accept. Furthermore, although little work has yet been attempted on the elastic hysteresis of single crystals, the experiments that have been made show that single crystal specimens display much the same hysteresis phenomena as ordinary aggregates.

The theory suggested in this paper perhaps helps to reconcile the apparent conflict with reason which arises if it must be accepted that hysteresis occurs in a strained crystal lattice. It has been estimated above that only about 1 in  $10^9$  of the atoms is involved in the loss of energy, and if this is the case it becomes clear that quite minute imperfections or discontinuities in the lattice structure, such as might be caused by impurities or sub-microscopic fissures, would be sufficient to lead to hysteresis. In this connexion it may also be repeated that the theory requires only extremely small displacements of the atoms, and it is on all points quite compatible with the occurrence of hysteresis in a crystal unit.

The author is indebted to Sir J. E. Petavel, Director of the National Physical Laboratory, for the experimental facilities and permission to publish the paper, and to Mr. J. E. Sears for his continued interest in the work. Useful help has also been received from his colleagues Dr. Gough and Messrs. Wright and Cox in the course of discussion of the subject.

### *References.*

- (1) Trans. Farad. Soc. "Discussion on Cohesion," xxiv. p. 53 (1928).
- (2) Phil. Mag. vii. p. 905 (1929).
- (3) Phys. Rev. xxx. p. 948 (1927).
- (4) Phys. Rev. xxxii. p. 486 (1928).
- (5) Proc. 2nd International Congr. for App. Mechanics, Zurich (1926).
- (6) Proc. Roy. Soc. lxxxvii. p. 502 (1912).
- (7) Proc. Roy. Soc. lxxxix. p. 528 (1913).
- (8) *Comptes Rendus*, p. 1066 (1909); p. 964 (1910).
- (9) Proc. Roy. Soc. civ. p. 538 (1923).

LXXXVI. *Redshift and Relativistic Cosmology.*

By HERMANN WEYL, Zurich (Switzerland)\*.

## ABSTRACT.

1. The de Sitter hyperboloid as homogeneous state of the world. Besides, on this solution of the gravitational equations, the cosmology depends on additional assumptions concerning the question which part of the hyperboloid corresponds to the real world, and, in connexion with this, concerning the undisturbed state of motion of the stars. The static coordinates used by most authors represent only a cuneiform sector.

2. Hypothesis of common origin in the infinitely distant past. The range of influence of a star covers only half the hyperboloid.  $\infty^3$  stars have their range of influence in common with it. Assumption that this half is the entire universe.

3. The universe then has the same topological character as in the special theory of relativity. Introduction of Robertson's coordinates. Computation of the redshift by means of these coordinates.

4. A homogeneous distribution of mass of infinitely small density is possible by which no point in space and time is distinguished. Computation of the density in static coordinates. Space is open, the total mass infinite.

---

RECENT observations made on spiral nebulae have ascertained their extra-galactic nature and confirmed the redshift of their spectral lines as systematic and increasing with the distance †. By these facts the cosmological questions about the structure of the world as a whole, to which the general theory of relativity gave rise in purely speculative form, have acquired an augmented and empirical interest. It is not my opinion that we can vouch for the correctness of the "geometrical" explanation which relativistic cosmology offers for this strange phenomenon with any amount of certainty at this time. Perhaps it will have to be interpreted in a more physical manner, in correspondence

\* Communicated by the Author.

† E. Hubble, Proc. Nat. Ac. xv. p. 168 (1929).

with the ideas of F. Zwicky\*. But the cosmologic-geometrical conception must on any account be examined seriously as a possibility. And this is my motive for saying a few words about the more recent discussion of the question by H. P. Robertson† and R. C. Tolman‡: firstly, to show that the cosmology proposed by Robertson is identical with the one proposed by me—this is the result of a conference with Professor Robertson at Princeton; and, secondly, to clarify and defend my or our point of view as opposed to the assertions of Professor Tolman§.

Like Mr. Tolman, I start from de Sitter's solution: the world, according to its metric constitution, has the character of a four-dimensional "sphere" (hyperboloid)

$$x_1^2 + x_2^2 + x_3^2 + x_4^2 - x_5^2 = a^2 \quad . \quad . \quad . \quad (1)$$

in a five-dimensional quasi-euclidean space, with the line element

$$ds^2 = dx_1^2 + dx_2^2 + dx_3^2 + dx_4^2 - dx_5^2. \quad . \quad . \quad (2)$$

The sphere has the same degree of metric homogeneity as the world of the special theory of relativity, which can be conceived as a four-dimensional "plane" in the same space. The plane, however, has only one connected infinitely distant "seam," while it is the most prominent topological property of the sphere to be endowed with two—the infinitely distant past and the infinitely distant future. In this sense one may say that space is closed in de Sitter's solution. On the other hand, however, it is distinguished from the well-known Einstein solution, which is based on a homogeneous distribution of mass, by the fact that the null cone of future belonging to a world-point does not overlap with itself; in this causal sense, the de Sitter space is open.

Tolman's careful investigation shows anew that nothing like a systematic redshift can be derived solely on the basis of the constitution of the metric field in its undisturbed state, i. e., from the de Sitter solution of the gravitational equations. I believe, however, that in a complete cosmology supplementary assumptions must be added:—(1) assumptions of topological character, which determine whether the entire

\* Phys. Rev. xxxiii. p. 1077 (1929). A detailed communication will appear in the Proc. Nat. Ac.

† Phil. Mag. v. Suppl. p. 835 (1928).

‡ Astroph. Journ. lxxix. p. 245 (1929).

§ Besides, in the fifth edition of 'Raum Zeit Materie' (Berlin, 1923), I have exposed my opinion in 'Was ist Materie?', p. 71 (Berlin, 1924), and defended it against L. Silberstein in Phil. Mag. [6] xlviii. p. 348 (1924).

de Sitter sphere or which part of it corresponds to the real world, and (2) closely connected with these an assumption about the "undisturbed" motion of the stars by which  $\infty^3$  geodesic world-lines are set off from the manifold of all these lines. As regards the first point, the static coordinates, *e. g.*, which belong to a star (the "observer"), and with which Mr. Tolman works by preference, represent only a cuneiform sector of the entire sphere.

The world-line of the observer A shall be given by

$$x_1 = x_2 = x_3 = 0, \quad x_4 > 0. \quad . \quad . \quad . \quad (3)$$

Let us put

$$x_4 = z \cdot \text{ch } t/a, \quad x_5 = z \cdot \text{sh } t/a. \quad . \quad . \quad . \quad (4)$$

Then we obtain

$$ds^2 = (dx_1^2 + dx_2^2 + dx_3^2 + dz^2) - \frac{z^2}{a^2} dt^2 \quad . \quad . \quad (5)$$

with the relation

$$x_1^2 + x_2^2 + x_3^2 + z^2 = a^2. \quad . \quad . \quad . \quad (6)$$

Space and time fall apart; space, with regard to its metric constitution, is the three-dimensional sphere (6) of radius  $a$  in a four-dimensional euclidean space with coordinates  $x_1 x_2 x_3 z$ , or rather the hemisphere  $z > 0$ . Our representation only exhibits the sector of the hyperboloid

$$x_4 + x_5 > 0, \quad x_4 - x_5 > 0. \quad . \quad . \quad . \quad (7)$$

The geodesics are cut out of the sphere by the two-dimensional planes passing through the origin in the five-dimensional space with the coordinates  $x_a$ . The null cones opening into the future, which issue from all the points of such a geodesic with time-like direction, from the world-line of a star, fill a region of the world which I shall call the *range of influence of the star*. It is a highly remarkable feature of the de Sitter cosmology that this range of influence covers only half the hyperboloid (while it coincides with the entire "plane" in the special theory of relativity). In the case of the observer star A, for example, the range of influence is characterized by  $x_4 + x_5 > 0$ . (The sector represented by the corresponding static coordinates is again only part of the range of influence, and more precisely that part which is accessible to observation from A.) There are  $\infty^3$  stars or geodesics to which the same range of influence belongs as to the arbitrarily chosen star A; they form a system that has been causally interconnected since eternity.

Stars that do not belong to it lie beyond the range of influence of A during their early history. On the other hand, it is true that if A' is a star of the system, A ceases to act upon A' from a certain moment of its history on, even though conversely A' remains in the range of influence of A during its entire history. Therefore the stars of the system may be described as stars "of common origin," but the common origin lies in an infinitely distant past. *Our assumption is that in the undisturbed state the stars form such a system of common origin.* Clearly this means neither continuous formation nor continuous entry in the sense of the two hypotheses mainly discussed by Mr. Tolman. By the assumption of the common range of influence the future acquires a different significance from the past. Moreover, it can be shown that this assumption (and the contrary one that results from it by the interchange of past and future) is the only one which sets off a system of  $\infty^3$  geodesics from the entire manifold of these lines in such a manner that all time moments remain equivalent.

If this hypothesis of common origin, according to which the stars have stood in a connexion of mutual interaction since eternity, is the correct one, it will be natural to consider only that part of the sphere which they cover, i. e., that half of the hyperboloid which represents their common sphere of influence as the real world. This is surely the smallest part of the hyperboloid that can be taken into consideration as the real world: a star existing from eternity to eternity and the propagation of the light emitted by it must have room in the universe. By the perfectly natural topological assumption that the world does not project over this minimum, the  $\infty^3$  geodesics referred to are immediately distinguished as those lines which have taken their course in the real world since eternity, which, therefore, demand neither formation of stars nor "entry from the border of the world" at a finite moment of time. Only when referring to the entire hyperboloid is it appropriate to describe the pencil of  $\infty^3$  world-lines of our system of stars as one that concentrates on an infinitely small part of the total extent of the sphere towards the infinitely distant past, while it spreads over it more and more towards the future.

But if only that half which is covered by the world-lines has real significance, it is convenient to follow Professor Robertson in introducing coordinates  $\tau, \xi_1, \xi_2, \xi_3$ , such that the world-lines expressed in terms of them appear as "parallel vertical straight lines" on which the three "spacial coordinates"  $\xi_1, \xi_2, \xi_3$  are constant and only the "time"  $\tau$



varies\*. All four coordinates are capable of the values from  $-\infty$  to  $+\infty$  independently of one another; the world has again exactly the same topological constitution as in the special theory of relativity, so that one can no longer reasonably speak of a "closed space." The introduction of these coordinates can be performed in such a manner that the line element assumes the form

$$ds^2 = e^{-2\tau/a} (d\xi_1^2 + d\xi_2^2 + d\xi_3^2) - d\tau^2. \quad (8)$$

If one asks for all the transformations which not only leave this expression of the metric field invariant but carry the system of the world-lines of our stars into itself, the answer reads: all euclidean motions of the space  $(\xi_1 \xi_2 \xi_3)$  combined with the transformation  $\tau \rightarrow \tau + \tau_0$ ,  $\xi_i \rightarrow e^{\tau_0/a} \cdot \xi_i$  ( $\tau_0$  an arbitrary constant). Thus full homogeneity prevails also with regard to the stellar motions.  $a$  cannot very well be regarded as the radius of space any longer; according to (8) its simplest interpretation is that of being the standard of measurement for the scattering of the stars or the redshift which corresponds to it as Doppler effect.

To arrive at the Robertson coordinates, we bear in mind that the world-line of a star in our system is defined by a set of equations

$$x_i = \xi_i (x_4 + x_5) / a \quad [i = 1, 2, 3]$$

with constant  $\xi_i$  (two-dimensional plane that goes through the line

$$x_1 = x_2 = x_3 = 0, \quad x_4 + x_5 = 0).$$

Let us add the definition

$$x_4 + x_5 = a \cdot e^{\tau/a},$$

which takes account of the restriction  $x_4 + x_5 > 0$ . The transformation can then be summed up in the form

$$x_i = \xi_i \cdot e^{\tau/a} \quad [i = 1, 2, 3], \quad x_4 + x_5 = a \cdot e^{\tau/a}. \quad (9)$$

On account of equation (1),

$$x_1^2 + x_2^2 + x_3^2 + (x_4 + x_5)(x_4 - x_5) = a^2,$$

$x_4 - x_5$  can then be expressed in the Greek coordinates. For  $ds^2$  one easily obtains the desired result (8). If one puts

$$x_1^2 + x_2^2 + x_3^2 = r^2, \quad \xi_1^2 + \xi_2^2 + \xi_3^2 = \rho^2,$$

then

$$z = \sqrt{a^2 - r^2}$$

\* The same coordinates have already been discovered by G. Lemaitre, Journ. Math. Massach. iv. p. 188 (1925).

in that region which can be referred to the static coordinates of the observer, and according to (4) the equations (9) furnish

$$r = \rho \cdot e^{\tau/a}, \quad \sqrt{1 - \left(\frac{r}{a}\right)^2} \cdot e^{t/a} = e^{\tau/a} \quad . \quad . \quad (10)$$

for the connexion which Robertson himself indicated as prevailing between his own and the static coordinates. But it is essential to take into consideration not only this part but the entire range of influence of the observer star. For the cosmology which regards it as the real world the coordinates introduced by Mr. Robertson are by far the most appropriate.

Since Mr. Tolman finds the derivation of my formula for the redshift unclear, it shall quickly be repeated here in the Greek coordinates. The final result, of course, depends on what one means by the distance of the observed star from the observer. If the equation of the infinitely small null cone issuing from an arbitrary point is written in the form

$$d\xi_1^2 + d\xi_2^2 + d\xi_3^2 - a^2(de^{-\tau/a})^2 = 0,$$

it is immediately seen that the equation of the finite null cone issuing from the point

$$\xi_1 = \xi_2 = \xi_3 = 0, \quad \tau = \tau_0,$$

is the following :

$$\xi_1^2 + \xi_2^2 + \xi_3^2 - a^2(e^{-\tau/a} - e^{-\tau_0/a})^2 = 0,$$

or the time  $\tau$  at which a light-signal must be dispatched from a star at the distance  $\rho$  in order to reach the observer at the moment  $\tau_0$  is given by

$$\rho = a(e^{-\tau/a} - e^{-\tau_0/a}).$$

To the radiation period  $d\tau$  therefore corresponds the observation period  $d\tau_0$ , which is furnished by

$$d(e^{-\tau/a} - e^{-\tau_0/a}) = 0 \quad \text{or} \quad e^{-\tau/a} d\tau = e^{-\tau_0/a} d\tau_0.$$

A radiation frequency  $\nu$  is observed as the distinct frequency  $\nu_0$ :

$$\frac{\nu_0}{\nu} = \frac{d\tau}{d\tau_0} = e^{(\tau - \tau_0)/a}.$$

This may be written

$$\frac{\nu_0}{\nu} = e^{\tau/a} \cdot e^{-\tau_0/a} = e^{\tau/a} \left( e^{-\tau/a} - \frac{\rho}{a} \right) = 1 - \frac{\rho}{a} e^{\tau/a}.$$

If the  $r$  of the star has the value  $r$  at the moment of light emission, then, according to (10),

$$\frac{\nu_0}{\nu} = 1 - \frac{r}{a}, \quad \frac{\Delta\nu}{\nu} = -\frac{r}{a}.$$

$r$  is the projection of the natural distance  $d$  on the sphere (6) onto the equatorial plane  $z=0$ ; therefore

$$\frac{r}{a} = \sin \frac{d}{a},$$

and we have the formula

$$\frac{\Delta\nu}{\nu} = -\sin d/a.$$

Mr. Tolman asks why I got the tan instead of the sin. The reason for this is as follows. In my earlier paper  $d$  meant the naturally measured distance of the star in the static space at the same moment  $t$  at which the observation takes place;  $t$  is the static time of the observer. We have

$$\begin{aligned} \frac{\nu}{\nu_0} &= e^{\tau_0/a} \cdot e^{-\tau/a} = e^{\tau_0/a} \left( e^{-\tau_0/a} + \frac{\rho}{a} \right) \\ &= 1 + \frac{\rho}{a} e^{\tau_0/a}. \quad . \quad . \quad . \quad (11) \end{aligned}$$

The time  $t$  of observation is  $=\tau_0$ . According to (10)

$$\frac{r}{\sqrt{a^2 - r^2}} = \frac{\rho}{a} \cdot e^{\tau/a}$$

holds. At the moment of observation  $t=\tau_0$ , the star  $\rho$  therefore has the distance  $r$  which is given by this equation with  $t=\tau_0$ , and one obtains from (11)

$$\frac{\nu}{\nu_0} = 1 + \frac{r}{\sqrt{a^2 - r^2}} = 1 + \tan d/a.$$

So long as one is only dealing with distances that are small compared with  $a$  the precise definition is of no consequence, and one obtains the law for the linear increase of

the redshift with the distance; but as soon as the order of magnitude of  $a$  is approached, an exact discussion is required as to which distance is determined by the indirect astronomical methods.

The de Sitter solution corresponds to an empty world or to an infinitely small density of the stars. Can this density be chosen so that the distribution of the stars distinguishes neither a definite centre in space nor a definite moment in time? This is actually possible; the density need only be assumed constant, say  $=\beta$ , in the Robertson coordinates. The total mass of the universe then becomes infinite. This shows clearly how impossible it has become to speak of a closed space. It is, of course, easy to reduce this density to static coordinates. We determine the mass which is contained at the static time  $t$  in the region  $r \leq r_0$  of static space. The world-lines of this mass cover that part of the world which is described by  $\rho \leq \rho_0$  in Robertson's coordinates,

$$\rho_0 = \frac{ar_0}{\sqrt{a^2 - r_0^2}} \cdot e^{-t/a}.$$

The desired mass is therefore

$$= \beta \cdot \frac{4\pi}{3} \rho_0^3 = \frac{4\pi\beta}{3} \left( \frac{r_0}{\sqrt{1 - r_0^2/a^2}} \right)^3 \cdot e^{-3t/a}.$$

In the region in which  $r$  lies between  $r$  and  $r+dr$  we consequently at the time  $t$  find the mass

$$4\pi\beta r^2 dr \cdot \frac{e^{-3t/a}}{(1 - r^2/a^2)^{5/2}}.$$

The naturally measured volume of this zone is

$$4\pi r^2 dr : (1 - r^2/a^2)^{1/2},$$

so that the quantity

$$\beta \cdot \frac{e^{-3t/a}}{(1 - r^2/a^2)^2}$$

is to be regarded as the density at the distance  $r$  and at the time  $t$ .

Berkeley, California,  
July 1929.

LXXXVII. *The Equilibrium of Dense Stars.* By EDMUND C. STONER, Ph.D. (Camb.), Reader in Physics, University of Leeds\*.

*Introduction.*

IN white dwarf stars the last stages of the ionization process are reached, so that at least in the central parts the molecules consist almost entirely of atomic nuclei and free electrons. Under these conditions very high densities are possible. The mean densities deduced from observations, though large (of the order 50 to 100 thousand), fall very far short of those corresponding to a "close-packed" arrangement, if a naive view of the "sizes" of electrons and nuclei is taken. It was suggested that some limitation might be introduced by the "jamming" of a few remaining atoms with K-ring electrons. In a previous paper †, however, it was shown that a limitation is imposed by the exclusion principle applying to free electrons, as embodied in the Fermi statistics. The number of electrons with momenta within a definite range cannot exceed a certain maximum. Any increase in density involves an increase of energy. In the limiting case, at absolute zero, the star can contract until the decrease in gravitational energy becomes insufficient to balance the increase of kinetic energy of the electrons. With a few simplifying assumptions, an expression was derived which indicated that the maximum density varied as the square of the mass of the star. It has been pointed out by Anderson‡ that in this calculation the effect of the relativity change of mass was neglected. He has taken this effect into account, but in a manner which seems open to criticism. His general conclusions, which seem to be correct, are that the simple expression holds provided the electron densities are not too large, but that the mass corresponding to large electron densities is smaller than that previously calculated, and that it reaches a limit. The correction becomes important for stars of mass about half that of the Sun, and so for the white dwarfs which were actually considered. The main purpose of this paper is to calculate the effect of the relativity change of mass, using a method which seems more rigorous than

\* Communicated by Prof. R. Whiddington, F.R.S.

† E. C. Stoner, Phil. Mag. vii. p. 63 (1929). (This paper will be referred to as I.)

‡ W. Anderson, Zeits. für Phys. lvi. p. 851 (1929).

that of Anderson. The conclusion drawn is that the range in which the simple expression holds approximately is wider than that indicated by Anderson's results, the "limiting mass" being somewhat greater, so that there is still an equilibrium state, under the particular conditions, for the stars under consideration. The significance of the results for very dense stars is discussed, and the effect of the electron gas following the Fermi statistics at the smaller densities found in normal stars is briefly considered.

*Effect of the Relativity Change of Mass on the Zero-point Energy of Electron Gas.*

Let  $E_g$  be the gravitational energy of the idealized star,  $E_k$  the total kinetic energy of the electrons,  $n$  the number of electrons per unit volume. Then, as previously shown, the equilibrium condition is given by

$$\frac{d}{dn}(E_g + E_k) = 0. \quad (1)$$

Let  $\bar{\epsilon}$  be the mean kinetic energy of the electrons at absolute zero,  $V$  the volume of the star, supposed to be of uniform density. (The distribution of density will be considered later.) When the relativity change of mass is neglected, the total kinetic energy at absolute zero is given by

$$E_k = nV\bar{\epsilon} = nV \frac{3}{40} \left(\frac{3}{\pi}\right)^{2/3} \frac{h^2 n^{2/3}}{m_0}. \quad (2)$$

It is this expression which has to be modified.

In Anderson's treatment  $m_0$  is replaced by  $m$ , where  $m$  is derived from the equation

$$c^2(m - m_0) = \frac{3}{40} \left(\frac{3}{\pi}\right)^{2/3} \frac{h^2 n^{2/3}}{m}. \quad (3)$$

It is thus assumed that the total kinetic energy can be expressed in the alternative forms

$$nVc^2(m - m_0) \quad \text{and} \quad nV \frac{3}{40} \left(\frac{3}{\pi}\right)^{2/3} \frac{h^2 n^{2/3}}{m},$$

where  $m$  has the same value in both expressions, being a "mean" mass; further, that this mean mass can be employed in subsequent calculations in place of  $m_0$ . The value of a mean mass, however, depends on the manner in which the mass enters into the particular expressions for which the appropriate mean value is being derived, and it is not legitimate to use one particular mean value indiscriminately

in more general calculations. (Perhaps the simplest illustration is that the arithmetic mean is not in general equal to the root mean square. The objection to Anderson's treatment has a similar basis.) It seems more satisfactory to attack the problem of determining the zero-point energy without introducing the idea of mean mass at all.

Let  $\epsilon$  be the kinetic energy of an electron,  $p$  the momentum, and let  $\beta = v/c$ ,

$$\epsilon = (m - m_0)c^2 = m_0c^2 \left( \frac{1}{\sqrt{1 - \beta^2}} - 1 \right), \quad . \quad . \quad (4)$$

$$p^2 = (m\beta c)^2 = m_0^2c^2 \left( \frac{1}{1 - \beta^2} - 1 \right). \quad . \quad . \quad . \quad (5)$$

Substituting for  $1/\sqrt{1 - \beta^2}$  in (4),

$$\epsilon = m_0c^2 \left[ \left( 1 + \frac{p^2}{m_0^2c^2} \right)^{1/2} - 1 \right] \quad . \quad . \quad . \quad (6)$$

In the completely condensed state there are two electrons in each cell of the 6-dimensional phase-space (of 6-volume  $h^3$ ), so that the number of electrons in a volume  $V$  with momenta between  $p$  and  $p + dp$  is equal to

$$2 \times \frac{4\pi p^2 dp}{h^3} \times V.$$

Thus for the total energy  $E_K$  of the electrons in a condensed state with maximum momentum  $p_0$

$$E_K = \int_0^{p_0} 2m_0c^2 \left[ \left( 1 + \frac{p^2}{m_0^2c^2} \right)^{1/2} - 1 \right] \frac{4\pi p^2 dp V}{h^3}. \quad . \quad (7)$$

Since  $nV$  is the total number of electrons (double the number of cells), the maximum momentum  $p_0$  is related to  $n$  by

$$(V/h^3) \int_0^{p_0} 4\pi p^3 dp = \frac{1}{2} nV.$$

$$\left. \begin{aligned} n &= \frac{8\pi p_0^3}{h^3}, & p_0 &= \left( \frac{3h^3 n}{8\pi} \right)^{1/3} \\ y &= \frac{p}{m_0c}, & x &= \frac{p_0}{m_0c} \end{aligned} \right\} \quad . \quad . \quad (8)$$

Let

Then

$$\begin{aligned} E_K &= \frac{8\pi V m_0 c^2}{h^3} \times (m_0 c)^3 \int_0^x \{(1+y^2)^{1/2} - 1\} y^2 dy, \\ &= \frac{8\pi V m_0^4 c^5}{h^3} \left[ -\frac{x^3}{3} + \int_0^x (1+y^2)^{1/2} y^2 dy \right] \quad . \quad (9) \\ &= \frac{8\pi V m_0^4 c^5}{h^3} \left[ -\frac{x^3}{3} + f(x) \right] \dots \dots \dots (9a) \end{aligned}$$

As long as  $x$  is small (i. e.,  $p_0 \ll m_0 c$ ),  $f(x)$  may be readily evaluated by integration in series,

$$\begin{aligned} [f(x)]_{x <} &= \frac{1}{3} x^3 + \frac{1}{10} x^5 - \frac{1}{56} x^7 \dots, \\ E_K &= \frac{8\pi V m_0^4 c^5}{10 h^3} x^5 \left( 1 - \frac{5}{28} x^2 \dots \right) \dots \dots (10) \end{aligned}$$

Substituting for  $x$

$$E_K = \frac{8\pi V}{3 h^3 m_0} p_0^5 \left( 1 - \frac{5}{28} \frac{p_0^2}{m_0^2 c^2} \dots \right), \quad \dots \dots (10a)$$

$$= n V \frac{3}{40} \left( \frac{3}{\pi} \right)^{2/3} \frac{h^2 n^{2/3}}{m_0} \left[ 1 - \frac{5 h^2}{112} \left( \frac{3}{\pi} \right)^{2/3} n^{2/3} \right], \dots (10b)$$

agreeing in the limit with (2) for  $n$  small.

The above expression may be used for  $p_0 \ll m_0 c$ , corresponding to  $n \ll \frac{8\pi}{3} \left( \frac{m_0 c}{h} \right)^3$ , or, substituting numerical values,  $n \ll 5.88 \times 10^{29}$ . For stars of mass .44 and .85 that of the Sun, the value of  $n$  came out on the simple theory as about  $1.86 \times 10^{29}$  and  $6.9 \times 10^{29}$ . The approximation given by series integration is thus inadequate, and it is necessary to use the complete expression for the integral

$$\begin{aligned} f(x) &= \int_0^x (1+y^2)^{1/2} y^2 dy, \\ &= \int_0^x (1+y^2)^{3/2} dy - \int_0^x (1+y^2)^{1/2} dy. \end{aligned}$$

The second integral is known, and the first may be reduced by noting that

$$\frac{d}{dy} \{y(1+y^2)^{1/2}\} = 4(1+y^2)^{3/2} - 3(1+y^2)^{1/2}.$$



The final result is

$$f(x) = \frac{1}{8} [x(1+x^2)^{1/2}(1+2x^2) - \log \{x + (1+x^2)^{1/2}\}]. \quad (11)$$

For  $x$  small this may be expanded (noting that the log is equal to

$$\int (1+x^2)^{-1/2} dx),$$

giving the result (10) on substitution in (9a).

The complete expression for the total kinetic energy of the electrons thus becomes

$$E_K = \frac{8\pi V m_0^4 c^5}{h^3} \left[ \frac{1}{8} x(1+x^2)^{1/2}(1+2x^2) - \frac{1}{8} x^3 - \log \{x + (1+x^2)^{1/2}\} \right], \quad (12)$$

with

$$x = \frac{p_0}{m_0 c} = \frac{1}{m_0 c} \left( \frac{3h^3 n}{8\pi} \right)^{1/3}.$$

The energy is less than that given by (2). In the limit when  $x$  is large ( $x \gg 1$ ,  $n \gg 5.88 \times 10^{29}$ ),

$$\begin{aligned} (E_K)_{x \gg 1} &= \frac{8\pi V m_0^4 c^5}{h^3} \frac{x^4}{4}, \\ &= \frac{2\pi V c}{h^3} p_0^4 = n V \frac{3}{8} \left( \frac{3}{\pi} \right)^{1/3} h c n^{1/3}. \quad (12a) \end{aligned}$$

These expressions may be compared with (10a) and (10b). They show that when  $n$  is large the mean kinetic energy increases as  $n^{1/3}$  (instead of  $n^2$ ). For a constant total number of electrons ( $nV$  constant),  $E_K$  then varies as  $n^{1/3}$ , as does also  $-E_G$ . When this is so there will obviously be no equilibrium under the conditions imposed.

### *The Equilibrium Condition.*

If the conditions are such that an equilibrium state is possible, there will be a limiting density—"limiting" because the calculation refers to a sphere of uniform density at zero temperature. The limiting density is that corresponding to the value of  $n$  when

$$\frac{d}{dn} (E_K + E_G) = 0. \quad (13)$$

It is more convenient, for the present application, to treat  $x$ , defined by (8), as the variable, so that the equilibrium condition becomes

$$\frac{d}{dx} (E_K + E_G) = 0. \quad (14)$$

For the gravitational potential energy (as shown in I.) with  $2.5 m_H$  as the mean molecular weight of the material of the star,

$$E_g = -\frac{3}{5} \frac{GM^2}{M^{1/3}} \left(\frac{4}{3}\pi n\right)^{1/3} (2.5 m_H)^{1/3}. \quad (15a)$$

Substituting  $\left(\frac{8\pi}{3}\right)^{1/3} \frac{m_0 c x}{h}$  for  $n^{1/3}$  from (8),

$$E_g = 3^{1/3} \left(\frac{4\pi}{5}\right)^{2/3} \frac{1}{h} GM^{5/3} m_H^{1/3} m_0 c x. \quad (15b)$$

From (12)  $E_K$  may be written as

$$E_K = \frac{8\pi V m_0^4 c^5}{h^3} f_1(x).$$

Substituting  $M/(2.5 m_H n)$  for  $V$ , and further substituting for  $n$  as above,

$$E_K = \frac{3M m_0 c^2}{2.5 m_H} \frac{f_1(x)}{x^3}. \quad (16)$$

Using the values (15) and (16) in (14), the result is

$$\frac{d}{dx} \left[ \frac{1}{x^3} f_1(x) \right] = 10^{1/3} \left(\frac{\pi}{3}\right)^{2/3} \frac{G m_H^{4/3} M^{2/3}}{hc}. \quad (17)$$

Inserting numerical values,

$$\frac{d}{dx} \left[ \frac{1}{x^3} f_1(x) \right] = F(x) = 1.483 \times 10^{-23} M^{2/3}, \quad (18)$$

$$M = 1.751 \times 10^{34} [F(x)]^{3/2}. \quad (18a)$$

$F(x)$  is obtained by straightforward differentiation of  $\frac{1}{x^3} f_1(x)$ , where  $f_1(x)$  is the bracketed quantity in (12).

The final result is

$$F(x) = \frac{1}{8x^3} \left[ \frac{3}{x} \log\{x + (1+x^2)^{1/2}\} + (1+x^2)^{1/2} (2x^2 - 3) \right]. \quad (19)$$

By means of equations (18a) and (19) the mass may be found corresponding to any value of  $x$ , and so to any limiting electron concentration. Since the mean molecular weight is about  $2.5 m_H$ , the limiting density is given by

$$\rho_0 = 2.5 m_H n = 4.15 \times 10^{-24} n. \quad (20)$$

*Numerical Results.*

The method of procedure adopted is to calculate  $F(x)$  for different values of  $x$ , from which a  $F(x)$ ,  $x$  curve may be plotted. From this, using (18a), an  $M$ ,  $x$  curve may be derived. If desired, this may be converted into an  $M$ ,  $n$  curve, using the relation

$$n = \left(\frac{8\pi}{3}\right) \left(\frac{m_0 c}{h}\right)^3 x^3,$$

giving

$$n = 5.876 \times 10^{29} x^3 \quad \text{or} \quad x = 1.194 \times 10^{-10} n^{1/3}. \quad (21)$$

The full expression for  $F(x)$  (19) is inconvenient to use when  $x$  is small. The expression may then be expanded, with the result

$$[F(x)]_{x \ll 1} = \frac{1}{5}x - \frac{1}{14}x^3 + \frac{1}{24}x^5 \dots \dots (19a)$$

When  $x$  is small enough for the first term in the expansion to be sufficient, the same result is obtained as before, namely,

$$n = 10^4 \left(\frac{\pi}{3}\right)^3 \frac{1}{h^6} G^3 M^2 m_H^4 m^3, \quad \dots (19a')$$

or, substituting numerical values from (18a), (20), and (21),

$$\left. \begin{aligned} n &= 2.396 \times 10^{-37} M^2, \\ \rho &= 9.95 \times 10^{-61} M^2. \end{aligned} \right\} \dots (22)^*$$

The first two terms in (19a) give  $F(x)$  correct to less than 1 per cent. up to  $x = .5$ , and form the most convenient expression for this range.

When  $x$  is large, as may be seen from (19),

$$\begin{aligned} [F(x)]_{x \gg 1} &= \frac{1}{8x^3} (2x^3 - 3x), \\ &= .2500 - \frac{3}{8x^2} \dots \dots (19b) \end{aligned}$$

This expression gives  $F(x)$  correct to 1 per cent. for  $x > 10$ . It indicates, moreover, the limiting mass for which an

\* This is in agreement with Anderson's result. In I., as pointed out by Anderson, a slight numerical error was made, and the result was given as  $n = 2.31 \times 10^{-37} M^2$ . Correspondingly, the result for the maximum density, given as  $\rho = 3.85 \times 10^8 (M/M_\odot)^2$ , should be  $\rho = 3.977 \times 10^8 (M/M_\odot)^2$ , with the Sun's mass,  $M_\odot$ , taken as  $2.0 \times 10^{33}$ .

equilibrium state can be attained under the conditions, namely, from (18a),

$$\begin{aligned} M_0 &= 1.751 \times 10^{34} (\cdot 25)^{3/2}, \\ &= 2.19 \times 10^{33}. \end{aligned} \quad (23)$$

TABLE I.

Corresponding values of  $x$ ,  $F(x)$ ,  $\log_{10} n$ , and  $\log_{10} M$ .

$$\begin{aligned} n &= 5.876 \times 10^{29} x^3, \\ M &= 1.751 \times 10^{34} [F(x)]^{3/2}. \end{aligned}$$

$x$ .	$F(x)$ .	$\log_{10} n$ .	$\log_{10} M$ .
·1	·0200	26·7690	31·6947
·2	·0394	27·6720	32·1364
·3	·0581	28·2003	·3895
·4	·0756	·5753	·5609
·6	·1071	29·1036	·7879
·8	·1330	·4783	·9291
1·0	·1537	·7690	33·0233
1·5	·1887	30·2973	·1569
2	·2085	·6720	·2220
3	·2280	31·2003	·2801
4	·2366	·5753	·3042
5	·2410	·8660	·3162
6	·2436	32·1036	·3233
8	·2463	·4783	·3303
10	·2476	·7690	·3339
20	·2494	33·6720	·3385
40	·2498	34·5753	·3396
60	·2499	35·1036	·3399
100	·2500	·7690	·3401

The value obtained by Anderson for  $M_0$  is  $1.37 \times 10^{33}$ , so that the range of mass in which this particular type of equilibrium can occur is shown by this method to be considerably greater than that indicated by Anderson's approximate treatment.

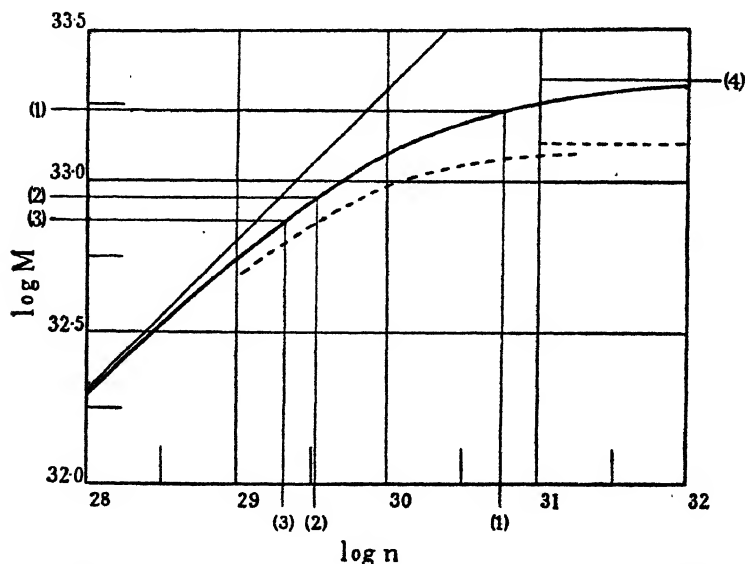
A series of corresponding values of  $x$  and  $F(x)$  calculated from (19), supplemented by (19a) and (19b), is shown in Table I. The relation required is that between  $n$  and  $M$ , related to  $x$  and  $F(x)$  by (21) and (18a). It is convenient

to use logarithms (base 10) when the following equations are obtained :

$$\log_{10} n = 29.7690 + 3 \log x, \quad . . . . (24)$$

$$\log_{10} M = 34.2432 + \frac{3}{2} \log F(x). \quad . . . . (25)$$

The conversion is then readily carried out. Corresponding values of  $n$  and  $M$  are shown in the last two columns of the table. It is unnecessary to give values for  $\log M$  less than 32, as no stars are known of mass less than a tenth that of the Sun ( $\log M_s = 33.3010$ ), and in any case, for stars of small mass, the approximate expression (22) will be sufficiently accurate. For any value of  $M$  the maximum value of  $\log n$  can be found by interpolation, and from that



Variation of limiting electron concentration ( $n$ ) with mass ( $M$ ) in a sphere of uniform density.

(1) Sirius B . . . . .	$\log M = 33.230$	$\log n = 30.748$
(2) $\alpha$ Eridani B . . . .	$\log M = 32.944$	$\log n = 29.524$
(3) Procyon B . . . . .	$\log M = 32.869$	$\log n = 29.313$
(4) Limiting $M$ . . . .	$\log M_0 = 33.340$	$(M_0 = 2.19 \times 10^{33})$

For the limiting density  $\log \rho_0 = \log n - 24 + 0.618$ .

The straight line corresponds to the formula in which the relativity effect is neglected. The dotted curve gives Anderson's results.

the value of  $n$ . If the density is required it can be found from (20), while  $\log \rho_0$  is given by

$$\log \rho_0 = \log n - 24 + 0.6180. \quad . . . . (26)$$

The relation between  $\log M$  and  $\log n$  is shown by the curve in the figure. The "positions" of a number of stars are indicated. The straight line is the result found by the original approximation, in which the relativity effect was neglected (giving  $n$  varying as  $M^2$ ). The main conclusion is that for stars for which this equilibrium can occur the limiting density is somewhat less than that calculated by Anderson, and that the "limiting mass" is larger; his results are indicated by the dotted line.

### White Dwarfs.

The number of stars known to be of the white dwarf type is small, but this does not necessarily indicate that stars of very high density are uncommon. Dense stars of ordinary mass will have a small radius, and so will be faint objects unless they are near the Sun (on the stellar scale of nearness) or have a high-surface temperature. "Black dwarfs" (to use Fowler's term) would not be observed. According to Jeans \*, four white dwarfs are known with certainty, but for one of these—the companion of the red giant  $\alpha$  Ceti—he does not give any quantitative data. Procyon B is a possible white dwarf, but its spectral type is unknown. In the following table are collected the relevant observational data derived from Jeans †. Procyon B is included because its mass is known. The four columns give the spectral type, the absolute visual and bolometric magnitudes, and the mass in terms of the Sun's mass ( $M_\odot$ ).

TABLE II.  
Observational Data.

	Spectral Type.	$M_{\text{vis.}}$	$M_{\text{bol.}}$	$M/M_\odot$
Sirius B .....	A 7	11.3	11.2	.85
$\alpha_2$ Eridani B .....	A 0	11.2	10.8	.44
Procyon B ... ..	—	16	—	.37
Van Maanen's star .....	F	14.3	14.3	—

\* J. H. Jeans, 'Astronomy and Cosmogony,' p. 63 (Camb. Univ. Press, 1928).

† *Loc. cit.* p. 59. I am indebted to Prof. Eddington for informing me that the value .21 given for the mass of  $\alpha_2$  Eridani B in his 'Internal Constitution of the Stars' is based on an earlier determination of the orbit, and that the value .44 is presumably the more trustworthy. Also to Sir James Jeans for confirming the value .44.

From these observational data deductions may be made as to other characteristics of the stars. From the spectral type the surface temperature ( $T_s$ ) may be estimated, and from the effective temperature and the absolute magnitudes the radius of the star. The following formulæ are given by Jeans for the radius in terms of that of the sun ( $r/r_s$  denoted by  $R$ ):—

$$\log R = -0.2 M_{\text{bol.}} - 2 \log T_s + 8.53, \quad . \quad . \quad (27a)$$

$$\log R = -0.2 M_{\text{vis.}} + \frac{5880}{T_s} - 0.01. \quad . \quad . \quad (27b)$$

It is further possible to calculate the total radiation of energy in ergs per second ( $E$ ),

$$\log E = -0.4 M_{\text{bol.}} + 35.52. \quad . \quad . \quad . \quad (28)$$

TABLE III.

Deduced Characteristics of Sirius B and  $\alpha_2$  Eridani B.

	$M/M_s$	$T_s$	$R$	$E'$	$\rho$	$\rho_0$ calc.
Sirius B .....	.85	8,000	.0312	.0065	$3.97 \times 10^4$	$2.3 \times 10^7$
$\alpha_2$ Eridani B...	.44	11,200	.0187	.0185	$9.55 \times 10^4$	$1.4 \times 10^6$

The amount of radiation per gram ( $E'$ ) is a quantity of great interest :

$$\begin{aligned} \log E' &= \log E - \log M, \\ &= \log E + \log (M_s/M) - \log M_s, \\ &= -0.4 M_{\text{bol.}} + 2.22 + \log (M_s/M). \quad . \quad (29) \end{aligned}$$

(The sun's mass is taken as  $2.0 \times 10^{33}$  grams.)

The mean density is given by

$$\begin{aligned} \rho &= \frac{3M}{4\pi r^3} = \left(\frac{M}{M_s}\right) \left(\frac{r_s}{r}\right)^3 \frac{3M_s}{4\pi r_s^3}, \\ &= (M/M_s) (1/R)^3 \rho_s = 1.42 (M/M_s) (1/R)^3. \quad . \quad (30) \end{aligned}$$

The values given in Table III. have been calculated from these equations. It may be noted that for Sirius B the radius deduced from the relativity shift is .03, in remarkable agreement with the value .0312 calculated in the way indicated. (In general the values are not significant to more than two figures.) The available data for Procyon B and Van Maanen's Star are insufficient for the calculation

of  $\rho$  or  $E'$ ; these stars will be discussed later. The value of  $M/M_s$  is included in the table, and also the value of the limiting density,  $\rho_0$ , calculated as already described.

The calculated limiting densities are considerably greater than those obtained by the simple formula (19a) (used in I.), which gives for stars of the mass of Sirius B and  $\alpha_2$  Eridani B the values  $\rho = 2.8 \times 10^6$  and  $7.5 \times 10^5$ . The order of magnitude of the difference for stars of different mass will be apparent from the figure.

The calculated radiation per gram ( $E'$ ) of  $\alpha_2$  Eridani B is about 10 times greater than the value given by Jeans. This will be discussed later. The mean density for Sirius B is somewhat smaller than that usually given (about  $5 \times 10^4$ ). This results from the use of a slightly larger value for the radius. Taking the relativity shift value ( $R = .03$ ), the mean density comes out as  $4.5 \times 10^5$ .

### Mean Molecular Weight.

The mean molecular weight has been taken as  $2.5 m_H$ . This is the value for completely ionized atoms of lead  $\left(\frac{207.2}{82+1}\right)$ . For atoms of lower atomic number the value is slightly smaller, and for those of high atomic number, larger. Jeans derives a value  $2.6 m_H$  on the assumption, for which there is strong evidence, that in many stars atoms of the atomic number equal to that of uranium, and even higher, are present. In condensed stars of the type considered, however, most of these atoms will have been transformed into atoms of an inert type, and the estimate  $2.5 m_H$  is probably sufficiently accurate. In any case, a small change will not affect the numerical results appreciably.

It might be thought that the change of mass of the electron would produce a not negligible effect, but it may readily be shown that the effect will be very small. Let  $m$  be the mass of an electron with momentum  $p$ . The molecular weight becomes  $2.5 m_H + \mu$ , where

$$2.5 m_H + \mu = m_H \left( 2.5 + \frac{m - m_0}{m_H} \right).$$

Now

$$m^2(1 - \beta) = m_0^2,$$

$$\beta = \frac{p}{mc} = \left( \frac{p}{m_0 c} \right) \frac{m_0}{m}$$



$$\frac{m-m_0}{m_0} = \left[ 1 + \left( \frac{p}{m_0 c} \right)^2 \right]^{1/2},$$

$$2.5 m_H + \mu = m_H \left[ 2.5 + \frac{1}{1845} \left\{ 1 + \left( \frac{p}{m_0 c} \right)^2 \right\}^{1/2} \right]. \quad (31)$$

From (8) the maximum momentum is given by

$$p_0 = \left( \frac{3h^3 n}{8\pi} \right)^{1/3},$$

so that

$$\frac{p_0}{m_0 c} = \frac{h}{m_0 c} \left( \frac{3}{8\pi} \right)^{1/3} n^{1/3},$$

$$= 1.194 \times 10^{-10} n^{1/3}. \quad (32)$$

For an electron concentration  $n = 10^{33}$  (corresponding to a density greater than  $10^9$ ) the maximum molecular weight is

$$2.5 m_H + \mu = m_H (2.5 + .0065). \quad (31a)$$

The correction is thus quite negligible for all the densities which come into consideration.

### Mean Density.

In the foregoing treatment the star has been idealized as having a uniform density. This seems legitimate when the aim has been to obtain an estimate of the maximum density under gravitational-kinetic equilibrium. In an actual star, however, the density will not be uniform, even in the condensed limit. When  $n$  is small the energy per unit volume is proportional to  $n^{5/3}$  (eq. 10 *b*), and when  $n$  is large, to  $n^{4/3}$  (eq. 12 *a*). Since the pressure is proportional to the energy per unit volume, and the density is proportional to  $n$ , the following relations hold between the pressure and density:—

$$n \ll 5.9 \times 10^{29}, \quad \rho \ll 2.4 \times 10^6, \quad p = \kappa \rho^{5/3}, \quad (33a)$$

$$n \gg 5.9 \times 10^{29}, \quad \rho \gg 2.4 \times 10^6, \quad p = \kappa \rho^{4/3}. \quad (33b)$$

In an ideal condensed star the distribution will thus be polytropic, the relation between pressure and density obeying the relation  $p = \kappa \rho^\gamma$ . The distributions in polytropic stars for a number of values of  $\gamma$  (or its equivalent  $n'$ , defined by  $\gamma = 1 + 1/n'$ ) have been worked out by Emden. The results are quoted by Eddington\*. Table IV. gives the ratio of the

\* A. S. Eddington, 'The Internal Constitution of the Stars,' p. 89 (C. U. P. 1926).

maximum (central) to the mean density. Uniform density corresponds to  $n'=0$ .

This table certainly indicates that the maximum mean density may be considerably less than the maximum central density, and it might seem that all that is necessary to convert the previously calculated results for limiting densities to mean densities is to divide by the appropriate ratio. There are a number of other factors, however, which have to be taken into consideration. The gravitational energy of a star is given by \*

$$E_g = -\frac{3}{5-n'} G \frac{M^2}{r} \dots \dots (34)$$

For uniform density the coefficient is  $3/5$ , the value used (eq. 15 a). For  $\gamma=5/3$  the factor becomes  $6/7$ , so that for a given  $M$  the calculated  $n$  would be increased. The whole

TABLE IV.

Ratio of Maximum to Mean Density in Polytropes.

$\gamma$ .....	$\infty$	5/3	3/2	7/5	4/3
$n'$ .....	0	3/2		5/2	3
$\rho_0/\rho$ .....	1	6.00	11.4	24.1	54.4

calculation, however, is based on the assumption that  $n$  is uniform, and different averaging processes would have to be carried out in deriving expressions for the gravitational and kinetic energies in terms either of  $n_0$  (the central electron concentration) or the mean  $n$ . Some rough calculations indicate that the values derived for the limiting concentrations approximate to those for  $n_0$ ; but a much more elaborate investigation would be necessary if the variation of density were to be properly taken into account. The indications are that the values obtained for the limiting density approach those for the limiting central density, and that the limiting mass may be slightly changed; that Sirius B still falls within the range for which gravitational-kinetic equilibrium can occur; and that the limiting mean densities may be smaller than those calculated approximately in the ratios suggested by the values in Table IV. These results, however, are somewhat uncertain, and for the present the calculations are left in the form which is strictly appropriate for the case of the homogeneous sphere.

\* Eddington, *loc. cit.* p. 87.

*Van Maanen's Star and Procyon B.*

Van Maanen's Star is of great interest, as it is the smallest star known, being about the same size as the earth. From the data in Table II. the radius may be calculated (eq. 27), the result being  $R = \cdot 00955$ , taking the surface temperature as 7000 corresponding to an F-type star. The mass is unknown, and since the star is not a binary component, there is no method available by which it may be estimated. It is, however, possible to calculate *compatible* values of the mass (giving the mean density) and of the radiation per gram ( $E'$ ) from the known data. From (29),

$$\log E' = -5\cdot72 + 2\cdot22 + \log (M_s/M),$$

$$E'(M/M_s) = 3\cdot162 \times 10^{-4}. \quad . \quad . \quad . \quad (35)$$

TABLE V.

Compatible Values for Van Maanen's Star.

 $T_s = 7000. \quad R = \cdot 00955.$ 

$M/M_s.$	$E'.$	$10^{-6}\rho.$	$10^{-6}\rho_0$ calc.
2	0016	33	19
4	0008	65	114
6	0005	98	37
8	0004	130	131
10	0003	163	104

In Table V. are given compatible values of  $M/M_s$ ,  $\rho$ , and  $E'$ , together with the calculated  $\rho_0$  for each value of the mass. Incidentally, this table gives the values of  $\rho_0$  for a range of masses.

As will be seen from the above table, the values which Jeans suggests as a pure guess \* for  $M/M_s$  and  $E'$ —2 and 00055—are not compatible with each other. The interesting point which emerges, however, is that unless the numerical results of the equilibrium theory are very wide of the mark owing to the essential factors being ignored, a lower limit for the mass of Van Maanen's Star can be roughly estimated. The mean density cannot be greater than the calculated limiting density, and it is probably several times smaller.

\* J. H. Jeans, 'The Universe Around Us,' p. 310 (C. U. P. 1929).

From this it is possible to draw the following conclusions for Van Maanen's Star :—

$$M/M_s > \cdot 4, \quad \rho > 650,000, \quad E' < \cdot 0008.$$

For Procyon B the spectral type is unknown, though it is probably M or K\*. It is, however, of interest to examine how far the star approaches the condensed type if a reasonable value of the surface temperature is assumed. For assumed temperatures of 3000 (M type) and 4000 (K type) the estimated correction† to convert  $M_{vis.}$  to  $M_{bol.}$  may be applied, and using (27), (29), and (30), the following results are obtained :—

TABLE VI.

Compatible Values for Procyon B.

$$M/M_s = \cdot 37. \quad \rho_0 \text{ calc.} = \cdot 84 \times 10^6.$$

$T_e$ .	$M_{bol.}$	R.	$\rho$ .	$E'$ .
3000	14	$\cdot 056$	$2\cdot 4 \times 10^3$	$\cdot 001$
4000	15\cdot 5	$\cdot 018$	$1\cdot 1 \times 10^5$	$\cdot 0003$

Of course nothing definite can be deduced from these results, as in the case of Van Maanen's Star. They simply serve to show that unless the surface temperature is considerably greater than 3000, Procyon B does not approach the limiting condensed state, the mean density being much smaller than that of other white dwarfs.

### *Generation of Energy.*

Some of the more important observed and deduced data for the three white dwarfs about which most is known are collected together, for convenience in comparison, in Table VII. The total energy radiated per second is symbolized by  $E$ , the energy per gram by  $E'$ .

As was to be expected, the calculated limiting density  $\rho_0$  is considerably greater than the "observed" mean density. The polytrope ratios (Table IV.) suggest that the maximum mean density may be something approaching 50 times smaller than  $\rho_0$  for Sirius B, and 6 times smaller for

\* J. H. Jeans, 'Astronomy and Cosmogony,' p. 128.

† *Ibid.* p. 46.

$\alpha_2$  Eridani B. If these ratios are approximately correct,  $\alpha_2$  Eridani B may be said to approach the limiting condensed state fairly closely, while Sirius B is still far removed from it. If the observational data (Table II.) and the essentials of the equilibrium theory are correct, Van Maanen's Star is certainly the most dense that is known, though it is impossible to say how nearly it approaches the condensed limit.

If the observational data are correct, again, there is for stars of this type no simple relation between the mass and luminosity—as is shown by the absolute bolometric magnitude of  $\alpha_2$  Eridani B being smaller than that of Sirius B, although its mass is smaller. The radiation per gram, moreover, does not decrease steadily with the mass of the star, as had been suggested\*.

TABLE VII.

Observed and Deduced Data for White Dwarfs.

	$M/M_\odot$	$T_s$	R.	$\rho$ .	$\rho_0$ calc.	$h$ .	$E'$ .
Sirius B .....	·85	8,000	0312	40,000	$23 \times 10^6$	$1.1 \times 10^{31}$	0065
$\alpha_2$ Eridani B .....	·44	11,200	·0187	95,000	$1.4 \times 10^6$	$1.6 \times 10^{31}$	·0185
Van Maanen's Star .	>·4	7,000	·0095	>650,000	$>1.1 \times 10^6$	$6.4 \times 10^{29}$	<·0008

According to Jeans's hypothesis, which, in spite of its speculative nature, certainly satisfies most of the conditions, the energy generation in stars is to be traced to electron-proton annihilation occurring in hyper-uranium atoms as a result of one of the extra-nuclear electrons of the atom falling into the nucleus. In completely ionized stars of the white dwarf type this process could not occur, so that the small radiation per gram of these stars is in complete accordance with the hypothesis. The radiation would be mainly due to the atoms in the outer layers of the star, so that there is not necessarily any simple relation between either the mass or the mean density and the amount of radiation per gram. It does none the less remain peculiar that  $\alpha_2$  Eridani B, which approaches the condensed state, should have a much higher surface temperature than Sirius B, and that it should generate more energy per gram. The material available in this connexion, however, is too slight to permit of any inductive generalizations being made.

\* J. H. Jeans, 'The Universe Around Us,' p. 310.

*The Fermi Statistics of Electron Gas at Lower Densities.*

The densities of white dwarfs are very much greater than those of other stars, in which the densities are too low and the temperatures too high for the electron gas to approach the condensed state. According to Jeans's theory of stellar evolution (outlined in I.), the tenanted portions of the Russell temperature-luminosity diagram correspond to stable states in which the pressures exceed considerably the perfect gas-pressures. There will be a range of stability for each successive stage of ionization of the atoms, and this, on the liquid-star hypothesis, corresponds to the "jamming" of the incompletely-ionized atoms. The difficulty about this hypothesis is that the size which must be attributed to the atoms is very much greater than that indicated by other evidence. Now, with the Fermi statistics the pressure is always greater than that of a perfect gas, and it is interesting to note that there will be a maximum deviation corresponding to each stage of ionization. When with increasing temperature there is an increase in the number of electrons through ionization, there will be a deviation from the perfect gas-relation between pressure and number of molecules. This deviation will decrease as the temperature increases, and will increase again when the next stage of ionization will increase. The deviations required, however, are much greater than those indicated by the Fermi statistics. This may be illustrated by taking a particular case and making the most favourable estimates. To ensure stability at the centre of the star, according to Jeans, the pressure must be at least 1.107 times the normal pressure \*. The pressure of electron gas is given by

$$p = nkT \left\{ 1 + \frac{1}{16 \times 2} \frac{nh^3}{(\pi mkT)^{3/2}} \dots \right\}. \quad (36)$$

Inserting numerical values

$$p = nkT \left\{ 1 + 3.62 \times 10^{-17} \frac{n}{T^{3/2}} \dots \right\}. \quad (37)$$

Taking  $\rho$  as  $2.5 \text{ } n m_H$ , Table VIII. gives the corresponding values of  $T$ ,  $n$ , and  $\rho$  for the pressure to exceed the normal by 10 per cent.

In stars generally, for a given central temperature the central density is of order of ten times less than that in

\* J. H. Jeans, 'Astronomy and Cosmogony,' p. 141.

the table. For the sun \* the central density is about 140, and the temperature can hardly be less than  $40 \times 10^6$ . This gives

$$p = nkT(1 + 0.48 \times 10^{-2}). \quad (38)$$

The pressure is thus about  $\frac{1}{2}$  per cent. above normal instead of the required 10 per cent. It would seem, therefore, that unless there are other parts of the theory requiring modification, a simple application of the Fermi statistics is unable to remove the difficulties, although it does lead to deviations from the perfect gas laws of the required type.

TABLE VIII.

Corresponding Values for the Pressure to exceed normal by 10 per cent.

T.	$n_e$	$\rho$ .
$10^3$	$2.76 \times 10^{28}$	$1.145 \times 10^{-3}$
$10^4$	$2.76 \times 10^{22}$	$1.145 \times 10^{-2}$
$10^5$	$2.76 \times 10^{24}$	$1.145 \times 10$
$10^6$	$2.76 \times 10^{27}$	$1.145 \times 10^4$

### Conclusion.

It is generally agreed that the dense dwarf stars represent an advanced stage of stellar evolution. It is reasonable to suppose that the *white* dwarf stage, corresponding to high surface temperature, will be a comparatively short one, and since the stars are small, it is probable that most condensed stars are too faint to be observed. From the mass luminosity relation, moreover, even treating this as a purely empirical generalization, the masses of condensed stars will in general be small. There is therefore a strong probability that stars of the type in which the gravitational kinetic equilibrium discussed in this paper is of importance are much more numerous than is suggested by the number of known examples. For these the theory may be said to account in a general way for the order of magnitude of the densities deduced from the observational data.

For more normal stars the application of the Fermi statistics shows that there will be an appreciable deviation from the perfect gas laws for the electron gas. Although the deviations will be of the kind required in Jeans's theory

\* *Ibid.* p. 104.

of stability, they are not nearly large enough. It would seem, therefore, either that the theory as to the conditions for stability requires modification, or that there are factors involved which are at present unrecognized.

### *Summary.*

In a previous paper the conclusion was reached that there was a limiting density for stars in which the atoms were completely ionized, varying as the square of the mass of the star. The limiting state occurs when the decrease in gravitational energy on contraction is equal to the increase in the total kinetic energy of the electron gas. In the treatment the relativity change of mass with velocity was neglected. Some approximate calculations by Anderson indicate the general effect of this change of mass, which necessitates a modification of the previous conclusions when the mass of the star becomes comparable with that of the sun.

In the present paper the effect of the relativity change of mass is worked out with more rigour for the idealized case for a sphere of uniform density. For spheres of increasing mass the limiting density varies at first as the square of the mass, and then more rapidly, there being a limiting mass ( $2.19 \times 10^{33}$ ) above which the gravitational kinetic equilibrium considered will not occur. Tables and curves are given showing the relation between mass and limiting density.

It is shown that the distribution of density in condensed stars will be polytropic, and rough estimates are made of the ratio of the central to the mean density.

The observational and deduced data for known white dwarfs are considered in some detail. The density of Sirius B is well below the limit calculated, while that of  $\alpha_2$  Eridani B approaches it. The theory enables a lower limit for the mass and density of Van Maanen's Star to be roughly estimated. The observational, deduced, and calculated data for these three stars, and also for Procyon B, are given in tables.

The deduced data indicate that the generation of energy per gram in known dense stars is not simply related to the mass of the star.

The application of the Fermi statistics to the electron gas in normal stars is briefly discussed in connexion with Jeans's theory of stability. There will be deviations from the perfect gas laws of the type required, but they are about twenty times too small to satisfy the stability conditions.

Physics Department,  
The University, Leeds.  
December 1929.



LXXXVIII. *Second Order Expressions for the Potentials of a Sphere.* By D. B. MAIR\*.

1. **T**HE measure  $ds$  of a timelike interval in the gravitational field of the sun being given in terms of polar coordinates by

$$ds^2 = -e^\lambda dr^2 - e^\mu (r^2 d\theta^2 + r^2 \sin^2 \theta d\phi^2) + e^\nu dt^2$$

$\Theta$  being the Newtonian potential of the sun (treated as a non-rotating sphere of perfect fluid, symmetrical about its centre), zero at infinity and negative elsewhere, and  $L$  being the product of the sun's mass and the gravitation constant, it is known that, to the first power of  $L$ , the set of values

$$\lambda = -2\Theta \quad \mu = -2\Theta \quad \nu = 2\Theta$$

give the potentials in matter and in the void, and that the set

$$\lambda = 2L/r \quad \mu = 0 \quad \nu = -2L/r$$

give the potentials in the void. The object of this paper is to extend the second set of expressions to matter, and to extend both sets of expressions to the second power of  $L$  for matter and the void.

2. In a reference system in which the sun is at rest the elements of the energy tensor are

$$T_{11} = pe^\lambda \quad T_{22} = pe^\mu r^2 \quad T_{33} = pe^\mu r^2 \sin^2 \theta \quad T_{44} = (\rho - p)e^\nu$$

$$T = \rho - 4p$$

The field equations

$$H_{\alpha\beta} \equiv G_{\alpha\beta} - \frac{1}{2}g_{\alpha\beta}G + \kappa T_{\alpha\beta} = 0$$

become in terms of  $\lambda \mu \nu$ , a dash denoting differentiation with respect to  $r$ ,

$$H_{11} \equiv \frac{e^{\lambda-\mu}-1}{r^2} - \frac{\mu' + \nu'}{r} - \frac{\mu'}{4}(\mu' + 2\nu') + \kappa pe^\lambda = 0$$

$$H_{22} \equiv r^2 e^{\mu-\lambda} \left\{ -\frac{\mu'' + \nu''}{2} + \frac{\lambda' - 2\mu' - \nu'}{2r} \right. \\ \left. + \frac{1}{4}(\lambda'\mu' + \lambda'\nu' - \mu'^2 - \mu'\nu' - \nu'^2) \right\} + \kappa p r^2 e^\mu = 0$$

\* Communicated by the Author.

$$H_{44} \equiv e^{\nu-\lambda} \left\{ \frac{1-e^{\lambda-\mu}}{r^2} + \mu'' + \frac{3\mu' - \lambda'}{r} + \frac{\mu'}{4}(-2\lambda' + 3\mu') \right\} + \kappa(\rho - p)e^{\nu} = 0$$

$H_{33}$  repeats  $H_{22}$  and all other equations  $H_{\alpha\beta}$  are identities. Along with these we have  $G = \kappa T$  or

$$H \equiv e^{-\lambda} \left[ \frac{2(e^{\lambda-\mu} - 1)}{r^2} - 2\mu'' - \nu'' + \frac{2\lambda' - 6\mu' - 2\nu'}{r} + \frac{1}{2} \{ (\lambda' - \nu')(2\mu' + \nu') - 3\mu'^2 \} \right] - \kappa T = 0$$

by which we may replace any one of the three.

3. As these equations contain the pressure  $p$  we must take account of the equations of matter

$$T_{\alpha\beta}^{\beta} = 0$$

For  $\alpha=1$  this is

$$p' + \frac{1}{2}\rho\nu' = 0$$

while the other equations are identities. This with the field equations constitute the equations that have to be satisfied.

As the field equations we take

$$H_{11} = 0 \quad H_{11} - \frac{e^{\lambda-\mu}}{r^2} H_{22} = 0 \quad e^{\lambda} H = 0$$

The four equations whose solution we seek are thus

$$J_1 \equiv -\frac{\mu' + \nu'}{r} + \frac{e^{\lambda-\mu} - 1}{r^2} - \frac{1}{4}\mu'(\mu' + 2\nu') + \kappa p e^{\lambda} = 0$$

$$J_2 \equiv \frac{\mu'' + \nu''}{2} - \frac{\lambda' + \nu'}{2r} + \frac{e^{\lambda-\mu} - 1}{r^2} + \frac{1}{4}(-\lambda'\mu' - \lambda'\nu' - \mu'\nu' + \nu'^2) = 0$$

$$J_3 \equiv -2\mu'' - \nu'' + \frac{2\lambda' - 6\mu' - 2\nu'}{r} + \frac{2}{r^2}(e^{\lambda-\mu} - 1) + \frac{1}{2}\{\lambda' - \nu'\}(2\mu' + \nu') - 3\mu'^2 - \kappa T e^{\lambda} = 0$$

$$J_4 \equiv p' + \frac{1}{2}\rho\nu' = 0$$

4. We first seek a solution of the first order in  $L$ , neglecting powers of  $L$ .  $J_1$  gives

$$\lambda = \mu + r(\mu' + \nu') \quad . \quad . \quad . \quad . \quad (4, 1)$$

With this value of  $\lambda$ ,  $J_2$  becomes an identity, and  $J_3$  becomes

$$\nu'' + \frac{2\nu'}{r} = \kappa T \quad (4, 2)$$

Since the Newtonian potential  $\Theta$  is given when the density is taken as  $T \equiv \rho - 4p$  by

$$\Theta'' + \frac{2\Theta'}{r} = 4\pi\chi T = \frac{1}{2}\kappa T \quad (4, 3)$$

in which  $\chi$  is the gravitation constant, equation (4, 2) shows that  $\nu$  is  $2\Theta$ , and the most general first order solution is thus

$$\lambda = \xi + r\xi' + 2r\Theta' \quad \mu = \xi + \nu = 2\Theta \quad (4, 4)$$

$\xi$  being such as to make  $\xi\xi'\lambda'$  continuous at the boundary of the sun, and otherwise at our disposal.

5. As second order solution we assume

$$\left. \begin{aligned} \lambda &= \xi + r\xi' + 2r\Theta' + \chi - \psi & \mu &= \xi + \chi - \psi + \omega \\ \nu &= 2\Theta + 2\psi - \chi \end{aligned} \right\} \quad (5, 1)$$

$\chi\psi\omega$  being second order quantities to be now determined. Substitution of these expressions in the equations of article 3 gives, to the second order,

$$K_1 \equiv -\left(\frac{\psi'}{r} + \frac{\omega'}{r} + \frac{\omega}{r^2}\right) + \frac{1}{4}\xi'^2 + \xi'\Theta' + 2\Theta'^2 + \kappa p = 0$$

$$K_2 \equiv \frac{1}{2}\left(\psi'' - \frac{\psi'}{r} + \omega'' - \frac{2\omega}{r^2}\right) + 2\Theta'^2 - \frac{r}{4}(\xi' + 2\Theta')(\xi'' + 2\Theta'') = 0$$

$$K_3 \equiv -\left(\chi'' + \frac{2\chi'}{r}\right) = 2\left(\omega'' + \frac{3\omega'}{r} + \frac{\omega}{r^2}\right) + \frac{3}{2}\xi'^2 + 6\xi'\Theta' + 4\Theta'^2$$

$$(1 + r(\xi' + \Theta'))(\xi'' + 2\Theta'') - \kappa T(\xi + r\xi' + 2r\Theta') = 0$$

$$K_4 \equiv p' + \rho\Theta' = 0$$

6. Integration of the equation  $2K_2/r = 0$  gives

$$\psi' + \omega' + \frac{\omega}{r} = \frac{r}{4}(\xi' + 2\Theta')^2 - 4r\Phi \quad (6, 1)$$

in which

$$\Phi' = \frac{\Theta'^2}{r} \quad (6, 2)$$

The use of this in equation  $K_1$  gives

$$\kappa p = -4\Phi - \Theta'^2 \quad (6, 3)$$

whence by differentiation and the use of equation (4, 3)

$$\kappa p' = -\frac{4\Theta'^2}{r} - 2\Theta'\Theta'' = -\kappa T\Theta' \quad (6, 4)$$

To the second order this is equation  $K_4$ , which is thus included in the other three and need not be considered further.

Integration of the equation  $r^2 K_3 = 0$  gives

$$\chi' + 2\left(\omega' + \frac{\omega}{r}\right) = \frac{\Psi}{r^2} \quad (6, 5)$$

in which

$$\begin{aligned} \Psi' &= r^2\left(\frac{3}{2}\xi'^2 + 6\xi'\Theta' + 4\Theta'^2\right) + r^3(\xi' + \Theta')(\xi'' + 2\Theta'') \\ &\quad - \kappa T r^2(\xi + r\xi' + 2r\Theta') \\ &= \frac{1}{2}(r^3\xi'^2)' + (r^3\xi'' + 2r^2\xi')\Theta' - \xi r^2\kappa T - r^3\kappa T\Theta' \quad (6, 6) \end{aligned}$$

7. The density  $T$  of the sun is assumed to be a function of the distance  $r$  from the centre. Let it be given by

$$\frac{1}{2}\kappa T = \frac{L}{a^3} \left\{ 3A_1 + 4A_2\frac{r}{a} + \dots + (g+2)A_g\left(\frac{r}{a}\right)^{g-1} \right\} \quad (7, 1)$$

in which  $a$  is the sun's radius. Since  $L$  is the sun's mass multiplied by  $\chi \equiv \kappa/8\pi$

$$L = \int_0^a \frac{1}{2}\kappa T r^2 dr = \int_0^a dr \frac{L}{a} \Sigma A_m(m+2) \left(\frac{r}{a}\right)^{m+1} = L \Sigma A_m$$

so that

$$\Sigma A_m \equiv A_1 + A_2 + \dots + A_g = 1 \quad (7, 2)$$

The differential equation for  $\Theta$  gives for  $\Theta_M$  in matter

$$(r^2\Theta'_M)' = \frac{1}{2}r^2\kappa T = \frac{L}{a} \Sigma A_m(m+2) \left(\frac{r}{a}\right)^{m+1}$$

$$\Theta'_M = \frac{L}{a^2} \Sigma A_m \left(\frac{r}{a}\right)^m$$

$$\Theta_M = \frac{L}{a} \Sigma A_m \frac{1}{m+1} \left(\frac{r}{a}\right)^{m+1} + B$$



so that

$$\Psi'_{\text{V}} = - \frac{2I_z^2}{r^2} . . . . . (9, 1)$$

$$\Psi'_M = \frac{2L^2}{a^2} \sum A_m A_n \left[ \left( \frac{2m+4}{n+1} - 1 \right) \left( \frac{r}{a} \right)^{m+n+2} - \frac{(2m+4)(n+2)}{n+1} \left( \frac{r}{a} \right)^{m+1} \right] \quad (9, 2)$$

and by integration

$$\Psi_V = \frac{2L^2}{r} + \frac{L^2}{a} C_2 \quad . \quad . \quad . \quad . \quad . \quad . \quad . \quad . \quad (9,3)$$

$$\Psi_M = \frac{2l^2}{a} \sum A_m A_n \left[ \left( \frac{2m+4}{n+1} - 1 \right) \frac{1}{m+n+3} \left( \frac{r}{a} \right)^{m+n+3} - \frac{2n+4}{n+1} \left( \frac{r}{a} \right)^{m+2} \right] \quad (9, 4)$$

In  $\Psi_M$  the integration constant is zero because  $\Psi/r^2$  is finite at the origin. The value of the constant  $C_2$  is given by the continuity of the  $\Psi$  at the sun's boundary and is

$$C_2 = -6 \sum A_m A_n \left( 1 + \frac{1}{m+n+3} \right) \quad . \quad . \quad (9, 5)$$

## 10. Writing

$$\Omega' = \omega' + \frac{\omega}{r}$$

we have from (6, 1) and (6, 5)

$$\psi'_V = -\Omega'_V + \frac{L^2}{r^3}$$

$$\psi'_M = -\Omega'_M - \frac{4L^2}{a^3} \sum A_m A_n \frac{1}{m+n} \left(\frac{r}{a}\right)^{m+n+1} - \frac{4L^2 r C_1}{a^4}$$

$$\chi'_{\nabla} = -2\Omega'_{\nabla} + \frac{2L^2}{r^3} + \frac{L^2 C_2}{ar^2}$$

$$\chi'_M = -2\Omega'_M + \frac{2L^2}{a^3} \sum A_m A_n \left[ \left( \frac{2m+n}{n+1} - 1 \right) \frac{1}{m+n+3} \left( \frac{r}{a} \right)^{m+n+1} - \frac{2n+4}{n+1} \left( \frac{r}{a} \right)^m \right]$$

Integrating these equations we have in the void

$$\psi_v = -\Omega_v - \frac{L^2}{2r^2}$$

$$\chi_v = -2\Omega_v - \frac{L^2}{r^2} - \frac{L^2 C_2}{ar}$$

the integration constants being zero because  $\psi$  and  $\chi$  vanish at infinity. The expressions for  $\psi_M$   $\chi_M$  in matter need not be written down. Each has an integration constant, and by means of them we make  $\psi$   $\chi$  continuous at the sun's boundary.

The quantity  $\omega$  is at our disposal. It and its first derivative must be made continuous at the sun's boundary. That done we have values of  $\psi$   $\chi$   $\omega$ , and therefore of  $\lambda$   $\mu$   $\nu$ , that satisfy the differential equations in matter and in the void, and are continuous together with their first derivatives across the boundary. Hence they give the values of the potentials to the second power of  $L$ .

11. From these values we have in the void, from equation (5, 1)

$$\lambda = \frac{L}{r} \left( 2 - \frac{L}{a} C_2 \right) - \frac{L^2}{2r^2} - \Omega$$

$$\mu = \frac{L}{r} \left( 2 - \frac{L}{a} C_2 \right) - \frac{L^2}{2r^2} + \omega - \Omega$$

$$\nu = -\frac{L}{r} \left( 2 - \frac{L}{a} C_2 \right)$$

$$e^\lambda = 1 + \frac{L}{r} \left( 2 - \frac{L}{a} C_2 \right) + \frac{3L^2}{2r^2} - \Omega$$

$$e^\mu = 1 + \frac{L}{r} \left( 2 - \frac{L}{a} C_2 \right) + \frac{3L^2}{2r^2} + \omega - \Omega$$

$$e^\nu = 1 - \frac{L}{r} \left( 2 - \frac{L}{a} C_2 \right) + \frac{2L^2}{r^2}$$

The simplest treatment of  $\omega$  is to make it zero everywhere, which makes  $\lambda$  and  $\mu$  equal. We may also take for  $\omega_v$  a series in negative powers of  $r$ . The third and higher powers of  $r$  introduce these powers in the expressions for  $\lambda$   $\mu$   $\nu$ , and are of no particular interest. We shall take

$$\left[ \frac{G}{1+r} \right] \omega_v = \frac{L^2}{a^2} \left( D \frac{a}{r} + E \frac{a^2}{r^2} \right)$$

to which corresponds in matter

$$\omega_M = \frac{L^2}{a^3} \left\{ 2D + 3E - (D + 2E) \frac{r}{a} \right\}$$

These give in the void

$$\Omega = \frac{L^2 E}{2r^2} \quad \omega - \Omega = \frac{L^2}{a^2} \left\{ D \frac{a}{r} + \frac{1}{2} E \left( \frac{a}{r} \right)^2 \right\}$$

and

$$e^\lambda = 1 + \frac{L}{r} \left( 2 - \frac{LC_2}{a} \right) + \frac{L^2}{r^2} \left( \frac{3}{2} - \frac{1}{2} E \right)$$

$$e^\mu = 1 + \frac{L}{r} \left( 2 - \frac{LC_2}{a} + \frac{LD}{a} \right) + \frac{L^2}{r^2} \left( \frac{3}{2} + \frac{1}{2} E \right)$$

$$e^\nu = 1 - \frac{L}{r} \left( 2 - \frac{LC_2}{a} \right) + \frac{2L^2}{r^2}$$

In these expressions  $C_2$  is given by equation (9, 5), and  $D$  and  $E$  are at our disposal. These are second order expressions to which the first set of values mentioned in article 1 have been extended.

12. The quantity  $\xi$  of expression (4, 4) being at disposal we now give it the value zero in the void. Since

$$\lambda' \equiv r(\xi'' + 2\Theta'') + 2\xi' + 2\Theta'$$

is to be continuous at the boundary,  $\xi''$  must be discontinuous to balance the discontinuity of  $\Theta''$ . We take

$$\xi_M = -Z \frac{L}{a} \left( \frac{r}{a} - 1 \right)^2 \quad \dots \quad (12, 1)$$

$$Z = \Sigma(m+2)A_m$$

which makes  $\xi \xi' \lambda'$  continuous.

The values in matter of certain expressions of equation (6, 6) are

$$(r^3 \xi'' + 2r^3 \xi') \Theta' = \frac{2L^2}{a^2} \Sigma A_m A_n \left[ -3(n+2) \left( \frac{r}{a} \right)^{m+3} + \left( \frac{r}{a} \right)^{m+2} \right]$$

$$-r^2 \xi \kappa T = \frac{2L^2}{a^2} \Sigma A_m A_n (m+2)(n+2)$$

$$\left[ \left( \frac{r}{a} \right)^{m+3} - 2 \left( \frac{r}{a} \right)^{m+2} + \left( \frac{r}{a} \right)^{m+1} \right]$$



$$-r^3 \kappa T \Theta' = -\frac{2L^2}{a^2} \Sigma A_m A_n (n+2) \left(\frac{r}{a}\right)^{m+n+2}$$

$$\frac{1}{2} r^3 \xi'^2 = \frac{2L^2}{a^2} \Sigma A_m A_n (m+2) (n+2)$$

$$\left[ \left(\frac{r}{a}\right)^5 - 2\left(\frac{r}{a}\right)^4 + \left(\frac{r}{a}\right)^3 \right]$$

Integrating the sum of the first three and adding the fourth we have

$$\Psi_M = \frac{2L^2}{a} \Sigma A_m A_n (n+2)$$

$$\left[ -\frac{1}{m+n+3} \left(\frac{r}{a}\right)^{m+n+3} + \frac{m-1}{m+4} \left(\frac{r}{a}\right)^{m+4} - \frac{2m+2}{m+3} \left(\frac{r}{a}\right)^{m+3} \right. \\ \left. + \left(\frac{r}{a}\right)^{m+2} + (m+2) \left\{ \left(\frac{r}{a}\right)^5 - 2\left(\frac{r}{a}\right)^4 + \left(\frac{r}{a}\right)^3 \right\} \right] \quad (12, 2)$$

The integration constant is zero because  $\Psi/r^2$  is finite at the origin.

Since in the void  $\xi$  and  $T$  are zero equation (6, 6) gives

$$\Psi_V = \text{const} = \frac{L^2}{a} C_2 \quad . \quad . \quad . \quad (12, 3)$$

and the continuity of  $\Psi$  at the sun's boundary gives for the value of  $C_2$

$$C_2 = \Sigma A_m A_n 2(n+2) \left( -\frac{1}{m+n+3} - \frac{5}{m+4} + \frac{4}{m+3} \right) \quad (12, 4)$$

13. By the help of equations (8, 1) (8, 2) and (12, 1) equation (6, 1) gives

$$\psi'_M = -\Omega'_M + \frac{L^2}{a^3} \Sigma A_m A_n$$

$$\left[ \left(1 - \frac{4}{m+n}\right) \left(\frac{r}{a}\right)^{m+n+1} - 2(m+2) \left\{ \left(\frac{r}{a}\right)^{n+2} - \left(\frac{r}{a}\right)^{n+1} \right\} \right. \\ \left. + (m+2)(n+2) \left\{ \left(\frac{r}{a}\right)^3 - 2\left(\frac{r}{a}\right)^2 + \frac{r}{a} \right\} \right] - \frac{4L^2 C_1 r}{a^4} \\ . \quad . \quad . \quad (13, 1)$$

$$\psi'_V = -\Omega'_V + \frac{3L^2}{r^3} \quad . \quad . \quad . \quad . \quad . \quad . \quad . \quad . \quad (13, 2)$$

and by the help of (12, 2) and (12, 3) equation (6, 5) gives

$$\chi'_m = -2\Omega'_m + \frac{2L^2}{a} \Sigma A_m A_n (n+2)$$

$$\left[ -\frac{1}{m+n+3} \left(\frac{r}{a}\right)^{m+n+1} + \frac{m-1}{m+4} \left(\frac{r}{a}\right)^{m+2} - \frac{2m+2}{m+3} \left(\frac{r}{a}\right)^{m+1} \right. \\ \left. + \left(\frac{r}{a}\right)^m + (m+2) \left\{ \left(\frac{r}{a}\right)^3 - 2\left(\frac{r}{a}\right)^2 + \frac{r}{a} \right\} \right] \quad (13, 3)$$

$$\chi'_v = -2\Omega'_v + \frac{L^2 C_2}{ar^2} \quad . \quad . \quad . \quad . \quad . \quad . \quad . \quad . \quad (13, 4)$$

The integration of these equations gives in the void

$$\psi_v = -\Omega_v - \frac{3L^2}{2r^2} \quad . \quad . \quad . \quad . \quad . \quad (13, 5)$$

$$\chi_v = -2\Omega_v - \frac{L^2 C_2}{ar} \quad . \quad . \quad . \quad . \quad . \quad (13, 6)$$

the integration constants being zero because  $\psi$  and  $\chi$  vanish at infinity. In matter integration gives expressions that we need not write down. The integration constants are determined by making  $\psi$  and  $\chi$  continuous at the sun's boundary.  $\omega$  being supposed so chosen as to satisfy the continuity conditions, we have in  $\psi \chi \omega$  a set of values that satisfy the differential equations in matter and in the void and also the continuity conditions. Hence the values of  $\lambda \mu \nu$  expressed in terms of  $\psi \chi \omega$  by equations (5, 1) give the values of the potentials everywhere.

These expressions furnish the extension to the second power of  $L$  of the second set of values mentioned in article 1.

14. If  $\omega$  is given the same values as in article 11 we have in the void

$$\left. \begin{aligned} e^\lambda &= 1 + \frac{L}{r} \left( 2 - \frac{LC_2}{a} \right) + \frac{L^2}{r^2} \left( \frac{7}{2} - \frac{E}{2} \right) \\ e^\mu &= 1 + \frac{L^2}{ar} (D - C_2) + \frac{L^2}{2r^2} (3 + E) \\ e^\nu &= 1 - \frac{L}{r} \left( 2 - \frac{LC_2}{a} \right) - \frac{L^2}{r^2} \end{aligned} \right\} \quad . \quad (14, 1)$$

If D and E are chosen to make  $\mu$  zero the other two expressions are

$$\left. \begin{aligned} e^{\lambda} &= 1 + \frac{L}{r} \left( 2 - \frac{LC_2}{a} \right) + \frac{5L^2}{r^2} \\ e^{\nu} &= 1 - \frac{L}{r} \left( 2 - \frac{LC_2}{a} \right) - \frac{L^2}{r^2} \end{aligned} \right\} \quad \dots \quad (14, 2)$$

the value of  $C_2$  being given by equation (12, 4).

15. It is well known that the values used for the potentials in the expression

$$ds^2 = (1 - 2L/r) dt^2 - (1 - 2L/r)^{-1} dr^2 - r^2 d\theta^2 - r^2 \sin^2 \theta d\phi^2$$

satisfy the differential equations in the void exactly. This is however not sufficient to prove them true potentials. To prove that it would be necessary to discover the complementary values of the potentials in matter, and to show that the two sets, along with their first derivatives, are continuous across the boundary of the matter. While some variation in the values given in article 14 for the potentials in the void can be obtained by varying the value of  $\xi$  of article 12, we have been unable to find a variation of  $\xi$  that makes the values in question true to the second power of  $L$ , and we see no reason to believe that these values are true beyond the first power of  $L$ .

LXXXIX. *Reducing Observations by the Method of Minimum Deviations.* By E. C. RHODES, D.Sc., Reader in Statistics, University of London \*.

THE writer recently was desirous of smoothing out the fluctuations in the series of figures set out below. A parabola was fitted by the method of Least Squares. The accompanying diagram shows clearly the effect of this smoothing.

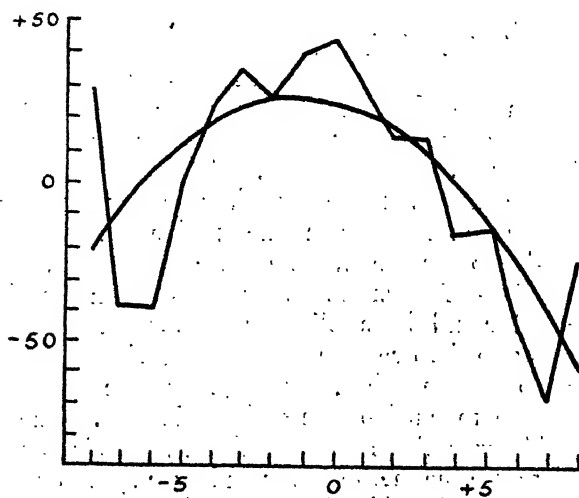
The result was not considered altogether satisfactory. The plus and minus deviations occurred practically in three sets; a set of minus, then a set of plus, then a set of minus. It was considered that the parabola was a bad fit. Two reasons suggested themselves for this: first, the original

\* Communicated by Sir J. J. Thomson, O.M., F.R.S.

data from which the series was obtained did not involve absolutely random fluctuations ; second, the parabola might

Series.		Parabola	Deviations.
<i>x.</i>	<i>y.</i>	(by Least Squares).	
-8	+28	-21	+49
-7	-39	-8	-31
-6	-40	+2	-42
-5	-1	+11	-12
-4	+23	+18	+5
-3	+34	22	+12
-2	+25	25	0
-1	+40	25	+15
0	+43	24	+19
1	+29	21	+8
2	+14	15	-1
3	+12	8	+4
4	-16	-2	-14
5	-14	-13	-1
6	-46	-26	-20
7	-68	-42	-26
8	-24	-59	+35

Fig. 1.



not be the best curve for use in smoothing. As to the first, it was definitely known that the original data, which were

observations at equal time-intervals, were subject to periodic fluctuations of varying intensity and changing phase, as well as to random variations. As to the second, there was no virtue in the parabola, as such, but associated series were reasonably represented by parabolas. It was therefore decided to concentrate on the first consideration, which meant that although we had obtained the parabola of best fit by the criterion of least squares, yet it might not really be the best parabola which would smooth out the fluctuations in the series. This led us to the question of what other methods of fitting there were available, and Edgeworth's description of the use of medians in this connexion led to the attempt to fit by the method of Minimum Deviations. This method may be briefly described. Suppose the equation to the parabola is

$$y = a_0 + a_1x + a_2x^2,$$

and the given  $y$ 's are  $y_{-8}, y_{-7}, \dots, y_{-1}, y_0, y_1, \dots, y_8$ , then instead of, as in the method of Least Squares, making

$$\sum_{x=-8}^{+8} (a_0 + a_1x + a_2x^2 - y_x)^2$$

a minimum, we make

$$\sum_{x=-8}^{+8} |a_0 + a_1x + a_2x^2 - y_x|$$

a minimum.

His description of the method and his arguments in its favour are briefly summarized in Bowley's 'Edgeworth's Contributions to Mathematical Statistics,' pp. 103 *et seq.* (1928), and are exposed by Edgeworth in the 'Philosophical Magazine,' xlv. (1923), xxv. (1888). Unfortunately, Edgeworth confined himself in the working of the method to a reliance on a diagram (he used as illustrations the problem of two variables), which means in practice a rather laborious piece of work, and apparently did not notice that the method could be applied in a more simple manner, without any need to rely on the position of straight lines in relation to one another, although at one stage in his argument he touched on this simplification. The writer, finding Edgeworth's method cumbrous, especially when he intended to use the method over and over again on different series, sought a simplification, which it is hoped will be of use to others, especially as there are many series which involve fluctuations which cannot on *à priori* grounds be

considered altogether adventitious, and where therefore the method of Least Squares does not strictly apply.

The simpler method is as follows:—Suppose we are dealing with a series of deviations, say, involving three unknowns,

$$A_1u + B_1v + C_1w + D_1, \quad A_2u + B_2v + C_2w + D_2, \dots \\ \dots A_nu + B_nv + C_nw + D_n,$$

and we want to find values of  $u$ ,  $v$ ,  $w$  which make

$$\sum_{s=1}^n |A_s u + B_s v + C_s w + D_s|$$

a minimum. First, find for what values of  $v$  and  $w$  the expression is a minimum when  $u$  is given by

$$-\frac{B_r v + C_r w + D_r}{A_r},$$

*i. e.* find a local minimum point in the plane

$$A_r u + B_r v + C_r w + D_r = 0,$$

where  $r$  is any one of the values  $s$  from 1 to  $n$ . This reduces the problem to one involving two variables only, *i. e.* what values of  $v$  and  $w$  will make

$$\sum_{t=1}^{n-1} |E_t v + F_t w + G_t|$$

a minimum, where the  $E$ 's,  $F$ 's,  $G$ 's are obtained from the  $A$ 's,  $B$ 's,  $C$ 's,  $D$ 's. To solve this, find for what value of  $w$  the expression is a minimum when  $v$  is given by

$$-\frac{F_p w + G_p}{E_p},$$

*i. e.* find a local minimum point in the line

$$E_p v + F_p w + G_p = 0,$$

where  $p$  is any one of the values of  $t$  from 1 to  $n-1$ . This reduces simply to the problem of finding a weighted median. The process is repeated until we arrive at a stage when we find that the local minimum in the plane

$$A_l u + B_l v + C_l w + D_l = 0$$

is the point where the planes

$$A_m u + B_m v + C_m w + D_m = 0 \quad \text{and} \quad A_n u + B_n v + C_n w + D_n = 0$$

meet it, and where the local minimum in the plane

$$A_mu + B_mv + C_mw + D_m = 0$$

is the point where the planes

$$A_nu + B_nv + C_nw + D_n = 0 \quad \text{and} \quad A_lu + B_lv + C_lw + D_l = 0$$

meet it, and the local minimum in the plane

$$A_nu + B_nv + C_nw + D_n = 0$$

is the point where the planes

$$A_lu + B_lv + C_lw + D_l = 0 \quad \text{and} \quad A_mu + B_mv + C_mw + D_m = 0$$

meet it. Then this point of intersection of these three planes is the true minimum point, and the values  $u$ ,  $v$ ,  $w$  obtained from solving these equations make

$$\sum_{s=1}^n | A_s u + B_s v + C_s w + D_s |$$

a minimum.

In the case of two variables, where a diagram is used by Edgeworth to illustrate the argument, the process is simply to proceed along one line until we arrive at the point on the line for which the values of the variables make the expression a minimum, this being a point of intersection with another line. Then proceed along this new line until we arrive at the minimum point on this line, which is a point of intersection of this second line with a third. Then proceed along this third line until we get to the minimum point, which will give another line. This goes until we reach the stage where the  $q$ th line leads to the  $q+1$ th and the  $q+1$ th leads to the  $q$ th again. The required values of the variables are given by the intersection of these  $q$ th and  $q+1$ th lines. The description of the process may appear to make it complicated, but in practice this is not so. In the first place, in tracing the course of these lines to the minimum point we are getting closer and closer to this point very quickly, and one or two attempts are alone necessary in practice. Further, in any problem we can start with a particular line which we suspect is near the heart of the mystery by getting some crude approximation to the minimum or by other considerations, and from this line there is probably little distance to go to the minimum.

The accompanying example will indicate the method and the amount of labour involved. The problem is to fit a parabola to the data on p. 975 by this method.

(1) Deviations.	(2)	(3)	(4) Values of $a_2$ .	(5) $a_2$ in order.	(6) Coefficient of $a_2$ in (3).	(7) Sums.
$a_0 - 8a_1 + 64a_2 - 28$	$-4a_1 + 48a_2 - 5$	$36a_2 - 9.8$	$+0.3$	$-4.3$	14	14 380
$a_0 - 7a_1 + 49a_2 + 39$	$-3a_1 + 33a_2 + 62$	$24a_2 + 58.4$	$-2.43$	$-3.8$	6	20 366
$a_0 - 6a_1 + 36a_2 + 40$	$-2a_1 + 20a_2 + 63$	$14a_2 + 60.6$	$-4.3$	$-3.8$	4	24 360
$a_0 - 5a_1 + 25a_2 + 1$	$-a_1 + 9a_2 + 24$	$6a_2 + 22.8$	$-3.8$	$-2.7$	6	30 356
$a_0 - 4a_1 + 16a_2 - 23$	0	0		$-2.45$	4	34 350
$a_0 - 3a_1 + 9a_2 - 34$	$a_1 - 7a_2 - 11$	$-4a_2 - 9.8$	$-2.45$	$-2.43$	24	58 346
$a_0 - 2a_1 + 4a_2 - 25$	$2a_1 - 12a_2 - 2$	$-6a_2 + 0.4$	$+0.1$	$-2.2$	6	64 322
$a_0 - a_1 + a_2 - 40$	$3a_1 - 15a_2 - 17$	$-6a_2 - 13.4$	$-2.2$	$-2.0$	21	88 316
$a_0$	$4a_1 - 16a_2 - 20$	$-4a_2 - 15.2$	$-3.8$	$-1.62$	50	138 292
$a_0 + a_1 + a_2 - 29$	$5a_1 - 15a_2 - 6$	0		$-1.58$	66	204 242
$a_0 + 2a_1 + 4a_2 - 14$	$6a_1 - 12a_2 + 9$	$6a_2 + 16.2$	$-2.7$	$-1.4$	14	218 176
$a_0 + 3a_1 + 9a_2 - 12$	$7a_1 - 7a_2 + 11$	$14a_2 + 19.4$	$-1.4$	$-1.3$	36	254 162
$a_0 + 4a_1 + 16a_2 + 16$	$8a_1 + 39$	$24a_2 + 48.6$	$-2.0$	$-0.7$	81	338 126
$a_0 + 5a_1 + 25a_2 + 14$	$9a_1 + 9a_2 + 37$	$36a_2 + 47.8$	$-1.3$	$+0.1$	6	344 42
$a_0 + 6a_1 + 36a_2 + 46$	$10a_1 + 20a_2 + 69$	$50a_2 + 81.0$	$-1.62$	$+0.3$	36	380 36
$a_0 + 7a_1 + 49a_2 + 68$	$11a_1 + 33a_2 + 91$	$66a_2 + 104.2$	$-1.58$			
$a^2 + 8a_1 + 64a_2 + 24$	$12a_1 + 48a_2 + 47$	$84a_2 + 61.4$	$-0.7$			



From the diagram (fig. 1) we might suspect that the parabola would go through the point  $x=-4, y=23$ . We therefore start by taking  $a_0-4a_1+16a_2-23=0$ , and obtain col. (2) by substituting for  $a_0$ . Considering col. (2), the diagram again suggests that the parabola might go through the point  $x=1, y=29$ ; we therefore substitute for  $a_1$  in col. (2) from  $5a_1-15a_2=6$ , which gives col. (3). Col. (3) gives us values of  $a_2$  from which we can obtain the weighted median, col. (5) shows the values of  $a_2$  in order, col. (6) the corresponding coefficients of  $a_2$  in col. (3) without sign, and col. (7) shows the sums of these coefficients starting from the top and bottom of col. (6) respectively. The best value of  $a_2$  is  $-1.58$ . This is the value corresponding to 66 in col. (6); the sum of col. (6) from the top to 66 is greater than the sum from the bottom to 14 (the figure below 66), the sum of col. (6) from the top to 50 (the figure above 66) is less than the sum from the bottom up to (66).

Thus we are led to the expression  $11a_1+33a_2+91$  in col. (2). The local minimum of the series of col. (2) in the line  $5a_1-15a_2=6=0$  is the point in this line where it intersects  $11a_1+33a_2+91=0$ . We now substitute in col. (2) the value of  $a_1$  obtained from  $11a_1+33a_2+91=0$ . This gives a new col. (3) and new values of  $a_2$ , and an examination of these gives the best. The work is set out below.

(3)	(4)	(5)	(6)	(7)
	Values of $a_2$ .	$a_2$ in order.	Coefficients of $a_2$ in (3).	Sums.
$60a_2+28.1$	$-0.4$	$-3$	26	26 372
$42a_2+86.8$	$-2.07$	$-2.7$	12	38 346
$26a_2+79.5$	$-3$	$-2.08$	18	56 334
$12a_2+32.3$	$-2.7$	$-2.07$	42	98 316
0		$-1.93$	10	108 274
$-10a_2-19.3$	$-1.93$	$-1.90$	28	136 264
$-18a_2-18.5$	$-1.0$	$-1.74$	24	160 236
$-24a_2-41.8$	$-1.74$	$-1.67$	28	188 212
$-28a_2-53.1$	$-1.90$	$-1.58$	30	218 184
$-30a_2-47.4$	$-1.58$	$-1.37$	10	228 154
$-30a_2-40.6$	$-1.35$	$-1.35$	30	258 144
$-28a_2-46.9$	$-1.67$	$-1.1$	24	282 114
$-24a_2-27.2$	$-1.1$	$-1.0$	18	300 90
$-18a_2-37.5$	$-2.08$	$-0.4$	60	360 72
$-10a_2-13.7$	$-1.37$	$+4.4$	12	372 12
0				
$12a_2-53.3$	$+4.4$			

This gives the best  $a_2 = -1.67$  from  $7a_1-7a_2+11=0$ .

We now substitute in the original col. (2) the value of  $a_1$  from  $7a_1 - 7a_2 + 11 = 0$  and get the following series. In what follows col. (5) is dispensed with, it is not really necessary to rewrite the values of  $a_2$ , and all the figures are not written in col. (7). Again, in the determination of the weighted median we are not really particular in what order the values of  $a_2$  are written, except in the immediate neighbourhood of the median itself.

(3)	(4)	(6)	(7)
	Values of $a_2$ .	Coefficients of $a_2$ in order of $a_2$ .	Sums.
$44a_2 + 1.3$	-0.03	18	18
$30a_2 + 66.7$	-2.22	8	26
$18a_2 + 66.1$	-3.7	8	34
$8a_2 + 25.6$	-3.2	30	64
0		12	76
$-6a_2 - 12.6$	-2.1	6	82
$-10a_2 - 5.1$	-0.51	12	94
$-12a_2 - 21.7$	-1.8	30	124
$-12a_2 - 26.3$	-2.2	44	168 192
$-10a_2 - 13.9$	-1.39	10	178 148
$-6a_2 - 0.4$	-0.07	18	138
0		10	120
$8a_2 + 26.4$	-3.3	60	110
$18a_2 + 22.9$	-1.27	6	50
$30a_2 + 53.3$	-1.78	44	44
$44a_2 + 73.7$	-1.68		
$60a_2 + 28.1$	-0.4		

This gives the best  $a_2 = -1.68$  from  $11a_1 + 33a_2 + 91 = 0$ .

This stage illustrates the procedure in the case of two variables. Starting from the original col. (2), involving  $a_1$  and  $a_2$ , we find the local minimum on the line

$$5a_1 - 15a_2 - 6 = 0$$

is at the intersection of this with

$$11a_1 + 33a_2 + 91 = 0.$$

The local minimum along

$$11a_1 + 33a_2 + 91 = 0$$

is at the intersection of this with

$$7a_1 - 7a_2 + 11 = 0.$$

The local minimum along

$$7a_1 - 7a_2 + 11 = 0$$

is at the intersection of this with

$$11a_1 + 33a_2 + 91 = 0.$$

Therefore the values of  $a_1$  and  $a_2$  obtained from

$$7a_1 - 7a_2 + 11 = 0 \quad \text{and} \quad 11a_1 + 33a_2 + 91 = 0$$

will make the series in col. (2) when summed without regard to sign a minimum.

Returning to our problem, we have found that starting from

$$a_0 - 4a_1 + 16a_2 - 23 = 0,$$

we are led to

$$a_0 + 7a_1 + 49a_2 + 68 = 0 \quad \text{and} \quad a_0 + 3a_1 + 9a_2 - 12 = 0.$$

Now start from col. (1) again, substituting

$$a_0 = -3a_1 - 9a_2 + 12;$$

we get a new col. (2):—

$$\begin{array}{r}
 (2) \\
 -11a_1 + 55a_2 - 16 \\
 -10a_1 + 40a_2 + 51 \\
 -9a_1 + 27a_2 + 52 \\
 -8a_1 + 16a_2 + 13 \\
 -7a_1 + 7a_2 - 11 \\
 -6a_1 \quad -22 \\
 -5a_1 - 5a_2 - 13 \\
 -4a_1 - 8a_2 - 28 \\
 -3a_1 - 9a_2 - 31 \\
 -2a_1 - 8a_2 - 17 \\
 -a_1 - 5a_2 - 2 \\
 0 \\
 a_1 + 7a_2 + 28 \\
 2a_1 + 16a_2 + 26 \\
 3a_1 + 27a_2 + 58 \\
 4a_1 + 40a_2 + 80 \\
 5a_1 + 55a_2 + 36
 \end{array}$$

In dealing with this we may use the information already acquired and try substituting for  $a_1$  in col. (2) from

$$4a_1 + 40a_2 + 80 = 0,$$

which comes from

$$a_0 + 7a_1 + 49a_2 + 68$$

of col. (1). This substitution gives us a new col. (3), from which we obtain the median  $a_2$ , which is the intersection of

$$4a_1 + 40a_2 + 80 = 0 \quad \text{with} \quad -10a_1 + 40a_2 + 51 = 0.$$

Substituting in col. (2) the value of  $a_1$  from this last equation gives a new col. (3), from which the median  $a_2$  is the intersection of this line with

$$4a_1 + 40a_2 + 48 = 0.$$

Thus we have arrived at the fact that the local minimum in

$$a_0 + 3a_1 + 9a_2 - 12 = 0$$

is where this meets

$$a_0 + 7a_1 + 49a_2 + 68 = 0 \quad \text{and} \quad a_0 - 7a_1 + 49a_2 + 39 = 0.$$

Now repeat the process from col. (1). Starting with a substitution of

$$a_0 = -7a_1 - 49a_2 - 68,$$

we get a new col. (2) :—

Col. (2).

$$\begin{array}{rcl} -15a_1 + 15a_2 & - & 96 \\ -14a_1 & - & 29 \\ -13a_1 - 13a_2 & - & 28 \\ -12a_1 - 24a_2 & - & 67 \\ -11a_1 - 33a_2 & - & 91 \\ -10a_1 - 40a_2 & - & 102 \\ -9a_1 - 45a_2 & - & 93 \\ -8a_1 - 48a_2 & - & 108 \\ -7a_1 - 49a_2 & - & 111 \\ -6a_1 - 48a_2 & - & 97 \\ -5a_1 - 45a_2 & - & 82 \\ -4a_1 - 40a_2 & - & 80 \\ -3a_1 - 33a_2 & - & 52 \\ -2a_1 - 24a_2 & - & 54 \\ -a_1 - 13a_2 & - & 22 \\ 0 & & \\ a_1 + 15a_2 & - & 44 \end{array}$$

Obtain from this col. (2) a value of  $a_1$  from

$$14a_1 + 29 = 0,$$

which has been obtained from

$$a_0 - 7a_1 + 49a_2 + 39 = 0.$$

This gives the best  $a_2$  from the intersection of

$$14a_1 + 29 = 0 \quad \text{with} \quad -6a_1 - 48a_2 - 97 = 0.$$

Using this last equation to give  $a_1$  for substitution in col. (2), we arrive at the best  $a_2$  from the intersection of this with

$$14a_1 + 29 = 0.$$

Thus the local minimum on

$$a_0 + 7a_1 + 49a_2 + 68 = 0$$

is where this meets

$$a_0 - 7a_1 + 49a_2 + 39 = 0 \quad \text{and} \quad a_0 + a_1 + a_2 - 29 = 0.$$

The field has now been narrowed down, and we find, when we get a new col. (2) from col. (1) by substituting

$$a_0 = 7a_1 - 49a_2 - 39,$$

that the local minimum in the plane

$$a_0 - 7a_1 + 49a_2 + 39 = 0$$

is where this meets

$$a_0 + a_1 + a_2 - 29 = 0 \quad \text{and} \quad a_0 + 7a_1 + 49a_2 + 68 = 0.$$

With the information available at this stage there is no wasted labour involved; in fact, we merely verify the statement. It follows now that the local minimum on

$$a_0 + a_1 + a_2 - 29 = 0$$

is where this meets

$$a_0 + 7a_1 + 49a_2 + 68 = 0 \quad \text{and} \quad a_0 - 7a_1 + 49a_2 + 39 = 0.$$

If the actual work is done, we find ourselves with a repetition of work previously done. This marks the end of the working of the new procedure, and we find that the best values of  $a_0, a_1, a_2$  to render the original series a minimum when summed without regard to sign are those obtained by solving

$$a_0 - 7a_1 + 49a_2 + 39 = 0,$$

$$a_0 + a_1 + a_2 - 29 = 0,$$

$$a_0 + 7a_1 + 49a_2 + 68 = 0,$$

which give

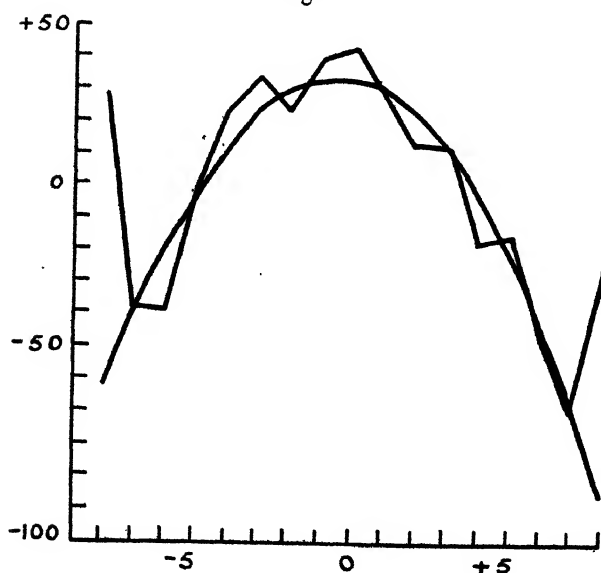
$$a_0 = 32\frac{5}{6}, \quad a_1 = -2\frac{1}{14}, \quad a_2 = -1\frac{18}{21}.$$

The table below shows again the original series and the smooth values from this parabola obtained by the method of Minimum Deviations.

A diagram (fig. 2) showing this parabola with the original data, when compared with fig. 1, will indicate clearly the

Series.		Parabola (by Minimum Deviations).		Deviations.
$x$ .	$y$ .			
-8	+28	-63		+91
-7	-39	-39		0
-6	-40	-18		-22
-5	-1	-1		0
-4	+23	+13		+10
-3	+34	+23		+11
-2	+25	+30		-5
-1	+40	+33		+7
0	+43	+33		+10
1	+29	+29		0
2	+14	+22		-8
3	+12	+11		+1
4	-16	-4		-12
5	-14	-22		+8
6	-46	-43		-3
7	-68	-68		0
8	-24	-96		+72

Fig. 2.



difference between the two parabolas obtained by Least Squares and Minimum Deviations as smooths of the original series. The second parabola is much more satisfactory. A glance at the diagrams and at the table of deviations

shows the important part of the two values of  $y$  associated with  $x=+8$  and  $x=-8$ . The importance of these compared with the other  $y$ 's has been exaggerated in the method of Least Squares; this method has forced the parabola to pay too much attention to these values and to neglect its duty towards the other observations. In the method of Minimum Deviations these large deviations are not given undue prominence, with the result that the parabola adequately describes the remaining observations.

The exposition above might appear to make the procedure laborious. Undoubtedly it is more so than the method of Least Squares. But the labour would have appeared less if one had been content to illustrate with an example involving only two variables. On the other hand, the illustration here shown indicates how the method can be used with three variables; and it has the advantage of being derived from a problem met with in the course of an investigation, with the accompanying illuminating diagrams, which call attention to the necessity for alternative methods, to that of Least Squares, where fluctuations are not random.

Pressing the advantages of this method further, it is not restricted to problems where the deviations involve only linear functions of the variables. Theoretically there is nothing to prevent the method from being extended to the case of a general problem of minimizing

$$\sum_{s=1}^n |f_s(u, v, w)|.$$

Here we choose a particular deviation, say  $f_s(u, v, w)$ , equate this to zero and find  $u$  in terms of  $v, w$ , and get a new series:

$$\sum_{t=1}^{n-1} |F_t(v, w)|,$$

from which we choose, say  $F_p(v, w)$ , and get a series involving only one variable. In practice the working would depend on the simplicity or otherwise of the functions  $f$ , but in certain cases the method can be applied without a great deal of labour, and gives a great advantage over the method of Least Squares, which can only be used in such cases in a modified manner, where the original foundation for the justification for the method of Least Squares now disappears. For instance, the curve  $y=Bx^a$  crops up as a theoretical method of describing data in a variety of ways. When the method of Least Squares is used for fitting this curve, the computer resorts to a trick and fits the line

$$\log y = a \log x + \log B$$

to the data, using as his variables  $\log x$  and  $\log y$ ; thus virtually asserting that the deviations of the logarithms of the original  $y$ 's from the logarithms of the  $y$ 's of the curve follow the normal law, instead of the deviations of the original  $y$ 's from the  $y$ 's of the curve. But in a comparatively simple case like this the method of minimum deviations may be used with fair ease. The method may be illustrated by the working on the data below, which relate to production ( $x$ ) and price ( $y$ ) of corn in the United States (Warren and Pearson, 'Inter-relationships of Supply and Price,' 1928, p. 188).

$x$ .	$y$ .	$x$ .	$y$ .
68	192	113	77
75	135	113	93
79	169	114	86
81	141	116	86
85	116	118	89
90	123	118	89
93	103	119	99
94	123	120	106
96	120	120	109
96	101	120	82
97	109	121	85
98	130	122	79
100	102	123	79
102	105	123	96
103	91	124	90
107	121	133	93
108	114	137	60
109	94	140	66
110	100	147	93
112	82		

A plot of these associated values of  $x$  and  $y$  suggests that a useful start would be given by taking  $x = 110$ ,  $y = 100$  as satisfying the equation  $y = Bx^a$ . From this we get  $B = 100/110^a$ . Substituting this value we get a series of deviations:

$$192 - 100 \left( \frac{68}{110} \right)^a,$$

$$135 - 100 \left( \frac{75}{110} \right)^a,$$

$$169 - 100 \left( \frac{79}{110} \right)^a,$$



From these we may obtain values of  $a$  by equating each to zero, and from these values of  $a$  we must pick out the best to make the sum of the deviations a minimum. At this stage the work is slightly different from that in the simpler case of a linear function considered first above and dealt with by Edgeworth. Suppose that we have obtained the values of  $a$  as described above, and suppose now they are arranged in order of size, and that the corresponding deviations are also so arranged. Take the general case where  $B = y_r/x_r^a$ , and we have :

$$\begin{array}{l|l} a_1 & y_1 - y_r \left( \frac{x_1}{x_r} \right)^a, \\ a_2 & y_2 - y_r \left( \frac{x_2}{x_r} \right)^a, \\ a_3 & y_3 - y_r \left( \frac{x_3}{x_r} \right)^a, \\ a_4 & y_4 - y_r \left( \frac{x_4}{x_r} \right)^a \\ \vdots & \vdots \end{array}$$

where  $a_1 < a_2 < a_3 \dots \leq a_n$ .

Now suppose that of these  $a$ 's, arranged in order,  $a_s$  is that which makes

$$\sum_t \left| y_t - y_r \left( \frac{x_t}{x_r} \right)^a \right|$$

a minimum, then the deviations in series above which occur before the  $s$ th will be negative and those after the  $s$ th will be positive. If we put  $a = a_s + \alpha$ , where  $\alpha$  is small and positive, the sum of the deviations may be written

$$\begin{aligned} & \left( y_r \left( \frac{x_1}{x_r} \right)^{a_s + \alpha} - y_1 \right) + \left( y_r \left( \frac{x_2}{x_r} \right)^{a_s + \alpha} - y_2 \right) + \dots + \left( y_r \left( \frac{x_s}{x_r} \right)^{a_s + \alpha} - y_s \right) \\ & \quad + \left( y_{s+1} - y_r \left( \frac{x_{s+1}}{x_r} \right)^{a_s + \alpha} \right) + \dots, \end{aligned}$$

and if we put  $a_s = a_s - \alpha$  where  $\alpha$  is small and positive, the sum of the deviations may be written

$$\left( y_r \left( \frac{x_1}{x_r} \right)^{a_s - \alpha} - y_1 \right) + \left( y_r \left( \frac{x_2}{x_r} \right)^{a_s - \alpha} - y_2 \right) + \dots$$

$$+ \left( y \left( \frac{x_{s-1}}{x_r} \right)^{a_s - a} - y_{s-1} \right) + \left( y_s - y_r \left( \frac{x_s}{x_r} \right)^{a_s - a} \right) \\ + \left( y_{s+1} - y_r \left( \frac{x_{s+1}}{x_r} \right)^{a_s - a} \right) + \dots$$

If we express

$$\left( \frac{x_t}{x_r} \right)^{a_s + a} = \left( \frac{x_t}{x_r} \right)^{a_s} \left( 1 + a \log \left( \frac{x}{x_r} \right) \right),$$

we see that since  $a_s$  makes the expression a minimum

$$\sum_{t=1}^s \left( \frac{x_t}{x_r} \right)^{a_s} \log \left( \frac{x_t}{x_r} \right) > \sum_{t=s+1}^n \left( \frac{x_t}{x_r} \right)^{a_s} \log \left( \frac{x_t}{x_r} \right)$$

and

$$\sum_{t=1}^{s-1} \left( \frac{x}{x_r} \right)^{a_s} \log \left( \frac{x_t}{x_r} \right) < \sum_{t=s}^n \left( \frac{x}{x_r} \right)^{a_s} \log \left( \frac{x_t}{x_r} \right).$$

Thus the "weights" to be used for finding the weighted median  $a$  are

$$\left( \frac{x_t}{x_r} \right)^{a_s} \log \left( \frac{x_t}{x_r} \right)$$

for values of  $t$  from 1 to  $n$ , and are proportional to

$$x_t^{a_s} \log \left( \frac{x_t}{x_r} \right).$$

Unfortunately, these weights to be used to determine  $a_s$  involve  $a_s$  itself, but we can get approximations to the weights by taking weights proportional to

$$y_t \log \left( \frac{x_t}{x_r} \right),$$

replacing  $x_t^{a_s}$  by  $y_t$ . Or we can see at a glance at the table of the  $a$ 's in order that the value required will be nearly  $a = -1$ , and we can take the weights proportional to

$$\log \left( \frac{x}{x_r} \right) / x_t.$$

Either of these will lead to the correct result, for we can always check these results by using the value of  $a_s$  so found to work out the correct weights and verify that our  $a_s$  is really the weighted median. In any other problem of curve fitting by this method a similar difficulty will arise, and can be overcome by some such device as described above.

Proceeding then with our illustration, we get values of  $a$ , arrange them in order, weight them, and get the weighted average.

Values of $a$ .	$a$ 's in order.	$\left(y_t \log \frac{x_t}{x_r}\right)$ .		$\left(\log \left(\frac{x_t}{x_r}\right) \middle  x_t\right)$ .	
		Weights.	Sums.	Weights.	Sums.
- 1.35	-10	1	1	1	1
- .78	- 9	1	2	1	2
- 1.58	- 7	1	3	1	3
- 1.12	- 6	1	4	1	4
- .5	- 4	1	5	1	5
- .98	- 2.8	2	7	2	7
- .1	- 2.7	1	8	1	8
- 1.31	- 2.32	6	14	7	15
- 1.34	- 2.28	4	18	4	19
- .07	- 2.28	3	21	3	22
- .7	- 2.28	7	28	5	27
- 2.28	- 2.11	4	32	4	31
- .2	- 1.72	7	39	7	38
- .6	- 1.70	4	43	3	41
+ 1	- 1.66	3	46	3	44
- 6	- 1.66	3	49	3	47
- 7	- 1.58	24	73	18	65
+ 6	- 1.35	40	113	34	99
...	- 1.34	7	120	6	105
-10	- 1.31	8	128	7	112
- 9	- 1.12	19	147	16	128
- 2.7	- .98	11	158	10	138
- 4	- .8	5	163	4	142
- 2.8	- .78	22	101	22	93
- 1.66	- .7	6	79	6	71
- 1.66	- .6	3	73	3	65
- .1	- .5	13	70	13	62
+ .7	- .3	5	57	4	49
+ .91	- .3	8	52	6	45
- 2.28	- .2	12	44	9	39
- 1.70	- .2	4	32	4	30
- 2.28	- .1	3	28	3	26
- 2.11	- .1	8	25	8	23
- .3	- .07	6	17	6	15
- .8	+ .7	4	11	3	9
- .3	+ .91	4	7	3	6
- 2.32	+ 1	3	3	3	3
- 1.72	+ 6	0	0	0	0
- .2					

Thus the best  $a$  is  $-1.12$  obtained from  $x=81$ ,  $y=141$ .

Now we start again by taking  $B=141/81^a$ . This gives us another series of  $a$ 's, from which we deduce the best  $a$  is  $-1.26$ , obtained by the intersection of  $141=B 81^a$  with  $85=B 121^a$ . Further, we find when we start from  $85=B 121^a$

that we arrive again at  $141 = B\ 81^a$ . Therefore  $a = -1.2610$ ,  $B = 35967$  are the  $a$ ,  $B$  which make a minimum, the sum of the deviations  $192 - B\ 68^a$ , etc., when the signs are ignored.

<i>x.</i>	<i>y.</i>	Minimum Deviation.		Least Square. Logs.	
		Curve.	Deviation.	Curve.	Deviation.
68	192	176	+16	168	+24
75	135	155	-20	150	-15
79	169	145	+24	141	+28
81	141	141	0	137	+ 4
85	116	133	-17	130	-14
90	123	124	- 1	123	0
93	103	118	-15	118	-15
94	123	117	+ 6	117	+ 6
96	120	114	+ 6	114	+ 6
96	101	114	-13	114	-13
97	109	112	- 3	112	- 3
98	130	111	+19	111	+19
100	102	108	- 6	109	- 7
102	105	105	0	106	- 1
103	91	104	-13	105	-14
107	121	99	+22	101	+20
108	114	98	+16	100	+14
109	94	97	- 3	99	- 5
110	100	96	+ 4	98	+ 2
112	82	94	-12	96	-14
113	77	93	-16	95	-18
113	93	93	0	95	- 2
114	86	92	- 6	94	- 8
116	86	90	- 4	92	- 6
118	89	88	+ 1	90	- 1
118	89	88	+ 1	90	- 1
119	99	87	+12	89	+10
120	106	86	+20	89	+17
120	109	86	+23	89	+20
120	82	86	- 4	89	- 7
121	85	85	0	88	- 3
122	79	84	- 5	87	- 8
123	79	83	- 4	86	- 7
123	96	83	+13	86	+10
124	90	82	+ 8	85	+ 5
133	93	75	+18	78	+15
137	60	73	-13	76	-16
140	66	71	- 5	74	- 8
147	93	67	+26	71	+22
Sum (Deviations) <sup>2</sup> .....		6339		6244	

The table above shows for comparison the values of  $y$  from the curve

$$y = 35967x^{-1.2610},$$

just obtained by the method of Minimum Differences, with the original  $y$ 's, also the values of  $y$  from the curve

$$y = 19083x^{-1.1220},$$

obtained by Warren and Pearson (*loc. cit.*) by fitting a straight line to the logarithms of the  $x$ 's and  $y$ 's, and the original  $y$ 's, with deviations.

It is interesting to compare the sum of the squares of the deviations, 6244 against 6339; and if it is felt in a case of this kind that the deviations were purely fortuitous, then the method of Least Squares on the logarithms of the originals gives a curve which is a better approximation to the true Least Square curve than the method of Minimum Deviations, and, in a sense, we may regard the preceding work as justifying the use of the Least Square Method in fitting a straight line to the logarithms of the original figures. But there is another point of view; if there is no more justification for the idea that the sums of the squares of the deviations from the fitting curve should be a minimum than there is for the idea that the sum of the deviations from the fitting curve, signs being ignored, should be a minimum, then the work here and that by Warren and Pearson bear comparison in an important particular, viz. the value of  $a$ . In the work done by these authors the important part related to this value, and we see that two different methods of reconciling the original data to a function of the form  $y = Bx^a$  lead to results which are approximately equal, but which really differ by about 10 per cent. of their values, viz.  $-1.122$  and  $-1.261$ , difference  $.139$ . These considerations indicate clearly that not too great a reliance may be placed on the absolute exactitude of such a figure when calculated by one of these methods.

The writer has used the method of Minimum Deviations in the case of 2 and 3 variables where the deviation function is linear, and in the case where the deviations are obtained from  $y = Bx^a$ . There are simpler problems than those illustrated here, where the method would not require such labour, *e.g.* fitting a hyperbola to a few observations; and it would be of interest if other workers would try this method, and make comparisons with results obtained by the method of Least Squares.

XC. *An X-ray Investigation of the Copper-Antimony System of Alloys.* By E. VYRON HOWELLS, *M.Sc. (Wales)* and W. MORRIS-JONES, *M.A., M.Sc., F.Inst.P. (Physics Department, University College, Swansea)\**.

### *Introduction.*

THE investigation described in this paper was undertaken with the object of determining the crystal structure of the Copper-Antimony Alloys. The structure of one member of the series— $\text{Cu}_3\text{Sb}$ —had already been determined by Morris Jones and Evans<sup>(1)</sup>, but the crystal structures of the complete system were unknown†. An X-ray examination of the system seemed, therefore, well worth carrying out, especially as the results of such a study should, in addition, serve to verify information concerning the metallurgy of the system obtained by thermal and micrographical methods.

The metallurgy of the copper-antimony system has engaged the attention of many workers. The most complete investigation is that of Sir H. C. Carpenter<sup>(2)</sup>, published in 1913. As a result of his work, Carpenter drew up the equilibrium diagram given in fig. 1, and this is the diagram taken as the basis of comparison in the research described below. The diagram shows the existence at normal temperatures of the following constituents :—

- (i.) The  $\alpha$  phase, a region of solid solution of antimony in copper up to 7 per cent. by weight of antimony.
- (ii.) The  $\gamma$  phase, extending between the composition 30 per cent. to 39 per cent. by weight of antimony; the latter limit being at the composition  $\text{Cu}_3\text{Sb}$ .
- (iii.) The intermetallic compound  $\text{Cu}_3\text{Sb}$ .
- (iv.) The  $\epsilon$  phase, consisting of a region of slight solution of copper in antimony.

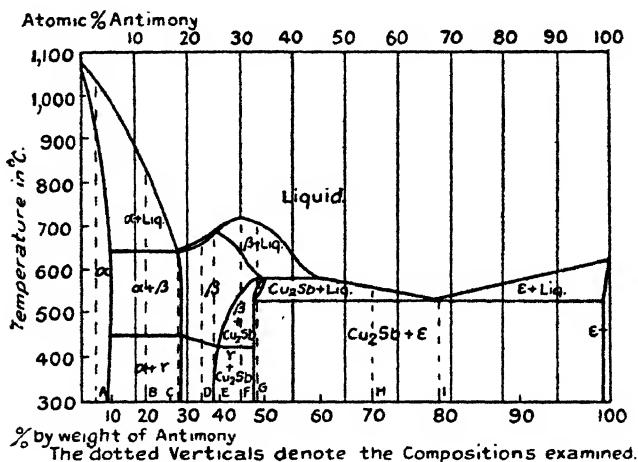
\* Communicated by W. Morris-Jones, Senior Lecturer in Physics, University College, Swansea.

† *Note added.*—Since the completion of the present investigation, in September 1929, a paper on the Copper-Antimony Alloys by Westgren, Hagg, and Erikson has appeared (*Zeit. für Phys. Chem.* B. iv. pt. 6, August 1929). Their results agree very satisfactorily with those of the present work.

At temperatures higher than  $430^{\circ}\text{C}$ . a phase  $\beta$  is formed ; but below this temperature the alloy assumed the character of the  $\gamma$  phase.

Previous investigators of this system of alloys had concluded from micrographical, thermal, and other data that, if copper can hold antimony in solution, the degree of solubility was very small, and in no case did it exceed 0.4 per cent. by weight of antimony ; whereas Carpenter, as his diagram shows, found that antimony is soluble in copper to the extent of 4 atoms per cent.—which is slightly over 7 per cent. by weight of antimony.

Fig. 1.



Carpenter's equilibrium diagram.

In agreement with previous workers Carpenter found, on the other hand, that antimony could hold very little copper in solution, and that the degree of solubility did not exceed 0.5 per cent. by weight of copper.

An earlier equilibrium diagram due to Guertler <sup>(3)</sup> showed copper and antimony to be completely insoluble in each other. In addition, there was no phase in this diagram corresponding to the  $\gamma$  phase of Carpenter.

In the course of the present X-ray investigation a study was therefore made of the crystal structure of the regions of solid solution at the copper and antimony ends of the diagram. The crystal structure of the compound  $\text{Cu}_2\text{Sb}$  was also investigated, and an examination made of the character of the  $\beta$  and the  $\gamma$  phases.

*Preparation of the Alloys.*

The copper used in making the alloys was of electrolytic origin, while the antimony was of 99.916 per cent. purity. In making the alloys the copper was placed in a salamander pot, under a layer of charcoal, and melted in a wind-furnace. The antimony, which melts at a much lower temperature, was then introduced quickly in small quantities, and the whole was well stirred with a carbon

TABLE I.

Alloy.	Composition per cent. Cu by weight.	Density grams. per c.c.	Crystal structure.	Dimensions of the unit-cell in Å.U.
Copper ....	100	8.93	Face-centred cubic.	$a_0$ —3.610
A .....	96	8.75	Face-centred cubic.	$a_0$ —3.644
B .....	80	8.26	Mixture of face-centred cubic and hexagonal close-packed lattices.	$a_0'$ —3.670 $a_0''$ —2.728 $c_0''$ —4.288
C .....	70	8.34	Hexagonal close-packed lattice.	$a_0$ —2.728 $c_0$ —4.288
D .....	65	8.64	Hexagonal close-packed.	$a_0$ —2.752 $c_0$ —4.326
E .....	61	8.66	Hexagonal close-packed.	$a_0$ —2.766 $c_0$ —4.348
F .....	55	8.30	Mixture of hexagonal close-packed and simple tetragonal lattices.	$a_0'$ —2.766 $c_0'$ —4.348 $a_0''$ —4.029 $c_0''$ —6.140
G .....	51	8.42	Simple tetragonal.	$a_0$ —4.029 $c_0$ —6.140
H .....	30	7.45	Mixture of simple tetragonal and face-centred rhombohedral lattices.	$a_0'$ —4.020 $c_0'$ —6.126 $a_0''$ —6.235
I .....	20	7.02	Mixture of simple tetragonal and face-centred rhombohedral lattices.	$a_0'$ —6.024 $c_0'$ —6.133 $a_0''$ —6.240
Antimony ..	0	6.62	Face-centred rhombohedral.	$a_0$ —6.235 angle 87° 24'

rod. To ensure homogeneity of each ingot the pot was replaced in the furnace and the alloy re-heated to a temperature above its melting-point.

The compositions of the alloys were determined electrolytically by estimation of the copper content, and the densities found by the specific gravity bottle method. To make certain that the alloys were in a definite state of



equilibrium the specimens were subjected to prolonged periods of annealing, at temperatures given in the equilibrium diagram.

In all nine alloys were prepared. Their compositions and densities are given in Table I.

### *Experimental Method.*

The crystal structures of the alloys were investigated by the X-ray powder method. Details of the apparatus used in the present investigation and the precaution observed to ensure the accuracy of measurements have been described in previous papers <sup>(1)</sup> and <sup>(4)</sup>. Following the experimental procedure there outlined, the accuracy of the measurements in the present investigation may be estimated as within  $\frac{1}{4}$  to  $\frac{1}{8}$  of 1 per cent.

To simplify as far as possible the examination of the powder photographs only the  $K_{\alpha}$  radiation of copper was used, the  $K_{\beta}$  radiation being absorbed by a thin nickel filter placed at the point of entry of the beam into the camera. One or two of the strong lines due to the  $K_{\beta}$  radiation could not be eliminated, though they were considerably reduced in intensity. Occasionally a line due to the  $L_{\alpha}$  radiation of tungsten was also present on the film; this happened after the tube had been used for some time, and was due to the slow deposition of tungsten on to the target as the filament slowly volatilized.

### *Results.*

The X-ray data supplied by the films of copper, of alloys of A to I, and of antimony are given in Tables II. to XII. The first column in each case gives the radiation producing the reflexion, the values taken for the wavelength being :—

$K_{\alpha}$ (copper).	1.540 Å.U.
$K_{\beta}$ „	1.389 Å.U.
$L_{\alpha}$ (tungsten).	1.484 Å.U.

The second column of the Tables gives the Miller indices of the reflecting planes, and the third column the intensities of the lines on the films. The symbol (St.) denotes strong; M. (medium); W. (weak); and V.W. (very weak).

The plane spacings deduced from measurements on the films are tabulated in the fourth column, while the calculated spacings for the structure found are given in column

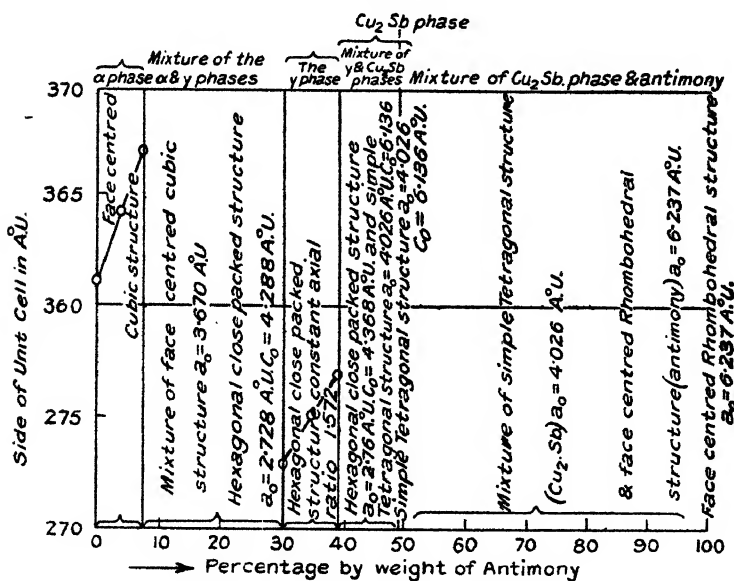
five. The composition, density, crystal structure, and the dimensions of the unit-cells for the nine alloys and for the two end elements copper and antimony are given in Table I.

Fig. 2 gives the crystal structure data found for the system.

### The $\alpha$ Phase.

According to the equilibrium diagram (fig. 1) the  $\alpha$  phase consists of a solid solution of antimony in copper up

Fig. 2.



Crystal structure data for the Cu-Sb alloys.

to over 7 per cent. by weight of antimony. As the atomic diameters of copper and antimony are 2.54 Å.U. and 2.87 Å.U. respectively, a change in the lattice constant of copper would therefore be expected on the introduction of antimony, the solution of antimony causing an expansion of the copper lattice, but accompanied by no change in the type of lattice.

Table II. gives the data supplied by films for electrolytic copper. The films, as was to be expected, gave the well-known pattern of lines associated with the face-centred

cubic structure of copper. The side of the unit-cell deduced from these lines was  $a_0 = 3.610 \text{ \AA.U.}$ —in agreement with the values obtained by other workers.

TABLE II.  
Pure Copper.

Radiation.	Plane.	Intensity.	Observed $d/n$ .	$a_0$ .	Calculated $d/n$ .
$K\beta$ . . . . .	111	W.	2.085 $\text{\AA.U.}$	3.611 $\text{\AA.U.}$	2.084 $\text{\AA.U.}$
$K\alpha$ . . . . .	111	St.	2.084	3.610	2.084
$K\alpha$ . . . . .	100 (2)	St.	1.807	3.614	1.805
$K\alpha$ . . . . .	110 (2)	St.	1.275	3.610	1.275
$K\alpha$ . . . . .	311	St.	1.087	3.610	1.087
$K\alpha$ . . . . .	111 (2)	M.	1.041	3.606	1.042
$K\alpha$ . . . . .	100 (4)	M.	.902	3.608	.902,
$K\alpha$ . . . . .	331	St.	.828	3.610	.828

Structure : face-centred cubic.

Dimensions of the unit-cell :  $a_0 = 3.610 \text{ \AA.U.}$

The crystal structure of the  $\alpha$  phase was investigated by the aid of alloys A and B, and the data obtained from measurements on the films are given in Tables III. and IV.

TABLE III.

Alloy "A."—Composition 96 per cent. copper, 4 per cent. antimony. (The  $\alpha$  phase.)

Radiation.	Plane.	Intensity.	Observed $d/n$ .	Calculated $d/n$ .
$L\alpha$ (tungsten) . . . .	111	W.	2.102 $\text{\AA.U.}$	2.104 $\text{\AA.U.}$
$K\alpha$ . . . . .	111	St.	2.106	2.104
$K\alpha$ . . . . .	100 (2)	St.	1.827	1.822
$K\alpha$ . . . . .	110 (2)	St.	1.291	1.289
$K\alpha$ . . . . .	311	St.	1.097	1.099
$K\alpha$ . . . . .	111 (2)	M.	1.048	1.052

Structure : face-centred.

Dimensions of the unit-cell :  $a_0 = 3.644 \text{ \AA.U.}$

It was found that alloy A (Table III.) produced lines on the film conforming to the face-centred cubic structure of copper, but there was a distinct displacement of the lines, indicating a definite increase in the size of the unit-cell, due to the antimony in solution. As there were no

other lines present on the films, it was evident that this alloy lay within the  $\alpha$  phase. The 4 per cent. antimony in solution caused an expansion of the copper lattice from  $a_0=3.610$  Å.U. to  $a_0=3.644$  Å.U.

The films of alloy B, 80 per cent. copper, 20 per cent. antimony (Table IV.), on the other hand, contained lines of both the  $\alpha$  and the  $\gamma$  phases, showing that the limit of solubility of antimony in copper is below this composition in antimony. The value of the lattice constant gives therefore the dimensions of the face-centred structure

TABLE IV.

Alloy "B."—Composition 80 per cent. copper, 20 per cent. antimony. (The Eutectic Mixture  $\alpha + \gamma$ .)

Radiation.	Plane.	Intensity.	Observed $d/n$ .	Calculated $d/n$ .
$K\beta$ .....	10 $\bar{1}0$	W.	2.364 Å.U.	2.363 Å.U.
$K\alpha$ .....	0002	M.	2.173	2.144
* $K\alpha$ .....	III	St.	2.121	2.116
$K\alpha$ .....	10 $\bar{1}1$	St.	2.073	2.069
* $K\alpha$ .....	100	M.	1.832	1.834
$K\alpha$ .....	10 $\bar{1}2$	M.	1.600	1.588
$K\alpha$ .....	11 $\bar{2}0$	W.	1.364	1.364
* $K\alpha$ .....	110	M.	1.298	1.298
$K\alpha$ .....	10 $\bar{1}3$	M.	1.233	1.223
$K\alpha$ .....	20 $\bar{2}1$	M.	1.153	1.151
* $K\alpha$ .....	311	W.	1.104	1.104
$K\alpha$ .....	0004	W.	1.081	1.072

Mixture of face-centred cubic lattice of side  $a_0=3.670$  Å.U. and a hexagonal close-packed lattice of sides :—

$$a_0=2.728 \text{ Å.U.}$$

$$c_0=4.288 \text{ Å.U.,}$$

corresponding to an axial ratio 1.572.

NOTE.—Lines of the face-centred cubic lattice of the  $\alpha$  phase are marked with an asterisk (\*).

at the limit of the  $\alpha$  phase. This value was found to be 3.670 Å.U., showing a further expansion of the lattice from that of alloy A.

As stated above, the addition of 4 per cent. by weight of antimony to pure copper expands the unit-cell from  $a_0=3.610$  Å.U. to 3.644 Å.U. If this increase follows a linear law with solution of antimony, as is the case with most solid solutions, then the side of the unit-cell increases by

1000 Messrs. E. V. Howells and W. Morris-Jones : *X-Ray*

$\cdot 0085 \text{ \AA.U.}$  per 1 per cent. by weight of antimony. At the limit of solution the total expansion is from  $3\cdot 610 \text{ \AA.U.}$  to  $3\cdot 770 \text{ \AA.U.}$ —i.e.,  $\cdot 06 \text{ \AA.U.}$  A simple calculation therefore fixes the boundary of the solid solution at 7 per cent. by weight of antimony. This agrees almost exactly with the result given by Carpenter, who stated that the upper limit of the  $\alpha$  phase was slightly over 7 per cent. by weight of antimony.

### *The $\gamma$ Phase.*

According to the equilibrium diagram the  $\gamma$  phase is a homogeneous phase, extending between the compositions 30 per cent. and 39 per cent. by weight of antimony. The phase, however, does not exist at temperatures above  $430^{\circ} \text{C.}$ , for, on heating the alloy above the segregation line in the diagram, a definite change has been found to take place and another phase  $\beta$  is formed. In Carpenter's diagram the boundary of the  $\gamma$  phase on the antimony side coincides with the composition  $\text{Cu}_3\text{Sb}$ .

In the examination of the crystal structure and character of the  $\gamma$  phase the five alloys B, C, D, E, and F were used; of these the alloy B, as indicated by the diagram (fig. 1), was a composition in the eutectic mixture  $\alpha + \gamma$ ; C, D, and E were compositions in the  $\gamma$  phase itself, E corresponding to the composition  $\text{Cu}_3\text{Sb}$ ; while F was a composition in the eutectic mixture  $\gamma + \text{Cu}_2\text{Sb}$ .

The films of alloy B contained lines of both the  $\alpha$  and the  $\gamma$  phases. The crystal structure data for this alloy, obtained by an examination of the films, corresponded with the dimensions of the structures at the adjoining boundaries of the  $\alpha$  and the  $\gamma$  phases. The lines corresponding with the  $\gamma$  phase in alloy B conformed to a crystal structure of the hexagonal close-packed class. The dimensions of the unit-cell are:—

$a_0 = 2\cdot 728 \text{ \AA.U.}$  and  $c_0 = 4\cdot 288 \text{ \AA.U.}$ , corresponding to an axial ratio  $1\cdot 572$  (Table IV.).

Lines corresponding to a hexagonal close-packed lattice only were present on the films of alloy C, the dimensions of the lattice (see Table V.) being the same as those obtained from the  $\gamma$  phase lines of alloy B. Starting from the copper end of the diagram, the  $\gamma$  phase can then be considered to commence near the composition 70 per cent. by weight of copper.

TABLE V.

Alloy "C."—Composition 70 per cent. copper, 30 per cent. antimony. (The  $\gamma$  Phase.)

Radiation.	Plane.	Intensity.	Observed $d/n$ .	Calculated $d/n$ .
$K\beta$ .....	$10\bar{1}0$	V.W.	2.361 Å.U.	2.363 Å.U.
$K\alpha$ .....	$10\bar{1}0$	V.W.	2.375	2.363
$K\alpha$ .....	0002	M.	2.170	2.144
$K\alpha$ .....	1011	St.	2.076	2.069
$K\alpha$ .....	$10\bar{1}2$	M.	1.600	1.588
$K\alpha$ .....	$1\bar{1}20$	M.	1.364	1.364
$K\alpha$ .....	$10\bar{1}3$	M.	1.232	1.223
$K\alpha$ .....	$1\bar{1}22$	M.	1.153	1.151
$K\alpha$ .....	$20\bar{2}1$	W.	1.149	1.139
$K\alpha$ .....	0004	V.W.	1.080	1.072
$K\alpha$ .....	2022	V.W.	1.035	1.035
$K\alpha$ .....	$10\bar{1}4$	V.W.	.982	.976
$K\alpha$ .....	$20\bar{2}3$	V.W.	.911	.911
$K\alpha$ .....	$2\bar{1}31$	V.W.	.871	.874
$K\alpha$ .....	$1\bar{1}24$	V.W.	.844	.844

Structure : close-packed hexagonal.

Dimensions of the unit-cell :  $a_0 = 2.728$  Å.U. $c_0 = 4.288$  Å.U.,

corresponding to an axial ratio 1.572.

TABLE VI.

Alloy "D."—Composition 65 per cent. copper, 35 per cent. Antimony. (The  $\gamma$  Phase.)

Radiation.	Plane.	Intensity.	Observed $d/n$ .	Calculated $d/n$ .
$K\beta$ .....	$10\bar{1}0$	W.	2.364 Å.U.	2.383 Å.U.
$K\alpha$ .....	0002	M.	2.185	2.163
$K\alpha$ .....	1011	St.	2.093	2.088
$K\alpha$ .....	$10\bar{1}2$	W.	1.610	1.602
$K\alpha$ .....	$1\bar{1}20$	M.	1.376	1.376
$K\alpha$ .....	$10\bar{1}3$	M.	1.239	1.231
$K\alpha$ .....	$1\bar{1}22$	M.	1.161	1.161
$K\alpha$ .....	$20\bar{2}1$	W.	1.147	1.149
$K\alpha$ .....	$20\bar{2}2$	V.W.	1.045	1.044
$K\alpha$ .....	$20\bar{2}3$	V.W.	.917	.918
$K\alpha$ .....	$2\bar{1}31$	V.W.	.878	.882
$K\alpha$ .....	$1\bar{1}24$	V.W.	.850	.851

Structure : hexagonal close-packed.

Dimensions of the unit-cell :  $a_0 = 2.752$  Å.U. $c_0 = 4.326$  Å.U.,

corresponding to an axial ratio 1.572.

Only lines of the  $\gamma$  phase were present, also on the films of alloy E. The data for this alloy are given in Table VII. The plane spacings derived from these lines again satisfied a hexagonal close-packed arrangement ; but, in this case, the sides calculated for the unit cell are :—

$$a_0 = 2.766 \text{ \AA.U. and } c_0 = 4.348 \text{ \AA.U.,}$$

TABLE VII.

Alloy "E" ( $\text{Cu}_3\text{Sb}$ ).—Composition 61 per cent. Cu, 39 per cent. Sb. (The  $\gamma$  phase.)

Radiation.	Plane.	Intensity.	Observed $d/n$ .	Calculated $d/n$ .
$K_\alpha$ .....	10 $\bar{1}$ 0	M.	2.400 $\text{\AA.U.}$	2.395 $\text{\AA.U.}$
$K_\alpha$ .....	0002	M.	2.181	2.177
$K_\alpha$ .....	10 $\bar{1}$ 1	St.	2.096	2.098
$K_\alpha$ .....	10 $\bar{1}$ 2	M.	1.610	1.610
$K_\alpha$ .....	11 $\bar{2}$ 0	M.	1.382	1.383
$K_\alpha$ .....	10 $\bar{1}$ 3	M.	1.240	1.240
$K_\alpha$ .....	20 $\bar{2}$ 0	W.	1.195	1.197
$K_\alpha$ .....	11 $\bar{2}$ 2	M.	1.167	1.167
$K_\alpha$ .....	20 $\bar{2}$ 1	W.	1.149	1.154
$K_\alpha$ .....	0004	V.W.	1.088	1.088
$K_\alpha$ .....	20 $\bar{2}$ 2	V.W.	1.043	1.049
$K_\alpha$ .....	10 $\bar{1}$ 4	V.W.	.989	.990
$K_\alpha$ .....	20 $\bar{2}$ 3	W.	.920	.923
$K_\alpha$ .....	21 $\bar{3}$ 1	W.	.882	.886
$K_\alpha$ .....	11 $\bar{2}$ 4	V.W.	.853	.856
$K_\alpha$ .....	21 $\bar{3}$ 2	V.W.	.832	.836
$K_\alpha$ .....	10 $\bar{1}$ 5	V.W.	.817	.817

Structure : hexagonal close-packed.

Dimensions of the unit cell :  $a_0 = 2.766 \text{ \AA.U.}$   
 $c_0 = 4.348 \text{ \AA.U.,}$

corresponding to an axial ratio 1.572.

corresponding to an axial ratio 1.572, showing an expansion of the lattice with increase of antimony content. Alloy E, as already pointed out, corresponds to the composition  $\text{Cu}_3\text{Sb}$ , and a more detailed account of it will be given at a later stage. The films of alloy F contained a mixture of lines due to the  $\gamma$  phase and to the alloy  $\text{Cu}_3\text{Sb}$ . Table VIII. gives the data for this alloy. The lines of the  $\gamma$  phase conformed to a hexagonal close-packed structure—the dimensions of the

TABLE VIII.

Alloy "F."—Composition 55 per cent. copper, 45 per cent. antimony. (Eutectic mixture  $\gamma + \text{Cu}_3\text{Sb}$ .)

Radiation.	Plane.	Intensity.	Observed $d/n$ .	Calculated $d/n$ .
$K_\alpha$ .....	101	V.W.	3.382 Å.U.	3.369 Å.U.
$K_\alpha$ .....	001 (2)	V.W.	3.058	3.070
$K_\beta$ .....	111	V.W.	2.612	2.584
$K_\alpha$ .....	110	V.W.	2.831	2.849
$L_\alpha$ (tungsten)	111	M.	2.596	2.584
* $K_\beta$ .....	10 $\bar{1}0$	M.	2.357	2.395
$K_\alpha$ .....	111	W.	2.568	2.584
* $K_\alpha$ .....	0002	V.W.	2.193	2.177
* $K_\alpha$ .....	10 $\bar{1}1$	W.	2.104	2.098
$K_\alpha$ .....	112	M.	2.088	2.088
$K_\alpha$ .....	001 (3)	V.W.	2.045	2.046
$K_\alpha$ .....	100 (2)	M.	2.016	2.015
$L_\alpha$ (tungsten)	201	V.W.	1.903	1.914
$K_\alpha$ .....	201	M.	1.879	1.914
$K_\alpha$ .....	103	V.W.	1.836	1.825
$K_\alpha$ .....	121	V.W.	1.727	1.729
$K_\alpha$ .....	101 (2)	V.W.	1.682	1.684
* $K_\alpha$ .....	10 $\bar{1}2$	V.W.	1.614	1.610
$K_\alpha$ .....	001 (4)	W.	1.537	1.535
$K_\alpha$ .....	203	V.W.	1.444	1.436
$K_\alpha$ .....	104	W.	1.431	1.434
* $K_\alpha$ .....	11 $\bar{2}0$	V.W.	1.383	1.383
$K_\alpha$ .....	100 (3)	V.W.	1.338	1.343
$K_\alpha$ .....	112 (2)	V.W.	1.289	1.292
$K_\alpha$ .....	130	V.W.	1.270	1.274
$K_\alpha$ .....	131	W.	1.246	1.247
$K_\alpha$ .....	102 (2)	V.W.	1.219	1.221
* $K_\alpha$ .....	20 $\bar{2}0$	W.	1.197	1.197
$K_\alpha$ .....	105	W.	1.173	1.175
* $K_\alpha$ .....	11 $\bar{2}2$	W.	1.166	1.167
$K_\alpha$ .....	115	W.	1.125	1.129
* $K_\alpha$ .....	20 $\bar{2}2$	V.W.	1.044	1.049
$K_\alpha$ .....	112 (2)	V.W.	1.039	1.044
$K_\alpha$ .....	100 (4)	V.W.	1.004	1.007

Mixture of a hexagonal close-packed lattice of dimensions :

$$\left. \begin{array}{l} a_0 = 2.766 \text{ Å.U.} \\ c_0 = 4.348 \text{ Å.U.} \end{array} \right\} \text{axial ratio 1.572 and a simple tetragonal lattice of dimensions :—}$$

$$\left. \begin{array}{l} a_0 = 4.029 \text{ Å.U.} \\ c_0 = 6.140 \text{ Å.U.} \end{array} \right\} \text{corresponding to axial ratio 1.524.}$$



unit-cell being in exact agreement with those obtained from alloy E. As the dimensions of the unit-cell calculated from the films of alloy F, which exists in the eutectic mixture  $\gamma + \text{Cu}_3\text{Sb}$ , are identical with those obtained from films of alloy E (composition  $\text{Cu}_3\text{Sb}$ ), which contains lines of the  $\gamma$  phase only, it follows that the boundary of the  $\gamma$  phase on the antimony side of the diagram is near the composition  $\text{Cu}_3\text{Sb}$ . This statement confirms the result of Carpenter.

To complete the examination of the  $\gamma$  phase it was considered that information should be obtained from the films of an alloy existing well inside the phase. Such an alloy was alloy D, of composition 35 per cent. by weight of antimony. A hexagonal close-packed lattice was found to be the arrangement for this alloy also, the dimensions of the unit-cell being  $a_0 = 2.752 \text{ \AA.U.}$  and  $c_0 = 4.326 \text{ \AA.U.}$ , corresponding to an axial ratio 1.572. As was expected, this unit-cell is intermediate in size between the unit-cells for alloys C and E.

The results obtained from the films of alloys B, C, D, E, and F all point to the fact that the  $\gamma$  phase is a region of solid solution, crystallizing in a close-packed hexagonal structure, the dimensions of the unit cell increasing from

$$\left. \begin{array}{l} a_0 = 2.728 \text{ \AA.U.} \\ c_0 = 4.288 \text{ \AA.U.} \end{array} \right\} \text{ to } \left\{ \begin{array}{l} a_0 = 2.766 \text{ \AA.U.} \\ c_0 = 4.348 \text{ \AA.U.} \end{array} \right.$$

with increase of antimony content. For all these alloys the axial ratio remained constant at 1.572. This result is of interest, as it shows that the hexagonal cell, like a cubic cell, expands proportionally in all directions when a solid solution is formed having this structure. If, as shown in fig. 2, the expansion of the hexagonal lattice of the  $\gamma$  phase follows a linear relationship with composition of antimony, and if one boundary of the  $\gamma$  phase is fixed at the  $\text{Cu}_3\text{Sb}$  composition, a simple calculation gives the other boundary to be at the composition 71 per cent. by weight of copper. On the other hand, by using the films of alloys B and C this boundary was found to be near 70 per cent. by weight of copper.

These results indicate that the boundary of the  $\gamma$  phase on the copper side is somewhere in the region of 70 per cent. by weight of copper, and on the antimony side at the composition  $\text{Cu}_3\text{Sb}$  (*i.e.*, 39 per cent. by weight of

antimony). These are also the limits of the phase found by Carpenter.

The crystal structure and lattice dimensions of the alloy  $\text{Cu}_3\text{Sb}$  had already been determined by Morris-Jones and Evans<sup>(1)</sup>, who assigned to it a hexagonal close-packed lattice, the dimensions of the unit-cell being  $a_0 = 2.777 \text{ \AA.U.}$ , and the axial ratio 1.572. From consideration of these values and of the density of the alloy they found that half a molecule of  $\text{Cu}_3\text{Sb}$  was associated with the cell. Many films of long exposures were taken to see whether the above unit was a sub-unit of a larger cell, but they did not detect the presence of any additional lines which would suggest such a cell. Proceeding then as if the alloy  $\text{Cu}_3\text{Sb}$  was a composition in a region of solid solution Morris-Jones and Evans placed two mean atoms of mass  $\frac{1}{2}$  of that of the  $\text{Cu}_3\text{Sb}$  molecule at the coordinates (000) and  $(\frac{1}{3}, \frac{2}{3}, \frac{1}{2})$ . This procedure enabled them to calculate the intensities of the lines on the films, and they found that the calculated intensities agreed very well with the observed intensities. As a result of their work Morris-Jones and Evans intimated that  $\text{Cu}_3\text{Sb}$  may not be a true compound, but an alloy in a range of solid solution.

In the present investigations the observations from the films of  $\text{Cu}_3\text{Sb}$  corroborated the work of Morris-Jones and Evans. The plane spacings calculated from the films of alloy E and given in Table VII. satisfied a close-packed hexagonal unit-cell, the dimensions being  $a_0 = 2.766 \text{ \AA.U.}$ , and the axial ratio 1.572, agreeing to  $\frac{1}{3}$  of 1 per cent. with the results of these workers.

If two mean atoms were placed at the coordinates given by these investigators the shortest inter-atomic distance was  $2.700 \text{ \AA.U.}$ , agreeing very well with  $2.705 \text{ \AA.U.}$ , the mean diameter of the copper and antimony atoms. There were no lines on any of the films which did not satisfy a hexagonal structure or would suggest a bigger cell.

In the present investigation no crystal structure data were discovered to indicate the existence of a definite compound at the composition  $\text{Cu}_3\text{Sb}$ . It appears that the alloy  $\text{Cu}_3\text{Sb}$  is just a composition in the range of solid solution  $\gamma$ , which extends from 30 to 39 per cent. by weight of antimony. The boundary of the  $\gamma$  phase on the antimony side happens to coincide with the composition  $\text{Cu}_3\text{Sb}$ , and the limit of the expansion of the hexagonal

lattice is at this composition. The work of Morris-Jones and Evans <sup>(1)</sup>, which has been confirmed, is therefore explained.

TABLE IX.

Alloy "G."—Composition 51 per cent. copper, 49 per cent. antimony. (The  $\text{Cu}_2\text{Sb}$  Phase.)

Radiation.	Plane.	Intensity.	Observed $d/n$ .	Calculated $d/n$ .
$\text{K}_\alpha$ .....	101	V.W.	3.382 Å.U.	3.369 Å.U.
$\text{K}_\beta$ .....	001 (2)	V.W.	3.071	3.070
$\text{K}_\alpha$ .....	111	V.W.	2.609	2.584
$\text{K}_\alpha$ .....	110	W.	2.854	2.849
$\text{L}_\alpha$ (tungsten)	102	V.W.	2.418	2.442
$\text{K}_\alpha$ .....	111	W.	2.584	2.584
$\text{K}_\alpha$ .....	102	V.W.	2.435	2.442
$\text{K}_\alpha$ .....	112	St.	2.088	2.088
$\text{K}_\alpha$ .....	001 (3)	V.W.	2.048	2.046
$\text{K}_\alpha$ .....	100 (2)	M.	2.016	2.015
$\text{K}_\alpha$ .....	201	W.	1.879	1.914
$\text{K}_\alpha$ .....	103	V.W.	1.836	1.825
$\text{K}_\alpha$ .....	121	V.W.	1.729	1.729
$\text{K}_\alpha$ .....	101 (2)	V.W.	1.684	1.684
$\text{K}_\alpha$ .....	001 (4)	V.W.	1.537	1.535
$\text{K}_\alpha$ .....	203	V.W.	1.444	1.436
$\text{K}_\alpha$ .....	104	M.	1.433	1.434
$\text{K}_\alpha$ .....	110 (2)	M.	1.424	1.424
$\text{K}_\alpha$ .....	100 (3)	V.W.	1.338	1.343
$\text{K}_\alpha$ .....	111 (2)	V.W.	1.289	1.292
$\text{K}_\beta$ .....	102 (2)	V.W.	1.219	1.221
$\text{K}_\gamma$ .....	130	V.W.	1.271	1.274
$\text{K}_1$ .....	131	W.	1.246	1.247
$\text{K}_1$ .....	102 (2)	W.	1.218	1.221
$\text{K}_\alpha$ .....	105	M.	1.174	1.175
$\text{K}_\alpha$ .....	115	M.	1.124	1.127
$\text{K}_\alpha$ .....	112 (2)	V.W.	1.041	1.044
$\text{K}_\alpha$ .....	100 (4)	V.W.	1.004	1.007
$\text{K}_\alpha$ .....	120 (2)	V.W.	.897	.901

Structure: simple tetragonal.

Dimensions of the unit-cell:  $a_0 = 4.029$  Å.U.

$c_0 = 6.140$  Å.U.

corresponding to an axial ratio 1.524.

Two molecules of  $\text{Cu}_2\text{Sb}$  to the unit-cell.

It may also be pointed out that the resistivity curve of Stephens and Evans <sup>(5)</sup> for the copper-antimony alloys shows only a slight increase in resistivity over the range

30 to 40 per cent. by weight of antimony corresponding to the  $\gamma$  phase.

### The $\text{Cu}_2\text{Sb}$ Phase.

The alloy  $\text{Cu}_2\text{Sb}$  has a characteristic purple-lilac colour and is extremely brittle. Its metallurgical and physical properties all point to the fact that it is a definite compound, existing at the composition represented by the formula.

TABLE X.

Alloy "H."—Composition 30 per cent. copper, 70 per cent. antimony. (Eutectic mixture  $\text{Cu}_2\text{Sb}$  and Sb.)

Radiation.	Plane.	Intensity.	Observed $d/n$ .	Calculated $d/n$ .
$K_\alpha$ .....	100 (2)	M.	3.110 Å.U.	3.111 Å.U.
* $K_\alpha$ .....	110	W.	2.822	2.843
* $K_\alpha$ .....	111 $\searrow$	M.	2.609	2.579 $\}$
	211 $\swarrow$			2.637 $\}$
$K_\alpha$ .....	110 (2)	W.	2.252	2.250
$K_\alpha$ .....	221	W.	2.155	2.159
* $K_\alpha$ .....	112	M.	2.086	2.084
* $K_\alpha$ .....	001 (3)	V.W.	2.032	2.042
* $K_\alpha$ .....	100 (2)	W.	2.008	2.010
$K_\alpha$ .....	112	V.W.	1.874	1.880
$K_\alpha$ .....	320	V.W.	1.777	1.755
* $K_\alpha$ .....	121	V.W.	1.720	1.725
$K_\alpha$ .....	100 (4)	V.W.	1.554	1.555
* $K_\alpha$ .....	110 (2)	V.W.	1.424	1.422
$K_\alpha$ .....	210 (2)	V.W.	1.418	1.416
$K_\alpha$ .....	332	V.W.	1.369	1.385

Mixture of a simple tetragonal lattice of dimensions :  $a_0 = 4.020$  Å.U.  
 $c_0 = 6.126$  Å.U.  
 corresponding to an axial ratio 1.524, and a face-centred rhombohedral lattice of antimony  $a_0 = 6.235$  Å.U. and angle  $87^\circ 24'$ .

NOTE.—The lines of the simple tetragonal lattice of  $\text{Cu}_2\text{Sb}$  are denoted by an asterisk (\*).

In the course of the present work X-ray photographs were taken of this phase (i.) to establish its crystal structure, and (ii.) to discover whether a region of solid solution exists on either side of the  $\text{Cu}_2\text{Sb}$  composition.

The crystal structure of the phase was deduced from the measurements of the films of the alloys F, G, H, and I, and

the X-ray data for these alloys are recorded in Tables VIII., IX., X., and XI. The composition of alloy C corresponds to the pure compound. These films showed that  $\text{Cu}_2\text{Sb}$  crystallizes in a simple tetragonal arrangement, the dimensions of the unit-cell being constant within the range of accuracy claimed for the measurements. This

TABLE XI.

Alloy "I."—Composition 20 per cent. copper, 80 per cent. antimony. (Eutectic mixture  $\text{Cu}_2\text{Sb} + \text{Sb}$ )

Radiation.	Plane.	Intensity.	Observed $d/n$ .	Calculated $d/n$ .
$\text{K}_\alpha$ .....	100 (2)	M.	3.113 Å.U.	3.114 Å.U.
$^*\text{K}_\alpha$ .....	111 } 211 }	V.W.	2.607	2.581 } 2.639 }
$\text{K}_\alpha$ .....	110 (2)	W.	2.255	2.251
$\text{K}_\alpha$ .....	221	W.	2.158	2.161
$^*\text{K}_\alpha$ .....	112	W.	2.086	2.086
$^*\text{K}_\alpha$ .....	001 (3)	V.W.	2.044	2.044
$^*\text{K}_\alpha$ .....	100 (2)	V.W.	2.011	2.012
$\text{K}_\alpha$ .....	111 (2)	W.	1.883	1.882
$\text{K}_\alpha$ .....	320	W.	1.772	1.763
$\text{K}_\alpha$ .....	100 (4)	V.W.	1.558	1.557
$\text{K}_\alpha$ .....	210 (2) }	W.	1.418	1.418 }
$^*\text{K}_\alpha$ .....	110(2) }			1.422 }
$\text{K}_\alpha$ .....	332	W.	1.370	1.386
$\text{K}_\alpha$ .....	431	V.W.	1.262	1.262
$\text{K}_\alpha$ .....	100 (5) }	V.W.	1.244	1.245 }
$^*\text{K}_\alpha$ .....	131 }			1.246 }

Mixture of a simple tetragonal lattice of dimensions :—

$a_0 = 4.024$  Å.U. } corresponding to an axial ratio of 1.524, and a face-  
 $c_0 = 6.133$  Å.U. } centred rhombohedral lattice of dimensions  $a_0 =$   
 6.240 Å.U. and angle  $87^\circ 24'$ .

NOTE.—The lines of the simple tetragonal lattice of  $\text{Cu}_2\text{Sb}$  are denoted by an asterisk (\*).

structure accounted for all the reflexions produced by the crystal planes. The dimensions of the unit-cell deduced from the films of the alloys of F, G, H, and I, are :—

F.  $a_0 = 4.029$  Å.U. } G.  $a_0 = 4.029$  Å.U. }  
 $c_0 = 6.140$  Å.U. }  $c_0 = 6.140$  Å.U. }  
 H.  $a_0 = 4.024$  Å.U. } I.  $a_0 = 4.020$  Å.U. }  
 $c_0 = 6.133$  Å.U. }  $c_0 = 6.126$  Å.U. }

corresponding to an unvarying axial ratio  $c = 1.524$ .

The maximum fluctuation in the values of the lattice constants is within the range of experimental error, being less than  $\frac{1}{4}$  of 1 per cent. This close agreement between the values of the lattice from the four alloys, which include the actual compound and compositions on either side of it, shows that the lattice structure is of unvarying dimensions.  $\text{Cu}_2\text{Sb}$  has therefore a unique structure, and the constancy of the unit-cell obtained from the alloys F, G, H, and I shows that neither copper nor antimony is soluble in it.

The mean values taken for the sides of the fundamental cell are

$$a_0 = 4.026 \text{ \AA.U.}$$

$$c_0 = 6.136 \text{ \AA.U.}$$

corresponding to an axial ratio  $c = 1.572$ .

The reflexions from the tetragonal faces, combined with the density of the compound, *i. e.*, 8.42 gms. per c.c., showed that two  $\text{Cu}_2\text{Sb}$  molecules are associated with the unit-cell. The Laue symmetry for  $\text{Cu}_2\text{Sb}$  was not determined, as we failed to obtain an isolated crystal of any size. However, the powder photograph shows that the unit-cell is obviously simple tetragonal, and the body-centre space-groups are thus excluded. To determine the space-group and atomic arrangement further measurements with single crystals are needed. The crystal structure and size of unit-cell determined in the present investigation were quoted by Stephens <sup>(6)</sup> in a paper dated April 1929.

### *Antimony.*

Carpenter, in his investigation of the antimony end of the diagram found that an alloy containing 0.98 of an atom per cent. of copper was inhomogeneous even after prolonged annealing, being an eutectic mixture of  $\text{Cu}_2\text{Sb}$  and antimony crystals. From a study of this alloy Carpenter states that the solubility of copper in antimony does not exceed one atom per cent., and he has drawn the solubility line at this composition, which is 0.5 per cent. by weight of copper. This phase of solution Carpenter called the " $\epsilon$ " phase.

A solution of 0.5 per cent. of copper in antimony should produce a slight but measurable change in the dimensions of the antimony cell—the change to be expected in this case being a contraction due to the smaller copper atom.

*References.*

- (1) Morris-Jones and Evans, *Phil. Mag.* iv. p. 1302 (Dec. 1927).
- (2) Carpenter, H. C., *Zeit. für Metallkunde*, iv. p. 300 (1913).
- (3) Guertler, *Zeit. Anorg. Chem. SI.* p. 418 (1906).
- (4) Grime and Morris-Jones, *Phil. Mag.* vii. p. 1118 (June 1929).
- (5) Stephens and Evans, *Phil. Mag.* viii. no. 48 (July 1929).
- (6) Stephens, *Phil. Mag.* viii. no. 50, p. 286 (September 1929).
- (7) James and Tunstall, *Phil. Mag.* xi. p. 233 (August 1920).
- (8) Ogr, *Phil. Mag.* xlii. p. 163 (1921).
- (9) Persson and Westgren, *Zeit. für Phys. Chem.* cxxxvi. p. 208 (September 1928).

January 1930.

XCI. *A Method of Investigating the Higher Atmosphere.*

By E. H. SYNGÉ\*.

REGULAR balloon observations of the upper atmosphere, as may be seen from the tables in any book on meteorology, do not extend beyond 20 km., at which height the density is from  $\frac{1}{12}$  to  $\frac{1}{14}$  that at sea-level. The density is falling rapidly at this point, and it is improbable that balloon observations could be carried to a much greater altitude. They must certainly fail long before that interesting region is attained, at about 50 km., where the density is about  $\frac{1}{1000}$  that at sea-level and the pressure similar to that at which electrical discharge in vacuum tubes takes place most readily. It is quite probable that the ionization of the lower atmosphere may be controlled by conditions here, so that a means of recording variations in the atmosphere at these altitudes might be of considerable importance to meteorologists. So far as the writer is aware the only method suggested for obtaining records at such altitudes has been that of sending up powerful rockets, loaded with apparatus, which, after recording the conditions at the height reached, would descend to the earth by means of parachutes†. The difficulties of this method are numerous and obvious, and it does not seem that any attempt has been made to obtain records in this way. The following method, on quite different lines, is, however,

\* Communicated by the Author.

† R. H. Goddard, "A Method of Reaching Extreme Altitudes," *Smithsonian Misc. Collections*, vol. lxxi. no. 2 (1921).

available to determine certain properties and variations of the upper atmosphere, as far as a density from  $\frac{1}{1000}$  to  $\frac{1}{10,000}$  that at sea-level. Nearly all the apparatus required exists in sufficient quantity; there are no formidable technical difficulties to be surmounted; and the theory appears quite unassailable.

The method depends on the scattering of light by the molecules of a gas; for a gas of constant composition this scattering is proportional, to a high approximation, to the density of the gas, and inversely proportional to the fourth power of the wave-length of the light. Thus, supposing the composition of the atmosphere to be unchanged at the heights investigated, its density at these heights will be known, after making various corrections, if we can project a sufficiently strong beam of light to allow of the light scattered in a given region being detected and measured by photo-electric apparatus after collection by a large reflector.

The sky of night is, of course, by no means perfectly dark, and even if we select the darkest part of the sky on a clear moonless night as a background, the light scattered by the beam of a single searchlight at any considerable height will be quite imperceptible to the eye. For instance; taking figures for the searchlight from Glazebrook's 'Dictionary of Applied Physics'; for the molecular scattering from Schuster and Nicholson's 'Optics'; and for the sky from Russell, Dugan, and Stewart's 'Astronomy,' it appears that, at a height of 30 km., where we may suppose the density to be about  $\frac{1}{50}$  that at sea-level, the light scattered from the beam of a 36-inch searchlight, with the most powerful arc, will only add about 1 part in 200 to the brightness of the darkest part of the sky. This proportion, although perfectly imperceptible to the eye, can be detected by photo-electric apparatus, which is sensitive to a difference of 1 part in 1000.

This is the case of a single searchlight, but the method involves the concentration of a large number of searchlights upon the same region in the upper atmosphere. The effect is additive. In the case considered, if a single searchlight enables a reading to be made with a probable error of 10 per cent., then ten searchlights will reduce the probable error to about 1 per cent. This leaves out of account various important considerations—for instance, the steadiness of the arcs and the absorption of the light by



the atmosphere in its double journey, first from the searchlights to the region of the upper atmosphere under investigation, and afterwards from this region to the collecting reflector. The latter effect, which differs for various wave-lengths, will usually be much more complicated if the emitting and receiving stations are at a low altitude. A table in Schuster and Nicholson's 'Optics,' 3rd ed. p. 324, makes this very evident. Figures are given which compare the observed mean, the observed clear-day readings, and the theoretical molecular scattering for Washington and Mount Wilson. The variation of the clear-day observations from the mean is about four times as great at the lower station as at Mount Wilson. At both stations clear-day observations differ very little from the calculated values for the short wave-lengths, which produce far the greatest effect on the photo-electric cell, so that even at a low altitude observations of this sort would require trifling corrections only, for atmospheric variations on clear days.

With regard to the steadiness of the arc, the high intensity Sperry arc is only moderately steady. Its intensity, however, appears to be a function of the current passing through the arc\*, and if this is known for the moment of observation the correction could be made at once. When a number of searchlights are employed together the irregularities would tend to neutralize one another, and this, the more effectively, the more numerous were the searchlights. Probably the total current used per second with a large assemblage of searchlights would hardly vary at all, and the amount of any small variation would indicate the necessary correction with sufficient accuracy.

Some remarks are necessary as to the collecting reflector and the design of photo-electric cell required. A parabolic mirror about 1 metre in diameter would seem well suited to the case, but it should be made with considerably greater care than an ordinary searchlight reflector, in which errors amounting to a divergence of  $1^\circ$  beyond theory are usual†. The error here should not exceed a few minutes of arc, and the mirror should be silvered on the face, as the dispersion of the glass and irregularities of two surfaces instead of one are no doubt responsible for the large error in the ordinary

\* "Colour and Spectral Composition of certain High-Intensity Searchlight Arcs," Bur. Stand. Tech. Pap. no. 168 (1920).

† Glazebrook's 'Applied Physics,' vol. iv. pp. 521, 522.

reflector. A focal length of about 1 metre would be suitable. With such a reflector a photo-electric cell-window of a little less than 2 cm. in diameter placed at the focus would admit light from a circle of the sky about  $1^\circ$  in diameter. In the approximate result given for a height of 30 km. it was supposed that the beam of the searchlight made an angle of about  $60^\circ$  with the horizontal, and that the axis of the receiving reflector made a similar angle with the horizontal. We can give an approximate figure for the amount of light entering the cell under these circumstances. No unit of photo-electric activity seems to be in use, but the photo-electric effectiveness depends so largely on the wave-length, blue light being more than 30 times as effective as yellow light for a potassium cell \*, that it is pointless to give a value for the light in ergs without specifying the wave-length. But making the necessary calculations, it appears that the light entering the cell from a single searchlight in the given circumstances may be taken as approximately equivalent in photo-electric activity to  $10^{-5}$  or  $1.5 \times 10^{-5}$  ergs of yellow light per second. The light from the night sky, which comes jointly from a faint zodiacal light spread over the whole sky, although strongest near the ecliptic; from a permanent auroral effect; from the stars, which contribute about a sixth part of the whole; and, finally, from the light scattered in the atmosphere by all these, may probably be taken as about the same in composition (practically speaking, in blueness), as the light scattered from the searchlight, and we may set it as photo-electrically equivalent to  $2 \times 10^{-3}$  or  $3 \times 10^{-3}$  ergs of yellow light per second entering the cell. These amounts are quite sufficient in themselves to allow of an accuracy to the degree mentioned. The light, however, which passes through the window diverges at an angle of  $60^\circ$ , and as the photo-electric surface is not sensitive to yellow light beyond  $10^7$  erg per sq. cm. per sec. the cell must be rather flatter than is usual. If the sensitive surface is 2 cm. distant from the cell-window, the concentration would be sufficient. By making the reflector larger, and the window proportionately larger, the depth of the cell can be increased in the same proportion, and the total current will be increased in the square of this proportion.

\* H. S. Allen, 'Photoelectricity,' p. 273.

A cell with so large a window is not suited for giving direct readings to the degree of accuracy aimed at, but the method of a substituted beam, on a similar principle to that outlined by the authors of 'Photographic Photometry' (Oxford University Press), seems adequate to ensure the required accuracy.

The question of a substituted equivalent beam appears essential to the method, and as it presents various difficulties it may be discussed here. The principle is very simple. The searchlight or searchlights are simultaneously occulted, and at the same time an equivalent light whose strength is known enters the cell. When this light is exactly equivalent in its effect to the light collected from the searchlight, the needle of the galvanometer will remain steady. And thus the strength of the light coming from the searchlight can be calculated from the strength of the known light, which is regulated by crossed optical wedges.

For accurate results, however, the lights should be exactly equivalent. They should have the same composition and strike the cell at the same angles. It is this which presents difficulties here, since the composition of the light from the searchlights as it reaches the receiving mirror varies according to the conditions of the atmosphere.

The most simple plan for meeting the difficulty might be the following:—A frame carrying some narrow strips of aluminium ribbon, painted white on the side facing the mirror and black on the other side, is suspended between the sky and the reflector. A beam is made up with a composition approximately the same as that reaching the reflector from the searchlight under the actual conditions. This beam is divided by mirrors, and the divided parts are each passed along the aluminium strips, with which they make small angles. A proportion of the light diffused from the strips strikes the mirror at the proper angles to bring it into the cell. The strength of the beam, before division, is regulated by passage through crossed optical wedges, and the effect on the photo-electric cell can be made approximately identical with the effect of the searchlights. The composition of the equivalent beam with the proper proportions of the various wave-lengths does not present any great difficulty. The source of light can be a standard incandescent wire. A spectrum of this is formed by a prism, and there is an arrangement of narrow shutters or flat pins which can be pushed down in the focal plane of

the spectrum, so as to cut off the desired portions of various wave-lengths; the beam is then reconstituted by reverse passage through a prism, passes through the optical wedges, is divided as described, and switched on at the same instant as the searchlights are occulted. The energy value and photo-electric value of different portions of the spectrum of the wire being supposed known, tables could be made out showing the proper amounts of each wave-length to be cut out for different conditions of the atmosphere, and the latter can be determined by observation on certain bright standard stars. The corrections would be much more complicated for a low-altitude station than for Mount Wilson, but they would not be so difficult as they appear at first sight. In practice they would take on a routine character. One would not, of course, determine the absolute density of the atmosphere directly in this way. To do this, one could compare the effect at the height under investigation with that at a height within the range of balloon observation. But we are far less concerned with the absolute density of the atmosphere at any height than with its variation from day to day, and the method suggested gives us the means of ascertaining this with great simplicity, to the degree of accuracy we are aiming at, say 1 part in 100.

If investigations of the atmosphere at very great heights were attempted (of course, with a great assemblage of searchlights) the general brightening of the atmosphere due to secondary and tertiary scattering from the beams would have to be allowed for. For an altitude where the density was  $\frac{1}{100}$ , that at sea-level, this effect would equal about  $\frac{1}{20}$  that of the direct scattering reaching the cell. Where the density was  $\frac{1}{10,000}$ , it might equal  $\frac{1}{2}$  that of the direct scattering. To eliminate this effect the receiving reflector would be turned a little aside from the spot under investigation, and the difference recorded by the cell when the beams were all on, and all occulted, would measure this effect, which could then be allowed for in the determination when the reflector was turned directly on the spot. A theoretical calculation would give the proper composition for the substituted beam, which would be required to measure the secondary and tertiary scatterings. It is, of course, only necessary to have a quite approximately correct composition of the substituted beam, *i. e.*, the beam

which is diffused from the aluminium ribbons, but it is important to know its relative photo-electric value in any arrangement.

If it were intended to carry out regular observations on the density of the atmosphere at a height of 50 km. (density about  $\frac{1}{1000}$  that at sea-level) a permanent assemblage of several hundred searchlights would be required. It would also be necessary to have some electrically controlled mechanism by which the observer at the receiving station could simultaneously occult the whole assemblage, about 30 km. distant. This offers no great difficulty, and since all the belligerent nations in the late war have many thousands of searchlights on their hands, the investigations could be carried out by their meteorological departments without any great outlay.

In such an assemblage it would be simplest to keep all the searchlight reflectors permanently fixed in the same direction, while the observer with his collecting reflector followed the course of their combined beam from kilometre to kilometre of altitude, choosing times for his observations when no bright star lay within the  $1^\circ$  circle whose light enters the photo-electric cell.

It is possible, of course, that the daily variations in density at 50 km. may be small, or that they may not be immediately related to the weather, in which case the method would only have an abstract scientific interest; but it is at least equally possible that the variations may be considerable and rapid, and may bear closely upon conditions in the lower atmosphere; and if so, the method might prove an important one in meteorology. It is certainly a simple and direct one, at all events for stations at high altitudes.

**XCH.** *Measurements of Sound-Velocities in Air, Oxygen, and Carbon Dioxide at Temperatures from  $900^\circ$  C. to  $1200^\circ$  C., with special reference to the Temperature-Coefficients of Molecular Heats.* By Dr. F. E. KING and Prof. J. R. PARTINGTON\*.

**T**HE present communication gives the results of measurements of sound-velocities at higher temperatures than those previously used, except in the case of air, for which

\* Communicated by the Authors.

measurements up to  $1300^{\circ}\text{C}$ . have been published. The method used and the way in which the results were calculated agree with those previously described (Shilling, *Phil. Mag.* iii. p. 273 (1927); Partington and Shilling, *Phil. Mag.* vi. Suppl. p. 920 (Nov. 1928)).

It was stated in the second reference (pp. 928 and 932) that the piston and central furnace tube of the most recent type of apparatus were of Pythagoras porcelain, and that these measurements were discontinued owing to fracture of the piston. A new piston was obtained, and, after fitting, was dried by passing dry air through the furnace, the temperature being gradually raised to a red heat. After drying, a series of measurements was made with air at room temperature, in which the value of the tube constant previously found, viz. 0.00136, was confirmed (*op. cit.* p. 937). An opportunity was also taken to recalibrate the valve oscillator against the standardized steel bar, when the value previously found was confirmed.

The experiments with air were continued with rising temperatures, and the values of the wave-lengths at temperatures above  $900^{\circ}$  were measured as an additional check on the apparatus. These values were in agreement with those previously found, as will be seen by comparing the velocities given in Table I. with those previously published.

The temperature of the furnace was maintained during the night, when the dynamo was not running, by using the 240-volt D.C. mains. On account of the higher voltage economical running was arranged by putting the furnace windings in series, instead of in parallel, the change-over being made by a large double-throw switch. In this way undue cooling of the furnace was prevented when the dynamo was shut off, but as the current was now the same in all windings the ends of the furnace now tended to cool off somewhat on account of the greater radiation losses there. When the dynamo was put in operation, with the windings in parallel, a uniform temperature throughout the working length of the tube was rapidly attained by suitable manipulation of the resistances.

A few measurements had been made, and a temperature of  $1100^{\circ}\text{C}$ . reached, when one of the end platinum windings fused. As this occurred overnight, when the resistances were in series, the whole furnace cooled rapidly. After removing some of the lagging, it was found that the cause of the breakdown was the penetration of a little of the outside lagging of bauxite to the surface of the outer winding, causing fusion of the platinum. At the same time the

sudden cooling had caused fracture of the central furnace tube. It was therefore necessary entirely to dismantle the whole furnace and erect it again.

A new tube was available, and the apparatus was re-assembled with every precaution against breakdown of the tube or platinum windings. It was clear, however, that there was considerable risk of breakdown at the higher temperatures used, and in order to economize time and thus minimize risk, apparatus for the delivery of the three gases used in a pure and dry condition was arranged. The constant of the new tube was determined, and found to be 0.00137. The procedure adopted was, when the furnace had reached a desired temperature, to pass each gas in turn through the furnace tube until analysis of the issuing gas showed that all air or foreign gas had been displaced, and measurements were then made with all the gases at this temperature. This was carried as far as  $1200^{\circ}$ , when it was noticed that gas was not issuing from the exit, and investigation showed that the new tube had also cracked. Since the assembly of another apparatus will be a lengthy operation, the results so far found, up to  $1200^{\circ}$ , are now published. The properties of the Pythagoras porcelain showed that, although small pieces would withstand very high temperatures and soften only superficially in the oxy-coal gas-flame, lengths of two metres were liable to sudden and unexpected fracture at temperatures in the neighbourhood of  $1100^{\circ}$ – $1200^{\circ}$  \*.

The results of the sound-velocity measurements are presented in tables, those in Table I. being for air. The two sets of figures refer to the two furnaces used. The good agreement between these results and those previously found is apparent when they are plotted against temperature. The new points fall reasonably closely on both sides of the smooth curve derived from the previous values (*op. cit.* p. 933), thus confirming the latter. Since the earlier results were from

\* In this connexion we wish to draw attention to the fact that after full inquiries we were unable, at the time the experiments were made, to obtain any material of English make which was suitable for the furnace tubes. After some delay we obtained specimens of material from a firm recommended to us, but they were in forms unsuitable for testing, and we were informed that the material could not be supplied in tubes which could be used under the conditions contemplated. It seems necessary to mention this in view of some communications on the subject which appeared since our experiments were completed ('Chemistry and Industry,' June 21 and July 5, 1929). One of the most difficult problems in this work is that of obtaining a suitable material for the tubes.

a continuous series of measurements made throughout the whole temperature range, and extend to higher temperatures than the present, they are probably to be preferred, and hence no calculations of molecular heats have been made from the present velocities.

TABLE I.  
Sound-velocities in Air.

Temperature °C.	Velocity m./sec.	Temperature °C.	Velocity m./sec.
939	691.4	1025	715.6
975	702.8	1074	729.9
864	670.8	1069	727.2
932	690.9	1119	739.5
1017	712.0	1167	750.4
1048	721.1	—	—

TABLE II.  
Oxygen. Sound-velocities and Molecular Heats.

Temperature °C.	Velocities m./sec.		$C_v$	$C_p$	$C_p/C_v$
	Observed.	Interpolated.			
959	664.1	663.3	5.319	7.306	1.3736
1024	679.8	680.0	5.350	7.337	1.3715
1052	686.7	687.1	5.356	7.343	1.3710
1085	695.6	695.4	5.369	7.356	1.3701
1139	708.8	708.7	5.394	7.381	1.3684
1171	716.7	716.4	5.411	7.398	1.3673

Table II. contains the results with oxygen. The observed velocities in the second column were plotted against the temperatures, and the values in column three found by graphical interpolation. The molecular heats and their ratio were calculated exactly as before. The last decimals



are of no real significance in these values but are included for purposes of comparison.

In calculating the results for carbon dioxide the method of correcting for the presence of 0.5 per cent. of air in the gas used differs from that employed by Shilling (*op. cit.* p. 293). In the latter it appears that the correction was determined by simple proportion from the measured velocities of sound in the carbon dioxide containing 0.5 per cent. of air and the velocity in pure air. The method now adopted is to calculate the molecular heat of the impure gas ( $C_v^i$  in the

TABLE III.

Sound-velocities and Molecular Heats for Carbon Dioxide.

Temperature °C.	Carbon dioxide + 0.5 per cent. of air.		Pure carbon dioxide.			
	Velocity m./sec.	$C_v^i$	$C_v$	$C_p$	$C_p/C_v$	Velocity m./sec.
15	265.01	6.732	6.741	8.782	1.3028	264.83
100	300.36	7.087	7.093	9.110	1.2835	300.13
200	336.30	7.524	7.536	9.536	1.2654	336.04
300	368.00	7.974	7.989	9.983	1.2496	367.72
400	397.70	8.220	8.236	10.228	1.2419	397.40
500	424.64	8.544	8.561	10.551	1.2324	424.31
600	449.90	8.829	8.848	10.837	1.2248	449.55
700	472.70	9.316	9.336	11.325	1.2131	472.34
800	495.26	9.555	9.576	11.564	1.2076	494.89
900	516.55	9.850	9.873	11.861	1.2014	516.16
1000	537.39	10.032	10.058	12.046	1.1977	536.97

Tables III. and IV.), using the appropriate constants, and to correct for the presence of the 0.5 per cent. of air by the mixture rule. The derivation of the sound-velocities in pure carbon dioxide from the corrected values of  $C_v$  thus obtained is simply the reverse of the usual calculations. The corrections for the earlier determinations have therefore been repeated, and the results are given in Table III., the values in which have been calculated from the velocities  $V'$  in Shilling's paper (Table VII.), which, when the tube correction has been applied, appear in column two in Table III. in the present paper. A comparison with Shilling's table will show that the differences between the corrected and

uncorrected figures are smaller than those given by the previous method of calculation, and this has resulted in some small modification in the corresponding values of the molecular heats. The present corrected values are closer to the values obtained by Dixon, to which reference was made in Shilling's paper (p. 293). Five-figure logarithms were used in the calculations, and a fifth figure has been included

TABLE IV.

Sound-velocities in Carbon Dioxide + 0.5 per cent. of Air.

Temperature ° C.	Velocity m./sec.	$C_v^I$	Temperature ° C.	Velocity m./sec.	$C_v^I$
946	526.05	9.973	1081	552.63	10.374
1020	541.83	9.982	1135	562.49	10.614
1050	546.98	10.211	1178	571.24	10.575

TABLE V.

Sound-velocities and Molecular Heats. Pure Carbon Dioxide.

Temperature ° C.	$C_v$	Velocities m./sec.		$C_v$	$C_p$	$C_p/C_v$
		Calculated.	Interpolated.			
946	9.997	525.64	525.60	10.005	11.993	1.1987
1020	10.005	541.40	540.40	10.230	12.218	1.1944
1050	10.233	546.56	546.40	10.272	12.260	1.1936
1081	10.400	552.19	552.35	10.369	12.357	1.1918
1135	10.640	562.04	562.70	10.491	12.479	1.1895
1178	10.601	570.81	570.80	10.601	12.589	1.1875

in order to show how the corrected and uncorrected values compare. The last figure, however, has no real significance.

The new values for carbon dioxide, uncorrected, are given in Table IV., whilst Table V. contains the figures for the pure gas, corrected for the presence of air as explained above. In Table V. the velocities obtained from the corrected values in column three by interpolation are given in

column four, and from these the values of  $C_v$ ,  $C_p$ , and  $C_p/C_v$  were calculated.

The values for oxygen and carbon dioxide at each hundred degrees from 900° to 1200°, to two decimal places, are given in Table VI. The values for oxygen and carbon dioxide are in good agreement with those previously found at 900 and 1000°.

TABLE VI.  
Molecular Heats of Oxygen and Carbon Dioxide.

Temperature ° C.	Oxygen.		Carbon dioxide.	
	$C_v$ .	$C_p$ .	$C_v$ .	$C_p$ .
900	5.30	7.29	9.90	11.89
1000	5.33	7.32	10.18	12.17
1100	5.37	7.36	10.42	12.41
1200	5.42	7.40	10.57	12.66

The authors desire to acknowledge the receipt of a grant from the Government Grant Committee of the Royal Society, which has defrayed part of the expense of the research. One of the authors (F. E. K.) also wishes to acknowledge the receipt of a grant from the Department of Scientific and Industrial Research.

Chemistry Department,  
East London College,  
University of London.

### XCIH. *The Magnetic Characteristics of Nickel.*

By F. TYLER\*, B.Sc.†

**D**URING the last thirty or forty years a large number of investigations on the magnetic properties of materials have been carried out, and extensive experimental data have been accumulated. Recently great advances have been made on the theoretical side, and for diamagnetism and paramagnetism a considerable amount of work has been done in

\* In receipt of a maintenance grant from the Department of Scientific and Industrial Research.

† Communicated by Prof. R. Whiddington, F.R.S.

correlating experiment and theory. For ferromagnetism the correlation has not been carried so far. In view of the many interesting points which arise in connexion with ferromagnetism, it seems desirable to consider how far the experimental results are in conformity with the various theories, and to discuss the significance of the data in the light of them. In this paper the magnetic characteristics of nickel, particularly in the neighbourhood of the Curie point, will be considered from this point of view, the data for nickel being the most reliable amongst those on ferromagnetics.

### *Theoretical Magnetization Curves.*

According to the classical treatment of magnetism given by Langevin in 1905 and extended by Weiss in 1907, paramagnetic behaviour generally (including ferromagnetism) should be determined by the following equations :

$$\frac{\sigma}{\sigma_0} = \coth a - \frac{1}{a}, \quad . \quad . \quad . \quad . \quad . \quad . \quad . \quad (1)$$

$$H = H_e + NI, \quad . \quad . \quad . \quad . \quad . \quad . \quad . \quad (2)$$

$$a = \frac{\mu H}{kT}, \quad . \quad . \quad . \quad . \quad . \quad . \quad . \quad (3)$$

where  $\sigma$  is the specific intensity of magnetization,  $\sigma_0$  the saturation intensity, and  $N$  the coefficient of the "molecular field" (postulated by Weiss to account for ferromagnetism, and for deviations from the simple Curie law shown by many paramagnetics). When the external field is zero ( $H_e=0$ ), the possibility arises of a substance becoming spontaneously magnetized if  $N$  is positive, and by a graphical method curves showing the relation between this magnetization and temperature can be obtained. (This magnetization corresponds to the extrapolated saturation value for zero external field at the particular temperature.) These curves are usually

drawn so as to represent  $\frac{\sigma}{\sigma_0}$  as a function of  $\frac{T}{\theta}$ , where  $\theta$  is the Curie temperature.

This treatment assumes that any orientation of the magnetic carriers with respect to the field is possible. According to the quantum theory, however, only certain discreet orientations (or rather discreet values of the resolved moment) are possible, and a knowledge of these is to be obtained from a study of the Zeeman effect. The magnetic moment in the field direction is given by  $mg$  (Bohr magnetons), where

$m = j, j-1, j-2, \dots -j$ . ( $j$  is the inner quantum number.)

The expression  $\frac{\mu H}{kT} \cos \theta$  appearing in Langevin's treatment then becomes

$$\frac{jg\mu_B H}{kT} \cdot \frac{m}{j} = \frac{mg\mu_B H}{kT} \quad (\mu_B = 1 \text{ Bohr magneton}).$$

Now, the number of atoms whose moment resolved parallel to the field is  $mg\mu_B$  is proportional to

$$e^{\frac{mg\mu_B H}{kT}} = e^{mgh} \left( \text{putting } h = \frac{\mu_B H}{kT} \right),$$

and hence for the mean resolved magnetic moment of the assembly

$$\bar{\mu} = \sum_{-j}^j e^{mgh} \cdot mg\mu_B \left| \sum_{-j}^j e^{mgh} \right|,$$

whence

$$\frac{\sigma}{\sigma_0} = \frac{1}{j} \sum_{-j}^j e^{mgh} \cdot m \left| \sum_{-j}^j e^{mgh} \right| \dots \dots \dots (4)$$

This is the function which must replace the classical expression for  $\frac{\sigma}{\sigma_0}$  appearing in (1).

The limiting quantum case is that in which the magnetic elements can only set themselves either parallel or anti-parallel with the field which occurs when the magnetic moment of the carriers is 1 Bohr magneton ( $jg=1$ ). Under these circumstances (4) reduces to the form

$$\frac{\sigma}{\sigma_0} = \tanh a. \quad \dots \dots \dots (5)$$

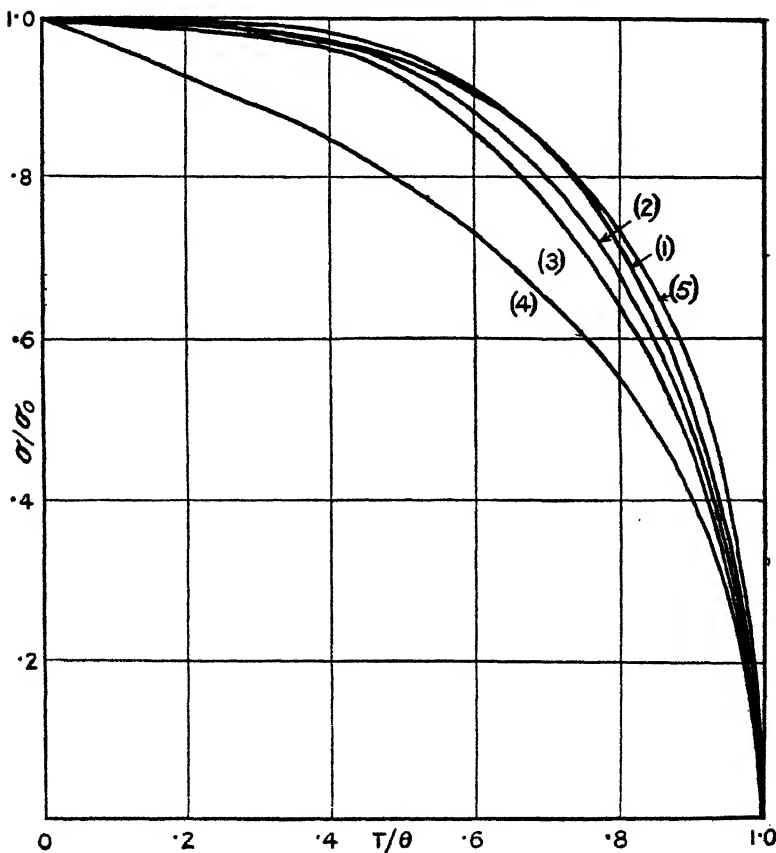
With this relation in place of (1) magnetization temperature curves can be obtained as before. The classical curve may be considered as the limiting quantum curve for  $j \rightarrow \infty$ .

An essential point which emerges from the foregoing discussion is that while the reduced magnetization temperature curves for the Weiss-Langevin theory should be the same for all substances, a series of curves are possible on the quantum theory, the form of the curves depending on the quantum state of the elementary carriers under consideration. These curves will now be discussed in relation to the experimental results.

*Experimental Results.*

The saturation values for ferromagnetics below the Curie point have been given by several investigators. Weiss \*, in collaboration with Onnes (1910), determined the saturation intensity of nickel, iron, cobalt, and magnetite down to 20° K.,

Fig. 1.  
Spontaneous magnetization curves.



- (1) Quantum theoretical curve for  $1 \mu_B$ .
- (2) " " "  $2 \mu_B$ .
- (3) " " "  $3 \mu_B$ .
- (4) Classical curve (Langevin).
- (5) Experimental curve for nickel (Weiss & Forrer).

---

\* P. Weiss and H. K. Onnes, *Comptes Rendus*, cl. pp. 686-687 (1910).

the method being based on the measurement of the maximum couple exerted on an ellipsoid of the material supposed isotropic. For temperatures above  $0^{\circ}\text{C}$ . the most satisfactory results for nickel are those recently given by Weiss and Forrer\* ; these results will be used in constructing a "corresponding state" curve for this metal. The values of  $\sigma$  are obtained by extrapolating the  $(\sigma, H)$  curves to zero field. The saturation intensity  $\sigma_0$  at absolute zero can also be found by extrapolation, and hence from Weiss's magnetic isothermals  $\frac{\sigma}{\sigma_0}$  may be obtained as a function of  $\frac{T}{\theta}$ . The value of  $\theta$

adopted is that obtained by Weiss from experiments on the magnetic-caloric effect. The resulting experimental corresponding state curve is shown in fig. 1 together with the theoretical curves discussed above. Included in fig. 1 are also theoretical curves for the cases of 2 and 3  $\mu_B$ .

From fig. 1 it will be seen that the experimental results fit reasonably closely with the 1  $\mu_B$  curve ; there is an appreciable divergence from the 2 and 3  $\mu_B$  curves, whilst there is little or no correspondence between the experimental and classical curves.

The quantum theory treatment of ferromagnetism thus gives a much more satisfactory representation of the facts for nickel than the older theory, if it is assumed that the carriers have a moment of 1  $\mu_B$ . There are, however, still slight discrepancies between the theoretical and experimental curves to be considered, as may be seen from the figure. The non-conformity of the two curves is most pronounced in the region just below the Curie point, the experimental values being appreciably higher than the theoretical. This may be attributed to a number of reasons ; but perhaps the chief reason lies in the uncertainty of the experimental curve in this region due to the difficulty of obtaining reliable extrapolated values for the quasi-saturation moment.

### *Magnetization near the Curie Point.*

In order to circumvent the uncertainty due to extrapolation in the curves for zero external field in the neighbourhood of the Curie point, it was decided to compare the theoretical and experimental curves giving the relation between  $\frac{\sigma}{\sigma_0}$  and  $\frac{T}{\theta}$  for an external field of a few thousand

\* P. Weiss and R. Forrer, *Annales de Physique*, X<sup>e</sup> Serie, Tome v. p. 153 (1926).

gauss. The experimental curves are obtainable directly from results; the theoretical curves, however, require more detailed consideration.

When the carriers have a moment of  $1\mu_B$ , the quantum theory gives the following equations:

$$\frac{\sigma}{\sigma_0} = \tanh a, \quad . \quad . \quad . \quad . \quad . \quad . \quad . \quad (6)$$

$$a = \frac{\mu H}{kT} = \frac{\sigma_0 H}{RT}, \quad . \quad . \quad . \quad . \quad . \quad . \quad (7)$$

$$H = H_e + N \frac{\rho \sigma}{m}. \quad . \quad . \quad . \quad . \quad . \quad . \quad (8)$$

Substituting for  $H$  in (7),

$$\begin{aligned} a &= \frac{\sigma_0}{RT} \left( H_e + \frac{N \rho \sigma}{m} \right) \\ &= \frac{\sigma_0}{RT} \cdot H_e + \frac{N \rho \sigma_0^2}{m RT} \cdot \frac{\sigma}{\sigma_0}. \quad . \quad . \quad . \quad . \quad . \quad (9) \end{aligned}$$

Now  $\theta$ , the Curie temperature, is given by

$$\theta = \frac{\sigma_0^2 N \rho}{m R}. \quad . \quad . \quad . \quad . \quad . \quad . \quad (10)$$

Hence, using (10), (9) becomes

$$a = \frac{\sigma_0 H_e}{RT} + \frac{\theta}{T} \cdot \frac{\sigma}{\sigma_0},$$

or, rewriting,

$$\begin{aligned} \frac{\sigma}{\sigma_0} &= \frac{T}{\theta} \cdot a - \frac{H_e \sigma_0}{R \theta} \\ &= \frac{a}{\theta} \left( T - \frac{H_e \sigma_0}{R a} \right). \quad . \quad . \quad . \quad . \quad . \quad (11) \end{aligned}$$

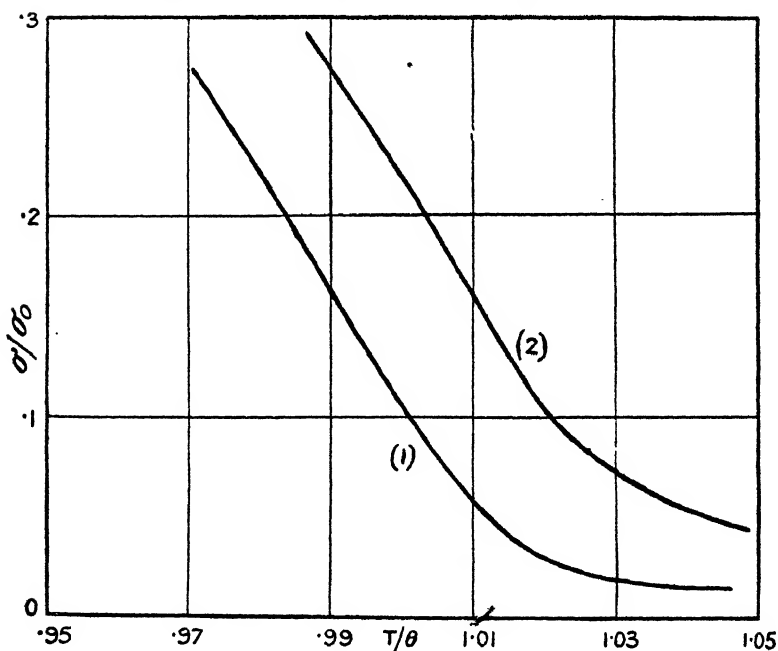
From (11) it follows that the state of a substance in an external field  $H_e$  and at a temperature  $T$  is the same as if the substance were subject solely to the intrinsic field, and at a slightly lower temperature, viz.,  $T - \frac{H_e \sigma_0}{R a}$ . A consideration

of this fact then enables the desired curves to be obtained from the appropriate corresponding temperature curves, without the uncertainty inherent in the usual graphical treatment. (This uncertainty is due to the fact that the term  $\frac{H_e \sigma_0}{R a}$  appearing in (11) is far too small to be represented with precision on a diagram.)



The experimental and theoretical curves thus obtained for  $H_c = 10,000$  gauss are shown in fig. 2. There is no coincidence between the two curves, although they are sensibly parallel. The relative position of the two curves depends on the choice of  $\theta$ , and it is found that by a judicious selection of the value of the Curie temperature the curves can be made to coalesce satisfactorily for a wide range below the Curie point; though whatever the value of  $\theta$  chosen, the

Fig. 2.  
Magnetization curves for  $H_c = 10,000$  gauss.



(1) Quantum theoretical curve for  $1\mu_B$ .

(2) Experimental curve for nickel (Weiss & Forrer).

experimental curves always lie above the theoretical for values of  $T > \theta$ .

Now, it is well known that there are wide discrepancies in the values of  $\theta$  as given by different investigators. This is partly due to variation of  $\theta$  with the chemical purity of the material, but from the observations on material of a high degree of purity it seems fairly certain that the value of  $\theta$  as derived from observations on the ferromagnetic properties of a substance is materially different from the value obtained

from the paramagnetic properties by extrapolation of the  $(\frac{1}{\chi}, T)$  curves. Forrer \* has recently discussed the significance of the ferromagnetic and paramagnetic Curie points, which in the case of nickel differ by about 16°C. He points out that in this immediate region there is still some effect due to hysteresis, and it is only above the upper point that the substance loses entirely its ferromagnetic properties and becomes truly paramagnetic. If this higher value of  $\theta$  is employed in dealing with the magnetization curves, then a satisfactory agreement can be obtained for a considerable range below the Curie point.

A problem closely associated with the magnetization values in the vicinity of the Curie point is the variation of specific heat of a ferromagnetic body. Thermodynamical considerations predict a sudden decrease in the specific heat at the Curie point, the magnitude depending on  $\frac{d\sigma^2}{dT}$  in the immediate neighbourhood. In the classical case for values of  $T$  just less than  $\theta$  the following approximate relation holds :

$$\frac{\sigma}{\sigma_0} = \sqrt{\frac{5}{3}\left(1 - \frac{T}{\theta}\right)}, \quad \dots \dots \dots (12)$$

whence

$$\left[ \frac{d\left(\frac{\sigma}{\sigma_0}\right)^2}{d\left(\frac{T}{\theta}\right)} \right]_{T=\theta} = \frac{5}{3}.$$

The corresponding relation for the quantum theory case when the carriers have a moment of  $I \mu_B$  is

$$\frac{\sigma}{\sigma_0} = \sqrt{3\left(1 - \frac{T}{\theta}\right)}, \quad \dots \dots \dots (13)$$

giving

$$\left[ \frac{d\left(\frac{\sigma}{\sigma_0}\right)^2}{d\left(\frac{T}{\theta}\right)} \right]_{T=\theta} = 3.$$

These values,  $\frac{5}{3}$  and 3, are the extreme values, and it would be expected *a priori* that the experimentally-obtained magnitude would not lie outside these limits ; a value close

\* R. Forrer, *Comptes Rendus*, clxxxviii. pp. 1242-1244 (May 6, 1929).

to 3 would be expected. From Weiss and Forrer's results a graph giving the relation between  $\left(\frac{\sigma}{\sigma_0}\right)^2$  and  $\frac{T}{\theta}$  can be drawn; from this it is found that

$$\left[ \frac{d\left(\frac{\sigma}{\sigma_0}\right)^2}{d\left(\frac{T}{\theta}\right)} \right]_{T=\theta} \doteq 5.$$

This value is considerably higher than the extreme upper limit indicated by theoretical considerations.

Heisenberg's \* recent theory of ferromagnetism essentially gives a satisfactory interpretation of the Weiss molecular field. This he shows may arise from the interchange interaction of the electrons outside closed groups in the atoms in the lattice. Equations are deduced similar to those appearing in the quantum modification of Weiss's theory for the  $I\mu_B$  case. The main differences are that an  $I^2$  term is introduced into the expression for the internal field, and that the quantity corresponding to  $N$  is dependent on the temperature. Although the expressions are admittedly approximations, the closeness of approximation should be greatest at fairly high temperatures, and it seemed of interest to carry out a calculation from them as to the variation of magnetization near the Curie point. They do actually give a value for

$$\left[ \frac{d\left(\frac{\sigma}{\sigma_0}\right)^2}{d\left(\frac{T}{\theta}\right)} \right]_{T=\theta}$$

materially greater than 3, but it is doubtful whether much significance can be attached to the result on account of the limited applicability of the formulæ resulting from some of the subsidiary assumptions made in the treatment of the problem.

#### *Above the Curie Point.*

The magnetic data for nickel above the Curie point are as tabulated below :—

	Temp. range °C.	C.	$\theta$ .	$C_M$ .	$p$ .
Ni $\beta_1$ .....	412-900	·0056	645	·325	8·02
Ni $\beta_2$ .....	900-	—	—	·403	8·96

\* W. Heisenberg, *Zeits. für Physik*, xlix. p. 619 (1928).

The  $p$  values given in the last column are computed from the Curie constant appearing in the Weiss-Curie law as follows:—

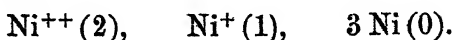
$$p = \frac{\sigma}{1123.5} = \frac{\sqrt{3RC_M}}{1123.5} = 14.07 \sqrt{C_M}.$$

If the carriers have not all the same magnetic moment, then the Weiss magneton number ( $p$ ) deduced from  $C_M$  is a root-mean square value  $p = \sqrt{\bar{p}^2}$ .

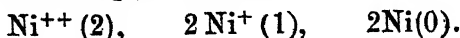
Now, in his investigations on ferromagnetics at low temperatures, Weiss deduced with reasonable certainty that the gramme-molecular moment of nickel extrapolated to zero temperature corresponded to a  $p$  value of 3. (For carriers of different moments the  $p$  value observed at low temperature will be an arithmetic mean  $p = \bar{p}$ .)

Weiss attempted to account for the discordance between the  $p$  values at high and low temperatures by supposing that there were carriers with moments of 3 and 8 whose relative number changed gradually as the temperature rose (there being no discontinuity in the quasi-saturation curve). The investigations above the Curie point, however, show that the magnetic properties usually occur discontinuously, and, further, if they are of considerable magnitude, that they are usually associated with changes in the crystalline structure.

Stoner\* has shown that both the results can be accounted for on the basis of the atomic theory of magnetism without the necessity in general of assuming a change in the constitution of the substance. He supposes that there are groups of atoms in the crystals, and that the magnetic properties are due to ions which have the same moment as those found from measurements on paramagnetic solutions and solid salts. Thus for nickel he considers groups of five Ni atoms, and suggests that the effective ions with  $\mu_B$  values constituting the group to be



This gives a  $p$  value for low temperatures ( $p = \bar{p}$ ) of 3 to agree with the observed value of 3, and for high temperatures ( $p = \sqrt{\bar{p}^2}$ ) the calculated  $p$  value is 8.2 against the observed value of 8.0 for  $\text{Ni}\beta_1$ . With the change in crystal structure in passing from  $\text{Ni}\beta_1$  to  $\text{Ni}\beta_2$ , the constitution of the group changes which he suggests is now



\* E. C. Stoner, Leeds Phil. Soc. i. p. 55 (1926).

This gives a calculated  $p$  value of 9.1, the observed value being 8.96.

### Discussion.

In view of the preceding discussion of the corresponding temperature curves for nickel, it may reasonably be supposed that the magnetic state of nickel is governed by the relation expressed in equation (5), implying that the magnetic moment of the elementary carriers is  $1 \mu_B$ . This assumption satisfactorily correlates the magnetization values below the Curie point, although there are a few uncertain features in the immediate neighbourhood of the Curie point; this region, however, presents a separate problem of its own. In order to account for the  $p$  value of 3 at low temperatures, it may be assumed that there are groups of 5 carriers, three of which have a moment of  $1 \mu_B$ ; this would give the necessary Weiss magneton value of 3. Little, however, can be said about the *nature* of the carriers. It has been seen that Weiss and Stoner, in discussing the magnetic data for nickel, definitely attribute the ferromagnetic properties of the metal to ions. The recent thermoelectric observations of Dorfmann\*, however, seem to indicate that it is the free or conduction electrons which play the role of the elementary magnets. The jump in the specific heat at the Curie point may be written  $\Delta_\theta C_a$  per atom, and this will be made up of  $\Delta_\theta C_i$  due to the positive ions and  $\Delta_\theta C_e$  due to the conduction electrons; i. e.,

$$\Delta_\theta C_a = \Delta_\theta C_i + n \Delta_\theta C_e,$$

where  $n$  = number of conduction electrons per atom.

$\Delta_\theta C_a$  is measured calorimetrically, and  $\Delta_\theta C_e$  is obtained from the sharp change in the thermoelectric magnitude

$T \frac{d^2 E}{dT^2}$  at the Curie point. These latter measurements were

of the same order of magnitude—implying that the conduction electrons are responsible for the ferromagnetism of nickel. Further, on substituting the value of  $\Delta_\theta C_e$  into the quantum theory expression for the jump in the specific heat at the Curie point, viz.

$$\Delta_\theta C_m = \frac{5}{2} k \cdot \frac{j(j+1)}{j^2 + j + \frac{1}{2}},$$

the  $j$  value obtained was approximately  $\frac{1}{2}$ . This is to be

\* J. Dorfmann and R. Jaanus, Pt. I.; J. Dorfmann and I. Kikoin, Pt. II., *Zeits. für Physik*, liv. pp. 277-296 (1929).

expected if the carriers are free electrons, for then  $l=0$  and  $j=s=\frac{1}{2}$ . Also for free electrons  $g=2$ , and hence they have an associate magnetic moment of  $1\mu_B$ —a fact in accordance with the previous discussion. To account for the  $p$  value of 3 at low temperatures, a concentration of 60 per cent. of free electrons to atoms is necessary. Above the Curie point, considering an electron, the  $p$  value can be obtained from Hund's expression :

$$p = 4.97g \sqrt{j(j+1)}$$

by putting  $g = 2$  and  $j = \frac{1}{2}$ . The value of  $p$  then obtained is 8.6. To account for the observed  $p$  values of 8.02 and 8.96 an electron concentration of approximately 80 per cent. (at the Curie point Dorfmann finds 78 per cent.) and 110 per cent. respectively is necessary. Under these circumstances the necessary facts can readily be accounted for.

On the free electron explanation of ferromagnetism, however, it is difficult to realise why ferromagnetism should be restricted to the metals iron, nickel, and cobalt, and certain alloys and compounds (though this objection might also be raised against Heisenberg's theory); the majority of the metals would be expected to share the characteristic properties of ferromagnetics, such metals as silver and copper manifesting them to a high degree. Further, Pauli has shown by applying the Fermi statistics to the assembly of free electrons in the alkali metals, that the slight residual paramagnetism shown by these metals can be satisfactorily accounted for. Far from producing marked ferromagnetic properties, free electrons appear to be responsible for a slight paramagnetism. Thus the nature of the carriers in a ferromagnetic body still remains an outstanding problem.

### Summary.

Quantum and classical theory curves for the variation of the spontaneous magnetization with temperature below the Curie point are obtained and compared with the experimental results for nickel. Curves corresponding to large external fields are also considered.

The comparison shows that the variation of  $\frac{\sigma}{\sigma_0}$  with  $a = \left(\frac{\mu H}{kT}\right)$  is closely given by a  $\tanh$  curve, indicating that the carriers have a moment of 1 Bohr magneton ( $j=\frac{1}{2}$ ,  $g=2$ ). There seem to be anomalies in the variation in magnetization close to the Curie point.

The magnetic data for temperatures above the Curie point are also discussed. It is possible to explain most of the magnetic characteristics by supposing that the carriers are free electrons whose numbers may vary, as suggested by Dorfmann's work on the variation of thermoelectric properties of nickel at the Curie point. There are, however, several objections to this hypothesis. No definite conclusions can be drawn until the relation between conduction electrons and interaction electrons is more fully worked out.

In conclusion I wish to express my indebtedness to Dr. E. C. Stoner for his valuable advice and constructive criticism.

Physics Department,  
University of Leeds.

XCIV. *The Turbulence in front of a Body moving through a Viscous Fluid.* By N. A. V. PIERCY, D.Sc., and E. G. RICHARDSON, B.A., Ph.D., D.Sc. \*

A PREVIOUS paper † relating to the generation of the large-scale turbulence in the wake of a circular cylinder moving through air at considerable Reynolds' numbers, incidentally showed the front stagnation point to be a region of maximum turbulence. Similar exploration near the front stagnation point of an aerofoil ‡ gave the same result. In both cases the unsteadiness of flow was damped out in the subsequent motion of the fluid.

The matter is of some interest in the theory of aerodynamics, if this instability is an essential feature of all stagnation points, because of its relation to an aspect of the stability of fluid motion in cylindrical layers studied by Kelvin, Rayleigh, and G. I. Taylor. According to a well-known analogy, "the varying centrifugal force of the different layers of fluid plays the part of gravity (in a fluid of variable density), and the resulting condition for stability is that the square of the circulation must increase continuously in passing from the inner to the outer cylinder, just as the density of a fluid under gravity must decrease continuously with height in order that it may be in stable

\* Communicated by the Authors.

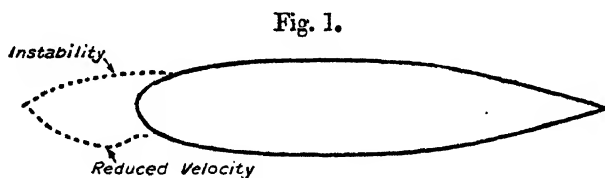
† Phil. Mag. vi. p. 970 (1928).

‡ Aero. Res. Comm. R. & M. no. 1224 (1928).

equilibrium"\*. So far as this simple feature of rotating fluids may find reflexion in the varying flow round a body in a stream, one might expect instability in a limited region surrounding the stagnation point where the stream-lines are convex to the axis and the pressure decreases outwards along a normal, and stability farther round the shoulder of the body where those conditions are reversed.

Both cases of motion that we have so far examined accord with these expectations, but both leave in doubt a question as to whether the instability observed may be a consequence of fluctuation in the circulation round the body. With the aerofoil the circulation had a large average value depending on lift, while in the case of the circular cylinder, although the average circulation was zero, it might conceivably have had a periodic value due to the large-scale eddies shed asymmetrically from the rear.

At Prof. Taylor's suggestion, we therefore explored the region in front of a cylinder of good "stream-line" section—



Section of strut.

an aeroplane strut—arranged with its axis of symmetry parallel to the wind. The shape of the section, given in fig. 1, and the Reynolds's number employed,  $4 \times 10^4$ , using maximum width across the stream to specify length, ensured that insignificant eddying only was shed from the tail, so that the periodic circulation round the cylinder, if any, was very small.

The strut was arranged in a two-dimensional fashion between the walls of the 4-ft. wind-channel working at 42 ft./sec. in the Aerodynamical Laboratory at East London College, and the hot-wire method employed in comparing the velocity fluctuation at any point near the body with that in the undisturbed stream was essentially the same as described in the earlier paper referred to.

Along the various lines that were explored round the nose of the cylinder measurements were made of the average value of the velocity as well as of its relative amplitude, and

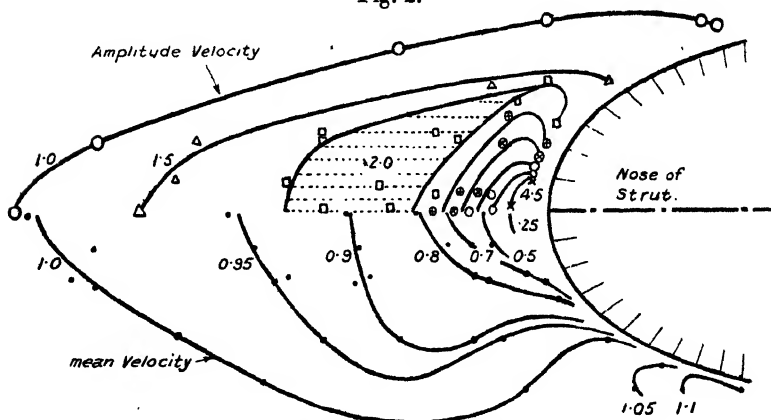
\* Taylor, Phil. Trans. Roy. Soc. A, cccxiii. pp. 291 & 327 (1923).



from this information fig. 2 has been prepared, which shows above the symmetrical axis contours of equal galvanometer response to velocity amplitude, and below the axis iso-average-velocity curves. The numbers attached to the amplitude contours give the amplitude in terms of its value at a distance in the stream, while those attached to the curves of average velocity give the average velocity in terms of its undisturbed value.

The question may be raised to what extent the magnitude of the temperature fluctuations set up in the hot-wire by fluctuations of velocity are influenced by the mean velocity round which these fluctuations take place. The calibration curve of a hot-wire in a steady wind shows (a) at low

Fig. 2.



Contours of mean velocity and velocity amplitude.

velocities an almost parabolic drop of resistance, merging into (b) a linear drop at high velocities. Anywhere over this second region a given change of velocity will produce an approximately constant change of resistance; in other words, a linear relation between the response of a vibration galvanometer and the fluctuation of velocity might be looked for.

Investigations have been in hand to test this point practically, in which hot-wires have been oscillated at various amplitudes approximately in S.H.M., both in stagnant air and in an air-stream. In some of these the wires have been oscillated in close proximity to a smooth brass surface. An early opportunity will be taken to describe in detail the results obtained, but it has been found that, although abnormal response occurs at low speeds, yet easily within

the limits of the mean velocities measured in the present investigation (fig. 2), the relation between velocity amplitude and galvanometer response at constant frequency is linear and independent of the mean velocity.

### CONCLUSION.

Fig. 2 shows a considerable area of instability extending upstream a distance about one quarter of the length of the strut section and roughly covering the area for which the mean velocity is sensibly reduced below its value in the undisturbed stream. The broken lines in fig. 1 show to scale the extent of the disturbance. The disturbance is quickly damped out over the shoulder of the strut.

Within the area explored, velocity amplitude increases rapidly as the stagnation point is approached. We therefore conclude that front stagnation points in general are centres of maximum turbulence.

XCV. *Experiments on the Apparent Deviation from Ohm's Law for Metals at High Current Densities.* By H. MONTEAGLE BARLOW, *Ph.D.*\*

### INTRODUCTION.

A NUMBER of experimental investigations have been made to test the validity of Ohm's law for a metallic conductor carrying a current of very high density †. All of these attempts, with the exception of a recent one by Bridgman, indicate that any departure from Ohm's law, if it exists at all, is exceedingly small, even at densities as large as  $10^7$  amp. per sq. cm. Prof. Bridgman, however,

\* Communicated by the Author.

† (a) Clerk Maxwell, J. D. Everett, and A. Schuster, *Brit. Assoc. Rep.* pp. 36-63 (1876).

(b) E. Lecher, *Sitzber. Wien Akad.* cxvi. (2a) i. p. 49 (1907).

(c) H. Rausch von Traubenberg, *Phys. Zeits.* xviii. p. 75 (1917).

(d) F. Wenner, *Phys. Rev.* (2) xv., p. 531 (1920).

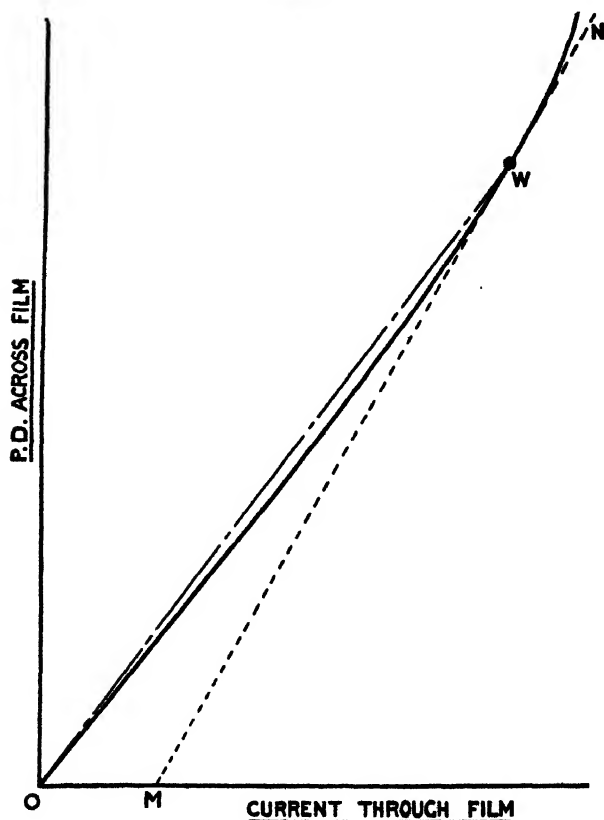
(e) P. W. Bridgman, *Proc. Am. Acad. Arts & Sci.* lvii. no. 6, p. 131 (1922), and a preliminary report in *Proc. Nat. Acad. Sci.* vii. p. 299 (1921).

See also J. J. Thomson, 'The Corpuscular Theory of Matter,' p. 54 (1907); W. F. G. Swann, *Phil. Mag.* xxviii. p. 467 (1914); K. T. Compton, *Nat. Acad. Sci. Proc.* xii. p. 548 (1926), and H. Margenau, *Zeits. f. Physik*, lvi. p. 259 (1920).

claims to have observed and measured a definite increase in the effective resistance of gold and silver films to currents of the order  $10^6$  amp. per sq. cm., and this after eliminating errors due to rise of temperature.

The method of investigation adopted by Bridgman is exceedingly ingenious. Measurements were made by passing a large direct current and a small audible frequency

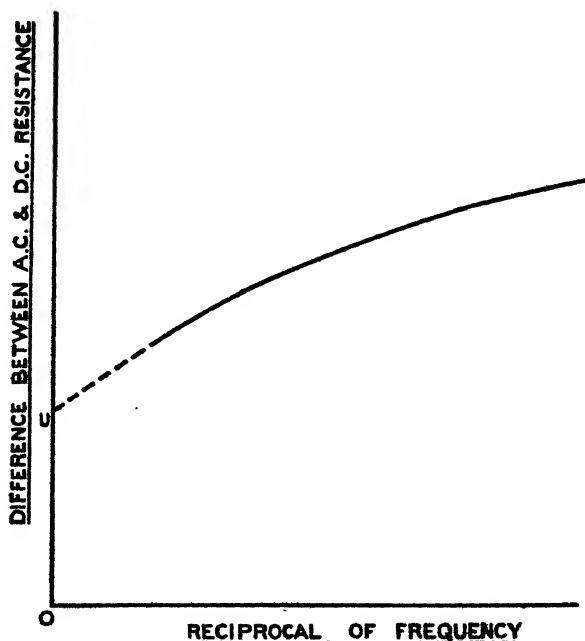
Fig. 1.



alternating current through the metal film at the same time. The P.D. between the ends of the film was balanced in a simple bridge circuit first with a moving coil galvanometer and then with a pair of telephones. The balancing resistances were exactly the same for the alternating current and the direct current until the density reached about  $10^5$  or  $10^6$  amp. per sq. cm., but after this small differences were observed.

This result naturally suggests that at very high current densities the curve representing the relation between the P.D. across the ends of the film and the current through it at constant temperature is no longer a straight line, but has a slightly increasing slope in accordance with the fact that the alternating current P.D. was greater than the corresponding direct current P.D. Thus in fig. 1 the D.C. balance gives a resistance at the point W represented by the slope of the straight line OW, whereas the A.C.

Fig. 2.



balance gives a resistance at the same point represented by the slope of the line MWN, which is a tangent to the curve at W.

Bridgman noticed that this apparent deviation from Ohm's law was a function of the frequency of the alternating current, and became smaller as the frequency was increased. He concluded that this effect was due to the periodic heating and cooling of the film with the alternating current. To eliminate the error introduced in this way he made a series of measurements with a given current density and different frequencies from 3750 periods per

sec. down to 320 periods per sec., plotted the difference between the A.C. and the D.C. resistance against the reciprocal of the frequency, and extrapolated to zero or infinite frequency (see fig. 2). The assumption was made that at very high frequencies the heating and cooling effect would become negligible, so that a true measure of the deviation from Ohm's law was given by the intercept OU on the curve.

So far as the magnitude of the alternating current was concerned, Bridgman did not find that this affected the apparent deviation over a range of ten- or twenty-fold. The average alternating current used was about 0.02 amp., being about one-thirtieth part of the maximum direct current employed.

To test the genuineness of the observed effect, an experiment was made with two different rates of flow of the cooling water traversing the surface of the film. With constant direct current the steady rise of temperature was 40 per cent. greater in one case than in the other. When the difference between the A.C. and D.C. settings in cm. of the bridge wire were plotted against the reciprocal of the frequency, it was found that the two curves appeared to extrapolate to the same value, indicating that the effect as measured by the intercept on the vertical axis was independent of temperature\*.

Although there was a marked change in the rise of temperature of the film for specimens of different width, this seemed to bear no relation to the extrapolated difference between the A.C. and D.C. resistance expressed as a percentage of the initial resistance.

On the other hand, the thickness of the film was an important factor and conductors of gold leaf  $16.7 \times 10^{-6}$  cm. thick gave a percentage deviation some seven times as much as the corresponding percentage deviation for gold leaf only  $8 \times 10^{-6}$  cm. thick. This variation of the effect with thickness was far more than could possibly be accounted for by errors in observation and seems to the author to have an important significance.

\* It is not quite clear whether the result would have been the same had the difference between the A.C. and D.C. resistances been plotted instead of the difference between the slide-wire readings. At the higher temperature the steady current resistance of the film must have been greater, so that the balance-point on the slide wire would be in a new position, and a given displacement would no longer correspond with the same change in resistance.

## EXPERIMENTAL WORK.

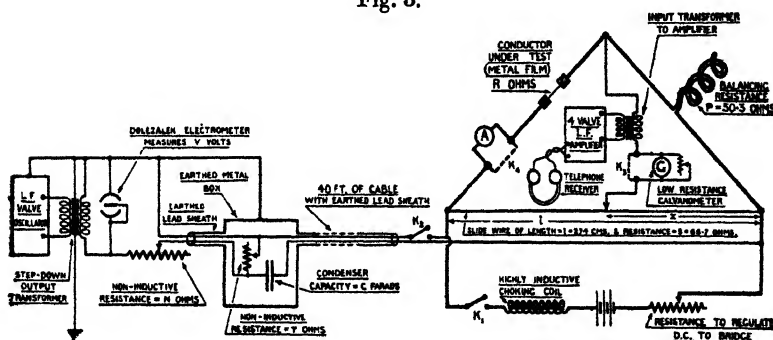
## (a) Description of Apparatus.

The following experiments were carried out with the object of confirming Bridgman's observations. The same method of investigation was employed, but certain refinements were introduced to obtain a higher degree of accuracy.

A four-valve audible frequency amplifier was used in conjunction with the telephone receiver, so that the A.C. balance of the bridge could be made effectively with very much smaller alternating currents. The frequency range employed was from 1000 to 14,000 cycles per sec.

The diagram of connexions for the bridge is shown in fig. 3. A Eureka slide wire 274 cm. long, and having a

Fig. 3.

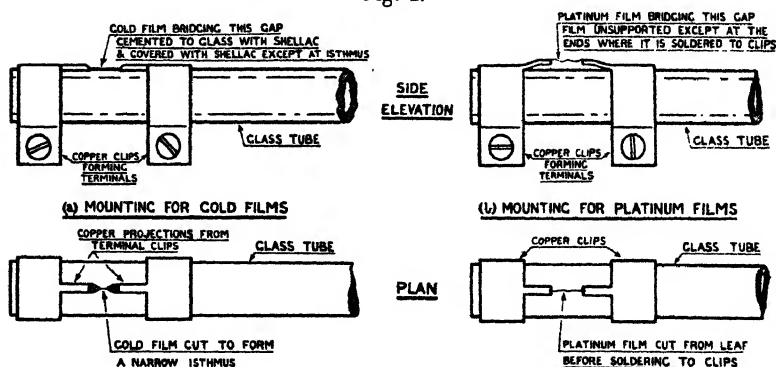


resistance of 66.7 ohms, was used, the only sliding contact in the bridge being the tapping-point to which the detector system was connected. Thus, only out-of-balance currents passed through this contact, which consisted of a very narrow ebonite trough filled with mercury, through which the wire was free to slide. The conductor under test was a thin metal film, in some cases of gold either  $5 \times 10^{-6}$  cm. or  $9 \times 10^{-6}$  cm. thick, and in others of platinum  $16.5 \times 10^{-6}$  cm. thick, whilst the balancing resistance P was a non-inductively wound Eureka wire of 50.3 ohms. The cross-section of every conductor, with the exception of the metal film under test, was sufficiently large to make special cooling devices unnecessary with the currents employed. The A.C. was derived from a valve oscillator, and a 25-mfd. condenser in the supply leads prevented the D.C. from getting back along these leads. A large inductance coil in

the D.C. supply wires was used to choke back the A.C. For the detector it was found best to connect the moving coil galvanometer in series with the primary of the transformer attached to the amplifier.

One of the important points in the investigation was to determine how the apparent departure from Ohm's law was affected by the magnitude of the A.C. through the film. With this in mind great care was taken to prevent direct induction from the valve oscillator, which was placed 40 feet away from the bridge and connected to it by a cable having an earthed lead sheath. The output from the oscillator was applied first to a step-down transformer on the secondary of which the voltage was measured with a Dolezalek electrometer, and then passed through a system of non-inductive resistances forming a potential

Fig. 4.



divider, so that the current flowing away to the bridge was reduced to a very small value. The oscillator and its accessories were enclosed in earthed metal boxes as shown in the diagram. With this arrangement it was not possible to detect any trace of A.C. in the bridge circuit when the key  $K_2$  connecting to the supply cable was open.

A low resistance moving coil milli-ammeter was joined in series with the metal film to measure the direct current passing through it. This instrument was short-circuited during the measurements.

Various methods of mounting the metal foils under test were tried. With the gold films it was not found possible to improve on Bridgman's arrangement. They were cemented to the outside of a glass tube with shellac dissolved in alcohol (see fig. 4 (a)). In some cases a

stream of pure distilled water flowing across the film at right angles to its length was used for cooling, but the author found that the water had a tendency to boil, causing irregular variations in the resistance of the film and noises in the telephone receiver. Much steadier conditions were obtained with no special cooling device apart from the surrounding air, and the current densities reached, about  $3 \times 10^{-6}$  amp. per sq. cm., were not far short of those possible with the flowing water.

Attempts were made to employ liquid-air cooling, but with gold this was unsuccessful on account of a change in structure at the reduced temperature. Experiment showed that only platinum would withstand immersion in liquid air and return to its original condition when brought back to room temperature. A very narrow strip of platinum was cut from the leaf and soldered to copper terminals mounted on a glass tube (see fig. 4 (b)). The film was entirely unsupported except at its ends, and formed an arched bridge at room temperature, so that the contraction, when immersed in liquid air, could take place without restriction. Tests on these platinum conductors were also made in absolute alcohol and air at room temperature, the natural convection currents in the cooling medium being relied upon to dissipate the heat. With platinum the current densities reached were comparatively small, but the apparent deviation from Ohm's law was large enough to measure accurately. In order to make a comparison between the observations it was essential not to submit the film to any treatment that caused a permanent change in its properties. Thus great care had to be taken to immerse the film in the liquid air gradually.

*(b) Procedure in making the Measurements.*

The galvanometer was short-circuited with the link  $K_3$ , and then both D.C. and A.C. were admitted to the bridge by closing keys  $K_1$  and  $K_2$ . A balance was first made with the telephones, and if, after opening the link  $K_3$ , the galvanometer showed a deflexion, the slider was re-set for the D.C. balance. Generally the observations were repeated several times before recording them. The voltage output and frequency of the valve oscillator were also noted, together with the resistances and capacity in the wires connecting to the bridge. This enabled the A.C.



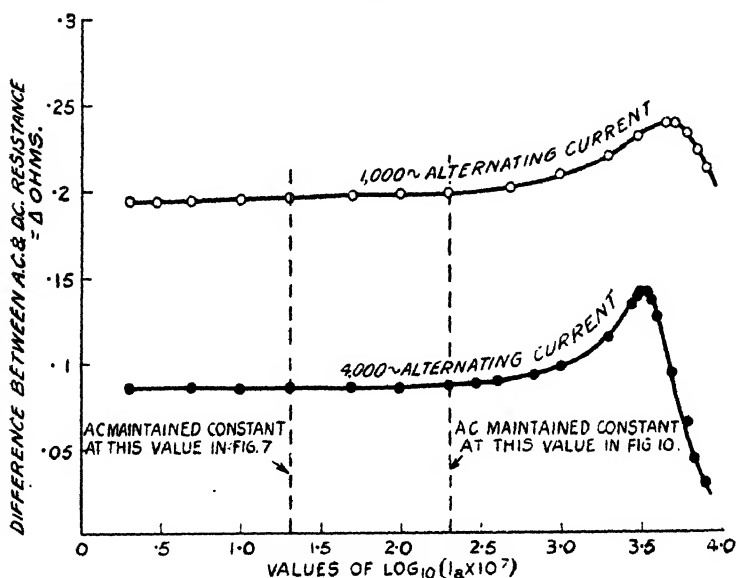
through the conductor under test to be calculated. Representing the constants of the circuit by symbols as indicated in fig. 3, it is easy to show that the alternating current  $I_a$  through the metal film is given by:—

$$I_a = \frac{QV}{(P+R)\sqrt{\left(Q^2 + \frac{1}{\omega^2 C^2}\right)\left(\frac{N+r}{r}\right)^2 + 2QN\left(\frac{N+r}{r}\right) + N^2}},$$

where

$$Q = \frac{(R+P)S}{R+P+S} \quad \text{and} \quad \omega = 2\pi \text{ (frequency).}$$

Fig. 5.



Platinum film,  $16.5 \times 10^{-8}$  cm. thick. Section  $2.47 \times 10^{-7}$  cm.<sup>2</sup>

Film immersed in absolute alcohol at room temperature.

Constant direct current = 0.024 amp. =  $0.97 \times 10^5$  amp. per cm.<sup>2</sup>

The value of the D.C. was obtained by removing the link  $K_4$  across the milli-ammeter, which was in series with the film.

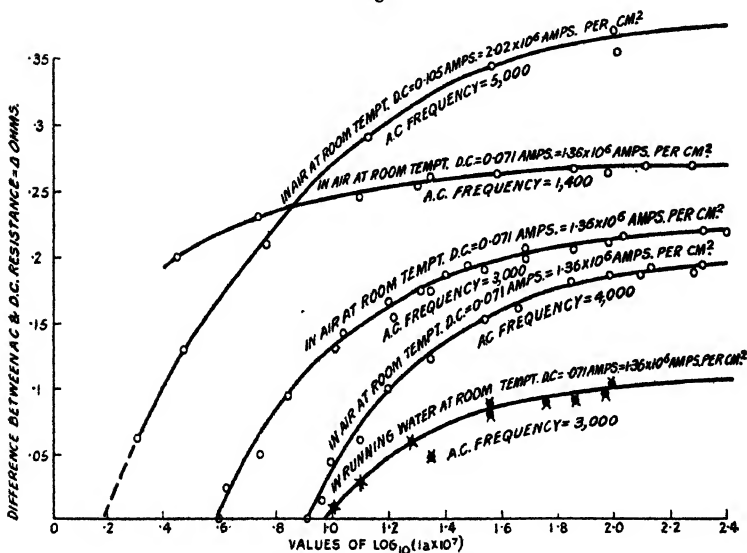
For each specimen preliminary tests were made with a small D.C., and under these conditions the balance position as shown by the galvanometer always agreed exactly with the balance position obtained with the telephones.

If  $x_1$  and  $x_2$  represent the distances from the balance point to the right-hand end of the slide wire (see fig. 3) for the direct current and alternating current respectively, then the difference between the A.C. and D.C. resistances of the conductor under test is given by :

$$\Delta = Pl \left( \frac{x_1 - x_2}{x_1 x_2} \right)$$

where  $l$  = total length of the slide wire.

Fig. 6.



Gold film  $9 \times 10^{-6}$  cm. thick. Section  $= 5.2 \times 10^{-8}$  cm.<sup>2</sup>

All the measurements were made with relatively small alternating currents, so that the D.C. balance was not appreciably altered by interrupting the A.C. supply.

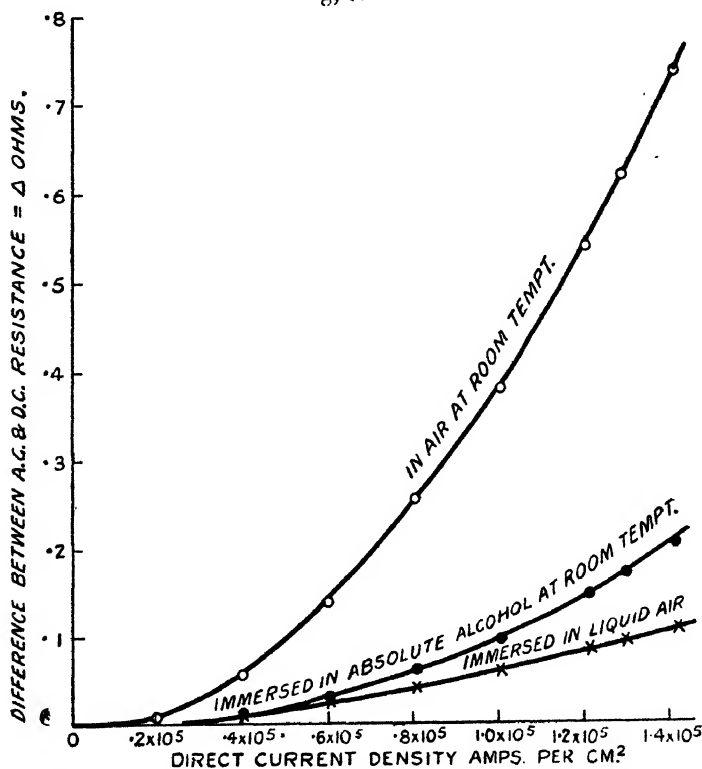
### (c) Experimental Results.

The curves figs. 5 and 6 show the manner in which the observed difference between the A.C. and D.C. resistances of the metal film varied with the magnitude of the alternating current passing through the film. The logarithm of the current has been plotted in order to cover the range within a reasonable space. The smallest alternating current that could be used to give sufficiently reliable

results was  $2 \times 10^{-7}$  amp., and the largest employed was  $8 \times 10^{-4}$  amp., the latter representing about one-thirtieth part of the D.C., this relative value being roughly the same as that used by Bridgman throughout his work.

It will be seen that in the case of platinum there was a curious increase in the difference between the A.C. and D.C. resistances for comparatively large alternating currents, but there was no indication that the effect would

Fig. 7.



Platinum film  $16.5 \times 10^{-6}$  cm. thick. Section  $2.47 \times 10^{-7}$  cm.<sup>2</sup>

Constant A.C. =  $2 \times 10^{-6}$  amp. = 8.1 amp. per cm.<sup>2</sup> Frequency = 4000.

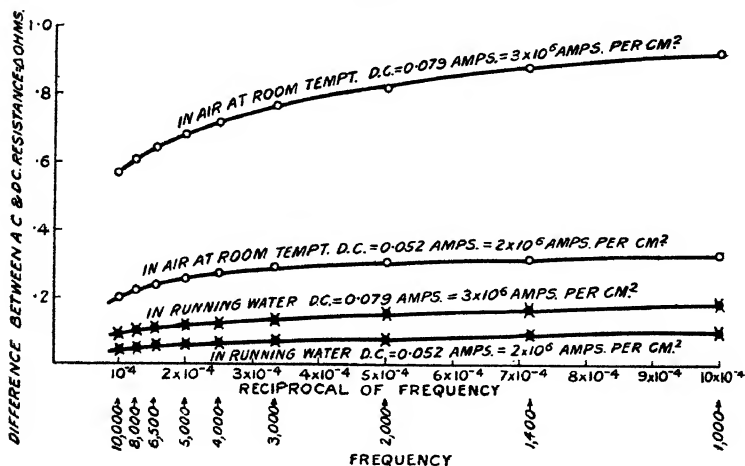
ultimately disappear with the smallest currents employed. On the other hand, with the gold film the difference between the A.C. and D.C. resistances became zero in some cases within the range of measurement, and in others showed definite signs of rapidly approaching that value at the lower end of the scale.

Fig. 7 refers to the platinum film with various cooling media, and shows the difference between the A.C. and D.C.

resistances as a function of the direct-current density. The A.C. had a value of about  $2 \times 10^{-6}$  amp. throughout this test, and the frequency was kept constant at 4000. Assuming a temperature coefficient of resistance for platinum of  $36.5 \times 10^{-4}$ , a calculation was made for the rise in temperature of the film. It was found that this rise in temperature was always directly proportional to the measured difference between the A.C. and D.C. resistances, suggesting that if the heating effect of the current could be completely eliminated there would be no apparent deviation from Ohm's law.

In attempting to deduce figures for the difference between the A.C. and D.C. resistances at infinite frequency

Fig. 8.



Gold film  $5 \times 10^{-6}$  cm. thick. Section =  $2.5 \times 10^{-3}$  cm.<sup>2</sup>

Constant A.C. =  $2 \times 10^{-5}$  amp. = 800 amp. per cm.<sup>2</sup>

the curves shown in figs. 8, 9, and 10 were obtained. The highest frequency employed by Bridgman was 3750, whereas in the author's experiments with gold measurements were made at 14,000 frequency.

The platinum film was, unfortunately, broken before the frequency was taken above 5000, but the results (fig. 10) serve to show the influence of the different cooling media. The effect of frequency is very much greater in air at room temperature than in liquid air.

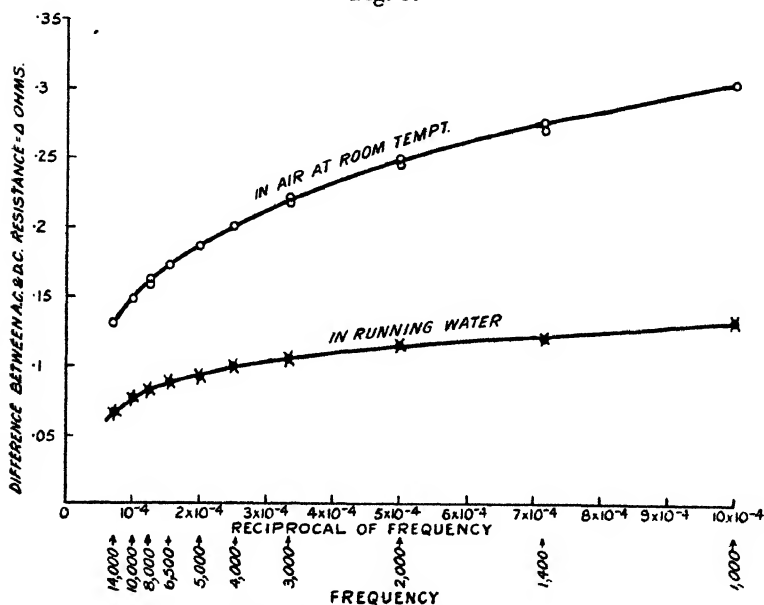
The A.C. was kept as nearly as possible constant during these tests, having the value  $2 \times 10^{-5}$  amp. for the platinum

film,  $2 \times 10^{-5}$  amp. for one of the gold films, and  $3 \times 10^{-5}$  amp. for the other gold film.

It will be seen that all the curves bend over rapidly towards the origin, and any extrapolation is subject to serious error.

The specimen of gold to which the curves shown in fig. 8 refer was cut from a specially thin part of the leaf (estimated at about  $5 \times 10^{-6}$  cm. thick), and it was possible in this case to reach a current density of about  $3 \times 10^6$  amp./cm.<sup>2</sup> with only the surrounding air for dissipating

Fig. 9.



Gold film  $9 \times 10^{-6}$  cm. thick. Section  $5.2 \times 10^{-4}$  cm.<sup>2</sup>  
 Constant D.C. = 0.0707 amp. =  $1.36 \times 10^6$  amp. per cm.<sup>2</sup>  
 Constant A.C. =  $3 \times 10^{-5}$  amp. = 577 amp. per cm.<sup>2</sup>

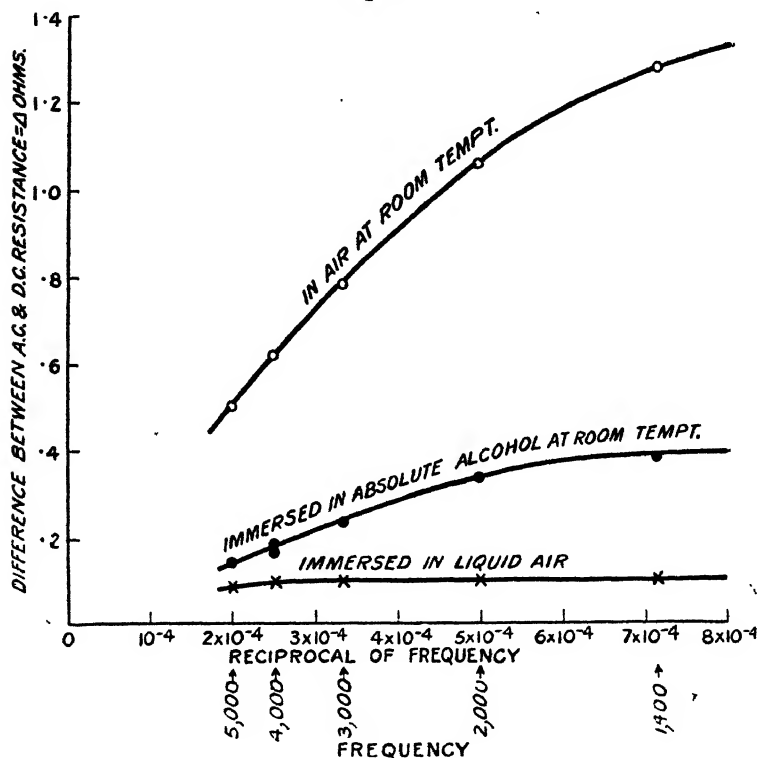
the heat. With a stream of distilled water for cooling, and the same current density, the difference between the A.C. and D.C. resistances was very much smaller.

Bridgman produced his curves with a straight line from the point corresponding to a frequency of 3750 to the vertical axis. Evidently this leads to entirely erroneous results, and, in any case, would give different values for the intercept on the vertical axis with the same current density when using natural air cooling and water cooling.

## CONCLUSION FROM EXPERIMENTS.

The foregoing observations prove that Ohm's law is rigidly true for a gold conductor carrying a current of density  $2 \times 10^6$  amp. per sq. cm., and leave little room for doubt that the law is equally true at  $3 \times 10^6$  amp. per sq. cm.

Fig. 10.



Platinum film  $16.5 \times 10^{-6}$  cm. thick. Section  $2.47 \times 10^{-7}$  cm.<sup>2</sup>

Constant D.C. = 0.032 amp. =  $1.3 \times 10^5$  amp. per cm.<sup>2</sup>

Constant A.C. =  $2 \times 10^{-5}$  amp. = 81 amp. per cm.<sup>2</sup>

The same conclusion is indicated for platinum at a current density of  $1.3 \times 10^5$  amp. per sq. cm.

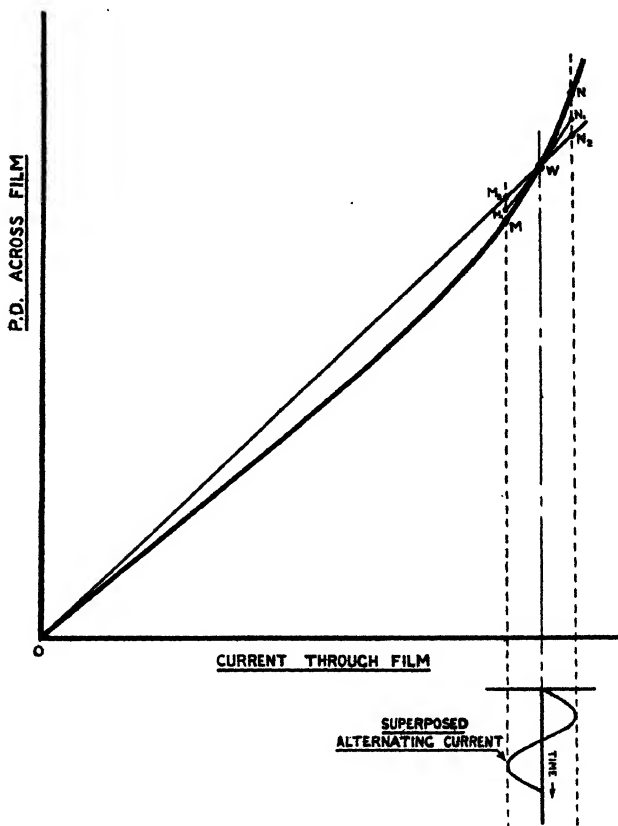
## DISCUSSION OF RESULTS.

Suppose that a curve (fig. 11) is plotted giving the change of P.D. across the metal film for various direct currents passing through it. The gradient of this curve

OMWN increases, due to the rising temperature with increase of current.

Now let a small A.C. be superposed on the D.C. If the frequency were sufficiently low, the corresponding alternating potential variations would be expected to follow the static characteristic, that is, along the line MWN.

Fig. 11.



Assuming that Ohm's law is strictly true, then the higher the frequency the more nearly will the potential variation approximate to the straight line through W from the origin, that is,  $M_2WN_2$ . For audible frequencies such as can be employed in these experiments, the alternating potential variation probably follows some curve such as  $M_1WN_1$ .

Again, the smaller the value of the alternating current the less it will influence the temperature of the conductor, so that the A.C. balance of the bridge is brought nearer to the D.C. balance. Bridgman, in analysing his experiments, assumed a sinusoidal variation of resistance with the alternating current. The author's observations on the effect of decreasing the magnitude of the A.C. suggest that Bridgman's hypothesis does not really represent the facts. During the tests the conductor was necessarily always at a higher temperature than its surroundings, and any reduction in current tended to produce a fall in temperature which was more rapid than the corresponding rise accompanying an increase of current.

In all cases the more efficient the cooling the smaller the difference between the A.C. and D.C. resistance.

As one would expect, it was only possible to get a minimum sound in the telephones for the A.C. balance, and this minimum was always sharper the less the values of the direct and alternating currents. Moreover, the A.C. balance was greatly improved by immersing the conductor in a good cooling medium such as water or liquid air.

In conclusion, the author desires to express his thanks to Prof. W. C. Clinton for placing the apparatus in the Pender Laboratory at his disposal.

University College, London.  
February, 1930.

---

#### *XCVI. Notices respecting New Books.*

*Speech and Hearing.* By Dr. HARVEY FLETCHER. [Pp. xv + 331, with 154 figures.] (New York: D. van Nostrand Co.; London: Macmillan & Co. 1929. Price 21s. net.)

FIFTEEN years ago a systematic investigation of speech and hearing was commenced in the Research Laboratories of the Bell Telephone System with a view to obtain data upon which to base the design of telephone apparatus. The investigation was planned on a comprehensive scale, and is still far from finished; as it has proceeded, many new problems requiring investigation have arisen. The investigation commenced with a study of the



constitution of speech in order to establish a description of average speech and to ascertain to what extent intelligibility was affected by small variations and imperfections in speech. A necessary adjunct was a study of the human ear and its mechanical operation.

As the investigation progressed the necessity of the design of better and more precise instruments than were already available became apparent. The problem of obtaining a reliable record of a complex sound was solved by means of electrical apparatus consisting of condenser, microphone, amplifier, and a special oscillograph. Apparatus was designed by means of which sound-waves can be converted into electrical form and reconverted again to sound with the least possible distortion. There are many examples in this book of beautiful experimental technique which emphasize the wide applications of the thermionic valve in acoustic problems.

For the measurement of the degree of precision with which speech sounds can be recognized and differentiated an essentially perfect reproduction system was employed which could be deteriorated step by step until the faults became noticeable; an estimate was made of the degree of dissatisfaction produced by measured imperfections.

The volume is divided into four parts. Part I. is devoted to speech, including the mechanism of speaking and the characteristics of speech waves. Many examples of speech waves, in the form of photographic oscillograms, are given. Part II. deals with the physical properties of musical sounds and of noise. Part III. is concerned with hearing; it includes an account of the mechanism of hearing, limits of audition, minimum perceptible differences in sound, and the methods by which acuity of hearing may be tested. Part IV. is entitled perception of speech and music; it is devoted mainly to the methods of measuring the recognition of speech sounds and to the effects of intensity changes of frequency distortion and of other types of distortion and of noise and deafness upon the recognition of speech sounds.

It is of interest to note that many of the instruments devised in connexion with these researches have found important commercial applications. "A surprising number of modern acoustical accomplishments have come about through the use of slightly modified forms of apparatus which was originally developed for these investigations. Modern phonographic records are produced with an electrical transmitter which was developed in the very early stages of these studies; and radio broadcasting has grown up around this same 'microphone.' The reproducing equipment of the modern phonograph and of the radio were predicated directly upon these investigations; and talking motion pictures owe their success and much of their apparatus to this same source."

Dr. Fletcher is to be congratulated upon such a fascinating account of an important series of investigations.

*The Life and Work of Sir Norman Lockyer.* By T. MARY LOCKYER and WINIFRED L. LOCKYER, with the assistance of Prof. H. DINGLE and contributions by Dr. CHARLES E. ST. JOHN; Prof. MEGH NAD SAHA, F.R.S., Sir NAPIER SHAW, F.R.S., Prof. H. N. RUSSELL, the Rev. J. GRIFFITH, Sir RICHARD GREGORY, and Prof. A. FOWLER, F.R.S. [Pp. xii+474, with 17 plates.] (London: Macmillan & Co. 1928. Price 18s. net.)

THE first half of this volume consists of a general biography of Sir Norman Lockyer, written by Prof. Dingle from material compiled by Lady Lockyer and Miss Lockyer. It presents the main facts of Lockyer's life, but as a biography it is singularly unsatisfying. The narrative is unrelieved by a single anecdote, and contains few extracts from letters written by Lockyer. It presents to us Lockyer the scientist, but not Lockyer the man.

The second portion consists of chapters contributed by several writers in appreciation of Lockyer's astronomical, archæological, and general scientific work. Of Lockyer's wholehearted and unselfish devotion to the cause of science, and of his far-sighted realization of the importance of scientific education and research to the industry and commerce of the country, there can be no denial. Science owes much to him for his unsparing advocacy of its importance for national advancement. Lockyer will also be remembered as the founder and first editor of 'Nature,' which he nursed with persistent devotion through a long period of struggle. It is difficult to realize at the present time that for thirty years this publication was not a financial success.

Lockyer's astronomical work is a curious mixture of grain and chaff. We can see now what was of permanent value in it and what was not, but it is more than doubtful whether Lockyer himself would have appraised his work in the same way. He was very prone to advance theories on incomplete and inconclusive evidence, and he therefore failed to influence current astronomical thought as he otherwise might have done. His laboratory work was of greater importance than his speculations, and his studies of the spectra of elements under varying conditions are of permanent value.

*National Physical Laboratory. Collected Researches.* Vol. xxi. 1929. (His Majesty's Stationery Office. Price £1 2s. 6d.)

THE researches brought together in this volume have, with one exception, appeared in the 'Proceedings of the Royal Society,' 'The Philosophical Magazine,' and other journals during the last three or four years. Members of the Electrical Department of the National Physical Laboratory and the Radio Research Board have contributed papers dealing with problems connected with the propagation of radio waves, the attenuation due to the resistance of the earth, errors in direction-finding, and measurements on waves received from the upper atmosphere. Several

papers included in this collection have an indirect bearing on wireless waves—piezo-electric quartz resonator, improved cathode ray-tube, and the measurement of inductances and capacities. The first paper gives a detailed description of the new standard of mutual inductance constructed at the National Physical Laboratory for presentation to the Japanese Government, the former standard having been destroyed in the 1923 earthquake.

*Dipolmoment und Chemische Struktur.* Herausgegeben von Prof. Dr. P. DEBYE. Leipziger Vorträge. 1929. Kartoniert R.M. 9. (Verlag von S. Hirzel in Leipzig.)

IN Prof. Debye's recently published book on Polar Molecules a considerable number of experimental results on the determination of molecular moments are given and compared with the calculations derived from the theoretical formulæ. These include the work of Errera on the molar polarization of free molecules and the relation between dissymmetry and chemical structure; Sänger on the determination of electric moments for gases and vapours using the temperature effect, and the polarization of mixtures; and Höjendahl's experiments to establish the connexion between the arrangement of atoms and the dissymmetry measured by the electric moment. Their later researches and those of Wolf, Ebert, and others are brought together in the present volume. Estermann's paper on the application of the molecular ray method for the measurement of molecular polarization is of special interest. The first experiments of this kind were undertaken by Wrede on the alkali salts. Estermann has developed and improved the experimental arrangements, and applied the method to a number of organic compounds. This collection of experimental data will be of service in keeping research workers in touch with the recent developments in the study of chemical structure, based upon Debye's dipole theory.

*Einführung in die Wellenmechanik, Louis de Broglie.* Übersetzt von RUDOLF FIEBELS. Geb. R.M. 13.80. (Akademische Verlagsgesellschaft, m.b.H., Leipzig.)

THE development of wave mechanics has proceeded at a rapid rate during the last three or four years, and notable contributions have been made by de Broglie, Schrödinger, and others. This volume gives an orderly and systematic account of the new mechanics, the theoretical basis for the understanding of atomic phenomena. In the preface the author has reproduced the paper read at the Glasgow meeting of the British Association. The subject is presented in the order of its development—the earlier dynamical theories, the analogy between dynamics and optics, the association of wave propagation with the motion of a particle, and the derivation of the Schrödinger differential equation of the wave function. Examples of wave motion are given in the case of

vibrating strings and membranes, rectangular and circular, followed by the determination of energy levels for the rotator, the harmonic oscillator, and the hydrogen atom whose eigen functions are the polynomials of Legendre, Hermite, and Laguerre. The experiments of G. P. Thomson on the diffraction of cathode rays through metal films are described in detail, and show close agreement with the wave mechanical theory. Brief reference is made to the work of Rupp, who has investigated this problem by photographic and electrical methods. Recent experiments on the relative intensities of the Stark components in hydrogen also show a remarkable agreement with Schrödinger's theoretical calculation. No better introduction to the study of wave mechanics can be recommended to students of modern physics, who require a clear exposition of the new theory and its application to atomic problems. An English translation would deservedly bring the book within the reach of a wider circle of readers.

---

## XCVII. *Proceedings of Learned Societies.*

### GEOLOGICAL SOCIETY.

[Continued from p. 864.]

January 22nd, 1930.—Prof. J. W. Gregory, LL.D., D.Sc.,  
F.R.S., President, in the Chair.

THE following communication was read:—

‘The Geology of some Salt-Plugs in Laristan (Southern Persia).’  
By John Vernon Harrison, B.Sc., F.G.S.

The area under consideration is contained in the rectangle between lat.  $27^{\circ}$  and lat.  $28^{\circ} 20'$  N. (85 miles) and between long.  $54^{\circ} 20'$  and long.  $57^{\circ}$  E. (175 miles). The two main towns are Bandar Abbas and Lar.

Much of this district is covered by normally folded rocks which range in age from Ordovician to Recent, and reach an aggregate thickness of as much as 25,000 feet. The lowest 1000 feet are chiefly shales and sandstones. From Carboniferous to Middle Miocene there are about 13,000 feet of strata which are mainly limestones. The silt, sand, and conglomerate of the Mio-Pliocene together reach a thickness of 11,000 feet. The only general angular unconformity occurs high in the Mio-Pliocene. On the north and east the frontal part of the nappes overrides and ploughs into the normally folded rocks.

South and west of the line of nappes the normal folds have been invaded by plugs of salt, which have brought up quantities of

gypsum and blocks of sedimentary and igneous rocks. The extrusive salt has come to the surface at different times, from Oligocene to late Mio-Pliocene. The intrusive salt-masses, sheathed with autochthonous sediments tilted around them, form in some cases brightly coloured mountains of very striking and characteristic appearance.

Where the sedimentary sheath has been broken or removed by erosion, tongue-like masses of salt and gypsum have moved outwards from the salt dome, and these are described as salt-gypsum 'glaciers'. Erosion has sometimes entirely removed the soluble upper portions of a salt-plug and left a corrie-like valley in a limestone hogback. In such a case the corrie-floor is covered with a layer of the insoluble material which has accompanied the salt to the surface.

This jumbled assemblage of rocks is designated the Hormuz Series. They comprise fœtid dolomites and limestones, dark calcareous shales, red sandstone and shale, variegated shales and sandstones, and igneous rocks which range from granite-porphry to basalt, all more or less epidotized. Dr. G. M. Lees first found Cambrian trilobites in the dark shales, and since then other geologists have discovered them in several other localities. The Hormuz Beds are believed to lie directly on the salt which has brought them to the surface, so that the salt and gypsum of the salt-plugs must be older than Middle Cambrian.

The formation of the salt-plugs is attributed to tangential forces acting on Cambrian salt, which, on account of its comparative plasticity, has acted as something analogous to an igneous magma in its behaviour.

February 21st, 1930.—Prof. J. W. Gregory, LL.D., D.Sc.,  
F.R.S., President, in the Chair.

In dealing in his Anniversary Address with the Geological History of the Pacific Ocean, the PRESIDENT remarked that widespread faith in the unity and permanence of the Pacific Ocean has been based on many features, such as its simple trigonal form, its marginal earthquake-zone, its volcanic girdle, and its coastal structure. The theory was rejected by Huxley in his Presidential Address to this Society in 1870. The view that the Pacific Basin is the hollow left when the moon was torn away from the Earth is untenable, as the moon is 37 times too big and 20 per cent. too heavy. The standard geological theory of the origin of the Pacific is that of Suess, who inferred, from the parallelism of the surrounding mountains, its unity of origin, and from the widespread marine Triassic rocks on the coasts, its Triassic age.

The geological evidence indicates, not a persistent Pacific Ocean, but a succession of variable narrow seas separated by land, and frequently with a predominant trend of west and east. Thus in the Lower Cambrian the *Olenellus* Sea on the north was separated from the *Redlichia* Sea on the south-west; in the Middle Cambrian one

sea spread from the Himalaya to the Rocky Mountains, and an arm of it in the Upper Cambrian overspread Eastern Australia. The whole of the Southern Pacific from New Zealand to South America may have been land, for the only Cambrian in South America was an arm of the Atlantic.

The Ordovician of Pupiao in Southern China has 'scarcely any trace of an American element', the fauna there is European. China and Western America had no direct marine connexion.

In the Devonian Period the East Indies and the China Sea were occupied by a land that extended into the Western Pacific and bounded the sea by which the European fauna reached South-Eastern China and Tongking. In the Middle Devonian the sea with the *Flabellites* fauna lay along western South America and in the valleys of the Amazon and Mississippi; but it did not reach Australia, where, in Upper Devonian times, the Chemung fauna of New York invaded New South Wales. The absence of this fauna from Asia and California shows the separation of the north-western and south-eastern Pacific seas.

The Carboniferous had the same separation of the Asiatic and West American marine faunas, and evidence of land is given by *Gigantopteris*, a member of the Gondwana flora, which is found in Southern and Eastern China and in Texas, and doubtless entered both from a Pacific land.

The Trias has a wide range around parts of the Pacific, but was deposited in separate seas—an Arctic Ocean with a gulf to British Columbia; the western end of a South European sea which reached Venezuela and Southern California; the eastern end of the same sea which extended past the Himalaya to New Zealand. It is represented in New Zealand by a distinct province in a gulf, and not the opening to a Pacific Ocean. Evidence of Transpacific lands in the Trias is given, according to F. von Huene, by the affinities of the Triassic reptiles of South America to those of India.

The Jurassic was the time of the main development of the Pacific Continent of Haug. The Liassic Sea of the North Pacific was separated from the contemporary seas in Central and South America. The Malm fauna of Chile ranged westwards to the Himalaya, but was different from that of the North Pacific and the European fauna in the Antillean region. The Pacific region in Upper Jurassic times, according to Uhlig, was occupied by faunas of four geographical provinces.

In the Cretaceous shallow water connected California and India, while later a land separated the Senonian fauna of California and Japan from that of Chile and New Zealand. The North Pacific was crossed by the giant Sauropods in their range between Mongolia and Montana, and a land-route in a suitable latitude was used thrice later by large quadrupeds. The South Pacific was crossed in the Cretaceous Period by reptiles that migrated between South America and Asia, as the route by way of North and Central America was not then available. Lands west of America allowed the diffusion of the Dakota flora (Turonian) southwards to the Argentine.

In the Kainozoic Era Transpacific lands seem to have lasted until the Oligocene or early Miocene, since the alligator, various reptiles, amphibia, insects, crayfish, land-mollusca, primitive mammals, etc., indicate routes of migration across the tropical and warm temperate zones. Land-plants show the same, for Asa Gray pointed out how much is common to the floras of China and to those of the southern humid areas of the United States. *Gordonia*, one of the plants with this distribution, helps to fix the date of the migration, as it has recently been discovered in the Miocene strata of the Rocky Mountains.

The occurrence of similar animals and plants on opposite sides of the southern oceans has been explained by their origin in a northern land or by their independent evolution. The northern monopoly of evolution is opposed by the theory of Ernst Schwarz of the southern origin of the mammals, and the evidence of the development of numerous animals and plants in the southern lands. The evidence of parasitology renders the alternatives to the spread of some animals across the Southern Pacific, according to Launelot Harrison, 'merely grotesque'.

The life of the Pacific islands, according to many authorities, can only be explained by the existence of extensive Pacific lands on which developed a Eu-Pacific fauna and flora. These lands must have been connected with Polynesia and Australia, and were probably united to the former extension of the Andes to the north-west of Peru; according to Steinmann, his Chimu-andes extended to Hawaii and Polynesia, and were cut off from South America at the end of the Eocene Period.

The coral-islands and the circum-Pacific river-systems also constitute evidence in favour of a subsidence of the Pacific area in the Middle and Upper Kainozoic Eras.

The evidence of the sedimentary rocks that the crust subsides to amounts up to 50,000 feet is opposed to that extreme form of isostasy which denies the possible uplift of an ocean-floor. The arguments in favour of that view, based on a sub-oceanic heavy stratum, as proved by the distribution of igneous rocks, gravity observations, and the speed of earthquake-waves, rest on assumptions so doubtful that geologists should be guided by the direct geological evidence.

February 26th, 1930.—Prof. E. J. Garwood, M.A., Sc.D.,  
F.R.S., President, in the Chair.

The following communication was read:—

'The Glaciation of Western Edenside and Adjoining Areas, and the Drumlins of Edenside and the Solway Basin.' By Sydney Ewart Hollingworth, M.A., B.Sc., F.G.S.

The first part of this paper deals with the glaciation and deglaciation of Western Edenside and of the eastern and north-

eastern parts of the Lake District. In the lowland areas the threefold sequence<sup>1</sup> of Early Scottish, Lake District-Edenside, and late Scottish glaciations is recognized. Almost the whole of the deposits are referable to the maximum of the second or main glaciation. At that time, Edenside acted not merely as a reservoir into which ice moved from the surrounding high ground, but was, with the latter, part of one vast area of accumulation. A great flood of ice travelled anti-clockwise around the northern end of the Lake District—first northwards towards the Solway, and then westwards and south-westwards into the Irish Sea Basin; it was joined en route by ice from the Lake District valleys. Other outlets were the Tyne Gap,<sup>2</sup> Stainmore, and the Lune Valley.

Some twenty stages in the retreat from the Eden back to the valley-glacier stage are recognized, those associated with the retreat from the Penrith Sandstone escarpment being particularly well defined. Although the ice in the lower ground received supplies from the hills throughout, movement during the later phases of the retreat was subordinate to decay, and in several areas the evidence suggests that lobes of ice died away *in situ* by progressive thinning.

The ice-fronts were, during the retreat, parallel to the trend of the drumlins over extensive areas. This unexpected result led to the study of the drumlins of the much wider area, embracing all Edenside and the Solway Basin, which forms the second part of the paper. It is shown conclusively that the drumlins were formed at the maximum of the Main or Lake District-Edenside glaciation and not—as has been frequently claimed for other areas—at a late stage. With rare exceptions, they show no evidence of modification by such transverse movements of ice as occurred during the phase of retreat. Even in the area south of the Solway that was covered by the Scottish Re-advance Ice, most of the drumlins are not due to that ice, but belong to the Lake District-Edenside maximum.

The existence is established of a parting or shed in the ground-ice of the low ground across Edenside near Appleby, from which the lower layers moved outwards, towards Stainmore and down Edenside, and a second similar shed near Carlisle, from which the ice moved eastwards and westwards. These ground-ice partings are independent of the position of the surface ice-sheds. When considered in conjunction with the boulder-dispersal, they imply extensive differential movements within the main body of the Edenside ice, and have important bearings on the movement of ice in general, and on glacial erosion.

Prof. W. T. GORDON exhibited a set of cellulose 'pulls' from coal-balls, on behalf of Mr. JAMES LOMAX, of Bolton. In doing so, he reminded Fellows that Mr. John Walton of

<sup>1</sup> & <sup>2</sup> See also F. M. Trotter, 'The Glaciation of Eastern Edenside, the Alston Block, & the Carlisle Plain,' Q. J. G. S. vol. lxxxv. (1929) pp. 549-612.



Manchester University and Dr. D. Koopmans of Heerlen had devised the process, and the former had given a description of the technique to the Society last session.<sup>1</sup> Since the discovery, several investigators had tried out the method, and the results obtained by Mr. Lomax represented some of the largest and best sections of coal-balls yet produced.

The essence of the process was the replacement of the matrix of the petrification by cellulose, and, in order to effect this, the surface of the fossil was smoothed and polished (the polish need only be a dull polish). If this surface was etched with hydrofluoric, hydrochloric, acetic, chromic, or other acid suited to the type of petrification, the etching produced a 'furry' surface, where the 'fur' was the insoluble part of the fossil and held together sufficiently well, so as not to crumble, when it was gently washed by immersion in water. The etching was continued to the extent desired, and, after washing and drying, a layer of cellulose in amyl acetate or cellulose acetate in acetone, or such other preparation as will give a cellulose film when it dries, was spread over the 'fur.' When thoroughly dry, the film could be stripped off, taking the 'fur' with it. In the case of plant-remains the 'fur' consisted, in part at all events, of carbon, and the cellulose was merely a new matrix replacing the old one of silica or calcite, etc. The film was then mounted in Canada balsam, or, as the specimens on exhibit, on paper, or on glass. One difficulty sometimes encountered was the presence of bubbles in the celluloid film.

Prof. Gordon further described a new technique which had been developed by Dr. B. F. Barnes & Mr. H. Duerden, of Birkbeck College. In it the cellulose film was made as in the Walton-Koopmans process; it was flattened by immersion in alcohol, then the back was coated with egg-albumen, and the whole laid on a glass slide. On hardening, the film was in close contact with the glass surface, and the cellulose was then removed by amyl acetate. Thus the original matrix was now replaced by egg-albumen, and the section rendered perfectly transparent. The process was completed by covering with Canada balsam and a cover-slip. This process will shortly be described by the two above-mentioned authors.

In conclusion, he said that it was possible to make fifty sections from 2 mm. thickness of material, and that a transverse, a longitudinal radial, and a longitudinal tangential section could be made at one and the same time by suitably squaring up the original specimen.

<sup>1</sup> Abstr. of Proc. No. 1189, December 13th, 1928, p. 16.

---

*[The Editors do not hold themselves responsible for the views expressed by their correspondents.]*

THE  
LONDON EDINBURGH AND DUBLIN  
PHILOSOPHICAL MAGAZINE  
AND  
JOURNAL OF SCIENCE.

---

[SEVENTH SERIES.]

---

JUNE 1930.

---

XCVIII. *Notes on Surface-Tension.* By ALFRED W. PORTER, D.Sc., F.R.S., F.Inst.P., Emeritus Professor of Physics in the University of London\*.

V. *On Jaeger's Maximum Pressure Method.*

IN determinations of the surface-tension of mercury by means of Jaeger's method (*i. e.*, the determination of maximum pressure in a gas-bubble before bursting occurs) an ambiguity arises. Sometimes the collapse of the bubble seems to be determined by the inside diameter of the delivery tube, sometimes by the outside diameter. Owing to the impossibility of seeing the growing bubble through the mercury, when this is the liquid, the choice of diameter to be used in the necessary calculation has to be determined by the experimental value of surface-tension expected. The following considerations appear to provide a criterion which removes this undesirable indeterminateness.

At the same time the usual assumption, that the results are always independent of the angle of contact, is shown to be erroneous. How this belief ever obtained credence is a matter of some surprise; it seems, however, to be very commonly held.

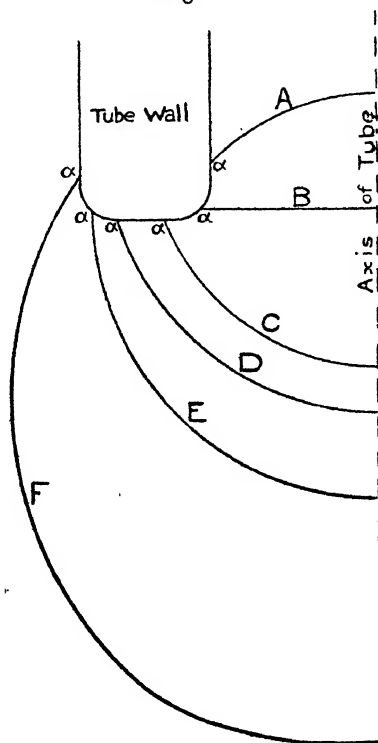
The first cases that will be considered are those in which the angle of contact (reckoned in the liquid) lies between

\* Communicated by the Author. For previous parts see *Phil. Mag.*, March and August 1929.

$90^\circ$  and  $180^\circ$ , as is the case for mercury, for which it is in the neighbourhood of  $135^\circ$ .

As the mercury is forced down the capillary tube, and in it a bubble of gas is ultimately formed, any *equilibrium* position of the bubble must be consistent with the angle of contact between the liquid and glass being of this constant value. Taking into consideration that even the sharpest ground surfaces are terminated by rounded edges, various possible

Fig. 1.



positions of the bubble are as shown in fig. 1. With a small pressure the liquid surface is inside the tube and is convex upwards (A); with increased pressure it reaches position B, making the contact angle  $\alpha$  with the rounded edge, and is then absolutely flat; the pressure inside must now be the same as the pressure at the same level outside the tube. With further increase of pressure the bubble begins to form with concave side upwards, and the point of contact moves along the rounded edge until the position C is reached. It will be assumed that the rounded edge is so

sharp that the radius of the line of contact in the C position can be taken as the internal radius of the tube. It now becomes a question as to whether it will require a greater pressure to cause the interface between liquid and gas to expand into positions such as D, E, F while the angle of contact remains constant. If the equilibrium pressures at D, E, F are less than at C, the bubble becomes unstable with the pressure that has increased it to C, and it will expand indefinitely. Thus the maximum pressure in this case is the pressure corresponding to the interface C, and the surface-tension can be calculated from the form of that interface. It is clear that only the internal radius will enter into the calculation. It turns out that the equilibrium pressure for the position D (just inside the curved *outer* edge) is always less than that at C (at any rate for such radii as can usefully be employed—the statement may not be true for very large radii), and consequently the expansion from C to D is always of a non-equilibrium type. At E, however, the equilibrium value may be less or greater than at C; in the latter case the expansion is resisted, and a fresh increase of pressure is required for further expansion to occur. It must be explained that the interface E is the one which has a vertical tangent at the line of contact; the line of contact is therefore such a position on the rounded outer edge that a vertical tangent corresponds to the true angle of contact; the radius of the line of contact is therefore sensibly the same as the external radius of the tube. Between E and F the equilibrium pressure is found always to diminish (except possibly for very large tubes). Hence the maximum pressure made use of will be either the pressure for case C or for case E, according to which pressure is the larger of the two.

The radius of the line of contact in any position will be denoted by  $C$ , the angle of contact by  $\alpha$ , the maximum semi-diameter of bubble in any position by  $X$ ; the coordinates of any point by  $y$  and  $x$ . It will be assumed that a sufficiently accurate expression for the inquiry is the Poisson-Rayleigh formula

$$y = X - \sqrt{X^2 - x^2} + \frac{1}{2} X^2 \log \frac{X + \sqrt{X^2 - x^2}}{2X},$$

*all distances* being given their *reduced values*, i. e., each true distance expressed in centimetres is to be divided by  $\beta$  (i. e.,  $\sqrt{\sigma/[g(\rho - \rho_0)]}$ ) before being inserted in the equation;  $X$  is (in reduced units) the maximum semi-width of the meniscus if it were extended in accordance with the

formula until it became vertical. In the same way the pressures will be expressed in terms of the reduced height of a column of the liquid concerned equivalent to it. The results obtained will then be applicable to any values of  $\sigma$ ,  $g$ ,  $\rho$ ; at any stage of the operations the equations may be transformed to ordinary c.g.s. units by making them homogeneous in regard to lengths, by multiplying the several terms by the appropriate powers of  $\beta$  which has the dimensions of a length.

Taking the Poisson-Rayleigh equation, we have

$$\tan \theta = \frac{dy}{dx} = \frac{x}{\sqrt{X^2 - x^2}} \left\{ 1 - \frac{X^3}{3(X + \sqrt{X^2 - x^2})} \right\},$$

and at the lowest point the meridional curvature is

$$\left( \frac{d^2y}{dx^2} \right)_0 = \frac{1}{X} \left( 1 - \frac{X^2}{6} \right) = \frac{h}{2},$$

where  $h$  is the reduced-pressure difference (inside minus outside) at the vertex. If  $d$  is the reduced depth of the tip below the surface of the liquid, we have, if  $p + A$  is the pressure inside,

$$p + A = A + d + y_c + h,$$

where  $A$  = atmospheric pressure and  $y_c$  the ordinate at line of contact.

Since we may regard  $d$  as fixed, the problem consists in calculating

$$p - d = y_c + h.$$

It must be noticed that in positions A, C, and D  $\theta_c = \alpha - \frac{\pi}{2}$

at contact; in position E,  $\theta_c = \frac{\pi}{2}$ ; at F,  $\theta_c = \alpha - \frac{\pi}{2}$ ; while at B it is zero.

#### Position E.

For this position and for any contact angle

$$y_c = c - \frac{1}{3}c^3 \log 2,$$

where  $c$  = ext. radius; and from the curvature at the vertex we have also

$$\frac{1}{c} \left( 1 - \frac{c^2}{6} \right) = \frac{h}{2},$$

so that

$$p - d = \frac{2}{3}c + \frac{2}{c} - .231c^3$$

Hence the following table of reduced values:—

<i>c.</i>	<i>p-d.</i>		<i>c.</i>	<i>p-d.</i>
·1	20·07		·5	4·276
·2	10·13		·6	3·684
·3	6·86		·7	3·245
·4	5·25 <sub>3</sub>		·8	2·916

*Positions between C and D.*

In these cases it is necessary to know the angle of contact  $\alpha$ .

$$\tan \theta = -\tan \alpha = \frac{c}{\sqrt{X^2 - c^2}} \left\{ 1 - \frac{1}{3} \frac{X^3}{(X + \sqrt{X^2 - c^2})} \right\};$$

whence, approximately,

$$X = \frac{c}{\sin \alpha} \left\{ 1 - \frac{c^2}{3 \tan^2 \alpha \cdot (1 - \cos \alpha)} \right\}.$$

From  $X$  can be calculated for any value of  $c$

$$h = \frac{2}{X} \left\{ 1 - \frac{X^2}{6} \right\},$$

and

$$y_c = X - \sqrt{X^2 - c^2} + \frac{1}{3} X^3 \log \frac{X + \sqrt{X^2 - c^2}}{2X};$$

and thence  $p-d$ . This has been done for  $\alpha = 120^\circ, 135^\circ, 150^\circ$ .

$$\alpha = 120^\circ.$$

<i>c.</i>	<i>X.</i>	<i>p-d.</i>		<i>c.</i>	<i>X.</i>	<i>p-d.</i>
·1	·115	17·46		·4	·454	4·47
·2	·230	8·72		·6	·672	3·01
·3	·342	5·91		·8	·876	2·43

$$\alpha = 135^\circ.$$

<i>c.</i>	<i>X.</i>	<i>p-d.</i>		<i>c.</i>	<i>X.</i>	<i>p-d.</i>
·1	·141	14·14		·5	·672	2·89
·2	·280	7·11		·6	·789	2·52
·3	·417	4·78		·7	·895	2·22
·4	·548	3·63		·8	·990	1·965

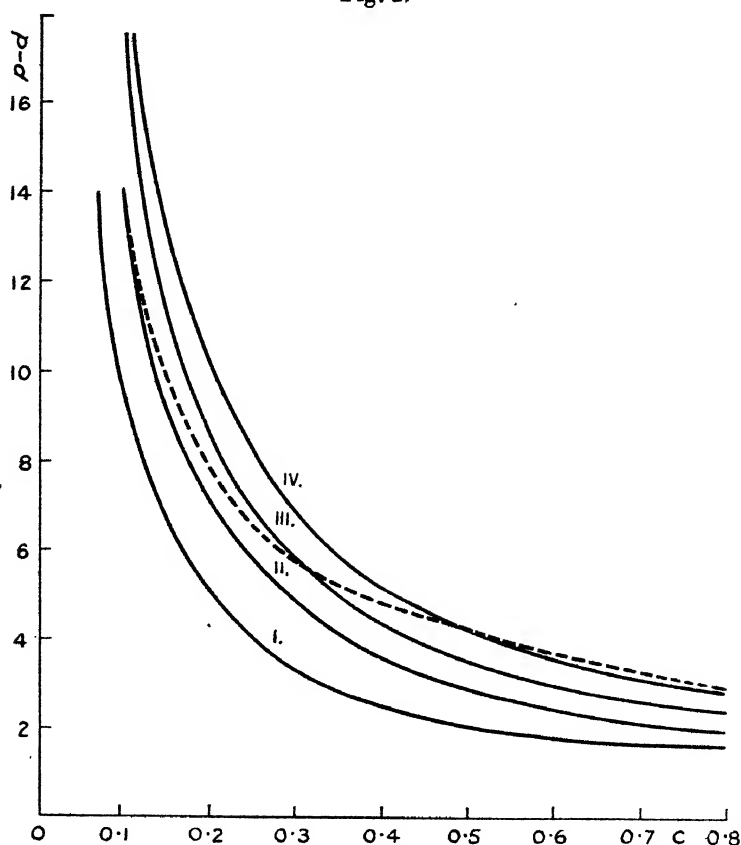
$$\alpha = 150^\circ.$$

<i>c.</i>	<i>X.</i>	<i>p-d.</i>		<i>c.</i>	<i>X.</i>	<i>p-d.</i>
·1	·199	9·75		·5	·866	2·11
·2	·392	5·01		·6	·968	1·90
·3	·571	3·25		·7	1·032	1·72
·4	·731	2·60				

The values in these tables are plotted in fig. 2 as follows :—

Curve.	From C to D.	At E.
I. ....	$\alpha = 150^\circ$	
II. ....	$\alpha = 135^\circ$	
III. ....	$\alpha = 120^\circ$	
IV. ....	$\alpha = 90^\circ$	$\alpha = \text{any value.}$

Fig. 2.



[Note: Curve IV., which was calculated for any  $\alpha$  at E, is identical with the curve for  $\alpha = 90^\circ$  at C to D.]

The use of the curves will now be explained.

Suppose  $\alpha = 135^\circ$ , which is approximately the value for mercury against air. Find the  $p$  on Curve II. corresponding to  $c = \text{int. rad.}$  Find the pressure on Curve IV. corresponding to  $c = \text{ext. rad.}$  If the latter is less than the

former, the pressure in position C is more than sufficient to expand the bubble beyond E; but if more, then the pressure must be further increased until it has the equilibrium value at E. The equilibrium value at F is always (at least within a range which is of practical use) less than at E, so it does not alter one's conclusions. The curve F is shown as a dotted line in fig. 2. The diagram is useful to interpolate from. In practice, however, the chief use is to enable a choice of suitable radii of tip to be made before actual use, and only rough values are required, because the choice should always be made so as to remove any possible doubt arising from the approximations made in calculating the curves. A table of selected values may therefore prove more useful. The accompanying table gives the radii which correspond to a series of selected equilibrium pressures—all being still expressed in "reduced" units. Values for Curves I., II., III., IV. correspond to points between C and D for the angles of contact named, while IV. is also valid for E and any angle of contact.

Values of  $c$ .

Red. Pressure.	I. 150°.	II. 135°.	III. 120°.	IV. 90°.
14	·07	·10	·12	·14
12	·08	·11	·14	·16 <sub>s</sub>
10	·09 <sub>s</sub>	·13 <sub>s</sub>	·17	·20 <sub>s</sub>
8	·12	·17 <sub>s</sub>	·22	·26
6	·17	·24	·29	·34 <sub>s</sub>
4	·25	·36	·44	·53
3	·33	·48	·60	·75

Examples:—Formercury at moderate temperatures  $B = \cdot 187$ ; hence an inner radius of  $\cdot 032$  cm. corresponds to  $c = \cdot 172$ . The table shows that for  $\alpha = 135^\circ$  this radius corresponds to an equilibrium pressure 8. If the outer reduced radius were  $\cdot 26$ , the last column shows that the pressure would still be 8. It is a moot point then as to whether the inside or outside radius would be the determining one. But if the outer radius were  $\cdot 345$ , the equilibrium pressure thereat would only be 6; hence the pressure 8 which had been impressed at C would be sufficient to cause indefinite expansion of the bubble. In 1926 Sauerwald and Drath (*Z. f. anorg. u. allgem. Chemie*, cliv. p. 79 (1926)) obtained the surface-tension of mercury with several tips, and in every case found that the *outer* radius was the effective one,



*i. e.*, calculations from it gave the value of the surface-tension as obtained by other workers by other methods. They give no reason, however, for this being the case. The above table shows that this must be the case for their tubes if the angle of contact is not far from  $135^\circ$ . The following table gives the inner ( $r_1$ ) and outer ( $r_2$ ) radii (reduced) for their tubes, and the corresponding reduced pressures as determined from the above data :—

$r_1$ .	$r_2$ .	Pressures.	
		Inner.	Outer.
·172	·225	8	9·1
·255	·342	5·7	6·0
·132	·166	10·4	12·0
·133	·164	10·4	12·0
·158	·204	8·9	10·0
·166	·214	8·4	9·5
·141	·196	9·6	10·3

The numbers in the last column are in every case greater than those in the last but one. It would have been safer to have chosen the radii so that the pressures would have been more decidedly different—*e. g.*, for the second row, with  $r_1 = \cdot 255$ ,  $r_2$  should be not more than  $\cdot 32$  for safety. It may be added that if the inner and outer radii are nearly alike, and mercury is the liquid, the outer edge is generally the effective one.

To calculate the surface-tension when the external edge is the effective one we have (position E)

$$p - d = \frac{2}{3}c + \frac{2}{c} - \cdot 231c^3.$$

Let  $(p - d)\beta = H$ ,  $c\beta = r_2 = \text{external radius}$  ;

$$\text{then } \beta^2 = \frac{Hr_2}{2} - \frac{r_2^2}{3} + \frac{\cdot 231}{2} \frac{r_2^4}{\beta^2},$$

and inserting an approximate value for  $\beta^2$  in the denominator,

$$\beta^2 = \frac{Hr_2}{2} \left( 1 - \frac{2}{3} \frac{r_2}{H} + \cdot 461 \frac{r_2^2}{H^2} \right),$$

and

$$\beta^2 = \sigma / (g(\rho - \rho_0)).$$

This formula differs in the last term from five formulæ that have previously been given. Whether this last term is of much significance is doubtful, although it is based on the

Poisson-Rayleigh formula, which should justify it being retained. For small values of  $r_2$  it can obviously be neglected; for larger values it is possible that uncertainties arise in connexion with the approximations made. The precise way in which the bubble breaks away may cause a fluctuation in the value of  $H$ . In any case, the problem is ultimately a kinetic, and not a static one. The possible range in  $H$  should be determined by experiment for slowly and quickly formed bubbles respectively, in order that some estimate of the possible error due to viscosity or inertia can be made.

It will be seen that when the external radius is the determining one the calculation of the surface-tension does not involve the angle of contact. *It is quite otherwise when the maximum pressure is determined by the internal radius.* Since it is now a case for numerical calculation, we will express in terms of true lengths, and the true head corresponding to  $p-d$  will be called  $H$ . Then, the formulæ for position C give

$$H = -\frac{X}{3} + X\left(1 - \sqrt{1 - \frac{r_1^2}{X^2}}\right) + \frac{2\beta^2}{X} + \frac{X^3}{3\beta^2} \log \left\{ \frac{1}{2} \left(1 + \sqrt{1 - \frac{r_1^2}{X^2}}\right) \right\},$$

whence

$$\beta^2 = \frac{HX}{2} \left\{ 1 - \frac{2X}{3H} + \frac{X}{H} \sqrt{1 - \frac{r_1^2}{X^2}} - \frac{2}{3} \frac{X^2}{H^2} \log \left\{ \frac{1}{2} \left(1 + \sqrt{1 - \frac{r_1^2}{X^2}}\right) \right\} \right\},$$

where

$$X = \frac{r_1}{\sin \alpha} \left[ 1 - \frac{r_1^2}{3\beta^2 \tan^2 \alpha (1 - \cos \alpha)} \right].$$

In the last formula  $\beta^2$  can be put approximately  $\frac{HX}{2}$ ,

where  $X$  is approximately  $\frac{r_1}{\sin \alpha}$ . *This reduction requires a knowledge of the angle of contact.*

The angles of contact considered in the above lie between  $90^\circ$  and  $180^\circ$ . The question for smaller angles requires separate discussion.

XCIX. *The Numerical Solution of Partial Differential Equations.* By GORAKH PRASAD, D.Sc., Reader in Mathematics, University of Allahabad, India \*.

### 1. Introduction.

**M**ETHODS for solving ordinary differential equations have long been known and have now found their way into text-books †. A method of solving integral equations was given by me some time ago ‡. But it appears that up till now no method for solving partial differential equations numerically has been published. The aim of the present paper is to find a method for such equations.

The method explained below is very accurate, fairly rapid, and pretty general.

### 2. Outline of the Method.

Consider first the partial differential equation

$$\frac{\partial^2 z}{\partial x \partial y} = f(x, y, z), \quad . . . . . (1)$$

and suppose that we want that solution of this equation, which is equal to  $\phi(y)$  when  $x=a$ , and which is equal to  $\psi(x)$  when  $y=b$ , where  $\phi$  and  $\psi$  are given functions. Of course, if  $z_{0,0}$  is the value of  $z$  when  $x=a$  and  $y=b$ , we must have

$$\phi(b) = \psi(a) = z_{0,0}.$$

Suppose that we want the solution of (1) in the region  $a < x < A$ ,  $b < y < B$ , it being assumed that a solution exists whose various differential coefficients up to the 4th, or the 5th, order are continuous. The solution will be obtained step by step. Suppose that a solution is in progress, and we have obtained the values of  $z$  and  $\frac{\partial z}{\partial x}$  for a network of points given by

$$x = a + kw, \quad k = 0, 1, 2, \dots n, \quad \text{where } a + nw \text{ is nearly equal to } A;$$

$$y = b + k'w', \quad k' = 0, 1, 2, \dots r', \quad b + r'w' < B;$$

\* Communicated by the Author.

† Whittaker, 'Calculus of Observations,' chap. xiv. Sanden, 'Practical Mathematical Analysis' (translated by Levy), chaps. x. and xi.

‡ See Proc. Edin. Math. Soc. xlii. pp. 46-59, where further references on the subject will be found.

and also for the points

$$x = a + kw, \quad k = 0, 1, 2, \dots, r, \quad a + rw < A,$$

$$y = b + (r' + 1)w'.$$

It is required to find the values of  $z$  and  $\frac{\partial z}{\partial x}$  for

$$x = a + (r + 1)w, \quad y = b + (r' + 1)w',$$

which, for the sake of brevity, will be denoted by  $z_{r+1, r'+1}$  and  $p_{r+1, r'+1}$ , respectively. These values will be expressed in terms of the values of  $p$  and  $z$  already determined and their differences. It is open for us to use either a formula involving central differences or one involving the differences lying along a sloping line in the difference table. The advantage of a central-difference formula lies in the fact that the series occurring in it is much more convergent. Indeed, it has been shown by Pearson\* that the central-difference interpolation formula, from which equation (2) below is derived by integration, is so remarkably convergent that a table containing only sixty-seven logarithms, say those of the whole numbers from 34 to 100, to eight figures, is an adequate frame for finding all logarithms to seven figures of all seven-figure numbers, and for this only the first central difference,  $\delta^2$ , has to be taken into account. But the disadvantage of the central-difference formula is that, as values of  $z_{k, k'}$  and  $p_{k, k'}$  for  $k > r$  and  $k' > r' + 1$  are not known, these central differences can only be estimated; their values cannot be found exactly in the first instance. Hence a method of successive approximations has to be used; but the second approximation can always be made sufficiently accurate to enable us to dispense with higher approximations. The formula involving only the backward differences does not necessitate the use of successive approximations; but, on the whole, the central-difference formulæ are much less laborious to work with†.

The formula for calculating  $p_{r+1, r'+1}$  is

$$p_{r+1, r'+1} = p_{r+1, r'} + w' \left\{ \frac{1}{2} - \frac{1}{24} \delta'^2 + \frac{11}{1440} \delta'^4 - \frac{191}{120960} \delta'^6 + \dots \right\} (s_{r+1, r'} + s_{r+1, r'+1}), \quad (2)$$

where  $s_{r, r'}$  denotes the value of  $\frac{\partial^2 z}{\partial x \partial y}$  when  $x = a + wr$ ,

\* K. Pearson, 'Tracts for Computers,' no. ii.

† Cf. Bosanquet, "On the Capillary Rise of Liquids in Wide Tubes," Phil. Mag. no. 28, 1928.

$y=b+w'r'$ , and an approximate extrapolated value of  $s_{r+1, r'+1}$  is used, as illustrated by the example below. The notation employed here for the differences is the same as that used by Pearson\*.

The formula for  $z_{r+1, r'+1}$  is

$$z_{r+1, r'+1} = z_{r, r'+1} + w \left\{ \frac{1}{2} - \frac{1}{24} \delta^2 + \frac{11}{1440} \delta^4 - \frac{191}{120960} \delta^6 + \dots \right\} (p_{r, r'+1} + p_{r+1, r'+1}), \quad (3)$$

where the approximate value of  $p$  found by (2) is used.

Small errors in the original extrapolated value of  $s$  will produce a much smaller error in the value computed for  $p$ , because of the factor  $\frac{1}{2}w'$ ; and this will give rise to a still smaller error in  $z$  for a similar reason. The value  $z_1$  thus obtained for  $z$  is, therefore, very nearly correct. The original extrapolated value of  $s$  should now be replaced by the value obtained by substituting in (1)  $z_1$  for  $z$  and the proper values of  $x$  and  $y$ , and the computation repeated. The value of  $z$  should change only by a very small amount now. In fact, this change should be so small that if the computation were to be repeated with this changed value of  $z$ , there would be no further alteration in the value of  $z$ . We thus get the correct value of  $z$ .

We see now that the process of solving partial differential equations is analogous to that of solving a pair of simultaneous ordinary differential equations of the first order.

If very large intervals are taken, it is possible that the extrapolated values of  $\delta^2$  and  $\delta'^2$  might be appreciably wrong. In such cases the computation should be revised at every few steps, using the new (computed) values of these differences.

### 3. An Example.

Consider the differential equation

$$\frac{\partial^2 z}{\partial x \partial y} = \frac{(\log_e 10)^2 \cdot z}{6x^{\frac{1}{2}}y^{\frac{1}{2}}}, \quad \dots \dots \dots (4)$$

and suppose we want that solution which is equal to  $25.9546.10^{y^{\frac{1}{2}}}$  when  $x=2$  and is equal to  $27.6853.10^{x^{\frac{1}{2}}}$  when  $y=3$ . Suppose that the values of  $z$  for

$$x = 2.0, 2.5, \dots 5.0, \dots,$$

$$y = 3.0, 3.8, \dots 6.2,$$

\* K. Pearson, 'Tracts for Computers,' no. iii. p. 10.

have been calculated, and that the values of  $z$  for

$$x = 2.0, 2.5, \dots 4.5,$$

$$y = 7.0$$

have also been calculated, and we want the value of  $z$  when  $x=5.0$ ,  $y=7.0$ . The computed values of  $z$ ,  $p$ , and  $s$  are given in the annexed tables.

TABLE I.  
Values of  $z$ .

$y \backslash x.$	2.0.	2.5.	3.0.	3.5.	4.0.	4.5.	5.0.
3.0 .....	718.562	1055.33	1493.83	2056.27	2768.53	3660.75	4767.80
3.8 .....	943.420	1385.58	1961.29	2699.73	3634.89	4806.30	6259.77
4.6 .....	1194.86	1754.86	2434.01	3419.26	4603.65	6087.27	7928.14
5.4 .....	1474.43	2165.46	3065.22	4219.30	5680.83	7511.58	9783.18
6.2 .....	1783.63	2619.57	3708.01	5104.10	6872.13	9086.80	11834.76
7.0 .....	2123.95	3119.39	4415.52	6077.99	8183.36	10820.60	?

TABLE II.  
Values of  $p$ .

$y \backslash x.$	2.0.	2.5.	3.0.	3.5.	4.0.	4.5.	5.0.
3.0 .....	584.971	768.432	992.947	1265.41	1593.70	1986.78	2454.82
3.8 .....	768.026	1008.89	1303.67	1661.39	2092.42	2608.50	3223.00
4.6 .....	972.720	1277.79	1651.12	2104.19	2650.08	3303.72	4081.91
5.4 .....	1200.32	1576.76	2037.45	2596.52	3270.14	4076.72	5037.09
6.2 .....	1452.03	1907.41	2464.70	3141.02	3955.91	4931.62	6093.40
7.0 .....	1729.08	2271.36	2934.99	3740.35	4710.72	5872.61	?
		121.35	141.73	165.01	191.52		
			2.90	3.23			

The figures below the main entries in these tables are the values of  $\delta^2$  and  $\delta^4$ , or  $\delta'^2$  and  $\delta'^4$ , as the case may be.

Looking at the values of  $\delta'^2$  in the column  $x=5.0$  in Table III., we can guess that an approximate value of the next  $\delta'^2$  is 6.40. This leads to the value

$$2 \times 1385.78 - 1256.07 + 6.40 = 1521.89$$

of  $s$  for the blank space in which there is the note of interrogation. We put down 6.60 as the value of  $\delta^2$  in this blank space. As the value 6.30 or 6.90 would produce a difference of only one unit in the last place in the values of  $p$ , we see it is not very important that our guess be quite right.

TABLE III.  
Values of  $s$ .

$y \backslash x$ .	2.0.	2.5.	3.0.	3.5.	4.0.	4.5.	5.0.
3.0 .....	215.849	283.544	366.387	466.924	588.059	733.104	905.81
3.8 .....	242.074	317.994	410.904	523.655	659.509	822.172	1015.86
							6.83
4.6 .....	269.926	354.581	458.180	583.904	735.386	916.767	1132.74
							6.45
							.31
5.4 .....	299.315	393.187	508.066	647.477	815.454	1016.59	1256.07
							6.38
6.2 .....	330.224	433.789	560.530	714.338	899.662	1121.56	1385.78
7.0 .....	362.671	476.411	615.604	784.528	988.062	1231.77	?

By formula (2) we now find the corresponding values of  $p$  to be

$$6093.41 + 0.8 \left\{ \frac{1}{2}(1385.78 + 1521.89) - \frac{1}{24}(6.40 + 6.60) \right\} \\ = 7256.04.$$

The last row of Table II. now becomes

$y \backslash x$ .	2.0.	2.5.	3.0.	3.5.	4.0.	4.5.	5.0.
7.0 .....	1729.08	2271.36	2934.99	3740.35	4710.72	5872.61	7256.04
		121.35	141.73	165.01	191.52	221.54	
			2.90	3.23	3.51		

We put down 4.00 as the value of the next  $\delta^4$ . This gives 255.56 as the value of  $\delta^2$  under  $x=5.0$ . Applying now formula (3), we have, finally, for the value of  $z$ ,

$$10820.60 + 0.5 \left\{ \frac{1}{2}(5872.61 + 7256.04) - \frac{1}{24}(221.54 + 255.56) \right\} \\ = 14092.82.$$

It is easy to verify that  $10x^{\frac{1}{2}}+y^{\frac{1}{2}}$  is the solution of the differential equation under consideration, and that the value of  $z$  found above is quite correct.

In general, the value of  $z$  found would be slightly inaccurate. With this value of  $z$  a better value of  $s$  could be calculated to replace the assumed value 1521.89. The calculation would then have to be repeated.

We see that, although our intervals are fairly large, viz. 0.5 and 0.8, we have been able to attain seven-figure accuracy at the very first approximation. Taking larger intervals and using the terms in  $\delta^4$  and  $\delta'^4$  also in the second approximation, it is evident that we could very rapidly tabulate the values of  $z$  for a large region. All intermediate values of  $z$  could be derived by the use of bi-variate central-difference interpolation formulæ\*.

#### 4. Initial Values for $z$ .

It remains now to see how a few initial values of  $z$  and  $\frac{\partial z}{\partial x}$  can be calculated to start the solution. By differentiating successively the equation (1), we find

$$\frac{\partial^3 z}{\partial x^2 \partial y}, \quad \frac{\partial^3 z}{\partial x \partial y^2}, \quad \frac{\partial^4 z}{\partial x^3 \partial y}, \quad \frac{\partial^4 z}{\partial x^2 \partial y^2}, \quad \frac{\partial^4 z}{\partial x \partial y^3}, \dots$$

Also by differentiating  $\phi(y)$  or  $\psi(x)$ , we find the values of

$$\frac{\partial z}{\partial x}, \quad \frac{\partial^2 z}{\partial x^2}, \quad \frac{\partial^3 z}{\partial x^3}, \dots; \quad \frac{\partial z}{\partial y}, \quad \frac{\partial^2 z}{\partial y^2}, \quad \frac{\partial^3 z}{\partial y^3}, \dots$$

at the point  $x=a, y=b$ . Thus the values of all necessary coefficients in the Taylor's expansion,

$$\begin{aligned} z_{r,r'} &= z_{0,0} + rw \left( \frac{\partial z}{\partial x} \right)_{0,0} + r'w' \left( \frac{\partial z}{\partial y} \right)_{0,0} \\ &\quad + \frac{1}{2} \left\{ r^2 w^2 \left( \frac{\partial^2 z}{\partial x^2} \right)_{0,0} + 2rr'ww' \left( \frac{\partial^2 z}{\partial x \partial y} \right)_{0,0} \right. \\ &\quad \left. + r'^2 w'^2 \left( \frac{\partial^2 z}{\partial y^2} \right)_{0,0} \right\} + \dots, \end{aligned}$$

become known; and substituting 1, 2, ... for  $r, r'$ , we can find a sufficient number of values of  $z$ . We can do the same for  $p$ .

\* K. Pearson, 'Tracts for Computers,' no. iii.



Another procedure is also possible. We might take  $w$  and  $w'$  so small in the beginning that  $\delta^2$ ,  $\delta'^2$  might become negligible, and we might thus be able to use formulæ (2) and (3) from the very beginning.

Thus, in the example considered above, take

$$w = w' = 0.1.$$

We know  $z_{0,0}$ ,  $z_{0,1}$ ,  $z_{1,0}$ ;  $p_{0,0}$ ,  $p_{1,0}$ ;  $s_{0,0}$ ,  $s_{0,1}$ ,  $s_{1,0}$ . To find  $z_{1,1}$  we notice that

$$s_{0,0} = 215.849, \quad s_{1,0} = 228.292,$$

$$s_{0,1} = 219.030.$$

Therefore, supposing that  $\Delta' \Delta s_{0,0}$  is constant, the extrapolated value of

$$\begin{aligned} s_{1,1} &= 219.030 + 12.443 \\ &= 231.473. \end{aligned}$$

We find, therefore, that an approximate value of

$$\begin{aligned} p_{0,1} &= p_{0,0} + \frac{1}{2}w'(s_{0,0} + s_{0,1}) \\ &= 606.715. \end{aligned}$$

Similarly

$$p_{1,1} = 641.667.$$

These values give

$$z_{1,1} = 807.689$$

by (3).

To see if a second approximation is required, we substitute this in (4). The value of  $s_{1,1}$  comes out to be 231.655. As there is an appreciable difference between this and the extrapolated value, we revise the calculation with the new value of  $s$  and get

$$z_{1,1} = 807.678.$$

If we compare this with the known solution, we find that it is quite correct. We see that by taking  $w$  and  $w'$  to be about 0.1, we can use formulæ (2) and (3) from the very beginning.

### 5. *A more general Equation.*

If instead of (1) we have the equation

$$\frac{\partial^2 z}{\partial x \partial y} = f(x, y, z, p, q), \quad . \quad . \quad . \quad (5)$$

the above method still gives the solution, but we have to calculate in this case  $q$  also at each of the points where  $z_{r,r'}$  is found. This can be done from the formula :

$$q_{r+1,r'+1} = q_{r,r'+1} + w \left\{ \frac{1}{2} - \frac{1}{24} \delta^2 + \frac{11}{1440} \delta^4 - \frac{191}{120960} \delta^6 + \dots \right\} (s_{r,r'+1}, s_{r+1,r'+1}). \quad (6)$$

Thus in this case the computation of  $s$ ,  $p$ ,  $q$ , and  $z$  all have to go along simultaneously, instead of the computation of  $s$ ,  $p$ , and  $z$  only.

### 6. Transformation of Equations.

By a slight modification of Laplace's method \* any partial differential equation of the form

$$Rr + Ss + Tt = F(x, y, z, p, q), \quad . \quad . \quad . \quad (7)$$

where  $R$ ,  $S$ , and  $T$  are functions of  $x$  and  $y$ , can, in general, be transformed into an equation of the form

$$\frac{\partial^2 z}{\partial x \partial y} = f(x, y, z, p, q).$$

We see thus that most of the partial differential equations which are linear in the second-order terms can be easily solved numerically.

Allahabad,  
October 2, 1929.

---

C. *The Scattering Powers of the Atoms in Magnesium Oxide for X-Rays and some Related Properties.* By G. W. BRINDLEY, M.Sc, Assistant Lecturer in Physics, University of Leeds †.

### 1. Introduction.

EXPERIMENTS have been made recently by R. W. G. Wyckoff and Miss A. H. Armstrong <sup>(1)</sup> on the intensity of reflexion of X-rays by powdered crystals of magnesium oxide and sodium fluoride, and from their results they have calculated the scattering powers of the atoms in these crystals. The scattering power of an atom for X-rays is

\* Forsyth, 'A Treatise on Differential Equations,' p. 504 (London, 1914).

† Communicated by Prof. R. Whiddington, F.R.S.

closely connected with the number and distribution of its electrons and with its amplitude of thermal vibration. References to work on this subject are given in a recent paper by the writer<sup>(2)</sup>, in which the amplitudes of vibration at room temperature are calculated for the atoms in the crystals NaCl, KCl, NaF, and LiF. For these crystals it was possible to assume that the atoms are singly ionized, but in the case of MgO it is not certain whether the lattice points are occupied by neutral atoms or by singly or doubly ionized atoms.

The present calculations were undertaken with the object of determining, if possible, the state of ionization of the atoms in MgO, and also of estimating their amplitudes of thermal vibration, from the experimental data of Wyckoff and Miss Armstrong.

## 2. *The Relation between the Scattering Power of an Atom and the Number and Distribution of its Electrons.*

The most direct way, theoretically, of determining the number of electrons associated with each atom would be to use the following equation, due originally to A. H. Compton<sup>(3)</sup>, which enables the electron distribution  $U(r)$  to be calculated from the scattering power  $F$ :

$$U(r) = \frac{8\pi r}{D^2} \sum_1^{\infty} n \cdot F_n \sin 2\pi nr/D. \quad . \quad . \quad (1)$$

If  $F_n$ , the scattering power in a direction  $\theta_n$ , the glancing angle of incidence for the spectrum of order  $n$  from planes of spacing  $D$ , is expressed in terms of the electron as unit, then  $U(r)$  is the radial electron density at distance  $r$  from the nucleus, and the total number of electrons in the atom

is  $\int_0^{\infty} U(r) dr$ . This method, however, suffers from the disadvantage that  $F_n$  can only be measured for a limited range of angles, and for the largest angles at which  $F$  can be measured  $F_n$  is quite appreciable. In consequence the series cannot be summed completely. This difficulty is magnified because  $n \cdot F_n$  occurs in the summation, and  $n \cdot F_n$  is still large when  $F_n$  is small. Whether the higher-order terms in the summation are neglected, or an extrapolation of  $F$  to zero is attempted, there is usually a very considerable uncertainty in  $U(r)$ .

Wyckoff and Miss Armstrong recognized these difficulties; they calculated the charge distribution along a cube edge of MgO, using an expression similar to (1), with and without

an extrapolation of  $F$  to zero, and their results were markedly different in the two cases. Their final conclusion was that "in view of the inexact nature of this extrapolation too much physical significance cannot be attached to the results of these series developments" (*op. cit.* p. 439). A short account has recently appeared of an investigation by E. O. Wollen<sup>(4)</sup>, who has used the radial Fourier series, and he finds that "the data indicate that the number of electrons associated with magnesium and oxygen is more nearly that of the neutral atoms than that of the ions."

In view, however, of the uncertainties inherently attached to the use of equation (1), an attempt has been made to solve the problem by a different method, using the experimental data of Wyckoff and Miss Armstrong.

### 3. An Alternative to the Method of Fourier Analysis.

The underlying theory, which has been fully discussed elsewhere<sup>(5)</sup>, is briefly as follows:—

Knowing the wave function  $\psi$  for an atom with central symmetry,  $U(r)$  can be calculated:

$$U(r) = 4\pi r^2 \cdot \psi \bar{\psi} \dots \dots \dots (2)$$

$F_0$ , the scattering power of the atom *at rest*, is then given by the equations

$$\begin{aligned} F_0 &= \int_0^\infty U(r) \cdot \frac{\sin \phi}{\phi} \cdot dr, \\ &= 4\pi \int_0^\infty \psi \bar{\psi} \cdot \left( \frac{\sin \phi}{\phi} \right) r^2 dr, \dots \dots (3) \end{aligned}$$

where

$$\phi = 4\pi r \left( \frac{\sin \theta}{\lambda} \right).$$

$F_T$ , the scattering power of the atom when vibrating at temperature  $T$ , is connected with  $F_0$  by the relation

$$F_T = F_0 \cdot e^{-M}, \dots \dots \dots (4)$$

where

$$M = \left( \frac{8\pi^2}{3} \right) \cdot \bar{u}^2 \cdot \left( \frac{\sin \theta}{\lambda} \right)^2 = \alpha \left( \frac{\sin \theta}{\lambda} \right)^2.$$

This expression for  $M$  was given by I. Waller<sup>(6)</sup>, and is true for crystals having cubic symmetry.  $\bar{u}^2$  is the mean square of the displacement of the atom from its equilibrium position;  $\sqrt{\bar{u}^2}$  may be regarded as the mean amplitude of vibration at temperature  $T$ .

The calculation of  $F_0$  and  $F_T$  from  $U(r)$  is not accompanied by the same disadvantages as the reverse calculation of  $U(r)$  from  $F$ , for since in equation (3)  $U(r)$  and  $(\sin \phi)/\phi$  both tend to zero as  $r$  becomes large,  $F_0$  can be calculated accurately.

The equations (2), (3), and (4) may be made the basis of a method for determining the state of ionization of the atoms in a crystal, *provided the experimental data are sufficiently extensive.*

A series of investigations by R. W. James and others on the scattering powers of the atoms in crystals of rock-salt, NaCl, sylvine, KCl, and aluminium<sup>(7)</sup> at different temperatures has shown that when the scattering powers  $F_T$  at room-temperature are corrected for thermal agitation and for zero-point energy, the resulting  $F_0$  values for the atoms at rest agree very well indeed with the theoretical  $F_0$  values obtained by use of equation (3) from the charge distributions calculated by the method of D. R. Hartree<sup>(8)</sup>, which is based on wave mechanical principles. Apart from the general evidence<sup>(9)</sup> showing that wave functions calculated by Hartree's method are correct to a fairly close approximation, the results obtained by James and his co-workers are strong evidence for the view that scattering powers calculated from Hartree charge distributions are approximately correct when the appropriate temperature factor,  $e^{-M}$ , is applied. This principle has been discussed more fully by the writer in a recent paper<sup>(2)</sup>.

In applying the principle to MgO, we require first the radial charge distribution and hence the  $F_0$  functions for neutral O, neutral Mg,  $O^{-2}$ , and  $Mg^{+2}$ . Secondly, we must estimate the temperature factors for the atoms in MgO, and so calculate the  $F_T$  functions by means of equation (4); this second step is, in general, the more difficult of the two. A comparison of the theoretical  $F_T$  values and the experimental values should then decide the degree of ionization of the atoms in the crystal. Whether it will be possible or not to make the final decision will depend on whether the theoretical  $F_0$  and  $F_T$  functions are appreciably different for the ionized and un-ionized atoms in the region of  $(\sin \theta)/\lambda$  where experimental measurements have been made.

A somewhat similar investigation to the present one has been made by R. W. James, the writer, and R. G. Wood for aluminium<sup>(7)</sup>. In that case it was not possible to determine whether the atoms in crystalline aluminium are singly, doubly; or trebly ionized, because it is only at very small scattering angles that  $F_0$  is appreciably different for the

three ions; this arises because the M electron(s) in  $\text{Al}^{+2}$  and  $\text{Al}^+$  are so diffuse.

The same difficulty will undoubtedly arise for  $\text{Mg}^{+2}$ ,  $\text{Mg}^+$ , and Mg owing to the diffuseness of the M electron(s) in  $\text{Mg}^+$  and Mg; but it is not at first sight evident whether there will be the same difficulty for oxygen, for whereas neutral Mg has two electrons *more* than the neon-like ion  $\text{Mg}^{+2}$ , neutral O has two electrons *less* than  $\text{O}^{-2}$ . It was therefore thought worth while to examine the theoretical  $F_0$  curves for neutral O and  $\text{O}^{-2}$ .

#### 4. The Scattering Powers of Neutral Oxygen and of $\text{O}^{-2}$ .

The distribution of charge in neutral oxygen has been calculated recently by Miss Black using Hartree's method, and James has calculated the  $F_0$  function\*, the atom being assumed to be spherically symmetrical.

The case of  $\text{O}^{-2}$  was more difficult. In Schrödinger's equation for the wave-function  $\psi$  of an electron in a central field, there occurs a parameter  $E$  which, considered physically, is the total negative energy of the electron in the potential field. Hartree uses a constant  $\epsilon$ , given by  $E = -\frac{1}{2}\epsilon$ , so that for an electron in a normal atom  $\epsilon$  is essentially positive. In a calculation of the charge distribution of  $\text{F}^-$  considerable difficulty was found in obtaining the wave function for the 22 electrons owing mainly to the charge on the outside of the ion being in a very weak attractive field and partly to  $\epsilon$  being very small. In the case of  $\text{O}^{-2}$  the charge on the outside of the ion would be in a repulsive field, and, from an inspection of  $\epsilon$  for other neon-like ions,  $\epsilon$  for  $\text{O}^{-2}$  would probably be *negative*, in which case there would be no solution of the wave equation of the required type; if  $\epsilon$  is just positive a solution of the required type will exist but will be difficult to calculate.

$F_0$  curves, however, have been calculated for the following neon-like ions from charge distributions obtained by Hartree's method,  $\text{F}^-$ , Ne,  $\text{Na}^+$ ,  $\text{Al}^{+3}$ , and  $\text{Si}^{+4}$ , and a method was therefore sought for determining the  $F_0$  curve for  $\text{O}^{-2}$  by extrapolation. Several quite different methods of extrapolation have been used which lead to almost identical results.

One method was as follows. The wave function obtained by Hartree's method for an electron in an atom of nuclear

\* I am indebted to Miss Black and Mr. James for these data.

charge  $Ze$  can be represented approximately by considering the electron to be in a central Coulomb field due to a charge  $Z'e$ . Now by choosing  $Z'$  rightly, the  $F_0$  curve calculated from the Hartree distribution of charge and the  $F_0'$  curve\* obtained from the "hydrogen-like" distribution can be made almost identical. Actually it was found best to choose  $Z'$  so that for each electron in the above series of neon-like ions the Hartree and the hydrogen-like  $F_0$  curves coincided at  $F_0=0.5$ . For a particular group of electrons,  $Z'$  was found to vary linearly with  $Z$ ; hence  $Z'$  could be obtained with a fair degree of certainty for  $O^{-2}$  by extrapolation. The differences between the Hartree  $F_0$  curves and the hydrogen-like  $F_0'$  curves were small, and so by extrapolation the difference between the Hartree  $F_0$  curve and the hydrogen-like  $F_0'$  curve for  $O^{-2}$  could be calculated. In this way the Hartree  $F_0$  curve was estimated for each group of electrons in  $O^{-2}$ . It was found that the  $F_0$  curve for the two 1s and the two 2s electrons was practically the same for neutral oxygen and for  $O^{-2}$ , but for a 2p electron in  $O^{-2}$  the  $F_0$  curve was found to fall to zero more quickly than for a 2p electron in neutral oxygen. As this point is of some importance, a few details may be given of the calculation.

For a 2p electron in a Coulomb field of charge  $Z'e$  <sup>(10)</sup>,

$$U(r) = \frac{Z'^5}{24} \cdot r^4 \cdot e^{-Z'r}.$$

Then

$$\begin{aligned} F_0' &= \int_0^\infty U(r) \cdot \frac{\sin \phi}{\phi} \cdot dr, \\ &= \frac{Z'^5}{24k} \int_0^\infty r^3 \cdot \sin kr \cdot e^{-Z'r} \cdot dr, \end{aligned}$$

where

$$k = \frac{\phi}{r} = 4\pi \left( \frac{\sin \theta}{\lambda} \right).$$

On evaluating the integral

$$F_0' = \frac{1 - \left( \frac{k}{Z'} \right)^2}{\left[ 1 + \left( \frac{k}{Z'} \right)^2 \right]^4}$$

$Z'$  was obtained by making  $F_0'$ , the hydrogen-like function,

\*  $F_0'$  is the scattering power for a hydrogen-like distribution of charge with nuclear charge  $Z'e$ .

and  $F_0$ , the Hartree function, coincide at  $F_0=0.5$ ; that is to say,  $Z'$  is given by

$$\left[1 + \left(\frac{k}{Z'}\right)^2\right]^4 = 2 \left[1 - \left(\frac{k}{Z'}\right)^2\right].$$

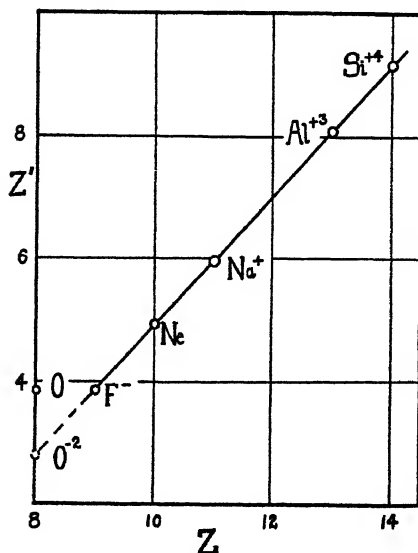
A graphical solution of this equation gives

$$\frac{k}{Z'} = 0.716,$$

whence

$$Z' = 17.5 \left(\frac{\sin \theta}{\lambda}\right)_{F_0=0.5},$$

Fig. 1.



The variation of  $Z'$ , the effective nuclear charge for X-ray scattering, with  $Z$ , the true nuclear charge, for the 2s electrons of neon-like ions.

where  $\left(\frac{\sin \theta}{\lambda}\right)_{F_0=0.5}$  is the value of  $(\sin \theta)/\lambda$ , ( $\lambda$  in Å.U.), for which the Hartree  $F_0$  function is 0.5.

The results obtained are shown in fig. 1, where  $Z'$  is plotted against  $Z$ ;  $Z'$  may be called the effective nuclear charge for X-ray scattering. The linearity of the variation of  $Z'$  with  $Z$  is clearly seen. It is of interest to observe how far the value of  $Z'$  for neutral oxygen lies from this line.

Another method by which  $F_0$  was estimated for O<sup>-2</sup> will be described fully in a later paper, but the principle of the



method is as follows. When  $F_0$  for a particular group of electrons is plotted as a function of  $\frac{1}{Z-s} \left( \frac{\sin \theta}{\lambda} \right)$ , where  $Ze$  is the true nuclear charge,  $F_0$  is practically independent of  $Z$  when  $s$  has the appropriate value. Values of  $s$  have now been obtained for the different groups of electrons in many atoms and ions. It is possible in the case of  $O^{-2}$  to estimate  $s$  with a considerable degree of certainty, and hence to calculate  $F_0$  for  $O^{-2}$ .

Other methods have also been used, but they all lead to essentially the same result for  $F_0$ . This may be taken as evidence that in estimating the  $F_0$  curve for  $O^{-2}$  from data for other neon-like ions no serious errors have been made. The error in  $F_0$  is probably nowhere greater than 0.1, and is probably less for those parts of the curve which are not steep with respect to the  $(\sin \theta)/\lambda$  axis.

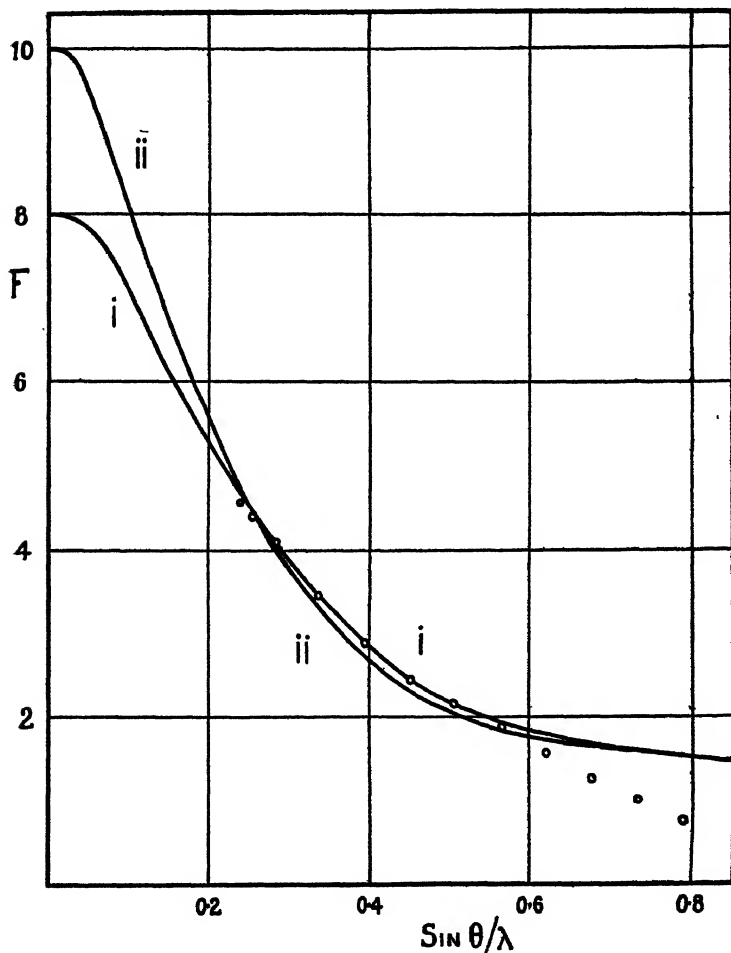
### 5. *A Discussion of the Results for Oxygen in MgO.*

In fig. 2 the theoretical  $F_0$  curves are drawn for neutral O and for  $O^{-2}$ . At small values of  $(\sin \theta)/\lambda$  the curves are quite different, owing to the number of electrons being different in the two cases. At large values of  $(\sin \theta)/\lambda$  the curves are practically coincident; this is due to the fact that only the 1s electrons scatter appreciably at large angles, and the 1s electrons in neutral O and  $O^{-2}$  have the same distribution of charge. The most interesting region is between  $(\sin \theta)/\lambda = 0.25$  and 0.65, where the two curves are slightly different. The physical significance of this result appears to be as follows. When two additional electrons are added to neutral oxygen to form  $O^{-2}$  there is an interaction between these electrons and those already present. Neutral oxygen is considered to have four 2s electrons, and  $O^{-2}$ , being neon-like, to have six 2s electrons. The interaction, therefore, of the two additional electrons in  $O^{-2}$  affects mainly the 2s group; owing to their mutual repulsion, the 2s electrons in  $O^{-2}$  have a more diffuse distribution of charge than the 2s electrons in neutral O. This may also be seen from the data given in fig. 1,  $Z'$  for neutral O being 3.86 and for  $O^{-2}$  2.80. Hence, although the scattering power of  $O^{-2}$  tends to be greater, owing to its greater number of electrons, the effect is more than counterbalanced by the greater diffuseness of the electrons in  $O^{-2}$ , and, except at small values of  $(\sin \theta)/\lambda$ ,  $F_0$  for  $O^{-2}$  is slightly *smaller* than  $F_0$  for neutral oxygen. The curves, however, are for the most part so nearly

coincident that it will be difficult to decide whether oxygen is ionized or not in  $\text{MgO}$ .

As stated above, before a comparison can be made between theory and experiment an estimate should be made of the temperature factor  $e^{-M}$  and the corresponding  $F_T$  curves

Fig. 2.



X-ray scattering curves for (i) neutral oxygen and (ii)  $\text{O}^{-2}$ .  
The circles show the experimental values of Wyckoff and Miss Armstrong.

calculated. However, it is seen from fig. 2 that there is a close agreement between the theoretical  $F_0$  curves and the experimental results of Wyckoff and Miss Armstrong, which are shown in the figure by circles.

The fact that the agreement between the experimental results and the theoretical  $F_0$  curves is so close without the application of a temperature correction indicates that the amplitude of thermal vibration of the oxygen atoms (or ions) in MgO is very small. This result is in accord with the general physical properties of MgO. Wyckoff and Miss Armstrong used artificial crystals, periclase, and in this form MgO is very hard. On Moh's scale of hardness periclase has a value approximately 6, a value which lies between the hardness of felspar and that of quartz. Other physical properties show that the atoms in MgO are very tightly bound together. For example, the fusion point is of the order of  $2000^\circ\text{C}$ . The coefficient of thermal expansion ( $\alpha=0.0000114$ ) is not much greater than that of quartz. The compressibility also is very small. In such a crystal it is not surprising to find that the oxygen atoms have a small amplitude of thermal vibration.

Since the theoretical curves are so close together in the region of  $(\sin \theta)/\lambda$  where experimental measurements have been made, it is difficult to draw a definite conclusion as to the state of ionization of the oxygen atoms. Between  $(\sin \theta)/\lambda=0.3$  and  $0.6$  the experimental results certainly fit the neutral oxygen curve better than the  $\text{O}^{-2}$  curve. Moreover, if some small allowance be made for thermal vibration, then it is possible to fit the neutral O curve *slightly better* to the experimental results, but any such allowance increases the difference between the  $\text{O}^{-2}$  curve and the experimental results. The closest agreement is obtained between the theoretical  $F_T$  curve for neutral oxygen and the experimental data when

$$F_T = F_0 \cdot e^{-0.20 (\sin^2 \theta)/\lambda^2},$$

$$\text{i. e., } \alpha=0.20, \text{ whence } \sqrt{u^2}=0.087 \text{ A.U.}$$

We may therefore draw the following conclusion. The experimental results are in agreement with the view that oxygen in MgO exists as neutral oxygen rather than as  $\text{O}^{-2}$ , and a comparison of theory with experiment points to neutral O rather than to  $\text{O}^{-2}$  as existing in MgO, but in view of the small difference between the theoretical results for neutral O and  $\text{O}^{-2}$  an unquestionable decision can hardly be given. This is in agreement with the result obtained by Wollen<sup>(4)</sup> using Fourier analysis. The present method shows clearly the uncertainty attached to the determination of the number of electrons in atoms from X-ray scattering data; in the analytical method there is also uncertainty, but in general it is not so evident.

There is one further point of interest. Beyond  $(\sin \theta)/\lambda = 0.6$  the experimental values fall rapidly. It is very difficult to find an explanation for this result, but it seems to be connected in some way with the use of powdered crystals. In the experiments of James single crystals were used, and although the measurements were made at larger values of  $(\sin \theta)/\lambda$  than are used with powdered crystals, there was no sign of any sudden falling off of  $F$  to zero at large  $(\sin \theta)/\lambda$ . Further, the results of James were in close agreement with theory. Attention has recently been directed to this point<sup>(2)</sup>, for similar measurements by R. J. Havighurst<sup>(11)</sup> with powdered crystals show the same effect.

## 6. The Scattering Powers of Neutral Magnesium and of $Mg^{+2}$ .

The scattering powers of  $Mg$  and of  $Mg^{+2}$  have been calculated by the method referred to in section 4, in which  $F_0$  is regarded as a function of  $\frac{1}{Z-s} \left( \frac{\sin \theta}{\lambda} \right)$ . The results are shown in fig. 3, and, as anticipated earlier, the curves do not differ except at very small values of  $(\sin \theta)/\lambda$ . The experimental results are shown in the figure by circles. No information concerning the state of ionization of magnesium can be obtained from this figure. It is of interest to note, however, that the magnesium atom (or ion) appears to have a much larger amplitude of thermal vibration than the oxygen atom. The closest agreement between  $F_T$ , the theoretical scattering curve for  $Mg$  (or  $Mg^{+2}$ ), and the experimental data is obtained by taking

$$F_T = F_0 e^{-0.33 (\sin^2 \theta)/\lambda^2},$$

$$i.e., \quad \alpha = 0.33, \quad \text{whence} \quad \sqrt{u^2} = 0.11, \text{ \AA.U.}$$

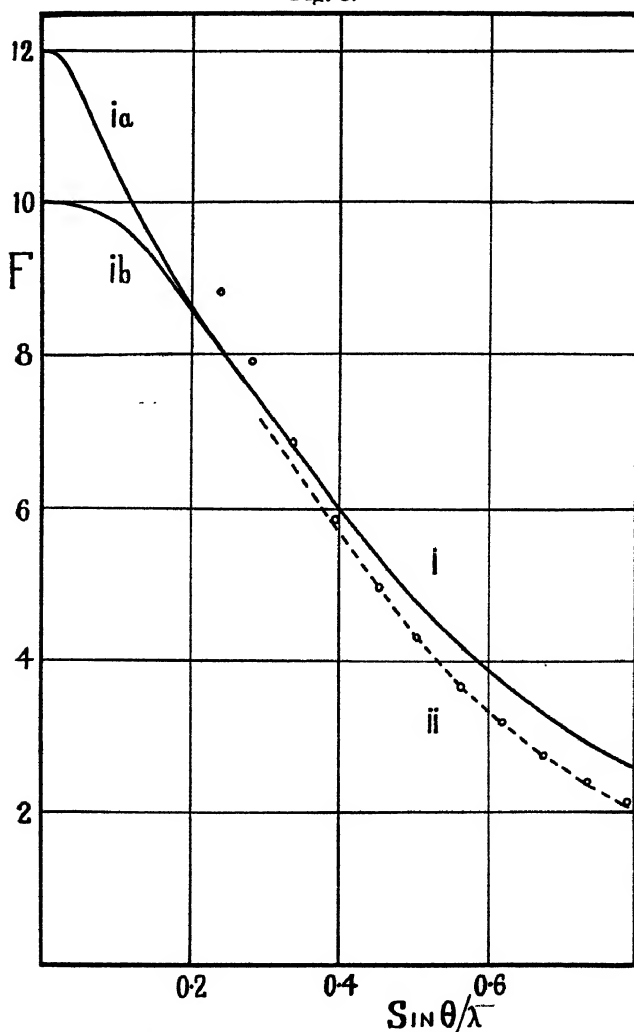
The difference between the estimated amplitudes of vibration,  $0.11 \text{ \AA.U.}$  for  $Mg$  and  $0.087 \text{ \AA.U.}$  for  $O$ , is not so great as might have been expected from a glance at figs. 2 and 3. However, since

$$\overline{u^2} = \frac{3\alpha}{8\pi^2} = \frac{5}{8\pi^2} \cdot \frac{\log_e(F_0/F_T)}{(\sin^2 \theta)/\lambda^2},$$

the amplitude of vibration,  $\sqrt{u^2}$ , depends on the ratio  $(F_0/F_T)$ ;  $F_0$  and  $F_T$  have a larger absolute difference in the case of magnesium, but this is counterbalanced by  $F_0$  and  $F_T$  each being about twice as big for  $Mg$  as for  $O$ , for  $(\sin \theta)/\lambda > 0.3$ . The values given above for the amplitudes of vibration must only be regarded as rough estimates

for the difference between  $F_T$  and  $F_0$ , particularly in the case of oxygen, is too small for accurate values to be obtained. It is, however, worth noting that in  $MgO$ , as in  $NaCl$  and  $LiF$ , the smaller ion has the larger amplitude of vibration.

Fig. 3.



X-ray scattering curves for (i a) neutral  $Mg$  and (i b)  $Mg^{+2}$ . Curve (ii) is given by  $F_T = F_0 e^{-0.33 (\sin^2 \theta) / \lambda^2}$ .

The circles show the experimental results of Wyckoff and Miss Armstrong.

In conclusion, I would like to take this opportunity to thank Professor Hartree for his kindness in allowing me to make use of his results for some of the neon-like ions.

## 7. Summary.

(i.) It is pointed out that the determination of the number of electrons associated with the atoms of magnesium and oxygen in  $\text{MgO}$  by means of Fourier analysis is not practicable owing to the uncertainties inherently connected with the method.

(ii.) An alternative method is suggested based on the principle that the scattering power of an atom for X-rays can be calculated, knowing the distribution of charge in the atom and a temperature factor to correct for the thermal vibration.

(iii.) Scattering curves are given for neutral O,  $\text{O}^{-2}$ , neutral Mg, and  $\text{Mg}^{+2}$ . Certain difficulties in the case of  $\text{O}^{-2}$  were surmounted by a method of extrapolation.

(iv.) In the case of oxygen, the scattering curves for O and  $\text{O}^{-2}$  are very similar, and there is good agreement with the experimental results. The data are in keeping with the view that the oxygen atom in  $\text{MgO}$  is un-ionized and, in fact, point to this conclusion, but the scattering curves for O and  $\text{O}^{-2}$  are not sufficiently different for a decisive answer to be given.

(v.) In the case of magnesium, no information can be obtained concerning the state of ionization of the atom.

(vi.) Estimates are made of the amplitudes of vibration of the atoms in the lattice, the results being  $0.11 \text{ \AA.U.}$  for Mg and  $0.09 \text{ \AA.U.}$  for O, the smaller ion having the larger vibration as in  $\text{NaCl}$  and  $\text{LiF}$ , but these values can only be regarded as *rough estimates*. Such small values for the amplitudes of vibration are in accord with the general physical properties of crystalline  $\text{MgO}$ .

## 8. References.

- (1) R. W. G. Wyckoff and A. H. Armstrong, *Zeit. f. Krist.* lxxii. p. 433 (1930).
- (2) G. W. Brindley, *Phil. Mag.* ix. p. 193 (Feb. 1930).
- (3) A. H. Compton, see 'X-rays and Electrons,' ch. v.
- (4) E. O. Wollen, *Phys. Rev.* xxxv. p. 127 (1930).
- (5) I. Waller and R. W. James, *Proc. Roy. Soc. A*, cxvii. p. 214 (1927); R. W. James, I. Waller, and D. R. Hartree, *Proc. Roy. Soc. A*, cxviii. p. 334 (1928); R. W. James and G. W. Brindley, *Proc. Roy. Soc. A*, cxxi. p. 155 (1928).
- (6) See I. Waller and R. W. James, *loc. cit.*
- (7) R. W. James, G. W. Brindley, and R. G. Wood, *Proc. Roy. Soc. A*, cxxv. p. 401 (1929).
- (8) D. R. Hartree, *Proc. Camb. Phil. Soc.* xxiv. pp. 89, 111 (1928).
- (9) J. A. Gaunt, *Proc. Camb. Phil. Soc.* xxiv. p. 328 (1928); J. C. Slater, *Phys. Rev.* xxxii. p. 343 (1928); also xxxv. p. 211 (1930).

(10) See E. Schrödinger, *Ann. d. Physik*, lxxix. p. 361 (1926), see equation (18), p. 369.

(11) R. J. Havighurst, *Phys. Rev.* xxviii. p. 869 (1926).

The Physical Laboratories,

The University of Leeds.

March 14, 1930.

*Note added in proof, April 26th.*—In a private communication Prof. Hartree has pointed out to me that a consideration of other physical properties of MgO indicates that the atoms in the crystal are ionized; *e.g.* NaF and MgO have the same structure, but AlN is different, which suggests that NaF and MgO are both formed of ionized atoms, but that AlN is different; the interatomic distance also agrees with Lennard-Jones's calculated value based on  $Mg^{+2}$  and  $O^{-2}$  (*Proc. Roy. Soc.* cix. p. 476, table vii.). If the atoms in MgO are really ionized, then it would seem that reliable information about the state of ionization of atoms in crystals cannot be obtained from X-ray scattering curves. Uncertainty arises both in the analytical method and in the alternative method discussed above owing to the difficulty of obtaining sufficiently extensive experimental data.

CI. *Problems of determining Initial and Maximum Stresses in Ties and Struts under Elastic or rigid End Constraints.*—

Part III.\* *By* W. H. BROOKS, B.Sc., Ph.D. (Eng.) Lond.†

*To establish Expressions for Y/X for Struts flexed by Various Methods*

THE strut equations are quickly derived from the tie results by substituting in the latter  $-P$  for  $P$ , and therefore  $i.n.$  for  $n$ , where  $i = \sqrt{-1}$ ; remembering that  $n = \sqrt{P/EI}$ , and that

$$\sinh i.n.l. = i.\sin nl.$$

$$\cosh i.n.l. = \cos nl.$$

$$\tanh i.n.l. = i.\tan n.l.$$

*Strut Method 1 A.* See fig. 4 (vol. viii. p. 947, 1929), with  $P$  reversed:—

From the tie equation (4) for deflexion  $\delta$  at C,

$$\begin{aligned}\delta/W &= -(L - \tanh inL/in)/2P = -(L - i.\tan nL/in)/2P \\ &= -(L - \tan nL/n)/2P = (\tan nL/n - L)/2P. \quad (70)\end{aligned}$$

\* See Part I., *Phil. Mag.* (7) viii. p. 943 (1929); and Part II., *Phil. Mag.* (7) ix. p. 426 (1930). Figs. 1-11 and Charts I.-VI. (referred to in this Part) appeared in Parts I. and II.

† Communicated by the Author.

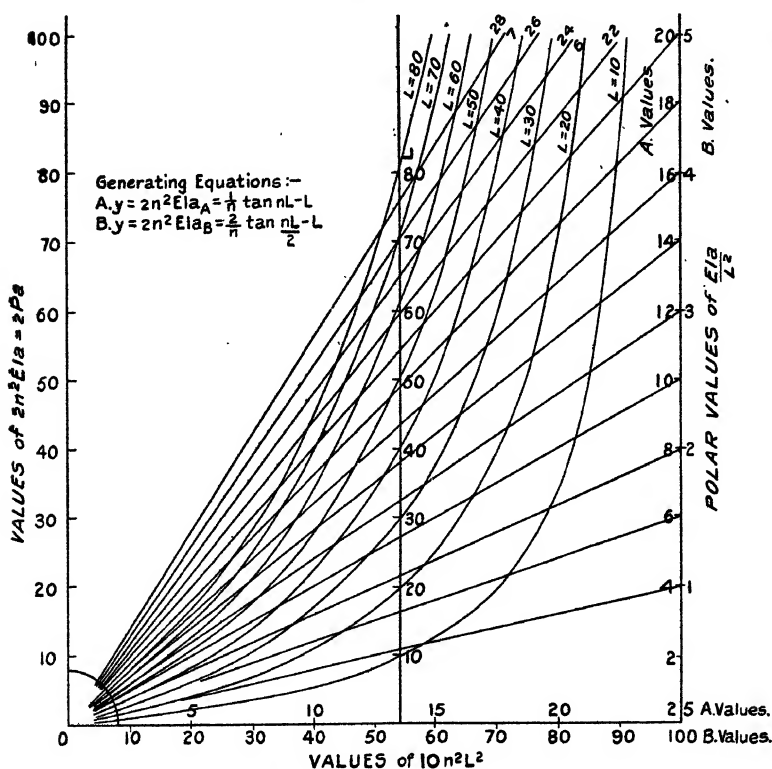
That is, initially, when  $\delta = 0$  and  $W = 0$ ,

$$"a" = (\tan n_a L_a / n_a - L_a) / 2n_a^2 \cdot EI. \quad (71)$$

(Strut equation  $A\delta$ .)

In equation (71), " $a$ " is the  $W.\delta$ . derivative, and is found experimentally as described in the general procedure. Having found " $a$ ," the solution to  $n_a^2 L_a^2$ , and thence the solution to  $P_a$ , i. e.,  $n_a^2 EI$ , may be readily obtained from

CHART VII.



Stress Chart for Struts A and B by deflexion.

Chart VII., on which the suffix  $a$  to  $n$  and to  $L$  is suppressed for reasons of clarity. To obtain a solution, the value of  $EI\alpha/L^2$  is located on the vertical scale of A values—drawn in where  $10n^2L^2 = 25$ ,—and a polar ray is drawn through the origin of the chart. The curve of  $L$  (the half-strut length) is next interpolated by aid of the vertical scale of  $L$  drawn in where  $10n^2L^2 = 13.5$ . The projection on to the abscissæ of the point of intersection of this latter curve with the former ray gives the solution sought.



Applying the expansion

$$\tan \beta = \beta + \beta^3/3 + 2\beta^5/15 + 17\beta^7/315 + \dots$$

to equation (70), and writing  $nL$  for  $\beta$ , it becomes

$$\delta/W = L(1 + n^2L^2/3 + 2n^4L^4/15 + 17n^6L^6/315 + \dots - 1)/2P,$$

and substituting

$$n^2 = \pi^2 P/4L^2 P_e,$$

$$\text{where } P_e = \pi^2 EI/4L^2,$$

the Euler buckling value of  $P$ ,

$$\begin{aligned} \delta/W &= L\{\pi^2/12 \cdot (P/P_e) + \pi^4/120 \cdot (P/P_e)^2 \\ &\quad + 17\pi^6/20160 \cdot (P/P_e)^3 + \dots\}/2P \\ &\doteq 2L\{(P/P_e) + (P/P_e)^2 + (P/P_e)^3 + \dots\}/5P. \end{aligned}$$

The latter expression in brackets is now a G.P. having a common ratio  $= P/P_e$  less than unity, and may therefore be summed to infinity. Thus

$$S_\infty = P/(P - P_e),$$

giving

$$\delta/W \doteq 2L/5(P_e - P), \quad \dots \dots (72)$$

or, initially, " $a$ "  $= 2L/5(P_e - P_a)$ ;

$$\therefore P_a \doteq P_e - 2L/5a. \quad \dots \dots (73)$$

This last expression may therefore be used for an approximate solution in this case, or as a first approximation when seeking for an exact solution to equation (71).

For a *strut* therefore, tested as in this case,

$$2L/5a < P, \quad \text{i.e., } 2L/a < 5\pi^2 EI/4L^2$$

approximately; and this result may be used to check a doubtful case of stress reversal (see section on Stress Reversal), for when  $2L/5a$  is found to be  $> P_e$ , i.e., when " $a$ " is found to be  $< 8L^3/5\pi^2 EI$ ,  $P_a$  is shown to be negative, and therefore the member is a *tie*.

Conversely, when " $a$ " is found to be  $> 8L^3/5\pi^2 EI$ , the member is a *strut*.

In other words, when  $P_a = 0$ , the above approximation shows that the value of " $a$ " (which would then be constant and  $= \delta/W$ ),

$$\doteq 8L^3/5\pi^2 EI. \quad \dots \dots (74)$$

The exact value of this ratio for the above case—as may readily be deduced for the equivalent simply supported beam—is  $L^3/6EI$ , and should preferably be used in a closer check for stress reversal. For any case the value of " $a$ "

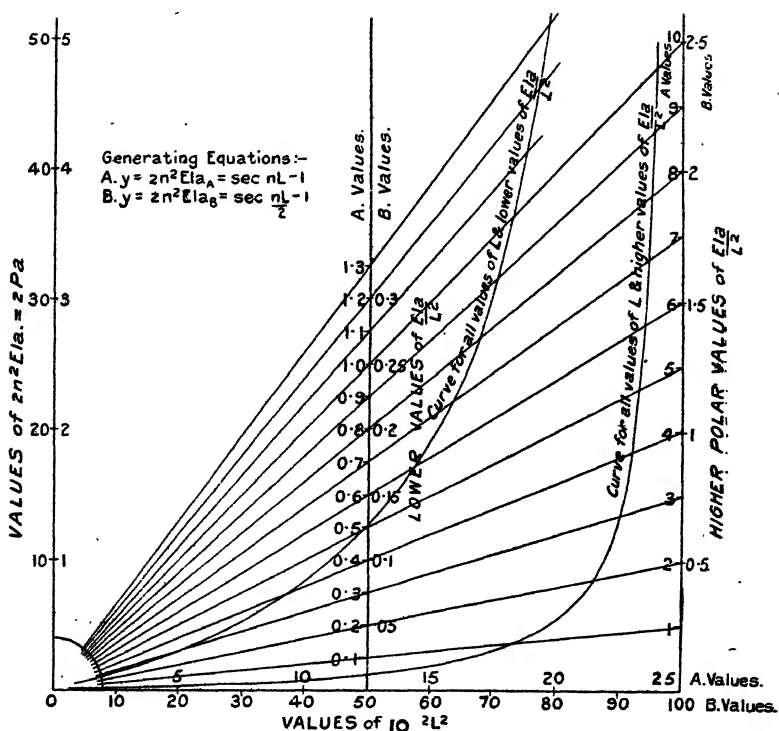
when  $P = 0$ , will hereinafter be referred to as the "reversal ratio," and is fully discussed in the section on Reversal Ratios, later.

*Strut Method 1 A. Alternatively by slope. See fig. 5*  
(vol. viii. p. 950, 1929), with  $P$  reversed:—

From the tie equation (8) for the slope  $\theta$  at A or B,

$$\begin{aligned}\theta/W &= -(1 - 1/\cosh nL)/2P = -(1 - 1/\cos nL)/2P \\ &= -(1 - \sec nL)/2P = (\sec nL - 1)/2P, \quad (75)\end{aligned}$$

CHART VIII.



Stress Chart for Struts A and B by slope.

or, initially, when  $\theta = 0$  and  $W$  also = 0,

$$"a" = (\sec n_a L_a - 1)/2n_a^2 \cdot EI, \quad \dots (76)$$

(Strut equation A $\theta$ )

where "a" is the  $W.\theta$  derivative.

Graphical solutions to  $n_a^2$  in this equation may be quickly obtained from the A values of Chart VIII., which is used in

a similar way to that described for Chart VII. Here also the suffix  $a$  is suppressed for reasons of clarity.

Applying the expansion

$$\sec \beta = 1 + \beta^2/2! + 5\beta^4/4! + 61\beta^6/6! + \dots$$

to equation (75), it becomes

$$\theta/W = (n^2 L^2/2! + 5n^4 L^4/4! + 61n^6 L^6/6! + \dots);$$

and substituting 
$$n^2 L^2 = \frac{\pi^2}{4} \cdot \frac{P}{P_e},$$

it becomes

$$\begin{aligned} & \{ \pi^2/8 \cdot (P/P_e) + 5\pi^4/16 \cdot 4! \times (P/P_e)^2 \\ & \quad + 61\pi^6/64 \cdot 6! \times (P/P_e)^3 + \dots \} / 2P \\ & \doteq 5/8 P_e \cdot \{ (P/P_e) + (P/P_e)^2 + (P/P_e)^3 + \dots \}; \end{aligned}$$

and, summing to infinity as before,

$$\theta/W \doteq 5/8 (P_e - P), \dots \dots \dots (77)$$

or, initially, 
$$P_a \doteq P_e - 5/8 a, \dots \dots \dots (78)$$

and may be used as a first approximation when seeking a solution to equation (76).

Equation (78) shows that in this case, where the member is a *strut*, approximately,  $5/8 a$  must be  $< P_e$ , i. e.,  $< \pi^2 EI/4L^2$ , or " $a$ "  $> 5L^2/2\pi^2 EI$ , and, when  $P_a = 0$ , " $a$ "  $\doteq 5L^2/2\pi^2 EI$ .

When  $P$  is reversed, the member becomes a *tie*, and then " $a$ "  $< 5L^2/2\pi^2 EI$ .

The exact value of this reversal ratio, i. e., the value of the  $W.\theta$ . derivative when  $P = 0$ , as deduced from the equivalent simply supported beam for this case, is  $L^2/4EI$ , and should preferably be used in a closer check.

That is, the member is a  $\left\{ \begin{array}{c} \text{strut} \\ \text{or} \\ \text{tie} \end{array} \right\}$  according as the initial

$W.\delta$ . derivative  $\left\{ \begin{array}{c} > \\ < \end{array} \right\}$  or  $L^2/6EI$  (fig. 4), or according as the

initial  $W.\theta$ . derivative  $\left\{ \begin{array}{c} > \\ < \end{array} \right\}$  or  $L^2/4EI$  (fig. 5) (see later section

on Stress Reversal and Reversal Ratios).

*Strut Method 1 B.* See fig. 6 (vol. viii. p. 952, 1929), with  $P$  reversed:—

From the tie equation (14) for the *deflexion*  $\delta$  at  $C$ ,

$$\begin{aligned} \delta/W &= -\{ L - 2/in. \tanh(inL/2) \} / 2P \\ &= -\{ L - 2/in. i. \tan(nL/2) \} / 2P \\ &= -(L - 2/n. \tan n\bar{L}/2) / 2P = (2/n. \tan n\bar{L}/2 - L) / 2P. \quad (79) \end{aligned}$$

That is, initially,

$$"a" = (2/n_a \cdot \tan n_a L_a/2 - L_a)/2 \cdot n_a^2 EI, \quad (80)$$

(Strut equation B<sub>δ</sub>)

where "a" is the W.δ. derivative.

Graphical solutions to  $n_a^2$  in this equation may be readily obtained from the B values of Chart VII. in a similar way to that described for Strut Method 1 A.

Expanding equation (79) similarly to the expansion of equation (70), it becomes

$$\delta/W = L/2P \cdot (1 + n^2 L^2/12 + n^4 L^4/120 + 17n^6 L^6/20160 + \dots - 1),$$

and substituting  $n^2 L^2 = \pi^2 \cdot P/P_e$ , where  $P_e = \pi^2 EI/L^2$  in this case,

$$\begin{aligned} \delta/W &= L/2P \cdot \{ \pi^2/12 \cdot (P/P_e) + \pi^4/120 \cdot (P/P_e)^2 \\ &\quad + 17/20160 \cdot (P/P_e)^3 + \dots \} \\ &\doteq 2L/5P \{ (P/P_e) + (P/P_e)^2 + (P/P_e)^3 + \dots \}, \end{aligned}$$

as in Method 1 A,—but with a different value for  $P_e$ , and therefore yielding the same equations (72) and (73) in  $P_e$ , to which corresponding deductions apply.

Hence, for a strut with clamped ends as in this case, the value of the initial W.δ. derivative must approximately be  $> 2L^3/5\pi^2 EI$ , i. e.,  $> \frac{1}{4}$  the approximate value obtained in Method 1 A.

When "a" is found to be approximately  $< 2L^3/5\pi^2 EI$ , the member is shown to be a tie.

When  $P_e = 0$ ,

$$\text{the constant value of "a"} = \delta/W \doteq 2L^3/5\pi^2 EI. \quad (81)$$

Here the exact value of the reversal ratio, as deduced from the equivalent encastred beam with  $P = 0$ , is  $L^3/24EI$ , or  $\frac{1}{4}$  the reversal ratio of Method 1 A, and should be used when a closer check is required. (See later section on Reversal Ratios.)

*Strut Method 1 B. Alternatively by slope  $\theta$  at  $\frac{1}{4}$  span.*

See fig. 7 (vol. viii. p. 952, 1929), with P reversed :—

From the tie equation (18),

$$\theta/W = -(1 - \operatorname{sech} nL/2)/2n^2 EI = (\sec nL/2 - 1)/2n^2 EI, \quad (82)$$

$$\text{or, initially, "a"} = (\sec n_a L_a/2 - 1)/2n_a^2 EI. \quad (83)$$

(Strut equation B<sub>θ</sub>)

Graphical solutions to  $n_a^2$  in this equation may readily be obtained from the B values of Chart VIII. in a similar way to that previously described for alternative Method 1 A.

Expanding equation (83) similarly to the expansion of equation (75), it becomes on substituting for  $P_s$ , which  $= \pi^2 EI/L^2$ ,

$$"a" \doteq 5/8 P_a \cdot \{ (P_a/P_s) + (P_a/P_s)^2 + (P_a/P_s)^3 + \dots \};$$

and, summing to infinity as before and making corresponding deductions, we get as approximate relationships

$$5/8 a < P_s, \quad i. e., < \pi^2 EI/L^2,$$

*i. e.*, approximately the  $W.\theta$ . derivative  $> 5L^2/8\pi^2 EI$ . That is, the approximate reversal ratio in this case is  $\frac{1}{4}$  of the corresponding ratio obtained by Method 1 A. Its exact value is  $L^2/16EI$ , as may readily be deduced from first principles when  $P = 0$ .

Hence a member with clamped ends is a  $\left\{ \begin{array}{c} \text{strut} \\ \text{or} \\ \text{tie} \end{array} \right\}$  according

as the initial  $W.\delta$ . derivative  $\left\{ \begin{array}{c} > \\ \text{or} \\ < \end{array} \right. L^2/24EI$  (fig. 6), or accord-

ing as the initial  $W.\theta$ . derivative  $\left\{ \begin{array}{c} > \\ \text{or} \\ < \end{array} \right. L^2/16EI$  (fig. 7).

*Strut Method 2 A.* See fig. 8 (vol. ix. p. 426, 1930), with  $P$  reversed :—

$$\begin{aligned} \text{From the tie equation (29) for the deflexion } \delta \text{ at C,} \\ \delta/W &= -[l - \{ \sinh inl - \tanh inL (\cosh inl - 1) \} / in] / 2P \\ &= -[l - \{ i \cdot \sin nl - i \cdot \tan nL (\cosh nl - 1) \} / in] / 2P \\ &= [\{ \sin nl - \tan nL (\cos nl - 1) \} / n - l] / 2P. \quad \dots \quad (84) \end{aligned}$$

That is, initially, when  $\delta = 0$  and  $W$  also  $= 0$ ,

$$"a" = [\{ \sin n_a l + \tan n_a L \quad \quad \quad a l \} / n_a - l] / 2n_a^2 EI, \quad \dots \quad (85)$$

(Strut equation Gd)

where " $a$ " = the initial  $W.\delta$ . derivative.

Solutions to  $n_a^2$  in equation (85) for an instrument constant  $l = 10$  units may be readily obtained from the G values of Chart IX. by finding the point of intersection of the appropriate polar ray of  $EI \cdot a/L^2$  with the correct curve of  $L$ , the length of the half-strut, which latter may be interpolated from the typical curves given. Here, as on

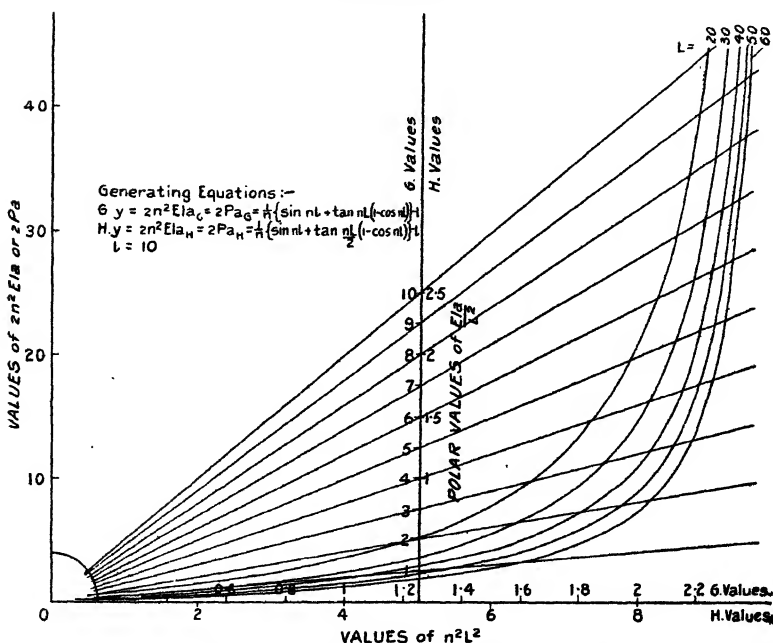
the other charts, the suffix  $a$  is suppressed for simplicity. Projecting from the point so found on to the abscissæ gives the solution to  $P_a = n_a^2 \cdot EI$  sought.

*Strut Method 2 A. Alternatively by the slope  $\theta$  at D :—*

From tie equation (32),

$$\begin{aligned}\theta/W &= -(\cosh nl - 1)(\cosh inl - \sinh inl \cdot \tanh inL)/2P \\ &= -(\cos nl - 1)(\cos nl - i \cdot \sin nl \cdot i \cdot \tan nL)/2P \\ &= (1 - \cos nl)(\cos nl + \sin nl \cdot \tan nL)/2P, \dots (86)\end{aligned}$$

CHART IX.



Stress Chart for Struts G and H by deflexion.

or, initially,

$$\begin{aligned}“a” &= (1 - \cos n_a l)(\cos n_a l + \sin n_a l \cdot \tan n_a L_a)/2n_a^2 EI, \\ &\dots (87) \\ &\text{(Strut equation } G_\theta)\end{aligned}$$

where “ $a$ ” is the initial  $W \cdot \theta$  derivative.

Equation (87) is the generating equation of the  $G$  curves and values of Chart X. from which solutions to  $n_a^2$  and thence solutions to  $P_a = n_a^2 EI$  may be obtained by interpolation in a similar way to that described for Chart IX.

*Strut Method 2 B.* See fig. 9 (vol. ix. p. 429, 1930), with P reversed:—

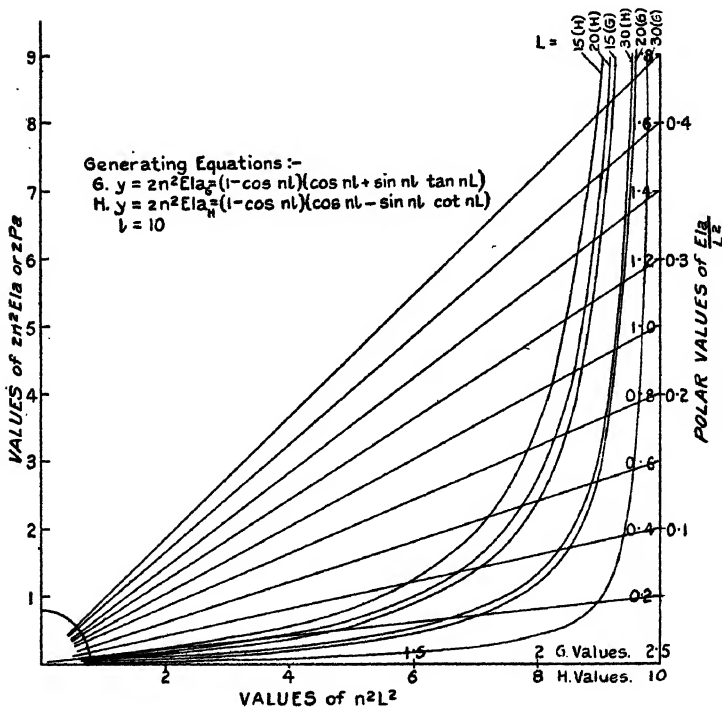
From the equation (41) for the deflection  $\delta$  at C,

$$\begin{aligned}\delta/W &= -[l - \{i \cdot \sin nl - i \cdot \tan \overline{nL/2} (\cos nl - 1)\} / in] / 2P \\ &= [\{\sin nl + \tan \overline{nL/2} (1 - \cos nl)\} / n - l] / 2P, \quad \dots (88)\end{aligned}$$

or, initially,

$$\begin{aligned}“a” &= [\{\sin n_a l + \tan \overline{n_a L_a/2} (1 - \cos n_a l)\} / n_a - l] / 2n_a^3 EI, \quad (89) \\ &\quad \text{(Strut equation H}\delta\text{)}\end{aligned}$$

CHART X.



Stress Chart for Struts G and H by slope.

where “a” is the  $W \cdot \delta$  derivative.

Solutions to this equation are given by the H values of Chart IX. to be used in a similar way to that described for Strut Method 2 A.

Alternatively, from the equation (42) for the slope  $\theta$  at D,

$$\begin{aligned}\theta/W &= -(\cos nl - 1) (\cos nl - i \cdot \sin nl / i \cdot \tan nL) / 2P \\ &= (1 - \cos nl) (\cos nl - \sin nl \cdot \cot nL) / 2P, \quad \dots (90)\end{aligned}$$

or, initially, when both  $\theta$  and  $W = 0$ ,

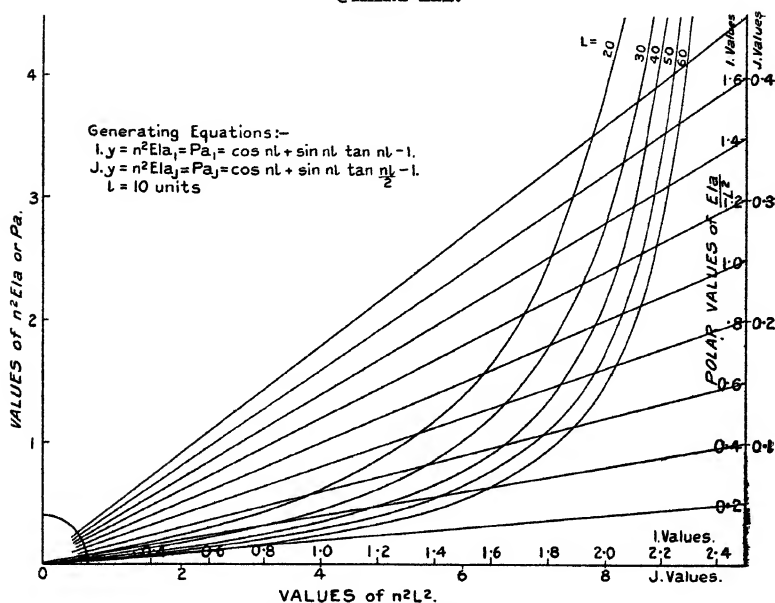
$$"a" = (1 - \cos n_a l) (\cos n_a l - \sin n_a l \cdot \cot n_a L_a) / 2n_a^2 EI; \quad (91)$$

(Strut equation H $\theta$ )

where " $a$ " in this case is the  $W \cdot \theta$  derivative.

Solutions to equation (91) are given by the H values and curves of Chart X., which are used in a similar way to that described in the alternative Strut Method 2 A.

CHART XI.



Stress Chart for Struts I and J by deflexion.

*Strut Method 3 A.* See fig. 10 (vol. ix. p. 431, 1930), with P reversed:—

Here the ratio of the deflexion  $\delta$  at C to  $M_1$  at D is obtained from the corresponding tie equation (48), and is

$$\begin{aligned} \delta/M_1 &= -(1 - \cosh inl + \sinh inl \cdot \tanh inL)/P \\ &= -(1 - \cos nL - \sin nL \cdot \tan nL)/P \\ &= (\cos nL + \sin nL \cdot \tan nL - 1)/P; \quad \dots \quad (92) \end{aligned}$$

and under initial conditions when  $\delta = 0$  and  $M_1$  also = 0,

$$"a" = (\cos n_a l - \sin n_a l \cdot \tan n_a L_a - 1) / n_a^2 EI, \quad (93)$$

where " $a$ " here is the  $M_1 \cdot \delta$  derivative and is obtained as described in the section on General Procedure.



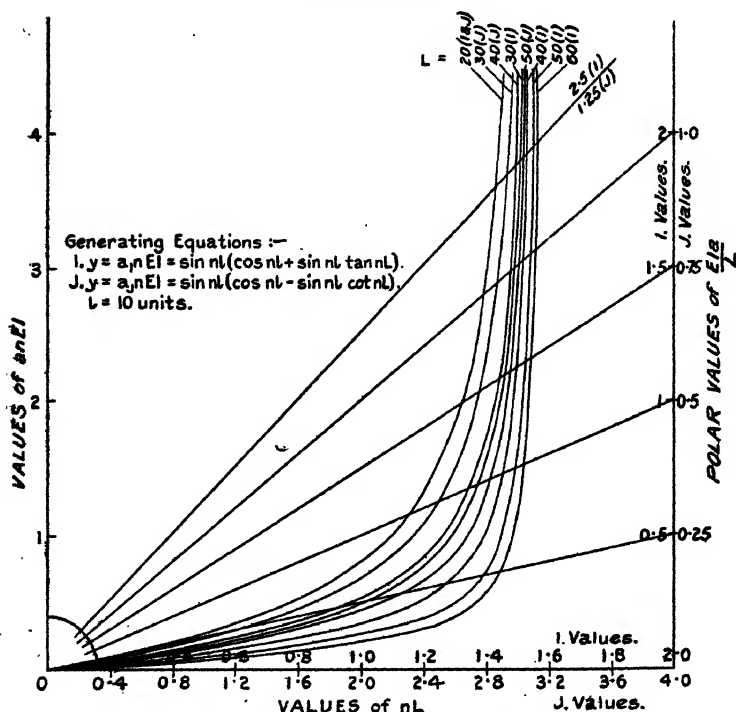
Solutions to  $n_a^2$  in the above equation are given by the I values of Chart XI., which has been drawn for an instrument constant  $l = 10$  units. The method of using this chart is similar to that previously described for the use of Chart IX. On this chart also the suffix "a" is suppressed.

*Strut Method 3A.* Alternatively from the ratio of the slope  $\theta$  at D to the couple  $M_1$  at D :—

From the equation (54),

$$\begin{aligned}\theta/M_1 &= i \cdot \sin nl / i \cdot n \cdot EI \cdot (\cos nl - i \cdot \sin nl \cdot i \cdot \tan nL) \\ &= \sin nl / n \cdot EI \cdot (\cos nl + \sin nl \cdot \tan nL), \quad . \quad . \quad (94)\end{aligned}$$

CHART XII.



Stress Chart for Struts I and J by slope.

or, initially,

$$"a" = \sin n_a l / n_a EI \cdot (\cos n_a l + \sin n_a l \cdot \tan n_a L_a), \quad (95)$$

(Strut equation I<sub>0</sub>)

where "a" = the  $M_1 \theta$  derivative to be substituted, and is found as described in the "General Procedure."

The foregoing equation is the generating equation I of Chart XII.—to be used for its solution—upon which, as on the other charts, the suffix “*a*” is suppressed for clearness. To obtain a solution to  $n_a$  and hence a solution to  $P_a = n_a^2 EI$ , the I value of  $ELa/L$  on the ordinate drawn in at  $nL = 2$  units on the abscissa is first located; then a polar ray is drawn to the origin through the point so found. Where this ray intersects, the I curve of  $L$ —which may be interpolated from the typical curves shown—locates a point vertically above a point on the abscissa scale of I values which gives the solution to  $P_a$  in terms of  $n_a L_a$ .

*Strut Method 3 B.* See fig. 11 (vol. ix. p. 435, 1930), with *P* reversed:—

Considering tie equation (63), which was established for the deflexion  $\delta$  at C, the derived corresponding strut equation here required is

$$\begin{aligned}\theta/M_1 &= -(1 - \cos nl + i \cdot \sin nl \cdot i \cdot \tan \overline{nL/2})/P \\ &= (\cos nl + \sin nl \cdot \tan \overline{nL/2} - 1)/P, \quad . \quad . \quad (96)\end{aligned}$$

or, initially,

$$\begin{aligned}“a” &= (\cos n_a l + \sin n_a l \cdot \tan \overline{n_a L_a/2} - 1)/n_a^2 EI. \quad (97) \\ &\quad (Strut equation J_\delta.)\end{aligned}$$

Here “*a*” is the  $M_1 \cdot \delta$  derivative, and is found as described in the “General Procedure.”

By substituting the value of “*a*” so found in equation (97), this equation may then be solved for  $n_a^2$ , and thus  $P_a = n_a^2 EI$  calculated, by the aid of the *J* values of Chart XI., which has been drawn for an instrument constant  $l = 10$  units, and is used in a similar way to that described for the corresponding Method 3 A.

*Strut Method 3 B. Alternatively by slope:—*

From the tie equation (65) for the slope  $\theta$  and couple  $M_1$  at D, the ratio obtaining here is seen to be

$$\begin{aligned}\theta/M_1 &= i \cdot \sin nl / i \cdot n EI \cdot (\cos nl - i \cdot \sin nl / i \cdot \tan nL) \\ &= \sin nl (\cos nl - \sin nl \cdot \cot nL) / n EI. \quad . \quad . \quad (98)\end{aligned}$$

That is, initially, when both  $\theta$  and  $M_1 = 0$ ,

$$\begin{aligned}“a” &= \sin n_a l (\cos n_a l - \sin n_a l \cdot \cot n_a L_a) / n_a EI, \quad (99) \\ &\quad (Strut equation J_\theta)\end{aligned}$$

where “*a*” is the  $M_1 \theta$  derivative. To effect a solution to this equation from any value of “*a*” experimentally deter-

mined, the J values and curves of Chart XII. should be used in a similar way to that described for Method 3A alternative.

An inspection of the foregoing equations for struts will show that, in the pin-jointed cases, the values of "a" become infinite when  $n_a L_a = \pi/2$ , and failure apparently occurs by flexing: i. e., for safety,

$$L_a(P/EI)^{1/2} \gtrless \pi/2, \text{ or } P_a \gtrless \pi^2 EI/4L_a^2,$$

which latter is the Euler buckling value.

Also, on inspecting the equations for struts with fixed ends, it will be seen that the values of "a" become infinite when  $n_a L_a = \pi$ , corresponding to the Euler buckling value of  $\pi^2 EI/L_a^2$ , as would be expected.

It must, however, be remembered, that in all cases the ends are elastically constrained, and, in the event of a strut commencing to buckle under a limiting end load, the initial compression in the strut will at once be reduced by the reactions of the end constraints as previously discussed.

It is also well known, and should here be borne in mind, that where initial eccentricity of  $P_a$  exists under weak constraints the critical values of  $P_a <$  the Euler value  $P_e$ . The fact that  $P_a$  may not be truly axial to the strut does not however affect the relations given by the equations—a deduction fully discussed in the Thesis, of which this is an abstract.

*Correction Factors for Non-central Loading of Struts by  
Methods 2 A and 2 B, 3 A and 3 B.*

In both deflexion and slope investigations by the foregoing tie methods it is shown in the Thesis that a correction factor

$$= (1 \pm \frac{\tanh nL_1 - \tanh nL}{\tanh nL_1 + \tanh nL})$$

appears in each of the final expressions obtained for non-central loading, which factor practically reduces to unity when  $nL > 3$ , as is most likely to obtain, i. e. initially, when  $n_a L_a > 3$ .  $L$  and  $L_1$  are the end distances from the non-central origin midway between the flexing loads or couples applied to the tie.

The corresponding correction factor applicable to struts is therefore

$$\begin{aligned} & (1 \pm \frac{\tanh inL_1 - \tanh inL}{\tanh inL_1 + \tanh inL}) \\ &= (1 \pm i \cdot \frac{\tan nL_1 - i \cdot \tan nL}{i \cdot \tan nL_1 + i \cdot \tan nL}) \\ &= (1 \pm \frac{\tan nL_1 - \tan nL}{\tan nL_1 + \tan nL}). \end{aligned}$$

Now this factor only reduces to unity when  $nL = nL_1$ , i. e., for central loading conditions only. Hence care must be exercised when making a strut test to ascertain that the flexing bridge or flexing couples are placed centrally, or, in particular cases where it is impossible to do so, the above correction factor must be introduced to obtain true results, using the stress charts as drawn to obtain first approximations only.

Obviously, the "a" expressions established by Methods 1A and 1B are only applicable to centrally tested cases—whether strut or tie—and so will not further be explored here.

### *Stress Reversal.*

Where deformation of a structure has occurred through perhaps the subsidence of a support, the partial failure of a member or through other causes, cases may arise in which certain members, originally tensile, may suffer a reversal of stress, and so be called upon to function as struts, and *vice versa*. Now the former state of affairs may be serious on account of the smaller cross-sectional area to resist buckling, and, if the reversed stress in the tie is of sufficient magnitude to cause buckling, the state of affairs will, of course, be apparent on inspection. When, however,  $-P_a < P_a$ , mere inspection will furnish no evidence of stress reversal either qualitatively or quantitatively.

By applying the principles of the foregoing methods, choosing, say, two methods to check the results of each, it should be possible to obtain complete evidence in doubtful cases of this nature both as regards the sign of the stress present and also as regards its magnitude.

Criteria for stress reversal have already been noted in two cases, under the treatment for struts, tested by Methods 1A and 1B. A third case is fully discussed in the Thesis. Tests applicable to all cases will now be considered.

#### *1. By the Reversal Ratio.*

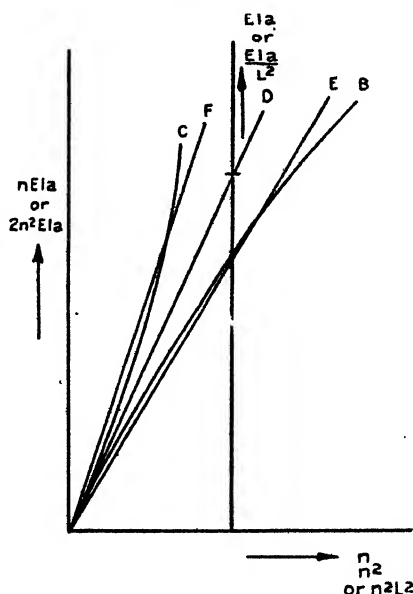
In the treatment by Methods 1A and 1B the term "reversal ratios" was introduced and explained in its natural sequence there. This term may be defined as "the value of the initial X.Y. derivative" when  $P_a = 0$ .

In the cases mentioned it was shown that a member is a *strut* or a *tie* according as the initial derivative  $>$  the reversal ratio or  $<$  the reversal ratio respectively. For reference purposes these reversal ratios are here tabulated with inclusion of the values for the remaining cases.

## Reversal Ratios.

By method.	Deflexion ratio.	Fig. No.	Slope ratio.	Fig. No.
1 A .....	$\delta_C/W = L^3/6EI$	4	$\theta_D/W = L^2/4EI$	5
1 B .....	$\delta_C/W = L^3/24EI$	6	$\theta_D/W = L^2/16EI$	7
2 A .....	$\delta_C/W = l^2(3L-l)/12EI$	8	$\theta_D/W = l^2/4EI$	8
2 B .....	$\delta_C/W = l^2(3L-2l)/24EI$	9	$\theta_D/W = l^2(L-l)/4 \cdot EI \cdot L$	9
3 A .....	$\delta_C/M_1 = l(2L-l)/2EI$	10	$\theta_D/M_1 = l/EI$	10
3 B .....	$\delta_C/M_1 = l(L-l)/2EI$	11	$\theta_D/M_1 = l(L-l)/EI \cdot L$	11

Fig. 12.



## 2. From the Stress Chart for the Method used.

Where a stress chart is used the evaluation of the reversal ratio will be obviated, since a multiple of this ratio is given by the limiting tangent to the appropriate curve of  $L$  at the origin, and on most of the charts appears as the product of  $EI \cdot a$  ("a" being the initial derivative when  $P_a = 0$ , and is consequently the reversal ratio).

Thus in fig. 12 a typical L curve OB from a tie chart, and a curve OC for the same value of L from a corresponding strut chart, are shown as though drawn to the same scale. When  $P_a = 0$ , the polar ray OD becomes the common tangent to both curves with its value indicated in terms of EI.a. If the member be a tie, its ray will be as OE, below OD, and consequently giving an intersection only on the tie curve OB. If the member be a strut, its ray will be as OF, above OD, so giving an intersection on the strut curve only.

That is, for any determined value of the initial derivative and given value of L only *one* intersection can be obtained, and a member is shown to be a tie or a strut according as the intersection is found on the appropriate tie chart or on the corresponding strut chart. If the tie chart yields no solution to a supposed tensile case, the member has suffered reversal of stress, and the magnitude of the stress obtaining can be found from the corresponding strut chart.

#### *General Deductions and Conclusions.*

This section is intended to form a summary to the foregoing investigations and conclusions thereto, and to draw further conclusions respecting the relative merits or limitations of adaptability—as the case may be—of the various methods discussed, and is therefore later divided for convenience of reference into two subsections: (a) dealing with the methods for the determinations of the stresses in ties, and (b) dealing with the similar methods for the determinations of the stresses in struts.

#### *Values of EI.*

Throughout this research it is very apparent that in any tie or strut investigation the degree of exactitude experimentally obtainable depends fundamentally upon knowing the value of the flexural rigidity (EI)—similarly to knowing the value of Young's Modulus (E) only, for the well-established methods of incremental stress determinations by the measurement of direct strains.

This quantity (EI) is therefore of fundamental importance, and, for the subsequent testing of a member, its value should be readily obtainable from specification and acceptance test data. When the factor E is unknown the usual handbook value for the material may be taken, and will give approximate results. It was found throughout the experimental work done and fully recorded in the complete Thesis that—broadly speaking—any percentage error in the value of E

taken gave approximately double that percentage error in the derivative "a."

Here it should perhaps be pointed out that, although known relationships exist between  $E$  and other physical quantities of a material <sup>(12), (13), (14)</sup>, the direct determination of  $E$  from such quantities may not be possible when dealing with a member *in situ*, on account of the possible objection to the removal of a small quantity of the material for its determination. The other rigidity factor  $I$ , the second moment of area of the section, is, of course, a purely geometrical quantity, and so is obtainable from average cross-sectional measurements.

### (a) Ties.

#### 1. Central Single-load Method.

This method is obviously of limited application, and, although it is apparently the simplest of the three general methods discussed, it can only be easily applied to particularly placed members.

For ties of uniform cross-section to which central lateral loads may be conveniently applied as indicated in figs. 4 to 7 inclusive, the stresses present may be determined from

- (i.) the load-deflexion derivative of Method 1A and Stress Chart I., A values ; or alternatively from
- (ii.) the load-slope derivative—where obtainable—of Method 1A and Stress Chart II., A values, in smoothly pinned ended cases ; and from
- (iii.) the load-deflexion derivative of Method 1B and Stress Chart I., B values ; or alternatively from
- (iv.) the load-slope derivative of Method 1B and Stress Chart II., B values, in firmly fixed ended cases.

#### 2. Flexing Bridge Method.

From the consistent experimental results obtained in the foregoing research, which results, together with the apparatus used, are fully recorded in the Thesis proper, it seems reasonable to infer that the Flexing Bridge Method—theoretically investigated by Methods 2A and 2B—will also give satisfactory experimental results, and may prove, as the analysis and resulting Stress Charts III. and IV. show, to have as wide and flexible an application as the following Couple Method, so that the former deductions of Method 1 should apply with equal verity to Methods 2 and 3 also.

### 3. Couple Method.

The stresses in ties to which it is not convenient or possible to apply independent lateral test loads may be determined by the application of simple flexing couples as indicated in figs. 10 and 11 (vol. ix. pp. 431, 435, 1930)—couples which may be applied anywhere along a continuous portion of the tie, irrespective of any tie joints on either side. The end conditions of fixity are immaterial in most actual cases.

For long or short ties of whatever inclination, flexible in any plane, the stresses present may be determined from

- (i.) the couple-deflexion derivative of Method 3 A and Stress Chart V. in smoothly pinned ended cases, or from
- (ii.) the couple-deflexion derivative of Method 3 B and Stress Chart V. in fixed ended cases.

Alternatively, the stresses present may be determined from

- (iii.) the couple-slope derivative of Method 3 A and Stress Chart VI. in smoothly pinned ended cases, or from
- (iv.) the couple-slope derivative of Method 3 B and Stress Chart VI. in fixed ended cases.

When in either Chart V. or Chart VI. the interpolated stress points lie on or near the dotted K curves, departures from the end conditions of fixity assumed are shown not to have affected the determinations.

#### (b) Struts.

##### 1. Central Single-load Method.

For uniform smoothly pinned ended struts to which single lateral loads may be conveniently applied, as indicated in figs. 4 and 5 (with P reversed), first approximations to the stresses present may be determined from

- (i.) the load-deflexion derivative of Method 1 A and Stress Chart VII., A values; or alternatively from
- (ii.) the load-slope derivative—where obtainable—of Method 1 A and Stress Chart VIII., A values.

For uniform firmly fixed ended struts the stresses present may be determined, as indicated in figs. 6 and 7 (with P reversed), from

- (iii.) the load-deflexion derivative of Method 1 B and Stress Chart VII., B values; or alternatively from
- (iv.) the load-slope derivative—where obtainable—of Method 1 B and Stress Chart VIII., B values.



**2. Flexing Bridge Method.**

As concluded for ties, the similar consistent results obtained in this research on struts leads to the conclusion that the Flexing Bridge Methods 2 A and 2 B will also yield satisfactory experimental results if care be taken to ensure that the assumed theoretical conditions are provided for as closely as possible.

**3. Couple Method.**

In cases where it is not practicable to apply single lateral loads, the stresses in pinned ended struts having any inclination whatever may be determined by the application of flexing couples, as indicated in fig. 10 (with P reversed) from

- (i.) the couple-deflexion derivative of Method 3 A and Stress Chart XI., I values ; or alternatively from
- (ii.) the couple-slope derivative of Method 3 A and Stress Chart XII., I values.

For struts having fixed ends and flexible in whatever planes, the stresses present may be found, as indicated in fig. 11 (with P reversed), from

- (iii.) the couple-deflexion derivative of Method 3 B and Stress Chart XI., J values ; or alternatively from
- (iv.) the couple-slope derivative of Method 3 B and Stress Chart XII., J values.

The experimental part of this research, fully described in the Thesis, was carried out by the author in the Mechanical Laboratories of the Northampton Polytechnic Institute, London, during the four years 1925 to 1928, and he here desires to record his thanks to C. E. Larard, Esq., M.I.C.E., M.I.Mech.E., Head of the Civil and Mechanical Engineering Department, for his encouragement throughout its prosecution.

*References.*

- (12) "The Physical Properties of Metals as Functions of each other." By Dr. A. H. Stuart. *Journal of the Institute of Metals*, no. 2, 1915.
- (13) "The Modulus of Elasticity and its Relation to other Physical Quantities." By Dr. A. H. Stuart. *Proc. Inst. of Mech. Engineers*, December 1912.
- (14) "Relation between Young's Modulus, Density, and Atomic Weight." By T. Peczalski. *Comptes Rendus*, clxxvi. pp. 500-502, Feb. 19, 1923.

CII. *A Hot-Wire Amplifier Method for the Measurement of the Distribution of Vortices behind Obstacles.* By E. TYLER, M.Sc., F.Inst.P., Lecturer, Physics Department, College of Technology, Leicester\*.

INTRODUCTION.

THE desirability of using a hot-wire method for measuring the longitudinal and lateral spacing of vortices behind obstacles of small section, such as cylinders and plates, when placed in a steady air stream, necessitates greater sensitivity being obtained for the detection of the velocity fluctuations caused by the vortex formation than when using larger models. When an electrically heated platinum wire of small diameter is employed for the detection of vortex frequency, if the periodic heating and cooling of it occurs at a frequency of 100/sec. or more, the sensitiveness of it as a detector is considerably decreased. Moreover, when small models are used, even at moderately low air speeds, the frequency of formation of the vortices is generally well above the lower limit of audibility, and again a reduction in sensitivity is produced.

In previous papers †, I have described methods in which the longitudinal and lateral spacing of vortices formed behind cylinders at low frequencies have been determined, and the methods described herein are the results of an attempt to obtain data in a much shorter time for smaller models than in the previous methods, combined with increased sensitivity.

The investigations are classified under three headings:—

- 1) Measurement of the longitudinal spacing of vortices behind cylinders, using a differential hot-wire method.
- (2) Measurement of the lateral spacing of vortices behind cylinders.
- (3) Estimation of frequency formation of vortices behind cylinders, inclined plates, and aerofoils.

(1) *Longitudinal Spacing of Vortices behind Cylinders in Air.*  
*Differential Hot-wire Method.*

The arrangement for the determination of such spacing of vortices is as in fig. 1.

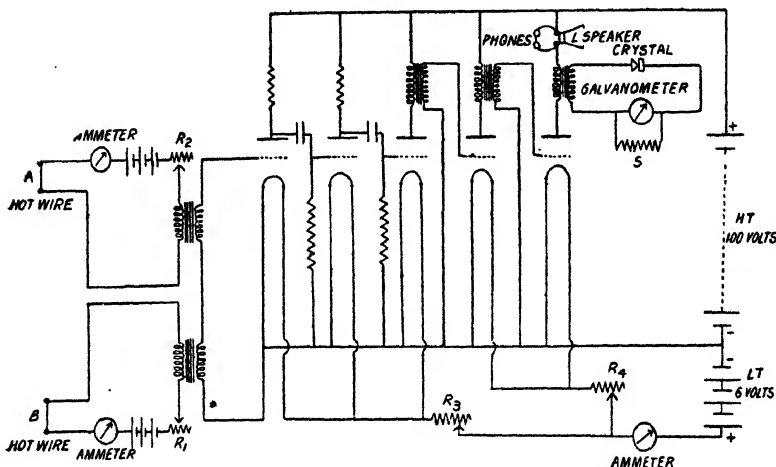
\* Communicated by the Author.

† Journal of Scientific Inst. iii. No. 12, Sept. 1926; Phil. Mag. v. March 1928; Journal of Scientific Inst. vi. No. 10, Oct. 1929.

Two electrically heated platinum wires A and B, each of length 1 inch and diameter .001 inch, supplied with constant heating currents of .35 amp., formed part of two similar electrical circuits. Each wire was coupled to the grid input circuit of a five-valve amplifier by means of separate primaries of a transformer, and the plate circuit of the last valve was transformer-coupled to a circuit consisting of a crystal rectifier and a shunted reflecting galvanometer.

The wires were arranged similarly, as in the previous method, each mounted vertically at the ends of prongs of separate forks, and placed behind the cylinder in the middle of a wind channel ( $1\frac{1}{2} \times 1\frac{1}{2} \times 15$  ft.), through which a steady stream of air flowed. Now, when each wire is suitably

Fig. 1.



placed, one in each vortex row, such that it is in a position where the velocity fluctuations are greatest, a periodic change in the resistance of the wire will occur of the same frequency as the frequency of formation of the vortices, and the resulting variations of P.D. across the wire, after being amplified, produce a fluctuating anode current superimposed upon the steady anode current in the plate circuit of the last valve. These fluctuations of anode current simultaneously produce induced currents in the crystal circuit of the same periodicity, and, after rectification by the crystal, produce a steady deflexion of the galvanometer, the sensitivity of which is controlled by the shunted resistance S.

The wire A was therefore kept stationary in a most favourable position in one vortex row giving maximum

steady deflexion of the galvanometer, while the other wire, B, was moved along a line up and down the stream in the opposite vortex row, which also gave a maximum steady deflexion of the galvanometer of the same magnitude as that produced by the wire A. The heating currents for both wires were kept constant for all positions of the wires, and the resulting deflexion of the galvanometer due to the periodic heating and cooling of both wires acting simultaneously was observed. When the two wires were in such positions that the velocity fluctuations at these points were in phase, the fluctuating P.D.s across the wires being also

TABLE I.

Amplifier Results for Cylinders.

$D = 4.20$  cm.  $N = 150$ .  $V = 317.5$  cm./sec.

$$\frac{V}{ND} = 5.05 \quad \frac{VD}{\nu} = 900.$$

Distance behind cylinder $x$ , cm.	$\frac{x}{D}$	$h$ , cm.	$l$ , cm.	$\frac{h}{l}$	$b = \frac{l}{D}$	$a = \frac{u}{V} \cdot \frac{b}{1-a} = \frac{V}{ND}$	
1.00	2.38	.375	1.375	.274	3.26	.353	5.03
2.20	5.24	.425	1.625	.263	3.86	.230	5.01
3.00	7.14	.450	1.675	.270	3.97	.212	5.06
3.85	9.17	.475	1.70	.284	4.05	.195	5.02
5.00	11.90	.500	1.75	.286	4.17	.170	5.02
5.65	13.45	.502	1.75	.287	4.17	.170	5.02

in phase after amplification produced a reinforcement of the fluctuating anode current, with a consequent maximum steady deflexion of the galvanometer after rectification. When the two wires were in relative positions corresponding to a phase difference of  $180^\circ$ , the fluctuating P.D.s across them opposed each other, resulting in a minimum rectification, and hence a minimum steady deflexion of the galvanometer.

Hence to obtain the longitudinal spacing of the vortices, the galvanometer deflexions due to the rectified currents were observed for corresponding positions of the movable hot wire downstream, and by plotting these deflexions against the distance of the movable hot wire behind the obstacle downstream, similar results were obtained to those

in the previous method, the graph exhibiting maximum and minimum values of deflexion.

The distance between two successive maxima or minima was assumed a measure of the longitudinal spacing between successive vortices in the same row.

TABLE II.

$$D = .650 \text{ cm. } N = 121. \quad V = 437 \text{ cm./sec.}$$

$$\frac{V}{ND} = 5.57. \quad \frac{VD}{v} = 1925.$$

Distance behind cylinder $x$ , cm.	$\frac{x}{D}$	$h$ , cm.	$l$ , cm.	$\frac{h}{l}$	$b = \frac{l}{D}$	$a = \frac{v}{V}$	$\frac{b}{1-a} = \frac{V}{ND}$
1.80	2.76	.580	2.325	.250	3.57	.358	5.57
2.50	3.85	.650	2.50	.260	3.85	.310	5.59
4.50	6.91	.730	2.675	.276	4.11	.260	5.56
6.50	10.00	.820	2.80	.293	4.30	.170	5.55

TABLE III.

$$D = .32 \text{ cm. } N = 186. \quad V = 298 \text{ cm./sec.}$$

$$\frac{V}{ND} = 5.01. \quad \frac{VD}{v} = 645.$$

Distance behind cylinder $x$ , cm.	$\frac{x}{D}$	$h$ , cm.	$l$ , cm.	$\frac{h}{l}$	$b = \frac{l}{D}$	$a = \frac{v}{V}$	$\frac{b}{1-a} = \frac{V}{ND}$
.75	2.34	.300	1.00	.300	3.13	.376	5.01
1.25	3.90	.350	1.275	.275	3.97	.210	5.02
1.90	5.93	.405	1.275	.317	3.97	.210	5.02
2.50	7.81	.420	1.30	.324	3.90	.223	5.00
4.50	14.10	.460	1.320	.349	4.12	.178	5.00

Results for cylinders are included in Tables I., II., III., and IV. and figs. 2, 3, and 4. It will be observed that each graph is characteristic of a decrease in the maximum value of the peaks, together with an increase in the longitudinal spacings for increasing distances behind the obstacle, evidently due to a widening out of the vortices, resulting in

a decrease in vortex strength as they move down the stream. Such an effect is consistent with the results observed by Fage and Johansen \* for a large plate, using a different method.

TABLE IV.

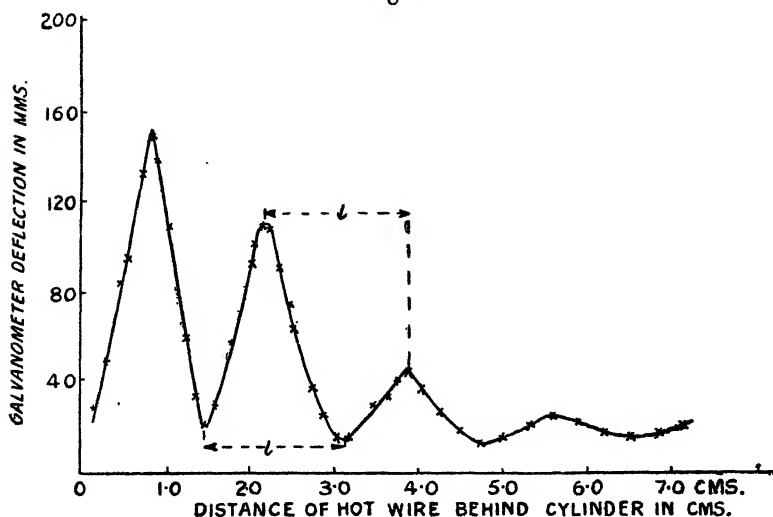
Results by Vibration Galvanometer Method.

$D=3.58$  cm.  $N=10$  cm.  $V=202.7$  cm./sec.

$$\frac{V}{ND}=5.66. \quad \frac{VD}{v}=4900.$$

Distance behind cylinder $x$ , cm.	$\frac{x}{D}$	$h$ , cm.	$l$ , cm.	$\frac{h}{l}$	$b=\frac{l}{D}$	$a=\frac{u}{V}$	$\frac{b}{1-a}=\frac{V}{ND}$
11.50	3.20	3.80	13.00	.292	3.64	.358	5.67
16.50	4.60	4.25	13.50	.314	3.77	.334	5.66
25.00	6.99	4.80	14.00	.342	3.90	.308	5.64
31.50	8.80	5.00	14.75	.339	4.12	.272	5.66

Fig. 2.



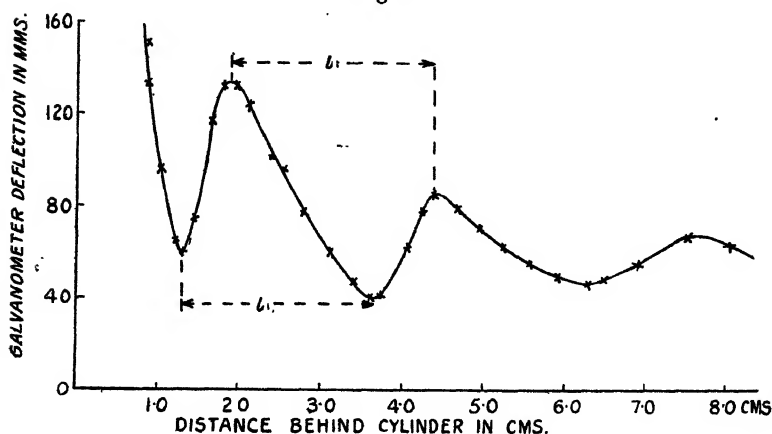
Cylinder  $D=.42$  cm.;  $V=317.5$  cm./sec.;  $N=150$ ;  $\frac{V}{ND}=5.05$ .

By using a loud speaker in the plate circuit of the last valve, the positions having the same phase and also  $180^\circ$  out

\* Proc. Roy. Soc. A, cxvi. (1927).

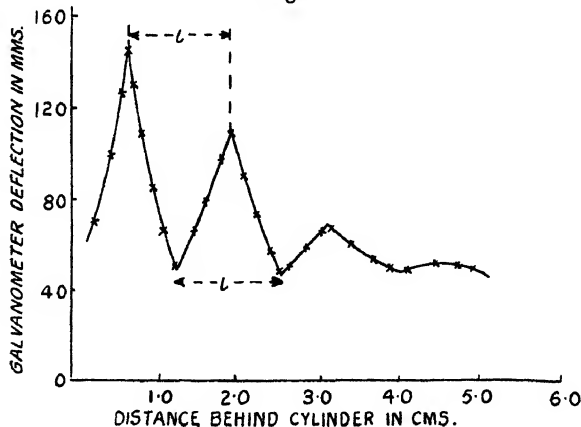
of phase, corresponding to maximum and minimum peaks on the curves, could easily be demonstrated by the audible note heard in the loud speaker; for since reinforcement of the

Fig. 3.



Cylinder  $D = .65$  cm.;  $V = 437$  cm./sec.;  $N = 121$ ;  $\frac{V}{ND} = 5.57$ .

Fig. 4



Cylinder  $D = .32$  cm.;  $V = 298$  cm./sec.;  $N = 186$ ;  $\frac{V}{ND} = 5.01$ .

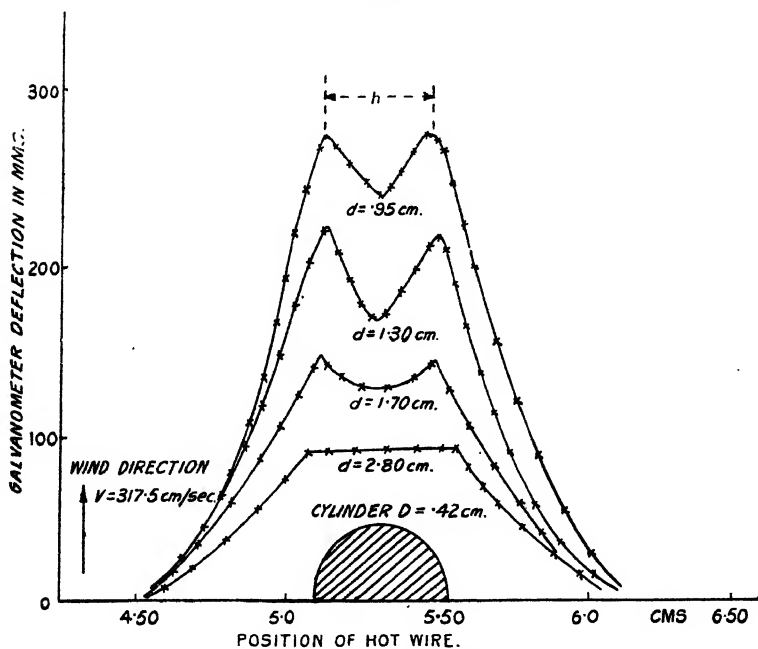
fluctuating P.D.'s across the wire occurs when the wires are in relative positions of same phase, maximum intensity of sound is heard in the loud speaker, whereas, when in positions corresponding to  $180^\circ$  out of phase, minimum resultant P.D. due to both wires produces minimum intensity of sound in the loud speaker. Thus, when the movable hot wire is traversed downstream, alternately maximum and minimum sound is

heard. As the distance of the movable hot wire downstream increased, the maximum intensity showed a gradual falling off, and at a distance of 8 cm. no sound was heard at all, again indicating a diminution in vortex strength.

## (2) Determination of the Lateral Spacing of Vortices behind Cylinders in Air.

By using one vertical hot wire transformer-coupled to the amplifier as in fig. 1, it was traversed laterally in a vertical plane at right angles to the wind stream at different distances behind the obstacle.

Fig. 5.



$d =$  distance of lateral traverse behind cylinder.

At each position of the wire, the heating current was kept constant, and the corresponding steady deflexions of the galvanometer observed. Figs. 5 and 6 are typical results for cylinders of  $D = .65 \text{ cm.}$  and  $.42 \text{ cm.}$

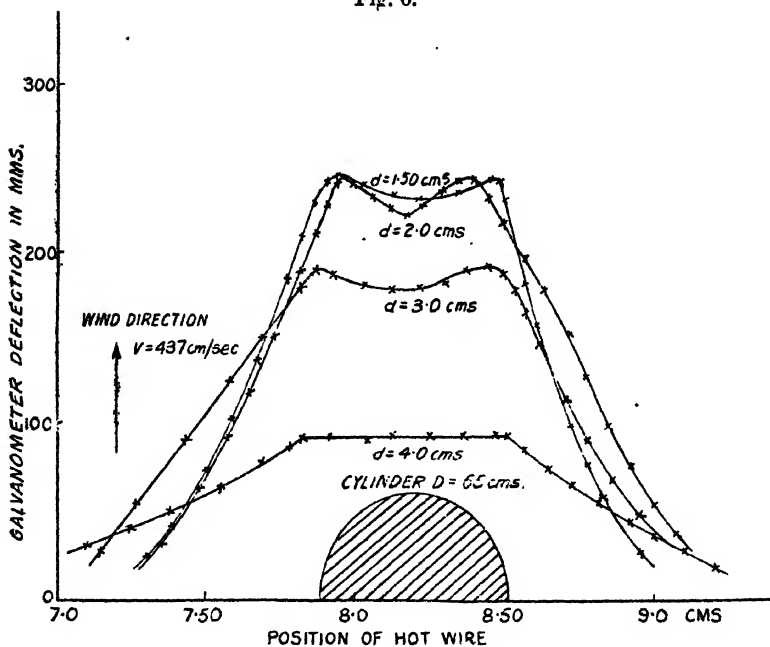
It will be observed that each traverse produces a curve exhibiting two maxima, similar to the curves obtained by a vibration galvanometer method described elsewhere\*

\* *Loc. cit.* ref. †, p. 1113. See also Table IV. for results.



and are similar to Dryden and Kuethe's\* results using a different arrangement. The distance between such maxima was again taken as a measure of the lateral distance ( $h$ ) between the centres of two rows of vortices, for this is true, assuming the maximum variation in velocity amplitude occurs along the paths of the centres of the vortices, which would therefore produce a maximum effect on the periodic heating and cooling of the wire, and hence a maximum deflexion of the galvanometer due to maximum rectification.

Fig. 6.



$a$  = distance of lateral traverse behind cylinder.

The peaks of figs. 5 and 6 also show that as the distance of the vortices behind the cylinders is increased there is a diminution in their peak values, indicating a decrease in vortex strength. At a distance of 4.0 cm., overlapping of the two rows of vortices is sufficient to produce a region of uniform velocity variation, for the traverses show no peaks, but are merely flat over this region.

Fig. 7 shows the variation of maximum velocity amplitude with increase in distance downstream behind a cylinder

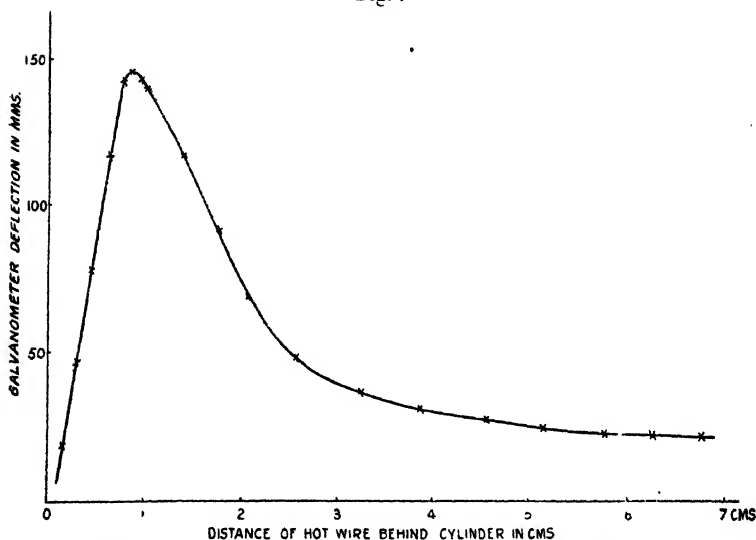
\* Report N. A. C. No. 329, Aeronautics, Bureau of Standards, Jan. 8th, 1929.

of  $D=0.65$  cm. From this figure it will be seen that at first the amplitude is small, but grows quickly, and reaches a maximum value at a distance of 1.0 cm. behind it. It then falls off gradually.

(3) *Frequency Determination of Vortices in Air behind Cylinders, Inclined Plates, and Aerofoils.*

The same arrangement as used in the previous section for the lateral spacings was now employed to determine the

Fig. 7



Variation of maximum velocity amplitude behind cylinder  $D=0.65$  cm. Traverse downstream at 325 cm. from centre of wake,  $V=445$  cm./sec;  $N=138$ .

frequency of formation of vortices, and in principle is similar to the method first successfully used by Piercy and Richardson\*, except that greater amplification was now produced.

By suitably placing the hot wire in one vortex row, where maximum variation in velocity amplitude occurs, and inserting in the plate circuit of the last valve either a pair of telephones or a loud-speaker, the small oscillating P.D.s produced across the wire by its periodic heating and cooling due to formation of vortices, after amplification were made to produce an audible note in either the phones or the loud speaker, of the same frequency as the vortex formation.

\* Phil. Mag. vi. Nov. 1928.

With such amplification the note heard was of sufficient intensity to be heard all over a large room, and demonstration to an audience could easily be made.

The value of this frequency was determined by comparing the note heard with a similar note produced on a monochord standardized with a 256 fork. Tables V., VI., and VII. incorporate results for cylinders, inclined plates, and aerofoils, and fig. 8 shows a comparison of results for plates and aerofoils.

TABLE V.  
Amplifier Results for Cylinders in Air.  
 $\nu$  for air = 148.

Diameter D, cm.	Frequency N, per sec.	Velocity V, cm./sec.	$\frac{V}{ND}$	$\frac{ND}{\nu}$
·61	86·5	268	5·10	1100
·61	57·7	182	5·18	750
·42	139	293	5·02	830
·42	110·7	238	5·12	677
·31	181	297	5·30	621
·31	100	165	5·32	345
·163	300	266	5·42	292
·163	360	327	5·58	360
·120	510	330	5·40	268
·120	265	185	5·80	150
·060	335	152·5	7·60	61·8
·060	730	278	6·35	113
·060	820	307·5	6·25	125
·046	373	150	8·75	46·8
·046	453	167	8·00	52·0
·046	645	208	7·02	65

It will be observed that the results are in good agreement with those obtained by other methods\*. In particular it is of interest to compare the cylinder results with those of Piercy and Richardson, who obtained a few results for thin rods at somewhat higher values of  $\frac{VD}{\nu}$ . Good agreement is shown for similar values of  $\frac{VD}{\nu}$ ; but, furthermore, the results

\* Relf and Simmons, Phil. Mag. xlix. p. 509 (1925); Richardson, Proc. Phys. Soc. xxxvii. p. 178 (1925).

in Table V. indicate that at low values of  $\frac{VD}{\nu}$  for the cylinders there is an increase in  $\frac{V}{ND}$  which is consistent with results obtained by other experimenters\*.

TABLE VI.  
Amplifier Results for Plates in Air.

Type of Plate.	Angle of Inclination, $\theta^\circ$ .	Frequency N, per sec.	Velocity V, cm./sec.	$\frac{Nb}{V}$ .	$\frac{Nb \cdot \sin \theta}{V}$ .
Length = 11 cm. Width b, = 4.25 cm. Thickness D, = 50 mm.	5	695	371	.783	.068
	10	422.5	265	.678	.118
	10	490	318	.656	.114
	15	299	287.5	.442	.114
	30	293	425.5	.292	.146
	45	214	425.5	.213	.150
	60	160.7	417.5	.163	.141
Length = 11 cm. Width b, = 59 cm. Thickness D, = 50 mm.	90	152	450	.144	.144
	0	656	384	1.01	0
	0	898	485	1.09	0
	0	579	375	.910	.079
	10	415	371	.660	.115
	17	372	480	.456	.134
	30	237	480	.292	.146
	45	160.5	465	.204	.144
	70	124.5	465	.158	.148
	90	116	465	.147	.147

# THEORY AND DISCUSSION OF RESULTS.

## Longitudinal and Lateral Spacing of Vortices behind Cylinders.

Referring to Tables I., II., III., and IV., it will be observed that the mean value of  $\frac{h}{l} = .288$  agrees fairly well with Karman's theoretical stability condition for two parallel

\* Benard, *Comptes Rendus*, cxlvii. p. 839 (1908); clxxxii. No. 25, June 21, 1926. Walton, *Scientific Proc. Roy Dublin Soc.* xviii. No. 47, Jan. 9, 1928.

rows of vortices, viz.,  $\frac{h}{l} = .283$ , although the variations are too large to be experimental errors. The widening out of the vortex rows is associated with a corresponding increase in the longitudinal spacings ( $l$ ), and both these effects produce a retardation in the relative speed ( $u$ ) of the vortices with

TABLE VII.  
Amplifier Results for Aerofoils in Air \*.

Type of Aerofoil.	Angle of Inclination, $\theta^\circ$ .	Frequency $N$ , per sec.	Velocity $V$ , cm./sec.	$\frac{Nb}{V}$ .	$\frac{V}{ND}$ .	$\frac{Nb \cdot \sin \theta}{V}$ .
Width $b$ , = 1.2 cm. Maximum thickness $D$ , = 1.88 mm.	0	264	278	1.13	5.62	0
	0	396	402.5	1.18	5.40	0
	5	377	445	1.02	6.30	.089
	10	290	358	.970	6.58	.104
	10	280	363	.928	6.89	.099
	15	230	363	.756	8.40	.195
	20	170	337.5	.600	10.55	.205
	25	156	390	.479	13.30	.202
	30	120	425	.339	18.80	.109
	45	100	571	.210	30.40	.148
Width $b$ , = .64 cm. Maximum thickness $D$ , = .82 mm.	0	758	475	1.02	7.66	0
	0	660	402	1.05	7.45	0
	5	661	435	.971	8.03	.089
	5	565	372	.974	8.06	.085
	15	352	382	.590	13.20	.152
	20	300	347	.553	14.18	.189
	20	390	450	.555	14.10	.190
	30	250	450	.355	22.00	.177
	45	145	450	.205	37.90	.145
	60	90	347	.166	47.00	.145

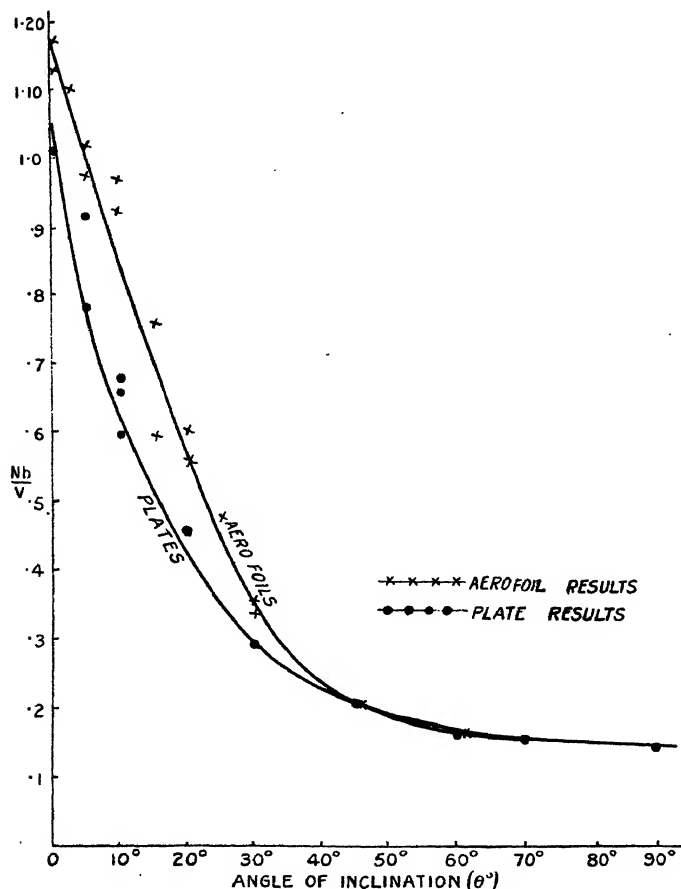
respect to the fluid stream as they recede from the cylinder, for there is a marked decrease in  $\frac{u}{V}$  as the distance downstream ( $x$ ) is increased.

\* Phil. Mag. v. March 1928. The following errata in that paper should be noted:—P. 453, Table III. Values of  $N$  given are only half correct values for aerofoil No. 1 (Brass). The corresponding values of  $\frac{V}{ND}$  should read half the values shown.

By plotting  $\frac{l}{D}$  against  $\frac{D}{x}$  for the different cylinders, as in fig. 9, the results are represented fairly well by the linear relation

$$\frac{l}{D} = 4.50 \left( 1 - 0.62 \frac{D}{x} \right), \dots \dots \dots (1)$$

Fig. 8.



Amplifier results for inclined plates and aerofoils.

which compares favourably with Karman and Rubach's\* value of  $\frac{l}{D} = 4.30$  for a cylinder in water and Fage's† value  $\frac{l}{D} = 4.27$  for a cylinder in air.

\* *Phys. Zeitschr.* xiii. p. 49 (1912).

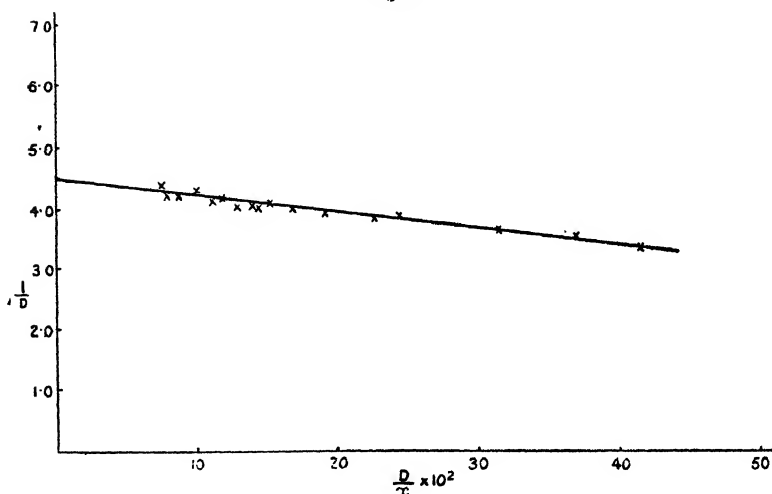
† *Roy. Aero. Soc.* Jan. 1929.

Beyond  $\frac{x}{D} = 12$ , the variations of  $\frac{l}{D}$  are of the same order as the experimental errors, and it is only at such distances behind the cylinders that the speed of the vortices relative to the surrounding fluid might be assumed constant.

*Frequency Formation of Vortices. Relation between  $\frac{ND}{V}$  and  $\frac{VD}{\nu}$  for Cylinders in Air.*

Following the method adopted by Rayleigh\* and others, by applying the theory of dimensional similarity, the

Fig. 9.



frequency of formation of the vortices,  $N$ , formed behind a stationary cylinder of diameter  $D$  cm. can be expressed as

$$\frac{ND}{V} = Kf\left(\frac{\nu}{VD}\right),$$

where  $V$  = velocity of the fluid stream,  
 $\nu$  = kinematic viscosity of the fluid,  
 $K$  = a constant,

and the function  $f\left(\frac{\nu}{VD}\right)$  is unknown, and is to be determined from the experimental results.

Assuming that  $\frac{ND}{V}$  would be affected by a change in

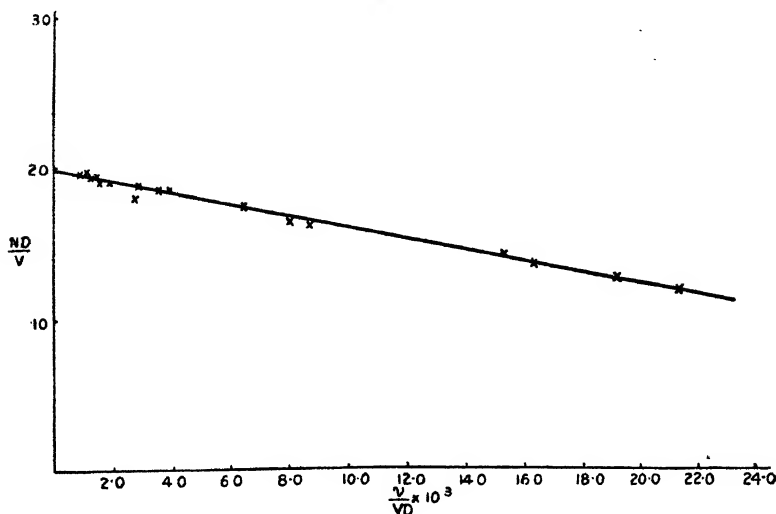
\* Rayleigh's 'Sound,' ii. pp. 413, 414.

viscosity  $\nu$ , and expanding  $f\left(\frac{\nu}{VD}\right)$  as a Maclaurin series, we get

$$\frac{ND}{V} = a + b \cdot \left(\frac{\nu}{VD}\right) + c \left(\frac{\nu}{VD}\right)^2 + \dots \text{etc.},$$

where  $a$ ,  $b$ , and  $c$  are constants.

Fig. 10.



Since generally  $\frac{\nu}{VD}$  is small with respect to  $\frac{ND}{V}$ , neglecting the higher power terms above the first order, we have

$$\begin{aligned} \frac{ND}{V} &= a + b \cdot \frac{\nu}{VD} \\ &= A_1 \left(1 + B_1 \frac{\nu}{VD}\right), \quad \dots \dots \dots (2) \end{aligned}$$

where  $A_1$  and  $B_1$  are also constants.

This is a linear equation in  $\frac{ND}{V}$  and  $\frac{\nu}{VD}$ , and by plotting the values of these non-dimensional quantities from Table V. a straight-line graph, as in fig. 10, is obtained, from which values of  $A_1 = 19.8$  and  $B_1 = -19.7$  are deduced.

Substituting these values in equation (2), the experimental results can be well represented by the equation

$$\frac{ND}{V} = 19.8 \left(1 - 19.7 \cdot \frac{\nu}{VD}\right), \quad \dots \dots (3)$$



which is nearly identical with that deduced by Rayleigh from Strouhal's\* results obtained by a different method,  $A_1$  and  $B_1$  having values of  $\cdot 195$  and  $20\cdot 1$  respectively.

*Results for Inclined Plates and Aerofoils.*

Analysis of the results for inclined plates suggests that at angles of inclination ( $\theta$ ) between  $20^\circ - 90^\circ$ ,  $\frac{Nb \cdot \sin \theta}{V} = \cdot 148$ , and is constant for different plates, whereas the aerofoils show this constancy at angles of  $30^\circ$  upwards. This is only true when the effect of viscosity is small, as will be shown later.

Between  $0^\circ$  and  $30^\circ$  there is, however, a difference between the plate and aerofoil results (see fig. 8) which is to be expected, since at low angles of inclination the maximum thickness  $D$  of the aerofoil plays a more important part in controlling the rate of formation of the vortices, and  $\frac{ND}{V}$  must now replace  $\frac{Nb \cdot \sin \theta}{V}$ . Variations of  $\frac{V}{ND}$  with  $\theta$  are included in Table VII. for the aerofoils.

A comparison of the results with those of Fage and Johansen† shows excellent agreement for  $30^\circ$  upwards. It is therefore highly probable that the vortex frequency formation behind an inclined plate at  $\theta^\circ$  to the fluid stream, and of width  $b$  cm., is similar to that behind a plate normal to the stream and having effective width  $b \cdot \sin \theta$ .

In such a case, both the lateral and longitudinal spacings will be modified proportionally. Confirmation of this has been made by Fage and Johansen, who found that  $\frac{l}{b \cdot \sin \theta} = 5\cdot 32$ , and is constant between angles  $30^\circ - 90^\circ$ . Some later work‡, by a different method, has also verified this constancy of  $\frac{l}{b \cdot \sin \theta}$ .

*Effect of Viscosity.*

By similar dimensional treatment to that used for the cylinders it can be shown by replacing the diameter  $D$  of the cylinder by  $b \cdot \sin \theta$ , the effective width of the plate, and neglecting the power terms of viscosity, that

$$\frac{Nb \cdot \sin \theta}{V} = A_2 \left( 1 + B_2 \frac{\nu}{V \cdot b \cdot \sin \theta} \right),$$

\* *Ann. der Phys.* v. p. 216 (1878).

† *Loc. cit.* ref. \*, p. 1117.

‡ To be published later.

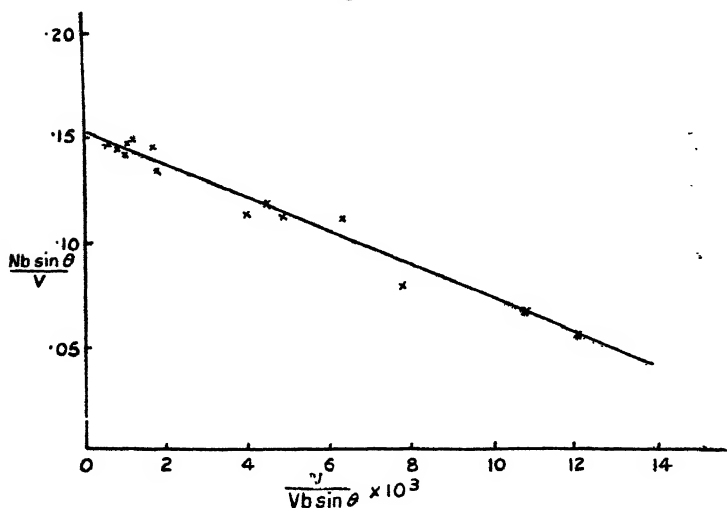
and a plot of  $\frac{Nb \cdot \sin \theta}{V}$  against  $\frac{v}{Vb \cdot \sin \theta}$  also gives a linear relation. Fig. 11 shows this quite well, the constants  $A_2$ ,  $B_2$  having values  $\cdot 152$  and  $-52\cdot 6$  respectively. Thus, retaining the viscosity term, the equation

$$\frac{Nb \cdot \sin \theta}{V} = \cdot 152 \left( 1 - 52\cdot 6 \frac{v}{Vb \cdot \sin \theta} \right)$$

is representative of the plate results over the whole range investigated.

It is of interest to compare these results with those of Karman and Rubach \* for a plate normal to a steady stream

Fig. 11.



of water, for without applying a correction for viscosity they obtained a value of  $\cdot 145$  for  $\frac{N \cdot b}{V}$ .

Further investigations are still in progress, the results of which will appear in a later paper.

#### SUMMARY.

A differential method, using two electrically heated platinum wires in conjunction with a valve amplifier is described for measuring the longitudinal spacing ( $l$ ) of vortices formed behind cylinders of small diameter placed in a steady air-stream. Measurements of the lateral

\* *Loc. cit.* ref. \*, p. 1125.

spacings ( $h$ ) of the vortex rows are also included, together with values of  $\frac{h}{\lambda}$ , and a comparison with theory shows fairly good agreement for the average results only. A determination of the frequency of formation of the vortices behind cylinders, inclined plates, and aerofoils is made by using the same amplifier, and empirical formulæ included to account for the results.

Physics Dept.,  
College of Technology,  
Leicester.  
January 1st, 1930.

CIII. *On the Mathematical Representation of Sensibility to Difference of Colour.* By R. A. HOUSTOUN, D.Sc.,  
*Lecturer on Physical Optics in the University of Glasgow* \*.

IT is well known that a colour possesses three qualities, hue, brightness, and saturation, and that it can consequently be specified by three independent variables. Also any light can be matched in colour and brightness by a superposition of three colours, the so-called primary colours. These may be real, if negative quantities are permitted in the mixture, but are otherwise imaginary. As independent variables we may choose the quantities of the primaries occurring in the mixture, measured in energy units. This was the method adopted by Helmholtz; thus according to Helmholtz the three variables are of exactly the same nature. According to Hering, on the other hand, the colour possesses brightness and two colour valencies, and two of the variables are of a different nature from the third.

The merits of these rival standpoints have been a subject of debate for years. Helmholtz's view had the advantage of a definite physical model, three different systems of nerves corresponding to his three primary colours, which made a stronger appeal to the imagination than Hering's somewhat vague physiological processes.

\* Communicated by the Author.

As the result of a paper already published \* and of some experimental work not yet published, I have found that the sensation of brightness is strictly proportional to the number of nerves excited. Colour may therefore be due to the number of impulses passing along each nerve per second. This gives a new standpoint on the subject, and there is also other recent work the bearing of which has not yet been investigated. I have therefore thought it worth while to re-examine the question.

The first requirement which a theory of colour-vision has to satisfy is the laws of colour mixing. The Young-Helmholtz theory does this in the most satisfactory manner on account of the definite picture which it gives of the process, but any other theory the variables of which are linear functions of the Young-Helmholtz variables gives the same numerical results as the latter does. This was pointed out specifically by Helmholtz † for the case of Hering's theory, and I have illustrated the point by some calculations ‡.

The next requirement to be satisfied is the perception of difference of colour. This point has not received so much attention in the discussion of the subject as the laws of colour mixing. The problem may be stated as follows: Let the three Young-Helmholtz variables, *i. e.*, the magnitudes of the stimuli affecting the three nerve systems, be laid off parallel to rectangular coordinate axes. Then to every colour there corresponds a point in space. How far must we move from any given point for the colour to become appreciably different? Or, putting it mathematically,  $x_1, x_2, x_3$  is given, and the quantities of the variables in the mixture are altered until there is a just appreciable change in sensation; what condition must  $dx_1, dx_2, dx_3$  satisfy?

Let  $dS$  be the change in the resultant sensation while  $dS_1, dS_2$ , and  $dS_3$  are the changes in the three fundamental sensations. Then Helmholtz assumed

$$dS^2 = dS_1^2 + dS_2^2 + dS_3^2 \\ = \frac{1}{3} \left( \frac{dx_1^2}{x_1^2} + \frac{dx_2^2}{x_2^2} + \frac{dx_3^2}{x_3^2} \right).$$

\* Phil. Mag. viii. p. 520 (1929).

† *Physiologische Optik*, Auflage ii., p. 376.

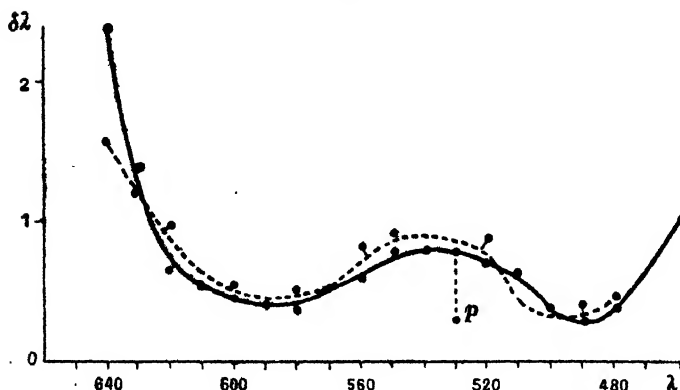
‡ Phil. Mag. xxxviii. p. 402 (1919).

This expression had the advantage that when  $x_2$  and  $x_3$  were zero it reduced to

$$dS = \frac{dx_1}{\sqrt{3x_1}},$$

which agreed with Fechner's law. Helmholtz tested the expression by applying it to König's\* measurements on the discrimination of hue in the spectrum. The results are shown in fig. 1, which is taken from Helmholtz's 'Physiological Optics,' fig. 1, 2nd Edition, p. 455. The

Fig. 1.



full line gives the difference of wave-length which according to König could just be discriminated at different points in the spectrum. The broken line shows what it should be according to the above assumption. König and Dieterici † had already determined  $S_1$ ,  $S_2$ ,  $S_3$  as functions of  $\lambda$ ; Helmholtz found that their primaries gave no agreement, and from their results calculated other primaries which gave the result shown.

With reference to the agreement it may be stated that the curve in the diagram shows only two points of maximum sensibility to change of wave-length in the spectrum, one in the yellow and one in the blue-green, whereas it is now known there are four such maxima. Also E. Schrödinger ‡ has pointed out that Helmholtz's

\* König and Dieterici, *Ann. d. Phys.* xxii. p. 579 (1884).

† König and Dieterici, *Berl. Ber.* p. 805 (1889).

‡ *Ann. d. Phys.* lxxiii. p. 481 (1920).

expression leads to a quite impossible value for the brightness of the solar spectrum, "a horrible camel's back with two well-marked maxima." Moreover, it has been shown by Abney and others that the brightness of colours is additive. This result, which is now appropriately known as Abney's law, is quite incompatible with Helmholtz's assumption.

Abney experimented with a spectrum falling upon a screen in which slits could be opened, so as to transmit different colours separately and together. These were allowed to illuminate a surface, and the intensity of the illumination falling on this surface was measured photometrically against white light from the same source. The red was thus, for example, equal to so many metre-candles of white light, the green to so many metre-candles, and the red and green together to a number of metre-candles equal to the sum of the separate values. Thus in computing the brightness of an illumination we can neglect the colour of the components.

Helmholtz's assumption is therefore out of the question, and Schrödinger has sought to replace it by

$$dS^2 = \frac{1}{a_1x_1 + a_2x_2 + a_3x_3} \left( \frac{a_1dx_1^2}{x_1} + \frac{a_2dx_2^2}{x_2} + \frac{a_3(dx_3^2)}{x_3} \right),$$

which is in agreement with Abney's law. He tests his expression by the experimental results shown in fig. 1, and finds that the agreement is about as good as that obtained by Helmholtz. When  $x_2, x_3, dx_2, dx_3$  are equal to zero his expression reduces to

$$dS = \frac{dx_1}{x_1},$$

which agrees with Fechner's law.

The fact that both Helmholtz's and Schrödinger's assumptions reduce to the conventional form for Fechner's law shows that they cannot hold for more than a limited range of intensities, for it is only over a limited range that this law represents the results even approximately.

Let us assume we are dealing with the colour for which

$$x_3=0 \text{ and } x_1=nx_2=\frac{n}{n+1} x \text{ say. Then}$$

$$dx_1=n dx_2=\frac{n}{n+1} dx,$$

and according to Helmholtz

$$dS^2 = \frac{1}{3} \left( \frac{dx_1^2}{x_1^2} + \frac{dx_2^2}{x_2^2} \right) = \frac{2}{3} \left( \frac{dx}{x} \right)^2,$$

whence 
$$dS = \sqrt{\frac{2}{3}} \frac{dx}{x}.$$

According to Schrödinger

$$\begin{aligned} dS^2 &= \frac{1}{a_1 x_1 + a_2 x_2} \left( \frac{a_1 dx_1^2}{x_1} + \frac{a_2 dx_2^2}{x_2} \right) \\ &= \frac{n+1}{a_1 n x + a_2 x} \left( \frac{a_1 n dx^2}{(n+1)x} + \frac{a_2 dx^2}{(n+1)x} \right) \\ &= \left( \frac{dx}{x} \right)^2, \end{aligned}$$

and

$$dS = \frac{dx}{x}.$$

Thus for a composite colour Helmholtz's assumption does not give the same expression for Fechner's law as it does for a primary colour, while Schrödinger's expression does. Now König and Brodhun \* tested this point specially, and found that the law was the same, no matter whether the colour was primary or composite. Thus on this point Schrödinger's expression is decidedly superior.

The criticism to which Schrödinger's expression might be subjected is that he abandons the standpoint of independent sensations. The three variables defining the stimulus,  $x_1, x_2, x_3$ , are independent, but the increment  $dS$  corresponding to a given  $dx$  depends not only on  $x_1$ , but also on  $x_2$  and  $x_3$ . The extent to which the red sensation is affected by a given change of stimulus depends on whether the green sensation is simultaneously stimulated or not. Thus the hypothesis of three independent sensations is fitted to Fechner's law by abandoning their independence. I feel certain that the adjustment cannot be made in any other way.

For let  $x_1$  be the energy absorbed per second in stimulating the one nerve system,  $x_2$  the energy absorbed per second in stimulating the other, and let  $S_1, S_2$  be the two

\* *Sitz. k. Akad. Wissensch.* (Berlin) p. 917 (1888).

sensations. Then by choosing different units for  $x_1$  and  $x_2$  we may write

$$S_1 = f(x_1), \quad S_2 = f(x_2).$$

The total sensation is given by

$$S = f(x_1) + f(x_2).$$

But, experimentally,

$$S = f(ax_1 + bx_2).$$

where  $a$  and  $b$  are constants, since it is necessary to express the energy absorbed in a third unit. This requires that  $S$  should be proportional to  $x$ , which is impossible.

The expressions which Helmholtz and Schrödinger postulate for  $dS^2$  represent both change of brightness and change of hue and saturation. Let us suppose that in a colour-matching apparatus the two fields are a perfect match as regards brightness, hue, and saturation, and let us increase the brightness of the one field. Then keeping the brightness constant let us change the colour. The eye recognizes the changes as different in kind. Consequently it seems wrong to combine them in the same expression.

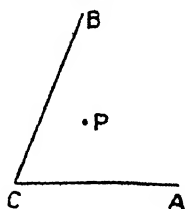
I think it desirable that one of the three variables defining the sensation should represent the brightness and nothing but the brightness. This satisfies Abney's law and Fechner's law automatically. It is an unusual standpoint for a physicist to adopt, but, as has been mentioned, I have obtained the result elsewhere that the brightness is proportional to the number of percipient elements active in the retina; thus Abney's law is satisfied, because there is always the same number of percipient elements on both sides of the equation. The mathematician will observe that my assumption makes it easier for the other two variables; they have now only to fulfil the requirements of colour mixing and colour sensitivity, and have nothing whatever to do with Abney's law or Fechner's law.

Let us now consider the nature of the other two variables. They have in the first place to satisfy the laws of colour mixing. These laws are summed up in the centre of gravity construction which was introduced in a sketchy manner in Newton's 'Optiks' and made into an accurate instrument of calculation by Maxwell and Helmholtz.



Let us assume that we have any three coloured lights, and that we superimpose  $\alpha$  units of the first,  $\beta$  of the second, and  $\gamma$  of the third. Then if we admit negative values of  $\alpha$ ,  $\beta$ , and  $\gamma$ , we can produce in this way all possible colours. Place  $\alpha$ ,  $\beta$ , and  $\gamma$  at the points A, B, and C (fig. 2), regard them as masses, and let P be their centre of gravity. The position of P depends obviously only on the ratios of  $\alpha$ ,  $\beta$ , and  $\gamma$ , not on their absolute magnitudes, *i.e.*, it depends only on the colour of the resultant light, not on its brightness. All colours occurring in nature are represented in the diagram, and it may be shown that, if we take any two colours and superimpose them, the colour of the resultant is obtained by placing masses on the diagram at the points representing the component colours equal in magnitude to the "quantities" of the components and taking the centre of gravity of these masses. It represents

Fig. 2.



the colour of the resultant. The "quantity" of a component is the sum of its  $\alpha$ ,  $\beta$ , and  $\gamma$  values and is thus usually not proportional to its brightness.

Once the colours are arranged on the diagram, any three points may be regarded as the primaries. The laws of colour mixing in themselves are independent of any particular choice of primaries, and the latter have been chosen from other considerations; for example, in order to make  $\alpha$ ,  $\beta$ ,  $\gamma$  always positive, to satisfy the phenomena of colour blindness, or to be easily produced in the laboratory. They may be real colours or colours not capable of actual production.

Once the colours are arranged on the diagram any two coordinates specifying the position of a point can be taken as the remaining variables of the theory. According to Hering these variables should be the red-green valency and the yellow-blue valency, and according to a recent

paper by Schrödinger \* the relations between Hering's valencies and the system of fundamental sensations adopted by König is mathematically both simple and interesting. The question arises as to whether the phenomena of the variation of colour sensibility require one system of coordinates in preference to another. Hering's valencies were chosen to explain the phenomena of simultaneous and successive contrast, but these phenomena are not of such a definite nature as the facts connected with the variation of colour sensibility, and if the latter could be described more easily with reference to Hering's theory, its position would be considerably strengthened.

Whenever the fundamental colours are chosen we are allowed considerable freedom in drawing the centre of gravity construction. We may place B (fig. 2) anywhere on the plane with reference to CA, *i. e.*, we have the two constants defining its position at our disposal. The intensities of the three colours are not necessarily measured in units of equal energy or equal brightness. Thus when we have the unit of  $\alpha$  fixed, we have the ratio of the units of  $\beta$  and  $\gamma$  at our disposal. There are thus four constants at our disposal, and there is consequently a fourfold infinity of constructions which will satisfy the laws of colour mixture. Is one of these constructions unique with reference to the phenomena of colour sensibility?

König's measurements on the discrimination of hue in the spectrum, *i. e.*, on the smallest difference in wave-length  $\delta\lambda$  which gives rise to an appreciable difference in hue, have already been referred to and represented in fig. 1. He and his collaborator Dieterici each found three maxima of sensibility one of which lies outside the range of the diagram. Their results were obtained by the method of mean error. Their work was repeated by a direct method both by Steindler † in 1906, and by L. A. Jones ‡ in 1917. The latter each found four maxima of sensibility. One set of results obtained by L. A. Jones is represented by the full curve in fig. 3, the ordinate in this case being proportional to  $1/\delta\lambda$ , so that the maxima represent maxima of sensibility. The results of Steindler and Jones are in good agreement, and there is no doubt whatever about

\* *Sitz. d. Wiener Akad.* cxxxiv. (ii. a) p. 470 (1925).

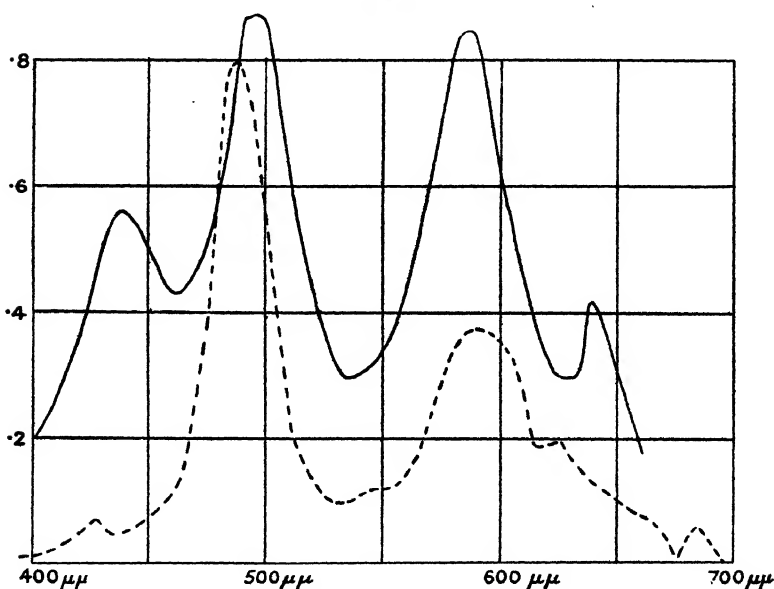
† *Sitz. d. Wiener Akad.* cxv. (ii. a) p. 115 (1906).

‡ *Journ. Op. Soc. of Amer.* p. 63 (1917).

the existence of the fourth maximum in the red ; I got it myself on the first attempt with an improvised apparatus. The sensibility to difference of hue throughout the spectrum does not vary appreciably with the intensity, until the latter becomes very small. It thus forms a very important test for any theory of colour vision. L. A. Jones found altogether 128 distinct hues between  $400\ \mu\mu$  and  $700\ \mu\mu$ .

L. A. Jones and E. M. Lowry \* have made a valuable series of determinations of retinal sensibility to saturation

Fig. 3.



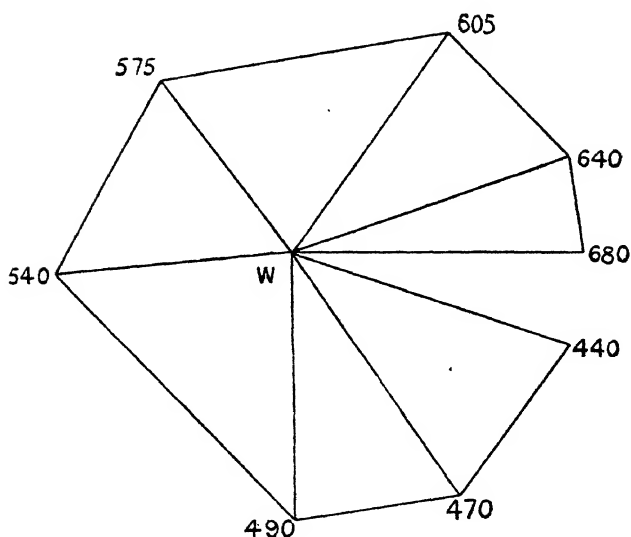
differences. Eight spectrum colours were employed, each was diluted with white, keeping the brightness constant, and the number of just perceptible steps necessary to reach white measured in each case. The apparatus had comparison fields with a sharp line of separation ; one side was diluted with white until there was a just perceptible difference, the other side was then made equal to the first, and a second step taken. Some of the results of Jones and of Jones and Lowry are represented in the following table and in fig. 4.

\* Journ. Op. Soc. Amer. xiii. p. 25 (1926).

TABLE.

$\lambda$ .	Steps to white.	Steps along spectrum.
440 $\mu\mu$	23	14
470	22	13
490	19	26
540	19	16
575	16	23
605	20	13
640	23	7
680	23	

Fig. 4.

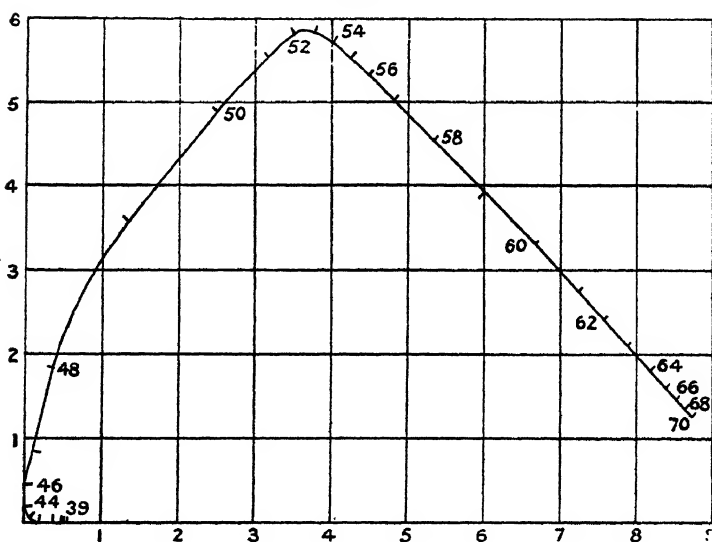


The first column in the table gives the eight wave-lengths employed by Jones and Lowry, the second column the number of steps required to reach white from the wave-length in question, and the third column the number of steps along the spectrum required to reach each wave-length from the next according to the measurements of Jones. In fig. 4 W represents white, and the distances between white and

the different wave-lengths and between consecutive wave-lengths are proportional to the number of steps. Thus fig. 4 represents a rough colour-sensibility diagram. The distance between two colours on it represents the number of just perceptible steps required to reach the one colour from the other.

Fig. 5 represents the König-Ives colour-mixture diagram in rectangular coordinates. It gives the position of the spectrum according to the data of König, as recalculated by Ives; the data of König are regarded at present as

Fig. 5.



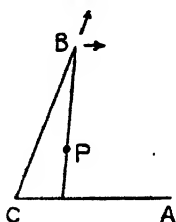
most authoritative, and this diagram is the most convenient way of employing them. Is it possible to modify fig. 5 by changing the four constants at our disposal, so as to make it also serve the same purpose as fig. 4?

Let us consider the effect of changing these four constants. Let  $P$  be the centre of gravity (fig. 6) of three masses situated at  $A$ ,  $B$ , and  $C$ . Displace  $B$  parallel to  $CB$ . Then  $P$  suffers a displacement parallel to  $CB$  proportional to its distance from  $CA$ . Displace  $B$  parallel to  $CA$ . Then  $P$  suffers a displacement parallel to  $CA$  proportional to its distance from  $CA$ . Thus in one case the diagram suffers an extension and in the other a shear. Straight lines remain straight, and the ratio of their parts is unaltered by the displacement.

Let us now diminish the unit in which the mass situated at B is measured. The apparent value of this mass increases, and P moves along PB towards B. Every straight line parallel to CA moves towards B keeping parallel to itself, but obviously the ratio of the parts of the straight line PB is altered by the change. It may be shown by considering the coordinates of three points that straight lines remain straight. Diminishing the unit in which one of the other masses is measured produces similar results.

Thus, no matter how we modify fig. 5, the straight part from the red end to  $540\ \mu\mu$  remains straight. Now the corresponding portion of fig. 4 is not straight, and cannot be made straight even if we take a different unit for the least perceptible step in two different directions. If different units of sensibility had been required in the

Fig. 6.



directions corresponding to Hering's colour valencies, that theory would naturally have been strengthened.

Since none of the variants of the colour-mixture diagram can be made to represent sensibility to both changes of hue and of saturation, it is interesting to inquire whether these requirements can be met separately. I have calculated the distances along the curve in fig. 5 which correspond to a difference of  $10\ \mu\mu$ , and plotted them in the broken curve in fig. 3 against their mean wave-lengths. The result gives the sensibility to difference of wave-length as recorded by the König-Ives diagram. It will be noticed that the curve gives three of the four maxima obtained by L. A. Jones in approximately the correct positions. The fourth one is not given; König's data have not been sufficiently accurate. But the same criticism applies to the evaluations of the colours of the spectrum in terms of the three primaries made by Maxwell, Dieterici, Abney, and Dow and myself\*. A redeter-

\* Phil. Mag. xlv. p. 169 (1923).

mination of the position of the spectrum on the diagram in the light of the desired result would probably reveal a correspondence in this point also.

On examining the König-Ives diagram it will be noticed that the spectrum curve is straight from  $690\ \mu\mu$  to  $540\ \mu\mu$  and approximately straight from  $520\ \mu\mu$  to  $440\ \mu\mu$ . If we assume these lines as sides of the triangle, it is obvious that by changing the scale of the second side the relative heights of the two principal maxima could be brought into agreement, and that by changing the units in which two of the three primaries are measured the positions of the maxima could be moved along the sides. So that doubtless, apart from the fourth maximum, quite a good agreement could be obtained between the two curves.

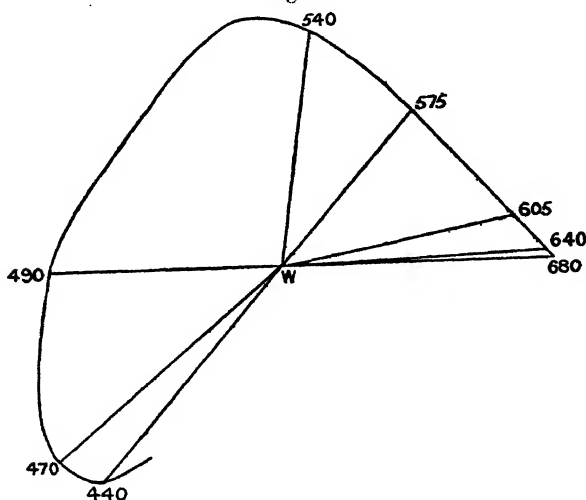
So much for the variation of hue along the spectrum. Let us now consider the sensibility to saturation differences. We have four constants at our disposal in the colour-mixture diagram. It is therefore possible to manipulate the diagram so as to get five lengths on it into a given ratio. According to Jones and Lowry between  $680\ \mu\mu$ ,  $575\ \mu\mu$ ,  $540\ \mu\mu$ ,  $490\ \mu\mu$ , and  $440\ \mu\mu$  and white there are 23, 16, 19, 19, and 23 steps respectively. I resolved therefore to adjust the diagram, so as to make the distances between these points take the ratio of the above numbers. Jones and Lowry employed a white of  $5200^\circ\text{K}$ . I found the coordinates of this point to be 0.302, 0.302, 0.396, on the König-Ives diagram. It was selected as origin, and  $680\ \mu\mu$  and  $575\ \mu\mu$  chosen as the points A and B of fig. 6. An extension of the diagram in the direction CB brought the distances of  $680\ \mu\mu$  and  $575\ \mu\mu$  into the correct ratio. The next point to adjust was  $490\ \mu\mu$ . It is very nearly on CA. The unit in which  $\alpha$  is measured was altered so as to make the distance of this point right. There then remained two constants at my disposal, the unit in which  $\beta$  was measured and the angle between CA and CB. The remaining two distances were expressed in terms of these constants, and the latter solved for. The details of the calculation are somewhat tedious, so I omit them and content myself with giving the result in fig. 7

This figure is a colour-mixture diagram which has the property, that the distances from white to five of the eight wave-lengths employed by Jones and Lowry are in the ratio of the numbers of steps of saturation difference necessary to reach these wave-lengths. It is found on

examination of the diagram, that the distances to the other three points are not far from the correct ratio. Consequently, the diagram, when drawn in this manner, in addition to representing the colours in terms of the primaries, states approximately their degree of saturation.

Jones and Lowry found that the steps were not equal, being smallest at complete saturation and at white. For example, if we take the case of  $680\text{ }\mu\mu$  when it was gradually diluted with white, just perceptible differences occurred at 97.0, 93.9, 90.5, 87.0, etc. per cent. of red, giving differences of 3.0, 3.1, 3.4, 3.5, etc. per cent. The differences gradually increase to a maximum of 6 per cent., and then diminish to 2.8 per cent. on reaching white. Two

Fig. 7.



of the wave-lengths investigated are almost complementaries,  $680\text{ }\mu\mu$  and  $490\text{ }\mu\mu$ . It is consequently possible to follow this direction across the diagram through white to saturation at the other side. The white used is, in units of equal luminosity, 40.5 per cent. of the red, and 59.5 per cent. of the blue at the ends of the path. If we specify the ends of the steps in percentages of this red and blue, the differences start from red at 1.8 per cent., rise to a maximum of 3.5 per cent., diminish to below 2 per cent. in passing through white, then rise to above 3 per cent., and finally diminish to 1.2 per cent. at the blue end. White is thus a point of maximum sensibility. It is impossible by any manipulation of the diagram to make these steps equal.



# 1144 *Representation of Sensibility to Difference of Colour.*

Let us now collect the results of this part of the investigation. If one of the three sensations is to specify brightness and the other two have to specify colour, it would involve the least disturbance to current practice if the sensations taken were

$$R + G + B, \quad \frac{R'}{R' + G' + B'}, \quad \frac{G'}{R' + G' + B'}$$

where  $R$ ,  $G$ , and  $B$  are the Young-Helmholtz fundamental sensations expressed in units of equal luminosity and  $R'$ ,  $G'$ ,  $B'$  the same sensations in units equal quantities of which make white. But when it comes to specifying sensibility to difference of colour, neither the second and third variables above nor the Hering colour valencies, are suitable. Polar coordinates seem indicated. The origin must be at white, and the scale of the diagram must be adjusted so that the distances to the five wave-lengths of Jones and Lowry are proportional to the number of steps to these wave-lengths. Then a step of sensation outwards will be given by

$$dS_r = f(r) dr,$$

where  $f(r)$  is a function which decreases to a minimum near the middle of the range. A step of sensation in a transverse direction will be given by

$$dS_\theta = \frac{F(\theta)}{r} d\theta,$$

where  $F(\theta)$  is chosen to bring the dotted curve of fig. 3 into agreement with the full curve. But, from the point of view of getting at the mechanism, at present it seems neither profitable to seek the exact form of these functions nor to investigate the connexion of  $dS_r$  and  $dS_\theta$  with the resultant step.

In the conventional representation of the colour triangle white is placed at the centroid, and the units are then said to be of "equal sensation value." No further definition has been given of what this phrase means. But the procedure has been due to the sound instinct to space difference in colour over the diagram as uniformly as possible. And the shape of the spectrum curve obtained in this way bears a rough resemblance to the curve obtained by the exact procedure of this paper and represented in fig. 7.

CIV. *Energies of Electrons in Gases.* By J. S. TOWNSEND,  
M.A., Wykeham Professor of Physics, Oxford\*.

1. THE investigations of the electrical properties of gases which have been carried out at the Electrical Laboratory, Oxford, include many experiments connected with phenomena observed with currents of various intensities when the mean energy of agitation of the electrons is of the order of the amount of energy corresponding to a potential of 5 volts.

In the experiments on the determination of the motion of electrons in gases with photo-electric currents it was found that, after the electrons have traversed a certain distance through a gas under the action of an electric force, a steady state of motion is established, where the mean energy of agitation  $E_1$  of the electrons and the mean velocity  $W_1$  in the direction of the electric force are functions of the ratio of the electric force  $Z$  to the gas-pressure  $p$ .

The energy  $E_1$  and the velocity  $W_1$  were thus obtained experimentally in terms of the ratio  $Z/p$ , without making any hypothesis as to the lengths of the mean free path or the amount of energy lost in a collision†.

The mean free path  $l$  and the mean loss of energy  $\lambda \cdot E_1$  of electrons in collisions with molecules of the gas may be found by the theory of the motion, in terms of the velocities  $W_1$  and the energy  $E_1$ .

The numerical factors that occur in the formulæ from which  $l$  and  $\lambda$  are derived have not been determined to a high degree of accuracy, but the most interesting results obtained from the experiments do not depend on the numerical factors, as they give the changes in  $l$  and  $\lambda$  obtained with different values of  $E_1$ , and the relative values of these quantities in different gases.

2. In each gas there is a range of forces and pressures where the coefficient  $\lambda$  and the mean free path at unit pressure  $L = l \times p$  are approximately constant. These

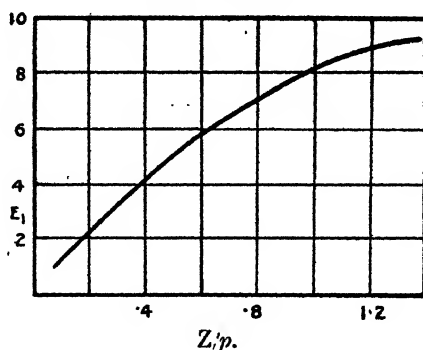
\* Communicated by the Author.

† A general description of these experiments and the tables of results obtained with several gases are given in the pamphlet on the 'Motion of Electrons in Gases.' Clarendon Press, Oxford.

ranges are well marked in helium \* and in neon †, where the mean energy of agitation  $E_1$  is approximately proportional to the ratio  $Z/p$ . At the upper limit to this range in neon,  $\lambda$  is approximately  $7 \times 10^{-5}$ , and the mean energy of agitation of the electrons is about 4 volts. In helium the upper limit to this range is near the point where the mean energy of agitation is 4 volts and  $\lambda$  is approximately  $2.5 \times 10^{-4}$ . With larger energies of agitation the values of  $\lambda$  are considerably increased, and the increases may be attributed to losses of energy in large amounts in some of the collisions where the kinetic energy of the electrons is much greater than the mean energy.

The effect of large losses of energy in neon and in helium may be seen directly from the curves (figs. 1 and 2), which give the mean energy of agitation  $E_1$  in the steady state

Fig. 1.—Neon.



of motion as found experimentally in terms of the ratio  $Z/p$ . The ordinates of the curves give the values of  $E_1$  in volts, and the abscissae the ratio  $Z/p$ ,  $Z$  being in volts per centimetre and  $p$  in millimetres of mercury.

In each gas there is a considerable portion of the curve which is almost in a straight line, and within this range the changes in  $L$  and  $\lambda$  are small. With the larger energies of agitation the rate of increase of  $E_1$  with  $Z/p$  diminishes, as is shown by the change of the slope of the curves. This indicates that the proportion of the energy of electrons which is lost in collisions increases with the energy of agitation.

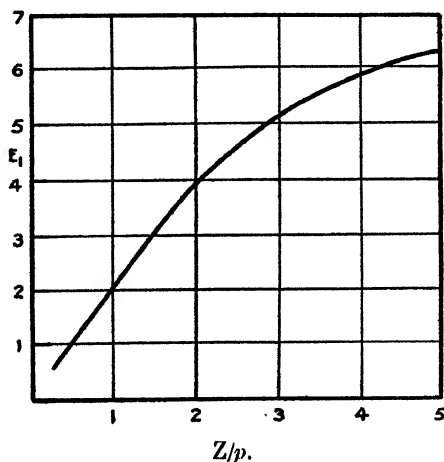
\* J. S. Townsend and V. A. Bailey, *Phil. Mag.* xlv. p. 657. (Oct. 1923).

† V. A. Bailey, *Phil. Mag.* xlvii. p. 379 (1924).

The curve (fig. 1), which gives the energy of agitation of electrons in neon, is approximately a straight line ( $E_1=10.5 \times Z/p$ ) from the point where  $E_1$  is 2 volts to  $E_1=4$  volts. At the point  $Z/p=.8$  the mean energy of agitation is 7.2 volts, which differs considerably from 8.4 volts, to be expected if there were no change in the proportion of the energy of an electron that is lost in a collision. This indicates that the energy of agitation of a considerable proportion of the total number of electrons is much below 7.2 volts.

The energies of agitation of electrons in helium are given by the curve (fig. 2). This curve is approximately in a straight line ( $E_1=2 \times Z/p$ ) from the point  $E_1=2$  volts

Fig. 2.—Helium.



to  $E_1=4$  volts. The energy of agitation is 4.7 volts at the point where  $Z/p=2.6$ , which is much below the 5.2 volts to be expected if  $\lambda$  were constant.

These results may be explained by the theory of ionization by collision as given by the author many years ago. In some of the collisions with the larger velocities of agitation the atoms acquire energy from the electrons in large amounts which may cause them to radiate, and in others the atoms may be ionized. But the transfer of energy in amounts which produce these effects occurs only in a small proportion of the total number of collisions with large energies of agitation.

3. This theory of ionization by collision gives a satisfactory explanation of luminous discharges which are maintained when the ratio of the electric force to the pressure of the gas is comparatively small\*.

This may be seen in a direct-current discharge in a long, wide tube containing gas at a few millimetres pressure. In the uniform positive column of the discharge where the current is maintained by the ionization of the gas the electric force is comparatively small.

Recent experiments† with high-frequency discharges of constant amplitude have also shown that the currents in long tubes which are accompanied by a uniform luminous glow are also maintained with small electric forces.

The theory which has been given to account for the long luminous columns indicates that positive ions and electrons are lost by diffusion to the sides of the tube, and these losses are balanced by the supply provided by the process of ionization by collision. In wide tubes containing gases at a few millimetres pressure the losses due to diffusion are small, so that the supply required to maintain continuity is provided by the ionization of the gas obtained with a small electric force‡. The theory shows that the mean force, in a high-frequency discharge of constant amplitude, is the same as the force in the direct-current discharge. This result has been obtained experimentally with nitrogen§ and neon, but the experiments with neon have not yet been completed for publication.

4. The forces in the uniform luminous columns of high-frequency discharges have been determined by Hayman|| for neon and helium at various pressures in a tube 2.9 cm. in diameter.

The mean force  $Z$  which is independent of the current is given in volts per centimetre, and the pressure  $p$  in millimetres of mercury in Table I. for discharges in neon, and in Table II. for discharges in helium. The ratios  $Z/p$  are given in the third line of each table, and the

\* 'Electricity in Gases,' p. 440. Clarendon Press, Oxford (1915).

† J. S. Townsend and R. H. Donaldson, *Phil. Mag.* v. p. 178 (Jan. 1928).

‡ *Comptes Rendus*, t. 186, p. 55 (9th Jan., 1928).

§ J. S. Townsend and W. Nethercot, *Phil. Mag.* vii. p. 600 (March 1929).

|| R. L. Hayman, *Phil. Mag.* vi. p. 586 (March 1929).

values of  $E_1$  in volts corresponding to these values of  $Z/p$ , as obtained from the curves figures 1 and 2, are given in the fourth line.

These experiments were made in a quartz tube with external electrodes, so that it was possible to heat the whole tube to a very high temperature in order to remove impurities. The gases were carefully prepared, and the tube was washed out several times with pure gas before the measurements of forces in the discharges were made. As far as could be seen with a direct-vision spectroscope, there were no impurities in the gases. The light from

TABLE I.—Neon.

$p$ .....	60	40	20	10	5	2
$Z$ .....	28.5	21	11.5	7.0	4.4	3.5
$Z/p$ .....	.47	.52	.57	.7	.88	1.75
$E_1$ .....	4.8	5.2	5.6	6.4	7.5	—

TABLE II.—Helium.

$p$ .....	20	10	5	2	1
$Z$ .....	32	19	11.5	6.4	5
$Z/p$ .....	1.6	1.9	2.3	3.2	5
$E_1$ .....	3.2	3.8	4.3	5.3	6.4

the electrodeless discharge was examined in each experiment, as this method of detecting impurities was found to be much more sensitive than the ordinary method with a small spectroscopic tube \*. These determinations of the forces in luminous discharges in pure gases are therefore very reliable.

In the discharge in neon at 20 mm. pressure the ratio of the force to the pressure is 0.57, and the mean energy of agitation of the electrons is 5.6 volts. This is about the point where losses of energy in large amounts have a noticeable effect on the mean energy of agitation in neon, as shown by the curve (fig. 1).

\* J. S. Townsend and S. P. MacCallum, *Phil. Mag.* v. p. 695 (April 1928).

In the discharge in helium at 5 mm. pressure the ratio of the force to the pressure is 2.3, and the mean energy of agitation of the electrons is 4.3 volts, which is near the point where large losses of energy in helium are shown by the curve (fig. 2).

5. It does not appear that these experiments can be explained by any hypothesis in agreement with the laws governing the impact of an electron on a molecule of a gas that have been given by Franck and Hertz. These laws, as described by Jeans\* and Atkinson†, are said to be very accurate and satisfactory, and are adopted by many writers, without questioning their validity.

There are, however, many phenomena which conflict with these laws of impact, and, if the methods by which they have been deduced from experimental data be examined, it is found that the evidence in support of them is not convincing.

The losses of energy which occur in the collisions of electrons with atoms of helium when the kinetic energy of the electrons is below a certain critical value has been estimated by finding the amount of energy lost in a comparatively small number of collisions. In these experiments the electrons move in an accelerating field, and lose energy in collisions with atoms of the gas while traversing a certain distance in the direction of the electric force. The experiments show that a small proportion of the total number of electrons lose a small amount of energy in traversing the gas, and this result is interpreted on the hypothesis that all the other electrons lose exactly the same amount as those comprised in the group which were found to have lost a small amount. The possibility of losses being distributed about a mean value is not considered, although, according to the ordinary dynamical theory of gases, there are many causes which give rise to inequalities in the amounts of energy lost by different groups of electrons in moving through the same distance in a gas. Also, if some electrons had lost energy in collisions with atoms in very large amounts, these losses would not have been detected. These experiments, however, are frequently quoted as proving that the loss of energy of electrons in collisions with atoms of monatomic

\* Jeans, 'Report on Radiation and the Quantum Theory,' 2nd ed. (1924).

† Atkinson, Proc. Roy. Soc. A, cxix. p. 335 (1928).

gases is *exactly* the same as if the atoms were perfectly elastic, when the energy of an electron is below a certain value. This critical value is stated to be 19.77 volts in helium and approximately 16 volts in neon.

What has been measured experimentally is a lower limit to the amount of energy that electrons may lose under certain conditions; and if the result were reliable, there would be an upper limit to the energy that electrons can acquire while moving in helium under the action of an electric force. If the gas were at 5 mm. pressure and the force 11.5 volts per cm., this upper limit to the energy of agitation would be about 4.6 volts. It is easy to see that this interpretation conflicts with the results of many simple experiments.

6. The other laws governing the impacts of electrons with atoms relate to the large amounts of energy that electrons may lose in collisions. When the energy of an electron exceeds a certain amount, it may lose a large proportion of its energy in a collision with an atom.

According to the laws of impact now adopted by many writers, these losses of energy in large amounts occur immediately the kinetic energy of an electron attains a certain exact value. This value corresponds to a certain critical potential, and for each gas there are said to be several critical potentials which have been determined to a high degree of accuracy.

The critical potentials in helium and neon, and the properties of the gases with which they have been associated, are briefly as follows. In helium the lowest critical potential is 19.77 volts and the ionizing potential is about 25 volts. In neon the lowest critical potential is 16 volts and the ionizing potential 21 volts. In consequence of the absorption of energy in amounts corresponding to some of the critical potentials; the atoms are caused to radiate, and these potentials are called resonance potentials. The others are called metastable potentials. When the atoms absorb energy in the amounts corresponding to these potentials they are thrown into a metastable state. The metastable atoms do not radiate, but possess the property of ionizing molecules of impurities which may be present in the gas.

This process of ionization is known as the "Stosse zweiter Art," and it is supposed to be very effective, especially in



helium, as the first critical potential in that gas is a metastable potential. In neon there are several critical potentials nearly the same as the first critical potential, and there seems to be some uncertainty as to whether the first critical potential is a metastable potential or a resonance potential.

As far as this discussion is concerned, it is of no importance whether the first critical potential is a resonance potential or a metastable potential.

The first resonance potential corresponds to a line in the ultra-violet spectrum, and according to the theory the full number of lines in the visible spectrum is not attained until the electrons acquire energy in amounts which may be 1 or 2 volts less than the ionizing potential. In both gases the ionizing potential is said to be about 5 volts greater than the first critical potential, so that when the energy of an electron increases gradually as it moves under the action of an electric force, it may lose all its energy in collisions with atoms in amounts corresponding to the first critical potentials before it attains the energy corresponding to one of the higher critical potentials. Under certain circumstances, therefore, it would be impossible to ionize the gas or to obtain lines in the visible spectrum. The ranges of the electric force and gas-pressure in which this result may be expected depend on the probability of an electron losing its energy in a collision, and on the difference between the ionizing potential and the first critical potential.

In the experiments on which the theory is based, changes in currents are obtained in helium with potentials of about 20 volts and in neon with potentials of 16 volts, and opinions have differed from time to time as to whether these effects were due to ionization by collision or to radiation from the gas, or to impurities. The point on which the advocates of this theory have always agreed is that the atoms of helium have a remarkable power of absorbing energy in amounts of about 20 volts, and the atoms of neon in absorbing energy in amounts of 16 volts, so that when the kinetic energy of the electrons just exceeds these critical amounts, very few can retain their energy after a few collisions with atoms of the gas.

There now seems to be some agreement on this point, and these potentials are said to be either metastable

potentials or resonance potentials, and the ionizing potentials are about 5 volts greater in each gas.

7. If these laws be true, there could be no appreciable effect due to ionization by collision or appreciable intensity in lines in the visible spectrum when the ratio  $Z/p$  is of the order of the values obtained in discharges accompanied by a uniform glow, in gases at a few millimetres pressure.

This may be seen by estimating the number of electrons which obtain energies above 20 volts in helium, when the gas is at 2 mm. pressure and the electric force 5 volts per cm. In this case the mean energy of agitation of the electrons is about 5 volts.

The electrons that diffuse in the direction of the force acquire energies greater than the mean energy  $E_1$ , but the number that acquire energies of 19 or 20 volts is very small, since they lose energy so rapidly in the amounts  $\lambda \cdot E$ , when  $E$  is four times the mean energy. These numbers are given by the formulæ for the distribution of the energy of electrons in terms of the mean energy of agitation. Also, the probability  $P$  that the energy of an electron may increase from 20 to 24 volts is very small, even when no collision results in a loss of energy greater than  $\lambda \cdot E$ . This probability depends on the number of free paths that the electron traverses after attaining the energy of 20 volts. After traversing 160 free paths  $P$  is about  $1.5 \times 10^{-5}$ , after 200 free paths  $P$  is about  $4.5 \times 10^{-5}$ , and after 240 free paths  $P$  is about  $10^{-4}$ . The probability increases with the number of free paths, and attains a maximum value about  $8 \times 10^{-4}$  when the electrons have traversed 800 free paths. Thus the number of electrons that attain energies of 23 or 24 volts is very small even when there are no losses of energy in large amounts. These calculations also show that if there were losses of energy in large amounts in 10 per cent. of the collisions when the energy of an electron exceeds 20 volts, the energy that an electron could attain would be limited, and no appreciable number would attain energies of 21 to 22 volts. Under these conditions most of the lines in the visible spectrum would be absent, whether the gas were pure or impure.

8. It has been suggested that in these cases the conductivity is due to impurities which are ionized by the

process known as the "Stosse zweiter Art," even when the amount of impurity is so small that it cannot be detected spectroscopically. The theory is nevertheless unsatisfactory for many reasons\*. It indicates that it would be impossible to obtain the ordinary lines in the visible spectrum of a monatomic gas at a few millimetres pressure, and if the gas were pure it would be impossible to have ionization. Also, the amount of impurity required to maintain the conductivity would be proportioned to the current, so that considerable amounts of impurity would be required to maintain currents of the order of 10 milliamps. Under these conditions, it would be necessary to suppose that there is a continuous supply of impurity to the gas in a discharge-tube, as it has been found that the current tends to remove impurities from monatomic gases.

It is thus quite clear that the laws of impacts of electrons on atoms of monatomic gas as given by Franck and Hertz are not in agreement with the electrical properties of currents in wide tubes as found experimentally. Also, as far as radiation from the gas is concerned, these laws are unsatisfactory, since they indicate that the lines in the visible spectrum of monatomic gases would not be excited, under the conditions in which bright luminous columns of gas are obtained in discharge-tubes.

It may also be seen that these modern theories of critical potentials are not based on reliable experimental evidence. The experiments which are quoted in support of them depend on the interpretation of effects observed at the boundary of a space containing a gas, when large currents of electrons are projected into the space through apertures in the boundary. It is supposed that the kinetic energies of the electrons in the collisions with molecules of the gas are the same as the kinetic energy with which the electrons enter the gas. No allowance is made for the effect of the negative charge in the gas due to the accumulation of electrons. This charge exerts a repulsive force which reduces the kinetic energy of the electrons so that the energy of the electrons when they collide with molecules of the gas is less than the energy at the boundary. Also, the reduction of the

\* J. S. Townsend and S. P. MacCallum, *Proc. Roy. Soc. A*, cxxiv. (1929).

energy is continuous as the electrons move from the boundary into the gas, so that no large proportion of the electrons collide with any particular velocity. Under these conditions it cannot be maintained that the potentials of the electrons as they enter the gas represent amounts of energy coinciding with critical properties of molecules.

9. In the experiments which have been made to determine the mean energy of agitation the electrons move in a uniform electric field, and the currents are small, so that there is no appreciable charge in the gas. The electric force is therefore undisturbed by the current, and the mean energy of agitation  $E_1$  is found accurately in terms of the ratio  $Z/p$ . These results give the mean energy of agitation in other experiments where the ratio  $Z/p$  can be found experimentally, but many phenomena which are observed in gases depend on the distribution of energy about the mean.

It is clear that in many discharges ionization by collision is due to electrons which have energies greater than the mean, and the experiments with electrodeless discharges also show that the colour of the discharge depends on the distribution of the energies of electrons. In neon the colour is red at the higher gas-pressures and changes to yellow as the pressure is reduced. In helium the colour is yellow at high pressures and becomes bright green as the pressure is reduced. Since the forces in these discharges have been determined experimentally, the changes in the intensities of the lines of the spectrum of the gas may be found in terms of the changes in the energy of agitation. The experiments show that the lines of long wave-lengths are very intense compared with those of short wave-lengths when the kinetic energy of the electrons is small, and as the kinetic energy increases, the intensities of short waves increase in comparison with the long waves.

These observations are in accordance with a theory of the radiation from a discharge which was well known many years ago.

It is therefore of interest to determine the rate at which electrons tend to acquire the mean energy of agitation, and the disturbing effects which cause some of the elec-

trons to have energies which exceed the mean energy by definite factors.

10. The kinetic energy of an electron in a gas depends on the amount of energy transferred in collisions and the number of collisions with molecules when the electron traverses a given distance in the direction of the electric force. Electrons may gain or lose energy in collisions, but the amounts of energy lost are generally greater than the amounts gained, so that the average effect of a large number of collisions may be represented by a loss of energy which is proportional to the kinetic energy  $E$  of the electron. If  $\lambda E$  be the average loss of energy in a collision, the coefficient  $\lambda$  is a small fraction, and the amounts of energy that may be lost or gained in collisions is much greater than  $\lambda E$  \*. Thus different groups of electrons may lose amounts of energy which are widely different from the average loss of energy, in traversing a given distance in the direction of the electric force even if all the electrons collided with the same number of molecules.

Under some conditions there are considerable differences in the numbers of collisions of electrons with molecules of the gas, since electrons may traverse several consecutive free paths which on an average may be either longer or shorter than the mean free path ( $l$ ). When the total number of collisions with molecules is not very large, there are large inequalities in the amounts of energy lost by electrons due to these causes.

11. In general, when electrons move in a field of force the motion is automatically regulated, so that in moving through a given distance in the direction of the force the number of collisions of an electron with molecules of a gas is proportional to the kinetic energy of the electron. Thus electrons with large energies of agitation tend to lose much more energy in moving through a given distance in the direction of the force than do those with small energies.

This controlling action has an equalizing effect which brings the mean energy of agitation of a group of electrons to a definite fixed value when the electrons move in a uniform electric field.

\* Proc. Roy. Soc. A, cxx. p. 511 (1928).

The inequalities arising from variations of the free paths about the mean free path  $l$  and the variations of the losses of energy in collisions about the mean value  $\lambda \cdot E_1$  are therefore counteracted when the electrons move in the direction of the electric force so that no large deviations from the mean energy of agitation can arise from these causes.

12. The following investigation of the motion due to diffusion shows that there are wide differences in the velocities of different groups of electrons in the direction of an electric force, which are accompanied by large inequalities in the amounts of energy lost by the different groups.

The electrons that diffuse in the direction of the electric force traverse a given distance in that direction in a shorter time, and have fewer collisions with molecules, than the groups that move with the average velocity in the direction of the electric force. Thus some electrons gain energy by diffusion in the direction of the electric force, while others lose energy by diffusion in the opposite direction. In fact, the controlling action which regulates the general motion and causes the energies of different groups to approach a definite mean value, is in reality an average effect, which determines a steady state of motion where there is a distribution of energy about the mean energy of agitation due to diffusion. This distribution is independent of differences in the energies that may arise from other causes, and would be obtained if all losses of energy in collisions were equal to the mean loss of energy, and all free paths equal to the mean free path.

The effect of the controlling action which tends to equalize the energies of electrons will be considered first, in order to estimate the rates at which the mean energy of a group of electrons tends to approach a certain definite value  $E_1$  which depends on the ratio  $Z/p$ .

13. In order to simplify these investigations, it will be assumed that there are no large losses of energy in the collisions of electrons with molecules of the gas, in the amounts required to ionize atoms of the gas or to excite radiation. It will also be assumed that the energies of the electrons are large compared with the energy of agitation of a molecule of the gas; that the loss of energy

of an electron in a collision is  $\lambda \cdot E$ , where  $E$  is the energy of the electron and  $\lambda$  a constant; and that the mean free path  $L$  of an electron in the gas at unit pressure is also constant and the same for all values of  $E$ .

In order to calculate the energies of different groups of electrons, it is convenient to represent the mean energy  $E$  of a group in terms of the mean energy  $E_1$  of all the groups corresponding to the steady motion in a uniform electric field. Within the ranges of the electric forces and gas-pressures where  $\lambda$  and  $L$  are constant,  $E_1$  is proportional to the ratio  $Z/p$ . The number of collisions of electrons with molecules of the gas in the space between two planes perpendicular to the electric force  $Z$  may be represented in terms of the average number of collisions  $C$  of electrons in the steady state of motion, when the planes are at the distance apart ( $a$ ) where  $Zea = E_1$ .

Let  $W_1$  be the mean velocity of the electrons in the direction of the electric force,  $T$  the time  $a/W_1$ , and  $U_1$  the mean velocity of agitation in the steady state of motion. The total distance traversed by an electron moving with the velocity  $U_1$  in the time  $T$  is, is  $U_1 a/W_1$ , and this distance is  $C \times l$ , where  $l$  is the mean free path. The number  $C$  is therefore given in terms of  $U_1$  and  $W_1$  by the formula  $C = U_1 a/W_1 l$ .

For the purpose of these investigations it is not necessary to know the values of  $\lambda$  and  $C$ , but it is important to know the product  $\lambda \cdot C$ .

In the steady state of motion the mean energy of agitation of the electrons is constant, so that the energy ( $Zea$ ) gained by the electrons in moving through the distance ( $a$ ) in the direction of the force is equal to the energy lost in collisions which is approximately  $\lambda \cdot C \cdot E_1$ .

Since  $Zea = E_1$ , the relation between the constants  $\lambda$  and  $C$  is given approximately by the formula  $\lambda \times C = 1$ . The degree of accuracy of this formula depends on the distribution of the velocities of agitation about the mean velocity  $U_1$ , and for first approximations  $\lambda$  may be taken to be  $1/C$ .

Hence, if the potential difference  $Za$  between two planes is equal to the energy  $E_1$  expressed in volts, the average number of collisions of electrons with molecules of the gas in the space between the planes is the same for all values of  $Z$  and  $p$ , and approximately equal to  $1/\lambda$ .

14. The mean velocity  $W$  of a group of electrons in the direction of the electric force, which is proportional to  $Z$ , is given in terms of the mean velocity of agitation  $U$  by an equation of the form

$$W = \frac{Z}{p} \times \frac{e}{m} \times \frac{L}{U} \times h, \dots \dots \dots (1)$$

where  $h$  is a numerical constant depending on the distribution of the velocities about the mean value  $U$ . The value of  $h$  for the Maxwellian distribution is 0.815,  $U$  being the root of the mean square of the velocity ( $U = \sqrt{2E/m}$ ). The distribution of the velocities of electrons about the mean velocity  $U$  is not the same as in the Maxwellian distribution, and in order to determine  $h$  it is necessary to find an appropriate formula for the distribution of the velocities.

Equation (1) shows that  $W$  is inversely proportional to  $U$ , so that when the energy  $E$  of a group of electrons changes as the group moves under an electric force through a gas, the product  $U \times W$  is approximately constant and equal to  $U_1 \times W_1$ . In cases where the distribution of the energies about the mean energy changes as the electrons move through the gas, the product  $U \times W$  is not accurately the same as  $U_1 \times W_1$ , since the factor  $h$  in equation (1) changes with the distribution. This applies to a group which begins to move through a gas when the energies of the electrons are approximately the same, since the distribution of the energy in the first stages of the motion is not the same as in the final stages. For this reason the formulæ which are obtained on the hypothesis that the product  $U \times W$  is a constant are only approximate, though in some cases the results approach a high degree of accuracy.

15. If the kinetic energy of a group of electrons be small, the energy increases as the electrons move through the gas\*.

Let the electrons start from the plane  $z=0$ , and let  $E$  be the mean energy of agitation of the group in passing through a plane perpendicular to the electric force at a distance  $z$  from the origin. Also let  $dc$  be the average

\* Proc. Roy. Soc. A, lxxxi. p. 461 (1908).



number of collisions of an electron with molecules of the gas in the space between the two planes  $z$  and  $z+dz$ . The electrons traverse the space  $dz$  in the time  $dz/W$ , and the number of collisions is proportional to  $Udz/W$ . Since  $C$  is the average number of collisions in the space between two planes at a distance apart  $a$  when the velocities are  $U_1$  and  $W_1$ , the number  $dc$  is given by the formulæ

$$\frac{dc}{C} = \frac{dz}{a} \cdot \frac{U}{U_1} \cdot \frac{W_1}{W} = \frac{E}{E_1} \cdot \frac{dz}{a}, \dots \dots (2)$$

and the loss of energy in the collisions is

$$\lambda \cdot E \, dc = E^2 dz / a E_1. \dots \dots (3)$$

The rate of increase of  $E$  with  $z$  is given by the equation

$$\begin{aligned} dE &= Ze \, dz - E^2 dz / a E_1 \\ &= Ze(1 - E^2/E_1^2) \, dz, \dots \dots (4) \end{aligned}$$

which on integration gives

$$\log (E_1 + E) / (E_1 - E) = 2Zez/E_1 = 2z/a. \dots (5)$$

This equation is represented by Curve 1 (fig. 3), the ordinates being the ratios  $E/E_1$  and the abscissæ the ratios  $z/a$ .

If the energy of agitation  $E$  be greater than the energy corresponding to steady motion, the electrons lose energy as they move through the gas. The relation between  $E$  and  $z$  is then given by the equation

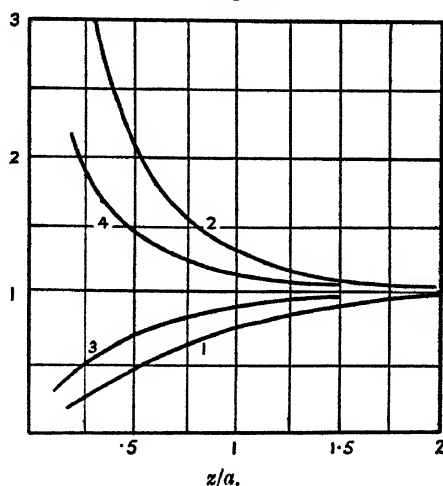
$$\log (E + E_1) / (E - E_1) = 2z/a, \dots \dots (6)$$

the constant of integration being chosen to make  $E$  very large compared with  $E_1$  at the plane  $z=0$ .

Equation (6) is represented by Curve 2 (fig. 3). It will be observed that the ordinates of Curve 2 are the reciprocals of the ordinates of Curve 1. The curves show that if the mean energy of the electrons in one group be  $0.25E_1$  and in another group  $4E_1$  at the plane  $z=0.55a$ , the energy of the first group increases and that of the second group diminishes as the electrons move in the direction of the electric force, so that at the plane  $z=0.55a$  the energies are  $.5E_1$  and  $2E_1$ , and at the plane  $z=2a$  the energies are  $.96E_1$  and  $1.04E_1$  in the two groups respectively.

16. The velocities of agitation of the two groups in passing a plane at the distance  $z$  from the origin are given by Curves 3 and 4 (fig. 3), the ordinates being the ratios  $U/U_1$  and the abscissæ the ratios  $z/a$ . These ordinates are the square roots of the ordinates of Curves 1 and 2 respectively. The time required for a group to traverse the distance  $dz$  is inversely proportional to  $W$  and therefore directly proportional to  $U$ . Hence the area between Curve 3 and the ordinates at the distances  $z_1$  and  $z_2$  from the origin is proportional to the time in which the first group moves through the distance  $(z_2 - z_1)$ , and the

Fig. 3.



Ordinates of Curves 1 and 2,  $E/E_1$ .  
Ordinates of Curves 3 and 4,  $U/U_1$ .

corresponding change in energy is given by the ordinates of Curve 1 at the points  $z_1$  and  $z_2$ .

Similarly the area between Curve 4 and the ordinates of two points of the curve gives the time in which a change of energy takes place in the second group. The unit of area represents the time  $T = a/W_1$ . The curves show that the energy of the first group increases from  $0.25E_1$  to  $0.5E_1$  in the time  $0.18 \times T$ , and the energy of the second group diminishes from  $4E_1$  to  $2E_1$  in the time  $0.5 \times T$ .

The velocities  $W$  for the two groups are given in terms of  $W_1$  by Curves 3 and 4, the ordinates being the ratios  $W/W_1$  for the groups with energies given by Curves 2 and 1 respectively.

Hence, in general when the energies of groups of electrons become large or small compared with the energy  $E_1$ , changes arise in the motion which tend to equalize the energies, so that the groups have approximately the same mean energy  $E_1$  after traversing the distance  $2a$  in the direction of the electric force.

17. In order to determine the effect of diffusion in causing inequalities in the energies of the electrons, the inequalities arising from variations of the free paths about the mean free path ( $l$ ) and variations of the losses of energy in collisions about the mean loss  $\lambda E_1$  may be left out of consideration.

In the actual motion in a field of force, different groups of electrons move with different velocities in the direction of the electric force. The distance that a group moves in that direction in the time  $dt$  is  $(W + w')dt$ ,  $W$  being the mean velocity due to the electric force and  $w'$  the velocity due to diffusion. The velocity  $w'$  is different for different groups of electrons, and in some groups containing small numbers of electrons  $w'$  may be very large compared with  $W$  for short intervals of time.

The motion of electrons in the direction  $z$  due to diffusion may be found by the theory of diffusion of particles where the coefficient of diffusion is taken to be constant. The space distribution at a given time may be expressed in terms of the number of free paths  $c$  traversed by the particles, and for this investigation it is convenient to express  $c$  in terms of the number  $C$  and the distances  $z$  in terms of  $a$ , where  $a$  is  $E_1/Z.e$ .

The ordinary equations of motion of electrons in an electric field of intensity  $Z$  may be written in the form

$$\frac{pw}{K} = -\frac{dp}{dz} + neZ, \quad . \quad . \quad . \quad . \quad (7)$$

where  $K$  is the coefficient of diffusion,  $n$  the number of electrons per cubic centimetre, and  $p$  the partial pressure of the electrons.

In the steady state of motion where  $E_1$  is the mean energy of agitation the partial pressure  $p$  is  $2nE_1/3$ , and  $w$  is the velocity  $W_1$  due to the electric force when  $dp/dz$  is zero.

Equation (7) therefore gives

$$K_1/W_1 = 2E_1/3Ze = 2a/3, \quad . \quad . \quad . \quad . \quad (8)$$

and the product  $4K_1T$  is therefore  $8a^2/3$ ,  $T$  being the time  $a/W_1$ , and  $K_1$  the mean coefficient of diffusion in the steady motion. This product may also be expressed in terms of the mean free path  $l$ ,  $4KT=4l^2C/3$ ,  $C$  being the number of free paths traversed by each electron in the time  $T$ .

Hence, if  $c$  be the number of free paths traversed in the time  $t$ , the product  $4K_1t$  is given in terms of the ratio  $c/C$  by the formula

$$4K_1t=8a^2c/3C \quad . \quad . \quad . \quad . \quad . \quad (9)$$

or

$$4K_1t=A c/C,$$

where  $A$  is  $8a^2/3$  or  $4l^2C/3$ .

18. The effect of diffusion in causing inequalities in the energies of agitation may be deduced from the space distribution due to diffusion when there is no electric force acting on the electrons. All the electrons may be supposed to be at the plane  $z=0$  at the time  $t=0$ , and it is required to find the motion due to diffusion when all the electrons are moving with a constant velocity of agitation. Under these conditions the coefficient of diffusion is constant and the same for each electron, and  $K$  may be taken to be equal to the mean coefficient of diffusion  $K_1$  in the steady state of motion.

The space distribution is thus obtained from the equation

$$\frac{dn}{dt} = K \cdot \frac{d^2n}{dz^2}, \quad . \quad . \quad . \quad . \quad . \quad (10)$$

$ndz$  being the number of electrons between the planes  $z$  and  $z+dz$  at the time  $t$ .

The solution of this equation, which satisfies the initial conditions, is

$$n/N=(4\pi Kt)^{-\frac{1}{2}}e^{-z^2/4Kt}, \quad . \quad . \quad . \quad . \quad . \quad (11)$$

which gives  $n=0$  for all values of  $z$  when  $t$  is zero except at the plane  $z=0$ . In this equation  $N$  is the total number of electrons which are near the plane  $z=0$  at the time  $t=0$ .

The ratio  $n/N$  is obtained in terms of  $z$ , and the number of free paths  $c$  traversed by the electrons in the time  $t$  by substituting in equation (11) the value of  $4Kt$  given by equation (9). Hence

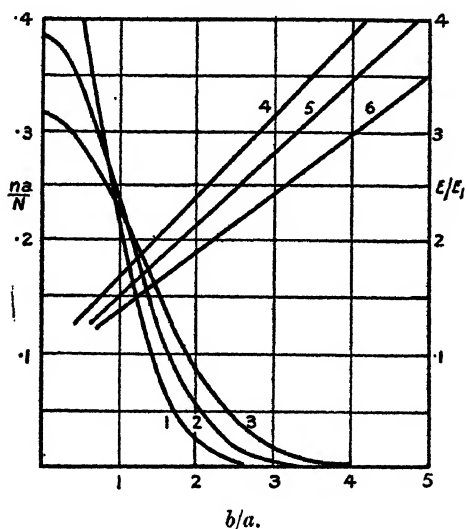
$$n/N=(8\pi c^2/3C)^{-\frac{1}{2}}e^{-3z^2C/8a^2c}. \quad . \quad . \quad . \quad . \quad (12)$$

19. The notation is simplified by writing  $f(t, z)$  and  $f(c, z)$  for the expressions on the right of equations (11) and (12) respectively.

Equation (11) gives the distribution at a given time  $t$  when the velocity of agitation is constant; but it is inconvenient to express the distribution in terms of  $t$ , since the energy of agitation of different groups of electrons changes when the motion takes place in an electric field.

Equation (12) gives the distribution after each electron has traversed a given number of free paths  $c$ . In this equation the distance  $z$  is the sum of the projections on

Fig. 4.



Ordinates of Curves 1, 2, 3,  $na/N$ .

Ordinates of Curves 4, 5, 6,  $E/E_1$ .

Curves 1 and 4,  $C_1 = .5 C$ .

Curves 2 and 5,  $C_1 = .8 C$ .

Curves 3 and 6,  $C_1 = 1.2 C$ .

the axis of  $z$  of the free paths of different electrons, the free paths being straight lines. This distribution is independent of the velocity of agitation, and equation (12) may be interpreted as giving the probability of the sum of the projections of the free paths being between the lengths  $z$  and  $z+dz$ . Equation (12) is therefore very convenient for determining the numbers in different groups when the motion takes place in an electric field.

The distribution given by equation (12) may be represented by a curve giving the positions of the electrons after traversing the number of free paths  $c$ . It is convenient to change the letter  $z$  in this equation to  $b$ , in order to indicate the distances of the electrons from the plane  $z=0$ , when each electron has traversed a given number of free paths  $c_1$ . The following expression is thus obtained for the ratio  $na/N$ ,

$$na/N = .346 \sqrt{C/c_1} \times e^{-1.2C/c_1 c_1}. \quad (13)$$

This equation is represented by Curves 1, 2, and 3 (fig. 4), which correspond to the three values of  $c_1$ , .5C, .8C, and 1.2C. (In neon the number C is approximately  $1.4 \times 10^4$ , and in helium  $4 \times 10^3$ .)

The ordinates of the curves are the ratios  $na/N^3$ , and the abscissæ the ratios  $b/a$ .

The curves show that the number of electrons that attain distances  $b$  greater than  $4a$  from the plane  $z=0$  is very small. When  $c_1$  is 1.2C the number that exceed this distance is  $8 \times 10^{-4}$ .

The mean distance  $\bar{b}$  from the plane  $z=0$  of the electrons ( $N/2$ ) on one side of the plane is

$$\bar{b} = 2 \int_0^\infty b f(c_1, b) db = a \sqrt{8c_1/3\pi C}. \quad (14)$$

When  $c_1$  is equal to C,  $\bar{b}$  is  $.92 \times a$ .

20. The electrons which diffuse from the plane  $z=0$  may be divided into groups which are at different distances  $b$  from the plane  $z=0$  when the number of free paths  $c_1$  have been traversed. In order to estimate the loss of energy in collisions, it is necessary to find the mean distance of a group from the plane  $z=0$  when a proportion  $c/c_1$  of the free paths have been traversed by each electron. Let  $n_1 db$  be the number of electrons in the group between the planes  $z=b$  and  $z=b+db$  after the number of free paths  $c_1$  have been traversed,  $n_1 db = N \times f(c_1 b) db$ ; also let  $c+c'=c_1$ .

The number of electrons in the space between the planes  $z$  and  $z+dz$  after the total number  $N$  have traversed the number of free paths  $c$  is  $ndz = N \times f(c, z) dz$ , which includes some of the electrons belonging to the group  $n_1 db$ . The number that belong to the group  $n_1 db$  is obtained by multiplying  $ndz$  by  $f(c', (b-z)) db$ , since the

electrons that belong to the group  $n_1 db$  must be at the distance  $(b-z)$  from the plane  $z$  when the remainder  $c'$  of the free paths have been traversed.

Let  $z=(bc/c_1+x)$ ,  $(b-z)=(bc'/c_1-x)$ , and  $dz=dx$ . When these values are substituted for  $z$ ,  $b-z$ , and  $dz$  in the above expressions, the number of electrons belonging to the group  $n_1 db$  which are between the planes  $z$  and  $z+dz$  after traversing the number  $c$  of free paths is

$$N dx db \times f(c, (cb/c_1+x)) \times f(c', (c'b/c_1-x)).$$

This expression may be written in the form

$$N \times (\pi A c_1)^{-\frac{1}{2}} e^{-b^2/\Delta c} db \times (\pi A c c'/c_1)^{-\frac{1}{2}} e^{-c_1 z^2/\Delta c c'} dx,$$

which reduces to

$$n_1 db \times f(cc'/c_1, x) dx. \quad . \quad . \quad . \quad (14)$$

These expressions show that the group  $n_1 db$  is distributed symmetrically about the plane  $z=cb/c_1$  when the electrons have traversed the number of free paths  $c$ . Thus  $dz=bdc/c_1$ ,  $z$  being the mean distance of the group from the plane  $z=0$ .

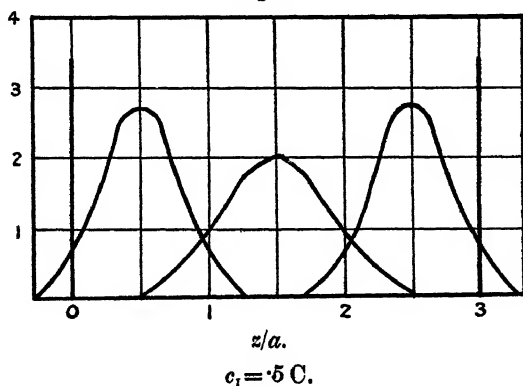
Also the distribution of the group about the central plane is the same as that attained when electrons diffusing from the plane have traversed the number of free paths  $cc'/c_1$ . Thus as the group moves away from the plane  $z=0$  the mean distance from the central plane increases and attains the maximum value  $a\sqrt{2c_1/3\pi C}$ , when  $c=c_1/2$ , and the central plane is at the distance  $b/2$  from the plane  $z=0$ . When the group passes through this position, the mean distance of the group from the central plane diminishes, and the electrons collect together as the central plane approaches the plane  $z=b$ .

21. The above results may also be obtained by taking the distributions as given in terms of the time  $t$  by equation 11, when the velocity of agitation is constant. The group of electrons  $n_1 db$  which are between the planes  $z=b$  and  $z=b+db$  at the time  $t_1$  is symmetrically distributed about the plane  $z=tb/t_1$  at any time  $t$  less than  $t_1$ . Thus the mean velocity of the group is a constant and equal to  $b/t_1$  while passing from the plane  $z=0$  to  $z=b$ . At any time  $t$  greater than  $t_1$  all directions of motion of the electron in the group  $n_1 db$  are equally probable, and the mean velocity of the group due to diffusion is zero.

These results are represented by the curves (fig. 5) which give the distributions of the group  $n_1 db$ , in three positions between the planes  $z=0$  and  $z=b$ . The distance  $b$  is taken as being  $3a$  and the total number of free paths  $c_1$  as  $C/2$ .

The ordinates of the curves are proportional to the numbers of electrons at the planes  $z$ , and the abscissæ are the ratios  $z/a$ . Curve 1 represents the distribution when the number of free paths  $c$  traversed by the electrons is  $c_1/6$ , and Curve 3, which is similar to Curve 1, gives the distribution when  $c$  is  $5c_1/6$ . The mean distance of the distribution from the central plane in these positions is  $\bar{x}=0.24 \times a$ . Curve 2 represents the distribution when  $c$  is  $c_1/2$ , the central plane being at the distance  $1.5a$  from

Fig. 5.



Motion of Group  $n_1 db$ .

the plane  $z=0$ . In this position the mean distance of the group from the central plane is  $x=0.325a$ .

22. When electrons start from a plane  $z=0$  and move in an electric field, the change of energy of different groups of electrons depends on the rate of diffusion in the direction of the electric force. The change in energy may be estimated in terms of the distance  $b$  that the electrons diffuse in the direction of the electric force while traversing a given number of free paths  $c_1$ . If all the electrons ( $N$ ) start with the same kinetic energy  $E_1$ , the numbers  $n_1 db$  in the groups that have approximately the same energy after traversing the given number of free paths  $c_1$  are given by equation (12) ( $n_1 db = Ndbf(c_1, b)$ ).



In order to find the rate of change of energy of the group ( $n_1 db$ ), as the electrons move away from the plane  $z=0$ , let the central plane of the group move through the distance  $dz$  while the electrons traverse the number of free paths  $dc$ . The mean increase of energy  $dE$  of the group is therefore

$$dE = Ze dz - \lambda E dc, \quad \dots \quad (15)$$

at any time during the motion while  $c$  is less than  $c_1$ .

The distance  $dz$  includes the distance  $bdc/c_1$  that the electrons diffuse, and the distance that the electrons move owing to the action of the electric force. The latter distance is the distance  $dz$  given by equation (2) in terms of  $dc$ , and is equal to  $aE_1 dc/EC$ .

Thus the distance  $dz$  in equation (15) is

$$dz = b dc/c_1 + aE_1 dc/EC. \quad \dots \quad (16)$$

Hence  $dE$  may be expressed either in terms of  $dz$  or  $dc$ . The latter is the most convenient variable to take, since the limits of integration are from  $c=0$  to  $c=c_1$ , and the number  $n_1$  is expressed in terms of  $c_1$  by equation (12).

Equation (15) thus becomes

$$dE = Ze(b/c_1 + aE_1/EC) dc - E dc/C$$

or

$$EdE = (EE_1 bC/ac_1 + E_1^2 - E^2) dc/C. \quad \dots \quad (17)$$

Let the constant  $bC/ac_1$  be represented by the expression  $(y-1/y)$ , where  $y$  is greater than unity, so that equation (17) becomes

$$EdE = (E_1 + yE)(E_1 - E/y)dc/C, \quad \dots \quad (18)$$

which on integration gives

$$\frac{y}{y^2 + 1} \left( y \log \left( \frac{yE_1 - E}{yE_1 - E} \right) - \frac{1}{y} \log \left( \frac{E_1 + yE}{E_1 + yE} \right) \right) = \frac{c}{C}, \quad (19)$$

$E_1$  being taken as the value of  $E$  when  $c=0$ .

This equation gives the values of  $E$  for the electrons in the group  $n_1 db = Ndbf(c_1, b)$  in terms of  $c$ , the number  $c_1$  which occurs in the constant  $bC/ac_1$  being the maximum value of  $c$ .

23. Equation (19) may be represented by a curve giving  $E/E_1$  in terms of  $c/C$  for a group corresponding to a given value of  $y$ . The curves thus obtained for eight

different values of  $y$  (or eight different groups of electrons) are given in fig. 6, the ordinates being the ratios  $E/E_1$  and the abscissæ the ratios  $c/C$ .

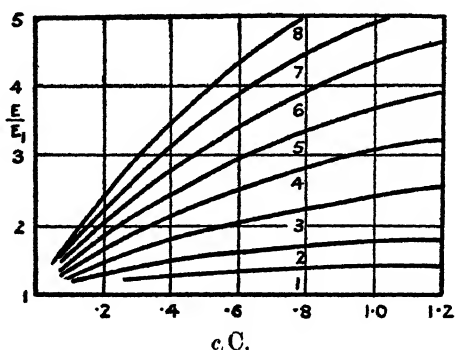
The values of  $y$  are 1.5, 2, 3, etc. . . . 8, and the corresponding values of  $bC/ac_1$  for the eight groups are (1.5—.66), (2—1/2), (3—1/3), and . . . (8—1/8).

The values of  $E/E_1$  for the different groups when all the electrons have traversed a given number of free paths  $c_1$  are given by the ordinates of the eight curves at the points when the abscissæ are equal to  $c_1/C$ , and the values of  $b/a$  for the different groups are obtained from the equation

$$b/a = (y - 1/y)c_1/C. \quad (20)$$

The results thus obtained when  $c_1$  is .8C are given in Table III.

Fig. 6



A similar set of figures may be obtained for any other value of  $c_1$  from the curves (fig. 6).

24. The values of  $E/E_1$  corresponding to the three values of  $c_1$ , .5C, .8C, and 1.2C are given in terms of the ratio  $b/a$  by Curves 4, 5, and 6 (fig. 4).

The ordinates are the ratios  $E/E_1$ , and the scale is given by the figures to the right of the diagram. The abscissæ are the ratios  $b/a$ , the scale being the same as for Curves 1, 2, and 3.

Thus the pair of Curves 1 and 4 give the numbers of electrons and the energies of the electrons in the different groups when the number of free paths traversed by each

electron is 0.5 C. Similar results are given by the pair of Curves 2 and 5 when the number of free paths traversed by the electrons is 0.8 C, and by the pair of Curves 3 and 6 when the number of free paths is 1.2 C.

The curves, 4, 5, and 6 are almost exactly straight lines for the values of the ratio  $E/E_1$  exceeding 1.2.

The equations of the lines are

$$\left. \begin{aligned} \text{Curve 4: } c_1 &= .5 \text{ C, } E/E_1 = .95 + .74 b/a, \\ \text{Curve 5: } c_1 &= .8 \text{ C, } E/E_1 = .85 + .65 b/a, \\ \text{Curve 6: } c_1 &= 1.2 \text{ C, } E/E_1 = .85 + .53 b/a. \end{aligned} \right\} \dots (21)$$

The agreement between these expressions for  $E/E_1$ , and the values of  $E/E_1$  obtained from Curves (fig. 6),

TABLE III.—( $c_1 = .8 \text{ C}$ ).

$y$ .	$b/a$ .	$E/E_1$ .	$.85 + .65b/a$ .
1.5.....	.66	1.32	1.28
2.....	1.20	1.65	1.63
3.....	2.14	2.25	2.24
4.....	3.0	2.80	2.80
5.....	3.84	3.34	3.34
6.....	4.67	3.86	3.88
7.....	5.5	4.4	4.42
8.....	6.3	4.95	4.93

is shown by the numbers in the last column of Table III. These numbers are the values of  $(.85 + .65b/a)$ , and are almost exactly the same as the values of  $E/E_1$  given in the third column of the table.

25. The equations of Curves 1, 2, and 3 (fig. 4) are given by equation (13). Thus the equation of Curve 2, where  $c_1 = 0.8 \text{ C}$ , is

$$na/N = .385 \times e^{-L^2/a^2 \times 2.13}, \dots (22)$$

and the number of electrons  $n_1 db$  in the group where the abscissæ are between  $b/a$  and  $(b+db)/a$  is

$$n_1 db = 0.385 N \times e^{-b^2/a^2 \times 2.13} db/a. \dots (23)$$

Let  $\Delta n$  be the number in the group where the energies are between the values  $E$  and  $E+dE$  after each electron has traversed the number of free paths  $c_1$ . Since the

values of  $b/a$  are given in terms of  $E/E_1$  by equations (21), the number  $\Delta n$  may be expressed in terms of  $E$  and  $dE$ .

When  $c_1$  is  $\cdot 8C$ , the expression for  $\Delta N$  obtained by substituting  $(E/E_1 - \cdot 85)/\cdot 65$  for  $b/a$  on the right of equation (23) is

$$\Delta N = 0\cdot 6 \times N \times e^{-1\cdot 1(E/E_1 - \cdot 85)^2} \times dE/E_1. \quad (24)$$

The formulæ corresponding to values of  $c_1$  from  $\cdot 8C$  to  $1\cdot 2C$  are exactly the same. Thus there is a considerable range of values of  $c_1$  where the distribution is constant, so that in the steady state of motion the numbers of electrons with energies exceeding  $1\cdot 2E_1$  are given by equation (24).

26. In the initial stages of the motion, when a number of electrons begin to move under the action of an electric force with the same kinetic energy  $E_1$ , very few electrons attain energies which are much greater than  $E_1$ . This investigation shows that the distribution given by equation (24) is not fully attained at the stage where all the electrons have traversed the number of free paths  $\cdot 5C$ . In the formula for  $\Delta N$  corresponding to the value of  $c_1 = \cdot 5C$  the logarithm of the exponential term is  $-1\cdot 36(E/E_1 - \cdot 95)^2$ , so that for the larger values of  $E/E_1$  the number  $\Delta N$  is less than that obtained when  $c_1$  is  $0\cdot 8C$ .

For values of  $c_1$  that are large compared with  $C$ , the groups with large energies are not separated in space from those with smaller energies, so that the distribution of energy is not represented in terms of  $b/a$  by equation (12). This is seen from the formulæ for  $\Delta N$ , corresponding to values of  $c_1$  greater than  $1\cdot 2C$ . The divergence from equation (24) begins to be appreciable when  $c_1$  is  $1\cdot 4 \times C$ , the logarithm of the exponential term being  $1\cdot 1(E/E_1 - 0\cdot 75)^2$  for this value of  $c_1$ .

27. The investigation shows that the final distribution is a function of the ratio  $E/E_1$ , which is the same for all gases and independent of the force  $Z$  and the pressure  $p$  of the gas, since the values of  $\lambda$ ,  $l$ ,  $Z$ , and  $p$  are not involved in the formulæ for  $\Delta N$ .

28. It is convenient to have a simple method of finding the proportion of the electrons with a given energy  $x_1 E_1$  that acquire energies greater than  $x_2 E_1$  after each electron

has traversed a given number of free paths  $c_1$ , when  $(x_2 - x_1)$  is small compared with  $(x_1 + x_2)$ . Let  $N$  be the total number of electrons with the energy  $x_1 E_1$ ,  $N_1$  the number that acquire energies greater than  $x_2 E_1$ , and let the motion along the free paths begin at the plane  $z=0$ . The distribution due to diffusion after each electron has traversed the given number  $c_1$  of free paths is given by equation (13) in terms of the ratio  $b/a$ . The electrons which acquire energies greater than  $x_2 E$  are at distances  $b$  from the plane  $z=0$ , which exceed a certain value.

The number  $N_1$  is found by integrating  $ndb$  (equation (13)); and since this quality is given in the form  $N \pi \int_0^\infty e^{-s} ds$ ,  $N_1/N$  is obtained from tables of the integrals of the function  $e^{-s} ds$ .

The value of  $b/a$  for the group which attain the energy  $x_2 E_1$  is obtained from equation (17) by taking  $dE$  to be  $(x_2 - x_1)E_1$ ,  $dc$  to be  $c_1$ , and  $E$  to be the average energy  $(x_1 + x_2) E_1/2$ . The following equation is thus obtained:

$$b/a = x_2 - x_1 + ((x_1 + x_2)/2 - 2/(x_1 + x_2))c_1/C, \quad (25)$$

which gives the lower limit of  $b/a$  in the integral

$$\int_b^\infty ndb = N_1.$$

The ratio  $N_1/N$  increases with  $c_1$ , when  $c_1/C$  is a small fraction, and attains a maximum value for a certain value of  $c_1$  depending on  $x_1$  and  $x_2$ . Equation (13) shows that  $N_1$  depends on the quantity  $b^2 C/a^2 c_1$  which occurs in the exponential term, and the minimum value of this quantity as obtained from equation (25) is

$$(b^2 C/a^2 c_1) = 2(x_2 - x_1)(x_1 + x_2 - 4/(x_1 + x_2)), \quad (26)$$

the corresponding value of  $c_1/C$  being

$$(c_1/C) = (x_2 - x_1)/(x_1 + x_2)/2 - 2/(x_1 + x_2)$$

and

$$(b/a) = 2(x_2 - x_1).$$

As an example of these formulæ, the electrons may be supposed to be moving in helium where the number  $C$  is approximately 4000, and that the energy of a group of  $N$  is  $4E_1$ . After each electron in this group has traversed 200 free paths,  $c_1/C = 1/20$ , the number  $N_1$  that have acquired energies greater than  $5E_1$  is  $1.6 \times N \times 10^{-6}$ .

The number  $N_1$  increases with  $c_1$  and attains a maximum value  $2 \times N \times 10^{-4}$  when  $c_1/C$  is  $1/4.3$ .

29. The accuracy of the formulæ for the distribution of the energy  $E$  about the mean energy  $E_1$  obtained by this method depends principally on the accuracy to which the product  $\lambda \times C$  may be found. A rough calculation shows that  $\lambda$  is less than  $1/C$ , and that the relation between  $\lambda$  and  $C$  is given more accurately by the formulæ  $\lambda = 1/1.1 \times C$ . As a first step towards finding a more accurate expression for the distribution of the energy,  $\lambda$  may be taken to be  $1/1.1 \times C$  instead of  $1/C$ , and this has the advantage of giving an expression for  $\Delta N$  which is simpler than the expression in the formulæ (24). This change affects equations (16) to (21), since they were obtained by substituting  $1/C$  for  $\lambda$  in equation (15). If  $1.1 C$  be substituted for  $C$  in these equations, it is found that the value of  $b/a = (E/E_1 - .85)/.65$  corresponds to the number of collisions  $c_1$  which is given in terms  $C$  by the formulæ  $c_1 = 0.88 C$ . When these values of  $b/a$  and  $c_1$  are substituted in equation (13), the following equation for  $\Delta N$  is obtained instead of equation (24):

$$\Delta N = N \pi^{-\frac{1}{2}} e^{-(E/E_1 - .85)^2} dE/E_1. \quad . \quad . \quad . \quad (27)$$

The number of electrons ( $N, E$ ) with energies greater than  $E$  is obtained by integrating equation (27). Table IV. gives the proportion  $(N, E)/N$  of the total number with energies exceeding the mean energy  $E_1$  by the factors given in the first line of the table.

TABLE IV.

$E/E_1 \dots$	1.5	2	2.5	3	3.5	4	4.5
$(N, E)/N \dots$	0.18	0.05	0.01	$1.2 \times 10^{-3}$	$9 \times 10^{-5}$	$5 \times 10^{-6}$	$1.5 \times 10^{-7}$

The figures show that only 1 per cent. of the total number  $N$  have energies greater than  $2.5 E_1$ . The average energy of the electrons with energies greater than  $E_1$  is  $1.5 E_1$  approximately.

There are other points of interest in connexion with this method of investigating the distribution of energy which will be considered in another paper.

CV. *Elastic Impact of a Pianoforte Hammer.*

By R. N. GHOSH, D.Sc.\*

[Plate XII.]

IN a series of papers † the author has shown that, in the case of felt hammers, the duration of contact of the hammer with the string, the displacement of the striking point, and the velocity of rebound can be calculated from the theory presented by him. In this theory the hammer was considered to be slightly elastic, and the free vibrations of the short portions of the string between the nearer fixed end and the striking point were considered to be negligible. Recent experiments ‡ show that slight modification is required in order that the theory may be applicable (1) when the free vibrations are finite, and (2) when the impact is very elastic.

It is found in case (1) that when the hammer is slightly elastic the pressure does not rise and fall continuously, but by jumps at  $\tau$ ,  $2\tau$ ,  $3\tau$ , etc., where

$$\tau = \frac{2a}{c},$$

where  $a$  = striking distance and  $c$  = transverse wave velocity.

The introduction of greater softness simply diminishes the sharp rise. For the sake of comparison two curves showing the relation between pressure and time during contact have been appended in this paper.

*Previous Results.*

The earliest theory was given by Helmholtz §, who assumed that the duration of contact was a very small fraction of the period of vibration of the whole string. Kaufmann ||, however, showed that the string is appreciably displaced during impact, and gave a theory for a hard hammer when the striking point was close to a fixed end. He assumed that the short portion of the string takes up a form during impact

$$y_1 = f(ct) \frac{x}{a}, \quad . . . . . (1)$$

\* Communicated by Prof. M. N. Saha, F.R.S.

† Phys. Rev. xxviii. p. 458 (1926).

‡ Phil. Mag. vii. p. 346 (1929).

§ Ellis, 'Sensation of Tone' (Translation), p. 380.

|| Ann. der Physik, liv. p. 675 (1895).

and on the longer side

$$y_2 = f(ct - x + a). \quad (2)$$

Profs. Raman\* and Banerji, however, gave a general theory for any striking distance, assuming that the form of the string is given by

$$\left. \begin{aligned} y_1 &= A_k \sin kx \sin k(l-a), & 0 < x < a \\ y_2 &= A_k \sin k(l-x) \sin ka, & a < x < l \end{aligned} \right\} \quad (3)$$

Equations (3) assume that the wave reflected from the further end reaches the striking point during impact, which experiment shows is not always true. The present author extended Kaufmann's theory to the case of an elastic hammer, and arrived at the following formula † :

$$\left. \begin{aligned} q^2 &= \frac{T_0}{aM} \frac{1}{X} - \frac{1}{4} k^2, \\ k &= \frac{T_0}{Mc} \frac{1}{X}, \\ X &= \left(1 + \frac{T_0}{\mu a}\right). \end{aligned} \right\} \quad (4)$$

Among other theories, Das's functional formulæ may be mentioned here. Dr. W. H. George has made a comparative study of other theories, and a complete account will be found in his paper ‡.

In the present paper modifications are introduced on account of free vibrations of the short portion of the string mentioned in the introduction.

Let us first take the case of a slightly elastic hammer of effective mass  $M$  and elasticity  $\mu$ . Divide the total duration of impact into two parts, viz.: (1) the interval during which the hammer is in contact with the string but the latter is not displaced from its initial position, and (2) the interval when the string is shifted from its equilibrium position with a finite velocity. Let one end of the string be the origin of  $x$  axis and the striking distance be  $a$ . Let  $\zeta$  be the displacement of the hammer measured from the point of contact; then during the first interval the equation of motion of the hammer is given by

$$M\ddot{\zeta} = -\mu\zeta. \quad (5)$$

\* Proc. Roy. Soc. xcvii. p. 99 (1919).

† Phil. Mag. xlvii. p. 1141 (1924).

‡ Proc. Ind. Assoc. Calcutta, vii. p. 13, and subsequent papers (1920). Also Proc. Phys. Soc. London, xl. p. 30 (1927).



Hence

$$\zeta = \frac{V_0}{n} \sin nt, \quad \dots \dots \dots (6)$$

$n^2 = \frac{\mu}{M}$ , and  $V_0$  is the initial velocity of the hammer.

The pressure due to impact is given by

$$p_0 = V_0(M\mu)^{\frac{1}{2}} \sin nt. \quad \dots \dots \dots (7)$$

This state of affairs continues till a velocity wave of magnitude  $V_1 \frac{\text{cm.}}{\text{sec.}}$  is produced. This happens when the pressure is

$$p_1 = \frac{2T_0 V_1}{c}, \quad \dots \dots \dots (8)$$

$c$  being the transverse wave velocity and  $T_0$  the tension. And we find from (7) and (8) that the wave is generated at a time  $t_1$  given by

$$\tan nt_1 = 2 \left( \frac{T_0}{\mu} \frac{\rho}{M} \right)^{\frac{1}{2}}. \quad \dots \dots \dots (9)$$

For  $\frac{T_0}{\mu} = 2, \quad \rho = .028, \quad M = 6.6 \text{ grm.},$   
 $t_1 = 1.8 \times 10^{-5} \text{ sec.}$

Total duration of impact  $= .95 \times 10^{-2} \text{ sec.}$

During the second régime, we assume that the displacement of any point on the short portion of the string is given by

$$y_x = y_a \sum \frac{\sin kx}{\sin ka} + \sum P_r \sin \frac{r\pi x}{a} \sin \frac{r\pi ct'}{a}, \quad \dots \dots (10)$$

$t' = t - t_1$ ,  $y_a$  = displacement at  $x = a$ . While on the longer side

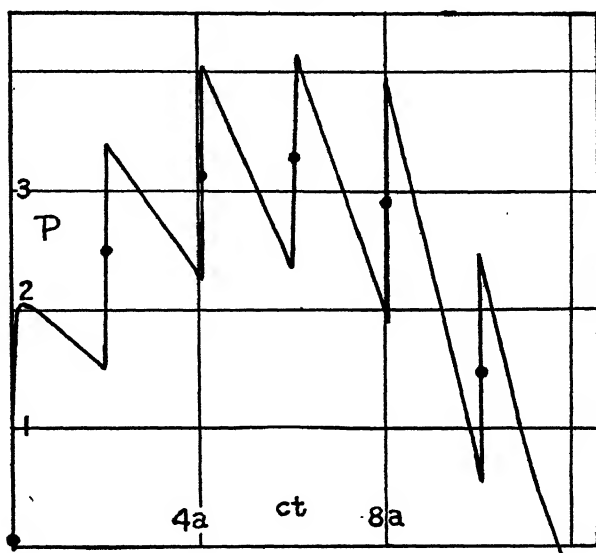
$$y_x = f(ct' - x + a), \quad \text{and} \quad f(ct') = y_a. \quad \dots \dots (11)$$

The second term in (10) is due to the free vibrations of the short portion of the string between the nearer end and the striking point, which is considered to be a nodal point for all the free vibrations of that portion. This is justified on experimental grounds, which indicate that the small part of the string between the nearer fixed end and the striking point vibrates with the latter point as nodes for various modes. Fig. 1 shows the phenomenon. It will be seen that, in addition to the hump due to the impact of the hammer, there are smaller kinks superposed on the hump. The figure also shows that the free vibrations form a two-step

zigzag curve, and it has also been found that the period is nearly equal to  $\frac{2a}{c}$ . (See Table at the end of this paper.)

The first term is due to the hump, the values of  $k$  being unknown at present. Equation (11) assumes that the other portion of the string is too long for the reflected wave from the further end to arrive during the time of contact of the hammer with the string. This assumption is generally true in the actual case of the pianoforte where  $a/l$  varies from  $\frac{1}{7}$  to  $\frac{1}{32}$ .

**Fig. 1.**



Now  $\zeta = y + \xi$  and  $p = \mu \xi$ , . . . . (12)

$$M\ddot{\xi} = -p.$$

## Also

$$p = T_0 \left\{ \frac{ky_a}{\tan ka} + \frac{\dot{y}_a}{c} \right\} + T_0 \sum \frac{r\pi}{a} (-1)^r \sin \frac{r\pi ct'}{a}, \quad (13)$$

$\zeta$  = compression of felt.

From (12) and (13) we obtain the equation of motion of the striking point,

$$\begin{aligned} & \frac{MT_0}{\mu c} \ddot{y}_a + M \left( 1 + \frac{T_0 k}{\mu \tan ka} \right) \ddot{y}_a + \frac{T_0}{c} \dot{y}_a + \frac{T_0 k y_a}{\tan ka} \\ & = \Sigma P_r T_0 \frac{r\pi}{a} (-1)^r \sin \frac{r\pi ct'}{a} \left\{ \frac{r^2 \pi^2 T_0 M}{a^2 \mu \rho} - 1 \right\}. \quad (14) \end{aligned}$$

We shall neglect the term in  $\ddot{y}_a$  as it is very small when  $\mu$  is large, and solve for  $y_a$  by trial. We find that for small values of  $a$ ,  $\tan ka$  is small, and is approximately equal to  $ka$ . In a case when  $a=15$  cm., and the other constants have the values as before,  $k=.0198$ ,  $\tan ka=.300$ , and  $ka=.297$ .

Thus for all practical purposes we may take  $\tan ka=ka$ , and then (14) reduces to

$$\frac{MT_0}{\mu c} \ddot{y}_a + M \left( 1 + \frac{T_0}{\mu a} \right) \ddot{y}_a + \frac{T_0}{c} \dot{y}_a + \frac{T_0}{a} y_a = \Sigma P_r \frac{r\pi}{a} (-1)^r T_0 \sin \frac{r\pi ct'}{a} \left\{ \frac{r^2 \pi^2 T_0 M}{a^2 \rho \mu} - 1 \right\}, \quad (15)$$

and (10) takes the form

$$y_x = \frac{y_a x}{a} + \Sigma P_r \sin \frac{r\pi x}{a} \cdot \sin \frac{r\pi ct'}{a}.$$

Let us now determine the values of  $P_r$  before solving (15) completely. We observe that  $t'=0$ ,

$$\dot{y}_x = \dot{y}_a \frac{x}{a} + \Sigma \frac{r\pi c}{a} P_r \sin \frac{r\pi x}{a},$$

$$\dot{y}_a = V_0 \left/ \left( 1 + \frac{4T_0 \rho}{\mu M} \right) \right. = V_1.$$

From the above we find

$$\int_0^a \dot{y}_x \sin \frac{r\pi x}{a} dx = \int_0^a V_1 \frac{x}{a} \sin \frac{r\pi x}{a} dx + P_r \frac{r\pi c}{2}.$$

Since at the beginning of the second state of affairs  $\dot{y}_x$  is everywhere zero except at  $x=a$ , we get

$$P_r = \frac{2a(-1)^r V_1}{c\pi^2 r^2}, \quad \dots \dots \dots (16)$$

$$\dot{y}_x = V_r \frac{x}{a} - \frac{2V}{\pi} \left\{ \sin \frac{\pi x}{a} \cos \frac{\pi ct'}{a} - \frac{1}{2} \sin \frac{2\pi x}{a} \cos \frac{2\pi ct'}{a} + \dots \right\}, \quad \dots \dots (16.1)$$

where  $V_r$  is the velocity of the striking point at time  $t'$ .

The above series can be evaluated for particular values of  $x$  or  $t'$  easily. For instance, when  $ct' = \frac{a}{2}$ ,

$$\dot{y}_x = \frac{x}{a} (V_r - V_1), \quad 0 < x < \frac{a}{2},$$

$$y_x = \left[ \frac{(V_r - V_1)x}{a} + V_1 \right], \quad \frac{a}{2} < x < a.$$

Now  $V_2$  will differ from  $V_1$  by a very small amount in the time  $ct' = \frac{a}{2}$ ; hence the portion of the string from  $x=0$  to  $x=\frac{a}{2}$  is at rest, while in the portion from  $x=\frac{a}{2}$  to  $x=a$  the points will have a velocity slightly less than the initial velocity of the point  $x=a$  by an amount proportional to its distance from the fixed end. Similarly the point  $x=\frac{a}{2}$  will have a velocity at any time  $t'$ ,

$$\dot{y}_{a/2} = \frac{(V_2 - V_1)}{2}, \quad 0 < ct' < \frac{a}{2},$$

$$\dot{y}_{a/2} = \frac{(V_2 + V_1)}{2}, \quad \frac{a}{2} < ct' < a.$$

Thus we find that the velocity of the point will sometimes be greater than, and sometimes less than, that which would be obtained at the same place when there were no free vibrations. This will repeat after an interval  $T = \frac{2a}{c}$ .

Solution of (15) :

$$y_a = \frac{V_1 e^{-\frac{k}{2}t'}}{q} \sin qt' - \frac{2V_1 T_0}{\pi c \mu} \sum \frac{1}{r} \sin \frac{r\pi ct'}{a} - \frac{2a^2 V_1 \rho}{c\pi^3 M} \sum \frac{1}{r^3} \sin \frac{r\pi ct'}{a} \quad (17)$$

The last two terms are due to free vibrations.

### I.

#### *Calculation of the Pressure due to Impact.*

From (13) we obtain, after substituting the values of  $y_a$  and  $\dot{y}_a$ ,

$$p = V_1 \rho c \left[ e^{-\frac{k}{2}t'} \frac{\sin qt'}{q} \left( \frac{c}{a} - \frac{k}{2} \right) + e^{-\frac{k}{2}t'} \cos qt' + \frac{2}{\pi} \left( 1 - \frac{T_0}{\mu a} \right) \sum \frac{1}{r} \sin \frac{r\pi ct'}{a} \right]. \quad (18)$$

(18) shows clearly the effect of free vibration, and in the case when  $\mu$  is infinite (hard hammer),

$$p \text{ (hard hammer)} = V_0 \rho c \left[ e^{-\frac{k}{2}t'} \frac{\sin qt'}{q} \left( \frac{c}{a} - \frac{k}{2} \right) + e^{-\frac{k}{2}t'} \cos qt' + \frac{2}{\pi} \sum \frac{1}{r} \sin \frac{r\pi ct}{a} \right]. \quad (19)$$

[Compare Das's formula, Proc. Phys. Lond. xxix. p. 29 (1927).]

The last term in (18) and (19) repeats after an interval of  $\frac{2a}{c}$ , and the resultant pressure can be obtained by algebraic summation of the two parts. In the case of a slightly elastic hammer we find that the pressure rises by  $V_1 \rho c \left(1 - \frac{T_0}{\mu a}\right)$  at intervals of  $\frac{2a}{c}$ ; while in the case of a hard hammer the rise is  $V_0 \rho c$ . Hence we find that for a slightly elastic hammer the pressure is initially zero; after a short interval  $t_1$  it rises to  $2V_1 \rho c$ ; the subsequent value of the pressure is given by (18). Fig. 1 shows (18) graphically; the sharp rise will diminish with softer hammer, and also with the diminution in the number of the harmonics. If, for instance, only ten harmonics are present, then the sharp peaks will be rounded off and the pressure at  $T = \frac{2a}{c}$  will be given by the first term only, the second term being zero.

*Amplitude of Free Vibration.*—The free vibration is given by

$$y_x = \frac{2aV_1}{c\pi^2} \sum \frac{1}{r^2} \sin \frac{r\pi x}{a} \sin \frac{r\pi ct'}{a},$$

which is a two-step zigzag curve with respect to time at a given point; further, the amplitude is proportional to  $V_1$ , diminishing with  $\mu$ ; thus, the softer the hammer the smaller is the free vibration. It is also proportional to the vibrating length.

This cannot be true beyond a certain limit, when our assumption  $\tan ka = ka$  does not hold good.

## II.

### *Highly Elastic Hammer.*

In this case also we assume

$$y_1 = y_a \frac{x}{a} + \sum P_r \sin \frac{r\pi x}{a} \sin \frac{r\pi ct}{a}; \quad . \quad . \quad . \quad (20)$$

but in the equation of motion the term in  $\ddot{y}_a$  is retained, but it is treated as small. Hence we find the solution

$$y_a = Ae^{-ut} + Be^{-\frac{k}{2}t} \sin qt + Ce^{-\frac{k}{2}t} \cos qt + \text{small terms},$$

where  $k$  and  $q$  have the same values as before and

$$u = -\frac{C\mu}{T_0} \left(1 + \frac{T_0}{\mu a}\right).$$

$A$ ,  $B$ , and  $C$  are constants to be determined from the initial conditions.

$$\text{At } t=0, \quad y_a = \dot{y}_a = 0, \quad p = 0$$

everywhere, and the initial velocity of the hammer is  $V_0$ .

On substituting these conditions in (20) we get

$$A = -C, \quad B = -\frac{A}{q} \left(u + \frac{k}{2}\right).$$

Further,

$$\dot{\xi} = y + \xi - \frac{1}{\mu} \frac{dp}{dt} = V_0 \quad \text{at } t=0.$$

Thus we get

$$A \left\{ u^2 + q^2 + 3\frac{k^2}{4} + ku \right\} + \sum P_r \frac{r^2 \pi^2 c}{a^2} (-1)^r = \frac{V_0 \mu c}{T_0}.$$

This is an indeterminate equation, but the value of  $P_r$  can be determined from the following considerations:—

- (1)  $P$  must be proportional to  $V_0$ .
- (2) It must have the dimension of length.
- (3) The series must be convergent.
- (4) The increase in the value of  $P_r$  should diminish  $A$ .
- (5) As regards the effect of  $\frac{T_0}{\mu}$  on the amplitude of vibra-

tion no definite experimental result is available at present; yet, borrowing the results for slightly elastic hammer, we find that  $P_r$  must diminish with softness of the hammer, and also the free vibration should be very small when the hammer mass is small. The effect of softness of the hammer on the free periods of the short piece of wire can be deduced from the results of § 135\*. It is found that when  $M=0$ ,

\* § 135, 'Theory of Sound,' i. (Lord Rayleigh).

and  $\mu$  is finite and great, the free periods are given by

$$\tan ka = -k \frac{T_0}{\mu}$$

When  $\mu = 0$  and  $M$  is finite, then

$$k \tan ka = \frac{T_0}{Ma^2}.$$

It is found that the effect will depend upon the mass of the hammer and its elasticity. In the case when the mass is small, and at the same  $\mu$  is large, the natural frequencies are lowered and the harmonic scale is not disturbed; while in the case when  $M$  is large, and  $\mu$  is small, the periods are lowered and at the same time the harmonic scale is disturbed.

From these considerations we find

$$P_r = \frac{V_0 a (-1)^r g}{\pi^3 c r^3}, \quad \dots \dots \dots (21)$$

$$g = \left(1 + \frac{T}{\mu} \frac{\rho}{M}\right)^{-\frac{1}{2}}.$$

Of course, in the case of a hard hammer, instead of  $\frac{1}{r^3}$  we shall have  $\frac{1}{r^2}$ .

From the above value of  $P_r$ ,

$$A(u^2 + q^2) = \frac{V_0 c \mu}{T_0} \left(1 - \frac{g}{\mu a} \sum \frac{1}{r}\right).$$

Now  $\sum \frac{1}{r}$  is a divergent series, but when only a few harmonics are present we can find a lower limit of  $\sum \frac{1}{r}$ , and for ten components the values come out to be 2.92, and (24) becomes

$$A(u^2 + q^2) = \frac{V_0 c \mu}{T_0} \left(1 - \frac{1.86}{\mu a}\right).$$

With the same values for the constants, the term in brackets has a value .88.

The above value of  $P_r$  satisfies all the conditions of the problem at  $t=0$  except one, viz. :

At  $t=0$ ,

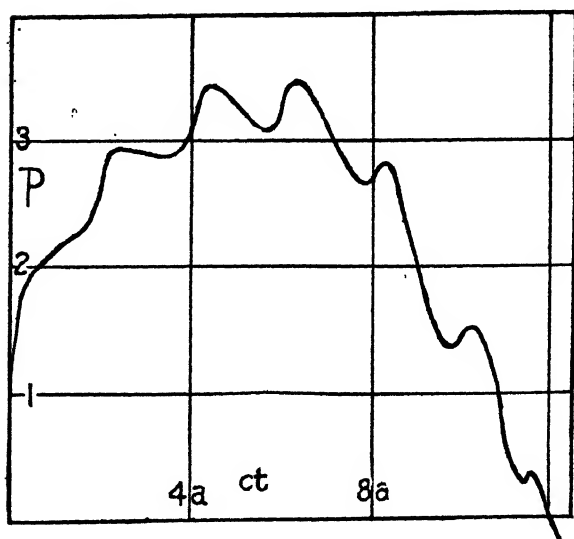
$$\begin{aligned} \dot{y}_x &= \dot{y}_a \frac{x}{a} + \sum \frac{g V_0 (-1)^r}{\pi^2 r^3} \sin \frac{r \pi x}{a}, \\ \dot{y}_x &= 0, \end{aligned}$$

but the second term does not vanish as it ought to do, since  $\dot{y}_x$  is everywhere zero. This is due to the fact that we have assumed two contradictory things, viz., that there are standing waves in the string which start in the string with zero displacement and zero velocity, which is not possible. Thus during a very short interval of time in the initial stages of motion our formulæ will not represent facts correctly.

The pressure is given by

$$p = T_0 \left[ \frac{y_a}{a} + \frac{\dot{y}_a}{c} + \frac{gV_0}{c\pi^2} \sum \frac{1}{r^2} \sin \frac{r\pi ct}{a} \right]. \quad (22)$$

Fig. 2.



The graph of (22) with the same values of the constants ( $\frac{T_0}{\mu} = 1$ ) is represented in fig. 2, where only ten terms have been included in the series. This curve shows that the pressure starts from zero value, rises considerably, then follows an irregular course, after which we find a regular rise and fall after an interval  $\frac{2a}{c}$ .

By comparison with (18) we find that the amplitude of vibration of the short portion diminishes when the hammer becomes softer, just as the rise and fall of pressure become rounded. This effect improves the tone-quality of the lower



notes in the instrument, where the hammer is generally very soft.

### *Summary and Conclusion.*

In the present paper free vibrations of the short portion of the string have been taken into consideration for calculating the pressure due to impact. It is found that in the case of (1) slightly elastic hammer, it rises suddenly at intervals of  $\frac{2a}{c}$  by an amount

$$V_0 \rho c \left(1 - \frac{T_0}{\mu a}\right) / \left(1 + \frac{4T_0 \rho}{\mu M}\right)^{\frac{1}{2}};$$

while in the case of a very soft hammer the rise is not sudden and the pressure is given by

$$p = T_0 \left\{ \frac{y_a}{a} + \frac{\dot{y}_a}{c} + \frac{gV_0}{c\pi^2} \sum \frac{1}{r^2} \sin \frac{r\pi ct}{a} \right\},$$

the softness has imposed greater convergence of the terms in series. In a subsequent paper the author intends to indicate the results of experiments carried out to verify the above theory in the case of a highly elastic hammer.

### TABLE.

Frequencies of free vibration of the short portion.

$T_\mu = 12.5$ ,  $l = 137$  cm.,  $P = .019$ ,  $V_0 = 1.04 \times 10^2$  cm./sec,

No.	$\phi$ .	$a$ cm.	M.	Freq. obs.	Freq. cal.
1.....	$1.5 \times 10^{-2}$	43	5 grms.	270	274
2.....	1.8 „	43	10 „	276	274
3.....	2.6 „	43	20.5 „	264	274
4.....	2.4 „	72	20.5 „	165	163
5.....	1.6 „	96	20.5 „	125	122

$\phi$  = Duration of contact.

CVI. *On the Relation of Electronic Waves to Light Quanta and to Planck's Law.* By Sir J. J. THOMSON, O.M., F.R.S.\*

SUMMARY.

THIS paper is an attempt to give, by the aid of electronic waves, a physical interpretation of light quanta, their relation to electrons, and the mechanism of light.

WE may regard an electron as consisting of two parts—one, which we shall call the core, carrying a charge of negative electricity equal to  $e$ , while the other is a system of waves surrounding the core, the velocity of the core being the group velocity of the waves in its neighbourhood. The wave system as well as the core may have both energy and momentum, and if the core is suddenly stopped the waves will go on and travel away from the charge. A somewhat similar effect was supposed to occur on the original theory of the production of Röntgen rays by the impact of cathode rays; part of the electric and magnetic field surrounding the moving electron in the cathode ray was supposed to travel on after the electron was stopped by its impact with a solid and constitute the Röntgen ray. Thus it would seem that the two parts which at any time make up an electron may, under certain conditions, be separated, and the original system of waves travel far from the core and form a wave system without any electric charge. The view taken in this paper is that light quanta consist of a special type of such wave systems, and thus that the structure of light quanta is very closely connected with that of electrons.

The system of waves associated with an electron which travels like those inside the atom round a closed path is of especial importance in this connexion. Take the case of electrons inside an atom under the action of a charge of positive electricity at its centre. The electronic waves in this case (see *Phil. Mag.* ser. 7, viii. p. 1073) travel round and round the atom, their wave fronts intersecting the paths of the core of the electron at right angles. The waves circulate in closed paths, and as the energy also travels in closed circuits none of it will escape, so that there is no loss of energy by radiation, and the waves when once started will persist for ever.

\* Communicated by the Author.

The mechanical properties of this system of waves have many analogies with those possessed by a fluid in which there is vortex motion, the group velocity of the waves corresponding to the velocity of the fluid. For if  $u, v, w$  are the components of the group velocity of the electronic waves at any point, then (see *Phil. Mag. loc. cit.*)

$$\oint (u dx + v dy + w dz) = \frac{c^2}{p} \times 2\pi,$$

where the integral is taken round a closed circuit.  $c$  is the velocity of light, and  $p$  is the frequency of the waves; thus, the integral on the left-hand side is constant both with regard to space and time.

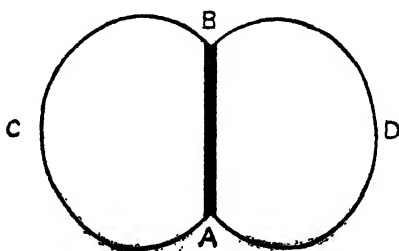
If  $u, v, w$  are the components of the velocity of a fluid, the above integral is called the "circulation" round the circuit; it also is constant and depends only on the strength of the vortices enclosed by the circuit. The results which follow from the constancy of the circulation in hydrodynamics have their analogies in the properties of the wave system; thus, for example, it follows from this principle that the motion of the liquid in which the vorticity originated carries along with it the vorticity, hence the motion of the medium in which the waves are produced will carry along with it the system of waves which were started in that medium.

For the sake of illustrating the use of this analogy we will consider one or two special cases. Take first the case of a long straight cylindrical vortex, which may be a cylinder of fluid in which the motion is rotational or a hollow cylinder round which circulation is established. The particles of fluid outside the vortex or hollow describe circles, with their centres on its axis and their planes at right angles to it; the magnitude of the velocity varies inversely as the distance from the axis. The system of waves corresponding to this case would be one where the group velocity of the waves at any point was equal in magnitude and direction to the velocity in the fluid. The fronts of the waves are everywhere at right angles to the group velocity, hence the wave fronts will be radial planes passing through the axis. The distance between two adjacent wave fronts measured along their normal is thus proportional to  $r$ , the distance from the axis; but this distance is also proportional to  $\lambda$ , where  $\lambda$  is the wave-length at the distance  $r$ ; hence  $\lambda \propto r$ , but  $r \propto 1/u$ , where  $u$  is the group velocity; hence  $\lambda u$  is constant, which agrees with the properties of

electronic waves. The waves, being electrical waves, have momentum, and the momentum at any point is perpendicular to the wave front through that point; hence the momentum will be tangential, and there will be a finite moment of momentum about the axis; the system of waves will, in this respect, resemble a top spinning about its axis. Since the energy is flowing round closed paths there will be no escape of energy.

The system of waves associated with an electron describing an orbit inside an atom is somewhat more complicated than the two-dimensional one we have just described. The hydrodynamical analogue to this system is shown in the figure, which represents the distribution of vorticity in a section of the fluid by a plane through the axis of symmetry AB.

The vorticity consists of closed vortex rings having a portion of their lengths AB in common. The toroidal



surface of which ACBDA is a section is one where the vortex lines are tangential to the surface, and when such a surface moves it carries its vorticity with it (Lamb's 'Hydrodynamics,' p. 186, 5th edit.). Inside this surface the liquid is revolving round the axis AB and has a finite moment of momentum about the axis, and neither energy nor fluid bursts through the surface. All these properties are possessed by the waves associated with an electron moving inside an atom under the influence of a central force varying inversely as the square of the distance, and the electron inside the atom will consist of its core and this system of waves, the core travelling with the group velocity of the waves in its neighbourhood. If the core is detached the wave system will persist and may escape from the atom, carrying with it the energy of the waves and the atmosphere of the electron. I regard this system of waves as a quantum of light, so that, on this view, light quanta are disembodied electrons. After the light quantum has escaped from the atom it will be surrounded by the normal ether and will

travel with the group velocity of waves through this medium, *i. e.*, with the velocity of light. Its direction of motion will be the direction of the group velocity in the ether, which will be determined by the light waves surrounding the quantum; thus these waves will guide the quantum along the path it has to travel. The light quantum on this view consists of a system of electronic waves flowing in closed circuits through a region filled with the atmosphere of the electron. Since the energy moves round the light quantum in closed circuits there is no escape of energy as it moves through space, and, as in the analogous case of vortex motion, the system will carry its medium along with it. No energy is given up by the quantum to the waves of light when once these are established, as they form a system of stationary waves with respect to the quantum. We shall suppose that the light quantum is symmetrical about an axis, and that the circuits round which the waves travel are circles with their centres on this axis and planes at right angles to it.

Any singularity in the wave field inside the light quantum will travel round the quantum with the group velocity of the waves in its neighbourhood. Before the light quantum was detached from the atom the singularity travelling round was the core of the electron. The path of the core will have a definite position in the system of waves, *i. e.*, it will be at a definite distance from the centre of the atom. Since the density of the energy in the waves will be greatest at the envelope of the rays in the wave system, and this is a circle whose radius depends on the energy content of the system, we should expect that this circle would be the path of the core and also the path of the singularity left when the core is detached.

The motion of such a singularity round the light quantum will produce a periodic effect whose period is the time taken by it to travel round the circuit, and is thus equal to the length of the circuit divided by the group velocity of the electronic waves. We regard this period as that of the waves of light associated with the quantum. There is also another period associated with this quantum—that of the electronic waves circulating round it. This period is infinitesimal in comparison with that of the waves of light; we shall see, however, that these electronic waves are of fundamental importance in determining the relation between the period of the light waves and their energy.

To determine this relation we proceed as follows:—the time taken to describe its circuit by a singularity at a distance  $r$  from the axis of the quantum is  $2\pi r/u$  if  $u$  is the group

velocity of the waves. Hence the frequency of the disturbance, i. e.,  $\nu$  the frequency of the light waves, is given by

$$\nu = \frac{u}{2\pi r} = \frac{u^2}{2\pi r}.$$

If  $V$  is the phase velocity of the *electronic waves inside the light quantum*,  $L$  their wave-length, and  $p$  their frequency,

$$u = \frac{c^2}{V} = \frac{c^2}{pL};$$

so that

$$2\pi r u = \frac{c^2}{p} \frac{2\pi r}{L}.$$

Now the circuit  $2\pi r$  must contain an integral number of wave-lengths; hence

$$\frac{2\pi r}{L} = n \text{ (an integer) ;}$$

so that

$$\nu = \frac{u^2}{2\pi r u} = \frac{pu^2}{nc^2}. \quad . \quad . \quad . \quad . \quad (1)$$

We now proceed to calculate  $E$ , the energy in the system of waves inside the light quantum. The energy in the electronic system in the atom before the core was detached was equal to the energy of the core +  $E$ . Suppose that this electronic system arose from the falling of an electron from a great distance into the atom. If  $m$  is the mass of the electron,  $u$  its velocity, then when the electronic system is inside the atom and the core is describing a circle of radius  $r$

$$mu^2 = \frac{e^2}{r}.$$

If the core had retained all the kinetic energy it acquired in its fall, then, neglecting relativity corrections,

$$\frac{1}{2}mu^2 = \frac{e^2}{r};$$

thus the core has lost by its fall an amount of energy equal to  $mu^2/2$ . We suppose that this has gone into the wave system, so

$$E = \frac{1}{2}mu^2 + E_0,$$

where  $E_0$  is the energy in the atmosphere of the electron when it is at rest and at an infinite distance from the atom;  $E_0$  is a constant, and will not appear in equations representing the transference of energy between light quanta or between a light quantum and an electron.

Thus, when the electronic system is in a steady state, the energy in the waves is equal to the kinetic energy of the core, and is thus equal to  $mu^2/2$ , where  $m$  is the mass of an electron and  $u$  the group velocity of the waves at the core of the electron.

From (1)

$$E = \frac{1}{2} \frac{mnc^2}{p} \nu + E_0.$$

If  $m_0$  is the mass of an electron at rest, and  $p_0$  the frequency of its vibration when in that state,

$$\frac{m}{p} = \frac{m_0}{p_0};$$

hence

$$E = \frac{n}{2} \frac{m_0 c^2}{p_0} \nu + E_0,$$

which is equivalent to

$$E = \frac{n}{2} \frac{m_0 c^2}{p_0} \nu = \frac{n}{2} h\nu, \quad \text{if } h = m_0 c^2 / p_0.$$

The resemblance of this equation to Planck's Law is obvious, in fact it becomes identical with it when  $n=2$  \*. On the view we have taken Planck's relation is a necessary consequence of the existence of electronic waves.

We can estimate the size of the light quanta as follows :—

Taking the case  $n=2$ , we have by (1)

$$\nu = \frac{pu^2}{2c^2} \quad \text{and} \quad \nu r^2 = \frac{pu^2 r^2}{2c^2} = \frac{c^2}{2\pi^2 p}.$$

When  $u/c$  is small, as it is for visible light,  $p$  is nearly equal to  $p_0$ , so that this equation becomes

$$\nu r^2 = \frac{h}{2\pi^2 m_0}.$$

\* If the time of vibration of the light quantum were measured by the time a disturbance took to travel over a distance equal to the wave-length of the electronic waves inside the quantum,  $n$  would not appear.

Now  $\nu = c/\lambda$ , where  $\lambda$  is the length of the light waves, so that

$$r^3 = \frac{h}{2\pi^2 cm_0} \cdot \lambda,$$

$$r^3 = \frac{10^{-10}}{8} \lambda,$$

$$r = .35\sqrt{\lambda} \times 10^{-5}.$$

Thus for the hydrogen lines

$$H_\alpha \quad r = 2.8 \times 10^{-8} \text{ cm.},$$

$$H_\delta \quad r = 2.24 \times 10^{-8} \text{ cm.}$$

Thus the quanta for visible light are of atomic dimensions. Since  $r \propto \sqrt{\lambda}$ , the size of the quantum varies much less rapidly than the wave-length.

If the light quanta have a finite size there will be a limit to the rate at which energy can be transmitted by light waves. For if  $r$  is the linear dimension of the quantum, the maximum number of quanta per unit volume may be taken as  $1/r^3$ . The energy in each quantum is  $hc/\lambda$ , so that the maximum energy per unit volume is  $hc/\lambda r^3$ , and the maximum rate at which energy can be transmitted across unit area is  $hc^2/\lambda r^3$ , or, substituting the value of  $r$ ,

$$1.3 \times 10^{11} \cdot \frac{1}{\lambda^{\frac{5}{2}}} \text{ ergs per sec. per square cm.}$$

Since the energy in the light quantum is equal to

$$\frac{m_0 c^2 \nu}{p_0},$$

its mass will equal  $m_0 \nu/p_0$ .

#### *Moment of Momentum of a Light Quantum about its Axes.*

The momentum per unit volume in the field of the electronic waves in the quantum is (see 'Beyond the Electron,' p. 41) equal to

$$(\text{energy per unit volume in the wave-field})/V,$$

where  $V$  is the phase velocity of the electronic waves. The moment of momentum about the axis is equal to

$$\frac{r}{V} (\text{energy per unit volume}),$$



but  $2\pi r = nL$ , where  $L$  is the length of the electronic wave, and therefore  $r/V = n/2\pi \cdot p$ . Thus the total moment of momentum is equal to

$$\frac{n}{2\pi p} \text{ (energy of quantum)} = \frac{a^2 h}{4\pi} \frac{v}{p}.$$

Since the light quantum has a finite moment of momentum about its axis, to fix the quantum we require, in addition to its energy, a vector to fix the position of its axis.

The case we have considered is one where one complete electronic system, *i. e.* core and waves, is deprived of its core and the whole of its wave-system goes to form the light quantum. The genesis of light quanta from atoms is somewhat more complicated than this. By doing work on an electronic system at one energy-level it is transferred to a higher level, and when it returns to its original level the work done to transfer it to the higher level appears in a light quantum. Whilst the electronic system is passing from the lower to the higher level it is not in a steady state, and there is no coordination between the core and the waves; the velocity of the core is not necessarily equal to the group velocity of the waves. We may suppose that during the transference the energy in the wave-system does not alter and is equal to  $\frac{1}{2} \frac{e^2}{r_1}$  where  $r_1$  is the radius of the first

energy-level. We have seen that when there is equilibrium between the wave-system and the core the energy in the waves is equal to  $e^2/2R$ , where  $R$  is the distance of the core from the centre. In the steady state at the second energy-

level  $r_2$  the energy in the waves round the core is  $\frac{1}{2} \frac{e^2}{r_2}$ ; hence

in this position there is an excess of energy in the wave system coming from the first energy level equal to  $\frac{1}{2} e^2 \left( \frac{1}{r_1} - \frac{1}{r_2} \right)$ . Let us suppose that this excess splits off

as a separate system, which is not so closely held by the core as the other. When the electron falls back to its former

level it carries with it the waves whose energy is  $\frac{1}{2} \frac{e^2}{r_2}$ , and the system whose energy is  $\frac{1}{2} e^2 \left( \frac{1}{r_1} - \frac{1}{r_2} \right)$  is free to escape as

a light quantum. The fall of the core from  $r_2$  to  $r_1$  leaves free an amount of energy  $\frac{1}{2} \left( \frac{e^2}{r_1} - \frac{e^2}{r_2} \right)$  which goes into the

system of waves attached to the core and increases its energy from  $\frac{1}{2} \frac{e^2}{r_2}$  to  $\frac{1}{2} \frac{e^2}{r_1}$ , the value it has when core and waves are in equilibrium.

The quantum of light on this theory is a system of electronic waves flowing round a closed circuit. This circuit must have been closed before the waves were detached from the core ; this is the case when the electron which supplied the waves was one of the electrons in an atom. It would not be so with a free electron like a cathode ray. When the core is detached from this system the only definite frequency in the wave-system is the frequency of the electronic waves themselves, and the Röntgen rays produced by the impact of cathode rays against a target must owe any definite frequency they possess to the influence of the target itself. The path of the electron, and therefore of the electronic waves, through the target, owing to collisions with the molecules of the target, will be very irregular, and may contain a loop ; the length of this loop must be an integral multiple of the wave-length of the electronic waves. The loop may be detached and escape, carrying with it the electronic waves which circulate round it. This system is of the same character as that given out by an atom when emitting one of its spectral lines. It will be quantized, because quantization is the result of having an integral number of wave-lengths round the circuit, and Planck's relation between period and energy will hold. As the velocity of the electron in the target is continually changing through collisions, the energy in the light quanta it emits will not be fixed, but will vary over a very wide range, and thus constitute a continuous spectrum. This corresponds to the white spectrum of the Röntgen rays. Those constituents of this spectrum, which are of any particular wave-length, will be of exactly the same character as the constituents of a monochromatic spectrum of that wave-length

The same thing applies to the continuous spectrum given out by a hot body ; this is due to the irregular motions of electrons in the body. We can also put the same reasoning into a form which brings it into close connexion with a method which has long been used to describe the origin of electrical waves. Consider an electron and a positive charge. Tubes of electric force stretch from the electron to the charge, and in these tubes lies the energy of the field. For any of this energy to travel away into space without carrying the electron

with it tubes must break away, and to do this they must form a loop. When the electron moves about the tubes move with it and may get looped. Since electronic waves are running along the tubes, the length of the loop must be an integral multiple of the length of these waves. When the loop gets detached electronic waves are travelling around its closed circuit, and we have just what on the theory we are considering is a light quantum. The frequency of the light is proportional to the energy in the quantum, and, as this depends on the velocity of the electron, the spectrum given by an irregularly moving collection of electrons will be continuous.

---

CVII. *Notices respecting New Books.*

*Mineralogy.* An Introduction to the Scientific Study of Minerals.

By Sir HENRY A. MIERS, M.A., D.Sc., F.R.S. Second Edition, revised by H. L. BOWMAN, M.A., D.Sc. [Pp. xx+658, with 761 illustrations.] (London: Macmillan and Co. 1929. Price 30s. net.)

THE second edition of Sir Henry Miers's 'Mineralogy' has been revised by Dr. Bowman, his successor in the Waynflete Chair of Mineralogy in Oxford. It follows the original plan of the book, with such changes and additions as have seemed necessary after the lapse of twenty-seven years. The volume is restricted to an account of the general properties of minerals,—crystalline, physical, and chemical—to the description of the more important mineral species, and to an account of the methods for the determination of minerals. No systematic account of the occurrence of minerals, their geological distribution and origin are given.

The volume is so well known to students of mineralogy that no detailed review of the contents of the second edition is necessary, the more so as the changes from the first edition are not extensive. The most important addition is an account of the analysis of crystal structure by means of X-rays. This is limited to twenty pages and might well have been expanded somewhat in view of the importance and power of the method. The idea of the wave-surface has been introduced into the chapter on the optical properties of crystals; this is a valuable and important addition. Numerous minor changes have been made and many new figures have been added.

The tables at the end of the volume—comprising a list of the principal minerals, tables of reactions, and tables of physical properties are very convenient for reference purposes. The index is excellent.

This text-book is one which no student of metallurgy can afford to dispense with.

*The Earth: its Origin, History, and Physical Constitution.* By HAROLD JEFFREYS, M.A., D.Sc., F.R.S. Second Edition. [Pp. x+346, with 16 figures.] (Cambridge: at the University Press. 1929. Price 20s. net.)

THE developments in the subjects dealt with in this volume during the four years which have elapsed since the first edition appeared have necessitated an increase in size and price of the new edition of about twenty-five per cent. The portion devoted to seismology has been completely rewritten and considerably extended. A full account is given of the important researches of Gutenberg and others. A chapter is devoted to general considerations and the structure of the upper layers, and another to the information as to the Earth's interior that is provided by seismology. The subject is thus brought into a more intimate relation with the other subjects dealt with. In particular, the conclusions provided by seismology have an important bearing on the thermal history of the Earth, and the chapter devoted to this subject has been rewritten.

The general question of isostasy receives a more extended discussion, and more definite conclusions are drawn as to the nature and degree of isostatic compensation. More attention has been given to the bodily tide in the Earth and to bodily tidal friction. Much fuller discussion is given of the contraction theory of mountain formation, and of theories of the origin of the continents and of the permanence of the continents. In addition, numerous minor additions and revisions have been made.

The result of these additions has been to increase considerably the value of the book. There is no other book which surveys in so authoritative a manner the work in many branches of geophysics and coordinates them. Astronomy, geology, seismology, and the general properties of matter are all called upon to contribute evidence. The style is lucid and clear, the mathematical portions are not unduly heavy, and the volume is eminently readable.

A new appendix entitled "The Relation of Mathematical Physics to Geology" has been added, replacing that on the hypothesis of the infinite deformability of the Earth by small stresses. It contains much common sense, and can be recommended to the serious attention of those geologists who are inclined to undervalue the evidence which can be derived from mathematical considerations.

**Magnetism.** By EDMUND C. STONER, Ph.D. (Methuen's Monographs on Physical Subjects.) [Pp. vii—117, with 20 diagrams.] (London: Methuen and Co. 1930. Price 2s. 6d. net.)

THEORIES of magnetism have been profoundly affected by modern views of atomic structure. This small monograph starts appropriately, therefore, with a consideration of the magnetic properties of atoms from the point of view of quantum mechanics. Diamagnetism, paramagnetism, and ferromagnetism are then dealt with in succession. A final chapter deals with the magnetic properties of the elements.

It will be seen that the book is intended for those who have some previous knowledge of the subject and describes some of the modern investigations and the present outlook on the subject. The development is necessarily somewhat condensed, though lucid and logical. The *résumé* of the modern outlook on the subject provides a fitting introduction to the subject for those who wish to pursue it further, and will be appreciated by workers in kindred subjects who find it difficult to keep in close contact with modern rapid developments. A summary of the more important books and articles on the subject of magnetism is given, and there are footnote references to more recent work, of which an account is not available in the books quoted.

*Catalogue of Lewis's Medical and Scientific Circulating Library.* Part I. Authors and Titles. Part II. Classified Index of Subjects, with Names of Authors who have written upon them. New edition, revised to the end of 1927. [Pp. 408+166.] (London: H. K. Lewis and Co. 1928. Price 15s. net; to subscribers, 7s. 6d. net.)

MESSRS. LEWIS'S Circulating Library was established in 1848, primarily to supply the needs of members of the medical profession. It has developed into a general scientific library, in which may be found books of scientific or philosophical interest which are not to be found in the ordinary circulating library. The catalogue deserves to be better known and has distinct value for reference purposes, quite apart from the library itself.

The first part is arranged alphabetically according to authors and gives the full name of the work, the editor, size of page, price, and date of publication. The second part consists of a useful classified subject catalogue; under each subject the arrangement is according to authors, with the addition of a word or two to indicate the name and scope of the book, and the date of publication. The latter enables most recent books to be identified at a glance. For such a classified index considerable cross referencing is desirable: this has been incompletely done. Under astronomy, for example, the names of neither Jeans nor Eddington are to be found. Eddington's 'Internal Constitution

of the Stars' is indexed under Stars, not under Astronomy. Arrhenius's 'Destinies of the Stars,' on the other hand, is given both under Astronomy and Stars. Other examples could be multiplied. In view of the incompleteness of the cross-referencing, a summary list of the headings in Part II. would save much turning of pages.

The library does not contain any foreign books, unless translated. Old standard classical works are also, in general, missing. These omissions limit the usefulness of both library and catalogue. Subject to these limitations, the Catalogue appears to be reasonably complete. Messrs. Lewis are to be congratulated upon the production of a useful volume.

### CVIII. *Proceedings of Learned Societies.*

#### GEOLOGICAL SOCIETY.

[Continued from p. 1064.]

March 12th, 1930.—Prof. E. J. Garwood, M.A., Sc.D., F.R.S.,  
President, in the Chair.

THE following communications were read:—

1. 'The Age of the Midland Basalts. By Roy Woodhouse Pocock, M.Sc., F.G.S.

Basic igneous rocks of Lower Carboniferous age are known to occur in the Bristol district, at Little Wenlock in Shropshire, in North Staffordshire, Derbyshire, and Cumberland. Rocks of similar type are present in the Upper Carboniferous of the Midlands, but hitherto no definite evidence of their age has been produced.

The object of this paper is to bring together all available data bearing on the age of the various igneous masses in the Upper Carboniferous, such as those of Kinlet, Shatterford, Clee Hill, Claverley, Rowley Regis, Wednesfield, etc.

The Kinlet basalt is shown, by the evidence of certain exposures, to be a flow of Yorkian age, probably near the top of that division, and this conclusion is supported by evidence from a recent boring east of the main basalt-mass.

The Shatterford basalt is shown to be extrusive, on the evidence of its relationship to the overlying and underlying Coal Measures.

The horizon of this basalt is somewhat lower in the Yorkian than that of Kinlet.

At Clee Hill the evidence shows the basalt to be extrusive, and that it suffered erosion during Yorko-Staffordian time.

The basic igneous rock in the Claverley boring is mentioned, as showing the association of igneous activity with the Coal Measures in the tract between Wyre Forest and South Staffordshire.

The Rowley basalt appears to lie just below the position of the unconformity, if such is present in the district, between the Etruria Marl and the Halesowen Beds. The evidence available for deciding whether the Rowley mass is extrusive or intrusive is discussed.

The rocks of Wednesfield and Pouk Hill are known to be definitely intrusive.

The age of these South Staffordshire rocks is considered, their close connexion (petrologically, stratigraphically, and structurally) with the Shropshire basic rocks is emphasized, and the conclusion is reached that the Shropshire and South Staffordshire basalts are of the same general age: namely, Yorko-Staffordian, whether extrusive or intrusive.

A volcanic belt is known to traverse the Midlands from Hanter and Stanner in Radnorshire to the Ashby Coalfield area. The main movement along this zone took place in Yorko-Staffordian time, and the basaltic masses in question are, without exception, situated along it.

2. 'The Origin of the Etruria Marl.' By Thomas Robertson, B.Sc., Ph.D.

The Etruria Marl Group of the Upper Coal Measures in the Midlands is mainly composed of chocolate-coloured to purple clay, mottled with green, yellow, etc., alternating with greenish sandstones (Espley Rock).

There is no earlier sedimentary rock in the district that could by decomposition yield so characteristic a facies as this Group presents, nor does the Group show characters definitely known to belong to deposits derived from arid regions.

In appearance and composition the Etruria Marl strongly resembles the denudation-products of basalt and basic tuff, and further examination shows that it contains fragments of basalt; that its position in the geological sequence is the same as that of the Coal-Measure vulcanicity in the Midland Province; and that it is best developed in those portions of the basins of deposition towards which the denudation-products of the Midland basalts would flow.

It is thus concluded that the Etruria Marl was formed by the decomposition of the Midland basalts; and certain subsidiary deductions are made regarding the general geological significance of the Etruria Marl facies.

March 26th, 1930.—Prof. E. J. Garwood, M.A., Sc.D., F.R.S.,  
President, in the Chair.

The following communication was read:—

‘A Classification of some Rhyolites, Trachytes, and Phonolites from part of Kenya Colony, with a Note on some associated Basaltic Rocks.’ By Walter Campbell Smith, M.C., T.D., M.A., Sec.G.S.

Comparison of specimens collected on two expeditions by Prof. J. W. Gregory in 1893 and 1919, previously described by Dr. G. T. Prior (1903) and Miss A. T. Neilson (1921), supported by some new analyses, has led to a revision of the somewhat confused nomenclature. The rocks are classified as follows:—

Rhyolites	{ Comendites. Pantellerites.
Trachytes	{ Soda-trachyte (Gibbelé type) Washington. Pantelleritic trachytes and kataphorite-trachytes.
Phonolites	{ (Kenya type) Prior and Neilson. (Losuguta type) Prior. Kenytes.

The pantelleritic trachytes include most of the phonolitic quartz-trachytes of Prior.

The ‘Kapitian phonolites’ are shown to be identical with the kenytes of Mount Kenya, which are found to contain phenocrysts of nepheline, as well as the more conspicuous well-known anorthoclase. Prior’s contention that the kenytes are basic members of the phonolite series is confirmed.

Basaltic rocks associated with the phonolites are relatively scarce. They include mugearites, alkali-basalts, and porphyritic types with abundant phenocrysts of augite and olivine.

April 9th, 1930.—Prof. E. J. Garwood, M.A., Sc.D., F.R.S.,  
President, in the Chair.

Prof. LÉON W. COLLET, For. Corresp. G.S., delivered a lecture on the Structure of the Canadian Rockies. The Lecturer said that Prof. K. F. Mather and Prof. P. Raymond of the Geological Department of Harvard University supervised in 1929, with the collaboration of Dr. Parejas of Geneva, a month’s Summer Course in the Canadian Rockies to investigate the stratigraphy along the Athabasca Valley (Jasper National Park) and round Mount Robson (B.C.). This course of 20 students did, in fact, the reconnaissance work for a two months’ expedition (financed by the Shaller Fund) in which the structures were studied under the leadership of the Lecturer, with the collaboration of Dr. Parejas and A. Lombard.



The Lecturer presented and described the section that he had made with Dr. Parejas along the Athabasca Valley, from the eastern border of the Rockies to Yellow Head Pass, that is, a complete section across the Rockies. This mountain-chain is made up of seven 'blocks' thrust one over the other from west to east, and separated by 'clean-cut thrusts' of the type of the North-West Highlands of Scotland.

From east to west, at Boule Roche the Carboniferous is overriding the Cretaceous of the Great Plains. On the eastern side of Roche Ronde one sees the Upper Cambrian on the Cretaceous of the former block. At the foot of Greenock Mountain, the Devonian is thrust over the Triassic. In Vine Creek the Devonian again overrides the Triassic. On the eastern side of Gargoyle the Devonian can be seen resting on the Jurassic. On the eastern side of Chetamon Mountain the Cambrian is pushed over the Carboniferous, and last but not least, at the foot of Pyramid Mountain, the pre-Cambrian is thrust over the Devonian.

In the Mount Robson region the Lecturer and Dr. Parejas detected a thrust-plane on the eastern side of Titkana Peak that had been imagined by Walcott, owing to the tremendous thickness of the Cambrian strata.

Comparing the structure of the Canadian Rockies with the structure of the Alps, the Lecturer showed that we were dealing with two different types of folding. The structure in blocks of the Canadian Rockies corresponds to Argand's 'ground folds' (*plis de fond*), while the Alps are made up of 'recumbent folds' developed in a geosyncline. In the Canadian Rockies the energy necessary for the folding was much greater than in the Alps, for in the former the strata have been cut into blocks as far down as the pre-Cambrian.

The Lecturer showed, moreover, that the Ordovician and the Silurian are missing in the eastern part of the Rockies. The Ordovician alone appears in the western part. He considered that this stratigraphical gap was a repercussion, across the Canadian Shield, of the Caledonian folding of the Canadian Appalachians.

The results arrived at by his expedition confirm the structure of the Canadian Rockies as shown by Prof. R. A. Daly's section along the 49th parallel, and the views expressed by Prof. E. Argand on the geology of North America in several chapters of his well-known '*Tectonique de l'Asie*'.

---

[*The Editors do not hold themselves responsible for the views expressed by their correspondents.*]

FIG. 1.

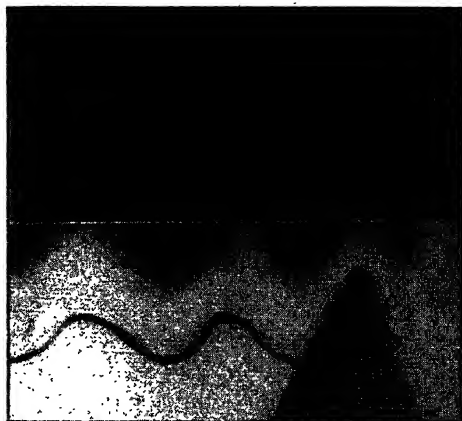
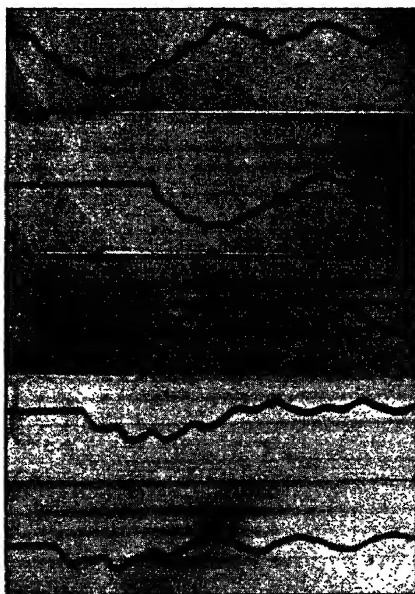


FIG. 2.





## INDEX TO VOL. IX.

- A**BATARAN ash, note on, 88.  
 Absolute zero, on the inaccessibility of the, 208.  
 Acoustical impedance, on, 346.  
 Air condensers, on the effect of occluded gases and moisture on the resistance of, 464; on sound-velocities in, 1020.  
 Algebraic curves, on some closed, 184.  
 Alkaline sulphates, on the space-group of the, 665.  
 Allen (J. F.) on the sense of vision, 817; on the sense of audition, 827; on the depression and enhancement of auditory sensitivity, 834.  
 Alpha-particles, on the scattering of, by light atoms, 273.  
 Aluminium, on the scattering of alpha-particles by, 286.  
 Ammonia, on the heat of dissociation of, 28.  
 Anand (C.) on experiments with carbon line resistances, 415.  
 Andrews (J. P.) on the collision of spheres of soft metals, 593.  
 Aniline, on the damping of a pendulum in, 502.  
 Annuli, on the free and forced oscillations of, 881.  
 Antimony-copper alloys, on an X-ray investigation of the, 993.  
 Antimony-lead alloys, on the Hall effect, electrical conductivity, and thermoelectric power of the, 547.  
 Atmosphere, on a method of investigating the higher, 1014.  
 Atoms, on the scattering of alpha-particles by light, 273.  
 Audition, on the sense of, 827.  
 Auditory sensitivity, on the depression and enhancement of, 834.  
 Bailey (Prof. V. A.) on the behaviour of electrons in magnetic fields, 560, 625.  
 Banerji (A. C.) on the scattering of  $\alpha$ -particles by light atoms, 273.  
 Banerji (D.) on the generation of pulses in vibrating strings, 88.  
 Barium, on the thermionic emission and electrical conductivity of, 440.  
 Barkas (W. W.) on the photo-phoresis of colloidal particles in aqueous solutions, 505.  
 Barlow (Dr. H. M.) on the deviation from Ohm's law for metals at high current densities, 1041.  
 Barratt (S.) on the band spectra of cadmium and bismuth, 519.  
 Bars, on the free and forced oscillations of thin, 881.  
 Bate (A. E.) on the end correction and conductance at the mouth of a stopped organ pipe, 23.  
 Bismuth, on the band spectrum of, 519.  
 Beam, on the effect of a circular hole on the stress distribution in a, 210.  
 Bonar (A. R.) on the band spectra of cadmium and bismuth, 519.  
 Bond (Dr. W. N.) on electrical and other dimensions, 842.  
 Books, new :—Bush's *Operational Circuit Analysis*, 191; Birtwistle's *La Nouvelle Mécanique de Quanta*, 191; Lorentz's *Die Relativitäts Theorie für gleichförmige Translationen*, 192; Smith's *A Source Book in Mathematics*, 668; Turnbull's *The Great Mathematicians*, 669; Schiller's *Logic for Use*, 669; Wien & Harms's *Handbuch der Experimental Physik*, 670; Bouny's *Leçons de Mécanique Rationnelle*, 671; Mellor's *A*

- Comprehensive Treatment on Inorganic and Theoretical Chemistry, 861; Banister's Elementary Applications of Statistical Method, 862; Fowler's The Elementary Differential Geometry of Plane Curves, 862; Fletcher's Speech and Hearing, 1055; The Life and Work of Sir Norman Lockyer, 1057; National Physical Laboratory. Collected Researches, 1057; Debye's Dipolmoment und Chemische Struktur, 1058; Peierls's Einführung in die Wellenmechanik, Louis de Broglie, 1058; Miers's Mineralogy, 1194; Jeffreys's The Earth: its Origin, History, and Physical Constitution, 1195; Stoner's Magnetism, 1196; Catalogue of Lewis's Medical and Scientific Circulating Library, 1196.
- Brentano (Dr. J.) on X-ray reflexions from crystal powders, 525.
- Brindley (G. W.) on the amplitude of vibration of ions in the crystals NaCl, NaF, LiF, and KCl, 193; on the scattering power of the carbon atom in diamond for X-rays, 204; on the scattering powers of the atoms in magnesium oxide for X-rays, 1081.
- Brooks (Dr. W. H.) on the initial and maximum stresses in ties and struts, 426, 1094.
- Cadmium, on the band spectrum of, 519.
- Carbon atom, on the scattering power of the, for X-rays, 204.
- dioxide, on sound-velocities in, 1020.
- line resistances, on, 415.
- Carrington (H.) on critical stresses for tubular struts, 668.
- Cataphoresis of small particles in water, on the, 769.
- Cathode dark space in the Geissler discharge, on the, 529.
- Cathode-rays, on the scattering and diffraction of, 641.
- Chalklin (Dr. F. C.) on the soft X-rays of manganese, 847.
- Chandrasekhar (S.) on the ionization-formula and the new statistics, 292; on the probability method in the new statistics, 621.
- Childs (E. C.) on the cathode dark space in the Geissler discharge, 529.
- Claassen (Dr. A.) on the calculation of absorption in X-ray powder photographs and the scattering power of tungsten, 57.
- Closed algebraic curves, on some, 184.
- Cobalt sulphate, on the paramagnetic rotatory dispersion of, 361.
- Collet (Prof. L. W.) on the structure of the Canadian Rockies, 1199.
- Collision, on the, of spheres of soft metals, 593.
- Colloidal particles, on the photo-phoresis of, in aqueous solutions, 505.
- Colour, on the mathematical representation of sensibility to difference of, 1130.
- Combustion, on luminosity in gaseous, 390; on temperature measurements in, 402.
- Condensers, on the effect of occluded gases and moisture on the resistance of air, 464.
- Conduction of heat, on the, 241.
- Contact of solids, on the, 610.
- Coordination, studies in, 131.
- Cormac (P.) on a skew double-slider-crank mechanism, 639.
- Copper-antimony alloys, on an X-ray investigation of the, 993.
- Cosmology, on redshift and relativistic, 936.
- Crookes's dark space in the Geissler discharge, on the, 529.
- Crystal powders, on precision measurements of X-ray reflexions from, 525.
- structure, on the, of the elements of the B subgroups, 65.
- Crystals, on the amplitude of vibration of ions in, 193.
- Current elements, on the mutual action of a pair of rational, 92.
- Curves, on some closed algebraic, 184.
- Cylinder, on the vortex system in the wake of a, 489.
- Damping, on forced vibrations with combined viscous and Coulomb, 801; on the, produced by eddy currents, 1, 16; on the, of a pendulum by viscous media, 502.

- David (Prof. W. T.) on luminosity in gaseous combustion, 390; on temperature measurements in gaseous combustion, 402.
- Davies (S.) on the damping produced by eddy currents induced in metal spheres and cylinders, 1.
- Davies (W.) on luminosity in gaseous combustion, 390; on temperature measurements in gaseous combustion, 402.
- Deming (W. E.) on temperature distribution along a heated filament, 28.
- Dense stars, on the equilibrium of, 944.
- Deodhar (Dr. D. B.) on new bands in the secondary spectrum of hydrogen, 37.
- Deviations, on reducing observations by the method of minimum, 974.
- Diamond, on the scattering power of the, for X-rays, 204.
- Diaphragms, on the free and forced oscillations of circular, 881.
- Dielectrics, on an anomalous after-effect of, for their apparent resistivity, 474; on dipoles and the anomalous properties of, 865.
- Differential equations, on the solution of partial, 1074.
- Dimensions, on electrical and other, 842.
- Dipole, on the effect of a, on the latent heat of vaporization of a liquid, 422.
- Dipoles in relation to the anomalous properties of dielectrics, on, 865.
- Displacements, on the measurement of small, 589.
- Double-slider-crank mechanism, on a skew, 639.
- Dufton (A. F.) on the effective temperature of a warmed room, 858.
- Dwerryhouse (Major A. R.) on the glaciation of Olun Forest and Radnor Forest, 328.
- Eckersley (T. L.) on the critical frequency in an ionized medium, 225.
- Eddy currents, on the damping produced by, 1, 16.
- Elastic hysteresis, on a molecular theory of, 913.
- Electric resistance of air condensers, on the effect of occluded gases and moisture on the, 464.
- Electrical conductivity of oxide cathodes, on the, 440.
- — —, on the, of the lead-antimony series of alloys, 547.
- dimensions, on, 842.
- Electricity, on frictional, 577.
- Electron density, on the distribution of, between two parallel infinite plates, 80.
- Electronic theory of valency, on the, 233.
- waves, on the relation of, to light quanta and to Planck's law, 1185.
- Electrons, on the behaviour of, in magnetic fields, 560, 625; on the energies of, in gases, 1145.
- Elements of the B subgroups, on the crystal structure of the, 65.
- Etch-figures of sylvine, on the, 233.
- Evans (Prof. E. J.) on the damping produced by eddy currents induced in metal spheres and cylinders, 1.
- Explosions, on the propagation of flame in gaseous, 260.
- Filament, on the temperature distribution along a heated, 28.
- Flame, on the propagation of, in gaseous explosions, 260.
- Fletcher (Miss H. M.) on the effect of occluded gases and moisture on the resistance of air condensers, 464.
- Force between two plates, on the variation with pressure of the, 97.
- Forced vibrations, on, with combined viscous and Coulomb damping, 801.
- Frequency, on the critical, in an ionized medium, 225.
- Friction, on the nature of, 628; on vibrations damped by solid, 329.
- Frictional electricity, on, 577.
- Gallium, on the crystal structure of, 65.
- Ganguli (R.) on the generation of pulses in vibrating strings, 88.
- Garrick (F. J.), studies in coordination, 131.
- Gaseous explosions, on the propagation of flame in, 260.

- Gases, on the energies of electrons in, 1145.
- Geissler discharge, on the cathode dark space in the, 529.
- Geological Society, proceedings of the, 326, 671, 863, 1059, 1196.
- Ghosh (Dr. P. K.) on the Carnmenellis granite, 326.
- Ghosh (Dr. R. N.) on the elastic impact of a pianoforte hammer, 1174.
- Ghosh (M.) on the theory of the pianoforte string struck by a hard hammer, 306, 321.
- Gordon (Prof. W. T.) on cellulose "pulls" from coal-balls, 1063.
- Green (Dr. G.) on problems in the conduction of heat, 241.
- Greenly (Dr. E.) on the Mona complex at Rhoscolyn, 863.
- Gregory (Prof. J. W.) on the geological history of the Pacific Ocean, 1060.
- Hall effect in the lead-antimony series of alloys, on the, 547.
- Hamilton's principle and the field equations of radiation, on, 568.
- Harrison (J. V.) on the geology of some salt-plugs in Laristan, 1059.
- den Hartog (J. P.) on forced vibrations with combined viscous and Coulomb damping, 801.
- Heat, on some problems in the conduction of, 241.
- Helium lines as standards of wavelength, on, 661.
- Herzfeld (K. F.) on the scattering of sound-waves by small elastic spheres, 741; on the propagation of sound in suspensions, 752.
- Hicks (Prof. W. M.) on the spectrum of Hg II., 673.
- Higuchi (Prof. S.) on some closed algebraic curves, 184.
- Hoare (F. E.) on the damping of a pendulum by viscous media, 502.
- Hole, on the effect of a circular, on the stress distribution in a, 210.
- Hollingworth (S. E.) on the glaciation of western Edenside, 1062.
- Hooker (S. G.) on the vortex system in the wake of a cylinder, 489.
- Hot-wire method for the measurement of the distribution of vortices, on a, 1113.
- Houstoun (Dr. R. A.) on the mathematical representation of sensibility to difference of colour, 1130.
- Howells (E. V.) on an X-ray investigation of the copper-antimony alloys, 993.
- Hume-Rothery (Dr. W.) on the crystal structures of the elements of the B subgroups, 65.
- Hydrodynamical inertia coefficients, on some, 161.
- Hydrogen, on new bands in the secondary spectrum of, 37  
— lines as standards of wavelength, on, 661.
- Hysteresis, on a molecular theory of elastic, 913.
- Impedance, on acoustical, 346.
- Inertia coefficients, on some hydrodynamical, 161.
- Ion hydrates, on, 131.
- Ionization-formula and the new statistics, on the, 292.
- Ionized medium, on the critical frequency in an, 225.
- Ions, on the amplitude of vibration of, in crystals, 193.
- Irons (Dr. E. J.) on the free periods of resonators, 346.
- Jaeger's maximum pressure method for surface tension, on, 1066.
- Kar (Dr. K. C.) on the theory of the pianoforte string struck by a hard hammer, 306, 321.
- Keeping (E. S.) on the damped oscillation of a conductor in a non-uniform magnetic field, 16.
- King (Dr. F. E.) on measurements of sound-velocities in air, oxygen, and carbon dioxide, 1020.
- Kirchhoff formula, on the, extended to a moving surface, 141.
- Kolossowsky (Prof. N. A.) on the inaccessibility of the absolute zero, 208.
- Krishnan (K. G.) on the application of the photoelectric cell to the measurement of small displacements, 589.
- Lamar (E. S.) on temperature distribution along a heated filament, 28.
- Lead-antimony series of alloys, on the Hall effect, electrical conductivity, and thermoelectric power of the, 547.

- Levy (Prof. H.) on the vortex system in the wake of a cylinder, 489.
- Light quanta, on the relation of electronic waves to, 1185.
- Liquid, on the effect of a dipole on latent heat of vaporization of a, 422.
- Lithium fluoride, on the amplitude of vibration of ions in, 193.
- Lowry (Prof. T. M.) on the electronic theory of valency, 233.
- Luminosity in gaseous combustion, on, 390.
- Macdonald (P. A.) on the sense of vision, 817; on the sense of audition, 827.
- Magnesium, on the scattering of alpha-particles by, 288.
- oxide, on the scattering powers of the atoms in, for X-rays, 1081.
- Magnetic characteristics of nickel, on the, 1026.
- fields, on the behaviour of electrons in, 560, 625.
- Mair (D. B.) on second-order expressions for the potentials of a sphere, 964.
- Majumdar (R. C.) on new methods in statistical mechanics, 584.
- Manganese, on the soft X-rays of, 847.
- Martin (Dr. A. E.) on the variation with pressure of the force between two plates, 97.
- Martin (Dr. A. R.) on the effect of a permanent dipole on the internal latent heat of vaporization of a liquid, 422.
- Mechanics, on new methods in statistical, 584.
- Meksyn (D.) on Hamilton's principle and the field equations of radiation, 568.
- Mercury, on the spectrum of, 673.
- Metals, on the collision of spheres of soft, 593; on the apparent deviation from Ohm's law for, at high current densities, 1041.
- Miller (A. A.) on the glaciation of Clun Forest and Radnor Forest, 328.
- Molecular free paths, on the determination of, 97.
- Molybdenum, on the temperature distribution along a heated filament of, 28.
- Morgans (W. R.) on the Kirchhoff formula extended to a moving surface, 141.
- Morris-Jones (W.) on an X-ray investigation of the copper-antimony alloys, 993.
- Murgoci (R.) on the thermionic emission and electrical conductivity of oxide cathodes, 440.
- Narkiewicz-Jodko (K.) on the Raman effect in the proximity of the critical point, 299.
- Newton (Miss D. A.) on the cataphoresis of small particles in water, 769.
- Nickel, on the magnetic characteristics of, 1026.
- Observations, on reducing, by the method of minimum deviations, 974.
- Ogg (Prof. A.) on the space-group of the alkaline sulphates, 665.
- Ohm's law, on the apparent deviation from, for metals at high current densities, 1041.
- Oil-drops in water, on the cataphoresis of, 769.
- Oldham (R. D.) on historic changes of level in the delta of the Rhone, 357.
- Organ pipe, on the end correction and conductance at the mouth of a stopped, 23.
- Oscillations, on the free and forced, of thin bars, circular diaphragms, and annuli, 881.
- Oxide cathodes, on the thermionic emission and electrical conductivity of, 440.
- Oxygen, on sound-velocities in, 1020.
- Paramagnetic rotatory dispersion of cobalt sulphate, on the, 361.
- Partial differential equations, on the numerical solution of, 1074.
- Partington (Prof. J. R.) on measurements of sound-velocities in air, oxygen, and carbon dioxide, 1020.
- Pendulum, on the damping of a, by viscous media, 502.
- Penney (W. G.) on hydrogen and helium lines as standards of wavelength, 661.
- Photoelectric cell, on the application of the, to the measurement of small displacements, 589.



- Photographic emulsions, on the quantum theory of X-ray exposures on, 787.
- Photophoresis, on the, of colloidal particles in aqueous solutions, 505.
- Pianoforte hammer, on the elastic impact of a, 1174.
- string, on the theory of the, struck by a hard hammer, 306, 321.
- Piercy (Dr. N. A. V.) on the turbulence in front of a body moving through a viscous fluid, 1038.
- Pipe, on the end correction and conduction at the mouth of a stopped, 23.
- Planck's law, on the relation of electronic waves to, 1185.
- Plates, on the variation with pressure of the force between two, 97.
- Pocock (R. W.) on the age of the Midland basalts, 1197.
- Porter (Prof. A. W.) notes on surface-tension, 1066.
- Potassium chloride, on the amplitude of vibration of ions in, 193; on the etch-figures of, 233.
- Potentials of a sphere, on second order expressions for the, 964.
- Prasad (Dr. G.) on the numerical solution of partial differential equations, 1074.
- Probability method, on the, in the new statistics, 621.
- Psychophysical law, on the, 817, 827.
- Pulses, on the generation of, in vibrating strings, 88.
- Puri (G. L.) on experiments with carbon line resistances, 415.
- Quantum theory of X-ray exposures on photographic emulsions, on the, 787.
- Radiation, on Hamilton's principle and the field equations of, 568; on the optical effects of isotropic, spread over elliptic space, 50.
- Rakshit (H.) on the distribution of space charge between a plane hot cathode and a parallel anode, 80.
- Raman effect, on the, in the proximity of the critical point, 299.
- Rational current elements, on the mutual action of a pair of, 92.
- Redshift and relativistic cosmology on, 936.
- Reimann (A. L.) on the thermionic emission and electrical conductivity of oxide cathodes, 440.
- Resistances, on carbon line, 415.
- Resistivity, on an anomalous after-effect of dielectrics for their apparent, 474; on the application of the damping produced by currents to the determination of, 1, 16.
- Resonators, on the free periods of, 346.
- Rhodes (Dr. E. C.) on reducing observations by the method of minimum deviations, 974.
- Richardson (Dr. E. G.) on the turbulence in front of a body moving through a viscous fluid, 1038.
- Roberts (R. W.) on the paramagnetic rotatory dispersion of aqueous solutions of cobalt sulphate, 361.
- Robertson (Dr. T.) on the origin of the Etruria marl, 1198.
- Robertson (Prof. A.) on the critical stress for tubular struts, 324.
- Room, on the effective temperature of a warmed, 858.
- Rotatory dispersion of cobalt sulphate, on the paramagnetic, 361.
- Saegusa (Prof. H.) on an anomalous after-effect of dielectrics for their apparent resistivity, 474.
- Saha (Prof. M. N.) on new methods in statistical mechanics, 584.
- Scattering powers of the atoms in magnesium oxide for X-rays, on the, 1081.
- Searle (Dr. G. F. C.) on the mutual action of a pair of rational current elements, 92.
- Seth (Prof. J. B.) on experiments with carbon line resistances, 415.
- Shaw (Prof. P. E.) on frictional electricity, 577; on the nature of friction, 628.
- Shimizu (S.) on an anomalous after-effect of dielectrics for their apparent resistivity, 474.
- Silberstein (Dr. L.) on illuminated space-time, 50; on the quantum theory of X-ray exposures on photographic emulsions, 787.

- Skew double-slider-crank mechanism, on a, 639.  
 Smith (W. C.) on rhyolites, trachytes, and phonolites from Kenya Colony, 1199.  
 Sodium chloride and fluoride, on the amplitude of vibration of ions in, 193.  
 Solid friction, on vibrations damped by, 329.  
 Solids, on the contact of, 610.  
 Sound, on the propagation of, in suspensions, 752.  
 Sound-velocities in air, oxygen, and carbon dioxide, on measurements of, 1020.  
 Sound-waves, on the scattering of, by small elastic spheres, 741.  
 Space charge, on the distribution of, between a plane hot cathode and a parallel anode, 80.  
 Space-group of the alkaline sulphates, on the, 665.  
 Spacetime, on illuminated, 50.  
 Spectrum, on new bands in the secondary, of hydrogen, 37<sup>2</sup>; on the band, of cadmium and of bismuth, 519; on the, of mercury, 673.  
 Sphere, on second order expressions for the potentials of a, 964.  
 Spheres of soft metals, on the collision of, 593.  
 Spheres, on the scattering of sound-waves by small elastic, 741.  
 Starr (A. T.) on the lag in a thermometer, 901.  
 Stars, on the equilibrium of dense, 944.  
 Statistical mechanics, on new methods in, 584.  
 Statistics, on the probability method in the new, 621.  
 Stephens (E.) on the Hall effect, electrical conductivity, and thermoelectric power of the lead-antimony alloys, 547.  
 Stone (W.) on some phenomena of the contact of solids, 610.  
 Stoner (Dr. E. C.) on the equilibrium of dense stars, 944.  
 Stress, on the critical, for tubular struts, 324, 686.  
 Stress distribution in a beam. effect of a circular hole on the, 210.  
 Stresses, on initial and maximum, in ties and struts, 426, 1094.  
 String, on the theory of the piano-forte, struck by a hard hammer, 306, 321.  
 Strings, on the generation of pulses in vibrating, 88.  
 Struts, on the critical stress for tubular, 324, 686; on initial and maximum stresses in, 426, 1094.  
 Surface tension, notes on, 1066.  
 Suspensions, on the propagation of sound in, 752.  
 Sylvine, on the amplitude of vibration of ions in, 193; on the etch-figures of, 233.  
 Synge (E. H.) on a method of investigating the higher atmosphere, 1014.  
 Taylor (Dr. J. L.) on some hydrodynamical inertia coefficients, 161.  
 Teegan (J. A. C.) on the application of the photoelectric cell to the measurement of small displacements, 589.  
 Temperature distribution along a heated filament, on the, 28.  
 — measurements in gaseous combustion, on, 402.  
 —, on the effective, of a warmed room, 858.  
 Thermionic emission of oxide cathodes, on the, 440.  
 Thermoelectric power, on the, of the lead-antimony series of alloys, 547.  
 Thermometer, on the lag in a, 901.  
 Thomas (S.) on vibrations damped by solid friction, 329.  
 Thompson (B.) on the upper estuarine series of Northamptonshire, 671.  
 Thomson (Sir J. J.) on the relation of electronic waves to light quanta and to Planck's law, 1185.  
 Thornton (Prof. W. M.) on the propagation of flame in gaseous explosions, 260.  
 Ties, on initial and maximum stresses in, 426, 1094.  
 Tomlinson (G. A.) on a molecular theory of elastic hysteresis, 913.  
 Townsend (Prof. J. S.) on the energies of electrons in gases, 1145.  
 Trivelli (A. P. H.) on the quantum theory of X-ray exposures on photographic emulsions, 787.

- Tungsten, on the scattering power of, 57.
- Turbulence in front of a body moving through a viscous fluid, on the, 1038.
- Tutton (Dr. A. E. H.) on the space-group of the alkaline sulphates, 867.
- Tuzi (Z.) on the effect of a circular hole on the stress distribution in a beam, 210.
- Tyler (E.) on the distribution of vortices behind obstacles, 1113.
- Tyler (F.) on the magnetic characteristics of nickel, 1026.
- Valency, on the electronic theory of, 233.
- Vaporization, on the effect of a dipole on the latent heat of, of a liquid, 422.
- Vernon (M. A.) on the electronic theory of valency, 233.
- Vibrations, on, damped by solid friction, 329; on forced, with combined viscous and Coulomb damping, 801.
- Vina, on the acoustics of the, 88.
- Viscous fluid, on the turbulence in front of a body moving through a, 1038.
- Vision, on the sense of, 817.
- Vortex system in the wake of a cylinder, on the, 489.
- Vortices, on the distribution of, behind obstacles, 1113.
- Walker (Dr. F.) on the geology of the Shiant Isles, 864.
- Warren (A. G.) on the free and forced symmetrical oscillations of thin bars, circular diaphragms, and annuli, 881.
- Water, on the cataphoresis of small particles in, 769.
- Wave-length, on hydrogen and helium lines as standards of, 661.
- Weber's law, note on, 817, 827.
- Weyl (Prof. H.) on redshift and relativistic cosmology, 936.
- White (P.) on the scattering and diffraction of cathode-rays, 641.
- Whitehead (S.) on dipoles in relation to the anomalous properties of dielectrics, 865.
- X-ray exposures, on the quantum theory of, on photographic emulsions, 787.
- investigation of the copper-antimony alloys, on an, 993.
- powder-photographs, on the absorption in, 57.
- reflexions, on precision measurements of, from crystal powders, 525.
- X-rays, on the scattering power of the carbon atom for, 204; on the soft, of manganese, 847; on the scattering powers of the atoms in magnesium oxide for, 1081.
- Zero, on the inaccessibility of the absolute, 208.
- Ziamecki (Dr. S. L.) on the Raman effect in the proximity of the critical point, 299.

END OF THE NINTH VOLUME.





INDIAN AGRICULTURAL RESEARCH  
INSTITUTE LIBRARY, NEW DELHI.

[illegible]

GIPNLK—H-4, I.A.R I.—29-4-55—15,000